Scientific and Technical Aerospace Reports

STAR

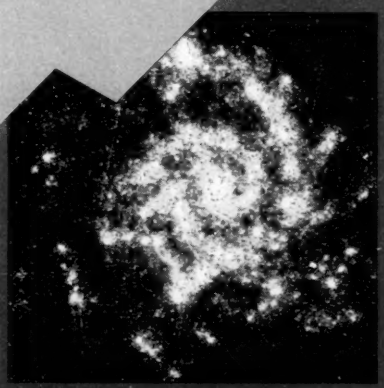

An Abstract Journal

NASA STI PROGRAM SCIENTIFIC & TECHNICAL INFORMATION

Volume 30, Number 19
October 8, 1992
N92-28223 to N92-29227

Scientific and Technical Aerospace Reports

Scientific and Technical Aerospace Reports (STAR) is an abstract journal that provides comprehensive coverage of worldwide aerospace-related reports. It is a major product of the International Aerospace Database managed by the NASA Scientific and Technical Information (STI) Program. The coverage includes reports on aeronautics, space, and supporting disciplines. *STAR* lists current, publicly available reports entered into the NASA STI Database during the 2-week period preceding publication. A typical citation and abstract appear on page viii. They explain how to read the items that are announced in this journal.

NASA sponsors a companion journal, *International Aerospace Abstracts (IAA)* (*NOVA* for internal NASA use) that lists abstracts of the open literature on aerospace subjects available worldwide. *IAA* is available for sale through the AIAA.

Entries found in *STAR* and *IAA* are available through NASA's online service, RECON, as the International Aerospace Database and through DIALOG as the Aerospace Database.

Information on aerospace and related subjects is gathered by the NASA STI Program through national and international agreements and exchanges and is made available to the NASA community as well as to the public in many forms through various outlets. The section on NASA STI Program Products and Services contains additional information.

For further information please contact:
NASA Center for AeroSpace Information (CASI)
P.O. Box 8757
Baltimore, Maryland 21240-0757
(301) 621-0390

US ISSN 0036-8741

Volume 30 Number 19 / October 8, 1992

TABLE OF CONTENTS

AERONAUTICS For related information see also *Astronautics.*

01 AERONAUTICS (GENERAL) **3221**

02 AERODYNAMICS **3226**
Includes aerodynamics of bodies, combinations, wings, rotors, and control surfaces; and internal flow in ducts and turbomachinery. For related information see also *34 Fluid Mechanics and Heat Transfer.*

03 AIR TRANSPORTATION AND SAFETY **3230**
Includes passenger and cargo air transport operations; and aircraft accidents. For related information see also *16 Space Transportation* and *85 Urban Technology and Transportation.*

04 AIRCRAFT COMMUNICATIONS AND NAVIGATION **3230**
Includes digital and voice communication with aircraft; air navigation systems (satellite and ground based); and air traffic control. For related information see also *17 Space Communications, Spacecraft Communications, Command and Tracking* and *32 Communications and Radar.*

05 AIRCRAFT DESIGN, TESTING AND PERFORMANCE **3231**
Includes aircraft simulation technology. For related information see also *18 Spacecraft Design, Testing and Performance* and *39 Structural Mechanics.* For land transportation vehicles see *85 Urban Technology and Transportation.*

06 AIRCRAFT INSTRUMENTATION **3235**
Includes cockpit and cabin display devices; and flight instruments. For related information see also *19 Space craft Instrumentation* and *35 Instrumentation and Photography.*

07 AIRCRAFT PROPULSION AND POWER **3236**
Includes prime propulsion systems and systems components, e.g., gas turbine engines and compressors; and onboard auxiliary power plants for aircraft. For related information see also *20 Spacecraft Propulsion and Power, 28 Propellants and Fuels,* and *44 Energy Production and Conversion.*

08 AIRCRAFT STABILITY AND CONTROL **3239**
Includes aircraft handling qualities; piloting; flight controls; and autopilots. For related information see also *05 Aircraft Design, Testing and Performance.*

09 RESEARCH AND SUPPORT FACILITIES (AIR) **3240**
Includes airports, hangars and runways; aircraft repair and overhaul facilities; wind tunnels; shock tubes; and aircraft engine test stands. For related information see also *14 Ground Support Systems and Facilities (Space).*

ASTRONAUTICS For related information see also *Aeronautics.*

12 ASTRONAUTICS (GENERAL) **3243**
For extraterrestrial exploration see *91 Lunar and Planetary Exploration.*

13 ASTRODYNAMICS **3244**
Includes powered and free-flight trajectories; and orbital and launching dynamics.

14 GROUND SUPPORT SYSTEMS AND FACILITIES (SPACE) **3244**
Includes launch complexes, research and production facilities; ground support equipment, e.g., mobile transporters; and simulators. For related information see also *09 Research and Support Facilities (Air).*

15 LAUNCH VEHICLES AND SPACE VEHICLES **3244**
Includes boosters; operating problems of launch/space vehicle systems; and reusable vehicles. For related information see also *20 Spacecraft Propulsion and Power.*

16 SPACE TRANSPORTATION **3245**
Includes passenger and cargo space transportation, e.g., shuttle operations; and space rescue techniques. For related information see also *03 Air Transportation and Safety* and *18 Spacecraft Design, Testing and Performance.* For space suits see *54 Man/System Technology and Life Support.*

17 SPACE COMMUNICATIONS, SPACECRAFT COMMUNICATIONS, COMMAND AND TRACKING . N.A.
Includes telemetry; space communications networks; astronavigation and guidance; and radio blackout. For related information see also *04 Aircraft Communications and Navigation* and *32 Communications and Radar.*

N.A.—no abstracts were assigned to this category for this issue.

18 SPACECRAFT DESIGN, TESTING AND PERFORMANCE **3246**
Includes satellites; space platforms; space stations; spacecraft systems and components such as thermal and environmental controls; and attitude controls. For life support systems see *54 Man/System Technology and Life Support.* For related information see also *05 Aircraft Design, Testing and Performance, 39 Structural Mechanics,* and *16 Space Transportation.*

19 SPACECRAFT INSTRUMENTATION ..... **N.A.**
For related information see also *06 Aircraft Instrumentation* and *35 Instrumentation and Photography.*

20 SPACECRAFT PROPULSION AND POWER **3248**
Includes main propulsion systems and components, e.g., rocket engines; and spacecraft auxiliary power sources. For related information see also *07 Aircraft Propulsion and Power, 28 Propellants and Fuels, 44 Energy Production and Conversion,* and *15 Launch Vehicles and Space Vehicles.*

CHEMISTRY AND MATERIALS

23 CHEMISTRY AND MATERIALS (GENERAL) **3250**

24 COMPOSITE MATERIALS **3250**
Includes physical, chemical, and mechanical properties of laminates and other composite materials. For ceramic materials see *27 Nonmetallic Materials.*

25 INORGANIC AND PHYSICAL CHEMISTRY **3254**
Includes chemical analysis, e.g., chromatography; combustion theory; electrochemistry; and photochemistry. For related information see also *77 Thermodynamics and Statistical Physics.*

26 METALLIC MATERIALS **3258**
Includes physical, chemical, and mechanical properties of metals, e.g., corrosion; and metallurgy.

27 NONMETALLIC MATERIALS **3261**
Includes physical, chemical, and mechanical properties of plastics, elastomers, lubricants, polymers, textiles, adhesives, and ceramic materials. For composite materials see *24 Composite Materials.*

28 PROPELLANTS AND FUELS **3266**
Includes rocket propellants, igniters and oxidizers; their storage and handling procedures; and aircraft fuels. For related information see also *07 Aircraft Propulsion and Power, 20 Spacecraft Propulsion and Power,* and *44 Energy Production and Conversion.*

29 MATERIALS PROCESSING ..... **N.A.**
Includes space-based development of products and processes for commercial application. For biological materials see *55 Space Biology.*

ENGINEERING For related information see also *Physics.*

31 ENGINEERING (GENERAL) **3268**
Includes vacuum technology; control engineering; display engineering; cryogenics; and fire prevention.

32 COMMUNICATIONS AND RADAR **3272**
Includes radar; land and global communications; communications theory; and optical communications. For related information see also *04 Aircraft Communications and Navigation* and *17 Space Communications, Spacecraft Communications, Command and Tracking.* For search and rescue see *03 Air Transportation and Safety,* and *16 Space Transportation.*

33 ELECTRONICS AND ELECTRICAL ENGINEERING **3278**
Includes test equipment and maintainability; components, e.g., tunnel diodes and transistors; microminiaturization; and integrated circuitry. For related information see also *60 Computer Operations and Hardware* and *76 Solid-State Physics.*

34 FLUID MECHANICS AND HEAT TRANSFER **3282**
Includes boundary layers; hydrodynamics; fluidics; mass transfer and ablation cooling. For related information see also *02 Aerodynamics* and *77 Thermodynamics and Statistical Physics.*

35 INSTRUMENTATION AND PHOTOGRAPHY **3287**
Includes remote sensors; measuring instruments and gauges; detectors; cameras and photographic supplies; and holography. For aerial photography see *43 Earth Resources and Remote Sensing.* For related information see also *06 Aircraft Instrumentation* and *19 Spacecraft Instrumentation.*

36 LASERS AND MASERS **3289**
Includes parametric amplifiers. For related information see also *76 Solid-State Physics.*

37 MECHANICAL ENGINEERING **3292**
Includes auxiliary systems (nonpower); machine elements and processes; and mechanical equipment.

38 QUALITY ASSURANCE AND RELIABILITY **3297**
Includes product sampling procedures and techniques; and quality control.

39 STRUCTURAL MECHANICS **3298**
Includes structural element design and weight analysis; fatigue; and thermal stress. For applications see *05 Aircraft Design, Testing and Performance* and *18 Spacecraft Design, Testing and Performance.*

GEOSCIENCES For related information see also *Space Sciences.*

42 GEOSCIENCES (GENERAL) **3305**

43 EARTH RESOURCES AND REMOTE SENSING **3305**
Includes remote sensing of earth resources by aircraft and spacecraft; photogrammetry; and aerial photography. For instrumentation see *35 Instrumentation and Photography.*

44 ENERGY PRODUCTION AND CONVERSION **3306**
Includes specific energy conversion systems, e.g., fuel cells; global sources of energy; geophysical conversion; and windpower. For related information see also *07 Aircraft Propulsion and Power, 20 Spacecraft Propulsion and Power,* and *28 Propellants and Fuels.*

45 ENVIRONMENT POLLUTION **3308**
Includes atmospheric, noise, thermal, and water pollution.

46 GEOPHYSICS **3308**
Includes aeronomy; upper and lower atmosphere studies; ionospheric and magnetospheric physics; and geomagnetism. For space radiation see *93 Space Radiation.*

47 METEOROLOGY AND CLIMATOLOGY **3318**
Includes weather forecasting and modification.

48 OCEANOGRAPHY **3320**
Includes biological, dynamic, and physical oceanography; and marine resources. For related information see also *43 Earth Resources and Remote Sensing.*

LIFE SCIENCES

51 LIFE SCIENCES (GENERAL) **3323**

52 AEROSPACE MEDICINE **3324**
Includes physiological factors; biological effects of radiation; and effects of weightlessness on man and animals.

53 BEHAVIORAL SCIENCES **3326**
Includes psychological factors; individual and group behavior; crew training and evaluation; and psychiatric research.

54 MAN/SYSTEM TECHNOLOGY AND LIFE SUPPORT **3329**
Includes human engineering; biotechnology; and space suits and protective clothing. For related information see also *16 Space Transportation.*

55 SPACE BIOLOGY ..... **N.A.**
Includes exobiology; planetary biology; and extraterrestrial life.

MATHEMATICAL AND COMPUTER SCIENCES

59 MATHEMATICAL AND COMPUTER SCIENCES (GENERAL) ..... **N.A.**

60 COMPUTER OPERATIONS AND HARDWARE **3332**
Includes hardware for computer graphics, firmware, and data processing. For components see *33 Electronics and Electrical Engineering.*

61 COMPUTER PROGRAMMING AND SOFTWARE **3333**
Includes computer programs, routines, algorithms, and specific applications, e.g., CAD/CAM.

62 COMPUTER SYSTEMS **3341**
Includes computer networks and special application computer systems.

63 CYBERNETICS **3344**
Includes feedback and control theory, artificial intelligence, robotics and expert systems. For related information see also *54 Man/System Technology and Life Support.*

64 NUMERICAL ANALYSIS **3346**
Includes iteration, difference equations, and numerical approximation.

65 STATISTICS AND PROBABILITY **3348**
Includes data sampling and smoothing; Monte Carlo method; and stochastic processes.

66 SYSTEMS ANALYSIS **3349**
Includes mathematical modeling; network analysis; and operations research.

67 THEORETICAL MATHEMATICS **3349**
Includes topology and number theory.

PHYSICS For related information see also *Engineering.*

70 PHYSICS (GENERAL) **3350**
For precision time and time interval (PTTI) see *35 Instrumentation and Photography;* for geophysics, astrophysics or solar physics see *46 Geophysics, 90 Astrophysics,* or *92 Solar Physics.*

71 ACOUSTICS **3351**
Includes sound generation, transmission, and attenuation. For noise pollution see *45 Environment Pollution.*

72 ATOMIC AND MOLECULAR PHYSICS **3354**
Includes atomic structure, electron properties, and molecular spectra.

73 NUCLEAR AND HIGH-ENERGY PHYSICS **3356**
Includes elementary and nuclear particles; and reactor theory. For space radiation see *93 Space Radiation.*

74 OPTICS **3357**
Includes light phenomena and optical devices. For lasers see *36 Lasers and Masers.*

75 PLASMA PHYSICS **3360**
Includes magnetohydrodynamics and plasma fusion. For ionospheric plasmas see *46 Geophysics.* For space plasmas see *90 Astrophysics.*

76 SOLID-STATE PHYSICS **3362**
Includes superconductivity. For related information see also *33 Electronics and Electrical Engineering* and *36 Lasers and Masers.*

77 THERMODYNAMICS AND STATISTICAL PHYSICS **3366**
Includes quantum mechanics; theoretical physics; and Bose and Fermi statistics. For related information see also *25 Inorganic and Physical Chemistry* and *34 Fluid Mechanics and Heat Transfer.*

SOCIAL SCIENCES

80 SOCIAL SCIENCES (GENERAL) ..... **N.A.**
Includes educational matters.

81 ADMINISTRATION AND MANAGEMENT **3366**
Includes management planning and research.

82 DOCUMENTATION AND INFORMATION SCIENCE **3367**
Includes information management; information storage and retrieval technology; technical writing; graphic arts; and micrography. For computer documentation see *61 Computer Programming and Software.*

83 ECONOMICS AND COST ANALYSIS **3370**
Includes cost effectiveness studies.

84 LAW, POLITICAL SCIENCE AND SPACE POLICY ..... **N.A.**
Includes NASA appropriation hearings; aviation law; space law and policy; international law; international cooperation; and patent policy.

85 URBAN TECHNOLOGY AND TRANSPORTATION **3370**
Includes applications of space technology to urban problems; technology transfer; technology assessment; and surface and mass transportation. For related information see *03 Air Transportation and Safety, 16 Space Transportation,* and *44 Energy Production and Conversion.*

SPACE SCIENCES For related information see also *Geosciences.*

88 SPACE SCIENCES (GENERAL) ..... **N.A.**

89 ASTRONOMY **3370**
Includes radio, gamma-ray, and infrared astronomy; and astrometry.

90 ASTROPHYSICS **3371**
Includes cosmology; celestial mechanics; space plasmas; and interstellar and interplanetary gases and dust. For related information see also *75 Plasma Physics.*

91 LUNAR AND PLANETARY EXPLORATION **3372**
Includes planetology; and manned and unmanned flights. For spacecraft design or space stations see *18 Spacecraft Design, Testing and Performance.*

92 SOLAR PHYSICS **3395**
Includes solar activity, solar flares, solar radiation and sunspots. For related information see *93 Space Radiation.*

93 SPACE RADIATION **3397**
Includes cosmic radiation; and inner and outer earth's radiation belts. For biological effects of radiation see *52 Aerospace Medicine.* For theory see *73 Nuclear and High-Energy Physics.*

GENERAL

Includes aeronautical, astronautical, and space science related histories, biographies, and pertinent reports too broad for categorization; histories or broad overviews of NASA programs.

99 GENERAL **3397**

SUBJECT INDEX **I-1**

PERSONAL AUTHOR INDEX **I-75**

CORPORATE SOURCE INDEX **I-83**

CONTRACT NUMBER INDEX **I-97**

REPORT NUMBER INDEX **I-99**

ACCESSION NUMBER INDEX **I-107**

APPENDIX **A-1**

TYPICAL CITATION AND ABSTRACT

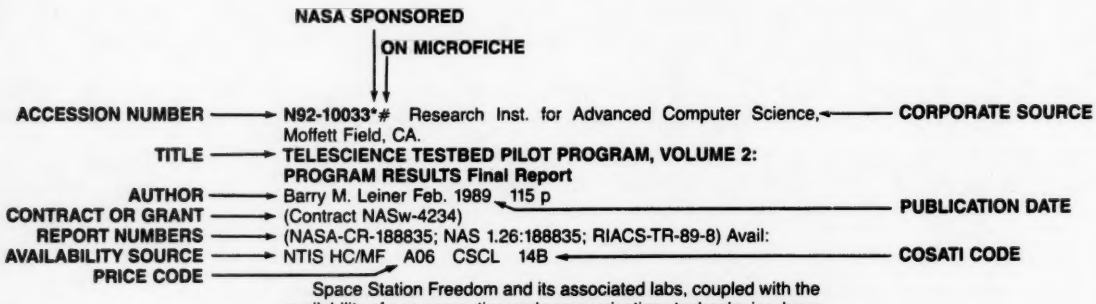

Space Station Freedom and its associated labs, coupled with the availability of new computing and communications technologies, have the potential for significantly enhancing scientific research. A Telescience Testbed Pilot Program (TTPP), aimed at developing the experience base to deal with issues in the design of the future information system of the Space Station era. The testbeds represented four scientific disciplines (astronomy and astrophysics, earth sciences, life sciences, and microgravity sciences) and studied issues in payload design, operation, and data analysis. This volume, of a 3 volume set, which all contain the results of the TTPP, contains the integrated results. Background is provided of the program and highlights of the program results. The various testbed experiments and the programmatic approach is summarized. The results are summarized on a discipline by discipline basis, highlighting the lessons learned for each discipline. Then the results are integrated across each discipline, summarizing the lessons learned overall.

Author

VOLUME 30 NUMBER 19 / OCTOBER 8, 1992

Scientific and Technical Aerospace Reports

A Semimonthly Publication of the National Aeronautics and Space Administration

01 AERONAUTICS (GENERAL)

N92-28348# Air Force Inst. of Tech., Wright-Patterson AFB, OH. School of Systems and Logistics.
LIFE CYCLE COSTS OF THE C-130 ELECTRICAL POWER SYSTEM UPGRADE M.S. Thesis
Theodore D. Seymour Sep. 1991 141 p
(AD-A246759; AFIT/GLM/LSQ/91S-57) Avail: NTIS HC/MF A07 CSCL 01/3

This research investigated the life cycle costs of three alternative electrical power systems for a planned electrical system upgrade to the C-130 transport aircraft. Research identified the contractors as Sundstrand, Westinghouse, and Leland. The literature review included discussions on the C-130, electrical power systems and the proposed alternatives, and the elements of life cycle cost analysis. In the discussion on supportability issues, this research evaluated changes in mission capable rates and the needed fleet size to perform the current mission. In estimating Operating and Support costs, this research used the analogy approach. Analogies were based on expert opinions of Air Force and industry engineers. Sensitivity analysis was then performed on these expert's predictions to help in the formation of conclusions. The system performance of all options netted similar results. However, Alternative 3 had the lowest total life cycle costs, making it the most cost effective option. This research concluded the Leland proposal to be the best choice and recommends implementation of the proposal. GRA

N92-28522# Advisory Group for Aerospace Research and Development, Neuilly-Sur-Seine (France). Flight Mechanics Panel.
PILOTED SIMULATION EFFECTIVENESS [L'EFFICACITE DE LA SIMULATION PILOTEE]
Feb. 1992 349 p In ENGLISH and FRENCH Symposium held in Brussels, Belgium, 14-17 Oct. 1991
(AGARD-CP-513; ISBN-92-835-0656-1) Copyright Avail: NTIS HC/MF A15

The ability of piloted simulators to represent military and civil aviation operational tasks with ever increasing levels of fidelity is leading to a steady growth in their use for all areas of aviation from new concept studies, through support for development and flight clearance, to training aircrews for complex missions. The papers here present a variety of experience of the effectiveness of simulation for many of the key areas of application. This session focuses on: the use of simulation in aircraft development programs; the use of simulation in developing piloting skills; the use and potential of simulation in full mission training for military roles; and the effectiveness of simulation for a variety of research tasks. For individual titles, see N92-28523 through N92-28552.

N92-28523# Federal Ministry for Defence, Bonn (Germany, F.R.). Armaments Technology Directorate.
OPPORTUNITIES FOR FLIGHT SIMULATION TO IMPROVE OPERATIONAL EFFECTIVENESS **c09**
J. Heyden *In* AGARD, Piloted Simulation Effectiveness Feb. 1992 15 p (For primary document see N92-28522 19-01)
Copyright Avail: NTIS HC/MF A15

The keynote address gives an overview over the opportunities of piloted simulation for the development of aircraft and for the training of aircrews to operate the aircraft. Based on the military flight mission requirements some critical issues of peacetime military operations in Europe are discussed and the resulting opportunities for application of flight simulation in development and training are presented. The address concludes on recommendations for piloted simulation. Author

N92-28524# Wright Lab., Wright-Patterson AFB, OH. Flight Dynamics Directorate.
PILOTED SIMULATION EFFECTIVENESS DEVELOPMENT APPLICATIONS AND LIMITATIONS **c09**
Richard A. Borowski *In* AGARD, Piloted Simulation Effectiveness Feb. 1992 3 p (For primary document see N92-28522 19-01)
Copyright Avail: NTIS HC/MF A15

The author of this brief note begins by describing how flight simulators were first developed, and the reasons that brought about this research. The remainder of his paper is a survey of some simulation systems used in the U.S. with the recognition that similar and in some cases superior systems exist elsewhere. Concentration is placed on simulators run by the government, the military, and NASA. H.A.

N92-28525# Air Force Flight Test Center, Edwards AFB, CA.
UTILITY OF GROUND SIMULATION IN FLIGHT CONTROL PROBLEM IDENTIFICATION, SOLUTION DEVELOPMENT, AND VERIFICATION **c09**
K. L. Keller, D. B. Janzen, and A. A. Asay *In* AGARD, Piloted Simulation Effectiveness Feb. 1992 8 p (For primary document see N92-28522 19-01)
Copyright Avail: NTIS HC/MF A15

The Air Force Flight Test Center (AFFTC) Flying Qualities Simulator is consistently used prior to and in conjunction with flight test to identify aircraft flight control problems and also to develop, test, and validate solutions to these problems. The subject of this paper is an example of how ground simulation was vital in developing an effective software modification to eliminate a potentially dangerous aircraft flight control anomaly. Through simulation, an in flight uncommanded pitch oscillation incident was investigated and the source of the problem was identified. A potential solution was tested and validated by utilizing the simulator prior to flight test. Additional benefits were gained due to simulation studies. The project pilots were able to practice test maneuvers and emergency procedures essential to the flight test program. The preliminary work accomplished by ground simulation correctly predicted the effectiveness of the software modifications and ensured the success of an efficient and valid flight test program. Author

N92-28526# Aerospatiale, Toulouse (France).
FLIGHT SIMULATION AND DIGITAL FLIGHT CONTROLS **c09**
D. Chatrenet *In* AGARD, Piloted Simulation Effectiveness Feb. 1992 4 p (For primary document see N92-28522 19-01)
Copyright Avail: NTIS HC/MF A15

The A-320 is the first civil airliner to make extensive use of digital flight controls. Despite previous experience with this technology, developing this system quickly has proven a challenge. Flight simulation with a high degree of fidelity has played a key role in flight control development. Simulation has also complemented the flight testing of the A-320-200. Digital flight

control has moved the critical areas from aerodynamic model accuracy to flight control system representation exactness. Simulator acceptance procedures had also to be adapted to address the case of closed loop controlled aircraft correctly.
Author

N92-28527# McDonnell-Douglas Helicopter Co., Mesa, AZ. Flight Mechanics/Performance Dept.
THE APPLICATION OF FLIGHT SIMULATION MODELS IN SUPPORT OF ROTORCRAFT DESIGN AND DEVELOPMENT **c09**
P. Shanthakumaran *In* AGARD, Piloted Simulation Effectiveness Feb. 1992 28 p (For primary document see N92-28522 19-01)
Copyright Avail: NTIS HC/MF A15

McDonnell Douglas Helicopter Company's overall approach to design development and flight evaluation through flight simulation models is presented. Flight simulation model description, validation against flight test data bases, and applications for rotorcraft design and development, are presented. Specific model refinements for each application are emphasized. Examples include power-off emergency landing, empennage design, maneuver envelope expansion, engine-airframe integration, and manned simulations.
Author

N92-28528# Messerschmitt-Boelkow-Blohm G.m.b.H., Munich (Germany, F.R.). Helicopter Div.
EXPERIENCE WITH PILOTED SIMULATION IN THE DEVELOPMENT OF HELICOPTERS **c09**
M. Obermayer, K. Kampa, W. Doehnel, and A. Faulkner *In* AGARD, Piloted Simulation Effectiveness Feb. 1992 11 p (For primary document see N92-28522 19-01)
Copyright Avail: NTIS HC/MF A15

Based on examples from several projects this paper reflects MBB's experience with applicability, limitations, acceptance, and effectiveness of helicopter simulation. Some of the key points are the objective and subjective validation of a simulator and various factors, which influence the acceptance by pilots. In this context it is very important to make a trade-off between simulator sophistication and required results. Other aspects of simulation effectiveness include evaluation and training of critical flight conditions prior to flight tests as well as involving the customer from early concept studies up to full mission simulations, which gives him more influence on the design and leads to better identification with the product.
Author

N92-28529# Thomson-CSF, Malakoff (France).
INTEREST IN REAL-TIME SIMULATIONS FOR THE DEVELOPMENT TERRAIN FOLLOWING FUNCTION OF RADAR SYSTEMS [INTERET DES SIMULATIONS 'TEMPS REEL' POUR LE DEVELOPPEMENT DE LA FONCTION SUIVI DE TERRAIN DES SYSTEMES RADAR] **c32**
T. Martinet *In* AGARD, Piloted Simulation Effectiveness Feb. 1992 5 p In FRENCH; ENGLISH summary (For primary document see N92-28522 19-01)
Copyright Avail: NTIS HC/MF A15

During a penetration mission, modern tactical aircraft have to fly over regions with heavy electromagnetic environments. To realize such a mission, a minimum knowledge of terrain elevation is needed. Terrain elevation knowledge can be obtained from real time sensors such as radar. The development of terrain following function becoming more and more complicated, it necessitates the use of simulations to analyze the performance of sophisticated data processing and flight control. The aim of this paper is to demonstrate the contribution of interactive real time simulations during the phase of development to optimize radar resources management, in different types of terrain and many configurations of electronic warfare. It is then shown how the operational people can take part to the definition of the radar to obtain the most appropriate comportment. It is finally described how to characterize the radar performances in the complete weapon system and observe the manifestation of error simulation on the security of the system.
Author

N92-28530# Naval Air Test Center, Patuxent River, MD. Strike Aircraft Test Directorate.
USE OF HIGH-FIDELITY SIMULATION IN THE DEVELOPMENT OF AN F/A-18 ACTIVE GROUND COLLISION AVOIDANCE SYSTEM **c03**
Timothy R. Fitzgerald and Michael T. Brunner *In* AGARD, Piloted Simulation Effectiveness Feb. 1992 13 p (For primary document see N92-28522 19-01)
Copyright Avail: NTIS HC/MF A15

An active Ground Collision Avoidance System (GCAS) was developed for the F/A-18 using the Naval Air Test Center's F/A-18 simulation. The simulation was used for the development of all three components of GCAS: (1) the algorithms used to determine the recovery initiation altitude; (2) the additional flight control laws (FCL's) necessary to perform the recovery maneuver; and (3) the visual and audio cues used to provide recovery status information to the pilot. The use of a simulation has allowed the rapid development of a viable F/A-18 GCAS that incorporates technology from the F/A-18 Integrated Fire and Flight Control (IFFC) simulation and the Advanced Fighter Technology Integration (AFTI) F-16 program. Complete system development and preliminary evaluations were performed using the simulation. This increased overall project safety while decreasing development and potential flight test costs significantly.
Author

N92-28531# Royal Aerospace Establishment, Bedford (England). FMS Div.
VALIDATION OF SIMULATION SYSTEMS FOR AIRCRAFT ACCEPTANCE TESTING **c05**
A. A. Woodfield *In* AGARD, Piloted Simulation Effectiveness Feb. 1992 4 p (For primary document see N92-28522 19-01)
Copyright Avail: NTIS HC/MF A15

There is currently a limited role for simulation in flight clearance of sub-systems in civil aircraft. However, the extensive use of simulation for manned space vehicle clearance shows the potential for simulation to join other rigs in flight clearance. There is a serious risk that simulation could prove inadequate if there is no systematic validation program. Simulation is a complex integration of models of vehicles and the environment, physical sensation devices and the pilot. Any of these can be modified to compensate for inadequacies in parts of the simulation. This can be acceptable for training simulators but is not acceptable for clearance activities because the influence of such modifications cannot be predicted in situations that are not going to be tested in flight. These issues are discussed.
Author

N92-28532# National Aerospace Lab., Amsterdam (Netherlands).
AIRCRAFT SIMULATION AND PILOT PROFICIENCY: FROM SURROGATE FLYING TOWARDS EFFECTIVE TRAINING **c09**
P. G. A. M. Jorna, E. R. A. vanKleef (Royal Netherlands Air Force, The Hague.), and W. P. deBoer *In* AGARD, Piloted Simulation Effectiveness Feb. 1992 8 p (For primary document see N92-28522 19-01)
Copyright Avail: NTIS HC/MF A15

Simulators are currently built as simple system 'look-a-likes' and a structured or experimentally validated approach to their use and implementation as part of a comprehensive training system is lacking. This is one reason why their use in training was not always as successful as expected. This paper reviews some experiences with the application of simulators in military flight training and it reports research strategies like the development of objective performance measures in support of validation trials and future simulator development. It is proposed to prototype simulator concepts before implementing them and relevant research initiatives in this area are reviewed.
Author

N92-28533# CAE Electronics Ltd., Montreal (Quebec). Tactical Systems Div.
THE USE OF A DEDICATED TESTBED TO EVALUATE SIMULATOR TRAINING EFFECTIVENESS **c09**
David Kurts and Charles Gainer (Army Research Inst. Aviation Research and Development Activity, Fort Rucker, AL.) *In* AGARD,

Piloted Simulation Effectiveness Feb. 1992 9 p (For primary document see N92-28522 19-01)
Copyright Avail: NTIS HC/MF A15

The Simulator Complexity Test Bed (SCTB) is being produced for the U. S. Army Research Institute Aviation Research and Development Activity (ARIARDA) to specifically address the question of the level of simulation fidelity required to ensure adequate transfer of training in a tactical helicopter simulator environment. This paper presents the objectives of the SCTB, the hardware and software architecture designed to facilitate these goals, and presents examples of some typical research that will be conducted. The simulator is based on the Apache AH-64A attack helicopter using aircraft parts and simulated avionics to provide a realistic replica of the pilot and copilot gunner positions. Author

N92-28534# Netherlands Aerospace Medical Centre, Soesterberg.
G-TOLERANCE AND SPATIAL DISORIENTATION: CAN SIMULATION HELP US? **c52**
J. Smit and Robert E. vanPatten (Van Patten, Robert E., Bellbrook, OH) *In* AGARD, Piloted Simulation Effectiveness Feb. 1992 7 p (For primary document see N92-28522 19-01)
Copyright Avail: NTIS HC/MF A15

Pilots of modern fighter aircraft are endangered by high G-forces, loss of situational awareness, and spatial disorientation. In order to prepare aircrew for these factors, ground based training facilities simulating some aspects of the relevant phenomena are used. The human centrifuge has proven to be rather effective in increasing G-tolerance, especially in conditions of high onset rate. Unrealistic simulations caused by the small radius of rotation in centrifuges can generate disturbing vestibular stimulation. During the development of the human centrifuge at the Netherlands Aerospace Medical Center an investigation was undertaken to find methods to suppress these detrimental effects. Smoothing of centrifuge motion and a realistic, computer-generated outside-vision system proved to be effective measures. Realistic target tracking and a cockpit-like environment are factors which enhance transfer of training. Author

N92-28535# Air Force Flight Test Center, Edwards AFB, CA. Test and Evaluation Simulator.
USE OF SIMULATION IN THE USAF TEST PILOT SCHOOL CURRICULUM **c09**
Daniel P. Ringenbach, Steven E. Louton (NSI Technology Services Corp., Research Triangle Park, NC.), and Daniel Gleason *In* AGARD, Piloted Simulation Effectiveness Feb. 1992 7 p (For primary document see N92-28522 19-01)
Copyright Avail: NTIS HC/MF A15

The six degree-of-freedom, real time, Test Pilot School (TPS) simulator at the Test and Evaluation Mission Simulator (TEMS) of the Air Force Flight Test Center (AFFTC) is an invaluable and versatile tool used by the TPS. It is an effective learning tool providing positive reinforcement on basic aircraft dynamics taught in the classroom and an efficient evaluation tool for flight control systems designed by the students. Author

N92-28536# Alenia, Torino (Italy). Flight Simulation Center.
AM-X FLIGHT SIMULATOR FROM ENGINEERING TOOL TO TRAINING DEVICE **c09**
A. Armando, P. Castoldi, and F. Fassi *In* AGARD, Piloted Simulation Effectiveness Feb. 1992 12 p (For primary document see N92-28522 19-01)
Copyright Avail: NTIS HC/MF A15

Effectiveness of Flight Simulation with pilot-in-the-loop can be intended rather differently depending on the context in which the simulation activities are carried out, namely in the two traditional areas of Research & Development (R&D) and Training. In the latter case, effectiveness can be considered the amount of training a simulator is able to transfer per time unit, while in the case of R&D simulation its effectiveness is related to the amount of confidence engineers can gain in the prediction of an airborne system behavior before releasing it to the real flight. Pursuing the maximization of effectiveness in these two different contexts leads to different approaches in applying simulation methodologies. This paper will show to what extent a simulation facility created and continuously improved to support the development of a new attack aircraft, the AM-X, was finally capable of training operational pilots during the conversion to that aircraft. Author

N92-28537# Sikorsky Aircraft, Stratford, CT.
FULL MISSION SIMULATION: A VIEW INTO THE FUTURE **c09**
Michael J. Ferranti and Stephen H. Silder, Jr. *In* AGARD, Piloted Simulation Effectiveness Feb. 1992 10 p (For primary document see N92-28522 19-01)
Copyright Avail: NTIS HC/MF A15

The use of engineering simulation as a design support tool is becoming more prevalent in assisting design engineers in prototyping new concepts in advanced integrated helicopters. The primary goal in using full mission simulation as a risk reduction tool is that it can provide significant insight into critical design areas. In this capacity, it allows the research engineer the means to review critical design issues and assess areas of high risk associated with air vehicle design. The use of the Engineering Development Full Mission Flight Simulator (EDFMFS) will allow the design engineers the opportunity to view the future performance of the design air vehicle. This includes areas of both aerodynamic and operational suitability. The use of representative flight simulators will allow major design issues to be resolved with a significant reduction in the cost normally associated with developmental flight testing. The performance of flight control laws and cockpit design can be evaluated in the safe and secure environment of the simulator before actual flight test. In this regard, the capabilities of EDFMFS's have shown themselves to be an outstanding tool in evaluating advanced design aircraft during the initial design phase. Today's use of statistical and multivarient analysis techniques provides the designers with a real time quantitative capability to collect and analyze data, thus, reducing the risk associated with new product development. The methodologies used that provide the designer and pilots with the unique opportunity to evaluate different aircraft configurations in the Full Mission Flight Simulator before the design is concluded are identified. Author

N92-28538# Wright Lab., Wright-Patterson AFB, OH.
FULL MISSION SIMULATION FOR RESEARCH AND DEVELOPMENT OF AIR COMBAT FLIGHT AND ATTACK MANAGEMENT SYSTEMS **c09**
Daniel G. Goddard and James M. Zeh *In* AGARD, Piloted Simulation Effectiveness Feb. 1992 13 p (For primary document see N92-28522 19-01)
Copyright Avail: NTIS HC/MF A15

A description is presented of the analysis approach for an advanced development program using a realtime, pilot-in-the-loop air combat simulation. The program is developing and demonstrating advanced onboard flight and attack management algorithms to assist the pilot when outnumbered in air-to-air combat. A highly flexible simulation architecture allows hosting the flight test computer code in general purpose simulation computers. The simulator cockpit stations are modified to emulate the advanced pilot vehicle interface. A data collection and analysis approach is described which isolates and measures the effects of the various systems making up the advanced fighter concept. Author

N92-28539# CAE Electronics Ltd., Saint Laurent (Quebec).
THE EVALUATION OF SIMULATOR EFFECTIVENESS FOR THE TRAINING OF HIGH SPEED, LOW LEVEL, TACTICAL FLIGHT OPERATIONS **c09**
Andrew Morris and Paul E. VanHemel (CAE-Link Corp., Alexandria, VA.) *In* AGARD, Piloted Simulation Effectiveness Feb. 1992 11 p (For primary document see N92-28522 19-01)
Copyright Avail: NTIS HC/MF A15

The German Government has initiated a three phase program to evaluate the use of an improved simulator for the Tornado aircraft. In the first phase of this program computer aided

engineering (CAE) has built a prototype simulator, referred to as the Evaluation Unit (EU). The improvements in the EU consist of visual system upgrades to provide a CAE Fiber-Optic Helmet Mounted Display (FOHMD) for the pilot and weapon system officer (WSO), with imagery from an Evans & Sutherland ESIG-1000 image generator, as well as a six-degree of freedom (DOF) motion system. The EU was installed at CAE Electronics GmbH in Stolberg, Germany. Military and industrial representatives are conducting an evaluation of the upgraded simulator to assess its capability to provide high speed, low level, tactical flight operations training capability. A factorial analysis of variance (ANOVA) design is being used to objectively assess recorded performance data and subjective impressions data collected during simulator flights by military crews from the German Air Force and Navy. Author

N92-28540# Ministry of Defence, London (England).
HARRIER GR MK 5/7 MISSION SIMULATORS FOR THE ROYAL AIR FORCE **c09**
B. R. Clifford and P. Jackson (Link-Miles, Lancing, England) *In* AGARD, Piloted Simulation Effectiveness Feb. 1992 6 p (For primary document see N92-28522 19-01)
Copyright Avail: NTIS HC/MF A15

IN 1985, in anticipation of the phased replacement of the Harrier GR MK 3 by the Harrier GR MK 5, the UK version of the AV8B, the UK Air Staff issued a requirement for two mission simulators capable of fulfilling a comprehensive pilot training and evaluation task. It identified the need for simulators which would provide a wide range of psycho-physical cues with accurate flight and systems simulation, integrated with a high resolution, wide field-of-view visual system compatible with the Harrier's operational roles and inherent speed and agility. It became apparent that this would require the utilization of new technology, particularly in the area of head and eye-slaved visual displays; studies within the MoD confirm this and conclude that although innovative, the application of such technology was feasible. Some of the background and selection process are reviewed, and the mission simulators selected to meet the Royal Air Force's training needs are briefly described. Author

N92-28541# Messerschmitt-Boelkow-Blohm G.m.b.H., Ottobrunn (Germany, F.R.).
DEVELOPMENT AND EVALUATION OF AN ATTACK AND MANEUVERING SYSTEM WITH COMBAT DEVELOPMENT SIMULATORS AS MAIN DEVELOPMENT TOOL **c09**
Herbert Eibl, Hans-Guenter Offenbeck, and Hans W. Pongratz *In* AGARD, Piloted Simulation Effectiveness Feb. 1992 17 p (For primary document see N92-28522 19-01)
Copyright Avail: NTIS HC/MF A15

As a result of conceptual design work on future fighter aircraft and of future air/air weapons it was concluded that in future air/air combat, especially in the beyond visual range (BVR) scenario, a pilot has to be supported by means of intelligent onboard processing equipment in order to fulfill his most demanding tasks by fully exploiting the weapon system capabilities. An integrated fire and tactical flight director control system was developed for the entire air combat arena by DASA MBB's Military Aircraft Division in its manned simulator facility. A description of the developed system and the used simulator facility is given. As a first step to verify this development, the Attack and Maneuvering System (AMS) for the BVR-air combat was successfully evaluated by the German Air Force in a large scale manned realtime simulation study. It was demonstrated that such a system can significantly improve the combat effectiveness of a modern fighter aircraft in the BVR-scenario by a factor of up to 6. Author

N92-28542# Naval Air Test Center, Patuxent River, MD. Rotary Wing Aircraft Test Directorate.
SHIPBOARD MISSION TRAINING EFFECTIVENESS OF THE NAVAL AIR TEST CENTER'S V-22 GOVERNMENT TEST PILOT TRAINER **c09**
G. Vandervliet, C. Miller, and P. Croisetiere *In* AGARD, Piloted Simulation Effectiveness Feb. 1992 12 p (For primary document see N92-28522 19-01)
Copyright Avail: NTIS HC/MF A15

Initial shipboard compatibility tests of the V-22 Osprey VSTOL tiltrotor aircraft were conducted aboard the USS Wasp (LHD-1) on 4-8 Dec. 1990. Pilot training and engineering analysis for the first shipboard launches and recoveries of the V-22 Osprey aircraft were conducted in the V-22 simulator at the Naval Air Test Center. During these sessions, workload data was recorded and the pilots made comments regarding the quality of the training. Quantitative comparisons of time history data were made using power spectral densities, averages, and maximum attained values. Qualitative comments were compared to the remarks made after the actual at-sea tests. Conclusions are drawn concerning the effectiveness of the training, and suggestions for future improvements are made. Author

N92-28543# Office National d'Etudes et de Recherches Aerospatiales, Paris (France).
USE OF A RESEARCH SIMULATOR FOR THE DEVELOPMENT OF NEW CONCEPTS OF FLIGHT CONTROL [UTILISATION D'UN SIMULATEUR DE RECHERCHE POUR LE DEVELOPPEMENT DE NOUVEAUX CONCEPTS DE COMMANDES DE VOL] **c09**
Ph. Guicheteau *In* AGARD, Piloted Simulation Effectiveness Feb. 1992 11 p In FRENCH; ENGLISH summary (For primary document see N92-28522 19-01)
Copyright Avail: NTIS HC/MF A15

Several studies performed at ONERA have shown the usefulness of testing the behavior of the whole aircraft with the pilot in the loop by using a research flight simulator as soon as the preliminary design of new FCE for future aircraft is undertaken. The communication presents three conceptual studies related to mission oriented control systems which were performed at ONERA's research flight facility. The description of the conceptual phase of each of these studies and, for two of them, of their further validation on full flight simulators allows a conclusion about the complementary roles of research and full flight simulators. Author

N92-28544# Dassault-Breguet Aviation, Saint Cloud (France).
THE ROLE OF SIMULATION FOR THE STUDY OF APIS (PILOTING SUPPORT BY SYNTHETIC IMAGERY) [LE ROLE DE LA SIMULATION POUR L'ETUDE APIS (AIDE AU PILOTAGE PAR IMAGERIE SYNTHETIQUE)] **c09**
Pierre Larroque, Pierre Pagniez, and Roland Miginiac *In* AGARD, Piloted Simulation Effectiveness Feb. 1992 12 p In FRENCH (For primary document see N92-28522 19-01)
Copyright Avail: NTIS HC/MF A15

This report presents different methods of simulation used at Dassault Aviation for the APIS (pilot support by synthetic imagery) study. The aim of this study was to define man-machine concepts for synthetic imagery derived from onboard information and updated in flight. The imagery system provides the pilot with a comprehension and decision tool that can be used for any flight conditions (low altitude, poor visibility...) and tactical conditions. This document describes: (1) the methods used to produce static images from needs analysis, enabling a preliminary selection of acceptable images; (2) the use of workstations to generate and pilot in real time the solutions retained and to improve the representations; (3) interfacing workstations with a real-time processor and a RAFALE type simulation cabin, permitting manual or automatic execution of a 3-D trajectory in a simple scenario and used after evaluation by 10 pilots; (4) scenarios retained and results obtained as a result of these evaluations; and (5) follow up future spinoffs for the engineering of Dassault fighter aircraft. Transl. by L.B.

N92-28545*# Systems Technology, Inc., Hawthorne, CA.
THE USE OF GROUND BASED SIMULATION FOR HANDLING QUALITIES RESEARCH: A NEW ASSESSMENT **c09**
David G. Mitchell, Roger H. Hoh (Hoh Aeronautics, Inc., Lomita, CA.), Adolph Atencio, Jr. (Army Aviation Systems Command, Moffett Field, CA.), and David L. Key (Army Aviation Systems

Command, Moffett Field, CA.) *In* AGARD, Piloted Simulation Effectiveness Feb. 1992 14 p (For primary document see N92-28522 19-01)
(Contract NAS2-13127)
Copyright Avail: NTIS HC/MF A15

A study was conducted on the NASA Ames Research Center's Vertical Motion Simulator to determine the effects of simulator characteristics on perceived handling characteristics. Differences in pilot opinion were found as the visual and motion parameters were changed, reflecting a change in the pilots' perceptions of handling qualities, rather than changes in the aircraft model itself. The results indicate a need for tailoring the motion without dynamics to suit the task, with reduced washouts for precision maneuvering as compared to aggressive maneuvering. Visual delay data are inconclusive, but suggest that it may be better to allow some time delay in the visual path to minimize the mismatch between vision and motion, rather than eliminate the visual delay entirely through lead compensation. The simulation results are compared with ratings from a similar in-flight simulation experiment. Author

N92-28546# Defence Research Agency, Bedford (England). Flight Systems Dept.
INITIAL VALIDATION OF A R/D SIMULATOR WITH LARGE AMPLITUDE MOTION **c09**
A. D. White, J. R. Hall, and B. N. Tomlinson *In* AGARD, Piloted Simulation Effectiveness Feb. 1992 24 p (For primary document see N92-28522 19-01)
Copyright Avail: NTIS HC/MF A15

The Advanced Flight Simulator (AFS) Complex at the Defense Research Agency (DRA) at Bedford was enhanced by the addition of a large displacement motion platform and a three channel Computer Generated Image (CGI) outside world visual system. The trial described here was the first in a series of trials aimed at validating the AFS in its present configuration and in particular at demonstrating its ability to address a wide variety of vehicle handling qualities with a high degree of fidelity and user confidence. It included a direct comparison between the ground based AFS and the Calspan Learjet in-flight simulator. The comparison between the AFS and Learjet involved three pilots flying the same offset approach landing tasks using the same aircraft model in both the AFS and in flight. The lateral handling qualities were varied by adjusting the time constant of a filter in the pilot's roll control loop. Pilot comments, handling quality, and PIO ratings indicate that the AFS reproduces the lateral handling qualities and roll PIO tendencies of the Learjet in-flight simulator with high fidelity. The degradation in handling qualities and increase in PIO tendencies with increasing filter time constant were clearly revealed in both the AFS and Learjet. The importance of good platform motion cueing and task design when evaluating handling qualities was also demonstrated. Author

N92-28547# Deutsche Airbus G.m.b.H., Hamburg (Germany, F.R.).
USE OF A VIRTUAL COCKPIT FOR THE DEVELOPMENT OF A FUTURE TRANSPORT AIRCRAFT **c09**
Dieter Kricke and Wilfried Quellmann *In* AGARD, Piloted Simulation Effectiveness Feb. 1992 10 p Sponsored in part by BMFT and Council of the European Community (For primary document see N92-28522 19-01)
Copyright Avail: NTIS HC/MF A15

A development tool called the 'visual cockpit' is discussed. A comparison of civil and military transport aircraft development shows a significant technology gap on the military tactical transport side during the last 30 years. Therefore, it seems very beneficial to consider a 'dual use' of well-proven 'civil technologies' for military applications. Specific military transport missions require aircraft capabilities, some of which are quite new and therefore challenging for transport aircraft (e.g. low level flight profiles in night and poor visibility conditions). The demonstration of the feasibility and an evaluation of technical solutions imply the need for suitable development tools. The Virtual Cockpit is explained in terms of its components (hardware/software), features, and capabilities. A major field of investigation in this context is the aircraft systems' central control and monitoring. Author

N92-28548# Deutsche Forschungsanstalt fuer Luft- und Raumfahrt, Brunswick (Germany, F.R.). Inst. fuer Flugmechanik.
THE ROLE OF SYSTEMS SIMULATION FOR THE DEVELOPMENT AND QUALIFICATION OF ATTAS **c09**
D. Hanke, H.-H. Lange, and P. Saager *In* AGARD, Piloted Simulation Effectiveness Feb. 1992 11 p (For primary document see N92-28522 19-01)
Copyright Avail: NTIS HC/MF A15

The Advanced Technologies Testing Aircraft System (ATTAS) is a flight test vehicle to be used as a flying simulator to demonstrate and validate new methods and technologies. In order to provide broad testing capabilities, ATTAS was heavily modified and equipped with a powerful digital fly-by-wire/light flight control system. Presented here is a technical description of the simulator structure and simulation capabilities. Also addressed is the specific role of system identification techniques for simulator validation. Several examples are given demonstrating system performance. Finally, conclusions concerning the merits of system simulation for the ATTAS development and operation are discussed. Author

N92-28549# Douglas Aircraft Co., Inc., Long Beach, CA.
THE USE AND EFFECTIVENESS OF PILOTED SIMULATION IN TRANSPORT AIRCRAFT RESEARCH AND DEVELOPMENT **c09**
J. Hodgkinson, K. F. Rossitto, and E. R. Kendall *In* AGARD, Piloted Simulation Effectiveness Feb. 1992 8 p (For primary document see N92-28522 19-01)
Copyright Avail: NTIS HC/MF A15

Simulation requirements for military and for commercial transport aircraft are contrasted. The special problems introduced by active control are discussed with reference to earlier fighter data. Transport simulator experiments to explore these problems are described. Author

N92-28550# Toronto Univ., Downsview (Ontario). Inst. for Aerospace Studies.
AN EVALUATION OF IFR APPROACH TECHNIQUES: GENERIC HELICOPTER SIMULATION COMPARED WITH ACTUAL FLIGHT **c09**
L. D. Reid, S. Advani, and J. H. deLeeuw *In* AGARD, Piloted Simulation Effectiveness Feb. 1992 18 p (For primary document see N92-28522 19-01)
(Contract W2207-7-AF69/01-SS)
Copyright Avail: NTIS HC/MF A15

Described here is a comparison process using a generic helicopter simulator and flight tests carried out in the National Aeronautical Establishment's Bell 205 research helicopter. The project was designed to establish some initial application boundaries for the newly commissioned helicopter simulator. Hence, the validation process took place in the reverse order, with the helicopter simulator runs performed after the flight tests. Author

N92-28551*# National Aeronautics and Space Administration. Langley Research Center, Hampton, VA.
APPLICATION OF PILOTED SIMULATION TO HIGH-ANGLE-OF-ATTACK FLIGHT-DYNAMICS RESEARCH FOR FIGHTER AIRCRAFT **c09**
Marilyn E. Ogburn, John V. Foster, and Keith D. Hoffler (Vigyan Research Associates, Inc., Hampton, VA.) *In* AGARD, Piloted Simulation Effectiveness Feb. 1992 16 p (For primary document see N92-28522 19-01)
Copyright Avail: NTIS HC/MF A15

The use of piloted simulation at Langley Research Center as part of the NASA High-Angle-of-Attack Technology Program (HATP), which was created to provide concepts and methods for the design of advanced fighter aircraft, is reviewed. A major research activity within this program is the development of the design processes required to take advantage of the benefits of

advanced control concepts for high angle of attack agility. Fundamental methodologies associated with the effective use of piloted simulation for this research are described, particularly those relating to the test techniques, validation of the test results, and design guideline/criteria development. Author

N92-28552# British Aerospace Public Ltd. Co., Lancashire (England). Military Aircraft Div.
EFFECTIVE CUEING DURING APPROACH AND TOUCHDOWN: COMPARISON WITH FLIGHT c09
Peter Beckett *In* AGARD, Piloted Simulation Effectiveness Feb. 1992 11 p (For primary document see N92-28522 19-01)
Copyright Avail: NTIS HC/MF A15

The importance of the various cues provided by flight simulators is a topic for continual debate. Designers of simulators must wrestle with the issue in order to create a sufficient illusion of flight that allows the pilot to carry out his tasks. Hopefully, he becomes stimulated in a similar manner to the real world and behaves accordingly. For training purposes, we are then reinforcing behavior patterns. In research and development simulation, we become more confident that problems or deficiencies of pilot/aircraft interaction are identified early. Clearly, if the cueing is identical to the real world, we would expect identical behavior from the pilot. Simulators invariably fall short of this in many ways. What are considered to be essential cueing requirements are often intuitive, sometimes based on experience and sometimes completely open to individual opinion. A good test of cueing effectiveness is a comparison with flight. The cueing issues for landing approach and touchdown of fast jets are discussed here and simulation results are compared with flight. Author

N92-28677* National Aeronautics and Space Administration, Washington, DC.
AERONAUTICAL ENGINEERING: A CONTINUING BIBLIOGRAPHY WITH INDEXES (SUPPLEMENT 278)
May 1992 128 p
(NASA-SP-7037(278); NAS 1.21:7037(278)) Avail: NTIS HC A07; NTIS standing order as PB92-914100, A04

This bibliography lists 414 reports, articles, and other documents introduced into the NASA scientific and technical information system in April 1992. Author

N92-28679* National Aeronautics and Space Administration, Washington, DC.
AERONAUTICAL ENGINEERING: A CONTINUING BIBLIOGRAPHY WITH INDEXES (SUPPLEMENT 275)
Feb. 1992 112 p
(NASA-SP-7037(275); NAS 1.21:7037(275)) Avail: NTIS HC A06; NTIS standing order as PB92-914100, A04

This bibliography lists 379 reports, articles, and other documents introduced into the NASA scientific and technical information system in Jan. 1991. Author

02 AERODYNAMICS

Includes aerodynamics of bodies, combinations, wings, rotors, and control surfaces; and internal flow in ducts and turbomachinery.

For related information see also *34 Fluid Mechanics and Heat Transfer.*

N92-28477*# National Aeronautics and Space Administration. Langley Research Center, Hampton, VA.
CALCULATION OF UNSTEADY TRANSONIC FLOWS WITH MILD SEPARATION BY VISCOUS-INVISCID INTERACTION
James T. Howlett Jun. 1992 39 p
(RTOP 509-10-02-03)
(NASA-TP-3197; L-16996; NAS 1.60:3197) Avail: NTIS HC/MF A03

This paper presents a method for calculating viscous effects in two- and three-dimensional unsteady transonic flow fields. An integral boundary-layer method for turbulent viscous flow is coupled with the transonic small-disturbance potential equation in a quasi-steady manner. The viscous effects are modeled with Green's lag-entrainment equations for attached flow and an inverse boundary-layer method for flows that involve mild separation. The boundary-layer method is used stripwise to approximate three-dimensional effects. Applications are given for two-dimensional airfoils, aileron buzz, and a wing planform. Comparisons with inviscid calculations, other viscous calculation methods, and experimental data are presented. The results demonstrate that the present technique can economically and accurately calculate unsteady transonic flow fields that have viscous-inviscid interactions with mild flow separation. Author

N92-28511*# Maryland Univ., College Park. Dept. of Aerospace Engineering.
STUDIES IN GENERAL AVIATION AERODYNAMICS Final Technical Report
Allen E. Winkelmann 1990 20 p
(Grant NAG1-681)
(NASA-CR-190431; NAS 1.26:190431) Avail: NTIS HC/MF A03

The Department of Aerospace Engineering at the University of Maryland has completed a research study for NASA Langley on the application of drooped leading edges to high aspect wings. The experimental study conducted for this grant was a natural extension of work previously conducted at NASA Ames, the University of Michigan, NASA Langley and the University of Maryland. Previous research had shown that wing planform modifications (commonly referred to as drooped leading edge mods) could have a significant effect on reducing or eliminating the stall/spin characteristics of General Aviation (GA) aircraft. All aircraft studied in the earlier work had relatively low aspect ratio wings (AR = 6). Since future GA aircraft will feature higher aspect ratio wings, the obvious question was: how well will the dropped leading edge work on higher aspect ratio wings? The focus of the current study was to examine the effectiveness of the drooped leading edge modifications to higher aspect ratio wings with AR = 9 to 12. Author

N92-28657# National Aerospace Lab., Amsterdam (Netherlands). Informatics Div.
ANALYSIS OF RESULTS OF AN EULER-EQUATION METHOD APPLIED TO LEADING-EDGE VORTEX FLOW
J. I. vandenBerg, H. W. M. Hoeijmakers, and J. M. J. W. Jacobs 30 Oct. 1990 17 p Presented at the AGARD Fluid Dynamics Panel Symposium on Vortex Flow Aerodynamics, Scheveningen, Netherlands, 1-4 Oct. 1990 Previously announced as N92-13000 Sponsored by Netherlands Agency for Aerospace Programs
(NLR-TP-90368-U; ETN-92-91450) Avail: NTIS HC/MF A03

The flow about a 65 deg sharp edged cropped delta wing with and without an underwing body is simulated by solving the Euler equations. Results are presented for the wing body configuration at a transonic free stream Mach number at incidences ranging from 10 to 20 deg for which in the flow field above the wing a strong vortex develops as well as shocks for the high incidence of 20 deg. Results for subsonic to transonic free stream Mach numbers at high incidence are obtained for the wing alone configuration for which, in the presence of a strong vortex, at transonic free stream Mach number, shocks appear in the solution. For the wing-body configuration, the computational results are compared with experimental data, and the solution in the near wake is investigated. ESA

N92-28658# National Aerospace Lab., Amsterdam (Netherlands). Fluid Dynamics Div.
COMPARISON OF LDA AND LTA APPLICATIONS FOR PROPELLER TESTS IN WIND TUNNELS
J. H. M. Gooden and J. W. Kooi 7 May 1988 10 p Presented at the 4th International Symposium on Applications of Laser Anemometry to Fluid Mechanics, Lisbon, Portugal, 11-14 Jul. 1988 Previously announced in IAA as A89-33381
(Contract NIVR-03601-N)
(NLR-MP-88031-U; ETN-92-91512) Avail: NTIS HC/MF A02

A study to investigate the performance of a two component Laser Doppler (LDA) and Laser Transit (LTA) Anemometer is presented. Both systems were compared under industrial testing conditions in the flow field of a propeller. Free stream flow speed was 40 m/s. The propeller, diameter 0.73 m, was operated at 3500 and 6000 rpm. Axial and tangential velocities were measured in front of, in between and behind the propeller blades. The results of the two systems were in good agreement within 1 m/s for the axial velocity. The error in the tangential velocity was about 1 to 2 m/s but of a different sign. The productivity and the capability of the LDA to measure in highly turbulent flows were superior. The high light concentration in the probe volumes of the LTA made artificial seeding superfluous. ESA

N92-28659# National Aerospace Lab., Amsterdam (Netherlands). Fluid Dynamics Div.

CALCULATION OF UNSTEADY SUBSONIC AND SUPERSONIC FLOW ABOUT OSCILLATING WINGS AND BODIES BY NEW PANEL METHODS

M. H. L. Hounjet 14 Apr. 1989 24 p Presented at the European Forum on Aeroelasticity and Structural Dynamics, Aachen, Fed. Republic of Germany, 17-19 Apr. 1989 Previously announced in IAA as A90-33359 Sponsored in part by Royal Netherlands Air Force

(NLR-TP-89119-U; ETN-92-91518) Avail: NTIS HC/MF A03

The unsteady aerodynamic loads in the subsonic and supersonic domain, obtained with two new panel methods, for lifting surfaces and for realistic aircraft configurations are presented. The General Unsteady Lifting (GUL) surface code and the Compressible Aerodynamic Response (CAR) methods were developed for calculations involving realistic aircraft configurations. A description of the methods is given. Results are presented and comparisons are made with results of existing methods and with experimental data for a fighter type wing with external stores. ESA

N92-28660# National Aerospace Lab., Amsterdam (Netherlands). Informatics Div.

CONSTRAINED SPANLOAD OPTIMIZATION FOR MINIMUM DRAG OF MULTI-LIFTING-SURFACE CONFIGURATIONS

R. F. vandenDam 10 Apr. 1989 19 p Presented at the AGARD Specialists Meeting on Computational Methods for Aerodynamic Design (Inverse) and Optimization, Loen, Norway, 22-23 May 1989

(Contract NIVR-01101-N)

(NLR-TP-89126-U; ETN-92-91519) Avail: NTIS HC/MF A03

The development of a interactive computer program system that can be used in aircraft drag minimization studies is addressed. It comprises algorithms for choosing the spanwise distributions of lift, pitching moment, chord and thickness to chord ratio of lifting elements. The choices are optimal in that they minimize induced plus viscous drag while satisfying constraints of aerodynamic, flight mechanical and structural natures. The configurations that can be dealt with may consist of a number of segments representing, for instance, wings or parts of wings, horizontal tails or canards, winglets, flaprail-fairings, etc. Also the interaction between propellers and lifting elements may be included in the procedure. The induced drag is computed using the Trefftz plane integral (farfield analysis), while the viscous drag follows from form factor methods. Novel mathematical formulations of the constrained optimization problems based on the calculus of variations are used. The method was integrated in an infrastructure that allows the capabilties of the method to be efficiently exploited in a multidisciplinary environment. The theoretical models and methods underlying the analysis and optimization capability, comparisons with other theories, information aspects, and some examples of applications are presented. ESA

N92-28674*# National Aeronautics and Space Administration. Lewis Research Center, Cleveland, OH.

EXPERIMENTAL AND COMPUTATIONAL ICE SHAPES AND RESULTING DRAG INCREASE FOR A NACA 0012 AIRFOIL

Jaiwon Shin and Thomas H. Bond Jan. 1992 12 p Presented at the 5th Symposium on Numerical and Physical Aspects of Aerodynamic Flows, Long Beach, CA, 13-16 Jan. 1992; sponsored in part by California State Univ.

(RTOP 505-68-10)

(NASA-TM-105743; E-7148; NAS 1.15:105743) Avail: NTIS HC/MF A03

Tests were conducted in the Icing Research Tunnel (IRT) at LeRC to document the repeatability of the ice shape over the range of temperatures varying from -15 to 28 F. Measurements of drag increase due to the ice accretion were also made. The ice shape and drag coefficient data, with varying total temperatures at two different airspeeds, were compared with the computational predictions. The calculations were made with the 2D LEWICE/IBL code which is a combined code of LEWICE and the interactive boundary layer method developed for iced airfoils. Comparisons show good agreement with the experimental data in ice shapes. The calculations show the ability of the code to predict drag increases as the ice shape changes from a rime shape to a glaze shape. Author

N92-28692# National Aerospace Lab., Amsterdam (Netherlands). Aerodynamics Div.

DEVELOPMENT AND VALIDATION OF A CHARACTERISTIC BOUNDARY CONDITION FOR A CELL-CENTERED EULER METHOD

J. I. vandenBerg and J. W. Boerstoel 6 May 1990 12 p Presented at the 17th ICAS Congress, Stockholm, Sweden, 9-14 Sep. 1990 Sponsored in part by Netherlands Agency for Aerospace Programs

(NLR-TP-90144-U; ETN-92-91535) Avail: NTIS HC/MF A03

The development and numerical validation of a solid wall boundary condition for the numerical solution of the Euler equations with a cell centered central difference scheme is presented. This solid wall boundary condition was obtained from the theory of characteristics, and was also formulated for a cell/centered central/difference scheme. The boundary condition was developed to clarify the question of what the effect is of various boundary/condition algorithms on the accuracy of the three dimensional numerical solution of the Euler equations. The numerical validation of the solid/wall boundary condition consists of a comparison of results obtained with the conventional and the new solid/wall boundary condition. Discretization and convergence errors as well as grid depency of the solution were investigated. As a test case, the NLR 7301 airfoil was chosen. Calculations were performed for the supercritical, shock free flow at M(sub infinity) = 0.721, alpha = 0.194 deg, and for a flow with a strong shock at M(sub infinity) = 0.70, alpha 2.0 deg. ESA

N92-28696*# National Aeronautics and Space Administration. Lewis Research Center, Cleveland, OH.

RESULTS OF A LOW POWER ICE PROTECTION SYSTEM TEST AND A NEW METHOD OF IMAGING DATA ANALYSIS

Jaiwon Shin, Thomas H. Bond, and Geert A. Mesander (Air Force Logistics Command, Tinker AFB, OK.) Jun. 1992 18 p Presented at the 48th Annual Forum and Technology Display, Washington, DC, 3-5 Jun. 1992; sponsored in part by the American Helicopter Society

(RTOP 505-68-10)

(NASA-TM-105745; E-6930; NAS 1.15:105745) Avail: NTIS HC/MF A03

Tests were conducted on a BF Goodrich De-Icing System's Pneumatic Impulse Ice Protection (PIIP) system in the NASA Lewis Icing Research Tunnel (IRT). Characterization studies were done on shed ice particle size by changing the input pressure and cycling time of the PIIP de-icer. The shed ice particle size was quantified using a newly developed image software package. The tests were conducted on a 1.83 m (6 ft) span, 0.53 m (221 in) chord NACA 0012 airfoil operated at a 4 degree angle of attack. The IRT test conditions were a -6.7 C (20 F) glaze ice, and a -20 C (-4 F) rime ice. The ice shedding events were recorded with a high speed video system. A detailed description of the image processing package and the results generated from this analytical tool are presented. Author

N92-28709# National Aerospace Lab., Amsterdam (Netherlands). Informatics Div.
WAVE DRAG DETERMINATION IN THE TRANSONIC FULL-POTENTIAL FLOW CODE MATRICS
J. vanderVooren and A. J. vanderWees 19 Feb. 1990 32 p
(Contract NIVR-RB-311.1-01501-N)
(NLR-TP-90062-U; ETN-92-91530) Avail: NTIS HC/MF A03

The mathematical background of a method developed to calculate wave drag in transonic potential flow is described. The method is a generalization and extension of Garabedian's and McFadden's idea of determining wave drag by volume integration of the artificial viscosity. The generalization of Garabedian's and McFadden's idea involves the introduction of a reference artificial viscosity which provides a solid theoretical basis. At the same time this ensures that calculated wave drag is to a certain extent independent of the specific details of the artificial viscosity in different diodes. The extension of Garabedian's and McFadden's idea accounts for the fact that artificial viscosity does not smear out supersonic/subsonic shock waves completely, but leaves room for a truly discontinuous sonic/subsonic 'shock remainder' that contributes substantially to the wave drag. Both fully conservative and nonconservative shock capture in potential flow are covered. The method can be extended to handle also pseudo Rankine-Hugoniot shock waves. An illustrative example for a transonic transport type wing is given. ESA

N92-28713# National Aerospace Lab., Amsterdam (Netherlands). Aerodynamics Div.
FLOW GRADIENT CORRECTIONS ON HOT-WIRE MEASUREMENTS USING AN X-WIRE PROBE
J. H. M. Gooden and M. vanLent (Fokker B.V., Schipol-Oost, Netherlands) 11 Jul. 1990 18 p Presented at 12th Symposium on Turbulence, Rolla, MO, 1990 Previously announced in IAA as A91-54278
(Contract NIVR-01502-N)
(NLR-TP-90255-U; ETN-92-91543) Avail: NTIS HC/MF A03

The development of a method to correct hot wire measurements by means of a single X-wire probe for the effect of gradients normal to the plane of the wires in the mean flow velocities as well as the turbulence intensities is reported. Data processing is performed in an iterative way, using the results of measurements with different probe rolling angles, to determine the gradient corrections along the traverse from the previous loop. The method is applied to measurements in the wake above the trailing edge flap of a wing. Substantial improvements in the results are shown. ESA

N92-28729* National Aeronautics and Space Administration. Langley Research Center, Hampton, VA.
NATURAL FLOW WING Patent
Richard M. Wood, inventor (to NASA) and Steven X. S. Bauer, inventor (to NASA) 12 May 1992 13 p Filed 31 Jul. 1990
(NASA-Case-LAR-14281-1; US-Patent-5,112,120;
US-Patent-Appl-SN-560923; US-Patent-Class-244-35R;
US-Patent-Class-244-36; Int-Patent-Class-B64C-3/14) Avail: US Patent and Trademark Office

The invention is a natural flow wing and a method for constructing the same. The method comprises contouring a three-dimensional upper surface and a three-dimensional lower surface of the natural flow wing independently of one another into a prescribed shape. Experimental data and theoretical analysis show that flow and pressure-loading over an upper surface of a wing tend to be conical about an apex of the wing, producing favorable and unfavorable regions of performance based on drag. The method reduces these unfavorable regions by shaping the upper surface such that the maximum thickness near a tip of the natural flow wing moves aft, thereby, contouring the wing to coincide more closely with the conical nature of the flow on the upper surface. Nearly constant compressive loading characterizes the flow field over a lower surface of the conventional wing. Magnitude of these compressive pressures on the lower surface depends on angle of attack and on a streamwise curvature of the lower surface of the wing and not on a cross-sectional spanwise curvature. The method, thereby, shapes the lower surface to create an area as large as possible with negative slopes. Any type of swept wing may be used to obtain the final, shaped geometry of the upper and lower surfaces of the natural flow wing.
Official Gazette of the U.S. Patent and Trademark Office

N92-28789# Office National d'Etudes et de Recherches Aerospatiales, Paris (France). Direction de lAerodynamique.
FEASIBILITY STUDY OF HYPERSONIC CLINOMETRIC MEASUREMENTS AT R3Ch Final Summury Report [ETUDE DE FAISIBILITE DE MESURES CLINOMETRIQUES EN HYPERSONIQUE A R3CH. RAPPORT DE SYNTHESE FINAL]
M. C. Merienne and M. Alaphilippe Jun. 1991 46 p In FRENCH
(Contract DRET-89-34-001)
(ONERA-RSF-136/1865-AY-728-A; ETN-92-91327) Avail: NTIS HC/MF A03

The feasibility of clinometric measurements in hypersonic flow was investigated, by a miniaturized probe with five holes, in a R3Ch wind tunnel. The phases of the study were: estimation of the response time, the design, the calibration, and the measurements on a flat plate. The probe, with one end of 2 mm diameter, has a short response time and a high thermal resistance. The clinometric calibration performed under an incidence angle, between -4 and +4 degrees, shows a sensibility coefficient of the probe with a 4 maximal uncertainty, which represents a measurement error between 0.3 and 0.7 degrees. ESA

N92-28865# Washington State Univ., Pullman.
STUDY OF THE LEADING-EDGE VORTEX DYNAMICS IN THE UNSTEADY FLOW OVER AN AIRFOIL Final Report, 1 Jan. 1990 - 31 Dec. 1991
B. R. Ramaprain 27 Feb. 1992 54 p
(Grant AF-AFOSR-0131-90)
(AD-A247532; AFOSR-92-0222TR) Avail: NTIS HC/MF A04

The two-year project to study the dynamics of the leading-edge vortex (LEV) over a pitching airfoil under conditions of dynamic stall, was started in January 1990. Several accomplishments have been made during these two years. The most significant of these are: (1) the construction of a special water channel suitable for the study of dynamic stall over a pitching airfoil; (2) the measurement of surface pressure distributions over the airfoil under several key operating conditions; and (3) development of the techniques of Particle Image Velocimetry (PIV) and its use in the measurement of instantaneous velocity and vorticity field in the two-dimensional flow around the airfoil. Some of these data which are the first of their kind have been used to understand the physics of unsteady vorticity dynamics over a pitching airfoil. These data are being made available to other investigators for use as database in validating their numerical models. GRA

N92-28883# Naval Postgraduate School, Monterey, CA.
FLOW VISUALIZATION STUDIES OF A SIDESLIPPING, CANARD-CONFIGURED X-31A-LIKE FIGHTER AIRCRAFT MODEL M.S. Thesis
Chang H. Kim Dec. 1991 125 p
(AD-A245940) Avail: NTIS HC/MF A06

A water tunnel flow visualization investigation was performed to study the vortex development and bursting phenomena on a 2.3 percent scale model of a X-31A-Like fighter aircraft. The main focus of this study was two-fold: first, to study the effects of angle of attack and static sideslip on the model vortical flow field; and secondly, to study the effects of dynamic sideslip motion at two reduced yaw rates. Results indicate that the wing root vortex bursting locations move upstream as the AOA increases; and at constant angle of attack (AOA less than 30 degrees) the leeward side vortex bursting location moves backward and outboard with sideslip inputs while the windward side vortex bursting location moves forward and inboard. The vortex asymmetry switches sides at higher angle of attack (AOA greater than 30 degrees). The dynamic lag effects, which cause the leeward side vortex to burst earlier than in the static case during the positive sideslipping motion

and later than in the static case during the negative sideslipping motion, increase with the magnitude of the sideslipping motion.
GRA

N92-28888# Ohio Univ., Athens. Dept. of Mechanical Engineering.
NONLINEAR NORMAL AND AXIAL FORCE INDICIAL RESPONSES FOR A TWO DIMENSIONAL AIRFOIL Final Report
G. M. Graham, M. Islam, and K. C. Fang 15 Nov. 1991 79 p
(Grant AF-AFOSR-0502-89)
(AD-A247196; AFOSR-92-0077TR) Avail: NTIS HC/MF A05

Normal and axial force indicial responses for a 2-D NACA 0015 airfoil undergoing small step changes in angle of attack have been measured in a tow tank. The airfoil was pitched about the quarter chord and the Reynolds number was 95,000. First order and second order tests were conducted. In the first order tests, the angle of attack prior to the step onset was held constant. In the second order study, the airfoil was ramped up at constant rate to the onset angle. Step onset angles in the range 0 less than alpha less than 60 deg were considered. The step responses have been integrated numerically to compute the loading during a ramp-up motion. The integrated results are compared with baseline load data taken with the same airfoil. GRA

N92-28980*# National Aeronautics and Space Administration. Lewis Research Center, Cleveland, OH.
LASER ANEMOMETER MEASUREMENTS AND COMPUTATIONS IN AN ANNULAR CASCADE OF HIGH TURNING CORE TURBINE VANES
Louis J. Goldman and Richard G. Seasholtz Jul. 1992 38 p
(RTOP 505-62-52)
(NASA-TP-3252; E-6354; NAS 1.60:3252) Avail: NTIS HC/MF A03

An advanced laser anemometer (LA) was used to measure the axial and tangential velocity components in an annular cascade of turbine stator vanes designed for a high bypass ratio engine. These vanes were based on a redesign of the first-stage stator, of a two-stage turbine, that produced 75 degrees of flow turning. Tests were conducted on a 0.771 scale model of the engine size stator. The advanced LA fringe system was designed to employ thinner than usual laser beams resulting in a 50-micron-diameter probe volume. Window correction optics were used to ensure that the laser beams did not uncross in passing through the curved optical access port. Experimental LA measurements of velocity and turbulence were obtained both upstream, within, and downstream of the stator vane row at the design exit critical velocity ratio of 0.896 at the hub. Static pressures were also measured on the vane surface. The measurements are compared, where possible with calculations from a 3-D inviscid flow analysis. The data are presented in both graphic and tabulated form so that they may be readily used to compare against other turbomachinery computations. Author

N92-28981*# National Aeronautics and Space Administration. Marshall Space Flight Center, Huntsville, AL.
A GENERALIZED REUSABLE GUIDANCE ALGORITHM FOR OPTIMAL AEROBRAKING
G. A. Dukeman Jul. 1992 19 p
(NASA-TM-103590; NAS 1.15:103590) Avail: NTIS HC/MF A03

A practical real-time guidance algorithm was developed for guiding aerobraking vehicles in such a way that the maximum heating rate, the maximum structural loads, and the post-aeropass delta-V requirements (for post-aeropass orbit insertion) are all minimized. The algorithm is general and reusable in the sense that a minimum of assumptions are made, thus minimizing the number of gains and mission-dependent parameters that must be laboriously determined prior to a particular mission. A particularly interesting feature is that inplane guidance performance is tuned by simply adjusting one mission-dependent parameter, the bank margin; similarly, the out-of-plane guidance performance is turned by simply adjusting a plane controller time constant. Other objectives in the algorithm development are simplicity, efficiency, and ease of use. The algorithm is developed for, but not necessarily restricted to, a single pass mission and a trimmed vehicle with a bank angle modulation as the method of trajectory control. Guidance performance is demonstrated via results obtained using this algorithm integrated into an aerobraking test-bed program. Comparisons are made with numerical results from a version of the aerobraking guidance algorithm that was to be flown onboard NASA's aeroassist flight experiment (AFE) vehicle. Promising results are obtained with a minimum of development effort.
Author

N92-29159# European Space Agency, Paris (France).
CALCULATION OF SUPPORT INTERFERENCES ON THE AERODYNAMIC COEFFICIENTS FOR A WIND TUNNEL CALIBRATION MODEL [BERECHNUNG DER SUPPORT-INTERFERENZEN FUER DIE AERODYNAMISCHEN BEIWERTE EINES WINDKANAL-EICHMODELLS]
Dieter Steinbach (Deutsche Forschungsanstalt fuer Luft- und Raumfahrt, Goettingen, Germany, F.R.) Feb. 1992 78 p Transl. into ENGLISH of German document (Goettingen, Fed. Republic of Germany, DLR), May 1990 p 1-63 Original language document was announced as N91-15998
(ESA-TT-1247; DLR-FB-90-26; ISSN-0171-1342; ETN-92-91207)
Avail: NTIS HC/MF A05; Original German Version available from DLR, Wissenschaftliches Berichtswesen, Postfach 90 60 58, Cologne, Fed. Republic of Germany, 23 DM

Model support interferences are calculated in the form of corrections to the aerodynamic coefficients for a calibration model to be tested in a subsonic cryogenic wind tunnel. Two different model support systems are investigated: a horizontal sting (rear sting) and a vertical sting (ventral sting). The results of earlier experiments using these configurations already exist and the corrections obtained in the present work are therefore applied to these measurements for verification. In addition, the effect of the sting on the static longitudinal stability of the model is investigated in more detail. A three dimensional panel method is used for the calculations. This permits the simultaneous calculation of thickness and lift effects when several bodies of almost any given shape are present in the flow. The aerodynamic coefficients are obtained by numerical integration of the surface pressure distribution on the model. ESA

N92-29206# Office National d'Etudes et de Recherches Aerospatiales, Paris (France). Direction de l'Aerodynamique.
DEVELOPMENT OF AN UNSTEADY THREE-DIMENSIONAL VISCOUS-INVISCID INTERACTION NUMERICAL METHOD FOR THE CALCULATION OF AIRFOILS VIBRATION Final Summary Report [DEVELOPPEMENT D'UNE METHODE NUMERIQUE D'INTERACTION VISQUEUX-NON VISQUEUX TRIDIMENSIONNELLE INSTATIONNAIRE POUR LE CALCUL DU TREMBLEMENT DES VOILURES. RAPPORT DE SYNTHESE FINALE]
P. Girodroux-Lavigne and J. C. LeBalleur Sep. 1991 44 p In FRENCH
(Contract STPA-85-95-009)
(ONERA-RSF-7/3617-AY-022A; ETN-92-91325) Avail: NTIS HC/MF A03

A study to predict the transonic vibration occurring in airfoils of a carrier aircraft is presented. The study was focused on the numerical technique of an inverse three dimensional unsteady boundary layer, as well as on the semi implicit unsteady coupling algorithm. The numerical results give a first approach of the coupling methods and the calculation of three dimensional separation, and restored the topology of the friction lines. The calculations were firstly performed for a subsonic flow in the following geometry conditions: a flat plate containing a wall hole with a very high three dimensionality. A separation through a transonic right wing type NACA0012 was predicted. ESA

N92-28820*# State Univ. of New York, Buffalo. Dept. of Mechanical and Aerospace Engineering.
MODELING OF THE REACTANT CONVERSION RATE IN A TURBULENT SHEAR FLOW

S. H. Frankel, C. K. Madnia, and P. Givi *In its* Large Eddy Simulations (LES) and Direct Numerical Simulations (DNS) for the Computational Analyses of High Speed Reacting Flows 30 Apr. 1992 14 p Submitted for publication (For primary document see N92-28817 19-34)
Avail: NTIS HC/MF A06

03 AIR TRANSPORTATION AND SAFETY

Includes passenger and cargo air transport operations; and aircraft accidents.

For related information see also *16 Space Transportation* and *85 Urban Technology and Transportation.*

N92-28655# National Aerospace Lab., Amsterdam (Netherlands). Informatics Div.
APPLICATION OF KNOWLEDGE-BASED SYSTEMS FOR DIAGNOSIS OF AIRCRAFT SYSTEMS [TOEPASSING VAN KENNISSYSTEMEN VOOR DIAGNOSE VAN VLIEGTUIGSYSTEMEN]
J. C. Donker and M. A. Piers 28 Apr. 1990 22 p In DUTCH Presented at the AI Applications Conference, Kerkrade, Netherlands, 10-15 Jun. 1991
(Contract NIVR-01708-N)
(NLR-TP-90192-U; ETN-92-91439) Avail: NTIS HC/MF A03

The applicability of knowledge based systems for the monitoring and diagnosis of aircraft systems was investigated in order to provide tools with which maintenance can be performed more effectively and efficiently. A knowledge based system was designed to support ground engineers in the maintenance of the Fokker 100 air conditioning system. The evaluation shows that the system performs well if complaints are described with enough detail. The main conclusion is that design and experience knowledge needed to support the maintenance personnel can be collected and implemented in a usable system. ESA

N92-28900# Federal Aviation Administration, Atlantic City, NJ.
DROP TEST: CESSNA GOLDEN EAGLE 421B Technical Report, Feb. - Nov. 1990
Robert McGuire, William Nissley, and Anthony Wilson May 1992 139 p
(DOT/FAA/CT-TN91/32) Avail: NTIS HC/MF A07

The results of two airplane vertical impact tests conducted at the Federal Aviation Administration (FAA) Technical Center, Atlantic City International Airport, New Jersey are presented. These tests entailed dropping a low wing, twin engine Cessna 421B aircraft from a vertical height of 11.2 feet, resulting in an impact velocity of approximately 26.0 feet per second (ft/s). In both tests, the aircraft was configured to simulate actual in-flight conditions including seats, occupants, and fuel. The structural response of the airframe, seats, and simulated occupants (anthropomorphic dummies) were measured throughout the tests, and the results are presented. The data collected in these tests and future tests of other commuter type aircraft will provide the basis for improved seat standards for commuter airplanes. These tests describe the impact response characteristics of commuter category airplane airframes, floor structures, seats, seat attachments, and occupant restraint systems. Author

N92-29182# Federal Aviation Administration, Washington, DC. Office of Aviation Policy and Plans.
FAA AVIATION FORECASTS
Feb. 1992 280 p
(AD-A250412; FAA-APO-92-1) Avail: NTIS HC/MF A13

This report contains forecasts of aviation activity at Federal Aviation Administration facilities. These include airports with FAA control towers, air route traffic control centers, and flight service stations. Detailed forecasts were made for the major users of the National Aviation System: air carriers, air taxi/commuters, military and general aviation. The forecasts have been prepared to meet the budget and planning needs of the constituent units of the FAA and to provide information that can be used by state and local authorities, the aviation industry, and the general public. The lethargy of the domestic and international economies over the past year have caused the aviation industry to experience its worst year ever. However, the outlook for the 12-year forecast period is for moderate economic growth, stable real fuel prices, and moderate inflation. Based on these assumptions, aviation activity by fiscal year 2003 is forecast to increase by 25.7 percent at towered airports, 28.3 percent at air route traffic control centers, and 4.8 percent in flight services performed. Hours flown by general aviation are forecast to increase 15.1 percent and domestic revenue passenger miles (RPM's) are forecast to increase 54.9 percent, with scheduled international RPM's forecast to increase by 112.8 percent and regional/commuter RPM's forecast to increase by 146.5 percent. GRA

N92-28530# Naval Air Test Center, Patuxent River, MD. Strike Aircraft Test Directorate.
USE OF HIGH-FIDELITY SIMULATION IN THE DEVELOPMENT OF AN F/A-18 ACTIVE GROUND COLLISION AVOIDANCE SYSTEM
Timothy R. Fitzgerald and Michael T. Brunner *In* AGARD, Piloted Simulation Effectiveness Feb. 1992 13 p (For primary document see N92-28522 19-01)
Copyright Avail: NTIS HC/MF A15

04 AIRCRAFT COMMUNICATIONS AND NAVIGATION

Includes digital and voice communication with aircraft; air navigation systems (satellite and ground based); and air traffic control.

For related information see also *17 Space Communications, Spacecraft Communications, Command and Tracking* and *Communications and Radar.*

N92-28317# Naval Postgraduate School, Monterey, CA.
ACCURACY OF SHIPBORNE KINEMATIC GPS SURVEYING M.S. Thesis
Barry Grinker Sep. 1991 120 p
(AD-A245942) Avail: NTIS HC/MF A06

In December 1990 an experiment was conducted at the Naval Postgraduate School in Monterey, California in which four different receivers, mounted on the mast of a ship, collected data simultaneously for several hours at a time. Ashtech LD - XII, Trimble 4000 ST, TI 4100 and Magnavox MX-4200 receivers were used. The reference system consisted of a Krupp Atlas Polarfix laser system set up on the shore at a pre-surveyed site. A two-axis vertical gyro system and a heading gyro gave the ship's 3-dimensional orientation at any instant in time, providing a connection between the laser reflector and the GPS antennas on the ship's mast. This enabled the reduction of the laser reflector's trajectory to the Ashtech and Trimble antennas for subsequent comparison to the kinematic GPS trajectories of these receivers determined by the postprocessing of the data collected. Each data set was processed once with the software provided by the manufacturer and once with an independent software package, OMNI, developed by the National Geodetic Survey. In addition to the software, six factors were examined to determine their effects on kinematic GPS surveys. They included: tropospheric corrections, initialization, satellite geometry, ephemeris type, data interval and multipath. GRA

N92-28718*# Ohio Univ., Athens. Dept. of Electrical and Computer Engineering.
LORAN-C PERFORMANCE ASSURANCE ASSESSMENT PROGRAM Final Report
Robert W. Lilley and N. Kent Brooks Jun. 1992 36 p
(Grant NAG1-816)
(NASA-CR-190469; NAS 1.26:190469; OU/AEC-EER-92-2)
Avail: NTIS HC/MF A03

The Federal Aviation Administration (FAA) has accepted the

Loran-C navigation system as a supplemental navigation aid for enroute use. Extension of Loran-C utilization to instrument approaches requires establishment of a process by which the current level of performance of the system is always known by the pilot. This system 'integrity' translates into confidence that, if the system is made available to the pilot, the guidance will be correct. Early in the consideration of Loran-C for instrument approaches, the Loran-C Planning Work-Group (LPW) was formed with membership from the FAA, the US Coast Guard, various state governments, aviation users, equipment manufacturers and technical experts. The group was hosted and co-chaired by the National Association of State Aviation Officials (NASAO). This forum was ideal for identification of system integrity issues and for finding the correct process for their resolution. Additionally, the Wild Goose Association (WGA), which is the international Loran-C technical and user forum, regularly brings together members of the FAA, Coast Guard, and the scientific community. Papers and discussions from WGA meetings have been helpful. Given here is a collection of the issues in which Ohio University became involved. Issues definition and resolution are included along with the recommendations in those areas where resolution is not yet complete. Author

N92-29103*# National Aeronautics and Space Administration. Ames Research Center, Moffett Field, CA.

A ROTORCRAFT FLIGHT DATABASE FOR VALIDATION OF VISION-BASED RANGING ALGORITHMS

Phillip N. Smith Apr. 1992 17 p

(RTOP 505-64-36)

(NASA-TM-103906; A-92021; NAS 1.15:103906) Avail: NTIS HC/MF A03

A helicopter flight test experiment was conducted at the NASA Ames Research Center to obtain a database consisting of video imagery and accurate measurements of camera motion, camera calibration parameters, and true range information. The database was developed to allow verification of monocular passive range estimation algorithms for use in the autonomous navigation of rotorcraft during low altitude flight. The helicopter flight experiment is briefly described. Four data sets representative of the different helicopter maneuvers and the visual scenery encountered during the flight test are presented. These data sets will be made available to researchers in the computer vision community. Author

05 AIRCRAFT DESIGN, TESTING AND PERFORMANCE

Includes aircraft simulation technology.

For related information see also *18 Spacecraft Design, Testing and Performance* and *39 Structural Mechanics*.For land transportation vehicles see *85 Urban Technology and Transportation*.

N92-28435*# National Aeronautics and Space Administration. Langley Research Center, Hampton, VA.

INTEGRATING AERODYNAMICS AND STRUCTURES IN THE MINIMUM WEIGHT DESIGN OF A SUPERSONIC TRANSPORT WING

Jean-Francois M. Barthelemy, Gregory A. Wrenn (Lockheed Engineering and Sciences Co., Hampton, VA.), Augustine R. Dovi (Lockheed Engineering and Sciences Co., Hampton, VA.), Peter G. Coen, and Laura E. Hall (Unisys Corp., Hampton, VA.) Apr. 1992 15 p Presented at the AIAA/ASCE/ASME/AHS/ASC 33rd Structures, Structural Dynamics and Materials Conference, Dallas, TX, 13-15 Apr. 1992

(RTOP 505-63-50-06)

(NASA-TM-107586; NAS 1.15:107586) Avail: NTIS HC/MF A03

An approach is presented for determining the minimum weight design of aircraft wing models which takes into consideration aerodynamics-structure coupling when calculating both zeroth order information needed for analysis and first order information needed for optimization. When performing sensitivity analysis, coupling is accounted for by using a generalized sensitivity formulation. The results presented show that the aeroelastic effects are calculated properly and noticeably reduce constraint approximation errors. However, for the particular example selected, the error introduced by ignoring aeroelastic effects are not sufficient to significantly affect the convergence of the optimization process. Trade studies are reported that consider different structural materials, internal spar layouts, and panel buckling lengths. For the formulation, model and materials used in this study, an advanced aluminum material produced the lightest design while satisfying the problem constraints. Also, shorter panel buckling lengths resulted in lower weights by permitting smaller panel thicknesses and generally, by unloading the wing skins and loading the spar caps. Finally, straight spars required slightly lower wing weights than angled spars. Author

N92-28468# Advisory Group for Aerospace Research and Development, Neuilly-Sur-Seine (France). Flight Mechanics Panel.

AIRCRAFT SHIP OPERATIONS [LE COUPLE AERONEF-NAVIRE DANS LES OPERATIONS]

J. G. Hoeg (Naval Air Test Center, Patuxent River, MD.) Apr. 1992 13 p Presented at the Flight Mechanics Panel Symposium, Seville, Spain, 20-23 May 1991

(AGARD-AR-312; ISBN-92-835-0668-5) Copyright Avail: NTIS HC/MF A03

Worldwide interest in the use of shipborne aircraft as a major weapons system is very broad. Many NATO countries operate fixed wing aircraft from ships. Additionally, the use of ships as helicopter platforms is extensive in the NATO community and brings another important dimension to the aircraft/ship interface issue. Thus, it seemed that both fixed and rotary wing aviation deserved equal billing in the Aircraft/Ship Interface Symposium which is the subject of this Technical Evaluation Report. The Symposium contained twenty-five presentations grouped under the following topics: Keynote Addresses; Ship Environment; Guidance, Controls, and Displays; Flight Test and Simulation Techniques; Launch, Recovery, and Handling Systems Development; and Operational Views and Future Developments. Author

N92-28469# Advisory Group for Aerospace Research and Development, Neuilly-Sur-Seine (France). Structures and Materials Panel.

INTEGRATED DESIGN ANALYSIS AND OPTIMISATION OF AIRCRAFT STRUCTURES [L'ANALYSE INTEGRALE DE LA CONCEPTION ET L'OPTIMISATION DES STRUCTURES DES AERONEFS]

May 1992 88 p Lectures held in Pasadena, CA, 8-9 Jun. 1992, in Lisbon, Portugal, 22-23 Jun. 1992, and in London, England, 25-26 Jun. 1992

(AGARD-LS-186; ISBN-92-835-0675-8) Copyright Avail: NTIS HC/MF A05

There is a lack of precise information on the effectiveness of specific methods in generating optimum designs for realistic aircraft structures. In this situation it is difficult for designers to make decisions on which systems to employ for a given design problem and which developments to pursue. Thus it is necessary for designers to be aware of the relative merits of the different methods currently used for the design optimization of advanced aircraft. This lecture series covers the methods available for the computer based design analysis and design optimization of aircraft structures. The lecture series deals with the principles and practices adopted to integrate the various factors which are considered in the design of advanced aircraft. These factors include: structural shape, aerodynamics, active control technology and aircraft performance. For individual titles, see N92-28470 through N92-28474.

N92-28470# Cranfield Inst. of Tech., Bedford (England). Dept. of Aerospace Science.

FUNDAMENTALS OF STRUCTURAL OPTIMISATION

A. J. Morris *In* AGARD, Integrated Design Analysis and Optimisation of Aircraft Structures May 1992 13 p (For primary document see N92-28469 19-05)

Copyright Avail: NTIS HC/MF A05

Structural optimization is concerned with the computerized automatic design of structures which are optimum with respect to some major design parameter. In the aircraft industry this parameter has usually been structural weight, though cost, performance, or other factors are now being considered. The general problem which is characterized here remains unchanged so that the basic nature of the optimization problem is the same for all applications. Also the structural optimization problem is always characterized by the finite element method (FEM). The use and application of these methods to computer aided design (CAD) requires some understanding of the underlying mathematical principles. It is shown that this process of developing solution methods use the optimization criteria as the basis for creating the up-date formulae which are the solution algorithm drivers. H.A.

N92-28471# Messerschmitt-Boelkow-Blohm G.m.b.H., Munich (Germany, F.R.). Military Aircraft Div.
PRACTICAL ARCHITECTURE OF DESIGN OPTIMISATION SOFTWARE FOR AIRCRAFT STRUCTURES TAKING THE MBB-LAGRANGE CODE AS AN EXAMPLE
J. Krammer *In* AGARD, Integrated Design Analysis and Optimisation of Aircraft Structures May 1992 16 p (For primary document see N92-28469 19-05)
Copyright Avail: NTIS HC/MF A05

The structural optimisation system MBB-Lagrange allows the optimization of homogeneous isotropic, orthotropic or anisotropic structures as well as fiber reinforced materials. With the simultaneous consideration of different requirements in the design of aircraft structures it is possible to reduce the number of iteration steps between design, analysis and manufacturing. Based on finite element methods for structures and panel methods for aerodynamics, the analysis with sensitivity includes modules for static, buckling, dynamic, static aeroelastic and flutter calculations. The optimization algorithms consists of mathematical programming methods and an optimization and analysis/sensitivity is the optimization model which leads to a very modular architecture. Typical application examples show the power and generality of the approach. Author

N92-28472# Dassault (E. M.) Co., Saint Cloud (France).
STRUCTURAL OPTIMIZATION OF AIRCRAFT
C. Cornuault and C. Petiau *In* AGARD, Integrated Design Analysis and Optimisation of Aircraft Structures May 1992 17 p (For primary document see N92-28469 19-05)
Copyright Avail: NTIS HC/MF A05

A general survey of Dassault experience and knowledge on Aircraft Design with Optimization Methods is depicted. This survey results from compiling the developments and the results already worked out and already presented in several papers. Part 1 gives a detailed description of the methodology. The special features of optimization with composite materials are shown. The organization of design resulting from use of optimization techniques is described and techniques neighboring optimization as model adjustment are reviewed, as well as further developments. Part 2 illustrates this methodology by an actual case study of an aircraft design by Dassault-Aviation with relevant examples of structural and aeroelastic optimization on carbon structures of a wing and a fin. Author

N92-28473*# National Aeronautics and Space Administration. Langley Research Center, Hampton, VA.
MULTIDISCIPLINARY DESIGN AND OPTIMIZATION
Jaroslaw Sobieszczanski-Sobieski *In* AGARD, Integrated Design Analysis and Optimisation of Aircraft Structures May 1992 15 p Presented as A System Approach to Aircraft Optimization, Paper No. 2 at the AGARD Workshop on Integrated Design Analysis and Optimization of Aircraft Structures, Bath, England, 1-2 May 1991 (For primary document see N92-28469 19-05)
(AGARD-Paper-2) Copyright Avail: NTIS HC/MF A05

Mutual couplings among the mathematical models of physical phenomena and parts of a system such as an aircraft complicate the design process because each contemplated design change may have a far reaching consequence throughout the system. This paper outlines techniques for computing these influences as system design derivatives useful to both judgmental and formal optimization purposes. The techniques facilitate decomposition of the design process into smaller, more manageable tasks and they form a methodology that can easily fit into existing engineering optimizations and incorporate their design tools. Author

N92-28474# Messerschmitt-Boelkow-Blohm G.m.b.H., Munich (Germany, F.R.). Military Aircraft Div.
MATHEMATICAL OPTIMIZATION: A POWERFUL TOOL FOR AIRCRAFT DESIGN
Otto Sensburg *In* AGARD, Integrated Design Analysis and Optimisation of Aircraft Structures May 1992 19 p (For primary document see N92-28469 19-05)
Copyright Avail: NTIS HC/MF A05

Formal mathematical optimization methods have been developed during the past 10 to 15 years for the structural design of aircraft. Together with reliable analysis programs like finite element methods they provide powerful tools for the structural design. They are efficient in at least two ways: (1) producing designs that meet all specified requirements at minimum weight in one step; and (2) relieving the engineer from a time consuming search for modifications that give better results, they allow more creative design modifications. MBB has developed a powerful optimization code called MBB-Lagrange which uses mathematical programming and gradients to fulfill different constraints simultaneously. Some examples depicting the successful application of the MBB-LAGRANGE code are presented. Also results of other optimization codes are shown. The paper closes with an outlook on how the optimization problem could be enlarged to include the shape and size of airplanes. Author

N92-28634# National Aerospace Lab., Amsterdam (Netherlands). Flight Div.
IMPROVEMENT OF SEPARATIONS OF PRACTICE BOMBS FROM A MULTIPLE BOMB ADAPTER
K. R. Rijzebol 31 Aug. 1990 32 p Presented at the 8th Aircraft/Stores Compatibility Symposium, Fort Walton Beach, FL, 23-28 Oct. 1990 Submitted for publication Sponsored by Royal Netherlands Air Force
(NLR-TP-90307-U; ETN-92-91447) Avail: NTIS HC/MF A03

In the search for a small and easy to handle practice bomb rack, the Multiple Practice Bomb Adapter (MBPA) to be used for training on the F-16 was investigated. An initial exploratory flight test program with this tandem two place MBPA did not show adverse characteristics. In a subsequent delivery flight test program, film recordings revealed bomb to pylon or bomb to adapter contact of both the Mk-106 and BDU-33D/B practice bombs. Flight tests with a rack with a heavily modified aerodynamically shape showed still unacceptable separation behavior. Additional mechanical modifications, consisting of spring type 'tail up restrictors', were applied. These modified bomb racks produced satisfactory separation characteristics for the BDU-33D/B practice bomb throughout the required release envelope. The Mk-106 produced considerable deflection of the tail up restrictors. A more rigid design of the tail up restrictor was then constructed for the original MPBA and was flight tested. The test results showed that the tail up restrictors do prevent collisions of bomb tails with the MPBA, the parent pylon, or the aircraft. The practice bombs separate positively and clear from the aircraft. ESA

N92-28649# National Aerospace Lab., Amsterdam (Netherlands). Structures and Materials Div.
THE USE OF LOAD ENHANCEMENT FACTORS IN THE CERTIFICATION OF COMPOSITE AIRCRAFT STRUCTURES
J. Lameris 22 Feb. 1990 60 p
(Contract OV/RLD-987)
(NLR-TP-90068-U; ETN-92-91432) Avail: NTIS HC/MF A04

In the full scale durability and damage tolerance tests of composite aircraft structures, the U.S. and European certification requirements demand among other things that the number of cycles applied are statistically significant and that the influence of the environment has been taken into account. Several certification

methods which take into account the requirement of having sufficient statistically reliable data are described. A review of the way in which these requirements are interpreted and applied in four composite aircraft certification programs in particular with regard to the application of so called enhancement factors is given. ESA

N92-28651# National Aerospace Lab., Amsterdam (Netherlands). Flight Div.

MODIFICATIONS AND RESULTS OF FLIGHT TESTS OF A PRACTICE BOMB ADAPTER

K. R. Rijzebol 30 Mar. 1990 11 p Sponsored by Royal Netherlands Air Force

(NLR-TP-90108-U; ETN-92-91434) Avail: NTIS HC/MF A03

The Royal Netherlands Airforce was searching for a small light and easy to handle practical bomb rack. Initial exploratory delivery flight tests with the tandem two place Multiple Practice Bomb Adapter (MPBA), carried at the outboard wing pylons of the F-16 aircraft, did not show adverse characteristics. A report on comparable flight tests with the A-7 Corsair was also positive. In a delivery flight test program to collect scoring data, high speed 16 mm movie recordings revealed bomb to pylon or bomb to adapter contact of both Mk-106 (at moderate airspeed) and BDU-33D/B (at higher speed) within the required release envelope. Subsequently, the aerodynamic shape of the practice adapter was modified. The internal, mechanical properties and the rack of aircraft interface remained unchanged. Flight tests with the modified rack showed still unacceptable separation behavior. After providing spring type 'tail up restrictors' to the original and to the aerodynamically modified bomb rack, satisfactory separation characteristics were demonstrated by the BDU-33D/B practice bomb throughout the required release envelope. A more rigid construction of the tail-up restrictor will probably produce satisfactory separation characteristics of the Mk-106 practice bomb as well. A comparison of the bomb adapter before and after modification and the results of the flight test programs are presented. ESA

N92-28687# National Aerospace Lab., Amsterdam (Netherlands). Aerodynamics Div.

LAH-MAIN ROTOR MODEL TEST AT THE DNW

J. W. G. vanNunen, C. Hermans, and H.-J. Langer (Deutsche Forschungsanstalt fuer Luft- und Raumfahrt, Brunswick, Germany, F.R.) 10 Aug. 1990 14 p Presented at the 16th European Rotorcraft Forum, Glasgow, Scotland, 18-21 Sep. 1990 Previously announced in IAA as A92-35771

(NLR-TP-90305-U; ETN-92-91446) Avail: NTIS HC/MF A03

In the context of a feasibility and cost definition study for the A129 LAH, a wind tunnel experiment was executed in the wind tunnel on a dynamically and Mach scaled mode of the main rotor. The tests aimed at getting more reliable answers to the question of which of the proposed rotor configurations would fulfil the stringent flight performance requirements of the new helicopter best. The rotor diameter amounted to 3.5 m. Four different rotor configurations were examined, the variations being either in the blade tip shape or in the twist distribution along the span of the blade. The dynamic characteristics of the various blade configurations were found to agree reasonably well. An exception in this respect should only be made for those blade configurations that have swept back tips. These specific blades exhibit definitely lower torsional frequencies than comparable blades with straight tips. The rotor torque measured on the model rotor correlates well up to 130 kts with the torque as determined during flight tests. Comparing the different rotor configurations considered during the present test, the high twist blade set is found to produce the highest vibration levels at the higher advance ratios. ESA

N92-28714# National Aerospace Lab., Amsterdam (Netherlands). Dept. of Flight Testing and Helicopters.

S-76B CERTIFICATION FOR VERTICAL TAKE-OFF AND LANDING OPERATIONS FROM CONFINED AREAS

J. M. G. F. Stevens and H. J. G. C. Vodegel 16 Aug. 1990 20 p Presented at 16th European Rotorcraft Forum, Glasgow, Scotland, 18-21 Sep. 1990 Previously announced in IAA as A92-35760

(NLR-TP-90286-U; ETN-92-91544) Avail: NTIS HC/MF A03

Data necessary for certification of vertical operations for the Sikorsky S-76B were generated. A computer simulation program was used to calculate two dimensional flight trajectories after an engine failure during takeoff or landing. Based on the initial results of computer simulations, flight tests were carried out during which single engine failure was simulated. Test data were recorded by video on board and on the ground. Calculated and flight test data were in good agreement over the considered range of masses, maneuvers and atmospheric conditions. Procedures for Category A vertical operations with the S-76B were determined with the use of the computer program. ESA

N92-28720*# Kansas Univ. Center for Research, Inc., Lawrence. Flight Research Lab.

IDENTIFICATION OF AERODYNAMIC MODELS FOR MANEUVERING AIRCRAFT Final Report

C. Edward Lan and C. C. Hu 30 Jun. 1992 101 p

(Grant NAG1-1087)

(NASA-CR-190444; NAS 1.26:190444; KU-FRL-872-5) Avail: NTIS HC/MF A06

The method based on Fourier functional analysis and indicial formulation for aerodynamic modeling as proposed by Chin and Lan is extensively examined and improved for the purpose of general applications to realistic airplane configurations. Improvement is made to automate the calculation of model coefficients, and to evaluate more accurately the indicial integral. Test data of large angle-of-attack ranges for two different models, a 70 deg. delta wing and an F-18 model, are used to further verify the applicability of Fourier functional analysis and validate the indicial formulation. The results show that the general expression for harmonic motions throughout a range of k is capable of accurately modeling the nonlinear responses with large phase lag except in the region where an inconsistent hysteresis behavior from one frequency to the other occurs. The results by the indicial formulation indicate that more accurate results can be obtained when the motion starts from a low angle of attack where hysteresis effect is not important. Author

N92-28721*# National Aeronautics and Space Administration. Ames Research Center, Moffett Field, CA.

THERMAL RESPONSE OF RIGID AND FLEXIBLE INSULATIONS AND REFLECTIVE COATING IN AN AEROCONVECTIVE HEATING ENVIRONMENT

D. A. Kourtides, S. A. Chiu, D. J. Iverson, and D. M. Lowe Mar. 1992 81 p

(RTOP 506-43-31)

(NASA-TM-103925; A-92064; NAS 1.15:103925) Avail: NTIS HC/MF A05

Described here is the thermal performance of rigid and flexible thermal protection systems considered for potential use in future Aeroassist Space Transfer Vehicles. The thermal response of these materials subjected to aeroconvective heating from a plasma arc is described. Properties that were measured included the thermal conductivity of both rigid and flexible insulations at various temperatures and pressures and the emissivity of the fabrics used in the flexible insulations. The results from computerized thermal analysis models describing the thermal response of these materials subjected to flight conditions are included. Author

N92-28771# Aeronautical Research Labs., Melbourne (Australia).

REDUCTION AND ANALYSIS OF F-111C FLIGHT DATA

P. Piperias Dec. 1991 51 p

(AD-A250341; ARL-STRUC-TM-544; DODA-AR-006-633) Avail: NTIS HC/MF A04

As part of a program to determine inspection intervals for the stiffener runout regions of the upper plates of the wing pivot fittings of RAAF F-111 aircraft, the possible influence on crack growth of stores carried and of low and negative g-spectrum loading has

been examined for reconnaissance aircraft, the remaining F-111 fleet, and for aircraft A8-148. Derived gust loading spectra for the same F-111 groups have also been determined. GRA

N92-28802# Naval Postgraduate School, Monterey, CA.
TASKING AND COMMUNICATION FLOWS IN THE F/A-18D COCKPIT: ISSUES, PROBLEMS, AND POSSIBLE SOLUTIONS M.S. Thesis
Mark F. McKeon Sep. 1991 77 p
(AD-A245977) Avail: NTIS HC/MF A05

The U.S. Marine Corps is replacing its A-6E TRAM aircraft with the two seat F/A-18D. With the exception of the F-15E Strike Eagle, never has a tactical aircraft been capable of processing such a vast amount of multi-mission data and displaying that fighter/attack information to the aircrew. These vast capabilities have led to some problems in the area of F/A-18D aircrew coordination. This thesis will review communication flows and tasking procedures that exist in many Group Decision Support Systems (GDSS) to develop guidelines that are applicable to tactical aircraft aircrew coordination procedures. These guidelines will then be applied to combat mission essential F/A-18D cockpit communication and tasking procedures that should be executed during various scenarios. Additionally, simulator flight profiles will be postulated to test, evaluate and verify these procedures. This study provides a framework on combat procedures that will not only benefit the Marine Corps' F/A-18D community, but as they start bringing into their inventory the two sea F/A-18E/F, the U.S. Navy as well. Author (GRA)

N92-28901# National Aerospace Lab., Tokyo (Japan). Flight Test Team.
AERODYNAMIC CHARACTERISTICS OBTAINED FROM ALPHA SWEEP TEST OF THE QUIET STOL EXPERIMENTAL AIRCRAFT ASKA
Toshio Bandou May 1991 67 p In JAPANESE
(NAL-TR-1112; ISSN-0389-4010; JTN-92-80381) Avail: NTIS HC/MF A04

Longitudinal aerodynamic characteristics are one of the most important considerations in aircraft design. Using the NAL Short Take Off and Landing (STOL) experimental aircraft, ASKA, an alpha sweep method was adopted instead of using the conventional discrete method to investigate ASKA's longitudinal aerodynamic characteristics. ASKA's longitudinal aerodynamic characteristics are described based on analysis of the test results. In addition, longitudinal aerodynamic coefficients obtained from flight tests are compared with the ASKA's wind tunnel design configuration. ASKA showed a pitch up phenomena during shallow Upper Surface Blowing (USB) flap angles, and also encountered path divergence in the flaps up configuration, being a significant phenomena for a powered lift aircraft. Powered lift aircraft's lift coefficient consists of basic lift due to wing and flaps, direct jet thrust, and supercirculation. This lift build-up is described using calculation results of flight test data. The powered lift factor, a key parameter for powered lift aircraft, is also described. Author (NASDA)

N92-28910*# National Aeronautics and Space Administration. Ames Research Center, Moffett Field, CA.
BINARY OPTICAL FILTERS FOR SCALE INVARIANT PATTERN RECOGNITION
Max B. Reid, John D. Downie, and Butler P. Hine Apr. 1992 12 p
(RTOP 506-51-31)
(NASA-TM-103902; A-92014; NAS 1.15:103902) Avail: NTIS HC/MF A03

Binary synthetic discriminant function (BSDF) optical filters which are invariant to scale changes in the target object of more than 50 percent are demonstrated in simulation and experiment. Efficient databases of scale invariant BSDF filters can be designed which discriminate between two very similar objects at any view scaled over a factor of 2 or more. The BSDF technique has considerable advantages over other methods for achieving scale invariant object recognition, as it also allows determination of the object's scale. In addition to scale, the technique can be used to design recognition systems invariant to other geometric distortions. Author

N92-28926*# National Aeronautics and Space Administration. Ames Research Center, Moffett Field, CA.
ROTORCRAFT IN-FLIGHT SIMULATION RESEARCH AT NASA AMES RESEARCH CENTER: A REVIEW OF THE 1980'S AND PLANS FOR THE 1990'S
Edwin W. Aiken, William S. Hindson, J. Victor Lebacqz, Dallas G. Denery, and Michelle M. Eshow (Army Aviation Systems Command, Moffett Field, CA.) Aug. 1991 15 p Presented at the International Symposium on In-Flight Simulation for the 1990's, Braunschweig, Germany, 1-3 Jul. 1991 Sponsored in part by Army Aviation Systems Command, St. Louis, MO
(RTOP 505-59-36)
(NASA-TM-103873; A-91178; NAS 1.15:103873) Avail: NTIS HC/MF A03

A new flight research vehicle, the Rotorcraft-Aircrew System Concepts Airborne Laboratory (RASCAL), is being developed by the U.S. Army and NASA at ARC. The requirements for this new facility stem from a perception of rotorcraft system technology requirements for the next decade together with operational experience with the Boeing Vertol CH-47B research helicopter that was operated as an in-flight simulator at ARC during the past 10 years. Accordingly, both the principal design features of the CH-47B variable-stability system and the flight-control and cockpit-display programs that were conducted using this aircraft at ARC are reviewed. Another U.S Army helicopter, a Sikorsky UH-60A Black Hawk, was selected as the baseline vehicle for the RASCAL. The research programs that influence the design of the RASCAL are summarized, and the resultant requirements for the RASCAL research system are described. These research programs include investigations of advanced, integrated control concepts for achieving high levels of agility and maneuverability, and guidance technologies, employing computer/sensor-aiding, designed to assist the pilot during low-altitude flight in conditions of limited visibility. The approach to the development of the new facility is presented and selected plans for the preliminary design of the RASCAL are described. Author

N92-28987 Department of the Navy, Washington, DC.
WING-EXTENDIBLE GLIDING STORE Patent
Samuel Greenhalgch, inventor (to Navy) 24 Dec. 1991 8 p Filed 21 Dec. 1990
(AD-D015233; US-Patent-5,074,493; US-Patent-Appl-SN-632442; US-Patent-Class-244-3.27) Avail: US Patent and Trademark Office

The instant invention discloses a gliding store with spring-actuated, extendible wings. Upon launch from an aircraft, and separation from the aircraft a safe distance, a launch lanyard and wing control device is separated from the store, allowing a pair of hinged wings to be forced open. Each wing is set on the store body at a predetermined position to cause the store to glide at a predetermined angle and with a predetermined flight path of free-fall. GRA

N92-29110*# National Aeronautics and Space Administration. Hugh L. Dryden Flight Research Center, Edwards, CA.
IN-FLIGHT SIMULATION STUDIES AT THE NASA DRYDEN FLIGHT RESEARCH FACILITY
Mary F. Shafer Jul. 1992 20 p Presented at the AIAA Simulation Technology Conference, New Orleans, LA, 12-14 Aug. 1991
(RTOP 505-64-30)
(NASA-TM-4396; H-1833; NAS 1.15:4396) Copyright Avail: NTIS HC/MF A03

Since the late 1950's, the National Aeronautics and Space Administration's Dryden Flight Research Facility has found in-flight simulation to be an invaluable tool. In-flight simulation has been used to address a wide variety of flying qualities questions, including low-lift-to-drag ratio approach characteristics for vehicles like the X-15, the lifting bodies, and the Space Shuttle; the effects of time

delays on controllability of aircraft with digital flight-control systems, the causes and cures of pilot-induced oscillation in a variety of aircraft, and flight-control systems for such diverse aircraft as the X-15 and the X-29. In-flight simulation has also been used to anticipate problems and to avoid them and to solve problems once they appear. Presented here is an account of the in-flight simulation at the Dryden Flight Research Facility and some discussion. An extensive bibliography is included. Author

N92-29180# Battelle Memorial Inst., Columbus, OH.
GENERATION OF SPECTRA AND STRESS HISTORIES FOR FATIGUE AND DAMAGE TOLERANCE ANALYSIS OF FUSELAGE REPAIRS Final Report
David Broek, Samuel H. Smith, and Richard C. Rice Oct. 1991 55 p
(Contract DTRS-57-89-C-00006)
(AD-A250390; DOT/VNTSC-FAA-91-16) Avail: NTIS HC/MF A04

This report describes a simplified procedure for the development of stress histories for use in the analysis of aircraft repairs. This report concentrates on stress histories for fuselage skin repairs. A description of typical fuselage loadings is provided, and basic fuselage stress histories are described. A method for development of an exceedance diagram for analysis of fuselage skin repairs is detailed. Subsequently, a methodology for generating detailed stress histories is reviewed. Some of the key features are (1) the inclusion of a range of flights of different severities, (2) the inclusion of deterministic loads where they occur, e.g., ground-air-ground cycles, (3) the use of a near-optimum number of stress levels (10-16 positive and negative), (4) the combination of positive and negative excursions of equal frequency, and (5) matching of the total number of flights and cycles with the total exceedance diagram. Two methods of estimating fuselage skin stresses are presented, the first based on static equilibrium requirements and the second based on a limit load analysis. A comparison of the proposed history generation scheme with that of an airframe manufacturer for the KC-135 is also presented. The predicted fatigue crack growth patterns for a hypothetical through crack at a fastener hole are compared for the two history generation schemes at three areas within a fuselage. GRA

N92-28531# Royal Aerospace Establishment, Bedford (England). FMS Div.
VALIDATION OF SIMULATION SYSTEMS FOR AIRCRAFT ACCEPTANCE TESTING
A. A. Woodfield *In* AGARD, Piloted Simulation Effectiveness Feb. 1992 4 p (For primary document see N92-28522 19-01)
Copyright Avail: NTIS HC/MF A15

06 AIRCRAFT INSTRUMENTATION

Includes cockpit and cabin display devices; and flight instruments.

For related information see also *19 Spacecraft Instrumentation* and *35 Instrumentation and Photography.*

N92-28376# Advisory Group for Aerospace Research and Development, Neuilly-Sur-Seine (France). Avionics Panel.
APPLICATIONS OF ASICS TO AVIONICS
Feb. 1992 49 p
(AGARD-AG-329; ISBN-92-835-0657-X) Copyright Avail: NTIS HC/MF A03

An overview of how Application Specific Integrated Circuits (ASICs) can be a key factor in avionics systems is presented. The technical capabilities and possibilities of ASICs in avionics applications are discussed along with the essential characteristics and various types of ASICs that are available. The computer aided design (CAD) tools necessary for the rapid development of ASICs are discussed. Two specific examples of applications are cited: (1) the imbedded computers necessary for airborne radar digital signal processing; and (2) the ASIC role in image processing for aircraft cockpits. For individual titles, see N92-28377 through N92-28380.

N92-28377# Thomson Composants, Saint Egreve (France).
WHAT IS AN ASIC?
J. M. Brice and J. Redolfi *In* AGARD, Applications of ASICs to Avionics Feb. 1992 7 p (For primary document see N92-28376 19-06)
Copyright Avail: NTIS HC/MF A03

Since the emergence of the first ASICs in 1975, many advances have occurred in this field. This has resulted in highly complex digital ASICs and very high speed analog circuits. This strong evolution did not really change the nature of the four ASIC families: full custom circuits, standard cells, programmable devices, and PLD's. Author

N92-28378# Thomson Composants, Saint Egreve (France).
THE SILICON COMPILER FOR DESIGNING MILITARY VLSI ASIC'S
J. M. Brice *In* AGARD, Applications of ASICs to Avionics Feb. 1992 14 p (For primary document see N92-28376 19-06)
Copyright Avail: NTIS HC/MF A03

The capabilities of present day military electronics are a direct result of the use of the following two technologies: (1) very large scale integration (VLSI) and (2) silicon integrated circuits (ICs). As a result, defense electronics manufacturers are able to design increasingly sophisticated digital electronics systems. A discussion of complexity in digital Application Specific Integrated Circuits (ASICs) is presented. D.R.D.

N92-28379# Micro Circuit Engineering Ltd., Tewkesbury (England).
APPLICATIONS OF SILICON HYBRID MULTI-CHIP MODULES TO AVIONICS
E. S. Eccles *In* AGARD, Applications of ASICs to Avionics Feb. 1992 14 p (For primary document see N92-28376 19-06)
Copyright Avail: NTIS HC/MF A03

Silicon-based multi-chip modules (MCMs) are an inevitable byproduct of reduced feature size and higher speed integrated circuit (IC) devices. Early versions are available and are being exploited in military and high performance commercial applications. Their use will proliferate rapidly over the next four years and is likely to extend the use of monolithic ICs into performance areas which were previously inaccessible. Author

N92-28380# Thomson-CSF, Montrouge (France). Direction Recherche et Technologie.
A RADAR SIGNAL PROCESSING ASIC AND A VME INTERFACE CIRCUIT
A. Chochod *In* AGARD, Applications of ASICs to Avionics Feb. 1992 6 p (For primary document see N92-28376 19-06)
Copyright Avail: NTIS HC/MF A03

The purpose of this circuit is to perform real time signal processing for radar applications such as a missile seeker. There are two operating modes (standard and sample accumulation) and a variety of options through user selectable parameters and control logic (i.e. detection with global, local, or fixed threshold). Author

N92-28644# National Aerospace Lab., Amsterdam (Netherlands). Flight Div.
A SIMPLE AND LOW COST SYSTEM TO MEASURE DELAY TIMES IN PNEUMATIC SYSTEMS
S. StormvanLeeuwen 19 May 1990 19 p
(NLR-TP-90174-U; ETN-92-91438) Avail: NTIS HC/MF A03

A methodology to measure pneumatic delay times based on the determination of the complex transfer function of the pressure line in the frequency range of interest is described. From the transfer function, the delay time as a function of the frequency can be calculated. The transfer function is established by measuring the amplitude and phase response of the pressure system at a number of discrete frequencies. The equipment to generate a

pneumatic stimulus and the equipment to determine the amplitude and phase response is described. ESA

N92-28654# National Aerospace Lab., Amsterdam (Netherlands). Flight Div.
POTENTIAL APPLICATIONS OF LASER DOPPLER ANEMOMETRY FOR IN-FLIGHT MEASUREMENTS
H. W. Jentink 9 May 1990 32 p
(NLR-TP-90163-U; ETN-92-91437) Avail: NTIS HC/MF A03

The application of laser anemometry for flight testing and other aircraft related measurements is addressed. The laser anemometry technique and previous work in this field are reviewed and applications are described. A comparison of possibilities of laser anemometry with conventional techniques shows some unique advantages of laser anemometry. ESA

N92-29222# Air Force Inst. of Tech., Wright-Patterson AFB, OH. School of Engineering.
DEVELOPMENT OF A FLIGHT INFORMATION SYSTEM USING THE STRUCTURED METHOD M.S. Thesis
Yeong-Lae Kwak Mar. 1992 106 p
(AD-A248207; AFIT/GCS/ENG/92M-03) Avail: NTIS HC/MF A06

This thesis documents the development of a database system for the Flight Information System (FIS) of the Korean Air Force. The scope of the FIS is too large to be covered by this thesis. Thus, this thesis covers only the core part of the FIS due to the limitation of time and man-power. This thesis uses the structured method. Structured analysis and structured design techniques are the two techniques most used. This thesis focused not only the development of the FIS but also the application of the software development method, the structured method, and its tools such as DFD, DD, ERD, and so on. Also, the use of ORACLE was an important part of this thesis too. GRA

07 AIRCRAFT PROPULSION AND POWER

Includes prime propulsion systems and systems components, e.g., gas turbine engines and compressors; and onboard auxilliary power plants for aircraft.

For related information see also *20 Spacecraft Propulsion and Power, 28 Propellants and Fuels,* and *44 Energy Production and Conversion.*

N92-28294# Southwest Research Inst., San Antonio, TX. Engine Fuel and Vehicle Research Div.
HIGH-TEMPERATURE MINIATURIZED TURBINE ENGINE LUBRICATION SYSTEM SIMULATOR Final Report, Sep. 1988 - May 1991
Clifford A. Moses, Pierre J. Gutierrez, Burl B. Baber, and John P. Cuellar Feb. 1992 50 p
(Contract F33615-88-C-2816)
(AD-A249259; WL-TR-91-2103) Avail: NTIS HC/MF A03

A high-temperature miniaturized turbine engine lubrication system simulator was designed and fabricated for the purpose of evaluating limited quantities, 1 quart or less, of candidate Integrated High Performance Turbine Engine Technology candidate lubricants. The computer-controlled simulator can determine a lubricant's functional and tribological properties under a wide variety of operating conditions. Metal test coupons can be added to the system to evaluate a lubricant's corrosive properties. Operating parameters are 10,000 rpm, 100 Ksi Hertz stress bulk oil temperatures to 750 F, bearing temperatures to 8500 F, and hot spots to 9500 F. The simulator also has the capability for inert atmosphere and once through lubrication operation. Validation of the simulator was accomplished with 48-hour test runs using high temperature polyester and polyphenylether lubricants. GRA

N92-28418*# National Aeronautics and Space Administration. Lewis Research Center, Cleveland, OH.
INTERNAL REVERSING FLOW IN A TAILPIPE OFFTAKE CONFIGURATION FOR SSTOVL AIRCRAFT
Jack G. McArdle, Barbara S. Esker, and James A. Rhodes (McDonnell Aircraft Co., Saint Louis, MO.) Jul. 1992 23 p Proposed for presentation at the 28th Joint Propulsion Conference and Exhibit, Nashville, TN, 6-8 Jul. 1992; sponsored by AIAA, SAE, ASME, and ASEE
(RTOP 505-68-32)
(NASA-TM-105698; E-7086; NAS 1.15:105698; AIAA Paper 92-3790) Avail: NTIS HC/MF A03

A generic one-third scale model of a tailpipe offtake system for a supersonic short takeoff vertical landing (SSTOVL) aircraft was tested at LeRC Powered Lift Facility. The model consisted of a tailpipe with twin elbows, offtake ducts, and flow control nozzles, plus a small ventral nozzle and a blind flange to simulate a blocked cruise nozzle. The offtake flow turned through a total angle of 177 degrees relative to the tailpipe inlet axis. The flow split was 45 percent to each offtake and 10 percent to the ventral nozzle. The main test objective was to collect data for comparison to the performance of the same configuration predicted by a computational fluid dynamics (CFD) analysis. Only the experimental results are given - the analytical results are published in a separate paper. Performance tests were made with unheated air at tailpipe-to-ambient pressure ratios up to 5. The total pressure loss through the offtakes was as high as 15.5 percent. All test results are shown as graphs, contour plots, and wall pressure distributions. The complex flow patterns in the tailpipe and elbows at the offtake openings are described with traversing flow angle probe and paint streak flow visualization data. Author

N92-28419*# National Aeronautics and Space Administration. Lewis Research Center, Cleveland, OH.
FULL NAVIER-STOKES ANALYSIS OF A TWO-DIMENSIONAL MIXER/EJECTOR NOZZLE FOR NOISE SUPPRESSION
James R. DeBonis Jul. 1992 17 p Proposed for presentation at the 28th Joint Propulsion Conference and Exhibit, Nashville, TN, 6-8 Jul. 1992; sponsored by AIAA, SAE, ASME, and ASEE
(RTOP 537-02-23)
(NASA-TM-105715; E-7109; NAS 1.15:105715; AIAA Paper 92-3570) Avail: NTIS HC/MF A03

A three-dimensional full Navier-Stokes (FNS) analysis was performed on a mixer/ejector nozzle designed to reduce the jet noise created at takeoff by a future supersonic transport. The PARC3D computational fluid dynamics (CFD) code was used to study the flow field of the nozzle. The grid that was used in the analysis consisted of approximately 900,000 node points contained in eight grid blocks. Two nozzle configurations were studied: a constant area mixing section and a diverging mixing section. Data are presented for predictions of pressure, velocity, and total temperature distributions and for evaluations of internal performance and mixing effectiveness. The analysis provided good insight into the behavior of the flow. Author

N92-28458# Advisory Group for Aerospace Research and Development, Neuilly-Sur-Seine (France). Propulsion and Energetics Panel.
STEADY AND TRANSIENT PERFORMANCE PREDICTION OF GAS TURBINE ENGINES [PREDICTION DES PERFORMANCES DES MOTEURS A TURBINE A GAZ EN REGIMES ETABLI ET TRANSITOIRE]
May 1992 189 p Lectures held in Cambridge, MA, 27-28 May 1992, in Neubiberg, Fed. Republic of Germany, 9-10 Jun. 1992, and in Chatillon/Bagneux, France, 11-12 Jun. 1992
(AGARD-LS-183; ISBN-92-835-0674-X) Copyright Avail: NTIS HC/MF A09

Aero-thermodynamic performance prediction methods for gas turbine engines with respect to steady and transient operation are discussed. This includes advanced cycle calculation methods, also taking into account variable cycle engine types. A very important objective is the consideration of installation effects, i.e. Reynolds number and inlet distortions, as well as advanced control concepts

for increasing engine surge margins. In addition to these topics, individual papers include practical considerations in designing the engine cycle, dynamic simulation, inlet distortion effects in aircraft propulsion system integration, 'smart' engines, and performance and health monitoring models. For individual titles, see N92-28459 through N92-28467.

N92-28459# Carleton Univ., Ottawa (Ontario). Dept. of Mechanical and Aerospace Engineering.
OVERVIEW ON BASIS AND USE OF PERFORMANCE PREDICTION METHODS
H. I. H. Saravanamuttoo *In* AGARD, Steady and Transient Performance Prediction of Gas Turbine Engines May 1992 18 p (For primary document see N92-28458 19-07)
Copyright Avail: NTIS HC/MF A09

The basic methods of component matching, which is central to the prediction of gas turbine performance, are outlined. Steady-state prediction of off-design performance must be done at the beginning of an engine development program. This ensures that the engine can satisfy all the mission requirements. The matching techniques can be extended to predict transient performance, which is essential for controls development and to ensure good engine handling. The large amount of computation required demands the use of computer modelling and the role of modelling in the development program and the basic requirements for performance modelling are described. Author

N92-28460# Royal Aerospace Establishment, Farnborough (England). Air Vehicle Performance Dept.
PRACTICAL CONSIDERATIONS IN DESIGNING THE ENGINE CYCLE
M. G. Philpot *In* AGARD, Steady and Transient Performance Prediction of Gas Turbine Engines May 1992 24 p Sponsored by Ministry of Defence (For primary document see N92-28458 19-07)
Copyright Avail: NTIS HC/MF A09

To define the cycle parameters and calculate the performance of a real engine, numerous practical constraints need to be taken into account. These fall into two main categories: the limitations of available component technologies; and the operational considerations that are dependent on aircraft application. The main technology limiters are discussed. How they are incorporated into the cycle definition process is indicated. Operational factors include the extent of the intended flight envelope and the range of the critical flight conditions for which performance must be assured, and the balance to be struck between minimizing fuel consumption, maximizing installed power, and constraining costs of ownership. Taking these technology and operational influences into account, the basic cycle characteristics and approach to cycle choice are examined for three main classes of aircraft: subsonic transports, military combat aircraft, and helicopters. Author

N92-28461# Societe Nationale d'Etude et de Construction de Moteurs d'Aviation, Moissy-Cramayel (France). Engineering Div.
STEADY AND TRANSIENT PERFORMANCE CALCULATION METHOD FOR PREDICTION, ANALYSIS, AND IDENTIFICATION
Jean Pierre Duponchel, Jean Loisy, and Rene Carrillo *In* AGARD, Steady and Transient Performance Prediction of Gas Turbine Engines May 1992 21 p (For primary document see N92-28458 19-07)
Copyright Avail: NTIS HC/MF A09

The detailed design and development of turbofans involves the prediction and identification, by means of test analysis, of the performance of the engine and its components. The thermodynamic simulation and analysis codes integrate existing knowledge and interpretations of the detailed operating procedure of the components of the engine being developed. The relevance of the predicted performance depends on the quality of the representation of the various physical phenomena affecting the characteristics of the components and, consequently, on the incorporation of experimental correlation in the modelling. In this context, the representation of compressor and turbine characteristics is particularly important. We will analyze the ability of corrected parameters to represent MACH similitude at the component inlet under various conditions. Author

N92-28462# Carleton Univ., Ottawa (Ontario). Dept. of Mechanical and Aerospace Engineering.
COMPONENT PERFORMANCE REQUIREMENTS
H. I. H. Saravanamuttoo *In* AGARD, Steady and Transient Performance Prediction of Gas Turbine Engines May 1992 10 p (For primary document see N92-28458 19-07)
Copyright Avail: NTIS HC/MF A09

Component data are essential for modelling the overall performance of gas turbines. The component characteristics are not easily obtained, and much of the data are proprietary and not available in the open literature. Several methods are available for estimating component characteristics and are briefly described. The requirements of users and manufacturers are quite different, but both can produce fully credible performance models. Author

N92-28463# Virginia Polytechnic Inst. and State Univ., Blacksburg. Dept. of Mechanical Engineering.
DYNAMIC SIMULATION OF COMPRESSOR AND GAS TURBINE PERFORMANCE
Walter F. OBrien *In* AGARD, Steady and Transient Performance Prediction of Gas Turbine Engines May 1992 28 p (For primary document see N92-28458 19-07)
Copyright Avail: NTIS HC/MF A09

Dynamic performance simulation models are discussed with emphasis on the fundamental principles of the models and the methods used to represent component and stage flow characteristics. Results of several simulations of the dynamic behavior of multistage compressors are shown with comparisons to experimental data. Possibilities for advanced computational techniques for near-real-time simulations of compressors and gas turbines are reviewed. Author

N92-28464*# Cambridge Univ. (England).
INLET DISTORTION EFFECTS IN AIRCRAFT PROPULSION SYSTEM INTEGRATION
J. P. Longley and E. M. Greitzer (Massachusetts Inst. of Tech., Cambridge.) *In* AGARD, Steady and Transient Performance Prediction of Gas Turbine Engines May 1992 18 p Sponsored by NASA. Lewis Research Center; GE; and Rolls-Royce Ltd. (For primary document see N92-28458 19-07)
Copyright Avail: NTIS HC/MF A09

A tutorial survey of inlet flow distortion effects on engine performance and stability is presented. Inlet distortions in aero engines arise through a variety of causes. They can be essentially steady, due to non-axisymmetric intake duct geometry, or time varying, for example from flow separation off the lip of the inlet during maneuvers or shock-induced separation during supersonic flight. Whatever the cause, the result is generally a decrease in performance and, more importantly, a lessening of the stable flow range of the compressor. The distortions are generally three-dimensional. It is an extremely useful simplification to break them, at least conceptually, into radial and circumferential non-uniformities and approach each separately. Purely radial distortions can be treated by the methods that were developed for designing compressors in nominally axisymmetric inlet flow, and this type of distortion will be only briefly discussed. Circumferential non-uniformities, however, introduce additional fluid dynamic features into the analysis of compressor behavior and often have the larger impact on performance and stability. Thus we concentrate mainly on the effects of steady circumferential inlet flow distortion. Author

N92-28465# Technische Univ., Munich (Germany, F.R.). Performance Dept.
CALCULATION OF INSTALLATION EFFECTS WITHIN PERFORMANCE COMPUTER PROGRAMS
J. Kurzke *In* AGARD, Steady and Transient Performance Prediction of Gas Turbine Engines May 1992 19 p (For

primary document see N92-28458 19-07)
Copyright Avail: NTIS HC/MF A09

Gas turbine engine components, such as compressors, burners, and turbines are usually tested on rigs prior to installation into an engine. In the engine, the component behavior is different for a variety of reasons. The installation effects are caused by small geometrical differences due to nonrepresentative rig operating temperatures and pressures, by different gas properties and Reynolds numbers and by radial as well as circumferential temperature and pressure profiles at the inlet to the component. For highly accurate performance predictions these rig-to-engine effects are taken into account. Traditionally the term 'installation' is also used for describing all the differences in engine operation and behavior between testbed and aircraft. Intake and afterbody drag, power offtake and bleed, as well as intake pressure losses and inlet flow distortion have significant impact on airflow, thrust, specific fuel consumption, and compressor stability. Using modern performance synthesis programs all these effects can be simulated. Author

N92-28466*# Massachusetts Inst. of Tech., Cambridge. Gas Turbine Lab.
DYNAMIC CONTROL OF AERODYNAMIC INSTABILITIES IN GAS TURBINE ENGINES
E. M. Greitzer, A. H. Epstein, G. R. Guenette, D. L. Gysling, J. Haynes, G. J. Hendricks, J. Paduano, J. S. Simon, and L. Valavani *In* AGARD, Steady and Transient Performance Prediction of Gas Turbine Engines May 1992 20 p Sponsored by NASA. Lewis Research Center; AFOSR; ONR; Pratt and Whitney Aircraft; and Army Aviation Systems Command (For primary document see N92-28458 19-07)
Copyright Avail: NTIS HC/MF A09

This lecture discusses the use of closed loop control at the component level to enhance the performance of gas turbine engines. The general theme is the suppression of flow instabilities (rotating stall and surge) through use of feedback, either actively or by means of the aeromechanical coupling provided by tailored structures. The basic concepts that underlie active control of turbomachinery instability, and their experimental demonstration, are first described for a centrifugal compressor. It is shown that the mechanism for stabilization is associated with damping of unsteady perturbations in the compression system, and the steady-state performance can thus remain virtually unaltered. Control of instability using a tailored structure is then discussed, along with experimental results illustrating the flow range extension achievable using this technique. A considerably more complex problem is presented by active control or rotating stall where the multi-dimensional features mean that distributed sensing and actuation are required. In addition, there are basic questions concerning unsteady fluid mechanics; these imply the need to resolve issues connected with identification of suitable signals as well as with definition of appropriate wave launchers for implementing the feedback. These issues are discussed and the results of initial successful demonstrations of active control of rotating stall in a single-stage and a three-stage axial compressor are presented. The lecture concludes with suggestions for future research on dynamic control of gas turbine engines. Author

N92-28467# GasTOPS Ltd., Gloucester (Ontario).
ENGINE PERFORMANCE AND HEALTH MONITORING MODELS USING STEADY STATE AND TRANSIENT PREDICTION METHODS
B. D. MacIsaac *In* AGARD, Steady and Transient Performance Prediction of Gas Turbine Engines May 1992 21 p (For primary document see N92-28458 19-07)
Copyright Avail: NTIS HC/MF A09

The role of computer modelling in the design, development, and validation of a performance monitoring system is discussed. The basic requirements of an engine health monitoring system are discussed in the context of the user environment. A form of model based on stage characteristics provides the basis for describing engine measurements. Faults are modelled in accordance with empirical data obtained from tests conducted at the stage level. The model is used to investigate various parameters that provide unambiguous identification of the fault in question. Fault libraries were developed for field use. Author

N92-28686# Science Applications International Corp., San Antonio, TX. Logistics Technology Div.
TURBINE AIRCRAFT ENGINE OPERATIONAL TRENDING AND JT8D STATIC COMPONENT RELIABILITY STUDY Final Report, 28 Mar. 1990 - 28 Mar. 1991
A. Bruce Richter, Margaret Ridenour-Bender, and Mike Tsao Mar. 1992 74 p
(Contract F04606-89-D-0036)
(DOT/FAA/CT-91/10) Avail: NTIS HC/MF A04

The engine subpanel of the June 1988 International Conference on Aging Airplanes identified the need to study aircraft turbine engine static components for reliability problems resulting from aging effects. This study trended in-flight shutdowns and unscheduled removal rates of JT8D, CF6, and JT3D turbine aircraft engines for the two year period of February 1988 through January 1990. Specific engine components on the JT8D engines of air carriers frequently exceeding the industry norm during the trending period were identified. This review noted the following types of component failures occurring: hard failures, wear and tear/inspection failures, structural failures, diagnostic troubleshooting, and maintenance errors. In addition to specific JT8D engine components being identified, an ultrasonic inspection procedure was developed for the JT8D engine outer combustor case boss. Author

N92-28711# National Aerospace Lab., Amsterdam (Netherlands). Structures and Materials Div.
DIFFUSER CASING UPGRADE FOR AN ADVANCED TURBOFAN
G. A. Kool, R. J. H. Wanhill, and C. E. W. Looije 26 Mar. 1990 14 p Presented at the Conference for Life Assessment and Repair Technology for Combustion Turbine Section Components, Phoenix, AZ, 17-19 Apr. 1990 Prepared in cooperation with Royal Netherlands Air Force, The Hague and Turbine Support Europa, Tilburg, Netherlands
(NLR-TP-90097-U; ETN-92-91531) Avail: NTIS HC/MF A03

A qualification program for upgrade modification and repair of diffuser casings for an advanced turbofan engine type is addressed. The methodology of setting up the program is described and technical aspects are surveyed, paying special attention to critical upgrade/repair items, capability demonstrations, supporting nondestructive inspection and mechanical and metallurgical testing. ESA

N92-28985*# National Aeronautics and Space Administration. Lewis Research Center, Cleveland, OH.
ELECTROMECHANICAL SYSTEMS WITH TRANSIENT HIGH POWER RESPONSE OPERATING FROM A RESONANT AC LINK
Linda M. Burrows and Irving G. Hansen 1992 6 p Proposed for presentation at the 27th Intersociety Energy Conversion Engineering Conference, San Diego, CA, 3-7 Aug. 1992; sponsored by SAE, ACS, AIAA, ASME, IEEE, AIChE, and ANS
(RTOP 906-11-03)
(NASA-TM-105716; E-7113; NAS 1.15:105716) Avail: NTIS HC/MF A02

The combination of an inherently robust asynchronous (induction) electrical machine with the rapid control of energy provided by a high frequency resonant AC link enables the efficient management of higher power levels with greater versatility. This could have a variety of applications from launch vehicles to all-electric automobiles. These types of systems utilize a machine which is operated by independent control of both the voltage and frequency. This is made possible by using an indirect field-oriented control method which allows instantaneous torque control in all four operating quadrants. Incorporating the AC link allows the converter in these systems to switch at the zero crossing of every half cycle of the AC waveform. This zero loss switching of the link allows rapid energy variations to be achieved without the usual

frequency proportional switching loss. Several field-oriented control systems were developed by LeRC and General Dynamics Space Systems Division under contract to NASA. A description of a single motor, electromechanical actuation system is presented. Then, focus is on a conceptual design for an AC electric vehicle. This design incorporates an induction motor/generator together with a flywheel for peak energy storage. System operation and implications along with the associated circuitry are addressed. Such a system would greatly improve all-electric vehicle ranges over the Federal Urban Driving Cycle (FUD). Author

08 AIRCRAFT STABILITY AND CONTROL

Includes aircraft handling qualities; piloting; flight controls; and autopilots.

For related information see also *05 Aircraft Design, Testing and Performance.*

N92-28457*# National Aeronautics and Space Administration. Ames Research Center, Moffett Field, CA.
COMPARISON OF THREE CONTROLLERS APPLIED TO HELICOPTER VIBRATION
Jane A. Leyland May 1992 79 p
(RTOP 505-61-51)
(NASA-TM-102192; A-89130; NAS 1.15:102192) Avail: NTIS HC/MF A05

A comparison was made of the applicability and suitability of the deterministic controller, the cautious controller, and the dual controller for the reduction of helicopter vibration by using higher harmonic blade pitch control. A randomly generated linear plant model was assumed and the performance index was defined to be a quadratic output metric of this linear plant. A computer code, designed to check out and evaluate these controllers, was implemented and used to accomplish this comparison. The effects of random measurement noise, the initial estimate of the plant matrix, and the plant matrix propagation rate were determined for each of the controllers. With few exceptions, the deterministic controller yielded the greatest vibration reduction (as characterized by the quadratic output metric) and operated with the greatest reliability. Theoretical limitations of these controllers were defined and appropriate candidate alternative methods, including one method particularly suitable to the cockpit, were identified. Author

N92-28584*# Systems Technology, Inc., Hawthorne, CA.
EFFECTS OF COCKPIT LATERAL STICK CHARACTERISTICS ON HANDLING QUALITIES AND PILOT DYNAMICS
David G. Mitchell, Bimal L. Aponso, and David H. Klyde Washington NASA Jun. 1992 208 p Prepared for PRC Kentron, Inc., Edwards, CA
(Contracts NAS2-12722; ATD-90-STI-6401; RTOP 505-64-30)
(NASA-CR-4443; H-1769; NAS 1.26:4443) Avail: NTIS HC/MF A10

This report presents the results of analysis of cockpit lateral control feel-system studies. Variations in feel-system natural frequency, damping, and command sensing reference (force and position) were investigated, in combination with variations in the aircraft response characteristics. The primary data for the report were obtained from a flight investigation conducted with a variable-stability airplane, with additional information taken from other flight experiments and ground-based simulations for both airplanes and helicopters . The study consisted of analysis of handling qualities ratings and extraction of open-loop, pilot-vehicle describing functions from sum-of-sines tracking data, including, for a limited subset of these data, the development of pilot models. The study confirms the findings of other investigators that the effects on pilot opinion of cockpit feel-system dynamics are not equivalent to a comparable level of added time delay, and until a more comprehensive set of criteria are developed, it is recommended that feel-system dynamics be considered a delay-inducing element in the aircraft response. The best correlation with time-delay requirements was found when the feel-system dynamics were included in the delay measurements, regardless of the command reference. This is a radical departure from past approaches. Author

N92-28652# National Aerospace Lab., Amsterdam (Netherlands). Flight Div.
SOME LONGITUDINAL HANDLING QUALITIES DESIGN GUIDELINES FOR ACTIVE CONTROL TECHNOLOGY TRANSPORT AIRCRAFT
W. P. deBoer, H. T. Huynh (Office National d'Etudes et de Recherches Aerospatiales, Paris, France), O. P. Nicholas (Royal Aerospace Establishment, Farnborough, England), D. Schafranek (Deutsche Forschungsanstalt fuer Luft- und Raumfahrt, Brunswick, Germany, F.R.), and J. A. J. vanEngelen 11 May 1990 21 p
(NLR-TP-90129-U; GARTEUR/TP-056; ETN-92-91435) Avail: NTIS HC/MF A03

The main conclusions and recommendations from extensive work performed by the Flight Mechanics Action Group on handling qualities (FM/AG01) of the Group for Aeronautical Research and Technology in Europe (GARTEUR) are presented. The work of this AG, which involved cooperation between research institutes of France, Germany, the United Kingdom, and the Netherlands, was performed with the ultimate aim of establishing handling qualities guidelines for future transport aircraft with advanced flight control and display system. The work of the AG started with the consultation of aircraft industries within the participating countries concerning their opinion on anticipated manual control aspects for future transport aircraft. The underlying report may be regarded as the overall result of the work performed on the basis of this consultation, which resulted in a number of handling qualities guidelines. ESA

N92-28653# National Aerospace Lab., Amsterdam (Netherlands). Structures and Materials Div.
RESPONSE OF HELICOPTERS TO GUSTS
R. Noback 27 Apr. 1990 98 p
(Contract RNLAF-RB-KLU-1990/A.5)
(NLR-TP-90159-U; ETN-92-91436) Avail: NTIS HC/MF A05

Equations to describe the response of helicopters to atmospheric gusts are derived. Results of calculations are compared to results as presented in the literature. The influence of various parameters is investigated, especially that of a mass parameter. Special attention is paid to the response to continuous sinusoidal turbulence. ESA

N92-28801# Naval Postgraduate School, Monterey, CA.
STABILITY AND CONTROL FLIGHT TESTING OF A HALF-SCALE PIONEER REMOTELY PILOTED VEHICLE M.S. Thesis
Kent Robert Aitcheson Sep. 1991 74 p
(AD-A245973) Avail: NTIS HC/MF A04

Stability and control flight testing was conducted on a half-scale Pioneer remotely piloted vehicle. The aircraft was instrumented with sensors to measure flight control deflections, angle of attack, side slip angle, and airspeed. A developmental telemetry transmitter was installed to send the information to a ground based receiver where it was recorded for computer processing. Flight tests were conducted to characterize longitudinal static stability by varying the center of gravity to determine the neutral point. Directional static stability was characterized using steady heading side slip flight tests. The telemetry system's performance was acceptable and the directional stability data correlated favorably with data gathered from wind tunnel testing and computational methods. Longitudinal stability was more difficult to characterize due to limitations of elevator deflection resolution and the amount of data gathered. Additional flight testing will be conducted to tune the telemetry system with the data collection sensors, and to increase the Pioneer static stability data base. GRA

09 RESEARCH AND SUPPORT FACILITIES (AIR)

Includes airports, hangars and runways; aircraft repair and overhaul facilities; wind tunnels; shock tubes; and aircraft engine test stands.

For related information see also *14 Ground Support Systems and Facilities (Space).*

N92-28248# Chemical Research and Development Center, Aberdeen Proving Ground, MD.

EXPERIMENTAL AERODYNAMIC FACILITIES OF THE AERODYNAMICS RESEARCH AND CONCEPTS ASSISTANCE BRANCH Final Report, Jan. - Feb. 1992

Miles C. Miller Feb. 1992 28 p

(AD-A247489; CRDEC-TR-309) Avail: NTIS HC/MF A03

This report is intended to acquaint researchers within the Department of Defense and approved U.S. Government contractors with the experimental aerodynamic facilities currently in use at the U.S. Army Chemical Research, Development and Engineering Center. GRA

N92-28388# Arizona Univ., Tucson. Coll. of Engineering and Mines.

EXPAND TURBULENCE LABORATORY FACILITIES TO MEET NEW DOD RESEARCH INTEREST Final Technical Report, 1 Oct. 1986 - 30 Sep. 1991

Frank H. Champagne 6 Mar. 1992 6 p

(Grant AF-AFOSR-0004-87)

(AD-A248581; AFOSR-92-0259TR) Avail: NTIS HC/MF A02

The expansion of our turbulence laboratory facility funded by this DOD-URI award is complete. Two new test sections and a translator have been acquired for our wind tunnel. The new translator is specially designed to permit measurement of three-dimensional wakes with a minimum of blockage. Fortlier, our MASSCOMP 500 series laboratory computer, was PRP upgraded to a 32-bit machine. GRA

N92-28407# Naval Aerospace Medical Research Lab., Pensacola, FL.

USE OF A COMMERCIALLY AVAILABLE FLIGHT SIMULATOR DURING AIRCREW PERFORMANCE TESTING Final Report

Scott A. Shappell and Brady J. Bartosh Nov. 1991 21 p

(AD-A245922; NAMRL-TM-91-2) Avail: NTIS HC/MF A03

Investigations of aircrew sustained operations (SUSOPS) have been criticized for employing tasks with no apparent external validity. Because measures obtained directly from aviators flying high-performance aircraft are difficult to obtain, a laboratory compromise is needed. High-fidelity flight simulators used for aircrew training offer the most realistic simulation, but their availability is limited. Personal computer-based flight simulators may provide adequate simulation in the laboratory at a reasonable cost. This report describes a representative research protocol using a commercially available flight simulator during a simulated aircrew SUSOP. GRA

N92-28579# Technische Univ., Delft (Netherlands). Faculty of Aerospace Engineering.

THE BASIC RESEARCH SIMULATOR PROGRAMME AND THE INDUSTRIAL AND AEROSPACE COMMUNITY: OPPORTUNITIES FOR COOPERATIVE RESEARCH

S. K. Advani Oct. 1991 69 p

(LR-662; ETN-92-91401) Avail: NTIS HC/MF A04

The configuration of the basic research simulator and the proposed applications of the facility are outlined. The benefits to industry of the simulator are: the dynamic behavior and control of motion platforms; the performance of vehicle simulations in a ground based environment; and the human factors of vehicle operation. The dynamic behavior of a motion platform can be improved by minimizing the mass of the moving components and by placing the center of gravity in a low vertical location. In practice, metal fiber laminates (hybrid materials) will form the primary structure of the basic research simulator in order to minimize its weight. To lower the center of gravity, the cockpit floor will be attached beneath the primary load bearing frame of the moving platforms and below its gimbals. Further improvements to the dynamic properties will be achieved through the application of multivariable control techniques to drive the six degrees of freedom motion system. A motion system with favorable dynamic properties can serve as an ideal tool for conducting basic research in vehicle simulation and in human factors: motion signal noise and parasitic displacements on the nondriven directions can be virtually cancelled by proper design and control techniques. The provision for flexible cockpit and instrument arrangements supports research into instrument display formats. ESA

N92-28661# National Aerospace Lab., Amsterdam (Netherlands). Aerodynamics Div.

THE WINDTUNNEL AS A TOOL FOR LAMINAR FLOW RESEARCH

A. Elsenaar 8 May 1990 17 p Presented at 17th ICAS Congress, Stockholm, Sweden, 9-14 Sep. 1990 Previously announced in IAA as A91-24324 Sponsored in part by Netherlands Agency for Aerospace Programs

(NLR-TP-90145-U; ETN-92-91536) Avail: NTIS HC/MF A03

Testing laminar airfoils or wings in the wind tunnel entails some specific experimental problems. These problems are discussed using the (limited) experience of laminar flow tests made in a high speed wind tunnel. Special measurement techniques like infrared imaging for transition detection and fast continuous wake rake traverses, are required for detailed drag assessment. Premature transition due to contamination of the airfoil surface appears to be a problem. The transition location in flight is unlikely to be duplicated in the wind tunnel due to flow quality and Reynolds number differences. Therefore a methodology to extrapolate the wind tunnel test result to flight conditions is discussed. ESA

N92-28669# National Aerospace Lab., Amsterdam (Netherlands). Fluid Dynamics Div.

INSTRUMENTATION REQUIREMENTS FOR LAMINAR FLOW RESEARCH IN THE NLR HIGH SPEED WIND TUNNEL HST

A. Elsenaar, P. B. Rohne, D. Rozendal, and R. Poestkoke 8 May 1989 14 p Presented at the 13th International Congress on Instrumentation in Aerospace Simulation Facilities, Goettingen, Fed. Republic of Germany, 18-21 Sep. 1989 Previously announced in IAA as A90-28283

(NLR-TP-89158-U; ETN-92-91520) Avail: NTIS HC/MF A03

The testing of laminar flow airfoils and wings in wind tunnels imposes very stringent requirements on the wind tunnel and the measurement techniques. Starting from experience obtained in high speed tunnels, typical aspects like scale effects, flow quality and model contamination are discussed. Different techniques of transition detection are revised, and the infrared technique in combination with continuous wake rake traverses is concluded to provide the best opportunities for a detailed experimental analysis of a particular laminar flow design. ESA

N92-28673*# National Aeronautics and Space Administration. Lewis Research Center, Cleveland, OH.

FLOW QUALITY STUDIES OF THE NASA LEWIS RESEARCH CENTER 8- BY 6-FOOT SUPERSONIC/9- BY 15-FOOT LOW SPEED WIND TUNNEL

E. Allen Arrington and Mark T. Pickett Jul. 1992 47 p Presented at the 17th Aerospace Ground Testing Conference, Nashville, TN, 6-8 Jul. 1992; sponsored in part by AIAA

(Contract NAS3-25266; RTOP 505-62-84)

(NASA-TM-105417; E-6827; NAS 1.15:105417; AIAA Paper 92-3916) Avail: NTIS HC/MF A03

A series of studies were conducted to determine the existing flow quality in the NASA Lewis 8 by 6 Foot Supersonic/9 by 15 Foot Low speed Wind Tunnel. The information gathered from these studies was used to determine the types and designs of flow manipulators which can be installed to improve overall tunnel flow quality and efficiency. Such manipulators include honeycomb flow straighteners, turbulence reduction screens, corner turning vanes, and acoustic treatments. The types of measurements,

instrumentation, and results obtained from experiments conducted at several locations throughout the tunnel loop are described.
Author

N92-28772# Wright Lab., Wright-Patterson AFB, OH.
A METHODOLOGY FOR THE EVALUATION OF RUNWAY ROUGHNESS FOR REPAIR
John T. Riechers Sep. 1991 39 p
(AD-A250407; WL-TM-02-307-FIBE) Avail: NTIS HC/MF A03

The Structural Integrity Branch has supported the evaluation of aircraft response to ground induced loadings through modeling since the 1970's. A methodology for the use of these modeling techniques to evaluate a runway for roughness, and to rate the prospective repairs by effectiveness is presented. This information can be used by local civil engineering to determine the extent of repairs required, and if these repairs can be accomplished under general maintenance funds allocations, or if a major construction request is necessary. GRA

N92-28828 Physics and Electronics Lab. TNO, The Hague (Netherlands).
EVALUATION OF DRIVE SIMULATOR SETTINGS FOR DAF YA-4440 Final Report [EVALUATIE RIJSIMULATOR-INSTELLINGEN VOOR DE DAF YA-4440]
T. M. Dokoupil Oct. 1991 23 p In NEPALI
(Contract A81KL131)
(FEL-91-B345; TD91-3887; ETN-92-91228) Copyright Avail: TNO Physics and Electronics Lab., P.O. Box 96864, 2509 JG The Hague, Netherlands

The algorithm developed to determine the so called k-factors for the simulation of the vehicle DAF YA-4440 was evaluated. For the drive simulation of a vehicle on the universal dynamometer bench, k-factors corresponding to friction coefficients of the vehicle were determined. The k-factor settings determined by using the estimation algorithm agree well with road measurements and simulator measurements. The corrections applied to the algorithm results are satisfactory for the DAF YA-4440, but it cannot be guaranteed that they are generally satisfactory for drive simulations. ESA

N92-28829# National Aerospace Lab., Tokyo (Japan). Aeroengine Div.
AIR EJECTOR EXPERIMENTS USING THE TWO-DIMENSIONAL SUPERSONIC CASCADE TUNNEL: ZERO SECONDARY FLOW PERFORMANCE Report No. 1
Susumu Takamori and Hajime Sakaguchi Feb. 1991 19 p In JAPANESE
(NAL-TM-632; ISSN-0452-2982; JTN-92-80350) Avail: NTIS HC/MF A03

The air ejector has almost limitless application possibilities in engineering practice due to its simplicity. To determine the feasibility of using an ejector as a suction pump for boundary layer air removal in the two dimensional supersonic cascade tunnel, especially when a portion of the tunnel's air supply is used for its primary flow, both subsonic and supersonic air ejector tests were conducted. The tested ejector was axially symmetrical and a center jet type, with its geometrical configuration being varied, i.e., the primary nozzle to mixing tube throat area ratio, and the straight mixing space (mixing tube) and diverging passage section (diffuser) lengths. These configuration changes enabled geometrical effects on ejector performance to be obtained. The following experimental results using a zero secondary flow air ejector are discussed: (1) the effects of the straight mixing and diverging passage section lengths on the relationship between secondary pressure (secondary vacuum chamber pressure) and primary stagnation pressure (primary pressure characteristics) during a zero secondary flow condition; (2) the effect of throat area ratio of primary nozzle to mixing tube on primary pressure characteristics; (3) the relationship between the minimum secondary pressure and throat area ratio; (4) the optimal operating conditions for a zero secondary flow subsonic ejector; and (5) the effect of primary Mach numbers on a zero secondary flow supersonic ejector performance.
Author (NASDA)

N92-28833# National Aerospace Lab., Tokyo (Japan). Advanced Aircraft Research Group.
UPGRADING THE DATA PROCESSING SECTION OF THE NAL GUST WIND TUNNEL DATA PROCESSING SYSTEM
Akihito Iwasaki, Toshimi Fujita, and Hirotoshi Fujieda May 1991 22 p In JAPANESE
(NAL-TM-635; ISSN-0452-2982; JTN-92-80352) Avail: NTIS HC/MF A03

The data processing system in NAL Gust Wind Tunnel is composed of data acquisition and data processing sections. The outline of the system used to upgrade the data processing section and secondary date processing for wind tunnel data are described. The new system includes an Eclipse MV/7800XP CPU, six megabytes of memory, and various peripheral devices. Performance enhancements were obtained using this upgrade.
Author (NASDA)

N92-28835# National Aerospace Lab., Tokyo (Japan). Aircraft Aerodynamics Div.
REPLACEMENT OF THE NAL HIGH PRESSURE AIR STORAGE SYSTEM
Shigeo Baba, Hisashi Suenaga, Masamitu Suzuki, and Nobuhiro Toda Mar. 1991 31 p In JAPANESE
(NAL-TM-634; ISSN-0452-2982; JTN-92-80362) Avail: NTIS HC/MF A03

The replacement process is described for the high pressure air storage vessel attached to the 2 m x 2 m Transonic Wind Tunnel of the NAL. The oldest two of three existing 10 m diameter vessel were dismantled and replaced by a new 13 m diameter vessel, thereby preserving the total capacity. Both the operational and maintenance histories of the old vessel are discussed, as well as the design construction features included in the new one, its initial test results, and the important issues related to future system operations. Author (NASDA)

N92-28975# Merit Technology, Inc., Plano, TX.
AIR COMBAT MANEUVERING EXPERT SYSTEM TRAINER Final Report, Jul. 1988 - Dec. 1991
Robert J. Bechtel Jan. 1992 40 p
(Contract F33615-88-C-0011)
(AD-A246459; AL-TP-1991-0058) Avail: NTIS HC/MF A03

Models of decision making can be useful in a number of applications. Building, validating, and creating the uses for such models is usually a significant undertaking for any domain of interesting size. The Air Combat Maneuvering Expert System Trainer (ACMEST) Project used knowledge acquisition techniques developed in artificial intelligence to construct models of pilot tactical decision making, and to implement those models as rule-based inference system. The model implementations were then used in a man-in-the-loop simulation environment to teach air combat maneuvering. The resulting system serves as a proof-of-concept demonstrator, but must have greater flexibility in knowledge representation, validated models, and improvements in display capability to become useful in operational training. GRA

N92-29204# National Aerospace Lab., Amsterdam (Netherlands). Flight Div.
NARSIM: A REAL-TIME SIMULATOR FOR AIR TRAFFIC CONTROL RESEARCH
W. denBraven and J. M. tenHave 25 May 1990 58 p Submitted for publication
(NLR-TP-90147-U; ETN-92-91537) Avail: NTIS HC/MF A04

The lack of capacity and efficiency in the present day air transportation system is noted. Developments towards a future integrated Air Traffic Management (ATM) system were initiated in order to reduce these deficiencies. Real time Air Traffic Control (ATC) simulators, such as the NLR ATC Research Simulator (NARSIM), will play an essential role in the research on this future ATC, thus describing the area of interest for ATC research simulation. NARSIM is described. Its functions are characterized, followed by a description of the air traffic controller's work environment, the hardware configuration, and the controller

workstations. An introduction to NARSIM's main research areas, which are integrated ATM and the man machine interface, is given. ESA

N92-28523# Federal Ministry for Defence, Bonn (Germany, F.R.). Armaments Technology Directorate.
OPPORTUNITIES FOR FLIGHT SIMULATION TO IMPROVE OPERATIONAL EFFECTIVENESS
J. Heyden *In* AGARD, Piloted Simulation Effectiveness Feb. 1992 15 p (For primary document see N92-28522 19-01)
Copyright Avail: NTIS HC/MF A15

N92-28524# Wright Lab., Wright-Patterson AFB, OH. Flight Dynamics Directorate.
PILOTED SIMULATION EFFECTIVENESS DEVELOPMENT APPLICATIONS AND LIMITATIONS
Richard A. Borowski *In* AGARD, Piloted Simulation Effectiveness Feb. 1992 3 p (For primary document see N92-28522 19-01)
Copyright Avail: NTIS HC/MF A15

N92-28525# Air Force Flight Test Center, Edwards AFB, CA.
UTILITY OF GROUND SIMULATION IN FLIGHT CONTROL PROBLEM IDENTIFICATION, SOLUTION DEVELOPMENT, AND VERIFICATION
K. L. Keller, D. B. Janzen, and A. A. Asay *In* AGARD, Piloted Simulation Effectiveness Feb. 1992 8 p (For primary document see N92-28522 19-01)
Copyright Avail: NTIS HC/MF A15

N92-28526# Aerospatiale, Toulouse (France).
FLIGHT SIMULATION AND DIGITAL FLIGHT CONTROLS
D. Chatrenet *In* AGARD, Piloted Simulation Effectiveness Feb. 1992 4 p (For primary document see N92-28522 19-01)
Copyright Avail: NTIS HC/MF A15

N92-28527# McDonnell-Douglas Helicopter Co., Mesa, AZ. Flight Mechanics/Performance Dept.
THE APPLICATION OF FLIGHT SIMULATION MODELS IN SUPPORT OF ROTORCRAFT DESIGN AND DEVELOPMENT
P. Shanthakumaran *In* AGARD, Piloted Simulation Effectiveness Feb. 1992 28 p (For primary document see N92-28522 19-01)
Copyright Avail: NTIS HC/MF A15

N92-28528# Messerschmitt-Boelkow-Blohm G.m.b.H., Munich (Germany, F.R.). Helicopter Div.
EXPERIENCE WITH PILOTED SIMULATION IN THE DEVELOPMENT OF HELICOPTERS
M. Obermayer, K. Kampa, W. Doehnel, and A. Faulkner *In* AGARD, Piloted Simulation Effectiveness Feb. 1992 11 p (For primary document see N92-28522 19-01)
Copyright Avail: NTIS HC/MF A15

N92-28532# National Aerospace Lab., Amsterdam (Netherlands).
AIRCRAFT SIMULATION AND PILOT PROFICIENCY: FROM SURROGATE FLYING TOWARDS EFFECTIVE TRAINING
P. G. A. M. Jorna, E. R. A. vanKleef (Royal Netherlands Air Force, The Hague.), and W. P. deBoer *In* AGARD, Piloted Simulation Effectiveness Feb. 1992 8 p (For primary document see N92-28522 19-01)
Copyright Avail: NTIS HC/MF A15

N92-28533# CAE Electronics Ltd., Montreal (Quebec). Tactical Systems Div.
THE USE OF A DEDICATED TESTBED TO EVALUATE SIMULATOR TRAINING EFFECTIVENESS
David Kurts and Charles Gainer (Army Research Inst. Aviation Research and Development Activity, Fort Rucker, AL.) *In* AGARD, Piloted Simulation Effectiveness Feb. 1992 9 p (For primary document see N92-28522 19-01)
Copyright Avail: NTIS HC/MF A15

N92-28535# Air Force Flight Test Center, Edwards AFB, CA. Test and Evaluation Simulator.
USE OF SIMULATION IN THE USAF TEST PILOT SCHOOL CURRICULUM
Daniel P. Ringenbach, Steven E. Louton (NSI Technology Services Corp., Research Triangle Park, NC.), and Daniel Gleason *In* AGARD, Piloted Simulation Effectiveness Feb. 1992 7 p (For primary document see N92-28522 19-01)
Copyright Avail: NTIS HC/MF A15

N92-28536# Alenia, Torino (Italy). Flight Simulation Center.
AM-X FLIGHT SIMULATOR FROM ENGINEERING TOOL TO TRAINING DEVICE
A. Armando, P. Castoldi, and F. Fassi *In* AGARD, Piloted Simulation Effectiveness Feb. 1992 12 p (For primary document see N92-28522 19-01)
Copyright Avail: NTIS HC/MF A15

N92-28537# Sikorsky Aircraft, Stratford, CT.
FULL MISSION SIMULATION: A VIEW INTO THE FUTURE
Michael J. Ferranti and Stephen H. Silder, Jr. *In* AGARD, Piloted Simulation Effectiveness Feb. 1992 10 p (For primary document see N92-28522 19-01)
Copyright Avail: NTIS HC/MF A15

N92-28538# Wright Lab., Wright-Patterson AFB, OH.
FULL MISSION SIMULATION FOR RESEARCH AND DEVELOPMENT OF AIR COMBAT FLIGHT AND ATTACK MANAGEMENT SYSTEMS
Daniel G. Goddard and James M. Zeh *In* AGARD, Piloted Simulation Effectiveness Feb. 1992 13 p (For primary document see N92-28522 19-01)
Copyright Avail: NTIS HC/MF A15

N92-28539# CAE Electronics Ltd., Saint Laurent (Quebec).
THE EVALUATION OF SIMULATOR EFFECTIVENESS FOR THE TRAINING OF HIGH SPEED, LOW LEVEL, TACTICAL FLIGHT OPERATIONS
Andrew Morris and Paul E. VanHemel (CAE-Link Corp., Alexandria, VA.) *In* AGARD, Piloted Simulation Effectiveness Feb. 1992 11 p (For primary document see N92-28522 19-01)
Copyright Avail: NTIS HC/MF A15

N92-28540# Ministry of Defence, London (England).
HARRIER GR MK 5/7 MISSION SIMULATORS FOR THE ROYAL AIR FORCE
B. R. Clifford and P. Jackson (Link-Miles, Lancing, England) *In* AGARD, Piloted Simulation Effectiveness Feb. 1992 6 p (For primary document see N92-28522 19-01)
Copyright Avail: NTIS HC/MF A15

N92-28541# Messerschmitt-Boelkow-Blohm G.m.b.H., Ottobrunn (Germany, F.R.).
DEVELOPMENT AND EVALUATION OF AN ATTACK AND MANEUVERING SYSTEM WITH COMBAT DEVELOPMENT SIMULATORS AS MAIN DEVELOPMENT TOOL
Herbert Eibl, Hans-Guenter Offenbeck, and Hans W. Pongratz *In* AGARD, Piloted Simulation Effectiveness Feb. 1992 17 p (For primary document see N92-28522 19-01)
Copyright Avail: NTIS HC/MF A15

N92-28542# Naval Air Test Center, Patuxent River, MD. Rotary Wing Aircraft Test Directorate.
SHIPBOARD MISSION TRAINING EFFECTIVENESS OF THE NAVAL AIR TEST CENTER'S V-22 GOVERNMENT TEST PILOT TRAINER
G. Vandervliet, C. Miller, and P. Croisetiere *In* AGARD, Piloted Simulation Effectiveness Feb. 1992 12 p (For primary document see N92-28522 19-01)
Copyright Avail: NTIS HC/MF A15

N92-28543# Office National d'Etudes et de Recherches Aerospatiales, Paris (France).
USE OF A RESEARCH SIMULATOR FOR THE DEVELOPMENT OF NEW CONCEPTS OF FLIGHT CONTROL [UTILISATION D'UN SIMULATEUR DE RECHERCHE POUR LE DEVELOPPEMENT DE NOUVEAUX CONCEPTS DE COMMANDES DE VOL]
Ph. Guicheteau *In* AGARD, Piloted Simulation Effectiveness Feb. 1992 11 p In FRENCH; ENGLISH summary (For primary document see N92-28522 19-01)
Copyright Avail: NTIS HC/MF A15

N92-28544# Dassault-Breguet Aviation, Saint Cloud (France).
THE ROLE OF SIMULATION FOR THE STUDY OF APIS (PILOTING SUPPORT BY SYNTHETIC IMAGERY) [LE ROLE DE LA SIMULATION POUR L'ETUDE APIS (AIDE AU PILOTAGE PAR IMAGERIE SYNTHETIQUE)]
Pierre Larroque, Pierre Pagniez, and Roland Miginiac *In* AGARD, Piloted Simulation Effectiveness Feb. 1992 12 p In FRENCH (For primary document see N92-28522 19-01)
Copyright Avail: NTIS HC/MF A15

N92-28545*# Systems Technology, Inc., Hawthorne, CA.
THE USE OF GROUND BASED SIMULATION FOR HANDLING QUALITIES RESEARCH: A NEW ASSESSMENT
David G. Mitchell, Roger H. Hoh (Hoh Aeronautics, Inc., Lomita, CA.), Adolph Atencio, Jr. (Army Aviation Systems Command, Moffett Field, CA.), and David L. Key (Army Aviation Systems Command, Moffett Field, CA.) *In* AGARD, Piloted Simulation Effectiveness Feb. 1992 14 p (For primary document see N92-28522 19-01)
(Contract NAS2-13127)
Copyright Avail: NTIS HC/MF A15

N92-28546# Defence Research Agency, Bedford (England). Flight Systems Dept.
INITIAL VALIDATION OF A R/D SIMULATOR WITH LARGE AMPLITUDE MOTION
A. D. White, J. R. Hall, and B. N. Tomlinson *In* AGARD, Piloted Simulation Effectiveness Feb. 1992 24 p (For primary document see N92-28522 19-01)
Copyright Avail: NTIS HC/MF A15

N92-28547# Deutsche Airbus G.m.b.H., Hamburg (Germany, F.R.).
USE OF A VIRTUAL COCKPIT FOR THE DEVELOPMENT OF A FUTURE TRANSPORT AIRCRAFT
Dieter Kricke and Wilfried Quellmann *In* AGARD, Piloted Simulation Effectiveness Feb. 1992 10 p Sponsored in part by BMFT and Council of the European Community (For primary document see N92-28522 19-01)
Copyright Avail: NTIS HC/MF A15

N92-28548# Deutsche Forschungsanstalt fuer Luft- und Raumfahrt, Brunswick (Germany, F.R.). Inst. fuer Flugmechanik.
THE ROLE OF SYSTEMS SIMULATION FOR THE DEVELOPMENT AND QUALIFICATION OF ATTAS
D. Hanke, H.-H. Lange, and P. Saager *In* AGARD, Piloted Simulation Effectiveness Feb. 1992 11 p (For primary document see N92-28522 19-01)
Copyright Avail: NTIS HC/MF A15

N92-28549# Douglas Aircraft Co., Inc., Long Beach, CA.
THE USE AND EFFECTIVENESS OF PILOTED SIMULATION IN TRANSPORT AIRCRAFT RESEARCH AND DEVELOPMENT
J. Hodgkinson, K. F. Rossitto, and E. R. Kendall *In* AGARD, Piloted Simulation Effectiveness Feb. 1992 8 p (For primary document see N92-28522 19-01)
Copyright Avail: NTIS HC/MF A15

N92-28550# Toronto Univ., Downsview (Ontario). Inst. for Aerospace Studies.
AN EVALUATION OF IFR APPROACH TECHNIQUES: GENERIC HELICOPTER SIMULATION COMPARED WITH ACTUAL FLIGHT
L. D. Reid, S. Advani, and J. H. deLeeuw *In* AGARD, Piloted Simulation Effectiveness Feb. 1992 18 p (For primary document see N92-28522 19-01)
(Contract W2207-7-AF69/01-SS)
Copyright Avail: NTIS HC/MF A15

N92-28551*# National Aeronautics and Space Administration. Langley Research Center, Hampton, VA.
APPLICATION OF PILOTED SIMULATION TO HIGH-ANGLE-OF-ATTACK FLIGHT-DYNAMICS RESEARCH FOR FIGHTER AIRCRAFT
Marilyn E. Ogburn, John V. Foster, and Keith D. Hoffler (Vigyan Research Associates, Inc., Hampton, VA.) *In* AGARD, Piloted Simulation Effectiveness Feb. 1992 16 p (For primary document see N92-28522 19-01)
Copyright Avail: NTIS HC/MF A15

N92-28552# British Aerospace Public Ltd. Co., Lancashire (England). Military Aircraft Div.
EFFECTIVE CUEING DURING APPROACH AND TOUCHDOWN: COMPARISON WITH FLIGHT
Peter Beckett *In* AGARD, Piloted Simulation Effectiveness Feb. 1992 11 p (For primary document see N92-28522 19-01)
Copyright Avail: NTIS HC/MF A15

12 ASTRONAUTICS (GENERAL)

For extraterrestrial exploration see *91 Lunar and Planetary Exploration.*

N92-28406# General Accounting Office, Washington, DC. Information Management and Technology Div.
SPACE STATION: DELAYS IN DEALING WITH SPACE DEBRIS MAY REDUCE SAFETY AND INCREASE COSTS
2 Jun. 1992 21 p
(GAO/IMTEC-92-50; B-237832) Avail: NTIS HC/MF A03; also available from GAO, PO Box 6015, Gaithersburg, MD 20877 HC first copy free, additional copies $2.00

The majority of NASA's current designs for protecting the space station and crew from debris are outdated and its overall debris protection strategy is insufficient. NASA's contractors have designed the station using a 1984 model of the space environment that is obsolete, significantly underestimating the increasing amount of debris that the station will encounter during its 30-year lifetime. In February 1992, NASA directed its space centers to incorporate an updated 1991 model into their designs. However, the agency has not yet made critical decisions on how to implement this change. Preliminary evaluations show that incorporating the 1991 model using currently established safety criteria could entail a major redesign of some components, with significant cost impact and schedule delays. NASA's overall protection strategy for space debris is insufficient. While NASA has concentrated its protection on shielding the space station from small debris and plans to augment this initial shielding in orbit, it has not yet developed designs or studied the cost and operational impact of augmenting its protection with additional shielding. Further, current designs do not provide the capability of warning or protecting the crew from imminent collision with mid-size debris. Finally, although some capabilities exist for maneuvering the station away from large debris, the agency lacks collision-avoidance plans and debris-tracking equipment. In developing a comprehensive strategy to protect the station from the more severe debris environment, NASA cannot avoid some difficult decisions. These decisions involve tradeoffs between how much the agency is willing to pay to protect the station, the schedule delays it may incur, and the risk to station safety it is willing to accept. It is important that these decisions be made before NASA completes its critical design

reviews in early 1993. At that time key designs will be made final and manufacturing will begin. Without a comprehensive strategy, NASA will have decided to build the station, knowing the consequences of this decision on station and crew safety, and on life-cycle station cost. Author

N92-29100*# Office of Space Science and Applications, Washington, DC. Life Sciences Div.
SPACE LIFE SCIENCES STRATEGIC PLAN
Arnauld E. Nicogossian 1992 60 p
(NASA-TM-107954; NAS 1.15:107954) Avail: NTIS HC/MF A04

Over the last three decades the Life Sciences Program has significantly contributed to NASA's manned and unmanned exploration of space, while acquiring new knowledge in the fields of space biology and medicine. The national and international events which have led to the development and revision of NASA strategy will significantly affect the future of life sciences programs both in scope and pace. This document serves as the basis for synthesizing the options to be pursued during the next decade, based on the decisions, evolution, and guiding principles of the National Space Policy. The strategies detailed in this document are fully supportive of the Life Sciences Advisory Subcommittee's 'A Rationale for the Life Sciences,' and the recent Aerospace Medicine Advisory Committee report entitled 'Strategic Considerations for Support of Humans in Space and Moon/Mars Exploration Missions.' Information contained within this document is intended for internal NASA planning and is subject to policy decisions and direction, and to budgets allocated to NASA's Life Sciences Program. Author

N92-28731*# North Carolina State Univ., Raleigh.
REVIEW OF MARS MISSION SCENARIOS
Gerald Walberg *In* NASA. Langley Research Center, Ongoing Progress in Spacecraft Controls Jul. 1992 p 1-11 (For primary document see N92-28730 19-18)
Avail: NTIS HC/MF A07

13 ASTRODYNAMICS

Includes powered and free-flight trajectories; and orbital and launching dynamics.

N92-28937# RADEX, Inc., Bedford, MA.
COORDINATE SYSTEMS FOR SPACE AND GEOPHYSICAL APPLICATIONS Scientific Report No. 9
K. H. Bhavnani and R. P. Vancour 11 Dec. 1991 76 p
(Contract F19628-89-C-0068)
(AD-A247550; AD-E200896; RXR-91121; PL-TR-91-2296) Avail: NTIS HC/MF A05

Many coordinate systems used at Phillips Laboratory for space and geophysical applications are described. This document describes astronomical, orbital, and geomagnetic systems, and special emphasis is given to magnetospheric coordinates in which radiation belt particle investigations may be made. An extensive list of terms and abbreviations is included. These coordinate systems are identified by their origins and the primary and secondary reference axes, which allows them to be systematically compared, categorized and diagrammed. Angle coordinate systems for defining attitude are intimately related, and are also covered. Transformation matrices are provided for several systems, for conversion from one coordinate system into another. GRA

14 GROUND SUPPORT SYSTEMS AND FACILITIES (SPACE)

Includes launch complexes, research and production facilities; ground support equipment, e.g., mobile transporters; and simulators.

For related information see also *09 Research and Support Facilities (Air).*

N92-28343*# National Aeronautics and Space Administration. Goddard Space Flight Center, Greenbelt, MD.
MODELING RADIATION FORCES ACTING ON TOPEX/POSEIDON FOR PRECISION ORBIT DETERMINATION
J. A. Marshall, S. B. Luthcke (Hughes STX, Inc., Lanham, MD.), P. G. Antreasian (Colorado Univ., Boulder.), and G. W. Rosborough (Colorado Univ., Boulder.) Jun. 1992 78 p
(NASA-TM-104564; Rept-92B00089; NAS 1.15:104564) Avail: NTIS HC/MF A05

Geodetic satellites such as GEOSAT, SPOT, ERS-1, and TOPEX/Poseidon require accurate orbital computations to support the scientific data they collect. Until recently, gravity field mismodeling was the major source of error in precise orbit definition. However, albedo and infrared re-radiation, and spacecraft thermal imbalances produce in combination no more than a 6-cm radial root-mean-square (RMS) error over a 10-day period. This requires the development of nonconservative force models that take the satellite's complex geometry, attitude, and surface properties into account. For TOPEX/Poseidon, a 'box-wing' satellite form was investigated that models the satellite as a combination of flat plates arranged in a box shape with a connected solar array. The nonconservative forces acting on each of the eight surfaces are computed independently, yielding vector accelerations which are summed to compute the total aggregate effect on the satellite center-of-mass. In order to test the validity of this concept, 'micro-models' based on finite element analysis of TOPEX/Poseidon were used to generate acceleration histories in a wide variety of orbit orientations. These profiles are then compared to the box-wing model. The results of these simulations and their implication on the ability to precisely model the TOPEX/Poseidon orbit are discussed. Author

N92-29098# Israel Aircraft Industries Ltd., Lod. MBT Systems and Space Technology.
VERIFICATION OF SATELLITE EGSE TEST-SOFTWARE USING AN APPLICATION GENERATOR
Avi Gutmanovitz and Zohar Yarchi 24 Oct. 1990 9 p
(ITN-92-85131) Avail: NTIS HC/MF A02

Electrical Ground Support Equipment (EGSE) is used to perform checkout and testing procedures during the integration and testing of satellite sub-systems. The EGSE is a computer-based system that implements the concepts and standards of satellite integration and testing. The verification of spacecraft software is a well covered subject area. Less literature is available concerning the Acceptance Test Procedure (ATP) to be performed on the EGSE data-base itself. This paper poses the problem of EGSE data-base and special software verification and suggests a solution implemented in the Offeq program. Author

15 LAUNCH VEHICLES AND SPACE VEHICLES

Includes boosters; operating problems of launch/space vehicle systems; and reusable vehicles.

For related information see also *20 Spacecraft Propulsion and Power.*

N92-28226# Sandia National Labs., Albuquerque, NM.
A COILGUN DESIGN PRIMER
B. Marder 1991 12 p Presented at the 6th Symposium on Electromagnetic Launch Technology, Austin, TX, 28-30 Apr. 1992
(Contract DE-AC04-76DP-00789)

(DE92-011149; SAND-91-2155C; CONF-9204102-3) Avail: NTIS HC/MF A03

How an induction coilgun works is explained, and the factors which go into its design are presented. Our purpose is to obtain algebraic expressions which, although crude, provide useful predictors of behavior, illustrate the dependence on various parameters, and suggest ways to optimize the design. Detailed prediction of the gun's behavior can be obtained from simulation codes, such as SLINGSHOT. DOE

N92-28254# Air Force Inst. of Tech., Wright-Patterson AFB, OH. School of Systems and Logistics.

A COST-BENEFIT ANALYSIS ON THE DELETION OF THE INERTIAL UPPER STAGE FACTORY ACCEPTANCE TESTING VERSUS A DECREASE IN MISSION RELIABILITY M.S. Thesis

Michael H. Horn Sep. 1991 82 p

(AD-A246620) Avail: NTIS HC/MF A05

This study investigated the benefits attributable to deleting the factory acceptance testing for the Inertial Upper Stage (IUS) space booster and the possible impacts on mission reliability. A review of the literature revealed limited research on the advantages or disadvantages of performing acceptance testing on commercial programs. However, a review of DoD policy recognized the advantages of cost and time savings when developmental and operational tests are combined. An analysis was performed on the anomalies that occurred during the acceptance testing for the vehicles involved in this study to determine whether all hardware defects would be detected by a later phase of testing. The research suggested that only two chance failures would be undetected by flight testing resulting in a decrease in reliability of .03 percent and a savings of $646,500 per IUS vehicle if acceptance testing was eliminated. The study concluded that current reliability could be maintained by additional flight testing but further research was necessary before a modification to the program could be implemented. GRA

N92-28861# Sandia National Labs., Albuquerque, NM.

A MOMENTUM LIMIT FOR ELECTROMAGNETIC RAILGUNS

M. Cowan 1991 6 p Presented at the 6th Symposium on Electromagnetic Launch Technology, Austin, TX, 28-30 Apr. 1992

(Contract DE-AC04-76DP-00789)

(DE92-011380; SAND-91-2285C; CONF-9204102-6) Avail: NTIS HC/MF A02

We postulate that there is a required velocity of magnetic flux into a plasma-armature railgun to keep the armature from expanding toward the breech and thereby changing the nature of the forward-going force. Testing this idea with data from several guns we find confirmation, provided the required flux velocity increases with the square of the linear current density. This leads to the conclusion that these guns have a momentum limit while they are operating as true electromagnetic launchers. That limit is derived. High-performance railguns reach this limit during current rise, and most of their momentum comes from a hybrid phase. The hybrid phase has a pressure limitation at high velocity similar to electrothermal, light-gas, and powder guns. The 6 km/s 'velocity limit' is explained by this pressure limitation. DOE

N92-29102# Sandia National Labs., Albuquerque, NM.

SPACE APPLICATIONS FOR CONTACTLESS COILGUNS

R. J. Lipinski, S. Beard, J. Boyes, E. C. Cnare, M. Cowan, B. W. Duggin, R. J. Kaye, R. M. Morgan, D. Outka, and D. Potter et al 1992 4 p Presented at the 6th Symposium on Electromagnetic Launch Technology, Austin, TX, 28-30 Apr. 1992

(Contract DE-AC04-76DP-00789)

(DE92-011156; SAND-92-0460C; CONF-9204102-4) Avail: NTIS HC/MF A01

Two space applications are considered for (electrically) contactless coilguns: launch of small satellites into low-earth orbit, and launch of lunar liquid oxygen (LLOX) from the moon to the stationary Lagrangian point L2. For the earth-to-orbit (ETO) application, the baseline conceptual design consists of a 960-m long gun sited in a tunnel at 25 degrees inclination. The gun launches an 1820-kg package that includes a 100-kg satellite and a 650-kg boost rocket for orbital insertion. For the lunar application, the launcher is 200 m long. A 100-kg load of LLOX is packaged in a 10-kg fiber-wrapped tank, accelerated at 2 kgees in an aluminum bucket (armature), and launched at 2.33 km/s at 30-minute intervals. The canisters arrive at L2 2.97 days later and are captured by robotic tugs that deliver them to a fuel depot. The total mass of LLOX derived per year is 867 Mg (metric tons). DOE

N92-29104*# National Aeronautics and Space Administration. Ames Research Center, Moffett Field, CA.

PERFORMANCE OF UNCOATED AFRSI BLANKETS DURING MULTIPLE SPACE SHUTTLE FLIGHTS

Paul M. Sawko and Howard E. Goldstein Apr. 1992 36 p

(RTOP 506-43-31)

(NASA-TM-103892; A-91237; NAS 1.15:103892) Avail: NTIS HC/MF A03

Uncoated Advanced Flexible Reusable Surface Insulation (AFRSI) blankets were successfully flown on seven consecutive flights of the Space Shuttle Orbiter OV-099 (Challenger). In six of the eight locations monitored (forward windshield, forward canopy, mid-fuselage, upper wing, rudder/speed brake, and vertical tail) the AFRSI blankets performed well during the ascent and reentry exposure to the thermal and aeroacoustic environments. Several of the uncoated AFRSI blankets that sustained minor damage, such as fraying or broken threads, could be repaired by sewing or by patching with a surface coating called C-9. The chief reasons for replacing or completely coating a blanket were fabric embrittlement and fabric abrasion caused by wind erosion. This occurred in the orbiter maneuvering system (OMS) pod sidewall and the forward mid-fuselage locations. Author

16 SPACE TRANSPORTATION

Includes passenger and cargo space transportation, e.g., shuttle operations; and space rescue techniques.

For related information see also *03 Air Transportation and Safety* and *18 Spacecraft Design, Testing and Performance.* For space suits see *54 Man/System Technology and Life Support.*

N92-28826# Deutsche Forschungsanstalt fuer Luft- und Raumfahrt, Lampoldshausen (Germany, F.R.). Inst. fuer Chemische Antriebe und Verfahrenstechnik.

EVALUATION OF FUTURE SPACE TRANSPORTATION SYSTEMS WITH REGARD TO THEIR RELIABILITIES AND COSTS Ph.D. Thesis - Technischen Univ. Berlin

Lutz vonEntress-Fuersteneck Jul. 1991 216 p In GEORGIAN

(DLR-FB-91-27; ISSN-0939-2963; ETN-92-91067) Avail: NTIS HC/MF A10; DLR, Wissenschaftliches Berichtswesen, VB-PL-DO, Postfach 90 60 58, 5000 Cologne, Fed. Republic of Germany, HC 74 DM

Functional correlations between feasibility, reliability, and costs of space transportation systems with regard to different expositions are derived and several parametric variations for optimum life cycles are developed. Reliability analysis reveals the existence of experience values, learning factors, and risk relations. Mass and cost analysis show the influence of different exposition factors in modified equations. All these factors are included in a multifunctional software package able to predict the system reliability of any space transportation system over a given number of takeoffs. The software package also calculates the planned costs and the additional costs of failures. ESA

N92-28956# Aerospace Corp., El Segundo, CA.

SPACE TRANSPORTATION ANALYSIS AND DESIGN

R. Hartunian, B. Moss, M. Wolfe, J. Statsinger, and L. Forrest 15 Mar. 1992 118 p

(Contract F04701-88-C-0089)

(AD-A250629; TOR-92(2464)-1) Avail: NTIS HC/MF A06

This TOR is intended to be a living document that will be updated at regular intervals, and will be linked to an ever-increasing

body of easily accessed space transportation corporate knowledge in the form of both paper, magnetic, and intellectual media. This body of knowledge will include reports, computer-based analytical tools, technical databases, and human skills/knowledge databases. It is expected that its growth will be very much influenced by customer demand and the evolving future role of Aerospace in the global space community. Consequently, the table of contents should in no way be assumed to be definitive. GRA

17 SPACE COMM., SPACECRAFT COMM., COMMAND & TRACKING

Includes telemetry; space communications networks; astronavigation and guidance; and radio blackout.

For related information see also *04 Aircraft Communications and Navigation* and *32 Communications and Radar.*

No abstracts in this category.

18 SPACECRAFT DESIGN, TESTING AND PERFORMANCE

Includes satellites; space platforms; space stations; spacecraft systems and components such as thermal and environmental controls; and attitude controls.

For life support systems see *54 Man/System Technology and Life Support.* For related information see also *05 Aircraft Design, Testing and Performance, 39 Structural Mechanics,* and *16 Space Transportation.*

N92-28368# Naval Postgraduate School, Monterey, CA.
PREDICTION OF ATTITUDE STABILITY OF ASYMMETRIC DUAL-SPIN STABILIZED SPACECRAFT USING IMPROVED LIQUID SLOSH MODEL M.S. Thesis
Michael J. Szostak Jun. 1991 51 p
(AD-A247023) Avail: NTIS HC/MF A04

The rigid slug method for modelling sloshing liquid fuel aboard dual-spin stabilized spacecraft has been shown to be inadequate by recent flight data. This rigid slug model and a uniform gravity model put forth by Abramson is examined in detail. The Abramson model is incorporated into a computer simulation written specifically to predict spacecraft attitude. An analysis is performed with both the modified and unmodified versions of this simulation to determine the boundaries of stability for rotor and platform asymmetries. The results show that the improved model is better able to predict spacecraft attitude stability. GRA

N92-28369*# National Aeronautics and Space Administration. Marshall Space Flight Center, Huntsville, AL.
PAYLOAD ISOLATION AND STABILIZATION BY A SUSPENDED EXPERIMENT MOUNT (SEM)
Wayne L. Bailey (Teledyne Brown Engineering, Huntsville, AL.), Carmine E. DeSanctis, Placide D. Nicaise, and David N. Schultz 30 Jun. 1992 23 p
(NASA-TM-107941; NAS 1.15:107941) Avail: NTIS HC/MF A03

Many Space Shuttle and Space Station payloads can benefit from isolation from crew or attitude control system disturbances. Preliminary studies have been performed for a Suspended Experiment Mount (SEM) system that will provide isolation from accelerations and stabilize the viewing direction of a payload. The concept consists of a flexible suspension system and payload-mounted control moment gyros. The suspension system, which is rigidly locked for ascent and descent, isolates the payload from high frequency disturbances. The control moment gyros stabilize the payload orientation. The SEM will be useful for payloads that require a lower-g environment than a manned vehicle can provide, such as materials processing, and for payloads that require stabilization of pointing direction, but not large angle slewing, such as nadir-viewing earth observation or solar viewing payloads. Author

N92-28370*# National Aeronautics and Space Administration. Marshall Space Flight Center, Huntsville, AL.
SCIENCE AND APPLICATION PAYLOADS IN THE 1990'S
Carmine E. DeSanctis 30 Jun. 1992 11 p
(NASA-TM-107937; NAS 1.15:107937) Avail: NTIS HC/MF A03

During the 90's with the operation of the Extended Duration Orbiter (EDO), Space Station Freedom (SSF), large platforms in polar and Geosynchronous orbits around the Earth, and supporting systems and technology, an infrastructure will exist that will offer a wide range of opportunities for science and applications payloads. The Marshall Space Flight Center (MSFC) is in a unique position of studying for NASA science missions for all of these systems. This paper will discuss a variety of payloads being studied for NASA at the MSFC that are scheduled for flight in the 90's, in support of space science and Mission to Planet Earth. These science payloads such as the Controls, Astrophysics and Structures Experiment in Space (CASES), Advanced Solar Observatory (ASO), Laser Atmospheric Wind Sounder (LAWS), and Lightning Imaging Sensor (LIS), etc. will fully utilize the capabilities of EDO, SSF, Earth Observing System (EOS), and Earth Science Geostationary Platform (ESGP). Emphasis will be placed on showing how these scientific payloads can fully exploit the great potential of these new capabilities for exciting new science and application missions. Author

N92-28560# Army Construction Engineering Research Lab., Champaign, IL.
STRUCTURAL DESIGN METHODOLOGY FOR LARGE SPACE STRUCTURES Final Report
Ralph J. Dornsife Feb. 1992 60 p
(AD-A247672; CERL-M-92/12) Avail: NTIS HC/MF A04

The Department of Defense requires research and development in designing, fabricating, deploying, and maintaining large space structures (LSS) in support of Army and Strategic Defense Initiative military objectives. Because of their large size, extreme flexibility, and the unique loading conditions in the space environment, LSS will present engineers with problems unlike those encountered in designing conventional civil engineering or aerospace structures. LSS will require sophisticated passive damping and active control systems in order to meet stringent mission requirements. These structures must also be optimally designed to minimize high launch costs. This report outlines a methodology for the structural design of LSS. It includes a definition of mission requirements, structural modeling and analysis, passive damping and active control system design, ground-based testing, payload integration, on-orbit system verification, and on-orbit assessment of structural damage. In support of this methodology, analyses of candidate LSS truss configurations are presented, and an algorithm correlating ground-based test behavior to expected microgravity behavior is developed. GRA

N92-28683*# National Aeronautics and Space Administration. Lewis Research Center, Cleveland, OH.
SOLAR ARRAY MODULE PLASMA INTERACTION EXPERIMENT (SAMPIE): TECHNICAL REQUIREMENTS DOCUMENT
G. Barry Hillard (Sverdrup Technology, Inc., Brook Park, OH.) and Dale C. Ferguson May 1992 25 p
(RTOP 589-01-1B)
(NASA-TM-105660; E-7033; NAS 1.15:105660) Avail: NTIS HC/MF A03

The Solar Array Module Plasma Interactions Experiment (SAMPIE) is a NASA shuttle space flight experiment scheduled for launch in early 1994. The SAMPIE experiment will investigate plasma interactions of high voltage space power systems in low earth orbit. Solar cell modules, representing several technologies, will be biased to high voltages to characterize both arcing and plasma current collection. Other solar modules, specially modified in accordance with current theories of arcing and breakdown, will

demonstrate the possibility of arc suppression. Finally, several test modules will be included to study the basic nature of these interactions. The science and technology goals for the project are defined in the Technical Requirements Document (TRD) which is presented here. Author

N92-28730*# National Aeronautics and Space Administration. Langley Research Center, Hampton, VA.
ONGOING PROGRESS IN SPACECRAFT CONTROLS
Dave Ghosh, ed. (Lockheed Engineering and Sciences Co., Hampton, VA.) Jul. 1992 143 p Workshop held in Hampton, VA, 13 Jan. 1992
(RTOP 506-59-61-01)
(NASA-CP-10099; NAS 1.55:10099) Avail: NTIS HC/MF A07

This publication is a collection of papers presented at the Mars Mission Research Center workshop on Ongoing Progress in Spacecraft Controls. The technical program addressed additional Mars mission control problems that currently exist in robotic missions in addition to human missions. Topics include control systems design in the presence of large time delays, fuel-optimal propulsive control, and adaptive control to handle a variety of unknown conditions. For individual titles, see N92-28731 through N92-28738.

N92-28731*# North Carolina State Univ., Raleigh.
REVIEW OF MARS MISSION SCENARIOS c12
Gerald Walberg *In* NASA. Langley Research Center, Ongoing Progress in Spacecraft Controls Jul. 1992 p 1-11 (For primary document see N92-28730 19-18)
Avail: NTIS HC/MF A07

The following paper is presented in viewgraph format and covers topics including: mission scenario; exposure to reduced gravity; exposure to space radiation; and initial mass in low Earth orbit. H.A.

N92-28732*# North Carolina State Univ., Raleigh. Dept. of Mathematics.
STABILITY AND OPTIMAL CONTROL THEORY OF HEREDITARY SYSTEMS WITH APPLICATIONS FROM OSCILLATING FLYING VEHICLES, MECHANICAL SYSTEMS, AND ROBOTICS
Ethelbert Nwakuche Chukwu *In* NASA. Langley Research Center, Ongoing Progress in Spacecraft Controls Jul. 1992 p 13-24 (For primary document see N92-28730 19-18)
Avail: NTIS HC/MF A07

The author derives an equation determining the dynamics of the deterministic model of a flying vehicle. He next examines a simplified mechanical problem whose optimal feedback control strategy is investigated. From there robotics are incorporated into the mathematical model to develop an equation describing optimal control of the dynamics. H.A.

N92-28733*# National Aeronautics and Space Administration. Langley Research Center, Hampton, VA.
SENSOR FILTER DESIGNS FOR LARGE FLEXIBLE SPACECRAFT
Nancy A. Nimmo *In its* Ongoing Progress in Spacecraft Controls Jul. 1992 p 25-37 (For primary document see N92-28730 19-18)
Avail: NTIS HC/MF A07

Traditional control methods may excite flexible modes causing degraded performance or instability of large flexible space structures (LFSS). Control techniques developed for control of LFSS requires a numerical model of the structure and some knowledge of model error. This will be increasingly difficult with the complex space structures planned for the future. If filters could be used to condition the sensor output, control design would be less demanding. This paper is presented in viewgraph format. Author

N92-28734*# National Aeronautics and Space Administration. Langley Research Center, Hampton, VA.
FUEL OPTIMAL PROPULSIVE REBOOST OF FLEXIBLE SPACECRAFT
Jim Redmond *In its* Ongoing Progress in Spacecraft Controls Jul. 1992 p 39-54 (For primary document see N92-28730 19-18)
Avail: NTIS HC/MF A07

The following paper is presented in viewgraph format and topics include: (1) exact solutions are difficult to obtain for higher order systems; (2) impulsive forces cannot be implemented directly; (3) exact solution provide the basis for judging the optimality of approximate techniques; and (4) properties of the exact solution can be used to develop improved approximations. Furthermore, the author discusses a floating harmonic oscillator whose model possesses rigid and flexible body motion characteristics of the proposed spacecraft. H.A.

N92-28735*# National Aeronautics and Space Administration. Langley Research Center, Hampton, VA.
FUEL OPTIMAL MANEUVER: EXPERIMENTAL TESTBEDS
John L. Meyer *In its* Ongoing Progress in Spacecraft Controls Jul. 1992 p 55-75 (For primary document see N92-28730 19-18)
Avail: NTIS HC/MF A07

The objective of this paper is to conduct experiments in fuel optimal propulsive maneuvers of flexible spacecraft in order to verify and extend recently developed theory and apply it to various classes of spacecraft. Topics covered in viewgraph format include: impulse damping control by experimental verification; impulse damping of the SCOLE reflector and mast; fuel optimal control of rotating flexible beam; fuel optimal aerobrake maneuvers. H.A.

N92-28736*# North Carolina State Univ., Raleigh. Dept. of Mechanical and Aerospace Engineering.
INITIAL INVESTIGATIONS OF AN ADAPTIVE DISCRETE-TIME CONTROLLER FOR NONLINEAR TIME-VARYING ROBOTIC MODELS c37
S. S. Giang and Gordon K. F. Lee *In* NASA. Langley Research Center, Ongoing Progress in Spacecraft Controls Jul. 1992 p 77-106 (For primary document see N92-28730 19-18)
Avail: NTIS HC/MF A07

The objective of this paper is to design a discrete-time controller which forces $y(t) = F(q(t),q'(t))$ to follow a desired trajectory, when non-linearities may be uncertain. A self-tuning adaptive control algorithm is then developed that addresses three types of errors: (1) error due to model linearization; (2) errors due to controlling a time-varying plant; and (3) errors due to discretization. H.A.

N92-28737*# North Carolina State Univ., Raleigh. Mars Mission Research Center.
IDENTIFICATION OF LINEAR SYSTEM MODELS AND STATE ESTIMATORS FOR CONTROLS
Chung-Wen Chen *In* NASA. Langley Research Center, Ongoing Progress in Spacecraft Controls Jul. 1992 p 107-122 (For primary document see N92-28730 19-18)
Avail: NTIS HC/MF A07

The following paper is presented in viewgraph format and covers topics including: (1) linear state feedback control system; (2) Kalman filter state estimation; (3) relation between residual and stochastic part of output; (4) obtaining Kalman filter gain; (5) state estimation under unknown system model and unknown noises; and (6) relationship between filter Markov parameters and system Markov parameters. H.A.

N92-28738*# North Carolina State Univ., Raleigh. Mars Mission Research Center.
FUZZY LOGIC CONTROLLER FOR MANIPULATOR SYSTEMS: PRELIMINARY RESULTS c63
D. Gerber, H. Roberts, R. J. Stanley, II, and J. C. Windsor *In* NASA. Langley Research Center, Ongoing Progress in Spacecraft Controls Jul. 1992 p 123-148 (For primary document see

N92-28730 19-18)
Avail: NTIS HC/MF A07

The following paper is presented in viewgraph format and covers topics that include: fuzzy control; center of gravity; and robotics. H.A.

N92-28750* National Aeronautics and Space Administration. Marshall Space Flight Center, Huntsville, AL.
CLOSED-LOOP AUTONOMOUS DOCKING SYSTEM Patent
Richard W. Dabney, inventor (to NASA) and Richard T. Howard, inventor (to NASA) 28 Apr. 1992 10 p Filed 20 Feb. 1990
Supersedes N90-26861 (28 - 21, p 2966)
(NASA-Case-MFS-28421-1; US-Patent-5,109,345; US-Patent-Appl-SN-481537; US-Patent-Class-364-459; US-Patent-Class-358-103; US-Patent-Class-244-161; Int-Patent-Class-B64G-1/64) Avail: US Patent and Trademark Office

An autonomous docking system is provided which produces commands for the steering and propulsion system of a chase vehicle used in the docking of that chase vehicle with a target vehicle. The docking system comprises a passive optical target affixed to the target vehicle and comprising three reflective areas including a central area mounted on a short post, and tracking sensor and process controller apparatus carried by the chase vehicle. The latter apparatus comprises a laser diode array for illuminating the target so as to cause light to be reflected from the reflective areas of the target; a sensor for detecting the light reflected from the target and for producing an electrical output signal in accordance with an image of the reflected light; a signal processor for processing the electrical output signal in accordance with an image of the reflected light; a signal processor for processing the electrical output signal and for producing, based thereon, output signals relating to the relative range, roll, pitch, yaw, azimuth, and elevation of the chase and target vehicles; and a docking process controller, responsive to the output signals produced by the signal processor, for producing command signals for controlling the steering and propulsion system of the chase vehicle.

Official Gazette of the U.S. Patent and Trademark Office

N92-28765# Amptek, Inc., Bedford, MA.
EMPIRICAL TECHNIQUES FOR THE STUDY OF ACCELERATION MECHANISMS IN THE SPACE ENVIRONMENT Final Report, 1 Sep. 1989 - 28 Feb. 1991
John O. McGarity, Alan C. Huber, and John A. Pantazis 22 May 1991 13 p
(Contract F19628-86-C-0029)
(AD-A249940; PL-TR-91-2273; AD-E200993) Avail: NTIS HC/MF A03

Particle correlation techniques used with pulse counting energetic particle detectors are reviewed. Three methods are proposed for use on an electrostatic analyzer to be flown on the Space Shuttle Tethered Satellite System 1 Mission. GRA

N92-28967# Florida Atlantic Univ., Boca Raton. Center for Applied Stochastics Research.
NONLINEAR SLOSHING AND THE COUPLED DYNAMICS OF LIQUID PROPELLANTS AND SPACECRAFT Final Report, 1 Oct. 1989 - 31 Dec. 1991
Tsung-Chow Su 29 Feb. 1992 84 p
(Grant AF-AFOSR-0444-89)
(AD-A250023; AFOSR-92-0229TR) Avail: NTIS HC/MF A05

Current and future space-based systems have rather complex mission requirements which demand the storage of large amounts of liquid propellants on board. With large controller bandwidths and rapid maneuvering of the spacecraft in a low gravity environment, potential coupling between the sloshing liquid, the spacecraft motion and structural modes need to be carefully evaluated to ensure the system design adequacy. For achieving the mission success, the first important step is to understand the nonlinear dynamics of the liquid sloshing. The report summarizes a two-year study on the development and application of the numerical method for three-dimensional liquid sloshing simulation. Fluid dynamics and fluid loading, including total force and impact for the vessel undergoing rapid movement were simulated. Effects of baffles and active baffles with or without feedback mechanism for sloshing control were compared. It was found that moving baffles can be very effective in suppressing large amplitude sloshing. Complicated swirling intensification by drainage was also numerically simulated. GRA

19 SPACECRAFT INSTRUMENTATION

For related information see also *06 Aircraft Instrumentation* and *35 Instrumentation and Photography.*

N92-28451*# National Aeronautics and Space Administration. Lewis Research Center, Cleveland, OH.
EARLY MISSION SCIENCE SUPPORT: SPACE ACCELERATION MEASUREMENT SYSTEM (SAMS)
Richard DeLombard *In its* International Workshop on Vibration Isolation Technology for Microgravity Science Applications May 1992 p 345-355 (For primary document see N92-28436 19-31)
Avail: NTIS HC/MF A18

20 SPACECRAFT PROPULSION AND POWER

Includes main propulsion systems and components, e.g., rocket engines; and spacecraft auxilliary power sources.

For related information see also *07 Aircraft Propulsion and Power, 28 Propellants and Fuels, 44 Energy Production and Conversion,* and *15 Launch Vehicles and Space Vehicles.*

N92-28366# Massachusetts Inst. of Tech., Lexington. Lincoln Lab.
SCATTERING MEASUREMENTS AND PREDICTIONS FOR A DELTA STAGE 2 ROCKET NOZZLE
Thomas G. Moore 3 Jan. 1992 33 p
(Contract F19628-90-C-0002)
(AD-A246776; TR-934; ESD-TR-91-161) Avail: NTIS HC/MF A03

The interaction between electromagnetic waves and cavities often exhibits very distinguishable scattering patterns. One method for extracting information from the scattered field is to form a radar image. This technique is very useful if the frequency of the incident field is not near a resonance of the cavity. One of the distinguishing features in an image of a cavity is a return that is visible downrange from the entrance of the cavity. This extended return is the result of energy trapped inside the cavity that later exits toward the radar. By measuring the characteristics of this extended return it may be possible to determine information about the cavity. In order to study the phenomenology of scattering from cavities, this report examines a common geometry (rocket nozzle). Rocket nozzles are commonly found on tumbling rocket bodies that are left in an earth orbit. At times it is useful to try to determine the condition, or shape/size, of a rocket nozzle on a tumbling rocket body. To derive such information, an understanding must be developed of how radar energy scatters from such nozzles. This report will examine the scattering from a non conic rocket nozzle and address the question of estimating the shape of the nozzle from measurements made from radar images. The predicted location and intensity of the scattered field are compared with those measured from a radar image. GRA

N92-28417*# National Aeronautics and Space Administration. Lewis Research Center, Cleveland, OH.
AN OVERVIEW OF IN-FLIGHT PLUME DIAGNOSTICS FOR ROCKET ENGINES
G. C. Madzsar, R. L. Bickford (Aerojet Solid Propulsion Co., Sacramento, CA.), and D. B. Duncan (Duncan Technologies, Auburn, CA.) Jul. 1992 25 p Proposed for presentation at

the 28th Joint Propulsion Conference and Exhibit, Nashville, TN, 6-8 Jul. 1992; sponsored by AIAA, SAE, ASME, and ASEE
(RTOP 590-21-41)
(NASA-TM-105727; E-7130; NAS 1.15:105727; AIAA Paper 92-3785) Avail: NTIS HC/MF A03

An overview and progress report of the work performed or sponsored by LeRC toward the development of in-flight plume spectroscopy technology for health and performance monitoring of liquid propellant rocket engines are presented. The primary objective of this effort is to develop technology that can be utilized on any flight engine. This technology will be validated by a hardware demonstration of a system capable of being retrofitted onto the Space Shuttle Main Engines for spectroscopic measurements during flight. The philosophy on system definition and status on the development of instrumentation, optics, and signal processing with respect to implementation on a flight engine are discussed. Author

N92-28682*# National Aeronautics and Space Administration. Lewis Research Center, Cleveland, OH.
NASA LEWIS STEADY-STATE HEAT PIPE CODE USERS MANUAL
Leonard K. Tower (Sverdrup Technology, Inc., Brook Park, OH.), Karl W. Baker, and Timothy S. Marks (Oregon State Univ., Corvallis.) Jun. 1992 45 p
(RTOP 590-13-21)
(NASA-TM-105161; E-6450; NAS 1.15:105161) Avail: NTIS HC/MF A03

The NASA Lewis heat pipe code was developed to predict the performance of heat pipes in the steady state. The code can be used as a design tool on a personal computer or with a suitable calling routine, as a subroutine for a mainframe radiator code. A variety of wick structures, including a user input option, can be used. Heat pipes with multiple evaporators, condensers, and adiabatic sections in series and with wick structures that differ among sections can be modeled. Several working fluids can be chosen, including potassium, sodium, and lithium, for which monomer-dimer equilibrium is considered. The code incorporates a vapor flow algorithm that treats compressibility and axially varying heat input. This code facilitates the determination of heat pipe operating temperatures and heat pipe limits that may be encountered at the specified heat input and environment temperature. Data are input to the computer through a user-interactive input subroutine. Output, such as liquid and vapor pressures and temperatures, is printed at equally spaced axial positions along the pipe as determined by the user. Author

N92-28693*# National Aeronautics and Space Administration. Lewis Research Center, Cleveland, OH.
INTEGRATED HEALTH MONITORING AND CONTROLS FOR ROCKET ENGINES
W. C. Merrill, J. L. Musgrave, and T. H. Guo Apr. 1992 7 p Presented at the SAE Aerospace Atlantic, Dayton, OH, 7-10 Apr. 1992; sponsored in part by the Engineering Society for Advancing Mobility Land, Sea, Air, and Space
(RTOP 506-42-72)
(NASA-TM-105763; E-7180; NAS 1.15:105763) Avail: NTIS HC/MF A02

Current research in intelligent control systems at the Lewis Research Center is described in the context of a functional framework. The framework is applicable to a variety of reusable space propulsion systems for existing and future launch vehicles. It provides a 'road map' technology development to enable enhanced engine performance with increased reliability, durability, and maintainability. The framework hierarchy consists of a mission coordination level, a propulsion system coordination level, and an engine control level. Each level is described in the context of the Space Shuttle Main Engine. The concept of integrating diagnostics with control is discussed within the context of the functional framework. A distributed real time simulation testbed is used to realize and evaluate the functionalities in closed loop. Author

N92-28747 Department of the Navy, Washington, DC.
SOLID-PROPELLANT-POWERED MANEUVERING SYSTEM FOR SPACECRAFT Patent
Charles W. Goddard, inventor (to Navy), John T. Lucas, inventor (to Navy), and Paul A. Galvan, inventor (to Navy) 5 Nov. 1991 11 p Filed 15 Feb. 1991
(AD-D015245; US-Patent-5,062,593; US-Patent-Appl-SN-660361; US-Patent-Class-244-169) Avail: US Patent and Trademark Office

An improvement to a variable-pressure solid-propellant-powered maneuvering system for spacecraft is presented. The new system is capable of operating for longer than one propellant burn cycle. At least two solid propellant gas generators are connected via a manifold to a plurality of nozzle valve clusters; at least one of the gas generators is connected to the manifold via a sequence valve which isolates that generator from the manifold until such time as it is desired to put that generator into operation. GRA

N92-28748 Department of the Navy, Washington, DC.
ROCKET NOZZLE SHIELD Patent
Carl A. Vollersen, inventor (to Navy), Thomas W. Anderson, inventor (to Navy), Wayne M. Brown, inventor (to Navy), and Lozelle L. Pratt, inventor (to Navy) 24 Dec. 1991 6 p Filed 8 Mar. 1991
(AD-D015248; US-Patent-5,074,187; US-Patent-Appl-SN-674271; US-Patent-Class-89-1.809) Avail: US Patent and Trademark Office

A shield for the nozzle of an underwater launched missile can be formed from a rigid plate. The plate is separated from the end of the nozzle by a gap that is at least equal to the throat area of the nozzle. The gap reduces overpressure of the missile during launch while keeping water out of the nozzle by being directed perpendicular to the water flow direction. Important advantages of the invention are its simplicity and low cost. A further advantage is its strength and the ability to absorb a blow from a water jar. Another advantage is the ability to block the flow of water from behind the rocket without blocking the flow of gas. GRA

N92-28780# Office National d'Etudes et de Recherches Aerospatiales, Paris (France).
ABLATION OF MATERIAL OF SOLID PROPELLANT MOTOR NOZZLES [ABLATION DES MATERIAUX DE TUYERES DE PROPULSEURS A PROPERGOL SOLIDE]
V. Borie, Y. Maisonneuve, D. Lambert, and G. Lengelle 1990 247 p In FRENCH
(ONERA-NT-1990-13; ISSN-0078-3781; ETN-92-91272) Avail: NTIS HC/MF A11

An aerothermochemical analysis of carbon-carbon composite material ablation near the nozzle throats of large advanced solid propellant rocket motors was conducted. The different steps of the approach consisted of chamber equilibrium calculations, nozzle inviscid flow calculations, boundary layer calculations, experimental work concerning the ablation rate and the surface roughness of a nozzle carbon-carbon material, chemical attack description of this material, nozzle heat transfer calculations and throat ablation evaluations. The experimental results are compared with other experimental results available in the literature concerning carbon materials, and the calculated results show good agreement between the measured data on large solid propellant rockets when the model assumes a flow transition between a laminar boundary layer existing on the 'smooth' virgin carbon-carbon material at the start of firing and a turbulent boundary layer existing in the very rough ablative carbon-carbon surface during stabilized motor operation. ESA

N92-28800# Army Missile Command, Redstone Arsenal, AL. Propulsion Directorate.
INTRODUCTION TO ROCKET PROPULSION Summary Report
J. M. Lyon Dec. 1991 234 p
(AD-A250424; AD-E951808; AMSMI-TR-RD-PR-91-17) Avail: NTIS HC/MF A11

The design process for solid propellant rocket motors is presented in an introductory text suitable for professional reference

as well as for instruction at the high school senior through college junior level. Beginning with a brief history of rocketry and a short discussion of the basic properties of matter, the text progresses through the development of the governing laws of rocket propulsion and utilization of important propulsion theories and equations. Design considerations for various motor components (propellants, grain, and inert hardware) are presented. Performance prediction using computers and instrumentation and testing are discussed. Numerous examples and problems are provided. GRA

N92-28931# Science Applications International Corp., McLean, VA.
INVESTIGATION OF ENERGY EXCHANGE MECHANISMS BETWEEN THE MEAN AND ACOUSTIC FLOW FIELDS IN SOLID ROCKET COMBUSTION CHAMBERS Final Report, Aug. 1989 - Aug. 1991
Joseph D. Baum 5 Nov. 1991 52 p
(Contract F49620-89-C-0124)
(AD-A247402; SAIC-91/1286) Avail: NTIS HC/MF A04

The objective of the research effort described in this final report was to investigate the physical mechanisms by which energy is exchanged between the mean and the acoustic flow fields in solid propellant rocket motors. During the first year of this research effort, we examined energy exchange mechanisms between the mean flow and the standing acoustic wave in the cold flow simulator. The effect of the actual burning of the solid propellant on the energy exchange mechanisms was examined in the second year. Among the major achievements of this investigation was the demonstration of acoustic streaming phenomena, shown via the examination of the instantaneous and the time-averaged solutions. In addition, it was shown that the instantaneous mechanical dissipation near the wall followed the local radial derivative of the axial acoustic velocity. Correspondingly, the time averaged dissipation function contours were confined to a region near the wall, with maximum values at the acoustic velocity anti-node location. Very little dissipation was observed near the acoustic velocity nodes, indicating that significant dissipation and vorticity production can only occur through the interaction between the acoustic velocity flow field with the mean flow injected through the periphery, thus pinpointing the source of acoustic energy dissipation due to the so called flow turning phenomenon. GRA

N92-28945# Pulse Sciences, Inc., Agoura Hills, CA.
SPEAR 2 SPACE POWER DATA ANALYSIS Technical Report, 17 May 1990 - 17 Mar. 1991
John R. Bayless 1 Apr. 1992 16 p
(Contract DNA001-90-C-0084)
(AD-A248057; PSI-FR-2567-1; DNA-TR-91-71) Avail: NTIS HC/MF A03

This project provided data analysis and support for the SPEAR II payload tests at the NASA Plum Brook Station in June, 1990. It also provided support for test preparation and overall data review. Independent analysis of the payload chamber tests with and without plasma indicated that: (1) when plasma is not present, the probability of arcing in the pulse transformer approached zero monotonically, and (2) with plasma present, pulse conditioning of the transformer was erratic and, at the highest voltages, arc-free operation appeared not to be attainable. GRA

N92-28983*# National Aeronautics and Space Administration. Lewis Research Center, Cleveland, OH.
DEVELOPMENT AND FLIGHT HISTORY OF SERT 2 SPACECRAFT
William R. Kerslake (Sverdrup Technology, Inc., Brook Park, OH.) and Louis R. Ignaczak 1992 53 p Proposed for presentation at the 28th Joint Propulsion Conference and Exhibit, Nashville, TN, 6-8 Jul. 1992; sponsored by AIAA, SAE, ASME, and ASEE
(RTOP 506-42-31)
(NASA-TM-105636; E-6839; NAS 1.15:105636; AIAA Paper 92-3516) Avail: NTIS HC/MF A04

A 25-year historical review of the Space Electric Rocket Test 2 (SERT 2) mission is presented. The Agena launch vehicle; the SERT 2 spacecraft; and mission-peculiar spacecraft hardware, including two ion thruster systems, are described. The 3 1/2-year development period, from 1966 to 1970, that was needed to design, fabricate, and qualify the ion thruster system and the supporting spacecraft components, is documented. Major testing of two ion thruster systems and related auxiliary experiments that were conducted in space after the 3 Feb. 1970, launch are reviewed. Extended ion thruster restarts from 1973 to 1981 are reported, in addition to cross-neutralization tests. Tests of a reflector erosion experiment were continued in 1989 to 1991. The continuing performance of spacecraft subsystems, including the solar arrays, over the 1970-1991 period is summarized. Finally, the knowledge of thruster-spacecraft interactions learned from SERT 2 is listed.
Author

23 CHEMISTRY AND MATERIALS (GENERAL)

N92-29141* National Aeronautics and Space Administration. Langley Research Center, Hampton, VA.
POLY(1,3,4-OXADIAZOLES) VIA AROMATIC NUCLEOPHILIC DISPLACEMENT Patent
John W. Connell, inventor (to NASA), Paul M. Hergenrother, inventor (to NASA), and Peter Wolf, inventor (to NASA) 2 Jun. 1992 9 p Filed 22 Jan. 1991 Supersedes N91-23237 (29 - 15, p 2391)
(NASA-Case-LAR-14427-1; US-Patent-5,118,781; US-Patent-Appl-SN-645089; US-Patent-Class-528-185; US-Patent-Class-548-143; Int-Patent-Class-C08G-73/08; Int-Patent-Class-C07D-271/10) Avail: US Patent and Trademark Office

Poly(1,3,4-oxadiazoles) (POX) are prepared by the aromatic nucleophilic displacement reaction of di(hydroxyphenyl) 1,3,4-oxadiazole monomers with activated aromatic dihalides or activated aromatic dinitro compounds. The polymerizations are carried out in polar aprotic solvents such as sulfolane or diphenylsulfone using alkali metal bases such as potassium carbonate at elevated temperatures under nitrogen. The di(hydroxyphenyl) 1,3,4-oxadiazole monomers are synthesized by reacting 4-hydroxybenzoic hydrazide with phenyl 4-hydrobenzoate in the melt and also by reacting aromatic dihydrazides with two moles of phenyl 4-hydroxybenzoate in the melt. This synthetic route has provided high molecular weight POX of new chemical structure, is economically and synthetically more favorable than other routes, and allows for facile chemical structure variation due to the large variety of activated aromatic dihalides which are available.
Official Gazette of the U.S. Patent and Trademark Office

24 COMPOSITE MATERIALS

Includes physical, chemical, and mechanical properties of laminates and other composite materials.
For ceramic materials see *27 Nonmetallic Materials*.

N92-28224# Department of the Navy, Washington, DC.
METHOD FABRICATING LOAD-BEARING COMPOSITES FREE FROM MICROBUCKLING DEFORMATION UP TO A PREDETERMINED LOAD Patent Application
Neil J. Dubois, inventor (to Navy) 3 Jul. 1991 20 p
(AD-D015212; US-Patent-Appl-SN-725717; Navy-Case-72815)
Avail: NTIS HC/MF A03

A method fabricating a continuous filament reinforced composite free from microbuckling deformation up to a predetermined load with a high degree of certainty is disclosed. A continuous filament is selected from among a group of appropriate types of filaments. A matrix material is selected from a group of appropriate types of matrix materials. Selected filaments are undirectionally embedded in the selected matrix to provide a uniaxially continuously reinforced composite. The Young's modulus

and the shear modulus are calculated for the composite. Mathematical formulas are provided for calculation of upper and lower bounds of transverse stiffness, B. A mathematical formula is provided for calculation of critical comprehensive stress, P(sub c). Transverse stiffness, B, is involved as one of the factors in this formula. Either one or the other of the upper bound of B or the lower bound of B are alternatively applied in calculating P(sub c) depending upon a consideration related to the shape of a cross section of the structural member into which the composite is to be formed. A structural member subjected to load values below P(sub c) will be free from load-induced microbuckling with a high degree of certainty. GRA

N92-28252# Case Western Reserve Univ., Cleveland, OH. Dept. of Macromolecular Science.
QUANTITATIVE INTERPHASE STUDY OF COMPOSITE MATERIALS. INTERPHASE ENGINEERING: A SCIENTIFIC WAY OF TAILORING THE MECHANOPHYSICAL PROPERTIES OF COMPOSITE MATERIALS Final Report, 1 Jul. 1988 - 31 Dec. 1991
Hatsuo Ishida and Jack L. Koenig 17 Mar. 1992 14 p
(Contract N00014-88-R-0330)
(AD-A247776) Avail: NTIS HC/MF A03

The projects covering Jul. 1988 - Dec. 1991 were concerned with the application of a new technique, NMR imaging, in the following areas: interface studies; preparation of composites with special innerlayers; and systematic surface treatment of carbon fibers and characterization of surfaces. We have studied all proposed areas and obtained several major breakthroughs as summarized in the formal Final Report. GRA

N92-28303# Army Armament Research, Development and Engineering Center, Watervliet, NY.
REVIEW AND UPDATE ON ELECTROCOMPOSITES Final Report
V. P. Greco Feb. 1992 49 p
(AD-A248050; ARCCB-TR-92005) Avail: NTIS HC/MF A03

The demand for metal matrix composites (MMC) is reaching a new height in the material community in view of their superior strength at elevated temperatures. Several methods are employed in producing these composites in which high strength inert particles, fibers, or filaments are incorporated in the matrix of a conventional metal. A critical problem in producing metal matrix composites is the handling and damaging of candidate brittle high strength fibers due to high process temperatures and pressures. A process for producing composites, which does not require high temperatures or pressures, is electrodeposition in aqueous solutions. This is a process which offers a number of other benefits. Electrocomposites are reinforced electrodeposits or electroforms with high strength inert particles, fibers, or continuous filaments. From a review of the literature, an updated evaluation of electrocomposites is given, followed by a review of their strengthening mechanisms and the proposed theories of particle encapsulation. The results and properties of electro composites previously reported are also reviewed and the future role that platers have in producing high performance composites, which outperform superalloys, is assessed. GRA

N92-28307# Northwestern Univ., Evanston, IL.
MICROMECHANICS OF DEFECTS Final Report, 15 Dec. 1988 - 14 Dec. 1991
T. Mura Mar. 1992 4 p
(Contract DAAL03-89-K-0019)
(AD-A248432; ARO-26057.16-EG) Avail: NTIS HC/MF A02

This report contains a brief outline of research findings and a list of publications and technical reports related to the micromechanics of defects, nondestructive testing, and cracking in fiber reinforced composites. GRA

N92-28416# Army Armament Research, Development and Engineering Center, Watervliet, NY.
X RAY DIFFRACTION STUDY OF RESIDUAL STRESSES IN METAL MATRIX COMPOSITE-JACKETED STEEL CYLINDERS SUBJECTED TO INTERNAL PRESSURE Final Report
S. L. Lee, M. Doxbeck, and G. Capsimalis Mar. 1992 23 p
(AD-A248449; ARCCB-TR-92007) Avail: NTIS HC/MF A03

The study of aluminum/silicon carbide metal matrix composite (MMC)-jacketed steel structural components was made because of their light weight and high stiffness. Steel 'liner' cylinders were wrapped with MMC 'jackets' with an all-hoop layup and put through various degrees of hydraulic autofrettage and thermal soak. The results from our x-ray diffraction residual stress measurements on cylinders using a position-sensitive scintillation detection system are discussed. Our experimental results are compared with theoretical predictions from a model based on the elastic-plastic analysis of a thick-walled cylinder subjected to internal pressure. Interpretation of the interference effect caused by the MMC jacket on the steel liner is also discussed. GRA

N92-28572# Technical Research Centre of Finland, Espoo. Metals Lab.
NONDESTRUCTIVE EVALUATION OF DAMAGES CAUSED BY IMPACT AND FATIGUE LOADING OF POLYMER COMPOSITES [LUJITEMOUVIN ISKU- JA VASYMISVAURIOIDEN HAVAITSEMINEN NDT-MENETELMILLA]
Pentti Kauppinen, Harri Jeskanen, and Reino Tarvainen Sep. 1991 35 p In FINNISH Sponsored by Technology Development Center and Finnish Industry
(VTT-RR-742; ISBN-951-38-3990-7; ISSN-0358-5077; ETN-92-91266) Copyright Avail: NTIS HC/MF A03

The damages of multilayer composite plates in impact loading were studied by using different ultrasonic techniques, holographic interferometry, and thermography in order to evaluate the resolution of different techniques and to estimate the applicability of these techniques to inspections in the field conditions. In the laboratory study, delaminations larger than 10 mm diameter were detected. Due to the beam width of the ultrasonic transducer used in the study, the sizes of delaminations having the diameter smaller than 10 mm could not be evaluated. The damages caused by fatigue loading were studied using glass fiber reinforced epoxy laminates. The creation of damages due to mechanical loading was too rapid and could not be monitored by using ultrasonic techniques. ESA

N92-28573# Technical Research Centre of Finland, Espoo. Metals Lab.
FATIGUE STRENGTH OF A GLASS FIBER REINFORCED LAMINATE STRUCTURE [LASIKUITULUJITTEISEN LAMINAATIRAKENTEEN KESTAVYYS VASYTTAVAN KUORMITUKSEN ALAISENA]
Pertti Auerkari, Pentti Kauppinen, Heikki Keinanen, Pekka H. Pankakoski, Kari Santaoja, and Tero Uuttu Sep. 1991 25 p In FINNISH Sponsored by Technology Development Center and Finnish Industry
(VTT-RR-743; ISBN-951-38-3991-5; ISSN-0358-5077; ETN-92-91267) Copyright Avail: NTIS HC/MF A03

The fatigue strength of laminated beams made of a fiber rich epoxy glass fiber reinforced composite was assessed from bending fatigue testing results. The results were compared with estimated strength requirements in service. Due to high stress sensitivity and relatively high loads in service, the fatigue life of the beams should be determined from in situ strain measurements. By measuring surface strains and displacements directly, complicating considerations of the orthotopic properties can be minimized in the the analysis. Also, the difficulties related to local damage in the region of failure initiation are avoided, when simulated testing of the whole structure can be related to in service loading. The fatigue behavior of the beams demonstrate a case where the Miner rule is not directly applicable. This was due to a sequence effect associated with step loading. ESA

N92-28577# Technische Univ., Delft (Netherlands).
THE INFLUENCE OF ELEVATED TEMPERATURE ON THE BONDING QUALITY OF DEFORMED GLARE
R. vanPraag Jul. 1991 23 p
(LR-659; ETN-92-91399) Avail: NTIS HC/MF A03

The influence of elevated temperatures on deformed GLARE, a metal laminate consisting of aluminum layers and fibers embedded in a resin (the so called prepreg) is addressed. The results of three types of GLARE are plotted. In particular, the determination of the relation between the amount of deformation and the temperature at which spontaneous delamination occurs is described. ESA

N92-28582# Technische Univ., Delft (Netherlands). Faculty of Aerospace Engineering.
THE COMPRESSIVE PROPERTIES OF GLARE
J. L. Verolme Nov. 1991 41 p
(LR-666; ETN-92-91404) Avail: NTIS HC/MF A03

An investigation of compressive properties from GLARE 1 to GLARE 4 is reported. Several layups were tested in longitudinal as well as in longitudinal transverse direction. To check whether Young's modulus and the yield stress can be predicted accurately theoretically, prediction methods based on simple formulas are developed. For this purpose, pure aluminum alloy and pure prepreg specimens were tested. Simple methods are shown to already lead to accurate (90 percent and more) predictions. To investigate the effect of the post stretch percentage on the yield stress of GLARE 1, as-cured material is also examined. As expected, the compressive yield stress lowers with increasing post stretch percentage. To show the abilities of GLARE in compression, structural efficiency curves were created. ESA

N92-28637# National Aerospace Lab., Amsterdam (Netherlands). Structures and Materials Div.
SIMPLE COMPUTER PROGRAMS FOR THE DESIGN AND SIZING OF FIBER REINFORCED COMPOSITES [REKENPROGRAMMA'S VOOR HET ONTWERPEN EN DIMENSIONEREN VAN VEZELVERSTERKTE KUNSTSTOFFEN]
J. Olthoff 4 Feb. 1990 15 p In DUTCH Presented at the Symposium Ontwerpen en Construeren met Composieten, Delft, Netherlands, 19 Jun. 1990
(NLR-TP-91050-U; ETN-92-91452) Avail: NTIS HC/MF A03

An inventory of computer programs for composite materials is given. The programs are divided into four groups: general laminate theory; specific laminate problems; general (finite element) analysis programs; and miscellaneous problems. ESA

N92-28702# Army Lab. Command, Watertown, MA. Material Technology Lab.
PREDICTION OF COMPOSITE MATERIAL PROPERTIES USING TWO-DIMENSIONAL FINITE ELEMENT MICROMECHANICAL ANALYSIS Final Report
Panagiotis Blanas Apr. 1992 28 p
(AD-A250300; MTL-TR-92-18) Avail: NTIS HC/MF A03

Two-dimensional finite element analysis is employed to predict the mechanical properties of unidirectional composite materials with isotropic constituents. The composite is treated as a transversely isotropic but homogeneous continuum, and linear elastic behavior is assumed for the analysis. Axisymmetric and plane strain finite element formulations along with the constitutive relations for transversely isotropic materials are used to obtain the apparent properties of the composite. The results are compared with results from micromechanics equations and experimental data. GRA

N92-28724# National Academy of Sciences - National Research Council, Washington, DC. Marine Board.
NATIONAL CONFERENCE ON THE USE OF COMPOSITE MATERIALS IN LOAD-BEARING MARINE STRUCTURES. VOLUME 1: SUMMARY REPORT
1991 88 p Conference held in Arlington, VA, 25-26 Sep. 1990 Sponsored in part by US Coast Guard
(Contract DTCG-23-88-C-20055)
(PB92-163831) Avail: NTIS HC/MF A05

The purpose of the conference was to bring together leaders from industry, government, and academia to exchange ideas and lay the groundwork for future marine applications of composite materials by U.S. industry. The goals of the conference were the following: to promote technology transfer from other industries where the application of composites is more advanced; to identify opportunities for marine applications of composite materials; and to assess and recommend developments and research needed to advance those applications. This volume is the summary report of the Steering Committee, based on the conclusions and recommendations reached during and after the conference. Author

N92-28725# National Academy of Sciences - National Research Council, Washington, DC. Marine Board.
NATIONAL CONFERENCE ON THE USE OF COMPOSITE MATERIALS IN LOAD-BEARING MARINE STRUCTURES. VOLUME 2: CONFERENCE PROCEEDINGS
1991 264 p Conference held in Arlington, VA, 25-26 Sep. 1990 Sponsored in part by US Coast Guard
(Contract DTCG-23-88-C-20025)
(PB92-163849) Avail: NTIS HC/MF A12

The purpose of the conference was to bring together leaders from industry, government, and academia to exchange ideas and lay the groundwork for future marine applications of composite materials by U.S. industry. The goals of the conference were the following: to promote technology transfer from other industries where the application of composites is more advanced; to identify opportunities for marine applications of composite materials; and to assess and recommend developments and research needed to advance those applications. This volume contains the 21 papers presented during the first day of the conference and synopses of the three technical briefings given on the second day. Author

N92-28898# Naval Postgraduate School, Monterey, CA.
EFFECT OF ALUMINA PARTICLE ADDITIONS ON THE AGING KINETICS OF 2014-ALUMINUM MATRIX COMPOSITES M.S. Thesis
Christopher P. Harper Sep. 1991 83 p
(AD-A245949) Avail: NTIS HC/MF A05

Differential Scanning Calorimetry (DSC) was conducted on 2014 aluminum, 2014 aluminum reinforced with 10 and 15 percent by volume of alumina particles, 2024 aluminum, and a A1/4 percent Cu alloy. Electrical resistivity and matrix micro-hardness measurements were conducted on the 2014 aluminum alloy and the metal matrix composites (MMC) during isothermal aging. Transmission Electron Microscopy (TEM) and DSC were used to identify the metastable phases formed in the 2014 aluminum alloy. The effect of alumina particle addition on the precipitation, growth and thermal stability of the metastability phases in the 2014 aluminum alloy and MMC were studied. Results were used to characterize the effect of the alumina reinforcement on the aging kinetics of the 2014 aluminum alloy matrix. GRA

N92-28917# Naval Research Lab., Washington, DC.
ENERGETICS OF NANOSCALE GRAPHITIC TUBULES Interim Report, 1 Sep 1991 - 30 Aug. 1992
D. H. Robertson, D. W. Brenner, and J. W. Mintmire Apr. 1992 20 p
(NR Proj. RR0-1301)
(AD-A250165; TR-5) Avail: NTIS HC/MF A03

Using both empirical potentials and first-principles total energy methods, we have examined the energetics and elastic properties of all possible graphitic tubules with radii less than 0.9 nm. We find that the strain energy per carbon relative to an unstrained graphite sheet goes as the inverse square of the tubule radius, R, and is insensitive to other aspects of the lattice structure, indicating that relationships derivable from continuum elastic theory persist well into the small radius limit. We also predict that this strain energy is much smaller than that in highly-symmetric fullerene clusters with similar radii, suggesting a possible thermodynamic

preference for tubular structures rather than cage structures. The empirical potentials further predict that the elastic constants along the tubule axis generally soften with decreasing tubule radius, although with a distinct dependence on helical conformation.
GRA

N92-28918# Naval Research Lab., Washington, DC.
ELECTRONIC STRUCTURE OF FULLERENE TUBULES Interim Report, 1 Sep. 1991 - 30 Aug 1992
J. W. Mintmire, D. H. Robertson, B. I. Dunlap, R. C. Mowrey, and D. W. Brenner Apr. 1992 10 p
(NR Proj. RR0-2203)
(AD-A250166; TR-4) Avail: NTIS HC/MF A02

Recent reports suggest that graphitic tubules with diameters on the order of fullerene diameters have been synthesized. Such small-diameter tubules should have electronic properties related to those of two-dimensional graphite. We demonstrate by comparison with results from a first principles, self-consistent, all electron Gaussian-orbital based local-density functional approach that an all-valence tightbinding model can be expected to give a reasonable description of the electronic states of these tubules. In analyzing both high-symmetry tubules and lower-symmetry chiral tubules, we see that a relatively high carrier density could be expected for many of these structures. GRA

N92-28921# Naval Air Development Center, Warminster, PA. Air Vehicle and Crew Systems Technology Dept.
TENSILE AND INTERLAMINAR PROPERTIES OF GLARE (TRADE NAME) LAMINATES Final Report, 1 Oct. 1990 - 1 Jul. 1991
Jeffrey Cook and Mary E. Donnellan 1 Sep. 1991 24 p
(AD-A250188; NADC-91087-60) Avail: NTIS HC/MF A03

The mechanical properties of several GLARE laminates were investigated as part of an AKZO-coordinated round robin evaluation program. Tensile, floating roller peel, and three-point bend tests were performed on GLARE to determine its tensile properties, peel strength, and interlaminar shear strength, respectively. Strength, elongation to failure, and elastic modulus of the GLARE configurations tested in tension compared favorably to ARALL-4 and monolithic 2024-T3. Peel strength of ARALL-4 was found to be very low in the longitudinal fiber direction due to uninhibited crack front propagation along the fiber/adhesive layer interface. The peel strength of GLARE was found to be ten times higher than for ARALL in the longitudinal direction. Three point bend tests revealed an interlaminar shear strength of over 70 MPa.
GRA

N92-28953# Naval Research Lab., Washington, DC.
EXPERIMENTAL DETERMINATION OF DISSIPATED ENERGY DENSITY AS A MEASURE OF STRAIN-INDUCED DAMAGE IN COMPOSITES
Phillip W. Mast, Gerald E. Nash, John Michopoulos, Ray W. Thomas, and Robert Badaliance 17 Apr. 1992 77 p
(DA Proj. RS3-4-S-91)
(AD-A250322; NRL/FR/6383-92-9369) Avail: NTIS HC/MF A05

An approach to characterizing failure behavior and degree of load induced internal damage in composite materials and structures is formulated. This approach is based on a systematic experimental procedure to observe the response of composite materials subjected to multiaxial load environments. The energy dissipated by internal failure mechanisms is employed as a measure of internal damage and is characterized by an energy dissipation function, which is identified by means of a deconvolution procedure. Use of this information as a failure analysis and prediction tool is demonstrated by simulating the structural response of some naval structural components made from several different composite materials. In addition, a general theory for the derivation of the constitutive behavior of the damaged composites is presented.
GRA

N92-28959# Naval Postgraduate School, Monterey, CA.
THE EFFECTS OF THERMOMECHANICAL PROCESSING PARAMETERS ON ELEVATED-TEMPERATURE BEHAVIOR OF A 6061 Al-Al2O3 METAL MATRIX COMPOSITE M.S. Thesis
Thomas J. Schauder Mar. 1992 64 p
(AD-A247889) Avail: NTIS HC/MF A04

The effects of thermomechanical processing parameters on the elevated temperature behavior of a 6061 aluminum, Al-Al2O3 metal-matrix composite (MMC) have been studied. The same processing parameters were employed with unreinforced 6061 Al to provide a comparison. These materials were both thermomechanically processed at either 350 C or 500 C using two rolling schedules. Both schedules involved a constant strain per pass. Subsequent mechanical tests were conducted at temperatures 200 to 500 C and strain rates ranging from 6.7 x 10(exp -3) s(exp -1) to 1.3 x 10(exp -1) s(exp -1). The materials processed at 500 C exhibited higher strength when compared to those processed at 350 C for deformation temperatures below 350 C. Materials stabilized by annealing after completion of rolling displayed higher ductilities when compared to the as-processed materials, especially at lower testing temperatures. The peak ductilities of the MMCs occurred at testing temperatures near the prior rolling temperatures. Solution treatment prior to rolling and additional strains during rolling in excess of 2.5 appeared to have no effect on strength or ductility. GRA

N92-29152* National Aeronautics and Space Administration. Lewis Research Center, Cleveland, OH.
METHOD OF INTERCALATING LARGE QUANTITIES OF FIBROUS STRUCTURES Patent
James R. Gaier, inventor (to NASA) 17 Dec. 1991 6 p Filed 2 Nov. 1990 Supersedes N92-16025 (30 - 7, p 1055)
(NASA-Case-LEW-15077-1; US-Patent-5,073,412; US-Patent-Appl-SN-608493; US-Patent-Class-427-294; US-Patent-Class-118-416; US-Patent-Class-252-502; US-Patent-Class-423-447.2; US-Patent-Class-423-448; US-Patent-Class-423-460; US-Patent-Class-427-443.2) Avail: US Patent and Trademark Office

A method of intercalating large quantities of fibrous structures uses a rotatable reaction chamber containing a liquid phase intercalate. The intercalate liquid phase is controlled by appropriately heating, cooling, or pressurizing the reaction. Rotation of the chamber containing the fiber sample enables total submergence of the fiber during intercalation. Intercalated graphite fibers having metal-like resistivities are achieved and are conceivably useful as electrical conductors.
Official Gazette of the U.S. Patent and Trademark Office

N92-29192# Air Force Inst. of Tech., Wright-Patterson AFB, OH. School of Engineering.
DEVELOPMENT OF A STRATIFIED PLATE MODEL FOR COMPOSITE PANELS M.S. Thesis
Alan L. Lesmerises Mar. 1992 113 p
(AD-A248206; AFIT/GA/ENY/92M-02) Avail: NTIS HC/MF A06

A new model for composites represents a composite panel as an alternating stack of isotropic matrix and orthotropic fiber-dominated layers. An energy approach results in a set of partial differential equations and boundary conditions where the mechanical properties of the matrix and fibers appear separately. Two solution methods are developed. The first, called Strata Theory is developed for general applications, while the second, called the Exact Stratified Plate, is used as a benchmark for comparison to Strata Theory. Both solutions assume zero gradients of displacement through the thickness of a fiber layer. They are compared for an isotropic material and a two-ply composite with cross-plies, using simply-supported cases of a square plate and cylindrical bending. GRA

N92-29220# Aeronautical Research Inst. of Sweden, Stockholm. Structures Dept.
ON THE USE OF STRUCTURAL DYNAMIC EXPERIMENTAL METHODS FOR DAMAGE INSPECTION OF A GLASS FIBRE REINFORCED PLASTIC PLATE

Magnus Alvelid and Lars Gustavsson Jan. 1992 92 p Sponsored by Swedish National Board for Industrial and Technical Developement
(FFA-TN-1992-02; ETN-92-91394) Avail: NTIS HC/MF A05

Structural dynamic methods were used to investigate the effects of a cross section damage in the dynamic behavior of a composite plate made from glass fiber reinforced plastic. The possibilities to use either of these methods for damage inspection, when such materials are used in wind turbine blades, are considered. The plate was clamped at two ends and was free at the other two ends. Electrodynamic shakers were used to create vibrations in the plate. Four different analysis methods were used for investigating the effect of the damages: two measures of the global behavior of the plate (Frequency Response Function (FRF) measurements and a single tone excitation) and two for investigating local behavior (cross correlation and impedance measurements). The FRF method does not require measurements of the damaged spots and is considered the best one for real structure experiments. Since a damage of a certain size affects waves with corresponding wavelength, the size of the damage can be estimated. ESA

25 INORGANIC AND PHYSICAL CHEMISTRY

Includes chemical analysis, e.g., chromatography; combustion theory; electrochemistry; and photochemistry.

For related information see also *77 Thermodynamics and Statistical Physics.*.

N92-28240# Georgia Inst. of Tech., Atlanta. School of Aerospace Engineering.
COMBUSTION MECHANISMS OF SOLIDS Final Report, Oct. 1985 - Aug. 1988
E. W. Price, R. K. Sigman, and C. P. Markou 24 Feb. 1992 150 p
(Contract N00014-85-K-0803)
(AD-A247088) Avail: NTIS HC/MF A07

This report summarizes the studies of ingredient decomposition and sandwich burning during the period October 1985 to September 1988. A CO2 laser pyrolysis facility was built and preliminary tests on propellant ingredients were conducted. Results showed presence of a liquid state or reacting froth on the surface of all ingredients tested (AP, AN, PBAN, NMMO and BAMO-THF). Ingredient combustion behavior was studied by the edge burning sandwich method using sandwiches of AP with PBAN, NMMO and BAMO-THF. The effects of Fe2O3, Fe2O4 and catocene (10 percent level in the binder lamina) were evaluated. Burning with BAMO-THF was qualitatively similar to that with PBAN, with the correspondingly high burning rate. GRA

N92-28261# Iowa Univ., Iowa City. Dept. of Chemistry.
NEW METHODOLOGY FOR FLUOROCARBON SYNTHESIS Final Report, 15 Nov. 1988 - 14 Nov. 1991
Donald J. Burton Dec. 1991 41 p
(Grant AF-AFOSR-0134-89)
(AD-A247163; AFOSR-92-0162TR) Avail: NTIS HC/MF A03

Novel, general methods for the preparation of thermally stable perfluorinated organometallic reagents were developed. F-vinyl iodides were prepared as precursors to F-vinyl organometallics. A variety of polyfluorinated cadmium, zinc, and copper reagents were developed as synthetic reagents for the introduction of polyfluorinated alkyl, aryl, and allyl groups. SET chemistry was developed for the regiospecific addition of iodofluoroacetates and iodofluoromethylphosphonates to functionalized alkenes, and to accomplish a useful preparation of allylsulfonyldifluoroacetates and acetamides. Alkylation reactions and acylation reactions of alpha-fluorocarboxy phosphorus ylides were developed as a useful entry to precursors which could be easily hydrolyzed to alpha-fluoro ester and alpha-fluoro-beta-keto esters. GRA

N92-28287# Texas A&M Univ., College Station. Research Foundation.
MACROCYCLIC POLYCATION COMPLEXES FOR SECONDARY ANION BINDING, MOLECULAR RECOGNITION, AND CATALYSIS Final Report, 1 Jul. 1988 - 30 Sep. 1991
Arthur E. Martell 7 Feb. 1992 5 p
(Contract N00014-88-K-0451)
(AD-A246690) Avail: NTIS HC/MF A01

For the Co(2)-BISDIEN systems it was previously found that a tribridged dinuclear Co(2) complex of the macrocyclic ligand BISDIEN, in which hydroxide, dioxygen (as peroxo), and oxalato anions are bound simultaneously to both metal centers, undergoes a facile redox reaction in which the dioxygen is reduced to water and the oxalate is oxidized to carbon dioxide. This work was later extended to the study of tribridged dicobalt-BISDIEN complexes containing bound dioxygen (as bridging peroxo) and bridging catecholate and disulfocatecholate as reducing substrates. The bifunctional reductants in these systems undergo two-electron oxidation, while the four-electron reduction of dioxygen to water is accomplished by conversion of the Co(2) centers to the inert dinuclear Co(3)-BISDIEN complex. This study has now been extended to catalytic systems involving four-electron reduction substrates. Thus mesoxalate (ketomalonate) is converted entirely to carbon dioxide by the loss of four electrons, while the dioxygen is reduced to water, and the metal centers remain as cobalt(2). The system 2 proved to be catalytic, and several turnovers were observed in the presence of excess mesoxalate. For the binulcear Cu(1) macrocyclic complexes, earlier work by this research group demonstrated that dioxygen is complexed and activated by a dinuclear Cu(1) tetra Schiff base macrocyclic ligand, resulting in oxygen insertion (hydroxylation) into a benzene ring of the macrocyclic ligand. GRA

N92-28290# Harvard Univ., Cambridge, MA. Dept. of Chemistry.
ORTHOGONAL SELF-ASSEMBLY OF REDOX ACTIVE MOLECULES ON Pt AND Au: SELECTIVE REACTION OF DISULFIDE WITH Au AND ISONITRILE WITH Pt
James J. Hickman, Paul E. Laibinis, David I. Auerbach, Chaofeng Zou, and Timothy J. Gardner Feb. 1992 17 p
(Contract N00014-86-K-0756)
(AD-A246698; TR-46) Avail: NTIS HC/MF A03

Surfaces of platinum and gold adsorb ferrocenyl-12-dodecyl isocyanide, 1, and di(10-ferrocenecarbonyl-decyl) disulfide, 2, and yield self-assembled, redox active monolayers incorporating ferrocene groups. The values of E(sub 1/2) for alkyl ferrocenyl centers from 1 are approximately 300 mV more negative than acyl ferrocenyl centers from 2. This difference allows easy electrochemical measurement of surface concentrations of ferrocene centers from 1 and 2 on Pt or Au. One adsorbs selectively on Pt or Au compared to 2, but with different degrees of selectivity. Further, for Pt the selectivity depends on the surface pretreatment. The affinity of 2 for a Pt surface first exposed to an O2 plasma (oxidized Pt) is lower than that for a Pt surface exposed first to an O2 plasma and then to a H2 plasma (reduced Pt). The same two plasma treatments of Pt do not affect the binding of 1 on Pt. Thus, the selectivity of Pt for 1 vs. 2 is higher for the oxidized Pt approximately (200:1) compared to that for the reduced Pt approximately (20:1). The two plasma treatments of Au do not influence the selectivity for binding 1 vs. 2; the selectivity for binding 1 vs 2. on Au is approximately 8:1. By using the O2 plasma pretreatment and a 40:1 solution of 2:1, orthogonal self-assembly of 2 onto Au and 1 onto Pt can be effected when the two samples are derivatized in the same solution. GRA

N92-28300# Emory Univ., Atlanta, GA.
RELAXATION DYNAMICS OF HIGHLY EXCITED HALOGENS IN THEIR ELECTRONIC GROUND STATES Final Report, 1 Aug. 1989 - 15 Oct. 1991
Michael Heaven 21 Jan. 1992 32 p
(Grant AF-AFOSR-0249-88)
(AD-A247312; AFOSR-92-0161TR) Avail: NTIS HC/MF A03

Highly excited vibrational levels of ground state iodine, and

all levels of the metastable state, are involved in processes leading to the dissociation of I2 in the chemical oxygen iodine laser (COIL). Populations in these vibrationally and vibronically excited levels can be sensitively monitored by exciting laser induced fluorescence (LIF) from the valance to ion-pair transitions. However, accurate spectroscopic constants are required for the extraction of population distributions from spectral intensity data. Constants for the systems were obtained from rotationally resolved spectra for jet cooled, metastable I2. Studies of matrix isolated I2 and IBr were undertaken in order to examine their electronic relaxation dynamics in simple cryogenic solids, and to determine the A and A' state radiative decay rates. Large matrix shifts were observed, caused by solvation of the excited state dipole. It is probable that an optically pumped laser, operating on the D'-A' transition of Ar matrix isolated I2, could be constructed. GRA

N92-28341# Sandia National Labs., Albuquerque, NM.
SELECTIVE SUPPRESSION OF PHOTOCHEMICAL ETCHING: RAMAN SPECTROSCOPY FOR PRE-ETCH PROCESS SELECTION
C. I. H. Ashby and D. R. Myers 1992 14 p Presented at the 2nd International Conference on Laser Advanced Materials Processing, Nagaoka City, Japan, 7-12 Jun. 1992
(Contract DE-AC04-76DP-00789)
(DE92-010955; SAND-92-0447C; CONF-920657-2) Avail: NTIS HC/MF A03

Carrier-driven photochemical reactions require direct participation of free carriers for the chemical reaction to proceed. Therefore, they can be selectively suppressed by increasing the carrier recombination rate through creation of defects using ion implantation. The residual defect concentration following ion implantation should correlate with etching suppression. Changes in the Raman LO-phonon lineshape correlate well with the degree of etching suppression and predict etching behavior better than defect concentrations calculated with the Monte Carlo code, TRIM. Raman spectroscopy may be a useful pre-etch diagnostic to predict the degree of etching suppression resulting from a given implantation treatment. DOE

N92-28374*# National Aeronautics and Space Administration. Langley Research Center, Hampton, VA.
AN ANALYSIS OF COMBUSTION STUDIES IN SHOCK EXPANSION TUNNELS AND REFLECTED SHOCK TUNNELS
Casimir J. Jachimowski Jul. 1992 12 p
(RTOP 505-62-40-04)
(NASA-TP-3224; L-17025; NAS 1.60:3224) Avail: NTIS HC/MF A03

The effect of initial nonequilibrium dissociated air constituents on the combustion of hydrogen in high-speed flows for a simulated Mach 17 flight condition was investigated by analyzing the results of comparative combustion experiments performed in a reflected shock tunnel test gas and in a shock expansion tunnel test gas. The results were analyzed and interpreted with a one-dimensional quasi-three-stream combustor code that includes finite rate combustion chemistry. The results of this study indicate that the combustion process is kinetically controlled in the experiments in both tunnels and the presence of the nonequilibrium partially dissociated oxygen in the reflected shock tunnel enhances the combustion. Methods of compensating for the effect of dissociated oxygen are discussed. Author

N92-28391# Purdue Univ., West Lafayette, IN. Dept. of Chemistry.
THE EVALUATION OF RATE CONSTANTS FOR RAPID ELECTRODE REACTIONS BY USING MICROELECTRODE VOLTAMMETRY: VIRTUES OF MEASUREMENT AT LOWER TEMPERATURE
Lance K. Safford and Michael J. Weaver 28 Feb. 1992 37 p
(Contract N00014-91-J-1409)
(AD-A246760; TR-120) Avail: NTIS HC/MF A03

The prospects of utilizing electrochemical kinetic measurements at lower temperatures for evaluating reliably the standard rate constants, k(sub s), of rapid redox couples in nonaqueous media, specifically using microelectrode voltammetry, have been examined by means of digital simulations along with experiment. Cyclic voltammetric measurements were made between 200 and 300 K at a gold microdisk, for ferrocenium-ferrocene (Fc(sup +/o)), o-nitrotoluene(sup o/-), and nitromesitylene(sup o/-) redox couples in acetone, propionitrile, and butyronitrile, at a gold microdisk with scan rates from 100 to 10(exp 4) V s(exp -1). The latter two couples were selected as examples of systems that exhibit rapid, yet still unambiguously measurable, k(sub s) values at ambient temperatures; the more facile Fc(sup +/o) system has been suspected to yield immeasurably fast electrode kinetics using conventional techniques under these conditions. Sample simulated voltammograms were generated between 200 and 300 K for a sequence of activation enthalpies for electron exchange accounting also for known temperature dependent diffusion coefficients, solution resistance, and double-layer capacitance. GRA

N92-28728* National Aeronautics and Space Administration. Marshall Space Flight Center, Huntsville, AL.
CONTROLLED METHOD OF REDUCING ELECTROPHORETIC MOBILITY OF MACROMOLECULES, PARTICLES, OR CELLS
Patent
James M. VanAlstine, inventor (to NASA) 28 Apr. 1992 11 p Filed 18 Oct. 1990 Continuation-in-part of US-Patent-Appl-SN-376487, filed 7 Jul. 1989
(NASA-Case-MFS-26049-2-NP; US-Patent-5,108,568; US-Patent-Appl-SN-599601; US-Patent-Appl-SN-376487; US-Patent-Class-204-180.1; US-Patent-Class-204-183.3; US-Patent-Class-204-299R; Int-Patent-Class-G01N-27/26) Avail: US Patent and Trademark Office

A method of reducing electrophoretic mobility of macromolecules, particles, cells, and other substances is provided which comprises interacting in a conventional electrophoretic separating procedure, the substances with a polymer-linked affinity compound comprised of a hydrophilic neutral polymer such as polyethylene glycol bound to a second component such as a hydrophobic compound, an immunocompound such as an antibody or antibody active fragment, or a ligand such as a hormone, drug, antigen, or a hapten. The reduction of electrophoretic mobility achieved is directly proportional to the concentration of the polymer-linked affinity compound employed, and such reduction can comprise up to 100 percent for particular particles and cells. The present invention is advantageous in that electrophoretic separation can now be achieved for substances whose native surface charge structure had prevented them from being separated by normal electrophoretic means. Depending on the affinity component utilized, separation can be achieved on the basis of the specific/irreversible, specific/reversible, semi-specific/reversible, relatively nonspecific/reversible, or relatively nonspecific/irreversible ligand-substance interactions.
Official Gazette of the U.S. Patent and Trademark Office

N92-28743*# National Aeronautics and Space Administration. Ames Research Center, Moffett Field, CA.
HIGH QUALITY GAUSSIAN BASIS SETS FOR FOURTH-ROW ATOMS
Harry Partridge and Knut Faegri, Jr. (Oslo Univ., Norway) Mar. 1992 74 p Submitted for publication
(RTOP 506-43-11)
(NASA-TM-103918; A-92056; NAS 1.15:103918) Avail: NTIS HC/MF A04

Energy optimized Gaussian basis sets of triple-zeta quality for the atoms Rb-Xe have been derived. Two series of basis sets are developed: (24s 16p 10d) and (26s 16p 10d) sets which were expanded to 13d and 19p functions as the 4d and 5p shells become occupied. For the atoms lighter than Cd, the (24s 16p 10d) sets with triple-zeta valence distributions are higher in energy than the corresponding double-zeta distribution. To ensure a triple-zeta distribution and a global energy minimum, the (26s 16p 10d) sets were derived. Total atomic energies from the largest basis sets are between 198 and 284 (mu)E(sub H) above the numerical Hartree-Fock energies. Author

N92-28756* National Aeronautics and Space Administration. Lyndon B. Johnson Space Center, Houston, TX.
WATER ELECTROLYSIS Patent
Franz H. Schubert, inventor (to NASA) and David J. Grigger, inventor (to NASA) 5 May 1992 5 p Filed 1 Feb. 1991
(NASA-Case-MSC-21572-1-SB; US-Patent-5,110,436; US-Patent-Appl-SN-648933; US-Patent-Class-204-129; Int-Patent-Class-C25B-1/04; Int-Patent-Class-C25B-1/12) Avail: US Patent and Trademark Office

This disclosure is directed to an electrolysis cell forming hydrogen and oxygen at space terminals. The anode terminal is porous and able to form oxygen within the cell and permit escape of the gaseous oxygen through the anode and out through a flow line in the presence of backpressure. Hydrogen is liberated in the cell at the opposing solid metal cathode which is permeable to hydrogen but not oxygen so that the migratory hydrogen formed in the cell is able to escape from the cell. The cell is maintained at an elevated pressure so that the oxygen liberated by the cell is delivered at elevated pressure without pumping to raise the pressure of the oxygen. Author

N92-28769# Rensselaer Polytechnic Inst., Troy, NY.
KINETIC STUDIES OF METAL COMBUSTION IN PROPULSION Final Report, 1 Dec. 1988 - 29 Feb. 1992
Arthur Fontijn 17 Apr. 1992 15 p
(Grant AF-AFOSR-0086-89)
(AD-A250207; AFOSR-92-0390TR) Avail: NTIS HC/MF A03

Advanced propulsion system designs require quantitative understanding of the temperature-dependent kinetics of the gas-phase oxidation reactions of the metallic fuel components. To this end, experimental rate coefficient measurements have been made on aluminum and boron species, in the 440-1830 K temperature range, in a high-temperature fast-flow reactor (HTFFR). Results are reported for the following individual reactions: Al + N2O; AlO + Cl2; AlO + HCl; AlO + CH4; AlCl + CO2; AlCl + N2O; AlCl + HCl; BCl + CO2; BCl + N2O; BCl + SO2. The reaction products are discussed. For several series of homologous exothermic reactions, correlations are established between the activation barriers and the sums of the s-p (or sigma-pie) promotion energies and the ionization potentials of the metallic reactants minus the electron affinities of the oxidants. These series are the reactions of alkali metal atoms with N2O, group 2 and transition metal atoms with N2O, boron group atoms with N2O, and AlCl, BCl, BF and BH with O2, CO2, N2O and SO2. These correlations are explained on the basis of chemical resonance theory. Calculations based on this semi-empirical approach are shown to agree well with experiment. GRA

N92-28822# Sandia National Labs., Livermore, CA.
STOCHASTIC SIMULATION OF THE STRUCTURE AND PROPAGATION RATE OF TURBULENT PREMIXED FLAMES
S. Menon (Quest Integrated, Inc., Kent, WA.) and A. R. Kerstein 1992 18 p Presented at the 24th International Symposium on Combustion, Sydney (Australia), 5-10 Jul. 1992
(Contract DE-AC04-76DR-00789)
(DE92-006682; SAND-91-8742; CONF-920707-14) Avail: NTIS HC/MF A03

A stochastic simulation model of the wrinkled flamelet regime of turbulent premixed combustion is shown to exhibit several postulated scaling properties governing flame structure and propagation rate. The model, based on the linear-eddy model of molecular mixing in turbulent flow, incorporates laminar burning of flamelets and the resultant decrease of flame surface area, and flamelet convection and surface area growth due to turbulent stirring. Simulated realization, implemented on a one-dimensional domain representing a longitudinal line through the turbulent flame brush, exhibit linear dependence of the turbulent flame speed u(sub T) on the turbulent velocity fluctuation u', fractal flame structure, and a lower cutoff of fractal scaling that can be plausibly characterized either by the Kolmogorov scale L(sub K) approximately Re(-)3/4)L, where Re is the turbulence Reynolds number and L is the integral scale, or by the Gibson sale L(sub G) approximately (u'/S(sub L))(exp 3)L, where S(sub L) is the laminar flame speed. The latter ambiguity indicates that the Re values investigated computationally (up to 1000) are not high enough to fully resolve the high-Re limiting behavior, reflecting an analogous limitation of typical experimental configurations. The experimentally observed decrease of the fractal dimension D at low u'/S(sub L) is reproduced, and is interpreted as reflecting insufficient dynamic range to fully resolve the fractal regime rather than an intrinsic dependence of D on u'/S(sub L). DOE

N92-28827# Georgia Inst. of Tech., Atlanta. School of Chemical Engineering.
HIGH TEMPERATURE MEMBRANES FOR H2S AND SO2 SEPARATIONS
J. Winnick 1991 34 p
(Contract DE-FG22-90PC-90293)
(DE92-010451; DOE/PC-90293/T3) Avail: NTIS HC/MF A03

High temperature membrane separation techniques were applied to gas mixtures involved in coal utilization. For coal gasification, H2S was removed from the syn-gas stream, split into hydrogen, which enriches the syn-gas, and sulfur, which can be condensed from an inert gas sweep stream. For coal combustion, SO2 was separated from the flue gas, with concentrated SO3 produced as a by-product. Both processes appear economically viable but each requires fundamental improvements. Both the H2S cell and the SO2 cell require more efficient membranes and the H2S cell needs a more efficient anode. Membranes will be fabricated by either hot-pressing, impregnation of sintered bodies or tape casting. Research conducted during the present quarter is highlighted, with an emphasis on progress towards these goals. DOE

N92-28882# Defence Research Establishment, Ottawa (Ontario).
AN INVESTIGATION INTO TECHNIQUES FOR THE DETERMINATION OF MOISTURE CONTENT ON ACTIVATED CARBON
L. E. Cameron and S. H. Liang Sep. 1991 35 p
(AD-A245938; DREO-TN-91-25) Avail: NTIS HC/MF A03

The current method employed in the determination of the moisture content of activated carbon is the American Standard Test Method (ASTM) D-2867 (1976), using xylene extraction. However, this test is time-consuming and requires an elaborate experimental set-up. Furthermore, the ASTM has been found to be unsuitable for ASC/T carbon which contains triethylenediamine (TEDA). For this reason, alternatives to the ASTM were considered in this study. The ASTM method has been modified by replacing the extracting solvent xylene with toluene, to reduce the quantity of TEDA being collected with the water. Another alternative is the use of a convection oven where carbon samples were dried under three conditions: 150 C for 3 hours, 105 C for 3 hours and 105 C for 16 hours, and the moisture content results compared. This alternate method proves to be more efficient and the results obtained are comparable to that of the ASTM method. The optimum drying conditions for the accurate determination of moisture content on BPL, ASC and ASC/T carbons were determined to be 105 C for 60 minutes, 150 C for 90 minutes and 105 C for 90 minutes respectively. The last alternative considered was the use of a thermal analytical technique, namely Differential Scanning Calorimetry (DSC). It has been determined in this study that DSC can be used as an analytical tool for the determination of moisture content on carbons. However, better resolution of the DSC thermogram is required for precise measurements in moisture content determination. GRA

N92-28893# Wisconsin Univ., Madison.
THERMODYNAMIC AND KINETIC ASPECTS OF SURFACE ACIDITY
J. A. Dumesic 1992 36 p
(Contract DE-FG02-84ER-13183)
(DE92-011194; DOE/ER-13183/T1) Avail: NTIS HC/MF A03

Our research in the general area of acid catalysis involves the characterization of solid acidity and the corresponding assessment of catalytic performance of acidic materials. Acid

characterization studies are required to provide essential information about the type of acid site (i.e., Lewis versus Bronsted), the strength of the sites, and the mobility of molecules adsorbed on the acid sites. An accurate measure of acid strength is given by the heat of adsorption of a basic probe molecule on the acid site. A thermodynamic representation of the mobility of adsorbed species on these sites is given by the entropy of adsorption. Important techniques used in these acid site characterization studies include microcalorimetry, thermogravimetric measurements, temperature programmed desorption, infrared spectroscopy and solid state nuclear magnetic resonance. The combination of these acid site characterization studies with reaction kinetics measurements of selected catalytic processes allows the elucidation of possible relationships between surface thermodynamic and kinetic properties of acidic sites. Such relationships are important milestones in formulating effective strategies for the effective utilization of solid acid catalysts. Current work in this direction involves methylamine syntheses over various zeolites, and the basic probe molecules employed include ammonia, methanol, water and mono-, di- and tri-methylamines. DOE

N92-28894# Westinghouse Savannah River Co., Aiken, SC.
UNDERWATER VAPOR PHASE BURNING OF ALUMINUM PARTICLES AND ON ALUMINUM IGNITION DURING STEAM EXPLOSIONS
M. Epstein (Fauske and Associates, Inc., Burr Ridge, IL.) Sep. 1991 79 p Presented at the DOE AERO Meeting, San Francisco, CA, 13 Nov. 1991 Prepared in cooperation with Fauske and Associates, Inc., Burr Ridge, IL
(Contract DE-AC09-89SR-18035)
(DE92-011196; WSRC-RP-91-1001; CONF-9111204-1) Avail: NTIS HC/MF A05

Recently reported experimental studies on aluminum-water steam explosions indicate that there may be a critical metal temperature at which the process changes over from a physical explosion to one which is very violent and involves the rapid liberation of chemical energy. In this report we examine the hypothesis that vapor-phase burning of aluminum is a necessary condition for the occurrence of such 'ignition-type' steam explosions. An available two-phase stagnation flow film-boiling model is used to calculate the steam flux to the vaporizing aluminum surface. Combining this calculation with the notion that there is an upper limit to the magnitude of the metal vaporization rate at which the reaction regime must change from vapor phase to surface burning, leads to prediction of the critical metal surface temperature below which vapor phase burning is impossible. The critical temperature is predicted for both the aluminum-water pre-mixture configuration in which coarse drops of aluminum are falling freely through water and for the finely-fragmented aluminum drops in the wake of the pressure shock that 'triggers' the explosion. Vapor phase burning is predicted to be possible during the pre-mixture phase but not very likely during the trigger phase of a steam explosion. The implications of these findings in terms of the validity of the hypothesis that ignition may begin with the vapor phase burning of aluminum is discussed. Recently postulated, alternative mechanisms of underwater aluminum ignition are also discussed. DOE

N92-28896# Purdue Univ., West Lafayette, IN. Dept. of Chemistry.
ASYNCHRONOUS OPTICAL SAMPLING FOR LASER-BASED COMBUSTION DIAGNOSTICS IN HIGH-PRESSURE FLAMES Final Report, 15 Dec. 1988 - 14 Dec. 1991
G. B. King, N. M. Laurendeau, and F. E. Lytle 23 Apr. 1992 12 p
(Grant AF-AFOSR-0051-89)
(AD-A250206; AFOSR-92-0391TR) Avail: NTIS HC/MF A03

This is the final report on the development of a new laser-based combustion diagnostic for the quantitative measurement of both major and minor species in high-pressure flames. The technique, Asynchronous Optical Sampling (ASOPS), is a state-of-the-art improvement in picosecond pump/probe spectroscopy. A method is presented for vastly improving the output of the synchronously mode-locked dye laser systems. The beat frequency is increased to 155.7 kHz. Subnanosecond excited-state lifetimes for Na are obtained with only 128 averages, for the first time allowing data to be obtained within the time scale of turbulence. The first quantitative evaluation of the ASOPS technique in a flame environment is presented. GRA

N92-28942# Cornell Univ., Ithaca, NY.
CONVERSION OF ACETIC ACID TO METHANE BY THERMOPHILES Progress Report
S. Zinder 1991 6 p
(Contract DE-FG02-85ER-13370)
(DE92-010652; DOE/ER-13370/T1) Avail: NTIS HC/MF A02

The objective of this project is to provide an understanding of thermophilic anaerobic microorganisms capable of breaking down acetic acid, the precursor of two-thirds of the methane produced by anaerobic bioreactors. Recent results include: (1) the isolation of Methanothrix strain CALLS-1, which grows much more rapidly than mesophilic strains; (2) the demonstration that thermophilic cultures of Methanosarcina and Methanothrix show minimum thresholds for acetate utilization of 1-2.5 mM and 10-20 microns respectively, in agreement with ecological data indicating that Methanothrix is favored by low acetate concentration; (3) the demonstration of high levels of thermostable acetyl-coA synthetase and carbon monoxide dehydrogenase in cell-free extracts of Methanothrix strains CALS-1; (4) the demonstration of methanogenesis from acetate and ATP in cell free extracts of strain CALS-1; (5) the demonstration that methanogenesis from acetate required 2 ATP/methane, and, in contrast to Methanosarcina, was independent of hydrogen and other electron donors; (6) the finding that entropy effects must be considered when predicting the level of hydrogen in thermophilic syntrophic cultures; and (7) the isolation and characterization of the Desulfotomaculum thermoacetoxidans. Current research is centered on factors which allow thermophilic Methanothrix to compete with Methanosarcina. DOE

N92-28954# Army Chemical Research and Development Center, Aberdeen Proving Ground, MD. Ballistic Lab.
MULTICOMPONENT COMPARISON OF OPTICAL AND MASS SPECTROMETRIC DIAGNOSTICS IN LOW-PRESSURE FLAMES Final Report, Oct. 1989 - Oct. 1991
Stephen L. Howard, Randy J. Locke, David C. Dayton, Rosario C. Sausa, and Andrzej W. Miziolek Apr. 1992 28 p
(DA Proj. 1L1-61102-AH-43)
(AD-A250323; BRL-TR-3328) Avail: NTIS HC/MF A03

A new generation flat flame burner system for characterization of one-dimensional premixed laminar flames has been developed to study the detailed flame chemistry relevant to gaseous flames of burning propellants. This instrument incorporates several spectral techniques in one apparatus so that various diagnostic techniques can be quantitatively compared and the usable detection range (both in terms of spatial resolution and species detection) expanded. Features include molecular beam sampling with triple quadrupole mass spectrometric detection (MB/MS), laser-induced fluorescence (LIF), resonance-enhanced multiphoton ionization (REMPI), and temperature analysis by thermocouple and LIF. The intercomparison of different diagnostic techniques was accomplished on a stoichiometric 20 Torr C2H4/O2/Ar flame. Profiles for 0, H, and OH were obtained. Temperature profiles were taken of the unperturbed as well as perturbed (quartz sampler present) flames. As expected, the quartz sampler acted as a heat sink (approximately 200 K lower in the highest temperature flame regions). In general, the comparison between the different diagnostic techniques, is fair. Possible reasons for the minor discrepancies observed are discussed and include diffusion and thermal effects for the mass spectrometric technique as well as photochemical and stimulated emission effects for the laser diagnostics. GRA

N92-28973# Texas A&M Univ., College Station. Dept. of Chemistry.
MOLECULAR RECOGNITION IN THE OXIDATION OF CATECHOLS BY DICOBALT-BISDIEN DIOXYGEN COMPLEXES
F. S. Cezar, Bruno Szpoganicz, and Arthur E. Martell 30 Jan. 1992 22 p
(Contract N00014-88-K-0451)
(AD-A246456; TR-14) Avail: NTIS HC/MF A03

Formation and degradation of molecular species of the substrate-receptor complex (mu-4 methylcatechol) mu-peroxdicobalt(III) BISDIEN were studied by UV-vis spectroscopy. The family of absorbance curves show an intense charge transfer band with a maximum at 367 nm. The degradation redox reaction showed first order behavior. The reactive intermediate has a peroxo bridge and a bridging substrate, 4-methylcatechol coordinated to the two metal centers in the macrocyclic cavity. In the presence of excess substrate and dioxygen, the reaction is catalytic and the product is 3-methyl-cis, cis-muconic acid, which was separated by HPLC and characterized by mass spectrometry. When 3,5-di-t-butylcatechol was used in place of 4-methylcatechol, the redox reaction was not observed. This substrate cannot coordinate to the bimetallic center in the cavity of BISDIEN, and is not oxidized. The results are discussed on the basis of the selectivity of the receptor complex. GRA

N92-28982# Minnesota Univ., Minneapolis. Dept. of Chemical Engineering and Materials Science.
SIMULATIONS OF SOLVENT EFFECTS ON CONFINED ELECTROLYTES Technical Report No. 8, period ending 1 Jan. 1991
Lianrui Zhang, H. T. Davis, and Henry S. White 26 Feb. 1992 20 p
(Contract N00014-91-J-1927)
(AD-A246851) Avail: NTIS HC/MF A03

Monte Carlo simulations are reported for the solvent primitive model (SPM) of the electrical double layer at electrically charged and neutral surfaces. Both solvent and ions are modeled as hard spheres with interactions governed by hard sphere and Coulomb interactions. Density profiles of solvent and ions and electrostatic potential profiles are presented for 1:1 electrolyte concentrations of 1 and 2M at 300 K. Comparison of results at charged and neutral walls indicates that the solvent structure contributes significantly to the layering of ions and decrease of potentials in the double layer (a result not obtainable from simulations of the conventional primitive model (PM) of the double layer). The solvent induced steric ordering of electrolyte ions at a neutral wall create a space charge layer. Author (GRA)

N92-29091# MSNW, Inc., San Marcos, CA.
CHEMICAL VAPOR SYNTHESIS OF NIOBIUM ALUMINIDES Final Report, Apr. 1989 - Jul. 1991
J. Chin, J. H. Norman, and G. H. Reynolds Jan. 1992 129 p
(Contract F33615-89-C-5607)
(AD-A250332; WL-TR-91-4103) Avail: NTIS HC/MF A07

Chemical vapor deposition of niobium aluminides, niobium silicides, metal-rich compositions containing dispersed metallic phases, and ternary compositions in the titanium-niobium aluminum system was performed by several techniques. Process chemistry models were used to select deposition conditions and for correlation with experimental results on deposit compositions. Conditions were identified which permitted direct chemical vapor deposition of small samples of intermetallic foils. GRA

N92-29126# Scientific Research Associates, Inc., Glastonbury, CT.
NUMERICAL STUDIES OF LOW TEMPERATURE GALLIUM ARSENIDE BUFFER LAYERS AND THEIR INFLUENCE ON DEVICE OPERATION Annual Report, 15 Feb. 1991 - 15 Feb. 1992
H. L. Grubin and J. P. Kreskovsky Apr. 1992 12 p
(Contract F49620-91-C-0023)
(AD-A250309; SRA-R92-910034-1; AFOSR-92-0311TR) Avail: NTIS HC/MF A03

This report summarizes recent work on the development and application of an algorithm for studying charge transport in low temperature gallium arsenide (LT GaAs) buffer layers and their influence on device operation. During this reporting period the drift and diffusion equations were modified to include the transient dependence of electrons and holes for gallium arsenide. Calculations were performed for two-terminal, one and two-dimensional structures. Studies with the one-dimensional structures focussed on the trap kinetics. The two-dimensional studies represent a first attempt to examine the effects of clusters on transport through the LT GaAs. The one-dimensional studies are very briefly summarized, as the results were presented at the recent MRS symposium on LT materials, and will appear in the conference proceedings. A copy of the paper accompanies this report. The newer clustering results are also included. We note that these latter results are very preliminary and are included to indicate the future direction of our LT studies. GRA

N92-29185# Minnesota Univ., Minneapolis. Dept. of Chemical Engineering and Materials Science.
SUBSTRATE INDUCED ORDERING OF MOLECULAR ADSORBATES ON Au(111) Technical Report No. 7, period ending 1 Jan. 1991
Joachim H. Scott, Claudia R. Arana, Hector D. Abruna, Helen H. Petach, and C. M. Elliott 27 Feb. 1992 12 p
(Contract N00014-91-J-1927)
(AD-A246850) Avail: NTIS HC/MF A03

Adsorbed monolayers of Ru(bpy)2bpy-(CH2)x-(bpy)2(+) (x = 4 and 5) on the unreconstructed and reconstructed surfaces of Au(111) were imaged by scanning tunneling microscopy in dimethylformamide. On the reconstructed surface, the adsorbed films display highly-ordered patterns that are commensurate with the measured corrugation patterns of the substrate, STM images reveal a random spatial distribution. The key finding in our study is that the observed supramolecular structures of electroactive films on the reconstructed surface are commensurate with the long range atomic corrugation of the underlying substrate. In contrast, long range ordering is absent in films of I adsorbed on the unreconstructed and atomically flat Au(111) surface. GRA

N92-28821*# State Univ. of New York, Buffalo. Dept. of Mechanical and Aerospace Engineering.
THE COMPOSITIONAL STRUCTURE AND THE EFFECTS OF EXOTHERMICITY IN AN UNPREMIXED PLANAR JET FLAME
C. J. Steinberger, T. J. Vidoni, and P. Givi *In its* Large Eddy Simulations (LES) and Direct Numerical Simulations (DNS) for the Computational Analyses of High Speed Reacting Flows 30 Apr. 1992 42 p (For primary document see N92-28817 19-34)
Avail: NTIS HC/MF A06

26 METALLIC MATERIALS

Includes physical, chemical, and mechanical properties of metals, e.g., corrosion; and metallurgy.

N92-28237# North Carolina Univ., Chapel Hill. Dept. of Chemistry.
SYNTHESIS AND CHARACTERIZATION OF NEW LOW-DIMENSIONAL TRANSITION METAL COMPLEX CONDUCTORS Final Report, 1 Mar. 1989 - 30 Nov. 1991
William E. Hatfield 22 Apr. 1992 9 p
(Contract N00014-89-J-1734)
(AD-A249263) Avail: NTIS HC/MF A02

This final report contains a recapitulation of accomplishments and conclusions. A listing of all technical reports and journal articles emanating from the contract is included along with the names of all personnel who participated in the research. GRA

N92-28241# Boeing Co., Seattle, WA. Defense and Space Group.
X RAY COMPUTED TOMOGRAPHY OF FULL-SCALE CASTINGS Interim Report, Mar. - Dec. 1990

Gary E. Georgeson and Richard H. Bossi 31 Oct. 1991 58 p
(Contract F33615-88-C-5404)
(AD-A247101; WL-TR-91-4049) Avail: NTIS HC/MF A04

Computed Tomography (CT) has been investigated for its potential to evaluate full-scale castings. Currently, casting manufacturers suffer from a number of shortfalls in inspection which affect the use of castings in the aircraft/aerospace industry. An earlier task assignment indicated that CT has superior sensitivity to casting defects in small test coupons than conventional film radiography. But, as casting size and geometric complexity is increased, the CT sensitivity and measurement accuracy are reduced. In this task, CT testing was conducted to quantify the detection sensitivity and measurement accuracies possible on full-scale castings and to establish the CT system performance factors necessary for defect detection. The identification of cost-effective applications for CT in the casting industry was also sought. This effort has identified four areas in which CT can be cost-effectively utilized in casting manufacturing. These areas are new product development, early screening, manufacturing of complex geometries and critical region inspection. A CT system may be cost effective if the foundry has: (1) a large production rate (greater than $100M/year); (2) a high percentage of parts requiring internal dimensional measurements; (3) a large percentage of complex aerospace castings; or (4) material review board (MRD) authority for engineering buy-off of rejected castings. GRA

N92-28338# Ames Lab., IA.
EVALUATION OF PLASMA SPRAYED CRUCIBLE COATINGS FOR MELT PROCESSING COPPER-REFRACTORY METAL ALLOYS
D. J. Sordelet, T. W. Ellis, and F. C. Laabs 1992 6 p Presented at the 1992 International Thermal Spray Conference, Orlando, FL, 1-5 Jun. 1992
(Contract W-7405-eng-82)
(DE92-010871; IS-M-700; CONF-9206135-2) Avail: NTIS HC/MF A02

A study was made to access the suitability of several plasma arc sprayed coatings applied to graphite for application as containment crucibles for melt processing copper-refractory metal alloys. Coatings of Ta, TaC, TaB2 and ZrO2*8w/oY2O3 were evaluated and compared to uncoated graphite. The ZrO2*8w/pY2O3 coating was sprayed over a tungsten bond coat. Prealloyed samples of Cu-15v/o Cr and Cu-15v/o Nb were placed within the crucibles and heated inductively to 1800 and 2100 C, respectively. Compatibility of the coating-alloy system was evaluated by optical and scanning electron microscopy, EDS, XRD, and combustion chromatography. DOE

N92-28390# Pennsylvania State Univ., University Park. Dept. of Materials Science and Engineering.
MECHANISMS OF FRACTURE AND CREEP OF STRUCTURAL ALLOYS Annual Report No. 4, 1 Dec. 1990 - 31 Dec. 1991
D. A. Koss 30 Mar. 1992 28 p
(Contract N00014-91-J-1414)
(AD-A248701) Avail: NTIS HC/MF A03

Progress is reviewed for a research program which focuses on two aspects which limit the performance of structural alloys. First, in a study generic to a wide range of materials, we are determining the mechanisms, as well as local failure criteria, by which voids or pores grow and link during ductile fracture due to damage accumulation. Secondly, in a study focused specifically at high temperature titanium alloys, we are examining the elevated temperature strength and deformation behavior of a novel, age-hardenable beta titanium alloy. Progress for the period December 1, 1990 to December 31, 1991 is reviewed for the following projects: (1) modeling the effects of stress state on void linking; (2) three-dimensional void growth and linking during ductile fracture; and (3) elevated temperature behavior of a novel age-hardenable beta titanium alloy. GRA

N92-28426# Reinhart and Associates, Inc., Austin, TX.
SURFACE RESIDUAL STRESS ANALYSIS OF METALS AND ALLOYS Final Report, 4 Apr. 1991 - 4 Feb. 1992
Teodoro Leon-Salamanca and Eugene R. Reinhart 4 Feb. 1992 31 p
(Contract N00019-91-C-0062)
(AD-A248372) Avail: NTIS HC/MF A03

The critically refracted longitudinal wave (CRLW) technique was used to establish how feasible it is to measure stress changes at the surface and interior of a material, in particular naval airframe metals such as Ti-6Al-4V, 6061-T651 aluminum, and 4340 steel. The CRLW propagation characteristics were found to be potentially practical if use of the 2P wave is implementable to have it as a reference wave. The CRLW technique was effective in detecting stress gradients in bent plates by measuring the acoustoelastic effect on the longitudinal wave velocity. The CRLW technique was applied in the range of 1.0 to 10 MHz and the expected longitudinal wave velocity changes followed the expected trends in the Al6061-T651 and 4340 steel plates (0.50 inch thick). The longitudinal wave velocity changes measured in the Ti-6Al-4V plate did not follow the expected trends probably due to its thickness (0.25 inch). GRA

N92-28574# Technische Univ., Delft (Netherlands). Faculty of Aerospace Engineering.
THE EFFECT OF INTERMEDIATE HEAT TREATMENTS ON OVERLOAD INDUCED RETARDATION DURING THE FATIGUE CRACK GROWTH IN AN Al-ALLOY
M. R. Ling and J. Schijve Mar. 1991 16 p
(LR-651; ETN-92-91396) Avail: NTIS HC/MF A03

Crack growth fatigue tests were carried out on 2024-T3 specimens. Constant amplitude loading was periodically interrupted by 10 overload cycles. Intermediate heat treatments (T4) were applied to remove the residual stress in the crack tip zone and the crack closure wake behind the crack tip. Retardation effects induced by crack closure due to the previous load history, were fully erased by the heat treatments. Overload effects were easily introduced again by new overload cycles afterwards. Crack growth rate results and fractographic observations indicate that primary crack tip plastic deformation (in virgin material) is more effective for crack extension than secondary plastic deformation in an existing plastic zone. This conclusion is significant for cycle by cycle crack prediction models for variable amplitude loading. ESA

N92-28576# Technische Univ., Delft (Netherlands).
THE APPLICATION OF CARBON FIBRES IN ARALL LAMINATES
C. A. J. R. Vermeeren Sep. 1991 61 p
(LR-658; ETN-92-91398) Avail: NTIS HC/MF A04

The mechanical properties of CARE (carbon reinforced) are evaluated. Results on tensile strength, elastic modulus, blunt notch properties, and several kinds of fatigue are demonstrated for CARE with six different carbon fibers. The results are compared with the existing aramid ARALL and GLARE materials. Solutions to solve the galvanic corrosion problem are discussed. An investigation of titanium alloys and thermoplastic adhesives, for elevated temperature ARALL (up to 250 C) are discussed. CARE offers superior mechanical properties: high strength, high modulus materials with excellent fatigue performance. Isolating the carbon prepreg with a thermoplastic adhesive, or with a glass prepreg, solves the potential galvanic corrosion problem. Good mechanical and fatigue properties are achieved up to 250 C for ARALL with thermoplastic adhesive, carbon fibers and titanium alloy sheets. ESA

N92-28578# Technische Univ., Delft (Netherlands). Faculty of Aerospace Engineering.
THE STRESS CORROSION CRACKING BEHAVIOR OF AlLi 2090-T83 IN SUBSTITUTE OCEAN WATER
A. Buis and J. Schijve Nov. 1991 32 p
(LR-661; ETN-92-91400) Avail: NTIS HC/MF A03

The stress-corrosion (SC) behavior of the alloy 2090-T83 was

evaluated in substitute ocean water (SOW) under constant immersion. For comparison, some tests were performed in a 3.5 wt percent NaCl solution, and, as a reference, the cracking behavior was also studied in N2 gas. Smooth specimens machined from a 4 mm thick sheet were tested in the longitudinal and in the long transverse direction utilizing both the constant load and the slow strain rate (SSR) techniques. Both methods suggested that alloy was susceptible to stress corrosion cracking (SCC), SOW being a much more aggressive solution for SCC than the NaCl solution. The SCC mechanism was studied employing the SSR method. The effects of strain rate, de-aeration of the solution, or electrode potential were examined. During SSR testing, either the corrosion potential or the current at constant potential was monitored. The fracture specimens were examined in a scanning electron microscope (SEM) equipped with a backscatter electron detector and an energy dispersive x-ray analysis system to distinguish various local cracking and corrosion morphologies. Both SEM and a transmission electron microscope were used for characterizing the microstructure of the alloy. Based on the observations, the SCC of 2090 in SOW is a result of local anodic dissolution along subgrain boundaries and is primarily induced by the preferential dissolution of T(1) precipitates. Al6(Fe, Cu) constituents played a minor role in the SCC process. ESA

N92-28691# National Aerospace Lab., Amsterdam (Netherlands). Structures and Materials Div.
EFFECT OF COOLING RATE ON CORROSION PROPERTIES OF HIGH STRENGTH ALUMINIUM ALLOYS UNDER ATMOSPHERIC CONDITIONS
L. Schra and W. G. J. tHart 19 Apr. 1990 33 p
(Contract NIVR-1869)
(NLR-TP-90138-U; ETN-92-91534) Avail: NTIS HC/MF A03

Long term outdoor exposure tests to investigate the effect of cooling rate on corrosion and stress corrosion properties of extruded rods of the high strength aluminum alloys, 2024-T4, 2023-T6, 7075-T6, and 7075-T73, are reported. The 2024 alloy exhibited a high susceptibility to Stress Corrosion Cracking (SCC) irrespective of best treatment and cooling rate, whereas 7075-T6 was susceptible to SCC only at high cooling rates. All tested alloys showed an abrupt change from low to high SCC growth resistance at specific cooling rates. The 2024 alloy proved to be more prone to exfoliation corrosion than 7075. The corrosion susceptibility decreased at high cooling rates for 2024-T4 and 7075-T6, whereas the cooling rate had no effect for 2024-T6 and 7075-T73. Both the SCC and exfoliation corrosion behavior could be predicted by accelerated laboratory test methods. ESA

N92-28763# Allied-Signal Aerospace Co., Kansas City, MO.
EROSION OF STAINLESS STEEL BY ULTRASONIC CLEANING: A PRELIMINARY STUDY
W. B. Harding Apr. 1992 7 p
(Contract DE-AC04-76DP-00613)
(DE92-012566; KCP-613-4547) Avail: NTIS HC/MF A02

The erosion of stainless steel during ultrasonic cleaning was measured using several ultrasonic frequencies and powers and several water-based and solvent cleaning liquids. DOE

N92-28794# National Aerospace Lab., Amsterdam (Netherlands). Structures and Materials Div.
OUTDOOR CORROSION TESTING OF ALUMINIUM-LITHIUM ALLOYS
L. Schra, W. G. J. tHart, and J. A. M. Boogers 1 Aug. 1990 62 p
(Contract NIVR-01404-N)
(NLR-TP-90272-U; ETN-92-91395) Avail: NTIS HC/MF A04

The results of outdoor corrosion and stress corrosion tests, conducted on Al-Li plate and sheet materials for 3 and almost 5 years respectively, are summarized. The results of outdoor corrosion experiments are given. The peak aged XXXA-T651 (8090-T651) exhibited greater exfoliation corrosion resistance than 2047-T351 and 2324-T39 plate. The 2091-T3 and 2024-T3 sheet were found to be unsuspectable to exfoliation corrosion. The exfoliation susceptibility of 2091 increased with increased ageing. The 8090-T8 sheet showed blistering rather than exfoliation corrosion. The exfoliation attack of the plate material was generally much more severe than that of the sheet material. The MASTMAASIS test seems to be most promising for predicting the exfoliation corrosion resistance of Al-Li alloys in natural environments. There is a need for a simple and rapid immersion test, because the EXCO test proved to be unreliable for characterizing the exfoliation susceptibility of Al-Li alloys. The results of the stress corrosion tests are given. The Stress Corrosion Cracking (SCC) initiation resistance of XXXA-T651 plate was similar to or slightly better than that of 2024-T351 and 2324-T39 plate. For SCC growth the ranking of materials depended on the influence of Corrosion Product Wedging (CPW) on SCC growth. When the influence was small, as in the first 1 1/2 years of testing, 2024-T351 and 2324-T39 exhibited slower crack growth; whereas XXXA-T651 was superior when there was a significant influence, as in the latter part of testing. Alternate immersion SCC initiation testing in synthetic seawater resulted in the same trends as outdoor exposure. SCC Growth in laboratory test environments was greatly influenced by CPW. ESA

N92-28823# Deutsche Forschungsanstalt fuer Luft- und Raumfahrt, Cologne (Germany, F.R.). Abt. Metallurgie.
EFFECT OF SOLIDIFICATION TECHNIQUE AND CONSOLIDATION METHOD ON THE PROPERTIES OF RAPIDLY SOLIDIFIED Al-Fe ALLOYS Ph.D. Thesis - Technische Hochschule Aachen
Susanna Hodiamont Jul. 1991 120 p In GEORGIAN Sponsored by DFG
(DLR-FB-91-24; ISSN-0939-2963; ETN-92-91065) Avail: NTIS HC/MF A06; DLR, Wissenschaftliches Berichtswesen, VB-PL-DO, Postfach 90 60 58, 5000 Cologne, Fed. Republic of Germany, HC 46.50 DM

The consolidation process of Al-Fe alloys is investigated and optimized. An attempt is made to preserve the beneficial microstructure of the as-atomized powders and ribbons. Due to the preservation of the as-atomized microstructure, the mechanical properties of the alloy can be significantly increased. Changes in microstructure which occur during consolidation are investigated and correlated to the values of the mechanical properties. Electron microscope images of alloy structures illustrate the results obtained using different alloying techniques. ESA

N92-28854# Pennsylvania Univ., Philadelphia. Dept. of Materials Science and Engineering.
DIFFUSION-CONTROLLED DECOHESION USING A Cu-Sn ALLOY AS A MODEL SYSTEM
D. Bika and C. J. McMahon, Jr. 1991 6 p Presented at the Annual Fall Meeting of the Materials Research Society, Boston, MA, 2-6 Dec. 1991
(Contract DE-FG02-87ER-45290)
(DE92-011645; CONF-911202-71) Avail: NTIS HC/MF A02

This research deals with a mode of brittle intergranular fracture in which a surface adsorbed embrittling element is driven into a grain boundary as a result of the application of a tensile stress across the boundary. A Cu-Sn(8 percent) alloy was employed to explore this phenomenon, since tin is a surface-active element, and this alloy is known to suffer intergranular weakness at elevated temperatures. Intergranular cracking occurred by brittle, discontinuous crack advance at 265 C in vacuum with an average rate of 0.1 micron/sec. This behavior is analogous to sulfur-induced stress-relief cracking in steels and several cases of liquid-metal embrittlement, suggesting that this phenomenon has a generic nature. DOE

N92-28856# Oak Ridge National Lab., TN.
COMPOSITIONAL DISORDER, MAGNETISM, AND THEIR INTERPLAY IN METALLIC ALLOYS
D. D. Johnson (Sandia National Labs., Albuquerque, NM.), J. B. Staunton (Warwick Univ., Coventry, England), F. J. Pinski (Cincinnati Univ., OH.), and B. L. Gyorffy (Bristol General Hospital, England) 1991 14 p Presented at the Annual Fall Meeting

of the Materials Research Society, Boston, MA, 2-6 Dec. 1991 (Contract DE-AC05-84OR-21400)
(DE92-011671; CONF-911202-74) Avail: NTIS HC/MF A03

Chemical disorder leads to many intriguing phenomena in alloys which have yet to be fully understood, particularly those phenomena occurring when chemical and magnetic effects interplay with one another. For example, magnetic order gives rise to chemical ordering in alloys, as in Ni-rich NiFe alloys. Two examples of the interplay of chemical disorder and magnetism will be discussed. Our recently developed ab-initio Landau (mean-field) theory for calculating the chemical-chemical, magneto-chemical, and magnetic-magnetic correlation functions in substitutional random alloys is used to describe electronic/magnetic mechanisms (e.g., in FeV) which give rise to the chemical short-range order as determined by neutron, X-ray, or electron diffuse scattering intensities. New developments within this approach that account for charge rearrangement effects will be mentioned. These calculations are performed within the multiple-scattering framework, developed by Korringa, Kohn, and Rostoker (KKR), combined with the coherent potential approximation (CPA) to describe the disorder. This approach allows a first-principles description of the electronic structure of the high-temperature, chemically disordered state and its instability in ordering at low temperatures. This method provides not only a direct comparison of diffuse scattering data with theory but a means to understand more fully the underlying mechanisms which drive chemical and/or magnetic ordering. DOE

N92-28976# Naval Postgraduate School, Monterey, CA.
PHASE TRANSFORMATIONS IN Ti3Al BASED ALLOY M.S. Thesis
Emmanuel Tsourdalakis Dec. 1991 67 p
(AD-A246464) Avail: NTIS HC/MF A04

A 'super alpha(sub 2)' titanium-aluminide based alloy, with additions of niobium, chromium, and tantalum, was studied with respect to phase transformations under different heat treatments, aging times, and temperatures. Samples were heated at temperatures ranging between 1000 - 1300 C and quenched to retain the high temperature microstructure. Quenched samples were aged between 500 - 850 C for various times, and transformations were studied using dilatometry, x-ray analysis, transmission electron microscopy, and microhardness testing. It was found that at around 650 C the transformation of beta yields alpha(sub 2) occurred after two hours of aging, while below this temperature, aging for up to 100 hours at 500 C produced only the beta yields omega transformation with very little alpha 2. Also, an 'omega-type' phase was observed at this aging temperature. Microhardness measurements and x-ray diffraction confirmed the above results. Quenching from high temperature showed the presence of lath-like features which were poor in Ta and Cr and had the B2 structure. GRA

N92-29094* National Aeronautics and Space Administration. Goddard Space Flight Center, Greenbelt, MD.
HIGH TEMPERATURE SOLDER DEVICE FOR FLAT CABLES Patent
Carl L. Haehner, inventor (to NASA) 30 Jun. 1992 7 p Filed 20 Jun. 1991 Supersedes N91-283363 (29 - 20, p 3317)
(NASA-Case-GSC-13344-1; US-Patent-5,126,527; US-Patent-Appl-SN-718046; US-Patent-Class-219-85.15; US-Patent-Class-219-85.19; Int-Patent-Class-B23K-1/00) Avail: US Patent and Trademark Office

A high temperature solder device for flat cables includes a microwelder, an anvil which acts as a heat sink and supports a flexible flat ribbon cable that is to be connected to a multiple pin connector. The microwelder is made from a modified commercially available resistance welding machine such as the Split Tip Electrode microwelder by Weltek, which consists of two separate electrode halves with a removable dielectric spacer in between. The microwelder is not used to weld the items together, but to provide a controlled compressive force on, and energy pulse to, a solder preform placed between a pin of the connector and a conductor of the flexible flat ribbon cable. When the microwelder is operated, an electric pulse will flow down one electrode, through the solder preform and back up the other electrode. This pulse of electrical energy will cause the solder preform to heat up and melt, joining the pin and conductor.
Official Gazette of the U.S. Patent and Trademark Office

N92-29164 National Physical Lab., Teddington (England). Div. of Materials Metrology.
SOME EXPERIMENTS TO DETERMINE THE EFFICIENCY OF COLLECTION OF ALUMINA PARTICLES BY ELECTRON BEAM BUTTON MELTING IN A NICKEL-BASE SUPERALLOY, AP1
S. Chakravorty and P. N. Quested Nov. 1991 79 p Sponsored in part by Cameron Iron Works Ltd; Howmet Inc.; Imphy S.A.; Inco Alloys Ltd.; Ireland Alloys Ltd.; Rolls-Royce Plc; Special Melted Products Ltd.; Stocksbridge Engineering Steels; and Willan Metals Ltd.
(NPL-DMM(A)-42; ISSN-0959-2423; ETN-92-91378) Copyright Avail: National Physical Lab., Teddington, Middlesex, TW11 0LW, England

Seeding experiments to determine collection efficiency of 50 micrometer size alumina particles in alloy AP1 by the Electron Beam Button Melting (EBBM) method were performed at three dopant levels, 50 ppm, 0.5 ppm and 0.05 ppm. The recovery of alumina particles doped at 50 ppm level were found to be greater than 90 percent by this method. However, at lower concentration, the recovery rate is less clearly defined due to high yttrium contamination in the manufactured material. The effects of mass, temperature and pressure during EBBM in the characterization and recovery of 50 ppm doped material were also investigated and remelting of buttons at all dopant levels was performed to reaffirm particle collection efficiency. ESA

N92-29170# Department of the Navy, Washington, DC.
VOLATILE CVD PRECURSORS BASED ON COPPER ALKOXIDES AND MIXED GROUP IIA-COPPER ALKOXIDES Patent Application
Andrew Purdy, inventor (to Navy) 31 Jan. 1992 10 p
(AD-D015264; US-Patent-Appl-SN-828634) Avail: NTIS HC/MF A02

This invention relates to novel chemical compositions for use in chemical vapor deposition. More specifically, it relates to fluorinated copper alkoxides and fluorinated calcium-copper, strontium-copper, and barium copper alkoxides having superior physical properties for application in chemical vapor deposition to form thin films. The compounds should also be useful for the preparation of calcium, strontium, and barium-copper oxides by sol-gel processes. Chemical vapor deposition is a process in which one or several precursor compounds and reactant gases are introduced into a reactor in the vapor phase. The reactor consists of a chamber containing the substrate upon which material is deposited from vapor as a thin films. GRA

27 NONMETALLIC MATERIALS

Includes physical, chemical, and mechanical properties of plastics, elastomers, lubricants, polymers, textiles, adhesives, and ceramic materials.

For composite materials see *24 Composite Materials*.

N92-28249# Army Materials Technology Lab., Watertown, MA.
Mg-Si-Al OXYNITRIDE GLASSES Final Report
Donald R. Messier and Robert P. Gleisner Feb. 1992 16 p
(DA Proj. 1L1-61102-AH-42)
(AD-A247593; MTL-TR-92-6) Avail: NTIS HC/MF A03

The glass-forming region at 1650 C was investigated for Mg-Si-Al-O-N compositions containing up to 20 equivalent percent N (16 atomic percent), and glass batches of up to 30 g were prepared and characterized. Glasses containing up to 8 atomic percent N were grey colored, but transparent, while crystal-free glasses with higher N contents were unattainable. Little, if any, N loss occurred during melting; glass density, microhardness, and elastic modulus all increased with N content. The origins and

consequences of the metallic precipitates that cause the grey color are discussed in the context of the literature on glasses prepared under reducing conditions. GRA

N92-28250# Army Materials Technology Lab., Watertown, MA.
MULTIPHASE STRUCTURE OF A SEGMENTED POLYURETHANE: EFFECTS OF TEMPERATURE AND ANNEALING
Yingjie Li (State Univ. of New York, Stony Brook.), Tong Gao (State Univ. of New York, Stony Brook.), Jian Liu (State Univ. of New York, Stony Brook.), Kung Linliu (State Univ. of New York, Stony Brook.), Benjamin Chu (State Univ. of New York, Stony Brook.), and C. R. Desper Feb. 1992 35 p
(DA Proj. 1L1-61102-AH-42)
(AD-A247594; MTL-TR-92-4) Avail: NTIS HC/MF A03

The multiphase structure and related relaxations of a segmented polyurethane were characterized by using a combination of differential scanning calorimetry (DSC), dynamical mechanical analysis (DMA), stress-strain test, thermally stimulated discharge current (TSDC), and synchrotron small-angle X-ray scattering (SAXS). The polymers studied consisted of 4,4'-diphenylmethane diisocyanate (MDI) and 1,4'-butanediol (BD) hard segments with soft segments comprised of PTMO end-capped with PPO at a 70/30 PTMO/PPO weight ratio. The results showed a soft segment glass transition temperature (Tg,s) which is significantly higher than the Tg,s (-84 C) of the corresponding pure soft segment, suggesting an incomplete phase separation behavior for the soft segments. The specimen lost its mechanical strength at above 200 C while DSC indicated an endotherm ca. 195 C due to the hard segment domain consisting of dissolution into the soft segment matrix. TSDC showed interfacial polarization due to the multiphase characteristics. Synchrotron SAXS scanning from 26 C to 250 C indicated that the sample structure remained stable with increasing temperature. A small change around 75 C was attributed to the glass transition of the amorphous hard segment domain. Phase mixing took place when the temperature was above 190 C, in agreement with the DSC and DMA results. GRA

N92-28251# Massachusetts Inst. of Tech., Cambridge. Dept. of Chemical Engineering.
CHAIN FOLDING IN EBEE SEMICRYSTALLINE DIBLOCK COPOLYMERS
K. C. Douzinas and R. E. Cohen 9 Mar. 1992 29 p
(Contract N00014-91-J-1045)
(AD-A247595; TR-7) Avail: NTIS HC/MF A03

X-ray pole figure analysis and small angle x-ray scattering were used to determine the lattice unit cell orientation with respect to the lamellar microstructure for semicrystalline diblock copolymers of ethylene co-butylene b-ethylethylene (EBEE). The x-ray data indicate that the orientation of the crystallized EB chains is perpendicular to the lamellar normals, unlike the chain cry folding which was observed in semicrystalline homopolymers and proposed for semicrystalline diblock copolymers where the crystallized chains align roughly parallel to the lamellar normals. The unusual chain folding observed for EBEE is attributed to the influence of topological constraints in the EB blocks which crystallize with the amorphous lamellar microdomains present in the heterogeneous melt phase of the block copolymers. GRA

N92-28291# Harvard Univ., Cambridge, MA. Dept. of Chemistry.
CORRELATION BETWEEN SURFACE FREE ENERGY AND SURFACE CONSTITUTION Interim Report
Manoj K. Chaudhury and George M. Whitesides Feb. 1992 19 p
(Contract N00014-86-K-0756)
(AD-A246699; TR-47) Avail: NTIS HC/MF A03

Self-assembled monolayers (SAMs) of alkylsiloxanes on elastomeric polydimethylsiloxane (PDMS) were used as model systems to study interactions between surfaces. Surface free energies of these chemically modified surfaces were estimated by measuring the deformations that resulted from the contact between small semispherical lenses and flat sheets of the elastomer under controlled loads. The measured surface free energies correlated with the surface chemical compositions of the SAMs and were commensurate with the values estimated from the measurements of contact angles. This study provides, for the first time, direct experimental evidence for the validity of estimates of the surface free energies of low-energy solids obtained from contact angles. GRA

N92-28323# California Univ., Irvine. Dept. of Chemistry.
SYNTHESIS AND STUDY OF METALLONITRIDE COMPLEXES AND POLYMERS Final Report, 1 Jan. - 30 Nov. 1991
Nancy M. Doherty 2 Mar. 1992 7 p
(Grant AF-AFOSR-0179-91)
(AD-A248577; AFOSR-92-0224TR) Avail: NTIS HC/MF A02

The synthesis and chemistry of compounds in which two transition metal centers are bridged by a single nitrogen atom, the bridging nitride ligand, has been investigated. These studies have focused on understanding the chemical and physical properties of the M(N)M unit in order to explore its use as a building block for new transition metal-containing polymers. The approach to this chemistry has involved parallel exploration of molecular nitride-bridged species, which serve as model systems for developing the chemistry of these compounds, and of extended structures incorporating metal-nitrogen-metal linkages. Supporting studies on the reactivity and spectroscopy of silylimido precursor compounds, which are used in the synthetic route to nitride-bridged structures, have been performed. Extension of this chemistry to phosphide-bridged species has been explored. GRA

N92-28339# Argonne National Lab., IL.
EFFECT OF METALLIC COATING PROPERTIES ON THE TRIBOLOGY OF OIL-LUBRICATED COATED-CERAMICS
O. O. Ajayi, G. R. Fenske, A. Erdemir, R. A. Erck, J. H. Hsieh, and F. A. Nichols 1992 11 p Presented at the International Conference on Practical Tribology, Moscow, USSR, 4-9 May 1992
(Contract W-31-109-eng-38)
(DE92-010904; ANL/CP-75375; CONF-9205132-1) Avail: NTIS HC/MF A03

The friction and wear behavior of zirconia ceramics lubricated with solid coatings (Ag, Au, and Nb), deposited by ion-beam-assisted-deposition (IBAD) techniques, and a polyol-ester-based synthetic oil are presented. Although the simultaneous use of soft (e.g., Ag and Au) solid lubricants in conjunction with the synthetic lubricant significantly reduces the friction and wear under boundary lubrication at temperatures up to 250 C, these results demonstrate that the durability of the soft films was poor. In contrast, durability of Nb coating (in terms of chemical reactivity and adhesion during the tribo-tests) was better than that of the Ag or Au films. However, the friction and wear behavior of the Nb-coated films was poorer than that of the ceramics coated with Ag or Au. DOE

N92-28360# Case Western Reserve Univ., Cleveland, OH.
PROCEEDINGS OF ASILOMAR CONFERENCE ON POLYMERIC MATERIALS Final Report
Eric Baer Mar. 1992 21 p Conference held in Pacific Grove, CA, 9-12 Feb. 1992
(Contract DAAL03-92-C-0028)
(AD-A249366; ARO-29648.1-MS-CF) Avail: NTIS HC/MF A03

The conference was held as scheduled. A report has been prepared which contains the program, a list of attendees and a copy of the abstracts of the papers presented at the conference. Polymeric materials, composites, carbonaceous materials, imines, polyester systems, and polyethylene fibers are among the topics covered. GRA

N92-28398# Dayton Univ., OH.
LUBRICANT EVALUATION AND PERFORMANCE 2 Interim Report, Jul. 1988 - Dec. 1990
Costandy S. Saba, M. A. Keller, H. A. Smith, R. E. Kauffman, and D. K. Toth Jan. 1992 576 p
(Contract F33615-88-C-2817)

(AD-A247464; UDR-TR-91-53; WL-TR-91-2111) Avail: NTIS HC/MF A25

The development of improved methods is described for defining, measuring, and assessing high temperature (500-750 F) lubricants for use in advanced aircraft turbine engines and the development of improved techniques for lubricant monitoring and lubricant condition monitoring for advanced lubricating fluids. Arrhenius plots were developed for describing the effective life of candidate 4 cSt lubricants, polyphenyl ethers, and other experimental fluids as a function of time and temperature for selected limiting values of changes in physical and chemical properties. Significant improvement in AE spectrometer sensitivity for analyzing wear metal was made. An in-line magnetic wear monitor was evaluated for possible application as a condition monitoring device for oil systems. Fluorescence, UV, dielectric constant, voltammetric, and thermal analysis techniques were developed and evaluated as high temperature lubricant monitoring devices. The tribological behavior of high temperature candidate fluids were evaluated and compared in the boundary lubrication regime using sliding four-ball test and various steel and ceramic specimens. GRA

N92-28405# Hampton Univ., VA.
IONIZED ASSISTED DEPOSITION OF ORGANIC FILMS FOR OPTOELECTRONIC APPLICATIONS Final Report
Calvin W. Lowe 20 Dec. 1991 2 p
(Contract N00014-91-J-1483)
(AD-A247744) Avail: NTIS HC/MF A01

This goal of this project was to deposit 2-methyl-4-nitroaniline (MNA) films on glass substrates. The experimental apparatus was operational with the exception of a suitable substrate holder and integration of the time of flight mass spectrometer into the system. In the 10 months of this project, we have designed and installed a liquid nitrogen cooled substrate holder and shutter. The time of flight mass spectrometer is complete and needs only to be calibrated. This is a straightforward process involving admitting a known gas such as Ar into the system and noting the time delay for its mass peak on the oscilloscope. GRA

N92-28412# Laser Photonics Technology, Inc., Amherst, NY.
SOL-GEL PROCESSED MULTIFUNCTIONAL ORGANIC POLYMER-INORGANIC OXIDE COMPOSITES FOR ELECTRONICS AND PHOTONICS Final Report, 1 Jun. 1991 - 31 Jan. 1992
Ryszard Burzynski and Martin K. Casstevens 4 Feb. 1992 45 p
(Contract F49620-91-C-0035)
(AD-A246773; AF030-FR-LPt(1/92); AFOSR-92-0007TR) Avail: NTIS HC/MF A03

This document includes a detailed description of efforts to develop sol-gel polymer composites for use in the fields of electronics and photonics. The central aim of the SBIR Phase 1 effort was to develop a multifunctional composite containing both oxides and organic polymers; both of the components in these materials are expected to perform active roles. A particular example that was investigated is one in which the inorganic component increases the charge carrier mobility while an organic component enhances its nonlinear optical response. Another example is the potential of organic and inorganic semiconductors becoming redox-coupled creating an entirely new class of multifunctional materials. The work involved: (1) the synthesis of several vanadium alkoxides and polymers; (2) developing protocols for the preparation of composite films of the highest optical quality; and (3) obtaining assessments of conductivity and nonlinear optical response. Spectroscopic data indicate the presence of specific absorption bands characteristic of charge transfer phenomena. High conductivity and a nonlinear optical response of the composites were observed. Further development and optimization of these systems will yield materials useful in such applications such as photorefractive media, antistatic coatings, large area electroluminescent panels or light emitting devices. GRA

N92-28415# Southwest Research Inst., San Antonio, TX.
STUDY OF HIGH TEMPERATURE FAILURE MECHANISM IN CERAMICS Final Report, Dec. 1989 - Sep. 1991
Richard A. Page, James Lankford, and Kwai S. Chan Jan. 1992 80 p
(Contract F49620-88-C-0081)
(AD-A247018; SWRI-2253/3; AFOSR-92-0012TR) Avail: NTIS HC/MF A05

This final report documents the results of a basic research program aimed at: (1) studying the high temperature failure mechanisms in ceramics; (2) establishing relationships between cavitation mechanisms and creep crack growth characteristics; and (3) developing a damage mechanism-based life prediction model. The growth rate, near-tip creep responses, and damage processes of creep cracks in a pyroceram glass-ceramic were studied under tensile loading at elevated temperatures. The results of these studies indicated that creep crack growth in the pyroceram glass-ceramic occurred both in continuous and discontinuous manners, with the damage processes manifested as the nucleation, growth, and coalescence of inhomogeneously distributed cavities and microcracks. Sintering of cavities led to the existence of a growth threshold below which the creep crack would open, blunt, but not propagate. Measurements of the total accumulated creep strain near the crack-tip revealed that creep crack extension followed a critical strain criterion. Relationships between cavitation mechanisms and creep crack growth characteristics of the glass-ceramic are discussed. GRA

N92-28553# Georgia Inst. of Tech., Atlanta. School of Chemical Engineering.
FORMATION, STRUCTURE, AND PROPERTIES OF BORON NITRIDE FIBERS FROM POLYMER PRECURSORS Final Report
A. S. Abhiraman, Prashant Desai, Bruce Wade, and N. Venkatasubramanian 25 Feb. 1992 65 p
(Contract N00014-88-K-0495)
(AD-A247679) Avail: NTIS HC/MF A04

A study of possible polymer precursor-based routes to oriented boron nitride fibers, with emphasis on the formation of continuous polyborate gel fibers and subsequent nitridation, is presented. Results from preliminary investigations of the use of polyborazylene, polyborazine, and decaborane-diamine as precursors for boron nitride fibers are also included. Formation, via a sol-gel route, of a polyborate gel fiber containing no metal counter ion is a major accomplishment of this research. Incorporation in the precursor of rheological aids that are fugitive during subsequent pyrolysis/nitridation is seen to be advantageous in the formation of processable polyborate fibers. Whether suitable schemes exist for generating high orientation in the trial boron nitride fiber remains an unanswered question with all the precursors. Nonoxide precursors suffer due to their high cost and chemical instabilities prior to their conversion to BN fibers. GRA

N92-28558# Michigan Univ., Ann Arbor. Dept. of Materials Science and Engineering.
MECHANISTIC STUDIES OF SUPERPLASTICITY OF STRUCTURAL CERAMICS Final Report
I.-Wei Chen 1 Feb. 1992 127 p
(Grant AF-AFOSR-0289-87)
(AD-A246951; AFOSR-92-0087TR) Avail: NTIS HC/MF A07

A comprehensive methodology for developing superplastic ceramics, evaluating superplastic formability, and understanding microstructural evolution and flow mechanisms during large deformation was developed. A summary of these accomplishments, which focuses on two important classes of structural ceramics, zirconia and silicon nitride, is provided here in the form of nine published journal papers, conference contributions and general reviews. GRA

N92-28563# Defence Research Establishment Atlantic, Dartmouth (Nova Scotia).
THE EFFECTS OF ALUMINA TRIHYDRATE ON THE FLAMMABILITY CHARACTERISTICS OF POLYESTER, VINYL ESTER, AND EPOXY GLASS REINFORCED PLASTICS
Richard M. Morchat Dec. 1991 25 p
(AD-A247707; DREA-TM-91/214) Avail: NTIS HC/MF A03

The effects of an inorganic fire-retardant additive, alumina trihydrate, on flammability characteristics and smoke generation of glass reinforced polyester, vinyl ester, and epoxy resins were evaluated. Information is presented on the flame spread index, limiting oxygen index, density of smoke generated, and toxic gases of combustion. Results indicated that the addition of the fire-retardant additive to the polymeric materials significantly decreased the flame spread index and increased the limiting oxygen index; however, the amount of smoke generated during pyrolytic and flaming combustion was high and unacceptable. Finally, the toxic gas evolution data indicated that the threshold limit values for some gases were exceeded. GRA

N92-28564# Defence Research Establishment, Ottawa (Ontario).
THERMAL ANALYSIS OF SELECTED COMMERCIAL THERMOPLASTIC RESINS
K. M. McCutcheon, J. C. Collyer, and S. V. Lowen Jun. 1991 21 p
(AD-A247711; DREO-TN-91-9) Avail: NTIS HC/MF A03

Thermogravimetric Analysis (TGA) and Differential Scanning Calorimetry (DSC) were used to characterize and identify several commercial thermoplastics used or considered for use in Canadian C4 gas masks. The goal was to build a database from which unknown thermoplastic samples could be fingerprinted. A secondary goal was to characterize the thermal transitions of the polymers to determine the effect of processing. Both TGA and DSC demonstrated characteristic thermal transitions of the particular polymer used in the sample. In some cases, the presence and amount of inorganic fillers could be detected, as well as polymer blend composition. The effect of thermal history was also determined for Noryl and Valox resins by heating and then quench cooling the samples. The thermal transitions of the more crystalline Valox were dependent on the thermal history whereas the amorphous Noryl could be repeatedly heated and cooled, maintaining reproducible thermal transitions. GRA

N92-28570# Pennsylvania State Univ., University Park.
PROCESSING AND PROPERTIES OF CHEMICALLY DERIVED CALCIUM SILICATE CEMENTS Final Report, 1 Apr. 1988 - 31 Aug. 1991
B. E. Scheetz, J. J. Mecholsky, and J. H. Adair 27 Feb. 1992 87 p
(Grant AF-AFOSR-0184-88)
(AD-A249106; AFOSR-92-0223TR) Avail: NTIS HC/MF A05

A chemical engineering approach has been employed to promote elimination of large size flaws and improve strength. A general philosophy in the program was to prepare advanced cements designated as chemically bonded ceramics and use fracture mechanics and fractography to determine the size and origin of the critical flaw. Flaws of a certain type were eliminated in subsequent materials by alteration in some stage of the processing scheme. One of the most important goals of the current program was to analyze the effectiveness of indentation techniques for evaluating the mechanical properties of cementitious materials. The indentation-strength technique was found applicable to MDF cements for measuring fracture toughness. The indentation-strength technique and fracture surface analysis were found applicable to MDF cements for measuring fracture toughness. By using both optical and electron microscopes, fractograph becomes a powerful tool to estimate toughness. Therefore, we suggest the small crack techniques are applicable for the measurement of crack growth resistance in cementitious materials as long as the crack size is a characteristic dimension of the microstructure. GRA

N92-28751* National Aeronautics and Space Administration. Langley Research Center, Hampton, VA.
POLYIMIDAZOLES VIA AROMATIC NUCLEOPHILIC DISPLACEMENT Patent
John W. Connell, inventor (to NASA) and Paul M. Hergenrother, inventor (to NASA) 26 May 1992 8 p Filed 19 Jul. 1991 Supersedes N90-26954 (28 - 21, p 2983) Division of US-Patent-Appl-SN-508316, filed 12 Apr. 1990
(NASA-Case-LAR-14145-1; US-Patent-5,116,934; US-Patent-Appl-SN-732884; US-Patent-Appl-SN-508316; US-Patent-Class-528-125; US-Patent-Class-528-126; US-Patent-Class-528-127; US-Patent-Class-528-128; US-Patent-Class-528-220; US-Patent-Class-528-224) Avail: US Patent and Trademark Office

Polyimidazoles (PI) are prepared by the aromatic nucleophilic displacement reaction of di(hydroxyphenyl) imidazole monomers with activated aromatic dihalides or activated aromatic dinitro compounds. The reactions are carried out in polar aprotic solvents such as N,N-dimethyl acetamide, sulfolane, N-methylpyrrolidinone, dimethylsulfoxide, or diphenylsulfone using alkali metal bases such as potassium carbonate at elevated temperatures under nitrogen. The di(hydroxyphenyl) imidazole monomers are prepared by reacting an aromatic aldehyde with a dimethoxybenzil or by reacting an aromatic dialdehyde with a methoxybenzil in the presence of ammonium acetate. The di(methoxyphenyl) imidazole is subsequently treated with aqueous hydrobromic acid to give the di(hydroxphenyl) imidazole monomer. This synthetic route has provided high molecular weight PI of new chemical structure, is economically and synthetically more favorable than other routes, and allows for facile chemical structure variation due to the availability of a large variety of activated aromatic dihalides and dinitro compounds.
Official Gazette of the U.S. Patent and Trademark Office

N92-28904# Research Triangle Inst., Research Triangle Park, NC.
LARGE-AREA, PLASMA-ASSISTED, HALOGEN-BASED DIAMOND DEPOSITION Quarterly Report No. 1-2, 31 Dec. 1991 - 3 Mar. 1992
R. A. Rudder 4 Mar. 1992 53 p
(Contract N00014-91-C-0177)
(AD-A247423; RTI/5123/91-29; RTI-83U-5123) Avail: NTIS HC/MF A04

A number of chemical systems have been evaluated for diamond growth in the parallel plate capacitive systems. Unlike previous work in the RF inductive systems, diamond growth from H2/CH4, H2/CH1, and H2O/CH3OH systems in the parallel plate was not forthcoming. Analysis of the critical differences between the RF inductive vs RF capacitive coupling identified the plasma density and the degree of plasma dissociation to be the substantial differences. We have embarked on a course to evaluate scale of the RF inductive technology by development of a planar inductive coil which would merely replace the capacitive plate on standard large area RF system. Preliminary results show that creation of a high density plasma at low pressures and modest power levels over a 100 nano-m area is feasible with the current 500 W power supply. No diamond growth shave yet been attempted. GRA

N92-28912# Naval Civil Engineering Lab., Port Hueneme, CA.
PAINT REMOVAL USING CRYOGENIC PROCESSES Final Report, Oct. 1989 - Jun. 1991
Richard E. Kirts and Philip L. Stone Jan. 1992 44 p
(AD-A247668; NCEL-TN-1839) Avail: NTIS HC/MF A03

The use of a high-pressure jet of cryogenic fluid (e.g., liquid nitrogen at -320 F) to remove paint and other protective coatings from Navy aircraft and ships was studied. The objective of the work was to explore the feasibility of developing a paint removal method that is less harmful to the environment than the chemical paint stripping methods presently in use. It was learned that only thick (t greater than 0.020 inch) films of paint can be effectively removed by the mechanism of thermal shock. Aircraft paint is too thin and flexible to be removed by cryogenic methods. Cryogenic methods are not recommended for use on ships because of the

danger of steel embrittlement by low temperatures. It was demonstrated that a jet of liquid nitrogen can effectively remove certain paints (regardless of thickness) by the mechanism of differential thermal contraction. The process may have application where control of paint waste is essential, for example, removal of thick films of lead base paint. GRA

N92-28916# Naval Research Lab., Washington, DC.
NANOSCALE INVESTIGATION OF INDENTATION, ADHESION, AND FRACTURE OF DIAMOND (111) SURFACES Interim Report, 1 Sep. 1991 - 30 Aug. 1992
J. A. Harrison, C. T. White, R. J. Colton, and D. W. Brenner Apr. 1992 27 p
(NR Proj. RR0-1301)
(AD-A250164) Avail: NTIS HC/MF A03

Molecular dynamics simulations have been used to model the dynamics of indentation and the resulting damage for a (111) surface of a (1 x 1) hydrogen terminated diamond tip interacting with the (111) surface of both a (1 x 1) hydrogen terminated diamond crystal and a non-hydrogen terminated diamond crystal. In both cases, indentation can result in a non-adhesive (i.e., elastic) or an adhesive (i.e., plastic) interaction depending on the maximum value of the applied load. Further, adhesion is usually accompanied by fracture and is independent of where the tip contacts the surface. In the case of the hydrogen terminated crystal, the diamond crystal structure is significantly disrupted as a result of the indentation. When the hydrogen is removed from the crystal's surface, adhesion occurs at lower loads than previously observed. However, the crystal structure is not significantly altered as a result of the indentation. The state of the surface dictates the type of indentation mechanism. GRA

N92-28972# George Washington Univ., Washington, DC. Dept. of Chemistry.
X RAY PHOTOELECTRON SPECTROSCOPY STUDY ON THE DOUBLE LAYER AT AN Al2O3-Al INTERFACE
David E. Ramaker and Hideo Sambe Jan. 1992 13 p
(Contract N00014-91-J-1896)
(AD-A246454; TR-56) Avail: NTIS HC/MF A03

Upon oxidation of a clean Aluminum (Al) surface, an electrical double layer (EDL) is formed at the aluminum-aluminum oxide (Al-Al2O3) interface. This EDL is investigated using X-ray Photoelectron Spectroscopy data available in the literature. The EDL strength, measured as a potential difference across the EDL, depends on the Al surface and the oxidation process. The polarity of the EDL is invariably the same: the Al2O3 side of the Al-Al2O3 interface is always positively charged. The reduction of the Al work function upon oxidation is attributed to this EDL. The asymmetry in the potential barrier shape formed in Al-Al2O3-Al sandwiches is also attributed to a strong EDL at the electron-film interface and a weaker EDL at the interface between the counter electrode and the film. Author (GRA)

N92-29090* National Aeronautics and Space Administration. Lewis Research Center, Cleveland, OH.
OXIDATION RESISTANT COATING FOR TITANIUM ALLOYS AND TITANIUM ALLOY MATRIX COMPOSITES Patent
William J. Brindley, inventor (to NASA), James L. Smialek, inventor (to NASA), and Carl J. Rouge, inventor (to NASA) 26 May 1992 5 p Filed 1 Apr. 1991 Supersedes N91-26375 (29 - 18, p 2966)
(NASA-Case-LEW-15155-1; US-Patent-5,116,690;
US-Patent-Appl-SN-682160; US-Patent-Class-428-614;
US-Patent-Class-428-660; US-Patent-Class-428-661;
Int-Patent-Class-B32B-5/02; Int-Patent-Class-B32B-15/01;
Int-Patent-Class-B32B-15/20) Avail: US Patent and Trademark Office

An oxidation resistant coating for titanium alloys and titanium alloy matrix composites comprises an MCrAlX material. M is a metal selected from nickel, cobalt, and iron. X is an active element selected from Y, Yb, Zr, and Hf.
Official Gazette of the U.S. Patent and Trademark Office

N92-29116# Case Western Reserve Univ., Cleveland, OH. Dept. of Macromolecular Science.
MOLECULAR ENGINEERING OF LIQUID CRYSTALLINE POLYMERS BY LIVING CATIONIC POLYMERIZATION. 21: SYNTHESIS AND CHARACTERIZATION OF POLY (3-((4-CYANO-4'-BIPHENYL)OXY) PROPYL VINYL ETHER) MACROMONOMERS
Virgil Perce, Myongsoo Lee, and Dimitris Tomazos 27 Mar. 1992 10 p
(Contract N00014-90-J-1828)
(AD-A248305; TR-59) Avail: NTIS HC/MF A02

This paper describes the synthesis and characterization of poly (3-((4-cyano-4'-biphenyl) oxy) propyl vinyl ether) poly(6-3) macromonomers obtained by the functionalization of the growing chain end of the corresponding living polymer obtained by the initiation of the cationic polymerization of 3-(4-cyano-4'biphenyl)oxy propyl vinyl ether with CF3SO3H/S(CH3)2, with 2-hydroxy ethyl methacrylate poly(6-3)-I, 2-2(2-allyloxyethoxy) ethoxyethanol poly 6-3-II and 10-undecen-1-ol poly(6-3)-III. GRA

N92-29145# University of Southern California, Los Angeles. Dept. of Chemistry.
SILICON POLYMERS Final Report
William P. Weber Apr. 1992 12 p
(Grant AF-AFOSR-0007-89)
(AD-A250201; AFOSR-92-0289TR) Avail: NTIS HC/MF A03

Unsaturated carbosilane polymers have been prepared by anionic as well as metathesis polymerization of silacyclopent-3-enes. Of particular interest is unsaturated carbosilane polymers with Si-H substitution which have been prepared. These complementary functionalities permit crosslinking by hydrosilation reactions to yield new coating materials which have low dielectric constants and moisture absorption. These polymers can be chemically modified by addition reaction, to the carbon-carbon double bonds. GRA

N92-29157* National Aeronautics and Space Administration. Langley Research Center, Hampton, VA.
POLYIMIDE PROCESSING ADDITIVES Patent
James C. Fletcher, inventor (to NASA), J. Richard Pratt, inventor (to NASA), Terry L. St.Clair, inventor (to NASA), Diane M. Stoakley, inventor (to NASA), and Harold D. Burks, inventor (to NASA) 26 May 1992 24 p Filed 11 Aug. 1987
(NASA-Case-LAR-13669-1; US-Patent-5,116,939;
US-Patent-Appl-SN-084064; US-Patent-Class-528-353;
US-Patent-Class-528-179; US-Patent-Class-528-185;
US-Patent-Class-528-352; US-Patent-Class-525-420;
US-Patent-Class-525-432; Int-Patent-Class-C08F-283/04) Avail: US Patent and Trademark Office

A process for preparing polyimides having enhanced melt flow properties is described. The process consists of heating a mixture of a high molecular weight poly-(amic acid) or polyimide with a low molecular weight amic acid or imide additive in the range of 0.05 to 15 percent by weight of additive. The polyimide powders so obtained show improved processability, as evidenced by lower melt viscosity by capillary rheometry. Likewise, films prepared from mixtures of polymers with additives show improved processability with earlier onset of stretching by TMA.
Official Gazette of the U.S. Patent and Trademark Office

N92-29189# Ohio Univ., Athens. Dept. of Physics and Astronomy.
THE IN SITU OBSERVATION OF DIAMOND FILM NUCLEATION AND GROWTH Semiannual Report, 1 Jul. 1991 - 1 Mar. 1992
Martin E. Kordesch 20 Mar. 1992 20 p
(Contract N00014-91-J-1596)
(AD-A248203) Avail: NTIS HC/MF A03

The growth of a two-dimensional ordered carbon monolayer on Mo(100) has been observed under conditions approaching those used for diamond chemical vapor deposition (CVD) using a photoelectron emission microscope. The method used is a combination of HFCVD and atomic layer epitaxy, using a strongly

chemisorbed oxygen layer as a nucleation inhibitor. Site-for-site place exchange of carbon for oxygen, that preserves the surface ordering, has been observed. Extension of this technique to surfaces that are templates for diamond epitaxy is being investigated. GRA

N92-29194# Technical Research Centre of Finland, Espoo. Metals Lab.
THE CHARACTERIZATION OF CERAMICS AND CERAMIC/METAL-JOINTS BY ULTRASONIC TECHNIQUES [KERAAMIEN JA KERAAMI-METALLILIITOSTEN OMINAISUUKSIEN MAARITTAMINEN ULTRAAANIMENETELMALLA]
Pentti Kauppinen and Harri Jeskanen Sep. 1991 52 p In FINNISH Sponsored by Technology Development Center and Finnish Industry
(VTT-RR-741; ISBN-951-38-3989-3; ISSN-0358-5077; ETN-92-91265) Copyright Avail: NTIS HC/MF A04

The applicability of different ultrasonic techniques for characterization of ceramics and ceramic/metal joints was studied. High frequency ultrasonics was used to evaluate flaws, porosity and elastic properties of ceramics. By changing the focussing conditions of the high frequency (30 to 50 MHz) transducers both microcracks opening to the surface and discontinuities in the material were detected. In aluminum oxide flaws and inclusions smaller than 100 micrometers were found. From the measured ultrasonic wave velocity the modulus of elasticity of aluminum oxide, zirconium oxide and silicon nitride was obtained as 344 GPa, 185 GPa and 374 GPa, respectively. High frequency ultrasonics was also used to evaluate the quality of both adhesively bonded and brazed ceramic/metal joints. Lack of bonding as well as laminar cracks caused by thermal stresses were detected. The results show that the reflection type acoustic microscope can be successfully used for the characterization of ceramics and ceramic/metal joints. A sufficient resolution for the detection of micro discontinuities can in most cases be achieved by using frequencies above 50 MHz. The ultrasonic measurement of the elastic properties of ceramics is based on the measurement of ultrasonic velocity in the material. The techniques for the accurate measurement of sound velocities must be further developed especially for porous ceramics and ceramic coatings. ESA

N92-29195# Sandia National Labs., Albuquerque, NM.
ION CONDUCTIVE POLYMER SOLID ELECTROLYTES
Hidekazu Izuchi and Tomohiko Noda 26 Feb. 1992 9 p Transl. into ENGLISH of Japanese Patent Application No. HE13-59058 (14 Mar. 1991)
(Contract DE-AC04-76DP-00789)
(DE92-010518; ALS/TR-92-009) Avail: NTIS HC/MF A02

The high polymer solid electrolyte is an immobile solvent formed of a lattice of mutually soluble polyvinylidene fluoride, solvent A, and ion-dissociable salt. The electrolyte is manufactured by dissolving in solution stoichiometric amounts of polyvinylidene fluoride, solvent A (mutually soluble with, and a swelling agent for polyvinylidene fluoride), solvent B, and an ion-dissociable salt. Solvent B is extracted in a subsequent step. An alternate manufacturing procedure by which to produce a high polymer solid electrolyte is to dissolve an ion-dissociable salt in solvent B. The high polymer solid electrolyte lattice consists of polyvinylidene fluoride solvated by roughly stoichiometrical amounts of solvent A and ion-dissociable salt. A novel feature of the electrolyte is that it is essentially solid, and yet ions released by dissociation of the salt when solvated by solvent A migrate mainly through solvent A, resulting in high ionic conductivity. DOE

28 PROPELLANTS AND FUELS

Includes rocket propellants, igniters, and oxidizers; their storage and handling procedures; and aircraft fuels.

For related information see also *07 Aircraft Propulsion and Power, 20 Spacecraft Propulsion and Power,* and *44 Energy Production and Conversion.*

N92-28433*# National Aeronautics and Space Administration. Lewis Research Center, Cleveland, OH.
HYDROGEN NO-VENT FILL TESTING IN A 5 CUBIC FOOT (142 LITER) TANK USING SPRAY NOZZLE AND SPRAY BAR LIQUID INJECTION
Matthew E. Moran and Ted W. Nyland Jul. 1992 10 p Proposed for presentation at the 28th Joint Propulsion Conference and Exhibit, Nashville, TN, 6-8 Jul. 1992; sponsored by AIAA, SAE, ASME, and ASEE
(RTOP 506-42-73)
(NASA-TM-105759; E-7173; NAS 1.15:105759; AIAA Paper 92-3063) Avail: NTIS HC/MF A02

A total of 38 hydrogen no-vent fill tests were performed in this test series using various size spray nozzles and a spray bar with different hole sizes in a 5 cubic foot receiver tank. Fill levels of 90 percent by volume or greater were achieved in 26 of the tests while maintaining a receiver tank pressure below 30 psia. Spray nozzles were mounted at the top of the tank, whereas, the spray bar was centered in the tank axially. The spray nozzle no-vent fills demonstrated tank pressure and temperature responses comparable to previous test series. Receiver tank pressure responses for the spray bar configuration were similar to the spray nozzle tests with the pressure initially rising rapidly, then leveling off as vapor condenses onto the discharging liquid streams, and finally ramping up near the end of the test due to ullage compression. Both liquid injection techniques tested were capable of filling the receiver tank to 90 percent under variable test conditions. Comparisons between the spray nozzle and spray bar configurations for well matched test conditions indicate the spray nozzle injection technique is more effective in minimizing the receiving tank pressure throughout a no-vent fill compared to the spray bar under normal gravity conditions. Author

N92-28739 Department of the Navy, Washington, DC.
PROPELLANT-TO-INHIBITOR BONDING SYSTEM Patent
Thomas F. Davidson, inventor (to Navy) and Evester Sullivan, inventor (to Navy) 15 Oct. 1991 12 p Filed 30 Nov. 1990
(AD-D015243; US-Patent-5,056,405; US-Patent-Appl-SN-621256; US-Patent-Class-82-20-14) Avail: US Patent and Trademark Office

A system for bonding solid propellant to the inhibitor, for use in replaceable propellant grain assemblies, is presented. The system makes use of an inhibitor sleeve that has one end attached to an end closure having interior insulation, made of the same rubber insulation material as the inhibitor, and forming a cylindrical cavity for receiving a poured propellant mix. The bonding system is employed prior to pouring the propellant mix. This bonding system involves cleaning the interior surface of the cavity with freon solvent and brush-applying a barrier coat (an epoxy resin with amine curing agents) to the interior surface of the cleaned inhibitor. Next, a liner is brush-coated onto the cured interior surface of the barrier coat. The liner is then cured and the propellant is then cast into the cavity formed by the lined inhibitor sleeve and insulated closure. It is important that the polymer and curing agent of the propellant and liner be the same to assure optimum compatibility and effective adhesive bonding. This is accomplished by providing common chemical constituents even though they are formed by different processes and have other different chemical constituents. GRA

N92-28914# Science Applications, Inc., McLean, VA.
IDENTIFICATION AND ANALYSIS OF FACTORS AFFECTING THE ADOPTION OF ALTERNATIVE TRANSPORTATION FUELS Final Report, Jul. 1990 - Dec. 1991
H. Chernoff and D. Friedman 1991 70 p
(Contracts GRI-5090-810-2037; DE-AC01-87EI-19800)
(PB92-164326; GRI-92/0064) Avail: NTIS HC/MF A04

Early adoption of alternative transportation fuels will be driven almost entirely by legislation rather than by the economic decisionmaking of vehicle users. However, given the legal and regulatory requirements for alternative transportation fuel use, the choices made between competing options will depend largely on the perceived benefits and risks of each vehicle/fuel type system. The analysis was performed shortly after passage of the Clean Air Act Amendments of 1990 under a jointly funded task with the DOE Energy Information Administration. The report generally reflects the contractor's point of view regarding the future of the alternative transportation fuels market which is still in its infancy. Given the many legal, regulatory, and technology-based uncertainties that exist, the report portrays a fairly pessimistic outlook for non-petroleum fuel use. Author

29 MATERIALS PROCESSING

Includes space-based development of products and processes for commercial applications.
For biological materials see *55 Space Biology*.

N92-28437*# Universities Space Research Association, Huntsville, AL.
NUMERICAL STUDIES OF CONVECTIVE TRANSPORT ASSOCIATED WITH CRYSTAL GROWTH IN MIRROGRAVITY
N. Ramachandran *In* NASA. Lewis Research Center, International Workshop on Vibration Isolation Technology for Microgravity Science Applications May 1992 p 99-114 (For primary document see N92-28436 19-31)
Avail: NTIS HC/MF A18

N92-28438*# National Aeronautics and Space Administration. Lewis Research Center, Cleveland, OH.
AN EXAMINATION OF ANTICIPATED g-JITTER ON SPACE STATION AND ITS EFFECTS ON MATERIALS PROCESSES
Emily Nelson *In its* International Workshop on Vibration Isolation Technology for Microgravity Science Applications May 1992 p 115-131 (For primary document see N92-28436 19-31)
Avail: NTIS HC/MF A18

N92-28439*# University Coll. of North Wales, Bangor.
THE MICROGRAVITY ISOLATION MOUNT (MGIM): A COLUMBUS FACILITY FOR IMPROVING THE MICROGRAVITY QUALITY OF PAYLOADS
R. G. Owen, D. I. Jones, A. R. Owens, G. Roberts, and P. Hadfield *In* NASA. Lewis Research Center, International Workshop on Vibration Isolation Technology for Microgravity Science Applications May 1992 p 133-161 (For primary document see N92-28436 19-31)
Avail: NTIS HC/MF A18

N92-28440*# Canadian Space Agency, Ottawa (Ontario). Astronaut Program Office.
KC-135 LARGE MOTION ISOLATION MOUNT (LMIM)
Bjarni V. Tryggvason *In* NASA. Lewis Research Center, International Workshop on Vibration Isolation Technology for Microgravity Science Applications May 1992 p 163-173 (For primary document see N92-28436 19-31)
Avail: NTIS HC/MF A18

N92-28441*# National Space Development Agency, Tokyo (Japan).
NASDA'S ACTIVITIES ON VIBRATION ISOLATION TECHNOLOGY
In NASA. Lewis Research Center, International Workshop on Vibration Isolation Technology for Microgravity Science Applications May 1992 p 175-192 Prepared in cooperation with Japan Space Utilization Promotion Center, Tokyo, Japan; Ishikawajima-Harima Heavy Industries Co. Ltd., Tokyo, Japan; and Nippon Electric Co., Tokyo, Japan (For primary document see N92-28436 19-31)
Avail: NTIS HC/MF A18

N92-28442*# National Aeronautics and Space Administration. Lewis Research Center, Cleveland, OH.
VIBRATION ISOLATION TECHNOLOGY DEVELOPMENT TO DEMONSTRATION
Carlos Grodsinsky *In its* International Workshop on Vibration Isolation Technology for Microgravity Science Applications May 1992 p 193-207 (For primary document see N92-28436 19-31)
Avail: NTIS HC/MF A18

N92-28443*# Applied Technology Associates, Inc., Albuquerque, NM.
NEW INERTIAL ACTUATOR PROVIDES ISOLATION AND STABILIZATION IN MICROGRAVITY CONDITIONS
John Blackburn *In* NASA. Lewis Research Center, International Workshop on Vibration Isolation Technology for Microgravity Science Applications May 1992 p 209-221 (For primary document see N92-28436 19-31)
Avail: NTIS HC/MF A18

N92-28444*# SatCon Technology Corp., Cambridge, MA.
A 6 DEGREE-OF-FREEDOM LORENTZ FORCE VIBRATION ISOLATOR WITH NONLINEAR CONTROLLER
Ralph Fenn and Bruce Johnson *In* NASA. Lewis Research Center, International Workshop on Vibration Isolation Technology for Microgravity Science Applications May 1992 p 223-240 (For primary document see N92-28436 19-31)
Avail: NTIS HC/MF A18

N92-28445*# Pennsylvania State Univ., University Park.
DIGITAL CONTROL ALGORITHMS FOR MICROGRAVITY ISOLATION SYSTEMS
Alok Sinha and Yung-Peng Wang *In* NASA. Lewis Research Center, International Workshop on Vibration Isolation Technology for Microgravity Science Applications May 1992 p 241-256 (For primary document see N92-28436 19-31)
Avail: NTIS HC/MF A18

N92-28446*# Virginia Univ., Charlottesville. Center for Magnetic Bearings.
MICROGRAVITY VIBRATION ISOLATION RESEARCH AT THE UNIVERSITY OF VIRGINIA
Carl R. Knospe, David W. Lewis, A. Peter Allan, Paul E. Allaire, Robert R. Humphris, Bibhuti B. Banerjee, and R. David Hampton *In* NASA. Lewis Research Center, International Workshop on Vibration Isolation Technology for Microgravity Science Applications May 1992 p 257-264 (For primary document see N92-28436 19-31)
Avail: NTIS HC/MF A18

N92-28447*# Virginia Univ., Charlottesville. Center for Magnetic Bearings.
EXTENDED H2 SYNTHESIS FOR MICROGRAVITY VIBRATION ISOLATION
R. David Hampton and Carl R. Knospe *In* NASA. Lewis Research Center, International Workshop on Vibration Isolation Technology for Microgravity Science Applications May 1992 p 265-268 (For primary document see N92-28436 19-31)
Avail: NTIS HC/MF A18

N92-28448*# National Aeronautics and Space Administration. Marshall Space Flight Center, Huntsville, AL.
ACAP: ACCELERATION CHARACTERIZATION AND ANALYSIS PROJECT
Charles R. Baugher *In* NASA. Lewis Research Center, International Workshop on Vibration Isolation Technology for Microgravity Science Applications May 1992 p 295-307 (For primary document see N92-28436 19-31)
Avail: NTIS HC/MF A18

N92-28449*# National Aeronautics and Space Administration. Lyndon B. Johnson Space Center, Houston, TX.
SHOCK AND VIBRATION ISOLATION FOR CYCLIC EXERCISE IN SPACECRAFT

W. Thornton *In* NASA. Lewis Research Center, International Workshop on Vibration Isolation Technology for Microgravity Science Applications May 1992 p 309-319 (For primary document see N92-28436 19-31)
Avail: NTIS HC/MF A18

N92-28450*# National Aeronautics and Space Administration, Washington, DC.
SPACE STATION FREEDOM MICROGRAVITY ENVIRONMENT REQUIREMENTS AND ASSESSMENT METHODS
Philip Bogert *In* NASA. Lewis Research Center, International Workshop on Vibration Isolation Technology for Microgravity Science Applications May 1992 p 321-344 (For primary document see N92-28436 19-31)
Avail: NTIS HC/MF A18

N92-28454*# Massachusetts Inst. of Tech., Cambridge. Dept. of Aeronautics and Astronautics.
MICROGRAVITY ISOLATION MOUNTS BASED UPON PIEZOELECTRIC FILM
Andreas vonFlotow *In* NASA. Lewis Research Center, International Workshop on Vibration Isolation Technology for Microgravity Science Applications May 1992 p 391-396 (For primary document see N92-28436 19-31)
Avail: NTIS HC/MF A18

N92-28455*# Jet Propulsion Lab., California Inst. of Tech., Pasadena.
PREDICTING MICROGRAVITY LEVELS FOR SPACE STATION USING VAPEPS
G. Badilla, T. Bergen, D. Kern, and T. Scharton *In* NASA. Lewis Research Center, International Workshop on Vibration Isolation Technology for Microgravity Science Applications May 1992 p 397-410 (For primary document see N92-28436 19-31)
Avail: NTIS HC/MF A18

31 ENGINEERING (GENERAL)

Includes vacuum technology; control engineering; display engineering; cryogenics; and fire prevention.

N92-28359# Carnegie-Mellon Univ., Pittsburgh, PA. Management Sciences Research Group.
SCHEDULING MULTIPLE VARIABLE-SPEED MACHINES
Michael A. Trick Nov. 1991 31 p Revised
(Contract N00014-85-K-0198)
(AD-A249362; MSRR-578) Avail: NTIS HC/MF A03

We examine scheduling problems where we control not only the assignment of jobs to machines, but also the time used by the job on the machine. For instance, many tooling machines allow control of the speed at which a job is run. Increasing the speed incurs costs due to machine wear but also increases throughput. We discuss some fundamental scheduling problems in this environment and give algorithms for some interesting cases. Some cases are inherently difficult so for these we give heuristics. Our approach illustrates the exploitation of underlying network structure in combinatorial optimization problems. We create heuristics that optimally schedule a large portion of the jobs and then attempt to fit in the remainder. This also gives a method for quickly finding valid inequalities violated by the linear relaxation solution. For the problem of minimizing the sum of makespan and production costs, a rounding heuristic is within a constant factor of optimal. Our heuristics are compared to other, classical, heuristics. GRA

N92-28436*# National Aeronautics and Space Administration. Lewis Research Center, Cleveland, OH.
INTERNATIONAL WORKSHOP ON VIBRATION ISOLATION TECHNOLOGY FOR MICROGRAVITY SCIENCE APPLICATIONS
Joseph F. Lubomski, ed. May 1992 405 p Workshop held in Cleveland, OH, 23-25 Apr. 1991
(RTOP 694-03-0C)
(NASA-CP-10094; E-7035; NAS 1.55:10094) Avail: NTIS HC/MF A18

The International Workshop on Vibration Isolation Technology for Microgravity Science Applications was held on April 23-25, 1991 at the Holiday Inn in Middleburg Heights, Ohio. The main objective of the conference was to explore vibration isolation requirements of space experiments and what level of vibration isolation could be provided both by present and planned systems on the Space Shuttle and Space Station Freedom and by state of the art vibration isolation technology. For individual titles, see N92-28437 through N92-28455.

N92-28437*# Universities Space Research Association, Huntsville, AL.
NUMERICAL STUDIES OF CONVECTIVE TRANSPORT ASSOCIATED WITH CRYSTAL GROWTH IN MIRROGRAVITY **c29**
N. Ramachandran *In* NASA. Lewis Research Center, International Workshop on Vibration Isolation Technology for Microgravity Science Applications May 1992 p 99-114 (For primary document see N92-28436 19-31)
Avail: NTIS HC/MF A18

Information on numerical studies of convective transport associated with crystal growth in microgravity is given in viewgraph form. Inferences drawn from the research are that protein crystals seem to grow at much larger relative supersaturations than small molecule crystals; growth rate is limited by attachment kinetics more than by transport; attachment kinetics are apparently influenced by convective flows, although the mechanism is uncertain; acceleration levels required to achieve D/L growth within Space Station Freedom specifications may not be achievable on manned vehicles; and D/L transport can help minimize incorporation of impurities, but growth cessation cannot be explained. Author

N92-28438*# National Aeronautics and Space Administration. Lewis Research Center, Cleveland, OH.
AN EXAMINATION OF ANTICIPATED g-JITTER ON SPACE STATION AND ITS EFFECTS ON MATERIALS PROCESSES **c29**
Emily Nelson *In its* International Workshop on Vibration Isolation Technology for Microgravity Science Applications May 1992 p 115-131 (For primary document see N92-28436 19-31)
Avail: NTIS HC/MF A18

Information on anticipated g-jitter on Space Station Freedom and the effect of the jitter on materials processes is given in viewgraph form. It was concluded that g-jitter will dominate the acceleration environment; that it is a 3D multifrequency phenomenon; and that it varies dramatically in orientation. Information is given on calculated or measured sources of residual acceleration, aerodynamic drag, Shuttle acceleration measurements, the Space Station environment, tolerable g-levels as a function of frequency, directional solidification, vapor crystal growth, protein crystal growth, float zones, and liquid bridges. Author

N92-28439*# University Coll. of North Wales, Bangor.
THE MICROGRAVITY ISOLATION MOUNT (MGIM): A COLUMBUS FACILITY FOR IMPROVING THE MICROGRAVITY QUALITY OF PAYLOADS **c29**
R. G. Owen, D. I. Jones, A. R. Owens, G. Roberts, and P. Hadfield *In* NASA. Lewis Research Center, International Workshop on Vibration Isolation Technology for Microgravity Science Applications May 1992 p 133-161 (For primary document see N92-28436 19-31)
Avail: NTIS HC/MF A18

The Microgravity Isolation Mount (MGIM) is a facility for providing active vibration isolation for sensitive experiments on the Columbus Attached Laboratory and the Columbus Free-Flying Laboratory. The facility is designed to be accommodated in a standard Columbus rack, and it iterfaces with existing rack utility services. The design is based on a non-contact strategy, whereby the

payload 'floats' inside the rack, and its position is controlled by a number of magnetic actuators. The main advantage of using this non-contact strategy is the improved microgravity quality available. The overall design of the facility and a description of its elements are given. Author

N92-28440*# Canadian Space Agency, Ottawa (Ontario). Astronaut Program Office.
KC-135 LARGE MOTION ISOLATION MOUNT (LMIM) **c29**
Bjarni V. Tryggvason *In* NASA. Lewis Research Center, International Workshop on Vibration Isolation Technology for Microgravity Science Applications May 1992 p 163-173 (For primary document see N92-28436 19-31)
Avail: NTIS HC/MF A18

Information on the Large Motion Isolation Mount (LMIM) to be used on the KC-135 is given in viewgraph form. Information given includes the cost per Kg-sec, program elements, the effect of aircraft acceleration level on free float time, and program objectives. Author

N92-28441*# National Space Development Agency, Tokyo (Japan).
NASDA'S ACTIVITIES ON VIBRATION ISOLATION TECHNOLOGY **c29**
In NASA. Lewis Research Center, International Workshop on Vibration Isolation Technology for Microgravity Science Applications May 1992 p 175-192 Prepared in cooperation with Japan Space Utilization Promotion Center, Tokyo, Japan; Ishikawajima-Harima Heavy Industries Co. Ltd., Tokyo, Japan; and Nippon Electric Co., Tokyo, Japan (For primary document see N92-28436 19-31)
Avail: NTIS HC/MF A18

The National Space Development Agency's (NASDA) activities in providing various vibration isolation technologies for the Space Station Mission are covered in viewgraph form. Technologies covered include an active vibration isolation system for extra sensitive missions in the low frequency range, a passive damping system consisting of a damping rack for the reduction of resonance amplification, and an isolator for vibration isolation from low frequencies. Information is given in viewgraph form on the active vibration isolation concept, voice coil type electromagnetic suspension, a profile of an active vibration isolation system, a three degree of freedom ground experiment, and acceleration feedback. Author

N92-28442*# National Aeronautics and Space Administration. Lewis Research Center, Cleveland, OH.
VIBRATION ISOLATION TECHNOLOGY DEVELOPMENT TO DEMONSTRATION **c29**
Carlos Grodsinsky *In its* International Workshop on Vibration Isolation Technology for Microgravity Science Applications May 1992 p 193-207 (For primary document see N92-28436 19-31)
Avail: NTIS HC/MF A18

The main thrust of these studies has resulted in an active inertial feedforward/feedback isolation system. This prototype magnetic suspension system has been demonstrated in a laboratory setting in six degrees-of-freedom and has been preliminarily characterized in its isolation performance with favorable results. This isolation system consists of a closed loop digital control system referencing a platform around six relative and six inertial sensors. These sensors control the isolated mass through nine attractive electromagnetic actuators with a system capability of +/- three-tenths of an inch travel in three dimensions. The development of a prototype system from design to fabrication leads directly into the demonstration phase of the project which will attempt a low gravity environmental demonstration of engineering hardware for the isolation of a scientific payload. The demonstration phase of the project will use an aircraft low gravity maneuver to establish a research testbed for the study of isolation hardware and control strategies in an off-loaded environment. In developing this demonstration capability the Lewis Learjet aircraft has been characterized through its parabolic flight maneuvers and a trunnioned experimental volume has been designed for the test of both active and passive isolation packages. This vibration isolation testbed is operational and has two data acquisition systems available for both autonomous and interactive operation, with a combined input capability of 32 channels. Author

N92-28443*# Applied Technology Associates, Inc., Albuquerque, NM.
NEW INERTIAL ACTUATOR PROVIDES ISOLATION AND STABILIZATION IN MICROGRAVITY CONDITIONS **c29**
John Blackburn *In* NASA. Lewis Research Center, International Workshop on Vibration Isolation Technology for Microgravity Science Applications May 1992 p 209-221 (For primary document see N92-28436 19-31)
Avail: NTIS HC/MF A18

Experiments in materials and fluids processing have been conducted, or are planned, that take advantage of the low-g environment offered by space-based platforms. While the specific goals of the experiments vary, a common objective is to see improved results from the processes over those that would be obtained from similar ground-based experiments. While the space-based processing environment does offer a low-g environment, it is not disturbance free. Results of experiments already conducted, particularly those in manned vehicles, show that spacecraft induced disturbances still limit what can be achieved in materials processing. The duration of actual micro-g level environments is shorter than desired and periods of milli-g activity levels are not uncommon. While small scale experiments can be configured to overcome some of the vehicle disturbance sources, larger scale processing devices and commercial activities will require alternative methods to reduce the influences of spacecraft vibrations. Applied Technology Associates, Inc., (ATA), in cooperation with NASA Lewis Research Center, is developing hardware to provide a sustained micro-g experiment environment. This work is being sponsored under a Small Business Innovation Research (SBIR) program, which is currently in the Phase 2 development stage. ATA's approach is based on an inertial actuator, which when used as part of a closed-loop stabilization system, rejects unwanted disturbances to the experiment package. A prototype of the actuator has been fabricated and used in a laboratory demonstration to prove the principle of operation. ATA's presentation emphasized the development and testing of the Digital Materials Processing Experiment (DAMPER) inertial actuator. Physical and performance characteristics of the device are presented. Technical issues, including further optimization of the actuator's performance and plans for additional laboratory experiments, are also covered. Author

N92-28444*# SatCon Technology Corp., Cambridge, MA.
A 6 DEGREE-OF-FREEDOM LORENTZ FORCE VIBRATION ISOLATOR WITH NONLINEAR CONTROLLER **c29**
Ralph Fenn and Bruce Johnson *In* NASA. Lewis Research Center, International Workshop on Vibration Isolation Technology for Microgravity Science Applications May 1992 p 223-240 (For primary document see N92-28436 19-31)
Avail: NTIS HC/MF A18

This program demonstrated the technical feasibility of constructing large-stroke magnetic suspensions that can meet the active vibration isolation requirements of Space Station. These requirements include: (1) strokes over 1 cm in all directions, (2) actuator bandwidths over 100 Hz, (3) isolator roll-off frequencies below 10(exp -2) Hertz, and (4) force capability over 1 Newton in all axes. The 100 Hz actuator bandwidth allows the suspension to reject any direct force disturbances that act on the microgravity experiment, for example forces created by cable connections. The low isolator roll-off frequency and large stroke allow the magnetic suspension to isolate the microgravity experiment from Space Station vibrations above the roll-off frequency. The capability to meet these requirements was demonstrated by designing, constructing and testing a six-degree-of-freedom, prototype magnetic suspension system that featured high-performance, Lorentz-force actuators and full multi-input, multi-output control. This prototype suspension is designed to isolate large orbiter locker

experiments under typical spacecraft constraints of size, weight, and power. Suspension in the full six-degrees-of-freedom was successfully demonstrated in this program while using a gravity-force unload mechanism to simulate a space environment. The prototype isolator is capable of space-based isolation service with relatively minor modification. The use of advanced, nonlinear control algorithms were investigated on a specially designed single-degree-of-freedom testbed. This low acceleration test facility simulates the Space Station vibration isolation problem in a single horizontal axis with low-friction, air-slide support. This allowed testing at the desired microgravity levels, without the gravity bias effects that are seen in a full six-degrees-of-freedom suspension. Precision components were used to reduce residual accelerations to microgravity levels so that the effects of sensor, actuator, and electronic noise could be evaluated. During the Phase 2 program, this testbed was used to demonstrate the advantages of nonlinear control algorithms to provide increased vibration isolation performance. Author

N92-28445*# Pennsylvania State Univ., University Park.
DIGITAL CONTROL ALGORITHMS FOR MICROGRAVITY ISOLATION SYSTEMS **c29**
Alok Sinha and Yung-Peng Wang *In* NASA. Lewis Research Center, International Workshop on Vibration Isolation Technology for Microgravity Science Applications May 1992 p 241-256 (For primary document see N92-28436 19-31)
Avail: NTIS HC/MF A18

New digital control algorithms were developed to achieve the desired acceleration transmissibility function. The attractive electromagnets have been taken as actuators. The relative displacement and the acceleration of the mass were used as feedback signals. Two approaches were developed to find that controller transfer function in Z-domain, which yields the desired transmissibility at each frequency. In the first approach, the controller transfer function is obtained by assuming that the desired transmissibility is known in Z-domain. Since the desired transmissibility H sub d(S) = 1/(tauS+1)(exp 2) is given in S-domain, the first task is to obtain the desired transmissibility in Z-domain. There are three methods to perform this task: bilinear transformation, and backward and forward rectangular rules. The bilinear transformation and backward rectangular rule lead to improper controller transfer functions, which are physically not realizable. The forward rectangular rule does lead to a physically realizable controller. However, this controller is found to be marginally stable because of a pole at Z=1. In order to eliminate this pole, a hybrid control structure is proposed. Here the control input is composed of two parts: analog and digital. The analog input simply represents the velocity (or the integral of acceleration) feedback; and the digital controller which uses only relative displacement signal, is then obtained to achieve the desired closed-loop transfer function. The stability analysis indicates that the controller transfer function is stable for typical values of sampling period. In the second approach, the aforementioned hybrid control structure is again used. First, an analog controller transfer function corresponding to relative displacement feedback is obtained to achieve the transmissibility as 1/(tauS+1)(exp 2). Then the transfer function for the digital control input is obtained by discretizing this analog controller transfer function via bilinear transformation. The stability of the resulting Z-domain closed loop system is analyzed. Also, the frequency response of the Z-domain closed-loop transfer function is determined to evaluate the performance of the control system. Author

N92-28446*# Virginia Univ., Charlottesville. Center for Magnetic Bearings.
MICROGRAVITY VIBRATION ISOLATION RESEARCH AT THE UNIVERSITY OF VIRGINIA **c29**
Carl R. Knospe, David W. Lewis, A. Peter Allan, Paul E. Allaire, Robert R. Humphris, Bibhuti B. Banerjee, and R. David Hampton *In* NASA. Lewis Research Center, International Workshop on Vibration Isolation Technology for Microgravity Science Applications May 1992 p 257-264 (For primary document see N92-28436 19-31)
Avail: NTIS HC/MF A18

Research at the University of Virginia on microgravity vibration isolation is reviewed. This work falls into three areas: the one degree of freedom isolation test rig and Lorentz actuator design, multiple degree of freedom active isolation system control, and innovative actuators for long stroke, non-contacting six degree of freedom isolation. Theoretical and design issues of multiple degree of freedom isolation are discussed. Author

N92-28447*# Virginia Univ., Charlottesville. Center for Magnetic Bearings.
EXTENDED H2 SYNTHESIS FOR MICROGRAVITY VIBRATION ISOLATION **c29**
R. David Hampton and Carl R. Knospe *In* NASA. Lewis Research Center, International Workshop on Vibration Isolation Technology for Microgravity Science Applications May 1992 p 265-268 (For primary document see N92-28436 19-31)
Avail: NTIS HC/MF A18

The vibration environment onboard current and planned manned orbiters requires isolation for microgravity science experiments. The disturbance frequencies are sufficiently low and the attenuation requirements sufficiently great so as to preclude a passive isolation system. Described here is a design procedure, known as extended H2 synthesis, for active isolation system controllers currently being developed by the University of Virginia. Author

N92-28448*# National Aeronautics and Space Administration. Marshall Space Flight Center, Huntsville, AL.
ACAP: ACCELERATION CHARACTERIZATION AND ANALYSIS PROJECT **c29**
Charles R. Baugher *In* NASA. Lewis Research Center, International Workshop on Vibration Isolation Technology for Microgravity Science Applications May 1992 p 295-307 (For primary document see N92-28436 19-31)
Avail: NTIS HC/MF A18

Information on the Acceleration Characterization and Analysis Project presentation to the Vibration Isolation Workshop is given in viewgraph form. Topics covered include the microgravity acceleration requirements curve, a schedule of major microgravity payload flights, and determination of shuttle orbiter center of gravity. Author

N92-28449*# National Aeronautics and Space Administration. Lyndon B. Johnson Space Center, Houston, TX.
SHOCK AND VIBRATION ISOLATION FOR CYCLIC EXERCISE IN SPACECRAFT **c29**
W. Thornton *In* NASA. Lewis Research Center, International Workshop on Vibration Isolation Technology for Microgravity Science Applications May 1992 p 309-319 (For primary document see N92-28436 19-31)
Avail: NTIS HC/MF A18

A unique feature of undisturbed space flight is vibration and weight free environments not available on Earth. On long flights, exercise and especially locomotor exercise will be required if the crew is to function in a relatively normal fashion and avoid lengthy rehabilitation on return to Earth. Exercise forces in the low frequency range can amount to 2 to 3 times crew body weight in the frequency range most critical to material science. Therefore, the amount of isolation will need to be orders of magnitude greater than present techniques. The following is a brief rationale of the need for these exercises and a description of exercise forces. Current isolation means and their deficiencies will be described, and a method capable of providing the isolation proposed and work to date will be mentioned. H.A.

N92-28450*# National Aeronautics and Space Administration, Washington, DC.
SPACE STATION FREEDOM MICROGRAVITY ENVIRONMENT REQUIREMENTS AND ASSESSMENT METHODS **c29**
Philip Bogert *In* NASA. Lewis Research Center, International Workshop on Vibration Isolation Technology for Microgravity

Science Applications May 1992 p 321-344 (For primary document see N92-28436 19-31)
Avail: NTIS HC/MF A18

An overview of the Space Station Freedom's microgravity requirements is provided in viewgraph form. Additionally, the following topics are covered: (1) quasi-steady assessment techniques; (2) low frequency vibration assessment techniques; and (3) vibroacoustic assessment techniques. Author

N92-28451*# National Aeronautics and Space Administration. Lewis Research Center, Cleveland, OH.
EARLY MISSION SCIENCE SUPPORT: SPACE ACCELERATION MEASUREMENT SYSTEM (SAMS) **c19**
Richard DeLombard *In its* International Workshop on Vibration Isolation Technology for Microgravity Science Applications May 1992 p 345-355 (For primary document see N92-28436 19-31)
Avail: NTIS HC/MF A18

The Space Acceleration Measurement System (SAMS) is discussed in viewgraph form. Applications of the SAMS are as follows: (1) measurement of low-g accelerations; (2) monitoring of low-g environment; (3) monitoring of experiment-induced vibrations; and (4) validation of vibration isolation techniques. Additionally, typical locations for the SAMS are given. Author

N92-28452*# National Aeronautics and Space Administration. Lyndon B. Johnson Space Center, Houston, TX.
MICROGRAVITY ACCELEROMETER CHARACTERIZATION ON COLUMBIA STS-32 MISSION **c35**
Jeff Schoess (Honeywell, Inc., Minneapolis, MN.), Don Thomas, and Bonnie Dunbar *In* NASA. Lewis Research Center, International Workshop on Vibration Isolation Technology for Microgravity Science Applications May 1992 p 357-368 (For primary document see N92-28436 19-31)
Avail: NTIS HC/MF A18

The Honeywell In-Space Accelerometer (HISA) is a three-axis microgravity accelerometer instrument package recently developed by Honeywell Systems and Research Center (SRC) to monitor oscillatory and transient accelerations onboard spacecraft and spaceborne structures. The HISA was designed to be co-located with materials and life sciences experiments to record real-time accelerometer event data, sampling time, and temperature. The HISA was originally developed to monitor the microgravity disturbances associated with a polymer morphology experiment developed by 3M Company in Minneapolis, Minnesota. The HISA was first flight tested with the 3M experiment on the Space Shuttle Atlantis STS-34 in October 1989. The HISA was successfully flown on a second shuttle mission (Columbia STS-32 in January 1990) in support of the NASA JSC-sponsored Microgravity Disturbances Experiment (MDE), which focused on the effects of microgravity disturbances on the growth of high-quality Indium crystals. The primary objective of the STS-32 MDE experiment was to investigate the effects of crew-induced gravity disturbances on the microstructure (crystal defects and uniformity of impurity distribution) of float-zone-grown crystals. The float-zone technique involves establishing a suspended molten zone between two cylindrical samples a pure, single-crystal sample and an impure, polycrystalline sample. Microgravity disturbances due to crew treadmill activity and orbiter maneuvering system thruster firings were sensed and recorded by the HISA to understand their effects on the stability of the float zone. The principle of operation of the HISA, the flight configuration of the HISA supporting the MDE experiment, and the characterization of STS-32 treadmill disturbance data are summarized. Author

N92-28453*# Alabama Univ., Huntsville. Center for Microgravity and Materials Research.
DEVELOPMENT OF A RESIDUAL ACCELERATION DATA REDUCTION AND DISSEMINATION PLAN **c82**
Melissa J. B. Rogers *In* NASA. Lewis Research Center, International Workshop on Vibration Isolation Technology for Microgravity Science Applications May 1992 p 369-382 (For primary document see N92-28436 19-31)
Avail: NTIS HC/MF A18

A major obstacle in evaluating the residual acceleration environment in an orbiting space laboratory is the amount of data collected during a given mission: gigabytes of data will be available as SAMS units begin to fly regularly. Investigators taking advantage of the reduced gravity conditions of space should not be overwhelmed by the accelerometer data which describe these conditions. We are therefore developing a data reduction and analysis plan that will allow principal investigators of low-g experiments to create experiment-specific residual acceleration data bases for post-flight analysis. The basic aspects of the plan can also be used to characterize the acceleration environment of earth orbiting laboratories. Our development of the reduction plan is based on the following program of research: the identification of experiment sensitivities by order of magnitude estimates and numerical modelling; evaluation of various signal processing techniques appropriate for the reduction, supplementation, and dissemination of residual acceleration data; and testing and implementation of the plan on existing acceleration data bases. The orientation of the residual acceleration vector with respect to some set of coordinate axes is important for experiments with known directional sensitivity. Orientation information can be obtained from the evaluation of direction cosines. Fourier analysis is commonly used to transform time history data into the frequency domain. Common spectral representations are the amplitude spectrum which gives the average of the components of the time series at each frequency and the power spectral density which indicates the power or energy present in the series per unit frequency interval. The data reduction and analysis scheme developed involves a two tiered structure to: (1) identify experiment characteristics and mission events that can be used to limit the amount of accelerator data an investigator should be interested in; and (2) process the data in a way that will be meaningful to the experiment objectives. A general outline of the plan is given. Author

N92-28454*# Massachusetts Inst. of Tech., Cambridge. Dept. of Aeronautics and Astronautics.
MICROGRAVITY ISOLATION MOUNTS BASED UPON PIEZOELECTRIC FILM **c29**
Andreas vonFlotow *In* NASA. Lewis Research Center, International Workshop on Vibration Isolation Technology for Microgravity Science Applications May 1992 p 391-396 (For primary document see N92-28436 19-31)
Avail: NTIS HC/MF A18

The topics are presented in viewgraph form and include the following: a polyvinylidene fluoride (PVDF) actuator; a semi-active soft mount; a 3-axis experiment; low frequency disturbance attenuation; the control problem; and a 6-axis laboratory prototype. Author

N92-28455*# Jet Propulsion Lab., California Inst. of Tech., Pasadena.
PREDICTING MICROGRAVITY LEVELS FOR SPACE STATION USING VAPEPS **c29**
G. Badilla, T. Bergen, D. Kern, and T. Scharton *In* NASA. Lewis Research Center, International Workshop on Vibration Isolation Technology for Microgravity Science Applications May 1992 p 397-410 (For primary document see N92-28436 19-31)
Avail: NTIS HC/MF A18

The topics are presented in viewgraph form and include: a vibroacoustic payload environment prediction system (VAPEPS); objectives of the JPL space station analysis effort; statistical energy analysis (SEA); VAPEPS Space Station Freedom (SSF) model description; noise control treatments; and SSF microgravity preliminary analysis results. Author

N92-28793# Technische Univ., Berlin (Germany, F.R.). Fachbereich Elektrotechnik.
HIGH RESOLUTION ELECTRON BEAM LITHOGRAPHY ON X RAY MASK SUBSTRATES. EFFECTS OF ELECTRON SCATTERING AND MEMBRANE HEATING Ph.D. Thesis [HOCHAUFLOESENDE ELEKTRONENSTRAHLLITHOGRAPHIE AUF ROENTGENMASKENSUBSTRATEN. EFFEKTE DER ELEKTRONENSTREUUNG UND DER MEMBRANERWAERMUNG]
Klaus Reimer 1991 140 p In GERMAN
(ETN-92-91336) Avail: NTIS HC/MF A07

The requirements of X-ray masks for a 64 megabit storage in electron beam lithography, with regard to resolution power and positioning accuracy were compared with the present state of electron beam systems. Electron scattering behavior in X-ray mask substrates was examined with special emphasis on the quantification of the proximity effect. A Monte Carlo simulation program was developed. The evaluation of all results led to a specification list for an electron beam recording instrument. ESA

N92-28902# Army Cold Regions Research and Engineering Lab., Hanover, NH.
USE OF SCRAP RUBBER IN ASPHALT PAVEMENT SURFACES
Robert A. Eaton, Richard J. Roberts, and Robert R. Blackburn Dec. 1991 21 p Prepared in cooperation with Midwest Research Inst., Kansas City, MO
(AD-A247419; CRREL-SR-91-27) Avail: NTIS HC/MF A03

Scrap tire rubber was mixed into an asphalt concrete wearing course to study the effect of ice disbonding from the pavement surface under traffic. Rubber contents of 0, 3, 6, and 12 percent by weight were studied. Initial laboratory ice disbonding test results led to the development of a new paving material, Chunk Rubber Asphalt Concrete (CRAC), that uses larger pieces of rubber in a much denser asphalt concrete mix. Strength values doubled and ice disbonding performance was enhanced. GRA

N92-29191# Air Force Inst. of Tech., Wright-Patterson AFB, OH. School of Engineering.
MODULAR SIMULATION OF HEI FRAGMENTS AND BLAST PRESSURE M.S. Thesis
Gordon L. Galloway Mar. 1992 257 p
(AD-A248205; AFIT/GOR/ENS/92M-11) Avail: NTIS HC/MF A12

The fragmentation and blast pressure of High Explosive Incendiary projectiles are major causes of aircraft fuel fires. Because Halon 1301 is being banned from DoD use as a fire suppressant, alternative fire suppressants must be developed and tested. These new suppressants must counteract the fire directly or eliminate one or more of the factors which cause the fire. To this end, this thesis takes a detailed look at the HEI processes that lead to a fire. A comprehensive review of the current knowledge and understanding of these processes is presented. In addition, hypothesized dependencies between the various processes are stated. These hypothesized dependencies can not be proved or disproved with data at this time. Therefore, tests and test set-ups are outlined to collect the necessary data. The evidence in support of these dependencies is also presented. To aid the testing of various fire suppressant system and the hypothesized HEI explosion dependencies a simulation of the HEI explosion was developed. This simulation allows the user to simulate any configuration of the aircraft dry bay, and any attack scenario for the projectile. Using this simulation one of the hypothesized dependencies was tested and shown to be possible. GRA

32 COMMUNICATIONS AND RADAR

Includes radar; land and global communications; communications theory; and optical communications.

For related information see also *04 Aircraft Communications and Navigation* and *17 Space Communications, Spacecraft Communications, Command and Tracking.* For search and rescue see *03 Air Transportation and Safety,* and *16 Space Transportation.*

N92-28253# Naval Training Systems Center, Orlando, FL.
AN ANALYSIS OF AIRCREW COMMUNICATION PATTERNS AND CONTENT Final Report, Aug. 1989 - Apr. 1990
Randall L. Oser, Carolyn Prince, Ben B. Morgan, Jr., and Steven S. Simpson 3 Sep. 1991 80 p
(NR Proj. RM3-3-T-21)
(AD-A246618; NTSC-TR-90-09) Avail: NTIS HC/MF A05

The findings reported here represent a detailed analysis of tactical rotary-wing aircrew communication patterns and content. This research is part of an extensive effort to investigate the nature of tactical aircrew coordination and to develop effective mission-oriented aircrew coordination training. The primary objectives of this research were to answer the following questions: (1) What specific communication patterns and content are demonstrated by different helicopter crewmembers (i.e., Helicopter Aircraft Commander - HAC and Helicopter 2nd Pilot - H2P)? (2) Do tactical aircrew communication patterns and content vary as a function of the performance demands and requirements of different flight conditions (i.e., routine and non-routine)? (3) Are the communication patterns and content of more effective aircrews different from those of less effective aircrews? (4) What similarities exist between the communication patterns and content of military rotary-wing aircrews and commercial fixed-wing aircrews? and (5) Can the results of the communication analyses have an impact on aircrew coordination training? GRA

N92-28304# Mitre Corp., Bedford, MA.
AN OTH RADAR CLUTTER SIMULATION
J. Providakes, T. J. Elkins, R. B. Godwin, and M. C. Kelley Dec. 1991 28 p
(Contract F19628-89-C-0001)
(AD-A248054; M91-114) Avail: NTIS HC/MF A03

A computer simulation is described which was developed with the objective of arriving at an understanding of OTH radar clutter originating in the equatorial ionosphere. This source of clutter is of particular interest in OTH radar, since all radar propagation paths must pass through the equatorial region, even if the desired targets are far removed from it. A central feature of the simulation is an ionospheric propagation model developed to synthesize OTH radar clutter by making use of state-of-the art models for global ionospheric structure, including small-scale irregularities, and combining these with efficient ray tracing procedures and a multiple phase-screen approach to computing the diffraction of radar energy by the irregular ionosphere. Simulated clutter data is compared to actual measurements using several radars, with generally satisfactory results. GRA

N92-28347# Naval Postgraduate School, Monterey, CA.
THE USE OF CONFORMAL SUBDOMAIN BASIS FUNCTIONS IN THE METHOD OF MOMENTS COMPUTATIONS FOR A THIN WIRE M.S. Thesis
Bruce A. Walter Dec. 1991 89 p
(AD-A245964) Avail: NTIS HC/MF A05

The purpose of this thesis is to investigate the use of Conformal Subdomain Basis Functions (CSBF) in the Method of Moments (MM) solution of a thin wire scatterer. The effect of using CSBF on the computed current and the scattered field is investigated by formulating and coding the MM solution for a thin wire loop and comparing the computed results for various loop sizes to measured data and two other MM codes. Significant reduction in the number of segments (and computer memory requirements) are found for loops with circumferences of less than one to two wavelengths for plane wave incidence. From these results, it is concluded that

the use of CSBF will significantly reduce the number of segments required for the MM solution of a spiral antenna. GRA

N92-28357# Naval Postgraduate School, Monterey, CA.
COMPARISON OF ELECTROMAGNETIC PROPAGATION PREDICTIONS FROM IREPS AND RPO ACROSS A COASTAL TRANSITION M.S. Thesis
Bryce Campbell and Stephan Siletzky Mar. 1992 89 p
(AD-A249331) Avail: NTIS HC/MF A05

The Navy's existing electromagnetic ion prediction software, the Integrated Refractive Effects Prediction System (IREPS), neglects signal leakage from a duct, approximates diffraction, and assumes atmospheric horizontal homogeneity. To ameliorate these deficiencies, the Radio Physics Optics (RPO) program is being developed. This thesis analyzes the significantly different propagation predictions of the two models. RPO predicts significantly shorter propagation ranges in a duct than does IREPS. RPO predicts variations in duct thickness and height which IREPS idealizes, and RPO also computes a signal strength above the duct. Only RPO predicts significant interactions between the duct's dM/dz gradient and frequency. RPO is capable of modeling propagation paths for an inhomogeneous atmosphere. Neglecting atmospheric inhomogeneities in a coastal region introduces significant propagation prediction errors. GRA

N92-28358# Michigan State Univ., East Lansing. Dept. of Electrical Engineering and Systems Science.
ADAPTIVE SET-MEMBERSHIP IDENTIFICATION IN 0(m) TIME FOR LINEAR-IN-PARAMETERS MODELS
J. R. Deller, Jr. and S. F. Odehl 3 Apr. 1992 46 p Revised
(Contract N00014-91-J-1329; NSF MIP-90-16734)
(AD-A249359) Avail: NTIS HC/MF A03

This paper describes some fundamental contributions to the theory and applicability of optimal bounding ellipsoid (OBE) algorithms for signal processing. AU reported OBE algorithms are placed in a general framework which fruitfully demonstrates the relationship between the set-membership principles and least square error identification. Within this framework, flexible measures for adding explicit adaptation capability are formulated and demonstrated through simulation. Computational complexity analysis of OBE algorithms reveals that they are of O(m2) complexity per data sample with m the number of parameters identified, in spite of their well-known propensity toward highly-selective updating. Two very different approaches are described for rendering a specific OBE algorithm, the set-membership weighted recursive least squares algorithm, of 0(m) complexity. The first approach involves an algorithmic solution in which a suboptimal test for innovation is employed. The performance is demonstrated through simulation. The second method is an architectural approach in which complexity is reduced through parallel computation. GRA

N92-28371*# Michigan Univ., Ann Arbor. Radiation Lab.
SCATTERING AND RADIATION ANALYSIS OF THREE-DIMENSIONAL CAVITY ARRAYS VIA A HYBRID FINITE ELEMENT METHOD
Jian-Ming Jin and John L. Volakis Jun. 1992 22 p
(Contract NCA2-543)
(NASA-CR-190408; NAS 1.26:190408; UMICH-027723-5-T)
Avail: NTIS HC/MF A03

A hybrid numerical technique is presented for a characterization of the scattering and radiation properties of three-dimensional cavity arrays recessed in a ground plane. The technique combines the finite element and boundary integral methods and invokes Floquet's representation to formulate a system of equations for the fields at the apertures and those inside the cavities. The system is solved via the conjugate gradient method in conjunction with the Fast Fourier Transform (FFT) thus achieving an O(N) storage requirement. By virtue of the finite element method, the proposed technique is applicable to periodic arrays comprised of cavities having arbitrary shape and filled with inhomogeneous dielectrics. Several numerical results are presented, along with new measured data, which demonstrate the validity, efficiency, and capability of the technique. Author

N92-28410# Naval Postgraduate School, Monterey, CA.
DESIGN ON AN ENHANCED INTERACTIVE SATELLITE COMMUNICATIONS SYSTEM ANALYSIS PROGRAM M.S. Thesis
Kevin Robert Andersen Sep. 1991 228 p
(AD-A245967) Avail: NTIS HC/MF A11

This thesis describes the design of a user-friendly interactive satellite communications analysis program for use on a personal computer. The user inputs the various parameters of a satellite orbit, ground station location and communications equipment. The output generated allows a user to view the satellite ground trace and footprint, calculate satellite rise and set times, and analyze the performance of the communications link. The link analysis allows the user to input various signal losses and jamming interference. Care was taken to ensure that the program is simple to operate and that it provides on-line help for each segment. A principle goal of this thesis effort is to provide an educational tool that familiarizes the user with the communications segment of a space system. The initial success of the program based upon student response validates the use of object-oriented like software tools that enhance user understanding of complex subjects. GRA

N92-28431*# Space Systems/Loral, Palo Alto, CA. Communications Systems Lab.
FUTURE BENEFITS AND APPLICATIONS OF INTELLIGENT ON-BOARD PROCESSING TO VSAT SERVICES Final Report
Kent M. Price, Robert K. Kwan, Ron Edward, F. Faris, and Tom Inukai May 1992 227 p
(Contract NAS3-25092; RTOP 144-50-50)
(NASA-CR-189185; NAS 1.26:189185; SS/L-TR00820) Avail: NTIS HC/MF A11

The trends and roles of VSAT services in the year 2010 time frame are examined based on an overall network and service model for that period. An estimate of the VSAT traffic is then made and the service and general network requirements are identified. In order to accommodate these traffic needs, four satellite VSAT architectures based on the use of fixed or scanning multibeam antennas in conjunction with IF switching or onboard regeneration and baseband processing are suggested. The performance of each of these architectures is assessed and the key enabling technologies are identified. Author

N92-28586*# Virginia Polytechnic Inst. and State Univ., Blacksburg. Satellite Communications Group.
FADE DURATIONS IN SATELLITE-PATH MOBILE RADIO PROPAGATION
Robert G. Schmier and Charles W. Bostian Dec. 1986 171 p
(Contract JPL-956512)
(NASA-CR-190484; JPL-9950-1382; NAS 1.26:190484;
EE-SATCOM-86-5) Avail: NTIS HC/MF A08

Fades on satellite to land mobile radio links are caused by several factors, the most important of which are multipath propagation and vegetative shadowing. Designers of vehicular satellite communications systems require information about the statistics of fade durations in order to overcome or compensate for the fades. Except for a few limiting cases, only the mean fade duration can be determined analytically, and all other statistics must be obtained experimentally or via simulation. This report describes and presents results from a computer program developed at Virginia Tech to simulate satellite path propagation of a mobile station in a rural area. It generates rapidly-fading and slowly-fading signals by separate processes that yield correct cumulative signal distributions and then combines these to simulate the overall signal. This is then analyzed to yield the statistics of fade duration. Author

N92-28699# Victoria Univ. (British Columbia). Dept. of Electrical and Computer Engineering.
CODING FOR FREQUENCY HOPPED SPREAD SPECTRUM SATELLITE COMMUNICATIONS Final Report, 1 Apr. 1989 - 31 Mar. 1990
Vijay K. Bhargava, Qiang Wang, Ian F. Blake (Waterloo Univ., Ontario), Gang Li, T. Aaron Gulliver (Defence Research Establishment, Ottawa, Ontario), and Olaf Dravnieks 15 Apr. 1990 140 p
(Contract DSS-36001-8-359/01-SS)
(ECE-90-1; CTN-91-60077) Avail: NTIS HC/MF A07

Work aimed at improving the jamming resistance of satellite communications is reviewed. The performance of Reed-Solomon (RS) error correcting codes with slow frequency hopped (SFH) differential phase shift keying (DPSK) signalling is analyzed and evaluated under worst case partial band noise and worst case multitone jamming. A representative set of performance curves is shown. Recommendation on the choice of RS code parameters is given. Two in-hop jamming cancellation schemes for SFH/DPSK systems are proposed. One scheme is based on balanced coding; the other one uses notch filter to cancel jamming tone. The performance of both schemes is illustrated. It is shown that both schemes can work well under certain conditions. Basic principles and techniques for designing interleavers are presented. Block, convolution, and the more recent helical interleavers are considered. The trade-off between diversity and coding for spread spectrum systems, where a low code rate is anticipated, is discussed. An error correction scheme is presented for an M-ary symmetric channel (MSC) characterized by a large error probability (Pe). The value of Pe can be near, but smaller than 1-1/M, for which the channel capacity is zero. Such a large Pe may occur, for example, in a jamming environment. Monte-Carlo simulation results are presented. For the binary symmetric channel (BSC), it is shown that the overall code rate is larger than 0.6 R sub 0, where R sub 0 is the cutoff rate of the channel. For BSC and a large diversity order (m), a method is presented for BER (bit error rate) approximation on the central limit theorem. CISTI

N92-28773# Georgia Inst. of Tech., Atlanta.
AN ACOUSTIC CHARGE TRANSPORT IMAGER FOR HIGH DEFINITION TELEVISION APPLICATION Semiannual Report
W. D. Hunt, K. F. Brennan, A. Torabi, and C. J. Summers Mar. 1992 30 p Sponsored by DARPA
(AD-A250433) Avail: NTIS HC/MF A03

The primary goal of this research is to demonstrate the feasibility of developing an acoustic charge transport (ACT) imager for high definition systems applications. The operation of the proposed camera chip can be subdivided into three distinct functions: image capture, charge collection and storage, and charge readout for image reconstruction. The image capture stage of the device will be a GaAs/AlGaAs multiple quantum well avalanche photodiode (APD). Following the APD device is a charge storage and overflow heterostructure transistor which controls charge transfer into the ACT channel for readout and processing. We discuss progress towards developing each of these three aspects of the chip as well as work towards integrating these components into a successful working device. GRA

N92-28792# Technische Univ., Berlin (Germany, F.R.). Fachbereich Elektrotechnik.
EXAMINATION OF PROSODIC FEATURES IN SPEECH SIGNAL USING SPEECH FUNDAMENTAL FREQUENCY AND LOUDNESS DURATION Ph.D. Thesis [ZUR UNTERSUCHUNG PROSODISCHER MERKMALE IM SPRACHSIGNAL ANHAND DER SPRACHGRUNDFREQUENZ UND DER LAUTDAUER]
Martin Rusch 1991 140 p In GERMAN
(ETN-92-91334) Avail: NTIS HC/MF A07

The most important prosodic parameters and their physical correlations in speech signal were evaluated. Processes for their acquisition, in particular the speech fundamental frequency, were described. Fundamental frequency structures in natural language were examined, using various syllabic forms in stressed and unstressed position. A hierarchic model was developed. The software used for the boundness duration measurement allowed the segmentation of speech signal in time domain. The fundamental frequency and loudness duration correlations were represented for the realization of accentuation structures. ESA

N92-28796# Naval Ocean Systems Center, San Diego, CA. Research, Development, Test and Evaluation Div.
NULL SHIFTING WITH FIXED DELAYS
M. H. Berry and D. M. Gookin Mar. 1992 7 p Sponsored by ONR
(AD-A250059) Avail: NTIS HC/MF A02

We demonstrate null shifting over a 1 GHz bandwidth using a fiber optic and integrated optic transversal filter. The null depth for our system is greater than 70 dB measured with a 10 kHz IF bandwidth. The null shifting is achieved by varying the tap weight values. Null shifting in the response of a transversal filter is directly related to null steering for a radar direction finder. The fixed delays consist of optical fibers cut at 10 centimeter increments. Integrated optical 2 x 2 couplers are used as the tap weights. The weighting is controlled by an applied voltage. The depth of the null is limited by the dynamic range of the source/detector combination. Ordinary fixed weight fiber optic transversal filters are subject to dynamic range and bandwidth limitations due to errors in cutting the fiber lengths. This problem can be remedied by using variable taps to shift the null frequency. The null depth and resolution is not detrimentally effected by using this approach. GRA

N92-28809# Argonne National Lab., IL.
APERTURE COUPLING MEASUREMENT IN A TEST CHAMBER FOR THE ADVANCED PHOTON SOURCE (APS)
J. J. Song, J. H. Zhou, and R. L. Kustom 1992 3 p Presented at the 3rd European Particle Accelerator Conference, Berlin, Fed. Republic of Germany, 24-28 Mar. 1992
(Contract W-31-109-eng-38)
(DE92-013059; ANL/CP-75862; CONF-920315-32) Avail: NTIS HC/MF A01

Aperture coupling measurements have been made using two identical rectangular chambers. A common wall between them has holes of various size, thickness, shape, and number. The transverse electromagnetic (TEM) wave, which propagates in one rectangular chamber, couples through the aperture and radiates into the other chamber. The measured results are compared with the diffraction model and used to estimate the coupling impedance of a circulating beam. The results of these measurements were applied to the detailed design of some of the vacuum components in the Advanced Photon Source. DOE

N92-28810# Argonne National Lab., IL.
RF IMPEDANCE MEASUREMENT STATUS FOR THE 7-GeV ADVANCED PHOTON SOURCE (APS)
J. J. Song and R. L. Kustom 1992 3 p Presented at the 3rd European Particle Accelerator Conference, Berlin, Fed. Republic of Germany, 24-28 Mar. 1992
(Contract W-31-109-eng-38)
(DE92-013060; ANL/CP-75861; CONF-920315-31) Avail: NTIS HC/MF A01

Beam-coupling impedances (Z) for the 7-GeV APS storage ring have been numerically estimated. In order to confirm these calculations, the wire method with a synthetic pulse technique was used to measure the beam coupling impedance of various vacuum components around the main storage ring. A section of the beam + antechambers, a vacuum isolation valve with and without the RF shielding screen, an insertion device, and a photon absorber were used as a device under test (DUT) to obtain the results. The results were compared with the computer simulations, and the Z or k-dependence onbunch lengths were studied. DOE

N92-28846# Washington Univ., Seattle.
PROPAGATION AND SCATTERING OF MICROWAVES AND MILLIMETER WAVES IN SNOW BASED ON DENSE RANDOM MEDIA THEORY Report, 15 Feb. 1989 - 14 Feb. 1992
Leung Tsang 15 Apr. 1992 9 p

(Contract DAAL03-89-K-0055)
(AD-A249300; ARO-26384.11-GS) Avail: NTIS HC/MF A02

The propagation and scattering of electromagnetic waves in snow terrain in the microwave and millimeter wave frequencies are strongly affected by both volume and surface scattering. We have studied the scattering in snow terrain in the frequency range of 5 GHz to 100 GHz. Snow terrain is classified as a dense medium because it is a mixture of ice particles and air with the ice particles occupying an appreciable fractional volume. Volume scattering in snow terrain has been studied with dense media theory. We have validated the dense media theory with Monte-Carlo simulations of pair-distribution functions and by numerical solutions of Maxwell's equations. Also, we have performed Monte Carlo simulations of rough surface scattering by the finite element and finite difference methods. GRA

N92-28873*# Ohio State Univ., Columbus. Dept. of Electrical Engineering.
DIGITAL COMPRESSION ALGORITHMS FOR HDTV TRANSMISSION
Kenneth C. Adkins, Mary Jo Shalkhauser (National Aeronautics and Space Administration. Lewis Research Center, Cleveland, OH.), and Steven B. Bibyk May 1990 7 p
(Grant NAG3-1082; RTOP 650-60-21)
(NASA-CR-190509; NAS 1.26:190509) Avail: NTIS HC/MF A02

Digital compression of video images is a possible avenue for high definition television (HDTV) transmission. Compression needs to be optimized while picture quality remains high. Two techniques for compression the digital images are explained and comparisons are drawn between the human vision system and artificial compression techniques. Suggestions for improving compression algorithms through the use of neural and analog circuitry are given. Author

N92-28876*# National Aeronautics and Space Administration. Langley Research Center, Hampton, VA.
WINDSHEAR RADAR CALIBRATION: TRANSMITTER POWER AND RECEIVER GAIN STABILITY
Anne I. Mackenzie Jun. 1992 16 p
(RTOP 505-64-12-02)
(NASA-TM-107589; NAS 1.15:107589) Avail: NTIS HC/MF A03

An experimental windshear Doppler radar was flown on 27 occasions during a series of flight experiments in 1991. Radar calibrations were performed by the flight team to monitor the transmitter power and receiver gain from pre-flight to post-flight and from one day to another. From the recorded calibration data, the receiver gain and effective receiver system noise were calculated and tabulated, together with the transmitter power. These quantities of interest are compared for two receiver/transmitter (R/T) units and two intermediate frequency (IF) bandwidths that were tested in various modes. It was found that, in most operating modes, gain stayed within a 2.5-dB range and transmitter power stayed within a 20-watt range. R/T number 1 had 0.8 dB more gain and 1.2 dBm less noise power than R/T number 2. The 7-MHz IF bandwidth resulted in 1 dB more gain and 1 dBm less noise than the 2-MHz IF bandwidth. Depending on the R/T unit and IF bandwidth, the effective system noise power averaged between -107.3 dBm and -109.5 dBm. Author

N92-28878# Georgia Inst. of Tech., Atlanta. School of Physics.
STUDIES OF THE POLARIMETRIC DEPENDENCE OF ENHANCED BACKSCATTERING FROM ONE-DIMENSIONAL SURFACES Final Report, 15 Jul. - 14 Nov. 1991
Kevin A. ODonnell and Thierry R. Michel 15 Dec. 1991 19 p
(Contract DAAL03-91-G-0220; DA Proj. 1L1-61102-BH-57)
(AD-A248431) Avail: NTIS HC/MF A03

We conduct theoretical calculations that study the diffuse scattering properties of surfaces that are randomly rough in one dimension. The four distinct elements of the Stokes matrix of such a surface are calculated using numerical techniques that employ exact methods to determine the scattered field. The behavior of the Stokes matrix elements are interpreted explicitly in terms of multiple scattering. The surface parameters chosen are the same as used in recent experiments. The investigations clarify the physical origins of disagreement between theoretical and experimental results in this field. GRA

N92-28887# Defence Research Establishment, Ottawa (Ontario).
THE USE OF A VECTOR NETWORK ANALYZER FOR MEASURING THE PERFORMANCE OF RADAR ABSORBING MATERIALS
Jeffrey Stanier Nov. 1991 20 p
(AD-A247194; DREO-TN-91-32) Avail: NTIS HC/MF A03

Testing the performance of Radar Absorbing Materials (RAM) is often a difficult task and in most cases the manufacturer's specifications are the only source of performance data. This paper presents a method of measuring the normal reflection coefficient of planar RAM using a Hewlett-Packard 8510A Vector Network Analyzer and a small horn antenna. The Vector Network Analyzer is used to cancel the reflections from discontinuities in the signal path from the source to the RAM sample leaving only the reflections from the RAM sample. Using this approach, information can be gathered over a wide bandwidth very quickly, and comparisons between RAM samples can be done easily. GRA

N92-28905# Johns Hopkins Univ., Laurel, MD. Applied Physics Lab.
SIMULATING RADAR PROPAGATION THROUGH ATMOSPHERIC TURBULENCE USING THE TROPOSPHERIC ELECTROMAGNETIC PARABOLIC EQUATION ROUTINE (TEMPER) Technical Memorandum Apr. 1990 - Oct. 1991
Daniel Rouseff 20 Nov. 1991 51 p
(Contract N00039-89-C-5301)
(AD-A247408; JHU/APL-TG-1381) Avail: NTIS HC/MF A04

The Tropospheric Electromagnetic Parabolic Equation Routine (TEMPER) being developed by the Fleet Systems Department at the Applied Physics Laboratory has proven to be a useful tool in predicting low-altitude radar propagation. A marching procedure is used to step the field through what has been assumed to be a deterministic spatially varying index of refraction profile. In an actual environment, small-scale random fluctuations from atmospheric turbulence are superimposed on the deterministic profile. In this report a method for coupling random refractivity fluctuations into TEMPER is proposed and tested numerically. Three-dimensional spectral models from the atmospheric literature are used to derive the one-dimensional transverse spectra of refractivity necessary for parabolic simulations. Realizations consistent with the spectra are generated using filtered white noise. Propagation studies are conducted for the canonical problem of a plane wave transmitted through homogeneous isotropic turbulence. Good agreement is observed between the numerical results and existing theory for the second moment of the scattered field. However, the agreement is less good for predicting the random fluctuations in the log-amplitude of the field as three-dimensional effects become significant. Methods for simulating inhomogeneous boundary layer turbulence are considered. The limits of spectral modeling for simulating turbulence are discussed. GRA

N92-28906*# Space Systems/Loral, Palo Alto, CA. Communications Systems Lab.
MASS AND POWER MODELING OF COMMUNICATION SATELLITES Final Report
Kent M. Price, David Pidgeon, and Alex Tsao Dec. 1991 91 p
(Contract NAS3-25092; RTOP 144-50-50)
(NASA-CR-189186; NAS 1.26:189186; SS/L-TR00821) Avail: NTIS HC/MF A05

Analytic estimating relationships for the mass and power requirements for major satellite subsystems are described. The model for each subsystem is keyed to the performance drivers and system requirements that influence their selection and use. Guidelines are also given for choosing among alternative technologies which accounts for other significant variables such as cost, risk, schedule, operations, heritage, and life requirements. These models are intended for application to first order systems analyses, where resources do not warrant detailed development

of a communications system scenario. Given this ground rule, the models are simplified to 'smoothed' representation of reality. Therefore, the user is cautioned that cost, schedule, and risk may be significantly impacted where interpolations are sufficiently different from existing hardware as to warrant development of new devices. Author

N92-28947# Naval Ocean Systems Center, San Diego, CA.
ANALYSIS OF ELECTROMAGNETIC PROPAGATION OVER VARIABLE TERRAIN USING THE PARABOLIC WAVE EQUATION Final Report, Oct. 1989 - Oct. 1991
Frank J. Ryan Oct. 1991 44 p
(AD-A248061; NOSC/TR-1453) Avail: NTIS HC/MF A03

This report describes the fundamental physics and basic numerical algorithms that form the basis of a range-dependent microwave propagation model. The model accounts for the effects of nonhomogeneous atmospheric refractivity fields, finite surface conductivity and variable surface terrain elevation. Both vertical and horizontal field polarization and general antenna radiation patterns are included in the analysis. The electromagnetic field propagation is modeled using the splitstep Fourier parabolic wave equation (SSFPE) algorithm, modified to account for an impedance-type boundary condition. The various approximations used in developing the SSFPE algorithm are discussed, along with local and global error estimates. GRA

N92-28979# Defence Research Establishment, Ottawa (Ontario).
DATA SELECTION FOR FAST PROJECTION TECHNIQUES APPLIED TO ADAPTIVE NULLING: A COMPARATIVE STUDY OF PERFORMANCE
Mylene Toulgoat and Ross M. Turner Dec. 1991 37 p
(AD-A246468; DREO-1100) Avail: NTIS HC/MF A03

This report describes simulation studies of fast projection techniques for adaptive nulling of jammer signals. These techniques are based on a data selection criterion applied directly to the data vectors obtained at the output of an antenna array. The selected data vectors are used in fast projection algorithms to estimate the antenna weighting vector that is orthogonal to the jamming vectors. Four such algorithms are described ranging from the fastest but least effective to the most computationally demanding but most effective. In effect, these algorithms provide a better trade-off of performance versus computational load than was previously available. Relative performance is compared with that of the standard Sample Matrix Inversion (SMI) technique for test cases which evaluate the effects of the number of jammers, the jammer strengths relative to the receiver noise, and the jammer angular positions. GRA

N92-29084# Naval Postgraduate School, Monterey, CA.
EFFECTS OF FADING AND DATA MODULATION ON NONCOHERENT M-SEQUENCE ACQUISITION SCHEMES M.S. Thesis
Patrick J. Vincent Mar. 1992 110 p
(AD-A247968) Avail: NTIS HC/MF A06

In direct-sequence spread-spectrum systems, successful communications require phase synchronization of the m-sequence in the incoming signal with a locally generated m-sequence at the receiver. Many acquisition schemes which extract the phase of an incoming m-sequence have been studied, but most of them assume coherent demodulation (which is usually not available during acquisition) and or independent samples (which introduce a loss in the effective signal to noise ratio (SNR)). This thesis investigates the performance of two m-sequence acquisition schemes in the presence of fading and data modulation. A fixed sample size test and a truncated sequential test are studied without the usual assumptions of coherent demodulation or independent samples. The effects of fading and data modulation on our schemes' probability of false alarm, probability of detection and test length are thoroughly explored. We find that channel fading in effect induces a loss of signal SNR, but the desired power of the tests can be restored by suitable adjustments in the decision processor. We find that the effects of data modulation are less severe, but more problematic to correct. GRA

N92-29085 Department of the Navy, Washington, DC.
CROSSTALK CORRECTION SCHEME Patent
Roy L. Streit, inventor (to NASA) and Foster L. Striffler, inventor (to Navy) 4 Feb. 1992 5 p Filed 5 Jul. 1989
(AD-D015251; US-Patent-5,086,423; US-Patent-Appl-SN-376270; US-Patent-Class-370-6) Avail: US Patent and Trademark Office

Crosstalk contamination of signals of a multichannel data transmission system is designated by a matrix which has unit values for the diagonal and small values for the off-diagonal terms. If this matrix satisfies the criteria for finding an inverse thereof, the matrix may be inverted and the results are used to find the values for the correction matrix electronic circuits. The correction electronic matrix circuits with their respective inputs from the telemetry receiver give their summed outputs for each channel to be the crosstalk contamination-free signals for various channels. GRA

N92-29115*# National Inst. of Standards and Technology, Gaithersburg, MD.
WAVENUMBER CALIBRATION TABLES FROM HETERODYNE FREQUENCY MEASUREMENTS Final Report
A. G. Maki and J. S. Wells Dec. 1991 647 p
(NASA-CR-190422; NAS 1.26:190422; NIST/SP-821) Avail: NTIS HC/MF A99; also available SOD $31.00 as 003-003-03136-4

The new calibration atlas is based on frequency rather than wavelength calibration techniques for absolute references. Since a limited number of absolute frequency measurements is possible, additional data from alternate methodology are used for difference frequency measurements within each band investigated by frequency measurement techniques. Data from these complementary techniques include the best Fourier transform measurements available. Included in the text portion of the atlas are a description of the heterodyne frequency measurement techniques, details of the analysis including the Hamiltonians and least-squares-fitting and calculation procedures. Also included are other relevant considerations such as intensities and lineshape parameters. A 350-entry bibliography which contains all data sources used and a subsequent section on errors conclude the text portion. The larger portion of the atlas consists of several hundred spectral-maps/facing-tables pages for the various calibration molecules. The spectral maps (as well as the facing tables) are calculated from the molecular constants derived for the work. The primary calibration molecules are the linear triatomics, carbonyl sulfide and nitrous oxide, which cover portions of the infrared spectrum ranging from 488 to 3120 cm. Some gaps in the coverage afforded by OCS and N2O are partially covered by NO, CO, and CS2. An additional region from 4000 to 4400 cm based on CO is also included. Author

N92-29124* National Aeronautics and Space Administration. Pasadena Office, CA.
METHOD AND APPARATUS FOR FREQUENCY SPECTRUM ANALYSIS Patent
Steven W. Cole, inventor (to NASA) (Jet Propulsion Lab., California Inst. of Tech., Pasadena.) 16 Jun. 1992 10 p Filed 25 Feb. 1991 Supersedes N92-10125 (30 - 1, p 25)
(NASA-Case-NPO-17759-1-CU; US-Patent-5,122,731; US-Patent-Appl-SN-660371; US-Patent-Class-324-77C; US-Patent-Class-324-77CS; US-Patent-Class-324-78F; US-Patent-Class-324-78D; Int-Patent-Class-G01R-23/16) Avail: US Patent and Trademark Office

A method for frequency spectrum analysis of an unknown signal in real-time is discussed. The method is based upon integration of 1-bit samples of signal voltage amplitude corresponding to sine or cosine phases of a controlled center frequency clock which is changed after each integration interval to sweep the frequency range of interest in steps. Integration of samples during each interval is carried out over a number of cycles of the center frequency clock spanning a number of cycles of an

input signal to be analyzed. The invention may be used to detect the frequency of at least two signals simultaneously. By using a reference signal of known frequency and voltage amplitude (added to the two signals for parallel processing in the same way, but in a different channel with a sampling at the known frequency and phases of the reference signal), the absolute voltage amplitude of the other two signals may be determined by squaring the sine and cosine integrals of each channel and summing the squares to obtain relative power measurements in all three channels and, from the known voltage amplitude of the reference signal, obtaining an absolute voltage measurement for the other two signals by multiplying the known voltage of the reference signal with the ratio of the relative power of each of the other two signals to the relative power of the reference signal.

Official Gazette of the U.S. Patent and Trademark Office

N92-29131# Lawrence Livermore National Lab., CA.
ANALYSIS AND OPTIMIZATION OF LOW-EARTH-ORBIT COMMUNICATION LINKS
G. C. Corynen and R. E. Glaser Apr. 1992 81 p
(Contract W-7405-eng-48)
(DE92-013393; UCRL-LR-109784) Avail: NTIS HC/MF A05

We have completed the development and testing of an algorithm for modeling, analyzing, and optimizing physical aspects of individual laser links in a low-earth-orbit (LEO) communication system. Called NETLINK, the algorithm provides a highly parametrized test bed for confirming system requirements and exploring design alternatives. Although NETLINK is currently configured as a probability processor that computes and propagates probabilities and statistical parameters directly, with minor modifications it can serve as a Monte Carlo simulator where only individual random samples are processed. A simplified form of the algorithm is also intended as a prototype for producing onboard real-time link performance predictions that will be required at the network level to achieve optimal routing and configuration protocols. Our NETLINK software is implemented in the C language, in which network nodes are conventionally represented as structures. These are used to account for detailed dynamic, geometric, and statistical attributes of individual network nodes and for various random and systematic (bias) errors in the associated acquisition, tracking, and pointing (ATP) system. To achieve both mathematical rigor and computational efficiency, we incorporated advanced numerical techniques. We have obtained useful results with NETLINK. For example, a laser peak power of about 40 watts seems adequate to achieve a link reliability of 0.999 (i.e., a message error rate of 0.001) over a communication range of 10 to 2000 km. Moreover, link reliability inside the acceptable range interval also appears better than currently believed. Our results also show that on-line detector threshold optimization is both practical and useful, although it is not necessary if communication distances are limited to the interval 20 to 200 km, in which the optimal threshold is 2960 counts. In using the algorithm to optimize message header structure, we found the optimal header length to be four frames.

DOE

N92-29165# Army Communications-Electronics Command, Fort Monmouth, NJ.
TACTICAL LINE-OF-SIGHT RADIO PROPAGATION RELIABILITY
Kenneth H. Brockel, William T. Barnett, Kenneth D. Chaney, Joseph R. Inserra, and Robert J. Locher Oct. 1991 81 p
(AD-A245909; CECOM-TR-91-3) Avail: NTIS HC/MF A05

Recent deployment to Southwest Asia (SWA) of tactical Line-of-Sight (LOS) radio links, such as those used with Mobile Subscriber Equipment (MSE) and other Tri-Service Tactical Communications (TRI-TAC) systems, and user feedback indicating time-varying performance have raised the question of link reliability. The climate encountered in SWA (desert terrain in proximity to bodies of water) is known to be very difficult for LOS radio because it causes frequent and large reductions in received signal strength, referred to as time-varying fading. This report provides predictions of propagation performance for the systems fielded based on the latest technical literature and validates them with current information collected from system users. The conditions that cause time-variant fades on LOS paths are also addressed. Particular focus will be directed at the tactical environment and the unique challenge that exists to achieve highly reliable links with the limited antenna gains and terrain clearances present in the tactical world. This report also addresses future work that should be accomplished to ensure that LOS operators and planners have the latest data available to optimize the effectiveness of their current LOS capability. GRA

N92-29166# Naval Postgraduate School, Monterey, CA.
METHOD OF MOMENTS ANALYSIS OF DISPLACED-AXIS DUAL REFLECTOR ANTENNAS M.S. Thesis
Nissan Vered Mar. 1992 79 p
(AD-A247970) Avail: NTIS HC/MF A05

Small symmetric dual reflector antennas suffer from low efficiency due to subreflector blockage of the main reflector and subreflector scattering. These can be reduced by slicing the main dish and translating its rotational axis, along with modifying the subreflector geometry. This type of design is usually applied to low-frequency reflectors, but high-frequency analysis techniques are used. Consequently the agreement between measured and computed data is not good as it would be for rigorous solution such as the method of moments. This thesis modifies an existing method of moments computer code to handle the displaced axis geometry, and computes the radiation pattern and the efficiency of this antenna as a function of geometrical and electrical design parameters. Optimum configurations are identified for several feed types. The paraboloidal antenna with a feed at the focus does not allow much control of the power distribution over the aperture surface, except for what can be accomplished by changing the focal length and feed pattern. Author (GRA)

N92-29169# Department of the Navy, Washington, DC.
TARGET MOTION DETECTING IMPULSE DOPPLER RADAR SYSTEM Patent Application
Robert E. Jehle, inventor (to Navy) and David F. Hudson, inventor (to Navy) 25 Mar. 1992 14 p
(AD-D015263; US-Patent-Appl-SN-857536) Avail: NTIS HC/MF A03

Radiant energy intermittently emitted from a transmitter is reflected as echo pulses from a moving target being interrogated to produce Doppler signals by counting of photons of the echo pulses during time domain intervals between emission from the transmitter. Such counting of photons is limited to the time domain intervals by operational control of a laser pump through which a reference beam is generated at an energy level activating detectors irradiated by such beam to count the photons absorbed therein after capture of the photons by a receiving antenna. GRA

N92-29199# Department of the Navy, Washington, DC.
HIGH POWER MICROWAVE GENERATOR Patent Application
Han S. Uhm, inventor (to Navy) 14 Jan. 1992 16 p
(AD-D015262; US-Patent-Appl-SN-819699) Avail: NTIS HC/MF A03

Conversion of electron beam energy into high power microwave energy is effected within the cavity of a Klystron device to which the electron beam is accelerated from a continuous supply source through an ion focussing channel. Ion focusing is achieved by establishment of a preionized background plasma within the channel to modulate the current of the electron beam in response to wake field effects and cause bunching of the electron beam during propagation to the Klystron device. Author (GRA)

N92-28529# Thomson-CSF, Malakoff (France).
INTEREST IN REAL-TIME SIMULATIONS FOR THE DEVELOPMENT TERRAIN FOLLOWING FUNCTION OF RADAR SYSTEMS [INTERET DES SIMULATIONS 'TEMPS REEL' POUR LE DEVELOPPEMENT DE LA FONCTION SUIVI DE TERRAIN DES SYSTEMES RADAR]
T. Martinet *In* AGARD, Piloted Simulation Effectiveness Feb. 1992 5 p In FRENCH; ENGLISH summary (For primary

document see N92-28522 19-01)
Copyright Avail: NTIS HC/MF A15

33 ELECTRONICS AND ELECTRICAL ENGINEERING

Includes test equipment and maintainability; components, e.g., tunnel diodes and transistors; microminiaturization; and integrated circuitry.

For related information see also *60 Computer Operations and Hardware* and *76 Solid-State Physics.*

N92-28239# Colorado State Univ., Fort Collins. Dept. of Chemistry.
MICROHOLE ARRAY ELECTRODES BASED ON MICROPOROUS ALUMINA MEMBRANES
Charles J. Brumlik, Charles R. Martin, and Koichi Tokuda 25 Feb. 1992 19 p
(Contract N00014-82-K-0612)
(AD-A247082; TR-65) Avail: NTIS HC/MF A03

A procedure for preparing microhole array electrodes is described. These electrodes are based on a microporous alumina filtration membrane. This membrane (Anopore) contains linear 200 nano-m diameter pores. These pores define the holes in the microhole array. The microelectrodes at the bottoms of the holes are formed by simply coating the back of the membrane with gold. This procedure yields an electrode with a high density of uniform microholes. Furthermore, this microhole array electrode combines very deep microholes with the smallest microhole diameters (200 nano-m) to be reported in the literature to date. Cyclic voltammetry was used to characterize these electrodes. GRA

N92-28262# Nationaal Inst. voor Kernfysica en Hoge Energiefysica, Amsterdam (Netherlands).
DELAYED PULSE GENERATOR
P. P. M. Jansweijer and J. Stolte 1991 56 p In DUTCH
(DIGEL-1991-2; ETN-92-91229) Avail: NTIS HC/MF A04

A Delayed Pulse Generator (DPG) was developed to produce an output pulse after a trigger pulse. The DPG is a VME module containing two separate delay channels. Each channel has a trigger input, an inhibit input, and an output. The delay between trigger pulse and output pulse can be set via the VME bus. The delay can be varied between 90 ns and 655 micros, in steps of 10 ns. ESA

N92-28263# Nationaal Inst. voor Kernfysica en Hoge Energiefysica, Amsterdam (Netherlands).
HIGH VOLTAGE SPLITTING UNIT FOR THE POWER SUPPLIES OF THE VACUUM PUMPS OF AmPS [HOOGSPANNINGS VERDEELEENHEID VOOR DE VACUUM VOEDINGEN VAN AMPS]
J. T. vanEs and J. H. vanTrigt 19 Apr. 1991 9 p In DUTCH
(DIGEL-1991-7; ETN-92-91235) Avail: NTIS HC/MF A02

A high voltage splitting circuit was developed to supply the small vacuum pumps of the bundle circuit of AmPS (Amsterdam Pulse Stretcher). Each pump needs 7 kV and the current is a measure for the vacuum. Since the price per Watt for small power supplies is high compared with large power supplies, it was decided to feed eight pumps from a single large power supply. The splitting unit contains eight current measuring circuits each with outputs for the local meter, a recorder, and a PLC module. The pump current is measured in the high voltage line. ESA

N92-28275# Cornell Univ., Ithaca, NY. School of Electrical Engineering.
FEMTOSECOND CARRIER PROCESSES IN COMPOUND SEMICONDUCTORS AND REAL TIME SIGNAL PROCESSING Annual Report, 1 May 1991 - 30 Apr. 1992
J. P. Krusius 25 Mar. 1992 50 p
(Contract F49620-90-C-0039)
(AD-A248053) Avail: NTIS HC/MF A03

This report is the annual report on research conducted under the auspices of the Joint Services Electronics Program at Cornell University. The research is grouped under two themes: femtosecond carrier processes in compound semiconductors, and real time signal processing. Results on OMVPE materials growth, femtosecond laser probing of hot carriers, and ensemble Monte Carlo simulations are reported on under the first theme. Accomplishments on VLSI algorithms, fault tolerant architectures, and architectures with multiple functional units for signal processing are given under the second theme. GRA

N92-28276# Dayton Univ. Research Inst., OH.
SIMULATION IN INFRARED IMAGING: USING ELECTRICAL CIRCUIT PRINCIPLES TO MODEL HEAT TRANSFER Final Report, May 1990 - Aug. 1991
Ronald J. Evans Jan. 1992 39 p
(Contract F33615-90-C-0005)
(AD-A248290; AL-TR-1991-0103) Avail: NTIS HC/MF A03

Simulation of thermal or infrared imaging involves modeling the heat exchange between database features and external sources of heat or radiation (e.g., the sun). One approach to computing differential scene irradiance, as viewed by a sensor, employs electrical circuit theory to model heat transfer between the database objects within the scene. In this report, practical shortcomings of this circuit approach and possible alternatives are introduced and analyzed. Heat storage (capacitance) was one process simulated. Results showed that the computational changes required to implement thermal capacitance are difficult to simulate numerically. Individual feature estimates of capacity were inconsistent with expectations. In addition, the temperature contribution from the capacity or time-varying component did not overcome the effect of the steady-state component, which contained a significant amount of error from assumptions made in the circuit model. Further work is required to identify approaches which provide less extreme object temperatures throughout a diurnal or daily cycle. GRA

N92-28295# Illinois Univ., Urbana. Coordinated Science Lab.
SCATTERING MECHANISMS FOR SEMICONDUCTOR TRANSPORT CALCULATIONS Report, 1 Jul. - 31 Dec. 1991
Jeff Bude and Karl Hess 31 Dec. 1991 44 p
(Contract DAAL03-89-K-0037)
(AD-A249260; ARO-26711.17-EL) Avail: NTIS HC/MF A03

We have applied our Monte Carlo approach to impact ionization to various important semiconductor materials including GaAs, InP, and InAs. We find that in all these materials the ionization mechanism is quantitatively different to what has been described in previous-simplified models, such as Shockley's lucky electron theory. With regard to quantum transport, we have continued our work on the electron-electron interaction in simple nanostructures. The main goal of this study is to investigate whether Coulomb blockade effects continue to exist at the molecular level when quantization effects become significant. GRA

N92-28305# Mitre Corp., Bedford, MA.
DIAGNOSTIC REASONING WITHIN SEQUENTIAL CIRCUITS, VOLUME 1
Richard A. Marcotte, Maurine J. Neiberg, Richard L. Piazza, and Lester J. Holtzblatt Jan. 1992 76 p
(Contract F19628-89-C-0001)
(AD-A248055; MTR-11227-Vol-1) Avail: NTIS HC/MF A05

A model-based diagnostic reasoning system makes use of a design model of the structure and behavior of a circuit to diagnose faults within the circuit. In this volume of the FY91 final report for MOIE Project 7020, we describe the Generic Model-based Diagnostic System (GMODS), which can use VHSIC Hardware Description Language (VHDL) models to diagnose single and multiple faults within digital sequential circuits. This volume describes the overall GMODS approach, contrasts the capabilities and processing performance of two GMODS diagnostic algorithms (a minimal envisionment algorithm and a conflict set algorithm), and concludes that the conflict set algorithm is most appropriate for diagnosing sequential circuits. GRA

N92-28326# Analytic Power Corp., Boston, MA.
MOBILE ELECTRIC POWER
Valerie J. Bloomfield, David P. Bloomfield, and Bradley Q. Johnson 30 Jan. 1992 30 p LIMITED REPRODUCIBILITY: Availability: Document partially illegible
(Contract DAAL03-91-C-0036)
(AD-A249354; ARO-28866.1-CH-SBI) Avail: NTIS HC/MF A03

Analytic Power has proven the feasibility of a mobile electric power unit in the form of a hydride fueled ion-exchange membrane (IEM) fuel cell stack. We have over 5 years experience building and testing IEM fuel cells. The power section of a 350 watt fuel cell stack weighs 4.65 pounds based on our five cell sub-stack component weights. The composite stack structure is fabricated from two components; a unitized flow field and catalyzed membrane. The lightweight unitized flow field concept was proven in the first three months of the contract. A single unit flow field weighs 0.155 pounds and can seal to 60 psi. The single cell catalyzed Nafion membrane exceeded our performance goal of 0.6 volts at 100 ASF. Stack performance points were 0.42 volts at 113 ASF and .75 volts at 96 ASF. GRA

N92-28351# California Inst. of Tech., Pasadena.
MULTIMETER-WAVE GRID OSCILLATORS Final Report, 1 Nov. 1988 - 31 Oct. 1991
David Rutledge 1 Jan. 1992 21 p
(Contract DAAL03-89-K-0003)
(AD-A248430) Avail: NTIS HC/MF A03

Active grids dramatically increase the power-handling ability of solid-state devices by quasi-optical power combining. We report progress in three areas - oscillator grids, mixer grids, and amplifier grids. Several different grids with up to 100 devices have been demonstrated and accurate circuit models have been developed. This work should make high-power millimeter-wave monolithic circuits for radars and communications systems possible. GRA

N92-28367# Johns Hopkins Univ., Laurel, MD. Applied Physics Lab.
COMPARISON OF VARIOUS TECHNIQUES IN THE ANALYSIS OF WAVEGUIDE TRANSITIONS
William A. Huting Aug. 1991 35 p
(Contract N00039-89-C-5301)
(AD-A247019; JHU/APL-TG-1379) Avail: NTIS HC/MF A03

The solution of the continuous waveguide transition problem can be obtained by discretizing the boundary and applying mode-matching or by using a system of ordinary differential equations. Both approaches involve approximate representations of the boundary. When using the differential equation approach, it was found necessary to consider the transition as several sections in series in order to avoid numerical instabilities. When this is done, one may cascade using a generalized scattering matrix approach or a generalized ABCD matrix method. Results are shown comparing the accuracy of the boundary discretization approach and the differential equation approach for the Marie transducer and for linear transitions of various lengths in rectangular waveguide; experimental results are also given for the Marie transducer. GRA

N92-28373# Naval Postgraduate School, Monterey, CA.
INVESTIGATION OF AN EQUIVALENT CIRCUIT FOR THE INDUCTIVE STRIP IN FINLINE WITH DIELECTRIC M.S. Thesis
Michael R. Linzey Jun. 1991 81 p
(AD-A247025) Avail: NTIS HC/MF A05

This thesis describes a circuit model for the inductive strip in inhomogeneous finline with the following geometry: fin and strip centered in the shield, dielectric material with er = 2.22, b/a = 4/9, 0.5 less than or equal to w/b less than or equal to 1.0, T/a greater than or equal to 0.01 and 0.0 less than or equal to d/a less than or equal to 0.1. The model is shown to produce results that agree with data computed using the spectral domain method. The model has been generated using WR(90) waveguide operating in the TE(sub 10) mode. GRA

N92-28427# Cornell Univ., Ithaca, NY. School of Electrical Engineering.
STUDY OF ULTRA SHORT HFET DEVICES WITH InP SUBSTRATES Final Report, 1 Dec. 1988 - 30 Nov. 1991
Lester F. Eastman, H. Park, and W. Haydl 30 Jan. 1992 26 p
(Contract DAAL03-89-K-0006)
(AD-A248448; Rept-26151-EL) Avail: NTIS HC/MF A03

This research covered modulation-doped field effect transistors (MODFET's) of AlInAs/GaInAs/AlInAs/InP grown by molecular beam epitaxy (MBE). These are the highest frequency transistors yet made, but generally suffer from problems. The problem studied is that of obtaining well-behaved current vs voltage characteristics for these transistors, including reducing the anomalous kink effect, and increasing breakdown voltage. The most important results are the near-elimination of the kink effect by using reduced arsenic flux in the MBE growth, and sharply (-100:1) reduction of the gate breakdown current by using a barrier-enhancement acceptor doping plane under the gate. Near pinch-off, the drain-source voltage at breakdown wits doubled. Additionally, the optimization of the fabrication technology of tile mushroom (or T) shaped gates was completed for these devices, and integrated circuits for millimeter amplifiers and oscillators were designed and fabricated. GRA

N92-28432*# National Aeronautics and Space Administration. Lewis Research Center, Cleveland, OH.
NEUTRON, GAMMA RAY, AND TEMPERATURE EFFECTS ON THE ELECTRICAL CHARACTERISTICS OF THYRISTORS
A. J. Frasca (Wittenberg Univ., Springfield, OH.) and G. E. Schwarze 1992 9 p Proposed for presentation at the 27th Intersociety Energy Conversion Engineering Conference, San Diego, CA, 3-7 Aug. 1992; sponsored by SAE, ACS, AIAA, ASME, IEEE, AIChE, and ANS
(RTOP 590-13-31)
(NASA-TM-105728; E-7131; NAS 1.15:105728) Avail: NTIS HC/MF A02

Experimental data showing the effects of neutrons, gamma rays, and temperature on the electrical and switching characteristics of phase-control and inverter-type SCR's are presented. The special test fixture built for mounting, heating, and instrumenting the test devices is described. Four SCR's were neutron irradiated at 300 K and four at 365 K for fluences up to 3.2 x 10 exp 13 n/sq. cm, and eight were gamma irradiated at 300 K only for gamma doses up to 5.1 Mrads. The electrical measurements were made during irradiation and the switching measurements were made only before and after irradiation. Radiation induced crystal defects, resulting primarily from fast neutrons, caused the reduction of minority carrier lifetime through the generation of R-G centers. The reduction in lifetime caused increases in the on-state voltage drop and in the reverse and forward leakage currents, and decreases in the turn-off time. Author

N92-28456*# National Aeronautics and Space Administration. Marshall Space Flight Center, Huntsville, AL.
TAGUCHI METHODS IN ELECTRONICS: A CASE STUDY
R. Kissel May 1992 22 p
(NASA-TM-103586; NAS 1.15:103586) Avail: NTIS HC/MF A03

Total Quality Management (TQM) is becoming more important as a way to improve productivity. One of the technical aspects of TQM is a system called the Taguchi method. This is an optimization method that, with a few precautions, can reduce test effort by an order of magnitude over conventional techniques. The Taguchi method is specifically designed to minimize a product's sensitivity to uncontrollable system disturbances such as aging, temperature, voltage variations, etc., by simultaneously varying both design and disturbance parameters. The analysis produces an optimum set of design parameters. A 3-day class on the Taguchi method was held at the Marshall Space Flight Center (MSFC) in May 1991. A project was needed as a follow-up after the class was over, and the motor controller was selected at that time. Exactly how to proceed was the subject of discussion for some months. It was not clear exactly what to measure, and design kept getting mixed with optimization. There was even some discussion about why the Taguchi method should be used at all. Author

N92-28561# Syracuse Univ., NY.
LEAKAGE CURRENT MEASUREMENTS IN SOI DEVICES Final Report, Apr. 1989 - Mar. 1990
Charles Surya Dec. 1991 17 p
(Contract F30602-88-D-0027)
(AD-A247694; RL-TR-91-340) Avail: NTIS HC/MF A03

Total dose response of both NMOS and PMOS FETs fabricated on SOI substrates were studied. Back channel leakage currents were studied. Two types of SOI substrates were investigated in the study of back channel leakage currents: SIMOX and ZMR. Subthreshold current-voltage characteristics were studied as a function of the total dose of the back channel and front channel of SIMOX and ZMR SOI substrates. Some preliminary reports on the buried oxide leakage current are also provided. GRA

N92-28568# Naval Surface Warfare Center, Silver Spring, MD.
LIMITING FACTORS TO ADVANCING THERMAL BATTERY TECHNOLOGY FOR NAVAL APPLICATIONS
Patrick B. Davis and Clinton S. Winchester Oct. 1991 28 p
(AD-A247773; NAVSWC-TR-91-614) Avail: NTIS HC/MF A03

Thermal batteries are primary reserve electrochemical power sources using molten salt electrolyte which experience little effective aging while in storage or dormant deployment. Thermal batteries are primarily used in military applications, and are currently used in a wide variety of Navy devices such as missiles, torpedoes, decays, and training targets, usually as power supplies in guidance, propulsion, and Safe/Arm applications. Technology developments have increased the available energy and power density ratings by an order of magnitude in the last ten years. Present thermal batteries, using lithium anodes and metal sulfide cathodes, are capable of performing applications where only less rugged and more expensive silver oxide/zinc or silver/magnesium chloride seawater batteries could serve previously. Additionally, these batteries are capable of supplanting lithium/thionyl chloride reserve batteries in a variety of specifically optimized designs. Increases in thermal battery energy and power density capabilities are not projected to continue with the current available technology. Several battery designs are now at the edge of feasibility and safety. Since future naval systems are likely to require continued growth of battery energy and power densities, there must be significant advances in battery technology. Specifically, anode alloy composition and new cathode materials must be investigated to allow for safe development and deployment of these high power, higher energy density batteries. GRA

N92-28675*# National Aeronautics and Space Administration. Lewis Research Center, Cleveland, OH.
HIGH TEMPERATURE DIELECTRIC PROPERTIES OF APICAL, KAPTON, PEEK, TEFLON AF, AND UPILEX POLYMERS
A. N. Hammoud (Sverdrup Technology, Inc., Brook Park, OH.), E. D. Baumann, E. Overton, I. T. Myers, J. L. Suthar (State Univ. of New York, Buffalo.), W. Khachen (State Univ. of New York, Buffalo.), and J. R. Laghari (State Univ. of New York, Buffalo.) 1992 8 p Prepared for presentation at the 1992 Conference on Electrical Insulation and Dielectric Phenomena, Victoria, British Columbia, 18-21 Oct. 1992; sponsored by IEEE
(RTOP 506-41-41)
(NASA-TM-105753; E-7161; NAS 1.15:105753) Avail: NTIS HC/MF A02

Reliable lightweight systems capable of providing electrical power at the magawatt level are a requirement for future manned space exploration missions. This can be achieved by the development of high temperature insulating materials which are not only capable of surviving the hostile space environment but can contribute to reducing the mass and weight of the heat rejection system. In this work, Apical, Upilex, Kapton, Teflon AF, and Peek polymers are characterized for AC and DC dielectric breakdown in air and in silicone oil at temperatures up to 250 C. The materials are also tested in terms of their dielectric constant and dissipation factor at high temperatures with an electrical stress of 60 Hz, 200 V/mil present. The effects of thermal aging on the properties of the films are determined after 15 hours of exposure to 200 and 250 C, each. The results obtained are discussed and conclusions are made concerning the suitability of these dielectrics for use in capacitors and cable insulations in high temperature environments. Author

N92-28723*# Sverdrup Technology, Inc., Brook Park, OH.
M-H CHARACTERISTICS AND DEMAGNETIZATION RESISTANCE OF SAMARIUM-COBALT PERMANENT MAGNETS TO 300 C
Janis M. Niedra Aug. 1992 8 p Prepared for presentation at the 27th Intersociety Energy Conversion Engineering Conference, San Diego, CA, 3-7 Aug. 1992; sponsored in part by SAE, ACS, AIAA, ASME, IEEE, AIChE, and ANS
(Contract NAS3-25266; RTOP 590-13-11)
(NASA-CR-189194; E-7144; NAS 1.26:189194) Avail: NTIS HC/MF A02

The influence of temperature on the M-H demagnetization characteristics of permanent magnets is important information for the full utilization of the capabilities of samarium-cobalt magnets at high temperatures in demagnetization-resistant permanent magnet devices. In high temperature space power converters, such as free-piston Stirling engine driven linear alternators, magnet demagnetization can occur as a long-term consequence of thermal agitation of domains and of metallurgical change, and also as an immediate consequence of too large an applied field. Investigated here is the short-term demagnetization resistance to applied fields derived from basic M-H data. This quasistatic demagnetization data was obtained for commercial, high-intrinsic-coercivity, Sm2Co17-type magnets from 5 sources, in the temperature range 23 to 300 C. An electromagnet driven, electronic hysteresigraph was used to test the 1-cm cubic samples. The observed variation of the 2nd quadrant M-H characteristics was a typical rapid loss of M-coercivity and a relatively lesser loss of remanence with increasing temperature. The 2nd quadrant M-H curve knee point is used to define the limits of operation safe against irreversible demagnetization due to an excessive bucking field for a given flux density swing at temperature. Such safe operating area plots are shown to differentiate the high temperature capabilities of the samples from different sources. For most of the samples, their 2nd quadrant M-H loop squareness increased with temperature, reaching a peak or a plateau above 250 C. Author

N92-28753* National Aeronautics and Space Administration. Pasadena Office, CA.
SECONDARY Li BATTERY INCORPORATING 12-CROWN-4 ETHER Patent
Ganesan Nagasubramanian, inventor (to NASA) (Jet Propulsion Lab., California Inst. of Tech., Pasadena.) and Salvador DiStefano, inventor (to NASA) (Jet Propulsion Lab., California Inst. of Tech., Pasadena.) 5 May 1992 8 p Filed 11 Oct. 1990 Supersedes N91-13621 (29 - 5, p 652)
(NASA-Case-NPO-17922-1-CU; US-Patent-5,110,694;
US-Patent-Appl-SN-596139; US-Patent-Class-429-192;
US-Patent-Class-252-62.2; Int-Patent-Class-H01M-10/40) Avail: US Patent and Trademark Office

A rechargeable lithium battery which utilizes a polyethylene oxide (PEO) solid polymeric electrolyte complexed with a lithium salt is disclosed. The conductivity is increased an order of magnitude and interfacial charge transfer resistance is substantially decreased by incorporating a minor amount of 12-Crown-4 ether in the PEO-lithium salt solid electrolyte film. Batteries containing the improved electrolyte permit operation at a lower temperature with improved efficiency.
Official Gazette of the U.S. Patent and Trademark Office

N92-28783# Institut National Polytechnique, Grenoble (France). Techniques de l'Informatique, des Mathematiques, de la Microelectronique et de la Microscopie.
A KNOWLEDGE BASED APPROACH FOR TESTING VLSI CIRCUITS: APPLICATION TO THE VALIDATION OF PROTOTYPES FOR A NON-CONTACT TEST Ph.D. Thesis [APPROCHES A BASE DE CONNAISSANCES POUR LE TEST DE CIRCUITS VLSI: APPLICATION A LA VALIDATION DE

PROTOTYPES DANS LE CADRE D'UN TEST SANS CONTACT]
Meryem Marzouki 1991 230 p In FRENCH
(ETN-92-91321) Avail: NTIS HC/MF A11

Algorithmic methods, currently used for Very Large Scale Integration (VLSI) circuit testing, are facing two major problems: the complexity of the devices under test, and the incompleteness of the classical fault models. These problems can be solved by using qualitative reasoning, based on partitioning and hierarchy concepts, and by taking into account very general fault models, like the occurrence of a discrepancy between the expected and the observed behavior of the device under test: such a solution is provided by the use of second generation knowledge based systems. These systems are presented and the assessment of the state of the art related to the use of knowledge based approaches to electronic circuits and systems test and testability is considered. The prototype validation of VLSI circuits is presented. It was observed using a scanning electron microscope used in the voltage contrast mode. An overview of electron beam testing possibilities and particularities is provided. Two different diagnostic approaches in this framework are described: the first approach is a knowledge based one, and the second approach is based on the use of a fault dictionary. These two approaches, and the two systems in which they are embedded, are evaluated and compared. ESA

N92-28784# Institut National Polytechnique, Grenoble (France). Techniques de l'Informatique, des Mathematiques, de la Microelectronique de de la Microscopie.
IMAGE PROCESSING FOR FAILURE ANALYSIS OF INTEGRATED CIRCUITS BY AN ELECTRON BEAM Ph.D. Thesis [TRAITEMENT D'IMAGES EN ANALYSE DE DEFAILLANCES DE CIRCUITS INTEGRES PAR FAISCEAU D'ELECTRONS]
Didier Conard 1991 248 p In FRENCH
(ETN-92-91322) Avail: NTIS HC/MF A11

An automated and integrated system for failure analysis using electron beam testing was designed and constructed. The principle of this analysis consists of comparing images showing the internal functioning in voltage contrast of the failed circuit against that of a golden circuit. The application of this test technique to unknown circuits required the development of an automatic tool which allows the extraction of contrast difference over the whole circuit. Automation came up against problems of alignment between the images to be superimposed. A pattern recognition technique based on corner detection was developed to automatically correct these problems. The work was validated by an experimental study performed on 68000 microprocessors. ESA

N92-28797# Duke Univ., Durham, NC. Dept. of Physics.
NEAR MILLIMETER WAVES AND MICROELECTRONICS Final Report
Frank C. DeLucia 16 Jan. 1992 5 p
(Contract DAAL03-86-G-0019)
(AD-A250384; ARO-23756.3-PH-F) Avail: NTIS HC/MF A01

This is the final report on an Army Research Office grant supporting a fellowship. Two fellows were supported by the grant. One of the fellows developed a new technique to study gas phase molecules at liquid helium temperatures. The second used time-resolved double resonance techniques to determine the state dependence and cross section of many rotational and vibrational processes in methyl halides. GRA

N92-28798# Michigan Univ., Ann Arbor.
HIGH-PERFORMANCE INTEGRATED CIRCUIT EVALUATION SYSTEM FOR A GALLIUM ARSENIDE MICROSUPERCOMPUTER Final Report, 1 Jul. - 31 Dec. 1991
Richard B. Brown Feb. 1992 2 p
(Contract DAAL03-91-G-0223)
(AD-A250385; ARO-29305.1-EL) Avail: NTIS HC/MF A01

This grant was used to extend an HP82000 High-Speed Digital IC Tester by adding 40 200-MHz channels and 16 400-MHz channels, along with associated power supplies, systems racking, and accessories. The current configuration has a total of 176 1/0 channels. GRA

N92-28814# Oak Ridge National Lab., TN.
ASSESSMENT OF VALVE ACTUATOR MOTOR ROTOR DEGRADATION BY FOURIER ANALYSIS OF CURRENT WAVEFORM
J. D. Kueck (Carolina Power and Light Co., Raleigh, NC.), J. C. Criscoe (Carolina Power and Light Co., Raleigh, NC.), and N. M. Burstein 1992 15 p Presented at the 54th Annual American Power Conference, Chicago, IL, 13-15 Apr. 1992
(Contract DE-AC05-84OR-21400)
(DE92-013233; CONF-920432-11) Avail: NTIS HC/MF A03

This paper presents a test report of a motor diagnostic system which uses Fourier Analysis of the motor current waveform to detect broken rotor bars in the motor or defects in the driven equipment. The test was conducted on a valve actuator motor driving a valve actuator which was in turn driving a dynamometer to measure the actuator torque output. The motor was gradually degraded by open circuiting rotor bars. The test confirmed the efficacy of the waveform analysis method for assessing motor rotor degradation and also provided data regarding the change in waveform characteristics as motor rotors are gradually degraded to failure. DOE

N92-28948# Superconductor Technologies, Inc., Santa Barbara, CA.
THE PROCESSING OF HIGH TEMPERATURE CERAMIC SUPERCONDUCTING DEVICES, VOLUME 2 Final Report
James H. Long, Jr. 31 Jan. 1992 274 p
(Contract N00014-88-C-0713; ARPA Order 06268)
(AD-A248159) Avail: NTIS HC/MF A12

BEI has completed the preliminary evaluation on the planar coil and conductor requirements for the brushless DC motor. Results indicate that current density is adequate. However, there is not enough cross section of the conductor using the thin film approach. Preliminary design was based on two planar coils attached on each side of a central chill plate filled with liquid nitrogen. Evaluation was further performed on the output anticipated in thick film substrates 100 times thicker than the 1 micron thin film. Estimates with thick film substrates yielded .168 watts output which is still inefficient for DC brushless motor design. Thick film designs appear to be the correct approach to achieve a high conductor cross section, enabling sufficient power levels to drive the actuator or motor. GRA

N92-29147# Stanford Univ., CA. Lab. of Physics.
STANFORD CENTER FOR RESEARCH ON SUPERCONDUCTIVITY AND SUPERCONDUCTIVE ELECTRONICS Final Report, 15 Oct. 1988 - 14 Oct. 1991
M. R. Beasley 23 Mar. 1992 18 p
(Contract F49620-89-C-0001)
(AD-A250204; AFOSR-92-0293TR) Avail: NTIS HC/MF A03

New techniques for growing epitaxial thin films of high temperature superconducting cuprates have been developed. The electrical and superconducting properties of the thin film have been investigated by transport, magnetic, optical, and tunneling measurements. Insights into the basic nature of the superconducting interaction and the physics of some superconducting devices have been gained. GRA

N92-29153* National Aeronautics and Space Administration. Goddard Space Flight Center, Greenbelt, MD.
USER FRIENDLY JOYSTICK Patent
Wayne D. Eklund, inventor (to NASA) and James J. Kerley, inventor (to NASA) 19 May 1992 10 p Filed 20 Feb. 1991
(NASA-Case-GSC-13187-1; US-Patent-5,113,714;
US-Patent-Appl-SN-657790; US-Patent-Class-74-471XY;
US-Patent-Class-248-65; US-Patent-Class-248-68.1;
US-Patent-Class-273-148B; US-Patent-Class-338-128;
Int-Patent-Class-G05G-9/00) Avail: US Patent and Trademark Office

A joystick control device having a lower U-shaped bracket, an

upper U-shaped bracket, a handle attached to the upper U-shaped bracket, with the upper U-shaped bracket connected to the lower U-shaped bracket by a compliant joint allowing six degrees of freedom for the joystick. The compliant joint consists of at least one cable segment affixed between the lower U-shaped bracket and the upper U-shaped bracket. At least one input device is located between the lower U-shaped bracket and the upper U-shaped bracket.

Official Gazette of the U.S. Patent and Trademark Office

N92-29178# Tuebingen Univ. (Germany, F.R.). Inst. fuer Astronomie.

SPLIT EVENTS AND THEIR INFLUENCE ON PN CCD ENERGY SPECTRA Thesis [SPLIT EVENTS UND IHR EINFLUSS AUF PN CCD ENERGIESPEKTREN]

Urban Raidt Aug. 1991 120 p In GERMAN

(ETN-92-91485) Avail: NTIS HC/MF A06

It is shown that the propagation of a signal charge produced by a photon, with regard to the diffusion and Coulomb repulsion in measured Charge Coupled Device (CCD) spectra, represents a visible interference effect. The charge splitting effect is shown for a homogeneous area and a point source radiation. The condition that only single events are to occur during the light exposure in the pixels, makes a constraint of the source strength necessary for the various sorting modes. The results are given for the maximal photon rate for a point source and an area radiation according to the sorting mode carried out. ESA

N92-29197# Fermi National Accelerator Lab., Batavia, IL.

OPERATION AND RADIATION RESISTANCE OF A FOXFET BIASING STRUCTURE FOR SILICON STRIP DETECTORS

M. Laakso, P. Singh, E. Engels, Jr., and P. Shepard (Pittsburgh Univ., PA.) Feb. 1992 31 p Presented at the 6th European Symposium on Semiconductor Detectors, Milano, Italy, 24-27 Feb. 1992 Prepared in cooperation with Helsinki Univ. (Finland)

(Contract DE-AC02-76CH-03000)

(DE92-011279; FNAL/C-92/66; CONF-920299-1) Avail: NTIS HC/MF A03

AC-coupled strip detectors biased with a FOXFET transistor structure were studied. Measurement results for the basic operational characteristics of the FOXFET are presented together with a brief description of the physics underlying its operation. Radiation effects were studied using photons from a Cs-137 source. Changes in the FOXFET characteristics as a function of radiation dose up to 1 MRad are reported. Results about the effect of radiation on the noise from a FOXFET biased detector are described. DOE

N92-29208# Laboratoire d'Automatique et d'Analyse des Systemes, Toulouse (France). Equipe Composants Bipolaires.

DESIGN AND REALIZATION OF POLYSILICON EMITTER BIPOLAR TRANSISTORS Ph.D. Thesis - Toulouse Univ. [CONCEPTION ET REALISATION DE TRANSISTORS BIPOLAIRES DE PUISSANCE A EMETTEUR POLYSILICIUM]

Mohamed Ibannain 1991 132 p In FRENCH

(LAAS-91360; ETN-92-91331) Avail: NTIS HC/MF A07

Power bipolar transistors are well adapted for very high current switching. These devices are fully controllable at turn on and turn off and exhibit fairly high switching speeds compared to thyristors. A key feature of these structures is the steady-state-/blocked-voltage tradeoff. For a forced gain and an imposed blocking-voltage, a high steady-state can only be obtained at the expense of an increased surface that may become critical for conventional transistors. The various models that describe the operation of polysilicon emitter transistors are compared. The role of the polysilicon layer/monocrystal interface is highlighted. The actual technological production of a polysilicon emitter power transistor is considered. To obtain a satisfactory voltage hold, a PP(-) termination was preferred. The analysis of the characteristics of the first devices obtained showed certain stages of the process to be particularly critical as they modify the properties of the monocrystal/polysilicon interface. A full process adapted to the production of polysilicon emitter power bipolar transistors is proposed. The results of the electric characterization of the devices produced confirmed the relevance of the theoretical studies. ESA

34 FLUID MECHANICS AND HEAT TRANSFER

Includes boundary layers; hydrodynamics; fluidics; mass transfer; and ablation cooling.

For related information see also *02 Aerodynamics* and *77 Thermodynamics and Statistical Physics.*

N92-28225# Yale Univ., New Haven, CT.

STUDIES IN TURBULENCE AND TURBULENCE CONTROL Final Technical Report, 15 Nov. 1986 - 14 Dec. 1991

K. R. Sreenivasan 15 Jan. 1992 7 p

(Grant AF-AFOSR-0116-87)

(AD-A247164; AFOSR-92-0145TR) Avail: NTIS HC/MF A02

Projects studied under this AFOSR grant are summarized. They concern the following aspects, and are believed to be of interest for both applications and fundamentals of fluid mechanics and aerospace sciences: (1) Flow control, (2) Chaos and universality in wakes behind circular cylinders, (3) Absolute instability and the dynamics of variable density jets, (4) Kinematics and dynamics of turbulent vorticity fluctuations in laboratory and atmospheric turbulence, and (5) Fractals and multifractals in fluid flows. The report lists the Ph.D. theses and principal publications arising from the work. Reprints of some of the important papers are attached. The report also contains a section on the impact of the research. A list of Ph.D. students funded at least partly from the grant is given. GRA

N92-28258# California Univ., Irvine. Dept. of Mechanical and Aerospace Engineering.

THE LINEAR AND NONLINEAR SHEAR INSTABILITY OF A FLUID SHEET

R. H. Rangel and W. A. Sirignano 1991 10 p

(Grant AF-AFOSR-0016-86)

(AD-A247092; AFOSR-92-0041TR) Avail: NTIS HC/MF A02

A theoretical and computational investigation of the inviscid Kelvin-Helmholtz instability of a two-dimensional fluid sheet is presented. Both linear and nonlinear analyses are performed. The study considers the temporal dilational (symmetric) and sinuous (antisymmetric) instability of a sheet of finite thickness, including the effect of surface tension and the density difference between the fluid in the sheet and the surrounding fluid. Previous linear-theory results are extended to include the complete range of density ratios and thickness-to wavelength ratios. It is shown that all sinuous waves are stable when the dimensionless sheet thickness is less than a critical value that depends on the density ratio. At low density ratios, the growth rate of the sinuous waves is larger than that of the dilational waves, in agreement with previous results. At higher density ratios, it is shown that the dilational waves have a higher growth rate. The nonlinear calculations indicate the existence of sinuous oscillating modes when the density ratio is of the order of 1. Sinuous modes may result in ligaments interspaced by half of a wavelength. Dilational modes grow monotonically and may result in ligaments interspaced by one wavelength. GRA

N92-28268# Los Alamos National Lab., NM.

A STUDY OF THE NORMAL INJECTION OF HYDROGEN INTO A HEATED SUPERSONIC FLOW USING PLANAR LASER-INDUCED FLUORESCENCE Ph.D. Thesis

A. D. Rothstein Apr. 1992 143 p

(Contract W-7405-eng-36)

(DE92-010701; LA-12287-T) Avail: NTIS HC/MF A07

A sonic, highly under-expanded, jet of hydrogen was injected transversely into a supersonic (Mach 1.5), high-temperature static temperature (approx. 1400 K) argon-oxygen free stream. Laser-based diagnostics were utilized to non-intrusively probe the

combustion of oxygen-hydrogen. Planar laser-induced fluorescence (PLIF) was used to image the flow. The images were used to determine both H2 jet penetration depth profiles and two-dimensional temperature maps of the combustion region. The hydroxyl radical (OH) was used as the PLIF target species in the flow because it is an important and prominent intermediary of the hydrogen-oxygen combustion reaction and it has many strong ro-vibrational lines suitable for laser excitation. The very short gate width of the camera used (approx. 30 nsec) results in images that are well resolved temporally. Good spatial resolution (51 by 22 microns) was achieved with a UV-intensified CCD camera and suitable optics. Jet boundary penetrations are measured for a range of injection (450-1000 torr) and free stream (12-55 torr) pressures. The primary parameter that determines the jet trajectory is the ratio of the dynamic pressures of the jet to the free stream, labeled q. Previous experiments dealt with values of q on the order of one, but this study involves values between 5.9 and 38.6. The penetration profiles are compared where appropriate to previous results for both reacting and nonreacting flows. Despite the large extrapolation, reasonable agreement between the results established in the present study and those of other investigators is found. DOE

N92-28269# Lawrence Livermore National Lab., CA.
FLUIDS AT HIGH SHOCK PRESSURES AND TEMPERATURES
W. J. Nellis and A. C. Mitchell Dec. 1991 7 p Presented at the 13th AIRAPT International Conference on High Pressure Science and Technology, Bangalore, India, 7-11 Oct. 1991
(Contract W-7405-eng-48)
(DE92-010709; UCRL-JC-109291; CONF-9110228-8) Avail: NTIS HC/MF A02

Equation-of state and electrical conductivity results of shock-compressed monatomic, diatomic, and mixed-ionic fluids are reviewed. Fluids of interest are He, Xe, H2, N2 and synthetic planetary 'ice'. DOE

N92-28274# Cornell Univ., Ithaca, NY. School of Mechanical and Aerospace Engineering.
MAPPING CLOSURES FOR TURBULENT MIXING AND REACTION
S. B. Pope 1991 17 p
(Grant AF-AFOSR-0052-88)
(AD-A247305; AFOSR-92-0032TR) Avail: NTIS HC/MF A03

The mapping closure for the one point probability density function (PDF) of an inert scalar in homogeneous turbulence is explained and developed. It is shown that the pdf's calculated from the closure are in excellent agreement with those obtained from direct numerical simulations. The closure is then extended to many reactive scalars. In a turbulent reactive flow, the fluid composition at a point changes with time due to three processes: convection, reaction, and molecular diffusion. In pdf methods (Pope, 1985, 1991) the first two of these processes are treated exactly, but the effects of molecular diffusion have to be modeled. These different models have different attributes, but they all share two fundamental shortcomings: none has a sound physical basis; and none yields satisfactory results for the basic test case of a decaying inert scalar field in isotropic turbulence. GRA

N92-28350# DCW Industries, La Canada, CA.
A NUMERICAL WIND TUNNEL STUDY OF VISCOUS-INVISCID INTERACTION Final Report, Sep. 1987 - Mar. 1991
David C. Wilcox Jan. 1992 92 p
(AD-A248429; DCW-R-33-01) Avail: NTIS HC/MF A05

Research results based on the Wilcox k-w and multiscale turbulence models aimed at analyzing viscous-inviscid interaction are presented. Surface boundary conditions for rough surfaces and for surface mass injection are developed and tested for the multiscale model. The multiscale model is also applied to three-dimensional ship-hull flows, flow over convex surfaces, and free shear flows. Both the k-w and multiscale models are applied to a variety of two-dimensional shock-separated flows using an extremely fast numerical algorithm. Results show that such computations can be routinely done on a fast desktop computer. Using perturbation methods, an alternative to wall functions is devised to circumvent integration through the viscous sublayer without significant loss of accuracy. Partially successful attempts at implementing the k-w and multiscale models in a three-dimensional time-averaged Navier-Stokes program are also described. GRA

N92-28361*# Old Dominion Univ., Norfolk, VA. Dept. of Mechanical Engineering and Mechanics.
VISCOUS EFFECTS ON A VORTEX WAKE IN GROUND EFFECT Final Report, period ending 31 May 1991
Z. Zheng and Robert L. Ash Jun. 1992 48 p
(Grant NAG1-987)
(NASA-CR-190400; NAS 1.26:190400) Avail: NTIS HC/MF A03

Wake vortex trajectories and strengths are altered radically by interactions with the ground plane. Prediction of vortex strength and location is especially important in the vicinity of airports. Simple potential flow methods have been found to yield reasonable estimates of vortex descent rates in an otherwise quiescent ambient background, but those techniques cannot be adjusted for more realistic ambient conditions and they fail to provide satisfactory estimates of ground-coupled behavior. The authors have been involved in a systematic study concerned with including viscous effects in a wake-vortex system which is near the ground plane. The study has employed numerical solutions to the Navier-Stokes equations, as well as perturbation techniques to study ground coupling with a descending vortex pair. Results of a two-dimensional, unsteady numerical-theoretical study are presented in this paper. A time-based perturbation procedure has been developed which permits the use of analytical solutions to an inner and outer flow domain for the initial flow field. Predictions have been compared with previously reported laminar experimental results. In addition, the influence of stratification and turbulence on vortex behavior near the ground plane has been studied. Author

N92-28555*# Mississippi State Univ., Mississippi State. Coll. of Engineering Administration.
COMPUTATION OF STEADY AND UNSTEADY QUASI-ONE-DIMENSIONAL VISCOUS/INVISCID INTERACTING INTERNAL FLOWS AT SUBSONIC, TRANSONIC, AND SUPERSONIC MACH NUMBERS Final Report
Timothy W. Swafford, David H. Huddleston, Judy A. Busby, and B. Lawrence Chesser Jun. 1992 109 p Sponsored in part by NSF
(Grant NAG3-1170)
(NASA-CR-189881; NAS 1.26:189881; MSSU-EIRS-ERC-91-1)
Avail: NTIS HC/MF A06

Computations of viscous-inviscid interacting internal flowfields are presented for steady and unsteady quasi-one-dimensional (Q1D) test cases. The unsteady Q1D Euler equations are coupled with integral boundary-layer equations for unsteady, two-dimensional (planar or axisymmetric), turbulent flow over impermeable, adiabatic walls. The coupling methodology differs from that used in most techniques reported previously in that the above mentioned equation sets are written as a complete system and solved simultaneously; that is, the coupling is carried out directly through the equations as opposed to coupling the solutions of the different equation sets. Solutions to the coupled system of equations are obtained using both explicit and implicit numerical schemes for steady subsonic, steady transonic, and both steady and unsteady supersonic internal flowfields. Computed solutions are compared with measurements as well as Navier-Stokes and inverse boundary-layer methods. An analysis of the eigenvalues of the coefficient matrix associated with the quasi-linear form of the coupled system of equations indicates the presence of complex eigenvalues for certain flow conditions. It is concluded that although reasonable solutions can be obtained numerically, these complex eigenvalues contribute to the overall difficulty in obtaining numerical solutions to the coupled system of equations. Author

N92-28694# National Aerospace Lab., Amsterdam (Netherlands). Fluid Dynamics Div.
TURBULENCE MODELING: SURVEY OF ACTIVITIES IN BELGIUM AND THE NETHERLANDS, AND APPRAISAL OF THE STATUS AND A VIEW ON THE PROSPECTS
B. vanderBerg 28 May 1990 12 p Presented at AGARD Fluid Dynamics Panel Technical Status Review on Appraisal of the Suitability of Turbulence Models in Flow Calculations, Friedrichshafen, Fed. Republic of Germany, 26 Apr. 1990
(NLR-TP-90184-U; ETN-92-91540) Avail: NTIS HC/MF A03

Some experimental results obtained in turbulent boundary layers, as occur on airplane wings, are considered in relation to the usual turbulence mode assumptions. The status of turbulence modeling is found not to be satisfactory. To support the development of semiempirical models of acceptable accuracy, a more extensive base of reliable turbulence data is desirable.
ESA

N92-28712# National Aerospace Lab., Amsterdam (Netherlands). Fluid Dynamics/Informatics Div.
BOUNDARY CONDITIONS FOR EULER EQUATIONS AT INTERNAL BLOCK FACES OF MULTI-BLOCK DOMAINS USING LOCAL GRID REFINEMENT
A. Kassies and R. Tognaccini (Aeritalia S.p.A., Naples, Italy) 10 Apr. 1990 19 p Presented at the AIAA 21st Fluid Dynamics, Plasma Dynamics and Lasers Conference, Seattle, WA, 18-20 Jun. 1990 Previously announced in IAA as A90-38725 Prepared in cooperation with Aeritalia S.p.A., Naples, Italy
(Contract NIVR-01604-N)
(NLR-TP-90134-U; ETN-92-91533) Avail: NTIS HC/MF A03

A method for the numerical treatment of boundary conditions for Euler equations at internal block faces of arbitrary complex three dimensional patched multiblock domains is developed. The method should allow cell length and skewness discontinuities of the grid normal to the internal faces, and local grid refinement in each block individually. The method is developed for multiblock flow solvers based on an explicit cell centered finite volume scheme with adaptive numerical dissipation. The discontinuities of the grid at internal block faces are treated by a boundary condition using the gradient vector of each flow variable to determine the flow state at the internal face. In case of local grid refinement, where a coarse grid cell may be connected to any number of fine grid cells, a unique value of the gradient vector is used for all fine grid cells connected to a coarse grid cell. The resulting scheme is fully conservative and may be easily extended to other types of flow solvers. By implementing the described method in a three dimensional multiblock solver, a powerful aerodynamic analysis tool for solving the Euler equations in an arbitrary flow domain is obtained. The ability of the flow solver to handle grid discontinuities over internal faces allows much freedom in the grid generation process. The use of local grid refinement per block offers the desired flow simulation accuracy with grids of reasonable size.
ESA

N92-28752* National Aeronautics and Space Administration. Langley Research Center, Hampton, VA.
HEAT EXCHANGER WITH OSCILLATING FLOW Patent
Stephen J. Scotti, inventor (to NASA), Max L. Blosser, inventor (to NASA), and Charles J. Camarda, inventor (to NASA) 28 Apr. 1992 11 p Filed 30 Mar. 1990 Supersedes N90-27072 (28 - 21, p 3004)
(NASA-Case-LAR-14033-1; US-Patent-5,107,920; US-Patent-Appl-SN-501909; US-Patent-Class-165-109.1; US-Patent-Class-165-41; US-Patent-Class-165-4; US-Patent-Class-165-104.31; US-Patent-Class-165-104.34; US-Patent-Class-165-110; Int-Patent-Class-F28D-17/00) Avail: US Patent and Trademark Office

Various heat exchange apparatuses are described in which an oscillating flow of primary coolant is used to dissipate an incident heat flux. The oscillating flow may be imparted by a reciprocating piston, a double action twin reciprocating piston, fluidic oscillators, or electromagnetic pumps. The oscillating fluid flows through at least one conduit in either an open loop or a closed loop. A secondary flow of coolant may be used to flow over the outer walls of at least one conduit to remove heat transferred from the primary coolant to the walls of the conduit.
Official Gazette of the U.S. Patent and Trademark Office

N92-28766# Phillips Lab., Kirkland AFB, NM.
SINGLET DELTA OXYGEN PUMPING OF IODINE MONOFLUORIDE IN A SUPERSONIC FLOW Final Report, 1 Jul. - 31 Oct. 1990
C. A. Helms, L. Hanko, G. P. Perram, and G. Hager Jan. 1992 32 p
(AF Proj. 3151)
(AD-A249946; AD-E200955; PL-TR-91-1044) Avail: NTIS HC/MF A03

The iodine monofluoride (IF) molecule is known to lase via optical pumping. This study describes the first demonstration of coupling high number densities of ground state IF (10 exp 15 /cubed cm) with a high concentration of singlet delta oxygen (10 exp 16/cubed cm) in a supersonic flow. Although lasing was not achieved, a qualitative description of experimental observations is presented.
GRA

N92-28768# Illinois Univ., Urbana. Dept. of Chemical Engineering.
WALL TURBULENCE Final Report
L. P. Purtell Apr. 1992 8 p
(Contract N00014-82-K-0324)
(AD-A249973) Avail: NTIS HC/MF A02

This research was aimed at understanding turbulence generated at a wall. The goals were to investigate the structure of turbulence in the viscous wall region, to understand how production of turbulence is related to measured structural parameters, to develop models that will allow the computation of velocity and temperature fields, and to explore how the characteristics of wall turbulence are changed by external influences. The principal tools that were used are electrochemical techniques that measure turbulence characteristics in the immediate vicinity of a wall without interfering with the flow, the laser Doppler velocimeter, computer experiments, and pulsed-laser velocimetry. External influences to be studied are imposed flow oscillations, wavy walls, and drag-reducing polymers.
GRA

N92-28788# Office National d'Etudes et de Recherches Aerospatiales, Paris (France). Direction de lAerodynamique.
CONSTRUCTION OF A NUMERICAL OPTIMIZATION METHOD FOR THE DEFINITION OF HYPERSUPPORTED PROFILES Final Summary Report [REALISATION DUNE METHODE DOPTIMISATION NUMERIQUE POUR LA DEFINITION DE PROFILES HYPERSUSTENTES. RAPPORT DE SYNTHESE FINAL]
F. Moens Jun. 1991 66 p In FRENCH
(Contract DRET-89-34-001)
(ONERA-RSF-43/1736-AY-146A; ETN-92-91326) Avail: NTIS HC/MF A04

The method for a two dimensional description of hyper-supported profiles by numerical optimization consists of a stress minimization program, named CONMIN, and the aerodynamic program, named VIS18. The viscous effects are taken into account by the strong coupling iterative method. The decision variables considered are the deflection values, slots and flap covers, and the incidence of the assembly. The aim of the study is to maximize the whole lift-slope coefficient, for given values of stresses of the overspeeds of different bodies. The importance of including the viscous effects was demonstrated for the optimization of the OALT25 laminar profile, with a two slit flap. The deflection values calculated are greater than those obtained by optimization in an inviscid fluid, and a separation on the second flap is observed. Problems concerning relative minimal values and of multiple solutions were found for the optimization of the OAULM02 profile, with a single slot flap. These effects can be reduced by increasing the coupling interactions, although the calculation time increases.
ESA

N92-28803# Naval Research Lab., Washington, DC.
COMPUTATIONS OF DETONATION STRUCTURE: THE INFLUENCE OF MODEL INPUT PARAMETERS Interim Report
Michel H. Lefebvre, Elaine S. Oran, and K. Kailasanath 10 Apr. 1992 22 p
(AD-A248634; NRL/MR/4404-92-6961) Avail: NTIS HC/MF A03

We describe analyses and numerical computations that examine the validity of certain common simplifications in the chemical and thermophysical model on the calculation of detonation properties. In particular, we examine the effects of (1) approximations of the temperature dependence of the specific heat C, and the ratio of specific heats Gamma = C(sub p) / C(sub v) in a detailed numerical simulation of detonation in a mixture of hydrogen and oxygen mixture, (2) varying the heat release, and (3) varying the chemical induction time, and compare all of those approximations to a computation that uses a detailed model of the chemical kinetics and correct thermophysics. Finally, we describe computations of detonations in mixtures of hydrogen and oxygen diluted with argon and carbon tetrafluoride and show how the numerical model correctly predicts the trends in the detonation as the percentage of carbon tetrafluoride is increased. GRA

N92-28808# Pittsburgh Energy Technology Center, PA.
JOINT DOE/NSF WORKSHOP ON FLOW OF PARTICULATES AND FLUIDS
S. I. Plasynski, ed., W. C. Peters, ed., and Mike C. Roco 1991 396 p Presented at the 3rd Joint DOE/NSF Workshop on Flow of Particulates and Fluids, Worcester, MA, 22-24 Oct. 1991 Prepared in cooperation with NSF, Washington, DC
(DE92-012692; CONF-9110369) Avail: NTIS HC/MF A17

These proceedings are the result of the third DOE-NSF Workshop on fundamental research in the area of particulate two-phase flow and granular flow. The present collection of 23 contributions from universities and national laboratories is based on research projects sponsored by either the Department of Energy or the National Science Foundation. These papers illustrate some of the latest advancements in theory, simulations, and experiments. The papers from the Workshop held October 22-24, 1991 have been separated into three basic areas: experiments, theory, and numerical simulations. A list of attendees at the workshop is included at the end of the proceedings. Topics discussed include multiphase flow, slurry flow, particle fluidization, properties of suspensions, boundary value problems, and numerical simulation. DOE

N92-28817*# State Univ. of New York, Buffalo. Dept. of Mechanical and Aerospace Engineering.
[LARGE EDDY SIMULATIONS (LES) AND DIRECT NUMERICAL SIMULATIONS (DNS) FOR THE COMPUTATIONAL ANALYSES3 OF HIGH SPEED REACTING FLOWS] Semiannual Report, 1 Nov. 1991 - 30 Apr. 1992
Peyman Givi, Cyrus K. Madnia, C. J. Steinberger, and S. H. Frankel 30 Apr. 1992 115 p
(Grant NAG1-1122)
(NASA-CR-190364; NAS 1.26:190364) Avail: NTIS HC/MF A06

The principal objective is to extend the boundaries within which large eddy simulations (LES) and direct numerical simulations (DNS) can be applied in computational analyses of high speed reacting flows. A summary of work accomplished during the last six months is presented. For individual titles, see N92-28818 through N92-28821.

N92-28818*# State Univ. of New York, Buffalo. Dept. of Mechanical and Aerospace Engineering.
LARGE EDDY SIMULATIONS AND DIRECT NUMERICAL SIMULATIONS OF HIGH SPEED TURBULENT REACTING FLOWS
P. Givi, C. K. Madnia, C. J. Steinberger, and S. H. Frankel *In its* Large Eddy Simulations (LES) and Direct Numerical Simulations (DNS) for the Computational Analyses of High Speed Reacting Flows 30 Apr. 1992 20 p (For primary document see N92-28817 19-34)
(Grant NAG1-1122)
Avail: NTIS HC/MF A06

The basic objective of this research is to extend the capabilities of Large Eddy Simulations (LES) and Direct Numerical Simulations (DNS) for the computational analyses of high speed reacting flows. In the efforts related to LES, we were primarily involved with assessing the performance of the various modern methods based on the Probability Density Function (PDF) methods for providing closures for treating the subgrid fluctuation correlations of scalar quantities in reacting turbulent flows. In the work on DNS, we concentrated on understanding some of the relevant physics of compressible reacting flows by means of statistical analysis of the data generated by DNS of such flows. In the research conducted in the second year of this program, our efforts focused on the modeling of homogeneous compressible turbulent flows by PDF methods, and on DNS of non-equilibrium reacting high speed mixing layers. Some preliminary work is also in progress on PDF modeling of shear flows, and also on LES of such flows. Author

N92-28819*# State Univ. of New York, Buffalo. Dept. of Mechanical and Aerospace Engineering.
REACTANT CONVERSION IN HOMOGENEOUS TURBULENCE: MATHEMATICAL MODELING, COMPUTATIONAL VALIDATIONS AND PRACTICAL APPLICATIONS
C. K. Madnia, S. H. Frankel, and P. Givi *In its* Large Eddy Simulations (LES) and Direct Numerical Simulations (DNS) for the Computational Analyses of High Speed Reacting Flows 30 Apr. 1992 37 p Submitted for publication (For primary document see N92-28817 19-34)
Avail: NTIS HC/MF A06

Closed form analytical expressions are obtained for predicting the limited rate of reactant conversion in a binary reaction of the type F + rO yields (1 + r) Product in unpremixed homogeneous turbulence. These relations are obtained by means of a single point Probability Density Function (PDF) method based on the Amplitude Mapping Closure. It is demonstrated that with this model, the maximum rate of the reactants' decay can be conveniently expressed in terms of definite integrals of the Parabolic Cylinder Functions. For the cases with complete initial segregation, it is shown that the results agree very closely with those predicted by employing a Beta density of the first kind for an appropriately defined Shvab-Zeldovich scalar variable. With this assumption, the final results can also be expressed in terms of closed form analytical expressions which are based on the Incomplete Beta Functions. With both models, the dependence of the results on the stoichiometric coefficient and the equivalence ratio can be expressed in an explicit manner. For a stoichiometric mixture, the analytical results simplify significantly. In the mapping closure, these results are expressed in terms of simple trigonometric functions. For the Beta density model, they are in the form of Gamma Functions. In all the cases considered, the results are shown to agree well with data generated by Direct Numerical Simulations (DNS). Due to the simplicity of these expressions and because of nice mathematical features of the Parabolic Cylinder and the Incomplete Beta Functions, these models are recommended for estimating the limiting rate of reactant conversion in homogeneous reacting flows. These results also provide useful insights in assessing the extent of validity of turbulence closures in the modeling of unpremixed reacting flows. Some discussions are provided on the extension of the model for treating more complicated reacting systems including realistic kinetics schemes and multi-scalar mixing with finite rate chemical reactions in more complex configurations. Author

N92-28820*# State Univ. of New York, Buffalo. Dept. of Mechanical and Aerospace Engineering.
MODELING OF THE REACTANT CONVERSION RATE IN A TURBULENT SHEAR FLOW **c02**
S. H. Frankel, C. K. Madnia, and P. Givi *In its* Large Eddy Simulations (LES) and Direct Numerical Simulations (DNS) for the Computational Analyses of High Speed Reacting Flows 30 Apr.

1992 14 p Submitted for publication (For primary document see N92-28817 19-34)
Avail: NTIS HC/MF A06

Results are presented of direct numerical simulations (DNS) of spatially developing shear flows under the influence of infinitely fast chemical reactions of the type A + B yields Products. The simulation results are used to construct the compositional structure of the scalar field in a statistical manner. The results of this statistical analysis indicate that the use of a Beta density for the probability density function (PDF) of an appropriate Shvab-Zeldovich mixture fraction provides a very good estimate of the limiting bounds of the reactant conversion rate within the shear layer. This provides a strong justification for the implementation of this density in practical modeling of non-homogeneous turbulent reacting flows. However, the validity of the model cannot be generalized for predictions of higher order statistical quantities. A closed form analytical expression is presented for predicting the maximum rate of reactant conversion in non-homogeneous reacting turbulence. Author

N92-28821*# State Univ. of New York, Buffalo. Dept. of Mechanical and Aerospace Engineering.
THE COMPOSITIONAL STRUCTURE AND THE EFFECTS OF EXOTHERMICITY IN AN UNPREMIXED PLANAR JET FLAME c25
C. J. Steinberger, T. J. Vidoni, and P. Givi *In its* Large Eddy Simulations (LES) and Direct Numerical Simulations (DNS) for the Computational Analyses of High Speed Reacting Flows 30 Apr. 1992 42 p (For primary document see N92-28817 19-34)
Avail: NTIS HC/MF A06

Results are presented of direct numerical simulations (DNS) of a randomly perturbed compressible, spatially developing planar jet under the influence of a finite rate Arrhenius chemical reaction of the type F + O yields Product + Heat. The objectives of the simulations are to assess the compositional structure of the flame and to determine the influence of reaction exothermicity by means of statistical sampling of the data generated by DNS. It is shown that even with this idealized kinetics model, the simulated results exhibit features in accordance with experimental data. These results indicate that the Damkoehler number is an important parameter in determining the statistical composition of the reacting field, and that the results are insensitive to the mechanism by which this parameter is varied. It is demonstrated that as the intensity of mixing is increased and the effect of finite rate chemistry is more pronounced, the magnitudes of the ensemble mean and rms of the product mass fraction decrease, and those of the reactants mass fraction increase. Also, at higher mixing rates the joint probability density functions of the reactants' mass fractions shift towards higher values within the composition domain indicating a lower reactedness. These trends are consistent with those observed experimentally and are very useful in portraying the statistical structure of non-equilibrium diffusion flames. The DNS generated data are also utilized to examine the applicability of the 'laminar diffusion flamelet model' in predicting the rate of the reactant conversion with finite rate chemistry. This examination indicates that the bounds of the product formation scale reasonably well with those obtained by the flamelet model. However, in the range of the relatively low values of the Damkoehler numbers considered, the scatter of the results is substantially more than that to be completely determined by the closure. Author

N92-28825# Deutsche Forschungsanstalt fuer Luft- und Raumfahrt, Goettingen (Germany, F.R.). Abt. Messphysik.
EXPERIMENTAL AND THEORETICAL INVESTIGATIONS ON THE PARTICLE LAG OF PARTICLES UNDER THE INFLUENCE OF LARGE VELOCITY GRADIENTS IN COMPRESSIBLE FLOW Ph.D. Thesis - Goettingen Univ.
Peter Thomas Jun. 1991 149 p In GEORGIAN
(DLR-FB-91-25; ISSN-0939-2963; ETN-92-91066) Avail: NTIS HC/MF A07; DLR, Wissenschaftliches Berichtswesen, VB-PL-DO, Postfach 90 60 58, 5000 Cologne, Fed. Republic of Germany, HC 25 DM

The ability of micro-scale seedling particles to follow large velocity gradients is studied. Application of this behavior to fluid flow velocity measuring techniques such as Laser Doppler Anemometry (LDA) is investigated. The equation of particle motion is numerically integrated for flows across oblique shocks. The influence of the Basset integral which accounts for the temporal evolution of the accelerated motion on the particle motion is examined in cases involving large vorticity gradients across shock. Different seedling materials and techniques are tested and the experimental results are compared with each other. ESA

N92-28879# Pennsylvania State Univ., University Park. Turbomachinery Lab.
EXPLICIT NAVIER-STOKES COMPUTATION OF TURBOMACHINERY FLOWS Final Report, 1 Aug. 1986 - 31 Dec. 1991
Robert Kunz and B. Lakshminarayana Jan. 1992 251 p
(Contract DAAL03-86-G-0044)
(AD-A249284; PSU-Turbo-R-9201) Avail: NTIS HC/MF A12

A new three-dimensional explicit Navier-Stokes procedure has been developed for computation of turbomachinery flows. Several numerical strategies and modelling techniques have been developed and incorporated which enable convergent and accurate predictions of high Reynolds number flowfields across a wide range of Mach numbers. These include incorporation of a compressible low Reynolds number form of the turbulence transport model and other physical and solution parameters, eigenvalue and local velocity artificial dissipation scalings, a compact flux evaluation procedure, and a hybrid low Reynolds number ke/algebraic Reynolds stress model. Detailed stability and order of magnitude analyses are performed on the discrete system of seven governing equations. Conclusions are drawn concerning the influence of system rotation and turbulence transport source terms, implicit source term treatment and the coupling of the discrete mean flow equation system to the turbulence model equations and its effect on the stability of the numerical scheme. Three-dimensional validation is provided by the results of an incompressible curved duct flow computation. A high Reynolds number axial rotor flow, for which extensive experimental data is also available, was computed. A backswept transonic centrifugal compressor flow, for which L2F meridional passage velocity measurements are available, is computed. Full Navier-Stokes solutions are presented which are shown to capture detailed viscous dominated flow features. GRA

N92-28890# Massachusetts Univ., Amherst. Dept. of Civil Engineering.
LAGRANGIAN TURBULENCE: STRUCTURES AND MIXING IN ADMISSIBLE MODEL FLOWS Final Technical Report, 1 Jan. 1989 - 1 Jun. 1991
Julio M. Ottino 18 Dec. 1991 7 p
(Grant AF-AFOSR-0251-89)
(AD-A247203; AFOSR-92-0080TR) Avail: NTIS HC/MF A02

The goal of our research was to bridge the gap between modern ideas from dynamical systems and chaos and more traditional approaches to turbulence. In order to reach this objective we conducted theoretical and computational work on two systems: (1) a perturbed-Kelvin cat eyes flow, and (2) prototype solutions of the Navier-Stokes equations near solid walls. The main results obtained are two-fold: we have been able to produce flows capable of producing complex distributions of vorticity, and we have been able to construct flowfields, based on solutions of the Navier-Stokes equations, which are capable of displaying both Eulerian and Lagrangian turbulence. These results exemplify typical mechanisms of mixing enhancement in transitional flows. GRA

N92-28908*# Toledo Univ., OH.
LOW REYNOLDS NUMBER MULTIPLE-TIME-SCALE TURBULENCE MODEL AND CALCULATIONS OF STEADY AND PULSATING SHEAR LAYERS Final Report
Sang-Wook Kim May 1992 38 p
(Contract NCC3-229)
(NASA-CR-189176; E-7038; NAS 1.26:189176) Avail: NTIS HC/MF A03

A low Reynolds number multiple-time-scale turbulence model (LMS) and its application to fully developed turbulent channel flows and pulsating pipe flows are presented. The LMS can describe the inequilibrium turbulence phenomena down to the viscous sublayer. The calculated fluid flow and turbulence fields for the channel flows are in better agreement with the direct numerical simulation (DNS) results than those obtained using a Reynolds stress turbulence model, and the calculated near-wall dissipation rates are in qualitatively correct agreement with the DNS results. The LMS also successfully predicts the rapidly varying phase-lead of the wall shearing stress that occurs in a narrow range of the dimensionless frequency omega (+) = (omega x nu)/(upsilon x tau(exp2)) for the pulsating pipe flows while various other turbulence models fail to predict this phenomenon, and the LMS yields significantly improved numerical results for a wide range of the dimensionless frequency compared with those obtained using a rapid distortion theory (RDT). Author

N92-28978# Defence Research Establishment, Ottawa (Ontario).
A 2-D ANALYSIS OF EVAPORATION IN LAMINAR FLOW
Brad Cain Nov. 1991 27 p
(AD-A246467; DREO-1093) Avail: NTIS HC/MF A03

This report documents a two-dimensional, finite element study of the evaporation of a liquid on a flat surface into a laminar air stream for three geometries: (1) a hemispherical drop on a flat plate; (2) a hemispherical drop between parallel plates; and (3) a smear on a flat plate. The problems are made dimensionless and the flux from the liquid is determined in a parametric analysis with a range of values of the resulting independent variables. A comparison is made with same experimental data and an example of the use of the results is given. GRA

N92-29118# Oxford Univ. (England).
TURBULENT SPOT GENERATION AND GROWTH RATES IN A TRANSONIC BOUNDARY LAYER Final Report, 15 May 1989 - 14 Oct. 1991
J. P. Clark, J. E. LeGraff, and T. V. Jones 18 Mar. 1992 24 p
(Grant AF-AFOSR-0427-89)
(AD-A250221; AFOSR-92-0365TR) Avail: NTIS HC/MF A03

Wide-bandwidth surface heat transfer instrumentation has been used to track the generation, convection and growth of turbulent spots in a laminar boundary layer undergoing transition to turbulence. The model was a flat plate subjected to a range of free stream conditions in a piston-driven isentropic compression heated transient wind tunnel at Oxford University. Freestream Mach number (subsonic to 2.0), freestream turbulence and streamwise pressure gradient (favorable to adverse) were varied. Preliminary analysis of the time-resolved heat transfer data allowed estimates of spot convection rates, generation rates and spreading angles to be estimated. Convection rates were little affected by Mach number, whereas spreading angles were narrowed by favorable pressure gradients and expanded by adverse gradients. GRA

N92-29125* National Aeronautics and Space Administration. Lewis Research Center, Cleveland, OH.
PULSE THERMAL ENERGY TRANSPORT/STORAGE SYSTEM Patent
Mark W. Weislogel, inventor (to NASA) 7 Jul. 1992 11 p
Filed 26 Jul. 1991 Supersedes N92-10167 (30 - 1, p 32)
(NASA-Case-LEW-15235-1; US-Patent-5,127,471;
US-Patent-Appl-SN-736145; US-Patent-Class-165-104.22;
US-Patent-Class-165-41; US-Patent-Class-165-104.14;
US-Patent-Class-417-209; Int-Patent-Class-F28D-15/02) Avail: US Patent and Trademark Office

A pulse-thermal pump is described. The pump has a novel fluid flow wherein heat admitted to a closed system raises the pressure in a closed evaporator chamber, while another interconnected evaporator chamber remains open. This creates a pressure differential, and at a predetermined pressure, the closed evaporator is opened and the opened evaporator is closed. The difference in pressure initiates fluid flow in the system.
Official Gazette of the U.S. Patent and Trademark Office

N92-29171# Air Force Inst. of Tech., Wright-Patterson AFB, OH.
DEVELOPMENT OF INSTRUMENTATION FOR BOUNDARY LAYER TRANSITION DETECTION M.S. Thesis
Steven B. Harrison 1991 164 p
(AD-A249982; AFIT/CI/CIA-91-100) Avail: NTIS HC/MF A08

A steady state heat transfer technique is developed and evaluated for detecting boundary layer transition on a flat plate in incompressible flow. The method involves adhering encapsulated temperature sensitive liquid crystals to a constant heat flux surface. A heater composed of unidirectional carbon fibers is developed and tested with the aim of in-flight boundary layer transition detection on a natural laminar flow nacelle. The individual and combined influences of surface heating and favorable pressure gradient on boundary layer transition are considered. Heating is found to be a destabilizing influence on the boundary layer, while a favorable pressure gradient is a stabilizing influence. A Stanton number correlates the movement of transition with heating for zero pressure gradient flat plate boundary layers. No similar correlation is found when a favorable pressure gradient accompanies the heating. Heating is more destabilizing in a favorable pressure gradient than in zero pressure gradient. Shear sensitive liquid crystal is used to detect transition and to obtain, for the first time, quantitative measurements of surface shear stress in a transitional boundary layer. This involves calibrating the time required for the liquid crystal film to experience a texture change when subjected to a shearing force. Using this technique, shear sensitive liquid crystal shows promise for full coverage measurement of surface shear stress in low speed flows. GRA

35 INSTRUMENTATION AND PHOTOGRAPHY

Includes remote sensors; measuring instruments and gages; detectors; cameras and photographic supplies; and holography.

For aerial photography see *43 Earth Resources and Remote Sensing.* For related information see also *06 Aircraft Instrumentation,* and *19 Spacecraft Instrumentation.*

N92-28322# Eidgenoessische Technische Hochschule, Zurich (Switzerland). Inst. of Geodesy and Photogrammetry.
ON-LINE POINT POSITIONING WITH SINGLE FRAME CAMERA DATA Final Report, 1 Jan. 1989 - 15 Mar. 1992
A. Gruen 15 Mar. 1992 84 p
(Contract DAJA45-89-C-0004; DA Proj. 1L1-61102-BH-57)
(AD-A248307; TR-84) Avail: NTIS HC/MF A05

The project on-line point positioning with single frame camera data was concluded. The goal of the project was to develop a data processing concept for an on-line high accuracy point positioning system. An operational on-line system, installed in a UNIX environment under the programming language C, for aerial phototriangulation working on an analytical plotter or on a digital workstation should provide high speed of operation, accuracy of results, and ease of data management. Established tests showed that the Sun Microsystems workstations have sufficient memory capacity and speed performance to run on-line triangulation applications. The adopted algorithms in the on-line triangulation system for the computation of initial values, for the sequential and simultaneous adjustment and for quality control will be presented in this report. A description of the developed software modules and the program will also be given. Although this system was designed and developed specifically for aerial triangulation, it is anticipated that future applications for on-line triangulation algorithms and methods will be found in robotics and industrial quality control. GRA

N92-28767# Yuma Proving Ground, AZ.
AUTOMATION AND REMOTE CONTROL INSTRUMENTATION DEVELOPMENT: ROCKET FIRST MOTION TIMING SYSTEM (RFMTS) Final Report, Oct. 1988 - Oct. 1990

Bruce Buzzo Mar. 1992 61 p
(AD-A249970) Avail: NTIS HC/MF A04

The Rocket First Motion System was designed and developed to record the time interval from the firing pulse until the launcher detent is raised due to the forward movement of the rocket.

GRA

N92-28812# Lawrence Livermore National Lab., CA.
WOELTER X RAY MICROSCOPE CHARACTERIZATION MEASUREMENTS ON NOVA
B. A. Remington, S. G. Glendinning, R. J. Wallace, S. Rothman, and R. Morales Apr. 1992 14 p Presented at the 9th Topical Conference on High-Temperature Plasma Diagnostics, Santa Fe, NM, 15-19 Mar. 1992
(Contract W-7405-eng-48)
(DE92-013207; UCRL-JC-109095; CONF-920362-28) Avail: NTIS HC/MF A03

We have made in situ measurements of the spatial resolution function for two sectors of the 22X magnification Woelter x-ray microscope. Our experimental technique using backlit grid shot on the Nova laser and our method of analysis are described.

DOE

N92-29097* National Aeronautics and Space Administration. Langley Research Center, Hampton, VA.
PRESSURE TRANSDUCER AND SYSTEM FOR CRYOGENIC ENVIRONMENTS Patent
John J. Chapman, inventor (to NASA) 26 May 1992 21 p Filed 23 Apr. 1991 Supersedes N91-28546 (29 - 20, p 3349)
(NASA-Case-LAR-14579-1; US-Patent-5,116,331;
US-Patent-Appl-SN-690198; US-Patent-Class-73-721;
US-Patent-Class-73-708; US-Patent-Class-73-727;
US-Patent-Class-73-756; US-Patent-Class-338-4;
Int-Patent-Class-G01L-7/08; Int-Patent-Class-G01L-9/06) Avail: US Patent and Trademark Office

A silicon pressure die is bonded to a borosilicate substrate above the pneumatic port. A Wheatstone bridge circuit is formed on the silicon pressure die and has bridge elements of silicon doped with boron to a deposit density level of approximately 1 x 10(exp 19)-10(exp 21) boron/cc. A current source is provided to excite the Wheatstone bridge circuit. In addition, a temperature sensor is provided to provide temperature readings. An array may be formed of the resulting pressure transducers. This unique solution of materials permits operation of a pressure transducer in cryogenic environments.

Official Gazette of the U.S. Patent and Trademark Office

N92-29105*# National Aeronautics and Space Administration. Lewis Research Center, Cleveland, OH.
A 4-SPOT TIME-OF-FLIGHT ANEMOMETER FOR SMALL CENTRIFUGAL COMPRESSOR VELOCITY MEASUREMENTS
Mark P. Wernet and Gary J. Skoch Jul. 1992 8 p Presented at the Sixth International Symposium on the Application of Laser Techniques to Fluid Mechanics, Lisbon, Portugal, 20-23 Jul. 1992; sponsored by the Instituto Superio Techico
(DA Proj. 1L1-62211-A-47-A; RTOP 505-62-50)
(NASA-TM-105717; E-7112; NAS 1.15:105717;
AVSCOM-TR-92-C-026) Avail: NTIS HC/MF A02

The application of laser anemometry techniques in turbomachinery facilities is a challenging dilemma requiring an anemometer system with special qualities. Here, we describe the use of a novel laser anemometry technique applied to a small 4.5 kg/s, 4:1 pressure ratio centrifugal compressor. Sample velocity profiles across the blade pitch are presented for a single location along the rotor. The results of the intra-blade passage velocity measurements will ultimately be used to verify CFD 3-D viscous code predictions.

Author

N92-29135* National Aeronautics and Space Administration. Marshall Space Flight Center, Huntsville, AL.
WATER WINDOW IMAGING X RAY MICROSCOPE Patent
Richard B. Hoover, inventor (to NASA) 21 Apr. 1992 9 p Filed 31 Oct. 1990 Supersedes N91-15519 (29 - 7, p 1005)
(NASA-Case-MFS-28485-1; US-Patent-5,107,526;
US-Patent-Appl-SN-606988; US-Patent-Class-378-43;
US-Patent-Class-378-210; Int-Patent-Class-G21K-7/00) Avail: US Patent and Trademark Office

A high resolution x ray microscope for imaging microscopic structures within biological specimens has an optical system including a highly polished primary and secondary mirror coated with identical multilayer coatings, the mirrors acting at normal incidence. The coatings have a high reflectivity in the narrow wave bandpass between 23.3 and 43.7 angstroms and have low reflectivity outside of this range. The primary mirror has a spherical concave surface and the secondary mirror has a spherical convex surface. The radii of the mirrors are concentric about a common center of curvature on the optical axis of the microscope extending from the object focal plane to the image focal plane. The primary mirror has an annular configuration with a central aperture and the secondary mirror is positioned between the primary mirror and the center of curvature for reflecting radiation through the aperture to a detector. An x ray filter is mounted at the stage end of the microscope, and film sensitive to x rays in the desired band width is mounted in a camera at the image plane of the optical system. The microscope is mounted within a vacuum chamber for minimizing the absorption of x rays in air from a source through the microscope.

Official Gazette of the U.S. Patent and Trademark Office

N92-29156* National Aeronautics and Space Administration. Pasadena Office, CA.
ULTRA-HIGH TEMPERATURE STABILITY JOULE-THOMSON COOLER WITH CAPABILITY TO ACCOMODATE PRESSURE VARIATIONS Patent
Steven Bard, inventor (to NASA) (Jet Propulsion Lab., California Inst. of Tech., Pasadena.), Jiunn-Jeng Wu, inventor (to NASA) (Jet Propulsion Lab., California Inst. of Tech., Pasadena.), and Curtis A. Trimble, inventor (to NASA) (Jet Propulsion Lab., California Inst. of Tech., Pasadena.) 9 Jun. 1992 8 p Filed 28 Dec. 1990
(NASA-Case-NPO-18184-1-CU; US-Patent-5,119,637;
US-Patent-Appl-SN-636076; US-Patent-Class-62-51.2;
US-Patent-Class-62.224; Int-Patent-Class-F25B-19/02) Avail: US Patent and Trademark Office

A Joule-Thomson cryogenic refrigeration system capable of achieving high temperature stabilities in the presence of varying temperature, atmospheric pressure, and heat load is provided. The Joule-Thomson cryogenic refrigeration system includes a demand flow Joule-Thomson expansion valve disposed in a cryostat of the refrigeration system. The expansion valve has an adjustable orifice that controls the flow of compressed gas therethrough and induces cooling and partial liquefaction of the gas. A recuperative heat exchanger is disposed in the cryostat and coupled to the expansion valve. A thermostatically self-regulating mechanism is disposed in the cryostat and coupled to the J-T expansion valve. The thermostatically self-regulating mechanism automatically adjusts the cross sectional area of the adjustable valve orifice in response to environmental temperature changes and changes in power dissipated at a cold head. A temperature sensing and adjusting mechanism is coupled to a cold head for adjusting the temperature of the cold head in response to the change in heat flow in the cold head. The temperature sensing and adjusting mechanism comprises a temperature sensitive diode, a wound wire heater, and an electrical feedback control circuit coupling the diode to the heater. An absolute pressure relief valve is interposed between the output of the cryostat and an exhaust port for maintaining a constant exhaust temperature in the refrigerating system, independent of the changes in atmospheric pressure.

Official Gazette of the U.S. Patent and Trademark Office

N92-29163 National Physical Lab., Teddington (England). Div. of Radiation Science and Acoustics.
THE MEASURING ASSEMBLY FOR THE NPL PRIMARY STANDARD ABSORBED DOSE GRAPHITE CALORIMETER AT THERAPY LEVELS
I. Stoker and A. R. DuSautoy 2 Dec. 1991 31 p

(NPL-RSA(EXT)-23; ISSN-0955-9655; ETN-92-91373) Copyright Avail: National Physical Lab., Teddington, Middlesex, TW11 0LW, England

A measuring assembly which forms together with a calorimeter, a stable and accurate means to measure local absorbed dose in high energy photon or electron beams, is described. The assembly contains AC bridges with phase sensitive detectors which provide good noise rejection and high sensitivity for the measurement of very small temperature changes sensed by thermistors in the calorimeter. The system is designed to function automatically under microcomputer control providing data collection and processing as well as the means for calibration by electrical heating. The circuits are described and operation of the calorimeters discussed. In practice, the system had to be reliable and easily maintained as it is suited to a tight time schedule in conjunction with other equipment. Experience with a prototype measurement assembly showed that the system should be as modular as possible allowing the use of spare modules and offline maintenance to reduce downtime. ESA

N92-28452*# National Aeronautics and Space Administration. Lyndon B. Johnson Space Center, Houston, TX.
MICROGRAVITY ACCELEROMETER CHARACTERIZATION ON COLUMBIA STS-32 MISSION
Jeff Schoess (Honeywell, Inc., Minneapolis, MN.), Don Thomas, and Bonnie Dunbar *In* NASA. Lewis Research Center, International Workshop on Vibration Isolation Technology for Microgravity Science Applications May 1992 p 357-368 (For primary document see N92-28436 19-31)
Avail: NTIS HC/MF A18

36 LASERS AND MASERS

Includes parametric amplifiers.
For related information see also *76 Solid-State Physics.*

N92-28228# International Centre for Theoretical Physics, Trieste (Italy).
NOISE REDUCTION IN RING LASER DRIVEN BY A BROAD BAND PUMP
Bang Doan Bui and Long Van Cao Aug. 1991 10 p
(DE92-622403; IC-91/234) Avail: NTIS HC/MF A02

By using the model of the nonlinear system subjected to a dichotomous noise studied by K. Kitahara et al., the steady state behavior of the ring-laser in a cavity was investigated. The interesting effect of noise reduction in Raman ring laser was shown. DOE

N92-28271# Michigan Univ., Ann Arbor. Intense Energy Beam Interaction Lab.
INTENSE ELECTRON BEAM CYCLOTRON MASERS WITH MICROSECOND PULSELENGTHS Final Report, 1 Aug. 1988 - 30 Nov. 1991
Ronald M. Gilgenbach 20 Dec. 1991 87 p
(Grant AF-AFOSR-0276-88)
(AD-A247060; AFOSR-92-0084TR) Avail: NTIS HC/MF A05

Results are reported for a three year research program with the goal of generating high power microwaves over long-pulselengths. Three types of cyclotron maser devices were developed and utilized in experiments on the Michigan Electron Long Beam Accelerator, (MELBA) at electron beam parameters of 0.6-0.9 MV, 0.52-2 kA, and 0.5-5 microsec. (1) The gyrotron backward-wave-oscillator, (gyro-BWO) produced the optimal combination of high power (1-8 MW) and long pulse (0.5-1.2 microsec) microwave generation. Due to these promising results, this gyro-BWO device was investigated most intensively during the final phase of this research program. (2) Bragg resonator cyclotron resonance masers were investigated with high quality, low current electron beams for high frequency microwave generation. These devices generated hundreds of kW for hundreds of ns, but it was found that microwaves originated from cyclotron harmonic generation on absolute instabilities. (3) Open cavity resonators of unslotted and slotted types generated microwave spikes (20-40 ns) in the X-band with peak power up to 15-25 MW. High peak microwave power (MW) was also generated in the K-band, most likely from the second cyclotron harmonic. GRA

N92-28299# Stanford Univ., CA. Lab. of Physics.
RESEARCH STUDIES ON EXTREME ULTRAVIOLET AND SOFT X RAY LASERS Final Report, 1 Sep. 1988 - 31 Jan. 1992
S. E. Harris 10 Jan. 1992 33 p
(Contract F49620-88-C-0120)
(AD-A247309; AFOSR-92-0014TR) Avail: NTIS HC/MF A03

This report describes studies concerned with the physics of short wavelength lasers and with applications of a new type of quantum mechanical interference. Highlights of this work include the operation of a traveling wave X-ray pump H2 116 nm laser; the development of a new type of depletion spectroscopy for core-excited states; and the proposal of lasers without inversion and related concepts applicable to nonlinear optics. GRA

N92-28315# Norwegian Defence Research Establishment, Kjeller.
A DIODE LASER PUMPED Nd:YAG LASER
Torolf C. Wedberg 30 Sep. 1991 90 p
(FFI-91/7020; ISSN-0802-2437; ETN-92-91242) Avail: NTIS HC/MF A05

The design, modeling, building and testing of a longitudinally laser pumped continuous wave Nd:YAG laser is reported. The diode laser is a temperature stabilized 200 mW, 100 micrometer wide bar operating at 810 nm wavelength. Nd:YAG laser operation is demonstrated both at 1.06 and 1.32 micrometers with transverse electromagnetic mode output powers of 59 and 19mW respectively, and optical conversion efficiencies of 42 and 13 percent respectively. Attempts to obtain lasing at 0.95 micrometers did not succeed. A 1.06 micrometer intracavity frequency doubling using a KTP crystal was investigated. The theory for Nd:YAG and diode laser operation is addressed and a theoretical model for the diode laser pumped laser which includes the effects of pump diode and Nd:YAG laser mode overlap is presented. Computer simulations using this model showed very good agreement with experimental results and were used to find optimum laser parameters both for minimum threshold and maximum output power. ESA

N92-28330# Northeast Semiconductor, Inc., Ithaca, NY.
STRAINED AlGaInAs SEMICONDUCTING MATERIAL FOR IMPROVED LASER PERFORMANCE Final Report, 1 Jul. - 31 Dec. 1991
William Shaff and Michael Frost 30 Jan. 1992 17 p
(Contract DAAL03-91-C-0031)
(AD-A249379; ARO-29004.1-EL-SBI) Avail: NTIS HC/MF A03

This program has been successful at demonstrating for the first time that strained AlGaInAs quantum well lasers grown by MBE can exhibit superior reliability to AlGaAs quantum well lasers. The benefits to device performance justify undertaking the development of a commercial process to bring this improved reliability to the market for DOD applications. There were 11 quantum well wafers characterized to help guide the selection of optimum growth conditions and to understand the growth of strained AlGaInAs by MBE for laser applications. A total of 4 laser wafers have been processed under this program. Three wafers produced working lasers and one exhibits pulsed lifetest performance beyond any measured in the history of this company. Lifetest data is still being collected for laser array CW operation. The laser array performance seen is superior to any array made by this company to date. The light output for a given operating current does not degrade at up to 108 pulses. In fact, output rises slightly because threshold falls under operation. GRA

N92-28662# Naval Postgraduate School, Monterey, CA.
THEORY FOR THE CEBAF AND SHIPBOARD FELS M.S.

Thesis
Carl A. Bice Dec. 1991 81 p
(AD-A245979) Avail: NTIS HC/MF A05

The development of the free electron laser (FEL) as a source of coherent radiation continues toward the fulfillment of its potential for high power, high efficiency and short wavelength. New experiments toward fulfillment of the FEL's potential present new phenomena to be studied by theoreticians and experimentalists. Two of these phenomena in short wavelength FELs are the shift in phase velocity resonance and the reduction in gain. The first part of this thesis presents an argument for the use of the FEL in a maritime military capacity. The advantages of the FEL over conventional kinetic systems and other high-energy laser systems are emphasized. The remainder of this thesis examines several effects of short wavelength FELs. In particular, Chapter 4 examines the characteristics of the proposed CEBAF UV FEL and presents alternative designs to assist in design selection. Chapter 5 analyses the resonant phase velocity shift and loss in gain that occurs in short wavelength FELs and presents a method to predict the resonant phase velocity and gain. Chapter 4 presents a new tool for examining the optical mode within the FEL. By removing the input optical field from the total optical field, only the excited optical field amplitude and phase remain. Chapter 6 presents a modification to a self-consistent three-dimensional simulation that will display the excited optical field. GRA

N92-28707*# Research Inst. for Computing and Information Systems, Houston, TX.
A CONTRIBUTION TO LASER RANGE IMAGING TECHNOLOGY Final Report
Rui J. P. deFigueiredo (Rice Univ., Houston, TX.) and Bradley S. Denney (Rice Univ., Houston, TX.) 4 Feb. 1991 14 p
(Contract NCC9-16; RICIS Proj. AI-11)
(NASA-CR-190501; NAS 1.26:190501) Avail: NTIS HC/MF A03

The goal of the project was to develop a methodology for fusion of a Laser Range Imaging Device (LRID) and camera data. Our initial work in the project led to the conclusion that none of the LRID's that were available were sufficiently adequate for this purpose. Thus we spent the time and effort on the development of the new LRID with several novel features which elicit the desired fusion objectives. In what follows, we describe the device developed and built under contract. The Laser Range Imaging Device (LRID) is an instrument which scans a scene using a laser and returns range and reflection intensity data. Such a system would be extremely useful in scene analysis in industry and space applications. The LRID will be eventually implemented on board a mobile robot. The current system has several advantages over some commercially available systems. One improvement is the use of X-Y galvonometer scanning mirrors instead of polygonal mirrors present in some systems. The advantage of the X-Y scanning mirrors is that the mirror system can be programmed to provide adjustable scanning regions. For each mirror there are two controls accessible by the computer. The first is the mirror position and the second is a zoom factor which modifies the amplitude of the position of the parameter. Another advantage of the LRID is the use of a visible low power laser. Some of the commercial systems use a higher intensity invisible laser which causes safety concerns. By using a low power visible laser, not only can one see the beam and avoid direct eye contact, but also the lower intensity reduces the risk of damage to the eye, and no protective eyeware is required. Author

N92-28761# Textron Defense Systems, Everett, MA.
CO2 LASER FREQUENCY MULTIPLICATION
Jan. 1992 2 p
(Contract N00014-91-C-2279)
(AD-A245915) Avail: NTIS HC/MF A01

The month has been spent in a series of harmonic generation experiments at increasing peak intensity and fluence. Second harmonic beam quality has been measured. Using the oscillator alone, with grating selection of the 9.55 micrometer line, the pulse train consisted of a spike containing about 10 pulses followed by a tail containing about 40 pulses. Both the spike and the tail contained approximately equal energy, the combined total going as high as 180 mJ. The crystal was located near to the plane exit mirror of the oscillator, where the near-parallel beam has a Gaussian (amplitude) spot parameter of 0.46 cm. The on-axis fluence was 0.5 J/sq. cm. and the peak intensity in the 2 nsec optical pulses was approximately 20 NW/sq. cm. The pulses were separated by 40 nsec. Energy conversion efficiency of up to 31 percent was recorded, with 56 mJ of second harmonic (outside the crystal) for 181 mJ of incident 9.55 micrometer radiation. The second harmonic energy depended on the 1.5 power of the fundamental in the fundamental energy range 50 mJ to 180 mJ. Time-dependent analysis showed that the conversion efficiency was close to 50 percent in the spike but generally less than 10 percent in the 'tail' as expected from their intensity ratio (in the range 4:1 to 8:1). GRA

N92-28852# Sandia National Labs., Livermore, CA.
DEGENERATE FOUR-WAVE MIXING USING A TUNABLE EXCIMER LASER TO DETECT COMBUSTION GASES
G. Meijer (Katholieke Univ., Nijmegen, Netherlands), M. Versluis (Katholieke Univ., Nijmegen, Netherlands), and D. W. Chandler 1991 22 p Presented at the 24th International Symposium on Combustion, Sydney (Australia), 5-10 Jul. 1992
(Contract DE-AC04-76DR-00789)
(DE92-005327; SAND-91-8712; CONF-920707-4) Avail: NTIS HC/MF A03

A simple degenerate four wave mixing with forward geometry (DFWM-FG) experiment is used to monitor weak absorptions of stable molecules of combustion interest in the gas phase. DFWM-FG with a tunable ArF excimer laser enables us to detect H2 via the two-photon allowed E,F (sup 1)Sigma(sub g)(+) approaches X(sup 1)Sigma(sub g)(+) transition, CO via the spin-forbidden a(sup 3)Pi approaches X(sup 1)Sigma(+) transition and O2 via the B (sup 3)Sigma(sub u)(-) approaches X (sup 3)(Sigma)(sub g)(-) (Schumann-Runge band) transition. The tunable KrF excimer laser was used to monitor H2O via the C(sup 1)B(sub 1) approaches X(sup 1)A(sup 1) transition. In all cases the molecules are detected state-selectively. Success of these initial experiments indicates that this technique may have wide application in combustion system. DOE

N92-28862*# National Aeronautics and Space Administration. Langley Research Center, Hampton, VA.
PHASE STABILITY OF INJECTION-LOCKED BEAM OF SEMICONDUCTOR LASERS
Jin Hyuk Kwon (Yeungnam Univ., Gyongsan, Republic of Korea), Do Hoon Kim (Yeungnam Univ., Gyongsan, Republic of Korea), Gregory Schuster, and Ja H. Lee Washington Feb. 1992 9 p Transl. into ENGLISH from Journal of Optical Society of Korea (Republic of Korea), v. 1, no. 2, Sep. 1990 p 191-197
(RTOP 506-41-41-01)
(NASA-TT-10001; L-16967; NAS 1.77:10001) Avail: NTIS HC/MF A02

An experiment on the phase stability of an injection locked beam was done by using AlGaAs semiconductor lasers. The coherence of two beams from master and slave lasers was measured by interference between the beams in the Twymann-Green interferometer. The phase change of the output beam of the slave laser as a function of the driving current was measured in a Mach-Zehnder interferometer consisting of the master and slave lasers, and a value of 2.5 radians/mA was obtained. Author

N92-28903# Aerodyne Research, Inc., Billerica, MA.
TUNING AND AUTOMATIC PHASE ADJUSTMENT IN EXTERNAL CAVITY DIODE LASER BEAM COMBINERS Final Report
Roger S. Putnam Feb. 1992 32 p
(Contract N00014-91-C-0025)
(AD-A247421) Avail: NTIS HC/MF A03

We report quantitative measurements of self correcting phase shift produced in phaselocked beam combiners using multiple antireflection coated diode lasers in an external cavity. The major

result is the demonstration that the primary automatic phase adjustment is produced by optical frequency changes acting on the difference in pathlengths to the individual diode lasers, and that secondary phase changes are produced by fluctuations of the internal optical power acting on any imbalance among the various diode lasers' saturation behaviors. This suggests that the worst condition for a beam combining external cavity using automatic phaselocking is a near perfect pathlength match of the multiple laser arms. Further, the dynamic instability of a two laser system is measured and shown to be at its worst as the cavity length mismatch approaches zero. A second demonstration is controlled tuning over a frequency range corresponding to the inverse of the cavity length difference by piezo control of the phase error. Finally, the advantage for automatic phaselocking of using geometrically increasing feed lengths for the various diode lasers in the cavity is modeled and demonstrated. GRA

N92-28932# Potomac Photonics, Inc., Lanham, MD.
COMPACT, SELF-CONTAINED ArF LASERS Final Report, 1 Jun. - 30 Nov. 1991
C. P. Christensen 20 Jan. 1992 19 p
(Contract F49620-91-0040)
(AD-A247403; AFOSR-92-0017TR) Avail: NTIS HC/MF A03

Key development issues associated with compact argon fluoride waveguide lasers have been investigated in a Phase 1 SBIR study. Average laser power of 4 milliwatts and pulse energy of 16 microjoules have been produced. Feasibility of a compact gas supply suitable for steady-state operation of the laser at very low gas flow rates has been demonstrated. Formation of dioxygen fluoride radicals in the laser gas mixture following excitation has been observed, and optical absorption by these species has been found to limit laser energy at high pulse repetition rates. Oxygen sources in the laser gas supply have been investigated. GRA

N92-28933# Textron Defense Systems, Everett, MA.
CO2 LASER FREQUENCY MULTIPLICATION
Feb. 1992 2 p
(Contract N00014-91-C-2279)
(AD-A247542) Avail: NTIS HC/MF A01

This month has seen increased second harmonic conversion efficiency, with a highest total energy conversion of 70 percent. The increased sensitivity of phase matching at high conversions was observed. The thermal conductivity of Silver Gallium Selenium was measured. The second harmonic conversion efficiency has been modeled and an experimental threshold for optical coating surface damage has been obtained. All of the harmonic generation experiments were performed with the grating-tuned oscillator heavily modulated (depth 1.0) to yield 1.0 nanosec pulses at 9.55 microns (spaced by 40 nsec). The gain switched 'spike' which contained about 10 pulses was isolated by reduction of the intracavity iris to a diameter of 0.96 cm, considerably below the 1.4 cm diameter needed for transverse mode selection, introducing sufficient loss to reject the pulse 'tail' of 2 microsec duration. The short pulse train was expanded and then directed off a converging mirror into the 80 cm amplifier gain length. At the exit the 1/32 spot radius was 9.25 cm and the AgGaSe2 crystal was exposed to fluences up to 1.7 J/cm(exp 2). Harmonic conversion efficiency up to 60 percent was measured in one run which has been used for modeling purposes, in which the maximum harmonic energy was 80 mJ. The peak intensity in the highest pulse of the most energetic pulse train was 170 MW cm(exp -2). GRA

N92-28941*# Jet Propulsion Lab., California Inst. of Tech., Pasadena.
SCIENTIFIC APPLICATIONS OF FREQUENCY-STABILIZED LASER TECHNOLOGY IN SPACE
Bonny L. Schumaker 1 Dec. 1990 281 p
(Contract NAS7-918)
(NASA-CR-190449; NAS 1.26:190449; JPL-Publ-90-50) Avail: NTIS HC/MF A13

A synoptic investigation of the uses of frequency-stabilized lasers for scientific applications in space is presented. It begins by summarizing properties of lasers, characterizing their frequency stability, and describing limitations and techniques to achieve certain levels of frequency stability. Limits to precision set by laser frequency stability for various kinds of measurements are investigated and compared with other sources of error. These other sources include photon-counting statistics, scattered laser light, fluctuations in laser power, and intensity distribution across the beam, propagation effects, mechanical and thermal noise, and radiation pressure. Methods are explored to improve the sensitivity of laser-based interferometric and range-rate measurements. Several specific types of science experiments that rely on highly precise measurements made with lasers are analyzed, and anticipated errors and overall performance are discussed. Qualitative descriptions are given of a number of other possible science applications involving frequency-stabilized lasers and related laser technology in space. These applications will warrant more careful analysis as technology develops. Author

N92-29139*# Old Dominion Univ., Norfolk, VA. Dept. of Electrical and Computer Engineering.
USE OF LASER RANGE FINDERS AND RANGE IMAGE ANALYSIS IN AUTOMATED ASSEMBLY TASKS Final Report, 16 Aug. 1989 - 15 Aug. 1990
Nicolas Alvertos and Ivan DCunha Sep. 1990 123 p
(Contract NAS1-18584; RTOP 590-11-21-02)
(NASA-CR-186957; NAS 1.26:186957) Avail: NTIS HC/MF A06

A proposition to study the effect of filtering processes on range images and to evaluate the performance of two different laser range mappers is made. Median filtering was utilized to remove noise from the range images. First and second order derivatives are then utilized to locate the similarities and dissimilarities between the processed and the original images. Range depth information is converted into spatial coordinates, and a set of coefficients which describe 3-D objects is generated using the algorithm developed in the second phase of this research. Range images of spheres and cylinders are used for experimental purposes. An algorithm was developed to compare the performance of two different laser range mappers based upon the range depth information of surfaces generated by each of the mappers. Furthermore, an approach based on 2-D analytic geometry is also proposed which serves as a basis for the recognition of regular 3-D geometric objects. Author

N92-29160 Physics and Electronics Lab. TNO, The Hague (Netherlands).
PERFORMANCE OF THE MULTIFUNCTIONAL CW CO2-LASER RADAR AT THE TNO-FEL LABORATORY AND DURING THE BEST TWO FIELD TEST Final Report
H. Hebers Jun. 1991 47 p
(Contract A90KL621)
(FEL-91-A163; TD91-2230; ETN-92-91215) Copyright Avail: TNO Physics and Electronics Lab., P.O. Box 96864, 2509 JG The Hague, Netherlands

Measurements performed with the multifunctional CW CO2 (Continuous Wave carbon dioxide) laser radar system are reported. The BEST TWO (Battle field Emmissive Sources Test under European Theatre Weather and Obscurants) trial was held in France, at Camp de Mourmelon, Jul. 26 to Aug. 10 1990, to test battlefield effects on long range target acquisition by electrooptical systems. The results and experience gained from these experiments are described and recommendations for further improvement of the multifunctional laser radar setup are given. ESA

N92-29168# Los Alamos National Lab., NM.
THE LOS ALAMOS POP PROJECT: FEL OSCILLATOR EXPERIMENTS IN THE ULTRAVIOLET AND BEYOND
B. E. Newnam, R. W. Warren, J. C. Goldstein, M. J. Schmitt, S. C. Bender, B. E. Carlsten, D. W. Feldman, and P. G. OShea 1992 12 p Presented at the 13th International Free-Electron Laser (FEL) Conference, Santa Fe, NM, 25-30 Aug. 1991
(Contract W-7405-eng-36)
(DE92-011286; LA-UR-92-754; CONF-9108118-48) Avail: NTIS HC/MF A03

The Los Alamos POP Project will include a series of proof-of-principle FEL oscillator experiments in 1992 designed to extend FEL operation into the ultraviolet (UV) and vacuum ultraviolet (VUV). With beam energy extended to 50 MeV, enhanced beam brightness with a photoinjector, and appropriate UV and VUV resonator optics, the Los Alamos FEL oscillator should have sufficient single-pass gain (20-30 percent) to reach below 200 nm. The first goal will be lasing at 250 nm utilizing a permanent-magnet undulator with 5-mm period or alternatively on the third harmonic with a 1-cm period. To operate at VUV wavelengths of 200 and 150 nm (third harmonic), pulsed electromagnetic microwigglers with periods of 5.7- and 4.3 mm will be employed. DOE

N92-29223# Rochester Univ., NY. Dept. of Physics and Astronomy.
BIG SKY WORKSHOP ON SUPER-INTENSE LASER-ATOM PHYSICS Final Report, 1 May 1991 - 30 Apr. 1992
J. H. Eberly 20 Mar. 1992 73 p Workshop held in Big Sky, MT, 22-25 Jun. 1991
(Contract N00014-91-J-1668)
(AD-A248225) Avail: NTIS HC/MF A04

A Workshop was convened in order to examine and discuss current theoretical understanding of the interaction of very high-intensity short-pulse laser light with material systems, and to assess the possibility of experimental study of new theoretical predictions. In order to provide a specific focus, attention was restricted to new aspects of single-electron phenomena in strong and super-strong laser fields. GRA

N92-29226# Northeast Semiconductor, Inc., Ithaca, NY.
INNOVATIVE TECHNIQUES FOR THE PRODUCTION OF LOW COST 2D LASER DIODE ARRAYS Monthly Report No. 4, 1-31 Mar. 1992
31 Mar. 1992 9 p
(Contract N00014-91-C-0222)
(AD-A248247) Avail: NTIS HC/MF A02

The primary objective of this program is to develop a low cost, high yielding methodology for processing, packaging and characterization of molecular beam epitaxy (MBE) grown to dimensional high power laser diode lasers would reduce manufacturing cost from the current $10 to $20 per peak watt to below $3 per peak watt. Emphasis will be placed on innovative packaging techniques that will utilize recent advances in diamond heat sinking technology. GRA

37 MECHANICAL ENGINEERING

Includes auxiliary systems (nonpower); machine elements and processes; and mechanical equipment.

N92-28233# Japan Atomic Energy Research Inst., Tokyo.
A SURVEY REPORT FOR THE DESIGN OF BIPED LOCOMOTION ROBOT: THE WL-12 (WASEDA LEG-12)
Atsuo Takanishi, Ichiro Kato (Waseda Univ., Tokyo, Japan), and Etsuo Kume Nov. 1991 47 p In JAPANESE; ENGLISH summary
(DE92-782046; JAERI-M-91-197) Avail: NTIS HC/MF A03

A mechanical design study of biped locomotion robots is going on at JAERI within the scope of the Human Acts Simulation Program (HASP). The design study at JAERI is of an arbitrarily mobile robot for inspection of nuclear facilities. A survey has been performed for collecting useful information from already existing biped locomotion robots. This is a survey report of the biped locomotion robot: the WL-12 designed and developed at Waseda University. This report includes the mechanical model and control system designs. DOE

N92-28284# Ballistic Research Labs., Aberdeen Proving Ground, MD.
A SYSTEM STRUCTURE FOR PREDICTIVE RELATIONS IN PENETRATION MECHANICS Final Report, Aug. 1989 - Oct. 1991
Thomas A. Korjack Feb. 1992 155 p
(AD-A246453; BRL-TR-3317) Avail: NTIS HC/MF A08

The availability of a software system yielding quick numerical models to predict ballistic behavior is a requisite for any research laboratory engaged in material behavior. What is especially true about accessibility of rapid prototyping for terminal impaction is the enhancement of a system structure which will direct the specific material and impact situation towards a specific predictive model. This is of particular importance when the ranges of validity are at stake and the pertinent constraints associated with the impact are unknown. Hence, a compilation of semiempirical predictive penetration relations for various physical phenomena has been organized into a data structure for the purpose of developing a knowledge-based decision aided expert system to predict the terminal ballistic behavior of projectiles and targets. The ranges of validity and constraints of operation of each model were examined and cast into a decision tree structure to include target type, target material, projectile types, projectile materials, attack configuration, and performance or damage measures. This decision system implements many penetration relations, identifies formulas that match user-given conditions, and displays the predictive relation coincident with the match in addition to a numerical solution. The physical regimes under consideration encompass the hydrodynamic, transitional, and solid; the targets are either semi-infinite or plate, and the projectiles include kinetic and chemical energy. A preliminary databases has been constructed to allow further development of inductive and deductive reasoning techniques applied to ballistic situations involving terminal mechanics. GRA

N92-28293# Naval Postgraduate School, Monterey, CA.
WELD POOL FLOW VISUALIZATION STUDIES DURING GAS TUNGSTEN ARC WELDING OF STEEL AND ALUMINUM M.S. Thesis
Peter E. Schupp Mar. 1992 68 p
(AD-A249204) Avail: NTIS HC/MF A04

A flow visualization study of current distribution effects on weld pool stirring in GTA steel welds is presented using a pulsed ultraviolet laser vision system. Weld pool stirring is almost eliminated in HY-80 steel by the use of symmetric current flow path within the weld samples. Periodic radial surface pulses are observed at low currents in stationary welds while flows of turbulent nature are observed at higher currents. Autogenous welds on 17.75 cm by 28.0 cm by 1.27 cm thick 6061 aluminum plates are also studied to determine resulting surface flow characteristics and weld pool growth rates. Clockwise stirring in conjunction with a vertical undulation is noted in stationary welds. Solidified weld zone exhibits a profound crater that was not present in welds on HY-80 Steel. GRA

N92-28362*# Battelle Columbus Labs., OH.
REPLACEMENT BEARING FOR ROCKETDYNE SSME HPOTPs USING ALTERNATE SELF-LUBRICATING RETAINER MATERIALS Final Report
J. Gleeson, K. Dufrane, and J. Kannel 1 Apr. 1992 68 p
Original contains color illustrations
(Contract NAS8-36996)
(NASA-CR-184328; NAS 1.26:184328) Avail: NTIS HC/MF A04; 1 functional color page

Research was conducted to develop replacement bearings for the Rocketdyne Space Shuttle main engine (SSME) high pressure oxidizer turbopumps (HPOTPs). The replacement bearings consisted of standard balls and races with a special Battelle Self-Lubricating Insert Configuration (BASIC) retainer. The BASIC retainer consists of a phosphor bronze housing with inserts consisting of a polytetrafluoretheylene (PTFE) and bronze compound. The PTFE contacts the balls and the land guiding surface on the outer race. A PTFE transfer film is formed on balls

and races, which lubricates the critical interfaces. The BASIC retainer is a one-to-one replacement for the current Armalon retainer, but has superior lubricating properties and is stronger over the broad temperature range anticipated for the HPOTP bearings. As a part of the project 40 sets of balls and races (two sizes) and 52 BASIC retainers were shipped to NASA/MSFC.
Author

N92-28384# Naval Postgraduate School, Monterey, CA.
VISUALIZATION OF GAS TUNGSTEN ARC WELD POOLS M.S. Thesis
Daniel C. Espinosa Sep. 1991 83 p
(AD-A245926) Avail: NTIS HC/MF A05

Surface flow visualization of gas tungsten arc weld pools for HY-80 steel is presented using a pulsed laser light source and a conventional night vision image-intensifier tube equipped video camera. Visualization of the weld pool free surface is made possible by seeding a flow with alumina particles for both stationary and moving arc welds. These visualizations reveal several new features not incorporated in the existing models for stationary welds. A strong clockwise stirring is observed contrary to the axisymmetric computational models. Also, the pool surface shows a bulge near the center. Complex flow patterns are observed for moving arc welding. Interpretations of the observed flows based on the driving forces are provided. GRA

N92-28434*# National Aeronautics and Space Administration. Lewis Research Center, Cleveland, OH.
APPLICATION OF FACE-GEAR DRIVES IN HELICOPTER TRANSMISSIONS
F. L. Litvin (Illinois Univ., Chicago.), J.-C. Wang (Illinois Univ., Chicago.), R. B. Bossler, Jr. (Lucas Western, Inc., City of Industry, CA.), Y.-J. D. Chen (McDonnell-Douglas Helicopter Co., Mesa, AZ.), G. Heath (McDonnell-Douglas Helicopter Co., Mesa, AZ.), and D. G. Lewicki 1992 10 p Proposed for presentation at the Sixth International Power Transmission and Gearing Conference, Scottsdale, AZ, 13-16 Sep. 1992; sponsored by ASME
(RTOP 505-63-36; DA Proj. 1L1-62211-A-47-A)
(NASA-TM-105655; E-7019; NAS 1.15:105655;
AVSCOM-TR-91-C-036) Avail: NTIS HC/MF A02

The use of face gears in helicopter transmissions was explored. A light-weight, split torque transmission design utilizing face gears was described. Face-gear design and geometry were investigated. Topics included tooth generation, limiting inner and outer radii, tooth contact analysis, contact ratio, gear eccentricity, and structural stiffness. Design charts were developed to determine minimum and maximum face-gear inner and outer radii. Analytical study of transmission error showed face-gear drives were relatively insensitive to gear misalignment, but tooth contact was affected by misalignment. A method of localizing bearing contact to compensate for misalignment was explored. The proper choice of shaft support stiffness enabled good load sharing in the split torque transmission design. Face-gear experimental studies were also included and the feasibility of face gears in high-speed, high-load applications such as helicopter transmissions was demonstrated.
Author

N92-28476*# National Aeronautics and Space Administration. Lewis Research Center, Cleveland, OH.
OPTIMUM DESIGN OF A GEARBOX FOR LOW VIBRATION
Katsumi Inoue, Dennis P. Townsend, and John J. Coy 1992 10 p Proposed for presentation at the Sixth International Power Transmission and Gearing Conference, Scottsdale, AZ, 13-16 Sep. 1992; sponsored by ASME
(RTOP 505-63-36; DA Proj. 1L1-62211-A-47-A)
(NASA-TM-105653; E-6622; NAS 1.15:105653;
AVSCOM-TR-91-C-027) Avail: NTIS HC/MF A02

A computer program was developed for designing a low vibration gearbox. The code is based on a finite element shell analysis, a modal analysis, and a structural optimization method. In the finite element analysis, a triangular shell element with 18 degrees-of-freedom is used. In the optimization method, the overall vibration energy of the gearbox is used as the objective function and is minimized at the exciting frequency by varying the finite element thickness. Modal analysis is used to derive the sensitivity of the vibration energy with respect to the design variable. The sensitivity is representative of both eigenvalues and eigenvectors. The optimum value is computed by the gradient projection method and a unidimensional search procedure under the constraint condition of constant weight. The computer code is applied to a design problem derived from an experimental gearbox in use at the NASA Lewis Research Center. The top plate and two side plates of the gearbox are redesigned and the contribution of each surface to the total vibration is determined. Results show that optimization of the top plate alone is effective in reducing total gearbox vibration.
Author

N92-28645# National Aerospace Lab., Amsterdam (Netherlands). Informatics Div.
DYNAMICS MOTION SIMULATION OF THE HERMES ROBOT ARM SUBJECTED TO CONSTRAINTS
M. J. H. Couwenberg and A. A. tenDam 3 Aug. 1990 52 p
(Contract NIVR-02506-N)
(NLR-TP-90282-U; ETN-92-91444) Avail: NTIS HC/MF A04

The formulation and discretization of the dynamics equations is adopted for constrained motion, based on an elementary collision model: the manipulator end effector is confined to a rigid, frictionless, and flat surface and the motion constraint is then specified by an algebraic equality; the manipulator end effector comes into contact with a rigid, frictionless, and flat surface; the motion constraint is now specified by an algebraic inequality; the collision between the end effector and the constrained surface is assumed inelastic and frictionless. Simulation studies are performed with the aid of the Machine Independent Model Oriented Simulation Environment (MIMOSE). As basis for the simulation model, an existing model of the Hermes Robot Arm (HERA), as developed for the HERA Simulation Facility Pilot (HSF-P), is used. From this study it can be concluded that the applied method to treat equality constraints shows good results in relation with the simulation of constrained HERA motion.
ESA

N92-28646# National Aerospace Lab., Amsterdam (Netherlands). Flight Div.
LINEAR RECURSIVE FORMULATION OF FLEXIBLE MULTI-BODY SPACE SYSTEM DYNAMICS
P. T. L. M. vanWoerkom 16 Jul. 1990 114 p
(Contract NIVR-02506-N)
(NLR-TP-90284-U; ETN-92-91445) Avail: NTIS HC/MF A06

The development of a recursive formulation of the dynamics of flexible spacecraft robot manipulator systems, suitable for efficient numerical simulation, is addressed. The rather well established nonrecursive and recursive multibody system dynamics formulations require a computational effort in numerical simulations, proportional to the third power of the number of system bodies (n, and n cubed). However, recent developments in robotic manipulator systems show that it is possible to obtain a recursive multibody system dynamics formulation which requires a computational effort in numerical simulations, only linearly proportional to n itself (order n). This is of special interest for systems with structural flexibility, where n is large. Other advantages of the recursive algorithm are: easy derivation, reduced risk of introduction of algorithmic errors, easy coding, and reuse of software for a large class of systems. The system considered, displays chain topology. Any of its constituent bodies may be rigid or flexible. The base body may move in space (spacecraft) or display prescribed motion (e.g., fixed base). The point of departure is the application of d'Alembert's principle of virtual work to a single body. The development of a recursive algorithm of order n for rigid bodies, described by Brandl et al, is generalized to account for flexibility. An extensive comparison with literature was carried out for the purpose of validation and evaluation.
ESA

N92-28705# National Aerospace Lab., Amsterdam (Netherlands). Space Div.
MODELLING AND REAL-TIME SIMULATION OF THE HERMES ROBOT ARM HERA
P. Dieleman, M. J. H. Couwenberg, and F. vanderLaan (Fokker Space and Systems, Amsterdam, Netherlands) 13 Aug. 1990 9 p Presented at the International Symposium of Artificial Intelligence, Robotics and Automation in Space, Kobe, Japan, 18-20 Nov. 1990 Previously announced in IAA as A92-23656 Sponsored in part by Netherlands Agency for Aerospace Programs
(Contract EAS-7222/87/NL)
(NLR-TP-90262-U; ETN-92-91442) Avail: NTIS HC/MF A02

The Hermes Robot Arm (HERA) is a sophisticated and highly automated space manipulator system developed to be launched with and operated from the European Spaceplane Hermes. During operational use HERA will be located at the Columbus Free Flying Laboratory which is part of the European In Orbit Infrastructure. The HERA Simulation Facility Pilot (HSF-P) is the first dedicated simulation facility built for research and development needed for HERA. The main objectives of the HSF-P are evaluation of teleoperator station requirements, evaluation of operator on the loop support software, experimentation on manipulator operations feasibility and visualization of manipulator opeations both in real time and in non real time. Simulation models of flight elements used for HSF-P are described with main attention to the models used for simulation of HERA. A description of the HSF-P architecture and its realization is given. ESA

N92-28727* National Aeronautics and Space Administration. Lyndon B. Johnson Space Center, Houston, TX.
PAYLOAD RETENTION DEVICE Patent
Leo G. Monford, Jr., inventor (to NASA) 30 Jun. 1992 19 p Filed 26 Dec. 1991
(NASA-Case-MSC-21906-1; US-Patent-5,125,601;
US-Patent-Appl-SN-813558; US-Patent-Class-244-161;
US-Patent-Class-294-65.5; US-Patent-Class-294-86.4;
US-Patent-Class-901-30; US-Patent-Class-901-46;
Int-Patent-Class-B64G-1/62) Avail: US Patent and Trademark Office

A payload retention device for grappling and retaining a payload in docked position on a supporting structure in the cargo bay of a space vehicle is presented. The device comprises a two-fault tolerant electromagnetic grappling system comprising electromagnets for attracting and grappling a grapple strike plate affixed to the payload when in proximity thereto and an electromechanical latching assembly comprising a pair of independent latching subassemblies. Each subassembly comprises a set of latching pawls which are driven into latching and unlatching positions relative to a grappled payload by a pair of gearmotors, each equipped with a ratchet clutch drive mechanism which is two-fault tolerant with respect to latching such that only one gearmotor of the four needs to be operational to effect a latch of the payload but is single fault tolerant with respect to release of a latched payload. Sensors are included for automatically sensing the magnetic grappling of a payload and for automatically de-energizing the gearmotors of the latching subassemblies when a latch condition is achieved.
Official Gazette of the U.S. Patent and Trademark Office

N92-28749 Department of the Navy, Washington, DC.
TRANSIENT IMPELLER TEST FACILITY Patent
Paul J. Lefebvre, inventor (to Navy) 7 Jan. 1992 4 p Filed 24 Dec. 1990
(AD-D015249; US-Patent-5,078,009; US-Patent-Appl-SN-632709;
US-Patent-Class-73-168) Avail: US Patent and Trademark Office

A system is described for testing a pump or a turbine impeller under transient operating conditions in a fluid flow. The system provides simultaneously, as a function of time, user defined impeller speeds, fluid flow rate, and rise in fluid pressure so as to simulate real conditions. This information can be used to analyze the performance of existing impellers or for designating new impellers. There are very few existing facilities which can operate a pump or turbine impeller under general and user defined transient conditions throughout the transient. Old facilities operated under either steady-state conditions or specific transient conditions with no provision for defining the desired conditions throughout the transient. Steady-state operations is defined here as when the impeller rotates at constant speeds with constant flow rate and pressure rise. Transient operation is defined as when the impeller undergoes acceleration or deceleration (such as at pump start-up or shut down) and the impeller speed, flow rate, and pressure rise all change with time. GRA

N92-28754* National Aeronautics and Space Administration. Goddard Space Flight Center, Greenbelt, MD.
DEVICE FOR APPLYING CONSTANT PRESSURE TO A SURFACE Patent
Eve M. Abrams, inventor (to NASA) 3 Dec. 1991 5 p Filed 31 May 1990 Supersedes N91-13734 (29 - 5, p 672)
(NASA-Case-GSC-13230-1; US-Patent-5,068,951;
US-Patent-Appl-SN-531374; US-Patent-Class-29-110.5;
US-Patent-Class-29-123; US-Patent-Class-29-132;
US-Patent-Class-15-230.11; Int-Patent-Class-B05C-17/02) Avail: US Patent and Trademark Office

A device for applying constant pressure to a surface is disclosed. The device includes a cylinder having a longitudinal axis greater than the diameter of the cylinder. A first wheel and a second wheel are coupled to each end, respectively, of the cylinder. The wheels have a diameter substantially greater than the diameter of the cylinder. An elastomeric covering surrounds the cylinder. The elastomeric covering has an outer diameter substantially greater than the diameter of the wheels. A handle is coupled to the wheels for rolling and applying pressure to the elastomeric covering.
Official Gazette of the U.S. Patent and Trademark Office

N92-28815# Argonne National Lab., IL. Energy Systems Div.
PRESENT STATUS OF COMPUTATIONAL TOOLS FOR MAGLEV DEVELOPMENT
Z. Wang, S. S. Chen, and D. M. Rote Oct. 1991 49 p
(Contract W-31-109-eng-38)
(DE92-013252; ANL/ESD/TM-24) Avail: NTIS HC/MF A03

High-speed vehicles that employ magnetic levitation (maglev) have received great attention worldwide as a means of relieving both highway and air-traffic congestion. At this time, Japan and Germany are leading the development of maglev. After fifteen years of inactivity that is attributed to technical policy decisions, the Federal government of the United States has reconsidered the possibility of using maglev in the United States. The National Maglev Initiative (NMI) was established in May 1990 to assess the potential of maglev in the United States. One of the tasks of the NMI, which is also the objective of this report, is to determine the status of existing computer software that can be applied to maglev-related problems. The computational problems involved in maglev assessment, research, and development can be classified into two categories: electromagnetic and mechanical. Because most maglev problems are complicated and difficult to solve analytically, proper numerical methods are needed to find solutions. To determine the status of maglev-related software, developers and users of computer codes were surveyed. The results of the survey are described in this report. DOE

N92-28924# Army Belvoir Research and Development Center, Fort Belvoir, VA.
FLOW RATE TESTING OF VALVES USED WITH THE 500 GALLON COLLAPSIBLE DRUM Final Report
William D. Perdue Apr. 1992 66 p
(AD-A250567; BRDEC-2525) Avail: NTIS HC/MF A04

This report covers the test and evaluation of four couplings/valves used with the 500-gallon collapsible drum: the existing poppet valve, a new redesigned poppet valve, a Carter refuel/defuel valve that works in conjunction with the single point refueling nozzle, and a Kamvalok dry-break coupling valve. The purpose of this testing was to determine maximum flow capability of each valve design and identify any new characteristics that may impact performance of the FARE system. GRA

N92-28925*# National Aeronautics and Space Administration. Lyndon B. Johnson Space Center, Houston, TX.
EVALUATION OF WHIPPLE BUMPER SHIELDS AT 7 AND 10 km/s
J. A. Ang (Sandia National Labs., Albuquerque, NM.), L. C. Chhabildas (Sandia National Labs., Albuquerque, NM.), B. G. Cour-Palais (McDonnell-Douglas Space Systems Co., Houston, TX.), E. L. Christiansen, and J. L. Crews 1991 8 p Presented at the American Institute of Astronautics and Aeronautics (AIAA) Space Programs and Technologies Conference, Huntsville, AL, 24-27 Mar. 1992
(Contract DE-AC04-76DP-00789)
(NASA-TM-107958; NAS 1.15:107958; DE92-010663;
SAND-91-1717C; CONF-920373-3) Avail: NTIS HC/MF A02

A series of experiments has been performed on the Sandia Hypervelocity Launcher to determine the performance limits of conventional Whipple shields against representative 0.8 g aluminum orbital debris plate-like fragments with velocities of 7 and 10 km/s. Supporting diagnostics include flash x-rays, high speed photography, and transient digitizers for timing correlation. Two Whipple shield designs were tested with either a 0.030 cm or a 0.127 cm thick front sheet and a 0.407 cm thick backsheet separated by 30.5 cm. These two designs bracket the ballistic penetration limit curve for protection against these debris simulants for 7 km/s impacts. DOE

N92-29092* National Aeronautics and Space Administration. Lewis Research Center, Cleveland, OH.
REMOVABLE HAND HOLD Patent
Robert D. Corrigan, inventor (to NASA) and Robert L. Hauer, inventor (to NASA) 30 Jun. 1992 9 p Filed 15 Apr. 1991 Supersedes N91-26543 (29 - 18, p 2995)
(NASA-Case-LEW-15196-1; US-Patent-5,126,131;
US-Patent-Appl-SN-687606; US-Patent-Class-16-114R;
US-Patent-Class-248-222.1; US-Patent-Class-248-251;
US-Patent-Class-256-59; US-Patent-Class-16-111R;
Int-Patent-Class-A47H-1/144) Avail: US Patent and Trademark Office

A hand hold utilizes joining means which comprises two different mounting brackets that are permanently fastened to a supporting structure. An alignment/capture bracket is disposed at one end of the hand rail or hand hold which mates with one of the mounting brackets. A securing bracket is disposed at the opposite end of the hand rail/hand hold which connects with the other mounting bracket by means of a locking device. The alignment/capture bracket has a central tapered tongue with two matching slots disposed on each side.
Official Gazette of the U.S. Patent and Trademark Office

N92-29099* National Aeronautics and Space Administration. Goddard Space Flight Center, Greenbelt, MD.
SUPERCONDUCTING BEARINGS WITH LEVITATION CONTROL CONFIGURATIONS Patent
Yury Flom, inventor (to NASA) and James D. Royston, inventor (to NASA) 26 May 1992 13 p Filed 17 Apr. 1991 Supersedes N91-28578 (29 - 20, p 3354)
(NASA-Case-GSC-13346-1; US-Patent-5,117,139;
US-Patent-Appl-SN-691609; US-Patent-Class-310-90.5;
US-Patent-Class-505-876; Int-Patent-Class-H02K-1/14;
Int-Patent-Class-F16C-32/04) Avail: US Patent and Trademark Office

An improved superconducting bearing is presented. Rotor is confined within two superconducting circular bearing structures, each of which has a number of embedded heating elements, and will levitate rotor which has embedded magnets in its end. Heating elements are connected to a feedback control unit, as are rotor position sensors. The temperature profiles of each circular bearing structure is then adjusted according to the information on rotor position provided to control unit by position sensors. Novelty is believed to reside in providing a superconducting circular bearing structure allowing for a control of the levitating forces.
Official Gazette of the U.S. Patent and Trademark Office

N92-29120* National Aeronautics and Space Administration. Goddard Space Flight Center, Greenbelt, MD.
COUPLING DEVICE WITH IMPROVED THERMAL INTERFACE Patent
Malcolm Bruce Milam, inventor (to NASA) 28 Apr. 1992 11 p Filed 13 Jun. 1991 Supersedes N91-28582 (29 - 20, p 3355)
(NASA-Case-GSC-13251-1; US-Patent-5,108,214;
US-Patent-Appl-SN-714814; US-Patent-Class-403-28;
US-Patent-Class-403-404; US-Patent-Class-285-381;
US-Patent-Class-411-909; US-Patent-Class-292-DIG.66;
Int-Patent-Class-F16C-9/00) Avail: US Patent and Trademark Office

The primary object of the present invention is to provide a simple, reliable, and lightweight coupling that will also have an efficient thermal interface. A further object of the invention is to provide a coupling that is capable of blind mating with little or no insertion forces. Another object of the invention is to provide a coupling that acts as a thermal regulator to maintain a constant temperature on one side of the coupling. Another object of the invention is to increase the available surface area of a coupling thus providing a larger area for the conduction of heat across the thermal interface. Another object of the invention is to provide a fluidic coupling that has no fluid passing across the interface, thus reducing the likelihood of leaks and contamination. The foregoing objects are achieved by utilizing, as in the prior art, a hot area (at an elevated temperature as compared to a cold area) with a need to remove excess heat from the hot area to a cold area. In this device, the thermal interface will occur not on a planar horizontal surface, but along a non-planar vertical surface, which will reduce the reaction forces and increase the thermal conductivity of the device. One non-planar surface is a surface on a cold pin extending from the cold area and the other non-planar surface is a surface on a hot pin extending from the hot area. The cold pin is fixed and does not move while the hot pin is a flexible member and its movement towards the cold pin will bring the two non-planar surfaces together forming the thermal interface. The actuating member for the device is a shape-memory actuation wire which is attached through an aperture to the hot pin and through another aperture to an actuation wire retainer. By properly programming the actuation wire, heat from the hot area will cause the actuation wire to bend the hot wire. Heat from the hot area will cause the actuation wire to bend the hot pin towards the cold pin forming the coupling and the desired thermal interface. The shape-memory actuation wire is made of a shape-memory-effect alloy such as Nitinol.
Official Gazette of the U.S. Patent and Trademark Office

N92-29134*# Nichols Research Corp., Huntsville, AL.
DEVELOPMENT OF AN AUTOMATED WIRE DELIVERY SYSTEM FOR ROBOTIC WELDING APPLICATIONS Final Report, 18 Apr. 1990 - 18 Jul. 1992
Timothy B. Morris 9 Jul. 1992 37 p
(Contract NAS8-38477)
(NASA-CR-190487; NAS 1.26:190487; NRC-TR-92-143) Avail: NTIS HC/MF A03

Our Phase 1 study showed new techniques and procedures are required for maintaining the delivery of filler wire into the weld pool for robotic variable polarity plasma arc welding (VPPAW) and gas tungsten arc (GTA) welding applications. Toward this end, the development and implementation of an autonomous wire delivery system appears very feasible utilizing existing proven technologies. In our Phase 1 research effort, we investigated the requirements necessary of a wire delivery system to assure a quality weldment. We also evaluated various sensing technologies for their ability to provide information related to delivery of the wire into the weld pool. Finally, we described the types of software necessary for the automatic wire delivery system. Several approaches for automating the wire delivery system have been suggested, and we recommend the building of a prototype system in our Phase 2 effort as a logical step in the application of this technology to robotic GTA and VPPA welding. Such a prototype would contain the necessary hardware components, sensors and control software for evaluating the performance of the system as

applied to the berthing port, main engine and external fuel tank. This tool would be used to demonstrate the worth and plausibility of automating the wire delivery system for each of these applications. Author

N92-29136*# National Aeronautics and Space Administration. Lewis Research Center, Cleveland, OH.
DYNAMICS OF A SPLIT TORQUE HELICOPTER TRANSMISSION
Majid Rashidi (Cleveland State Univ., OH.) and Timothy Krantz (Army Aviation Systems Command, Cleveland, OH.) 1992 14 p Prepared for presentation of the 6th International Power Transmission and Gearing Conference, Scottsdale, AZ, 13-16 Sep. 1992; sponsored in part by ASME
(DA Proj. 1L1-62211-A-47-A; RTOP 505-63-36)
(NASA-TM-105681; E-7060; AVSCOM-TR-91-C-043; NAS 1.15:105681) Avail: NTIS HC/MF A03

A high reduction ratio split torque gear train has been proposed as an alternative to a planetary configuration for the final stage of a helicopter transmission. A split torque design allows a high ratio of power-to-weight for the transmission. The design studied in this work includes a pivoting beam that acts to balance thrust loads produced by the helical gear meshes in each of two parallel power paths. When the thrust loads are balanced, the torque is split evenly. A mathematical model was developed to study the dynamics of the system. The effects of time varying gear mesh stiffness, static transmission errors, and flexible bearing supports are included in the model. The model was demonstrated with a test case. Results show that although the gearbox has a symmetric configuration, the simulated dynamic behavior of the first and second compound gears are not the same. Also, results show that shaft location and mesh stiffness tuning are significant design parameters that influence the motions of the system. Author

N92-29138* National Aeronautics and Space Administration. Goddard Space Flight Center, Greenbelt, MD.
ROLLING FRICTION ROBOT FINGERS Patent
John M. Vranish, inventor (to NASA) 9 Jun. 1992 23 p Filed 17 Dec. 1990 Supersedes N91-17401 (29 - 9, p 1347)
(NASA-Case-GSC-13261-1; US-Patent-5,120,101;
US-Patent-Appl-SN-628529; US-Patent-Class-294-119.1;
US-Patent-Class-294-902; US-Patent-Class-901-39;
Int-Patent-Class-B66C-1/62) Avail: US Patent and Trademark Office

A low friction, object guidance, and gripping finger device for a robotic end effector on a robotic arm is disclosed, having a pair of robotic fingers each having a finger shaft slideably located on a gripper housing attached to the end effector. Each of the robotic fingers has a roller housing attached to the finger shaft. The roller housing has a ball bearing mounted centering roller located at the center, and a pair of ball bearing mounted clamping rollers located on either side of the centering roller. The object has a recess to engage the centering roller and a number of seating ramps for engaging the clamping rollers. The centering roller acts to position and hold the object symmetrically about the centering roller with respect to the X axis and the clamping rollers act to position and hold the object with respect to the Y and Z axis.
Official Gazette of the U.S. Patent and Trademark Office

N92-29140* National Aeronautics and Space Administration. Goddard Space Flight Center, Greenbelt, MD.
CONNECTION SPACE REDUCTION MECHANISM Patent
Malcolm Bruce Milam, inventor (to NASA) 12 May 1992 10 p Filed 31 Dec. 1990 Supersedes N91-21525 (29 - 13, p 2093)
(NASA-Case-GSC-13220-1; US-Patent-5,112,154;
US-Patent-Appl-SN-636532; US-Patent-Class-403-13;
US-Patent-Class-403-24; Int-Patent-Class-B25G-3/00) Avail: US Patent and Trademark Office

A connector assembly comprised of two halves, each respectively including a shell type connector subassembly, one being an active half and the other being a passive half is described. The active half includes an alignment cusp that causes a coupling motion in response to coming in contact with the outer portion of the other half, which causes the respective connectors within the two subassemblies to move toward each other into coupling relationship at twice the rate at which the two subassemblies come together. Both halves are adapted to rotate about and translate along respective mutually orthogonal axes to facilitate an interconnection.
Official Gazette of the U.S. Patent and Trademark Office

N92-29150* National Aeronautics and Space Administration. Lyndon B. Johnson Space Center, Houston, TX.
QUICK APPLICATION/RELEASE NUT WITH ENGAGEMENT INDICATOR Patent
Jay M. Wright, inventor (to NASA) 2 Jun. 1992 10 p Filed 13 Sep. 1991 Supersedes N92-11359 (30 - 2, p 244)
(NASA-Case-MSC-21799-1; US-Patent-5,118,237;
US-Patent-Appl-SN-759367; US-Patent-Class-411-433;
US-Patent-Class-411-14; US-Patent-Class-411-267;
Int-Patent-Class-F16B-37/08) Avail: US Patent and Trademark Office

A composite nut is shown which permits a fastener to be inserted or removed from either side with an indicator of fastener engagement. The nut has a plurality of segments, preferably at least three segments, which are internally threaded, spring loaded apart by an internal spring, and has detents on opposite sides which force the nut segments into operative engagements with a threaded member when pushed in and release the segments for quick insertion or removal of the nut when moved out. When the nut is installed, end pressure on one of the detents presses the nut segments into operative engagement with a threaded member where continued rotation locks the structure together with the detents depressed to indicate positive locking engagement of the nut. On removal, counterclockwise rotation of the nut relieves the endwise pressure on the detents, permitting internal springs to force the detents outward and allowing the nut segments to move outward and separate to permit quick removal of the fastener.
Official Gazette of the U.S. Patent and Trademark Office

N92-29151* National Aeronautics and Space Administration. Goddard Space Flight Center, Greenbelt, MD.
CRYOGENIC SHUTTER Patent
Richard D. Barney, inventor (to NASA) and Thomas J. Magner, inventor (to NASA) 7 Jul. 1992 9 p Filed 15 Nov. 1990 Division of US-Patent-Appl-SN-331119, filed 31 Mar. 1989
(NASA-Case-GSC-13189-2; US-Patent-5,128,796;
US-Patent-Appl-SN-613188; US-Patent-Appl-SN-331119;
US-Patent-Class-359-236; US-Patent-Class-359-230;
Int-Patent-Class-G02B-26/02) Avail: US Patent and Trademark Office

A magnetically operated shutter mechanism is provided that will function in cryogenic or cryogenic zero gravity environments to selectively block radiation such as light from passing through a window to a target object such as a mirror or detector located inside a cryogenic container such as a dewar. The mechanism includes a shutter paddle blade that is moved by an electromagnetically actuated torquing device between an open position where the target object is exposed to ambient radiation or light and a closed position where the shutter paddle blade shields the ambient radiation or light from the target object. The purpose of the shuttering device is to prevent the mirror or other target object from being directly exposed to radiation passing through the window located on the side wall of the dewar, thereby decreasing or eliminating any temperature gradient that would occur within the target object due to exposure to the radiation. A special nylon bearing system is utilized to prevent the device from binding during operation and the paddle blade is also thermally connected to a reservoir containing cryogen to further reduce the internal temperature. Author

N92-29217# Universiteit Twente, Enschede (Netherlands). Faculteit der Werktuigbouwkunde.
THE 1991 RESEARCH PROGRAM (OF THE FACULTY OF MECHANICAL ENGINEERING) Annual Report, 1991

[ONDERZOEK-PROGRAMMA 1991]
May 1991 88 p In DUTCH
(ETN-92-91353) Avail: NTIS HC/MF A05

The main research activities and programs are overviewed. The following domains are covered: production techniques, production organization, transportation and storage, mechanical engineering automation, design and construction, ergonomics, design in plastics, thermal mechanics, heat transfer and fluid mechanics, biomedical mechanical engineering, materials science, and technical mechanics and tribology. ESA

N92-28736*# North Carolina State Univ., Raleigh. Dept. of Mechanical and Aerospace Engineering.
INITIAL INVESTIGATIONS OF AN ADAPTIVE DISCRETE-TIME CONTROLLER FOR NONLINEAR TIME-VARYING ROBOTIC MODELS
S. S. Giang and Gordon K. F. Lee *In* NASA. Langley Research Center, Ongoing Progress in Spacecraft Controls Jul. 1992 p 77-106 (For primary document see N92-28730 19-18)
Avail: NTIS HC/MF A07

38 QUALITY ASSURANCE AND RELIABILITY

Includes product sampling procedures and techniques; and quality control.

N92-28425# Army Lab. Command, Watertown, MA. Material Technology Lab.
A SENSITIVITY ANALYSIS ON COMPONENT RELIABILITY FROM FATIGUE LIFE COMPUTATIONS Final Report
Donald M. Neal, William T. Matthews, Mark G. Vangel, and Trevor Rudalevige Feb. 1992 23 p
(AD-A247430; MTL-TR-92-5) Avail: NTIS HC/MF A03

Some uncertainties in determining high component reliability at a specified lifetime from a case study involving the fatigue life of a helicopter component are identified. Reliabilities are computed from results of a simulation process involving an assumed variability (standard deviation) of the load and strength in determining fatigue life. The uncertainties in the high reliability computation are then examined by introducing small changes in the variability for the given load and strength values in the study. Results showed that for a given component lifetime, a small increase in variability of load or strength produced large differences in the component reliability estimates. Among the factors involved in computing fatigue lifetimes, the component reliability estimates were found to be most sensitive to variability in loading. Component fatigue life probability density functions were obtained from the simulation process for various levels of variability. The range of life estimates were very large for relatively small variability in load and strength. GRA

N92-28726*# Illinois Univ., Urbana-Champaign. Coordinated Science Lab.
DEPEND: A SIMULATION-BASED ENVIRONMENT FOR SYSTEM LEVEL DEPENDABILITY ANALYSIS
Kumar Goswami and Ravishankar K. Iyer 26 Jun. 1992 44 p
(Grant NAG1-613)
(NASA-CR-189752; NAS 1.26:189752; UILU-ENG-92-2217; CRHC-92-11) Avail: NTIS HC/MF A03

The design and evaluation of highly reliable computer systems is a complex issue. Designers mostly develop such systems based on prior knowledge and experience and occasionally from analytical evaluations of simplified designs. A simulation-based environment called DEPEND which is especially geared for the design and evaluation of fault-tolerant architectures is presented. DEPEND is unique in that it exploits the properties of object-oriented programming to provide a flexible framework with which a user can rapidly model and evaluate various fault-tolerant systems. The key features of the DEPEND environment are described, and its capabilities are illustrated with a detailed analysis of a real design. In particular, DEPEND is used to simulate the Unix based Tandem Integrity fault-tolerance and evaluate how well it handles near-coincident errors caused by correlated and latent faults. Issues such as memory scrubbing, re-integration policies, and workload dependent repair times which affect how the system handles near-coincident errors are also evaluated. Issues such as the method used by DEPEND to simulate error latency and the time acceleration technique that provides enormous simulation speed up are also discussed. Unlike any other simulation-based dependability studies, the use of these approaches and the accuracy of the simulation model are validated by comparing the results of the simulations, with measurements obtained from fault injection experiments conducted on a production Tandem Integrity machine. Author

N92-28851# Wayne State Univ., Detroit, MI. Inst. for Manufacturing Research.
THERMAL WAVE IMAGING AND CHARACTERIZATION OF SOLIDS Final Report, 15 Jul. 1988 - 31 Dec. 1991
R. L. Thomas, P. K. Kuo, and L. D. Favro 31 Dec. 1991 33 p
(Contract DAAL03-88-K-0089)
(AD-A249297; ARO-24981.33-MS) Avail: NTIS HC/MF A03

Accomplishments are reported for a program of research to develop several thermal wave techniques and to explore applications of those techniques to the imaging of sub-surface features and the characterization of a variety of materials. Both experimental and theoretical studies were carried out, and the experiments included both CW and pulsed thermal wave excitation. The mirage effect (optical probe beam) technique was used to determine thermal diffusivities in a variety of materials including diamond and polymers. The results of our measurements on single crystal diamond showed a nearly 50 percent increase in thermal diffusivity at room temperature on (IR) thermal wave imaging for nondestructive evaluation (NDE), including synchronous imaging in the time domain. A technique for thermal wave tomography was developed, the inverse scattering problem was solved, and an algorithm developed to implement the solution on digitally acquired images. A U.S. Patent was issued to Wayne State University on the lock-in video technique. Instrumental development was carried out, culminating in a Beta-site development at an aerospace company and negotiations with several companies towards commercialization of the instrumentation for technology transfer. GRA

N92-29112# Polytechnic Univ., Farmingdale, NY. Research Inst.
IN-SITU FAULT DETECTION BY THE HYBRID RAY-MODE METHOD Final Technical Report, 1 Mar. 1990 - 30 Sep. 1991
Leopold B. Felsen 20 Apr. 1992 104 p
(Grant AF-AFOSR-0088-90)
(AD-A250213; POLY-WRI-1589-92; AFOSR-92-0349TR) Avail: NTIS HC/MF A06

The objective of this research effort has been to develop algorithms for in-situ location and identification, by ultrasound, of flaws in plates or laminated layered elastic materials. Achieving this objective requires detailed knowledge of the excitation propagation, scattering and detection of high frequency sound waves in unflawed and flawed environments. Based on an understanding of these fundamental wave phenomena, one may then attempt to construct analytical models with accompanying algorithms, so as to parametrize the NDE problem in terms of good observables. During this final period, the research program under the predecessor Grant No. AFOSR-86-0318 was phased out. Major effort was expanded on completing research items initiated under the predecessor grant, and on preparing, final manuscripts for publication. For the description of these previous studies, the readers should refer to the Final Report on the predecessor grant. A new phase was initiated during the current period, namely, a systematic study of nonspecular reflection of ultrasonic acoustic beams impinging from a fluid onto planar and cylindrical layered elastic materials. The nonspecular effect occurs when the incident beam is phase matched to a leaky mode in the structure and thereby causes the reflected field to be dominated

by strong interaction between the specularly reflected beam profile and the leaky mode. GRA

N92-29154* National Aeronautics and Space Administration. Goddard Space Flight Center, Greenbelt, MD.
METHOD FOR ADVANCED MATERIAL CHARACTERIZATION BY LASER INDUCED EDDY CURRENT IMAGING Patent
Engmin J. Chern, inventor (to NASA) 23 Jun. 1992 6 p Filed 5 Sep. 1991 Supersedes N92-23376 (29 - 14, p 2386)
(NASA-Case-GSC-13386-1; US-Patent-5,124,640; US-Patent-Appl-SN-758977; US-Patent-Class-324-224; US-Patent-Class-324-226; US-Patent-Class-324-262; US-Patent-Class-356-432; US-Patent-Class-374-4; US-Patent-Class-374-45; Int-Patent-Class-G01R-35/00) Avail: US Patent and Trademark Office

An improved nondestructive evaluation (NDE) method uses a laser source with modulator and scanning mirror, a pancake shape eddy current detecting coil, a lock-in amplifier, a system controller, and an impedance gain/phase analyzer. The laser is directed by the scanning mirror to a specimen to be analyzed. A very localized or small area of the specimen is impacted directly by the laser beam, creating a thermal or stress wave in the specimen. An impedance gain/phase analyzer is connected to the eddy current detecting coil and to a lock-in amplifier through the system controller. The lock-in amplifier is also synchronized to the laser modulator. The system controller is used to control the lock-in amplifier, scanning mirror, and to process data from the analyzer. Raster scanning of the laser beam across the specimen allows the detection by the coil of the laser generated thermal and elastic strains induced in the specimen by the laser. The rastering of the laser beam is controlled by the controller by positioning the mirror. Official Gazette of the U.S. Patent and Trademark Office

39 STRUCTURAL MECHANICS

Includes structural element design and weight analysis; fatigue; and thermal stress.

For applications see *05 Aircraft Design, Testing and Performance* and *18 Spacecraft Design, Testing and Performance.*

N92-28296*# General Electric Co., Cincinnati, OH. Aircraft Engines.
COUPLED STRUCTURAL/THERMAL/ELECTROMAGNETIC ANALYSIS/TAILORING OF GRADED COMPOSITE STRUCTURES Final Status Report
M. S. Hartle, R. L. McKnight, H. Huang, and R. Holt Apr. 1992 53 p
(Contract NAS3-24538; RTOP 505-62-91)
(NASA-CR-189153; NAS 1.26:189153) Avail: NTIS HC/MF A04

Described here are the accomplishments of a 5-year program to develop a methodology for coupled structural, thermal, electromagnetic analysis tailoring of graded component structures. The capabilities developed over the course of the program are the analyzer module and the tailoring module for the modeling of graded materials. Highlighted accomplishments for the past year include the addition of a buckling analysis capability, the addition of mode shape slope calculation for flutter analysis, verification of the analysis modules using simulated components, and verification of the tailoring module. Author

N92-28320# Georgetown Univ., Washington, DC.
CONTROL AND STABILIZATION OF DISTRIBUTED PARAMETER SYSTEMS IN STRUCTURAL DYNAMICS Final Report, 1 Sep. 1988 - 30 Nov. 1991
John E. Lagnese 30 Nov. 1991 5 p
(Grant AF-AFOSR-0337-88)
(AD-A247097; AFOSR-92-0079TR) Avail: NTIS HC/MF A01

The main purpose of this research is to develop a rigorous mathematical framework for the design of control laws for feedback stabilization and for controllability of the transient behavior of flexible structures based on distributed parameter models of such structures. This work has entailed deriving accurate distributed parameter models for elastic structures and understanding the implications of the various models for the controllability and stabilizability of structures. Substantial progress has been made for models of multiple-link constructions that are composed of elastic beams, plates, shells or combinations of such elastic elements. Such structures are representative of trusses, frames, robot arms, solar panels, antennae, deformable mirrors, etc., currently in use. GRA

N92-28327# California Univ., San Diego, La Jolla. Dept. of Applied Mechanics and Engineering Sciences.
INSTRUMENTATION FOR ULTRAHIGH STRAIN RATE EXPERIMENTS Final Technical Report, 4 Jan. 1988 - 31 Dec. 1991
S. Nemat-Nasser 31 Dec. 1991 40 p
(Contract DAAL03-88-G-0007)
(AD-A249358; ARO-25786.1-MS-A) Avail: NTIS HC/MF A03

This report outlines instruments acquired and fabricated at UCSD, under Grant No. DAAL03-88-G-0007, as part of the URI on Ultrahigh Dynamic Performance Materials. The URI was awarded by ARO in October, 1986. The instrumentation developed under this grant includes a computer control system for safe operation of gas gun; dedicated interferometry recording system for gas gun; an ultrasonic system; a 3OOkV flash X-ray system; an image-converter camera system capable of 20 million frames per second; a high-speed framing and streak-recording camera capable of up to two million frames per second, 85 high-resolution frames; a complete image-processing system dedicated to dynamic quantitative holography; and necessary dedicated wave-form digitizers. In addition, a novel system is developed to generate laser-induced high amplitude, short duration stress pulses, using much of the facilities which already existed at UCSD. Included in this report is a brochure entitled The Experimental Facilities of the Center of Excellence for Advanced Materials which includes brief descriptions and photographs of many of the instruments reported herein. GRA

N92-28352# Rensselaer Polytechnic Inst., Troy, NY. Dept. of Mechanical Engineering, Aeronauticel Engineering and Mechanics.
A COMBINED EXPERIMENTAL AND ANALYTICAL INVESTIGATION OF THE THEORY OF PLASTICITY INVOLVING STRAIN INDUCED ANISOTROPY Final Report, 1 Oct. 1988 - 30 Sep. 1991
E. H. Lee, E. Krempl, and T. L. Sham 3 Mar. 1992 43 p
(Contract DAAL03-88-K-0041)
(AD-A248440) Avail: NTIS HC/MF A03

Experiments were carried out which subjected tubes of ductile metals to histories of straining in combined tension/compression/torsion space. The computer controlled servo-hydraulic testing machine recorded the resulting stress histories together with the imposed strain histories. Intermittently along the path, the straining was halted to probe for the current yield locus. The nose of the yield locus in the direction of straining exhibited quite accurately a circular geometry, which implied isotropic-kinematic hardening. The centers of the fitted yield circles in generalized tension-shear space, define the back stress which expresses the anisotropic component of the hardening, and expresses the strength and orientation of the impediment to dislocation flow through the crystal, i.e., the yield stress required to maintain plastic flow. Application of a polygonal closed straining path caused the back sum tensor to rotate about 330 degrees while the material rotation due to shear was only about 1 degree. Thus, plastic spin, which in the literature has been considered to cause spin of the plastic anisotropy, sums out to be very much smaller. Measurements of stress response to linear and nonlinear strain paths have been used to generate the evolution law for the back stress and hence the constitutive relation. GRA

N92-28424# Purdue Univ., West Lafayette, IN.
PLANE WAVE PROPAGATION IN RANDOM GRANULAR MEDIA Final Report

Martin Ostoja-Starzewski Feb. 1992 48 p
(Contract DACA39-89-M-1309)
(AD-A247300; WES/CR/SL-92-2) Avail: NTIS HC/MF A03

A Markov property of disturbance propagation forms the basis for a study of wavefronts in graph representable microstructures. Stochastic Huygens' minor principle is developed to analyze wavefront propagation in 1-D, 2-D, and 3-D models of material microstructures. A diffusion approximation is obtained for microstructures with grains described by piecewise linear constitutive laws. A new general method of solution to transient wave problems in such microstructures is developed. The method uses solutions from deterministic problems as a reference basis for an analysis of field fluctuations and scatter in stochastic media. The wavefront is modeled as a random field in space-time governed by a Markovian propagator. Explicit formulas for random arrivals in space-time and random modulation of pulses are obtained from this diffusion approximation. The key coefficients appearing in these formulas are calculated in the dimensionless setting of a 1-D linear elastic setting for a wide range of statistics of material properties. Finally, a local averaging process is proposed to obtain various smoothing approximations of this random field. GRA

N92-28575# Technische Univ., Delft (Netherlands).
PROGRAMMING OF THE COMPLEX LOGARITHM FUNCTION IN THE SOLUTION OF THE CRACKED ANISOTROPIC PLATE LOADED BY A POINT FORCE
K. J. J. M. Zaal Jun. 1991 43 p
(LR-657; ETN-92-91397) Avail: NTIS HC/MF A03

In programming solutions of complex function theory, the complex logarithm function is replaced by the complex logarithmic function, introducing a discontinuity along the branch cut into the programmed solution which was not present in the mathematical solution. Recently, Liaw and Kamel presented their solution of the infinite anisotropic centrally cracked plate loaded by an arbitrary point force, which they used as Green's function in a boundary element method intended to evaluate the stress intensity factor at the tip of a crack originating from an elliptical home. Their solution may be used as Green's function of many more numerical methods involving anisotropic elasticity. In programming applications of Liaw and Kamel's solution, the standard definition of the logarithmic function with the branch cut at the nonpositive real axis cannot provide a reliable computation of the displacement field for Liaw and Kamel's solution. Either the branch cut should be redefined outside the domain of the logarithmic function, after proving that the domain is limited to a part of the plane, or the logarithmic function should be defined on its Riemann surface. A two dimensional line fractal can provide the link between all mesh points on the plane essential to evaluate the logarithm function on its Riemann surface. As an example, a two dimensional line fractal is defined for a mesh once used by Erdogan and Arin. ESA

N92-28580# Technische Univ., Delft (Netherlands). Faculty of Aerospace Engineering.
GROWTH OF SURFACE CRACKS UNDER FATIGUE LOADING: A LITERATURE SURVEY
Ichsan S. Putra Nov. 1991 41 p
(LR-664; ETN-92-91402) Avail: NTIS HC/MF A03

Topics related to the growth of surface cracks under fatigue loading are reviewed. The topics include: the stress intensity factor of surface cracks; crack growth and shape development under constant amplitude loading; and fatigue life prediction. ESA

N92-28583# Technische Univ., Delft (Netherlands). Faculty of Aerospace Engineering.
THE BUCKLING BEHAVIOR OF A CENTRAL CRACK IN A PLATE UNDER TENSION
E. Riks, C. C. Rankin (Lockheed Missiles and Space Co., Palo Alto, CA.), and F. A. Brogan (Lockheed Missiles and Space Co., Palo Alto, CA.) Nov. 1991 37 p
(LR-667; ETN-92-91405) Avail: NTIS HC/MF A03

A finite element procedure for the analysis of the buckling and postbuckling behavior of cracks in plates loaded in tension is presented. The procedure is applied to the problem of the centrally cracked plate in tension where the loading direction is perpendicular to the crack faces. The results of the analysis show that the buckling deformations can cause a considerable amplification of the stress intensity around the crack tip. This effect, which is due to a redistribution of the stress field in the plate, increases with the length of the crack. ESA

N92-28620*# National Aeronautics and Space Administration. Goddard Space Flight Center, Greenbelt, MD.
TYPES AND CHARACTERISTICS OF DATA FOR GEOMAGNETIC FIELD MODELING
R. A. Langel, ed. and R. T. Baldwin, ed. (Hughes STX, Inc., Lanham, MD.) Washington Jun. 1992 353 p Symposium held in Vienna, Austria, 23 Aug. 1991
(NASA-CP-3153; Rept-92B00061; NAS 1.55:3153) Avail: NTIS HC/MF A16

Given here is material submitted at a symposium convened on Friday, August 23, 1991, at the General Assembly of the International Union of Geodesy and Geophysics (IUGG) held in Vienna, Austria. Models of the geomagnetic field are only as good as the data upon which they are based, and depend upon correct understanding of data characteristics such as accuracy, correlations, systematic errors, and general statistical properties. This symposium was intended to expose and illuminate these data characteristics. For individual titles, see N92-28621 through N92-28633.

N92-28621*# Oxford Univ. (England). Dept. of Earth Sciences.
HISTORICAL DATA FOR GEOMAGNETIC FIELD MODELLING
c46
Andrew Jackson *In* NASA. Goddard Space Flight Center, Types and Characteristics of Data for Geomagnetic Field Modeling Jun. 1992 p 1-30 Sponsored in part by Royal Society (For primary document see N92-28620 19-39)
Avail: NTIS HC/MF A16

Described here are the various types of historical data (by which we mean actual measurements of the field taken in the past) which are available for geomagnetic field modelling, concentrating exclusively on observations made prior to the 20th century. These data take quite diverse forms, being derived from voyages of discovery or scientific expeditions, from surveys on land, or from observatories after the formation of the Gottingen Magnetic Union. Toward the latter part of the 19th Century, declination was measured quite regularly by various naval vessels for the purpose of constructing charts. Prior to the invention of a method for measuring field intensities by Gauss in 1832, all measurements were of declination or inclination. During the 19th Century over 40,000 observations are available in one year (the first International Polar Year 1882-83). Prior to 1800 there are only of the order of 12,000 measurements. We discuss measurement methods and the types of instruments used, and focus on specific problems which have been noted, such as those associated with the measurement of intensity on iron ships in the late 19th Century. Author

N92-28622*# Finnish Meteorological Inst., Helsinki. Geomagnetism Div.
MEASUREMENTS OF DECLINATION AT THE HELSINKI MAGNETIC-METEOROLOGICAL OBSERVATORY 1844-1853
c46
Heikki Nevanlinna, Anneli Ketola, and Tuulikki Kangas *In* NASA. Goddard Space Flight Center, Types and Characteristics of Data for Geomagnetic Field Modeling Jun. 1992 p 31-39 (For primary document see N92-28620 19-39)
Avail: NTIS HC/MF A16

A project was started with the goal of putting into computer readable form all the old unpublished magnetic data at the Finnish Meteorological Institute (FMI), the successor of the Helsinki magnetic-meteorological observatory. Altogether there are available about 2.5 million visual observations of D, H and Z made during the time interval 1844-1905. The first 10 year period (1844-1853) of declination data now converted to electronic form, includes

observations made at every tenth minute. The total number of observations is 489,152. We present some examples of declination observations in forms of tables and graphs showing hourly, daily, monthly, and annual means. Secular variations of the declination in 1844-1853 have been extremely linear, showing a steady eastward increase of 8 prime/year that is more than two times larger than the present annual rate of secular change in Finland. The standard deviation of the daily and monthly residuals, after removing the secular variation trend for the whole time period, is about 1 prime, demonstrating the high stability and reliability of the observations. For this reason the data may be suitable for deriving a 3-hour activity index K and daily Ak numbers, giving new information for extending the existing long series of activity characters backwards in time. Author

N92-28623*# National Environmental Research Council, Edinburgh (Scotland). Geomagnetism Group.
SURVEY DATA FOR GEOMAGNETIC FIELD MODELLING c46
D. R. Barraclough and S. Macmillan *In* NASA. Goddard Space Flight Center, Types and Characteristics of Data for Geomagnetic Field Modeling Jun. 1992 p 41-73 (For primary document see N92-28620 19-39)
Avail: NTIS HC/MF A16

The survey data discussed here are based on observations made relatively recently at points on land. A special subset of land survey data consists of those made at specially designated sites known as repeat stations. This class of data will be discussed in another part of this document (Barton, 1991b), so only the briefest of references will be made to repeat stations here. This discussion of 'ordinary' land survey data begins with a description of the spatial and temporal distributions of available survey data based on observations made since 1900. (The reason for this rather arbitrary choice of cut-off date is that this was the value used in the production of the computer file of magnetic survey data (land, sea, air, satellite, rocket) that is the primary source of data for geomagnetic main-field modeling). This is followed by a description of the various types of error to which these survey data are, or may be, subject and a discussion of the likely effects of such errors on field models produced from the data. Finally, there is a short section on the availability of geomagnetic survey data, which also describes how the data files are maintained.
Author

N92-28624*# National Aeronautics and Space Administration. Goddard Space Flight Center, Greenbelt, MD.
SATELLITE DATA FOR GEOMAGNETIC FIELD MODELING c46
R. A. Langel and R. T. Baldwin (Hughes STX, Inc., Lanham, MD.) *In its* Types and Characteristics of Data for Geomagnetic Field Modeling Jun. 1992 p 75-135 (For primary document see N92-28620 19-39)
(RTOP 579-31-02)
Avail: NTIS HC/MF A16

Satellite measurements of the geomagnetic fields began with the launch of Sputnik 3 in May of 1958 and have continued sporadically. Spacecraft making significant contributions to main field geomagnetism will be reviewed and the characteristics of their data discussed, including coverage, accuracy, resolution and data availability. Of particular interest are Vanguard 3; Cosmos 49, Ogo's -2, -4, and -6; Magsat; DE-2; and POGS. Spacecraft make measurements on a moving platfrom above the ionosphere as opposed to measurements from fixed observatories and surveys, both below the ionosphere. Possible future missions, such as Aristoteles and GOS are reviewed. Author

N92-28625*# National Geophysical Data Center, Boulder, CO. Marine Geology and Geophysics Div.
MARINE MAGNETIC DATA HOLDINGS OF WORLD DATA CENTER-A FOR MARINE GEOLOGY AND GEOPHYSICS c46
George F. Sharman and Dan Metzger *In* NASA. Goddard Space Flight Center, Types and Characteristics of Data for Geomagnetic Field Modeling Jun. 1992 p 137-148 (For primary document see N92-28620 19-39)
Avail: NTIS HC/MF A16

The World Data Center-A for Marine Geology and Geophysics is co-located with the Marine Geology & Geophysical Data Center, Boulder, CO. Fifteen million digital marine magnetic trackline measurements are managed within the GEOphysical DAta System (GEODAS). The bulk of these data were collected with proton precision magnetometers under Transit Satellite navigational control. Along-track sampling averages about 1 sample per kilometer, while spatial density, a function of ship's track and survey pattern, range from 4 to 0.02 data points/sq. km. In the near future, the entire geophysical data set will be available on CD-ROM. The Marine Geology and Geophysics Division (World Data Center-A for MGG), of the National Geophysical Data Center, handles a broad spectrum of marine geophysical data, including measurements of bathymetry, magnetics, gravity, seismic reflection subbottom profiles, and side-scan images acquired by ships throughout the world's oceans. Digital data encompass the first three, while the latter two are in analog form, recorded on 35mm microfilm. The marine geophysical digital trackline data are contained in the GEODAS data base which includes 11.6 million nautical miles of cruise trackline coverage contributed by more than 70 organizations worldwide. The inventory includes data from 3206 cruises with 33 million digital records and indexing to 5.3 million track miles of analog data on microfilm. Author

N92-28626*# Hughes STX, Inc., Lanham, MD.
REDUCTION OF MARINE MAGNETIC DATA FOR MODELING THE MAIN FIELD OF THE EARTH c46
R. T. Baldwin, J. R. Ridgway, and W. M. Davis (National Geophysical Data Center, Boulder, CO.) *In* NASA. Goddard Space Flight Center, Types and Characteristics of Data for Geomagnetic Field Modeling Jun. 1992 p 149-202 (For primary document see N92-28620 19-39)
Avail: NTIS HC/MF A16

The marine data set archived at the National Geophysical Data Center (NGDC) consists of shipborne surveys conducted by various institutes worldwide. This data set spans four decades (1953, 1958, 1960-1987), and contains almost 13 million total intensity observations. These are often less than 1 km apart. These typically measure seafloor spreading anomalies with amplitudes of several hundred nanotesla (nT) which, since they originate in the crust, interfere with main field modeling. The source for these short wavelength features are confined within the magnetic crust (i.e., sources above the Curie isotherm). The main field, on the other hand, is of much longer wavelengths and originates within the earth's core. It is desirable to extract the long wavelength information from the marine data set for use in modeling the main field. This can be accomplished by averaging the data along the track. In addition, those data which are measured during periods of magnetic disturbance can be identified and eliminated. Thus, it should be possible to create a data set which has worldwide data distribution, spans several decades, is not contaminated with short wavelengths of the crustal field or with magnetic storm noise, and which is limited enough in size to be manageable for the main field modeling. The along track filtering described above has proved to be an effective means of condensing large numbers of shipborne magnetic data into a manageable and meaningful data set for main field modeling. Its simplicity and ability to adequately handle varying spatial and sampling constraints has outweighed consideration of more sophisticated approaches. This filtering technique also provides the benefits of smoothing out short wavelength crustal anomalies, discarding data recorded during magnetically noisy periods, and assigning reasonable error estimates to be used in the least square modeling. A useful data set now exists which spans 1953-1987. Author

N92-28627*# Cambridge Univ. (England).
SECULAR VARIATION ACROSS THE OCEANS: A RETROSPECTIVE STUDY FROM 35 YEARS OF SHIPBOARD TOTAL FIELD MEASUREMENTS IN THE NE ATLANTIC c46
C. A. Williams, J. Verhoef (Geological Survey of Canada, Dartmouth, Nova Scotia), and R. Macnab (Geological Survey of Canada,

Dartmouth, Nova Scotia) *In* NASA. Goddard Space Flight Center, Types and Characteristics of Data for Geomagnetic Field Modeling Jun. 1992 p 203-214 (For primary document see N92-28620 19-39)
(Grant NERC-GR3/7704)
Avail: NTIS HC/MF A16

This is a pilot study to determine whether secular variation information can be retrieved from underway shipboard total field measurements with sufficient accuracy to complement geomagnetic data from land-based observatories. Applying the various new techniques described in this report, we extracted values of the total field at 42,677 crossovers or ship track intersection points contained in data sets collected between 18 degrees N and 50 degress N in the NE Atlantic, and extending temporally from 1955 to 1990. We used an edited subset of these total field values to derive the secular variation at 30,140 different locations in the study area, and compared the results with DGRF secular variation over the study area, calculated at 5 year intervals. The derived and DGRF values agree well, showing that indeed marine data can be a source for secular variations. However the analysis demonstrated that due to inherent noise in the marine data, only minor improvements on the DGRF values for the secular variation can be achieved. Author

N92-28628*# Naval Oceanographic Office, Bay Saint Louis, MS. Geopotential Div.
PROJECT MAGNET HIGH-LEVEL VECTOR SURVEY DATA REDUCTION c46
Rachel J. Coleman *In* NASA. Goddard Space Flight Center, Types and Characteristics of Data for Geomagnetic Field Modeling Jun. 1992 p 215-248 (For primary document see N92-28620 19-39)
Avail: NTIS HC/MF A16

Since 1951, the U.S. Navy, under its Project MAGNET program, has been continuously collecting vector aeromagnetic survey data to support the U.S. Defense Mapping Agency's world magnetic and charting program. During this forty-year period, a variety of survey platforms and instrumentation configurations have been used. The current Project MAGNET survey platform is a Navy Orion RP-3D aircraft which has been specially modified and specially equipped with a redundant suite of navigational positioning, attitude, and magnetic sensors. A review of the survey data collection procedures and calibration and editing techniques applied to the data generated by this suite of instrumentation will be presented. Among the topics covered will be the determination of its parameters from the low-level calibration maneuvers flown over geomagnetic observatories. Author

N92-28629*# Geological Survey of Canada, Ottawa (Ontario). Mineral Resources Div.
SURVEY PARAMETERS AND AVAILABILITY OF LOW-LEVEL AEROMAGNETIC DATA FOR GEOMAGNETIC FIELD MODELLING c46
Peter Hood *In* NASA. Goddard Space Flight Center, Types and Characteristics of Data for Geomagnetic Field Modeling Jun. 1992 p 249-286 (For primary document see N92-28620 19-39)
Avail: NTIS HC/MF A16

Since aeromagnetic surveying started immediately after World War II, a considerable area of the earth's surface both onshore (in excess of 25 million sq. km) has been magnetically surveyed. For about the first 15 years or so, fluxgate magnetometers were employed in aeromagnetic surveys, but the introduction of proton free-precession magnetometers resulted in absolute readings being recorded. Proton precession magnetometers have now been replaced to a large extent by the more sensitive optical absorption magnetometers. Some care has to be taken to calibrate aeromagnetic survey systems and this is best done using a calibration range tied to a magnetic observatory so that accuracies of 10nT or better are achieved for the total field values recorded. Survey navigation has always posed a problem for aeromagnetic surveys, especially offshore. Over land, vertically pointed 35 mm cameras were initially used to recover the aircraft track using a combination of aerial photos and topographic maps. Over featureless areas, it was necessary to utilize existing electronic positioning systems such as Loran C or set up special navigation systems. The advent of the satellite-based Global Positioning Systems (GPS) has to a larger extent solved the navigational problem because there is now almost continuous worldwide coverage to 10 m accuracy in the differential mode. The resultant aeromagnetic data is normally compiled into contour maps in which the diurnal variation and aircraft heading effects are removed. The resultant digital data are normally made publicly available both in gridded and profile form along with the published contour maps. Most aeromagnetic coverage has been obtained in the developed western countries, but elsewhere a considerable amount of surveying has been carried out; as an example, some 80 percent of Africa has been surveyed mostly as a result of aid programs. The data is usually held by the national geological survey or equivalent organizations, but in a number of cases the data (e.g., for the Magnetic Anomaly Map of North America) is also held by the World Data Centres. Author

N92-28630*# Bureau of Mineral Resources, Geology and Geophysics, Canberra (Australia).
MAGNETIC REPEAT STATION DATA c46
C. E. Barton *In* NASA. Goddard Space Flight Center, Types and Characteristics of Data for Geomagnetic Field Modeling Jun. 1992 p 287-319 (For primary document see N92-28620 19-39)
Avail: NTIS HC/MF A16

The nature, purpose, availability and distribution of magnetic repeat stations data are reviewed. Attention is paid to how repeat station data are obtained, sources of errors and limitations on accuracy. Repeat station results cannot achieve the accuracy of magnetic observatory estimates of the secular variation, but are, nevertheless, essential for improving the limited spatial coverage provided by observatories. The lack of appropriate standards and reporting procedures have meant that most global field molders have made little, or no, use of repeat data. Partly to rectify this problem, IAGA Working Group V-4 has instigated a scheme for systematic reporting and classification of magnetic repeat station data. The scheme will help to ensure that proper use is made of the wealth of repeat data that is available, and will also promote better observational practices. Author

N92-28631*# Geological Survey, Denver, CO.
GEOMAGNETIC DATA FROM THE US MAGNETIC OBSERVATORY NETWORK c46
Donald C. Herzog *In* NASA. Goddard Space Flight Center, Types and Characteristics of Data for Geomagnetic Field Modeling Jun. 1992 p 321-332 (For primary document see N92-28620 19-39)
Avail: NTIS HC/MF A16

The United States operates a network of, at present, 13 ground-based magnetic observatories. Continuous, one-minute digital vector and scalar geomagnetic field values have been recorded for the last decade, and extend about five years further back for several stations. Periodic, 3-component absolute measurements of the magnetic field are made to provide baseline reference data with which to determine calibrated field view values at all intervals. These data are now being made available on CD-ROM. The quality of the data depends upon a number of factors, including the types of instrumentation used to monitor and measure the field, the procedures and equipment used to collect and process the data, and the quality controls employed to check the data for erroneous values. These various factors are described here for the U.S. digital geomagnetic observatory data. The observatories have been undergoing an evolution over the last 15 years that will continue to significantly improve the accuracy, precision, and availability of geomagnetic data. Author

N92-28632*# Institute of Geodynamics, Bucharest (Romania).
MAGNETIC AND ELECTROMAGNETIC INDUCTION EFFECTS IN THE ANNUAL MEANS OF GEOMAGNETIC ELEMENTS c46
Crisan Demetrescu and Maria Andreescu *In* NASA. Goddard

Space Flight Center, Types and Characteristics of Data for Geomagnetic Field Modeling Jun. 1992 p 333-340 (For primary document see N92-28620 19-39)
Avail: NTIS HC/MF A16

The solar-cycle related (SC) variation in the annual means of the horizontal and vertical components of the geomagnetic field at European observatories is used to infer information on the magnetic and electric properties of the interior, characteristic of the observatory location, by identifying and analyzing the magnetic induction component and respectively the electromagnetic induction component of the SC variation. The obtained results and the method can be used to better constrain the anomaly bias in main field modelling and to improve the reliability of secular variation models beyond the time interval covered by data. Author

N92-28633*# Academy of Sciences, Potsdam (German D.R.). Central Inst. for Physics of the Earth.
INDEPENDENT CONSTITUENTS IN OBSERVATORY TIME SERIES IN CHARACTERIZING THE SECULAR VARIATION
c46
W. Webers *In* NASA. Goddard Space Flight Center, Types and Characteristics of Data for Geomagnetic Field Modeling Jun. 1992 p 341-349 (For primary document see N92-28620 19-39)
Avail: NTIS HC/MF A16

By an ansatz of a finite set of N superimposed oscillations, observatory time series are fitted. This start model is optimized for the independence of the used 2N-dimensional functional system as a criterion. Here, the contributions of each of the dimensions to the volume of the corresponding 2N-dimensional parallelpiped of the functional space is to be evaluated. Independence and an equal standard for the constituents are achieved by the optimizing procedure varying the start values of frequencies in the fitting ansatz when quotients of successively constructed Gram-determinants are beyond a definite threshold and of nearly the same numerical value. Results for globally distributed observatories characterize the secular variation. Author

N92-28643# National Aerospace Lab., Amsterdam (Netherlands). Structures and Materials Div.
SPACECRAFT SUSTAINED LOAD FRACTURE CONTROL
R. J. H. Wanhill 10 May 1989 89 p
(Contract ESA-A0/2-1162-NL/PH)
(NLR-TP-89163-U; ETN-92-91521) Avail: NTIS HC/MF A05

The opportunities for sustained load fracture control in spacecraft are indicated. Emphasis is given to verification by small scale laboratory testing. Sustained load fracture must be eliminated or controlled in service. For this purpose, a comprehensive fracture control plan is outlined. Materials and environments in aerospace structures and systems are considered and stress corrosion cracking, hydrogen embrittlement, and liquid metal embrittlement are discussed as major sustained load fracture. The laboratory testing is defined and placed in categories of major importance which provides the plans for preparing detailed test plans and proposals to systematically investigate the various categories of materials, environments, and types of test. ESA

N92-28650# National Aerospace Lab., Amsterdam (Netherlands). Structures and Materials Div.
CORRELATION, ERROR-LOCALISATION, AND UPDATING OF THE SECOND PROBLEM DEFINED IN GARTEUR AG11
A. deBoer and M. H. W. Ellenbroek 12 Feb. 1990 28 p
(Contract NIVR-02904-N)
(NLR-TP-90070-U; ETN-92-91433) Avail: NTIS HC/MF A03

A clamped free truss structure problem, defined in the GARTEUR (Group for Aeronautical Research and Technology in Europe) Action Group 11 refinement of structure dynamics computational methods, is described. The measured and calculated modal data of the structure are correlated, the locations of the errors are determined, and the finite element model of the structure is updated. These analyses are performed with the B2000 validation processor and the program TANCO. ESA

N92-28688# National Aerospace Lab., Amsterdam (Netherlands). Informatics Div.
MODAL ANALYSIS OF PLATES USING BOUNDARY INTEGRAL EQUATIONS
H. Schippers and W. L. Wendland (Stuttgart Univ., Germany, F.R.) 14 Jun. 1989 30 p Presented at the ESA Workshop on Modal Representation of Flexible Structures by Continuum Methods, Noordwijk, Netherlands, 15-16 Jun. 1989
(NLR-TP-89211-U; ETN-92-91522) Avail: NTIS HC/MF A03

Boundary integral equation methods are advocated for the modal analysis of vibrating plates. The integral equations are obtained by transforming the boundary value problem using the explicit fundamental solution for plate vibration. The dimensions of the original equation methods versus other continuum methods. The derivation of the integral equations is by no means unique; the two most popular methods are the direct method and the method of potentials. The direct method, which is based on the Betti representation formula, is usually applied in boundary element software packages. Here, the method of potentials is preferred. An indirect 'ansatz' for the transverse displacement of the vibrating plate and the application of appropriate boundary conditions yield a nonlinear eigenvalue problem for the boundary equations. The nonlinear eigenvalue problem can be solved by searching for the frequencies which make the determinant of the matrix equal to zero. As a result, the eigenvalues (i.e., the natural frequencies) and the corresponding eigenfunctions (modal vectors) are obtained. The two boundary integral equations define so called 'strongly elliptic' equations, which can be numerically solved by a boundary Galerkin method: the boundary is decomposed into a finite number of segments and the boundary potentials are approximated by finite elements in the boundary. The numerical simulation errors are estimated by giving convergence results for the eigenfunction and the eigenvalues. ESA

N92-28701*# National Aeronautics and Space Administration. Lewis Research Center, Cleveland, OH.
ELEVATED TEMPERATURE AXIAL AND TORSIONAL FATIGUE BEHAVIOR OF HAYNES 188
Peter J. Bonacuse (Army Aviation Systems Command, Cleveland, OH.) and Sreeramesh Kalluri (Sverdrup Technology, Inc., Brook Park, OH.) Jun. 1992 23 p
(RTOP 553-13-00)
(NASA-TM-105396; E-6788; NAS 1.15:105396; AVSCOM-TR-91-C-045) Avail: NTIS HC/MF A03

The results of high-temperature axial and torsional low-cycle fatigue experiments performed on Haynes 188, a wrought cobalt-base superalloy, are reported. Fatigue tests were performed at 760 C in air on thin-walled tubular specimens at various ranges under strain control. Data are also presented for coefficient of thermal expansion, elastic modulus, and shear modulus at various temperatures from room to 1000 C, and monotonic and cyclic stress-strain curves in tension and in shear at 760 C. The data set is used to evaluate several multiaxial fatigue life models (most were originally developed for room temperature multiaxial life prediction) including von Mises equivalent strain range (ASME boiler and pressure vessel code), Manson-Halford, Modified Multiaxiality Factor (proposed here), Modified Smith-Watson-Topper, and Fatemi-Socie-Kurath. At von Mises equivalent strain ranges (the torsional strain range divided by the square root of 3, taking the Poisson's ratio to be 0.5), torsionally strained specimens lasted, on average, factors of 2 to 3 times longer than axially strained specimens. The Modified Multiaxiality Factor approach shows promise as a useful method of estimating torsional fatigue life from axial fatigue data at high temperatures. Several difficulties arose with the specimen geometry and extensometry used in these experiments. Cracking at extensometer probe indentations was a problem at smaller strain ranges. Also, as the largest axial and torsional strain range fatigue tests neared completion, a small amount of specimen buckling was observed. Author

N92-28757* National Aeronautics and Space Administration. Langley Research Center, Hampton, VA.
METHOD AND APPARATUS FOR USING MAGNETO-ACOUSTIC REMANENCE TO DETERMINE EMBRITTLEMENT Patent
Sidney G. Allison, inventor (to NASA), Min Namkung, inventor (to NASA), William T. Yost, inventor (to NASA), and John H. Cantrell, inventor (to NASA) 9 Jun. 1992 10 p Filed 15 Apr. 1991 Continuation-in-part of abandoned US-Patent-Appl-SN-449211, filed 12 Dec. 1989 which is a division of US-Patent-Appl-SN-210486, filed 23 Jun. 1988
(NASA-Case-LAR-13817-5; US-Patent-5,121,058; US-Patent-Appl-SN-686263; US-Patent-Appl-SN-449211; US-Patent-Appl-SN-210486; US-Patent-Class-324-235; US-Patent-Class-73-601; US-Patent-Class-324-226; Int-Patent-Class-G01R-33/12; Int-Patent-Class-G01N-27/80) Avail: US Patent and Trademark Office

A method and apparatus for testing steel components for temperature embrittlement uses magneto-acoustic emission to nondestructively evaluate the component are presented. Acoustic emission signals occur more frequently at higher levels in embrittled components. A pair of electromagnets are used to create magnetic induction in the test component. Magneto-acoustic emission signals may be generated by applying an AC current to the electromagnets. The acoustic emission signals are analyzed to provide a comparison between a component known to be unembrittled and a test component. Magnetic remanence is determined by applying a DC current to the electromagnets and then by turning the magnets off and observing the residual magnetic induction. Author

N92-28776# Technical Research Centre of Finland, Espoo. Nuclear Engineering Lab.
PRE-TEST ANALYSES FOR PRESSURIZED THERMOSHOCK TESTS, VESSEL 1
Heli Talja and Heikki Keinanen Oct. 1991 44 p Sponsored by Finnish Center for Radiation and Nuclear Safety; Imatran Voima Oy; and Finnish Ministry of Trade and Industry
(VTT-RR-746; ISBN-951-38-3994-X; ISSN-0358-5077; ETN-92-91268) Copyright Avail: NTIS HC/MF A03

The pretest analyses performed for the thermoshock tests with the first model pressure vessel are described. The temperature calculation was made using both a computer code based on the Fourier series and the finite element method. As the next step the stresses due to internal pressure and thermal transient were calculated using both analytical formulas and the finite element method. To evaluate the structural integrity, the VTTSIF program, based on the influence function method, was applied to obtain the stress intensity factor values, which were compared to material toughness values. Five tests were made with the same model pressure vessel using four different geometries. In the first three tests, the flaw was actually a blunt notch. In the last two tests a sharp pre crack was produced before the test. The calculated temperatures and stresses are presented. When these are compared to measured values, a good correlation is observed. For each flaw the assessment is performed and for the last flaw geometry the calculated stress intensity is presented as a function of loading time and crack tip temperature. When this stress intensity factor is compared to the material fracture initiation toughness values obtained, crack initiation is clearly predicted. ESA

N92-28836# National Aerospace Lab., Tokyo (Japan). Space Technology Research Group.
QUATERNION AND EULER ANGLES IN KINEMATICS
Isao Yamaguchi, Takashi Kida, Osamu Okamoto, and Yoshiaki Ookami Jun. 1991 18 p In JAPANESE
(NAL-TM-636; ISSN-0452-2982; JTN-92-80363) Avail: NTIS HC/MF A03

A summary of quaternion in the kinematics of rigid body dynamics is presented. Quaternion is a four parameter system for specifying the orientation of a rigid body. Four parameters of quaternion are updated by integrating linear differential equations whose coefficients are the angular velocity of the body. After describing the coordinate systems and vectors, quaternion is introduced. Then, using a comparison with the Euler angles, typical presentation of body orientation and the relationships between quaternion and angular velocity are discussed. Finally, a computer simulation algorithm is derived to solve rigid body dynamics using quaternion. Author (NASDA)

N92-28850# National Aerospace Lab., Amsterdam (Netherlands). Structures and Materials Div.
CRACK RESISTANCE, FRACTURE TOUGHNESS AND INSTABILITY IN DAMAGE TOLERANT Al-Li ALLOYS
R. J. H. Wanhill, L. Schra, and W. G. J. tHart 10 May 1990 29 p Presented at ASTM Symposium on Cyclic Deformation Fracture, and Nondestructive Evaluation of Advanced Materials, San Antonio, TX, Nov. 1990
(NLR-TP-90172-U; ETN-92-91538) Avail: NTIS HC/MF A03

A comparison of the crack resistance (R curve), fracture toughness and instability behavior of candidate damage tolerant aluminum lithium alloys, 2091 and 8090, and the widely used conventional 2024-T3 alloy is addressed. The 2091 alloy was in three heat treatment conditions, T8X, TX and TY, all artificially aged. The 8090 alloy was in the T81 condition. The crack resistances and fracture toughnesses of 2091-T8X and 8091-T81 were similar to those of 2024-T3, but at a 50 MPa lower strength level. The crack resistances and fracture toughnesses of 2091-TX and 2091-TY were much inferior. In all cases, stable (slow) crack growth was ductile, but unstable crack growth in 2091-TX and 2091-TY was 100 percent intergranular and macroscopically brittle. Unstable crack growth in 2091-T8X was 50 percent intergranular and macroscopically ductile. Fractographic analysis indicated the 2091-TX and 2091-TY alloys to be sensitive to dynamic effects, such that the dynamic fracture toughness could be significantly lower than the quasistatic fracture toughness. This may also be true of 2091-T8X. These results point out that fail safe crack arrest tests should be included in any evaluation of damage tolerant Al-Li sheet alloys for aircraft structures. ESA

N92-28855# Sandia National Labs., Albuquerque, NM.
STRESS ANALYSIS OF PLATED-THROUGH-HOLES IN RIGID FLEX MULTILAYER PRINTED WIRING BOARDS
S. N. Burchett 1992 22 p Presented at the 35th Inst. for Interconnecting and Packaging Electronic Circuits Annual Meeting, Bel Harbor, FL, 5-10 Apr. 1992
(Contract DE-AC04-76DP-00789)
(DE92-011659; SAND-92-0271C; CONF-9204115-1) Avail: NTIS HC/MF A03

A rigid/flex printed wiring board is a hybridized system of wiring interconnects utilizing the concepts of both multilayer and flexible circuit technology. This type of printed wiring board offers significant advantages in the production of complex electronic assemblies. In contrast to standard printed wiring board assemblies which are homogeneous in material composition, rigid/flex assemblies have a combination of different laminates, films, and adhesives arranged to accomplish the electrical and mechanical design goals. After lamination, the circuit layers are interconnected using plated-through-hole technology. Associated with the plated-through-holes are at least two observed failure modes, barrel cracks and inner layer foil cracks, that develop during thermal testing of completed printed wiring board assemblies. Due to these failures, there is concern about the reliability of such systems. This paper presents the results from finite element stress analyses employed to assist in the understanding of failure modes in a plated-through-hole of a rigid/flex multilayer printed wiring board. The results of the analyses provided substantial insight about the thermal-structural response of the assembly and provided guidance to process improvements aimed at eliminating the failures. DOE

N92-28892# California Univ., San Diego. Dept. of Applied Mechanics and Engineering S ciences.
EXPLOMET 90 INTERNATIONAL CONFERENCE ON SHOCK-WAVE AND HIGH-STRAIN-RATE PHENOMENA IN MATERIALS
Marc A. Meyers, Lawrence E. Murr, and Karl P. Staudhammer

10 Jan. 1992 34 p
(Contract DAAL03-90-G-0068)
(AD-A248665) Avail: NTIS HC/MF A03

This report describes the major components and activities of EXPLOMET 90, an international conference on shock-wave and high-strain-rate effects held at UCSD August 12-17, 1990. The conference was attended by approximately 200 scientists and engineers from throughout the world and was enriched by invited/keynote lectures by a group of world-renowned scientists. Over 110 talks were presented and twenty posters were displayed. The proceedings are being published by M. Dekker and will appear in February 1992. Sessions were devoted to the following topics: (1) High Strain Rate Deformation; (2) Shock and Combustion Synthesis; (3) Dynamic Consolidation; (4) Shaped Charge Phenomena; (5) Shear Localization; (6) Dynamic Fracture; (7) Shock Phenomena and Superconductivity; (8) Shock Waves and Shock Loading; (9) Shock and Dynamic Phenomena in Ceramics; and (10) Explosive Welding and Metalworking. GRA

N92-29081# Naval Research Lab., Orlando, FL. Underwater Sound Reference Detachment.
ANALYSIS OF CONSTRAINED-LAYER DAMPING OF FLEXURAL AND EXTENSIONAL WAVES IN INFINITE, FLUID-LOADED PLATES
Pieter S. Dubbelday Mar. 1992 8 p
(AD-A247936) Avail: NTIS HC/MF A02

This study contains a mathematical analysis of constrained-layer damping (CLD) in plates of infinite extent, with an emphasis on the physical understanding of some special features, including fluid loading. Previous work is expanded to cover extensional waves. Some essential aspects of fluid loading may be understood by applying thin-plate theory. Therefore, thin-plate theory of extensional waves in a fluid-loaded plate was developed as a counterpart to that for flexural waves. The description and examples of CLD follow three models: the first is an extension of Kerwin's 1959 model, the second a hybrid model for which the base plate is treated by exact elasticity theory, and finally a fully exact model for all three layers. Examples and comparisons are given. GRA

N92-29101* National Aeronautics and Space Administration. Langley Research Center, Hampton, VA.
MAGNETIC REMANENCE METHOD AND APPARATUS TO TEST MATERIALS FOR EMBRITTLEMENT Patent
Sidney G. Allison, inventor (to NASA), Min Namkung, inventor (to NASA), William T. Yost, inventor (to NASA), and John H. Cantrell, inventor (to NASA) 26 May 1992 10 p Filed 2 Nov. 1990 Division of abandoned US-Patent-Appl-SN-449211, filed 12 Dec. 1989 which is a division of US-Patent-Appl-SN-210486, filed 23 Jun. 1988
(NASA-Case-LAR-13817-4; US-Patent-5,117,184;
US-Patent-Appl-SN-608504; US-Patent-Appl-SN-449211;
US-Patent-Appl-SN-210486; US-Patent-Class-324-239;
Int-Patent-Class-G01R-33/12; Int-Patent-Class-G01R-27/72)
Avail: US Patent and Trademark Office

A method and apparatus for testing steel components for temper embrittlement uses magneto-acoustic emission to nondestructively evaluate the component. Acoustic emission signals occur more frequently at higher levels in embrittled components. A pair of electromagnets are used to create magnetic induction in the test component. Magneto-acoustic emission signals may be generated by applying an AC current to the electro-magnets. The acoustic emission signals are analyzed to provide a comparison between a component known to be unembrittled and a test component. Magnetic remanence is determined by applying a DC current to the electromagnets, then turning the magnets off and observing the residual induction.

Official Gazette of the U.S. Patent and Trademark Office

N92-29155* National Aeronautics and Space Administration. Langley Research Center, Hampton, VA.
MAGNETO ACOUSTIC EMISSION METHOD FOR TESTING MATERIALS FOR EMBRITTLEMENT Patent
Sidney G. Allison, inventor (to NASA), Min Namkung, inventor (to NASA), William T. Yost, inventor (to NASA), and John H. Cantrell, inventor (to NASA) 28 Apr. 1992 10 p Filed 12 Dec. 1989 Division of US-Patent-Appl-SN-210486, filed 23 Jun. 1988
(NASA-Case-LAR-13817-2; US-Patent-5,109,195;
US-Patent-Appl-SN-449209; US-Patent-Appl-SN-210486;
US-Patent-Class-324-235; US-Patent-Class-73-801;
US-Patent-Class-324-209; US-Patent-Class-324-226;
US-Patent-Class-324-227; US-Patent-Class-324-239) Avail: US Patent and Trademark Office

A method and apparatus for testing steel components for temper embrittlement uses magneto-acoustic emission to nondestructively evaluate the component. Acoustic emission signals occur more frequently at higher levels in embrittled components. A pair of electromagnets are used to create magnetic induction in the test component. Magneto-acoustic emission signals may be generated by applying an ac current to the electromagnets. The acoustic emission signals are analyzed to provide a comparison between a component known to be unembrittled and a test component. Magnetic remanence is determined by applying a dc current to the electromagnets, then turning the magnets off and observing the residual magnetic induction.

Official Gazette of the U.S. Patent and Trademark Office

N92-29176# National Aerospace Lab., Emmeloord (Netherlands). Aerodynamics Div.
EXPLORATORY FLEXURAL POWER FLOW MEASUREMENTS ON A BAR
H. M. M. vanderWal 17 May 1990 13 p Presented at the 3rd International Congress on Intensity Techniques, Senlis, France, 27-29 Aug. 1990
(Contract NIVR-01808-N)
(NLR-TP-90178-U; ETN-92-91539) Avail: NTIS HC/MF A03

Exploratory experiments in a bar with an absorptive termination were performed. The bar was excited in a transversal direction. The flexural power flow in the bar was measured at various positions, applying the two transducer technique (2TT) and the four transducer technique (4TT). The separation distance between the accelerometers was varied. The power flow at the excitation point was determined from a force and an acceleration measurement (Fv). When comparing the 2TT power flow with the 4TT or Fv power flow, the discretization error (i.e. the error due to a finite accelerometer separation) is an important parameter, particularly for separations larger than one sixth of a wavelength. In order to quantify the effect of this error, a prediction of the measured power flows on the basis of an analytical solution of the bending wave equation for the far field is performed. For most cases a good agreement is found between the predicted and the measured power flow ratios (i.e. 4TT/2TT and 2TT/Fv). However, for accelerometer separations smaller than about one sixth of a wavelength, a larger scatter is observed in the power flow data, measured with the 4TT, due to loss of significant digits. This effect may result in limitations for multiple transducer techniques in two or three dimensional structures. ESA

N92-29181# Aeronautical Research Labs., Melbourne (Australia).
EXPERIMENTS IN PASSIVE VIBRATION REDUCTION
A. Goldman, P. Piperias, and C. D. Rider Dec. 1991 56 p
(AD-A250397; ARL-STRUC-TM-531; DODA-AR-006-150) Avail: NTIS HC/MF A04

Damping has been under investigation for many years. A search of the literature reveals an increase in activity in the period from 1960 to 1970. This report sets out the progress in recent years at ARL and evaluates some of the materials that are available in Australia. A number of practical applications are described. Tests were carried out on an aluminum plate with dimensions of 600 x 200 x 5mm and 600 x 200 x 6mm. Several identical pieces were cut from the same sheet such that they all had the same lengthwise grain structure. No experiments have been carried out to determine whether there is any difference, in stiffness or damping properties, between pieces of aluminum cut in different directions from the same sheet. The test procedure was in two stages. First, a random input was applied to establish the resonant frequencies of the

plate, simply supported on soft foam. In the second stage, the plate was excited sinusoidally at the first resonant frequency, and a decaying acceleration time history was captured on removal of the excitation. Both stages were conducted with and without constraining layers attached to the plate. GRA

42 GEOSCIENCES (GENERAL)

N92-28950*# Jet Propulsion Lab., California Inst. of Tech., Pasadena.
TOPEX/POSEIDON SCIENCE INVESTIGATIONS PLAN
1 Sep. 1991 184 p Original contains color illustrations
(Contract NAS7-918)
(NASA-CR-190456; NAS 1.26:190456; JPL-Publ-91-27) Avail: NTIS HC/MF A09; 21 functional color pages

TOPEX/POSEIDON is a satellite mission that will use the technique of radar altimetry to make precise measurement of sea level with a primary goal of studying the global ocean circulation. The mission represents the culmination of the development of satellite altimetry over the past two decades. The major thrust of the mission is a commitment to measuring sea level with an unprecedented accuracy such that the small-amplitude, basinwide sea level changes that bear significant effects on global change can be detected. The mission will be conducted jointly by NASA and the French Space Agency. The 3 to 5 year mission will study the long-term mean and variability of ocean circulation. An international team of 38 principal investigators was established to conduct scientific investigations in ocean circulation, tides, and Marine geophysics using data from the mission. Brief descriptions of the planned investigations as well as a summary of the major elements of the mission are provided. Author

43 EARTH RESOURCES AND REMOTE SENSING

Includes remote sensing of earth resources by aircraft and spacecraft; photogrammetry; and aerial photography.

For instrumentation see *35 Instrumentation and Photography.*

N92-28690# National Aerospace Lab., Amsterdam (Netherlands). Remote Sensing Div.
MULTITEMPORAL ANALYSIS OF A BRAIDING RIVER
H. H. S. Noorbergen 3 Jul. 1989 12 p Presented at the 15th Annual Conference on Operational Applications of Remote Sensing, Bristol, England, 13-15 Sep. 1989
(NLR-TP-89235-U; ETN-92-91524) Avail: NTIS HC/MF A03

The behavior of the Jamuna braiding river in Bangladesh is considered, in order to predict future changes of the river channels. A database is built which provides a useful potential for multitemporal research. For the remote sensing analysis, ten LANDSAT MSS (Multispectral Scanner) images were selected between 1973 and 1987. In addition to the normal selection criteria (cloud cover, quality), a specific criterion was used to select only images from seasons with comparable, low water levels in the main river channels. From each year a user defined classification was made into four color coded categories: water, sand, vegetation, and bare soil. Differences between two successive years were derived by combining their classification results. ESA

N92-28697# National Aerospace Lab., Amsterdam (Netherlands). Informatics Div.
TRANSPUTER-BASED EMBEDDED SYSTEM FOR METEOSAT IMAGE DATA COMPRESSION
M. H. J. B. Versteeg, R. A. Hogendoorn, and A. Monkel 20 Jun. 1990 15 p Presented at SPIE Conference on Visual Communications and Image Processing '90: Fifth in a Series, Lausanne, Switzerland, 2-4 Oct. 1990
(NLR-TP-90228-U; ETN-92-91542) Avail: NTIS HC/MF A03

A system to demonstrate the feasibility of using data compression for the Meteosat dissemination link is realized. The compression method used double the amount of image data that can be disseminated to the users via the existing channel without introducing any errors in the reconstructed image after decompression. The compression and decompression functions are performed in real time during the Meteosat dissemination (116 Kbit/sec). A multi processor system based on the Inmos Transputer was selected to provide the required processing power. ESA

N92-28708# National Aerospace Lab., Amsterdam (Netherlands). Space Div.
QUANTITATIVE UPDATING OF LAND USE INFORMATION ON 1:50,000 SCALE TOPOGRAPHIC MAPS USING SPOT LANDSAT THEMATIC MAPPER IMAGERY
F. B. vanderLaan and P. G. Meijer 30 Jan. 1989 43 p
(NLR-TP-89061-U; ETN-92-91516) Avail: NTIS HC/MF A03

The results of a study concerning the updating of land use on topographic maps using remote sensing information are reported and maps of change in land use are given. It was found that SPOT multispectral imagery is less suitable for land use classification purposes than LANDSAT Thematic Mapper data due to the lack of a spectral band in the mid-infrared. The most promising approach for updating land use information on topographic maps on a raster image processing system seems to be the use of digitized topographic map information at 10 m resolution together with LANDSAT Thematic Mapper data resampled to the same resolution. Such end product maps can technically be produced at a rate of 1 to 2 maps per week. The main technical problem in the production of maps is the limited availability of cloud free (summer) imagery. This availability was statistically assessed to be once per two years on the average. ESA

N92-28715*# Colorado Univ., Boulder. Center for Astrodynamics Research.
SEA SURFACE VELOCITIES FROM VISIBLE AND INFRARED MULTISPECTRAL ATMOSPHERIC MAPPING SENSOR IMAGERY Final Report
P. A. Pope, W. J. Emery, and M. Radebaugh 10 Jun. 1992 45 p
(Grant NAG8-806)
(NASA-CR-190398; NAS 1.26:190398) Avail: NTIS HC/MF A03

High resolution (100 m), sequential Multispectral Atmospheric Mapping Sensor (MAMS) images were used in a study to calculate advective surface velocities using the Maximum Cross Correlation (MCC) technique. Radiance and brightness temperature gradient magnitude images were formed from visible (0.48 microns) and infrared (11.12 microns) image pairs, respectively, of Chandeleur Sound, which is a shallow body of water northeast of the Mississippi delta, at 145546 GMT and 170701 GMT on 30 Mar. 1989. The gradient magnitude images enhanced the surface water feature boundaries, and a lower cutoff on the gradient magnitudes calculated allowed the undesirable sunglare and backscatter gradients in the visible images, and the water vapor absorption gradients in the infrared images, to be reduced in strength. Requiring high (greater than 0.4) maximum cross correlation coefficients and spatial coherence of the vector field aided in the selection of an optimal template size of 10 x 10 pixels (first image) and search limit of 20 pixels (second image) to use in the MCC technique. Use of these optimum input parameters to the MCC algorithm, and high correlation and spatial coherence filtering of the resulting velocity field from the MCC calculation yielded a clustered velocity distribution over the visible and infrared gradient images. The velocity field calculated from the visible gradient image pair agreed well with a subjective analysis of the motion, but the velocity field from the infrared gradient image pair did not. This was attributed to the changing shapes of the gradient features, their nonuniqueness, and large displacements relative to the mean distance between them. These problems implied a lower repeat time for the imagery was needed in order to improve the velocity field derived from gradient imagery. Suggestions are given for optimizing the repeat time of sequential imagery when using the

MCC method for motion studies. Applying the MCC method to the infrared brightness temperature imagery yielded a velocity field which did agree with the subjective analysis of the motion and that derived from the visible gradient imagery. Differences between the visible and infrared derived velocities were 14.9 cm/s in speed and 56.7 degrees in direction. Both of these velocity fields also agreed well with the motion expected from considerations of the ocean bottom topography and wind and tidal forcing in the study area during the 2.175 hour time interval. Author

N92-28717*# Brown Univ., Providence, RI. Dept. of Geological Sciences.
RELATIONSHIPS OF SOIL, GRASS, AND BEDROCK OVER THE KAWEAH SERPENTINE MELANGE THROUGH SPECTRAL MIXTURE ANALYSIS OF AVIRIS DATA Final Report
John F. Mustard Dec. 1991 27 p
(Grant NAGw-1118)
(NASA-CR-190445; NAS 1.26:190445) Avail: NTIS HC/MF A03

A linear mixing model is used to model the spectral variability of an AVIRIS scene from the western foothills of the Sierra Nevada and calibrate these radiance data to reflectance. Five spectral endmembers from the AVIRIS data, plus an ideal 'shade' endmember were required to model the continuum reflectance of each pixel in the image. Three of the endmembers were interpreted to model the surface constituents green vegetation, dry grass, and illumination. These are the main transient surface constituents that are expected to change with shifts in land use or climatic influences and viewing conditions ('shade' only). The spectral distinction between the other three endmembers is very small, yet the spatial distributions are coherent and interpretable. These distributions cross anthropogenic and vegetation boundaries and are best interpreted as different soil types. Comparison of the fraction images to the bedrock geology maps indicates that substrate composition must be a factor contributing to the spectral properties of these endmembers. Detailed examination of the reflectance spectra of the three soil endmembers reveals that differences in the amount of ferric and ferrous iron and/or organic constituents in the soils is largely responsible for the differences in spectral properties of these endmembers. Author

N92-28791# Naval Postgraduate School, Monterey, CA.
APPLICATIONS OF PASSIVE MICROWAVE SATELLITE DATA FOR ARCTIC SEA ICE STUDIES M.S. Thesis
William A. Wright Dec. 1991 127 p
(AD-A245966) Avail: NTIS HC/MF A07

Passive microwave satellite data provides all-weather, continuous observations of the polar ice cover. Multichannel radiometer data sets extending back to 1978 are readily available and distributed on CD-ROM media. Current algorithms can extract information on ice cover, concentration and type. Two applications of these data sets for polar studies are explored: (1) the possible detection of altered ice morphology due to anomalous tidal currents in the Yermak Plateau region; and (2) the tracking of multiyear ice features to infer ice motion. No evidence of altered ice morphology in the Yermak Plateau region was detected. Either the reported anomalous currents do not affect ice morphology or the limitations inherent to passive microwave imagery (poor spatial resolution) prevent detection. On the other hand, distinct multiyear ice features are observed to move in the direction of mean ice flow and are well correlated with the motion of nearby data buoys. Short term ice motion vectors are unreliable because of the low spatial resolution of the passive microwave data. However, long term averages are indicative of ice flow trajectories and can be used, for example, to increase our knowledge of the interannual variability of heat and salinity budgets in specific regions, including Fram Strait, the principal outflow region of the arctic basin. GRA

N92-28807# Los Alamos National Lab., NM.
REMOTE SENSING APPLICATIONS OF THE EXTENDED RADIOSITY METHOD
S. A. W. Gerstl and C. C. Borel 1992 3 p Presented at the 1992 International Geoscience and Remote Sensing Symposium, Houston, TX, 26-29 May 1992
(Contract W-7405-eng-36)
(DE92-011356; LA-UR-92-708; CONF-9205136-2) Avail: NTIS HC/MF A01

In this paper we describe the progress made in the last three years on developing the radiosity method for remote sensing applications. The research covered canopy modeling, volumetric scattering, and atmospheric corrections for future analysis of EOS imaging spectrometer data. DOE

N92-28834# Los Alamos National Lab., NM.
A NEW RADIOMETER FOR EARTH RADIATION BUDGET STUDIES
P. G. Weber 1992 4 p Presented at the 1992 International Geoscience and Remote Sensing Symposium, Houston, TX, 26-29 May 1992
(Contract W-7405-eng-36)
(DE92-011267; LA-UR-92-764; CONF-9205136-1) Avail: NTIS HC/MF A01

A critical need for the US Global Change Research Program is to provide continuous, well-calibrated radiometric data for radiation balance studies. This paper describes a new, compact, relatively light-weight, adaptable radiometer which will provide both spectrally integrated measurements and data in selected spectral bands. The radiometer design is suitable for use on (small) satellites, aircraft, or Unmanned Aerospace Vehicles (UAVs). Some considerations for the implementation of this radiometer on a small satellite are given. DOE

N92-28840# Los Alamos National Lab., NM.
ATMOSPHERIC CORRECTIONS OF LAND IMAGERY USING THE EXTENDED RADIOSITY METHOD
C. C. Borel and S. A. W. Gerstl 1992 5 p Presented at the 1992 International Geoscience and Remote Sensing Symposium, Houston, TX, 26-29 May 1992
(Contract W-7405-eng-36)
(DE92-011355; LA-UR-92-709; CONF-9205136-3) Avail: NTIS HC/MF A01

In this paper we describe an application of the extended radiosity method to compute atmospheric scattering effects over heterogeneous surfaces. Additionally, this method is able to perform the inverse operation: to correct for such atmospheric effects. The radiosity method is used to compute point-spread-functions (PSF). PSF's determine how much light is scattered from an adjacent surface into the field-of-view (FOV) of a sensor above the atmosphere. We show that the PSF's are in general asymmetric for pointable airborne or satellite sensors. A Fourier transform based method can be used to correct adjacency-effect-blurred images for these atmospheric distortions. DOE

44 ENERGY PRODUCTION AND CONVERSION

Includes specific energy conversion systems, e.g., fuel cells; global sources of energy; geophysical conversion; and windpower.

For related information see also *07 Aircraft Propulsion and Power, 20 Spacecraft Propulsion and Power,* and *28 Propellants and Fuels.*

N92-28277# Midwest Research Inst., Golden, CO.
THIN FILM CADMIUM TELLURIDE PHOTOVOLTAIC CELLS
A. Compaan (Toledo Univ., OH.) and R. Bohn (Toledo Univ., OH.) Apr. 1992 37 p
(Contract DE-AC02-83CH-10093)
(DE92-001239; NREL/TP-451-4797) Avail: NTIS HC/MF A03

This report describes research to develop vacuum-based growth techniques for CdTe thin-film solar cells: (1) laser-driven physical vapor deposition (LDPVD), and (2) radio-frequency (rf) sputtering. The LDPVD process was successfully used to deposit thin films of CdS, CdTe, and CdCl(sub 2), as well as related alloys and doped semiconductor materials. The laser-driven deposition process readily permits the use of several target

materials in the same vacuum chamber and, thus, complete solar cell structures were fabricated on SnO2-coated glass using LDPVD. The rf sputtering process for film growth became operational, and progress was made in implementing it. Time was also devoted to enhancing or implementing a variety of film characterization systems and device testing facilities. A new system for transient spectroscopy on the ablation plume provided important new information on the physical mechanisms of LDPVD. The measurements show that, e.g., Cd is predominantly in the neutral atomic state in the plume but with a fraction that is highly excited internally (greater than or equal to 6 eV), and that the typical neutral Cd translational kinetic energies perpendicular to the target are 20 eV and greater. DOE

N92-28383# Naval Postgraduate School, Monterey, CA.
ARCJET PLUME IONIZATION EFFECTS ON EXPOSED SOLAR ARRAY CONDUCTING SURFACES M.S. Thesis
Richard W. Evert Sep. 1991 71 p
(AD-A245912) Avail: NTIS HC/MF A04

High efficiency arcjet propulsion will be used in the near future for satellite orbit adjustment and eventually for orbit transfer. Testing is currently being conducted to explore spacecraft interface difficulties with this method of propulsion. This thesis looks at one aspect of this interface. Since most earth orbiting spacecraft use solar arrays for power generation, it is of interest to investigate how exposed, biased conducting surfaces will interact with the slightly ionized plume environment of the arcjet thruster. It was found that with the arcjet thruster mounted 25.4 cm above the solar array, firing along its axis at a 20 degree cant angle, electrical currents were indeed collected. The effect of having a constricted area exposed to the plume was to increase the current density. The electron densities at typical solar array distances were found to be 10 to the 10th to 10 to the 12th power/cu.m. An estimate of the total power lost for an array in this configuration showed that 0.05 percent of the overall power is lost due to collected currents. GRA

N92-28422# Department of Energy, Washington, DC. Geothermal Div.
GEOTHERMAL PROGRESS MONITOR, REPORT NO. 13
Feb. 1992 79 p
(DE92-010697; DOE/CE-0532) Avail: NTIS HC/MF A05

Geothermal Progress Monitor (GPM) Issue No. 13 documents that most related factors favor the growth and geographic expansion of the US geothermal industry and that the industry is being technologically prepared to meet those challenges into the next century. It is the function of GPM to identify trends in the use of this resource and to provide a historical record of its development pathway. The information assembled for this issue of GPM indicates that trends in the use of geothermal energy in this country and abroad continue to be very positive. Favorable sentiments as well as pertinent actions on the part of both government and industry are documented in almost every section. The FEDERAL BEAT points up that the National Energy Strategy (NES) developed at the highest levels of the US government recognizes the environmental and energy security advantages of renewable energy, including geothermal, and makes a commitment to 'substantial diversification' of US sources of energy. With the announcement of the construction of several new plants and plant expansions, the INDUSTRY SCENE illustrates industry's continued expectation that the use of geothermal energy will prove profitable to investors. In DEVELOPMENT STATUS, spokesmen for both an investor-owned utility and a major geothermal developer express strong support for geothermal power, particularly emphasizing its environmental advantages. DEVELOPMENT STATUS also reports that early successes have been achieved by joint DOE/industry R & D at The Geysers which will have important impacts on the future management of this mature field. Also there is increasing interest in hot dry rock. Analyses conducted in support of the NES indicate that if all the postulated technology developments occur in this field, the price of energy derived from hot dry rock in the US could drop. DOE

N92-28837*# National Aeronautics and Space Administration. Lewis Research Center, Cleveland, OH.
NASA LEWIS STIRLING SPRE TESTING AND ANALYSIS WITH REDUCED NUMBER OF COOLER TUBES
Wayne A. Wong, James E. Cairelli, Diane M. Swec, Thomas J. Doeberling, Thomas F. Lakatos, and Frank J. Madi (Sverdrup Technology, Inc., Brook Park, OH.) Aug. 1992 9 p Proposed for presentation at the 27th Intersociety Conversion Engineering Conference, San Diego, CA, 3-7 Aug. 1992; sponsored by SAE, AIAA, ASME, IEEE, ACS, AIChE, and ANS
(RTOP 590-13-11)
(NASA-TM-105767; E-7184; NAS 1.15:105767) Avail: NTIS HC/MF A02

Free-piston Stirling power converters are candidates for high capacity space power applications. The Space Power Research Engine (SPRE), a free-piston Stirling engine coupled with a linear alternator, is being tested at the NASA Lewis Research Center in support of the Civil Space Technology Initiative. The SPRE is used as a test bed for evaluating converter modifications which have the potential to improve the converter performance and for validating computer code predictions. Reducing the number of cooler tubes on the SPRE has been identified as a modification with the potential to significantly improve power and efficiency. Experimental tests designed to investigate the effects of reducing the number of cooler tubes on converter power, efficiency and dynamics are described. Presented are test results from the converter operating with a reduced number of cooler tubes and comparisons between this data and both baseline test data and computer code predictions. Author

N92-28863*# New Mexico Univ., Albuquerque. Dept. of Chemical and Nuclear Engineering.
NATURAL CIRCULATION DECAY HEAT REMOVAL FROM AN SP-100, 550 kWe POWER SYSTEM FOR A LUNAR OUTPOST Final Report
Mohamed S. El-Genk and Huimin Xue Jun. 1992 88 p
(Grant NAG3-992)
(NASA-CR-190421; NAS 1.26:190421; UNM-ISNPS-4-92) Avail: NTIS HC/MF A05

This research investigated the decay heat removal from the SP-100 reactor core of a 550-kWe power system for a lunar outpost by natural circulation of lithium coolant. A transient model that simulates the decay heat removal loop (DHRL) of the power system was developed and used to assess the system's decay heat removal capability. The effects of the surface area of the decay heat rejection radiator, the dimensions of the decay heat exchanger (DHE) flow duct, the elevation of the DHE, and the diameter of the rise and down pipes in the DHRL on the decay heat removal capability were examined. Also, to determine the applicability of test results at earth gravity to actual system performance on the lunar surface, the effect of the gravity constant (1 g and 1/6 g) on the thermal behavior of the system after shutdown was investigated. Author

N92-28974# State Univ. of New York, Buffalo. Dept. of Chemistry.
ELECTROCHEMICAL STUDIES OF LEWIS ACID-BASE SYSTEMS FOR USE IN THERMALLY REGENERABLE FUEL CELLS Final Report, 30 Apr. 1989 - 31 Dec. 1991
Robert A. Osteryoung 12 Feb. 1992 7 p
(Contract N00015-89-K-0056)
(AD-A246457) Avail: NTIS HC/MF A02

Electrochemical, NMR, and FT-IR studies in an ambient temperature chloroaluminate molten salt, consisting of 1-methyl 3-ethylimidazolium chloride, ImCl, mixed with aluminum chloride, are summarized. This work was related to the development of a thermally regenerative fuel cell. Particular emphasis was placed on studies of proton in the molten salt system and physical properties of imidazolium hydrogen dichloride, ImHCl2. GRA

N92-29143* National Aeronautics and Space Administration. Lewis Research Center, Cleveland, OH.
SOLAR THERMAL ENERGY RECEIVER Patent

Karl W. Baker, inventor (to NASA) and Miles O. Dustin, inventor (to NASA) 19 May 1992 9 p Filed 27 Mar. 1991 Supersedes N91-23617 (29 - 15, p 2457)
(NASA-Case-LEW-14949-1; US-Patent-5,113,659; US-Patent-Appl-SN-676910; US-Patent-Class-60-641.8; US-Patent-Class-60-659; US-Patent-Class-126-433; US-Patent-Class-126-436; Int-Patent-Class-F03G-6/00) Avail: US Patent and Trademark Office

A plurality of heat pipes in a shell receive concentrated solar energy and transfer the energy to a heat activated system. To provide for even distribution of the energy despite uneven impingement of solar energy on the heat pipes, absence of solar energy at times, or failure of one or more of the heat pipes, energy storage means are disposed on the heat pipes which extend through a heat pipe thermal coupling means into the heat activated device. To enhance energy transfer to the heat activated device, the heat pipe coupling cavity means may be provided with extensions into the device. For use with a Stirling engine having passages for working gas, heat transfer members may be positioned to contact the gas and the heat pipes. The shell may be divided into sections by transverse walls. To prevent cavity working fluid from collecting in the extensions, a porous body is positioned in the cavity.

Official Gazette of the U.S. Patent and Trademark Office

45 ENVIRONMENT POLLUTION

Includes atmospheric, noise, thermal, and water pollution.

N92-28272# Aerospace Corp., El Segundo, CA.
REACTIONS OF HYDRAZINES WITH CHEMICALS FOUND IN ENVIRONMENT
Henry S. Judeikis and Donald E. Damschen 24 Jan. 1992 24 p
(Contract F04701-88-C-0089)
(AD-A247064; TR-0091(6448)-1; SSD-TR-92-03) Avail: NTIS HC/MF A03

Reactions of hydrazine, monomethylhydrazine and unsymmetrical dimethylhydrazine with selected species of interest that are found in the environment have been investigated. Included are aqueous phase reactions that can occur in atmospheric aerosols, groundwater, or soils in contact with groundwater, as well as selected gas phase reactions. Reactants include oxygen and hydrogen peroxide (both reactants in the presence and absence of catalysts), ozone, nitrous acid, sulfur dioxide, and acetone (as a model for environmental ketones and aldehydes). Rate constants for the reactions have been determined, or upper limits set. In several instances, reaction products have been identified. By far, the fastest reactions measured were those involving the hydrazines and ozone with (second-order) rate constants up to 2.4 x 107 liter/mole-sec. GRA

N92-28811# Edgerton, Germeshausen and Grier, Inc., Idaho Falls, ID.
MONITORING ACTIVITIES REVIEW OF THE RADIOLOGICAL ENVIRONMENTAL SURVEILLANCE PROGRAM
P. D. Ritter Mar. 1992 37 p
(Contract DE-AC07-76ID-01570)
(DE92-013103; EGG-ESQ-10167) Avail: NTIS HC/MF A03

The 1992 Monitoring Activities Review (MAR) is directed at the Radiological Environment Surveillance Program (RESP) activities at the Radioactive Waste Management Complex (RWMC) of Idaho Engineering Laboratory (INEL). MAR panelists studied RESP documents and discussed their concerns with Environmental Monitoring Unit (EMU) staff and other panel members. These concerns were subsequently consolidated into a collection of recommendations with supporting discussions. Recommendations focus on specific monitoring activities, as well as the overall program. The MAR report also contains pertinent comments that should not require further action. DOE

N92-29173# Princeton Univ., NJ. Dept. of Chemical Engineering.
RECENT ADVANCES IN GLOBAL OPTIMIZATION Final Report, 1 Jan. - 31 Dec. 1991
C. A. Floudas and P. M. Pardalos 31 Dec. 1991 7 p
(Grant AF-AFOSR-0116-91)
(AD-A250211; AFOSR-92-0354TR) Avail: NTIS HC/MF A02

The conference, Recent Advances In Global Optimization, took place during May 10-11, 1991 at Princeton University. It was organized by Professor C.A. Floudas (Princeton University) and P.M. Pardalos (Penn State) and supported by AFOSR under grant AFOSR-91-0116. The conference was very successful and attracted researchers with interests in applied mathematics, computer sciences, operations research, chemical, civil, mechanical and electrical engineering, biochemistry and chemistry. It represents the first truly international conference devoted exclusively on the subject of global optimization. There were 80 participants from the USA, Germany, Finland, Italy, France, Vietnam, Russia, Canada, Portugal and Mexico. Princeton University recently published a book (Eds. Floudas and Pardalos) with the referred papers presented at the conference, and the Journal of Global Optimization is going to devote two issues on selected papers of this conference. GRA

N92-29183# Systems Applications International, San Rafael, CA.
REGIONAL ENVIRONMENTAL IMPACTS OF METHANOL-FUELED VEHICLES Final Report
T. Belian, R. E. Morris, M. P. Ligocki, and G. Z. Whitten 27 Dec. 1991 238 p Sponsored in part by Coordinating Research Council, Inc., Atlanta, GA
(PB92-176569; SYSAPP-91/151) Avail: NTIS HC/MF A11

The objectives of the study were to obtain, through simulation modeling, preliminary estimates of the regional environmental impacts methanol-fueled vehicles and to estimate the sensitivity of the model to important parameters and assumptions that affect the calculation of the impacts. The regional environmental effects of the use of M85 fuel (85 percent methanol and 15 percent gasoline) and M100 (neat methanol) relative to gasoline (an indoline blend) were estimated using a Lagrangian (trajectory) acid deposition model. The Comprehensive Chemistry Acid Deposition Model (CCADM), contains a detailed treatment of gas-phase and aqueous-phase chemistry and associated mass transfer, but provides for a less comprehensive representation of advection and diffusion. Two different meteorological regimes were analyzed: clear sky conditions and cloudy skies with a rain event. The study also included a review of gas- and aqueous-phase chemistry, with particular emphasis on methanol. The CCADM chemical mechanism was updated to include state-of-the-science (as 0f 1990) gas- and aqueous-phase chemistry including methanol chemistry. The CCADM was then used to analyze the regional environmental impacts from the use of methanol fuels. In performing such as an analysis it was necessary to make several assumptions. The sensitivity of the analysis was examined through a series of simulations that varied key input parameters within their ranges of uncertainty. Author

46 GEOPHYSICS

Includes aeronomy; upper and lower atmosphere studies; ionospheric and magnetospheric physics; and geomagnetism.

For space radiation see *93 Space Radiation.*

N92-28257# Texas Univ., El Paso. Dept. of Geological Sciences.
A SEISMIC AND INTEGRATED GEOPHYSICAL STUDY OF THE LITHOSPHERE OF THE COLORADO PLATEAU Final Report, 1 Jun. 1989 - 30 Sep. 1991
G. Randy Keller, Mark R. Baker, Diane I. Doser, and Juan H. Hinojosa 30 Nov. 1991 102 p

(Contract F49620-89-C-0076)
(AD-A247091; AFOSR-92-0009TR) Avail: NTIS HC/MF A06

The major effort of this project was field data collection, data processing, and interpretation for the Pacific to Arizona Crustal Experiment (PACE) seismic experiment. The massive data set gathered during this experiment have been analyzed by a variety of techniques. The results show a gradual thickening of the crust from about 30 km in the Basin and Range to about 40 km along the southwestern margin of the Colorado Plateau. Lateral variations along the transition zone were found to be small. Work along a long profile extending from the Nevada Test Site to White Sands Missile Range included collection of new data, waveform modeling of data from the Albuquerque, NM digital seismograph station and a crustal structure study of western New Mexico. These results document: thin (approximately 35 km) crust beneath the central portion of the Rio Grande rift; extension of the lithospheric anomaly associated with this rift well east of the physiographic rift valley; a broad transitional zone to thick crust on the western margin of the rift; and delineation of a batholithic mass in the upper crust of western New Mexico. GRA

N92-28319# Naval Postgraduate School, Monterey, CA.
AN ANALYSIS OF MIDDLE ULTRAVIOLET DAYGLOW SPECTRA M.S. Thesis
Billie S. Walden Dec. 1991 231 p
(AD-A245965) Avail: NTIS HC/MF A11

Middle ultraviolet spectra from 1800 to 3400A are analyzed. These spectra were obtained from the March 1990 rocket flight of the NPS MUSTANG instrument over the altitudes 105km to 315km. The data were compared with computer generated synthetic spectra. A least squares fitting procedure was developed for this purpose. Each data point was weighted using the standard deviation of the means. Synthetic spectra were generated for the following emissions: N2 Vegard-Kaphan; N2 Lyman-Birge-Hopfield; NO gamma, delta, and epsilon; OI 2972A, OII 2470A; and NII 2143A. Altitude profiles for the emissions were obtained. Tentative identification was made of the OIII 2853A emission. A comparison of VK and LBH profiles demonstrates the process of N2 A-state quenching by atomic oxygen. GRA

N92-28386# California Univ., Santa Cruz. Inst. of Tectonics.
ANALYSIS OF THE EFFECTS OF EURASIAN CRUSTAL AND UPPER MANTLE STRUCTURE ON REGIONAL PHASES USING BROADBAND SEISMIC DATA
Susan Schwartz and Thorne Lay 25 Oct. 1991 46 p
(Contract F19628-90-K-0041)
(AD-A248383; PL-TR-91-2281; AD-E200947; SR-1) Avail: NTIS HC/MF A03

This study represents the results of the first phase of a two year investigation of the effects of upper mantle structure on the propagation of regional phases. The first year of effort has been directed at improving the understanding of the PP phase observed at upper mantle distances, and developing a methodology by which this phase can be used to map out large-scale variations in uppermost mantle velocity gradients and absolute velocity levels. There was quite a success in quantifying the complex wavefield associated with PP, and a preliminary application of PP waveform analysis across the North American continent, where there is lots of independent knowledge of the structure with which to assess the resulting models, is presented. The next effort will be directed at application of the new methodology to mapping lid structure variations in Eurasia, combined with assessment of how these lid variations influence regional phase propagation and the behavior of various discriminant procedures such as Pn/Lg spectral behavior. GRA

N92-28394# Colorado Univ., Boulder.
STUDIES OF REGIONAL WAVE PROPAGATION USING DIFFERENTIAL SEISMOGRAMS AND RANDOMIZED STRUCTURAL MODELS Final Report, 1 Mar. 1990 - 1 Mar. 1991
Danny J. Harvey 7 May 1991 37 p
(Contract F19628-90-K-0023)
(AD-A247011; AD-E200869; PL-TR-91-2126) Avail: NTIS HC/MF A03

In order to improve our abilities to discriminate low yield nuclear explosions and to obtain accurate yield estimates, a study has been undertaken to infer detailed source and structural parameters by direct inversion of broad band seismic data using laterally homogeneous forward modeling methods. Three key problems have been identified which must be solved: the development of an accurate and efficient algorithm for computing differential seismograms, which are necessary for the inversion procedure, the development of better methods for incorporating anelastic attenuation into modal synthesis computations, and the determination of starting solutions that will produce synthetic seismograms which have the same general characteristics that we see in the data. An exact differential seismogram algorithm has been developed and implemented which produces accurate differential seismograms at arbitrary frequencies and phase velocities. An exact complex pole based algorithm has been developed to account for anelastic attenuation. A new representation of earth upper mantle and crustal structure has been used which provides an explainable, plausible and implementable method for modeling the features that we see in regional broad band data. GRA

N92-28567# Pennsylvania State Univ., University Park. Dept. of Meteorology.
SAR-RELATE STRESS VARIABILITY IN THE MARINE ATMOSPHERIC BOUNDARY LAYER (MABL)
Hampton N. Shirer and George S. Young 1992 8 p
(AD-A247772) Avail: NTIS HC/MF A02

By stressing the sea surface, the marine atmospheric boundary layer (MABL) wind field can alter the sea surface wave field and so can produce discernable signatures on Synthetic Aperture Radar images of the ocean. Among the resulting signatures, the quasi-linear and cellular microscale patterns still require adequate explanation. The ubiquitous MABL two- and three-dimensional convective circulations provide promising candidates for the forcing phenomena producing these signatures. These microscale circulations have horizontal wavelengths on the order of one to ten times the boundary layer depth, or approximately one to ten km, and temporal scales on the order of one to ten hours. Thus, they produce stress variations on the spatial and temporal scales of the quasi-linear and cellular SAR signatures. The goal is to develop methods of diagnosing both the form of MABL convection and its effect on the sea surface stress variability patterns given only the values of the large-scale meteorological and oceanographic parameters. As briefly summarized below, we are making good progress on this problem in several interacting, complementary ways, which range from data analysis to model development. GRA

N92-28569# Royal Norwegian Council for Scientific and Industrial Research, Kjeller.
NORSAR BASIC SEISMOLOGICAL RESEARCH
Svein Mykkeltveit 29 Nov. 1991 72 p
(Contract F49620-89-C-0038)
(AD-A248616; PL-TR-92-2005; AD-E200950; SR-11) Avail: NTIS HC/MF A04

This annual report describes the work accomplished during the period 1 October 1990-30 September 1991. The inversion of NORSAR travel time data constituted one of the first examples of seismic tomography. It is now becoming apparent that these data are influenced by wave diffraction effects, and hence that ordinary (ray based) tomography may be inadequate. A newly developed tomographic method that takes diffraction effects into account is applied. Data from the NORSAR array in its original form (22 subarrays; aperture 100 km) have been used and results are compared with those of the ray-based inversion experiments undertaken around 15 years ago. To facilitate comparison with earlier results, we inverted for velocity structure in the same boxlike structure as was used on the previous investigations. Discriminating between earthquakes and underground explosions is formulated

as an exercise in pattern recognition approach analysis. The analysis has been applied to a learning set of 44 nuclear explosions (8 test sites) and 35 earthquakes in Eurasia recorded at the NORESS array. The signal features considered were the normalized power in 8 spectral bands in the 0.2-5.0 Hz range of the P-wave (6 sec) and the P-coda (30 sec). Physically, it means that we exploit potential differences in the shape of earthquake and explosion spectra, respectively. Other features included are peak P and P-coda amplitude frequencies and relative P/P-coda power. GRA

N92-28587*# Lunar and Planetary Inst., Houston, TX.
WORKSHOP ON THE PHYSICS AND CHEMISTRY OF MAGMA OCEANS FROM 1 BAR TO 4 MBAR
Carl B. Agee, ed. (Harvard Univ., Cambridge, MA.) and John Longhi, ed. (Lamont-Doherty Geological Observatory, Palisades, NY.) 1992 85 p Workshop held in Burlingame, CA, 6-8 Dec. 1991; sponsored by NASA. Johnson Space Flight Center and LPI
(Contract NASw-4574)
(NASA-CR-190419; NAS 1.26:190419; LPI-TR-92-03) Avail: NTIS HC/MF A05

Evidence for the existence of magma oceans is discussed in great detail, and among the many new items introduced were high-pressure phase equilibrium experiments, calculations of depth of impact-produced melting, models incorporating crystal growth rates with degree of crystallinity and convection, and models of hard turbulent convection. It was agreed that before we can point to some present-day observable parameters and confidently establish the existence of magma oceans, we must learn much more about their phase equilibria and solidification dynamics. For individual titles, see N92-28588 through N92-28619.

N92-28588*# Nagoya Univ. (Japan). Water Research Inst.
THERMAL EVOLUTION AND CHEMICAL DIFFERENTIATION OF THE TERRESTRIAL MAGMA OCEAN
Y. Abe *In* Lunar and Planetary Inst., Workshop on the Physics and Chemistry of Magma Oceans from 1 Bar to 4 Mbar 1992 p 9-10 (For primary document see N92-28587 19-46)
Avail: NTIS HC/MF A05

The release of gravitational energy resulted in global melting and formation of a magma ocean during accretion of the Earth. Although it is believed that the formation of the magma ocean resulted in gravitational differentiation of melt and solid, the differentiation might be disturbed by the following processes: (1) convective mixing; (2) cooling and solidification; and (3) growth of the earth, which results in secular increase of pressure, and stirring by planetesimal impacts. The purpose of this study is to investigate the differentiation processes of the terrestrial magma ocean by taking into account various disturbing processes. Author

N92-28589*# Harvard Univ., Cambridge, MA. Dept. of Earth and Planetary Sciences.
HIGH-PRESSURE MELTING OF CARBONACEOUS CHONDRITE Abstract Only
Carl B. Agee *In* Lunar and Planetary Inst., Workshop on the Physics and Chemistry of Magma Oceans from 1 Bar to 4 Mbar 1992 p 11-12 (For primary document see N92-28587 19-46)
Avail: NTIS HC/MF A05

Phase equilibria experiments investigating the melting and differentiation of the primordial Earth require a realistic 'initial' chemical composition. Carbonaceous chondrites are good analogues for the initial bulk chemical composition of an accreting early Earth because they contain approximately solar abundances of the non-volatile elements and are the most primitive objects yet sampled in the solar system. Author

N92-28590*# California Inst. of Tech., Pasadena. Lab. of Experimental Geophysics.
A MAGMA OCEAN AND THE EARTH'S INTERNAL WATER BUDGET Abstract Only
Thomas J. Ahrens *In* Lunar and Planetary Inst., Workshop on the Physics and Chemistry of Magma Oceans from 1 Bar to 4 Mbar 1992 p 13-14 (For primary document see N92-28587 19-46)
Avail: NTIS HC/MF A05

There are lines of evidence which relate bounds on the primordial water content of the Earth's mantle to a magma ocean and the accompanying Earth accretion process. We assume initially (before a magma ocean could form) that as the Earth accreted, it grew from volatile- (H_2O, CO_2, NH_3, CH_4, SO_2, plus noble) gas-rich planetesimals, which accreted to form an initial 'primitive accretion core' (PAC). The PAC retained the initial complement of planetesimal gaseous components. Shock wave experiments in which both solid, and more recently, the gaseous components of materials such as serpentine and the Murchison meteorite have demonstrated that planetesimal infall velocities of less than 0.5 km/sec, induce shock pressures of less than 0.5 GPa and result in virtually complete retention of planetary gases. Author

N92-28591*# Academy of Sciences (USSR), Moscow. Inst. of Geochemistry.
EXPERIMENTAL DETERMINATION OF THE SOLUBILITY OF IRIDIUM IN SILICATE MELTS: PRELIMINARY RESULTS Abstract Only
Alexander Borisov, Donald B. Dingwell (Bayreuth Univ., Germany, F.R.), Hugh St.C. ONeill (Bayreuth Univ., Germany, F.R.), and Herbert Palme (Max-Planck-Inst. fuer Chemie, Mainz, Germany, F.R.) *In* Lunar and Planetary Inst., Workshop on the Physics and Chemistry of Magma Oceans from 1 Bar to 4 Mbar 1992 p 15-16 (For primary document see N92-28587 19-46)
Avail: NTIS HC/MF A05

Little is known of the geochemical behavior of iridium. Normally this element is taken to be chalcophile and/or siderophile so that during planetary differentiation processes, e.g., core formation, iridium is extracted from silicate phases into metallic phases. Experimental determination of the metal/silicate partition coefficient of iridium is difficult simply because it is so large. Also there are no data on the solubility behavior of iridium in silicate melts. With information on the solubility of iridium in silicate melts it is possible, in combination with experimental data for Fe-Ir alloys, to calculate the partition coefficient between a metallic phase and a silicate melt. Author

N92-28592*# Arizona Univ., Tucson. Lunar and Planetary Lab.
Mg-PEROVSKITE/SILICATE MELT AND MAGNESIOWUESTITE/SILICATE MELT PARTITION COEFFICIENTS FOR KLB-1 AT 250 KBARS Abstract Only
Michael J. Drake, David C. Rubie (Bayreuth Univ., Germany, F.R.), and Elisabeth A. McFarlane *In* Lunar and Planetary Inst., Workshop on the Physics and Chemistry of Magma Oceans from 1 Bar to 4 Mbar 1992 p 17-18 (For primary document see N92-28587 19-46)
Avail: NTIS HC/MF A05

The partitioning of elements amongst lower mantle phases and silicate melts is of interest in unraveling the early thermal history of the Earth. Because of the technical difficulty in carrying out such measurements, only one direct set of measurements was reported previously, and these results as well as interpretations based on them have generated controversy. Here we report what are to our knowledge only the second set of directly measured trace element partition coefficients for a natural system (KLB-1). Author

N92-28593*# Cologne Univ. (Germany, F.R.). Inst. fuer Geophysik und Meteorologie.
THE ROLE OF HARD TURBULENT THERMAL CONVECTION IN THE EARTH'S EARLY THERMAL EVOLUTION Abstract Only
Ulli Hansen, David A. Yuen (Minnesota Univ., Minneapolis.), Wuling Zhao (Minnesota Univ., Minneapolis.), and Andrei V. Malevsky (Minnesota Univ., Minneapolis.) *In* Lunar and Planetary Inst., Workshop on the Physics and Chemistry of Magma Oceans from 1 Bar to 4 Mbar 1992 p 19 (For primary document see N92-28587 19-46)
Avail: NTIS HC/MF A05

In the last several years great progress was made in the study of a new transition in thermal convection, called hard turbulence. Initial experiments were conducted with helium gas, then with water. It was shown that for base-heated Newtonian convection a transition occurred at Rayleigh numbers between 10(exp 7) and 10(exp 8). This transition is characterized by the appearance of disconnected plume structures in contrast to continuous plumes with mushroom-shaped tops found for lower Rayleigh numbers. This new hydrodynamic transition is expected to play an important role in reshaping our concepts of mantle convection in the early stages of planetary evolution. We have conducted two-dimensional calculations for large and small aspect-ratio configuration to see whether such a transition would take place for infinite Prandtl number fluids. Author

N92-28594*# Lunar and Planetary Inst., Houston, TX.
THE DISTRIBUTION OF ANORTHOSITE ON THE NEARSIDE OF THE MOON Abstract Only **c91**
B. R. Hawke (Hawaii Univ., Honolulu.), P. G. Lucey (Hawaii Univ., Honolulu.), G. J. Taylor (Hawaii Univ., Honolulu.), and P. D. Spudis *In its* Workshop on the Physics and Chemistry of Magma Oceans from 1 Bar to 4 Mbar 1992 p 20-21 (For primary document see N92-28587 19-46)
Avail: NTIS HC/MF A05

Remote sensing studies of lunar basin and crater deposits were conducted in order to determine the composition of surface units and to investigate the stratigraphy of the lunar crust. These studies have combined both visible and near-IR spectral observations with multispectral imaging in order to determine the lithology of relatively small portions (2-10 km) of the lunar surface. Numerous deposits of pure anorthosite (plagioclase greater than 90 percent) were identified and an interesting pattern has emerged. The purposes of this report are as follows: (1) to summarize the results of our previous studies of the distribution of anorthosite; (2)to present new findings concerning the modes of occurrence of lunar anorthosite; and (3) to assess the implication for the magma ocean hypothesis. Author

N92-28595*# Rutgers - The State Univ., New Brunswick, NJ. Dept. of Geological Sciences.
PHASE EQUILIBRIA AND TRACE ELEMENT PARTITIONING IN A MAGMA OCEAN TO 260 KILOBARS Abstract Only
Claude Herzberg *In* Lunar and Planetary Inst., Workshop on the Physics and Chemistry of Magma Oceans from 1 Bar to 4 Mbar 1992 p 22-23 (For primary document see N92-28587 19-46)
Avail: NTIS HC/MF A05

A magma ocean can solidify in a way that is intermediate between perfect equilibrium and perfect fractional crystallization. In order to model quantitatively any fractional crystallization scenario, it is necessary to understand the geochemical characteristics of the phases that crystallize from a magma ocean, and how they vary with pressure. The crystallizing phase is called the liquidus phase, and their identities were determined by numerous experiments utilizing the multianvil apparatus. For chondritic compositions the liquidus phases are as follows: olivine at 1 atmosphere to 100 kilobars; garnet from 100 to about 260 kilobars; silicate perovskite from 260 kilobars to possibly the core-mantle boundary in the Earth. Author

N92-28596*# Arizona Univ., Tucson. Lunar and Planetary Lab.
ORIGIN OF THE MOON AND LUNAR CORE FORMATION Abstract Only **c91**
Valerie J. Hillgren *In* Lunar and Planetary Inst., Workshop on the Physics and Chemistry of Magma Oceans from 1 Bar to 4 Mbar 1992 p 24-25 (For primary document see N92-28587 19-46)
Avail: NTIS HC/MF A05

In a recent version of the giant impact hypothesis by O'Neill, the initial abundances of the siderophile elements in the lunar mantle were established not only by combining impactor material and proto-Earth material, but also by adding a late reduced veneer. O'Neal also appealed to the possible volatilities of some elements (Mo and W) under conditions of lunar accretion, and required the segregation of a small Ni-rich metallic core. An attempt to more rigorously model lunar core formation in the O'Neill scenario is made by correlating degree of partial melting to temperature and extrapolating the 1260 C partition coefficients to the appropriate temperatures along a constant redox buffer. Author

N92-28597*# Lunar and Planetary Inst., Houston, TX.
SUPERHEAT IN MAGMA OCEANS Abstract Only
Petr Jakes *In its* Workshop on the Physics and Chemistry of Magma Oceans from 1 Bar to 4 Mbar 1992 p 26-27 Prepared in cooperation with Houston Univ., TX (For primary document see N92-28587 19-46)
Avail: NTIS HC/MF A05

The existence of 'totally molten' planets implies the existence of a superheat (excess of heat) in the magma reservoirs since the heat buffer (i.e., presence of crystals having high latent heat of fusion) does not exist in a large, completely molten reservoir. Any addition of impacting material results in increase of the temperature of the melt and under favorable circumstances heat is stored. The behavior of superheat melts is little understood; therefore, we experimentally examined properties and behavior of excess heat melts at atmospheric pressures and inert gas atmosphere. Highly siliceous melts (70 percent SiO2) were chosen for the experiments because of the possibility of quenching such melts into glasses, the slow rate of reaction in highly siliceous composition, and the fact that such melts are present in terrestrial impact craters and impact-generated glasses. Results from the investigation are presented. Author

N92-28598*# Washington Univ., Saint Louis, MO. Dept. of Earth and Planetary Sciences.
A NEW ANGLE ON LUNAR FERROAN-SUITE DIFFERENTIATION Abstract Only **c91**
B. L. Jolliff *In* Lunar and Planetary Inst., Workshop on the Physics and Chemistry of Magma Oceans from 1 Bar to 4 Mbar 1992 p 28-29 (For primary document see N92-28587 19-46) (Grant NAG9-56)
Avail: NTIS HC/MF A05

Small fragments of rock found among soil particles in sample 67513 from Station 11 on the southern rim of North Ray Crater at Apollo 16 yield information regarding the mafic, ferroan rocks from which they drive. We have identified a set of particles that have distinctive trace element geochemistry and whose bulk and mineral compositions indicate a genetic relationship to one another. These include polymict as well as monomict lithologies. Igneous members range from fragments with abundant anorthite to some with abundant exsolved pigeonite and augite. Consideration of this set of rock fragments, combined with mafic ferroan clasts from large breccias and from lunar-highlands meteorites suggests that there may be separate differentiation trends within the ferroan suite which are subparallel and which are less steem in Fe-Mg vs. An fractionation that the vertical trend obtained when the entire ferroan suite is taken together. This may result from a complex magma system with isolated reservoirs or separate, independently evolving magmas. Mineral compositional and textural variations are consistent with a model set forth by Longhi and Boudreau wherein the anorthite-rich samples reflect adcumulus growth with mafic crystals forming only from trapped liquid, and the more mafic samples by anorthite and pyroxene orthocumulate development. Author

N92-28599*# National Aeronautics and Space Administration. Lyndon B. Johnson Space Center, Houston, TX.
ESTIMATION OF HIGH TEMPERATURE METAL-SILICATE PARTITION COEFFICIENTS Abstract Only
John H. Jones, Christopher J. Capobianco (Arizona Univ., Tucson.), and Michael J. Drake (Arizona Univ., Tucson.) *In* Lunar and Planetary Inst., Workshop on the Physics and Chemistry of Magma Oceans from 1 Bar to 4 Mbar 1992 p 30-32 (For primary document see N92-28587 19-46)
Avail: NTIS HC/MF A05

It has been known for some time that abundances of siderophile

elements in the upper mantle of the Earth are far in excess of those expected from equilibrium between metal and silicate at low pressures and temperatures. Murthy (1991) has re-examined this excess of siderophile element problem by estimating liquid metal/liquid silicate partition coefficients reduces from their measured values at a lower temperature, implying that siderophile elements become much less siderophilic at high temperatures. Murthy then draws the important conclusion that metal/silicate equilibrium at high temperatures can account for the abundances of siderophile elements in the Earth's mantle. Of course, his conclusion is critically dependent on the small values of the partition coefficients he calculates. Because the numerical values of most experimentally-determined partition coefficients increase with increasing temperature at both constant oxygen fugacity and at constant redox buffer, we think it is important to try an alternative extrapolation for comparison. We have computed high temperature metal/silicate partition coefficients under a different set of assumptions and show that such long temperature extrapolations yield values which are critically dependent upon the presumed chemical behavior of the siderophile elements in the system.

Author

N92-28600*# California Univ., Los Angeles. Dept. of Earth and Space Sciences.

MAGMA OCEAN: MECHANISMS OF FORMATION Abstract Only

W. M. Kaula *In* Lunar and Planetary Inst., Workshop on the Physics and Chemistry of Magma Oceans from 1 Bar to 4 Mbar 1992 p 33 (For primary document see N92-28587 19-46)

Avail: NTIS HC/MF A05

The thermal state of the Earth at the time relevant to formation of a magma ocean was dominated by the great impact that created the Moon. As shown in computer experiments, the iron in the impacting bodies quickly sank to the core of the proto-Earth, while a significant fraction of silicates was pushed far enough out beyond the geosynchronous limit to constitute the main material of the Moon. Most of any atmosphere would have been pushed aside, rather than being expelled in the impact. However, the energy remaining in the material not going to the core or expelled was still sufficient to raise its temperature some 1000's of degrees, enough to vaporize silicates and to generate a strong 'planetary wind': a hydrodynamic expansion carrying with it virtually all volatiles plus appreciable silicates. This expansion was violent and uneven in its most energetic stage, but probably the resulting magma ocean was global. The duration, until cooling, was sufficient for silicates to condense to melt and the duration was probably short. Comparison of the Earth and Venus indicates that the great impact was extraordinarily effective in removing volatiles from the proto-Earth; in particular, the enormous differences in primordial inert gases between the planets demand a catastrophic difference in origin circumstances. On the other hand, the comparison limits the amount of silicates lost by the Earth to a rather minor fraction; most of that expelled in the wind must have condensed soon enough for the silicate to fall back to Earth or be swept up by the proto-Moon. So the Earth was left with a magma ocean. The question is whether sufficient water was retained to constitute a steam atmosphere. Probably not, but unknowns affecting this question are the efficiencies of outgassing in great impacts and in subsequent convective churnings deep in the mantle. During the stage when mantle convection is turbulent, an appreciable fraction of volatiles were also retained at depth, perhaps in some mineral phases not yet well-defined. We still have primordial helium being outgassed.

Author

N92-28601*# Arizona Univ., Tucson. Lunar and Planetary Lab.

Mg-PEROVSKITE/SILICATE MELT PARTITION COEFFICIENTS IN THE CMS SYSTEM AT 2430 C AND 226 KBARS Abstract Only

Elisabeth A. McFarlane, Michaei J. Drake, and Tibor Gasparik (State Univ. of New York, Stony Brook.) *In* Lunar and Planetary Inst., Workshop on the Physics and Chemistry of Magma Oceans from 1 Bar to 4 Mbar 1992 p 34-35 (For primary document see N92-28587 19-46)

Avail: NTIS HC/MF A05

The partitioning of elements among lower mantle phases and silicate melts is of interest in unraveling the early thermal history of the Earth. Because of the technical difficulty in carrying out such measurements, only one direct set of measurements has been reported, and these results as well as interpretations based on them have generated controversy. The first set of direct measurements on a synthetic system in the CaO-MgO-SiO2 (CMS) is reported. An experiment was conducted at Stony Brook, using the USSA-2000 split sphere anvil apparatus. An experiment in the CMS system doped with oxides of Al, Ti, Sc, and Sm and run at a nominal temperature of 2380 C and pressure of 226 kbars is reported. Nominal temperatures were measured with a W 3 percent Re/W 25 percent Re thermocouple. The hot spot temperature, where the liquidus is located, is estimated to be at 2430 C. A 10 mm MgO octahedron was used in concert with 4 mm truncation edge lengths on the WC cubes. The sample was contained in a Re capsule which was inserted into a LaCrO3 furnace. Pressure was calibrated at 2000 C. Run duration was approximately 3 minutes. The charge was mounted in epoxy and analyzed using a CAMECA SX-50 electron microprobe. Standard operating conditions were employed, although counting time for the less abundant elements was increased to improved counting statistics. The melt is unquenchable, and forms a dendritic intergrowth of quench crystals and residual melt. It was analyzed using a 30 micron raster. The structural identity of the Mg-perovskite phase was confirmed using x ray microdiffractometry. The results of the investigation are presented.

Author

N92-28602*# Massachusetts Univ., Amherst.

FATE OF A PERCHED CRYSTAL LAYER IN A MAGMA OCEAN Abstract Only

S. A. Morse *In* Lunar and Planetary Inst., Workshop on the Physics and Chemistry of Magma Oceans from 1 Bar to 4 Mbar 1992 p 36-37 (For primary document see N92-28587 19-46)

Avail: NTIS HC/MF A05

The pressure gradients and liquid compressibilities of deep magma oceans should sustain the internal flotation of native crystals owing to a density crossover between crystal and liquid. Olivine at upper mantle depths near 250 km is considered. The behavior of a perched crystal layer is part of the general question concerning the fate of any transient crystal carried away from a cooling surface, whether this be a planetary surface or the roof of an intrusive magma body. For magma bodies thicker than a few hundred meters at modest crustal depths, the major cooling surface is the roof even when most solidification occurs at the floor. Importation of cool surroundings must also be invoked for the generation of a perched crystal layer in a magma ocean, but in this case the perched layer is deeply embedded in the hot part of the magma body, and far away from any cooling surface. Other aspects of this study are presented.

Author

N92-28603*# Minnesota Univ., Minneapolis. Dept. of Geology and Geophysics.

EVIDENCE FOR A HIGH TEMPERATURE DIFFERENTIATION IN A MOLTEN EARTH: A PRELIMINARY APPRAISAL Abstract Only

V. Rama Murthy *In* Lunar and Planetary Inst., Workshop on the Physics and Chemistry of Magma Oceans from 1 Bar to 4 Mbar 1992 p 38-39 (For primary document see N92-28587 19-46)

Avail: NTIS HC/MF A05

If the earth were molten during its later stages of accretion as indicated by the present understanding of planetary accretion process, the differentiation that led to the formation of the core and mantle must have occurred at high temperatures in the range of 3000-5000 K because of the effect of pressure on the temperature of melting in the interior of the earth. This calls into question the use of low-temperature laboratory measurements of partition coefficients of trace elements to make inferences about earth accretion and differentiation. The low temperature partition coefficients cannot be directly applied to high temperature fractionations because partition coefficients refer to an equilibrium

specific to a temperature for a given reaction, and must change in some proportion to exp 1/RT. There are no laboratory data on partition coefficients at the high temperatures relevant to differentiation in the interior of the earth, and an attempt to estimate high temperature distribution coefficients of siderophile elements was made by considering the chemical potential of a given element at equilibrium and how this potential changes with temperature, under some specific assumptions. Author

N92-28604*# Arizona Univ., Tucson. Lunar and Planetary Lab.
FORSTERITE/MELT PARTITIONING OF ARGON AND IODINE: IMPLICATIONS FOR ATMOSPHERE FORMATION BY OUTGASSING OF AN EARLY MARTIAN MAGMA OCEAN Abstract Only
Donald S. Musselwhite, Michael J. Drake, and Timothy D. Swindle *In* Lunar and Planetary Inst., Workshop on the Physics and Chemistry of Magma Oceans from 1 Bar to 4 Mbar 1992 p 40-41 (For primary document see N92-28587 19-46)
(Grant NAG9-39)
Avail: NTIS HC/MF A05

Argon and Xe in the Martian atmosphere are radiogenic relative to the Martian mantle if the SNC meteorites are from Mars. Decay of the short lived isotope I-129 to Xe-129 (t sub 1/2 = 16 m.y.) is the most plausible source of the radiogenic Xe. This short half life constrains any process responsible for the elevated Xe-129/Xe-132 ratio of the Martian atmosphere to occur very early in solar system history. Musselwhite et al. proposed that the differential solubility of I and Xe in liquid water played a key role in producing the radiogenic signature in the Martian atmosphere. Here we explore an alternative hypothesis involving purely igneous processes, and motivated in part by new experimental results on the partitioning of I and Xe between minerals and melt. Author

N92-28605*# New Mexico Univ., Albuquerque. Dept. of Geology.
PRESSURE REGIMES AND CORE FORMATION IN THE ACCRETING EARTH Abstract Only
H. E. Newsom *In* Lunar and Planetary Inst., Workshop on the Physics and Chemistry of Magma Oceans from 1 Bar to 4 Mbar 1992 p 42-43 (For primary document see N92-28587 19-46)
Avail: NTIS HC/MF A05

Recent work suggests that a large degree of melting is required to segregate metal from silicates, suggesting a connection with the formation of magma oceans. At low pressures metallic liquids do not wet silicate minerals, preventing the metal from aggregating into large masses that can sink. At high pressures, above 25 GPa, the dihedral angles of grains in contact with oxygen-rich metallic liquids may be reduced enough to allow percolation of metal, but this has not been confirmed. Physical models of core formation and accretion may therefore involve the formation of magma oceans and the segregation of metal at both high and low pressures. Models of core formation involving different pressure regimes are discussed as well as chemical evidence bearing on the models. Available geophysical data is ambiguous. The nature of the 670 km boundary (chemical difference or strictly phase change) between the upper and lower mantle is in doubt. There is some evidence that plumes are derived from the lower mantle, and seismic tomography strongly indicates that penetration of subducting oceanic crust into the lower mantle, but the tomography data also indicates that the 670 km discontinuity is a significant barrier to general mantle convection. The presence of the D' layer at the base of the lower mantle could be a reaction zone between the mantle and core indicating core-mantle disequilibrium, or D' layer could be subducted material. The abundance of the siderophile elements in the mantle could provide clues to the importance of high pressure processes in Earth, but partition coefficients at high pressures are only beginning to be measured. Author

N92-28606*# Tohoku Univ., Sendai (Japan). Inst. of Mineralogy, Petrology, and Economic Geology.
TERRESTRIAL MAGMA OCEAN AND CORE SEGREGATION IN THE EARTH Abstract Only
Eiji Ohtani and Naoyoshi Yurimoto (Tsukuba Univ., Japan) *In* Lunar and Planetary Inst., Workshop on the Physics and Chemistry of Magma Oceans from 1 Bar to 4 Mbar 1992 p 44-45 (For primary document see N92-28587 19-46)
Avail: NTIS HC/MF A05

According to the recent theories of formation of the earth, the outer layer of the proto-earth was molten and the terrestrial magma ocean was formed when its radius exceeded 3000 km. Core formation should have started in this magma ocean stage, since segregation of metallic iron occurs effectively by melting of the proto-earth. Therefore, interactions between magma, mantle minerals, and metallic iron in the magma ocean stage controlled the geochemistry of the mantle and core. We have studied the partitioning behaviors of elements into the silicate melt, high pressure minerals, and metallic iron under the deep upper mantle and lower mantle conditions. We employed the multi-anvil apparatus for preparing the equilibrating samples in the ranges from 16 to 27 GPa and 1700-2400 C. Both the electron probe microanalyzer (EPMA) and the Secondary Ion Mass spectrometer (SIMS) were used for analyzing the run products. We obtained the partition coefficients of various trace elements between majorite, Mg-perovskite, and liquid, and magnesiowustite, Mg-perovskite, and metallic iron. The examples of the partition coefficients of some key elements are summarized in figures, together with the previous data. We may be able to assess the origin of the mantle abundances of the elements such as transition metals by using the partitioning data obtained above. The mantle abundances of some transition metals expected by the core-mantle equilibrium under the lower mantle conditions cannot explain the observed abundance of some elements such as Mn and Ge in the mantle. Estimations of the densities of the ultrabasic magma Mg-perovskite at high pressure suggest existence of a density crossover in the deep lower mantle; flotation of Mg-perovskite occurs in the deep magma ocean under the lower mantle conditions. The observed depletion of some transition metals such as V, Cr, Mn, Fe, Co, and Ni in the mantle may be explained by the two stage process, the core-mantle equilibrium under the lower mantle conditions in the first stage, and subsequent downwards separation of the ultrabasic liquid (and magnesiowustite) and flotation of Mg-perovskite in the lower mantle. Author

N92-28607*# Bayreuth Univ. (Germany, F.R.). Bayerisches Geoinstitut.
ESTIMATION OF THE VISCOSITIES OF SILICATE LIQUIDS AT HIGH PRESSURE FROM MEASUREMENTS OF OXYGEN DIFFUSIVITY Abstract Only
D. C. Rubie, C. R. Ross, II, M. R. Carroll (Bristol Univ., England), and S. C. Elphick (Edinburgh Univ., Scotland) *In* Lunar and Planetary Inst., Workshop on the Physics and Chemistry of Magma Oceans from 1 Bar to 4 Mbar 1992 p 46 (For primary document see N92-28587 19-46)
Avail: NTIS HC/MF A05

The dynamics and evolution of a magma ocean depend significantly on the structure and physical properties of silicate liquids at high pressure. Viscosity is particularly important because of its effect on the dynamics of convection and crystal setting. Traditionally, the viscosities of silicate liquids have been measured at high pressure by falling sphere viscometry but, due to some limitations of this technique, few measurements have been made at pressures exceeding 2.5 GPa. An alternative approach, which has previously been proven up to 2 GPa, is to use high pressure measurements of oxygen self-diffusivity (D) to estimate viscosity (eta) from the Eyring relationship eta = kT/D lambda (where k is the Boltzmann constant, T is absolute temperature, and lambda is the diffusive jump distance). We have performed preliminary experiments on Na2Si4O9 liquid in order to explore the feasibility of this method up to pressures in excess of 10 GPa. Diffusion couples were prepared from glass starting materials with one half of the sample enriched in O-18 and the other half containing the natural abundance (0.2 wt percent). Diffusion experiments were performed at 1600 to 1800 C at pressures in the range of 2.5 to 10 GPa for times up to 6 minutes using a 1200 ton multianvil apparatus. Oxygen diffusivities were derived from the resulting O-18

concentration profiles, which were analyzed using an ion microprobe. At 1800 C, oxygen diffusivities increase continuously from 1 x 10(exp -10) m(exp -2) s(exp -1) at 2.5 Gpa to 5 x 10(exp -10) m(exp -2) s(exp -1) at 10 GPa. From the Eyring relationship, the viscosity of Na2SiO9 liquid is predicted to decrease by approx. 0.7 log units over this pressure range at 1800 C. These trends, which can be related to changes in the structure of the liquid at high pressure, are in agreement with results of molecular dynamics calculations. These results suggest that it should be possible to estimate the viscosities of silicate liquids up to at least 15 GPa and 2200 C by this method. Author

N92-28608*# Hiroshima Univ. (Japan). Dept. of Earth and Planetary Systems Sciences.
COOLING OF THE MAGMA OCEAN DUE TO ACCRETIONAL DISRUPTION OF THE SURFACE INSULATING LAYER Abstract Only
Sho Sasaki *In* Lunar and Planetary Inst., Workshop on the Physics and Chemistry of Magma Oceans from 1 Bar to 4 Mbar 1992 p 47-48 (For primary document see N92-28587 19-46)
Avail: NTIS HC/MF A05

Planetary accretion has been considered as a process to heat planets. Some fraction of the kinetic energy of incoming planetesimals is trapped to heat the planetary interior (Kaula, 1979; Davies, 1984). Moreover, blanketing effect of a primary atmosphere (Hayashi et al., 1979; Sasaki, 1990) or a degassed atmosphere (Abe and Matsui, 1986; Zahnle et al., 1988) would raise the surface temperature of the Earth-size planets to be higher than the melting temperature. The primordial magma ocean was likely to be formed during accretion of terrestrial planets. In the magma ocean, if crystallized fractions were heavier than melt, they would sink. But if solidified materials were lighter than the melt (like anorthosite of the lunar early crust) they would float to form a solid shell surrounding the planet. (In an icy satellite, solidified water ice should easily float on liquid water because of its small density.) The surface solid lid would prevent efficient convective heat transfer and slow the interior cooling. Consider that the accretion of planetesimals still continues in this cooling stage. Shock disruption at planetesimal impact events may destroy the solid insulating layer. Even if the layer survives impacts, the surface layer is finally overturned by Rayleigh-Taylor instability, since accreting materials containing metals are heavier than the surface solidified lid of silicates. Author

N92-28609*# California Univ., Los Angeles. Dept. of Earth and Space Sciences.
EARLY PLANETARY DIFFERENTIATION: GEOPHYSICAL CONSEQUENCES Abstract Only
G. Schubert *In* Lunar and Planetary Inst., Workshop on the Physics and Chemistry of Magma Oceans from 1 Bar to 4 Mbar 1992 p 49-50 (For primary document see N92-28587 19-46)
Avail: NTIS HC/MF A05

Differentiation of a planet can have profound consequences for its structure and thermal evolution, including core formation and crystal growth. Recent theories for the origin and evolution of the terrestrial planets and the Moon have all these bodies forming hot and cooling thereafter. Early core formation, and in the cases of Earth and Moon, a deep magma ocean possibly encompassing the entire mantle are characteristic features of these models. Secular cooling of Mars from a hot origin and cooling of Moon from a hot initial state with a deep magma ocean have been criticized on the basis of their tectonic implications. The cases of Mars and the Moon are discussed. Author

N92-28610*# Tennessee Univ., Knoxville. Dept. of Geological Sciences.
IMPERFECT FRACTIONAL CRYSTALLIZATION OF THE LUNAR MAGMA OCEAN AND FORMATION OF THE LUNAR MANTLE: A REALISTIC CHEMICAL APPROACH Abstract Only
Gregory A. Snyder and Lawrence A. Taylor *In* Lunar and Planetary Inst., Workshop on the Physics and Chemistry of Magma Oceans from 1 Bar to 4 Mbar 1992 p 51-52 (For primary document see N92-28587 19-46)
Avail: NTIS HC/MF A05

It is generally considered that lunar mare basalts were generated by the melting of a cumulate mantle formed in an early Moon-wide magma ocean or magmasphere. However, the nature and chemistry of this cumulate mantle and the logistics of its origin have remained elusive. Extensive studies of terrestrial layered mafic intrusions over the past sixty years have emphasized the imperfection of fractional crystallization and attendant crystal-crystal and crystal-liquid separation in a convecting magma chamber. These separations were similarly inefficient during evolution of the lunar magmasphere, allowing for the trapping of interstitial melt and entrainment of a small proportion of less-dense plagioclase into the more-dense mafic cumulate mush. Indeed, petrography of lunar highlands samples demonstrates this well for anorthosites (with 1-10 percent olivine). Therefore, we propose a 'realistic' model for the evolution of the lunar mantle, which takes these observations into consideration, by the imperfect fractional crystallization of an early lunar magma ocean. Author

N92-28611*# California Inst. of Tech., Pasadena. Div. of Geological and Planetary Sciences.
EVOLUTION OF A TERRESTRIAL MAGMA OCEAN: THERMODYNAMICS, KINETICS, RHEOLOGY, CONVECTION, DIFFERENTIATION Abstract Only
V. S. Solomatov and D. J. Stevenson *In* Lunar and Planetary Inst., Workshop on the Physics and Chemistry of Magma Oceans from 1 Bar to 4 Mbar 1992 p 53-54 (For primary document see N92-28587 19-46)
Avail: NTIS HC/MF A05

The evolution of an initially totally molten magma ocean is constrained on the basis of analysis of various physical problems in the magma ocean. First of all an equilibrium thermodynamics of the magma ocean is developed in the melting temperature range. The equilibrium thermodynamical parameters are found as functions only of temperature and pressure and are used in the subsequent models of kinetics and convection. Kinematic processes determine the crystal size and also determine a non-equilibrium thermodynamics of the system. Rheology controls all dynamical regimes of the magma ocean. The thermal convection models for different rheological laws are developed for both the laminar convection and for turbulent convection in the case of equilibrium thermodynamics of the multiphase system. The evolution is estimated on the basis of all the above analysis.
H.A.

N92-28612*# California Inst. of Tech., Pasadena. Div. of Geological and Planetary Sciences.
DYNAMICS AND EVOLUTION OF A MAGMA OCEAN Abstract Only
D. J. Stevenson *In* Lunar and Planetary Inst., Workshop on the Physics and Chemistry of Magma Oceans from 1 Bar to 4 Mbar 1992 p 55 (For primary document see N92-28587 19-46)
Avail: NTIS HC/MF A05

The prevailing view of very large impacts during earth accretion suggests an initial state for earth evolution that was totally molten or nearly so. The problem confronted is to understand the evolution from this state to an almost completely solidified mantle. Two crucial questions are asked by the author: (1) is the resulting endstate of magma ocean freezing compatible with geological record, inferred mantle structure and evidence from geochemistry; and (2) does the freezing event leave a signature that can be discerned in the present earth. The emphasis on this keynote introduction will be to set the stage for the more detailed analyses to follow and to clarify the crucial questions and uncertainties.
H.A.

N92-28613*# Tokyo Inst. of Tech. (Japan). Earth and Planetary Sciences.
EVIDENCES FOR THE TERRESTRIAL MAGMA OCEAN FROM HIGH-PRESSURE MELTING EXPERIMENTS Abstract Only
Eiichi Takahashi *In* Lunar and Planetary Inst., Workshop on the

Physics and Chemistry of Magma Oceans from 1 Bar to 4 Mbar 1992 p 56-57 (For primary document see N92-28587 19-46)
Avail: NTIS HC/MF A05

In order to study the early evolutionary history of our planet, the author has carried out a series of melting experiments on primitive mantle peridotites. Using a new multi-anvil apparatus (SPI-1000), the author revisited the melting study on mantle peridotites and also started a melting study for representative chondrite compositions in the pressure range of 25 Gpa. The updated phase diagram for the peridotite is shown as is the preliminary melting phase diagram for Allende C3 chondrite. The liquidus and solidus of the Allende chondrite are extrapolated based on experimental results at 24 to 26 GPa on the same rock. H.A.

N92-28614*# Hawaii Univ., Honolulu. Planetary Geosciences.
EVIDENCE FOR MAGMA OCEANS ON ASTEROIDS, THE MOON, AND EARTH
G. Jeffrey Taylor and Marc D. Norman *In* Lunar and Planetary Inst., Workshop on the Physics and Chemistry of Magma Oceans from 1 Bar to 4 Mbar 1992 p 58-65 (For primary document see N92-28587 19-46)
Avail: NTIS HC/MF A05

There are sound theoretical reasons to suspect that the terrestrial planets melted when they formed. For Earth, the reasons stem largely from the hypothesis that the moon formed as a result of the impact of a Mars-sized planetesimal with the still accreting Earth. Such a monumental event would have led to widespread heating of the Earth and the materials from which the moon was made. In addition, formation of a dense atmosphere on the Earth (and possibly the Moon) would have led to retention of accretional heat and, thus, widespread melting. In other words, contemporary theory suggests that the primitive Moon and terrestrial planets had magma oceans. Author

N92-28615*# Arizona Univ., Tucson. Lunar and Planetary Lab.
MAGMA OCEAN FORMATION DUE TO GIANT IMPACTS Abstract Only
W. B. Tonks and H. J. Melosh *In* Lunar and Planetary Inst., Workshop on the Physics and Chemistry of Magma Oceans from 1 Bar to 4 Mbar 1992 p 66-67 (For primary document see N92-28587 19-46)
Avail: NTIS HC/MF A05

The effect of giant impacts on the initial chemical and thermal states of the terrestrial planets is just now being explored. A large high speed impact creates an approximately hemispherical melt region with a radius that depends on the projectile's radius and impact speed. It is shown that giant impacts on large planets can create large, intact melt regions containing melt volumes up to a few times the volume of the projectile. These large melt regions are not created on asteroid sized bodies. If extruded to the surface, these regions contain enough melt to create a magma ocean of considerable depth, depending on the impact speed, projectile radius, and gravity of the target planet. H.A.

N92-28616*# California Univ., Los Angeles. Inst. of Geophysics and Planetary Physics.
INHERITANCE OF MAGMA OCEAN DIFFERENTIATION DURING LUNAR ORIGIN BY GIANT IMPACT Abstract Only
Paul H. Warren *In* Lunar and Planetary Inst., Workshop on the Physics and Chemistry of Magma Oceans from 1 Bar to 4 Mbar 1992 p 68-69 (For primary document see N92-28587 19-46)
Avail: NTIS HC/MF A05

The giant impact model for the Moon has won widespread support. It seems to satisfactorily explain the high angular momentum of the Earth-Moon system, and the strong depletion of FeNi in the Moon. This model is usually assumed to entail no significant fractionation of nonvolatile lithophile elements relative to a simple binary mixture of impactor silicates plus protoearth silicates. Although the Earth may have been hot enough before the impact to be completely molten, analysis of the likely number and timing of major impacts in the prehistory of the impactor indicates that a fully molten, undifferentiated condition for that relatively small body is unlikely. Given selective sampling by the giant impact, any significant vertical differentiation within the noncore portion of the impactor would have been largely inherited by the Moon. Author

N92-28617*# California Univ., Los Angeles. Inst. of Geophysics and Planetary Physics.
THE THREE STAGES OF MAGMA OCEAN COOLING Abstract Only
Paul H. Warren *In* Lunar and Planetary Inst., Workshop on the Physics and Chemistry of Magma Oceans from 1 Bar to 4 Mbar 1992 p 70-71 (For primary document see N92-28587 19-46)
Avail: NTIS HC/MF A05

Models of magma ocean (MO) cooling and crystallization can provide important constraints on MO plausibility for a given planet, on the origin of long term, stable crusts, and even on the origin of the solar system. Assuming the MO is initially extensive enough to have a mostly molten surface, its first stage of cooling is an era of radiative heat loss from the surface, with extremely rapid convection below, and no conductive layer in between. The development of the chill crust starts the second stage of MO cooling. Heat loss is now limited by conduction through the crust. The third stage of cooling starts when the near surface MO evolves compositionally to the point of saturation with feldspar. At this point, the cooling rate again precipitously diminishes, the rate of crustal thickness growth as a function of temperature suddenly increases. More work on incorporating chemical constraints into the evolving physical models of MO solidification would be worthwhile. H.A.

N92-28618*# California Univ., Los Angeles. Inst. of Geophysics and Planetary Physics.
THE FERROAN-ANORTHOSITIC SUITE AND THE EXTENT OF PRIMORDIAL LUNAR MELTING Abstract Only **c91**
Paul H. Warren and Gregory W. Kallemeyn *In* Lunar and Planetary Inst., Workshop on the Physics and Chemistry of Magma Oceans from 1 Bar to 4 Mbar 1992 p 72-73 (For primary document see N92-28587 19-46)
Avail: NTIS HC/MF A05

The Apollo highlands rock collection includes more than 100 'pristine' fragments that survived the intense meteoritic bombardment of the ancient lunar crust with unmixed, endogenously igneous compositions. The geochemical anomaly manifested by the 'ferroan-anorthositic suite' (FAS) appears to reflect a geochemical, and probably also a genetic, bimodality among the ancient lunar cumulates. Early models that purported to account for this bimodality as a product of a single magma have been discredited. The model of the present paper implies that the Mg-suite rocks formed by a comparatively normal variety of basaltic fractional crystallization (FC) shortly after the era of magma ocean (MO) crystallization and FAS genesis. H.A.

N92-28619*# Carnegie Institution of Washington, DC.
GIANT AND LARGE IMPACTS IN THE CONTEXT OF PLANETARY FORMATION THEORY Abstract Only **c91**
G. W. Wetherill *In* Lunar and Planetary Inst., Workshop on the Physics and Chemistry of Magma Oceans from 1 Bar to 4 Mbar 1992 p 74-75 (For primary document see N92-28587 19-46)
Avail: NTIS HC/MF A05

Of particular relevance to the subject of this workshop is the expected size and velocity distribution of the interplanetary projectiles during the late stages of planet formation. This will in turn be determined by the evolution of these distributions throughout the planet forming process. Even at this early stage of understanding, it seems clear that assumption of simple power-law mass distributions are certain to lead to incorrect conclusions. Furthermore, the lunar cratering evidence, valuable as it is for relatively late (i.e., less than 4.2 b.y.) events, cannot provide information regarding stochastic events of potentially moon-destroying energy expected to be experienced by the early Earth. The early stages of terrestrial planet formation are discussed in more detail. Author

N92-28689# National Aerospace Lab., Amsterdam (Netherlands). Structures and Materials Div.
ATMOSPHERIC TURBULENCE SPECTRA AND CORRELATION FUNCTIONS
R. Noback 13 Jun. 1989 73 p
(Contract OV/RLD-937/1)
(NLR-TP-89217-U; ETN-92-91523) Avail: NTIS HC/MF A04

The derivation of one, two, and three dimensional spectra and correlation functions for isotropic (atmospheric) turbulence and the mutual relations were collected from various sources. Aircraft loads usually are determined using a one dimensional turbulence description. In some cases, a two or even three dimensional description might be preferable. Aircraft loads can then be determined using two dimensional spectra and cross spectra. These types of spectra are described, and an outline of methods to determine aircraft loads is given. ESA

N92-28703# Toronto Univ. (Ontario).
GROUND DEPOSITION OF LIQUID DROPLETS RELEASED FROM A POINT SOURCE IN THE ATMOSPHERIC SURFACE LAYER Ph.D. Thesis
Bernard Panneton 26 Jan. 1989 265 p
(ISBN-0-315-51071-4; CTN-92-60460) Copyright Avail: Micromedia Ltd., Technical Information Centre, 165 Hotel de Ville, Place du Portage, Phase 2, Hull, Quebec J8X 3X2, Canada HC $45.00 CAN, MF $15.00 CAN

A series of field experiments is presented in which the ground deposition of liquid droplets, 120 and 150 microns in diameter, released from a point source at 7 m above ground level, was measured. A detailed description of the experimental technique is provided, and the results are presented and compared to the predictions of a few models. A new rotating droplet generator is described. Droplets are produced by the forced breakup of capillary liquid jets and droplet coalescence is inhibited by the rotational motion of the spray head. The two dimensional deposition patterns are presented in the form of plots of contours of constant density, normalized arcwise distributions and crosswind integrated distributions. The arcwise distributions follow a Gaussian distribution whose standard deviation is evaluated using a modified Pasquill's technique. Models of the crosswind integrated deposit from Godson, Csanady, Walker, Bache and Sayer, and Wilson et al are evaluated. The results indicate that the Wilson et al random walk model is adequate for predicting the ground deposition of the 150 micron droplets. In one case, where the ratio of the droplet settling velocity to the mean wind speed was largest, Walker's model proved to be adequate. Otherwise, none of the models were acceptable in light of the experimental data.
Author (CISTI)

N92-28740# Oesterreichisches Forschungszentrum Seibersdorf G.m.b.H., Vienna. Inst. fuer Landwirtschaft.
HUMIC SUBSTANCES IN SOILS FROM BANGLADESH, NAMIBIA, AND CANADA
Martin H. Gerzabek and Shah M. Ullah Apr. 1991 9 p Repr. from International Agrophysics, v. 5, no. 3-4, 1989 p 197-203
(OEFZS-4574; ETN-92-90643) Copyright Avail: NTIS HC/MF A02

Humic substances are extracted from four dystric fluvisols in Bangladesh, an orthic solonschak in Canada and a rhodo-chromic cambisol on Namibia. They are analyzed by chromatography on controlled pore glass. Humic systems are characterized by low contents of high molecular weight humic substances, large amounts of low molecular weight humic substances, and exceedingly high percentages of low molecular weight non-humic substances compared with literature from Central Europe. The differences are probably due to the poor microbial activity in the analyzed soils, caused by anaerobic conditions, salinity, or dryness. ESA

N92-28853# State Univ. of New York, Albany. Atmospheric Sciences Research Center.
DEVELOPMENT OF ROTATING SHADOWBAND SPECTRAL RADIOMETERS AND GCM RADIATION CODE TEST DATA SETS IN SUPPORT OF ARM
J. Michalsky and L. Harrison 17 Mar. 1992 7 p
(Contract DE-FG02-90ER-61072)
(DE92-011438; DOE/ER-61072/2) Avail: NTIS HC/MF A02

Two tasks are included in the second year of this project. One task continues the collection of high quality data sets for the testing of radiation codes within climate models. The other task involves the development of accurate spectral instruments for the measurement of shortwave radiation. A third task was completed in the second half of the first year of the project and is briefly summarized. DOE

N92-28911*# Alabama Univ., Huntsville. Dept. of Physics.
THEORETICAL AND EXPERIMENTAL STUDIES RELEVANT TO INTERPRETATION OF AURORAL EMISSIONS Annual Report
Charles E. Keffer 29 Jun. 1992 66 p
(Grant NAG8-834)
(NASA-CR-190521; NAS 1.26:190521) Avail: NTIS HC/MF A04

The results obtained in the second year of a three year collaborative effort with MSFC are summarized. A succession of experimental studies was completed to determine the effects of the natural and induced space vehicle environment on the measurement of auroral images from space-based platforms. In addition, a global model which incorporates both auroral and dayglow emission sources is being developed to allow interpretation of measured auroral emissions. A description of work completed on these two tasks is presented. Author

N92-28935# Australian National Univ., Canberra. Research School of Earth Sciences.
THE DISTANCE DEPENDENCE OF REGIONAL PHASE DISCRIMINANTS Scientific Report No. 1, 30 Sep. 1990 - 29 Sep. 1991
Brian L. Kennett 4 Oct. 1991 38 p
(Grant AF-AFOSR-0352-90)
(AD-A247546; AD-E200901; PL-TR-91-2250) Avail: NTIS HC/MF A03

A number of proposed discriminants for distinguishing the character of seismic sources use the amplitude of the phase Pn as a reference. The merit of Pn is that it constitutes the onset of regional seismograms, but the behavior of the arrivals at an individual station can be quite complex. Results from long-range refraction experiments in Eurasia suggest that the complexity arises from the superimposition of a number of sub-phases returned from fine-scale structure in the uppermost mantle. The behavior is consistent with fine scale horizontal variations superimposed on a gentle increase in seismic velocity with depth, so that equivalent one-dimensional models will show multiple low velocity zones. Long range refraction data for Sn is much less common but similar trends can be discerned. As frequency increases such complexity is likely to become more important. Sn is often observed at distance beyond 300 km but emerges from Sg(Lg) much less clearly in general than Pn emerges from Pg. However some refraction profiles in the Finnish Shield areas show very clear Sn arrivals at short distances. The differences in character can be associated with differing velocity gradients for S in the uppermost mantle. The variability in Sn behavior means that it may prove difficult to generate discriminants based on amplitudes which can be readily transportable between different regions. GRA

N92-28964# Naval Oceanographic and Atmospheric Research Lab., Monterey, CA.
EVALUATION OF SIMPLE MESOSCALE MODELS FOR USE IN TESS Final Report
R. J. Miller and C. R. Sampson Nov. 1991 47 p
(AD-A247914; NOARL-TN-195) Avail: NTIS HC/MF A03

Prediction of wind flow in a complex coastal environment is a challenging task that continues to be of interest to the U.S. Navy, specifically for use in the Tactical Environmental Support System (TESS). TESS is a computer workstation which provides environmental information for the Navy's tactical decision makers and is discussed in detail in Phegley and Crosiar (1991). According to Mass and Dempsey (1986), global and regional models have improved to the point where the adequately predict larger scale

synoptic conditions; however, conversion of these forecasts into local and mesoscale weather is still a problem. One solution is to increase the resolution of a global or regional model to that desired for mesoscale prediction. The problem with this is that computational requirements for the model would far exceed the capability of TESS. Another solution is to run simple mesoscale models which use observations or output from the more complex models for initialization. Until recently, computational requirements of simple mesoscale models were beyond the capabilities of TESS. However, the TESS hardware has been upgraded to a system which is now capable of running simple mesoscale models.

GRA

N92-28621*# Oxford Univ. (England). Dept. of Earth Sciences.
HISTORICAL DATA FOR GEOMAGNETIC FIELD MODELLING
Andrew Jackson *In* NASA. Goddard Space Flight Center, Types and Characteristics of Data for Geomagnetic Field Modeling Jun. 1992 p 1-30 Sponsored in part by Royal Society (For primary document see N92-28620 19-39)
Avail: NTIS HC/MF A16

N92-28622*# Finnish Meteorological Inst., Helsinki. Geomagnetism Div.
MEASUREMENTS OF DECLINATION AT THE HELSINKI MAGNETIC-METEOROLOGICAL OBSERVATORY 1844-1853
Heikki Nevanlinna, Anneli Ketola, and Tuulikki Kangas *In* NASA. Goddard Space Flight Center, Types and Characteristics of Data for Geomagnetic Field Modeling Jun. 1992 p 31-39 (For primary document see N92-28620 19-39)
Avail: NTIS HC/MF A16

N92-28623*# National Environmental Research Council, Edinburgh (Scotland). Geomagnetism Group.
SURVEY DATA FOR GEOMAGNETIC FIELD MODELLING
D. R. Barraclough and S. Macmillan *In* NASA. Goddard Space Flight Center, Types and Characteristics of Data for Geomagnetic Field Modeling Jun. 1992 p 41-73 (For primary document see N92-28620 19-39)
Avail: NTIS HC/MF A16

N92-28624*# National Aeronautics and Space Administration. Goddard Space Flight Center, Greenbelt, MD.
SATELLITE DATA FOR GEOMAGNETIC FIELD MODELING
R. A. Langel and R. T. Baldwin (Hughes STX, Inc., Lanham, MD.) *In its* Types and Characteristics of Data for Geomagnetic Field Modeling Jun. 1992 p 75-135 (For primary document see N92-28620 19-39)
(RTOP 579-31-02)
Avail: NTIS HC/MF A16

N92-28625*# National Geophysical Data Center, Boulder, CO. Marine Geology and Geophysics Div.
MARINE MAGNETIC DATA HOLDINGS OF WORLD DATA CENTER-A FOR MARINE GEOLOGY AND GEOPHYSICS
George F. Sharman and Dan Metzger *In* NASA. Goddard Space Flight Center, Types and Characteristics of Data for Geomagnetic Field Modeling Jun. 1992 p 137-148 (For primary document see N92-28620 19-39)
Avail: NTIS HC/MF A16

N92-28626*# Hughes STX, Inc., Lanham, MD.
REDUCTION OF MARINE MAGNETIC DATA FOR MODELING THE MAIN FIELD OF THE EARTH
R. T. Baldwin, J. R. Ridgway, and W. M. Davis (National Geophysical Data Center, Boulder, CO.) *In* NASA. Goddard Space Flight Center, Types and Characteristics of Data for Geomagnetic Field Modeling Jun. 1992 p 149-202 (For primary document see N92-28620 19-39)
Avail: NTIS HC/MF A16

N92-28627*# Cambridge Univ. (England).
SECULAR VARIATION ACROSS THE OCEANS: A RETROSPECTIVE STUDY FROM 35 YEARS OF SHIPBOARD TOTAL FIELD MEASUREMENTS IN THE NE ATLANTIC
C. A. Williams, J. Verhoef (Geological Survey of Canada, Dartmouth, Nova Scotia), and R. Macnab (Geological Survey of Canada, Dartmouth, Nova Scotia) *In* NASA. Goddard Space Flight Center, Types and Characteristics of Data for Geomagnetic Field Modeling Jun. 1992 p 203-214 (For primary document see N92-28620 19-39)
(Grant NERC-GR3/7704)
Avail: NTIS HC/MF A16

N92-28628*# Naval Oceanographic Office, Bay Saint Louis, MS. Geopotential Div.
PROJECT MAGNET HIGH-LEVEL VECTOR SURVEY DATA REDUCTION
Rachel J. Coleman *In* NASA. Goddard Space Flight Center, Types and Characteristics of Data for Geomagnetic Field Modeling Jun. 1992 p 215-248 (For primary document see N92-28620 19-39)
Avail: NTIS HC/MF A16

N92-28629*# Geological Survey of Canada, Ottawa (Ontario). Mineral Resources Div.
SURVEY PARAMETERS AND AVAILABILITY OF LOW-LEVEL AEROMAGNETIC DATA FOR GEOMAGNETIC FIELD MODELLING
Peter Hood *In* NASA. Goddard Space Flight Center, Types and Characteristics of Data for Geomagnetic Field Modeling Jun. 1992 p 249-286 (For primary document see N92-28620 19-39)
Avail: NTIS HC/MF A16

N92-28630*# Bureau of Mineral Resources, Geology and Geophysics, Canberra (Australia).
MAGNETIC REPEAT STATION DATA
C. E. Barton *In* NASA. Goddard Space Flight Center, Types and Characteristics of Data for Geomagnetic Field Modeling Jun. 1992 p 287-319 (For primary document see N92-28620 19-39)
Avail: NTIS HC/MF A16

N92-28631*# Geological Survey, Denver, CO.
GEOMAGNETIC DATA FROM THE US MAGNETIC OBSERVATORY NETWORK
Donald C. Herzog *In* NASA. Goddard Space Flight Center, Types and Characteristics of Data for Geomagnetic Field Modeling Jun. 1992 p 321-332 (For primary document see N92-28620 19-39)
Avail: NTIS HC/MF A16

N92-28632*# Institute of Geodynamics, Bucharest (Romania).
MAGNETIC AND ELECTROMAGNETIC INDUCTION EFFECTS IN THE ANNUAL MEANS OF GEOMAGNETIC ELEMENTS
Crisan Demetrescu and Maria Andreescu *In* NASA. Goddard Space Flight Center, Types and Characteristics of Data for Geomagnetic Field Modeling Jun. 1992 p 333-340 (For primary document see N92-28620 19-39)
Avail: NTIS HC/MF A16

N92-28633*# Academy of Sciences, Potsdam (German D.R.). Central Inst. for Physics of the Earth.
INDEPENDENT CONSTITUENTS IN OBSERVATORY TIME SERIES IN CHARACTERIZING THE SECULAR VARIATION
W. Webers *In* NASA. Goddard Space Flight Center, Types and Characteristics of Data for Geomagnetic Field Modeling Jun. 1992 p 341-349 (For primary document see N92-28620 19-39)
Avail: NTIS HC/MF A16

47 METEOROLOGY AND CLIMATOLOGY

Includes weather forecasting and modification.

N92-28340# Colorado State Univ., Fort Collins. Dept. of Atmospheric Science.
PARAMETERIZATION OF CONVECTIVE CLOUDS, MESOSCALE CONVECTIVE SYSTEMS, AND CONVECTIVE-GENERATED CIRRUS
W. R. Cotton 3 Mar. 1992 14 p
(Contract DE-FG02-90ER-61066)
(DE92-010951; DOE/ER-61066/T1) Avail: NTIS HC/MF A03

A level 2.5 w deep convection updraft/downdraft parameterization scheme has been refined and tested against 3D simulations of sea-breeze generated convection over S. Florida. Cases for explicit simulation of MCS's in mid-latitudes and tropics have been encouraging. After a few refinements in those cases, fine resolution explicit simulations of deep convection and mesoscale, stratiform clouds will be begun. DOE

N92-28421# Copenhagen Univ. (Denmark). Geophysical Inst.
POLAR LOWS OVER THE NORTHEAST GREENLAND SEA
Erik A. Rasmussen and Torben S. Pedersen Dec. 1991 142 p
(Contract N00014-87-G-0232)
(AD-A245360) Avail: NTIS HC/MF A07

The purpose of the project reported on in this report has been to increase our knowledge of polar low occurrence, structure and dynamics in the Greenland region. To achieve this, different methods have been applied, including the use of diagnostic studies, theoretical analysis, and numerical modelling studies. Polar lows are small scale cyclonic storms with gale or storm winds which occur in high latitudes. These storms are still not regularly depicted on the traditional meteorological charts and are often too small for detection by operational numerical weather analysis models, and therefore, rarely predicted. Improved satellite observational capability combined with advanced numerical mesoscale weather analysis and prediction models will provide the basis for better detection and more accurate forecasting of these storms. Detailed case studies of polar lows development are relatively few because of lack of data. One relatively well documented development from December 1982 in the region around Bear Island in the Northeastern part of the Norwegian Sea has been used for validation purposes for the numerical experiments carried out as part of the project. GRA

N92-28423# Naval Postgraduate School, Monterey, CA.
MESOSCALE VERTICAL STRUCTURE OF AN EXPLOSIVE OCEANIC CYCLONE M.S. Thesis
Elizabeth B. Gardner Jun. 1991 88 p
(AD-A245927) Avail: NTIS HC/MF A05

The mesoscale vertical structure of an explosively deepening oceanic cyclone on 19-20 January 1989 during the Experiment on Rapidly Intensifying Cyclones over the Atlantic (ERICA) was studied. Hand analyses of height, temperature, and dew point, and cross-sections of theta and theta sub e were prepared using aircraft and sounding data through the warm-frontal region in order to document the vertical structure. The results showed that the initial disturbance formed under a region of strong upper-level confluence between a southern jet streak and an approaching upper-level short-wave from the northwest. Upper-level frontogenesis associated with the confluent flow was strong enough to produce tropopause folding and stratospheric extrusion as low as 700 mb about 750 km upstream from the surface low prior to rapid deepening. The mesoscale analyses during the initial occlusion phase showed the upper-level temperature and moisture patterns spiraling around the low center with strong warm air advection occurring under a pocket of cold air, aloft, producing significant convective instability. The cross-sections of theta sub e throughout the rapid deepening period showed unstable conditions, which suggests that moist potential instability in the warm frontal region was a factor in the rapid development of this storm. GRA

N92-28517# Naval Postgraduate School, Monterey, CA.
SIMULATION OF ATMOSPHERIC FRONTOGENESIS WITH A SEMI-LAGRANGIAN NUMERICAL MODEL M.S. Thesis
Ricardo CarvalhodeAlmeida Sep. 1991 70 p
(AD-A247151) Avail: NTIS HC/MF A04

In this study a numerical model based on the hydrostatic Boussinesq equations is used to simulate atmospheric frontogenesis driven by an irrotational non-divergent deformation wind field. The equations are numerically integrated by using the semi-Lagrangian technique associated with two different time schemes: explicit and semi. Both schemes produce realistic fronts after approximately 40 hours of model integration. The semi-Lagrangian semi-implicit scheme is more successful in handling the sharp gradients associated with the front. Also, the semi-Lagrangian semi-implicit equations are integrated with time steps as long as 3600 sec. producing solutions with relatively small errors. This indicates that this numerical scheme is appropriate for use in mesoscale regional models. GRA

N92-28668# Colorado State Univ., Fort Collins. Dept. of Electrical Engineering.
MULTIPARAMETER RADAR AND AIRCRAFT BASED STUDIES OF THE MICROPHYSICAL, KINEMATIC, AND ELECTRICAL STRUCTURE OF CONVECTIVE CLOUDS Annual Report, 15 Jan. 1991 - 14 Jan. 1992
V. N. Bringi 14 Jan. 1992 9 p
(Grant AF-AFOSR-0141-91)
(AD-A247497; AFOSR-92-0220TR) Avail: NTIS HC/MF A02

The installation of SUN workstations, disks, and Exabyte tape readers, so as to be compatible for NCAR radar analysis software, is described. Additionally, the installation of software to read the PMS data tapes from the Wyoming and NCAR King Airs is discussed. While the Wyoming aircraft data is on the NCAR mass store, the NCAR data is still in the process of transfer to mass store. We are planning to install software to read the T-28 aircraft tapes. We spent substantial time validating and calibrating the CP-2 multiparameter radar data. Time series data from 24 Aug. 1991 was evaluated in detail. We chose time series data for evaluation. GRA

N92-28745 European Organization for the Exploitation of Meteorological Satellites, Darmstadt (Germany, F.R.).
EUMETSAT: THE EUROPEAN ORGANIZATION FOR METEOROLOGICAL SATELLITES
1988 57 p
(ETN-92-91069) Copyright Avail: EUMETSAT, Am Elfengrund 45, D-6100 Darmstadt-Eberstadt, Fed. Republic of Germany

Information about EUMETSAT, an intergovernmental organization with sixteen European member states, whose primary objective is to establish, maintain, and exploit European systems of operational meteorological satellites, are presented. The origins, history, and organization of EUMETSAT are described. A description of the initial system of Meteosat satellites is given together with some examples of the ways in which satellites are used operationally by the meteorological services of Europe. Information given includes details on data collection and relay, data processing, image processing, the Meteosat meteorological products, and ocean observation. Possible future activities for EUMETSAT are also given. ESA

N92-28799# Naval Postgraduate School, Monterey, CA. Dept. of Physics.
A SELF-AFFINE MULTI-FRACTAL WAVE/TURBULENCE DISCRIMINATION METHOD USING DATA FROM SINGLE POINT FAST RESPONSE SENSORS IN A NOCTURNAL ATMOSPHERIC BOUNDARY LAYER Technical Report, Oct. 1990 - Sep. 1991
R. F. Kamada 10 Apr. 1992 49 p
(Contract MIPR-FY76169100412)
(AD-A250419; NPS-PH-92-008) Avail: NTIS HC/MF A03

We present D sub A, a self-affine, multi-fractal which may become the first routine wave/turbulence discriminant for time series data. Using nocturnal atmospheric data, we show the

advantages of D sub A over self-similar fractals and standard turbulence measures such as FFT's, Richardson number, Brunt Vaisala frequency, buoyancy length scale, variances, turbulent kinetic energy, and phase averaging. D sub A also shows promise in resolving wave-break events. Since it uses local basis functions, D sub A may be ideal tool to detect intermittent turbulence, coherent structures, and discrete wave trains in general. D sub A may also be a measure of chaos in general. GRA

N92-28830# Massachusetts Inst. of Tech., Cambridge.
DEVELOPMENT OF AN ADVANCED REPRESENTATION OF CUMULUS CONVECTION
K. A. Emanuel 1992 4 p
(Contract DE-FG02-91ER-61220)
(DE92-011031; DOE/ER-61220/1) Avail: NTIS HC/MF A01

Development of the new representation of cumulus convection, emphasizing the role of microphysical parameters, was completed. The newly developed cumulus scheme was coupled with a detailed representation of radiative transfer, in the context of a one-dimensional radiative-convective equilibrium model that includes the ocean as part of the calculations. The adjustable parameters of the scheme are microphysical in nature. They include the parcel precipitation efficiencies, epsilon(sub i), which are defined as the fraction of condensed water converted to precipitation in samples of air lifted reversibly from the subcloud layer; sigma(sub d), the areal fraction covered by unsaturated downdraft; and sigma(sub s), the fraction of precipitation assumed to fall outside of cloud. DOE

N92-28884# Naval Postgraduate School, Monterey, CA.
MESOSCALE SURFACE ANALYSIS OF THE ERICA IOP-5 CYCLONE M.S. Thesis
Susan N. Greer Jun. 1991 73 p
(AD-A245946) Avail: NTIS HC/MF A04

The mesoscale surface structure of an explosively deepening storm that developed during Intensive Observation Period (IOP) 5 (18-20 January 1989) of the Experiment on Rapidly Deepening Cyclones over the Atlantic (ERICA) was examined to determine the influence of surface forcing on explosive cyclogenesis. Aircraft, buoy and ship observations were converted to a 20 km gridded data set in order to generate objective analyses of the surface pressure and temperature fields comparable to the best hand analyses. The Brown-Liu boundary layer model was then used to calculate surface sensible heat fluxes from the gridded data sets. These analyses showed that the most significant feature that distinguished the IOP-5 storm from a typical nonexplosive storm was the region of sustained positive heat fluxes that occurred east of the low center. This feature, combined with substantial warm advection and conditions of moist symmetric neutrality in the baroclinic zone of the warm front, supports destabilization of the boundary layer and enhanced low-level baroclinicity. Thus, the positive heat fluxes fuel the convective transport of heat and moisture to the upper atmosphere and enhance the sensible and condensation heating that contribute to explosive cyclogenesis. GRA

N92-28922# Air Force Inst. of Tech., Wright-Patterson AFB, OH.
MICROWAVE DERIVED RAINRATES IN TYPHOONS AND THEIR USE IN THE DIAGNOSIS AND PREDICTION OF TYPHOON INTENSITY M.S. Thesis
Paul D. MacArthur 1991 88 p
(AD-A250556; AFIT/CI/CIA-91-118) Avail: NTIS HC/MF A05

An algorithm to convert satellite measured microwave radiances to rainfall rates was used to analyze the rainfall patterns of western North Pacific Ocean typhoons. These rainfall rates and patterns were correlated to the typhoon's Dvorak intensities (both present and future) in search of diagnostic insights and prognostic aids. The number of local maxima of mean annular rainfall rates correlated strongly with the filling or deepening of a typhoon. Storms with multiple peaks filled, indicating the existence of the barrier effect. An effective radius which demarks two regions where latent heat release either raises or depresses the central pressure was postulated. Cross-sections of convective and stratiform rainfall indicated both the importance of stratiform rain and the need for an active convective core in growing typhoons. The ratio of convective to total precipitation also showed the importance of stratiform rain to storm intensification and illustrated the barrier effect. Finally, northwesterly moving typhoons were examined in detail. Stable regression estimates of storm intensification were found. GRA

N92-28934# Air Force Environmental Technical Applications Center, Scott AFB, IL.
WIND-SPEED FORECASTING STUDY FOR WESTOVER AFB, MASSACHUSETTS
William R. Schaub, Jr. Dec. 1991 32 p
(AD-A247545; USAFETAC/PR-91/023) Avail: NTIS HC/MF A03

This report describes the results of a wind speed forecasting study for Westover Air Force Base, located in the Connecticut River valley of western Massachusetts. The purpose of this study is to identify useful tools for forecasting winds speeds at Westover Air Force Base. The results were five models that can be used as guides to forecasting maximum Westover winds for 6-hour periods starting at any 3-hourly time (OOZ, O3Z, etc.) in any season. GRA

N92-28965# Naval Oceanographic and Atmospheric Research Lab., Monterey, CA.
SEGMENTATION OF SATELLITE IMAGERY USING HIERARCHICAL THRESHOLDING AND NEURAL NETWORKS Final Report
James E. Peak Nov. 1991 63 p
(AD-A247915; NOARL-TN-185) Avail: NTIS HC/MF A04

A significant task in the automated interpretation of cloud features on satellite imagery is the segmentation of the image into separate cloud features to be identified. A new technique, Hierarchical Threshold Segmentation (HTS) is presented. In HTS, region boundaries are defined over a range of grayshade thresholds. The hierarchy of the spatial relationships between colocated regions from different thresholds is represented in tree form. This tree is pruned, using a neural network, such that the regions of appropriate sizes and shapes are isolated. These various regions from the pruned trees are then collected to form the final segmentation of the entire image. GRA

N92-28966# Naval Oceanographic and Atmospheric Research Lab., Monterey, CA.
A PROBABILISTIC NEURAL NETWORK APPROACH TO CLOUD CLASSIFICATION Final Report
R. L. Bankert, P. Rabindra, and S. K. Sengupta Oct. 1991 35 p
(AD-A247916; NOARL-TN-173) Avail: NTIS HC/MF A03

Automated satellite image interpretation would be useful in many forecasting operations. One aspect of that interpretation, cloud classification, is examined. Ten classes, composed of low, middle, high, and precipitation cloud types plus clear, are used as output nodes in a Probabilistic Neural Network (PNN) approach to classification of data using four Advanced Very High Resolution Radiometer (AVHRR) subscenes. Input to the neural network consists of 12 features that include a mixture of spectral, textural, and physical measures. There measures are selected, using a feature selection routine, from a collection of over 200 features. An overall accuracy of 85.15 percent is the result. Four classes have agreement of 90 percent or better. The two classes with the poorest accuracies were presented to the classifier with the smallest sample sizes. An increase in the number of samples should increase the accuracy of the classifier. GRA

N92-29087*# Utah Univ., Salt Lake City. Dept. of Meteorology.
ETO CLOUD STUDIES FOR FIRE 2, PART 1 Final Report, 1 Jun. 1990 - 31 May 1992
Kenneth Sassen 24 Jun. 1992 30 p Original contains color illustrations

(Grant NAG1-868)
(NASA-CR-190472; NAS 1.26:190472) Avail: NTIS HC/MF A03; 8 functional color pages

This research program in support of Project FIRE (First ISCCP Regional Experiment) involved two efforts. The results of the first effort, which were in direct support of the Extended Time Observations (ETO) component, are described here. Over the period from June 1990 through May 1991, our remote sensing systems were applied to providing ground-truth cirrus cloud observations for a total of 71 NOAA polar orbiting satellite overpasses. (Chronological tables of this effort are provided.) The primary remote sensor was a dual-polarization ruby (0.694 microns wavelength) lidar, although mid-way through the program we added a number of radiometers to assess the surface radiation budget and cirrus cloud infrared emittance, and some supplemental observations from a Ka-band (8.6 mm) radar were also collected. These studies were conducted from the Facility for Atmospheric Remote Sensing (FARS) at 40 degrees 46 minutes 00 seconds north latitude and 111 degrees 49 minutes 38 seconds east longitude. We also investigated the unusual characteristics of a subset of ETO case studies involving cirrus that generated solar and lunar corona displays. As we reported recently (reprint attached), these cirrus were atypically high and cold in relation to our total midlatitude cloud sample, and were comprised of unexpectedly small ice crystals from 10 to 30 microns in dimension. This finding lends some credence to the so-called cirrus small particle radiative anomaly, but only for very cold (less than -60 C) cirrus clouds. In a supplement, we will describe the design and testing of a prototype cirrus cloud polar nephelometer, which we constructed as part of our second research effort, to allow scattering phase functions to be obtained in future in situ cirrus research. Author

N92-29148* National Aeronautics and Space Administration. Pasadena Office, CA.
MICROWAVE TEMPERATURE PROFILER FOR CLEAR AIR TURBULENCE PREDICTION Patent
Bruce L. Gary, inventor (to NASA) (Jet Propulsion Lab., California Inst. of Tech., Pasadena.) 2 Jun. 1992 16 p Filed 27 Nov. 1990 Supersedes N91-23662 (29 - 15, p 2465)
(NASA-Case-NPO-18115-1-CU; US-Patent-5,117,689; US-Patent-Appl-SN-618790; US-Patent-Class-73-178R; US-Patent-Class-364-443; US-Patent-Class-374-112; Int-Patent-Class-G01C-21/00) Avail: US Patent and Trademark Office

A method is disclosed for determining Richardson Number, Ri, or its reciprocal, RRi, for clear air prediction using measured potential temperature and determining the vertical gradient of potential temperature, d(theta)/dz. Wind vector from the aircraft instrumentation versus potential temperature, dW/D(theta), is determined and multiplies by d(theta)/dz to obtain dW/dz. Richardson number or its reciprocal is then determined from the relationship Ri = K(d theta)/dz divided by (dW/dz squared) for use in detecting a trend toward a threshold value for the purpose of predicting clear air turbulence. Other equations for this basic relationship are disclosed together with the combination of other atmospheric observables using multiple regression techniques.
Official Gazette of the U.S. Patent and Trademark Office

48 OCEANOGRAPHY

Includes biological, dynamic, and physical oceanography; and marine resources.

For related information see also *43 Earth Resources and Remote Sensing.*

N92-28266# Norwegian Defence Research Establishment, Kjeller.
A DOMAIN DECOMPOSITION METHOD FOR OCEAN/BOTTOM INTERACTION PROBLEMS
Ivar Lie 7 Nov. 1991 35 p
(FFI-91/7022; ISSN-0802-2437; ETN-92-91244) Avail: NTIS HC/MF A03

A domain decomposition method for numerical simulation of ocean/bottom interaction problems is considered. The acoustic propagation in sea water is modeled by the compressible Euler equations for a stratified fluid and an equation of state. The bottom is modeled by the equations of linear elasticity. The coupling between the two sets of equations is constructed by imposing the physical boundary conditions between the two media on the characteristic variables. The general method of domain decomposition for such problems, allowing an arbitrary configuration of nonoverlapping domain in both media, is detailed. ESA

N92-28283# Naval Postgraduate School, Monterey, CA.
A DIAGNOSTIC STUDY OF THE VELOCITY STRUCTURE OF A MEANDERING JET IN THE CALIFORNIA CURRENT SYSTEM USING A PRIMITIVE EQUATION MODEL M.S. Thesis
James R. Mallette, Jr. Jun. 1991 98 p
(AD-A246039) Avail: NTIS HC/MF A05

A high resolution 20-level, primitive equation model is initialized using sigma-theta data acquired during a Coastal Transition Zone (CTZ) cruise from July 6 to 12, 1988 near Point Arena, California for the purpose of diagnosing the three-dimensional dynamically balanced flow field for the region. The major feature in the region during the cruise period was a strong meandering jet which flowed equatorward and offshore, oriented in a northeast to southwest direction. A density diagnostic version of the model, in which the sigma-theta is held constant during the 72 hour integration time, is compared with a robust diagnostic version of the model, in which the sigma-theta field is allowed to adjust dynamically within the constraints of a damping time scale. The density diagnostic version of the model produces vertical velocities which are an order of magnitude larger than vertical calculated from bio-optical data collected in the same location and at the same time as the CTZ cruise. The robust diagnostic version produced vertical velocities within the range of vertical velocities calculated from the bio-optical data. The horizontal pattern of vertical velocity from the robust diagnostic version also compared well with patterns seen in trough/ridge systems in the Gulf Stream. In particular, there is horizontal convergence and downwelling all along the offshore directed part of the meandering jet. Vertical cross-section comparisons between model velocity data and ADCP velocity data collected during the cruise revealed differences which may be caused by factors neglected by the models. GRA

N92-28316# Naval Postgraduate School, Monterey, CA.
OPTICAL EFFECTS ON OCEAN MIXED LAYER DYNAMICS M.S. Thesis
Jonathan W. White Jun. 1991 96 p
(AD-A245941) Avail: NTIS HC/MF A05

Improvements to the specification of ocean optical characteristics in mixed layer dynamics are explored. The effects of reflection (albedo), refraction and attenuation of solar radiation on mixed layer dynamics are examined. Parameterization schemes are developed to characterize the attenuation of individual spectral components of total solar radiation and the refraction of direct solar radiation. The effect of these parameterization schemes on mixed layer processes is evaluated analytically and numerically. A one-dimensional mixed layer model is used to examine the sensitivity of predicted mixed layer thermal structure to individual parameterizations. The thermal structure differences that result over long and short periods using the different parameterizations show that the accuracy of mixed layer predictions is significantly affected by the method used to describe the penetration of solar radiation into the ocean. GRA

N92-28318# Naval Postgraduate School, Monterey, CA.
AN EVALUATION OF THE NAVAL OCEANIC VERTICAL AEROSOL MODEL DURING KEY90 M.S. Thesis
Thomas H. Cecere Jun. 1991 63 p
(AD-A245943) Avail: NTIS HC/MF A04

An experiment was conducted in the Florida Keys from 2 to

19 July 1990 to test the performance of the Naval Oceanic Vertical Aerosol Model (NOVAM) in a weak-convective regime. Meteorological data collected by aircraft and boat was used to generate the surface and vertical profile information files required by NOVAM. Using this information, NOVAM predicts the aerosol extinction 1/km for a vertical cross-section of the atmosphere. Aircraft-observed aerosol extinction profiles were also obtained. Comparisons between observed and NOVAM aerosol extinction profiles revealed major deviations above the cloud top. From the surface to the top of the cloud layer, NOVAM generally did an excellent job in predicting profile shape, with the magnitude of aerosol extinction tied to the extinction matched at the surface. In a few cases, observed extinction increased more rapidly than NOVAM predicted extinction from the surface to the base of the cloud layer. This is attributed to rain scavenging associated with thunderstorm activity in the area. Comparison between different aerosol extinction profiles revealed much spatial and temporal variation that was verified by Lidar profiles of atmospheric structure. Thunderstorm activity, multiple cloud-layers, and the spatial variation in the atmospheric structure have led to a hypothesis that deep-convection was responsible for the major differences between observed and predicted aerosol extinction profiles. GRA

N92-28321# Naval Oceanographic and Atmospheric Research Lab., Bay Saint Louis, MS.

A NEW OCEAN BOTTOM MAGNETOMETER SYSTEM FOR CONTINENTAL SHELF MEASUREMENTS Final Report

Will Avera, Dan Fraley, Juan Reynaud, David Byman, and Richard Burgett Nov. 1991 8 p

(AD-A247644; NOARL-PR-91-054-352) Avail: NTIS HC/MF A02

The Naval Oceanographic and Atmospheric Research Laboratory (NOARL) initiated the development of an Ocean Magnetometer System (OMS) to conduct research measurements of the ocean magnetic environment on the continental shelf and in shallow marginal seas. Little is known of the magnetic environment on the shallow continental shelf areas. Most vector magnetic measurements conducted in the ocean are from the deep ocean basins. Motion of the magnetic sensor is a major limiting factor in shallow water vector magnetic measurements. The new technology incorporates motion sensors with a vector magnetometer to improve the signal/noise of the vector magnetic measurements. In an experiment in the Gulf of Mexico, the signal/noise of the vector magnetic measurements are improved by as much as 20 dB utilizing the motion sensor data. GRA

N92-28365# Naval Postgraduate School, Monterey, CA.

A NUMERICAL STUDY OF TIME-DEPENDENT WIND FORCING OFF THE WEST COAST OF PORTUGAL, 1987-1988 M.S. Thesis

Stephen L. Buss Jun. 1991 121 p

(AD-A246775; NPS-OC-91-002) Avail: NTIS HC/MF A06

A process-oriented numerical study of time-dependent wind forcing is conducted using a ten-layer, beta-plane, primitive equation ocean model to provide insight into mesoscale eddy generation and duration off the west coast of Portugal from 1987 to 1988. The wind forcing used was derived from synoptic surface pressure analyses off Lisbon, Portugal. Results obtained show that eddies generated during the coastal upwelling season (generally occurring during the spring and summer) decay during the winter. Only cyclonic eddies form during the 1987 and 1988 upwelling seasons. The eddies are generated through a combination of barotropic and baroclinic instability mechanisms. Since the wind forcing of the five-month-long 1987 upwelling season generates larger and stronger eddies than the wind forcing of the seven-month-long 1988 upwelling season, eddy characteristics appear to be more influenced by the characteristics (e.g., intensity, duration and frequency of occurrence) of the wind forcing than by the total length of the upwelling season. This study affirms the importance of wind stress forcing to the overall surface circulation and eddy generation in the coastal ocean regime off the west coast of Portugal. GRA

N92-28402# Scripps Institution of Oceanography, La Jolla, CA. Marine Physical Lab.

TEST OF THE NEW ONR OCEAN BOTTOM SEISMOGRAPHS ON THE JUAN DE FUCA RIDGE Final Report, 1 May 1990 - 30 Sep. 1991

Leroy M. Dorman and John A. Hildebrand Jan. 1992 6 p

(Contract N00014-90-J-1881)

(AD-A247733; MPL-U-10/92) Avail: NTIS HC/MF A02

Sea tests are vital to debug the ONR ocean bottom seismographs OBS performance, especially if the instruments are to perform reliably during the early ONR funded ULF/VLF experiments. These instruments were tested in a realistic deep-sea deployment under conditions where there was little experimental risk. The SERA Expedition (Seismic Experiments on the Rise Axis) was an ideal setting for testing these instruments since the EPR Natural Laboratory provided both local and distant earthquakes as well as airgun sources from the R/V Washington. The instruments recorded seismic data continuously during a four day deployment. This experiment provided an excellent variety of signals upon which to refine the instruments. GRA

N92-28566# Planning Systems, Inc., Slidell, LA.

THE NAVY LAYERED OCEAN MODEL USERS GUIDE Final Report

Alan J. Wallcraft Dec. 1991 28 p

(Contract N00014-89-C-6002)

(AD-A247754; NOARL-35) Avail: NTIS HC/MF A03

This report is a users guide to the Navy's hydrodynamic (isopycnal) nonlinear, primitive equation, layered ocean circulation model. The model retains the free surface and uses a semi-implicit time scheme that treats all gravity waves implicitly. It can handle full-scale bottom topography, provided it is confined to the lowest layer, and an arbitrary coastline geometry. The model was first used at the Naval Oceanographic and Atmospheric Research Laboratory more than 10 years ago for simulations of the ocean circulation in the Gulf of Mexico, the Caribbean Sea, the Alboran Sea, the western Mediterranean Sea, and the global oceans. In conjunction with the issuance of this report, the model code is being made available to the ocean modeling community. The vertically integrated equations of motion and their finite difference discretization on a C-grid is presented, as is a description on the semi-implicit time scheme, the boundary conditions, and the external forcing. The model code contains internal documentation that fully describes the user-specified model parameters and data sets. This report also contains general information about how to use the model, in particular, how to set it up for a new ocean region and how to port it to a new computer system. GRA

N92-28867*# State Univ. of New York, Binghamton. Dept. of Geological Sciences.

OCEAN TIDE MODELS FOR SATELLITE GEODESY AND EARTH ROTATION Final Technical Report, Mar. 1981 - Dec. 1991

Steven R. Dickman Dec. 1991 31 p

(Grant NAG5-145)

(NASA-CR-190468; NAS 1.26:190468) Avail: NTIS HC/MF A03

A theory is presented which predicts tides in turbulent, self-gravitating, and loading oceans possessing linearized bottom friction, realistic bathymetry, and continents (at coastal boundaries no-flow conditions are imposed). The theory is phrased in terms of spherical harmonics, which allows the tide equations to be reduced to linear matrix equations. This approach also allows an ocean-wide mass conservation constraint to be applied. Solutions were obtained for 32 long and short period luni-solar tidal constituents (and the pole tide), including the tidal velocities in addition to the tide height. Calibrating the intensity of bottom friction produces reasonable phase lags for all constituents; however, tidal amplitudes compare well with those from observation and other theories only for long-period constituents. In the most recent stage of grant research, traditional theory (Liouville equations) for determining the effects of angular momentum exchange on Earth's rotation were extended to encompass high-frequency excitations (such as short-period tides). Author

N92-28913# Naval Oceanographic and Atmospheric Research Lab., Bay Saint Louis, MS.
A COUPLED REGIONAL TIDE MODEL Final Report
J. K. Lewis, G. A. Vayda, and Y. L. Hsu Jan. 1992 25 p
(AD-A247917; NOARL-TN-221) Avail: NTIS HC/MF A03

Two dimensional numerical models were used to further study appropriate conditions at the open boundaries for regional models forced by parameters from a global tidal model. The open boundary condition of Reid and Bodine (1968) was applied to regional models of the western Florida shelf, north-central Gulf of Mexico, and the Kenya Coast. In addition, two semienclosed basins were modeled, the Persian Gulf, and the entire Gulf of Mexico. A number of tests were conducted to determine how well forcing, using the tidal constants from the 1 degree by 1 degree Schwiderski global model (1981, 1983) could reproduce regional tides as determined from observations. As seen in our previous work, the Reid and Bodine formulation was quite effective in driving the regional models while still allowing wave energy to propagate through the open boundaries and out of the model. The western Florida shelf is known to resonate with the M(sub 2) tide. Under such circumstances, the bottom friction becomes quite important in obtaining correct predictions of the observed tidal amplitudes. Several bottom friction schemes with varying drag coefficients were tested for both the north-central gulf and Florida shelf models. The results are discussed in light of the fact that we seek one scheme that would be applicable for both resonant and nonresonant situations. GRA

N92-28938# Scripps Institution of Oceanography, La Jolla, CA.
AUTONOMOUS OCEAN PROFILER Interim Report, Jun. - Sep. 1991
Sep. 1991 3 p
(Contract N00014-89-C-6014)
(AD-A247657; NOARL-CR-011-92) Avail: NTIS HC/MF A01

Six of the original ten Autonomous Lagrangian Circulation Explorers (ALACEs) deployed in Drake Passage in January 1990 were still operational at the end of September 1991. After 20 months and 40 vertical cycles these ALACEs are nearing their design life of 25 months and 50 cycles. Since the Drake passage deployment, ALACE has been extensively improved. The redesigns appear to be successful and of 36 ALACEs deployed during early 1991, only one has suffered infant mortality; two of the 10 Drake Passage ALACEs died in their first cycle. GRA

N92-28939# California Univ., San Diego, La Jolla.
SEAFLOOR PRESSURE ARRAY STUDIES AT ULTRA-LOW FREQUENCIES Final Report
John A. Orcutt 1991 25 p
(Contract N00014-90-J-1228)
(AD-A247663) Avail: NTIS HC/MF A03

Broadband inertial measurements of environmental noise on the seafloor have always been difficult technically and few examples of successful measurements are available. A knowledge of environmental noise processes, however, is essential for future broadband instrument design and deployment. In order to measure broadband noise routinely, a low frequency pressure gauge designed for deep ocean recording was adapted for use with the Scripps' OBSs and calibrated in the laboratory. The instruments were deployed twice in array configurations along with other pressure sensors in 4.1 km deep ocean southwest of San Diego, California. Spectra from the hydrophones showed a stable 0.15 Hz microseism peak throughout the deployment period with some evidence of dispersion. Smaller peaks at 0.3-1 Hz appeared when the local wind became stronger. Highly coherent peaks at 0.085 Hz, originally interpreted as 'single frequency microseisms', were found to be Rayleigh wavetrains from large earthquakes. Reverberations in the water column caused by P-wave arrivals from the earthquakes were also observed. Coherence in the microseism band was significant only for instruments separated by less than 6 km, lending support to the hypothesis that the source is at least in part isotropic and random. Wavenumber analysis was successful only for the well-defined earthquake signals while for the microseism band, low coherence and the location of the sensors reduced the array's useful azimuthal resolution. GRA

N92-28951# Institute for Naval Oceanography, Bay Saint Louis, MS.
OCEANOGRAPHIC DATA DICTIONARY FOR NETCDF FILES
A. L. Perkins Jan. 1992 24 p
(AD-A250017; INO-TM-7) Avail: NTIS HC/MF A03

This document presents a data dictionary for oceanographic netCDF data files. Commonly used words are abbreviated. Abbreviations are then combined to make sentence-like variable names that describe the contents of the variable. The goal is to facilitate netCDF file use by making the CDF form of the data self-documenting. GRA

N92-28963# Naval Oceanographic and Atmospheric Research Lab., Bay Saint Louis, MS.
NEURAL NETWORK PARAMETER ESTIMATION FOR THE MODIFIED BISTATIC SCATTERING STRENGTH MODEL (BISSM) Final Technical Report
B. S. Bourgeois Dec. 1991 74 p
(AD-A247913; NOARL-TN-214) Avail: NTIS HC/MF A04

This technical note investigates the estimation of environmental parameters in the Bistatic Scattering Strength Model (BISSM) given backscatter strength and bathymetric data. A monostatic version of the model is derived, since this will be the form of data provided by acoustic imaging sensors. Feedforward neural networks, using the backpropagation learning algorithm, are used to perform the estimation of parameters for the nonlinear BISSM equation. The parameters that can be estimated are identified, and neural networks have been developed to estimate these parameters. Using noise-free artificial data generated with the BISSM equation, the networks provided excellent estimates of the desired parameters. The primary impetus for this work is a need for the Naval Oceanographic Office (NAVOCENO) to provide relevant survey support for Low-Frequency Active Acoustics (LFAA) programs and future Low-Frequency Active (LFA) operational systems. It has been recognized by the Commander, Naval Oceanographic Command (CNOC) that such support will require knowledge of certain bottom and subbottom properties and high-resolution geomorphology. The BISSM model has been proposed as a model for aspects of active bottom reverberation. GRA

N92-28977# Naval Postgraduate School, Monterey, CA.
MODELING PULSE TRANSMISSION IN THE MONTEREY BAY USING PARABOLIC EQUATION METHODS M.S. Thesis
Eric L. Westreich Dec. 1991 38 p
(AD-A246465) Avail: NTIS HC/MF A03

Acoustic tomography signal transmissions in Monterey Bay are modelled using the time-domain parabolic equation method. Comparison of the model output with the measured arrival structures obtained in Monterey Bay in 1988 shows that this Fourier synthesis can produce good agreement with data. Furthermore, identification of the measured modal arrivals is possible by decomposing the PE model output into individual normal modes. Modal identification provides for the application of tomography in shallow water. GRA

N92-29211# Institute of Oceanographic Sciences, Wormley (England).
CTD DATA FROM THE NORTH EAST ATLANTIC, APRIL 1989, COLLECTED ON RRS DISCOVERY CRUISE 181
J. F. Read, R. T. Pollard, and C. Hirst 1991 156 p
(IOS-285-1991; ETN-92-91346) Avail: NTIS HC/MF A08; Institute of Oceanographic Sciences, Deacon Lab., Wormley, Godalming, Surrey GU8 5UB, England, HC 37 Sterling pounds

Conductive temperature depth (CTD) data collected in the north east Atlantic Ocean is presented. Four major sections were worked; the first in the Bay of Biskay down 7 deg west, then from the coast of Portugal out to 20 deg west along 41.5 deg north, the section along 20 deg west from 41.5 to 54 deg north was worked

in conjunction with BIOFS (Biogeochemical Ocean Flux Study), and the last section crossed the Rockall Trough at 54 deg north. Additional stations were worked in other locations and a total of 55 profiles are presented. Calibration and processing of the CTD data are described and the data are presented in profile plots of temperature, salinity and oxygen with listings at standard pressure levels of basic and derived variables. Discrete samples from each CTD cast are tabulated separately. ESA

N92-29212# Institute of Oceanographic Sciences, Wormley (England).
MOORED CURRENT MEASUREMENTS MADE IN THE ICELAND FAEROES REGION DURING JULY-AUGUST 1990
G. Griffiths, N. A. Crisp, and L. A. Povey 1991 47 p
(IOS-286-1991; ETN-92-91347) Avail: NTIS HC/MF A03;
Institute of Oceanographic Sciences, Deacon Lab., Wormley, Godalming, Surrey GU8 5UB, England, H 15 Sterling pounds

Current measurements at a fixed location (64 deg 23.8 north, 11 deg 55.7 west) just off the Iceland shelf near the Iceland Faeroes front are presented. A moored, upward looking, self contained ADCP recorded a 300 m profile of the current. Additional data, including temperature and pressure, were recorded by an S4 current meter and an Aanderaa rotor vane instrument. Data from all instruments were recovered error free, and the consistency of the data is supported by good correlation of the statistical analyses performed on each data set. During the deployment, a large change in the mean current was observed. This may be associated with the Iceland Faeroes front meandering over the mooring. ESA

N92-29213# Institute of Oceanographic Sciences, Wormley (England).
EVALUATION OF A SOLENT SONIC ANEMOMETER ON RRS CHARLES DARWIN CRUISE 43
M. J. Yelland, P. K. Taylor, K. G. Birch, R. W. Pascal, and A. L. Williams 1991 52 p Sponsored in part by Ministry of Agriculture, Fisheries and Food and Admiralty Research Lab.
(IOS-288-1991; ETN-92-91348) Avail: NTIS HC/MF A04;
Institute of Oceanographic Sciences, Deacon Lab., Wormley, Godalming, Surrey GU8 5UB, England, HC 16 Sterling pounds

A prototype Solent sonic anemometer was evaluated by comparison with a propelier vane anemometer and a Kaijo-Denki anemometer and by postcruise wind tunnel tests. The Solent sonic anemometer is a newly available instrument. Its low power consumption means that it would be suitable for buoy mounting. Following the trials, changes were made to the production model design. Using the calibration procedures used for production models, the Solent sonic should measure the mean wind to better than the 1.5 specified. The spectra from the prototype showed an increase in level at frequencies above about 2 Hz which is believed to be due to noise. This problem appears to have been overcome in production models by the faster sonic sampling rate. Wind stress values, determined from the observed spectral levels using the dissipation technique, were not significantly different from those determined by the Kaijo-Denki. The use of the asymmetrical head model is recommended to minimize the occurrence of spectral distortion when the relative wind direction is within 20 deg of one of the instrument struts. ESA

N92-29215# Bidston Observatory, Merseyside (England).
AN INVENTORY OF DATA COLLECTED DURING THE NERC'S NORTH SEA COMMUNITY RESEARCH PROJECT, 1987-1992
M. W. L. Blackley, R. K. Lowry, and L. J. Rickards 1991 74 p
(Rept-21-1991; ETN-92-91344) Avail: NTIS HC/MF A041;
Proudman Oceanographic Lab., Bidston Observatory, Birkenhead, Merseyside L43 7RA, England, HC 16 Sterling pounds

The data gathered as part of the Natural Environment Research Council (NERC) North Sea Community Research Project is presented. The aim of this project was a series of prognostic water quality models to aid management of the North Sea. The survey was planned to cover a 15 month period needed to resolve the seasonal cycle. Seasonal changes dominate events within the North Sea (winter storms, spring floods, and summer sunshine). Understanding the effects of these phenomena is essential for the development of water quality models. In between the survey cruises, a process study cruise looked at some particular aspect of the science of the North Sea. Data from these cruises are incorporated into the North Sea database. ESA

N92-29216# Institute of Oceanographic Sciences, Wormley (England).
DIRECTIONAL WAVE DATA RECORDED OFF FLAMBOROUGH HEAD (ENGLAND)
C. H. Clayson and J. A. Ewing 1990 44 p Sponsored by Dept. of Energy (UK)
(IOS-273-1990; ETN-92-91345) Avail: NTIS HC/MF A03;
Institute of Oceanographic Sciences, Deacon Lab., Wormley, Godalming, Surrey GU8 5UB, England, HC 14 Sterling pounds

A directional wave buoy was deployed 7.7 nm north-east of Flamborough Head, in the southern North Sea during the period from Dec. 1984 - May 1986. The deployments of the Datawell WAVEC buoy were carried out on behalf of the United Kingdom Department of Energy. The operational history, analytical techniques, and the results obtained during the measurement period are reported. The basic nondirectional information consists of measurements of the frequency spectrum from which wave height and period statistics are computed. In addition to this information, the directional wave buoy provides estimates of the directional spectrum from which the mean wave direction and directional spread are calculated. The results of this study are contained in a set of tables and figures which, in addition to wave height and period statistics, provide statistics of the joint occurrence of wave height, wave period, and wave direction. Information is given for each of the four seasons and for the whole data set. ESA

N92-29225# North Carolina Univ., Chapel Hill. Venable Lab.
STRUCTURE ENERGETICS AND DYNAMICS OF GULF STREAM VARIABILITY Final Report, 1 Jan. 1990 - 31 Dec. 1991
John M. Bane 11 Mar. 1992 7 p
(Contract N00014-90-J-1596)
(AD-A248246) Avail: NTIS HC/MF A02

This contract supported research on the physical oceanography of the Gulf Stream as part of the SYNoptic Ocean Prediction (SYNOP) Program. The objective of the research was to increase our understanding of the structure, energetics and dynamics of the Gulf Stream in the western portion of the SYNOP study area, which is between 75 deg W and 67 deg W, where Gulf Stream meanders are of large amplitude and still growing, and where the activity of the adjacent ring and eddy field is vigorous. To address this objective, direct measurements were made with an array of current meter moorings and inverted echo sounders (IESs) with bottom pressure sensors, arranged to observe the oceanic time-varying velocity, temperature, and pressure fields on a three dimensional grid of sites. GRA

51 LIFE SCIENCES (GENERAL)

N92-28247# Army Armament Research, Development and Engineering Center, Picatinny Arsenal, NJ.
EFFECTS OF EXTREMELY HIGH G ACCELERATION FORCES ON NASA'S CONTROL AND SPACE EXPOSED TOMATO SEEDS Special Publication
Roger Wentling and Carl DeFranco Dec. 1991 76 p
(AD-A247488; ARAED-SP-91002) Avail: NTIS HC/MF A05

An experiment to expose tomato seeds to high levels of mechanical shock after they had spent six years in space aboard NASA's Long Duration Exposure Facility was conducted in the High 'G' Air gun Test Facility at Picatinny Arsenal. A group of control seeds that did not go into space were also exposed to high levels of shock. The object of this test was to determine if high levels of gravity affected the growth of the plants grown

from this seed or the seeds from these plants. The tomato seeds were exposed from 1,258 times gravity (g) to 119,380 times gravity. Germination occurred at every level of testing and seeds from these plants will be saved to grow plants next year. In general, seeds from the higher shock levels produced higher quality tomatoes, and some abnormalities in developing of green tomatoes were observed at intermediate levels. Genetic effects, if any, are expected to be observed in the next generation which will be grown next year. GRA

N92-28382# Oak Ridge National Lab., TN.
PRIMER ON MOLECULAR GENETICS
Apr. 1992 28 p Prepared in cooperation with DOE, Washington, DC
(Contract DE-AC05-84OR-21400)
(DE92-010680; ORNL/M-2026) Avail: NTIS HC/MF A03

This report is taken from the April 1992 draft of the DOE Human Genome 1991-1992 Program Report, which is expected to be published in May 1992. The primer is intended to be an introduction to basic principles of molecular genetics pertaining to the genome project. The material contained herein is not final and may be incomplete. Techniques of genetic mapping and DNA sequencing are described. DOE

N92-29089# Naval Oceanographic and Atmospheric Research Lab., Bay Saint Louis, MS.
BIOLUMINESCENCE IN THE WESTERN ALBORAN SEA IN APRIL 1991 Final Report
D. M. Lavoie, D. K. Young, and M. S. Hulbert Feb. 1992 99 p
(AD-A250016; NOARL-TN-212) Avail: NTIS HC/MF A05

This document reports on the results of an expedition to study bioluminescence in the western Alboran Sea of the Mediterranean in April of 1991. Two oceanographic research vessels and a research submersible were involved in making extensive measurements of bioluminescence and optical properties, as well as related biological and physical parameters. The primary research tool used was the HIDEX, a high resolution, state-of-the-art bathyphotometer. The results reported here cover only bioluminescence and related biological measurements made from the USNS Bartlett. Recommendations are given for survey requirements needed to extend measurements seasonally and geographically in this region of the Mediterranean. GRA

52 AEROSPACE MEDICINE

Includes physiological factors; biological effects of radiation; and effects of weightlessness on man and animals.

N92-28242# Army Biomedical Research and Development Lab., Fort Detrick, MD.
ENVIRONMENTAL TESTING OF THE XI SCAN 1000, PORTABLE FLUOROSCOPIC AND RADIOGRAPHIC IMAGING SYSTEM Final Report, Dec. 1990 - Oct. 1991
David D. Baker, Jr., James H. Nelson, and David L. Danley 14 Feb. 1992 32 p
(DA Proj. 3M1-62787-A-874)
(AD-A247167; USABRDL-9201) Avail: NTIS HC/MF A03

The Xi Scan 1000, Portable Fluoroscopic and Radiographic Imaging System is a hand-held unit which can be configured as a 2.6 inch, direct view fluoroscope or a standard X-ray machine for 8 by 10 inch film. This study used the System 3 package including a C-arm, cassette tray, image Intensifier, and rechargeable battery power supply which weigh 30 pounds in the commercial carrying case. Although this system could not replace existing military radiography equipment, it could enhance current capability. The fluoroscope would benefit surgeons during procedures in far-forward facilities and it could provide instant feedback to other medical personnel as to the severity of common injuries. Although the Xi Scan 1000 appears robust, it was not designed for harsh environmental conditions. For this study, a container was procured that meets the Deployable Medical Systems (DEPMEDS) packaging standard (MIL-D-42048). With this container, the system was subjected to environmental tests IAW MIL-STD-810E, Environmental Test Methods and Engineering Guidelines, to include: storage and operation at high and low temperatures, transit shock, and vibration. After each environmental insult, performance tests were conducted to determine whether the system continued to meet specifications. Whereas the results showed the system susceptible to damage from temperature extremes and shock, the failure modes were related to design features currently being addressed. GRA

N92-28278# California Univ., Berkeley. Lawrence Berkeley Lab.
PROBLEMS IN MECHANISTIC THEORETICAL MODELS FOR CELL TRANSFORMATION BY IONIZING RADIATION
A. Chatterjee and W. R. Holley Oct. 1991 8 p Presented at the Workshop on Biophysical Modelling of Radiation Effects, Padua, Italy, 2-5 Sep. 1991
(Contract DE-AC03-76SF-00098)
(DE92-010265; LBL-31398; CONF-9109107-5) Avail: NTIS HC/MF A02

A mechanistic model based on yields of double strand breaks has been developed to determine the dose response curves for cell transformation frequencies. At its present stage the model is applicable to immortal cell lines and to various qualities (x-rays, neon and iron) of ionizing radiation. Presently, we have considered four types of processes which can lead to activation phenomena: (1) point mutation events on a regulatory segment of selected oncogenes; (2) inactivation of suppressor genes, through point mutation; (3) deletion of a suppressor gene by a single track; and (4) deletion of a suppressor gene by two tracks. DOE

N92-28288# Army Research Inst. for the Behavioral and Social Sciences, Alexandria, VA.
EFFECTS OF HIGH TERRESTRIAL ALTITUDE ON MILITARY PERFORMANCE
Louis E. Banderet and Richard L. Burse 1991 31 p Submitted for publication
(AD-A246695; USARIEM-T2-92) Avail: NTIS HC/MF A03

When people travel to terrestrial altitudes greater than 3000 m, their well being is usually compromised. At high altitude, the decreased atmospheric pressure results in a reduction of the partial pressure of oxygen and lowers the rate at which oxygen can diffuse into the blood. This decreases the oxygen supply to the brain, muscles, and other parts of the body and reduces the maximum rate at which the body can use oxygen to perform physical work. The main medical programs at high altitude which impact physical and mental performance are acute mountain sickness, high altitude cerebral edema (HACE), and high-altitude pulmonary edema. These disorders can usually be prevented by ascending slowly to 3000 m and then climbing 500 m on each subsequent ascent, allowing 1-2 days to acclimatize at each altitude. High altitude exposure can have profound effects on mental processes. Judgment may be severely impaired, especially if an individual is exposed to an extremely high altitude or has signs of HACE. Typically, the rate of performance on many tasks slows. On others, people more frequently neglect conceptual, computational, and procedural strategies. The use of optimal ascent profiles, medications, psychological strategies, and nutrients can facilitate coping and functioning in high-altitude environments. GRA

N92-28397# Arizona Univ., Tucson.
THE COORDINATED NONINVASIVE STUDIES (CNS) PROJECT, PHASE 1 Final Report, 8 Sep. 1988 - 7 Sep. 1991
Judith L. Lauter Dec. 1991 86 p
(Grant AF-AFOSR-0352-88)
(AD-A247159; AFOSR-92-0146TR-Phase-1) Avail: NTIS HC/MF A05

The CNS Project combines several noninvasive methods for monitoring brain structure and function in a test battery. Phase One (1988-1991) focussed on neuroanatomical and neurophysiological correlates of behavioral ear advantages for two sets of complex sounds. Fifteen subjects neurologically normal

according to conventional standards were tested with dichotic listening (2 measures), NM (2 measures), evoked potentials (2 measures), and qEEG (4 measures). One subject was also tested under similar conditions with PET. Results indicated: (1) Each individual had a distinct sidedness bias articulated in terms of a combination of anatomical and physiological variables; (2) These individual patterns cut across conventional categories such as gender and handedness; (3) In some of the subjects, these CNS profiles comprised internally consistent patterns of asymmetries linking subcortical physiology, cortical anatomy and cortical physiology; (4) In others, departures from such consistency signalled evidence of a variety of subtle neuropathologies, such as stuttering, mild learning disorder, central auditory dysfunction, or a history of hyperactivity and/or substance abuse. GRA

N92-28420*# National Aeronautics and Space Administration. Ames Research Center, Moffett Field, CA.
THERMOREGULATION DURING SPACEFLIGHT
John E. Greenleaf and Suzanne M. Fortney (National Aeronautics and Space Administration. Lyndon B. Johnson Space Center, Houston, TX.) Jan. 1992 34 p
(RTOP 199-18-12-07)
(NASA-TM-103913; A-92043; NAS 1.15:103913) Avail: NTIS HC/MF A03

The purpose of this flight proposal is to investigate human thermoregulatory parameters during exercise in microgravity. The hypothesis to be tested is that microgravity-adopted astronauts will exhibit accentuated increases in their core temperature (excess hyperthermia) during exercise because of altered heat loss responses due to reduced sweating and/or accentuated vasodilation. The specific aims are (1) to compare core and skin temperature responses during moderate exercise before flight and inflight; (2) to determine whether the hypothesized inflight excessive hyperthermia is due to increased heat production, reduced, sweating, impaired peripheral vasodilation, or to some combination of these factors; and (3) to determine whether heat production at an exercise load of 60 percent of the maximal working capacity is similar preflight and inflight. It is expected that the astronauts will exhibit excessive hyperthermia during exposure to microgravity which will be caused by decreased sweating and decreased skin blood flow. Author

N92-28515# Oregon Health Sciences Univ., Portland. Dept. of Biochemistry and Molecular Biology.
STRUCTURAL CHARACTERIZATION OF CROSS-LINKED HEMOGLOBINS DEVELOPED AS POTENTIAL TRANSFUSION SUBSTITUTES Final Report, 1 Nov. 1988 - 31 Oct. 1991
Richard T. Jones 30 Nov. 1991 101 p
(Contract DAMD17-89-C-9002; DA Proj. 3M1-62787-A-874)
(AD-A246777) Avail: NTIS HC/MF A06

Structural and functional studies of chemically modified hemoglobins have been done in an effort to find reagents and conditions that are suitable to produce cross-linked hemoglobin derivatives that would be suitable for use as acellular substitutes for the transfusions of erythrocytes. The effects of modifying hemoglobin with five different dicarboxylic bis(methyl phosphate) and three tricarboxylic tris(methyl phosphate) reagents provided by Professor Ronald Kluger have been examined by ion exchange separation of hemoglobin products, globin chain separation, peptide pattern analysis, and oxygen equilibrium measurements. The extent of reaction varied depending on the conformational state of the hemoglobin and the size of the reagent. Both cross-linked and uncross-linked products have been found and characterized structurally and functionally. Several have reduced oxygen affinities. A strong correlation was found between the oxygen affinities and the bridging distances of the beta1-x-82beta crosslinked hemoglobins. GRA

N92-28685# Lawrence Livermore National Lab., CA.
SOMATIC GENE MUTATION IN THE HUMAN IN RELATION TO RADIATION RISK
M. L. Mendelsohn Jan. 1992 10 p Presented at the 27th National Council on Radiation Protection and Measurements Annual Meeting on Genes, Cancer and Radiation Protection, Washington, DC, 2-3 Apr. 1991
(Contract W-7405-eng-48)
(DE92-009459; UCRL-JC-109513; CONF-9104298-2) Avail: NTIS HC/MF A02

This report discusses the measurement of somatic gene-mutation frequencies in the human. Questions were asked concerning their measurement, response to radiation, ability to function as a dosimeter, and what they tell us about the somatic mutation theory of carcinogenesis. DOE

N92-28755* National Aeronautics and Space Administration. Lyndon B. Johnson Space Center, Houston, TX.
PORTABLE DYNAMIC FUNDUS INSTRUMENT Patent
Gerald R. Taylor, inventor (to NASA), Richard T. Meehan, inventor (to NASA), Norwood R. Hunter, inventor (to NASA), Michael P. Caputo, inventor (to NASA), and C. Robert Gibson, inventor (to NASA) 30 Jun. 1992 9 p Filed 29 Jun. 1990 Supersedes N91-13865 (29 - 5, p 694)
(NASA-Case-MSC-21675-1; US-Patent-5,125,730;
US-Patent-Appl-SN-562095; US-Patent-Class-351-206;
US-Patent-Class-351-221; Int-Patent-Class-A61B-3/14) Avail: US Patent and Trademark Office

A portable diagnostic image analysis instrument is disclosed for retinal funduscopy in which an eye fundus image is optically processed by a lens system to a charge coupled device (CCD) which produces recordable and viewable output data and is simultaneously viewable on an electronic view finder. The fundus image is processed to develop a representation of the vessel or vessels from the output data.
Official Gazette of the U.S. Patent and Trademark Office

N92-28844# Office National d'Etudes et de Recherches Aerospatiales, Paris (France). Direction de l'Energetique.
STUDY OF THE LOSS OF CONSCIOUSNESS INFLIGHT BY FIGHTER AIRCRAFT PILOTS [ETUDE THEORIQUE DE LA PERTE DE CONNAISSANCE EN VOL DES PILOTES D'AVIONS DE CHASSE]
Daniel Gaffie and P. Quandieu (Centre d'Enseignement et de Recherches de Medecine Aeronautique, Paris, France) 15 Nov. 1990 64 p In FRENCH
(Contract DRET-89-1208)
(ONERA-RTS-11/3446-EY; ETN-92-91328) Avail: NTIS HC/MF A04

A model for studying the blood flow in a flexible blood vessel is proposed. From the symptotic analysis of the flow equations, a one dimensional simplified equation is obtained. In this simplified equation, the flow mean velocity, the blood vessel cross section, and the blood vessel wall mean shear stress are considered. A numerical solution is calculated, by means of a finite volume method, which includes a flow decomposition technique. The results show that the rate of the acceleration of the voluminal force induced by the motion of the aircraft is one of the most important parameters concerning the pilot's loss of conciousness. ESA

N92-28886# Jewish Hospital of Brooklyn, NY.
STUDY OF SCN NEUROCHEMISTRY USING IN VIVO MICRODIALYSIS IN THE CONSCIOUS BRAIN: CORRELATION WITH OVERT CIRCADIAN RHYTHMS Annual Report, 1 Nov. 1990 - 31 Oct. 1991
David J. Glass 31 Oct. 1991 9 p
(Grant AF-AFOSR-0047-90)
(AD-A247172; AFOSR-92-0104TR) Avail: NTIS HC/MF A02

We have completed the assessment of the diurnal variation in serotonergic activity in the SCN and its temporal relationship to wheel-running behavior under lightentrained (LD 14:10) and free-running (DD) conditions. First, under LD there was a marked diurnal rhythm in serotonergic activity with peak levels occurring at lightoff during the animals' initial bout of wheel-running activity. Thereafter, serotonergic activity decreased to daytime levels by the next morning, despite robust bouts of nocturnal wheel running behavior. Also, daytime periods of activity exhibited by some individuals was not associated with increased serotonergic activity.

From these results, it is hypothesized that serotonin in the SCN does not acutely trigger motor activity. Instead, it appears that serotonin is involved in coordinating light-entrained activity rhythms with the LD cycle, which is consistent with the findings of other researches using lesions or pharmacological approaches. Our second original finding is that the diurnal rhythm is serotonergic activity that is lost, or greatly diminished, in free-running hamsters held under DD for 3 wks. Thus, the rhythm in serotonergic activity seen under LD probably is not circadian in nature, but is passively driven by an external influence, i.e., the light-dark cycle. GRA

N92-28920# Texas Univ. Health Science Center, San Antonio.
INVESTIGATION OF LASER-INDUCED RETINAL DAMAGE Annual Report, 1 Apr. 1991 - 31 Mar. 1992
Randolph D. Glickman and Kwok-Wai Lam 22 Apr. 1992 34 p
(Grant AF-AFOSR-0208-91)
(AD-A250173; AFOSR-92-0316TR) Avail: NTIS HC/MF A03

Laser-induced, photooxidative damage in ocular tissue was studied with a quantitative assay using high performance liquid chromatography (HPLC) to separate oxidized and reduced ascorbic acid in exposed tissue components. We demonstrated that ascorbic acid, incubated with whole, bovine retinal pigment epithelial (RPE) cells, was oxidized when the reaction mixture was exposed to the output of an argon-ion continuous wave laser The amount of ascorbic acid oxidized was proportional to the irradiance of the sample, and the reaction was wavelength-dependent, with short-wavelength visible light more effective than long-wavelengths in driving the reaction. The photosensitizing activity was associated with the RPE melanin pigment granules, and was not lost after disrupting or heating the RPE cells. Because melanin was known to form free radicals when illuminated, we hypothesized that ascorbic acid detoxified the light-activated melanin free radicals while being itself oxidized in process. If the supply of reduced ascorbic acid were exhausted, however, the activated melanin could have been the source of tissue-damaging radicals. This model was consistent with a photochemical damage mechanism involving light-activated melanin. GRA

N92-29123# Arizona Univ., Tucson.
THE CHRONIC EFFECTS OF JP-8 JET FUEL EXPOSURE ON THE LUNGS Annual Report, 1 Apr. 1991 - 1 Apr. 1992
Mark L. Witten 23 Apr. 1992 17 p
(AD-A250308; AFOSR-92-0314TR) Avail: NTIS HC/MF A03

This research has resulted in four separate projects. The first was the exposure of Fischer 344 rats to JP-8 jet fuel for 7 or 28 days. This exposure resulted in changes in pulmonary function and lung chemical mediators, specifically Substance P, after 28 days of exposure. The second project dealt with blocking the increase in SP in these rats by a pretreatment regimen with capsaicin before jet fuel exposure. Capsaicin caused a further increase in lung permeability and a million-fold increase in airway sensitivity to histamine after the 7-day jet fuel exposure. The third project dealt with the effects of a 7-day jet fuel exposure in congenic mice who are deficient in the inducibility of the aryl hydrocarbon hydroxylase enzyme. These mice are relatively resistant to the effects of jet fuel-induced lung injury. The fourth project investigated the effects of the jet fuel exposure on secondary organs, specifically the liver, spleen, and kidneys. There were pathological differences in the liver, spleen, and kidneys between the 7-day jet fuel exposure group and baseline controls. However, some of these differences were not apparent in the 28-day exposure group, possibly indicating compensatory mechanisms to the exposure. GRA

N92-29179# Massachusetts Univ., Worcester. Dept. of Neurology.
NON-LINEAR ANALYSIS OF VISUAL CORTICAL NEURONS Final Report, 1 Jan. 1989 - 31 Dec. 1991
Lowell D. Jacobsen, James P. Gaska, and Daniel A. Pollen 7 Apr. 1992 26 p
(Grant AF-AFOSR-0247-89)
(AD-A250233; AFOSR-92-0307TR) Avail: NTIS HC/MF A03

Quantitative procedures were developed for testing block-structured models for multi-input nonlinear visual circuits studied with spatiotemporal white noise. A linear-nonlinear (LN) model test index was found to be suitable for classifying cells as simple versus complex. Although simple cells were better modeled as LN systems than complex cells, most simple cells deviated considerably from LN behavior. A nonlinearity of cortical origin would appear to be responsible, possibly activated more strongly by broadband noise than by sinewave grating stimuli. Also, two classes of binocular complex cells were identified. Whereas all binocular complex cells necessarily have a non-zero second-order same-eye interaction kernel, their second-order cross-eye interaction kernel could, it was found, be either non-zero or identically zero. GRA

N92-28534# Netherlands Aerospace Medical Centre, Soesterberg.
G-TOLERANCE AND SPATIAL DISORIENTATION: CAN SIMULATION HELP US?
J. Smit and Robert E. vanPatten (Van Patten, Robert E., Bellbrook, OH) *In* AGARD, Piloted Simulation Effectiveness Feb. 1992 7 p (For primary document see N92-28522 19-01)
Copyright Avail: NTIS HC/MF A15

53 BEHAVIORAL SCIENCES

Includes psychological factors; individual and group behavior; crew training and evaluation; and psychiatric research.

N92-28396# Human Engineering Labs., Aberdeen Proving Ground, MD.
PROGRAM CLUSTER: AN IDENTIFICATION OF FIXATION CLUSTER CHARACTERISTICS
Ramakrishna S. Pillalamarri, B. D. Barnette, Robert Karsh, and Deborah P. Birkmire Jan. 1992 30 p
(AD-A247014; HEL-TN-1-92) Avail: NTIS HC/MF A03

Innovative software techniques to advance methods of analysis in eye movement research have not kept pace with the development of hardware for collecting the samples of eye position. Eye fixation and duration have been the primary measures focused upon to glean knowledge of subjects' performance while engaged in cognitive visual tasks. Program cluster was developed as a means of investigating the dynamics of target examination characteristics that did not lend themselves to traditional eye movement analysis methods. The development of this tool proved to be a valuable means of assessing visual activity at a micro level as compared to the gross measures of distribution of visual attention in various areas of the visual field. This report describes the history surrounding the development of program cluster as an analysis tool, the source of input required for its execution, the mechanics of the execution as an interactive process, the program's products of visual displays and data file output, and potential application of such a tool for analysis of visual activity. GRA

N92-28408# Naval Postgraduate School, Monterey, CA.
A PROFILE OF SCIENTIST AND ENGINEER TRAINING CONDUCTED BY THE NAVAL AVIONICS CENTER M.S. Thesis
Michael L. Gregory Dec. 1991 425 p
(AD-A245925) Avail: NTIS HC/MF A18

This thesis provides an assessment of the training program from the perspective of civilian scientists and engineers working at the Naval Avionics Center (NAC). This assessment can be used in conjunction with other studies to provide NAC management with a basis on which to evaluate its return on investment from training. The author used a questionnaire to survey scientists and engineers in order to reveal training related trends across departments, job categories, paygrade levels, gender, ethnic origin, age, experience at NAC, and marital status. The author concluded that there is a good organizational climate for and support of the training program at NAC, that most of the job needs of scientists and engineers are being met by NAC's training program, and that there are some administrative changes needed to improve the training program. In addition, the kinds of NAC training that are

most useful to scientists and engineers are identified. The author presented several recommendations to improve the training program at NAC. GRA

N92-28557# Naval Aerospace Medical Research Lab., Pensacola, FL.
DELAYS IN LASER GLARE ONSET DIFFERENTIALLY AFFECT TARGET-LOCATION PERFORMANCE IN A VISUAL SEARCH TASK Interim Report, 1 Oct. 1990 - 30 Sep. 1991
M. D. Reddix, J. A. DAndrea, and P. D. Collyer Jun. 1991 23 p
(AD-A246708; NAMRL-1367) Avail: NTIS HC/MF A03

The present study examined the effects of low-intensity argon-laser glare on the visual search performance of aviators. Using a modified backward-masking paradigm, subjects were exposed to laser glare, either while seated in a cockpit simulation trainer with attached F-15 windscreen assembly. Brief exposure to laser glare, either 25 or 50 ms after a visual scene's onset, produced significant decrements in target-detection performance relative to a no-glare control whereas a 300-ms delay of laser glare onset had very little effect. The intensity of the light entering the eye (.38 micro-W/cm(exp 2)) and producing these effects was far below the Maximum Permissible Exposure (MPE) limit for safe viewing of coherent light. In addition, these effects were modulated by a target's distance from the center of the beam path (also center of the visual display). Specifically, targets closest to the center of the beam path were responded to the most slowly and with the least accuracy. This study demonstrated that the presence of the laser glare is not sufficient, in and of itself, to diminish target-detection performance. The time at which laser glare is experienced is an important factor in determining the probability and extent of visually mediated performance decrements. GRA

N92-28744*# National Aeronautics and Space Administration. Ames Research Center, Moffett Field, CA.
CREW STATION RESEARCH AND DEVELOPMENT FACILITY TRAINING FOR THE LIGHT HELICOPTER DEMONSTRATION/VALIDATION PROGRAM
Joy Hamerman Matsumoto (Bio-Dynamics Research and Development Corp., Eugene, OR.), Steven Rogers, Michael McCauley (Monterey Technologies, Inc., Carmel, CA.), and Al Salinas (Army Materiel Systems Analysis Activity, Aberdeen Proving Ground, MD.) Mar. 1992 10 p
(Contract NAS2-12849; RTOP 505-61-51)
(NASA-TM-103865; A-91153; NAS 1.15:103865; USAAVSCOM-TR-92-A-003) Avail: NTIS HC/MF A02

The U.S. Army Crew Station Research and Development Branch (CSRDB) of the Aircraft Simulation Division (AVSCOM) was tasked by the Light Helicopter Program Manager (LH-PM) to provide training to Army personnel in advanced aircraft simulation technology. The purpose of this training was to prepare different groups of pilots to support and evaluate two contractor simulation efforts during the Demonstration/Validation (DEM/VAL) phase of the LH program. The personnel in the CSRDB developed mission oriented training programs to accomplish the objectives, conduct the programs, and provide guidance to army personnel and support personnel throughout the DEM/VAL phase. Author

N92-28775# Argonne National Lab., IL.
A STRATEGY FOR MINIMIZING COMMON MODE HUMAN ERROR IN EXECUTING CRITICAL FUNCTIONS AND TASKS
L. Beltracchi (Nuclear Regulatory Commission, Washington, DC.) and R. W. Lindsay 1992 7 p Presented at the 8th Power Plant Dynamics, Control and Testing Symposium, Knoxville, TN, 27-29 May 1992
(Contract W-31-109-eng-38)
(DE92-011839; ANL/CP-75335; CONF-920538-18) Avail: NTIS HC/MF A02

Human error in execution of critical functions and tasks can be costly. The Three Mile Island and the Chernobyl accidents are examples of results from human error in the nuclear industry. There are similar errors that could no doubt be cited from other industries. A strategy to minimize common mode human error in the execution of critical functions and tasks is discussed. The strategy consists of the use of human redundancy, and also diversity in human cognitive behavior: skill-, rule-, and knowledge-based behavior. The authors contend that the use of diversity in human cognitive behavior is possible, and it minimizes common mode error. DOE

N92-28787# Technische Univ., Berlin (Germany, F.R.). Fachbereich Informatik.
IMPROVEMENT OF CONNECTIONNIST LEARNING PROCESSES, WORKING ACCORDING TO THE GRADIENTS METHOD Ph.D. Thesis [VERBESSERUNG KONNEKTIONISTISCHER LERNVERFAHREN, DIE NACH DER GRADIENTENMETHODE ARBEITEN]
Ralf Salomon 1991 142 p In GERMAN
(ETN-92-91335) Avail: NTIS HC/MF A07

The method developed automatically adapts the parameters without unusefully raising the computing costs. Known gradient processes are combined with the 'mutation' and 'selection' principles of the strategy of evolution. Prior to each iteration step, a set of learning and strategy parameters is produced by mutation from the present values. A dynamic adaptation is obtained to the constantly changing optical values of the learning parameters during the learning process. Detailed practical examinations show that this new process strongly reduces the number of necessary learning cycles with regard to other known improvements. ESA

N92-28877# Howard Univ., Washington, DC.
NEUROPSYCHOLOGICAL COMPONENTS OF OBJECT IDENTIFICATION Annual Technical Report, 1 Dec. 1990 - 31 Dec. 1991
Stephen M. Kosslyn 10 Jan. 1992 33 p
(Grant AF-AFOSR-0100-91)
(AD-A247049; AFOSR-92-0136TR) Avail: NTIS HC/MF A03

Four kinds of investigations of the structure of high-level visual processing were conducted during the past year. First, we carried out case studies of individual brain-damaged patients, finding evidence that curved edges are processed separately from straight edges, that location information sometimes can be used to encode some characteristics of shape, and that a decrease in overall activation level can selectively impair performance on some tasks. Second, we administered a set of 27 tasks to a group of 17 brain-damaged patients; these tasks were designed to assess the efficacy of specific subsystems. We have preliminary evidence that most (89 percent) of the subsystems double-dissociate, suggesting that these subsystems are in fact distinct. Third, we constructed computer simulation models to explore properties of the high-level visual system, and found support for the distinction between subsystems that compute two distinct kinds of spatial relations. Finally, some of the tasks we had developed to study deficits in brain-damaged patients were used to study the visual-spatial abilities of air force pilots; we found that pilots are particularly good at mental rotation and encoding metric distance information. GRA

N92-28880# California State Univ., Chico. Coll. of Communication.
INTEGRATING THE AFFECTIVE DOMAIN INTO THE INSTRUCTIONAL DESIGN PROCESS Interim Report, Jun. - Aug. 1991
Robert G. Main Mar. 1992 27 p
(Contract F49620-90-C-0076)
(AD-A249287; AL-TP-1992-0004) Avail: NTIS HC/MF A03

This study develops a model of instructional design that incorporates the affective domain as an integral component. The model combines Keller's ARCS model of motivation for learning with the five phased military instructional design model. The proposed model provides a framework for organizing instructional principles, strategies and techniques concerning the affective domain and furnishes a theoretical base to aid in formulating research hypotheses and collecting empirical data. Attention to the affective domain is particularly important for technology based instruction that removes teacher/student interaction from the

lesson delivery. This model should be helpful because it provides for the systematic consideration of the affective domain in every aspect of the instructional design process. The study concludes with recommendations for additional research needed to operationalize the model for use by instructional designers. GRA

N92-28940# Naval Health Research Center, San Diego, CA.
LAPSES IN ALERTNESS: BRAIN-EVOKED RESPONSES TO TASK-IRRELEVANT AUDITORY PROBES Final Report, Jun. 1989 - Sep. 1990
Scott Makeig, F. S. Elliott, Mark Inlow, and David Kobus Jan. 1992 31 p
(AD-A247669; NHRC-90-39) Avail: NTIS HC/MF A03

Thirteen subjects participated in an auditory simulation of a passive sonar target detection environment. Targets were 300 ms noise bursts presented at near threshold levels in a noise background at a mean rate of 10 per minute. Task irrelevant probe tones were also presented at inter-stimulus intervals of 2-4 seconds. Each subject participated in two 28 minute test sessions, pressing a button whenever they detected a noise target. Prominent minute-scale fluctuations in performance (computed as changes in local error rate using a 32-s moving window) occurred in many of the sessions. Evoked responses to the irrelevant probe tones in thirteen runs with highest number of performance lapses were sorted by current local error rate and smoothed using a moving-average. The amplitude of the grand mean N2 response to the irrelevant probe tones increased monotonically with error rate. Averaged evoked responses to relatively frequent, task-irrelevant probe tones appear to allow an accurate estimate of level of alertness if adequate number of trials are available. GRA

N92-28957# McGill Univ., Montreal (Quebec). Computer Vision and Robotics Lab.
CURVATURE ESTIMATION IN ORIENTATION SELECTION Final Report, 1 Feb. 1989 - 31 Jan. 1992
Steven W. Zucker and Max S. Cynader 31 Jan. 1992 12 p
(Grant AF-AFOSR-0260-89)
(AD-A247862; AFOSR-92-0211TR) Avail: NTIS HC/MF A03

To summarize, progress has been made on a family of related problems, including: A model of endstopped visual cortical neurons was extended to include complex components; An extensive simulation of the model was completed with regard to orientation, positional, spatial frequency, curvature, chevron, and end-line sensitivity; Orientation discontinuities were extended into the motion domain, and psychological and computational experiments were performed to confirm the hypothesis of multiple directions being represented at a point of discontinuity; A theory was developed to capture the non-linearities necessary for early measurement of orientation and curvature; A totally different theory has begun to take shape for functionally characterizing cytochrome oxidase blobs; and The mathematical foundations were laid for a theory of shape. GRA

N92-29119# Oregon State Univ., Newport. Marine Science Center.
IN SEARCH OF A UNIFIED THEORY OF BIOLOGICAL ORGANIZATION: WHAT DOES THE MOTOR SYSTEM OF A SEA SLUG TELL US ABOUT HUMAN MOTOR INTEGRATION? Report, 15 Jan. 1989 - 14 Jan. 19992
George J. Mpitsos and Seppo Soinila 7 Apr. 1992 71 p
(Grant AF-AFOSR-0262-89)
(AD-A250223; AFOSR-92-0299TR) Avail: NTIS HC/MF A04

We summarize the behavioral, electrophysiological, and immunohistochemical findings in the sea slug, Pleurobranchaea, and compare these finding to those obtained in other invertebrate animals, in higher animals, and in humans. The findings show that there is massive distribution and sharing of information occurring, respectively, through diverging and converging network connections. We examine the findings of reductionist approaches and find them inadequate to answer the problems arising from such widely distributed, multifunctional, and highly converging networks whose activity may be variable. Such findings indicate that cooperative actions among groups of neurons may arise dynamically and nonlinearly in shifting contexts or consensuses of response in which individual neurons may have different functions, even during times when the behaviors are similar. Control of these systems is emergent, fuzzy, and error-prone rather than being reflexive or following explicit causes and effects that can be read from the switchboard circuit of the connections between neurons. A unified theoretical perspective is needed that accounts for both the emergent and switch-board systems. Two problems apply in both cases. First, animals may have evolved highly specialized behaviors whose underlying neural networks may not necessarily reflect generally applicable principles. Second, owing to their complexity, it may not be possible to characterize biological networks in sufficient detail to permit an understanding of the system through simulation of the system itself. GRA

N92-29142# University of Southern Illinois, Springfield. School of Medicine.
LEARNING, TEACHING, AND TESTING FOR COMPLEX CONCEPTUAL UNDERSTANDING Technical Report, 1 Dec. 1987 - 30 Nov. 1990
Paul J. Feltovich, Rand J. Spiro, and Richard L. Coulson 4 Oct. 1991 56 p
(Contract N00014-88-K-0077)
(AD-A248728; TR-6) Avail: NTIS HC/MF A04

Drawing upon our research, which has revealed problems among medical students in their understanding of complex material, we propose that new visions of instruction and assessment are required if education is to promote deep and usable understanding of complex, difficult subject matter. In the main, we argue that instruction and testing should be congruent with the cognitive goals for students that are desired--that if what is desired is that students obtain accurate understanding, instruction and testing should focus on this; that if what is desired is that students be able to apply knowledge, instruction and testing should focus on knowledge application; that if what is desired is that students acquire a structure of knowledge that they will not easily forget, education should concentrate on building and assessing robust knowledge structures. We propose some desirable characteristics of learning, teaching and testing for achieving this combination of goals. Tied to this, we suggest that educational goals for understanding can be aided by knowing how understanding is likely to break down, and we present numerous examples of ways that students misunderstand. GRA

N92-29144# Utah Univ., Salt Lake City. Dept. of Psychology.
STUDIES OF PERCEPTUAL MEMORY Final Technical Report, 1 Feb. 1989 - 31 Jan. 1992
William A. Johnston, Kevin J. Hawley, and James M. Farnham 31 Jan. 1992 44 p
(Grant AF-AFOSR-0275-89)
(AD-A250200; AFOSR-92-0308TR) Avail: NTIS HC/MF A03

Perceptual memory refers to experience-induced changes in perceptual processing of particular objects or scenes. Part 1 of this report summarizes the results of 8 studies of the role of perceptual memory in recognition memory. The hypothesis was confirmed that perceptual memory-contributes to the feeling of familiarity that observers sometimes experience even when they lack explicit memory for previously encountered objects. Part 2 summarizes the results of 14 studies of a by-product of perceptual memory called novel popout. The theory was confirmed that novel popout arises from the automatic disinhibition of processing of objects that fail to match top-down effects of perceptual memory. GRA

N92-29146# Ohio State Univ., Columbus.
DEMODULATION PROCESSES IN AUDITORY PERCEPTION Annual Report, 1 Dec. 1989 - 30 Nov. 1990
Lawrence L. Feth 1 Mar. 1992 6 p
(Grant AF-AFOSR-0227-89)
(AD-A250203; AFOSR-92-0300TR) Avail: NTIS HC/MF A02

The development of a multi-channel version of the EWAIF model has begun. The revised model is the IWAIF (Intensity Weighted

Average of Instantaneous Frequency) model. The intensity is proportional to the square of the amplitude (or envelope) and in an earlier paper the PI had shown that envelope squared weighting worked at least as well as simple envelope weighting. Anantharaman's work, which he used as his masters thesis, led to a much more efficient calculation scheme. The model helps understand the intuitive notion that a signal's IWAIF value is its spectral center of gravity. Thus, EWAIF calculations may indeed have application to spectral shape discriminations . GRA

N92-29174*# National Aeronautics and Space Administration. Ames Research Center, Moffett Field, CA.

ACQUISITION AND IMPROVEMENT OF HUMAN MOTOR SKILLS: LEARNING THROUGH OBSERVATION AND PRACTICE

Wayne Iba (RECOM Technologies, Inc., Moffett Field, CA.) Oct. 1991 121 p

(NASA-TM-107878; RIA-91-29; NAS 1.15:107878) Avail: NTIS HC/MF A06

Skilled movement is an integral part of the human existence. A better understanding of motor skills and their development is a prerequisite to the construction of truly flexible intelligent agents. We present MAEANDER, a computational model of human motor behavior, that uniformly addresses both the acquisition of skills through observation and the improvement of skills through practice. MAEANDER consists of a sensory-effector interface, a memory of movements, and a set of performance and learning mechanisms that let it recognize and generate motor skills. The system initially acquires such skills by observing movements performed by another agent and constructing a concept hierarchy. Given a stored motor skill in memory, MAEANDER will cause an effector to behave appropriately. All learning involves changing the hierarchical memory of skill concepts to more closely correspond to either observed experience or to desired behaviors. We evaluated MAEANDER empirically with respect to how well it acquires and improves both artificial movement types and handwritten script letters from the alphabet. We also evaluate MAEANDER as a psychological model by comparing its behavior to robust phenomena in humans and by considering the richness of the predictions it makes. Author

N92-29186# Minnesota Univ., Minneapolis. Dept. of Psychology.

PSYCHOPHYSICAL ANALYSES OF PERCEPTUAL REPRESENTATIONS Annual Report, 15 Apr. 1990 - 14 May 1991

Irving Biederman 3 Dec. 1991 8 p

(Grant AF-AFOSR-0105-92)

(AD-A246945; AFOSR-92-0105TR) Avail: NTIS HC/MF A02

A number of collaborative projects have been launched during the first year and a half of the grant. Consistent with the original proposal, the common theme to all these projects is the linkages between early sensory (psychophysical) processes and perceptual representations that provide access to cognition. The individual project are summarized in the body of the report. In addition to the research projects, two informal weekly seminars were held throughout the first year among center personnel and those with closely related interests. One was concerned with the development of a front end for the kind of object recognition model described by RBC. The other was a general examination of recent research in neural net type models. GRA

54 MAN/SYSTEM TECHNOLOGY AND LIFE SUPPORT

Includes human engineering; biotechnology; and space suits and protective clothing.

For related information see also *16 Space Transportation.*

N92-28286# Air Force Inst. of Tech., Wright-Patterson AFB, OH. School of Systems and Logistics.

A STUDY OF PILOT ATTITUDES REGARDING THE IMPACT ON MISSION EFFECTIVENESS OF USING NEW COCKPIT AUTOMATION TECHNOLOGIES TO REPLACE THE NAVIGATOR/WEAPON SYSTEM OFFICER/ELECTRONIC WARFARE OFFICER M.S. Thesis

William K. Starr and Donald A. Welch Sep. 1991 258 p

(AD-A246683; AFIT/GLM/LSR/91S-62) Avail: NTIS HC/MF A12

This study analyzed the self-reported survey responses of 404 Air Force pilots concerning their perceptions of using advanced cockpit technologies to replace the Navigator, Weapon System Officer, and Electronic Warfare Officer (Nav/WSO/EWO) and the impact of advanced cockpit technologies on combat mission effectiveness. The first objective of this study was to compare, by aircraft type, the mission effectiveness factors that are always critical and almost always critical to the success of a combat mission. The second objective was to examine, from the pilot's point of view, the Nav/WSO/EWO's contribution (NAVCRIT) to enhancing the combat mission effectiveness factors. The third objective was to examine the Nav/WSO/EWO's contribution (REQ) to overall combat mission success. A stepwise regression model for predicting NAVCRIT and REQ utilizing surveyed pilot demographics was also explored. Research conclusions were mixed, since aircraft type impacted on almost all results. Mission effectiveness factors that were always critical were, however, similar across all aircraft types. Examination of NAVCRIT and REQ revealed distinct differences, by aircraft type, of the pilot's perception of Nav/WSO/EWO contribution to combat mission effectiveness. GRA

N92-28346# Defence Research Establishment, Ottawa (Ontario).

MODELLING OF HEAT AND MOISTURE LOSS THROUGH NBC ENSEMBLES

Brad Cain and Randall Osczevski Nov. 1991 30 p

(AD-A245939) Avail: NTIS HC/MF A03

This report summarizes work done to model the heat and moisture transport through various nuclear, bacteriological, chemical (NBC) clothing ensembles. The analysis involves simplifying the three dimensional physical problem of clothing on a person to that of a one dimensional problem of flow through parallel layers of clothing and air. Body temperatures are calculated based on prescribed work rates, ambient conditions and clothing properties. Sweat response and respiration rates are estimated based on empirical data to provide appropriate boundary conditions at the skin. Core and skin temperatures are calculated during the analysis and reported as functions of time for four different clothing ensembles. Evaporative heat loss was found to be the dominant heat loss mechanism. Estimates of the rate of sweat evaporation through the clothing ensembles is made. The predicted temperature responses, although not exact, are comparable to results from physiological experiments but somewhat lower. Work tolerance times were predicted to be longer than that found experimentally. GRA

N92-28518# Naval Postgraduate School, Monterey, CA.

CORRELATIONAL ANALYSIS OF SURVEY AND MODEL-GENERATED WORKLOAD VALUES M.S. Thesis

James J. Galvin, Jr. Sep. 1991 98 p

(AD-A247153) Avail: NTIS HC/MF A05

This study examines the accuracy of an Army helicopter pilot workload measuring model called the Task Loading Model. The model is a submodel of the Army-NASA Aircrew/Aircraft Integration

Program's Man-Machine Integration Design and Analysis System. The model's workload level output was correlated with the subjective workload measurements of several groups of pilots evaluating a variety of flight tasks. Seventy-one Army aviators completed surveys requiring scaled ratings and paired comparisons of workload related to common flight tasks conducted during typical missions. Their responses were examined for internal consistency and pooling by means of nonparametric tests. Aviator-supplied data was found to be robust and reliable. Pooled response data was correlated with model-generated data to determine the accuracy of the model. Results of this study show that the Task Loading Model is presently inadequate, but displays promising trends and should be further refined. GRA

N92-28521*# National Aeronautics and Space Administration. Marshall Space Flight Center, Huntsville, AL.

ANTHROPOMORPHIC TELEOPERATION: CONTROLLING REMOTE MANIPULATORS WITH THE DATAGLOVE Final Report

J. P. Hale, II Jun. 1992 31 p

(Proj. 89-06)

(NASA-TM-103588; NAS 1.15:103588) Avail: NTIS HC/MF A03

A two phase effort was conducted to assess the capabilities and limitations of the DataGlove, a lightweight glove input device that can output signals in real-time based on hand shape, orientation, and movement. The first phase was a period for system integration, checkout, and familiarization in a virtual environment. The second phase was a formal experiment using the DataGlove as input device to control the protoflight manipulator arm (PFMA) - a large telerobotic arm with an 8-ft reach. The first phase was used to explore and understand how the DataGlove functions in a virtual environment, build a virtual PFMA, and consider and select a reasonable teleoperation control methodology. Twelve volunteers (six males and six females) participated in a 2 x 3 (x 2) full-factorial formal experiment using the DataGlove to control the PFMA in a simple retraction, slewing, and insertion task. Two within-subjects variables, time delay (0, 1, and 2 seconds) and PFMA wrist flexibility (rigid/flexible), were manipulated. Gender served as a blocking variable. A main effect of time delay was found for slewing and total task times. Correlations among questionnaire responses, and between questionnaire responses and session mean scores and gender were computed. The experimental data were also compared with data collected in another study that used a six degree-of-freedom handcontroller to control the PFMA in the same task. It was concluded that the DataGlove is a legitimate teleoperations input device that provides a natural, intuitive user interface. From an operational point of view, it compares favorably with other 'standard' telerobotic input devices and should be considered in future trades in teleoperation systems' designs. Author

N92-28670*# Bionetics Corp., Cocoa Beach, FL.

COUPLING PLANT GROWTH AND WASTE RECYCLING SYSTEMS IN A CONTROLLED LIFE SUPPORT SYSTEM (CELSS)

Jay L. Garland 25 Mar. 1992 57 p

(Contract NAS10-11624)

(NASA-TM-107544; NAS 1.15:107544) Avail: NTIS HC/MF A04

The development of bioregenerative systems as part of the Controlled Ecological Life Support System (CELSS) program depends, in large part, on the ability to recycle inorganic nutrients, contained in waste material, into plant growth systems. One significant waste (resource) stream is inedible plant material. This research compared wheat growth in hydroponic solutions based on inorganic salts (modified Hoagland's) with solutions based on the soluble fraction of inedible wheat biomass (leachate). Recycled nutrients in leachate solutions provided the majority of mineral nutrients for plant growth, although additions of inorganic nutrients to leachate solutions were necessary. Results indicate that plant growth and waste recyling systems can be effectively coupled within CELSS based on equivalent wheat yield in leachate and Hoagland solutions, and the rapid mineralization of waste organic material in the hydroponic systems. Selective enrichment for microbial communities able to mineralize organic material within the leachate was necessary to prevent accumulation of dissolved organic matter in leachate-based solutions. Extensive analysis of microbial abundance, growth, and activity in the hydroponic systems indicated that addition of soluble organic material from plants does not cause excessive microbial growth or 'biofouling', and helped define the microbially-mediated flux of carbon in hydroponic solutions. Author

N92-28671*# Iowa State Univ. of Science and Technology, Ames. Dept. of Chemical Engineering.

SPACE LIFE SUPPORT ENGINEERING PROGRAM Annual Progress Report, 1 Jul. 1991 - 30 Jun. 1992

Richard C. Seagrave 30 Jun. 1992 36 p

(Grant NAG2-722)

(NASA-CR-190448; NAS 1.26:190448) Avail: NTIS HC/MF A03

A comprehensive study to develop software to simulate the dynamic operation of water reclamation systems in long-term closed-loop life support systems is being carried out as part of an overall program for the design of systems for a moon station or a Mars voyage. This project is being done in parallel with a similar effort in the Department of Chemistry to develop durable accurate low-cost sensors for monitoring of trace chemical and biological species in recycled water supplies. Aspen-Plus software is being used on a group of high-performance work stations to develop the steady state descriptions for a number of existing technologies. Following completion, a dynamic simulation package will be developed for determining the response of such systems to changes in the metabolic needs of the crew and to upsets in system hardware performance. Author

N92-28681*# Texas Univ., Arlington.

A STUDY OF THE CONTROL PROBLEM OF THE SHOOT SIDE ENVIRONMENT DELIVERY SYSTEM OF A CLOSED CROP GROWTH RESEARCH CHAMBER

C. C. Blackwell and A. L. Blackwell Jun. 1992 113 p

(Contract NCA2-484)

(NASA-CR-177597; A-92138; NAS 1.26:177597) Avail: NTIS HC/MF A06

The details of our initial study of the control problem of the crop shoot environment of a hypothetical closed crop growth research chamber (CGRC) are presented in this report. The configuration of the CGRC is hypothetical because neither a physical subject nor a design existed at the time the study began, a circumstance which is typical of large scale systems control studies. The basis of the control study is a mathematical model which was judged to adequately mimic the relevant dynamics of the system components considered necessary to provide acceptable realism in the representation. Control of pressure, temperature, and flow rate of the crop shoot environment, along with its oxygen, carbon dioxide, and water concentration is addressed. To account for mass exchange, the group of plants is represented in the model by a source of oxygen, a source of water vapor, and a sink for carbon dioxide. In terms of the thermal energy exchange, the group of plants is represented by a surface with an appropriate temperature. Most of the primitive equations about an experimental operating condition and a state variable representation which was extracted from the linearized equations are presented. Next, we present the results of a real Jordan decomposition and the repositioning of an undesirable eigenvalue via full state feedback. The state variable representation of the modeling system is of the nineteenth order and reflects the eleven control variables and eight system disturbances. Five real eigenvalues are very near zero, with one at zero, three having small magnitude positive values, and one having a small magnitude negative value. A Singular Value Decomposition analysis indicates that these non-zero eigenvalues are not results of numerical error. Author

N92-28831# National Aerospace Lab., Tokyo (Japan). Control System Development Team.

THE SECOND FLIGHT SIMULATOR TEST OF THE HEAD-UP DISPLAY FOR NAL QSTOL EXPERIMENTAL AIRCRAFT (ASKA)

Keiji Tanaka, Kenji Yazawa, and Kazuya Masui Feb. 1991 27 p In JAPANESE

(NAL-TM-633; ISSN-0452-2982; JTN-92-80351) Avail: NTIS HC/MF A03

A Head Up Display (HUD) designed by the NAL and manufactured for the NAL Quiet Short Take Off and Landing (QSTOL) experimental aircraft, ASKA, was evaluated for the second time using the STOL flight simulator. The objectives of these simulator tests were: (1) to confirm the display format which was modified after flight test results of the Beechcraft Queen-Air (a NAL research aircraft); (2) to evaluate the radar guidance functions which telelink information displayed in the HUD; and (3) to study the QSTOL's Instrument Flight Rules (IFR) approach capability using the HUD's radar guidance ability. Results of about 300 simulated approach and landing flights which were evaluated by five test pilots showed: (1) display format modifications improved readability and smoothness of the display's motion; (2) the radar guidance algorithm which obtains aircraft position using a tracking radar that is complemented by inertial information was determined to be satisfactory for use in actual flight; and (3) by using the HUD, and especially its indicated runway image, pilots were able to make precise approaches to the runway under Instrument Meteorological Conditions. In addition, other beneficial suggestions for display format final adjustments were obtained prior to HUD's use in the QSTOL flight test series. Author (NASDA)

N92-28897*# National Aeronautics and Space Administration. Lyndon B. Johnson Space Center, Houston, TX.

EXPERIMENTAL MEASUREMENT OF THE ORBITAL PATHS OF PARTICLES SEDIMENTING WITHIN A ROTATING VISCOUS FLUID AS INFLUENCED BY GRAVITY

David A. Wolf and Ray P. Schwarz (Krug Life Sciences, Inc., Houston, TX.) Jun. 1992 19 p

(RTOP 694-01-23-05)

(NASA-TP-3200; S-668; NAS 1.60:3200) Avail: NTIS HC/MF A03

Measurements were taken of the path of a simulated typical tissue segment or 'particle' within a rotating fluid as a function of gravitational strength, fluid rotation rate, particle sedimentation rate, and particle initial position. Parameters were examined within the useful range for tissue culture in the NASA rotating wall culture vessels. The particle moves along a nearly circular path through the fluid (as observed from the rotating reference frame of the fluid) at the same speed as its linear terminal sedimentation speed for the external gravitational field. This gravitationally induced motion causes an increasing deviation of the particle from its original position within the fluid for a decreased rotational rate, for a more rapidly sedimenting particle, and for an increased gravitational strength. Under low gravity conditions (less than 0.1 G), the particle's motion through the fluid and its deviation from its original position become negligible. Under unit gravity conditions, large distortions (greater than 0.25 inch) occur even for particles of slow sedimentation rate (less than 1.0 cm/sec). The particle's motion is nearly independent of the particle's initial position. Comparison with mathematically predicted particle paths show that a significant error in the mathematically predicted path occurs for large particle deviations. This results from a geometric approximation and numerically accumulating error in the mathematical technique. Author

N92-28944# Army Aeromedical Research Lab., Fort Rucker, AL.

METHODS OF VISUAL SCANNING WITH NIGHT VISION GOGGLES Final Report

John C. Kotulak Feb. 1992 20 p

(DA Proj. 3M1-62787-A-879)

(AD-A247470; USAARL-92-10) Avail: NTIS HC/MF A03

This report describes recommended methods for scanning the flight path and cockpit instruments for pilots wearing night vision goggles (NVGs) while flying Army helicopters. The impetus for this report was a task force sponsored by the Office of the Deputy Chief of Staff of the Army for Plans and Operations, which determined that the development of scanning methods was the Army's top training priority for night helicopter operations. The recommended methods of scanning were derived from published scientific works, interviews with scientists, and interviews with aviators from field tactical units, training units, and from the research and development community. The proposed scanning methods recommend free search as opposed to formalized scan patterns. In addition, they place equal weight on crew coordination and individual technique. The proposed methods stress actions taken before flight, such as premission planning and NVG preflight adjustments. Furthermore, the proposed methods are intended to build an awareness of: NVG performance limits, and how to maximize performance; common problems encountered while scanning with NVGs, and the conditions which elicit them; and the scientific basis for scanning. Separate scanning methods were developed for individuals and for crews. In addition, the relevant scientific literature was reviewed. GRA

N92-29121# Massachusetts Inst. of Tech., Cambridge. Research Lab. of Electronics.

SUPER AUDITORY LOCALIZATION FOR IMPROVED HUMAN-MACHINE INTERFACES Final Report, 1 Jun. 1990 - 28 Feb. 1992

Nathaniel Durlach 28 Apr. 1992 5 p

(Grant AF-AFOSR-0312-90)

(AD-A250288; AFOSR-92-0392TR) Avail: NTIS HC/MF A01

Work by Dr. Durlach and his collaborators is summarized here. The creation of a serious journal for continuing publication of peer-reviewed papers seemed essential for the development of the field (both technically and academically.) Thus, the funds in the grant were used to support the creation of a journal rather than a book. The journal is 'Presence: teleoperators and virtual environments,' published by MIT Press. The work performed to start the journal has occurred in two phases. The first consisted of establishing the journal as an organization entity. The second, which has only been completed within the past month, consisted of generating the first issue. GRA

N92-29129* National Aeronautics and Space Administration. Pasadena Office, CA.

METHOD AND APPARATUS FOR PREDICTING THE DIRECTION OF MOVEMENT IN MACHINE VISION Patent

Teri B. Lawton, inventor (to NASA) (Jet Propulsion Lab., California Inst. of Tech., Pasadena.) 28 Apr. 1992 16 p Filed 30 Sep. 1988

(NASA-Case-NPO-17552-1-CU; US-Patent-5,109,425; US-Patent-Appl-SN-251500; US-Patent-Class-382-1; US-Patent-Class-358-105; US-Patent-Class-364-424.01; US-Patent-Class-382-22; US-Patent-Class-901-1; Int-Patent-Class-G06K-9/00) Avail: US Patent and Trademark Office

A computer-simulated cortical network is presented. The network is capable of computing the visibility of shifts in the direction of movement. Additionally, the network can compute the following: (1) the magnitude of the position difference between the test and background patterns; (2) localized contrast differences at different spatial scales analyzed by computing temporal gradients of the difference and sum of the outputs of paired even- and odd-symmetric bandpass filters convolved with the input pattern; and (3) the direction of a test pattern moved relative to a textured background. The direction of movement of an object in the field of view of a robotic vision system is detected in accordance with nonlinear Gabor function algorithms. The movement of objects relative to their background is used to infer the 3-dimensional structure and motion of object surfaces.

Official Gazette of the U.S. Patent and Trademark Office

N92-29137* National Aeronautics and Space Administration. Lyndon B. Johnson Space Center, Houston, TX.
WHOLE BODY CLEANING AGENT CONTAINING N-ACYLTAURATE Patent
Steven E. Lentsch, inventor (to NASA) 26 May 1992 5 p Filed 29 May 1990 Supersedes N91-16566 (29 - 8, p 1195)
(NASA-Case-MSC-21589-1; US-Patent-5,116,543; US-Patent-Appl-SN-529427; US-Patent-Class-252-545; US-Patent-Class-252-547; US-Patent-Class-252-DIG.5; US-Patent-Class-252-DIG.14; US-Patent-Class-252-DIG.13; US-Patent-Class-424-70; US-Patent-Class-4-661) Avail: US Patent and Trademark Office

The subject invention relates to a human cleansing agent particularly suitable for use in long duration spaceflight and to a method of bathing with the agent. The agent of the subject invention is in the form of a paste having a pH of 5.0 to 7.9 which comprises an acyltaurate, a skin conditioner, a hair conditioner, and a preservative. More specifically, it includes sodium N-coconut acid-N-methyl taurate, in combination with soybean lecithin, polyquaternium 16, and formalin. This particular combination satisfies the following objectives: (1) that it be usable with a minimum amount of water per shower (approximately 1 gallon); (2) that it be easily separated from the water for purposes of water reclamation; (3) that it be pH compatible with skin and hair; (4) that it rinse well in deionized water; (5) that it be mild to skin and eyes; (6) that it effectively clean both skin and hair; (7) that it be suitable for use in zero gravity; and (8) that it provide ease of combing of wet and dry hair. The method of the invention includes the steps of wetting the skin and hair with a small quantity of water, lathering the skin with the paste, rinsing the lather from the skin and hair with a small quantity of water to produce a rinse water containing the cleansing agent, defoaming the rinse water, and supplying the defoamed rinse water to a water reclamation unit for recycling the water. The novelty of the invention appears to lie in the particular formulation of the cleansing agent and its method of use which provide optimal results under the given constraints and objectives.

Official Gazette of the U.S. Patent and Trademark Office

N92-29227# Harvard Coll. Observatory, Cambridge, MA.
THE ENERGETICS AND MECHANICS OF LOAD CARRYING Final Report, 1 Feb. 1988 - 31 Jan. 1989
Norman C. Heglund 16 Jan. 1992 5 p
(Contract DAAL03-88-K-0032)
(AD-A248441) Avail: NTIS HC/MF A02

African women commonly carry prodigious loads (70 percent or more of their body weight) supported by their heads for long distances. This method of load carriage is very economical; in a comparison of the metabolic cost of carrying large head-supported loads (by African women) to large back-supported loads (by American army recruits), it was found that the army recruits had to increase their metabolism twice as much as the women for the same load at the same walking speed. The mechanism by which these women carry loads so economically is unknown. The purpose of this study was to develop a quantitative understanding of how these women are able to carry head-supported loads so cheaply.

GRA

55 SPACE BIOLOGY

Includes exobiology; planetary biology; and extraterrestrial life.

No abstracts in this category.

59 MATHEMATICAL AND COMPUTER SCIENCES (GENERAL)

No abstracts in this category.

60 COMPUTER OPERATIONS AND HARDWARE

Includes hardware for computer graphics, firmware, and data processing.

For components see *33 Electronics and Electrical Engineering.*

N92-28236# Colsa, Inc., Huntsville, AL.
DIGITAL HARDWARE ARCHITECTURE IMPLEMENTATION Annual Report, Apr. 1991 - Apr. 1992
Lance Cooper, George Paramithas, Max Patin, and Stuart Venters 15 Apr. 1992 42 p
(Contract DASG60-91-C-0006)
(AD-A249194; CI-2071-92-0012) Avail: NTIS HC/MF A03

The work documented in this report was performed for US Army Strategic Defense Command Ground Based Radar Project (GBR). COLSA performed extensive analysis of the digital hardware and computer architectures of the data and signal processing equipment. Included in the analysis is a detailed evaluation of critical throughput for highly parallel computer systems. GRA

N92-28514# Pittsburgh Univ., PA. Dept. of Computer Science.
COINCIDENT PULSE TECHNIQUES FOR HYBRID ELECTRONIC OPTICAL COMPUTER SYSTEMS Annual Report, Jul. 1990 - Jul. 1991
D. M. Chiarulli, R. G. Melhem, and S. P. Levitan 31 Aug. 1991 98 p
(Grant AF-AFOSR-0469-89)
(AD-A246774; AFOSR-92-0137TR) Avail: NTIS HC/MF A05

This research was an investigation of the application of coincident pulse techniques to multiprocessor interconnection networks. The research focused on three main areas: an examination of the applicability of coincident pulse techniques and required hardware to multiprocessor applications; an investigation of the limits of scalability; and an exploration of various interconnection structures which can be created using these techniques. GRA

N92-28891# Naval Research Lab., Washington, DC.
A SURVEY OF HIGH DENSITY PACKAGING FOR HIGH PERFORMANCE COMPUTING SYSTEM
Nhi-Anh Chu and Henry Dardy 10 Apr. 1992 38 p
(AD-A248633; NRL/FR/5560-92-9329) Avail: NTIS HC/MF A03

In this age of modern warfare when precision-smart weapons and avionics are in high demand, there is a need for a dramatic increase of throughput density, defined loosely as the computation throughput per unit volume/weight of the electronic system. To date, the main approach has been the monolithic wafer scale integration (MWSI) approach. Over the last decades, monolithic integration circuit (IC) density has increased by several orders of magnitudes, and the monolithic IC area by 10 times, to approach the dimension of the semiconductor wafer. The growth trends for both circuit density and IC area have leveled off significantly. Hybrid wafer scale integration (HWSI) overcomes many of these limitations. This approach includes techniques to put monolithic chips very close together while maintaining or improving inter-chip signal quality. Major portions of the report survey techniques, performance and availability of HWSI technologies. The survey finds that HWSI can provide from one to two orders of magnitude of increase to the throughput density of current systems. There is

a major trend in the industry to invest in this technology, and it is expected to be available to the industrial as well as military systems at competitive prices within a few years. GRA

N92-28899*# National Aeronautics and Space Administration. Marshall Space Flight Center, Huntsville, AL.
FUNCTIONAL REQUIREMENTS DOCUMENT FOR THE EARTH OBSERVING SYSTEM DATA AND INFORMATION SYSTEM (EOSDIS) SCIENTIFIC COMPUTING FACILITIES (SCF) OF THE NASA/MSFC EARTH SCIENCE AND APPLICATIONS DIVISION, 1992
Michael E. Botts (Alabama Univ., Huntsville.), Ron J. Phillips (Alabama Univ., Huntsville.), John V. Parker, and Patrick D. Wright (Universities Space Research Association, Huntsville, AL.) Jun. 1992 87 p
(NASA-TM-4392; M-692; NAS 1.15:4392) Avail: NTIS HC/MF A05

Five scientists at MSFC/ESAD have EOS SCF investigator status. Each SCF has unique tasks which require the establishment of a computing facility dedicated to accomplishing those tasks. A SCF Working Group was established at ESAD with the charter of defining the computing requirements of the individual SCFs and recommending options for meeting these requirements. The primary goal of the working group was to determine which computing needs can be satisfied using either shared resources or separate but compatible resources, and which needs require unique individual resources. The requirements investigated included CPU-intensive vector and scalar processing, visualization, data storage, connectivity, and I/O peripherals. A review of computer industry directions and a market survey of computing hardware provided information regarding important industry standards and candidate computing platforms. It was determined that the total SCF computing requirements might be most effectively met using a hierarchy consisting of shared and individual resources. This hierarchy is composed of five major system types: (1) a supercomputer class vector processor; (2) a high-end scalar multiprocessor workstation; (3) a file server; (4) a few medium- to high-end visualization workstations; and (5) several low- to medium-range personal graphics workstations. Specific recommendations for meeting the needs of each of these types are presented. Author

N92-29083# Naval Postgraduate School, Monterey, CA.
TECHNOLOGICAL ENHANCEMENTS FOR PERSONAL COMPUTERS M.S. Thesis
Marvin G. Fuller Mar. 1992 62 p
(AD-A247962) Avail: NTIS HC/MF A04

This research is concerned with the usability and compatibility of many of the aftermarket enhancements commercially available to agencies using microcomputers in their workplace. These devices include biometric access devices, data input devices, storage device, and data transfer equipment. A limited number of associated software packages will be evaluated along with the hardware involved. This study explores the feasibility of add-on equipment for the Desktop III PC, the Unisys government contract. Due to delays in availability of a Unisys machine most of the research was done on an 80286 based Packard Bell PB-800D running the MS-DOS 3.3 operating system. Most of the applications were later installed on a Desktop III machine. Security considerations for Physical area, data access, and transmission media are discussed as this topic should be a vital concern for DOD computer users. The report concludes with a limited number of application scenarios that represent some of what can be accomplished with personal computers. GRA

N92-29132* National Aeronautics and Space Administration. Goddard Space Flight Center, Greenbelt, MD.
DISK MEMORY DEVICE Patent
Ronald M. Muller, inventor (to NASA) 5 May 1992 7 p Filed 26 May 1989
(NASA-Case-GSC-13196-1; US-Patent-5,111,345; US-Patent-Appl-SN-357928; US-Patent-Class-360-48; US-Patent-Class-369-32; US-Patent-Class-369-95; US-Patent-Class-360-98.01; Int-Patent-Class-G11B-5/09; Int-Patent-Class-G11B-17/22; Int-Patent-Class-G11B-3/74) Avail: US Patent and Trademark Office

A disk memory device is discussed. The device will maximize the storage capacity of a memory disk and at the same time will maximize the record and playback data rate. Two recording disks are mounted upon a common shaft that is rotated at a fixed speed. Each disk has a recording area including a surface upon which data can be recorded/read in the form of tracks arranged either in concentric tracks or in a spiral. The recording area surfaces are divided into multiple concentric track groups. Two read/write heads and two head positioning servos are mounted such that each disk recording surface can be read out or written by the read/write heads. Each track of the multiple track groups of the first disk are given designated numbers beginning with the outer track of the outermost or edge track group and continuing in higher consecutive numbers until the inner track of the innermost track group is designated. However, each track of the multiple track groups of the second disk are given designated numbers in the exact reverse order of the first disk, such that the combined length of a track from the first disk, when added to the length of the same numbered track of the second disk is a constant, generating a constant data rate for the disk memory device.
Official Gazette of the U.S. Patent and Trademark Office

61 COMPUTER PROGRAMMING AND SOFTWARE

Includes computer programs, routines, alogorithms, and specific applications, e.g., CAD/CAM.

N92-28243# Naval Postgraduate School, Monterey, CA.
OBJECT-ORIENTED PROGRAMMING: AN ASSESSMENT OF FUNDAMENTAL CONCEPTS AND DESIGN CONSIDERATIONS M.S. Thesis
Alan L. Fink Mar. 1992 175 p
(AD-A247480) Avail: NTIS HC/MF A08

The latest buzzword penetrating the professional computer science literature is Object-Oriented Programming. Computer scientists extol its theoretical virtues while developers explore its potential for streamlining the process of software development. Amidst all this activity there remains substantial confusion about fundamental concepts and the programming language mechanisms which implement these concepts. Too often, students of object-oriented programming mistake proficiency in an object-oriented language for efficient application of object-oriented techniques. The immediate consequence is poorly conceived, sometimes conflicting, efforts at exploiting reusability, information hiding, and other object-oriented capabilities. This thesis reviews the benefits attributed to object-oriented programming, arrives at definitions for fundamental concepts, advances recommendations for conducting object-oriented analysis and object-oriented design, and reviews some tradeoffs which designers need to consider when developing object-oriented classes and hierarchies. GRA

N92-28245# Naval Postgraduate School, Monterey, CA.
NPSNET: FLIGHT SIMULATION DYNAMIC MODELING USING QUATERNIONS M.S. Thesis
Joseph M. Cooke Mar. 1992 62 p
(AD-A247484) Avail: NTIS HC/MF A04

The Naval Postgraduate School (NPS) has actively explored the design and implementation of networked, realtime, three-dimensional battlefield simulations on low cost, commercially available graphics workstations. The most recent system, NPSNET, has improved in functionality to such an extent, that it is considered a low cost version of the Defense Advanced Research Project Agency's (DARPA) SIMNET system. In order to reach that level, it was necessary to economize in certain areas of the code so that real-time performance occurred at an acceptable level. One of those areas was in aircraft dynamics. However, with 'off-the-shelf' computers becoming faster and cheaper, real-time and realistic

dynamics are no longer an expensive option. The realistic behavior can now be enhanced through the incorporation of an aerodynamic model. To accomplish this task, a prototype flight simulator was built that is capable of simulating numerous types of aircraft simultaneously within a virtual world. Beside being easily incorporated into NPSNET, such a simulator will also provide the base functionality for the creation of a general purpose aerodynamic simulator that is particularly useful to aerodynamic students for graphically analyzing differing aircraft's stability and control characteristics. This system is designed for use on a Silicon Graphics workstation and uses the GL libraries. GRA

N92-28265# Norwegian Defence Research Establishment, Kjeller.
CESAR ADDRESS GENERATOR
Harald Blom and Roar Skogstroem 20 Oct. 1991 73 p
(FFI-91/7021; ISSN-0802-2437; ETN-92-91243) Avail: NTIS HC/MF A04

A detailed description of the CESAR address generator is presented. The CESAR system was developed for fast delivery SAR (Synthetic Aperture Radar) processing. The address generator is a dedicated ASIC (Application Specific Integrated Circuit) and is tailor made for addressing data sequences in BUF. The design is heavily pipelined. ESA

N92-28267*# National Aeronautics and Space Administration. Goddard Space Flight Center, Greenbelt, MD.
THE FATHER CHRISTMAS WORM
James L. Green and Patricia L. Sisson (Science Applications Research, Lanham, MD.) Jun. 1989 8 p Submitted for publication
(NASA-TM-107938; NAS 1.15:107938) Avail: NTIS HC/MF A02

Given here is an overview analysis of the Father Christmas Worm, a computer worm that was released onto the DECnet Internet three days before Christmas 1988. The purpose behind the worm was to send an electronic mail message to all users on the computer system running the worm. The message was a Christmas greeting and was signed 'Father Christmas'. From the investigation, it was determined that the worm was released from a computer (node number 20597::) at a university in Switzerland. The worm was designed to travel quickly. Estimates are that it was copied to over 6,000 computer nodes. However, it was believed to have executed on only a fraction of those computers. Within ten minutes after it was released, the worm was detected at the Space Physics Analysis Network (SPAN), NASA's largest space and Earth science network. Once the source program was captured, a procedural cure, using the existing functionality of the computer operating systems, was quickly devised and distributed. A combination of existing computer security measures, the quick and accurate procedures devised to stop copies of the worm from executing, and the network itself, were used to rapidly provide the cure. These were the main reasons why the worm executed on such a small percentage of nodes. This overview of the analysis of the events concerning the worm is based on an investigation made by the SPAN Security Team and provides some insight into future security measures that will be taken to handle computer worms and viruses that may hit similar networks. Author

N92-28285# Air Force Inst. of Tech., Wright-Patterson AFB, OH. School of Systems and Logistics.
AN APPLICATION OF INTERACTIVE COMPUTER GRAPHICS TO THE STUDY OF INFERENTIAL STATISTICS AND THE GENERAL LINEAR MODEL M.S. Thesis
Stephen D. Pearce Sep. 1991 170 p
(AD-A246668; AFIT/GSM/ENC/91S-22) Avail: NTIS HC/MF A08

This research created a learning environment, known as the Pearce Projection Modeling Environment (PPME) which is used as a tool by a teacher and student. The PPME was developed in an effort to create a new approach to the study of the General Linear Model through a constructive and projective, geometric approach. While the geometric approach to the GLM was developed over the past century, it has not been used extensively because of the inherent complexities associated with visualizing vector spaces. With the PPME, visualization is accomplished effortlessly. The PPME is a computer program that allows the student to enter response vectors and other vectors and data associated with the GLM and observe the relationships of those vectors interactively and in three-dimensions. The PPME encourages learning through constructive development by allowing the student to modify the vectors and observe the results of his actions. To validate the PPME as a learning tool, several data sets were generated and used to study three scenarios: The Sample Mean and Variance, A General Linear Test of the Population Mean, and An Ordinary Least Squares Simple Linear Regression. GRA

N92-28289# Tulane Univ., New Orleans, LA.
A UNIFORM APPROACH TO THE SEMANTICS OF CONCURRENCY Final Report, 1 Jul. 1988 - 31 Dec. 1991
Michael W. Mislove 31 Dec. 1991 17 p
(Contract N00014-88-K-0499)
(AD-A246697) Avail: NTIS HC/MF A03

The role of semantics is to allow reasoning about high-level programming languages through the use of models. Our research focuses on two approaches to semantics, Denotational Semantics and Operational Semantics, and their applications to languages supporting concurrent computation. In Denotational Semantics, mathematical models are studied which have the same operations on them as those that are available in the language (such as sequential composition and parallel composition, etc.) and a function is defined which assigns meanings in the model to programs in the language. This function should be compositional, i.e., a homomorphism with respect to the operations of the language. In this way, the meaning of a complicated program is made up as the composite of the meanings of its constituent parts, so the meanings of complicated programs can be understood in terms of the meanings of their simpler constituents. The other approach we study is Operational Semantics, where the meaning of a program is given by means of a Labelled Transition System which reflects the transitions of the program on an abstract machine. In the approach, and idealized implementation of the program is developed, and problems associated with implementation can be addressed in an abstract setting. GRA

N92-28301# Wisconsin Univ., Madison. Center for Mathematical Sciences.
THE STRUCTURE OF FINITELY GENERATED SHIFT-INVARIANT SPACES IN L2(IR SUP d)
Carl DeBoor, Ronald A. DeVore (South Carolina Univ., Columbia.), and Amos Ron Feb. 1992 35 p
(Contract DAAL03-G-90-0090; NSF DMS-90-00053)
(AD-A247314; CMS-TSR-92-08) Avail: NTIS HC/MF A03

A simple characterization is given of finitely generated subspaces of L2(IR(d)) which are invariant under translation by any (multi)integer, and used to give conditions under which such a space has a particularly nice generating set, namely a basis, and, more than that, a basis with desirable properties, such as stability, orthogonality, or linear independence. The last property makes sense only for 'local' spaces, i.e., shift-invariant spaces generated by finitely many compactly supported functions, and special attention is paid to such spaces. As an application, we prove that the approximation order provided by a given local space is already provided by the shift-invariant space generated by just one function, with this function constructible as a finite linear combination of the finite generating set for the whole space, hence compactly supported. GRA

N92-28309# Los Alamos National Lab., NM.
PROPX: AN X RAY MANIPULATION PROGRAM
G. A. Kyrala 1992 17 p Presented at the 9th Topical Conference on High-Temperature Plasma Diagnostics, Santa Fe, NM, 15-19 Mar. 1992
(Contract W-7405-eng-36)
(DE92-011264; LA-UR-92-837; CONF-920362-15) Avail: NTIS HC/MF A03

An interactive microcomputer program that performs some

manipulations on an input x ray spectrum is introduced and described. The program is used to calculate the effect of absorption of filters, transmission through fibers, responsivity of photocathodes, responsivity of absorptive detectors, folding of responses, plotting of cross sections, and calculation, as a function of electron temperature, of the response due to a bremsstrahlung spectrum. Fluorescence from the targets is not included. Two different x ray libraries are offered, one covers the x ray range 30-10,000 eV with 288 energy points, and the other covers the energy range 10 eV to 1 MeV with 250 energy points per decade. DOE

N92-28332# Westinghouse Savannah River Co., Aiken, SC.
AUDIT TRAILS AND PC CONTROL ON NOVELL NETWORKS
A. Cabot 1991 7 p Presented at the 14th DOE Computer Security Group Conference, Concord, CA, 7-9 May 1991
(Contract DE-AC09-89SR-18035)
(DE92-010695; WSRC-MS-91-086; CONF-9105126-6) Avail: NTIS HC/MF A02

Although Novell Netware 286 provides excellent access control at both the server and the directory level, the record they make available through the accounting function leaves much to be desired. Two programs are presented: (1) a BASIC program that converts the output of Novell's PAUDIT command into single line audit trails, providing an auditable record of server access; and (2) a program written in dBase III+ that can be used to insure that all PC's accessing the LAN are recorded in an inventory data base. The subject network consists of six file servers connecting approximately 500 users at the main office of WSRC's Engineering and Projects Division. DOE

N92-28342# Sandia National Labs., Albuquerque, NM.
LESSONS FROM ARCHIMEDES, A SYSTEM FOR PLANNING AND EXECUTING MECHANICAL ASSEMBLIES
D. Strip 1992 12 p Presented at the 1992 Institute of Electrical and Electronics Engineers (IEEE) International Conference on Robotics and Automation, Nice, France, 10-15 May 1992
(Contract DE-AC04-76DP-00789)
(DE92-010957; SAND-92-0520C; CONF-920540-16) Avail: NTIS HC/MF A03

Archimedes is a prototype mechanical assembly system which generates and executes robot assembly programs from a CAD model input. The system seeks to increase flexibility in robotic mechanical assembly applications by automating the programming task. Input is a solid model of the finished assembly, augmented by additional design information such as weld specifications. Parts relationships and geometric constraints are deduced from the solid model. A rule-based planner generates a 'generic' assembly plan that satisfies the geometric constraints, as well as other constraints embodied in the rules. A plan compiler then converts the generic plan into code specific to an application environment. Other outputs include fixture designs, workcell layout information, object-recognition (vision) routines, grasp plans, and executable code for controlling the robot and workcell accessories. Lessons from operating and demonstrating the system are presented with a particular emphasis on the implications for future systems. DOE

N92-28353# Naval Postgraduate School, Monterey, CA. Dept. of Electrical and Computer Engineering.
MULTIPLE-VALUED PROGRAMMABLE LOGIC ARRAY MINIMIZATION BY SIMULATED ANNEALING Technical Report, Jul. 1991 - Feb. 1992
Gerhard W. Dueck, Robert C. Earle, Parthasarathy Tirumalai, and Jon T. Butler 10 Feb. 1992 34 p
(AD-A248620; NPS-EC-92-004) Avail: NTIS HC/MF A03

We propose a solution to the minimization problem of multiple-valued programmable logic arrays (PLA) that uses simulated annealing. The algorithm accepts a sum-of-products expression, divides and recombines the product terms, gradually progressing toward a minimal solution. The input expression can be user-specified or one produced by another heuristic. The process is termed simulated annealing because it has an analog in the statistical mechanical model of annealing in solids. That is, the slow cooling of certain solids results in a state of low energy, a crystalline state rather than an amorphous state that results from fast cooling. In a PLA, the crystalline state is analogous to a realization with a small number of product terms. Unlike recently studied minimization techniques (which are classified as direct cover methods), our technique manipulates product terms directly, breaking them up and joining them in different ways, while reducing the total number of product terms. GRA

N92-28385# Naval Postgraduate School, Monterey, CA.
AN EXPERIMENTAL INVESTIGATION OF THE EFFECTS OF SOFTWARE SIZE INCREASE ON SOFTWARE PROJECT MANAGEMENT BEHAVIOR M.S. Thesis
Diana L. Baker Mar. 1992 74 p
(AD-A248362) Avail: NTIS HC/MF A04

Increasing demand for software and increasing shortfalls of programmers have focused efforts to improve software project productivity on the role of the software project manager. The complex dynamics of software project development, and the visibility of the project, affect decision making and performance to a large degree. Using the System Dynamics Model for software project management, these and other issues can be evaluated with low financial risk or outlays through simulation of software projects. This thesis investigates the effect of changing one of the dynamics (i.e., size) on the behavior and performance of the project manager by using a simulation of an actual software project in a game environment. Analysis of the results indicates that increased visibility significantly improves project schedule. GRA

N92-28428# Rutgers - The State Univ., New Brunswick, NJ.
NUMERICAL METHODS OF LINEAR AND NONLINEAR OPTIMIZATION Final Report, 1 Jul. 1987 - 30 Sep. 1991
David F. Shanno 30 Sep. 1991 32 p
(Grant AF-AFOSR-0215-87)
(AD-A248579; AFOSR-92-0263TR) Avail: NTIS HC/MF A03

The project has been concerned with developing new numerical techniques to solve large scale linear and nonlinear programming problems. Early work focused on sequential quadratic programming techniques for nonlinear programming. Subsequently, all work was focused on interior point methods for large scale linear and nonlinear programming. Initially, the focus of the research was on both dual-affine and primal-dual algorithm for linear programming. Substantial computational experience demonstrated the superiority of the primal-dual methods, and subsequent research focused on improving the efficiency of these methods, both by adding higher order methods via predictor-corrector techniques and by improving the linear algebra to take advantage of both sparsity and machine architecture. Most recently, research has focused on large scale quadratic programming. A primal-dual predictor-corrector method has been devised and shown to be very promising computationally for problems with diagonal or sparsely structured Hessian matrices. For problems with dense Hessians, a pure primal conjugate projected gradient algorithm shows promise on small problems. It remains to be tested on large-scale problems. GRA

N92-28519# Naval Postgraduate School, Monterey, CA.
CALCULATION OF CHIP TEMPERATURES USING ELLPACK M.S. Thesis
Vincent J. vanJoolen Jun. 1991 192 p
(AD-A247156) Avail: NTIS HC/MF A09

In this thesis we report on an experiment to solve a three dimensional elliptic problem using ELLPACK software. The physical problem arises when calculating the distribution of temperatures within an electronic package in order to assist in the design of appropriate cooling. ELLPACK software is modified here to solve three dimensional problems more general than the ones it was originally designed for. GRA

N92-28562# Naval Ocean Systems Center, San Diego, CA.
EXTENSIBILITY EXPERIMENTS WITH THE SOFTWARE

LIFE-CYCLE SUPPORT ENVIRONMENT Final Report
S. A. Parker and R. H. Mumm Nov. 1991 122 p
(AD-A247696; NOSC-TR-1463) Avail: NTIS HC/MF A06

This report describes the research carried out on the Software Life-Cycle Support Environment (SLCSE) by the Software Engineering Environment (SEE) prototypes task of the Software Engineering for C3 Systems project. The focus of this investigation is to perform extensibility experiments with the SLCSE. These experiments included the development of an interface to the ALS/N ADAVAX compiler and the integration of a number of public domain and other no-cost software tools into the SLCSE. One goal of this research was to determine of the SLCSE could be tailored to meet the needs of a specific project. GRA

N92-28585*# Research Triangle Inst., Research Triangle Park, NC.
INTEGRATION OF TOOLS FOR THE DESIGN AND ASSESSMENT OF HIGH-PERFORMANCE, HIGHLY RELIABLE COMPUTING SYSTEMS (DAHPHRS), PHASE 1
C. Scheper, R. Baker, G. Frank, S. Yalamanchili (Honeywell, Inc., Minneapolis, MN.), and G. Gray (Virginia Polytechnic Inst., Blacksburg.) May 1992 187 p Sponsored in cooperation with Rome Lab., Griffiss AFB, NY
(Contract NAS1-17964; RTOP 505-64-54-01)
(NASA-CR-189621; NAS 1.26:189621) Avail: NTIS HC/MF A09

Systems for Space Defense Initiative (SDI) space applications typically require both high performance and very high reliability. These requirements present the systems engineer evaluating such systems with the extremely difficult problem of conducting performance and reliability trade-offs over large design spaces. A controlled development process supported by appropriate automated tools must be used to assure that the system will meet design objectives. This report describes an investigation of methods, tools, and techniques necessary to support performance and reliability modeling for SDI systems development. Models of the JPL Hypercubes, the Encore Multimax, and the C.S. Draper Lab Fault-Tolerant Parallel Processor (FTPP) parallel-computing architectures using candidate SDI weapons-to-target assignment algorithms as workloads were built and analyzed as a means of identifying the necessary system models, how the models interact, and what experiments and analyses should be performed. As a result of this effort, weaknesses in the existing methods and tools were revealed and capabilities that will be required for both individual tools and an integrated toolset were identified. Author

N92-28636# National Aerospace Lab., Amsterdam (Netherlands). Informatics Div.
SOFTWARE DEVELOPMENT USING A METHOD BASE SYSTEM
S. deJong 30 Nov. 1990 22 p Presented at the CAPE Nederland 1991 Conference, Rotterdam, Netherlands, 26 Feb. 1991
(NLR-TP-90387-U; ETN-92-91451) Avail: NTIS HC/MF A03

CASE (Computer Aided Software Engineering) tools are presented. Activities to integrate a large part of the software engineering process with the CASE tools are shown. The software engineering process is based on the decomposition of a software system into functions to be performed. From each of the obtained functions, separate software components called methods are derived. Methods are stored in method bases to improve the reuse of software components. A method base system which supports management of methods is introduced. The method based system is one of the tools in use for information system production. Its role in the software engineering process is described, in combination with two other tools. The relation between methods and objects, as in 'object oriented' is discussed. Experiences with the various concepts and tools are presented. ESA

N92-28638# Technische Univ., Eindhoven (Netherlands). Dept. of Mathematics and Computing Science.
A NETWORK FLOW ALGORITHM FOR JUST-IN-TIME PROJECT SCHEDULING
E. V. Levner and A. S. Nemirovsky (Academy of Sciences, USSR, Moscow) Sep. 1991 24 p Revised
(Memo-COSOR-91-21; ISSN-0926-4493; ETN-92-91455) Avail: NTIS HC/MF A03

The polynomial solvability of the PERT-COST project scheduling problem is shown in the case of: the objective being a piecewise linear, convex (possibly, nonmonotone) function of the job durations as well as of job start/finish times; and the precedence relations between jobs being presented on the form of a general (not necessary, acyclic) directed graph with arc lengths of any sign. For the latter problem, a network flow algorithm (of pseudolinear complexity), which is easy to implement and which behaves well when the objective values grow slowly with the growth of the problem size while the number of breakpoints in the objective grows fast, is presented. ESA

N92-28639# Technische Univ., Eindhoven (Netherlands). Dept. of Mathematics and Computing Science.
GENETIC ALGORITHMS IN CODING THEORY: A TABLE FOR A3 (n, d)
R. J. M. Vaessens, E. H. L. Aarts (Philips Gloeilampenfabrieken N.V., Eindhoven, Netherlands), and J. H. vanLint (Philips Gloeilampenfabrieken N.V., Eindhoven, Netherlands) Sep. 1991 21 p
(Memo-COSOR-91-22; ISSN-0926-4493; ETN-92-91456) Avail: NTIS HC/MF A03

The problem of finding values of A(sub 3)(n, d) the maximal size of a ternary code of length n and minimum distance d is considered. The approach is based on a search for good lower bounds and a comparison of these bounds with known upper bounds. Several lower bounds are obtained using a genetic local search algorithm. Other lower bounds are obtained by constructing codes. For these cases in which lower and upper bounds coincide, this yields exact values of A(sub 3)(n,d). A table containing the known values of the upper and lower bounds for A(sub 3)(n,d), with n less than or equal to 16, is included. For some values of n and d the corresponding codes are given. ESA

N92-28666# ORA Corp., Ithaca, NY.
SPECTOOL: A COMPUTER-AIDED VERIFICATION TOOL FOR HARDWARE DESIGNS, VOLUME 1 Final Report, Jun. 1990 - Feb. 1991
Mandayam Srivas and Mark Bickford Dec. 1991 94 p Prepared for Harris Corp., Melbourne, FL
(Contract F30602-89-D-0096)
(AD-A247492; RL-TR-91-339-Vol-1) Avail: NTIS HC/MF A05

This report describes a computer-aided verification tool, SPECTOOL, for a class of synchronous hardware designs. The tool reduces the effort required for verifying a design in the targeted class by automating most of the routine, but cumbersome, parts of the verification process. The input to the tool is a circuit diagram of the design. This diagram is drawn using the graphical user-interface provided by the tool. SPECTOOL was used on several examples including a large pipelined microprocessor design. GRA

N92-28667# ORA Corp., Ithaca, NY.
SPECTOOL: USER'S MANUAL, VOLUME 2 Final Report, Jun. 1990 - Feb. 1991
Mandayam Srivas and Mark Bickford Dec. 1991 83 p Prepared for Harris Corp., Melbourne, FL
(Contract F30602-89-D-0096)
(AD-A247493; RL-TR-91-339-Vol-2) Avail: NTIS HC/MF A05

This report describes a computer-aided verification tool, SPECTOOL, for a class of synchronous hardware designs. The tool reduces the effort required for verifying a design in the targeted class by automating most of the routine, but cumbersome, parts of the verification process. The input to the tool is a circuit diagram of the design. This diagram is drawn using the graphical user-interface provided by the tool. SPECTOOL was used on several examples including a large pipelined microprocessor design. GRA

N92-28684*# National Aeronautics and Space Administration. Lewis Research Center, Cleveland, OH.
PC GRAPHICS GENERATION AND MANAGEMENT TOOL FOR REAL-TIME APPLICATIONS
Long V. Truong Jul. 1992 10 p Presented at the 23rd Conference on Modeling and Simulation, Pittsburgh, PA, 30 Apr. - 1 May 1992
(RTOP 506-41-41)
(NASA-TM-105749; E-7053; NAS 1.15:105749) Avail: NTIS HC/MF A02

A graphics tool was designed and developed for easy generation and management of personal computer graphics. It also provides methods and 'run-time' software for many common artificial intelligence (AI) or expert system (ES) applications. Author

N92-28700# Centre de Recherches Scientifiques et Techniques de l'Industrie des Fabrications Metalliques, Brussels (Belgium). Section Construction Mecanique.
THREE DIMENSIONAL MEASUREMENTS OF PRISMATIC BODIES: PROGRAMMING BY MEANS OF A CAD SYSTEM [LES MEASURES TRIDIMENSIONNELLES DE PIECES PRISMATIQUES: PROGRAMMER A L'AIDE D'UN SYSTEME CAO]
Geert vandenHoudt Aug. 1991 16 p In FRENCH Sponsored by l'Inst. pour l'Encouragement de la Recherche Scientifique dans l'Industrie et l'Agriculture
(CRIF-MC-91; ETN-92-91022) Avail: NTIS HC/MF A03

The use of computer assisted design (CAD) to perform 3-D measurements is discussed. The use of data from CAD to operate 3-D measuring machines is stressed. The method is applied for defining and controlling accurately the dimensions of objects to be manufactured. The principles, the advantages, and the disadvantages of some of the available software interfaces are underlined, and examples are given. The requirements that justify the use of 3-D measuring machines monitored by CAD software and data for quality controlling prismatic objects are underlined. The method is suitable for manufacturing a small number of complex objects. Author

N92-28704# Minnesota Univ., Minneapolis. Dept. of Computer Science.
GLOBAL MINIMUM SOLUTION OF ENGINEERING DESIGN PROBLEMS Final Report, 1 Feb. 1987 - 31 Aug. 1991
J. B. Rosen 31 Aug. 1991 6 p
(Grant AF-AFOSR-0127-87)
(AD-A247496; AFOSR-92-0216TR) Avail: NTIS HC/MF A02

Two algorithms to solve non-ionvex geometrical programming problems were developed and tested. Computational results were obtained. GRA

N92-28710*# Research Inst. for Computing and Information Systems, Houston, TX.
GROUND SYSTEMS DEVELOPMENT ENVIRONMENT (GSDE) SOFTWARE CONFIGURATION MANAGEMENT
Victor E. Church (Computer Sciences Corp., Beltsville, MD.), D. Long (Computer Sciences Corp., Beltsville, MD.), Ray Hartenstein (Computer Sciences Corp., Beltsville, MD.), and Alfredo Perez-Davila (Houston Univ., Clear Lake, TX.) 30 Apr. 1992 43 p
(Contract NCC9-16; RICIS Proj. SE-34)
(NASA-CR-190503; NAS 1.26:190503; CSC/TR-92/6054) Avail: NTIS HC/MF A03

This report presents a review of the software configuration management (CM) plans developed for the Space Station Training Facility (SSTF) and the Space Station Control Center. The scope of the CM assessed in this report is the Systems Integration and Testing Phase of the Ground Systems development life cycle. This is the period following coding and unit test and preceding delivery to operational use. This report is one of a series from a study of the interfaces among the Ground Systems Development Environment (GSDE), the development systems for the SSTF and the SSCC, and the target systems for SSCC and SSTF. This is the last report in the series. The focus of this report is on the CM plans developed by the contractors for the Mission Systems Contract (MSC) and the Training Systems Contract (TSC). CM requirements are summarized and described in terms of operational software development. The software workflows proposed in the TSC and MSC plans are reviewed in this context, and evaluated against the CM requirements defined in earlier study reports. Recommendations are made to improve the effectiveness of CM while minimizing its impact on the developers. Author

N92-28719# University of Southern California, Los Angeles. School of Engineering.
CENTER FOR THE INTEGRATION OF OPTICAL COMPUTING Annual Report No. 2, 15 Feb. 1991 - 14 Feb. 1992
A. A. Sawchuk and W. H. Steier 15 Mar. 1992 59 p
(Grant AF-AFOSR-0133-90)
(AD-A250306; AFOSR-92-0279TR) Avail: NTIS HC/MF A04

Topics reviewed include optical connections, lenslet array processors, generalization neural networks, spatial light modulators, MBE growth of quantum well structures, ultralow threshold laser array, charge transport optical nonlinearities, wave mixing at the bandedge in III-V semiconductors and photorefractive optical interconnections, optical computing, laser arrays, spatial modulators, and optical neural interconnections. GRA

N92-28741# Rolls-Royce Ltd., Derby (England). Materials and Mechanical Technology Dept.
KNOWLEDGE-BASED MATERIAL SELECTION IN DESIGN
R. J. Bamkin and B. J. Piercey 1990 5 p Repr. from Materials and Design, v. 11, no. 1, Feb. 1990 p 25-28 Presented at the Open Forum on Material Selection and the Role of Expert Systems, Birmingham, England, Jun. 1989
(PNR-90823; ETN-92-90846) Copyright Avail: NTIS HC/MF A01

The nature of material selection within the design process was studied to obtain a better understanding of the factors involved. This study justified the development of a 'Design Assistant' program for the selection of materials. The study concentrated on a component as a working part of larger assembly. This is modeled using object orientated software techniques. These cover the effects of contact between components (joints, wear, corrosion); a rule base of comparative materials and processes; recognition of the material shortlists already in use within companies; and how to interact with other disciplines within the design process. ESA

N92-28758*# National Aeronautics and Space Administration. Ames Research Center, Moffett Field, CA.
MoCog1: A COMPUTER SIMULATION OF RECOGNITION-PRIMED HUMAN DECISION MAKING, CONSIDERING EMOTIONS
William B. Gevarter Apr. 1992 51 p
(NASA-TM-107859; FIA-92-13; NAS 1.15:107859) Avail: NTIS HC/MF A04

The successful results of the first stage of a research effort to develop a versatile computer model of motivated human cognitive behavior are reported. Most human decision making appears to be an experience-based, relatively straightforward, largely automatic response to situations, utilizing cues and opportunities perceived from the current environment. The development, considering emotions, of the architecture and computer program associated with such 'recognition-primed' decision-making is described. The resultant computer program (MoCog1) was successfully utilized as a vehicle to simulate earlier findings that relate how an individual's implicit theories orient the individual toward particular goals, with resultant cognitions, affects, and behavior in response to their environment. Author

N92-28760*# Institute for Computer Applications in Science and Engineering, Hampton, VA.
VIENNA FORTRAN: A LANGUAGE SPECIFICATION, VERSION 1.1 Final Interim Report
Hans Zima (Wien Univ., Austria), Peter Brezany (Wien Univ., Austria), Barbara Chapman (Wien Univ., Austria), Piyush Mehrotra, and

Andreas Schwald (Wien Univ., Austria) Mar. 1992 90 p
Sponsored by Austrian Research Foundation and Austrian Ministry for Science and Research
(Contract NAS1-18605; RTOP 505-90-52-01)
(NASA-CR-189629; NAS 1.26:189629; ICASE-IR-21) Avail: NTIS HC/MF A05

The syntax and semantics of Vienna FORTRAN, a machine-independent language extension to FORTRAN 77, which allows the user to write programs for distributed-memory systems using global addresses are presented. Vienna Fortran includes high-level features for specifying virtual processor structures, distributing data across sets of processors, dynamically modifying distributions, and formulating explicitly parallel loops. The language is based upon the Single-Program Multiple-Data (SPMD) paradigm, which exploits the parallelism inherent in many scientific codes. A substantial subset of the language features has already been implemented. Author

N92-28779# Office National d'Etudes et de Recherches Aerospatiales, Paris (France).
VECTOR AND PARALLEL SUPERCOMPUTING PROGRAMMING [PROGRAMMATION DES SUPER-CALCULATEURS SCIENTIFIQUES VECTORIELS ET PARALLELES]
Francois-Xavier Roux 1991 152 p In FRENCH
(ONERA-NT-1991-11; ISSN-0078-3781; ETN-92-91271) Avail: NTIS HC/MF A08

The architecture of today's vector and parallel supercomputers and their programming environments are presented. A number of detailed examples of scientific algorithms, such as the assembly and solution of linear sets of equations occurring in numerical models based on finite difference or finite element discretizations, are illustrated. The three main kinds of architectures studied are pipelined vector computers, shared memory vector parallel commputers, and distributed memory massively parallel MIMD systems. The programming tools for vectorization and loop level parallelization of the Alliant and Cray machines with the 'autotasking' environment are presented. For coarse grain parallelization, the multitasking environment of the Cray machines is introduced along with the message passing programming of INTEL iPSC machines. The main examples of scientific algorithms detailed are the construction of a finite element matrix, the block Gaussian factorization of a dense matrix, the inversion of a coarse symmetric linear set of equations by an iterative method, the conjugate gradient algorithm, and a direct solver, the Crout factorization. Domain decomposition methods are also introduced. ESA

N92-28785# Institut National Polytechnique, Grenoble (France). Lab. Bull-IMAG.
COMPILATION AND OPERATION ENVIRONMENT OF AN OBJECT BASED LANGUAGE Ph.D. Thesis [COMPILATION ET ENVIRONNEMENT D'EXECUTION D'UN LANGAGE A BASE D'OBJETS]
Hiep NguyenVan 1991 207 p In FRENCH
(ETN-92-91323) Avail: NTIS HC/MF A10

Investigations performed on the scope of the GUIDE (Grenoble University Integrated and Distributed Environment) project are presented. The GUIDE project is the framework for research in the area of distributed applications. It is based on the development of an experimental distributed object based operating system. It provides a high degree of integration, and especially location transparancy. The GUIDE object based language specifically allows distributed applications to be written and executed easily using all elements of the model and the system. The compiling principles of GUIDE sources in executable objects are presented. Objects are dynamically created while executing applications and they remain permanent. Therefore a garbage collector must be present to automatically gather garbages. The study of garbage collector algorithm families and their adaptation for the GUIDE system is included. ESA

N92-28790# Office National d'Etudes et de Recherches Aerospatiales, Paris (France). Direction des Structures.
A CONTINUATION METHOD FOR CALCULATING THE EQUILIBRIUM POSITIONS OF NONLINEAR STRUCTURES [UNE METHODE DE CONTINUATION POUR LE CALCUL DES POSITIONS DEQUILIBRE DES STRUCTURES NONLINEAIRES]
R. Girard and D. Louis Sep. 1991 31 p In FRENCH
(Contract DRET-89-34-001)
(ONERA-RT-24/3542-RY-091-R; ETN-92-91329) Avail: NTIS HC/MF A03

A method of continuation applied to the solution of nonlinear structural problems is presented: parameterization of equilibrium paths, predictor correction for the equilibrium position search. Algorithms used to detect and overcome the bifurcation points were developed and tested. The tests were carried out on analytical problems of nonlinear phenomena, such as boundary points with or without bifurcation, and simple bifurcation points. ESA

N92-28795# Johns Hopkins Univ., Laurel, MD. Applied Physics Lab.
UNWRAPPING TWO-DIMENSIONAL PHASE DATA IN CONTOUR MAPS
William H. Carter 13 Nov. 1991 17 p
(Contract N00039-91-C-0001)
(AD-A249988; JHU/APL-TG-1380) Avail: NTIS HC/MF A03

A computer algorithm has been discovered for unwrapping two-dimensional phase data and producing perfect contour maps without holes or dark bands of erroneous contour lines. The method employs local, temporary unwrapping within single grid squares of rectangular sampled data and the addition of extra contour levels outside the 0 to 2 range to fill holes. GRA

N92-28841# Colorado Univ., Denver.
FAST ALGORITHMS FOR TRANSPORT MODELS
T. Manteuffel Apr. 1992 7 p
(Contract DE-FG02-90ER-25086)
(DE92-011432; DOE/ER-25086/2) Avail: NTIS HC/MF A02

The first two years of this project were focused on developing fast algorithms for the solution of the equations arising from models of single group isotropic transport of neutrally charged particles in slab geometry. In this context, the equation governing transport is an integral-differential equation involving one space variable and one angle variable. This paper discusses the solution of the equations. DOE

N92-28842# Institut National Polytechnique, Grenoble (France). Lab. d'Informatique Fondamentale et d'Intelligence Artificielle.
OPTIMIZATION BY RENAMING IN THE SOLUTION METHOD Ph.D. Thesis [OPTIMISATIONS PAR RENOMMAGE DANS LA METHODE DE RESOLUTION]
Thierry BoydelaTour 1991 114 p In FRENCH
(ETN-92-91324) Avail: NTIS HC/MF A06

The renaming technique allows a clausal form polynomial to be obtained. The technique is partially applied in order to minimize certain syntax criteria, in particular the number of clauses, and at the same time, preserve the polynomial complexity. It is shown that an efficient algorithm allows the optimum number of clauses on the linear expressions to be obtained. The influence of these transformations, on the resolution refutations method are theoretically and experimentally studied. ESA

N92-28845# California Univ., Berkeley. Space Sciences Lab.
ARCHIVAL OF THE ECOM-721 DATA Final Report, 29 Oct. 1990 - 28 Oct. 1991
Supriya Chakrabarti 15 Apr. 1992 3 p
(Contract DAAL03-90-G-0233)
(AD-A249299; ARO-28637.1-GS-EQ) Avail: NTIS HC/MF A01

The Army grant, number DAAL03-90-G-0233, has funded the procurement of an erasable optical disk drive and media for the archiving of the data taken from the ECOM instrument which flew aboard the P78-1 STP satellite. The data which was previously stored in 1/4 inch magnetic tape format is currently being transferred to a random access optical disk format. Although this

is a simple process, it is very important to the ultimate data analysis. With random access to the data and a much smaller volume of storage media, the data will now be accessible for long term studies of the extreme ultraviolet (EUV) and far ultraviolet (FUV) aurora and airglow. About 1100 orbits have been archived, and work is continuing on archiving the rest of the data with support from elsewhere. GRA

N92-28875*# Research Inst. for Advanced Computer Science, Moffett Field, CA.
KANERVA'S SPARSE DISTRIBUTED MEMORY WITH MULTIPLE HAMMING THRESHOLDS
Seppo Pohja (Tampere Univ. of Technology, Finland) and Kimmo Kaski (Tampere Univ. of Technology, Finland) Mar. 1992 9 p Sponsored by NASA. Ames Research Center
(NASA-CR-190552; NAS 1.26:190552; RIACS-TR-92-06) Avail: NTIS HC/MF A02

If the stored input patterns of Kanerva's Sparse Distributed Memory (SDM) are highly correlated, utilization of the storage capacity is very low compared to the case of uniformly distributed random input patterns. We consider a variation of SDM that has a better storage capacity utilization for correlated input patterns. This approach uses a separate selection threshold for each physical storage address or hard location. The selection of the hard locations for reading or writing can be done in parallel of which SDM implementations can benefit. Author

N92-28943# Naval Postgraduate School, Monterey, CA.
SPEEDS: AN APPROACH TO SUPPORT PROGRAMMING ENVIRONMENTS USING EXPERT DATABASE SYSTEMS M.S. Thesis
Ronald A. Boxall Sep. 1991 80 p
(AD-A247469) Avail: NTIS HC/MF A05

Programming decisions, such as scheduling, planning and coordinating, are made in every type of organization. In situations where these decisions are made by an expert who uses information contained in large databases, it could be advantageous for the organization to employ an expert system coupled with a database to assist in the decision process. This thesis proposes an approach for building expert database systems to support programming environments. To test this approach, a prototype expert database system is developed for a typical programming environment at a classical music radio station that employs experts to select music. The process of acquiring and representing the expert knowledge and the development, testing and implementation of the prototype are discussed in the context of this case study. The lessons learned in the development of this expert database system are also presented. GRA

N92-28946# Naval Ocean Systems Center, San Diego, CA.
STUDIES OF ITERATED TRANSFORM IMAGE COMPRESSION AND ITS APPLICATION TO COLOR AND DTED Final Report, Oct. 1990 - Sep. 1991
R. D. Boss and E. W. Jacobs Dec. 1991 38 p
(DA Proj. RV3-6-I-21)
(AD-A248060; NOSC/TR-1468) Avail: NTIS HC/MF A03

A new classification technique based on archetypes can reduce encoding time and still maintain compression and fidelity. The use of different metrics has shown little differences in the final encoding quality, thus implying that the use of the root mean square metric is preferred. Also presented is the Digital Terrain Elevation Database (DTED) that is more accurate after using an iterated transform algorithm modified to encode the coastlines. The results compare favorably with an adaptive discrete cosine transformation (ADCT) and mean residual vector quantization algorithm. Additionally, results of two iterated transform algorithms for encoding 24-bit/pixel color images are presented. The first method transforms the red, green, blue (RGB) to the luminancechrominance representation before encoding, showing results similar to ADCT algorithms. The second method encodes RGB subimages directly using common transformations, and does not perform as consistently as the luminance-chrominance method. GRA

N92-28952# Aeronautical Research Labs., Melbourne (Australia).
DIGITAL ENHANCEMENT AND RESTORATION OF IMAGES DERIVED FROM FLOW VISUALIZATION EXPERIMENTS
M. F. Lee Dec. 1991 33 p
(AD-A250317; ARL-FLIGHT-MECH-TM-452; DODA-AR-006-656) Avail: NTIS HC/MF A03

The Pixedit program has been rewritten to enable image processing of raster image files residing on the IRIS 4D workstations. Such techniques as spectral filtering, edge detection and enhancement and false coloring techniques have been incorporated into the new version of the program. These techniques are usefully applied in enhancing the quality of photographic images obtained from flow visualization experiments. This report describes the techniques used, giving examples of their application to flow visualization and provides instructions for operating the revised Pixedit program. GRA

N92-28969# AEDAR Corp., Landover, MD.
COMPUTER DERIVATION OF GREEN'S FUNCTIONS FOR STRUCTURAL DYNAMIC ANALYSIS Final Report, 1 Sep. 1989 - 31 Aug. 1991
James A. Fabunmi 21 Oct. 1991 80 p
(Contract F49620-89-C-0112)
(AD-A250249; AEDAR-FTR-91-02; AFOSR-92-0342TR) Avail: NTIS HC/MF A05

This research program has been concerned with the development of a new generation of computer-aided techniques for the dynamic analysis of complex structural systems. These techniques which use powerful symbolic processors such as MACSYMA are expected to facilitate the derivation and analysis of Green's functions of interconnected distributed parameter structures. The present approach uses integral methods to combine the transfer functions of the baseline structure with those of discrete substructure attachments in order to obtain the transfer function of the interconnected system. This resultant transfer function is then transformed into a form which lends itself easily to inverse Laplace transformation, yielding the Green's function of the interconnected system. Such algebraic results are expected to improve the understanding of the effects of substructure attachments e.g., active and passive vibration controllers, on the dynamics of large flexible structures. GRA

N92-28971# Aeronautical Research Labs., Melbourne (Australia).
COMPUTER RECOGNITION AND ANALYSIS OF PHOTOGRAMMETRIC TARGETS
B. A. Woodyatt and T. G. Ryall Mar. 1992 48 p
(AD-A250313; ARL-STRUC-TM-549; DODA-AR-006-659) Avail: NTIS HC/MF A03

This Technical Memorandum is a continuation of earlier work into the application of photogrammetric techniques for the modal analysis of vibrating structures. Methods are developed for the computer processing of photogrammetric negatives. The negatives capture the positions of retro-reflective targets located on the vibrating structure. With the relative distances between targets known, the distorted structure can be reconstructed. All targets are given a Global coordinate, thus reducing the accumulation of errors over the negative. The techniques used to establish the Global Coordinate System are discussed as are the methods used to determine accurately the location of the retro-reflective targets. GRA

N92-29106*# Research Inst. for Advanced Computer Science, Moffett Field, CA.
USING GAUSSIAN WINDOWS TO EXPLORE A MULTIVARIATE DATA SET
Louis A. Jaeckel Dec. 1991 62 p
(Contracts NCC2-408; NCC2-387)
(NASA-CR-190556; NAS 1.26:190556; RIACS-TR-91.22) Avail: NTIS HC/MF A04

In an earlier paper, I recounted an exploratory analysis, using Gaussian windows, of a data set derived from the Infrared

Astronomical Satellite. Here, my goals are to develop strategies for finding structural features in a data set in a many-dimensional space, and to find ways to describe the shape of such a data set. After a brief review of Gaussian windows, I describe the current implementation of the method. I give some ways of describing features that we might find in the data, such as clusters and saddle points, and also extended structures such as a 'bar', which is an essentially one-dimensional concentration of data points. I then define a distance function, which I use to determine which data points are 'associated' with a feature. Data points not associated with any feature are called 'outliers'. I then explore the data set, giving the strategies that I used and quantitative descriptions of the features that I found, including clusters, bars, and a saddle point. I tried to use strategies and procedures that could, in principle, be used in any number of dimensions. Author

N92-29107*# Research Inst. for Advanced Computer Science, Moffett Field, CA.
USER'S MANUAL FOR THE GAUSSIAN WINDOWS PROGRAM
Louis A. Jaeckel Feb. 1992 43 p
(Contracts NCC2-408; NCC2-387)
(NASA-CR-190554; NAS 1.26:190554; RIACS-TR-92.05) Avail: NTIS HC/MF A03

'Gaussian Windows' is a method for exploring a set of multivariate data, in order to estimate the shape of the underlying density function. The method can be used to find and describe structural features in the data. The method is described in two earlier papers. I assume that the reader has access to both of these papers, so I will not repeat material from them. The program described herein is written in BASIC and it runs on an IBM PC or PS/2 with the DOS 3.3 operating system. Although the program is slow and has limited memory space, it is adequate for experimenting with the method. Since it is written in BASIC, it is relatively easy to modify. The program and some related files are available on a 3-inch diskette. A listing of the program is also available. This user's manual explains the use of the program. First, it gives a brief tutorial, illustrating some of the program's features with a set of artificial data. Then, it describes the results displayed after the program does a Gaussian window, and it explains each of the items on the various menus. Author

N92-29113*# Research Inst. for Advanced Computer Science, Moffett Field, CA.
A LOOK-AHEAD VARIANT OF THE LANCZOS ALGORITHM AND ITS APPLICATION TO THE QUASI-MINIMAL RESIDUAL METHOD FOR NON-HERMITIAN LINEAR SYSTEMS Ph.D. Thesis - Massachusetts Inst. of Technology, Aug. 1991
Noel M. Nachtigal Oct. 1991 111 p
(Contract NCC2-387)
(NASA-CR-190557; NAS 1.26:190557; RIACS-TR-91.19)
Copyright Avail: NTIS HC/MF A06

The Lanczos algorithm can be used both for eigenvalue problems and to solve linear systems. However, when applied to non-Hermitian matrices, the classical Lanczos algorithm is susceptible to breakdowns and potential instabilities. In addition, the biconjugate gradient (BCG) algorithm, which is the natural generalization of the conjugate gradient algorithm to non-Hermitian linear systems, has a second source of breakdowns, independent of the Lanczos breakdowns. Here, we present two new results. We propose an implementation of a look-ahead variant of the Lanczos algorithm which overcomes the breakdowns by skipping over those steps where a breakdown or a near-breakdown would occur. The new algorithm can handle look-ahead steps of any length and requires the same number of matrix-vector products and inner products per step as the classical Lanczos algorithm without look-ahead. Based on the proposed look-ahead Lanczos algorithm, we then present a novel BCG-like approach, the quasi-minimal residual (QMR) method, which avoids the second source of breakdowns in the BCG algorithm. We present details of the new method and discuss some of its properties. In particular, we discuss the relationship between QMR and BCG, showing how one can recover the BCG iterates, when they exist, from the QMR iterates. We also present convergence results for QMR, showing the connection between QMR and the generalized minimal residual (GMRES) algorithm, the optimal method in this class of methods. Finally, we give some numerical examples, both for eigenvalue computations and for non-Hermitian linear systems. Author

N92-29172# Institute for Naval Oceanography, Bay Saint Louis, MS.
HYPER: A DOMAIN DECOMPOSITION PROGRAM, VERSION 1.0 (USER'S MANUAL)
A. L. Perkins Mar. 1992 33 p
(AD-A250018; INO-SP-4) Avail: NTIS HC/MF A03

This document describes the details for a set of utilities programs and subroutines that are collectively referred to as HYPER. The utility HYPER is designed to provide an environment for heterogeneous domain decomposition methods. In this user's manual, we describe the philosophy behind the code, how to use the code, and the data structures used for implementation. GRA

N92-29187# Mei Associates, Inc., Lexington, MA.
DESIGN SPECIFICATIONS FOR THE ADVANCED INSTRUCTIONAL DESIGN ADVISOR (AIDA), VOLUME 1 Final Report, Aug. 1989 - Jul. 1991
Albert E. Hickey, J. M. Spector, and Daniel J. Muraida Jan. 1992 180 p
(Contract F33615-88-C-0003)
(AD-A248201; AL-TR-1991-0085-Vol-1) Avail: NTIS HC/MF A09

This is the final report for the second phase effort on the Advanced Instructional Design Advisor (AIDA) project. An experimental system called XAIDA is described. The proposed XAIDA is intended to assist subject-matter experts in the design and development of computer-based instructional materials. The functional requirements for an automated and intelligent advisor that would be appropriate for Air Force technical development are presented, along with a system specification. GRA

N92-29188# Mei Associates, Inc., Lexington, MA.
DESIGN SPECIFICATIONS FOR THE ADVANCED INSTRUCTIONAL DESIGN ADVISOR (AIDA), VOLUME 2 Final Report, Aug. 1989 - Jul. 1991
Albert E. Hickey, J. Michael Spector, and Daniel J. Muraida Jan. 1992 132 p
(Contract F33615-88-C-0003)
(AD-A248202; AL-TR-1991-0085-Vol-2) Avail: NTIS HC/MF A07

This is the final report for the second phase effort or the Advanced Instructional Design Advisor (AIDA) project. An experimental system called XAIDA is described. The proposed XAIDA is intended to assist subject-matter experts in the design and development of computer-based instructional materials. The functional requirements for an automated and intelligent advisor that would be appropriate for Air Force technical development are presented, along with a system specification, automated instruction, instructional development, computer-based instruction, interactive technology, courseware design. At the request of the 857th Strategic Hospital Bioenvironmental Engineering Services the Armstrong Laboratory Occupational and Environmental Health Directorate (AL/OE) conducted a Hazardous Waste Technical Assistance Survey at Minot AFB on 24-28 Jun. 1991. The scope of this survey was to address hazardous waste management practices, to explore opportunities for waste minimization, and to determine waste streams. The survey team performed a shop-by-shop determination of hazardous waste streams and met with hazardous waste managers to discuss their waste programs. Recommendations include: (1) employ proven waste reduction techniques in 857 TRANS shops, 857 CES vehicle maintenance and equipment maintenance shops, and 5 FMS aircraft maintenance shops; and (2) install locking devices on each accumulation drum or tank at accumulation points. GRA

N92-29198# Yale Univ., New Haven, CT. Dept. of Computer Science.
NEW NEURAL ALGORITHMS FOR SELF-ORGANIZED LEARNING Interim Report, Dec. 1988 - Nov. 1991
John E. Moody Nov. 1991 4 p
(AD-A249816) Avail: NTIS HC/MF A01

This interim report describes work completed from December 1988 to November 1991. The original purpose of the research program funded by this grant was to study self-organized systems which adapt and learn. The originally proposed research fell into two main categories: (1) Biological Models of Self-Organization; and (2) New Self-Organized Learning Systems. During the period for which this grant was funded, significant progress was made in both areas. In addition, some new areas related to neural network learning are being explored as an outgrowth of the original proposal. These include: (1) Model Selection Techniques; and (2) Estimating Generalization Performance. GRA

N92-29200*# Research Inst. for Computing and Information Systems, Houston, TX.
REPOSITORY-BASED SOFTWARE ENGINEERING PROGRAM: CONCEPT DOCUMENT
14 Apr. 1992 54 p Prepared in cooperation with Applied Expertise, Inc., Arlington, VA
(Contract NCC9-16; RICIS Proj. RB-04)
(NASA-CR-190384; NAS 1.26:190384) Avail: NTIS HC/MF A04

This document provides the context for Repository-Based Software Engineering's (RBSE's) evolving functional and operational product requirements, and it is the parent document for development of detailed technical and management plans. When furnished, requirements documents will serve as the governing RBSE product specification. The RBSE Program Management Plan will define resources, schedules, and technical and organizational approaches to fulfilling the goals and objectives of this concept. The purpose of this document is to provide a concise overview of RBSE, describe the rationale for the RBSE Program, and define a clear, common vision for RBSE team members and customers. The document also provides the foundation for developing RBSE user and system requirements and a corresponding Program Management Plan. The concept is used to express the program mission to RBSE users and managers and to provide an exhibit for community review. Author

N92-29209# Laboratoire d'Automatique et d'Analyse des Systemes, Toulouse (France).
CONTRIBUTION TO THE DESIGN OF FLEXIBLE MANUFACTURING SYSTEMS: APPLICATION OF THE FORMAL DESCRIPTION TECHNIQUE ESTELLE Ph.D. Thesis - Toulouse Univ. [CONTRIBUTION A LA CONCEPTION DE SYSTEMES FLEXIBLES DE PRODUCTION: APPLICATION DE LA TECHNIQUE DE DESCRIPTION FORMELLE ESTELLE]
Vitorio Bruno Mazzola 1991 151 p In FRENCH Sponsored by CAPES, Brazil, and Univ. Federal de Santa Catarina
(LAAS-91378; ETN-92-91332) Avail: NTIS HC/MF A08

The study of flexible manufacturing systems is presented, and a method, based on the use of the Estelle formal description technique is proposed. Flexible manufacturing systems are composed of heterogeneous equipment which cooperate to perform a given production task. Due to its distributed nature, control of such a system requires solutions to the complex problems related to the synchronization and the interconnection of these devices. The study covers the different design steps of a flexible assembly cell, starting from the initial specification of an assembly task until the implementation of the cell driving system. This methodology allows the user to validate, by applying a verification technique by abstraction, the different design steps and the driving system levels (in particular, the task and the action levels). The use of two Estelle support tools, ESTIM and EWS, led to automating the proposed methodology and implementation of the flexible assembly cell driving system. Estelle was applied for specifying and validating a subset of the MMS (Manufacturing Message Services) services, defined for satisfying communication requirements within the flexible assembly cell. ESA

N92-29221# Technische Univ., Delft (Netherlands). Faculty of Technical Mathematics and Informatics.
APPLICATIONS AND BENEFITS OF FORMAL METHODS IN SOFTWARE DEVELOPMENT
Nico Plat, Jan vanKatwijk, and Hans Toetenel 1991 44 p
(Rept-91-33; ISSN-0922-5641; ETN-92-91408) Copyright Avail: NTIS HC/MF A03

A detailed examination is made of the application of and the benefits resulting from one particular formal method (VDM (Vienna Development Method)) in a standard model for software development (DoD-STD-2167A). Currently, there is no general agreement on how formal methods should be used, but in order to analyze the use of formal methods in the software development process a clear view of such use is essential; therefore, it is shown what 'using VDM' means. The different activities of DoD-STD-2167A are analyzed with regard to their suitability for applying VDM, and the benefits that may be the result from applying VDM for that activity. Based on this analysis, an overall view on the usage of VDM on the software development process is formulated. ESA

N92-29224# Maryland Univ. Baltimore County, Catonsville. Dept. of Mathematics and Statistics.
MAXIMIZING THE CONVERGENCE RATE OF THE EM ALGORITHM FOR THE MULTIPLE BROAD-BAND SIGNAL ESTIMATION AND DETECTION Final Report, 1 Jul. 1988 - 31 Jan. 1991
James T. Lo 26 Mar. 1992 9 p
(Contract N00014-88-K-0490)
(AD-A248230) Avail: NTIS HC/MF A02

The following results were obtained under the contract: numerical acceleration of convergence for the EM algorithm; a characterization of the rank-n ambiguity; a characterization of the phase delay ambiguity; determination of the minimal number of known and unknown signals for sensor location observability; a large class of cyclic regression algorithms for multiple signal direction finding; array sensor localization and calibration by cyclic regression; cyclic regression for the weighted subspace fitting for direction finding: cyclic regression for harmonic retrieval from colored noise; a statistical approach to training multilayer perceptrons. GRA

62 COMPUTER SYSTEMS

Includes computer networks and special application computer systems.

N92-28279# Oak Ridge National Lab., TN.
HeNCE: GRAPHICAL DEVELOPMENT TOOLS FOR NETWORK-BASED CONCURRENT COMPUTING
A. Beguelin, J. Dongarra, A. Geist, R. Manchek (Tennessee Univ., Knoxville.), K. Moore (Tennessee Univ., Knoxville.), and R. Wade (Tennessee Univ., Knoxville.) 1992 8 p Presented at the Scalable High Performance Computing Conference, Williamsburg, VA, 26-29 Apr. 1992
(Contracts DE-AC05-84OR-21400; DE-FG05-91ER-25105)
(DE92-011061; CONF-9204106-3) Avail: NTIS HC/MF A02

HeNCE (Heterogeneous Network Computing Environment) is an X Window based graphical parallel programming environment that was created to assist scientists and engineers with the development of parallel programs. HeNCE provides a graphical interface for creating, compiling, executing, and debugging parallel programs, as well as configuring a distributed virtual computer (using PVM). HeNCE programs can be run on a single Unix workstation or over a network of heterogeneous machines. This paper describes the purpose and use of the HeNCE software. DOE

N92-28306# Naval Postgraduate School, Monterey, CA.
THE TESTING, ANALYSIS, AND CORRECTION OF THE UPDATE OPERATION OF A PARALLEL, MULTI-BACKEND

DATABASE SUPERCOMPUTER M.S. Thesis
Michael A. Williams Mar. 1992 33 p
(AD-A248320) Avail: NTIS HC/MF A03

The Multi-Backend Database Supercomputer (MBDS) is designed to provide high-performance database management parallely for applications with very large and growing databases. This thesis is a testing, analysis, and correction of the primary database operation UPDATE of MBDS. We provide an overview of the entire MBDS system and then focus on the parallel UPDATE operation in an attempt to discover and correct the deficiencies of the original UPDATE algorithm. GRA

N92-28334# Lawrence Livermore National Lab., CA.
SISAL: TOWARD RESOLVING THE PARALLEL PROGRAMMING CRISIS
D. Cann, R. Wolski, and J. Feo 2 Mar. 1992 8 p Presented at the WHP92 on Heterogeneous Processing, Beverly Hills, CA, 23-24 Mar. 1992
(Contract W-7405-eng-48)
(DE92-010716; UCRL-JC-109774; CONF-920390-2) Avail: NTIS HC/MF A02

SISAL (Streams and Iterations in Single Assignment Language) is a functional language for numerical computation on both conventional and novel multiprocessor systems. We discuss the Sisal project; illustrate SISAL's performance in comparison to sequential and parallel FORTRAN; and identify the project's future directions. We demonstrate that one can raise the level of program abstraction without sacrificing performance. SISAL programs are efficient, portable, determinate, and free of the burden thwarting parallel program in development. Without question, functional programming can resolve today's parallel programming crisis. DOE

N92-28381# Lawrence Livermore National Lab., CA.
AN ELROS PRIMER
M. L. Branstetter, J. A. Guse, and D. M. Nessett 30 Oct. 1991 99 p
(Contract W-7405-eng-48)
(DE92-010661; UCRL-MA-108543) Avail: NTIS HC/MF A05

This document provides an introduction to ELROS and its use in building distributed applications. A thorough reading will equip a programmer with the necessary information to write simple distributed applications using the ELROS language. For a more comprehensive description of ELROS, including its advanced features, consult the ELROS user's manual that is in preparation. DOE

N92-28642# Technische Univ., Eindhoven (Netherlands). Dept. of Mathematics and Computing Science.
ANALYSING MULTIPROGRAMMING QUEUES BY GENERATING FUNCTIONS
I. J. B. F. Adan, J. Wessels (International Inst. for Applied Systems Analysis, Laxenburg, Austria), and W. H. M. Zijm (Universiteit Twente, Enschede, Netherlands) Oct. 1991 13 p
(Memo-COSOR-91-25; ETN-92-91459) Avail: NTIS HC/MF A03

The generating function approach for analyzing queueing systems has a longstanding tradition. One of the highlights is the seminal paper by Kingman on the shortest queue problem, where the author shows that the equilibrium probabilities p(sub m, n) of the queue lengths can be written as an infinite sum of products of powers. The same approach is used by Hifri to prove that for a multiprogramming model with two queues the boundary probability P(sub 0, n) can be expressed as an infinite sum of powers. A study which shows that the latter representation does not always hold, which implies that the multiprogramming problem is essentially more complicated than the shortest queue problem, is presented. However, it appears that the generating function approach is very well suited to show when a representation is available and when not. ESA

N92-28676*# Virginia Univ., Charlottesville. Dept. of Computer Science.
MENTAT/A: MEDIUM GRAIN PARALLEL PROCESSING Final Report
Andrew S. Grimshaw 16 Jul. 1992 50 p
(Grant NAG1-1181)
(NASA-CR-190486; NAS 1.26:190486) Avail: NTIS HC/MF A03

The objective of this project is to support the Algorithm to Architecture Mapping Model (ATAMM) firing rules using the Mentat run-time system and the Mentat Programming Language (MPL). Specifically, this required changes to (1) modify the run-time system to control queue length and inhibit actor firing until required data tokens are available and space is available in the input queues of all of the direct descendent actors, (2) disallow the specification of persistent object classes in the MPL, and (3) permit only decision free graphs in the MPL. We have been successful in implementing the spirit of the plan, although some goals changed as we came to better understand the problem. Here, we report on what we accomplished and the lessons we learned. The Mentat/A runtime system, the compiler, results for three applications, and a summary and some observations are given. Appendix A contains a list of technical reports and published papers partially supported by the grant. Appendix B contains listings for the three applications. Author

N92-28706# National Aerospace Lab., Amsterdam (Netherlands). Informatics Div.
SUPERCONDUCTING AT NLR: NEC SX-2 CAPABILITIES IN NLR'S TERMINAL AND FILE-TRANSFER NETWORK
G. J. Hameetman 11 Jan. 1989 14 p Presented at the Superconducting Europe 1989, Utrecht, Netherlands, 21-23 Feb. 1989
(NLR-TP-89007-U; ETN-92-91515) Avail: NTIS HC/MF A03

The improvements introduced at the NLR in information systems for aerospace and related applications are discussed. As the result of a continuous evaluation, a NEC SX-2 supercomputer was added and the computer network was extended. The purpose of the supercomputer was to bring about a more extensive digital simulation method. The purpose of the integration of workstations was to make flexible interaction possible with the multitude of computer systems, and to create man machine interface allowing control of the complex integrated information systems. ESA

N92-28746 Institute for Perception RVO-TNO, Soesterberg (Netherlands). Cognitive Psychology Group.
MODELS FOR RECALL AND RECOGNITION Final Report [MODELLEN VOOR HERINNERING EN HERKENNING]
J. G. W. Raaijmakers and R. M. Shiffrin May 1991 37 p Prepared in cooperation with Indiana Univ., Bloomington
(Grants NIMH-12717; AF-AFOSR-0089-87)
(IZF-1991-B-4; TD91-2156; ETN-92-91230) Copyright Avail: TNO Inst. Perception, Kampweg 5, P.O. Box 23, 3769 ZG Soesterberg, Netherlands

The state of the art concerning models for recall and recognition is reviewed. A distinction is made between network models, search or separate trace models, and composite/distributed memory models. The models are compared on a number of aspects, such as whether they are based on separate or composite traces, the nature of the memory representation, context dependency, etc. A comparison is made with respect to the ability to predict basic findings in memory research. The advantages and disadvantages of quantitative models of memory are discussed. ESA

N92-28770# Princeton Univ., NJ.
DEVELOPMENT OF A HIGH-PERFORMANCE FORTRAN COMPILER FOR PORTING CFD CODES TO THE NAVIER-STOKES COMPUTER Final Report, 1 Nov. 1990 - 31 Oct. 1991
Daniel M. Nosenchuck 31 May 1992 7 p
(Grant AF-AFOSR-0003-91)
(AD-A250208; AFOSR-92-0389TR) Avail: NTIS HC/MF A02

Research on developing a high-performance FORTRAN compiler for the Navier-Stokes Computer (NSC) was performed

during the contractual period. The thrust of the work was to develop a prototype compiler the NSC MiniNode. The NSC MiniNode is an operational prototype hardware node, that represents the key building block of a parallel-processing supercomputer whose architecture was designed to support the efficient simulation of large-scale complex fluid flows. GRA

N92-28782# Institut National Polytechnique, Grenoble (France). Lab. Conception de Systemes Integres.
FLEXIBLE INTEGRATED ARCHITECTURE FOR NEURAL NETWORKS Ph.D. Thesis [ARCHITECTURE INTEGREE FLEXIBLE POUR RESEAUX DE NEURONES]
Jamel Eddine Ouali 1991 196 p In FRENCH
(ETN-92-91320) Avail: NTIS HC/MF A09

A distributed, synchronous architecture, based on the existence of autonomous neural processor is proposed. The processor is to be customized according to the neural network to be implemented and can be easily connected to other neurons to constitute a network with fixed structure and size. This neuron is presented as a dedicated fabricated circuit in a short time in a silicon compiler environment. Such a neuron was designed and fabricated and proved completely operational. It is shown that without any modification of the architecture, learning possibilities can be included. For this, a learning algorithm using the back propagation was studied. Its implementation is shown on the proposed neural network, specifying the adjunction in the controller of the neuron to be implemented. The possibility of realizing very large circuits is explored. The possibility of wafer scale integration is considered. In fact, there is an intrinsic defect tolerance to neural computation, and regular physical implementation must allow the isolation and exclusion of the defective neurons. The possibilities of physical implementation of wafer scale architecture are presented. ESA

N92-28915# Yale Univ., New Haven, CT. Dept. of Computer Science.
CRYSTALLIZING FORTRAN
Dong-Yuan Chen, Marina C. Chen, Ron Y. Pinter, and Shlomit S. Pinter 26 Nov. 1991 15 p
(Contract N00014-91-J-1559; NSF CCR-89-08285)
(AD-A250162) Avail: NTIS HC/MF A03

The parallelization techniques embodied in source to source tools (that are customarily applied to FORTRAN programs) and in compilers for high level functional languages (such as crystal) can and should be combined under a common framework. Traditionally, the former tools target shared memory machines, whereas the latter distributed memory (or data parallel) machines. One effect of the combination is the ability to run sequential FORTRAN programs on a whole new class of machines; it also provides a good way to separate between different parallelization concerns and deal with them at the appropriate level. We describe the design and an implementation of a prototypical system that enables such a combination. The design is modular and extendible; its implementation entails, among other challenges, bridging the gap between imperative and functional program semantics. We have developed several techniques that solve these and other fundamental problems, and present them with this concrete framework. Experimental results, as achieved by the prototype and as presented hereby, are most encouraging and substantiate the usefulness of this approach. GRA

N92-28958# Texas Univ., Arlington. Dept. of Computer Science Engineering.
FAULT-TOLERANT PARALLEL COMPUTER SYSTEMS FOR REAL-TIME APPLICATIONS Final Report
S. M. Yang and Bill D. Carroll Feb. 1992 175 p
(Contract N00014-88-K-0622)
(AD-A247887) Avail: NTIS HC/MF A08

The objective of our research was to investigate techniques for designing fault-tolerant parallel computer systems for critical real-time applications. The focus of our research was to develop the practical fault tolerance design, implementation and analysis technology with the considerations of real-time recovery, structuring of recoverable interactions, and handling of software as well as hardware failure in distributed/parallel computing environments. We also investigate techniques for scheduling of real-time messages as well as real-time tasks in fault-tolerant distributed systems. GRA

N92-29096# Department of the Navy, Washington, DC.
ASYNCHRONOUS BIDIRECTIONAL NETWORK INTERFACE ENABLING SEAMLESS CONCURRENT PROCESSING IN A DISTRIBUTED HETEROGENEOUS MULTIPROCESSOR SYSTEM Patent Application
Bruce W. Stevens, inventor (to Navy) 28 Oct. 1991 28 p
(AD-D015274; US-Patent-Appl-SN-783661) Avail: NTIS HC/MF A03

A network interface resident on one processor enables heterogenous processors interconnected by a common network to exchange control and data information via virtual circuits created and maintained by the network interface between sockets defined at the communicating processors. Different kinds of messages are discriminated and their length is determined to enable the same network virtual circuit to multiplex data and control information in a manner that, being message specific, conserves network resources. Data conversion is implemented to enable heterogeneous processors to communicate over the network virtual circuit. Asynchronous, bidirectional communication is provided by the network interface for tightly-coupled, moderately-coupled, and loosely-coupled hardware architecture conformance types. GRA

N92-29109*# Research Inst. for Advanced Computer Science, Moffett Field, CA.
MAPPING UNSTRUCTURED GRID COMPUTATIONS TO MASSIVELY PARALLEL COMPUTERS Ph.D. Thesis - Rensselaer Polytechnic Inst., Feb. 1992
Steven Warren Hammond Jun. 1992 149 p
(Contract NCC2-387)
(NASA-CR-190551; NAS 1.26:190551; RIACS-TR-92.14) Avail: NTIS HC/MF A07

Investigated here is this mapping problem: assign the tasks of a parallel program to the processors of a parallel computer such that the execution time is minimized. First, a taxonomy of objective functions and heuristics used to solve the mapping problem is presented. Next, we develop a highly parallel heuristic mapping algorithm, called Cyclic Pairwise Exchange (CPE), and discuss its place in the taxonomy. CPE uses local pairwise exchanges of processor assignments to iteratively improve an initial mapping. A variety of initial mapping schemes are tested and recursive spectral bipartitioning (RSB) followed by CPE is shown to result in the best mappings. For the test cases studied here, problems arising in computational fluid dynamics and structural mechanics on unstructured triangular and tetrahedral meshes, RSB and CPE outperform methods based on simulated annealing. Much less time is required to do the mapping and the results obtained are better. Compared with random and naive mappings, RSB and CPE reduce the communication time two fold for the test problems used. Finally, we use CPE in two applications on a CM-2. The first application is a data parallel mesh-vertex upwind finite volume scheme for solving the Euler equations on 2-D triangular unstructured meshes. CPE is used to map grid points to processors. The performance of this code is compared with a similar code on a Cray-YMP and an Intel iPSC/860. The second application is parallel sparse matrix-vector multiplication used in the iterative solution of large sparse linear systems of equations. We map rows of the matrix to processors and use an inner-product based matrix-vector multiplication. We demonstrate that this method is an order of magnitude faster than methods based on scan operations for our test cases. Author

N92-29114# Texas Univ., El Paso. Dept. of Mathematical Sciences.
ESTIMATION OF THE POINT OF INCIPIENT DETERIORATION AND A CLASS OF LIFE DISTRIBUTION WITH APPLICATION TO CANNIBALIZATION Final Report, 1 Jul. 1989 - 30 Sep. 1991

Javier Rojo 20 Jan. 1992 10 p
(Contract F49620-89-C-0085)
(AD-A250216; AFOSR-92-0291TR) Avail: NTIS HC/MF A02

The training problem for feedforward neural networks is nonlinear parameter estimation that can be solved by a variety of optimization techniques. Much of the literature on neural networks has focused on variants of gradient descent. The training of neural networks using such techniques is known to be a slow process with more sophisticated techniques not always performing significantly better. It is shown that feedforward neural networks can have ill-conditioned Hessians and that this ill-conditioning can be quite common. The analysis and experimental results lead to the conclusion that many network training problems are ill-conditioned and may not be solved more efficiently by higher order optimization methods. The analyses are for completely connected layered networks; they extend to networks with sparse connectivity as well. The results suggest that neural networks can have considerable redundancy in parameterizing the function space in a neighborhood of a local minimum, independently of whether or not the solution has a small residual. GRA

63 CYBERNETICS

Includes feedback and control theory, artificial intelligence, robotics and expert systems.

For related information see also *54 Man/System Technology and Life Support.*

N92-28325# Rochester Univ., NY. Dept. of Computer Science.
REINFORCEMENT LEARNING FOR THE ADAPTIVE CONTROL OF PERCEPTION AND ACTION Ph.D. Thesis
Steven D. Whitehead Feb. 1992 182 p
(Contract N00014-80-C-0190; NSF IRI-89-03582)
(AD-A249351; TR-406) Avail: NTIS HC/MF A09

This dissertation applies reinforcement learning to the adaptive control of active sensory-motor systems. Active sensory-motor systems, in addition to providing for overt action, also support active, selective sensing of the environment. The principal advantage of this active approach to perception is that the agent's internal representation can be made highly task specific, thus, avoiding wasteful sensory processing and the representation of irrelevant information. One unavoidable consequence of active perception is that improper control can lead to internal states that confound functionally distinct states in the external world. This phenomenon, called perceptual aliasing, is shown to destabilize existing reinforcement learning algorithms with respect to optimal control. To overcome these difficulties, an approach to adaptive control, called the Consistent Representation (CR) method, is developed. This method is used to construct systems that learn not only the overt actions needed to solve a task, but also where to focus their attention in order to collect necessary sensory information. The principle of the CR-method is to separate control into two stages: an identification stage, followed by an overt stage. The identification stage generates the task-specific internal representation that is used by the overt control stage. Adaptive identification is accomplished by a technique that involves the detection and suppression of perceptually aliased internal states. GRA

N92-28375*# National Aeronautics and Space Administration. Langley Research Center, Hampton, VA.
SOFTWARE DESIGN FOR AUTOMATED ASSEMBLY OF TRUSS STRUCTURES
Catherine L. Herstrom, Carolyn Grantham, Cheryl L. Allen, William R. Doggett, and Ralph W. Will Jun. 1992 47 p
(RTOP 506-43-41-02)
(NASA-TP-3198; L-16983; NAS 1.60:3198) Avail: NTIS HC/MF A03

Concern over the limited intravehicular activity time has increased the interest in performing in-space assembly and construction operations with automated robotic systems. A technique being considered at LaRC is a supervised-autonomy approach, which can be monitored by an Earth-based supervisor that intervenes only when the automated system encounters a problem. A test-bed to support evaluation of the hardware and software requirements for supervised-autonomy assembly methods was developed. This report describes the design of the software system necessary to support the assembly process. The software is hierarchical and supports both automated assembly operations and supervisor error-recovery procedures, including the capability to pause and reverse any operation. The software design serves as a model for the development of software for more sophisticated automated systems and as a test-bed for evaluation of new concepts and hardware components. Author

N92-28387# Jackson State Univ., MS.
TEMPORAL REASONING AND PROBLEM SOLVING Final Report, 1 Oct. - 30 Sep. 1991
V. N. Gudivada and R. Loganantharaj 28 Jan. 1992 13 p
(Contract DAAL03-90-G-0217)
(AD-A248457; ARO-28197.9-MA-SAH) Avail: NTIS HC/MF A03

Temporal Reasoning involves the study of a general theory of time and an associated reasoning. Representation of time plays an important role in acquiring and manipulating temporal knowledge. Within the artificial intelligence community, there are two popular approaches to representing time: intervals and points. However, very little work has been done to combine the best aspects of these systems under a single framework. The main accomplishments of this project are to: (1) develop a temporal framework that combines the advantages of both the point-based and the interval-based systems which allow metric bounds on an event's duration; (2) design algorithms for satisfying temporal constraints; (3) develop an efficient algorithm for propagating temporal constraints, and explore the feasibility of applying parallelism; and (4) design and implement a primitive point-based temporal reasoning system. GRA

N92-28401# Naval Health Research Center, San Diego, CA.
COMPUTER ASSISTED IMPROVEMENT OF THE ESTIMATION MEAN SQUARED ERROR WITH APPLICATION TO BACK PROPAGATION NEURAL NETWORKS Final Report
J. E. Angus 24 Jul. 1991 11 p
(AD-A247724; NHRC-91-17) Avail: NTIS HC/MF A03

A computer assisted method for improving the mean squared error (MSE) in estimation for parametric models is presented. Assuming the existence of nontrivial sufficient statistics, the method involves generation of Monte Carlo samples from the conditional distribution of the observables, given the sufficient statistic(s). The method is illustrated in connection with a simple back-propagation neural network model for estimating a logistic regression function. Key words and phrases are: parametric estimation, exponential families, nonlinear models, nonlinear least squares, neural networks, Monte Carlo simulation, computer intensive statistical methods. GRA

N92-28429# Washington Univ., Saint Louis, MO.
ADAPTIVE AND NONLINEAR CONTROL Final Report, 15 Aug. 1988 - 14 Aug. 1991
Christopher I. Byrnes 29 Feb. 1992 36 p
(Grant AF-AFOSR-0309-88)
(AD-A248580; AFOSR-92-0262TR) Avail: NTIS HC/MF A03

This final report surveys the research accomplishments of a three year effort on the adaptive stabilization and control of distributed parameter systems and on the development of a systematic feedback design methodology for nonlinear control systems. In both areas, significant advances have been made by the use of concepts and techniques from dynamical systems theory, developing enhancements of classical frequency domain ideas (e.g., transmission zeroes, root locus methods, etc.) for both classes of systems. Indeed, for DPS the rigorous development of a root locus theory for parabolic systems is one of our most significant achievements. For nonlinear control design, we have enjoyed three unanticipated breakthroughs. First, the development of a nonlinear enhancement of transmission zeroes enabled the solution of a major open problem in nonlinear control - the nonlinear regulator

problem - for systems operating near an equilibrium. Second, the geometric techniques underlying the solution of the regulator problem have been successfully applied to obtain 'off-line' feedback laws which solve nonlinear optimal control problems via a nonlinear analogue of the Riccati equation. Third, these advances, combined with the work described in this report, have led successfully to the development of a nonlinear robust control theory analogous to the development of H robust control for linear systems. GRA

N92-28581# Technische Univ., Delft (Netherlands). Faculty of Aerospace Engineering.
INVERSE CONTROL PROBLEMS: MATHEMATICAL PRELIMINARIES, SYSTEM THEORETICAL APPROACHES, AND THEIR APPLICATIONS TO AIRCRAFT DYNAMICS
E. S. L. H. WiryoHadiatmojo Oct. 1991 160 p
(LR-665; ETN-92-91403) Avail: NTIS HC/MF A08

The concept of inverse control problems in multivariable systems is to determine the characteristics of unknown inputs when the characteristics of outputs are known a priori or prescribed. An attempt to provide systematically the necessary mathematical models to describe such problems is reported. By adopting the system theoretical approach, system inverses are constructed using transfer function and state space methods to study the behavior of the dynamics of such systems. The unknown inputs are found to be the outputs of these inverses. Additionally necessary and sufficient conditions for a class of reproducible outputs and for system invertibility are derived. ESA

N92-28648# National Aerospace Lab., Amsterdam (Netherlands). Space Div.
QUASI-RECURSIVE DYNAMICS EQUATIONS FOR SPACECRAFT-BASED FLEXIBLE ROBOTIC MANIPULATORS
P. T. L. M. vanWoerkom 16 Jan. 1990 78 p
(Contract NIVR-02506-N)
(NLR-TP-90028-U; ETN-92-91431) Avail: NTIS HC/MF A05

The development of the dynamics equations of a spacecraft manipulator system with chain topology is described. The spacecraft may be flexible; the attached manipulator consists of an arbitrary number of links, connected by single degree of freedom rotational joints; none, any, or all of the links may be flexible; a rigid or flexible payload can be accommodated as part of the last link. D'Alembert's principle is used as a starting point for the derivation of the dynamics equations. The equations obtained hold for arbitrary geometry and arbitrary mass properties. By expressing the virtual displacement of an elementary mass in recursive form, algebraic complexity of the resulting equations is also reduced. ESA

N92-28716# National Aerospace Lab., Amsterdam (Netherlands). Informatics Div.
WHAT IS ON THE MACHINE'S MIND? MODELS FOR REASONING WITH INCOMPLETE AND UNCERTAIN KNOWLEDGE Ph.D. Thesis - Tech. Univ. Delft
N. Roos 27 Feb. 1991 132 p
(NLR-TP-91099-U; ETN-92-91545) Avail: NTIS HC/MF A07

A logic for reasoning with inconsistent knowledge is described, and a proposal for an alternative way of reasoning is reported. The development of such a logic is performed, considering that promises are assumptions about the world. The semantics of this logic are based on the ideas of Shoham. It possesses all the properties of an ideal nonmonotonic logic. A reasoning process is presented as a process of constructing a partial model of the world. Based on a partial model, a 'probability' and an 'unlikelihood' measure are concluded. The former is used for conclusions expressing an expectation and the latter for conclusions expressing an explanation. ESA

N92-28759*# National Aeronautics and Space Administration. Ames Research Center, Moffett Field, CA.
LEARNING AND TUNING FUZZY LOGIC CONTROLLERS THROUGH REINFORCEMENTS
Hamid R. Berenji (Sterling Software, Moffett Field, CA.) and Pratap Khedkar (California Univ., Berkeley.) Jan. 1992 56 p
(NASA-TM-107875; FIA-92-02; NAS 1.15:107875) Avail: NTIS HC/MF A04

A new method for learning and tuning a fuzzy logic controller based on reinforcements from a dynamic system is presented. In particular, our Generalized Approximate Reasoning-based Intelligent Control (GARIC) architecture: (1) learns and tunes a fuzzy logic controller even when only weak reinforcements, such as a binary failure signal, is available; (2) introduces a new conjunction operator in computing the rule strengths of fuzzy control rules; (3) introduces a new localized mean of maximum (LMOM) method in combining the conclusions of several firing control rules; and (4) learns to produce real-valued control actions. Learning is achieved by integrating fuzzy inference into a feedforward network, which can then adaptively improve performance by using gradient descent methods. We extend the AHC algorithm of Barto, Sutton, and Anderson to include the prior control knowledge of human operators. The GARIC architecture is applied to a cart-pole balancing system and has demonstrated significant improvements in terms of the speed of learning and robustness to changes in the dynamic system's parameters over previous schemes for cart-pole balancing. Author

N92-28895# Kentucky Univ., Lexington. Dept. of Computer Science.
INVESTIGATIONS OF LOGIC OF INTROSPECTION AND RELATED MODES OF REASONING WITH APPLICATIONS Final Report, 1 Aug. 1989 - 31 Dec. 1991
Victor W. Marek and Miroslaw Truszczynski 17 Feb. 1992 6 p
(Contract DAAL03-89-K-0124)
(AD-A249286; ARO-26438.16-EL) Avail: NTIS HC/MF A02

We investigated symbolic aspects of common sense reasoning. The formalisms studied - nonmonotonic logics - go beyond the classical logic and encompass such reasoning mechanisms as circumscription, default logic, autoepistemic logic, reason maintenance, and logic programming with negation. The area of nonmonotonic logics is currently one of the most active topics in Artificial Intelligence and has potential applications in the next generation of Expert Systems and general reasoning software. Main results of our research provide understanding of the dependence of nonmonotonic modal logics on the underlying monotonic modal logics, explain the relationships between most important modes of non-monotonic reasoning, and provide algorithms for automated nonmonotonic reasoning as well as computational complexity results. Several pilot implementations of nonmonotonic reasoning engines were produced. GRA

N92-28970# California Inst. of Tech., Pasadena. Dept. of Electrical Engineering.
MONOLITHIC OPTOELECTRONIC IMPLEMENTATION OF NEURAL PLANES Final Technical Report
Demetri Psaltis, Steven Lin, and Annette Grot 18 Mar. 1992 102 p
(Contract N00014-88-K-2023)
(AD-A250286) Avail: NTIS HC/MF A06

The implementation of a neural computing system, whose structure and function is motivated by natural intelligence, will provide a unique way to solve problems that are typically too difficult for the conventional electronic computers to tackle. Interest in this type of computer has emerged, largely because it is hoped that by building a computer that shares some of the characteristics of the biological systems, we will be able to address problems such as image recognition which animals do exceedingly well but current computers do not. There has been considerable progress on the theoretical research in neural networks to justify the optimism of future applications. This has resulted in a focused attention on the hardware realization of neural architectures. The computational power of neural computers arises from matching the computer architecture and the physical properties of the devices used in the implementation to the requirements of the problem. GRA

N92-29082# Wright Lab., Wright-Patterson AFB, OH.
STRETCH AND HAMMER NEURAL NETWORKS FOR N-DIMENSIONAL DATA GENERALIZATION Final Report, May - Oct. 1991
Peter G. Raeth, Steven C. Gustafson, Gordon R. Little, and Todd S. Puterbaugh 15 Jan. 1992 102 p Prepared in cooperation with Dayton Univ., OH
(AD-A247941; WL-TR-91-1146) Avail: NTIS HC/MF A06

A hypersurface stretch and hammer neural network has been developed that generalize data from processes that have one output variable and one or more input variables. This network achieves several desirable properties through a novel combination of standard methods. The methods incorporate principal components, linear least squares, Gaussian radial basis functions, and diagonnally dominant matrices. An easily visualized physical model of network function ensures that the combination of methods is appropriate and practical. The model has natural potential for parallel implementation and for n-dimensional classification and other pattern recognition tasks. These tasks include smoothing (interpolation), filtering, and prediction (extrapolation). The model can be extended to accommodate multiple outputs. Unlike many other neural networks (such as backpropagation-trained networks), the training and performance characteristics of the stretch and hammer neural network. The trials on three-dimensional surface interpolation are also presented, as are notes on other potential applications. GRA

N92-29149# Virginia Polytechnic Inst. and State Univ., Blacksburg. Dept. of Electrical Engineering.
CONTROL OF NONLINEAR DISTRIBUTED PARAMETER SYSTEMS WITH APPLICATION TO FLOW CONTROL Final Technical Report, 1 Aug. 1989 - 31 Dec. 1991
William T. Baumann and Antoni S. Banach 30 Mar. 1992 8 p
(Grant AF-AFOSR-0495-89)
(AD-A250212; AFOSR-92-0371TR) Avail: NTIS HC/MF A02

The goal of this project was to put the intuitive idea of gain-scheduling on a rigorous foundation for a class of nonlinear, distributed-parameter systems. This involved a study of the existence and characterization of the ideal, infinite-dimensional, feedback control. Since in most applications the feedback function cannot be computed in closed form, it was necessary to study the convergence of approximate feedback functions, based on increasingly higher order finite-dimensional approximations of the system, to the ideal function. Finally, the results were applied to Burgers' Equation, which can be viewed as a low-order approximation to a wide variety of physical phenomena, including viscous compressible flow. GRA

N92-29175*# National Aeronautics and Space Administration. Ames Research Center, Moffett Field, CA.
BUILDING THE SCIENTIFIC MODELING ASSISTANT: AN INTERACTIVE ENVIRONMENT FOR SPECIALIZED SOFTWARE DESIGN
Richard M. Keller May 1991 13 p
(Contract NAS2-13210)
(NASA-TM-107844; FIA-91-13; NAS 1.15:107844) Avail: NTIS HC/MF A03

The construction of scientific software models is an integral part of doing science, both within NASA and within the scientific community at large. Typically, model-building is a time-intensive and painstaking process, involving the design of very large, complex computer programs. Despite the considerable expenditure of resources involved, completed scientific models cannot easily be distributed and shared with the larger scientific community due to the low-level, idiosyncratic nature of the implemented code. To address this problem, we have initiated a research project aimed at constructing a software tool called the Scientific Modeling Assistant. This tool provides automated assistance to the scientist in developing, using, and sharing software models. We describe the Scientific Modeling Assistant, and also touch on some human-machine interaction issues relevant to building a successful tool of this type. Author

N92-28738*# North Carolina State Univ., Raleigh. Mars Mission Research Center.
FUZZY LOGIC CONTROLLER FOR MANIPULATOR SYSTEMS: PRELIMINARY RESULTS
D. Gerber, H. Roberts, R. J. Stanley, II, and J. C. Windsor *In* NASA. Langley Research Center, Ongoing Progress in Spacecraft Controls Jul. 1992 p 123-148 (For primary document see N92-28730 19-18)
Avail: NTIS HC/MF A07

64 NUMERICAL ANALYSIS

Includes iteration, difference equations, and numerical approximation.

N92-28297*# National Aeronautics and Space Administration. Goddard Space Flight Center, Greenbelt, MD.
A FAST DIRECT SOLVER FOR A CLASS OF TWO-DIMENSIONAL SEPARABLE ELLIPTIC EQUATIONS ON THE SPHERE
Shrinivas Moorthi and R. Wayne Higgins May 1992 35 p
(RTOP 578-41-16-20)
(NASA-TM-104567; NAS 1.15:104567; Rept-92B00092) Avail: NTIS HC/MF A03

An efficient, direct, second-order solver for the discrete solution of two-dimensional separable elliptic equations on the sphere is presented. The method involves a Fourier transformation in longitude and a direct solution of the resulting coupled second-order finite difference equations in latitude. The solver is made efficient by vectorizing over longitudinal wavenumber and by using a vectorized fast Fourier transform routine. It is evaluated using a prescribed solution method and compared with a multigrid solver and the standard direct solver from FISHPAK. Author

N92-28311# International Centre for Theoretical Physics, Trieste (Italy).
THE PRINCIPAL PART OF PLANE VECTOR FIELDS WITH FIXED NEWTON DIAGRAM
F. Berezovskaya Sep. 1991 18 p
(DE92-622408; IC-91/304) Avail: NTIS HC/MF A03

Considering the main part of a plane vector field in a neighborhood of a singular point 0(0,0) it is well known that if the singularity real parts of eigenvalues are non-zero, the linear part of the vector field provides the topological normal form and tangents of all the o-curves. The problem is to find the main part of a plane vector field which would provide the topological orbital normal form in a neighborhood of singular point and asymptotics of all characteristics trajectories. The solution to the problem for the generic case of so-called nondegenerate vector fields, using the Newton diagram is given. DOE

N92-28329# Cornell Univ., Ithaca, NY.
A CENTER OF EXCELLENCE IN THE MATHEMATICAL SCIENCES Final Report, 1 Jan. 1986 - 31 Jan. 1992
Anil Nerode Mar. 1992 96 p
(Contract DAAG29-85-C-0018)
(AD-A249365; ARO-23306.531-MA) Avail: NTIS HC/MF A05

Significant discoveries were made concerning the role of symmetry in dynamical systems, work on the dynamics of low-dimensional dynamical systems (one and two dimensional real and complex systems), and progress in the use of symbolic computation tools for the study of dynamical systems. The development of the visualization tool and interface for studying dynamical systems, kaos, was partially funded through MSI. Research in interacting particle systems increased as they are attractive models useful in a wide variety of situations in physics, biology, and image processing. One of the great breakthroughs in the subject in the past five years was R. Durrett's development of methods for treating large classes of these models if one is willing to assume that the range of interaction is large or that the particles are moving at a fast rate. These assumptions are satisfied in many biological and physical systems and provide a reliable guide

to the qualitative features of other systems, as well. Very significant work was done in the area of polytopes, generalized discriminants, and resultants. They established a conjecture of Baues arising in the geometry of loop spaces in homotopy theory. Research and development was done on Macaulay which has become one of the major computer algebra systems for computations in algebraic geometry and commutative algebra. The system is in use world-wide. GRA

N92-28399# Texas A&M Univ., College Station. Dept. of Civil Engineering.
PROBABILISTIC FINITE ELEMENT ANALYSIS Final Report
John M. Niedzwecki 28 Feb. 1992 104 p
(Contract N00014-89-J-1586)
(AD-A247721) Avail: NTIS HC/MF A06

The finite element method is used extensively in structural analyses. Traditionally, the properties of the systems which are modeled using finite elements are assumed to be deterministic. The uncertainties in the structural response behavior estimates which result from uncertainties in the properties of the system were accounted for by using safety and reduction factors. As structures become more complex and industry makes use of materials such as composites, which are known to have random material properties, an alternative approach to design which quantifies the distributions in response may be required. Probabilistic finite element techniques, which are capable of assessing the distributions in response behavior for systems with random material properties, loads and boundary conditions are presented in this thesis. One particular method termed second-moment analysis is examined in detail. This method includes perturbation techniques and is used to compute the expected values and covariance matrices of probabilistic response behavior. Second-moment analyses in conjunction with the finite element method require as input the expected values of the random processes inherent to the system and their covariance matrices. Methods are also presented to compute these parameters for local element averages of the random processes which describe the uncertainty in the system. GRA

N92-28411# Wisconsin Univ., Madison. Center for Mathematical Sciences.
FOURIER ANALYSIS OF THE APPROXIMATION POWER OF PRINCIPAL SHIFT-INVARIANT SPACES
Carl deBoor and Amos Ron Jul. 1991 36 p
(Contract DAAL03-90-G-0090)
(AD-A246713; CMS-TSR-92-01) Avail: NTIS HC/MF A03

Spaces spanned by finitely or countably many translates of one or several basic functions play an important role in spline theory, radial basis function theory, sampling theory and wavelet theory. Spline theory stresses the case when the basic functions are compactly supported, while sampling theory single out the case when the spectrum (i.e., the support of the Fourier transform) of the basic functions is compact. In the radial basis function theory, neither of these is assumed, and instead, the computational simplicity as well as the positive definiteness (i.e., the positivity of the Fourier transform) of the basic functions is preferred. Finally, wavelet theory focuses on the interrelation between the initial space and its dyadic dilates. In all these areas, the underlying space s is meant for approximation or decomposition of functions, and thus, the determination of its approximation properties is of basic significance. GRA

N92-28635# National Aerospace Lab., Amsterdam (Netherlands). Fluid Dynamics Div.
HYPERBOLIC GRID GENERATION WITH BEM SOURCE TERMS
M. H. L. Hounjet 9 Oct. 1990 14 p Presented at the International Association for Boundary Element Methods, Rome, Italy, 15-19 Oct. 1990
(Contract NIVR-01904-N)
(NLR-TP-90334-U; ETN-92-91448) Avail: NTIS HC/MF A03

A method for the generation of O type grids about transverse cross sections of transport type aircraft is presented. The method combined a hyperbolic grid generation scheme with source terms obtained with a Boundary Element Method (BEM) in such a way that O type grids around fairly complex shapes with concavities can be generated easily. The component of the method, a boundary element method, a method to generate grids with a boundary element method, and the hyperbolic grid generation scheme are described, and applications are shown. ESA

N92-28641# Technische Univ., Eindhoven (Netherlands). Dept. of Mathematics and Computing Science.
MATRIX-GEOMETRIC ANALYSIS OF THE SHORTEST QUEUE PROBLEM WITH THRESHOLD JOCKEYING
I. J. B. F. Adan, J. Wessels (International Inst. for Applied Systems Analysis, Laxenburg, Austria), and W. H. M. Zijm (Universiteit Twente, Enschede, Netherlands) Oct. 1991 12 p
(Memo-COSOR-91-24; ETN-92-91458) Avail: NTIS HC/MF A03

A system consisting of c parallel servers with possibly different service rates is studied. Jobs arrive according to a Poisson stream and generate an exponentially distributed workload. An arriving job joins the shortest queue, where in case of multiple shortest queues, one of these queues is selected according to some arbitrary probability distribution. If the maximal difference between the lengths of the c queues exceeds some threshold value T, then one job switches from the longest to the shortest queue, where in case of multiple longest queues, the queue loosing a job is selected according to some arbitrary distribution. The matrix geometric approach is shown to be very well suited to find the equilibrium probabilities of the queue lengths. The interesting point is that for one partitioning of the state space an explicit ergodicity condition can be derived from Neuts' mean drift condition, whereas for another partitioning the associated R matrix can be determined explicitly. Both partitionings used are different from the one suggested by the conventional way by applying the matrix geometric approach. The study is seen as a plea for giving more attention to the question of the selection of a partitioning in the matrix geometric approach. ESA

N92-28777# Office National d'Etudes et de Recherches Aerospatiales, Paris (France).
WAVELETS AND NUMERICAL SIMULATION Ph.D. Thesis - Paris VI Univ. [ONDELETTES ET SIMULATION NUMERIQUE]
Valerie Perrier 1991 237 p In FRENCH
(ONERA-NT-1991-8; ISSN-0078-3781; ETN-92-91269) Avail: NTIS HC/MF A11

The study of the feasibility of wavelet based techniques in scientific computation, and especially for the numerical simulation of turbulence, is addressed. A survey of recent results concerning the wavelet transform and the decomposition of an orthonormal wavelet base is presented. Applications to filtering that illustrate the properties of time frequency localization of wavelet coefficients are presented. Fast analysis reconstruction algorithms are developed in the framework of periodic functions. Numerical algorithms based on wavelets for solving partial differential equations are defined: a spectral-like method, which dynamically optimizes the number of wavelet coefficients required to discretize the solution, and a traveling wavelet method which computes the solution as a sum of particles evolving in the position scale half plane. ESA

N92-28824# Lawrence Livermore National Lab., CA.
A COMPARATIVE STUDY OF THE ACCURACY OF VARIOUS TIME DOMAIN NONORTHOGONAL MESH METHODS
S. L. Ray and P. W. Rambo 21 Jan. 1992 6 p Presented at the Institute of Electrical and Electronic Engineers-American Physical Society (IEEE-APS) International Symposium, Chicago, IL, 18-25 Jul. 1992
(Contract W-7405-eng-48)
(DE92-007300; UCRL-JC-109505; CONF-920750-1) Avail: NTIS HC/MF A02

In recent years, a number of researchers have developed numerical methods for solving Maxwell's equations on irregular (nonuniform and nonorthogonal) meshes. These include curvilinear coordinate extensions of the FDTD method, staggered mesh finite

volume and discrete surface integration methods, and Voronoi (Dirichlet/Delaunay) mesh methods. Some of these methods are applicable to meshes of quadrilaterals (in 2D), others to triangular grids, and others to either type of element. While all of these methods appear to work well, little is known about their relative accuracy. The standard method for studying the accuracy of discrete wave propagation methods is through dispersion analysis. This type of analysis provides practical information about the accuracy of a given discretization by quantifying the amount of dispersion, dissipation, and anisotropy that is introduced into the solution by the numerical scheme. It also provides a stability limit for the maximum stable time step size. Unfortunately, this analysis can not be applied on an irregular mesh. One can, however, analyze the dispersion characteristics of the uniform nonorthogonal meshes. These skewed meshes present an idealized but representative situation which can be treated analytically, thus providing a simple and powerful means for comparing disparate schemes. DOE

N92-28949# Yale Univ., New Haven, CT. Dept. of Computer Science.
DIAGONAL FORMS OF TRANSLATION OPERATORS FOR HELMHOLTZ EQUATION IN THREE DIMENSIONS
V. Rokhlin 25 Mar. 1992 31 p
(AD-A248422; YALEU/DCS/RR-894) Avail: NTIS HC/MF A03

Fourier techniques have been a popular analytical tool in the study of physics and engineering for more than two centuries. A reason for the usefulness of such techniques is that certain trigonometric functions are eigenfunctions of the differentiation operator and can be effectively used to model solutions of differential equations which arise in the fields mentioned above. More recently, the arrival of digital computers and the development of the Fast Fourier Transform (FFT) algorithm in the 1960s have established Fourier analysis as a powerful and practical numerical tool. The FFT, which computes discrete Fourier transforms (DFTs), is now central to many areas, most notably spectral analysis and signal processing. In some applications, however, the input data is not uniformly spaced, a condition which is required for the FFT. Here, we present a set of algorithms for computing more efficiently some generalizations of the DFT, namely the forward and inverse transformations described by certain equations. GRA

N92-29193# Norwegian Defence Research Establishment, Kjeller.
ON SOME SPLITTING SCHEMES FOR WAVE EQUATIONS
Ivar Lie 20 Nov. 1991 47 p
(FFI-91/7023; ISSN-0802-2437; ETN-92-91245) Avail: NTIS HC/MF A03

Some splitting schemes for hyperbolic partial differential equations (PDEs) and in particular those equations with wave like solutions are presented. The purpose of the splitting is to decouple different types of waves, fast and slow waves. The splitting schemes to be discussed can therefore be categorized as time splitting. Two different splitting techniques are considered in detail, and it is shown how analytic solutions can be used as a part of one of these techniques, the operator integration factor approach. ESA

N92-29214# Amsterdam Univ. (Netherlands). Inst. for Language, Logic and Information.
GENERALIZED QUANTIFIERS AND MODAL LOGIC
Wiebe vanderHoek (Vrije Univ., Amsterdam, Netherlands) and Maarten deRijke Jun. 1991 32 p Sponsored in part by Netherlands Organization for Applied Scientific Research TNO
(ITLI-LP-91-01; ISSN-0924-2082; ETN-92-91349) Avail: NTIS HC/MF A03

Several modal languages in which some (sets of) generalized quantifiers can be represented are studied. The main language considered is suitable for defining by first order definable quantifier, but a sublanguage thereof is considered, as well as a language for dealing with the modal couterparts of some higher order quantifiers. These languages are studied both from a modal logic perspective and from a quantifier perspective. Thus, the issues addressed include normal forms, expressive power completeness both on modal systems and of systems in the quantifier tradition, and complexity as well as syntactic characterizations of special semantic constraints. Several techniques current in the theory of generalized quatifiers are used to obtain results in modal logic. ESA

65 STATISTICS AND PROBABILITY

Includes data sampling and smoothing; Monte Carlo method; and stochastic processes.

N92-28273# Educational Testing Service, Princeton, NJ.
THE VARIANCE OF RASCH ABILITY ESTIMATES FROM PARTIALLY-KNOWN ITEM PARAMETERS
Robert J. Mislevy Jan. 1992 20 p
(Contract N00014-88-K-0304)
(AD-A247065; ETS-RR-92-9-ONR) Avail: NTIS HC/MF A03

A closed-form approximation is given for the variance of examinee proficiency estimates in the Rasch model for dichotomous items, under the condition that only estimates, rather than true values, of item difficulty parameters are available. The term that must be added to the usual response-sampling variance is inversely proportional to both the number of examinees in the item calibration sample and the length of the test. Illustrative numerical values suggest that the impact of uncertainty about Rasch item parameters on subsequent estimates of examinee proficiencies is less than has been observed in the 2- and 3-parameter logistic IRT models. GRA

N92-28516# San Diego State Univ., CA. Center for Research in Mathematics and Science Education.
COMPUTER-BASED ASSESSMENT OF SCHEMA KNOWLEDGE IN A FLEXIBLE PROBLEM-SOLVING ENVIRONMENT
Technical Report, 1 Jun. 1990 - 1 Mar. 1991
Sandra P. Marshall Jan. 1992 25 p
(Contract N00014-90-J-1143)
(AD-A246779; CRMSE-91-01) Avail: NTIS HC/MF A03

This report describes assessment of students' schema knowledge for arithmetic word problems. The assessment takes place on-line as students interact with the computer program. The instruction that precedes the assessment, the environment in which students exhibit their knowledge, and the assessment of that knowledge all derive from one core theory of learning and memory, schema theory. This report outlines the schema theory briefly and describes the assessment environment, the student responses upon which the assessment is based, and the strategies of students observed through such assessment. GRA

N92-28640# Technische Univ., Eindhoven (Netherlands). Dept. of Mathematics and Computing Science.
DISTRIBUTION THEORY FOR SELECTION FROM LOGISTIC POPULATIONS
Paul vanderLaan Sep. 1991 16 p Presented at the Symposium on Biostatistics and Statistics in Honour of Charles W. Dunette, Hamilton, Ontario, 29 May - 1 Jun. 1991
(Memo-COSOR-91-23; ISSN-0926-4493; ETN-92-91457) Avail: NTIS HC/MF A03

Assume k (integer k greater than or equal to 2) independent populations pi(sub 1), pi(sub 2)..., pi(sub k) are given. The associated independent random variables X(sub 1), X(sub 2)..., X(sub k) are logistically distributed with unknown means mu(sub 1), mu(sub 2)..., mu(sub k) respectively, and common known variance. The goal is to select the best population with the largest mean. Some distributional results are derived for subset selection as well as for the indifference zone approach. The probability of correct selection is determined. Exact and numerical results concerning the expected subset size are presented for the subset selection approach. Some remarks are made for a generalized selection goal using subset selection. This goal is to select a nonempty subset of populations that contains at least one epsilon best (almost best) treatment with confidence level P. For a set of populations an epsilon best treatment is defined as a treatment

with location parameter on a distance less than or equal to epsilon (epsilon, greater than or equal to 0) from the best population. ESA

N92-28647# Technische Univ., Delft (Netherlands).
SOME AEROSPACE APPLICATIONS OF ESTIMATION THEORY Ph.D. Thesis
Geert Moek 1991 185 p
(ETN-92-91281) Avail: NTIS HC/MF A09

The application of estimation theory to three problems from aerospace research is described. The applications considered deal with spacecraft attitude estimation, software reliability modeling and estimation, and with a satellite based navigation algorithm. Maximum likelihood estimation is used in the software reliability case and mean square estimation in the other two applications. An adaptive iterated extended Kalman filter is evaluated on the basis of simulated and real spacecraft attitude measurement data. Results based on different combinations of attitude measurements and sensor models are compared. A satellite based navigation algorithm using a spline approximation of a vehicle trajectory and a non-recursive nonlinear least squares estimation algorithm are described. Their application to simulated pseudo range measurements shows the potential of accurate position determination. Maximum likelihood parameter estimation for four software reliability models is analyzed. Conditions are derived pertaining to the existence of bounded solutions of the likelihood equations. Uniqueness of such solutions is proved for two of the four models. Some results of the application of both simulated and real software failure time data are given. ESA

N92-28778# Office National d'Etudes et de Recherches Aerospatiales, Paris (France).
IDENTIFICATION OF WEAKLY NON-LINEAR DYNAMICAL SYSTEMS BY MEANS OF RANDOM EXCITATIONS Ph.D. Thesis - Ecole Centrale de Paris [IDENTIFICATION DES SYSTEMES DYNAMIQUES FAIBLEMENT NON-LINEAIRES A PARTIR D'EXCITATIONS ALEATOIRES]
Olivier Fillatre 1991 146 p In FRENCH
(ONERA-NT-1991-10; ISSN-0078-3781; ETN-92-91270) Avail: NTIS HC/MF A07

The identification of second order, weakly nonlinear, dynamical systems, in which the nonlinearity is a function of velocity and displacement components, is addressed. Though an a priori modeling of a nonlinearty might be imaginable when it is located on the structure, such an approach seems in fact particularly difficult, or even impossible, in the case of distributed nonlinearities. When these are sufficiently small, however, it is both justifiable and highly advantageous to use a linear system that is close to the original one, and that is physically satisfactory too. In the search for ways of defining such linearized systems that could be as close as possible to the original nonlinear one, the concept of True Stochastic Linearization (TSL) is developed. Observation of the variation of the resulting linearized system, as the excitation bandwidth tended toward infinity, led to the proposal and investigation of systems that are more satisfactory in terms of the similarity between the mass matrices of the two systems. A theoretical and numerical study was made of systems having from one to ten degrees of freedom, with localized and distributed cubic stiffness nonlinearities. ESA

N92-28961# Wright Lab., Wright-Patterson AFB, OH.
VHDL AND WAVES DESCRIPTIONS FOR A PSEUDO-RANDOM PATTERN GENERATOR Final Report, 5 Apr. - 28 Oct. 1991
Karen M. Serafino and Michael A. Dukes Jan. 1992 44 p
(AF Proj. 6096)
(AD-A247891; WL-TR-91-5037) Avail: NTIS HC/MF A03

A VHDL model for a 32-bit linear feedback shift register is documented, along with a WAVES dataset that provides test vectors for it. The register operates with a leading-edge dual clock, an asynchronous reset, and control bits to enable shifting (to the right) and loading. Other inputs are a polynomial and a seed value; the output is a bit pattern. The feedback feature is controlled by the polynomial. For each polynomial bit position with a value of '1', the value of the register corresponding to that is fed through feedback before being shifted. The WAVES dataset is used to generate input test vectors for the register, and to provide a utility to compare actual outputs to predicted outputs. There are three different architectures for the register: structural behavioral, and structural with multiple component instantiations produced by the VHDL generate statement. There are also two architectures for the test bench: one that uses the WAVES dataset, and one that produces input vectors internally. The WAVES test bench uses a built-in utility to check outputs from each of the three register architectures against each other, and the non-WAVES test bench does these checks internally. GRA

66 SYSTEMS ANALYSIS

Includes mathematical modeling; network analysis; and operations research.

N92-28313# Prins Maurits Lab. TNO, Rijswijk (Netherlands).
OPTIMALIZATION OF GRENADES WITH PRE-FORMED FRAGMENTS AGAINST AIR-TARGETS, PART 2 Thesis - Koninklijk Inst. voor de Marine Final Report [OPTIMALISATIE VAN GRANATEN MET VOORGEVORMDE SCHERVEN TEGEN LUCHTDOELEN (DEEL 2)]
A. P. Wildenberg May 1990 69 p In DUTCH
(Contract A85/KM/118)
(PML-1990-24-Pt-2; TD-90-1700-Pt-2; ETN-92-98303) Avail: Prins Maurits Lab. TNO, P.O. Box 45, 2280 AA Rijswijk ZH, Netherlands

Experiments and simulations were performed to improve the knowledge of the behavior of prefragmented shells. Based upon the 76 mm DIEHL grenade four types of model shells were defined. The effectiveness of these shells was experimentally checked, and the results were compared with those of simulations. The results of this comparison are discussed and evaluated in order to find the optimum shell types Author

67 THEORETICAL MATHEMATICS

Includes topology and number theory.

N92-28672*# National Aeronautics and Space Administration. Ames Research Center, Moffett Field, CA.
A DISCRETE FOURIER TRANSFORM FOR VIRTUAL MEMORY MACHINES
David C. Galant Mar. 1992 29 p
(RTOP 506-59-31)
(NASA-TM-103914; A-92048; NAS 1.15:103914) Avail: NTIS HC/MF A03

An algebraic theory of the Discrete Fourier Transform is developed in great detail. Examination of the details of the theory leads to a computationally efficient fast Fourier transform for the use on computers with virtual memory. Such an algorithm is of great use on modern desktop machines. A FORTRAN coded version of the algorithm is given for the case when the sequence of numbers to be transformed is a power of two. Author

N92-28927# Carnegie-Mellon Univ., Pittsburgh, PA. Graduate School of Industrial Administration.
DECOMPOSITION OF BALANCED MATRICES. PART 1: INTRODUCTION
Michele Conforti (Padua Univ., Italy), Gerard Cornuejols, and M. R. Rao (New York Univ., New York.) Oct. 1991 30 p
(Grants NSF DDM-89-01495; NSF DDM-88-00281; NSF DDM-90-01705)
(AD-A247397; MSRR-569) Avail: NTIS HC/MF A03

This study concerns 0,1 matrices that do not contain a square submatrix of odd order with two ones per row and per column. Such matrices are called balanced. They were first introduced by

Berge and we summarize here their relevance in combinatorial optimization. GRA

N92-28928# Carnegie-Mellon Univ., Pittsburgh, PA. Graduate School of Industrial Administration.
DECOMPOSITION OF BALANCED MATRICES. PART 2: WHEEL-AND-PARACHUTE-FREE GRAPHS
Michele Conforti (Padua Univ., Italy), Gerard Cornuejols, and M. R. Rao (New York Univ., New York.) Oct. 1991 12 p
(Grants NSF DDM-89-01495; NSF DDM-88-00281; NSF DDM-90-01705)
(AD-A247398; MSRR-570) Avail: NTIS HC/MF A03

The authors consider bipartite graphs G containing neither a wheel nor a parachute. These bipartite graphs are said to be WP-free. It is proven that is G is a WP-free bipartite graph, which is signable to be balanced and contains a cycle with a unique chord, then G contains a strong 2-join. This shows that if G is a WP-free balanced bipartite graph which is not strongly balanced, then G contains a strong 2-join. H.A.

N92-28929# Carnegie-Mellon Univ., Pittsburgh, PA. Graduate School of Industrial Administration.
DECOMPOSITION OF BALANCED MATRICES. PART 6: EVEN WHEELS
Michele Conforti (Padua Univ., Italy), Gerard Cornuejols, and M. R. Rao (New York Univ., New York.) Oct. 1991 26 p
(Grants NSF DDM-89-01495; NSF DDM-88-00281; NSF DDM-90-01705)
(AD-A247399; MSRR-574) Avail: NTIS HC/MF A03

In this part, we prove that if a balanced bipartite graph G contains an even wheel as an induced subgraph, then it has an extended star cutset. The proof is divided into two parts, treated in Sections 2 and 3 respectively. In Section 2, we give properties of the strongly adjacent nodes to even wheels. In particular, for an even wheel (W,v) with the smallest number of spokes and, subject to this, the smallest number of nodes, we prove that at least two nodes of W, say w sub 1 and w sub 2, are adjacent to all nodes with more than two neighbors in W. In Section 3, we prove that, for the above choice of W and an appropriate choice of v, the nodes with more than two neighbors in W together with the nodes of N(v) form an extended star cutset of G. GRA

N92-28930# Carnegie-Mellon Univ., Pittsburgh, PA. Graduate School of Industrial Administration.
DECOMPOSITION OF BALANCED MATRICES. PART 7: A POLYNOMIAL RECOGNITION ALGORITHM
Michele Conforti (Padua Univ., Italy), Gerard Cornuejols, and M. R. Rao (New York Univ., New York.) Oct. 1991 25 p
(Grants NSF DDM-89-01495; NSF DDM-88-00281; NSF DDM-90-01705)
(AD-A247400; MSRR-575) Avail: NTIS HC/MF A03

In this seven part paper, we prove the following theorem: At least one of the following alternatives occurs for a bipartite graph G: (1) The graph G has no cycle of length $4k + 2$; (2) The graph G has a chordless cycle of length $4k + 2$, (3)There exist two complete bipartite graphs K(sub 1), K(sub 2) in G having disjoint node sets, with the property that the removal of the edges in K(sub 1), K(sub 2) disconnects G; and (4) There exists a subset S of the nodes of G with the property that the removal of S disconnects G, where S can be partitioned into three disjoint sets T, A, N. GRA

70 PHYSICS (GENERAL)

For precision time and time interval (PTTI) see *35 Instrumentation and Photography;* for geophysics, astrophysics or solar physics see *46 Geophysics, 90 Astrophysics,* or *92 Solar Physics.*

N92-28238# Naval Research Lab., Washington, DC.
A GENERALIZATION OF THE K-V EQUILIBRIUM FOR AN INTENSE, RELATIVISTIC BEAM PROPAGATING IN A SOLENOID
S. Slinker, G. Joyce, J. Krall, and M. Lampe 25 Feb. 1992 23 p
(AD-A247067; NRL-MR-6922) Avail: NTIS HC/MF A03

A generalization of the Kapchinskij-Vladimirskij (K-V) equilibrium for an electron beam in a solenoid is derived by keeping higher order terms in an expansion of a Vlasov equilibrium. The radial profile of the charge density increases with r, whereas the radial profile of the K-V is flat. Space charge depression effects, the shear in longitudinal momentum and the self-induced longitudinal diamagnetic field are included. Numerical simulations of the beam transport in the Spiral Line Induction Accelerator (SLIA) illustrate the results. GRA

N92-28363# National Academy of Sciences - National Research Council, Washington, DC. Inst. of Medicine.
RESPONSIBLE SCIENCE: ENSURING THE INTEGRITY OF THE RESEARCH PROCESS, VOLUME 1
1992 216 p
(ISBN-0-309-04731-5; LC-92-10780) Avail: NTIS HC/MF A10

This report thoughtfully examines the challenges posed in ensuring that the search for truth reflects adherence to ethical standards. In recent years, we have learned, sometimes painfully, that not all scientists adhere to this obligation. Reports of falsified research results and plagiarism involving both junior and senior scientists have stimulated doubts and criticism about the ways in which misconduct in science is addressed by the research community. Misconduct in science is now being publicly examined in all of its aspects; how misconduct is defined, the process by which misconduct is discovered, and procedures for judging innocence or guilt and assessing penalties. Also being explored are the appropriate roles of individuals, research institutions, journals, government research agencies, and the legal system. Issues of misconduct and integrity in science present complex questions. These issues require the sustained attention of all members of the research community as well as of leaders in the public and private sector who are concerned with safeguarding the health of science. In this regard ensuring the integrity of the research process is similar to assuring safety in the workplace: it is a process that requires continued participation from all levels of the entire research enterprise--the practitioners, the host institutions, the sponsors in government, and the legislators who provide the funds. Author

N92-28400# Naval Research Lab., Washington, DC.
ANGULAR MOMENTUM: CAN BE USED IN BALLISTIC TRACKING Summary Report
R. L. Kolbe 5 Mar. 1992 15 p Sponsored by ONR
(AD-A247722; NRL/MR/4440-92-6952) Avail: NTIS HC/MF A03

The correlation and tracking problem for ballistic objects is a major concern for the Strategic Defense Initiative (SDI). In this report, the use of angular momentum for gating and assignment of reports and tracks of ballistic objects is proposed. The various errors and appropriate statistical tests that could be used on angular momentum to potentially improve the tracking and correlation, multi-track hypothesis, and Kalman filters are studied. The investigation is performed in earth centered inertial Cartesian coordinates for position, velocity, and acceleration in tracking, gating, and assignment. A discussion is given of a brief investigation, the theory developed, the results of a numerical test, and the conclusions. GRA

N92-29130* National Aeronautics and Space Administration. Pasadena Office, CA.
PRECISION MEASUREMENT OF MAGNETIC CHARACTERISTICS OF AN ARTICLE WITH NULLIFICATION OF EXTERNAL MAGNETIC FIELDS Patent
Shawn B. Honess, inventor (to NASA) (Jet Propulsion Lab., California Inst. of Tech., Pasadena.), Pablo Narvaez, inventor (to NASA) (Jet Propulsion Lab., California Inst. of Tech., Pasadena.), and James M. McAuley, inventor (to NASA) (Jet Propulsion Lab., California Inst. of Tech., Pasadena.) 30 Jun. 1992 14 p Filed 27 Nov. 1990
(NASA-Case-NPO-18187-1-CU; US-Patent-5,126,669; US-Patent-Appl-SN-618789; US-Patent-Class-324-261; US-Patent-Class-324-244; US-Patent-Class-324-205; US-Patent-Class-361-148; US-Patent-Class-361-149; US-Patent-Class-361-267; Int-Patent-Class-G01N-27/72) Avail: US Patent and Trademark Office

An apparatus for characterizing the magnetic field of a device under test is discussed. The apparatus is comprised of five separate devices: (1) a device for nullifying the ambient magnetic fields in a test environment area with a constant applied magnetic field; (2) a device for rotating the device under test in the test environment area; (3) a device for sensing the magnetic field (to obtain a profile of the magnetic field) at a sensor location which is along the circumference of rotation; (4) a memory for storing the profiles; and (5) a processor coupled to the memory for characterizing the magnetic field of the device from the magnetic field profiles thus obtained.
Official Gazette of the U.S. Patent and Trademark Office

71 ACOUSTICS

Includes sound generation, transmission and attenuation. For noise pollution see *45 Environmental Pollution*.

N92-28292# Army Construction Engineering Research Lab., Champaign, IL.
OPERATIONAL NOISE DATA FOR OH-58D ARMY HELICOPTERS Final Report
L. J. Benson, Micheal J. White, and Kevin J. Murphy Jan. 1992 57 p
(AD-A246822; CERL-N-92/07) Avail: NTIS HC/MF A04

The Army needs helicopter noise source emission data for use in the Installation Compatible Use Zone (ICUZ) program and for environmental assessments. This research gathered noise source emission data for the OH-58D helicopter. The data were normalized to 250 ft for use in noise maps. The data were also used to develop sound exposure level (SEL) versus distance curves for comparison with other helicopter data. The data show that the A-weighted maximum noise level increases with airspeed for level flight, but the A weighted SEL increases only slightly. The highest A-weighted maximum level was produced by the out-of-ground effect hover. Landings produce the largest A-weighted SEL.
GRA

N92-28302# Army Engineer Waterways Experiment Station, Vicksburg, MS. Environmental Lab.
PASSIVE ACOUSTIC RANGE ESTIMATION OF HELICOPTERS Final Report
Reo Olson and Daniel H. Cress Feb. 1992 80 p
(AD-A248033; WES/TR/EL-92-13) Avail: NTIS HC/MF A05

A passive acoustic method is presented that determines the velocity of a moving helicopter and its range at the closest point of approach. This method requires only the use of a single microphone if the fundamental blade rotation frequency of the helicopter is known, or two spatially separated microphones if it is not. The blade rotation frequency is generally adequately known after the helicopter is correctly classified using acoustic signature characteristics other than those discussed herein. The range estimate is considered valid for ranges of a few hundred meters with the attendant assumptions that: (1) the helicopter is traveling in a straight line, (2) the helicopter is moving at a constant velocity, and (3) the main rotor of the helicopter has a stable revolution rate typical of present operational helicopters. The technique was successfully tested on an example helicopter.
GRA

N92-28314# Norwegian Defence Research Establishment, Kjeller.
SIMULATION OF THE PROPAGATION OF ACOUSTICAL WAVES THROUGH AN INTERFACE SEPARATING A COMPRESSIBLE FLUID AND AN ELASTIC MEDIUM
Oeyvind Andreassen and Ivar Lie 13 Nov. 1991 45 p
(FFI-91/7017; ISSN-0802-2437; ETN-92-91241) Avail: NTIS HC/MF A03

A strategy for numerical simulation of wave propagation through an interface separating two media, water and ocean bottom, is carried out using spectral collocation. The propagation of acoustical waves in water is modeled by the Euler equations applied to a stratified fluid, while the elastic waves are modeled by the equations of elasticity. The transmission of the waves through the interface is managed through physical boundary conditions, continuous normal velocity component and normal stress, implemented by aid of characteristic boundary conditions. Domain decomposition procedures are used to solve the equations in each of the two physically different domains and to match the solutions at the boundary. At the interface modeling the ocean surface, free boundary conditions are used. The conditions at the lower and vertical boundaries are constructed to give free transmission of the wave modes, making no influence on the wave propagation. Some test cases are discussed, the simplest based upon a plane interface, the second with a piecewise linear interface made up of a horizontal and an inclined part.
ESA

N92-28324# Naval Oceanographic and Atmospheric Research Lab., Bay Saint Louis, MS.
UNDER-ICE BROADBAND TRANSIENT MEASUREMENTS AND PROCESSING Final Report
Roger W. Meredith Jan. 1992 26 p
(AD-A248609; NOARL-15) Avail: NTIS HC/MF A03

This report examines the horizontal spatial coherence of broadband acoustic energy in the frequency range 100-1200 Hz from explosive sources under the ice pack. The data were recorded on four hydrophone pairs with a nominal sensor separation of 370 m from source ranges from 3 to 25 km. Mean-square coherence is computed separately for the direct and ice-reflected propagation paths, and octaveband frequency averaging reduces variability inherent in the coherence estimation associated with explosive acoustic sources. Coherence varies significantly with sensor depth, range, and frequency. Background noise coherence is also examined briefly. Changes in coherence because of under-ice reflection are smallest for the 100-200 Hz octave band, but the change may be as high as 50 percent for the higher frequency bands.
GRA

N92-28364# Materials Research Labs., Ascot Vale (Australia).
ULTRASONIC AMBIENT NOISE IN AUSTRALIAN SHALLOW WATERS AT FREQUENCIES UP TO 200 kHz
Douglas H. Cato and Michael J. Bell Feb. 1992 27 p
(MRL-TR-91-23; AR-006-376) Avail: NTIS HC/MF A03

Little is known of ambient noise in the ocean at frequencies above 50 kHz and there are few measurements above 20 kHz. The results of this study indicate that the sustained ambient noise at frequencies up to 200 kHz in temperate and tropical waters of depths less than about 60 m is characterized by the numerous sharp transient sound of snapping shrimps. These transients have pulse widths of typically 3 to 8 micro-s (at one-third the peak voltage) and their bandwidth extends to well in excess of 200 kHz. Large variations in shrimp noise are to be expected over relatively short distances (hundreds of meters) as habitats change and hence shrimp numbers vary. Highest noise levels are to expected near the bottom and where there are coral or rock outcrops, shells, sponges or debris to provide shelter for shrimps. Noise measured under these conditions exceeded a peak level of 140 dB re 1 micro-Pa(exp 2) at an average of about 20 pulses per second and exceeded 150 dB re 1 micro-Pa(exp 2) at an

average of 3 to 4 pulses a second. Lowest noise levels have been observed over uncluttered mud or sand. Shrimp noise shows little diurnal or seasonal variation. Author

N92-28409# Naval Postgraduate School, Monterey, CA.
ADAPTIVE NOISE CANCELLATION APPLIED TO THE NUWES TEST RANGES M.S. Thesis
Dale W. Herdegen Dec. 1991 80 p
(AD-A245961) Avail: NTIS HC/MF A05

This thesis investigates the application of adaptive filtering at the NUWES test ranges. Two adaptive algorithms, least-mean-squares and recursive-least-squares, are studied. To facilitate the investigation, a model of the test ranges was developed. This model accounts for spherical spreading and linear attenuation of the propagated acoustic signals as well as the effects of Doppler shift, multipath, and finite propagation delay time. After describing the model, the adaptive filtering algorithms are briefly explained. Then, two schemes of adaptive filtering, adaptive noise cancellation and adaptive line enhancement, are applied to the model. Simulation results of the noise cancellation and line enhancement schemes are presented for several scenarios. GRA

N92-28413# Naval Air Development Center, Warminster, PA. Mission Avionics Technology Dept.
FUNDAMENTAL NOISE LIMITS IN MINIATURE ACOUSTIC AND VIBRATION SENSORS
Thomas B. Gabrielson 31 Dec. 1991 100 p
(AD-A247016; NADC-91113-50) Avail: NTIS HC/MF A05

Conventional noise analysis for acoustic and vibration sensors has focused either on the ambient noise floor imposed by the environment or the electrical noise floor imposed by the preamplifier. Microminiature sensors are, however, particularly sensitive to thermal (molecular) agitation because of their small moving parts. This mechanical-thermal noise can easily dominate the noise performance of these sensors. The purposes of this report are to review the fundamental noise sources in a sensor system and to illustrate the importance of noise sources intrinsic to the sensor's design. In particular, thermal noise, shot noise, 1/f noise, and amplifier noise components are discussed as they relate to the sensor system. GRA

N92-28556*# McDonnell-Douglas Corp., Long Beach, CA.
EVALUATION OF OUTDOOR-TO-INDOOR RESPONSE TO MINIMIZED SONIC BOOMS
David Brown and Louis C. Sutherland Jun. 1992 42 p Presented at the First Annual High-Speed Research Workshop, Williamsburg, VA, 14-16 May 1991 Prepared in cooperation with Wyle Labs., Inc., El Segundo, CA
(Contract NAS1-19060; RTOP 537-03-21-03)
(NASA-CR-189643; NAS 1.26:189643; Wyle-TN-91-8) Avail: NTIS HC/MF A03

Various studies were conducted by NASA and others on the practical limitations of sonic boom signature shaping/minimization for the High-Speed Civil Transport (HSCT) and on the effects of these shaped boom signatures on perceived loudness. This current effort is a further part of this research with emphasis on examining shaped boom signatures which are representative of the most recent investigations of practical limitations on sonic boom minimization, and on examining and comparing the expected response to these signatures when experienced indoors and outdoors. Author

N92-28559# Naval Postgraduate School, Monterey, CA.
IMAGE PROCESSING TECHNIQUES FOR ACOUSTIC IMAGES M.S. Thesis
Brian P. Murphy Jun. 1991 77 p
(AD-A247303) Avail: NTIS HC/MF A05

The primary goal of this research is to test the effectiveness of various image processing techniques applied to acoustic images generated in MATLAB. The simulated acoustic images have the same characteristics as those generated by a computer model of a high resolution imaging sonar. Edge detection and segmentation are the two image processing techniques discussed in this study. The two methods tested are a modified version of the Kalman filtering and median filtering. GRA

N92-28695# National Aerospace Lab., Amsterdam (Netherlands). Fluid Dynamics Div.
EXPERIMENTAL VALIDATION OF A LINE-DUCT ACOUSTICS MODEL INCLUDING FLOW
E. R. Rademaker 25 Jun. 1990 14 p Presented at ASME Conference on Duct Acoustics, Dallas, TX, Nov. 1990
(Contract NIVR-01803-N)
(NLR-TP-90223-U; ETN-92-91541) Avail: NTIS HC/MF A03

In the spinning mode synthesizer which was coupled to the flow nozzle of the small anechoic wind tunnel, an experimental program for the validation of a theoretical duct acoustics model was carried out. This model, LINDA, calculates the sound propagation in a cylindrical flow duct of finite length, which includes an acoustically lined section between two hard walled sections. Measurements of the circumferential and radial acoustic pressure distribution downstream and upstream of the lined sections, and of the radial distribution halfway of a lined section were made with flow at several frequencies and acoustic mode adjustments. From these measurements, quantities which characterize the net damping attained by the liners (the insertion loss and transmission loss) were derived. These values and the radial distribution of the transmitted field are compared with the theoretical results. The agreeement is good (plus or minus 1dB). ESA

N92-28722*# Florida Atlantic Univ., Boca Raton. Dept. of Ocean Engineering.
MOBILITY POWER FLOW ANALYSIS OF COUPLED PLATE STRUCTURE SUBJECTED TO MECHANICAL AND ACOUSTIC EXCITATION Final Report
J. M. Cuschieri Jun. 1992 42 p
(Grants NAG1-685; NAG1-1077; RTOP 505-63-36-05)
(NASA-CR-189635; NAS 1.26:189635) Avail: NTIS HC/MF A03

The mobility power flow approach that was previously applied in the derivation of expressions for the vibrational power flow between coupled plate substructures forming an L configuration and subjected to mechanical loading is generalized. Using the generalized expressions, both point and distributed mechanical loads on one or both of the plates can be considered. The generalized approach is extended to deal with acoustic excitation of one of the plate substructures. In this case, the forces (acoustic pressures) acting on the structure are dependent on the response of the structure because of the scattered pressure component. The interaction between the plate structure and the acoustic fluid leads to the derivation of a corrected mode shape for the plates' normal surface velocity and also for the structure mobility functions. The determination of the scattered pressure components in the expressions for the power flow represents an additional component in the power flow balance for the source plate and the receiver plate. This component represents the radiated acoustical power from the plate structure. For a number of coupled plate substrates, the acoustic pressure generated by one substructure will interact with the motion of another substructure. That is, in the case of the L-shaped plate, acoustic interaction exists between the two plate substructures due to the generation of the acoustic waves by each of the substructures. An approach to deal with this phenomena is described. Author

N92-28889# Connecticut Univ., Farmington. Health Center.
MONAURAL AND BINAURAL PROCESSING OF COMPLEX WAVEFORMS Final Report, 1 Nov. 1988 - 31 Oct. 1991
Constantine Trahiotis and Leslie R. Bernstein 5 Jan. 1992 12 p
(Grant AF-AFOSR-0030-89)
(AD-A247199; AFOSR-92-0116TR) Avail: NTIS HC/MF A03

Our research concerned the manners by which the monaural and binaural auditory systems process information in complex sounds. Substantial progress was made in three areas, consistent with the ojectives outlined in the original proposal. (1) New electronic equipment, including a NeXT computer was purchased,

installed and interfaced with the existing laboratory. Software was developed for generating the necessary complex digital stimuli and for running behavioral experiments utilizing those stimuli. (2) Monaural experiments showed that the CMR is not obtained successively and is reduced or non-existent when the flanking bands are pulsed rather than presented continuously. Binaural investigations revealed that the detectability of a tonal target in a masking level difference paradigm could be degraded by the presence of a spectrally remote interfering tone. (3) In collaboration with Dr. Richard Stern, theoretical efforts included the explication and evaluation of a weighted-image model of binaural hearing, attempts to extend the Stern-Colburn position-variable model to account for many crucial lateralization and localization data gathered over the past 50 years, and the continuation of efforts to incorporate into a general model notions that lateralization and localization of spectrally-rich stimuli depend upon the patterns of neural activity within a plane defined by frequency and interaural delay. GRA

N92-28909*# National Aeronautics and Space Administration. Ames Research Center, Moffett Field, CA.

THE DESIGN OF TEST-SECTION INSERTS FOR HIGHER SPEED AEROACOUSTIC TESTING IN THE AMES 80- BY 120-FOOT WIND TUNNEL

Paul T. Soderman and Larry E. Olson Jan. 1992 13 p Proposed for presentation at the DGLR/AIAA 14th Aeroacoustics Conference, Aachen, Germany, 11-14 May 1992

(RTOP 505-59-52)

(NASA-TM-103915; A-92052; NAS 1.15:103915) Avail: NTIS HC/MF A03

An engineering feasibility study was made of aeroacoustic inserts designed for large-scale acoustic research on aircraft models in the 80- by 120-Foot Wind Tunnel at NASA Ames Research Center. The goal was to find test-section modifications that would allow improved aeroacoustic testing at airspeeds equal to and above the current 100 knots limit. Results indicate that the required maximum airspeed drives the design of a particular insert. Using goals of 200, 150, and 100 knots airspeed, the analysis led to a 30 x 60 ft open-jet test section, a 40 x 80 ft open-jet test section, and a 70 x 110 ft closed test section with enhanced wall lining respectively. The open-jet inserts would be composed of a nozzle, collector, diffuser, and acoustic wedges incorporated in the existing 80 x 120 ft test section. The closed test section would be composed of approximately 5-ft acoustic wedges covered by a porous plate attached to the test-section walls of the existing 80 x 120. All designs would require a double row of acoustic vanes between the test section and fan drive to attenuate fan noise and, in the case of the open-jet designs, to control flow separation at the diffuser downstream end. The inserts would allow virtually anechoic acoustics studies of large helicopter models, jets, and V/STOL aircraft models in simulated flight. Model scale studies would be necessary to optimize the aerodynamic and acoustic performance of any of the designs. Successful development of acoustically transparent walls, though not strictly necessary to the project, would lead to a porous-wall test section that could be substituted for any of the open-jet designs, and thereby eliminate many aerodynamic and acoustic problems characteristic of open-jet shear layers. Author

N92-28984*# National Aeronautics and Space Administration. Lewis Research Center, Cleveland, OH.

MODAL ELEMENT METHOD FOR SCATTERING OF SOUND BY ABSORBING BODIES

Kenneth J. Baumeister and Kevin L. Kreider (Akron Univ., OH.) 1992 14 p Proposed for presentation at the ASME Winter Annual Meeting, Anaheim, CA, 8-13 Nov. 1992

(RTOP 505-62-52)

(NASA-TM-105722; E-7126; NAS 1.15:105722) Avail: NTIS HC/MF A03

The modal element method for acoustic scattering from 2-D body is presented. The body may be acoustically soft (absorbing) or hard (reflecting). The infinite computational region is divided into two subdomains - the bounded finite element domain, which is characterized by complicated geometry and/or variable material properties, and the surrounding unbounded homogeneous domain. The acoustic pressure field is represented approximately in the finite element domain by a finite element solution, and is represented analytically by an eigenfunction expansion in the homogeneous domain. The two solutions are coupled by the continuity of pressure and velocity across the interface between the two subdomains. Also, for hard bodies, a compact modal ring grid system is introduced for which computing requirements are drastically reduced. Analysis for 2-D scattering from solid and coated (acoustically treated) bodies is presented, and several simple numerical examples are discussed. In addition, criteria are presented for determining the number of modes to accurately resolve the scattered pressure field from a solid cylinder as a function of the frequency of the incoming wave and the radius of the cylinder. Author

N92-29196*# Virginia Polytechnic Inst. and State Univ., Blacksburg.

DETECTION OF IN-PLANE DISPLACEMENTS OF ACOUSTIC WAVE FIELDS USING EXTRINSIC FIZEAU FIBER INTERFEROMETRIC SENSORS

R. Dhawan, M. F. Gunther, and R. O. Claus 1991 4 p

(Grant NAG1-1348)

(NASA-CR-190493; NAS 1.26:190493) Avail: NTIS HC/MF A01

Quantitative measurements of the in-plane particle displacement components of ultrasonic surface acoustic wave fields using extrinsic Fizeau fiber interferometric (EFFI) sensors are reported. Wave propagation in materials and the fiber sensor elements are briefly discussed. Calibrated experimental results obtained for simulated acoustic emission events on homogeneous metal test specimens are reported and compared to previous results obtained using piezoelectric transducers. Author

N92-29201# Cambridge Univ. (England). Dept. of Engineering.

BOUNDARY LAYER INDUCED NOISE IN AIRCRAFT

W. R. Graham May 1992 345 p

(ISSN-0309-7293; CUED/A-Aero/TR-18) Avail: NTIS HC/MF A15

The aim of this research is to investigate ways of controlling boundary layer induced noise at the design stage, as the problem is much harder to treat after it has become apparent. In order to achieve this, it is essential to be able to model the noise generation process successfully, preferably in such a way that our physical understanding of the problem is enhanced, since without this understanding the formulation of general design guidelines is almost impossible. At present, although a large body of research germane to the problem exists, there is no such model, and the development of one is, thus, the first requirement of this work. Once the model is complete and validated, the question of noise limitation may be addressed. The reduction of the boundary layer induced noise problem in aircraft to an initial model problem, which may be formulated in general terms, and the subsequent further approximations that may be made to achieve a form simple enough to facilitate understanding of the results while retaining the necessary features of the problem are described. Author

N92-29203# Southampton Univ. (England). Audiology and Human Effects Group.

ANNOYANCE DUE TO DISCRETE TONES IN BROADBAND BACKGROUND NOISE. PART 2: ANALYSIS

D. W. Robinson Apr. 1992 72 p Sponsored by Dept. of the Environment

(ISVR-TR-202-Pt-2) Copyright Avail: NTIS HC/MF A04

A series of subjective tests of annoyance of tonal noises was described in a companion report (Robinson and Wright, 1991). Each stimulus consisted of a pure tone superimposed on a broadband noise. The present report analyses the results and derives from them a general algebraic formula accommodating all the variables (frequency and sensation level of the tonal component, level and spectrum shape of the broadband component). Annoyance of each tone/noise combination was determined as an overall tone penalty, that is, the equivalent

increment in decibels of the broadband component alone which was required to match the annoyance of the combination. These increments varied with the parameters of the stimuli in a complicated manner. Heuristic means revealed and underlying pattern of comparative simplicity: the overall tone penalty consists of the sum of two terms. The first term is a constant sub-multiple of the A-weighted level increase caused by adding the tonal component to the broadband noise and appears to be related to the corresponding increase of loudness level in phons. The second term is a multiple product of non-interactive factors expressing the dependence on the four parameters of the signal. The tone-frequency factor is given as a polynomial in log frequency. Sensation level appears directly in the formula as a proportionality factor; its magnitude has to be derived from the difference between the sound pressure level of the tone and that of the 1/3-octave band of the broadband component embracing the tone frequency, together with a detection ratio in decibels which is given as a quadratic function of frequency. The factor for broadband noise level is a negative exponential of level, falling by 22 percent for each 10 dB(A) increase in level. Finally, spectrum shape is accommodated by an empirical function which is linear in the difference between the C and A weighted sound pressure levels of the broadband noise. The algebraic formula reproduces the experimental data to a good accuracy (root-mean-square deviation 1.2 dB). Most of the residual deviation is implicit in the experimental uncertainties of the input data. The range of applicability of the formula is specified; it embraces a wide range of each variable but is, of course, limited to cases with single tones or, at least, to those where one tone is dominant. Author

72 ATOMIC AND MOLECULAR PHYSICS

Includes atomic structure, electron properties, and molecular spectra.

N92-28259# United Technologies Research Center, East Hartford, CT.

THEORETICAL STUDIES OF THE ELECTRONIC AND RESONANCE STRUCTURE OF ATOMIC AND MOLECULAR NEGATIVE IONS Final Technical Report, 15 Nov. 1988 - 15 Nov. 1991

Michels H. Harvey Jan. 1992 78 p
(Contract F49620-89-C-0019)
(AD-A247093; R92-928101; AFOSR-92-0016TR) Avail: NTIS HC/MF A05

This technical program constitutes a theoretical research investigation of the electronic structure of atomic and molecular ions and of radiative and collisional processes describing their formation and/or destruction. This study is directed toward elucidating the structure of both thermodynamically stable cations and anions, and resonance or metastable excited states in such systems. In addition, this study will include an analysis of the effects of both static E-fields and time dependent laser fields on resonance excitation, stimulated autodetachment and radiative electron attachment processes in negative ion systems and ion-pair production in Rydberg atom collisions. The goals of this research program are to develop accurate computational techniques which are applicable to studies of the electronic structure and radiative properties of small atomic and molecular ions and to carry out detailed calculations of the structure of several prototype species, including light element alkalis, alkaline earths and the noble gases. It is anticipated that the results of this program will furnish fundamental data and provide a better understanding of several detailed experimental studies that are currently in progress in this area, including work at SRI and ORNL. Areas of application of this research work include thermonuclear reactor programs, neutral and negative ion particle beam source development, high current switching devices and discharge plasma devices. GRA

N92-28260# Tennessee Univ., Knoxville. Dept. of Chemistry.

MOLECULAR DYNAMICS CALCULATIONS OF OPTICAL NONLINEAR PROPERTIES OF MATERIALS Final Report, 1 Oct. 1988 - 30 Sep. 1991

J. E. Bloor 20 Dec. 1991 62 p
(Contract N00019-88-C-0174)
(AD-A247095) Avail: NTIS HC/MF A04

The conductivity and nonlinear optical properties of small molecules beginning with the water molecule and further developed for hydrides and simple polymer molecules, including metal-ion containing polymers, are predicted based on ab initio techniques. These calculations are extended to the prediction, understanding, and improved design of polymer molecules for enhanced or controlled nonlinear properties. Specific predictions are provided for dipole polarizabilities and the first and second hyperpolarizabilities for small molecules. GRA

N92-28310# Los Alamos National Lab., NM.

EVIDENCE FOR PHYSICS BEYOND THE QUASI-DEUTERON MODEL IN PION ABSORPTION

C. L. Morris, J. D. Zumbro, R. D. Ransome (Rutgers Univ., Piscataway, NJ.), B. G. Ritchie (Arizona State Univ., Tempe.), D. L. Watson (York Univ., England), and C. Fred Moore (Texas Univ., Austin.) 1991 10 p Presented at the International Workshop on Pions in Nuclei, Penyscola (Spain), 2-9 Jun. 1991
(Contract W-7405-eng-36)
(DE92-011285; LA-UR-92-751; CONF-9106194-8) Avail: NTIS HC/MF A02

Cross sections for pion absorption of T(sub pi) = 100 MeV on a range of nuclei leading to two or more energetic protons are presented. A large fraction of the total absorption cross section leads to events with large missing energies, presumably to neutrals. A comparison of the fraction of the total absorption cross section which appears to be the result of an undisturbed two-body mechanism with predictions of a simple semi-classical model of the attenuation of protons through final-state interactions leads to the conclusion that most of the absorption cross section on heavy nuclei is not due to a two-body absorption mechanism followed by final-state interactions but must be the result of pion absorption on three or more nucleons. DOE

N92-28337# Continuous Electron Beam Accelerator Facility, Newport New, VA.

ELECTROPRODUCTION OF LIGHT QUARK BARYONS

V. D. Burkert 1991 44 p Presented at the Workshop on Baryon Spectroscopy and the Structure of the Nucleon, Saclay, France, 23-25 Sep. 1991
(Contract DE-AC02-83ER-40105)
(DE92-010853; DOE/ER-40105/181; CEBAF-PR-92-001; CONF-9109127-1) Avail: NTIS HC/MF A03

The status of electromagnetic excitation of light quark (u, d) baryon states is reviewed and confronted with results of calculations within the framework of microscopic models of the baryon structure and the photon-baryon coupling. Prospects for a qualitative improvement of our knowledge in this sector using photon and electron beams at the new, intermediate energy continuous wave electron machines are discussed. DOE

N92-28414# SRI International Corp., Menlo Park, CA.

EXCITED NEGATIVE IONS AND MOLECULES AND NEGATIVE ION PRODUCTION Final Report, 15 Nov. 1988 - 14 Nov. 1991

James R. Peterson Jan. 1992 63 p
(Contract F49620-89-K-0002)
(AD-A247017; AFOSR-92-0011TR) Avail: NTIS HC/MF A04

Research has been performed to determine fundamental properties of negative ions; decay mechanisms and products of molecular Rydberg states; and mechanisms affecting H(-) production in ion source discharges. Experiments were performed on both stable and metastable states of Ca(-), Cs(-), He2(-), and WO3(-); on the dissociative decay of Rydberg states of H3, D3, D2H, H2D, NeH, NeD, NH, CH, and O2; on the product states of dissociative recombination of Ar2(+) and Kr2; and on the vibrational

distribution of O2(+) resulting from the reaction O(+) + C02 yields O2(+) + CO. GRA

N92-28764# Texas A&M Univ., College Station. Cyclotron Inst.
EXCITATION OF ATOMS AND MOLECULES IN COLLISIONS WITH HIGHLY CHARGED IONS
R. L. Watson 1 Mar. 1992 6 p
(Contract DE-FG05-84ER-13262)
(DE92-012658; DOE/ER-13262/8) Avail: NTIS HC/MF A02

This report discusses research of multicharged nitrogen, oxygen and carbon monoxide molecular ions produced in collision with multicharged argon ions. Properties like ionization, dissociation, and excitation are investigated. DOE

N92-28839# Fermi National Accelerator Lab., Batavia, IL.
THE 17 keV NEUTRINO AND NEUTRINO TAGGING
R. H. Bernstein Feb. 1992 3 p Presented at the Workshop on Long-Baseline Neutrino Oscillations, Batavia, IL, 17-20 Nov. 1991
(Contract DE-AC02-76CH-03000)
(DE92-011281; FNAL/C-92/62; CONF-9111141-6) Avail: NTIS HC/MF A01

P-788 at FNAL proposed to search for neutrino oscillations in a tagged neutrino line. A K(sub L) beam and the decay modes K(sub L) yields pi(mu)nu(sub mu) and K (sub L) yields (pi)e(nu)(sub e) provides the neutrino flux. An upstream tagging spectrometer then identifies the hadron and lepton and reconstructs the K(sub L) decay; the lepton identification specifies the neutrino as nu(sub e) or nu(sub mu) and distinguishes nu from bar-nu at the decay vertex. A neutrino detector modeled after an existing deep-inelastic scattering spectrometer (rates were worked out for the CCFR apparatus) can be used to associate the K(sub L) with a neutrino interaction, measure the neutrino energy, and analyze outgoing muons. Monte Carlo studies show that 30K nu(sub e) and 20K nu(sub mu) could be obtained in two fixed target runs at the Tevatron. DOE

N92-28858# Fermi National Accelerator Lab., Batavia, IL.
THE MANY ASPECTS OF NEUTRINO PHYSICS
J. A. Frieman Jan. 1992 15 p Presented at the Many Aspects of Neutrino Physics; Workshop on Long-Baseline Neutrino Oscillations, Batavia, IL, 14-17 Nov. 1991; 17-20 Nov. 1991
(Contract DE-AC02-76CH-03000)
(DE92-011735; FNAL/C-92/26A; CONF-9111210-Summ; CONF-9111141-Summ) Avail: NTIS HC/MF A03

In mid-November, over seventy physicists gathered at Fermilab for an informal workshop on the Many Aspects of Neutrino Physics, which dovetailed with and also helped lay the groundwork for the succeeding conference on Long Baseline Neutrino Oscillations. The workshop indeed covered many of the interrelated aspects of neutrino physics: 17 keV neutrinos (experiments, theoretical models, and astrophysical constraints), neutrino properties (double beta decay experiments, neutrino magnetic moments), neutrinos from/as weakly interacting massive particles (WIMPs) in cosmology and astrophysics, atmospheric neutrinos, and solar neutrinos. In the following, I provide a brief and thoroughly biased account of only some of the many interesting developments discussed at the workshop. DOE

N92-28860# Lawrence Livermore National Lab., CA.
THE NONEQUILIBRIUM MOLECULAR DYNAMICS
W. G. Hoover Mar. 1992 14 p Presented at the International Workshop on Dynamical Fluctuations and Correlations in Nuclear Collisions, Aussois (France), 12-16 Mar. 1992
(Contract W-7405-eng-48)
(DE92-011760; UCRL-JC-110189; CONF-920318-1) Avail: NTIS HC/MF A03

Molecular dynamics is generalized in order to simulate a variety of nonequilibrium systems. This generalization was achieved by adopting microscopic mechanical definitions of macroscopic thermodynamic and hydrodynamic variables, such as temperature and stress. Some of the problems already treated include rapid plastic deformation, intense heat conduction, strong shockwaves simulation, and far-from-equilibrium phase transformations. Continuing advances in technique and in the modeling of interatomic forces, coupled with qualitative improvements in computer hardware, are enabling such simulations to approximate real-world microscale and nanoscale experiments. DOE

N92-28881# Naval Research Lab., Washington, DC.
ATOMISTIC SIMULATION OF THE NANOINDENTATION OF DIAMOND AND GRAPHITE SURFACES
J. A. Harrison, R. J. Colton, C. T. White, and D. W. Brenner Apr. 1992 11 p
(AD-A249296; NRL-TR-3) Avail: NTIS HC/MF A03

Molecular dynamics simulations which make use of a many-body analytic potential function have been used to study the nanometer-scale indentation of diamond and graphite. We find that the simulation correctly reproduces experimentally determined trends in load versus penetration data. As a result, trends in mechanical properties, e.g., Young's modulus, are also reproduced. GRA

N92-28936# Lowell Univ., MA. Center for Atmospheric Research.
CALCULATIONS AND DATABASING OF MOLECULAR ABSORPTION PARAMETERS FOR HITRAN Final Report, 30 Jun. 1989 - 30 Jun. 1991
Robert R. Gamache 25 Aug. 1991 76 p
(Contract F19628-88-K-0030)
(AD-A247549; AD-E200862; PL-TR-91-2216) Avail: NTIS HC/MF A05

Total internal partition sums of the species on the HITRAN database are presented. The development of maintenance programs and update programs for the 1991 version of the HITRAN database is given as well as the construction of the 1991 version; new data and developments are presented. The creation of new maintenance programs for updating halfwidths of O3 and H2O is discussed. Calculations are shown for the pressure broadened halfwidths of H2O and CO2 via several theoretical models. A summary of the 1991 HITRAN workshop is given with some recommendations for the future development. GRA

N92-28986*# National Aeronautics and Space Administration. Marshall Space Flight Center, Huntsville, AL.
THE EFFECT OF INDUCED CHARGES ON LOW-ENERGY PARTICLE TRAJECTORIES NEAR CONDUCTING AND SEMICONDUCTING PLATES
Victoria N. Coffey and Thomas E. Moore May 1992 23 p
(NASA-TM-103589; NAS 1.15:103589) Avail: NTIS HC/MF A03

The effect of the induced charge was found on particles less than 1 eV as they passed through simulated parallel, grounded channels that are comparable in dimension to those that are presently in space plasma instruments which measure the flux of low-energy ions. Applications were made to both conducting and semiconducting channels that ranged in length from 0.1 to 50 mm and in aspect ratio from 1 to 100. The effect of the induced charge on particle trajectories from simple straight lines. Several configurations of channel aspect ratio and detector locations are considered. The effect is important only at very low energies with small dimensions. Author

N92-29190# Oak Ridge National Lab., TN.
A USER'S MANUAL FOR MASH 1.0: A MONTE CARLO ADJOINT SHIELDING CODE SYSTEM
J. O. Johnson, ed., M. B. Emmett, W. A. Rhoades, R. L. Childs, W. H. Scott, Jr. (Science Applications International Corp., Oak Ridge, TN.), and J. A. Stoddard (Science Applications International Corp., Oak Ridge, TN.) Mar. 1992 449 p
(Contract DE-AC05-84OR-21400)
(AD-A248204; ORNL/TM-11778) Avail: NTIS HC/MF A19

The Monte Carlo Adjoint Shielding Code System, MASH, calculates neutron and gamma-ray environments and radiation protection factors for armored military vehicles, structures, trenches, and other shielding configurations by coupling a forward discrete ordinates air-overground transport calculation with an adjoint Monte

Carlo treatment of the shielding geometry. Efficiency and optimum use of computer time are emphasized. The code system includes the GRTUNCL and DORT codes for air-overground transport calculations, the MORSE code with the GIFT5 combinatorial geometry package for adjoint shielding calculations, and several peripheral codes that perform the required data preparations, transformations, and coupling functions. MASH is the successor to the Vehicle Code System (VCS) initially developed at Oak Ridge National Laboratory (ORNL). The discrete ordinates calculation determines the fluence on a coupling surface surrounding the shielding geometry due to an external neutron/gamma-ray source. The Monte Carlo calculation determines the effectiveness of the fluence at that surface in causing a response in a detector within the shielding geometry, i.e., the dose importance of the coupling surface fluence. A coupling code folds the fluence together with the dose importance, giving the desired dose response. The coupling code can determine the dose response as a function of the shielding geometry orientation relative to the source, distance from the source, and energy response of the detector. GRA

73 NUCLEAR AND HIGH-ENERGY PHYSICS

Includes elementary and nuclear particles; and reactor theory.

For space radiation see *93 Space Radiation.*

N92-28264# Nationaal Inst. voor Kernfysica en Hoge Energiefysica, Amsterdam (Netherlands).
BUNDLE DIMENSIONS AROUND THE INTERNAL TARGET AREA [BUNDELAFMETINGEN RONDOM INTERNAL TARGET AREA]
R. Maads Nov. 1991 8 p In DUTCH
(NIKHEF-K/AmPS/91-06; ETN-92-91237) Avail: NTIS HC/MF A02

The bundle dimensions in the area around the Internal Target (IT) of the accelerator AmPS (Amsterdam Pulse Stretcher) are treated with a view to the design of the hardware for the IT. The importance of the knowledge of these dimensions is discussed in case of the stretcher mode as well as the storage mode (i.e., without extraction). ESA

N92-28270# Stanford Linear Accelerator Center, CA.
ACCELERATOR SIMULATION USING COMPUTERS
M. Lee, Y. Zambre, and W. Corbett Jan. 1992 5 p Presented at the International Conference CUM Workshop on Current Trends in Data Acquisition and Control of Accelerators, Calcutta, India, 19-21 Nov. 1991
(Contracts DE-AC03-76SF-00515; DE-AC03-76SF-00098; DE-AM03-76SF-00010)
(DE92-010729; SU-SLAC-PUB-5701; CONF-9111203-1) Avail: NTIS HC/MF A01

Every accelerator or storage ring system consists of a charged particle beam propagating through a beam line. Although a number of computer programs exit that simulate the propagation of a beam in a given beam line, only a few provide the capabilities for designing, commissioning and operating the beam line. This paper shows how a 'multi-track' simulation and analysis code can be used for these applications. DOE

N92-28308# Nationaal Inst. voor Kernfysica en Hoge Energiefysica, Amsterdam (Netherlands).
INJECTION: ON-AXIS/OFF-AXIS [INJEKTIE: ON AXIS/OFF-AXIS]
R. Maas 13 Nov. 1991 6 p In DUTCH
(NIKHEF-K/AmPS/91-07; ETN-92-91238) Avail: NTIS HC/MF A02

The injection of the accelerometer AmPS (Amsterdam Pulse Stretcher) 91-06 is discussed. It is proposed to displace the local (in the horizontal plane) Closed Orbit (CO) around the injection point to the injection septum using four orbit correctors. In this way injection can occur on axis without displacing the injection septum. The uncertainty of the settings of the magnets that influence the local bump give an uncertainty in the bump parameters, although this uncertainty is smaller than the expected deviation due to misalignment effects of the whole machine. The required strength of the orbit correctors used is higher than the specifications of these elements. ESA

N92-28356# Los Alamos National Lab., NM.
THE SOLENOIDAL DETECTOR COLLABORATION SILICON DETECTOR SYSTEM
H. J. Ziock, M. T. Gamble, W. O. Miller, A. P. T. Palounek, and T. C. Thompson 1992 9 p Presented at the International Industrial Symposium on the Super Collider, New Orleans, LA, 4-6 Mar. 1992
(Contract W-7405-eng-36)
(DE92-011237; LA-UR-92-936; CONF-920331-3) Avail: NTIS HC/MF A02

Silicon tracking systems will be fundamental components of the tracking systems for both planned major SSC experiments. Despite its seemingly small size, it occupies a volume of more than 5 meters in length and 1 meter in diameter and is an order of magnitude larger than any silicon detector system previously built. This report discusses its design and operation. DOE

N92-28813# Oak Ridge National Lab., TN.
REPRESENTATION OF NEUTRON NOISE DATA USING NEURAL NETWORKS
K. Korsah, B. Damiano, and R. T. Wood 1992 9 p Presented at the 8th Power Plant Dynamics, Control and Testing Symposium, Knoxville, TN, 27-29 May 1992
(Contract DE-AC05-84OR-21400)
(DE92-013232; CONF-920538-24) Avail: NTIS HC/MF A02

This paper describes a neural network-based method of representing neutron noise spectra using a model developed at the Oak Ridge National Laboratory (ORNL). The backpropagation neural network learned to represent neutron noise data in terms of four descriptors, and the network response matched calculated values to within 3.5 percent. These preliminary results are encouraging, and further research is directed towards the application of neural networks in a diagnostics system for the identification of the causes of changes in structural spectral resonances. This work is part of our current investigation of advanced technologies such as expert systems and neural networks for neutron noise data reduction, analysis, and interpretation. The objective is to improve the state-of-the-art of noise analysis as a diagnostic tool for nuclear power plants and other mechanical systems. DOE

N92-29210# Oesterreichisches Forschungszentrum Seibersdorf G.m.b.H., Vienna. Bereich Lebenswissenschaften.
DETERMINATION OF FIELD RELATED TRANSFER FACTORS FOR Cs-137 AND Sr-90, FROM THE FALLOUT OF THE REACTOR ACCIDENT IN CHERNOBYL (USSR) [ERMITTLUNG PRAXISBEZOGENER TRANSFERFAKTOREN FUER 137CS UND 90SR AUS DEM FALLOUT DES REAKTORUNFALLES IN TSCHERNOBYL]
Christoph Artner, Martin H. Gerzabek, Othmar Horak, and Konrad Mueck May 1991 9 p Repr. from VDLUFA-Schriftenreihe 32 (Berlin, Fed. Republic of Germany, Kongressband 1990) 1990 p 881-886 In GERMAN Presented at the 102nd Verband Deutscher Landwirtschaftlicher Untersuchungs- und Forschungsanstalten 'Landwirtschaft im Spannungsfeld von Belastungsfaktoren und Gesellschaftlichen Anspruechen', Berlin, Fed. Republic of Germany, 17-22 Sep. 1990
(OEFZS-4581; ETN-92-91340) Copyright Avail: NTIS HC/MF A02

The plant ground transfer factor (TF) is defined. The resulting activity of the ground after radionuclide distribution causes a measurable absorption of both isotopes, Cs-137 and Sr-90, by the plants and allows to obtain TF in field conditions. Two hundred specimens of various plants were chosen. The corresponding ground specimens were taken from a zero to twenty centimeters ground layer. A survey of Cs-137 TF of various plants is given.

The TF's for Sr-90 are, at least, an order of magnitude higher than those for Cs-137. In most cases, the correlation between Cs-137 TF and the measured ground activity concentration is negative. The TF's obtained for Cs-137 and Sr-90 are, in general, comparable with data which were determined long before the reactor accident by various tests with artificially contaminated grounds. ESA

74 OPTICS

Includes light phenomena; and optical devices.
For lasers see *36 Lasers and Masers.*

N92-28223# Department of the Navy, Washington, DC.
THREE-AXIS FIBER OPTIC VECTOR MAGNETOMETER Patent Application
K. P. Koo, inventor (to Navy), G. H. Sigel, inventor (to Navy), and Frank Bucholtz, inventor (to Navy) 30 Sep. 1991 21 p
(AD-D015199; US-Patent-Appl-SN-767955; Navy-Case-68711)
Avail: NTIS HC/MF A03

This patent application discloses an optical fiber for magnetostrictive responsive detection of magnetic fields. The strength of the protective magnetic field is determined by standard interferometry techniques by comparing the phase or mode properties of the light from a light source exiting the fiber having a magnetostrictive jacket against the phase or mode properties of light from a light source exiting a reference fiber having pre-determined or identical light transmission properties. The sensitivity of magnetic effect upon the magnetostrictively affected fiber is enhanced by subjecting the magnetostrictive material to a quantitative low-level magnetic field. GRA

N92-28328# Stanford Univ., CA. Lab. of Physics.
TUNABLE OPTICAL SOURCES AND SYNTHETIC NONLINEAR MEDIA/GROWTH AND CHARACTERIZATION OF NONLINEAR OPTICAL MATERIALS Final Technical Report, 15 Jul. 1988 - 31 Oct.
Robert L. Byer and Robert S. Feigelson 13 Feb. 1992 32 p
(Contract DAAL03-88-K-0113)
(AD-A249363; ARO-25408.17-PH) Avail: NTIS HC/MF A03

The results of a joint research program in the development of nonlinear optical devices for the generation of tunable coherent radiation and the growth and processing of the nonlinear optical materials used in these devices is described. Continuous-Wave (CW) external-resonant-cavity harmonic generation and optical parametric oscillation have demonstrated the requirement for low losses and good resistance to optical damage in nonlinear optical materials. We have extended CW harmonic conversion to the generation of 1.7 watts of 532-nm radiation using periodically poled lithium niobate and lithium-diffused lithium niobate. We are continuing to investigate the growth technology of the bulk chalcopyrite materials AgGaSe2 and ZnGep2 and quantum well structures in GaAs for nonlinear infrared applications. A substantial effort has been placed in the characterization of nonlinear materials. Nonlinear optical coefficients have been remeasured in a number of materials to resolve discrepancies that have persisted for two decades, and the optical properties of the lithium diffused lithium niobate have been accurately characterized. GRA

N92-28355# Sandia National Labs., Albuquerque, NM.
PERSPECTIVES OF ION IMPLANTATION FOR OPTICS
G. W. Arnold 1992 8 p Presented at the 1992 Optics International Conference, Padova, Italy, 9-12 Jun. 1992
(Contract DE-AC04-76DP-00789)
(DE92-010664; SAND-92-0393C; CONF-9206141-1) Avail: NTIS HC/MF A02

Energetic ions incident on insulators produce refractive-index changes as a result of damage, compound formation, or phase separation. These alterations allow waveguides to be formed in crystals and glasses. Nonlinear optical properties allow second-harmonic generation in waveguides in crystals (e.g., quartz) and intensity-dependent refractive index changes due to metal colloids implanted into glass. Waveguide lasers have been realized by MeV He beam formation of guides in rare-earth containing materials and by direct implantation of rare-earths into waveguides regions. Hardness changes in glasses result from implantation-induced surface stresses and from crystallization. DOE

N92-28372# Kent Univ., Canterbury (England).
IN LINE OPTICAL FIBRE FREQUENCY SHIFTER PROJECT Final Report, 1 Jan. - 31 Dec. 1991
M. Berwick and D. A. Jackson 5 Feb. 1992 39 p
(Grant AF-AFOSR-0114-91)
(AD-A246714; EOARD-TR-92-04) Avail: NTIS HC/MF A03

This report describes the results of research directed towards improving the performance of the torsional-birefringent optical fiber frequency shifter. A detailed account is given of the experimental procedures required to construct and test a fiber-optic frequency shifter utilizing a travelling torsional acoustic wave to couple the polarization eigenmodes of a highly linearly birefringent optical fiber. The frequency shifter configurations such that the acoustic wave generator and optical fiber are co-axial. The device is thus more rugged than previous 'free fiber' frequency shifters where the acoustic wave is coupled into the fiber via an acoustic horn bonded to the edge of the optical fiber. Results are presented for the best device constructed thus far. The optical frequency shift was 3.204 MHz and an optical coupling efficiency of 12 percent was obtained with 4W of electrical power applied to the acoustic transducer. Carrier and sideband suppressions of 25 and 30 dB were attained. The coupling efficiency, carrier and sideband suppressions achieved for this device, while significantly improved on previous similar devices, are significantly lower than theoretical prediction and this is attributed to the difficulties in manufacturing the unit. GRA

N92-28475*# National Aeronautics and Space Administration. Lewis Research Center, Cleveland, OH.
ROCKET PLUME FLOWFIELD CHARACTERIZATION USING LASER RAYLEIGH SCATTERING
Frank J. Zupanc and Jonathan M. Weiss (Pennsylvania State Univ., University Park.) Jul. 1992 20 p Proposed for presentation at the 28th Joint Propulsion Conference and Exhibit, Nashville, TN, 6-8 Jul. 1992; sponsored by AIAA, SAE, ASME, and ASEE
(RTOP 506-42-31)
(NASA-TM-105739; E-7145; NAS 1.15:105739; AIAA Paper 92-3351) Copyright Avail: NTIS HC/MF A03

A Doppler-resolved laser Rayleigh scattering diagnostic was applied to a 111 N thrust, regenerative and fuel-film cooled, gaseous hydrogen/gaseous oxygen rocket engine. The axial and radial mean gas velocities were measured from the net Doppler shifts observed for two different scattering angles. Translational temperatures and number densities were estimated from the Doppler widths and scattered intensities, respectively, by assuming that water was the dominant scattering species in the exhaust. The experimental results are compared with theoretical predictions from a full Navier-Stokes code (RD/RPLUS) and the JANNAF Two-Dimensional Kinetics (TDK) and Standardized Plume Flowfield (SPF-II) codes. Discrepancies between the measured and predicted axial velocities, temperatures, and number densities are evident. Radial velocity measurements, however, show excellent agreement with predictions. The discrepancies are attributed primarily to inefficient mixing and combustion caused by the injection of excessive oxidizer along one side of the thrust chamber. Thrust and mass flow rate estimates obtained from the Rayleigh measurements show excellent agreement with the globally measured values. Author

N92-28554# Stanford Univ., CA. Optical Communications Research Lab.
ADVANCED OPTICAL FIBER COMMUNICATION SYSTEMS Status Report, 1 Sep. 1991 - 29 Feb. 1992
Leonid Kazovsky 29 Feb. 1992 4 p
(Contract N00014-91-J-1857)
(AD-A247683) Avail: NTIS HC/MF A01

Our research is focused on four aspects of advanced optical fiber communication systems: dynamic wavelength division multiplexing (WDM) networks, linewidth insensitive coherent optical analog links, video distribution systems using direct frequency modulation of semiconductor laser, and impact of fiber nonlinearities on optical communication systems. In the area of WDM networks, we investigated, designed, and are currently implementing a coherent optical network with a total throughput of 12 Gbit/s. In the study of coherent optical analog links, we analyzed two linewidth-insensitive schemes that could overcome the impact of phase noise of semiconductor laser diodes. In the area of video distribution systems, we investigated the performance of novel systems using direct frequency modulation of semiconductor lasers for subcarrier-multiplexed video distribution. In the area of fiber nonlinearities, we evaluated the performance of optical WDM systems in the presence of four-wave mixing, and are analyzing the impact of stimulated Brillouin scattering on such networks. GRA

N92-28571* National Aeronautics and Space Administration. Lewis Research Center, Cleveland, OH.
MONOLITHIC mm-WAVE PHASE SHIFTER USING OPTICALLY ACTIVATED SUPERCONDUCTING SWITCHES Patent
Robert R. Romanofsky, inventor (to NASA) and Kul B. Bhasin, inventor (to NASA) 26 May 1992 6 p Filed 25 Sep. 1990 Supersedes N91-13996 (29 - 5, p 716)
(NASA-Case-LEW-14878-1; US-Patent-5,116,807; US-Patent-Appl-SN-587921; US-Patent-Class-505-1; US-Patent-Class-505-703; US-Patent-Class-505-848; US-Patent-Class-505-866; US-Patent-Class-333-161; US-Patent-Class-333-995; Int-Patent-Class-H01P-1/18) Avail: US Patent and Trademark Office

A phase shifter is disclosed having a reference path and a delay path, light sources, and superconductive switches. Each of the superconductive switches is terminated in a virtual short circuit, which may be a radial stub. Switching between the reference path and delayed path is accomplished by illuminating the superconductive switches connected to the desired path, while not illuminating the superconductive switches connected to the other path.
Official Gazette of the U.S. Patent and Trademark Office

N92-28656# National Aerospace Lab., Amsterdam (Netherlands). Space Div.
TELESCIENCE EXPERIMENTS USING THE PROTOTYPE OPTICAL DIAGNOSTIC INSTRUMENT (PODI)
E. A. Kuijpers 19 Jun. 1990 9 p Sponsored by Netherlands Agency for Aerospace Programs
(NLR-TP-90199-U; ETN-92-91441) Avail: NTIS HC/MF A02

The breadboard called Prototype Optical Diagnostic Instrument (PODI) was developed following a study for a general facility for fluid experimental research on fluid physics on a space laboratory. PODI was developed further for the study of telescience and image processing related to microgravity instrumentation. The extended breadboard (TelePODI) is being used for various telescience experiments. Some intermediate results are reported and discussed. ESA

N92-28698*# Optivision, Inc., Palo Alto, CA.
FIBER-OPTIC INTERCONNECTION NETWORKS FOR SPACECRAFT Final Report, 22 May 1990 - 21 May 1992
Robert S. Powers May 1992 42 p Original contains color illustrations
(Contract NAS5-30896)
(NASA-CR-190531; NAS 1.26:190531) Avail: NTIS HC/MF A03; 1 functional color page

The overall goal of this effort was to perform the detailed design, development, and construction of a prototype 8x8 all-optical fiber optic crossbar switch using low power liquid crystal shutters capable of operation in a network with suitable fiber optic transmitters and receivers at a data rate of 1 Gb/s. During the earlier Phase 1 feasibility study, it was determined that the all-optical crossbar system had significant advantages compared to electronic crossbars in terms of power consumption, weight, size, and reliability. The result is primarily due to the fact that no optical transmitters and receivers are required for electro-optic conversion within the crossbar switch itself. Author

N92-28868*# Virginia Polytechnic Inst. and State Univ., Blacksburg. Dept. of Electrical Engineering.
ELLIPTICAL-CORE TWO MODE FIBER SENSORS AND DEVICES INCORPORATING PHOTOINDUCED REFRACTIVE INDEX GRATINGS
Jonathan A. Greene, Mark S. Miller, Suzanne E. Starr, Brian R. Fogg, Kent A. Murphy, Richard O. Claus, and Ashish M. Vengsarkar (Bell Telephone Labs., Inc., Murray Hill, NJ.) 1991 6 p
(Grant NAG1-1348)
(NASA-CR-190495; NAS 1.26:190495) Avail: NTIS HC/MF A02

Results of experiments performed using germanium-doped, elliptical core, two-mode optical fibers whose sensitivity to strain was spatially varied through the use of chirped, refractive-index gratings permanently induced into the core using Argon-ion laser light are presented. This type of distributed sensor falls into the class of eighted-fiber sensors which, through a variety of means, weight the strain sensitivity of a fiber according to a specified spatial profile. We describe results of a weighted-fiber vibration mode filter which successfully enhances the particular vibration mode whose spatial profile corresponds to the profile of the grating chirp. We report on the high temperature survivability of such grating-based sensors and discuss the possibility of multiplexing more than one sensor within a single fiber. Author

N92-28968# Naval Ocean Systems Center, San Diego, CA. Research, Development, Test, and Evaluation Div.
THE 2.0 GHz SAMPLING RATE TRANSVERSAL FILTER
M. H. Berry and D. M. Gookin Mar. 1992 5 p
(AD-A250244) Avail: NTIS HC/MF A01

A variable weight transversal filter was used to process analog signals in real time. The length of the delay lines between filter taps determined the sampling rate. The delay lines were made from optical fibers. The variable tap weights were implemented using integrated optical couplers under computer control. An electronic RF signal was input to the transversal filter by externally modulating a laser diode. The RF power out of the transversal filter was measured using a spectrum analyzer. The dynamic range of the filter was found to be greater than 70 dB. The factors which limit the operating performance of the filter were calculated. The actual filter response agreed well with predictions based on computer simulations. This work can be extended up to 16 GHz sampling rates using current technology. GRA

N92-29088*# Virginia Polytechnic Inst. and State Univ., Blacksburg. Materials Response Group.
DEVELOPMENT OF AN EMBEDDED FABRY PEROT FIBER OPTIC STRAIN ROSETTE SENSOR (FP-FOSRS)
Gregory P. Carman, John J. Lesko, Scott W. Case, Brian Fogg, and Richard O. Claus 1992 6 p
(Grant NAG1-1348)
(NASA-CR-190490; NAS 1.26:190490) Avail: NTIS HC/MF A02

We investigate the feasibility of utilizing a Fabry-Perot Fiber Optic Strain Rosette Sensor (FP-FOSRS) for the evaluation of the internal strain state of a material system. We briefly describe the manufacturing process for this sensor and point out some potential problem areas. Results of an embedded FP-FOSRS in an epoxy matrix with external resistance strain gauges applied for comparative purposes are presented. We show that the internal and external strain measurements are in close agreement. This work lays the foundation for embedding this sensor in actual composite laminas. Author

N92-29095# Department of the Navy, Washington, DC.
MULTI-CHANNEL FIBER OPTIC ROTARY JOINT FOR SINGLE-MODE FIBER Patent Application
Gregory H. Ames, inventor (to Navy) 16 Sep. 1991 21 p
(AD-D015273; US-Patent-Appl-SN-760635) Avail: NTIS HC/MF A03

A fiber optic rotary joint device is described. The device includes a rotor connected to either an input or output fiber optic array and a stator connected to the remaining unconnected input or output fiber optic array. A prism is mounted within the rotor for derotating an image of the input array to allow coupling to the output array. A prism rotor and a gear system are provided for rotating the prism at half the speed of the rotor. Optical means are provided for two adjustment tiers (small angular adjustment and fine adjustment) of alignment of the light propagation path for each channel of the array. Mechanical structural features provide maintenance of accurate alignment of optical elements under rotation of the joint. Further mechanical structural features provide resiliency of the gear system to isolate its operation from maintenance of mechanical alignment of optical elements. GRA

N92-29117* National Aeronautics and Space Administration. Langley Research Center, Hampton, VA.

NON-MECHANICAL OPTICAL PATH SWITCHING AND ITS APPLICATION TO DUAL BEAM SPECTROSCOPY INCLUDING GAS FILTER CORRELATION RADIOMETRY Patent

Glen W. Sachse, inventor (to NASA) and Liang-Guo Wang, inventor (to NASA) 7 Jul. 1992 11 p Filed 11 Feb. 1991 Supersedes N91-23889 (29 - 15, p 2507)
(NASA-Case-LAR-14588-1-CU; US-Patent-5,128,797; US-Patent-Appl-SN-653605; US-Patent-Class-359-246; US-Patent-Class-356-370; US-Patent-Class-356-414; US-Patent-Class-359-247; US-Patent-Class-359-281; Int-Patent-Class-G02F-1/01) Avail: US Patent and Trademark Office

A non-mechanical optical switch is developed for alternately switching a monochromatic or quasi-monochromatic light beam along two optical paths. A polarizer polarizes light into a single, e.g., vertical component which is then rapidly modulated into vertical and horizontal components by a polarization modulator. A polarization beam splitter then reflects one of these components along one path and transmits the other along the second path. In the specific application of gas filter correlation radiometry, one path is directed through a vacuum cell and one path is directed through a gas correlation cell containing a desired gas. Reflecting mirrors cause these two paths to intersect at a second polarization beam splitter which reflects one component and transmits the other to recombine them into a polarization modulated beam which can be detected by an appropriate single sensor.

Official Gazette of the U.S. Patent and Trademark Office

N92-29122* National Aeronautics and Space Administration. Pasadena Office, CA.

METHOD AND APPARATUS FOR PHASING SEGMENTED MIRROR ARRAYS Patent

Paul K. Manhart, inventor (to NASA) (Jet Propulsion Lab., California Inst. of Tech., Pasadena.) 12 May 1992 10 p Filed 6 Mar. 1991 Supersedes N91-32923 (29 - 24, p 4102)
(NASA-Case-NPO-18095-1-CU; US-Patent-5,113,064; US-Patent-Appl-SN-665509; US-Patent-Class-250-201.9; US-Patent-Class-359.849; Int-Patent-Class-G01J-1/20) Avail: US Patent and Trademark Office

A method and an apparatus are disclosed for edge phasing an array of segments in a segmented primary telescope mirror using white light from a far field source and starting with the inner edge of each segment in the first ring of segments. The segments are individually phased for zero piston and tilt error with respect to the edge of a reference surface in the open center position of the telescope mirror. After edge phasing of all segments in the telescope mirror array is completed, full surface phasing can be achieved by using a conventional Shack-Hartmann technique followed by finding the RMS best fit for each segment of the mirror array.

Official Gazette of the U.S. Patent and Trademark Office

N92-29133* National Aeronautics and Space Administration. Goddard Space Flight Center, Greenbelt, MD.

LASER OPTICAL DISK POSITION ENCODER WITH ACTIVE HEADS Patent

Eric P. Osborne, inventor (to NASA) 21 Apr. 1992 23 p Filed 30 Mar. 1990 Supersedes N91-14001 (29 - 5, p 717)
(NASA-Case-GSC-13175-1; US-Patent-5,107,107; US-Patent-Appl-SN-506636; US-Patent-Class-250-231.14; US-Patent-Class-369-44.26; Int-Patent-Class-G01D-5/34) Avail: US Patent and Trademark Office

An angular position encoder is provided that minimizes the effects of eccentricity and other misalignments between the disk and the read stations by employing heads which incorporate beam steering optics with the ability to actively track the disk in directions along the disk radius and normal to its surface. The device adapts features prevalent in optical disk technology toward the application of angular position sensing. A reflective disk and the principles of interferometry are employed. The servo-controlled steering optics move so as to acquire a track on the disk lying at a predetermined radius and distance below the head, and then adjust position and orientation in order to maintain the view of the disk track as required. Thus, the device is actively self-aligning.

Official Gazette of the U.S. Patent and Trademark Office

N92-29158* National Aeronautics and Space Administration. Langley Research Center, Hampton, VA.

SINGLE LAYER MULTI-COLOR LUMINESCENT DISPLAY AND METHOD OF MAKING Patent

James B. Robertson, inventor (to NASA) 14 Apr. 1992 8 p Filed 30 Apr. 1991 Continuation-in-part of abandoned US-Patent-Appl-SN-337768, filed 13 Apr. 1989 which is a division of US-Patent-Appl-SN-140185, filed 31 Dec. 1987
(NASA-Case-LAR-13616-3; US-Patent-5,104,683; US-Patent-Appl-SN-693049; US-Patent-Appl-SN-337768; US-Patent-Appl-SN-140185; US-Patent-Class-427-38; US-Patent-Class-427-66; US-Patent-Class-427-68; US-Patent-Class-427-108; US-Patent-Class-427-109) Avail: US Patent and Trademark Office

The invention is a multi-color luminescent display comprising an insulator substrate and a single layer of host material, which may be a phosphor deposited thereon that hosts one or more different impurities, therein forming a pattern of selected and distinctly colored phosphors such as blue, green, and red phosphors in a single layer of host material. Transparent electrical conductor means may be provided for subjecting selected portions of the pattern of colored phosphors to an electric field, thereby forming a multi-color, single layer electroluminescent display. A method of forming a multi-color luminescent display includes the steps of depositing on an insulator substrate a single layer of host material, which itself may be a phosphor, with the properties to host varying quantities of different impurities and introducing one or more of said different impurities into selected areas of the said single layer of host material by thermal diffusion or ion implantation to form a pattern of phosphors of different colors in the said single layer of host material.

Official Gazette of the U.S. Patent and Trademark Office

N92-29167# Naval Oceanographic and Atmospheric Research Lab., Bay Saint Louis, MS.

IMPACT ON THE MEDIUM MTF BY MODEL ESTIMATION OF BETA

Lee Estep and R. Arnone 1991 14 p
(AD-A247985; NOARL-PR-91-024-352) Avail: NTIS HC/MF A03

The effect of suspended particles in a water medium on the transport of light is normally dichotomized into two processes. Namely, the dual effects of absorption and scattering. Absorption simply acts to remove photons which might have contributed to image formation. Such attrition effects might be overcome for a given system by increasing the source flux or by using a more sensitive receiver. Scattering, however, produces two more pernicious effects. Scattering can produce a foreground veiling glare which reduces the effective contrast of the target with respect to the background, and by causing a redistribution of the trajectories of image forming photons, scrambles the information content originally presented by the target and background. The modulation transfer function (MTF) is used to characterize the effects the

medium has on the passage of image forming light. Wells has derived a transformation which converts the medium volume scattering function, Beta(theta), into a medium MTF expression via the use of a 'decay' function. The MTF expression so derived requires the value of the total (volume) scattering coefficient, b.
GRA

N92-29205# Department of the Navy, Washington, DC.
OPTICAL SWITCHING DEVICES Patent Application
Michael E. Boyle, inventor (to Navy) and James S. Shirk, inventor (to Navy) 12 Sep. 1991 16 p
(AD-D015261; US-Patent-Appl-SN-758143) Avail: NTIS HC/MF A03

An optical switching device employs a rare earth bis-phthalocyanine having third-order nonlinear susceptibilities. In a preferred optical switch, the rare earth bis-phthalocyanine is employed as a nonlinear optical material body that fills the space between two partially reflecting mirrors. When light incident on the switch is below a given intensity level, light passes through the switch and the switch is in an open state. When light is above a given intensity level, light is trapped in the nonlinear optical material and the switch is in a closed state.
Author (GRA)

75 PLASMA PHYSICS

Includes magnetohydrodynamics and plasma fusion.
For ionospheric plasmas see *46 Geophysics*. For space plasmas see *90 Astrophysics*.

N92-28234# National Inst. for Fusion Science, Nagoya (Japan).
DEVELOPMENT OF NEGATIVE HEAVY ION SOURCES FOR PLASMA POTENTIAL MEASUREMENT
M. Sasao, Y. Okabe, A. Fujisawa, H. Iguchi, J. Fujita, H. Yamaoka, and M. Wada Oct. 1991 16 p
(DE92-782102; NIFS-112) Avail: NTIS HC/MF A03

A plasma sputter negative ion source was studied for its applicability to the potential measurement of a fusion plasma. Both the beam current density and the beam energy spread are key issues. Energy spectra of a self extracted Au(-) beam from the source were measured under the condition of a constant work function of the production surface. The full width of half maximum (FWHM) increases from 3 to 9 eV monotonically as the target voltage increases from 50 V to 300 V, independently from the target surface work function of 2.2 - 3 eV.
DOE

N92-28298# Stanford Univ., CA. High Temperature Gasdynamics Lab.
ADVANCED DIAGNOSTICS FOR REACTING FLOWS Annual Report, 1 Oct. 1990 - 31 Oct. 1991
R. K. Hanson 20 Nov. 1991 42 p
(Grant AF-AFOSR-0067-89)
(AD-A247059; AFOSR-92-0123TR) Avail: NTIS HC/MF A03

Progress is reported for the past year of an interdisciplinary program aimed at establishing advanced optical diagnostic techniques applicable to combustion gases and plasmas, with some emphasis on high speed flows. The primary flowfield parameters of interest are species concentrations (including electrons), temperature, mass density, pressure, and velocity, and quantities derivable from these parameters such as mass flow rate (from the product of density and velocity). The techniques under study are based on laser spectroscopy, particularly laser absorption and laser-induced fluorescence, with the latter capable of providing both single-point and multi-point (2-d and 3-d) measurements. Laser sources include tunable CW lasers (ring dye and semiconductor diode lasers) and tunable pulsed lasers (excimer-pumped dye and narrow-linewidth excimer). The CW lasers are spectrally narrow, allowing study of a new class of techniques based on spectral lineshapes and shifts, while the pulsed lasers provide intense bursts of photons needed for techniques based on light-scattering phenomena. Accomplishments of note include: the first optical measurement of mass flux in high speed air flows; the first applications of tunable semiconductor diode lasers to absorption and fluorescence measurements in high temperature plasmas and supersonic flows, and to the measurement of water vapor in high temperature combustion gases; the first application of the planar laser-induced fluorescence (PLIF) technique to nonequilibrium shock tunnel flows; and further advances in the development of shock tube diagnostics for rate constant measurements of elementary combustion reactions.
GRA

N92-28335# Lawrence Livermore National Lab., CA.
A COMPARISON OF RESULTS FROM AN EDGE-PLASMA MODEL WITH THOSE FROM A TWO-DIMENSIONAL FLUID CODE
W. L. Barr, R. H. Bulmer, L. J. Perkins, S. A. Cohen (Princeton Univ., NJ.), and K. A. Werley (Los Alamos National Lab., NM.) 3 Mar. 1992 7 p Presented at the 10th Topical Meeting on Technology of Fusion Energy, Boston, MA, 7-12 Jun. 1992
(Contract W-7405-eng-48)
(DE92-010718; UCRL-JC-109808; CONF-920607-6) Avail: NTIS HC/MF A02

We have just completed a comparison of predictions for the scrape-off layer (SOL) plasma, from a physics model with the more accurate ones from a two-dimensional fluid code, the B2 code. The presented results show rather good agreement on values of plasma temperature in the SOL and of divertor heat load, for a rather wide range of Tokamak sizes and parameters. Therefore, we are confident that this model will provide a suitable divertor module for both the new ITER systems code, SUPERCODE, and other applications requiring fast but accurate modelling of edge plasma parameters at least within the range of the present benchmarks.
DOE

N92-28354# Naval Research Lab., Washington, DC.
SECONDARY INSTABILITY IN 3D MAGNETIC RECONNECTION Interim Report
R. B. Dahlburg, S. K. Antiochos, and T. A. Zang 6 Apr. 1992 46 p
(AD-A248630; NRL/MR/4440-92-6966) Avail: NTIS HC/MF A03

We consider the transition to turbulence in three dimensional reconnection of a magnetic neutral sheet. We find that the transition can occur via a three-step process. First, the sheet undergoes the usual tearing instability. Second, the tearing mode saturates to form a two-dimensional quasi-steady state. Third, this secondary equilibrium is itself unstable when it is perturbed by three-dimensional disturbances. Most of this paper is devoted to the analysis and simulation of the three-dimensional linear stability properties of the two-dimensional saturated tearing layer. The numerical simulations are performed with a semi-implicit, pseudospectral-Fourier collocation algorithm. We identify a three-dimensional secondary liner stability which grows on the ideal timescale. An examination of the modal energetics reveals that the largest energy transfer is from the mean field to the three-dimensional field, with the two-dimensional field acting as a catalyst.
GRA

N92-28664# Saskatchewan Univ., Saskatoon. Plasma Physics Lab.
OHMIC IGNITION IN A TOKAMAK REACTOR WITH THE CONFINEMENT DEGRADATION EFFECT DUE TO ALPHA HEATING
Osamu Mitarai (Kumamoto Inst. of Tech., Japan), Akira Hirose, and Harvey M. Skarsgard Aug. 1991 39 p Sponsored by Japanese Science Promotion Society and Natural Sciences and Engineering Research Council
(PPL-124; FFP-4-91; CTN-92-60500) Avail: NTIS HC/MF A03

The criterion for ohmic ignition in tokamaks is described in terms of the operation path on the generalized ignition contour map. The formula for the ohmic heating power and its dependence on the current density profile are presented. The ohmic ignition on the generalized ignition contour map is shown for the cases with and without a confinement degradation effect due to alpha heating. It is shown that a tokamak with a major radius larger

than about 6 m and a toroidal field of 10 tesla can reach ignition by ohmic heating alone at a surprisingly low peak density confinement degradation due to alpha heating, provided that a confinement enhancement factor of about 2 over the Goldston scaling is assumed. The critical toroidal field and plasma curent required for ohmic ignition have been estimated for tokamaks with major radii of 2 m (compact), 6 m (ITER class), and 10 m (large tokamaks). Author (CISTI)

N92-28665# Saskatchewan Univ., Saskatoon. Plasma Physics Lab.

IGNITION ACCESS CONDITION BASED ON THE GENERALIZED SADDLE POINT IN A MAGNETIC FUSION REACTOR

Osamu Mitarai (Kumamoto Inst. of Tech., Japan), Akira Hirose, and Harvey M. Skarsgard Feb. 1990 42 p
(PPL-109; CTN-92-60513) Avail: NTIS HC/MF A03

A major concern in fusion reactor studies is to calculate the confinement enhancement factor, relative to L-mode scaling, required for reaching ignition. An ignition access condition is proposed, based on the generalized saddle point for the confinement scaling law. The concept of the operation path of a reactor is described as given by a generalized global power balance equation. The ignition access condition is then derived. The height of the generalized saddle point is calculated for various plasma parameters, and the height of the operation paths for next-generation tokamaks and a stellarator reactor are presented. The confinement enhancement factors required to reach ignition in these machines are obtained using the ignition access condition previously derived. The operation path method using the generalized ignition contour map is compared to the conventional POPCON method, and their relationship and respective advantages are discussed. It is shown that a confinement enhancement factor up to about 2.5 is needed to reach ignition in the machines considered. Author (CISTI)

N92-28742# Institute of Plasma Physics, Prague (Czechoslovakia). Academy of Sciences.

THE THEORY OF THE LONG WAVEGUIDE STRUCTURES RADIATING THE LH WAVES INTO A PLASMA

O. Hurtak and J. Preinhaelter Sep. 1991 21 p
(IPPCZ-314) Avail: NTIS HC/MF A03

It has been shown that the radiation into a plasma from the structures composed of many waveguides is described well by the theory of the infinite structures. This theory results in the efficient numerical code which is appropriate namely for the study of the nonlinear response of the plasma in front of the grill. Both the infinite conventional grill and the structure built up from the infinite series of the identical N-waveguide multijunction sections are investigated. It is proved that the spectrum of the last structure is the superposition of N spectra of the infinite conventional grills with the specially selected phase shifts. The theoretical results for three long structures (24-waveguide conventional grill on ASDEX and two multijunction arrays, 32-waveguide grill on JET and 30-waveguide grill proposed for T15) are compared with the predictions of the theory of the corresponding infinite structures and the agreement is good. Author

N92-28805# Edgerton, Germeshausen and Grier, Inc., Idaho Falls, ID.

CRYOGENIC SYSTEM OPERATING EXPERIENCE REVIEW FOR FUSION APPLICATIONS

L. C. Cadwallader Jan. 1992 102 p
(Contract DE-AC07-76ID-01570)
(DE92-012509; EGG-FSP-10048) Avail: NTIS HC/MF A06

This report presents a review of cryogenic system operating experiences, from particle accelerator, fusion experiment, space research, and other applications. Safety relevant operating experiences and accident information are discussed. Quantitative order-of-magnitude estimates of cryogenic component failure rates and accident initiating event frequencies are presented for use in risk assessment, reliability, and availability studies. Safety concerns with cryogenic systems are discussed, including ozone formation, effects of spills, and modeling spill behavior. This information should be useful to fusion system designers and safety analysts, such as the team working on the International Thermonuclear Experimental Reactor design. DOE

N92-28816# Academy of Sciences of the Ukrainian SSR, Kiev. Inst. Teoreticheskoj Fiziki.

HYDRODYNAMIC ECHO IN STRONGLY INHOMOGENEOUS MAGNETIZED PLASMA

V. I. Lapshin and E. A. Fedutenko 1991 29 p In RUSSIAN
(DE92-621530; ITF-91-28) Avail: NTIS HC/MF A03

The possibility of the hydrodynamical echo existence in a strongly inhomogeneous, magnetized plasma is investigated. Values of generation time, electromagnetic field, energy flow density, surface charges, and density of plasma responses on two and three impulses resulting from external perturbations are obtained. The hydrodynamical echo is shown to be possible only in the case when initial impulses propagate in opposite directions along the magnetic field. DOE

N92-28847# Saskatchewan Univ., Saskatoon. Plasma Physics Lab.

PLASMA DENSITY SCALING AT THE CURRENT REVERSAL IN THE STOR-1M TOKAMAK WITH AC OPERATION

Osamu Mitarai (Kumamoto Inst. of Tech., Japan), Akira Hirose, and Harvey M. Skarsgard Feb. 1992 25 p Sponsored by Japan Society for the Promotions of Science and Natural Sciences and Engineering Research Council
(PPL-127; CTN-92-60497) Avail: NTIS HC/MF A03

Plasma density behavior in the STOR-1M tokamak with alternating current operation is described in the Murakami-Hugill diagram. At the current reversal, the density remains finite. Gas puffing before current reversal allows alternating current operation with larger currents, and improves its reproducibility. A qualitative explanation for the finite plasma density at the current reversal is presented, based on a short-circuit effect by the limiter.
Author (CISTI)

N92-28848# Saskatchewan Univ., Saskatoon. Plasma Physics Lab.

IMPROVED CONFINEMENT AND EDGE PLASMA FLUCTUATIONS IN THE STOR-M TOKAMAK

W. Zhang, C. Xiao, G. D. Conway, Akira Hirose, Osamu Mitarai (Kumamoto Inst. of Tech., Japan), A. Sarkissan (Quebec Univ., Varennes.), Harvey M. Skarsgard, and L. Zhang Dec. 1991 26 p Sponsored by Natural Sciences and Engineering Research Council
(PPL-126; CTN-92-60498) Avail: NTIS HC/MF A03

An improved ohmic confinement phase has been observed in the STOR-M tokamak after application of a turbulent heating (TH) pulse. This phase is characterized by increased average electron density, reduced H-alpha radiation from the edge, reduced density and magnetic fluctuations at the edge, a steeper density profile at the edge, and a more negative radial electric field. Almost complete suppression of sawtooth oscillations during the improved confinement phase has also been observed. A linear dispersion relation describes the density and magnetic fluctuations in the frequency range up to 350 kHz. In the edge region of the main discharge, the propagation direction of the density fluctuations is in the electron diamagnetic direction, and in the scrape-off layer the propagation direction is in the ion diamagnetic direction. The reduction of root mean square density and magnetic fluctuations after the TH pulse is largely due to suppression of relatively high frequency (under or equal to 500 kHz) components. The density fluctuations in the scrape-off layer remain intact after the pulse.
Author (CISTI)

N92-28849# Saskatchewan Univ., Saskatoon. Plasma Physics Lab.

ALTERNATING CURRENT TOKAMAK REACTOR WITH OHMIC IGNITION AND BOOTSTRAP CURRENT

Osamu Mitarai (Kumamoto Inst. of Tech., Japan), Akira Hirose,

and Harvey M. Skarsgard Apr. 1991 30 p
(PPL-120; FFP-2-91; CTN-92-60504) Avail: NTIS HC/MF A03

An alternating current tokamak reactor with ohmic ignition and long pulses due to the bootstrap current is proposed as a simple and quasi continuous fusion power plant. An ohmic plasma current of 23 MA with a high toroidal field of around 10 tesla in the ACTR-U tokamak (major radius 10 m, minor radius 2 m) provides the ohmic ignition. After entering the ignition regime, the plasma current is reduced by one half to enhance the bootstrap current with a high beta poloidal for prolongation of the pulse length. When the ohmic transformer reaches the maximum flux, the plasma current is ramped down and reversed, and then alternating current operation follows subsequently. It is thus demonstrated that an ohmic transformer alone is in principle sufficient for a quasi continuous deuterium-tritium fusion reactor. CISTI

N92-28962# Air Force Systems Command, Kirtland AFB, NM. Weapons Lab.
PLASMA BEAM MEASUREMENTS Final Report, Jan. - Oct. 1989
J. H. Degnan, D. Dietz, J. L. Holmes, G. F. Kiuttu, and D. W. Price Aug. 1991 176 p
(AF Proj. 5797)
(AD-A247892; WL-TR-90-83) Avail: NTIS HC/MF A09

Coaxial plasma gun plasma parameters were determined using a diagnostic array to observe electron density, temperature, luminosity, beam target interactions, target luminosity, magnetic fields and ion species. Diagnostics included He-Ne and CO2 laser and 94 GHz microwave interferometry, visible spectrometry using an optical multichannel analyzer, rotating mirror fast framing camera, gated microchannel plate framing cameras, optical vacuum photodiodes, X-ray diodes aad inductive magnetic probes. The plasma gun was operated with 126 or 252 microfarads, 18 kV discharges with Ar or H gas. For these conditions, 70-80 km/s average plasma velocity and 0.5-2 eV plasma electron temperature was observed. The dominant plasma ionic species was Si(sup +1) with a quartz insulator; with an alumina insulator, Al(sup +1) and Al(sup +2) were the dominant species. The plasma was self-luminous for 1.5-3 m. Interferometry showed averaged electron densities of 10 to the 15th power/cc. The plasma showed MHD instabilities. Plasma currents were 0.5-1.5 kA. Fast plasma velocities contributed less than 1 percent of the total beam energy. GRA

N92-29086# Sandia National Labs., Albuquerque, NM.
ANALYZING NOISY SPECTRAL LINE SHAPES
A. B. Filuk and J. E. Bailey 1992 7 p Presented at the 9th Topical Conference on High-Temperature Plasma Diagnostics, Santa Fe, NM, 15-19 Mar. 1992
(Contract DE-AC04-76DP-00789)
(DE92-011153; SAND-92-0066C; CONF-920362-10) Avail: NTIS HC/MF A02

In many situations it is necessary to analyze spectral line shapes where the data contain significant amounts of noise or statistical fluctuations. Our visible spectroscopy measurements exploring ion diode physics on the PBFA II accelerator typically result in noisy spectra because the harsh environment limits the number of photons collected. The spectral line profiles include contributions from Doppler (T approximately 1-3 keV), Stark (n sub e)(approximately 10(exp 17) cm(exp minus 3)), and instrument broadening, as well as from Stark shifting (E approximately 3-10 MV/cm) and Zeeman spliting (B approximately 2-10 T). We extract information about the physical parameters (e.g., ion temperature from Doppler broadening) by determining a range of fits that are consistent with the data, including the uncertainty due to the noise. The range of fits is generated by a Monte-Carlo technique. This method effectively distinguishes between actual spectral features and artifacts due to noise. It provides not only estimates of physical parameters, but also their uncertainties. We evaluated the technique over a range of signal-to-noise ratios and found that it works well for our application. DOE

N92-29093# SRI International Corp., Menlo Park, CA.
MICROWAVE INTERACTIONS WITH PLASMAS Final Report, Jun. 1989 - Jun. 1992
D. J. Eckstrom, R. J. Vidmar, and K. R. Stalder Apr. 1992 69 p
(Contract F49620-90-C-0041)
(AD-A250333; AFOSR-92-0343TR) Avail: NTIS HC/MF A04

Microwave interactions with a cold, collisional plasma having gradual density gradients were studied. The plasma was created by the photoionization of tetrakisdimethylaminoethylene (TMAE) vapor seeded into atmospheric pressure helium. Photoionization was provided primarily by sparkboard Spatial scans of the absorption of a microwave probe beam along chords across the plasma, with subsequent Abel inversion. Three-dimensional plasma density profiles were obtained that showed a gradual decrease in the peak plasma density versus distance away from the sparkboard. When a 58cm-diameter reflector was illuminated with 10-GHz microwaves in an anechoic chamber, the plasma sorbed as much as 28 dB in direct reflection, with similar attenuation of the normally weak side-scattered and cross-polarized radiation. The attenuation was compared with model predictions. Detailed analysis of the temporal and spatial dependence of the electron density following ionization indicated that both recombination and attachment processes influenced the plasma decay. The recombination rate of TMAE was found to be (9.0 +/- 1.1) x 10(exp -6) cm3 s(exp -1) for 300 K electrons. This work confirms the effectiveness of a cold, collisional plasma as a broadband, switchable wave absorber. GRA

76 SOLID-STATE PHYSICS

Includes superconductivity.

For related information, see also *33 Electronics and Electrical Engineering* and *36 Lasers and Masers.*

N92-28231# International Centre for Theoretical Physics, Trieste (Italy).
PERCOLATION CONDUCTIVITY OF PENROSE TILING BY TRANSFER-MATRIX MONTE CARLO
F. V. Babalievski Sep. 1991 12 p
(DE92-622792; IC-91/292) Avail: NTIS HC/MF A03

A generalization of Derrida and Vannimenus transfer-matrix Monte Carlo for calculations of percolation conductivity of Penrose Tiling was applied. The strips used were 10(exp 4) long and widths varied between 3 and 19. The results show that in spite of differences for strip widths 3-7 the percolative conductivity of Penrose tiling is very close to that of square lattice. The estimation of the percolation transport exponent once more confirms the universality conjecture for 0-1 distribution of resistors. DOE

N92-28280# International Centre for Theoretical Physics, Trieste (Italy).
WEIGHTED-DENSITY FUNCTIONAL APPROACH FOR THE SOLID-LIQUID INTERFACES IN ELECTROLYTES
T. A. Cherepanova, A. V. Stekolnikov, and P. Bennema Sep. 1991 35 p
(DE92-622662; IC-91/308) Avail: NTIS HC/MF A03

A weighted-density functional method is proposed to describe the atomic structure of the crystal-melt interface in electrolytes based on a charged-hard-sphere model of salt. The contribution of long-range Coulomb interaction is taken into account in the field formulation: the electrostatic field potential is determined from the Poisson equation. The ion density profiles and crystalline order parameter at the crystal-melt interface in the 1:1 symmetric electrolytes are calculated. The structurization of liquid near the solid surface is described. The results are compared to those for the neutral hard sphere system. The impurity distributions of extremely small concentrations are calculated both for the neutral and charged hard sphere systems. DOE

N92-28281# International Centre for Theoretical Physics, Trieste (Italy).
QUASI-REGULAR IMPURITY DISTRIBUTION DRIVEN BY CHARGE-DENSITY WAVE
I. Baldea, M. Badescu, and M. Moise Sep. 1991 32 p
(DE92-622799; IC-91/282) Avail: NTIS HC/MF A03

The displacive motion of the impurity distribution immersed into the one-dimensional system has recently been studied in detail as one kind of quasi-regularity driven by CDW. As a further investigation of this problem, we develop a microscopical model for a different kind of quasi-regular impurity distribution driven by CDW, consisting of the modulation in the probability of occupied sites. The dependence on impurity concentration and temperature of relevant CDW quantities is obtained. Data reported in the quasi-1D materials NbSe3 and Ta2NiSe7 (particularly, thermal hysteresis effects at CDW transition) are interpreted in the framework of the present model. Possible similarities to other physical systems are also suggested. DOE

N92-28282# Japan Atomic Energy Research Inst., Tokyo.
GADOLINIUM METASTABLE STATES POPULATION DISTRIBUTIONS AND ATOMIC DENSITY UNDER HIGH-RATE ELECTRON BEAM EVAPORATION
Akihiko Nishimura, Takashi Arisawa, Hironori Ohba, and Takemasa Shibata Oct. 1991 19 p In JAPANESE; ENGLISH summary
(DE92-782008; JAERI-M-91-178) Avail: NTIS HC/MF A03

Metastable states population distributions of gadolinium atoms under high-rate electron beam evaporation were measured by laser light absorption. The experiments were carried out under high atomic density of 10(exp 12) approximately 10(exp 13) atoms/cm(exp 3) at the light absorption zone and following several vapor characteristics were found: (1) the atomic excitation temperature derived from metastable states population distribution was considerably lower than the evaporation surface temperature and decreased with increasing the evaporation rate; (2) atomic vapor is almost free from the cluster formation caused by a rapid expansion into a high vacuum; and (3) the atomic density is in reciprocal proportion to the square of the distance from the evaporation surface. DOE

N92-28312# International Centre for Theoretical Physics, Trieste (Italy).
SHALLOW STATES OF DONOR IMPURITIES ON PERIODICALLY STRUCTURED SEMICONDUCTORS INTERFACES
Sun Hong and Shiwei Gu (Jiaotong Univ., Shanghai, China) Sep. 1991 17 p
(DE92-622791; IC-91/287) Avail: NTIS HC/MF A03

Ground state energies of shallow states of donor impurities on cosine-shaped, periodically structured interfaces formed by two semiconductors, such as GaAs/Ga(1-x)Al(x)As and Si/SiO2 interfaces, are calculated variationally with the approximation that interfaces represent infinitely high potential barriers. The results show that the ground state energies of interface impurity states are strongly affected by interface structures in GaAs/Ga(1-x)Al(x)As Lateral-Surface-Superlattices produced by Molecular-Beam-Epitaxy growth of AlAs/GaAs fractional-layer superlattices on (001) vicinal GaAs substrates, while effects of interface defects on interface impurity states are negligible for Si/SiO2 interfaces when the density of interface defects is less than 10(exp 10)/cm(exp 2). DOE

N92-28331# Sandia National Labs., Albuquerque, NM.
GROWTH AND OPTICAL CHARACTERIZATION OF Zn(1-x)Mn(x)Te GROWN BY MOLECULAR BEAM EPITAXY
J. L. Reno and E. D. Jones 1992 2 p Presented at the Electronic Materials Conference, Cambridge, MA, 24-26 Jun. 1992
(Contract DE-AC04-76DP-00789)
(DE92-010667; SAND-92-0384C; CONF-920676-1) Avail: NTIS HC/MF A01

We have grown Zn(1-x)Mn(x)Te alloys by molecular beam epitaxy and characterized them using x-ray diffraction and low temperature magnetoluminescence. Zn(1-x)Mn(x)Te is a dilute magnetic semiconductor (DMS) whose bandgap ranges from the green through the blue part of the spectrum and is therefore of interest for blue LED's. DOE

N92-28333# Lawrence Livermore National Lab., CA.
MICROSTRUCTURES OF SHOCKED QUARTZ
A. J. Gratz and W. J. Nellis Dec. 1991 5 p Presented at the 1991 American Physical Society (APS) Conference on Shock Compression of Condensed Matter, Williamsburg, VA, 17-20 Jul. 1991
(Contract W-7405-eng-48)
(DE92-010710; UCRL-JC-109289; CONF-9107105-59) Avail: NTIS HC/MF A01

Shock recovery experiments show three phases in shocked single-crystal quartz: melt-glass in a thin network connecting quartz crystallites containing transformation lamellae of diapletic glass. Both melting and solid-state amorphization occur, but in separate regions of the sample. These results are consistent with real-time measurements and suggest that the high-pressure of shocked quartz is six-coordinated glass. Stishovite probably is not synthesized in more than trace amounts along the Hugoniot. DOE

N92-28349# Purdue Univ., West Lafayette, IN. Dept. of Chemistry.
DYNAMICAL SOLVENT EFFECTS ON ACTIVATED ELECTRON-TRANSFER REACTIONS: PRINCIPLES, PITFALLS, AND PROGRESS
Michael J. Weaver Feb. 1992 58 p
(Contract N00014-91-J-1409)
(AD-A246764; TR-115) Avail: NTIS HC/MF A04

Recent experimental and conceptual progress in our understanding of dynamical solvent effects in activated electron-transfer processes are critically reviewed. Understanding the various influences exerted by the solvating environment upon the kinetics of electron-transfer (ET) processes, either in homogeneous solution or at metal-solution and related interfaces, has long captured the attention of experimentalists and theoreticians alike. These roles have been perceived primarily in terms of energetic factors, whereby the solvent is considered to affect the reaction rates via its influence on the net activation barrier to electron transfer, delta. Indeed, such considerations form a mainstay of the well-known Marcus and related theoretical treatments. In these approaches, solvent effects upon delta are separated into so-called intrinsic and extrinsic (or thermodynamic) factors. Author (GRA)

N92-28392# Purdue Univ., West Lafayette, IN. Dept. of Chemistry.
SURFACE CRYSTALLOGRAPHIC DEPENDENCE OF VOLTAMMETRIC OXIDATION OF POLYHYDRIC ALCOHOLS AND RELATED SYSTEMS AT MONOCRYSTALLINE GOLD-ACIDIC AQUEOUS INTERFACES
Antoinette Hamelin, Yeunghaw Ho, Si-Chung Chang, Xiaoping Gao, and Michael J. Weaver Feb. 1992 21 p
(Contract N00014-91-J-1409)
(AD-A246763; TR-114) Avail: NTIS HC/MF A03

The voltammetric oxidation in aqueous 0.1 Molar perchloric acid of four polyhydric alcohols, ethylene glycol, glycerol, meso-erythritol, and d-mannitol, on seven oriented gold surfaces is reported with the objective of assessing the role of surface crystallographic orientation on the catalytic electrooxidation of such poly-functional reactants. The automatically well-ordered nature of these gold surfaces has been scrutinized by in-situ scanning tunneling microscopy. In particular, the Au(221) and (533) faces were selected since they provide stepped surfaces, 4(111)-(111) and 4(111)-(100), respectively. The results are compared with corresponding data for simple unifunctional reactants, specifically for formic acid oxidation and with results reported previously for carbon monoxide oxidation. In contrast to the last reaction, the electrooxidation rates for both the polyhydric alcoholic and formic acid are greatest on Au(111), with Au(110) displaying unusually

low activity. While formic acid electrooxidation is insensitive to the presence of monoatomic surface steps, the polyhydric alcohols (especially mannitol) are substantially less reactive on AU(221) and (533) relative to Au(111). GRA

N92-28395# Georgia Inst. of Tech., Atlanta.
CHEMICAL VAPOR DEPOSITION OF YTTRIUM BORIUM(2) COPPER(3) OXYGEN(x) THIN FILMS FOR WIRE APPLICATIONS Final Report, May 1988 - Dec. 1991
W. J. Lackey, J. A. Hanigofsky, D. N. Hill, W. B. Carter, and E. K. Barefield Dec. 1991 312 p Prepared in cooperation with American Magnetics, Inc., Oak Ridge, TN
(Contract N00014-88-C-0615)
(AD-A247013) Avail: NTIS HC/MF A14

The chemical vapor deposition of superconducting yttrium barium copper oxide thin films onto continuous lengths of ceramic fiber tows has been investigated. This project couples two areas of current interest in the materials field continuous fiber coating and the deposition of one of the unique high temperature superconducting oxides. The YBa2Cu3O(x) material has zero resistance at temperatures above 77 K (the boiling point of nitrogen), and the film form has been shown to have high critical current densities. By coating ceramic fiber tows, a strong, flexible superconducting material in the form of wire can be developed and used for several applications, including coils for magnets and transmission lines. Over 900 deposition runs were completed using a horizontal CVD furnace and over 150 continuous fiber coating experiments were completed. The deposition was performed on fiber tows, flat samples, and flexible tapes; the continuous substrates were moved and held stationary in the furnace. GRA

N92-28512# Purdue Univ., West Lafayette, IN. Dept. of Chemistry.
THE EMERGENCE OF ATOMIC-LEVEL STRUCTURAL INFORMATION FOR ORDERED METAL-SOLUTION INTERFACES: SOME RECENT CONTRIBUTIONS FROM IN-SITU INFRARED SPECTROSCOPY AND SCANNING TUNNELING MICROSCOPY
Xiaoping Gao, Si-Chung Chang, Xudong Jiang, Antoinette Hamelin, and Michael J. Weaver 28 Feb. 1992 32 p
(Contract N00014-91-J-1409)
(AD-A246765; TR-118) Avail: NTIS HC/MF A03

The utilization of infrared reflection-absorption spectroscopy (IRAS) and scanning tunneling microscopy (STM) to extract atomic-resolution information for ordered metal-solution interfaces in a related (and relatable) fashion to metal-ultrahigh vacuum (UHV) surfaces is illustrated by means of some recent results from our laboratory. Two specific topics are addressed. The first involves the potential-dependent properties of saturated carbon monoxide adlayers on low-index platinum and rhodium electrodes in aqueous and nonaqueous media. The central role of the surface potential in controlling the CO adlayer structure is discussed on the basis of in-situ IRAS data, especially in comparison with the properties of corresponding metal-uhv interfaces. The application of in-situ atomic-resolution STM in tandem with IRAS for elucidating real-space adsorbate structures is noted for saturated CO adlayers on Rh(111) and Rh(110) electrodes. The second topic concerns the application of in-situ STM to probe potential induced reconstruction at gold-aqueous interfaces. All three low-index gold surfaces are seen to undergo reconstruction at potentials corresponding to small negative electrode charges. GRA

N92-28513# Cornell Univ., Ithaca, NY. Lab. of Atomic and Solid State Physics.
PHYSICS AND TECHNOLOGY FOR THE INVESTIGATION OF PROPERTIES OF ULTRA SMALL SYSTEMS Final Report, 15 Jan. 1990 - 14 Jan. 1992
J. M. Parpia and R. C. Richardson 17 Feb. 1992 16 p
(Grant AF-AFOSR-0111-90)
(AD-A246772; AFOSR-92-0165TR) Avail: NTIS HC/MF A03

In superconducting thin films, the long range proximity effect and the observation of a novel resistance anomaly are new physical phenomena exposed through the development of a technique to precisely modify the transition temperature in a well defined region. Free standing metallic structures were fabricated to understand thermal transport in thin films. In this latter work, the electron-phonon interaction should be modified due to the thermal cut-off of excitations. Using two different techniques, we have determined that the electron-phonon interaction does not display the expected thermal cut-off, a fact which may be of significance in thermalizing electronic components. We have also observed a reduction of the electron-impurity-spin interaction due to size effects, which should have interesting consequences for the magnetism of ultrasmall structures. GRA

N92-28762# California Univ., Berkeley. Lawrence Berkeley Lab.
MONTE CARLO OPTIMIZATION OF DEPTH-OF-INTERACTION RESOLUTION IN PET CRYSTALS
T. A. DeVol, W. W. Moses, and S. E. Derenzo Nov. 1991 5 p Presented at the IEEE Nuclear Science Symposium, Santa Fe, NM, 5-9 Nov. 1991
(Contract DE-AC03-76SF-00098)
(DE92-011147; LBL-31457; CONF-911106-92) Avail: NTIS HC/MF A01

The light distribution along one edge of a PET scintillation crystal was investigated with a Monte Carlo simulation. This position-dependent light can be used to measure the 511 keV photon interaction position in the crystal on an event by event basis, thus reducing radial elongation. The expected full width at half maximum (FWHM) of the light distribution on the 3 x 30 mm(exp 2) surface of a 3 x 10 x 30 mm(exp 3) bismuth germanate (BGO) crystal surrounded by a diffuse reflector was determined to be 3.0 mm. This light distribution does not change as the width (originally 3 mm) is varied from 1 to 6 mm, but decreases monotonically from 3.0 to 1.8 mm FWHM as the height (originally 10 mm) is reduced to 3 mm. Other geometrical modifications were simulated, including numerous corner reflectors on the opposing 3 x 30 mm(exp 2) surface, which reduced the FWHM to 2.4 mm. The response of a dual wedge photodiode combined with the predicted light distribution for the 3 x 10 x 30 mm(exp 3) BGO simulation crystal results in an expected depth of interaction resolution of 7.5 mm FWHM. DOE

N92-28786# Technische Univ., Berlin (Germany, F.R.). Fachbereich Physik.
HETEROEPITAXY OF InP ON Si (001) Ph.D. Thesis [HETEROEPITAXIE VON INP AUF SI(001)]
Marius Grundmann 1991 169 p In GERMAN
(ETN-92-91333) Avail: NTIS HC/MF A08

A low pressure Metal Organic Chemical Vapor Deposition (MOCVD) process was developed for the epitaxy of antiphase domain free InP on Si (001). This process does not include any high temperature annealing of silicon. The systematic examination of the influence of preliminary treatment of a vicinal silicon surface in the MOVCD gas environment at various temperatures led to the detection of phase transfer of the silicon surface between mono and diatomic stages. The indium phosphide epitaxy layers were examined with complementary methods (X-ray diffractometry and electron microscopy) and characterized. ESA

N92-28806# California Univ., Santa Barbara.
BIFURCATIONS AND PATTERNS IN NONLINEAR DISSIPATIVE SYSTEMS
Guenter Ahlers and David S. Cannell 26 Feb. 1992 5 p
(Contract DE-FG03-87ER-13738)
(DE92-013502; DOE/ER-13738/T2) Avail: NTIS HC/MF A01

This report discusses the following topics: Rayleigh-Benard convection with an imposed horizontal flow; Rayleigh-Benard convection in a gas under non-Boussinesq conditions; electro-convection in a nematic liquid crystal; and Rayleigh-Benard convection in a nematic liquid crystal. DOE

N92-28857# Oak Ridge National Lab., TN.
THE OXIDATION STABILITY OF BORON NITRIDE THIN FILMS ON MgO AND TiO2 SUBSTRATES

Xiaomei Qiu, A. K. Datye, R. T. Paine (New Mexico Univ., Albuquerque.), and L. F. Allard 1991 5 p Presented at the Annual Fall Meeting of the Materials Research Society, Boston, MA, 2-6 Dec. 1991
(Contract DE-AC05-84OR-21400)
(DE92-011686; CONF-911202-72) Avail: NTIS HC/MF A01

The stability of BN thin film coatings (2-5 nm) on MgO and TiO2 substrates was investigated using transmission electron microscopy (TEM). The samples were heated in air for at least 16 hours at temperatures ranging from 773-1273 K. On MgO supports, the BN thin film coating was lost by 1073 K due to a solid state reaction with the substrate. This lead to the formation of Mg2B2O5. No such reaction occurred with the TiO2 substrate and the BN was stable even at 1273 K. However, the coating appeared to ball up and phase segregate into islands of near-graphitic BN and clumps of TiO2 (rutile). The oxidizing treatment appears to promote the transformation from turbostratic BN to graphitic BN. DOE

N92-28874# Los Alamos National Lab., NM.
MAGNETIC HYSTERESIS AND RELAXATION IN Ag-SHEATHED TlBaCaCuO (1223) AND Bi(Pb)SrCaCuO (2223) SUPERCONDUCTING TAPES
P. J. Kung, M. P. Maley, J. Y. Coulter, J. O. Willis, D. E. Peterson, and M. E. McHenry (Carnegie-Mellon Univ., Pittsburgh, PA.) 1992 7 p Presented at the High Tc SUH Workshop on High Temperature Superconductivity (HTS) Materials, Bulk Processing and Bulk Applications, Houston, TX, 27-28 Feb. 1992
(Contract W-7405-eng-36)
(DE92-011357; LA-UR-92-706; CONF-920240-4) Avail: NTIS HC/MF A02

Magnetic hysteresis (7-75 K in magnetic fields up to 5 T) and relaxation characteristics (5-50 K in magnetic fields up to 2 T) were measured with the field perpendicular to the surface of Ag-sheathed TlBaCaCuO (1223 phase) and Bi(Pb)SrCaCuO (2223 phase) superconducting tapes. A study of the difference in the magnetic hysteresis between precursor powders and as-processed tapes was also carried out. The relaxation data were curve-fit using a rate equation for thermally activated flux motion, U(sub eff)/(kG(T)) = (-)T(ln(dM/dt) - ln (H(omega)(sub o) a/2(pi)d)) with the temperature dependence of U(sub eff) scaled by the functional form G(T) = 1 (-) (T/Tx)(exp 2). By comparing the results obtained from magnetic characterization with those from transport current measurement, these observations suggest the following: (1) Tl-1223 tapes have a weaker field dependence for J(sub c) at T greater than 35 K than Bi-2223 tapes due to the special crystal structure of the 1223 phase; and (2) weak links limit the transport critical current densities in Tl-1223 tapes to 10(exp 3) A/sq cm at 5 T and 35 K, for instance. DOE

N92-28885# Rensselaer Polytechnic Inst., Troy, NY. Dept. of Chemistry.
STUDIES OF 1,3-DISILACYCLOBUTANES AS SINGLE-SOURCE CVD PRECURSORS TO SILICON CARBIDE
David J. Larkin and Leonard V. Interrante Dec. 1991 10 p
(Contract N00014-91-J-1917)
(AD-A247111; Rept-2) Avail: NTIS HC/MF A02

Substituted 1,3-disilacyclobutanes were studied as potential low temperature single-source CVD precursors to silicon carbide. These studies were carried out in a cold-wall LPCVD system maintained at a total reactor pressure of 1.0 Torr using a mass flow controlled argon carrier gas. The precursor was decomposed on resistively heated Si(100) substrates at temperatures ranging from 700 C to 1100 C. Gas chromatography-Fourier transform infrared spectroscopy and quadrupole mass spectrometry were used to identify the volatile pyrolysis byproducts from each precursor. The decomposition onset temperature was separately determined for each precursor by monitoring the major pyrolysis byproducts, by using quadrupole mass spectrometry, while slowly increasing the substrate temperature. Scanning and transmission electron microscopy were used to determine the cross-sectional and surface morphology and also the deposition rate, which ranged from ca.0.035 micron/h to 12.0 micron/h. GRA

N92-28919# Rockwell International Science Center, Thousand Oaks, CA.
ELECTRODEPOSITION OF HIGH TEMPERATURE SUPERCONDUCTORS Quarterly Research and Development Report, 1 Jan. - 31 Mar. 1992
D. M. Tench 23 Apr. 1992 3 p
(Contract N00014-90-C-0225)
(AD-A250171) Avail: NTIS HC/MF A01

The overall objective of this project is to develop a process for direct electrodeposition of Y-Ba-Cu superconducting oxides from a molten salt at relatively low temperatures (300-550 C). The approach entails establishing a sequence of electrochemical steps for the layered deposition of Y, Ba, and Cu oxide species from a eutectic Na-K nitrate melt. GRA

N92-28923# United Kingdom Atomic Energy Authority, Harwell (England).
REPORT ON THE WORKSHOP ON ION IMPLANTATION AND ION BEAM ASSISTED DEPOSITION
G. Dearnaley Mar. 1992 3 p Workshop held in Corpus Christi, TX, 9-11 Mar. 1992
(AD-A250561; R/D-6907-EE-06) Avail: NTIS HC/MF A01

This workshop was organized by the Corpus Christi Army Depot (CCAD), the major helicopter repair base within AVSCOM. Previous meetings had revealed a strong interest throughout DoD in ion beam technology as a means of extending the service life of military systems by reducing wear, corrosion, fatigue, etc. The workshop opened with an account by Dr. Bruce Sartwell of the successful application of ion implantation to bearings and gears at NRL, and the checkered history of the MANTECH Project at Spire Corporation. Dr. James Hirvonen (AMTL) continued with a summary of successful applications to reduce wear in biomedical components, and he also described the processes of ion beam-assisted deposition (IBAD) for a variety of protective coatings, including diamond-like carbon (DLC). GRA

N92-29207# Laboratoire d'Automatique et d'Analyse des Systemes, Toulouse (France). Composants et Circuits a Effet de Champ.
FEASIBILITY OF METAL-OXIDE-SEMICONDUCTOR STRUCTURES ON Si-LPCVD THIN FILMS BY LOW TEMPERATURE (600 C) PROCESS Ph.D. Thesis - Inst. National des Sciences Appliquees de Toulouse [FAISABILITE DE STRUCTURES METAL-OXIDE-SEMICONDUCTEUR SUR FILMS MINCES DE SI-LPCVD PAR PROCEDE TECHNOLOGIQUE A BASSE TEMPERATURE (600 C)]
Philippe Taurines 1991 131 p In FRENCH
(LAAS-91307; ETN-92-91330) Avail: NTIS HC/MF A07

The feasibility of metal oxide semiconductor structure on polycrystalline silicon thin films obtained from Low Pressure Chemical Vapor Decomposition (LPCVD) is investigated. The electrical quality of 600C thermal oxide and the effect of deposition conditions on the film oxidation kinetics and crystalline structure are analyzed. The advantages of disilane on silane, as deposition gas, are lower deposition temperature, higher deposition rate and larger grain size when the films are deposited in the quasi amorphous state and crystallized by 600C annealing. The 600C steam oxidation, first realized on (100)-oriented monocrystalline silicon, shows the possibility of obtaining, by this process, a 10 nm thick pad oxide with very good electrical quality: 13 to 15 MV breakdown field, 3 eV chromium oxide barrier height. Concerning the silicon film oxidation, it is shown that oxide, with the highest values of the electical breakdown field and barrier height (metal oxide and oxide semiconductor), is obtained from the films which show the largest grain size and the lowest oxidation rate, i.e., the films deposited at 555C (300 mT) from silane pyrolysis. Moreover, the 600C thermal oxidation allows the gate pad oxide to be realized and the LPCVD silicon films to be crystallized, simultaneously. ESA

77 THERMODYNAMICS AND STATISTICAL PHYSICS

Includes quantum mechanics; theoretical physics; and Bose and Fermi statistics.

For related information see also *25 Inorganic and Physical Chemistry* and *34 Fluid Mechanics and Heat Transfer.*

N92-28227# International Centre for Theoretical Physics, Trieste (Italy).
CLASSICAL AND QUANTUM LIOUVILLE THEORY ON THE RIEMANN SPHERE WITH n GREATER THAN 3 PUNCTURES (II)
Jianmin Shen and Zhonghua Wang Dec. 1991 11 p
(DE92-622380; IC-91/396) Avail: NTIS HC/MF A03

Starting from the classical Liouville theory on the Riemann sphere with n greater than 3 punctures, we have studied the quantum Liouville theory near an arbitrary but fixed puncture via canonical quantization. We show that a kind of arbitrariness for the matrices dominating the classical and quantum exchange algebra relations appears in our theory. Starting from our formalism, we have found a sequency of solutions for the Classical and Quantum Yang-Baxter equations. DOE

N92-28229# International Centre for Theoretical Physics, Trieste (Italy).
THE EXCHANGE ALGEBRA FOR LIOUVILLE THEORY ON PUNCTURED RIEMANN SPHERE
Jianmin Shen and Zhengmao Sheng Nov. 1991 10 p
(DE92-622409; IC-91/376) Avail: NTIS HC/MF A02

We consider in this paper the classical Liouville field theory on the Riemann sphere with n punctures. In terms of the uniformization theorem of Riemann surface, we show explicitly the classical exchange algebra (CEA) for the chiral components of the Liouville fields. We find that the matrice which dominate the CEA is related to the symmetry of the Lie group SL(n) in a nontrivial manner with n greater than 3. DOE

N92-28230# International Centre for Theoretical Physics, Trieste (Italy).
HYPER-RAMAN SCATTERING AND 3-PHOTON RESONANT IONIZATION: COMPETITIVE EFFECTS
A. M. Guzman and C. Ramirez (Universidad Nacional de Colombia, Bogota.) Sep. 1991 19 p
(DE92-622671; LAMP-91/9) Avail: NTIS HC/MF A03

A semiclassical theory of hyper-Raman scattering and three-photon resonant ionization via the coupled density-matrix and Maxwell equations is presented. A simplified three-level atom model is obtained, which includes two-photon resonant pumping and time dependent photoionization rates. We consider conditions typically encountered in atomic vapors to simulate numerically pulse propagation. A strong depletion of the photoionization probability in the hyper-Raman field saturation regime is predicted. DOE

N92-28232# International Centre for Theoretical Physics, Trieste (Italy).
THE INFLUENCE OF THE RESONANT ELECTROMAGNETIC FIELD ON THE LIGHT ABSORPTION BY EXCITON AND BIEXCITON IN QUANTUM WELLS
Hong Quang Nguyen and A. I. Bobrysheva (Academy of Sciences of the Moldavian SSR, Kishinev.) Dec. 1991 8 p
(DE92-622801; IC-91/389) Avail: NTIS HC/MF A02

The influence of a resonant electromagnetic field on the light absorption by the exciton and biexciton in semiconductor quantum wells is investigated. The probabilities of exciton one-photon and biexciton two-photon absorption are calculated. DOE

N92-28235# Tokyo Univ., Tanashi (Japan). Inst. for Nuclear Study.
PROCEEDINGS OF THE WORKSHOP ON QUANTUM GRAVITY AND TOPOLOGY
Ichiro Oda, ed. Oct. 1991 186 p Workshop held in Tanashi, Japan, 21-23 Feb. 1991
(DE92-782191; INS-T-506; CONF-9102158) Avail: NTIS HC/MF A09

The workshop on Quantum Gravity and Topology was held at INS on February 21-23, 1991. Several introductory lectures and more than 15 talks were delivered for about 100 participants. The main subjects discussed were: (1) topological quantum field theories and topological gravity; (2) low dimensional and four dimensional gravity; (3) topology change; and (4) superstring theories etc. DOE

80 SOCIAL SCIENCES (GENERAL)

Includes educational matters.

No abstracts in this category.

81 ADMINISTRATION AND MANAGEMENT

Includes management planning and research.

N92-28256# Air Force Inst. of Tech., Wright-Patterson AFB, OH. School of Systems and Logistics.
IMPROVED DECISION MAKING THROUGH GROUP COMPOSITION M.S. Thesis
William E. Page, III Sep. 1991 215 p
(AD-A246622; AFIT/GSM/LSM/91S-21) Avail: NTIS HC/MF A10

This experimental study attempted to prove that teams formed with dissimilar personality types would have better decision making than teams which were not formed by dissimilar types. The Myers-Briggs Type Indicator (MBTI), based on Jung's Theory of Psychological Type, was used to determine the subject's personality type preferences. Subjects' perceptions of team processes were also investigated. The sample population consisted of military officers and civil servants who attended the Advanced Program Management course at the Air Force Institute of Technology. Decision making effectiveness was determined from team performance on the Time-by-Event-by-Member-Pattern-Observation system (TEMPO). The design for this research consisted of comparing the scores from teams formed by dissimilar MBTI personality types to scores from teams which were not formed by dissimilar MBTI personality types. The T-test was used to determine the differences between the teams' mean scores at an alpha equal to 0.1. The research concluded that teams formed by dissimilar MBTI personality types were statistically no more effective than teams formed without the MBTI; however, the teams formed by dissimilar MBTI personality types did score higher than the teams that were not formed with the MBTI. GRA

N92-28864*# National Aeronautics and Space Administration. Marshall Space Flight Center, Huntsville, AL.
SECOND NATIONAL SPACE GRANT CONFERENCE REPORT, 1991
Jeffrey T. Heimsoth, ed., E. Julius Dasch, ed., Richard F. Devon, ed., and Lynne Keffer, ed. 1991 165 p Conference held in Huntsville, AL, 11-15 Mar. 1991
(NASA-EP-278; NAS 1.19:278) Avail: NTIS HC/MF A08

The conference goals were: (1) to provide a setting for Space Grant College/Consortia leaders to meet and discuss program plans; (2) to provide participants with updates on major NASA science and engineering programs and educational affairs activities; and (3) to hold workshops on themes of critical importance to the program. The conference agenda focused primarily on a series of 15 workshops in which program directors or their designees discussed components of the Space Grant Program. These components - outreach, pre-college education, publicity, and

organization - were earlier incorporated in very specific ways within individual program plans. The conference, thus, afforded those attending an opportunity to exchange information and concerns regarding program elements while exploring ways to structure, enhance and perhaps broaden their program plans. Space Grant representatives also discussed with headquarters officials ways in which the Space Grant Program itself should be evaluated.

Author

N92-29111*# National Academy of Public Administration, Washington, DC.
MAINTAINING THE PROGRAM BALANCE, VOLUMES 1 AND 2
Harold Finger Jan. 1991 165 p
(Contract NASw-4254)
(NASA-CR-190269; NAS 1.26:190269) Avail: NTIS HC/MF A08

In March of 1990, the NASA Administrator asked the Academy to perform a study to address the following questions: (1) has NASA contracted too much of its technical work; (2) has NASA's in-house technical capability eroded over time; (3) is in-house engineering and scientific work important to the development of scientists and engineers; and (4) is NASA still able to attract quality scientists and engineers. A panel from the Academy addressed each question separately and came up with the following recommendations: (1) prepare and issue guidance on technical functional areas reserved for in-house performance; (2) convert contracted technical functions to in-house performance if critical to agency programs; (3) provide policy guidance to the centers to retain in-house projects; (4) examine the project mix at each center against agency goals and objectives; (5) institute an annual critical review for all technical disciplines; (6) modify the agency's contractor accountability process; and (7) seek opportunities for greater delegation of resources and technical decision making.

H.A.

N92-29161 Institute for Perception RVO-TNO, Soesterberg (Netherlands). Cognitive Psychology Group.
TIME PRESSURE EFFECTS ON DECISION MAKING IN A DYNAMIC TASK ENVIRONMENT Final Report [HET EFFECT VAN TIJDSDRUK OP BESLISSINGSGEDRAG IN EEN DYNAMISCHE TAAKSITUATIE]
J. H. Kerstholt 26 Jul. 1991 19 p Sponsored by TNO Defence Research
(IZF-1991-B-8; TD91-2168; ETN-92-91231) Copyright Avail: TNO Inst. for Perception, Kampweg 5, P.O. Box 23, 3769 ZG Soesterberg, Netherlands

Time pressure effects on both the quality of task performance and the underlying cognitive processes are investigated. The task used is dynamic in nature such that the environment changes over time both automatically and as a result of actions taken by the decision maker. Twenty subjects are required to monitor the fitness level of an athlete, that continually changes over time, and to recover the athlete whenever fitness decline has a physiological cause. Their major decision problem is to tradeoff the costs of requesting information and applying treatments on the one hand, and increasing changes of a serious consequence on the other. The results show that time pressure drastically reduces task performance under severe time pressure. Severe time pressure is caused by reacting too late to declines in fitness level. Subjects requested the smallest amount of information under moderate time pressure. Time pressure had no significant effect on the speed of information processing.

ESA

82 DOCUMENTATION AND INFORMATION SCIENCE

Includes information management; information storage and retrieval technology; technical writing; graphic arts; and micrography.

For computer documentation see *61 Computer Programming and Software.*

N92-28244# Naval Postgraduate School, Monterey, CA.
CONVERSION AND RETRIEVABILITY OF HARD COPY AND DIGITAL DOCUMENTS ON OPTICAL DISKS M.S. Thesis
Lawrence P. Bittner Mar. 1992 82 p
(AD-A247481) Avail: NTIS HC/MF A05

Paper documents can be converted into digital form, as a collection of images, or a combination of ASCII text and images. Full text and image document databases, display advantages and disadvantages during scanning and conversion processes. Conversion of paper thesis documents could be eliminated, if thesis documents could be submitted in digital form, for storage on optical disks. Utilizing existing paper thesis documents, image and full text databases were developed and evaluated to determine the best digital form for storage of paper documents. Analysis was performed on a thesis document in digital form, to determine the most feasible format for digital document submission. This thesis concludes that conversion of paper documents to digital form should not be pursued. Instead, thesis documents should be submitted in digital form for direct conversion and storage on optical disks. Follow on thesis research is recommended to build an in-house CD-ROM mastering system for this purpose.

GRA

N92-28246# Naval Postgraduate School, Monterey, CA.
THE INSTRUMENTATION OF A PARALLEL, DISTRIBUTED DATABASE OPERATION, RETRIEVE-COMMON, FOR MERGING TWO LARGE SETS OF RECORDS M.S. Thesis
Gregory A. Hammond Jun. 1992 67 p
(AD-A247486) Avail: NTIS HC/MF A04

The Naval Postgraduate School's Laboratory for Database Systems Research is the site of the multi-backend database supercomputer (MBDS). Originally, MBDS supported a prototype primary operation (retrieve-common) which merged two sets of records in a distributed, parallel database environment. This thesis presents the testing, and modification of that prototyped primary operation. First, the design rationale of the MBDS is reviewed. Specifically, this review examines the reasons for a database-oriented supercomputer, the MBDS primary processes, and the methodology of distributing a database within loosely coupled and highly parallel database stores. Then, this study explains the methodology involved in developing theories on the cause of retrieve-common's defects and bottlenecks. Finally, in validating our theories, this study relates the process of discovering and correcting these discrepancies.

GRA

N92-28389# Clemson Univ., SC. Apparel Research.
AUTOMATED APPAREL SPECIFICATION RETRIEVAL SYSTEM Final Report, 1 Jun. 1990 - 30 Jun. 1991
Gene A. Tagliarini 5 Feb. 1992 14 p
(Contract DLA900-87-D-0017)
(AD-A248619) Avail: NTIS HC/MF A03

This research investigated an information management program that was used to provide access to garment specifications. In particular, the requirements for producing and evaluating a military shift were used to explore the potential of hypermedia for providing immediate access to related segments of shirt construction and evaluation specifications. In addition, a hypermedia program was used to investigate the efficacy of augmenting the written requirements with graphics.

GRA

N92-28403# Naval Surface Warfare Center, Dahlgren, VA.
INFORMATION STRATEGY PLAN
W. R. Burrell and C. B. Wilson Jan. 1992 178 p
(AD-A247740; NSWCDD/TR-92/47) Avail: NTIS HC/MF A09

An enterprise-wide Information Strategy Plan (ISP) and model

was developed for a 5000-person, Navy research and development (R&D) center, spanning four geographically dispersed sites. The ISP included Naval Surface Warfare Center (NSWCDD) in its entirety and did not restrict itself to support functions but included the technical mission of the Center. The ISP provides a basis for delivering systems that are relevant to the enterprise and are targeted at supporting the principle business directions. The work analyzed the total business goals for NSWCDD with respect to how information technology does or could enhance its abilities to meet its goals. Using teams of people representing many viewpoints and levels within the enterprise, models were developed showing what information and functions NSWCDD needs to perform its business. GRA

N92-28404# Lockheed Missiles and Space Co., Austin, TX.
VALIDATION OF KNOWLEDGE BASED SYSTEMS Final Report, Mar. 1989 - Jun. 1990
Dec. 1991 137 p
(Contract F30602-88-C-0130)
(AD-A247741; RL-TR-91-361) Avail: NTIS HC/MF A07

Knowledge-based systems (KBS) technology has emerged from applied Artificial Intelligence as a means for modeling complex systems. KBS's have consequently become more and more integrated into large complex software systems in defense, industry, business, and science. Failures in these systems could be critical, but methods for validating conventional software systems do not take into account the incremental life cycles and other peculiarities of KBS engineering. The objective of this contract was to define and develop a KBS validation system, DEVA, that enables a user to check the redundancy, consistency, completeness and correctness of DARPA-Sponsored KBS'S. This report describes the implementation of the DEVA modules developed under this contract: a KEE translator, a rule refiner, a validation and verification of nonmonotonic reasoning module and structure, logic, extended structure, extended logic, semantics, omission, and control checkers. GRA

N92-28430# University of Southern California, Marina del Rey. Information Sciences Inst.
ORGANIZING PLAN LIBRARIES IN SUBSUMPTION HIERARCHIES: SPECIFICITY BASED PLAN SELECTION
Vibhu Mittal, Cecil Paris, Ramesh Patil, and William Swartout 1992 35 p
(Contract DABT63-91-C-0025)
(AD-A248711) Avail: NTIS HC/MF A03

As the number of plans in a plan library grows, the importance of selecting a plan efficiently also increases. Previous planners have not addressed this issue in great detail, because they typically had only tens of plans - as domain models grow more and more specialized, and planners incorporate new macro-operators through learning, plan libraries can become more than a magnitude greater in size. The issue of organizing plan libraries in specificity based hierarchies is addressed. In particular, we look at how a plan library can be represented in a frame-based KL-ONE style system. Such systems offer powerful mechanisms to handle dynamically changing knowledge bases. In particular, the subsumption classifier mechanism in such systems, offers a simple and efficient means of indexing new plans and goals into the hierarchy. We illustrate the feasibility of this approach by using examples from an implemented system, and describe some of the other advantages that accrue from the use of such a framework for organizing large plan libraries. GRA

N92-28565# Wright Lab., Wright-Patterson AFB, OH.
THE MECHANICAL PROPERTY DATA BASE FROM AN AIR FORCE/INDUSTRY COOPERATIVE TEST PROGRAM ON ADVANCED ALUMINUM ALLOYS (IN905XL AND AL905XL FORGINGS) Interim Report, Jan. 1987 - Mar. 1991
Mary A. Phillips and Steven R. Thompson Dec. 1991 156 p
(AF Proj. 2418)
(AD-A247752; WL-TR-91-4132) Avail: NTIS HC/MF A08

The development of a mechanical property database on Inco Alloys International aluminum-lithium structural alloys is detailed. Aluminum-lithium alloys tested were IN905XL Forgings and AL905XL Forgings. Basic mechanical property data consisted of tension, compression, bearing, shear, and fracture toughness. Fatigue data were developed for both smooth and notched specimens. Constant amplitude fatigue crack growth rate data and spectrum test data were generated. Limited corrosion characteristics were also obtained. All other data developed by the participants are documented. GRA

N92-28663# Air Force Academy, CO.
OVERVIEW OF TWO COMMON STATISTICAL COMPUTER PACKAGES: SAS AND BMDP
Kaye A. deRuiz Dec. 1991 20 p
(AD-A245982; USAFA-TR-91-19) Avail: NTIS HC/MF A03

This report provides a brief introduction to two statistical computer packages, SAS and BMDP. The overall approach used by these packages to input data, perform statistical analyses, etc., is discussed. A common data set is provided and used to give examples of programming steps and the corresponding output. Examples of simple statistical computations such as descriptive statistics, linear regression, and analysis of variance, are all presented along with a reference for more advanced techniques. This paper is not meant to replace the associated manuals, but to provide a beginner with enough information to read the manuals easily. GRA

N92-28804# Department of Energy, Washington, DC. Office of Information Resources Management Policy, Plans, and Oversight.
INFORMATION RESOURCES MANAGEMENT LONG-RANGE PLAN
Feb. 1992 260 p
(DE92-012408; DOE/AD-0019) Avail: NTIS HC/MF A12

The Department of Energy (DOE) has consolidated the Information Technology Resources (ITR) plans of its sites into a single document, the Department of Energy Information Resources Management (IRM) Long-Range Plan. This plan is the product of a long-range planning process used to project both future information technology requirements and the resources necessary to meet those requirements. It encompasses the plans of the various organizational components within the Department and its management and operating contractors over the next 5 fiscal years, 1993 through 1997. The annual long-range planning cycle for supporting this plan was initiated by a call in August 1990 for site plans to be submitted in February 1991 by those departmental components and contractors with major ITR requirements. The site plans were reviewed by the appropriate DOE Field Office, the Office of IRM Policy, Plans, and Oversight, program offices, and other senior management officials. During this review process, consideration was given to the validity of the programmatic requirements, the reasonableness of funding estimates, identification and resolution of any issues, and other alternatives available. Publication of this plan is the culmination of the above process. DOE

N92-28832# Sandia National Labs., Albuquerque, NM.
FILES IMPROVEMENT THE NARA WAY
C. Pasterczyk 19 Mar. 1992 5 p Presented at the 1992 Spring Seminar Rio Grande Chapter Association of Records Managers and Administrators, Albuquerque, NM, 19 Mar. 1992
(Contract DE-AC04-76DP-00789)
(DE92-011139; SAND-92-0477C; CONF-9203113-1) Avail: NTIS HC/MF A01

The purpose of this presentation is to set the scene with a definition of records management, records, and federal records. It is also to introduce some techniques to ensure that office files are properly organized and maintained, rapidly retrievable, complete, and ready for appropriate disposition the NARA (National Archives and Records Administration) way. DOE

N92-28838# Los Alamos National Lab., NM.
INFORMATION SYSTEMS FOR ENGINEERING SUSTAINABLE DEVELOPMENT
R. S. Leonard 27 Feb. 1992 35 p Presented at the Workshop

on Engineering Partnerships for Sustainable Development in Conjunction with Prep Con 4 of the United Nations Conference on Environment and Development, New York, NY, 1-3 Mar. 1992
(Contract W-7405-eng-36)
(DE92-011271; LA-UR-92-653; CONF-9203126-1) Avail: NTIS HC/MF A03

The ability of a country to follow sustainable development paths is determined to a large extent by the capacity or capabilities of its people and its institutions. Specifically, capacity-building in the UNCED terminology encompasses the country's human, scientific, technological, organizational, institutional, and resource capabilities. A fundamental goal of capacity-building is to enhance the ability to pose, evaluate, and address crucial questions related to policy choices and methods of implementation among development options. Hence, the United Nations Conference on Environment and Development (UNCED) Agenda 21 planning process has identified the need for better methods by which information can be transferred between industrialized nations and developing nations. The reasons for better methods of information transfer include facilitating decisions related to sustainable development and building the capacity of developing nations to better plan their future in both an economical and environmentally sound manner. This paper is a discussion on mechanisms for providing information and technologies available for presenting the information to a variety of cultures and levels of technical literacy. Consideration is given to access to information technology as well as to the cost to the user. One concept discussed includes an 'Engineering Partnership' which brings together the talents and resources of private consulting engineers, corporations, non-profit professional organizations, government agencies, and funding institution which work in partnership with each other and associates in developing countries. Concepts which are related to information technologies include a hypertext based, user configurable cultural translator, and information navigator and the use of multi-media technologies to educate engineers about the concepts of sustainability, and the adaptation of the concept of metabolism to creating industrial systems. DOE

N92-28866# Systems Exploration, Inc., Dayton, OH.
A THEORY OF AUTOMATED DESIGN OF VISUAL INFORMATION PRESENTATIONS Interim Report, Jun. 1990 - May 1991
Stephen Westfold and Cordell Green Feb. 1992 40 p
(Contract F33615-88-C-0004)
(AD-A247425; AL-TP-1991-0050) Avail: NTIS HC/MF A03

This paper reports on an elaborated theory of graphical display that describes how to automate the generation of tables and diagrams to represent relations occurring in technical data. This theory is an extension and reformulation of our earlier theory. It includes a semantic framework for expressing the translation of relations into graphics. The framework allows for fine-grained control of synthesis and for human factors guidance. Methods are presented for synthesis of multi-page and multi-screen graphics, for the graceful integration of tables and diagrams, for composite maps such as used for color coding, and for development of plot charts. GRA

N92-28955# Electronics Research Lab., Adelaide (Australia).
INFORMATION TECHNOLOGY IN PLAIN WORDS
A. Rattray Jan. 1992 78 p
(AD-A250324; ERL-0594-GD; DODA-AR-006-927) Avail: NTIS HC/MF A05

This document is a glossary of IT-related (Information Technology-related) terms directed specifically at the non-specialist reader. It is not for scientific professionals in any specific area, although their input has been invaluable in compiling this work. Further, it is not a formal Defense glossary in the sense of providing approved formal definitions of terms, and does not replace such definitions. This is a supplementary, and to some extent complementary, work. GRA

N92-28960# Naval Postgraduate School, Monterey, CA.
ANALYSIS OF MULTIMEDIA INFORMATION SYSTEMS FOR THE US COAST GUARD M.S. Thesis
Andrew C. Metcalf Mar. 1992 81 p
(AD-A247890) Avail: NTIS HC/MF A05

This is a descriptive study of multimedia information systems, their current and potential uses, benefits, and drawbacks to provide the basis for implementation of multimedia technology in the U.S. Coast Guard. Multimedia is generally considered to be a mix of text, graphics, sound, and static or full-motion video in an information system. In recent years, there has been a dramatic surge in the introduction of new multimedia products and the integration of multimedia with more conventional computing. These new applications include databases that use video images or audio recordings, teleconferencing, PC based video production editors, and audio/music synthesizers plus many more. Multimedia was found to be a positive development in information technology and is expected to be popularly accepted in very short order. The Coast Guard is not now implementing multimedia in its mainstream information processing functions, although several research and development projects involving multimedia are currently in progress. Recommendations are made for earliest evaluation of the new technology and some general implementation guidelines.
Author (GRA)

N92-29162 Institute for Perception RVO-TNO, Soesterberg (Netherlands). Cognitive Psychology Group.
IS CHOICE ACCURACY RELATED TO INFORMATION SEARCH PATTERNS? Final Report [IS DE JUISTHEID VAN EEN KEUZE GERELATEERD AAN HET INFORMATIEZOEKPATROON?]
J. H. Kerstholt 29 Jul. 1991 19 p Sponsored by TNO Defence Research
(IZF-1991-B-9; TD91-2169; ETN-92-91232) Copyright Avail: TNO Inst. for Perception, Kampweg 5, P.O. Box 23, 3769 ZG Soesterberg, Netherlands

A hypothesis that changing information search patterns, that are observed when task complexity increases, can be explained by an adaptive response to the choice environment, is tested. Two factors are manipulated: task complexity (number of alternatives and number of dimensions) and type of task (a multidimensional task requiring a choice between apartments and a unidimensional task requiring a choice between shopping baskets). Forty subjects made choices by means of computerized information boards. The results show the effects of both complexity and type of task on the information search patterns. The lowest proportion of requested information and the most variable search pattern is observed for the 'apartments' task on the complex conditions. Accuracy remained constant over all complexity conditions. The results suggest that under high task complexity levels subjects try to work smarter rather than harder. Topdown approaches, such as making use of prior knowledge, the structure of the task, and the kind of goal, allow them to maintain accuracy and to avoid the integration of large amounts of information.
ESA

N92-29202*# Jet Propulsion Lab., California Inst. of Tech., Pasadena.
PUBLICATIONS OF THE JET PROPULSION LABORATORY, 1989
15 Dec. 1990 39 p
(Contract NAS7-918)
(NASA-CR-190457; NAS 1.26:190457; JPL-Bibl-39-31) Avail: NTIS HC/MF A03

JPL Bibliography 39-31 describes and indexes by primary author the externally distributed technical reporting, released during calendar year 1989, that resulted from scientific and engineering work performed, or managed, by the Jet Propulsion Laboratory. Three classes of publications are included. The first is JPL Publications (87-, 88-, 89-series, etc.), in which the information is complete for a specific accomplishment. Publications can be tailored to wide or limited audiences and be presented in an established standard format or special format to meet a unique requirement. The second is articles from the quarterly

Telecommunications and Data Acquisition (TDA) Progress Report (42-series). Each collection of articles in this class of publication presents a periodic survey of current accomplishments by the Deep Space Network as well as other developments in Earth-based radio technology. The third is articles published in the open literature. Author

N92-28453*# Alabama Univ., Huntsville. Center for Microgravity and Materials Research.
DEVELOPMENT OF A RESIDUAL ACCELERATION DATA REDUCTION AND DISSEMINATION PLAN
Melissa J. B. Rogers *In* NASA. Lewis Research Center, International Workshop on Vibration Isolation Technology for Microgravity Science Applications May 1992 p 369-382 (For primary document see N92-28436 19-31)
Avail: NTIS HC/MF A18

83 ECONOMICS AND COST ANALYSIS

Includes cost effectiveness studies.

N92-28255# Air Force Inst. of Tech., Wright-Patterson AFB, OH. School of Systems and Logistics.
A REVIEW OF COST PERFORMANCE INDEX STABILITY M.S. Thesis
Scott R. Heise Sep. 1991 95 p
(AD-A246621; AFIT/GSM/LSY/91S-12) Avail: NTIS HC/MF A05

This study examines approaches currently used to determine when Cost Performance Index (CPI) stability occurs. The CPI indicates the cost performance efficiency of the work the contractor has accomplished to date; however it has value as a predictor of future contractor cost performance given that the CPI can be declared stable. Knowing that the CPI is stable allows government personnel to project the final cost of the contract and, if a cost overrun is projected, to determine the likelihood that the contractor can recover. The range method was used to test for stability of cumulative and non-cumulative (three month, six month, and six month moving average) CPI values. The method measured the range of the CPI values that occurred after the 50 percent contract completion point. The results (range method sensitivity analysis) indicated that the cumulative CPI is more stable than the other CPIs examined, stabilizing from the 20 percent completion point. As a caveat however, the method of least squares showed that the cumulative CPI does tend to decline within the allowable range limit as the contract proceeds. Thus the final cumulative CPI value can be expected to be lower than the cumulative CPI value observed at the 20 percent contract completion point. GRA

84 LAW, POLITICAL SCIENCE AND SPACE POLICY

Includes NASA appropriation hearings; aviation law; space law and policy; international law; international cooperation; and patent policy.

No abstracts in this category.

85 URBAN TECHNOLOGY AND TRANSPORTATION

Includes applications of space technology to urban problems; technology transfer; technology assessment; and surface and mass transportation.

For related information see also *03 Air Transportation and Safety, 16 Space Transportation,* and *44 Energy Production and Conversion.*

N92-29108*# Research Inst. for Computing and Information Systems, Houston, TX.
CONSULTING REPORT ON THE NASA TECHNOLOGY UTILIZATION NETWORK SYSTEM
Marjorie M. K. Hlava (Access Innovations, Inc., Albuquerque, NM.) 13 Feb. 1992 16 p Prepared in cooperation with Applied Expertise, Inc., Arlington, VA
(Contract NCC9-16; RICIS Proj. RB-04)
(NASA-CR-190387; NAS 1.26:190387) Avail: NTIS HC/MF A03

The purposes of this consulting effort are: (1) to evaluate the existing management and production procedures and workflow as they each relate to the successful development, utilization, and implementation of the NASA Technology Utilization Network System (TUNS) database; (2) to identify, as requested by the NASA Project Monitor, the strengths, weaknesses, areas of bottlenecking, and previously unaddressed problem areas affecting TUNS; (3) to recommend changes or modifications of existing procedures as necessary in order to effect corrections for the overall benefit of NASA TUNS database production, implementation, and utilization; and (4) to recommend the addition of alternative procedures, routines, and activities that will consolidate and facilitate the production, implementation, and utilization of the NASA TUNS database. Author

88 SPACE SCIENCES (GENERAL)

No abstracts in this category.

89 ASTRONOMY

Includes radio, gamma-ray, and infrared astronomy, and astrometry.

N92-28680*# Smithsonian Astrophysical Observatory, Cambridge, MA.
SCIENTIFIC INVESTIGATIONS WITH THE DATA BASE HEAO-1 SCANNING MODULATOR COLLIMATOR Final Report, 1 Oct. 1984 - 30 Sep. 1991
Daniel A. Schwartz Jun. 1992 48 p
(Grant NAG8-496)
(NASA-CR-190477; NAS 1.26:190477) Avail: NTIS HC/MF A03

The hardware specification for the Scanning Modulation Collimator (MC) experiment on HEAO-1 was to measure positions of bright (greater than 10(exp -11) ergs/cm(exp 2)s), hard (1 to 15 keV) x-ray sources to 5-10 arcsec, and to measure their size and structure in three energy bands down to 10 arcsec resolution. The scientific purpose of this specification was to enable the identification of these x-ray sources with optical and radio objects in order to elucidate the x-ray emission mechanism and the nature of the candidate astronomical system. The experiment was an outstanding success. Hardware systems functioned perfectly although loss of one (out of eight) proportional counters degraded our sensitivity by about 10 percent. Our aspect solution of 7 arcsec precision, allowed us to achieve statistic-limited location precision for all but the strongest sources. We vigorously pursued a strategy of determining the scientific importance of each identification, and of publishing each scientific result as it came along. Author

N92-28781# European Space Agency, Paris (France).
A Be STAR ATLAS OF FAR UV AND OPTICAL HIGH-RESOLUTION SPECTRA
V. Doazan (Observatoire de Paris-Meudon, France), G. Sedmak (Osservatorio Astronomico, Trieste, Italy), M. Barylak (European Space Agency, Villafranca, Spain), L. Rusconi (Trieste Univ., Italy), and Bruce Battrick, ed. Nov. 1991 370 p
(ESA-SP-1147; ISBN-92-9092-025-4; ETN-92-91276) Copyright Avail: NTIS HC/MF A15; ESA, EPD, ESTEC, Noordwijk, Netherlands, HC 75 Dutch guilders

An overview of the spectral characteristics of Be stars in both the far UV and optical wavelength ranges is provided and details of their variable behavior are given when data are available. Line profiles of H alpha and/or H beta are given for the majority of these stars. The Be star variability is illustrated in the broadest possible wavelength range, from 1230 to 3030A. Because Be-Be shell transitions of Ne stars in the optical regions are spectacular and have important modeling implications, it was intended to present a complete Be and Be-shell type spectrum in the far UV. The recent phase transition of Pleione from Be-shell to Be enabled two types of spectra to be presented for the same star. Selected spectral regions containing lines of special interest for Be star modeling are presented for all the Be stars observed with the International Ultraviolet Explorer (IUE) up to 1988; that is, 166 Be stars. ESA

N92-29128# Tuebingen Univ. (Germany, F.R.). Inst. fuer Astronomie.
ANALYSIS OF MIR-HEXE OBSERVATIONS: PULSATION AND ENERGY SPECTRA OF THE X RAY DOUBLE STAR SMC X-1 IN 20 TO 80 keV ENERGY FIELD Thesis [ANALYSE VON MIR-HEXE-BEOBACHTUNGEN: PULSATION UND ENERGIESPEKTRUM DES ROENTGENDOPPELSTERNS SMC X-1 IM ENERGIEBEREICH 20-80 KEV]
Mathias Kunz Nov. 1991 107 p In GERMAN
(ETN-92-91487) Avail: NTIS HC/MF A06

Hardware and software of the x-ray astronomy experiment, and the observations of the x-ray pulsar SMC X1 with HEXE (High Energy X Ray Experiment) are presented. The results of HEXE observations of SMC X1 are discussed with regard to already published observations and theoretical models of the physics of x-ray double stars. Statistical methods for detecting periodical signals, in particular Epoch Folding (EF) and Rayleigh Test (RT) are considered for the pulse period determination of SMC X1. Both methods give the same results. The pulse period of the x-ray signal is determined for three observation groups. It is found that hydrogen absorption by the material compassing the neutron stars is low. ESA

N92-29177# Tuebingen Univ. (Germany, F.R.). Inst. fuer Astronomie.
CALIBRATION OF HIGH ENERGY X RAY DETECTORS AT THE SPECTRUM OF THE CRAB NEBULA, AND X RAY PULSAR A0535+26 EXAMINATIONS Thesis [KALIBRATION VON HOCHENERGIEROENTGENDETEKTOREN AM SPEKTRUM DES CRAB-NEBELS UND UNTERSUCHUNGEN AM ROENTGENPULSAR A0535+26]
Peter Kretschmar Jul. 1991 106 p In GERMAN
(ETN-92-91484) Avail: NTIS HC/MF A06

A series of observations for the transient pulsar A0535+26 were analyzed with regard to the x ray spectrum and the pulse behavior of the source. The first spectral Crab examinations gave an extremely hard Crab spectrum, far from other published results, and great deviations between the theoretical law and measuring data, in particular at the lower edge of the High Energy X-ray Experiment (HEXE) energy field. The proper calibration parameters were tentatively determined, using existing data and Crab nebula measurement. The pulse period of the source was determined as P equal to 103.244 +/- 0.008 seconds. ESA

90 ASTROPHYSICS

Includes cosmology; celestial mechanics; space plasmas; and interstellar and interplanetary gases and dust.
For related information see also *75 Plasma Physics*.

N92-28774# Fermi National Accelerator Lab., Batavia, IL.
THE PHYSICS OF STRANGE MATTER
A. V. Olinto (Chicago Univ., IL.) Dec. 1991 27 p Presented at the Relativistic Aspects of Nuclear Physics, Rio de Janeiro (Brazil), 2-30 Aug. 1991
(Contracts DE-AC02-76CH-03000; DE-FG02-91ER-40606)
(DE92-011734; FNAL/C-91/349-A; CONF-9108186-3) Avail: NTIS HC/MF A03

Strange matter may be the ground state of matter. We review the phenomenology and astrophysical implications of strange matter, and discuss the possible ways for testing the strange matter hypothesis. DOE

N92-28843# Massachusetts Univ., Amherst. Dept. of Physics and Astronomy.
OBSERVATIONAL STUDY AND ANALYSIS OF POINT SOURCES FOUND BY THE INFRARED ASTRONOMY SATELLITE Final Technical Report, 1 Dec. 1987 - 30 Apr. 1991
S. G. Kleinmann 30 Apr. 1991 15 p
(Grant AF-AFOSR-0070-88)
(AD-A248416; AFOSR-92-0194TR) Avail: NTIS HC/MF A03

Results are presented of studies of the space distribution and other properties of two significant classes of compact astrophysical sources which are bright at midinfrared wavelengths: stars with excess infrared emission due to heated dust, and galaxies with nuclei that heat surrounding dust to anomalously high temperatures. The stellar studies reveal a complex structure for the galactic disk, which must be taken into account in the development of realistic infrared sky models. The extragalactic studies have been temporarily stalled by the remarkable discovery of low-luminosity stars with strong far-infrared spectral energy distributions mimicking warm galaxies. Much further observational work is needed to understand the origin of this emission. GRA

N92-28859# Fermi National Accelerator Lab., Batavia, IL.
QUARK MATTER AND COSMOLOGY
D. N. Schramm (Chicago Univ., IL.), B. Fields, and D. Thomas (Chicago Univ., IL.) Jan. 1992 16 p Presented at the Quark Matter 1991, Gatlinburg, TN, 11-15 Nov. 1991
(Contracts DE-AC02-76CH-03000; DE-FG02-91ER-40606)
(DE92-011736; FNAL/C-92/20-A; CONF-9111165-12) Avail: NTIS HC/MF A03

The possible implications of the quark-hadron transition for cosmology are explored. Possible surviving signatures are discussed. In particular, the possibility of generating a dark matter candidate such as strange nuggets or planetary mass black holes is noted. Much discussion is devoted to the possible role of the transition for cosmological nucleosynthesis. It is emphasized that even an optimized first order phase transition will not significantly alter the nucleosynthesis constraints on the cosmological baryon density nor on neutrino counting. However, it is noted that Be and B observations in old stars may eventually be able to be a signature of a cosmologically significant quark-hadron transition. It is pointed out that the critical point in this regard is whether the observed B/Be ratio can be produced by spallation processes or requires cosmological input. Spallation cannot produce a B/Be ratio below 7.6. A supporting signature would be Be and B ratios to oxygen that greatly exceed galactic values. At present, all data is still consistent with a spallagenic origin. DOE

N92-29127# Tuebingen Univ. (Germany, F.R.). Inst. fuer Astronomie.
THERMAL ACCRETION DISK MODELS FOR ACTIVE GALAXIES Thesis [THERMISCHE AKKRETIONSSCHEIBENMODELLE FUER AKTIVE GALAXIEN]
Thomas Doerrer Oct. 1991 94 p In GERMAN
(ETN-92-91486) Avail: NTIS HC/MF A05

The thermal emission of accretion disks in Active Galactic Nuclei (AGN) is examined. Medium broadband AGN spectra are shown in order to explain the emission mechanism proposed. Basic behaviors from radiation theory and from hydrodynamics of importance for the calculations are represented. The spectrum of the accretion disk is determined. ESA

N92-29184# Fermi National Accelerator Lab., Batavia, IL.
INVERSE PHASE TRANSITIONS: DOES BARYOGENESIS LEAD TO DARK MATTER?
S. Dodelson, B. R. Greene (Cornell Univ., Ithaca, NY.), and L. M. Widrow (Toronto Univ., Ontario) Feb. 1992 8 p Presented at the 15th Johns Hopkins Workshop on Current Problems in Particle Theory, Baltimore, MD, 26-28 Aug. 1991
(Contract DE-AC02-76CH-03000)
(DE92-013022; FNAL/C-92/72-A; CONF-9108175-3; CLNS-92-1133) Avail: NTIS HC/MF A02

The phase structure of a field theory can have two qualitatively different forms- the less familiar of which involves high temperature symmetry breaking and low temperature symmetry restoration and is dubbed an inverse phase transition. After a general discussion of such inverse phase transitions, we present an application of this phenomenon in which the symmetry under consideration is baryon number. The model has the virtues of generating the observed quark-antiquark asymmetry (with no explicit baryon number violating interactions) while simultaneously providing the dark matter known to exist in galactic halos and clusters of galaxies. Constraints from cosmology and particle physics highly constrain the mass of this dark matter candidate: 40GeV less than m(sub phi) less than 50GeV. In this way we demonstrate our main conclusion: the exotic phase structure of the inverted form can give rise to novel, predictive and testable cosmological phenomenon. DOE

91 LUNAR AND PLANETARY EXPLORATION

Includes planetology; and manned and unmanned flights. For spacecraft design or space stations see *18 Spacecraft Design, Testing and Performance.*

N92-28345*# National Aeronautics and Space Administration, Washington, DC.
PLANETARY GEOSCIENCES, 1989-1990
Maria T. Zuber, ed. (National Aeronautics and Space Administration. Goddard Space Flight Center, Greenbelt, MD.), Odette B. James, ed. (Geological Survey, Washington, DC.), Jonathan I. Lunine, ed. (Arizona Univ., Tucson.), Glenn J. MacPherson, ed. (Smithsonian Institution, Washington, DC.), and Roger J. Phillips, ed. (Southern Methodist Univ., Dallas, TX.) 1992 81 p LIMITED REPRODUCIBILITY: More than 20% of this document may be affected by color photographs Original contains color illustrations
(NASA-SP-508; NAS 1.21:508; LC-91-33408; ISBN-0-16-036173-7) Avail: NTIS HC/MF A05; 18 functional color pages

NASA's Planetary Geosciences Programs (the Planetary Geology and Geophysics and the Planetary Material and Geochemistry Programs) provide support and an organizational framework for scientific research on solid bodies of the solar system. These research and analysis programs support scientific research aimed at increasing our understanding of the physical, chemical, and dynamic nature of the solid bodies of the solar system: the Moon, the terrestrial planets, the satellites of the outer planets, the rings, the asteroids, and the comets. This research is conducted using a variety of methods: laboratory experiments, theoretical approaches, data analysis, and Earth analog techniques. Through research supported by these programs, we are expanding our understanding of the origin and evolution of the solar system. This document is intended to provide an overview of the more significant scientific findings and discoveries made this year by scientists supported by the Planetary Geosciences Program. To a large degree, these results and discoveries are the measure of success of the programs. Author

N92-28393# Naval Postgraduate School, Monterey, CA.
TRADE STUDY OF THREE OXYGEN PROCESSORS FOR THE MARTIAN ATMOSPHERE M.S. Thesis
Steven R. Plystak Sep. 1991 80 p
(AD-A246854) Avail: NTIS HC/MF A05

This thesis is focused toward the Mars atmosphere and its potential resource use for life support systems which provide oxygen to astronauts during all phases of a mission. The weight required to send numerous oxygen tanks to Mars would drastically increase the cost of the mission and might even take up space in the rocket for other needed items on Mars. The solution to this problem is to design a processor that will convert Martian resources to oxygen. Utilization of resources to support life in the Martian environment is performed through the development of life support systems. Life support systems which provide oxygen belong to the Air Revitalization functional area of the Environmental Control Life Support System for Space Station Freedom which will be analyzed in this thesis. Since the Martian atmosphere is primarily composed of carbon dioxide, this thesis will look at three oxygen processors under development which will convert carbon dioxide to oxygen. These three candidate technologies are the Electrochemical Oxide Cell, Sabatier, and Bosch carbon dioxide reductors. The oxide cell is a self-containing carbon dioxide to oxygen system, but the other two produce water. This suggests that other subsystems must be attached to the output to produce oxygen from water. A trade study is performed using parameters such as power, weight, mass, etc. in order to find the most suitable oxygen processor for the Martian atmosphere. The trade study suggests that the electrolyte oxide cell is the most effective alternative. GRA

N92-28478*# Lunar and Planetary Inst., Houston, TX. MSATT Study Group.
PAPERS PRESENTED TO THE WORKSHOP ON THE EVOLUTION OF THE MARTIAN ATMOSPHERE Abstracts Only
1992 37 p Workshop held in Kona, Hawaii, 29 Jun. - 1 Jul. 1992
(Contract NASw-4574)
(NASA-CR-190508; NAS 1.26:190508; LPI-Contrib-787) Avail: NTIS HC/MF A03

This volume contains papers that have been accepted for the Workshop on the Evolution of the Martian Atmosphere. The abstracts presented in the paper cover such topics as: modeling of the mars atmosphere from early development to present including specific conditions affecting development; studies of various atmospheric gases such as O2, SO2, CO2, NH3, and nitrogen; meteorite impacts and their effects on the atmosphere; and water inventories and cycles. For individual titles, see N92-28479 through N92-28510.

N92-28479*# California Inst. of Tech., Pasadena. Div. of Geological and Planetary Sciences.
THE IMPACT OF TEMPERATURE DEPENDENT CO2 CROSS SECTION MEASUREMENTS: A ROLE FOR HETEROGENEOUS CHEMISTRY IN THE ATMOSPHERE OF MARS? Abstract Only
A. D. Anbar, M. Allen, H. Nair, M-T. Leu, and Y. L. Yung *In* Lunar and Planetary Inst., Papers Presented to the Workshop on the Evolution of the Martian Atmosphere 1992 p 1 (For primary document see N92-28478 19-91)
Avail: NTIS HC/MF A03

Carbon dioxide comprises over 95 percent of the Mars atmosphere, despite continuous photolysis of CO2 by solar ultraviolet (UV) radiation. Since the direct recombination of CO and O is spinforbidden, the chemical stability of CO2 in the Martian atmosphere is thought to be the result of a HO(x)-catalyzed recombination scheme. Thus the rate of CO oxidation is sensitive to the abundance and altitude distribution of OH, H, and HO2. Most Martian atmospheric models assume that HO(x) abundances are governed purely by gas phase chemistry. However, it is well

established that reactive HO(x) radical are adsorbed by a wide variety of surfaces. The authors have combined laboratory studies of H, OH, and HO2 adsorption on inorganic surfaces, observational data of aerosol distributions, and an updated photochemical model to demonstrate that adsorption on either dust or ice aerosols is capable of reducing HO(x) abundances significantly, thereby retarding the rate of CO oxidation. H.A.

N92-28480*# Jet Propulsion Lab., California Inst. of Tech., Pasadena.
SURFACE VS. ATMOSPHERIC ORIGIN OF 2.1-2.5 MICRON ABSORPTION FEATURES IN THE MARTIAN SPECTRUM Abstract Only
James F. Bell, III (Hawaii Univ., Honolulu.) and David Crisp *In* Lunar and Planetary Inst., Papers Presented to the Workshop on the Evolution of the Martian Atmosphere 1992 p 1-3 (For primary document see N92-28478 19-91)
Avail: NTIS HC/MF A03

For 20 years the origin of subtle absorption features in the spectrum of Mars near 2.3 micro-m ('K' band: 1.9-2.5 micro-m) has been debated. This spectral region contains gaseous absorption features predominantly from CO2 and CO on Mars and from telluric H2O and CO2. The authors have obtained new higher spectral resolution telescopic K band spectra of 10 surface regions using the Infrared Telescope Facility (IRTF) at Mauna Kea during 1990. The goals were to confirm the existence of broad features seen at lower spectral resolution and to determine whether these bands are caused by atmospheric gases, surface (or airborne dust) minerals, or a combination of both. H.A.

N92-28481*# Pennsylvania State Univ., University Park. Dept. of Geosciences.
PHOTOCHEMICAL MODEL FOR NH3 IN AN EARLY MARTIAN ATMOSPHERE Abstract Only
L. L. Brown and J. F. Kasting *In* Lunar and Planetary Inst., Papers Presented to the Workshop on the Evolution of the Martian Atmosphere 1992 p 3 (For primary document see N92-28478 19-91)
Avail: NTIS HC/MF A03

A warm and wet climate scenario for early Mars has been explained by invoking a 5-bar CO2 atmosphere; however, Kasting has shown that CO2 will condense in the Martian atmosphere at these pressures. The formation of CO2 clouds will reduce the convection lapse rate and reduce the magnitude of the greenhouse effect. It is possible that additional greenhouse gases such as methane and ammonia were present in the early Mars atmosphere. We are using a one dimensional photochemical model to estimate the magnitude of the ammonia source required to maintain a given ammonia concentration in a dense CO2 atmosphere. Because CO2 is 2.5 times more efficient at Rayleigh scattering than Earth's N2 atmosphere, we anticipate increased scattering opacities and decreased photolytic destruction rates of ammonia on early Mars. The reduced gravity on Mars means that a 1 bar atmosphere will be approximately 3 times as thick as on Earth. It is possible that ammonia could have been shielded from photolysis by hydrocarbon aerosols which form as a product of methane photolysis. Author

N92-28482*# Massachusetts Inst. of Tech., Cambridge. Dept. of Earth, Atmospheric and Planetary Sciences.
OXYGEN IN THE MARTIAN ATMOSPHERE: REGULATION OF PO2 BY THE DEPOSITION OF IRON FORMATIONS ON MARS Abstract Only
Roger G. Burns *In* Lunar and Planetary Inst., Papers Presented to the Workshop on the Evolution of the Martian Atmosphere 1992 p 3-5 (For primary document see N92-28478 19-91)
Avail: NTIS HC/MF A03

During Earth's early history, and prior to the evolution of its present day oxygenated atmosphere, extensive iron rich siliceous sedimentary rocks were deposited, consisting of alternating layers of silica (chert) and iron oxide minerals (hematite and magnetite). The banding in iron formations recorded changes of atmosphere-hydrosphere interactions near sea level in the ancient ocean, which induced the oxidation of dissolved ferrous iron, precipitation of insoluble ferric oxides and silica, and regulation of oxygen in Earth's early atmosphere. Similarities between the Archean Earth and the composition of the present day atmosphere on Mars, together with the pervasive presence of ferric oxides in the Martian regolith suggest that iron formation might also have been deposited on Mars and influenced the oxygen content of the Martian atmosphere. Such a possibility is discussed here with a view to assessing whether the oxygen content of the Martian atmosphere has been regulated by the chemical precipitation of iron formations on Mars. H.A.

N92-28483*# Geological Survey, Menlo Park, CA.
WATER INVENTORIES ON EARTH AND MARS: CLUES TO ATMOSPHERE FORMATION Abstract Only
M. H. Carr *In* Lunar and Planetary Inst., Papers Presented to the Workshop on the Evolution of the Martian Atmosphere 1992 p 6 (For primary document see N92-28478 19-91)
Avail: NTIS HC/MF A03

Water is distributed differently on Earth and on Mars and the differences may have implications for the accretion of the two planets and the formation of their atmospheres. The Earth's mantle appears to contain at least several times the water content of the Martian mantle even accounting for differences in plate tectonics. One explanation is that the Earth's surface melted during accretion, as a result of development of a steam atmosphere, thereby allowing impact-devolitalized water at the surface to dissolve into the Earth's interior. In contrast, because of Mars' smaller size and greater distance from the Sun, the Martian surface may not have melted, so that the devolatilized water could not dissolve into the surface. A second possibility is suggested by the siderophile elements in the Earth's mantle, which indicates the Earth acquired a volatile-rich veneer after the core formed. Mars may have acquired a late volatile-rich veneer, but it did not get folded into the interior as with the Earth, but instead remained as a water rich veneer. This perception of Mars with a wet surface but dry interior is consistent with our knowledge of Mars' geologic history. Author

N92-28484*# Centre National de la Recherche Scientifique, Meudon-Bellevue (France). Lab. de Geographie Physique.
DISTRIBUTION OF MARTIAN GROUND-ICE TABLE: PRELIMINARY RESULTS ABOUT CLIMATIC VARIATIONS Abstract Only
F. M. Costard *In* Lunar and Planetary Inst., Papers Presented to the Workshop on the Evolution of the Martian Atmosphere 1992 p 6-7 (For primary document see N92-28478 19-91)
Avail: NTIS HC/MF A03

Rampart craters seem to have been emplaced by flows around craters over the surface just after the impact event by melting of volatiles. Such rampart craters are considered to be good ground-ice indicators. A map shows a latitudinal distribution of Martian ground-ice with a deep ground-ice table at equatorial latitudes and subsurface ground-ice tables at mid and high latitudes. Some studies suggest the presence of large amounts of ground-ice on Mars, with near surface ground-ice in the northern plains and a permafrost at low latitudes containing a large amount of volatiles at depth. Spatial variations in the spin axis of the planet affect the latitudinal distribution of the Sun's isolation, and therefore the Martian ground-ice distribution. H.A.

N92-28485*# National Air and Space Museum, Washington, DC. Center for Earth and Planetary Studies.
NATURE AND EVOLUTION OF THE EARLY MARTIAN ATMOSPHERE: EVIDENCE FROM HIGHLAND CRATER POPULATIONS Abstract Only
Robert A. Craddock and Ted A. Maxwell *In* Lunar and Planetary Inst., Papers Presented to the Workshop on the Evolution of the Martian Atmosphere 1992 p 7-8 (For primary document see N92-28478 19-91)
Avail: NTIS HC/MF A03

Release of water in a CO2 rich atmosphere by precipitation and channel forming processes has led to speculation on the creation of Martian carbonate deposits. On Mars water probably was not on the surface long enough to allow eroded material to

concentrate, raise the pH, and induce the formation of carbonates. This suggests that the Martian primordial atmosphere could be thinner (approximately 5 bars) and still allow highland degradation to occur over a long period of time (.45 to 1.2 billion years).
H.A.

N92-28486*# Los Alamos National Lab., NM. Space Plasma Physics Group.
AN ION MASS SPECTROMETER FOR MEASURING ISOTOPIC ADUNDANCES AND LOSS RATES OF O, C AND H IN MARS' UPPER ATMOSPHERE Abstract Only
R. C. Elphic, B. L. Barraclough, D. J. McComas, and J. E. Nordholt *In* Lunar and Planetary Inst., Papers Presented to the Workshop on the Evolution of the Martian Atmosphere 1992 p 8-9 (For primary document see N92-28478 19-91)
Avail: NTIS HC/MF A03

The history of Mars' climate is clearly intimately linked to the evolution of its store of volatiles, particularly H2O, and CO2. The global CO2-H2O system is complex, with a number of production, loss, exchange, and buffering mechanisms operating between the atmosphere and the surface. For example, loss of these volatiles takes place through solar wind interaction with the upper atmosphere/ionosphere, ionospheric chemistry, and thermal escape. The atmospheric water inventory is, in turn, influenced by the exchange with polar water ice deposits and high latitude ground-ice. Atmospheric CO2, on the other hand, can be lost through adsorption in the regolith and in the formation of carbonates. Finally, oxygen is exchanged between atmospheric CO2 and H2O. Author

N92-28487*# Washington Univ., Saint Louis, MO. Dept. of Earth and Planetary Sciences.
CHEMICAL MODELS OF VOLCANIC OUTGASSING ON MARS Abstract Only
Bruce Fegley, Jr. *In* Lunar and Planetary Inst., Papers Presented to the Workshop on the Evolution of the Martian Atmosphere 1992 p 9-11 (For primary document see N92-28478 19-91)
Avail: NTIS HC/MF A03

During the MSATT workshop in Boulder, CO, several participants emphasized the importance of constraints on the composition and temporal evolution of outgassed volatiles on Mars. I present the results of some preliminary calculations that model the composition of volcanic gases as a function of temperature, pressure, oxygen fugacity, and quench function of temperature. These results can be used in combination with cosmochemical models for the accretion of Mars to assess the plausibility of different atmospheric compositions during the planet's early history. Author

N92-28488*# Los Alamos National Lab., NM.
REDISTRIBUTION OF SUBSURFACE NEUTRONS CAUSED BY GROUND ICE ON MARS Abstract Only
W. C. Feldman, W. V. Boynton (Arizona Univ., Tucson.), B. M. Jakosky (Colorado Univ., Boulder.), and M. T. Mellon (Colorado Univ., Boulder.) *In* Lunar and Planetary Inst., Papers Presented to the Workshop on the Evolution of the Martian Atmosphere 1992 p 11-12 (For primary document see N92-28478 19-91)
Avail: NTIS HC/MF A03

The purpose of this study is to build on that of Squyres and Evans to approach the specific problem of the buried ice deposits explored by Mellon and Jakosky. Therefore, we calculated the depth dependence of equilibrium neutron energy spectra and related neutron-capture gamma ray production rates for a semi-infinite layer of regolith having a Chryse-fines composition containing 5, 10, and 18 wt percent of water. This high water-content layer was buried beneath the same regolith containing 1 percent water at depths of 20, 40, and 80 g/ sq. cm. A 16-g/sq. cm atmosphere having the abundances measured by Owen et al. was included throughout. We also calculated the effects of a 30-g/sq. cm-thick layer containing 18 percent water embedded within a semi-finite regolith containing 1 percent water, at depths of 20, 40, and 80 g/sq. cm below the atmosphere-surface interface. Author

N92-28489*# State Univ. of New York, Plattsburgh. Dept. of Physics.
TIME VARIATION OF THE METEORITIC CONTRIBUTION TO THE ATMOSPHERE OF MARS Abstract Only
G. J. Flynn *In* Lunar and Planetary Inst., Papers Presented to the Workshop on the Evolution of the Martian Atmosphere 1992 p 12-13 (For primary document see N92-28478 19-91)
Avail: NTIS HC/MF A03

The meteoritic contribution to the planets of the inner solar system varies significantly with time. During the first billion years, the flux of meteoritic material was significantly greater than present. Over the past 3.6 billion years, the background flux has been relatively constant, but shorter periods of significantly enhanced flux are associated with discrete events such as major impacts of large bodies onto the planets or their moons and passage through cometary debris streams. The topics covered include the following (1) the last 3.6 billion years; (2) large impacts; (3) passage through comet tail; and (4) major collision in the main-belt. Author

N92-28490*# State Univ. of New York, Stony Brook. Inst. for Terrestrial and Planetary Atmospheres.
THE PRODUCTION AND ESCAPE OF NITROGEN ATOMS ON MARS Abstract Only
J. L. Fox *In* Lunar and Planetary Inst., Papers Presented to the Workshop on the Evolution of the Martian Atmosphere 1992 p 13-14 (For primary document see N92-28478 19-91)
Avail: NTIS HC/MF A03

The lack of agreement between our previously computed values and those measured by Viking of the N-15:N-14 isotope enhancement ratio has led us to reevaluate our model of the Martian ionosphere. In previous models, we were unable to reproduce the ion profiles measured by the RPA on Viking using electron temperatures that were higher that the ion temperatures. When we increased the electron temperatures to 2500-3000 K and with a zero flux upper boundary condition, the ion densities at high altitudes exceeded the measured values by a large factor. We found that we can better fit the observed profiles if we impose a loss process at the upper boundary of our model. If the horizontal fluxes of ions do not constitute a net loss of ions, then the escape of N due to dissociative recombination is also inhibited and better agreement with the measured isotope ratio is found. The production of escaping nitrogen atoms is closely related to the production of thermospheric odd nitrogen; therefore, the densities of NO measured by Viking provide a convenient check on our nitrogen escape model. Our standard model NO densities are less that the measured values by a factor of 2-3, as are those of previous models. We find that reasonable agreement can be obtained by assuming that the rate coefficient for loss of odd nitrogen in the reaction of N with NO is smaller at temperatures that prevail in the lower Martian thermosphere than the standard value, which applies to temperatures of 200-400 K. Other aspects of this investigation are presented. Author

N92-28491*# National Aeronautics and Space Administration. Ames Research Center, Moffett Field, CA.
HIGH PRESSURE EXPERIMENTS WITH A MARS GENERAL CIRCULATION MODEL Abstract Only
R. M. Haberle, J. B. Pollack, J. R. Murphy, J. Schaeffer, and H. Lee *In* Lunar and Planetary Inst., Papers Presented to the Workshop on the Evolution of the Martian Atmosphere 1992 p 14-15 (For primary document see N92-28478 19-91)
Avail: NTIS HC/MF A03

The interaction of three physical processes will determine the stability of the Martian polar caps as the surface pressure increases: the greenhouse effect, atmospheric heat transport, and the change in the CO2 frost point temperature. The contribution of each is readily determined in the Mars general circulation model (GCM). Therefore, we have initiated experiments with the GCM to determine how these processes interact, and how the atmosphere-polar cap system responds to increasing surface pressure. The experiments are carried out for northern winter solstice and generally assume the atmosphere to be free of dust. Each experiment starts from resting isothermal conditions and runs for 50 Mars days. Mars'

current orbital parameters are used. The experiments are for surface pressures of 120, 480, and 960 mb, which represent 16, 64, and 128 times the current value. To date we have analyzed the 120 mb experiment and the results indicate the contrary to the simpler models, the polar caps actually advance instead of retreat. Other aspects of this investigation are presented. Author

N92-28492*# Colorado Univ., Boulder. Lab. for Atmospheric and Space Physics.
MARS VOLATILE EVOLUTION: IMPLICATIONS OF THE RECENT MEASUREMENT OF O-17 IN WATER FROM THE SNC METEORITES Abstract Only
Bruce M. Jakosky *In* Lunar and Planetary Inst., Papers Presented to the Workshop on the Evolution of the Martian Atmosphere 1992 p 15 (For primary document see N92-28478 19-91)
Avail: NTIS HC/MF A03

Oxygen, carbon, and hydrocarbon isotopes in water and carbon dioxide in the Martian environment can fractionate due to processes involving escape to space, exchange between atmospheric and non-atmospheric species, and exchange of atoms between different molecules. As a result, the ratios of O-18/O-17/O-16, C-13/C-12 and D/H in atmospheric and surface species are sensitive indicators of the integrated effects of outgassing and volatile evolution over geologic time. Previously, I summarized all of the available observations of isotopic abundances and compared them with models of fractionation in order to see which scenarios of volatile evolution were most plausible. Presently, I have included in the models the possible evolution of O-17 due to loss to space in order to see whether these measurements are consistent with various scenarios for atmospheric evolution. Author

N92-28493*# Colorado Univ., Boulder. Lab. for Atmospheric and Space Physics.
THE MARS WATER CYCLE AT OTHER EPOCHS: HISTORY OF THE POLAR CAPS AND LAYERED TERRAIN Abstract Only
Bruce M. Jakosky, Bradley G. Henderson, and Michael T. Mellon *In* Lunar and Planetary Inst., Papers Presented to the Workshop on the Evolution of the Martian Atmosphere 1992 p 15-16 (For primary document see N92-28478 19-91)
Avail: NTIS HC/MF A03

The atmospheric water cycle at the present epoch involves summertime sublimation of water from the north polar cap, transport of water through the atmosphere, and condensation on one or both winter CO2 caps. Exchange with the regolith is important seasonally, but the water content of the atmosphere appears to be controlled by the polar caps. The net annual transport through the atmosphere, integrated over long timescales, must be the driving force behind the long-term evolution of the polar caps; clearly, this feeds back into the evolution of the layered terrain. We have investigated the behavior of the seasonal water cycle and the net integrated behavior at the pole for the last 10 exp 7 years. Our model of the water cycle includes the solar input, CO2 condensation and sublimation, and summertime water sublimation through the seasonal cycles, and incorporates the long-term variations in the orbital elements describing the Martian orbit. Author

N92-28494*# National Aeronautics and Space Administration. Marshall Space Flight Center, Huntsville, AL.
MARS GLOBAL REFERENCE ATMOSPHERE MODEL (MARS-GRAM) Abstract Only
C. G. Justus (Georgia Inst. of Tech., Atlanta.) and Bonnie F. James *In* Lunar and Planetary Inst., Papers Presented to the Workshop on the Evolution of the Martian Atmosphere 1992 p 16-17 (For primary document see N92-28478 19-91)
Avail: NTIS HC/MF A03

Mars-GRAM is an empirical model that parameterizes the temperature, pressure, density, and wind structure of the Martian atmosphere from the surface through thermospheric altitudes. In the lower atmosphere of Mars, the model is built around parameterizations of height, latitudinal, longitudinal, and seasonal variations of temperature determined from a survey of published measurements from the Mariner and Viking programs. Pressure and density are inferred from the temperature by making use of the hydrostatic and perfect gas laws relationships. For the upper atmosphere, the thermospheric model of Stewart is used. A hydrostatic interpolation routine is used to insure a smooth transition from the lower portion of the model to the Stewart thermospheric model. Other aspects of the model are discussed. Author

N92-28495*# Pennsylvania State Univ., University Park. Dept. of Geosciences.
A REDUCED ATMOSPHERE FOR EARLY MARS? Abstract Only
J. F. Kasting *In* Lunar and Planetary Inst., Papers Presented to the Workshop on the Evolution of the Martian Atmosphere 1992 p 17-18 (For primary document see N92-28478 19-91)
Avail: NTIS HC/MF A03

One-dimensional, radiative-convective climate calculations indicate that the old model of a warm, dense, CO2 atmosphere on early Mars is no longer viable. The magnitude of the greenhouse effect in a CO2/H2O atmosphere is limited by condensation of CO2 clouds; this phenomenon is not important for Mars today, but has a pronounced cooling effect at the low solar luminosities thought to apply during early solar system history. The failure of this model indicates one of four things: (1) the new climate calculations are incorrect; (2) current solar evolution models are incorrect; (3) the idea that early Mars was warm and wet is incorrect; or (4) the atmosphere of early Mars contained other greenhouse gases (or particles) in addition to CO2 and H2O. Of these explanations, the most plausible is number (4) and the rest of the investigation is a further explanation of number (4). Author

N92-28496*# Warsaw Univ. (Poland). Inst. of Geophysics.
INFLUENCES OF CO2 SUBLIMATION/CONDENSATION PROCESSES ON THE LONG-TERM EVOLUTION OF THE MARTIAN ATMOSPHERE Abstract Only
K. Kossacki and J. Leliwa-Kopystynski *In* Lunar and Planetary Inst., Papers Presented to the Workshop on the Evolution of the Martian Atmosphere 1992 p 18 (For primary document see N92-28478 19-91)
Avail: NTIS HC/MF A03

The accumulation process of frozen CO2 within the Martian regolith is analyzed. The boundary conditions are taken to be the periodically variable temperature at the Mars surface and the constant heat flux at the bottom of the regolith layers, some hundred meters thick. The mean value of temperature as well as its amplitude are assumed to be dependent on latitude and could be variable with the geological time scale. The flux of gaseous CO2 within the regolith is controlled by the mechanism of gas transport through the porous medium. An appropriate initial geometry of distribution of pores is assumed. The porosity and flux change due to condensation/sublimation processes. The equations of heat and mass transfer are solved numerically for a given latitude. Next, the local (over the parallel of latitude belt) annual balance of CO2 is calculated. The procedure is repeated over the whole Martian surface and next the total annual net flux is calculated. Author

N92-28497*# Alberta Univ., Edmonton. Dept. of Geology.
CO2 AND CLATHRATE AS PAST EROSIVE AGENTS ON MARS Abstract Only
R. St.J. Lambert and V. E. Chamberlain (Idaho Univ., Moscow.) *In* Lunar and Planetary Inst., Papers Presented to the Workshop on the Evolution of the Martian Atmosphere 1992 p 18-19 (For primary document see N92-28478 19-91)
Avail: NTIS HC/MF A03

The debate on the history of the Martian atmosphere continues without resolution. Much hinges on a satisfactory solution to the problem of what liquid was responsible for the extensive development of canyons, channels, fretted terrain, and similar features. The 1960s and 1970s saw much debate about the roles of various fluids, namely water or brine, liquid CO2, or H2O sources in CO2 clathrate (CC), or magma. The last was discounted long ago, CC is largely ignored, and the most recent look at CO2 was

by ourselves, utilizing the phase diagrams for the CO2-H2O system. In this article, we will further investigate this dilemma. Author

N92-28498*# California Univ., Los Angeles. Inst. of Geophysics and Planetary Physics.
HISTORY OF OXYGEN AND CARBON ESCAPE FROM THE MARTIAN ATMOSPHERE Abstract Only
J. G. Luhmann, M. H. G. Zhang (Academy of Sciences, Graz, Austria), R. E. Johnson (Virginia Univ., Charlottesville.), S. W. Bougher (Arizona Univ., Tucson.), and A. F. Nagy (Michigan Univ., Ann Arbor.) *In* Lunar and Planetary Inst., Papers Presented to the Workshop on the Evolution of the Martian Atmosphere 1992 p 19-20 (For primary document see N92-28478 19-91)
Avail: NTIS HC/MF A03

A fraction of the oxygen in the Martian atmosphere continually escapes to space because dissociative recombination of the O2(+) ions in the ionosphere can impart sufficient energy to the product O atoms. In addition, ionization of the extended atomic oxygen corona resulting from the above process adds to escape since the solar wind can carry away O(+) ions born above a few hundred km altitude. A further by-product of this ion-pickup by the solar wind is an additional population of escaping oxygen atoms that are sputtered from the atmosphere near the exobase by pickup ions that are on reentry rather than escaping trajectories. This sputtering process can also remove carbon in the form of intact or dissociated CO2 since all atoms and molecules in the 'target' gas are subject to the collisional energy transfer that characterizes sputtering. We have estimated the present rates of escape of oxygen and carbon due to these mechanisms, as well as the rates at several epochs in the history of the solar system.
Author

N92-28499*# Lowell Observatory, Flagstaff, AZ.
USING THE HISTORICAL RECORD TO DETERMINE DUST SOURCES Abstract Only
L. J. Martin *In* Lunar and Planetary Inst., Papers Presented to the Workshop on the Evolution of the Martian Atmosphere 1992 p 20 (For primary document see N92-28478 19-91)
Avail: NTIS HC/MF A03

We have recently completed a study of virtually all reported dust activity noted in contemporary and historical records of Mars observations. This study included the compilation of maps showing the locations of these events to the degree that they could be determined. Whenever possible, regional (major) storms were individually mapped, as well as on a composite map. Areas of local events were shown only on a composite map. The four mappable plane-encircling storms were each given separate treatment on maps that portray their development around the planet. Author

N92-28500*# National Aeronautics and Space Administration. Ames Research Center, Moffett Field, CA.
LIQUID WATER HABITATS ON EARLY MARS Abstract Only
Christopher P. McKay and Wanda L. Davis *In* Lunar and Planetary Inst., Papers Presented to the Workshop on the Evolution of the Martian Atmosphere 1992 p 21 (For primary document see N92-28478 19-91)
Avail: NTIS HC/MF A03

Although the Viking results may indicate that Mars has no life today, the possibility exists that Mars may hold the best record of the events that led to the origin of life. There is direct geomorphological evidence that in the past Mars had large amounts of liquid water on its surface. Atmospheric models would suggest that this early period of hydrological activity was due to the presence of a thick atmosphere and the resulting warmer temperatures. From a biological perspective the existence of liquid water by itself motivates the question of the origin of life on Mars. From studies of the Earth's earliest biosphere, we know that by 3.5 Gyr ago life had originated on Earth and reached a fair degree of biological sophistication. Surface activity and erosion on Earth make it difficult to trace the history of life before the 3.5 Gyr timeframe. If Mars did maintain a clement environment for longer than it took for life to originate on Earth, then the question of the origin of life on Mars follows naturally. Based upon simple models of the evolution of the Martian climate, we divide the history of liquid water habitats on the Martian surface into four epochs based upon the atmospheric temperature and pressure. Author

N92-28501*# California Inst. of Tech., Pasadena. Div. of Geological and Planetary Sciences.
MARTIAN ATMOSPHERIC CHEMISTRY DURING THE TIME OF LOW WATER ABUNDANCE Abstract Only
Hari Nair, Mark Allen, Yuk L. Yung, and R. Todd Clancy (Colorado Univ., Boulder.) *In* Lunar and Planetary Inst., Papers Presented to the Workshop on the Evolution of the Martian Atmosphere 1992 p 21-22 (For primary document see N92-28478 19-91)
Avail: NTIS HC/MF A03

The importance of odd hydrogen (or HO(x)) radicals in the catalytic recombination of carbon monoxide and oxygen in the Martian atmosphere is a well known fact. The inclusion of recent chemical kinetics data, specifically temperature-dependent CO2 absorption cross sections, into our one dimensional photochemical model shows that HO(x) is too efficient in this regard. The absorption cross sections of CO2 are smaller than previously assumed; this leads to a reduction in the photolysis rate of CO2 while the photolysis rate of H2O has increased. As a consequence the predicted mixing ratio of CO in our models is substantially less than the observed value of 6.5(10)(exp -4). Simultaneous measurements of water, ozone, and carbon monoxide were obtained in the Martian atmosphere in early Dec. 1990 (L(sub s) for Mars was 344 deg.). Author

N92-28502*# Minnesota Univ., Minneapolis. School of Physics and Astronomy.
THE EARLY MARTIAN ATMOSPHERE Abstract Only
Robert O. Pepin *In* Lunar and Planetary Inst., Papers Presented to the Workshop on the Evolution of the Martian Atmosphere 1992 p 22-23 (For primary document see N92-28478 19-91)
Avail: NTIS HC/MF A03

Atmospheric noble gases on Mars, Earth, and Venus are severely and variably depleted with respect to solar abundances, and are characterized by isotopic signatures that differ from planet to planet and from meteoritic and inferred solar compositions. Earlier theories based on simple accretion of meteoritic veneers as planetary volatile sources are unable to replicate these distributions, and so attention is now focusing on evolutionary processes that can fractionate both elements and isotopes, operating either on the early planets themselves or in large preplanetary planetesimals. Author

N92-28503*# National Aeronautics and Space Administration. Ames Research Center, Moffett Field, CA.
ASTRONOMICAL VARIATION EXPERIMENTS WITH A MARS GENERAL CIRCULATION MODEL Abstract Only
J. B. Pollack, R. M. Haberle, J. R. Murphy, J. Schaeffer, and H. Lee *In* Lunar and Planetary Inst., Papers Presented to the Workshop on the Evolution of the Martian Atmosphere 1992 p 24 (For primary document see N92-28478 19-91)
Avail: NTIS HC/MF A03

In time scales of a hundred thousand to a million years, the eccentricity of Mars orbit varies in a quasi-periodic manner between extremes as large as 0.14 and as small as 0 and the tilt of its axis of rotation with respect to the orbit normal also varies quasi-periodically between extremes as large as 35 deg and as small as 15 deg. In addition, the orientation of the axis precesses on comparable time scales. These astronomical variations are much more extreme than those experienced by the Earth. These variations are thought to have strongly modulated the seasonal cycles of dust, carbon dioxide, and water. One manifestation of the induced quasiperiodic climate changes may be the layered terrain of the polar regions, with individual layers perhaps recording variations in the absolute and/or relative deposition rates of dust and water in the polar regions, most likely in association with the winter time deposition of carbon dioxide ice. In an attempt to understand the manner in which atmospheric temperatures and

winds respond to the astronomical forcings, we have initiated a series of numerical experiments with the NASA/Ames general circulation model of the Martian Atmosphere. Author

N92-28504*# Oklahoma Univ., Norman. School of Meteorology.

REGIONAL CLIMATIC EFFECTS OF ATMOSPHERIC SO2 ON MARS Abstract Only

S. E. Postawko and F. P. Fanale (Hawaii Univ., Honolulu.) *In* Lunar and Planetary Inst., Papers Presented to the Workshop on the Evolution of the Martian Atmosphere 1992 p 24-25 (For primary document see N92-28478 19-91)
Avail: NTIS HC/MF A03

The conditions under which the valley networks on Mars may have formed remains controversial. The magnitude of an atmospheric greenhouse effect by an early massive CO2 atmosphere has recently been questioned by Kasting. Recent calculations indicate that if solar luminosity were less than about 86 percent of its current value, formation of CO2 clouds in the Martian atmosphere would depress the atmospheric lapse rate and reduce the magnitude of surface warming. In light of recent revisions of magma generation on Mars during each Martian epoch, and the suggestions by Wanke et al. that the role of liquid SO2 should be more carefully explored, we have recalculated the potential greenhouse warming by atmospheric SO2 on Mars, with an emphasis on more localized effects. In the vicinity of an active eruption, the concentration of atmospheric SO2 will be higher than if it is assumed that the erupted SO2 is instantaneously globally distributed. The local steady-state concentration of SO2 is a function of the rate at which it is released, its atmospheric lifetime, and the rate at which local winds act to disperse the SO2. We have made estimates of eruption rates, length of eruption, and dispersion rates of volcanically released SO2, for a variety of atmospheric conditions and atmospheric lifetimes of SO2 to explore the maximum regional climatic effect of SO2. Author

N92-28505*# Jet Propulsion Lab., California Inst. of Tech., Pasadena.

THE THERMAL STRUCTURE, DUST LOADING, AND MERIDIONAL TRANSPORT IN THE MARTIAN ATMOSPHERE DURING LATE SOUTHERN SUMMER Abstract Only

M. Santee (California Inst. of Tech., Pasadena.) and D. Crisp *In* Lunar and Planetary Inst., Papers Presented to the Workshop on the Evolution of the Martian Atmosphere 1992 p 25-26 (For primary document see N92-28478 19-91)
Avail: NTIS HC/MF A03

We have derived a comprehensive picture of the thermal structure and dust loading of the Martian atmosphere in a relatively clear period during late southern summer. Using a new technique for the simultaneous retrieval of atmospheric temperatures and airborne dust abundances, we examined a subset of the Mariner 9 infrared interferometer spectrometer (IRIS) thermal emission spectra spanning L sub s = 343 degrees to 348 degrees. Global maps of temperature and dust optical depth as functions of latitude (plus or minus 90 degrees), altitude (approx. 0-60 km), and Mars local time of day were constructed from the profiles from individual spectra. One of the principal conclusions from this work is that both dayside and nightside atmospheric temperatures at altitudes above about 40 km are warmer over the winter (north) polar regions than over the equator or the summer (south) polar regions. These anomalous temperatures are consistent with ground-based observations of polar warming at higher altitudes (50-85 km), and they indicate that the atmosphere is not in radiative equilibrium. Zonal-mean zonal winds are derived from the observed meridional gradients of the zonally averaged temperatures assuming geostrophy and zero surface zonal wind. The intense eastward jets (with velocities exceeding 120 m/s) correspond to regions of strong horizontal temperature gradients. Similar calculations have been reported previously, but they were not global in coverage. Both the zonal-mean meridional circulation and large-scale waves contribute to the north-south atmospheric transport. Author

N92-28506*# National Aeronautics and Space Administration. Goddard Space Flight Center, Greenbelt, MD.

VOLCANIC RECYCLING OF CARBONATE DEPOSITS ON MARS Abstract Only

M. W. Schaefer *In* Lunar and Planetary Inst., Papers Presented to the Workshop on the Evolution of the Martian Atmosphere 1992 p 26 Prepared in cooperation with Maryland Univ., College Park (For primary document see N92-28478 19-91)
Avail: NTIS HC/MF A03

One question of great interest to those who study the evolution of the Martian atmosphere is: if there was an early, dense atmosphere that was removed, is there any mechanism that could restore it? In the case of an atmosphere removed largely by the formation of carbonates, the only obvious means of restoring it is by the thermal decomposition of the carbonates. Decomposition of carbonates under turbulently flowing lava holds great promise as a means of resupplying the atmosphere with CO2. Huppert and colleagues have modeled the emplacement of terrestrial komatiite flows and found that komatiites, even when flowing over previously emplaced and cooled komatiite flows, could melt and erode this rock to a significant depth. Based on this work, I have begun modeling the erosion of Martian carbonate deposits under turbulently flowing, komatiitic lava. Initial results from this modeling indicate that a high-volume lava flow, emerging at a temperature of, say, 1600 degrees, is capable of eroding several meters of carbonate deposits per day. If such a flow is active for a hundred days, several hundreds of meters of carbonate could be decomposed. If this process occurred over a large area, a bar or more of CO2 could be injected back into the atmosphere over an extremely short period of time. The implications of such an occurrence are intriguing. For instance, if a relatively late pulse of volcanism (such as is suggested by Frey) were to cause a large flow of lava over carbonate deposits in the northern lowlands, the resulting pulse of CO2 into the atmosphere could conceivably restore the climate to one in which liquid water could exist on the surface, or ice could flow. Author

N92-28507*# Max-Planck-Inst. fuer Chemie, Mainz (Germany, F.R.).

THE ROLE OF SO2 ON MARS AND ON THE PRIMORDIAL OXYGEN ISOTOPE COMPOSITION OF WATER ON EARTH AND MARS Abstract Only

H. Waenke, G. Dreibus, E. Jagoutz, and L. M. Mukhin *In* Lunar and Planetary Inst., Papers Presented to the Workshop on the Evolution of the Martian Atmosphere 1992 p 26-28 (For primary document see N92-28478 19-91)
Avail: NTIS HC/MF A03

We stress the importance of SO2 on Mars. In the case that water should have been supplied in sufficient quantities to the Martian surface by a late veneer and stored in the near surface layers in form of ice, temporary greenhouse warming by SO2 after large SO2 discharges may have been responsible for melting of ice and break-out of water in areas not directly connected to volcanic activity. Aside from water, liquid SO2 could explain at least some of the erosion features on the Martian surface.
Author

N92-28508*# Open Univ., Milton (England). Dept. of Earth Sciences.

MARTIAN SURFICIAL CARBON-CONSTRAINTS FROM ISOTOPIC MEASUREMENTS OF SHOCK-PRODUCED GLASS IN EET A79001 Abstract Only

I. P. Wright, C. P. Hartmetz, and C. T. Pillinger *In* Lunar and Planetary Inst., Papers Presented to the Workshop on the Evolution of the Martian Atmosphere 1992 p 28-29 (For primary document see N92-28478 19-91)
Avail: NTIS HC/MF A03

At the highest temperatures of extraction, trapped Martian atmospheric CO2 is released. For this component, delta C-13 rises to +27 percent (compared to +15 percent previously). Because of the possibilities that C-13 rich atmospheric CO2 is released along with C-13 depleted crustal carbon, the highest delta C-13 value measured represents a lower limit to the true isotopic

composition of the atmospheric species. Thus, the new delta C-13 determination is considered to best represent Martian atmospheric CO2. Based on a delta C-13 of +27 percent, and a release temperature of 1000-1200 C, the new analysis shows the glass to contain 2.4 ppm C as CO2, compared to 5.5 ppm C previously. Thus, it would seem that trapped CO2 is distributed rather unevenly throughout the glass. Author

N92-28509*# National Aeronautics and Space Administration. Ames Research Center, Moffett Field, CA.
HOW MARS LOST ITS ATMOSPHERE Abstract Only
Kevin Zahnle *In* Lunar and Planetary Inst., Papers Presented to the Workshop on the Evolution of the Martian Atmosphere 1992 p 29-30 (For primary document see N92-28478 19-91)
Avail: NTIS HC/MF A03

There is a widespread suspicion that Mars thin atmosphere is in some way attributable to the planet's size. Another possibility is that the atmosphere was never degassed or outgassed in the first place. I prefer escape. Hydrodynamic escape (vigorous thermal escape) and impact erosion (expulsion of atmosphere by impacts) are two processes that should have been operative early. Although in principle hydrodynamic escape could have shrunk Mars atmosphere a hundredfold while leaving the composition of the remnant atmosphere nearly unaltered, very high escape fluxes are required. The implicated escape mechanism must have been efficient, nearly non-fractionating, and vastly more potent for Mars than for Earth or Venus. Impact erosion is an appealing candidate. Noble gases are the obvious first test. Noble gases are the most volatile elements and so are the most likely to have been affected by impact erosion and the easiest to address quantitatively. Xenon in particular imposes three constraints on how Mars lost its atmosphere: (1) the very low abundance of nonradiogenic Xe abundance of nonradiogenic Xe compared to Earth, Venus, and likely meteoritic sources; (2) its nonradiogenic isotopes distinct from likely meteoritic sources; and (3) the relatively high absolute abundance of radiogenic daughter of the extinct radionuclide I-129 (half-life 17 Myr). In impact erosion, the first two become constraints on the composition, mass distribution, and orbital elements of the impactors. The third requires that Mars lost its nonradiogenic Xe early, probably before it was 100 Myr old. Impact erosion can explain Mars by any of three stories. (1) Mars in unlikely. In a sort of planetary brinkmanship, impact erosion almost removed the entire atmosphere but was arrested just in time. (2) Martian noble gases are cometary and cometary Xe is as isotopically mass fractionated as Martian and terrestrial Xe. This is most easily accomplished if a relatively thick geochemically controlled CO2 atmosphere protected trace atmophiles against escape. (3) Mars was indeed stripped of its early atmosphere but a small remnant was safely stored in the regolith, later released as a byproduct of water mobilization. Author

N92-28510*# National Aeronautics and Space Administration. Ames Research Center, Moffett Field, CA.
SPECTRAL IDENTIFICATION OF CHEMISORBED CO2 AND APPLICATION TO MARS ANALOG MATERIALS Abstract Only
A. P. Zent and T. L. Roush (San Francisco State Univ., CA.) *In* Lunar and Planetary Inst., Papers Presented to the Workshop on the Evolution of the Martian Atmosphere 1992 p 30-31 (For primary document see N92-28478 19-91)
Avail: NTIS HC/MF A03

The goal of this work is to identify the spectral signature of chemisorbed CO2, to test the efficacy of carbonate formation on Mars-analog materials via CO2 chemisorption, and to identify the surface-chemical characteristics of good chemisorbents, with the intent of assessing the possible geochemical importance of CO2 chemisorption as a quasipermanent CO2 sink in the Martian environment. Our approach is to search for infrared spectral bands that result from chemisorption of CO2 molecules onto chemical reagents and Mars-analog materials, and to identify the salient differences in adsorbents that favor strong, permanent CO2 chemisorption. The total amount of CO2 in the early Martian atmosphere, and consequent surface temperatures, are unknown. A CO2 greenhouse may not have been an adequate mechanism under any circumstances; however, it if were, then most of that CO2 must still be in the near-surface environment; no escape mechanism that could remove it after the decline of channeling has been identified. The only plausible reservoir is carbonate, and there are various remote sensing techniques that can be used to search for it. We are investigating CO2 chemisorption as a permanent CO2 sink, and to aid in interpretation of remotely sensed IR spectra of Mars. A common effect reported in CO2 adsorption studies is the formation of a layer of carbonate or bicarbonate anions on adsorbents that have OH- groups available on their surfaces. Inorganic hydroxyls occur on phyllosilicates, amorphous silicates, metal oxides and hydroxides; it is the most abundant and reactive surface functional group on the surfaces of terrestrial silicates. The process responsible for the reaction is chemisorption. Chemisorption is distinguished from physical adsorption in that there is a transfer of electrons between species, and the formation of a chemical bond. The heat of chemisorption is typically of the same order as heats of chemical reaction (i.e., a few hundred to a few thousand kJ/mole), as opposed to heats of physical adsorption (a few kJ per mole). Chemisorption is an activated process that is promoted by an increase in temperature - quite the opposite of physical adsorption. Chemisorption is not reversible in the sense that physical adsorption is. Author

N92-28988*# Lunar and Planetary Inst., Houston, TX.
WORKSHOP ON THE MARTIAN SURFACE AND ATMOSPHERE THROUGH TIME Progress Report
Robert M. Haberle, ed. (National Aeronautics and Space Administration. Ames Research Center, Moffett Field, CA.) and Bruce M. Jakosky, ed. (Colorado Univ., Boulder.) 1992 198 p Workshop held in Boulder, CO, 23-25 Sep. 1991; sponsored by LPI and Colorado Univ.
(Contract NASw-4574)
(NASA-CR-190418; NAS 1.26:190418; LPI-TR-92-02) Avail: NTIS HC/MF A09

The purpose of the workshop was to bring together the Mars Surface and Atmosphere Through Time (MSATT) Community and interested researchers to begin to explore the interdisciplinary nature of, and to determine the relationships between, various aspects of Mars science that involve the geological and chemical evolution of its surface, the structure and dynamics of its atmosphere, interactions between the surface and atmosphere, and the present and past states of its volatile endowment and climate system. For individual titles, see N92-28989 through N92-29080.

N92-28989*# Alabama Univ., Birmingham. Dept. of Physics.
IRON MOESSBAUER SPECTROSCOPY: SUPERPARAMAGNETISM IN HYDROTHERMAL VENTS AND THE SEARCH FOR EVIDENCE OF PAST LIFE ON MARS
David G. Agresti and Thomas J. Wdowiak *In* Lunar and Planetary Inst., Workshop on the Martian Surface and Atmosphere Through Time 1992 p 9-10 (For primary document see N92-28988 19-91)
Avail: NTIS HC/MF A09

In view of the demonstrated value of Iron Moessbauer Spectroscopy (FeMS) in the study of extraterrestrial iron and the fact that, after silicon and oxygen, iron is the most abundant element on the surface of Mars, we proposed, and have under development, a backscatter Moessbauer spectrometer with x ray fluorescence capability (BaMS/XRF) for use on Mars as a geophysical prospecting instrument. Specifically, we have proposed BaMS/XRF as part of the geochemistry instrumentation on NASA's Mars Environment Survey (MESUR) mission. BaMS/XRF will have applications in: (1) the study of past environments through the examination of sedimentary material; (2) the study of the contemporary Martian environment; and (3) the study of iron-containing minerals of possible biogenic origin. Development of a reference library from a geophysical point of view for putative Martian surface materials at appropriate temperatures is now underway. We carried out preliminary optical reflectance and FeMS measurements on mineral products (iron oxyhydroxides) of

deep-sea hydrothermal activity. Various aspects of this investigation are presented. Author

N92-28990*# National Aeronautics and Space Administration. Ames Research Center, Moffett Field, CA.
THE NANOPHASE IRON MINERAL(S) IN MARS SOIL
A. Banin (Hebrew Univ. of Jerusalem, Rehovot, Israel), T. Ben-Shlomo (Hebrew Univ. of Jerusalem, Rehovot, Israel), L. Margulies (Hebrew Univ. of Jerusalem, Rehovot, Israel), D. F. Blake, and A. U. Gehring (California Univ., Berkeley.) *In* Lunar and Planetary Inst., Workshop on the Martian Surface and Atmosphere Through Time 1992 p 11-12 (For primary document see N92-28988 19-91)
Avail: NTIS HC/MF A09

Iron-enriched smectites have been suggested as important mineral compounds of the Martian soil. They were shown to comply with the chemical analysis of the Martian soil, to simulate many of the findings of the Viking Labeled Release Experiments on Mars, to have spectral reflectance in the VIS-NIR strongly resembling the bright regions on Mars. The analogy with Mars soil is based, in a number of aspects, on the nature and behavior of the iron oxides and oxyhydroxides deposited on the surface of the clay particles. A summary of the properties of these iron phases and some recent findings are presented. Their potential relevance to Mars surface processes is discussed. Author

N92-28991*# National Aeronautics and Space Administration. Lyndon B. Johnson Space Center, Houston, TX.
MARTIAN IMPACT CRATER DEGRADATION STUDIES: IMPLICATIONS FOR LOCALIZED OBLITERATION EPISODES
N. G. Barlow *In* Lunar and Planetary Inst., Workshop on the Martian Surface and Atmosphere Through Time 1992 p 13-14 (For primary document see N92-28988 19-91)
Avail: NTIS HC/MF A09

Early spacecraft missions to Mars revealed that impact craters display a range of degradational states, but full appreciation of the range of preservational characteristics was not revealed until the Mariner 9 and Viking missions in the 1970's. Many studies have described the spatial and temporal distribution of obliteration episodes based on qualitative descriptions of crater degradation. Recent advances in photoclinometric techniques have led to improved estimates of crater morphometric characteristics. The present study is using photoclinometry to determine crater profiles and is comparing these results with the crater geometry expected for pristine craters of identical size. The result is an estimate of the degree of degradation suffered by Martian impact craters in selected regions of the planet. Size-frequency distribution analyses of craters displaying similar degrees of degradation within localized regions of the planet may provide information about the timing of obliteration episodes in these regions. Author

N92-28992*# Oregon State Univ., Corvallis. Dept. of Atmospheric Sciences.
MIDLATITUDE WEATHER SYSTEMS ON MARS: IS THERE A HEMISPHERIC ASYMMETRY?
J. R. Barnes *In* Lunar and Planetary Inst., Workshop on the Martian Surface and Atmosphere Through Time 1992 p 15-16 (For primary document see N92-28988 19-91)
Avail: NTIS HC/MF A09

The Viking Lander meteorology observations confirmed that midlatitude weather systems are present in the Northern Hemisphere of Mars during the autumn, winter, and early spring. These systems have properties consistent with a development through baroclinic instability of the wintertime zonal-mean circulation. It is known that the weather systems must be of importance for the zonal-mean circulation by virtue of their heat and momentum transports. Observations show that they are associated with dust raising, and they must be involved in the transport of dust; the weather systems almost certainly must act to produce significant water transports as well. Recent simulations with the ARC Mars General Circulation Model (GCM) show that the heat transports by the weather system (and by the zonal-mean circulation) during northern winter can be very substantial: large enough to significantly reduce the CO2 condensation at polar latitudes. This could be largely responsible for the observed early spring halt in the north polar cap recession and for the presence of westerly winds near the cap edge during this season. Author

N92-28993*# Hawaii Univ., Honolulu. Div. of Planetary Geosciences.
MARS: COMPOSITIONAL VARIABILITY OF FERRIC/FERROUS MINERALS AND POLAR VOLATILES FROM GROUNDBASED IMAGING SPECTROSCOPY
James F. Bell, III *In* Lunar and Planetary Inst., Workshop on the Martian Surface and Atmosphere Through Time 1992 p 17-18 Prepared in cooperation with Washington Univ., Seattle (For primary document see N92-28988 19-91)
Avail: NTIS HC/MF A09

In an attempt to further constrain the ferric and ferrous mineralogy of Mars, Bell et al. (1989; 1990) obtained high resolution imaging spectroscopic data of much of the Martian surface in the visible and near-infrared (0.4-1.1 micron) during the 1988 opposition. Preliminary analysis of these data showed further evidence of crystalline hematite absorption features at 0.8-0.9 microns and 0.6-0.7 microns. Additionally, the 0.6-0.7 micron Fe(III) band was shown to vary across the surface, with a substantial correlation with albedo in the region studied. Calibration of this 1988 data set (along with a similar data set obtained during the 1990 opposition) has been ongoing, and some of the most recent results of the analysis of these data using linear spectral mixture modeling are reported. Author

N92-28994*# California Inst. of Tech., Pasadena.
THERMALLY DISTINCT EJECTA BLANKETS FROM MARTIAN CRATERS
B. H. Betts and B. C. Murray *In* Lunar and Planetary Inst., Workshop on the Martian Surface and Atmosphere Through Time 1992 p 19-20 (For primary document see N92-28988 19-91)
Avail: NTIS HC/MF A09

The study of ejecta blankets on Mars gives information about the Martian surface, subsurface, geologic history, atmospheric history, and impact process. In Feb. and Mar. 1989, the Termoskan instrument on board the Phobos 1988 spacecraft of the USSR acquired the highest spatial resolution thermal data ever obtained for Mars, ranging in the resolution from 300 meters to 3 km per pixel. Termoskan simultaneously obtained broad band visible channel data. The data covers a large portion of the equatorial region from 30 degrees S latitude to 6 degrees N latitude. Utilizing the data set we have discovered tens of craters with thermal infrared distinct ejecta (TIDE) in the equatorial regions of Mars. In order to look for correlations within the data, we have compiled a database which currently consists of 110 craters in an area rich in TIDE's and geologic unit variations. For each crater, we include morphologic information from Barlow's Catalog of Large Martian Impact Craters in addition to geographic, geologic, and physical information and Termoskan thermal infrared and visible data. Author

N92-28995*# Jet Propulsion Lab., California Inst. of Tech., Pasadena.
INFRARED IMAGING OF MARS FOR VOLATILE DISTRIBUTION AND SEASONAL VARIABILITY BETWEEN 2.4 AND 5.1 MICRONS
Diana L. Blaney *In* Lunar and Planetary Inst., Workshop on the Martian Surface and Atmosphere Through Time 1992 p 21 (For primary document see N92-28988 19-91)
Avail: NTIS HC/MF A09

Recent advances in ground-based infrared imaging now allow for sub-arc second spectral imaging. Data collected at the NASA Infrared Telescope Facility using protocam, a 62 x 58 InSb array camera with a circular variable filter and a plate scale 0.2 arc-seconds/pixel, are discussed. These images are a first attempt at extended seasonal infrared coverage of Mars to look for seasonal variations. Currently, data collected in Jun. 1990 at Ls = 241 (southern spring) and in Jan. 1991 Ls = 360 (late southern summer) are being reduced and analyzed. The 3 micron bound water band

is the strongest surface absorption feature on Mars in the infrared. Infrared spectroscopy can also be useful in the detection of ice and frost deposits, especially in the polar regions. While imaging and spectroscopy at visible wavelengths allows for the detection of condensates, infrared information is needed to distinguish between water and CO2 ice/frost deposits. In the Jun. images, the southern polar cap totally disappears in the 3.4 micron CO2 frost band and is bright in the 3.1 micron water ice band, indicating that water ice is not a detectable component of the southern polar cap at this season. Further investigations are currently under way to look for residual water ice after the disappearance of the seasonal south polar cap in the Jan. images. The Jun. images that were focused on had a sub-earth point located at 184 longitude, and 23.8 S latitude which put the center of the disk in the southern highland region between Elysium and Amazonis. Examination of the Jun. images show that there are four surface units identifiable: a CO2 frost deposit, a northern plains unit, an equatorial unit, and a southern highland unit. At this resolution there does not appear to be any latitudinal variations in the 3 micron band that is independent of the 2.4 micron albedo features. The northern planes unit and the southern highland unit have very similar 'color' in the three micron band as demonstrated by the rise out of the band, but different brightness levels. The equatorial unit has a distinct three micron color implying a compositional difference. The albedo features at 2.4 microns have decreased contrast at longer wavelengths, till they are unrecognizable at 4 microns. Author

N92-28996*# Arizona State Univ., Tempe. Dept. of Geology.
INFLUENCE OF AERODYNAMIC ROUGHNESS LENGTH ON AEOLIAN PROCESSES: EARTH, MARS, VENUS
Dan G. Blumberg and Ronald Greeley *In* Lunar and Planetary Inst., Workshop on the Martian Surface and Atmosphere Through Time 1992 p 22 (For primary document see N92-28988 19-91)
Avail: NTIS HC/MF A09

The aerodynamic roughness length (z sub 0) is the height at which a wind profile assumes a zero velocity. The lower part of the atmospheric boundary layer will be impeded by friction with the surface. An increase in surface roughness will also increase the shear stress required to initiate particle entrainment by the wind. Bagnold (1941) estimated z sub 0 as being 1/30 of the mean particle size. In Nature, surface roughness is composed of nonerodible elements as well as sand-size erodible particles. To assess z sub 0 values as a function of terrain, field experiments were conducted to obtain wind profiles monitored over natural surfaces at 15 sites in the Mojave Desert, Death Valley, and Nye County, Nevada. These sites span a variety of arid-land terrains, including smooth playas, alluvial fans, and lava flows; z sub 0 values ranged from 0.0001 cm to 1 cm. These values were incorporated in a threshold model and a flux model to assess transport efficiency over such terrains in three planetary environments (Venus, Earth, and Mars), and for particle sizes ranging from 60-500 micron. Threshold and flux are a function of planetary environment, particle density and size (Dp), and z sub 0, and the shear velocity of 1.2 x U sub *t (for Dp = 250 micron and z sub 0 = 0.84). Results show that flux on Mars is approximately 14 g/(cm x s), on Earth it is approximately 3 g/(cm x s), and on Venus 0.5 g/(cm x s). Under all planetary environments, the results also show a dramatic decrease in the flux for particles greater than 200 microns when z sub 0 increases above 0.0085 cm (corresponding to sites consisting of alluvium). When z sub 0 approaches 0.03 cm (corresponding to a mantled pahoehoe lava), the flux diminishes. Author

N92-28997*# Arizona Univ., Tucson.
DUST STORM DRIVEN VARIATIONS OF THE MARS THERMOSPHERE AND EXOSPHERE: COUPLING OF ATMOSPHERIC REGIONS
S. W. Bougher, C. G. Fesen (Dartmouth Coll., Hanover, NH.), and R. W. Zurek (Jet Propulsion Lab., California Inst. of Tech., Pasadena.) *In* Lunar and Planetary Inst., Workshop on the Martian Surface and Atmosphere Through Time 1992 p 23 (For primary document see N92-28988 19-91)
Avail: NTIS HC/MF A09

The National Center for Atmospheric Research (NCAR) thermospheric general circulation model (TGCM) for the Earth was modified to examine the 3-D structure and circulation of the upper atmosphere of Mars (MTGCM). The solar, orbital, and seasonal responses of the Mars thermosphere above 100 km were examined for various combinations of input parameters. Author

N92-28998*# National Aeronautics and Space Administration. Ames Research Center, Moffett Field, CA.
SIMULATIONS OF SURFACE WINDS AT THE VIKING LANDER SITES USING A ONE-LEVEL MODEL
Alison F. C. Bridger (San Jose State Univ., CA.) and Robert M. Haberle *In* Lunar and Planetary Inst., Workshop on the Martian Surface and Atmosphere Through Time 1992 p 24-25 (For primary document see N92-28988 19-91)
Avail: NTIS HC/MF A09

The one-level model developed by Mass and Dempsey for use in predicting surface flows in regions of complex terrain was adapted to simulate surface flows at the Viking lander sites on Mars. In the one-level model, prediction equations for surface winds and temperatures are formulated and solved. Surface temperatures change with time in response to diabatic heating, horizontal advection, adiabatic heating and cooling effects, and horizontal diffusion. Surface winds can change in response to horizontal advection, pressure gradient forces, Coriolis forces, surface drag, and horizontal diffusion. Surface pressures are determined by integration of the hydrostatic equation from the surface to some reference level. The model has successfully simulated surface flows under a variety of conditions in complex-terrain regions on Earth. Author

N92-28999*# Massachusetts Inst. of Tech., Cambridge. Dept. of Earth, Atmospheric and Planetary Sciences.
RATES OF OXIDATIVE WEATHERING ON THE SURFACE OF MARS
Roger G. Burns *In* Lunar and Planetary Inst., Workshop on the Martian Surface and Atmosphere Through Time 1992 p 26-27 (For primary document see N92-28988 19-91)
Avail: NTIS HC/MF A09

Implicit in the mnemonic 'MSATT' (Mars surface and atmosphere through time) is that rates of surface processes on Mars through time should be investigated, including studies of the kinetics and mechanism of oxidative weathering reactions occurring in the Martian regolith. Such measurements are described. Two major elements analyzed in the Viking Lander XRF experiment that are most vulnerable to atmospheric oxidation are iron and sulfur. Originally, they occurred as Fe(2+)-bearing silicate and sulfide minerals in basaltic rocks on the surface of Mars. However, chemical weathering reactions through time have produced ferric- and sulfate-bearing assemblages now visible in the Martian regolith. Such observations raise several question about: (1) when the oxidative weathering reactions took place on Mars; (2) whether or not the oxidized regolith is a fossilized remnant of past weathering processes; (3) deducting chemical interactions of the ancient Martian atmosphere with its surface from surviving phases; (4) possible weathering reactions still occurring in the frozen regolith; and (5) the kinetics and mechanism of past and present-day oxidative reactions on Mars. These questions may be addressed experimentally by studying reaction rates of dissolution and oxidation of basaltic minerals, and by identifying reaction products forming on the mineral surfaces. Results for the oxidation of pyrrhotite and dissolved ferrous iron are reported. Author

N92-29000*# Observatoire de Paris-Meudon (France). Lab. de Physique du Systeme Solaire.
MARTIAN CHANNEL NETWORKS: A REVISED STRAHLER APPROACH FOR QUANTITATIVE MORPHOMETRY
N. A. Cabrol and E. A. Grin (Centre National de la Recherche Scientifique, Meudon-Bellevue, France) *In* Lunar and Planetary Inst., Workshop on the Martian Surface and Atmosphere Through

Time 1992 p 28-29 (For primary document see N92-28988 19-91)
Avail: NTIS HC/MF A09

To characterize the Martian channel tributary networks, empirical rules of Strahler are applied. The proposed statistical analysis is based upon the relationship between the number of network tributaries (branches) and the network order (N). Author

N92-29001*# University Coll., London (England). Planetary Image Centre.
ICE IN THE NORTHERN LOWLANDS AND SOUTHERN HIGHLANDS OF MARS AND ITS ENRICHMENT BENEATH THE ELYSIUM LAVAS
Julie A. Cave *In* Lunar and Planetary Inst., Workshop on the Martian Surface and Atmosphere Through Time 1992 p 30-31 (For primary document see N92-28988 19-91)
Avail: NTIS HC/MF A09

The simultaneously examination of ejecta mobility, crater morphology, and surface features has enabled several conclusions to be drawn regarding the location of subsurface ice in the region. The ice distribution is shown to be highly dependent upon latitude and geological situation; in particular, pronounced differences in the distribution between the highland and lowlands are seen, and concentrations of ice were detected beneath the Elysium lavas. Author

N92-29002*# European Space Agency. European Space Research and Technology Center, ESTEC, Noordwijk (Netherlands). Dept. of Space Science.
MARSNET SURFACE AND ATMOSPHERE INVESTIGATIONS
A. F. Chicarro *In* Lunar and Planetary Inst., Workshop on the Martian Surface and Atmosphere Through Time 1992 p 32-33 (For primary document see N92-28988 19-91)
Avail: NTIS HC/MF A09

Following an ESA preliminary study on the possible areas of European participation in the future international exploration of Mars and a recent ESA in-depth scientific and technical assessment study, MARSNET was selected for further phase-A studies as a potential European contribution to such exploration. The MARSNET mission consists of a network of small stations to be landed on the surface of Mars. All surface stations will have identical design and payload, and will be located several thousand km apart from each other. The required operational lifetime on the surface of Mars for all landers is one Martian year (687 days) to carry out long-term meteorological and seismological measurements. The availability of a data relay orbiter at low altitude is assumed. The instruments are mounted on a platform under the semi-hard lander solar array. The main scientific goals of the mission during the atmospheric descent and on the surface are outlined. Author

N92-29003*# Colorado Univ., Boulder. Lab. for Atmospheric and Space Physics.
MARS DUST AND CLOUD OPACITIES AND SCATTERING PROPERTIES
R. T. Clancy and S. W. Lee *In* Lunar and Planetary Inst., Workshop on the Martian Surface and Atmosphere Through Time 1992 p 34 (For primary document see N92-28988 19-91)
Avail: NTIS HC/MF A09

We have recently completed an analysis of the visible emission-phase function (EPF) sequences obtained with the solar-band channel of the Infrared Thermal Mapping (IRTM) instrument onboard the two Viking Orbiters. Roughly 100 of these EPF sequences were gathered during the 1977-1980 period, in which the total broadband (.3-3.0 microns) reflectances of the atmosphere/surface above specific locations on Mars were measured versus emission angle as the spacecraft passed overhead. A multiple scattering radiative transfer program was employed to model the EPF observations in terms of the optical depths of dust/clouds, their single scattering albedos and phase functions, and the Lambert albedos and phase coefficient of the underlying surfaces. Due to the predominance of atmospheric scattering at large atmospheric pathlengths and/or large dust opacities, we were able to obtain strong constraints on the scattering properties of dust/clouds and their opacities for a wide range of latitudes, longitudes, and seasons on Mars. Author

N92-29004*# Colorado Univ., Boulder.
VLA MAPPING OF 1.35 cm WATER EMISSION FROM THE MARS ATMOSPHERIC LIMB
R. T. Clancy, A. W. Grossman (Maryland Univ., College Park.), and D. O. Muhleman (California Inst. of Tech., Pasadena.) *In* Lunar and Planetary Inst., Workshop on the Martian Surface and Atmosphere Through Time 1992 p 35 (For primary document see N92-28988 19-91)
Avail: NTIS HC/MF A09

We report preliminary results of 1.35 cm spectral line observations, in which we employed the NRAO Very Large Array (VLA) interferometer to map the horizontal and vertical distributions of water vapor around the Mars atmospheric limb in early Dec. of 1990. The increased atmospheric pathlengths presented near the limb of Mars and the high angular resolution afforded by the VLA at centimeter wavelengths lead to a remarkably sensitive, remote measurement of water in the atmosphere of Mars. We achieve approximately 300 km horizontal resolution on Mars, operating in the C configuration of the VLA, when Mars was 17.3 inches in diameter. This allows us to resolve the latitudinal and diurnal variations in atmospheric water emission around the limb of Mars. We derive the vertical distribution of atmospheric water from observed pressure broadening in the spectrally resolved lineshapes. These observations, which consist of two eight-hour integrations obtained on Dec. 3-4 and Dec. 6-7, correspond to late winter in the Northern Hemisphere of Mars (L sub s = 344 degrees). Author

N92-29005*# Lunar and Planetary Inst., Houston, TX.
MARS ATMOSPHERIC WATER
R. T. Clancy, A. W. Grossman, and D. O. Muhleman (Geological Survey, Menlo Park, CA.) *In its* Workshop on the Martian Surface and Atmosphere Through Time 1992 p 36 (For primary document see N92-28988 19-91)
Avail: NTIS HC/MF A09

We indicate the Dec. 3-4 spectrum averaged over the morning limb of Mars. Two synthetic spectra indicate the expected line emission for 3 precipitable microns of water with a uniform vertical distribution (dotted) and a vertical distribution in which water decreases rapidly above 20 km altitude if Mars atmospheric temperatures are approximately 20 K cooler than implied by the Viking Infrared Thermal Mapping (IRTM) and lander descent observations. Such cooler atmospheric temperatures have been argued on the basis of ground-based microwave observations of Mars atmospheric CO. Our 3 pr micron column abundance for water can be compared to the global value of approximately 6 pr microns, observation for the same season with the Viking MAWD experiment in 1977. We will investigate the latitude and diurnal variations when the data corresponding to the second day of observations are reduced. We also plan to compare these VLA water observations with a very complementary set of Hubble Space Telescope ozone observations. Ultraviolet (220-330 nm) spectra and imates of Mars were obtained on Dec. 13 1990 as part of a general Mars observing program with the Hubble Space Telescope. Author

N92-29006*# Lunar and Planetary Inst., Houston, TX.
THE SUBSURFACE HYDROLOGIC RESPONSE OF MARS TO THE THERMAL EVOLUTION OF ITS EARLY CRUST
S. M. Clifford and M. H. Carr (Geological Survey, Menlo Park, CA.) *In its* Workshop on the Martian Surface and Atmosphere Through Time 1992 p 37-38 (For primary document see N92-28988 19-91)
Avail: NTIS HC/MF A09

The Martian valley networks and outflow channels provide persuasive evidence that large bodies of groundwater were present on Mars throughout much of its early geologic history. However, little attention was focused on how these volatile reservoirs may have responded to the thermal evolution of the early Martian crust.

In this regard, one process that has likely been of critical importance to the subsurface hydrologic evolution of Mars is thermal vapor diffusion. Various aspects of the thermal vapor diffusion process on Mars are discussed. Author

N92-29007*# Jet Propulsion Lab., California Inst. of Tech., Pasadena.
ANALYSIS OF MARTIAN ATMOSPHERIC AND SURFACE OPTICAL PROPERTIES BETWEEN 4.4 AND 5.1 MICRONS
Dave Crisp and Diana L. Blaney *In* Lunar and Planetary Inst., Workshop on the Martian Surface and Atmosphere Through Time 1992 p 39-40 (For primary document see N92-28988 19-91)
Avail: NTIS HC/MF A09

Spectra of several regions of Mars were taken by Blaney and McCord in Aug. of 1988 with the Cooled Grating Array Spectrometer (CGAS) at the NASA Infrared Telescope Facility (IRTF). The resulting spectra show several distinct absorption features at wavelengths between 4.4 and 5.1 microns. Many of these features can be attributed to gases in the Martian atmosphere, but others are more difficult to identify. To analyze these spectra more completely, we used a line-by-line multiple scattering model that was developed for studies of Venus night-side emission. This model includes all atmospheric and surface radiative processes that are known to be important on Mars, including absorption, emission, and multiple scattering by CO2, H2O, CO, and airborne dust, and a spectrally-dependent surface albedo. A Mie-scattering algorithm was used to derive dust optical properties from the optical constants of palagonic and basalt. Results from our preliminary efforts to simulate the spectra taken near Tharsis and Solis Planum are shown. Author

N92-29008*# Jet Propulsion Lab., California Inst. of Tech., Pasadena.
MICRO WEATHER STATIONS FOR IN SITU MEASUREMENTS IN THE MARTIAN PLANETARY BOUNDARY LAYER
D. Crisp, W. J. Kaiser, T. W. Kenny, T. R. VanZandt, and J. E. Tillman (Washington Univ., Seattle.) *In* Lunar and Planetary Inst., Workshop on the Martian Surface and Atmosphere Through Time 1992 p 41-42 (For primary document see N92-28988 19-91)
Avail: NTIS HC/MF A09

Viking Lander meteorology measurements show that the Martian planetary boundary layer (PBL) has large diurnal and seasonal variations in pressure, wind velocity, relative humidity, and airborne dust loading. An even larger range of conditions was inferred from remote sensing observations acquired by the Mariner 9 and Viking orbiters. Numerical models indicate that these changes may be accompanied by dramatic vertical and horizontal wind shears (100 m/s/km) and rapid changes in the static stability. In-situ measurements from a relatively small number surface stations could yield global constraints on the Martian climate and atmospheric general circulation by providing ground truth for remote sensing instruments on orbiters. A more complete understanding of the meteorology of the PBL is an essential precursor to manned missions to Mars because this will be their working environment. In-situ measurements are needed for these studies because the spatial and temporal scales that characterize the important meteorological processes near the surface cannot be resolved from orbit. The Mars Environmental Survey (MESUR) Program will provide the first opportunity to deploy a network of surface weather stations for a comprehensive investigation of the Martian PBL. The feasibility and utility of a network of micro-weather stations for making in-situ meteorological measurements in the Martian PBL are assessed. Author

N92-29009*# Observatoire de Paris-Meudon (France).
SOIL TEXTURE AND GRANULOMETRY AT THE SURFACE OF MARS
A. Dollfus, M. Deschamps, and J. Zimbelman (National Air and Space Museum, Washington, DC.) *In* Lunar and Planetary Inst., Workshop on the Martian Surface and Atmosphere Through Time 1992 p 43-44 (For primary document see N92-28988 19-91)
Avail: NTIS HC/MF A09

The microtexture of the near-surface Martian soil was sensed with three diagnostic parameters: (1) the albedo A at normal incidence and phase angle 5 degrees, which relates to the composition of the top surface exposed layer; (2) the polarization parameter b characterizes the texture of the top surface layer in terms of grain size; and (3) the thermal inertia parameter I which refers to the soil compaction through the first few decimeters below the top surface sensed by polarimetry, in terms of size for the pieces making a granular regolith. Parameter b was derived from instrument VPM on board the Soviet spacecraft MARS-5, inertial I is from IRTM on the American Viking, and albedo A from both. The polarimetric scans racked strips covering two contrasted regions, the dark hued Mare Erythraeum, and the adjacent bright orange Thaumasia. Erythraem is characterized everywhere by a same type of terrain, despite the large geomorphological diversity of the surface. There is an ubiquitous coating or mantling with small dark grains, of both albedo 12.7 percent and particle size 10 to 20 microns, above a subsurface dislocation in pieces around 300 to 600 microns. A simple model is with sand-size particles completely coated with 15 micron dark grains. Author

N92-29010*# Arizona State Univ., Tempe. Dept. of Geology.
THE COMPOSITION OF MARTIAN AEOLIAN SANDS: THERMAL EMISSIVITY FROM VIKING IRTM OBSERVATIONS
Kenneth S. Edgett and Philip R. Christensen *In* Lunar and Planetary Inst., Workshop on the Martian Surface and Atmosphere Through Time 1992 p 45-46 (For primary document see N92-28988 19-91)
Avail: NTIS HC/MF A09

Aeolian sands provide excellent surfaces for the remote determination of the mineralogic composition of Martian materials, because such deposits consist of relatively well-sorted, uniform particle sizes and might consist of chemically unaltered, primary mineral grains derived from bedrock. Dark features on the floors of Martian craters are controlled by aeolian processes and many consist largely of unconsolidated, windblown sand. Measurement of the thermal emissivity of geologic materials provides a way to identify mid-infrared absorption bands, the strength and positions of which vary with mineral structure and composition. The Viking Infrared Thermal Mapper (IRTM) had four surface-sensing mid-IR bands, three of which, the 7, 9, and 11 micron channels, correspond to absorption features characteristic of carbonates, sialic, and mafic minerals, respectively. In this study, the highest quality IRTM data were constrained so as to avoid the effects of atmospheric dust, clouds, surface frosts, and particle size variations (the latter using data obtained between 7 and 9 H, and they were selected for dark intracrater features such that only data taken directly from the dark feature were used, so as to avoid thermal contributions from adjacent but unrelated materials. Three-point emissivity spectra of Martian dart intracrater features were compared with laboratory emission spectra of minerals and terrestrial aeolian sands convolved using the IRTM response function to the four IRTM spectral channels. Author

N92-29011*# Centre National de la Recherche Scientifique, Orsay (France). Inst. d'Astrophysique Spatial.
INFRARED PHOTOMETRIC BEHAVIOR AND OPPOSITION EFFECT OF MARS
S. Erard, J-P. Bibring, and P. Drossart (Observatoire de Paris-Meudon, France) *In* Lunar and Planetary Inst., Workshop on the Martian Surface and Atmosphere Through Time 1992 p 47-48 (For primary document see N92-28988 19-91)
Avail: NTIS HC/MF A09

Although the instrument wasn't designed for this purpose, data from the imaging spectrometer ISM may be used for studying photometric variations of Mars reflectance, that are related to the surface materials and aerosols physical properties. ISM flew aboard the Phobos-2 spacecraft which orbited Mars from January to March, 1989. About 40,000 spectra were acquired in 128 channels ranging from 0.76 to 3.16 micro-m, with a spatial resolution of 25 km and a signal-to-noise ratio ranging up to 1000. Analysis of the results leads to the following conclusions: width variations of the opposition surge can be related to differences in porosity or grain size

distribution on the various domains, with little or no effect from suspended dust. As the biggest effects are observed on dark and bright materials, intermediate behaviors on average-bright regions cannot result from a mixing process, but are more likely to come from either cementation processes or modification of the grain size distribution under the influence of wind, which under Martian conditions preferentially removes the biggest particles. Thus, a surface dust consisting in big bright and small dark grains could explain the observations. Author

N92-29012*# Washington Univ., Saint Louis, MO. Dept. of Earth and Planetary Sciences.
ATMOSPHERE-SURFACE INTERACTIONS AND ATMOSPHERIC EVOLUTION ON MARS
Bruce Fegley, Jr. *In* Lunar and Planetary Inst., Workshop on the Martian Surface and Atmosphere Through Time 1992 p 49-50 (For primary document see N92-28988 19-91)
Avail: NTIS HC/MF A09

A knowledge of the original volatile endowment of Mars is essential for any discussion of atmospheric loss on this planet. Cosmochemical models which postulate that planetary bulk compositions and volatile contents were controlled by the radial temperature profile in the solar nebula, and estimated bulk compositions based on the assumption that Mars is the parent body for the SNC meteorites predicts that Mars is volatile-rich. However, contrary views can also be found. For illustrative purposes, it is assumed that Mars was volatile-rich initially like the Earth. Taking terrestrial volatiles as the sum of the atmospheric, crustal, and oceanic volatiles and assuming that Mars accreted with the same volatile content on a g/g basis, the volatile endowments for an Earth-like Mars correspond to approximately 14 bars CO2, 800 mbars N2, and 1.2 km H2O. Subsequent topics discussed are: composition of outgassing volatiles; rates of present day atmospheric-surface reactions; constraints on CO2 loss via carbonate formation; constraints on H2O loss; and loss of other volatiles. H.A.

N92-29013*# State Univ. of New York, Plattsburgh. Dept. of Physics.
THE METEORITIC CONTRIBUTION TO DUST AND AEROSOLS IN THE ATMOSPHERE OF MARS
G. J. Flynn *In* Lunar and Planetary Inst., Workshop on the Martian Surface and Atmosphere Through Time 1992 p 51-52 (For primary document see N92-28988 19-91)
Avail: NTIS HC/MF A09

The continuous, planet-wide accretion of meteoritic material onto the Earth and Moon has been established by stratospheric sampling on Earth and chemical abundance analysis of the lunar soils. Meteoritic material must contribute in a similar manner to the atmospheres of all the planets and moons of the inner solar system. Although meteorites that survive planetary entry unmelted are the primary contributors, secondary contributions come from: (1) recondensed vapor in meteorite trails; and (2) fragmentation debris from low density meteoroids. These three contributions provide a constant planet-wide source of atmospheric particulates on Mars. In the size range greater than 1 micro-m in diameter micrometeorites which survive atmospheric entry unmelted are the major contributor, accounting for about 8.6 x 10(exp 6) kg/year of material. For particles less than 1 micro-m in diameter the majority of the mass is likely to come from recondensed meteoric vapor, which could account for approx. 2 x 10(exp 6) kg/year. H.A.

N92-29014*# State Univ. of New York, Stony Brook. Inst. for Terrestrial and Planetary Atmosphere.
NITROGEN ESCAPE FROM MARS
J. L. Fox *In* Lunar and Planetary Inst., Workshop on the Martian Surface and Atmosphere Through Time 1992 p 53-54 (For primary document see N92-28988 19-91)
Avail: NTIS HC/MF A09

The mass spectrometer on the Viking spacecraft measured anomalous N-15:N-14 ratio of about 1.62 times the terrestrial value. This enhancement presumably results from differential escape of N-15. The escape of N is non-thermal and potential escape mechanisms include photodissociation, photoionization, and electron impact dissociative ionization of N2, and ion-molecule reactions and dissociative recombination of N2(+). The authors propose some calculations to explain the N ratio, but even with all escape mechanisms considered, the ratios don't balance. This leads to the assumption that some other escape mechanisms must exist that are unexplained. H.A.

N92-29015*# National Aeronautics and Space Administration. Goddard Space Flight Center, Greenbelt, MD.
IMPLICATIONS OF EARLY HESPERIAN AGES FOR PRESUMED NOACHIAN AGE VOLCANIC FLOWS ON MARS
H. V. Frey *In* Lunar and Planetary Inst., Workshop on the Martian Surface and Atmosphere Through Time 1992 p 55-56 (For primary document see N92-28988 19-91)
Avail: NTIS HC/MF A09

Volcanic resurfacing has been important in Martian history. Major common-age resurfacing events are recorded in the cumulative frequency curves for the highland/lowland transition zone in eastern Mars and elsewhere. Most obvious in all these regions is a major resurfacing at the early hesperian (EH) time of ridged plains (unit Hr) eruption in Lunae Planum and elsewhere. This event seems to have occurred with greater or lesser efficiency in nearly all terrains studied: ridged plains, knobby terrain, smooth plains, and adjacent cratered terrain. Volcanic processes have apparently dominated all other sources of resurfacing (aeolian, periglacial, impact, fluvial) throughout all Martian history. H.A.

N92-29016*# Jet Propulsion Lab., California Inst. of Tech., Pasadena.
MARTIAN SURFACE SIMULATIONS
R. W. Gaskell *In* Lunar and Planetary Inst., Workshop on the Martian Surface and Atmosphere Through Time 1992 p 57-58 (For primary document see N92-28988 19-91)
Avail: NTIS HC/MF A09

Current scenarios for a Mars landing involve the extensive analysis of the surface near the landing site. Pinpoint landing, for example, requires a detailed mapping of the area from orbit for landmark identification and landing site selection, and the use by the lander of its own imaging data to recognize these landmarks and to guide itself safely to the surface. Hazard avoidance requires sufficient orbital imaging to ensure that safe landing sites exist, with the lander using its sensory data to find one of them. Once on the surface, a rover must be able to avoid or surmount obstacles, travel across surfaces with varying compositions and slopes, and navigate to a desired destination. Computer simulated Martian surfaces are being constructed to aid in the development of these exploration technologies. These surface simulations attempt to mimic the specific geologic episodes that built the surface, such as cratering, lava flows, and aeolian activity. Each episode takes a preexisting surface as a starting point, alters it in some way, and stores the new surface for further processing. This modular construction makes it possible for new processes to be included without altering existing software. Author

N92-29017*# National Aeronautics and Space Administration. Lyndon B. Johnson Space Center, Houston, TX.
MARS SURFACE WEATHERING PRODUCTS AND SPECTRAL ANALOGS: PALAGONITES AND SYNTHETIC IRON MINERALS
D. C. Golden, D. W. Ming, R. V. Morris, and H. V. Lauer, Jr. (Lockheed Engineering and Sciences Co., Houston, TX.) *In* Lunar and Planetary Inst., Workshop on the Martian Surface and Atmosphere Through Time 1992 p 59-60 (For primary document see N92-28988 19-91)
Avail: NTIS HC/MF A09

There are several hypotheses regarding the formation of Martian surface fines. These surface fines are thought to be products of weathering processes occurring on Mars. Four major weathering environments of igneous rocks on Mars have been proposed; (1) impact induced hydrothermal alterations; (2) subpermafrost igneous intrusion; (3) solid-gas surface reactions; and (4) subaerial igneous intrusion over permafrost. Although one or more of these processes may be important on the Martian

surface, one factor in common for all these processes is the reaction of solid or molten basalt with water (solid, liquid, or gas). These proposed processes, with the exception of solid-gas surface reactions, are transient processes. The most likely product of transient hydrothermal processes are layer silicates, zeolites, hydrous iron oxides and palagonites. The long-term instability of hydrous clay minerals under present Martian conditions has been predicted; however, the persistence of such minerals due to slow kinetics of dehydration, or entrapment in permafrost, where the activity of water is high, can not be excluded. Anhydrous oxides of iron (e.g., hematite and maghemite) are thought to be stable under present Martian surface conditions. Oxidative weathering of sulfide minerals associated with Martian basalts has been proposed. Weathering of sulfide minerals leads to a potentially acidic permafrost and the formation of Fe(3) oxides and sulfates. Weathering of basalts under acidic conditions may lead to the formation of kaolinite through metastable halloysite and metahalloysite. Kaolinite, if present, is thought to be a thermodynamically stable phase at the Martian surface. Fine materials on Mars are important in that they influence the surface spectral properties; these fines are globally distributed on Mars by the dust storms and this fraction will have the highest surface area which should act as a sink for most of the absorbed volatiles near the surface of Mars. Therefore, the objectives of this study were to: (1) examine the fine fraction mineralogy of several palagonitic materials from Hawaii; and (2) compare spectral properties of palagonites and submicron sized synthetic iron oxides with the spectral properties of the Martian surface. Author

N92-29018*# Brown Univ., Providence, RI.
STYLES OF CRATER GRADATION IN SOUTHERN ISMENIUS LACUS, MARS: CLUES FROM METEOR CRATER, ARIZONA
J. A. Grant and P. H. Schultz *In* Lunar and Planetary Inst., Workshop on the Martian Surface and Atmosphere Through Time 1992 p 61-62 (For primary document see N92-28988 19-91)
Avail: NTIS HC/MF A09

Impact craters on the Earth and Mars provide a unique opportunity to quantify the gradational evolution of instantaneously created landforms in a variety of geologic settings. Unlike most landforms, the initial morphology associated with impact craters on both planets is uncomplicated by competition between construction and degradation during formation. Furthermore, pristine morphologies are both well-constrained and similar to a first order. The present study compares styles of graduation at Meteor Crater with those around selected craters (greater than 1-2 km in diameter) in southern Ismenius Lacus. Emphasis is placed on features visible in images near LANDSAT TM resolution (30-50 m/pixel) which is available for both areas. In contrast to Mars, vegetation on the Earth can modify gradation, but appears to influence overall rates and styles by 2X-3X rather than orders of magnitude. Further studies of additional craters in differing settings will refine the effects of this and other factors (e.g., substrate). Finally, by analogy with results from other terrestrial gradational surfaces this study should help provide constraints on climate over crater histories. Author

N92-29019*# Arizona Univ., Tucson. Dept. of Geosciences and Planetary Sciences.
MAGMATIC INTRUSIONS AND HYDROTHERMAL SYSTEMS ON MARS
V. C. Gulick *In* Lunar and Planetary Inst., Workshop on the Martian Surface and Atmosphere Through Time 1992 p 63-64 (For primary document see N92-28988 19-91)
Avail: NTIS HC/MF A09

We are continuing our investigation of Martian hydrothermal systems and the formation of fluvial valleys on Mars. Here we present our initial numerical modeling results of hydrothermal systems associated with magmatic intrusions on Mars. To model such hydrothermal systems, we consider single, cylindrical intrusions of 4 km height 2 km below the surface. Our preliminary results of modeling hydrothermal systems associated with magmatic intrusions in the Martian environment suggest that such systems, if associated with intrusions of several 10(exp 2) km(exp 3) or larger, in the presence of permeable, water-rich subsurface should be able to provide adequate discharges of water over the time periods needed to form fluvial valleys. However, it is important to note that the amount of water ultimately available for erosion also depends on the surface and subsurface lithology. Author

N92-29020*# Northeast Artificial Intelligence Consortium, Arecibo (Puerto Rico).
MARS: WAVELENGTH-DEPENDENT DUAL POLARIZATION GLOBAL SCATTERING
J. K. Harmon, M. A. Slade, and R. S. Hudson *In* Lunar and Planetary Inst., Workshop on the Martian Surface and Atmosphere Through Time 1992 p 65-66 (For primary document see N92-28988 19-91)
Avail: NTIS HC/MF A09

During the 1988 and 1990 Mars oppositions, the first continuous-wave (CW) multi-wavelength radar observations were performed that include the entire echo in both polarizations. These observations, coordinated in subradar coverage when possible, were made with the Arecibo S-band (12.6 cm lambda) and Goldstone X-band (3.5 cm lambda) facilities. The CW spectra obtained during these oppositions have been studied using a variety of techniques to explore the spatial and wavelength dependence of both the Same-sense Circular (SC) and Opposite-sense Circular (OC) polarization returns. Earlier multi-wavelength comparisons dealt primarily with the quasispecular component of the echoes. Our work in contrast has much new information (at high signal-to-noise) for the SC 'depolarized component. The unique value of these radar observations lies in their potential for probing the subsurface scattering behavior in 'appropriate' terrain. The clearest case for wavelength dependence in the SC component is the scattering behavior over Tharsis, where the X-band features are significantly weaker than the S-band features. This hypothesis was advanced to account for the low thermal inertia of Tharsis, but also can explain the S/X differences if the layer is about 40 cm thick. In contrast to the Tharsis result, the depolarized echo from the heavily cratered terrain is actually stronger at X-band. The obvious interpretation is that more scatterers exist at the scale of the shorter wavelength, either at the surface or as a distributed subsurface scatterers. The strongest depolarized feature of the X-band spectra is associated with the south residual polar cap. The radar cross section of this feature corresponds to an equivalent full-disk albedo of unity. Author

N92-29021*# Open Univ., Milton (England). Planetary Sciences Unit.
THE STABLE ISOTOPIC COMPOSITIONS OF INDIGENOUS CARBON-BEARING COMPONENTS IN EETA 79001
C. P. Hartmetz, I. P. Wright, and C. T. Pillinger *In* Lunar and Planetary Inst., Workshop on the Martian Surface and Atmosphere Through Time 1992 p 67-68 (For primary document see N92-28988 19-91)
Avail: NTIS HC/MF A09

It is now widely accepted that the most likely source of SNC meteorites is Mars. An oblique impact on Mars, or vaporization of permafrost, by an impactor seem to be the most likely ejection mechanisms capable of accelerating material to the 5 km/s velocity needed to overcome the gravitational field of Mars. These ejection mechanisms involve a large shock event in the SNC class, the shergottites EETA 79001 and ALHA 77055 are the most likely shocked samples, in which whole rock pressures of 35 to 45 GPa have been estimated. Martian weathering products have also been identified in EETA 79001. Here, the author started a series of analyses of EETA 79001 using a high-sensitivity static mass spectrometer capable of measuring sub-nanogram quantities of carbon. Recent measurements of lithology C confirm that the shock-implanted atmospheric CO2 is released during the 1100 to 1200 C step. H.A.

N92-29022*# Cornell Univ., Ithaca, NY.
GREENHOUSE WARMING BY MINOR GASES ON EARLY MARS
M. N. Heinrich, W. R. Thompson, and C. Sagan *In* Lunar and

Planetary Inst., Workshop on the Martian Surface and Atmosphere Through Time 1992 p 69 (For primary document see N92-28988 19-91)
Avail: NTIS HC/MF A09

The early atmospheres of Earth and Mars were non-oxidizing mixtures likely derived from volcanic outgassing of a silicate mantle, with some fraction of the volatiles also contributed by impacting comets and meteorites. Here the authors investigate the potential of minor atmospheric constituents produced by ultraviolet and auroral chemistry to contribute to the thermal opacity of early Earth and Mars atmospheres. Using a very simple two-stream thermal opacity model, the authors show that HCN at 10 parts per million (ppm) and N2O at 100 ppm can each block radiation in thermal infrared windows sufficiently to increase the surface temperature by 7 K separately, or 14 K together. Small quantities of other species are also produced in such experiments. Some of these have especially complex infrared spectra and should be further investigated for their potential to help close windows in the CO2 + H2O infrared transmission. Enhancement of greenhouse warming by minor atmospheric species different from those present in today's atmosphere may have played important roles in the climate of early Earth and Mars. H.A.

N92-29023*# Colorado Univ., Boulder. Lab. for Atmospheric and Space Physics.
THE MARTIAN POLAR CAPS: STABILITY AND WATER TRANSPORT AT LOW OBLIQUITIES
B. G. Henderson and B. M. Jakosky *In* Lunar and Planetary Inst., Workshop on the Martian Surface and Atmosphere Through Time 1992 p 70-71 (For primary document see N92-28988 19-91)
Avail: NTIS HC/MF A09

The seasonal cycle of water on Mars is regulated by the two polar caps. In the winter hemisphere, the seasonal CO2 deposits at a temperature near 150 K acts as a cold trap to remove water vapor from the atmosphere. When summer returns, water is pumped back into the atmosphere by a number of mechanisms, including release from the receding CO2 frost, diffusion from the polar regolith, and sublimation from a water-ice residual cap. These processes drive an exchange of water vapor between the polar caps that helps shape the Martian climate. Thus, understanding the behavior of the polar caps is important for interpreting the Martian climate both now and at other epochs. Mars' obliquity undergoes large variations over large time scales. As the obliquity decreases, the poles receive less solar energy so that more CO2 condenses from the atmosphere onto the poles. It has been suggested that permanent CO2 condenses from the atmosphere onto the poles. It has been suggested that permanent CO2 caps might form at the poles in response to a feedback mechanism existing between the polar cap albedo, the CO2 pressure, and the dust storm frequency. The year-round presence of the CO2 deposits would effectively dry out the atmosphere, while diffusion of water from the regolith would be the only source of water vapor to the atmosphere. We have reviewed the CO2 balance at low obliquity taking into account the asymmetries which make the north and south hemispheres different. Our analysis linked with a numerical model of the polar caps leads us to believe that one summertime cap will always lose its CO2 cover during a Martian year, although we cannot predict which cap this will be. We conclude that significant amounts of water vapor will sublime from the exposed cap during summer, and the Martian atmosphere will support an active water cycle even at low obliquity. Author

N92-29024*# Jet Propulsion Lab., California Inst. of Tech., Pasadena. Geology and Planetology Section.
DARK MATERIAL IN THE POLAR LAYERED DEPOSITS ON MARS
Ken Herkenhoff *In* Lunar and Planetary Inst., Workshop on the Martian Surface and Atmosphere Through Time 1992 p 72-73 (For primary document see N92-28988 19-91)
Avail: NTIS HC/MF A09

The Martian polar layered deposits probably record periodic variations in the deposition of dust and ice caused by climate changes over the past 10 to 100 million years. The polar layered deposits appear to be the source of dark, saltating material that has been distributed over the surface of Mars, but the mechanisms by which this material is incorporated and eroded from the layered deposits is unknown. These mechanisms must be understood before the processes that formed and modified the layered deposits can be inferred and related to Martian climate changes. In summary, weathering of the Martian layered deposits by sublimation of water ice may account for the geologic relationships observed in the Martian polar regions. The non-volatile components of the layered deposits appears to consist mainly of bright red dust, with small amounts of dark dust or sand. Alternatively, dark sand-sized basaltic particles may occasionally be transported onto the layered deposits, forming thin layers. Once eroded, particles of either type may saltate to form the dark dunes found in both polar regions. H.A.

N92-29025*# National Aeronautics and Space Administration. Ames Research Center, Moffett Field, CA.
MARS ENVIRONMENTAL SURVEY (MESUR): SCIENCE OBJECTIVES AND MISSION DESCRIPTION
G. Scott Hubbard, Paul F. Wercinski, George L. Sarver, Robert P. Hanel, and Ruben Ramos *In* Lunar and Planetary Inst., Workshop on the Martian Surface and Atmosphere Through Time 1992 p 74-75 (For primary document see N92-28988 19-91)
Avail: NTIS HC/MF A09

In-situ observations and measurements of Mars are objectives of a feasibility study beginning at the Ames Research Center for a mission called the Mars Environmental SURvey (MESUR). The purpose of the MESUR mission is to emplace a pole-to-pole global distribution of landers on the Martian surface to make both short- and long-term observations of the atmosphere and surface. The basic concept is to deploy probes which would directly enter the Mars atmosphere, provide measurements of the upper atmospheric structure, image the local terrain before landing, and survive landing to perform meteorology, seismology, surface imaging, and soil chemistry measurements. MESUR is intended to be a relatively low-cost mission to advance both Mars science and human presence objectives. Mission philosophy is to: (1) 'grow' a network over a period of years using a series of launch opportunities, thereby minimizing the peak annual costs; (2) develop a level-of-effort which is flexible and responsive to a broad set of objectives; (3) focus on science while providing a solid basis for human exploration; and (4) minimize project cost and complexity wherever possible. In order to meet the diverse scientific objectives, each MESUR lander will carry the following strawman instrument payload consisting of: (1) Atmospheric structure experiment, (2) Descent and surface imagers, (3) Meteorology package, (4) Elemental composition instrument, (5) 3-axis seismometer, and (6) Thermal analyzer/evolved gas analyzer. The feasibility study is primarily to show a practical way to design an early capability for characterizing Mars' surface and atmospheric environment on a global scale. The goals are to answer some of the most urgent questions to advance significantly our scientific knowledge about Mars, and for planning eventual exploration of the planet by robots and humans. Author

N92-29026*# Jet Propulsion Lab., California Inst. of Tech., Pasadena.
OBSERVATIONS OF MARS USING HUBBLE SPACE TELESCOPE
Philip B. James (Toledo Univ., OH.), R. Todd Clancy (Colorado Univ., Boulder.), Steven W. Lee (Colorado Univ., Boulder.), Ralph Kahn, Richard Zurek, Leonard Martin (Lowell Observatory, Flagstaff, AZ.), and Robert Singer (Arizona Univ., Tucson.) *In* Lunar and Planetary Inst., Workshop on the Martian Surface and Atmosphere Through Time 1992 p 76-77 (For primary document see N92-28988 19-91)
Avail: NTIS HC/MF A09

The lack of a continuous record of Martian meteorology or of volatile cycles on Mars for extended periods of several Martian years seriously hinders efforts to understand the physics of the Martian atmosphere and surface system. The spacecraft observations are limited to only a few isolated time periods, and

the Earth based record is limited by the relatively short periods surrounding oppositions when telescopic observations can yield useful data. To remedy this situation, the authors have embarked on a three year program of Mars observations using the Hubble Space Telescope (HST). Several scientific investigations are being carried out using the images, including: a study of the albedo variations; unit mapping of spectral reflectances; determination of optical depths due to aerosols and condensates; a study of the properties of condensate clouds and hoods; comparison of surface and atmospheric features; observation of size and shape of the polar caps; and investigation of surface atmospheric phenomena. H.A.

N92-29027*# National Aeronautics and Space Administration. Lyndon B. Johnson Space Center, Houston, TX.
DISTRIBUTION OF WATER ON MARS: IMPLICATIONS FROM SNC METEORITES
J. H. Jones *In* Lunar and Planetary Inst., Workshop on the Martian Surface and Atmosphere Through Time 1992 p 78-79 (For primary document see N92-28988 19-91)
Avail: NTIS HC/MF A09

There has been much speculation about the abundance of water and other volatiles on Mars. Attempts to calculate abundances of water on Mars indicate that Mars contains approx. 10-100 m of water. Numerous models have been put forth to determine the amount of water on Mars more closely. Some researchers infer that Chassigny parent magma contained greater than 1.5 percent water by weight and that the Martian mantle contained greater than 1000 parts per million water. This is too much water for a depleted region. Perhaps some of the water in Chassigny was assimilated at shallow depths, either in a crustal magma chamber or by interaction with superficial permafrost. Either is possible and provides an alternative to the dilemma of water-rich to depleted regions. H.A.

N92-29028*# National Aeronautics and Space Administration. Lyndon B. Johnson Space Center, Houston, TX.
A LIQUIDUS PHASE DIAGRAM FOR THE GROUNDMASS OF EETA 79001A (Eg), A PRIMITIVE SHERGOTTITE COMPOSITION
J. H. Jones, A. J. G. Jurewicz (Lockheed Engineering and Sciences Co., Houston, TX.), and L. Le (Lockheed Engineering and Sciences Co., Houston, TX.) *In* Lunar and Planetary Inst., Workshop on the Martian Surface and Atmosphere Through Time 1992 p 80-81 (For primary document see N92-28988 19-91)
Avail: NTIS HC/MF A09

Shergottites are members of the SNC meteorite suite, which may be samples of Mars. If so, the shergottite in our collection that most likely represents primitive liquid from the Martian mantle is EETA 79001. EETA 79001 has the Nd isotopic signature of a long-term depleted mantle, a relatively high Mg number, and a slightly olivine-normative composition. The authors have performed experiments on the composition of EETA 79001 for traces of Eg. Other topics discussed include: comparison of calculated phase equilibria; nature of the olivine-pyroxene boundary; and interstitial liquids. H.A.

N92-29029*# Arizona Univ., Tucson. Lunar and Planetary Lab.
GLACIAL GEOMORPHIC EVIDENCE FOR A LATE CLIMATIC CHANGE ON MARS
J. S. Kargel and R. G. Strom *In* Lunar and Planetary Inst., Workshop on the Martian Surface and Atmosphere Through Time 1992 p 82-83 (For primary document see N92-28988 19-91)
Avail: NTIS HC/MF A09

In a series of preliminary reports, we documented evidence of former glacial epochs on Mars. Apparent glacial landforms seemed to be concentrated primarily at middle to high southern latitudes. We now have additional evidence supporting the view that Martian glaciation appears to have been more extensive than previously recognized. The growth and collapse of ice sheets on Mars seems closely analogous to the growth and decline of Earth's great Pleistocene ice sheets. This implies that climate change was probably somewhat comparable on the two planets, although in the case of Mars the entire planet seems to have changed rapidly to a cold, dry present-day environment after the collapse of the ice sheets. Author

N92-29030*# National Aeronautics and Space Administration. Ames Research Center, Moffett Field, CA.
WAS EARLY MARS WARMED BY AMMONIA?
J. F. Kasting (Pennsylvania State Univ., University Park.), L. L. Brown (Pennsylvania State Univ., University Park.), J. M. Acord (Pennsylvania State Univ., University Park.), and J. B. Pollack *In* Lunar and Planetary Inst., Workshop on the Martian Surface and Atmosphere Through Time 1992 p 84-85 (For primary document see N92-28988 19-91)
Avail: NTIS HC/MF A09

Runoff channels and valley networks present on ancient, heavily cratered Martian terrain suggests that the climate of Mars was originally warm and wet. One explanation for the formation of these channels is that the surface was warmed by the greenhouse effect of a dense, CO2 atmosphere. However, recent work shows that this theory is not consistent for the early period of the solar system. One way to increase the surface temperature predicted is to assume that other greenhouse gases were present in Mars' atmosphere in addition to CO2 and H2O. This possible gas is ammonia, NH3. If ammonia was present in sufficient quantities, it could have raised the surface temperature to 273 K. An adequate source would have been volcanic outgassing if the NH3 produced was shielded from photolysis by an ultraviolet light absorber. H.A.

N92-29031*# Arizona Univ., Tucson.
EROSIONAL LANDFORMS ON THE LAYERED TERRAINS IN VALLES MARINERIS
G. Komatsu, R. G. Strom, V. C. Gulick, and T. J. Parker (University of Southern California, Los Angeles.) *In* Lunar and Planetary Inst., Workshop on the Martian Surface and Atmosphere Through Time 1992 p 86-87 (For primary document see N92-28988 19-91)
Avail: NTIS HC/MF A09

Many investigators have proposed potential lakes in Valles Marineris based on the relationship with outflow channels, and a proposed lacustrine origin of layered deposits. We have investigated the erosional style of the layered terrains and evaluated their potential origins as sedimentation in and erosional modification by these lakes. The erosional features that will be discussed are distributed in the central canyon area and classified into terraces and layered depressions. Many terraces can be explained by coastal erosion in lakes as well as by eolian erosion. The lack of terraces on the canyon walls is probably due to more recent sapping and mass wasting of materials with different mechanical response to erosion than the layered terrains. Catastrophic water discharges in Valles Marineris as hypothesized by an ocean model may have been the source of the lakes and the eventual catastrophic release of water from the canyons. Author

N92-29032*# Colorado Univ., Boulder. Lab. for Atmospheric and Space Physics.
MARS: CORRECTING SURFACE ALBEDO OBSERVATIONS FOR EFFECTS OF ATMOSPHERIC DUST LOADING
S. W. Lee and R. T. Clancy *In* Lunar and Planetary Inst., Workshop on the Martian Surface and Atmosphere Through Time 1992 p 88 (For primary document see N92-28988 19-91)
Avail: NTIS HC/MF A09

We have developed a radiative transfer model which allows the effects of atmospheric dust loading on surface albedo to be investigated. This model incorporates atmospheric dust opacity, the single scattering albedo and particle phase function of atmospheric dust, the bidirectional reflectance of the surface, and variable lighting and viewing geometry. The most recent dust particle properties are utilized. The spatial and temporal variability of atmospheric opacity (Tan) strongly influences the radiative transfer modelling results. We are currently using the approach described to determine Tan for IRTM mapping sequences of selected regions. This approach allows Tan to be determined at

the highest spatial and temporal resolution supported by the IRTM data. Applying the radiative transfer modelling and determination of Tan described, IRTM visual brightness observations can be corrected for the effects of atmospheric dust loading a variety of locations and times. This approach allows maps of 'dust-corrected surface albedo' to be constructed for selected regions. Information on the variability of surface albedo and the amount of dust deposition/erosion related to such variability results. To date, this study indicates that atmospheric dust loading has a significant effect on observations of surface albedo, amounting to albedo corrections of as much as several tens of percent. This correction is not constant or linear, but depends upon surface albedo, viewing and lighting geometry, the dust and surface phase functions, and the atmospheric opacity. It is clear that the quantitative study of surface albedo, especially where small variations in observed albedo are important (such as photometric analyses), needs to account for the effects of the atmospheric dust loading. Maps of 'dust-corrected surface albedo' will be presented for a number of regions. Author

N92-29033*# Atmospheric and Environmental Research, Inc., Cambridge, MA.

SIMULATIONS OF THE SEASONAL POLAR CAPS ON MARS

Bernhard Lee Lindner *In* Lunar and Planetary Inst., Workshop on the Martian Surface and Atmosphere Through Time 1992 p 89-90 (For primary document see N92-28988 19-91)

Avail: NTIS HC/MF A09

One of the most puzzling mysteries about the planet Mars is the hemispherical asymmetry in the polar caps. Every spring the seasonal polar cap of CO2 recedes until the end of the summer, when only a small part, the residual polar cap, remains. Scientists have sought to explain this asymmetry by modeling observations of the latitudinal recession of the polar cap and seasonal variations in atmospheric pressure (since the seasonal polar caps are primarily frozen atmosphere, they are directly related to changes in atmospheric mass). These models reproduce most aspects of the observed annual variations in atmospheric pressure fairly accurately. Furthermore, the predicted latitudinal recession of the northern polar cap in the spring agrees well with observations, including the fact that the CO2 ice is predicted to completely sublime away during the summer in the Southern Hemisphere, unlike what is observed. This power will show how the radiative effects of ozone, clouds, and airborne dust, light penetration into and through the polar caps, and the dependence of albedo on solar zenith angle affect CO2 ice formation and sublimation, and how they help explain the hemispherical asymmetry in the residual polar caps. These effects have not been studied with prior polar cap models. Author

N92-29034*# California Univ., Los Angeles. Inst. of Geophysics and Planetary Physics.

MARS ATMOSPHERE EVOLUTION: ESCAPE TO SPACE

J. G. Luhmann *In* Lunar and Planetary Inst., Workshop on the Martian Surface and Atmosphere Through Time 1992 p 91-92 (For primary document see N92-28988 19-91)

Avail: NTIS HC/MF A09

The loss mechanisms and the rates of escape, to space, of Martian atmosphere constituents have changed throughout the history of the solar system. For the first billion years, Mars' atmosphere escape was probably dominated by impact erosion related to the presence of debris left over from the accretionary phase. This loss was further augmented by hydrodynamic outflows related to the presence of an early denser atmosphere and a sun that was brighter in the EUV wavelengths. Following this initial 'catastrophic' phase, during which a large fraction of the original atmosphere was lost but then replaced by volcanism and cometary impact, the 'modern' loss mechanisms which still operate today would have taken over. Those mechanisms that now contribute to escape to space consist of classical thermal or Jeans escape, nonthermal escape due to chemical reaction in the atmosphere, and solar wind-related losses. Both the loss mechanisms and the rates of escape are discussed. Author

N92-29035*# California Univ., Los Angeles. Inst. of Geophysics and Planetary Physics.

DISCOVERY CONCEPTS FOR MARS

J. G. Luhmann, C. T. Russell, L. H. Brace (Michigan Univ., Ann Arbor.), A. F. Nagy (Michigan Univ., Ann Arbor.), B. M. Jakosky (Colorado Univ., Boulder.), C. A. Barth (Colorado Univ., Boulder.), and J. H. Waite (Southwest Research Inst., San Antonio, TX.) *In* Lunar and Planetary Inst., Workshop on the Martian Surface and Atmosphere Through Time 1992 p 93 (For primary document see N92-28988 19-91)

Avail: NTIS HC/MF A09

Two focused Mars missions that would fit within the guidelines for the proposed Discovery line are discussed. The first mission would deal with the issue of the escape of the atmosphere (Mars') to space. A complete understanding of this topic is crucial to deciphering the evolution of the atmosphere, climate change, and volatile inventories. The second mission concerns the investigation of remanent magnetization of the crust and its relationship to the ionosphere and the atmosphere. Author

N92-29036*# National Aeronautics and Space Administration. Ames Research Center, Moffett Field, CA.

NONLINEAR STRATIFIED FLOW OVER LOCALIZED TOPOGRAPHIC OBSTACLES ON MARS

J. A. Magalhaes and R. E. Young *In* Lunar and Planetary Inst., Workshop on the Martian Surface and Atmosphere Through Time 1992 p 94-95 (For primary document see N92-28988 19-91)

Avail: NTIS HC/MF A09

The current dynamical influence of the Martian atmosphere on the surface is clearly revealed by dark surface albedo features which are associated with localized topographic relief and were described in detail and classified as Type I(d) wind streaks. The contrast of the streaks diminishes or disappears during the global dust storms, and the streaks are observed to quickly reform after the termination of the storms; the streaks remain stable after L(sub S) = 0 deg until the next dust storm. These observations, together with the ragged edges of the streaks, were used to infer that the dark streaks are formed by the removal of bright dust from a darker substrate. Author

N92-29037*# National Aeronautics and Space Administration. Goddard Space Flight Center, Greenbelt, MD.

VOLATILE TRACERS OF MARTIAN ATMOSPHERIC EVOLUTION: PRESENT MEASUREMENT STATUS AND REQUIREMENTS FOR FUTURE INVESTIGATIONS

Paul Mahaffy and Konrad Mauersberger (Minnesota Univ., Minneapolis.) *In* Lunar and Planetary Inst., Workshop on the Martian Surface and Atmosphere Through Time 1992 p 96 (For primary document see N92-28988 19-91)

Avail: NTIS HC/MF A09

One of the most significant contributions to the detailed characterization of the molecular, atomic, and isotopic composition of the Martian atmosphere came from the Viking mass spectrometer experiments. Measurement of the abundance of the noble gases Ne, Ar, Kr, and Xe, as well as major molecular species was achieved together with some of the important isotopic compositions such as N-15/N-14, Ar-36/Ar-40, and others. The isotopic characterization, a key element to an understanding of atmospheric evolution, advanced further with recent measurements of the deuterium/hydrogen (D/H) ratio from HDO as well as the detailed study of gases contained in meteorites thought to be Martian origin. Author

N92-29038*# Georgia Southwestern Coll., Americus.

AN EJECTION MODEL FOR SNC METEORITES: AN INDICATION FOR RECENT VOLCANISM ON MARS

J. P. Manker *In* Lunar and Planetary Inst., Workshop on the Martian Surface and Atmosphere Through Time 1992 p 97-98 (For primary document see N92-28988 19-91)

Avail: NTIS HC/MF A09

When compared to other achondrites, Shergotty-Nakhla-Chassigny (SNC) meteorites are viewed as anomalous objects. This conclusion is based mainly on their

extremely young crystallization ages and their short cosmic ray exposure times. Further, SNC's noble gas and nitrogen components indicate a martian origin for these objects. If these meteorites are from Mars, then the most confounding question facing the planetary science community is how were they ejected from the planet's surface. The following is an investigation of that question.
Author

N92-29039*# Lowell Observatory, Flagstaff, AZ.
OBSERVED CHANGES IN LIMB CLOUDS IMMEDIATELY PRIOR TO THE ONSET OF PLANET-ENCIRCLING DUST STORMS
L. J. Martin, P. B. James (Toledo Univ., OH.), and R. W. Zurek (Jet Propulsion Lab., California Inst. of Tech., Pasadena.) *In* Lunar and Planetary Inst., Workshop on the Martian Surface and Atmosphere Through Time 1992 p 99-100 (For primary document see N92-28988 19-91)
(Grant NAGw-2257)
Avail: NTIS HC/MF A09

Of the several size and nomenclature groupings of Martian dust storms, it is the plane-encircling or truly runaway dust storms that are of most concern to both the theoreticians and mission planners. Once believed to be regularly seasonal, it is now known that they are not annual occurrences and that the few we know about occurred within at least one-third of Mars' seasonal cycle. We cannot confirm that any were observed before 1956, and not one has been observed since 1982 (the classification of that event as 'encircling' is an interpretation of observation from a single point on the planet's surface). If these storms occur in cycles, we do not know the lengths or causes of the cycles. Regional and local dust storms occur more frequently and throughout the Martian year, but the underlying question is how do some become runaways, encircling the planet, while the others die out, usually within a few days. An investigation of this topic is presented. Author

N92-29040*# Jet Propulsion Lab., California Inst. of Tech., Pasadena.
NEW DUST OPACITY MAPS FROM VIKING IR THERMAL MAPPER DATA
T. Z. Martin and M. I. Richardson (Imperial Coll. of Science and Technology, London, England) *In* Lunar and Planetary Inst., Workshop on the Martian Surface and Atmosphere Through Time 1992 p 101-102 (For primary document see N92-28988 19-91)
Avail: NTIS HC/MF A09

Mapping of dust opacity of the Martian atmosphere, using the silicate-induced absorption of 9 micron radiation, was performed with the Viking Infrared Thermal Mapper (IRTM) data for several local dust storms and in a global sense. We present here the first results from an effort to extend the earlier mapping work to the period of the 1977b major storm, and to concentrate attention on the details of opacity behavior during the initial phases of the 1977a and b storms. Author

N92-29041*# Geological Survey, Flagstaff, AZ.
TEMPORAL VARIABILITY OF THE SURFACE AND ATMOSPHERE OF MARS: VIKING ORBITER COLOR OBSERVATIONS
A. S. McEwen *In* Lunar and Planetary Inst., Workshop on the Martian Surface and Atmosphere Through Time 1992 p 103-104 (For primary document see N92-28988 19-91)
Avail: NTIS HC/MF A09

We are near the final stages in the processing of a large Viking Orbiter global color dataset. Mosaics from 57 spacecraft revolutions (or 'revs' hereafter) were produced, most in both red and violet or red, green, and violet filters. Phase angles range from 13 deg to 85 deg. A total of approximately 2000 frames were processed through radiometric calibration, cosmetic cleanup, geometric control, reprojection, and mosaicking into single-rev mosaics at a scale of 1 km/pixel. All of the mosaics are geometrically tied to the 1/256 deg/pixel Mars Digital Image Mosaic (MDIM). Photometric normalization is in progress, to be followed by production of a 'best coverage' global mosaic at a scale of 1/64 deg/pixel (0.923 km/pixel). Global coverage is near 100 percent in red-filter mosaics and 98 percent and 60 percent in corresponding violet- and green-filter mosaics, respectively. Soon after completion, all final datasets (including single-rev mosaics) will be distributed to the planetary community on compact disks.
Author

N92-29042*# Colorado Univ., Boulder. Lab. for Atmospheric and Space Physics.
REGIONAL VARIATIONS IN THE STABILITY AND DIFFUSION OF WATER-ICE IN THE MARTIAN REGOLITH
Michael T. Mellon and Bruce M. Jakosky *In* Lunar and Planetary Inst., Workshop on the Martian Surface and Atmosphere Through Time 1992 p 105-106 (For primary document see N92-28988 19-91)
Avail: NTIS HC/MF A09

Geologic evidence suggests subsurface water-ice has played an important role in the formation of Martian landforms. Forms of mass-wasting such as debris aprons and flow patterns on valley floors suggest creep deformation of ice-laden soil, while thermokarst and chaotic terrain suggest once extensive deposits of ground ice that were later removed. The global distribution of ice-related morphology was mapped. The mapping showed regional variation, in both latitude and longitude, in the distribution of debris aprons, concentric fill craters, and 'softened' crater profiles.
Author

N92-29043*# Arizona Univ., Tucson. Lab. of Planetary Image Research.
EXPLORING COMPOSITIONAL VARIATIONS ON THE SURFACE OF MARS APPLYING MIXING MODELING TO A TELESCOPIC SPECTRAL IMAGE
E. Merenyi, J. S. Miller, and R. B. Singer *In* Lunar and Planetary Inst., Workshop on the Martian Surface and Atmosphere Through Time 1992 p 107-108 (For primary document see N92-28988 19-91)
Avail: NTIS HC/MF A09

The linear mixing model approach was successfully applied to data sets of various natures. In these sets, the measured radiance could be assumed to be a linear combination of radiance contributions. The present work is an attempt to analyze a spectral image of Mars with linear mixing modeling. Author

N92-29044*# Deutsche Forschungsanstalt fuer Luft- und Raumfahrt, Cologne (Germany, F.R.). Inst. fuer Raumsimulation.
SIMULATION OF MARTIAN SURFACE-ATMOSPHERE INTERACTION IN A SPACE-SIMULATOR: TECHNICAL CONSIDERATIONS AND FEASIBILITY
D. Moehlmann and H. Kochan *In* Lunar and Planetary Inst., Workshop on the Martian Surface and Atmosphere Through Time 1992 p 109 (For primary document see N92-28988 19-91)
Avail: NTIS HC/MF A09

The Space Simulator of the German Aerospace Research Establishment at Cologne, formerly used for testing satellites, is now, since 1987, the central unit within the research sub-program 'Comet-Simulation' (KOSI). The KOSI team has investigated physical processes relevant to comets and their surfaces. As a byproduct we gained experience in sample-handling under simulated space conditions. In broadening the scope of the research activities of the DLR Institute of Space Simulation an extension to 'Laboratory-Planetology' is planned. Following the KOSI-experiments a Mars Surface-Simulation with realistic minerals and surface soil in a suited environment (temperature, pressure, and CO2-atmosphere) is foreseen as the next step. Here, our main interest is centered on thermophysical properties of the Martian surface and energy transport (and related gas transport) through the surface. These laboratory simulation activities can be related to space missions as typical pre-mission and during-the-mission support of the experiments design and operations (simulation in parallel). Post mission experiments for confirmation and interpretation of results are of great value. The physical dimensions of the Space Simulator (cylinder of about 2.5

m diameter and 5 m length) allows for testing and qualification of experimental hardware under realistic Martian conditions. Author

N92-29045*# National Aeronautics and Space Administration. Ames Research Center, Moffett Field, CA.
MARS DUST STORM SIMULATIONS: ANALYSIS OF SURFACE STRESS
J. R. Murphy and C. B. Leovy (Washington Univ., Seattle.) *In* Lunar and Planetary Inst., Workshop on the Martian Surface and Atmosphere Through Time 1992 p 110 (For primary document see N92-28988 19-91)
Avail: NTIS HC/MF A09

The primary mechanism by which dust is inserted into the Martian atmosphere is the interaction of low-level atmospheric motions with the planet's surface. Near-surface winds exert a shear stress upon dust particles resting on the Martian surface, and at some lower threshold limit of stress magnitude, approximately 0.04 N-m(exp -2), particles are set into motion. Wind tunnel studies indicate that the first particles are too large to remain in suspension in the Martian atmosphere, but their impact back upon the surface can set smaller suspendable particles into motion. This process is termed saltation. Numerical simulations of Martian dust storms were carried out via the interactive coupling of the NASA Ames Mars general circulation Model with an aerosol transport/microphysical model. Author

N92-29046*# California Univ., Los Angeles. Dept. of Earth and Space Sciences.
IS GROUND ICE STABLE NEAR THE MARTIAN EQUATOR?
D. A. Paige *In* Lunar and Planetary Inst., Workshop on the Martian Surface and Atmosphere Through Time 1992 p 111-112 (For primary document see N92-28988 19-91)
Avail: NTIS HC/MF A09

Determining the present distribution of subsurface water ice on Mars will undoubtedly be a prime objective for future spacecraft missions. Past theoretical studies have predicted that Martian ground ice should be stable to evaporation only at latitudes poleward of approximately +/- 50 deg. Presented here are a new set of calculations which show that bright surficial dust deposits can protect subsurface ice deposits from evaporation at much lower latitudes than previously expected. Author

N92-29047*# University of Southern California, Los Angeles. Dept. of Geological Sciences.
DISTRIBUTION OF COASTAL MORPHOLOGY IN THE MARTIAN NORTHERN LOWLANDS
T. J. Parker and D. S. Gorsline *In* Lunar and Planetary Inst., Workshop on the Martian Surface and Atmosphere Through Time 1992 p 113-114 (For primary document see N92-28988 19-91)
Avail: NTIS HC/MF A09

The northern plains of Mars exhibit boundary morphologies that were interpreted as shorelines of a sea that formed as a result of flooding from the major outflow channel along the periphery of the lowlands. Earlier work focused on a morphologic description based on the very high resolution images available in the west Deuteronilus Mensae region where these boundaries and their relationships to pre-existing features could be most readily characterized. Here, we wish to describe the criteria used in the earlier identification. Author

N92-29048*# Jet Propulsion Lab., California Inst. of Tech., Pasadena.
RECENT ELYSIUM VOLCANISM: EFFECTS ON THE MARTIAN ATMOSPHERE
J. B. Plescia and J. Crisp *In* Lunar and Planetary Inst., Workshop on the Martian Surface and Atmosphere Through Time 1992 p 115-116 (For primary document see N92-28988 19-91)
Avail: NTIS HC/MF A09

A vast area of smooth plains in southeastern Elysium near 5 deg N, 195 deg was identified as young volcanic plains. These plains represent flood eruptions of very low viscosity lavas at a point in time much later than the volcanism that produced the major volcanoes of Elysium. Since volcanism is a principal mechanism by which gases are supplied to the atmosphere, and since these gases can have important climatic effects, it is important to consider the amount of H2O, CO2, and other gases that were possibly released. We present estimates of input and release rates from this volcanic episode. The age is defined by the density of superposed craters; there are 89 +/- 15 craters greater than or equal to 1 km per 10(exp 6) sq km corresponding to the Upper Amazonian making this the youngest major volcanic episode. Lavas, covering 1.5 x 10(exp 6) sq km and presumably erupted through fissures, filled a topographic low and then flowed through knobby terrain into westernmost Amazonis. The western plains are characterized by scattered low shields having radial lava flows. Unit thickness is uncertain, individual flows are about 10 m thick; the entire deposit buries older knobby terrain having local relief of 200-400 m (estimated by Earth-based radar data); hence the volcanics must be thick enough to bury that relief. On the basis of unit morphology, length of flows, and the extent of the deposit, it can be inferred that the lava was of low viscosity and mafic to ultramafic composition. The age and petrology of the shergottites suggest they may have come from this unit. Author

N92-29049*# Worcester Polytechnic Inst., MA.
DETERMINING THE pH OF MARS FROM THE VIKING LABELLED RELEASE REABSORPTION EFFECT
Robert C. Plumb *In* Lunar and Planetary Inst., Workshop on the Martian Surface and Atmosphere Through Time 1992 p 117 Prepared in cooperation with Brown Univ., Worcester, MA (For primary document see N92-28988 19-91)
Avail: NTIS HC/MF A09

The acid-base properties and redox potentials of solids are two of the more fundamental chemical parameters characterizing a material. Knowledge of these parameters for martian regolith fines would be of considerable value in determining what specific compounds are present and making judgements on what reactions are possible. Author

N92-29050*# Geological Survey, Denver, CO.
CHEMICAL REACTION PATH MODELING OF HYDROTHERMAL PROCESSES ON MARS: PRELIMINARY RESULTS
Geoffrey S. Plumlee and W. Ian Ridley *In* Lunar and Planetary Inst., Workshop on the Martian Surface and Atmosphere Through Time 1992 p 118-119 (For primary document see N92-28988 19-91)
Avail: NTIS HC/MF A09

Hydrothermal processes are thought to have had significant roles in the development of surficial mineralogies and morphological features on Mars. For example, a significant proportion of the Martian soil could consist of the erosional products of hydrothermally altered impact melt sheets. In this model, impact-driven, vapor-dominated hydrothermal systems hydrothermally altered the surrounding rocks and transported volatiles such as S and Cl to the surface. Further support for impact-driven hydrothermal alteration on Mars was provided by studies of the Ries crater, Germany, where suevite deposits were extensively altered to montmorillonite clays by inferred low-temperature (100-130 C) hydrothermal fluids. It was also suggested that surface outflow from both impact-driven and volcano-driven hydrothermal systems could generate the valley networks, thereby eliminating the need for an early warm wet climate. We use computer-driven chemical reaction path calculation to model chemical processes which were likely associated with postulated Martian hydrothermal systems. Author

N92-29051*# National Aeronautics and Space Administration. Ames Research Center, Moffett Field, CA.
SHORT- AND LONG-TERM CLIMATE CHANGES ON MARS
James B. Pollack *In* Lunar and Planetary Inst., Workshop on the Martian Surface and Atmosphere Through Time 1992 p 120 (For primary document see N92-28988 19-91)
Avail: NTIS HC/MF A09

The present climate of Mars is dominated by the seasonal

cycles of dust, water vapor, and carbon dioxide. Understanding these cycles represents a first step towards interpreting climate changes in the past. Past climates on Mars were probably different from the present one due to astronomical variations of orbital and axial properties, to major changes in atmospheric pressure and/or composition, and to long-term changes in solar luminosity.

Author

N92-29052*# Hawaii Univ., Honolulu. Planetary Geosciences.
INFLUENCE OF HEAT FLOW ON EARLY MARTIAN CLIMATE
Susan Postawko and Fraser P. Fanale *In* Lunar and Planetary Inst., Workshop on the Martian Surface and Atmosphere Through Time 1992 p 121 (For primary document see N92-28988 19-91)
Avail: NTIS HC/MF A09

Previous arguments have suggested that the formation of the valley networks on Mars may be explained by higher internal regolith temperatures associated with a much higher heat flow early in the planet's history. It is possible that this higher heat flow could cause groundwater to be closer to the martian surface 3.8 billion years ago, and thus allow the formation of the valley networks by groundwater sapping, without having to invoke surface warming due to an atmospheric greenhouse effect. It was previously shown that, in fact, it may not be possible to completely separate the effects of higher heat flow and atmospheric greenhouse on early Mars. We have more fully explored the parametric space of our set of equations to better determine the sensitivity of the system to variations in any of the factors. The limiting factor in the effectiveness of an atmospheric greenhouse is the total CO2 available in the system. We find that a combination of higher heat flow and atmospheric greenhouse effect on early Mars may more easily explain valley network formation and distribution, even for a cool early sun, than either of these mechanisms separately.

Author

N92-29053*# Arizona State Univ., Tempe. Dept. of Geology.
MID-INFRARED SPECTRA OF MARTIAN KOMANTIITE
David P. Reyes *In* Lunar and Planetary Inst., Workshop on the Martian Surface and Atmosphere Through Time 1992 p 122-123 (For primary document see N92-28988 19-91)
Avail: NTIS HC/MF A09

Synthetic mid-infrared emissive spectra of basalts of possible Martian komatiitic compositions were generated to show what might be seen in data returned from the Thermal Emission Spectrometer (TES). TES is flying on the Mars Observer arriving at Mars in late 1993. The synthetic Martian komatiite spectra were generated using mineralogy based on Shergottite, Nakhlite, and Chassigny (SNC) meteorites and Viking X-Ray Fluorescence (XRF) data. These data sets provide strong evidence for the existence of ultramafic lavas on Mars, particularly lavas of komatiitic composition. Author

N92-29054*# Geological Survey, Flagstaff, AZ.
CHRYSE PLANITIA REGION, MARS: CHANNELING HISTORY, FLOOD-VOLUME ESTIMATES, AND SCENARIOS FOR BODIES OF WATER IN THE NORTHERN PLAINS
Susan L. Rotto and Kenneth L. Tanaka *In* Lunar and Planetary Inst., Workshop on the Martian Surface and Atmosphere Through Time 1992 p 124-125 (For primary document see N92-28988 19-91)
Avail: NTIS HC/MF A09

The Chryse Planitia region of Mars includes several outflow channels that debouched into a single basin. Here we evaluate possible volumes and areal extents of standing bodies of water that collected in the northern lowland plains, based on evidence provided by topography, fluvial relations, and channel chronology and geomorphology. Author

N92-29055*# Arizona State Univ., Tempe. Dept. of Geology.
DORSA ARGENTEA TYPE SINUOUS RIDGES, MARS: EVIDENCE FOR LINEAR DUNE HYPOTHESIS
Steven W. Ruff *In* Lunar and Planetary Inst., Workshop on the Martian Surface and Atmosphere Through Time 1992 p 126 (For primary document see N92-28988 19-91)
Avail: NTIS HC/MF A09

Unusual ridges with sinuous, dendritic, and braided morphologies near the south pole of Mars as well as in the Argyre basin have recently begun to receive attention. These ridges were originally thought to be glacially formed eskers, and recent work continues to argue for this hypothesis. Indeed, an entire glacial model was built around these ridges. A brief examination of possible ridge forming processes included an esker origin but also examined other mechanisms. Of the alternative hypotheses, an origin as linear dunes is the most reasonable. The current study focuses on evidence for this mode of origin. Author

N92-29056*# Jet Propulsion Lab., California Inst. of Tech., Pasadena.
ATMOSPHERIC AND SURFACE TEMPERATURES AND AIRBORNE DUST AMOUNTS DURING LATE SOUTHERN SUMMER FROM MARINER 9 IRIS DATA
M. Santee (California Inst. of Tech., Pasadena.) and D. Crisp *In* Lunar and Planetary Inst., Workshop on the Martian Surface and Atmosphere Through Time 1992 p 128-129 (For primary document see N92-28988 19-91)
Avail: NTIS HC/MF A09

The temperature structure and dust loading of the Martian atmosphere are investigated using thermal emission spectra recorded in 1972 by the Mariner 9 infrared interferometer spectrometer (IRIS). The analysis focuses on a subset of data consisting of approximately 2400 spectra obtained near the end of the southern summer season (L(sub s) equal to 343 deg to 348 deg), after the global dust storm had largely abated and airborne dust amounts were subsiding to background values. Simultaneous retrieval of the vertical distribution of both atmospheric temperature and dust optical depth is accomplished through an iterative procedure which is performed on each individual spectrum. The atmospheric transmittances are calculated using a Voigt quasi-random band model, which includes absorption by CO2 and dust, but neglects the effects of multiple scattering. Vertical profiles of temperature and dust optical depth are obtained using modified algorithms. These profiles are used to construct global maps of temperature and dust optical depth as functions of latitude (+/- 90 deg), altitude (approximately 0-50 km), and local time of day. Author

N92-29057*# National Aeronautics and Space Administration. Goddard Space Flight Center, Greenbelt, MD.
A CARBONATE-SILICATE AQUEOUS GEOCHEMICAL CYCLE MODEL FOR MARS
M. W. Schaefer (Maryland Univ., College Park.) and H. Leidecker *In* Lunar and Planetary Inst., Workshop on the Martian Surface and Atmosphere Through Time 1992 p 130-131 (For primary document see N92-28988 19-91)
Avail: NTIS HC/MF A09

A model for the carbonate-silicate geochemical cycle of an early, wet Mars is under development. The results of this study will be used to constrain models of the geochemical history of Mars and the likely mineralogy of its present surface. Although Mars today is a cold, dry planet, it may once have been much warmer and wetter. Values of total outgassed CO2 from several to about 10 bars are consistent with present knowledge (Pollack et al. 1987), and this amount of CO2 implies an amount of water outgassed at least equal to an equivalent depth of 500-1000 meters (Carr 1986). Pollack et al. (1987), in addition, estimate that a thick CO2 atmosphere may have existed for an extended period of time, perhaps as long as a billion years. The greenhouse effect of such an atmosphere would permit the presence of liquid water on the surface, most likely in the form of a shallow sea in the lowest regions of the planet, such as the northern plains (Schaefer 1990). The treatment of geochemical cycles as complex kinetic chemical reactions has been undertaken for terrestrial systems in recent years with much success (Lasaga 1980, 1981; Berner et al. 1983; Lasaga et al. 1985). Although the Martian system is vastly less well understood, and hence less well-constrained, it is also a much simpler system, due to the lack of biogenic reactions

that make the terrestrial system so complex. It should be possible, therefore, to use the same techniques to model the Martian system as have been used for terrestrial systems, and to produce useful results. A diagram of the carbonate-silicate cycle for Mars (simplified from the terrestrial system) is given. Author

N92-29058*# Geological Survey, Flagstaff, AZ.
AMAZONIS AND UTOPIA PLANITIAE: MARTIAN LACUSTRINE BASINS
David H. Scott, James W. Rice, Jr., James M. Dohm, and Mary G. Chapman *In* Lunar and Planetary Inst., Workshop on the Martian Surface and Atmosphere Through Time 1992 p 132-133 (For primary document see N92-28988 19-91)
Avail: NTIS HC/MF A09

Amazonis and Utopia Planitiae are two large (greater than 10(exp 6) sq. km) basins on Mars having morphological features commonly associated with former lakes. The investigation of these areas is an extension of our previous paleolake studies in the Elysium basin. Using Viking images, we are searching for familiar geologic forms commonly associated with standing bodies of water on Earth. Like Elysium, the two basins exhibit terraces and lineations resembling shorelines, etched and infilled floors with channel-like sinuous markings in places, inflow channels along their borders, and other geomorphic indicators believed to be related to the presence of water and ice. In some areas these features are better displayed than in others where they may be very tenuous; their value as indicators can be justified only by their association with related features. Even though these postulated paleolakes are very young in the Martian stratigraphic sequence, their shoreline features are poorly preserved and they are probably much older than large Pleistocene lakes on Earth. Author

N92-29059*# Arizona Univ., Tucson. Lab. of Planetary Image Research.
EVIDENCE FOR CRYSTALLINE HEMATITE AS AN ACCESSORY PHASE IN MARTIAN SOILS
R. B. Singer and J. S. Miller *In* Lunar and Planetary Inst., Workshop on the Martian Surface and Atmosphere Through Time 1992 p 134-135 (For primary document see N92-28988 19-91)
Avail: NTIS HC/MF A09

Based on visible and near-IR spectral images of Mars obtained by us in 1988, we have confirmed the occurrence of bulk crystalline hematite as a minor or accessory phase on the surface. This hematite is not uniformly distributed, being less abundant or absent in certain northern low-albedo regions. Even where most abundant, bulk hematite is not the primary coloring agent of heavily weathered materials on Mars. The primary coloring agent is apparently an amorphous or nanophase Fe3(+) phase, analogous to the coloring agent in certain Hawaiian palagonites (e.g. Adams and Evans, 1980; Singer, 1982; Morris et al, 1989). Based on these results, we can say with considerable certainty that bulk crystalline hematite exists on Mars in small amounts, in addition to the more ubiquitous nanophase or poorly crystalline ferric oxide phase(s). We conclude that Type 2 low-albedo regions (typified by Acidalia Planitia) contain less of this hematite than Type 1 regions (typified by Meridiani Sinus). Oxia Palus shows indication of slightly more oxidation and bulk hematite than Acidalia. This may be a real compositional difference, indicating that Oxia is in some sense transitional between Type 2 and Type 1 regions, but we cannot rule out the possibility of some optical mixing with surrounding higher-albedo regions. We are currently investigating the relationship of ferric-oxides in high-albedo regions to both types of low-albedo regions. As expected, spectral ratios of data from western Arabia to dark regions show considerably greater Fe3(+) in Arabia. There are not obvious spectral indications of a difference in ferric-oxide composition between Arabia and Type 1 low-albedo regions, implying that Arabia also contains minor bulk hematite. Author

N92-29060*# California Inst. of Tech., Pasadena. Div. of Geological and Planetary Sciences.
CARBONATE FORMATION ON MARS: HISTORY OF THE CO2 ATMOSPHERE FROM MODELS OF DIFFUSION-LIMITED GROWTH IN NON-AQUEOUS ENVIRONMENTS
Stuart K. Stephens and David J. Stevenson *In* Lunar and Planetary Inst., Workshop on the Martian Surface and Atmosphere Through Time 1992 p 136-137 (For primary document see N92-28988 19-91)
Avail: NTIS HC/MF A09

We conducted preliminary experiments designed to measure the amount of CO2 reacted from a simulated Martian atmosphere to form carbonate on silicate grains. Warm experiments at constant T (300-350 K) and with no water (vapor or liquid) yielded no detectable reaction, suggesting the following result. If we are indeed operating in the thermodynamically-favorable regime (supported by Gooding (1978) for the gas-solid reaction), then the lack of a reaction at warm temperatures suggests that a reaction in the 200-300 K regime will be less favored if reaction kinetics dominate. The completely dry scenario is thus not favored. An additional experiment, with abundant water vapor and at T approx. 300 K (constant), yielded a negative result as well. However, this is not inconsistent with Booth's findings, since lower temperatures may be required for the absorption of a monolayer of water. We plan further (lower-T) experiments. Author

N92-29061*# Colorado Univ., Boulder.
ATOMIC OXYGEN IN THE MARTIAN THERMOSPHERE
A. I. F. Stewart, M. J. Alexander, R. R. Meier (Naval Research Lab., Washington, DC.), L. J. Paxton (Johns Hopkins Univ., Laurel, MD.), S. W. Bougher (Arizona Univ., Tucson.), and C. G. Fesen (Dartmouth Coll., Hanover, NH.) *In* Lunar and Planetary Inst., Workshop on the Martian Surface and Atmosphere Through Time 1992 p 138-139 (For primary document see N92-28988 19-91)
Avail: NTIS HC/MF A09

The Mariner 9 Ultraviolet Spectrometer (UVS) made extensive observations of air-glow emissions from the thermosphere of Mars throughout the nominal mission (November 1971 - February 1972), during late summer in the southern hemisphere. Limb and disc measurements of the 130 nm triplet emission from thermospheric atomic oxygen were modelled by Strickland et al. Recently, the thermospheric general circulation models (TGCMs) developed for the Earth and Venus have been applied to Mars; we refer to it as the MTGCM. Our analysis shows that the oxygen mixing ratio is the fundamental unknown controlling the 130 nm brightness. Our radiative transport calculation shows that the emergent intensity at 130 nm is not very sensitive to variations in thermospheric temperature. The pattern of diurnal variation derived from our analysis is roughly the same as Strickland et al. although with somewhat lower values for the O mixing ratio. The main reasons for this difference are the more important role played by the photoelectron source in our model, and the somewhat larger 130 nm solar flux; thus, we require less oxygen to match the observed brightnesses. Strickland et al. also found that the OI 130 nm emission on Mars is correlated with solar activity. We find that the correlation is virtually non-existent during the early orbits when the planet was covered with a thick global dust storm, but later orbits, during the clearing of the storm, show a persistent correlation. Author

N92-29062*# Scientific Measurement Systems, Inc., Austin, TX.
PHYSICAL INTERPRETATION OF THERMAL AND REFLECTED DATA ON MARTIAN SURFACE UNITS
Edwin L. Strickland, III *In* Lunar and Planetary Inst., Workshop on the Martian Surface and Atmosphere Through Time 1992 p 140-141 (For primary document see N92-28988 19-91)
Avail: NTIS HC/MF A09

None of the available Viking Orbiter Infrared Thermal Mapper's thermal datasets can be uniquely interpreted in isolation from other data in terms of variations of a single, simple physical parameter of the martian surface. Other thermal datasets of a target area, thermal observations of adjacent materials, and visible and

near-infrared observations of the same region can often sufficiently constrain interpretations to obtain one that is nearly unique. The major datasets, their derived information, and their ambiguities are given. Author

N92-29063*# Scientific Measurement Systems, Inc., Austin, TX.
PHYSICAL PROPERTIES OF DEUCALIONIS, EOS, XANTHE-TYPE UNITS IN THE CENTRAL EQUATORIAL REGION OF MARS
Edwin L. Strickland, III *In* Lunar and Planetary Inst., Workshop on the Martian Surface and Atmosphere Through Time 1992 p 142-143 (For primary document see N92-28988 19-91)
Avail: NTIS HC/MF A09

Classification and mapping of surficial units in the central equatorial region of Mars (30 degrees N to 20 degrees S, 57 degrees E to 75 degrees W) using enhanced color images and Mars Consortium data, identified three distinct, high albedo, relatively red surficial units in regions with intermediate to high thermal inertias. These units have distinctive properties and morphologies, occur in different, well-defined areas, and show different seasonal and secular patterns of albedo change. Deucalionis units occupy the classical albedo area of Deucalionis Regio, south of Meridiani Sinus and Sabaeus Sinus, and adjacent areas. Eos forms a bright band that separates the dark, relatively blue Meridiani-type units that dominate the southern part of the study area from intermediate albedo, relatively red Oxia units common in the north. Xanthe forms moderately bright, relatively red, Type 1B crater-streaks and uniform sheet-deposits in and adjacent to parts of Chryse Planitia, including the Viking 1 landing site. Xanthe is always associated with Oxia deposits, and has significantly lower albedos than the Eos materials, which it can be confused with. Author

N92-29064*# Scientific Measurement Systems, Inc., Austin, TX.
PHYSICAL PROPERTIES OF MERIDIANI SINUS-TYPE UNITS IN THE CENTRAL EQUATORIAL REGION OF MARS
Edwin L. Strickland, III *In* Lunar and Planetary Inst., Workshop on the Martian Surface and Atmosphere Through Time 1992 p 144-145 (For primary document see N92-28988 19-91)
Avail: NTIS HC/MF A09

Classification and mapping of surficial units in the central equatorial region of Mars (30 degrees N to 20 degrees S, 57 degrees E to 75 degrees W) using enhanced color images and Mars Consortium data identified four major color/albedo units in the dark, reddish-gray regions that form the classical dark albedo markings of Mars, including Meridiani Sinus. The darkest, least red (relatively 'blue') materials form splotches (some with dune forms) in craters, inter-crater depressions, and part of Valles Marineris. These form the 'Dark Blue' Meridiani unit. Abundant materials that have higher albedos and are somewhat redder than the 'Dark Blue' unit have uniquely high green/(violet + red) color ratios in Viking Orbiter images. These materials, named 'Green-blue' Meridiani surround and mix with 'Dark Blue' Meridiani patches and are abundant on crater rims and local elevations. Discontinuous, patchy deposits with still higher albedos and much redder colors have morphologies classified of the Type Ib bright depositional dust streaks and sheets that were classified by Thomas et al. These dust deposits, which appear to be optically thin and patchy and are darker and not as red as other Type Ib dust deposits on Mars, and their Meridiani substrates, were designated the 'Red' Meridiani unit. Distinctive deposits that form highly eroded mesas and escarpments in northern Meridiani Sinus were named 'Light Blue' Meridiani, since they are not as red as other materials with moderately high albedos. Large areas dominated by these units form Meridiani Province in the central equatorial region of Mars. Author

N92-29065*# Scientific Measurement Systems, Inc., Austin, TX.
PHYSICAL PROPERTIES OF OXIA/LUNAE PLANUM AND ARABIA-TYPE UNITS IN THE CENTRAL EQUATORIAL REGION OF MARS
Edwin L. Strickland, III *In* Lunar and Planetary Inst., Workshop on the Martian Surface and Atmosphere Through Time 1992 p 146-147 (For primary document see N92-28988 19-91)
Avail: NTIS HC/MF A09

Classification and mapping of surficial units in the central equatorial region of Mars Consortium data identified the relatively dark but 'red' materials that cover Lunae Planum and surround the Meridiani materials of Oxia Palus inertia region of Arabia. Oxia Province consists of the regions dominated by the characteristically dark 'red' Oxia materials, but it includes darker streaks and splotches of relatively 'blue' Meridiani materials and brighter 'red' deposits of dust belonging to Eos Province (the bright 'red' border between Oxia and regional Meridiani deposits to the south) and Xanthe Province (the moderately bright 'red' dust deposits in western Chryse Planitia and its vicinity, including the VL-1 landing site). Two Oxia units were recognized: a darker unit present on Lunae Planum and east of Oxia Palus that have intermediate to high inertias. Oxia Province surrounds the extremely low thermal inertia Arabia Province in the east part of the study area, and occurs as isolated patches within Arabia (often including splotches of Meridiani materials within the Oxia patches). Arabia Province's materials have been widely interpreted as unconsolidated dust deposits which are currently forming at this stage of Mars' precessional climate cycle, although the persistence of stable, moderately strong albedo contracts among Arabia materials has not been addressed in those models. A systematic interpretation of Oxia and Arabia Province materials based on currently available remote sensing data is given. Author

N92-29066*# Scientific Measurement Systems, Inc., Austin, TX.
SURFACE PHOTOMETRIC PROPERTIES AND ALBEDO CHANGES IN THE CENTRAL EQUATORIAL REGION OF MARS
Edwin L. Strickland, III *In* Lunar and Planetary Inst., Workshop on the Martian Surface and Atmosphere Through Time 1992 p 148-149 (For primary document see N92-28988 19-91)
Avail: NTIS HC/MF A09

Comparison of the Viking Orbiter 2 Approach mosaic taken 11 Mars months later provides qualitative information on the photometric properties of the martian albedo features, and the distribution of dust and sand deposits responsible for the atmosphere near the northern summer solstice. The approach mosaic was taken at L (sub s) 106 degrees (early N. summer), phase angle 106 degrees; and airmasses varying from 4.6 at 30 degrees N to 3.3 near 10 degrees S. The apoapsis mosaic was taken in four sequences between L (sub s) 72 degrees and 76 degrees (late N. spring), near phase angles of 47 degrees, and at airmasses near 2.5. Systematic differences in the photometric decalibrations used to generate these mosaics may induce multiplicative errors of 5-10 percent of the observed albedos in comparisons of the mosaics, but they are probably nearer 3 percent of the albedos. In the study area (30 degrees N to 20 degrees S, 57 degrees E to 75 degrees W), scene-average approach Minnaert albedos were about 10 percent greater than apoapsis albedos and slightly less 'red'. The preferred explanation for the observed approach-apoapsis albedo difference is that both Arabia and Meridiani materials are smoother on millimeter and larger scales than other units in the study area. This is in good agreement with preliminary conclusions of Thorpe and (for dark intracrater Meridiani splotches) Regner et al. This is also consistent with reasonable models of these surfaces. 'Dark Blue' Meridiani surfaces are interpreted as consisting of sand dunes and sand sheets, which would be expected to have macroscopically smooth, nonshadowing surfaces. Viking Lander images of the surfaces at both landing sites show that smooth drift area's brightnesses are close to those of adjacent rough soil areas at low phase angles, but drifts become much brighter than rough soils when looking up-sun at high phase angles. Smooth patches of duricrust at both landing sites, interpreted by Strickland as eolian deposits (regardless of how they became salt enriched and cemented), also show this behavior. Author

N92-29067*# Arizona Univ., Tucson. Lunar and Planetary Lab.
GLACIAL AND MARINE CHRONOLOGY OF MARS

Robert G. Strom, Jeffrey S. Kargel, Natasha Johnson, and Christine Knight *In* Lunar and Planetary Inst., Workshop on the Martian Surface and Atmosphere Through Time 1992 p 150-151 (For primary document see N92-28988 19-91)
Avail: NTIS HC/MF A09

A summary is given of the glacial and marine chronology of Mars. Hydrological models of oceans and ice sheets, the cratering record, hydrological cycling, and episodic glaciation are discussed. Evidence for a Noachian ocean is evaluated. Author

N92-29068*# Arizona State Univ., Tempe. Dept. of Geology.
CHARACTERIZATION OF MARTIAN NEAR-SUBSURFACE MATERIALS BY DETERMINATION OF COHESION AND ANGLE OF INTERNAL FRICTION
R. J. Sullivan *In* Lunar and Planetary Inst., Workshop on the Martian Surface and Atmosphere Through Time 1992 p 152-153 (For primary document see N92-28988 19-91)
Avail: NTIS HC/MF A09

Back-analysis (reconstruction) of the stability of thirty avalanche chutes was performed in the very limited areas where high resolution imaging overlapped with available 1:500 K topographic map coverage. A new technique was developed to incorporate the third dimension (width) of an avalanche chute in stability back-analysis in order to yield unambiguous values of cohesion and angle of internal friction. The procedure is based upon extending the ordinary method of slices to three dimensions, in order to construct avalanche chute cross-sections whose widths and depths vary as a function of gradient, gravity, density of material, and phi and c. Applying the technique to the well documented slide at Lodalen, Norway as a test produces excellent correspondence with reality. Generally, the technique reveals that the width:depth ratio of any avalanche chute decreases with increasing contrast between the average slope angle and the angle of internal friction. Applying this technique to the martian avalanche chute yields results consistent with indications from earlier work, but with greater certainty. Values of cohesion and angle of internal friction identify the materials at the time of failure as moderately cohesive debris. If Sharp's identification of these features as avalanche chutes is correct, then the results here imply that weathering processes have had a significant effect to depths of tens of meters (where failure has occured) below the martian surface. It is also implied that on relatively steep slopes within Valles Marineris, sizable, unaltered, unmantled bedrock exposures for high resolution spectral and spatial scanning by Mars Observer may be scarce. Author

N92-29069*# Open Univ., Milton (England). Dept. of Earth Sciences.
TOPOGRAPHY OF APOLLINARIS PATERA AND MA'ADIM VALLIS
G. D. Thornhill, D. A. Rothery, J. B. Murray, T. Day (University Coll., London, England), A. Cook (University Coll., Loundon, England), J.-P. Muller (University Coll., London, England), and J. C. Iliffe (University Coll., London, England) *In* Lunar and Planetary Inst., Workshop on the Martian Surface and Atmosphere Through Time 1992 p 154-155 (For primary document see N92-28988 19-91)
Avail: NTIS HC/MF A09

Digital elevation models of the northern part of Ma'adim Vallis (603a41 607m/pix, 639a91 721m/pix), and Apollinaris Patera (603a42 612m/pix, 639a92 717m/pix), covering the area between 180 degrees to 190 degrees long and -2 degrees to -20 degrees lat. were obtained using a method described here. The results for the Ma'adim Vallis area show broad agreement with the United States Geological Survey (USGS) topographic map of the area with a channel depth of 1 to 2 km. A detailed study of the variations in the channel depth along its course and calculations of its discharge rate from channel cross section and slope are currently being undertaken. Results for Apollinaris Patera have been obtained, although the absolute heights relative to the Mars datum are not well constrained. However, the relative heights are sufficient for some analysis. Again, the topographic map is in reasonable agreement with the USGS map of the area, although there are significant differences. Author

N92-29070*# Washington Univ., Seattle. Dept. of Atmospheric Sciences.
TURBULENT SPECTRA, FLUXES, STABILITY AND GROWTH OF THE MIXED LAYER IN THE BOUNDARY LAYER OF MARS
James E. Tillman, Lars Landberg (Risoe National Lab., Roskilde, Denmark), and Soren E. Larsen (Risoe National Lab., Roskilde, Denmark) *In* Lunar and Planetary Inst., Workshop on the Martian Surface and Atmosphere Through Time 1992 p 156-158 (For primary document see N92-28988 19-91)
Avail: NTIS HC/MF A09

Spectra of wind and temperature from high frequency measurements in the atmospheric surface layer of Mars are presented for the first time. Heat and momentum fluxes, and stability are calculated for early spring from estimates of the surface temperature and mean Viking Lander 2 temperature and wind at 44 degrees N, using similarity theory. This study provides the first estimates of (1) the height of the mixed layer, (2) spectra of wind and temperature, (3) the validity of similarity theories on Mars, and (4) bounds of effective measuring height and surface roughness. It confirms and extends the universiality of model wind spectra. Finally and more important, we provide the ability to estimate and determine the self-consistency of Martian atmospheric mixed layer fluxes, stability and heights on a diurnal and annual basis. This can be used to initialize and validate the various models, which previously could only be compared with each other or the efforts of Sutton, Leovy and Tillman: these were restricted in season and limited by the results from the surface temperature model available at that time. Analysis of additional data can better estimate z(sub 0) values directly from the measurements and provide the parameters necessary to calculate the vertical profiles of wind and temperature on a daily, seasonal and annual basis. Author

N92-29071*# National Aeronautics and Space Administration. Lyndon B. Johnson Space Center, Houston, TX.
AQUEOUS-ALTERATION PRODUCTS IN S-N-C METEORITES AND IMPLICATIONS FOR VOLATILE/REGOLITH INTERACTIONS ON MARS
A. H. Treiman and J. L. Gooding *In* Lunar and Planetary Inst., Workshop on the Martian Surface and Atmosphere Through Time 1992 p 159-160 (For primary document see N92-28988 19-91)
Avail: NTIS HC/MF A09

The shergottite, nakhlite, and Chassigny (SNC) meteorites are inferred to be samples from the Martian surface, and so provide a wealth of information on Martian petrology and geochemistry. Because the SNCs are igneous rocks, it has not been obvious that they could reveal much about low-temperature geochemical processes and atmosphere surface interactions on Mars. However, five of the eight SNCs are known to contain low-temperature hydrous minerals and related phase of likely martian origin. Here, we review these martian weathering and alteration products in SNCs and outline possible implications for volatile/regolith interactions and regolith sinks for volatiles on Mars. Author

N92-29072*# Tokyo Univ., Sagamihara (Japan). Inst. of Space and Astronautical Science.
PLANET-B: A JAPANESE MARS AERONOMY OBSERVER
K. Tsuruda *In* Lunar and Planetary Inst., Workshop on the Martian Surface and Atmosphere Through Time 1992 p 161 (For primary document see N92-28988 19-91)
Avail: NTIS HC/MF A09

An introduction is given to a Japanese Mars mission (Planet-B) which is being planned at the Institute of Space and Aeronautical Science (ISAS), Japan. Planet-B aims to study the upper atmosphere of Mars and its interaction with the solar wind. The launch of Planet-B is planned for 1996 on a new launcher, M-L, which is being developed at ISAS. In addition to the interaction with the solar wind, the structure of the Martian upper atmosphere is thought to be controlled by the meteorological condition in the lower atmosphere. The orbit of Planet-B was chosen so that it

will pass two important regions, the region where the solar wind interacts with the Martian upper atmosphere and the tail region where ion acceleration is taking place. Considering the drag due to the Martian atmosphere, the periapsis altitude of 150 km and apoapsis of 10 Martian radii are planned. The orbit plane will be nearly parallel to the ecliptic plane. The altitude of the spacecraft will be spin stabilized and its spin axis will be controlled to the point of the earth. The dry weight of the spacecraft will be about 250 kg, including the scientific payload which consists of a magnetometer, plasma instruments, HF sounder, UV imaging spectrometer, and lower atmosphere monitor. Author

N92-29073*# California Univ., Los Angeles. Dept. of Earth and Space Science.

MICROCRATERS ON MARS: EVIDENCE OF PAST CLIMATIC VARIATIONS

A. R. Vasavada, T. J. Milavec, and D. A. Paige *In* Lunar and Planetary Inst., Workshop on the Martian Surface and Atmosphere Through Time 1992 p 162-163 (For primary document see N92-28988 19-91)

Avail: NTIS HC/MF A09

On Mars, we do not expect to see the full spectrum of crater sizes that we see on the Moon, because the Martian atmosphere decelerates smaller incoming meteorites. Mars climate models predict thirty-fold variations in Mars' atmospheric pressure due to large amplitude quasi-periodic variations in Mars' obliquity. More recent studies have shown that uncertainties in Mars' moment of inertia may have resulted in an underestimation of this range. In this study, we find that potential variations in the mass of the Martian atmosphere should have dramatic effects on the production rates of centimeter sized craters on the surface of Mars, and suggest that observations of the densities of Martian microcraters would provide an important validation of the astronomical theory for Martian climate change. Author

N92-29074*# Brookhaven National Lab., Upton, NY.

THE ULTRAVIOLET ALBEDO OF MARS

R. Wagener *In* Lunar and Planetary Inst., Workshop on the Martian Surface and Atmosphere Through Time 1992 p 164 (For primary document see N92-28988 19-91)

Avail: NTIS HC/MF A09

Ultraviolet observations have proven successful at studying the composition and structure of the upper atmospheres of the giant planets and Venus. In the case of Mars, the analysis of UV data has concentrated on the spatial distribution and temporal behavior of ozone. The potential of far ultraviolet (FUV) data (shortward of 200 nm) for measuring the atmospheric structure, in particular the vertical distribution of aerosols, is demonstrated. For illustrative purposes, a simple two layer model (atmosphere and surface) is computed using the atmospheric composition measured at the Viking landing sites. This model is then compared to the albedo observed with the International Ultraviolet Explorer (IUE). This comparison clearly shows that a clear atmosphere with the nominal Viking mixing ratios of CO2, O2, and H2O is incompatible with the IUE data shortward of 200 nm. To obtain a better match between data and model, an aerosol has to be introduced that effectively scatters at these wavelengths. The required reduction in effective CO2 pathlength is a factor of 5. The comparison also points out the inadequacy of the IUE to provide data in the critical wavelength region between 195 nm and 210 nm. Such data will be forthcoming from the Hubble Space Telescope and will provide the opportunity to infer the vertical distribution of aerosols on Mars on a global scale. Author

N92-29075*# California Inst. of Tech., Pasadena. Div. of Geological and Planetary Sciences.

HYDROGEN AND CARBON ISOTOPIC COMPOSITION OF VOLATILES IN NAKHLA: IMPLICATIONS FOR WEATHERING ON MARS

L. L. Watson, S. Epstein, and E. M. Stolper *In* Lunar and Planetary Inst., Workshop on the Martian Surface and Atmosphere Through Time 1992 p 165-166 (For primary document see N92-28988 19-91)

Avail: NTIS HC/MF A09

Gases were collected at 120, 200, 300, 415, and 600 and 850 C. Hydrogen yields for the 600 and 850 C aliquots were measured separately and then the gases were combined for isotopic analysis. CO2 samples collected at the two lowest temperature steps amounted to less than 0.5 mu mole and were not analyzed isotopically. Excluding the 120 C temperature step, the bulk delta D of the sample was + 187 percent. Delta D values increase from -91 percent in the 120 C step to +518 percent in the 315 to 850 C step. The hydrogen content is greatest in the 120 C step and is roughly constant in the 200, 300, and 415 C aliquots. Between 415 C and 850 C, the yield drops off considerably. From 850 C to 950 C, virtually no H2 and only minor CO2 (less than 1 mu mole) were extracted. Using the isotopic analysis from the 300, 415, 600, and 850 C temperature collections, the bulk delta C-13 sub (PDB) is 0.0 percent. The heaviest component (delta C-13 sub (PDB) of +29 percent) was collected between 300 and 415 C. The release of hydrogen at the low temperatures reported here is consistent with the breakdown of the phases that constitute the alteration product between approx. 250 and 650 C. Although not as high as the present Martian atmosphere, the high delta D values are consistent with a Martian origin for the meteorites in question. Author

N92-29076*# California Univ., Los Angeles. Dept. of Earth and Space Sciences.

MODELING THE SEASONAL CYCLE OF CO2 ON MARS: A FIT TO THE VIKING LANDER PRESSURE CURVES

S. E. Wood and D. A. Paige *In* Lunar and Planetary Inst., Workshop on the Martian Surface and Atmosphere Through Time 1992 p 167-168 (For primary document see N92-28988 19-91)

Avail: NTIS HC/MF A09

We have constructed a more accurate Mars thermal model, similar to the one used by Leighton and Murray in 1966, which solves radiative, conductive, and latent heat balance at the surface as well as the one-dimensional heat conduction equation for 40 layers to a depth of 15 meters every 1/36 of a Martian day. The planet is divided into 42 latitude bands with a resolution of two degrees near the poles and five degrees at lower latitudes, with elevations relative to the 6.1 mbar reference areoid. This estimate of the Martian zonally averaged topography was derived primarily from radio occultations. We show that a realistic one-dimensional thermal model is able to reproduce the VL1 pressure curve reasonably well without having to invoke complicated atmospheric effects such as dust storms and polar hoods. Although these factors may cause our deduced values for each model parameter to differ from its true value, we believe that this simple model can be used as a platform to study many aspects of the Martian CO2 cycle over seasonal, interannual, and long-term climate timescales. Author

N92-29077*# Open Univ., Milton (England). Planetary Sciences Unit.

ON THE ISOTOPIC COMPOSITION OF MAGMATIC CARBON IN SNC METEORITES

I. P. Wright, M. M. Grady, and C. T. Pillinger *In* Lunar and Planetary Inst., Workshop on the Martian Surface and Atmosphere Through Time 1992 p 169-170 (For primary document see N92-28988 19-91)

Avail: NTIS HC/MF A09

SNC meteorites are thought, from many lines of evidence, to come from Mars. A line of investigation which has been pursued in our laboratory over the years involves measurement of the stable isotopic composition of carbon, in its various forms, in SNC meteorites. In order to establish a firm basis for studying the isotopic systematics of carbon in the martian surface environment, it is first necessary to try and constrain the delta C-13 of bulk Mars. Taking all of the available information, it would seem that the delta C-13 of the Earth's mantle lies somewhere in the range of -5 to -7 percent. Preliminary assessment of magnetic carbon in SNC meteorites, would tend to suggest a delta C-13 of 20 to 30

percent, which is conspicuously different from that of the terrestrial mantle. It is not obvious why there should be such a difference between the two planets, although many explanations are possible. One of these possibilities, that previous delta C-13 measurements for magnetic carbon in SNC meteorites are in error to some degree, is being actively investigated. The most recent results seem to constrain the theta C-13 of the magnetic carbon in SNC meteorites to about -20 percent, which is not at odds with previous estimates. As such, it is considered that a detailed investigation of the carbon isotopic systematics of martian surface materials does have the necessary information with which to proceed. Author

N92-29078*# Arizona State Univ., Tempe. Dept. of Geology.
COMPARISON OF DRIFT POTENTIAL DERIVED FROM MARS GCM WITH ROCK ABUNDANCE FROM IRTM
Pengyang Xu and Ronald Greeley *In* Lunar and Planetary Inst., Workshop on the Martian Surface and Atmosphere Through Time 1992 p 171-172 (For primary document see N92-28988 19-91)
Avail: NTIS HC/MF A09

A General Circulation Model (GCM) for Mars developed at the Ames Research Center makes global predictions of wind shear stress as a function of season and dust optical depth. The surface shear stress, pressure and temperature from the GCM are used here to calculate the drift potential, or the amount of sediment that could be moved by the wind. A map of sand roses based on the calculations was generated for comparison with predictions of the distribution of rocks on Mars from Christensen, which is derived from infrared thematic mapper (IRTM) data. The drift potential was defined for Earth as the amount of sand moved at a given place for a stated period of time, and was adapted here for Mars. Author

N92-29079*# National Aeronautics and Space Administration. Ames Research Center, Moffett Field, CA.
CLIMATIC IMPLICATIONS OF THE SIMULTANEOUS PRESENCE OF CO2 AND H2O IN THE MARTIAN REGOLITH
A. P. Zent *In* Lunar and Planetary Inst., Workshop on the Martian Surface and Atmosphere Through Time 1992 p 173-174 (For primary document see N92-28988 19-91)
Avail: NTIS HC/MF A09

The current paradigm for quasi-periodic climate change on Mars holds that perhaps a few hundred millibars of CO2 are available for exchange between the atmosphere and regolith, and that a vast majority of that CO2 is presently absorbed into the regolith. The CO2 is partitioned between the regolith and atmosphere according to an equilibrium adsorptive relationship. If the atmospheric pressure exceeds the frost point at or near the poles, then quasi-permanent polar caps form and buffer the atmospheric pressure. This model was developed based upon laboratory studies of CO2 adsorption where no other adsorbates are present. We will conduct laboratory measurements of the simultaneous adsorption of H2O and CO2 under Mars-like conditions, and develop numerical expressions for use in climate modeling based upon our results. Author

N92-29080*# California Univ., Los Angeles.
THE ANCIENT OXYGEN EXOSPHERE OF MARS: IMPLICATIONS FOR ATMOSPHERE EVOLUTION
M. H. G. Zhang, J. G. Luhmann, A. F. Nagy (Michigan Univ., Ann Arbor.), and S. W. Bougher (Arizona Univ., Tucson.) *In* Lunar and Planetary Inst., Workshop on the Martian Surface and Atmosphere Through Time 1992 p 175 (For primary document see N92-28988 19-91)
Avail: NTIS HC/MF A09

This study involves the calculation, by the 2-stream method of Nagy and Cravens, of 'hot' oxygen exosphere density profiles for 'ancient' atmospheres and ionospheres (e.g., different extreme ultraviolet fluxes) and the associated escaping fluxes. We computed the total production rates above different 'nominal' ionopause altitudes (not taking into account the fact that some will reenter the atmosphere). We do not consider the additional neutral escape due to the sputtering process described by Luhmann and Kozyra. The results presented here thus represent conservative estimations of the neutral escape fluxes, but generous estimates of ion loss rates (except that here we do not consider charge exchange and impact ionization ion production processes). Further work along the lines of Luhmann and Kozyra can lead to estimates of sputtering losses over time and the roles played by impact ionization and charge exchange. Author

N92-28594*# Lunar and Planetary Inst., Houston, TX.
THE DISTRIBUTION OF ANORTHOSITE ON THE NEARSIDE OF THE MOON Abstract Only
B. R. Hawke (Hawaii Univ., Honolulu.), P. G. Lucey (Hawaii Univ., Honolulu.), G. J. Taylor (Hawaii Univ., Honolulu.), and P. D. Spudis *In its* Workshop on the Physics and Chemistry of Magma Oceans from 1 Bar to 4 Mbar 1992 p 20-21 (For primary document see N92-28587 19-46)
Avail: NTIS HC/MF A05

N92-28596*# Arizona Univ., Tucson. Lunar and Planetary Lab.
ORIGIN OF THE MOON AND LUNAR CORE FORMATION Abstract Only
Valerie J. Hillgren *In* Lunar and Planetary Inst., Workshop on the Physics and Chemistry of Magma Oceans from 1 Bar to 4 Mbar 1992 p 24-25 (For primary document see N92-28587 19-46)
Avail: NTIS HC/MF A05

N92-28598*# Washington Univ., Saint Louis, MO. Dept. of Earth and Planetary Sciences.
A NEW ANGLE ON LUNAR FERROAN-SUITE DIFFERENTIATION Abstract Only
B. L. Jolliff *In* Lunar and Planetary Inst., Workshop on the Physics and Chemistry of Magma Oceans from 1 Bar to 4 Mbar 1992 p 28-29 (For primary document see N92-28587 19-46) (Grant NAG9-56)
Avail: NTIS HC/MF A05

N92-28618*# California Univ., Los Angeles. Inst. of Geophysics and Planetary Physics.
THE FERROAN-ANORTHOSITIC SUITE AND THE EXTENT OF PRIMORDIAL LUNAR MELTING Abstract Only
Paul H. Warren and Gregory W. Kallemeyn *In* Lunar and Planetary Inst., Workshop on the Physics and Chemistry of Magma Oceans from 1 Bar to 4 Mbar 1992 p 72-73 (For primary document see N92-28587 19-46)
Avail: NTIS HC/MF A05

N92-28619*# Carnegie Institution of Washington, DC.
GIANT AND LARGE IMPACTS IN THE CONTEXT OF PLANETARY FORMATION THEORY Abstract Only
G. W. Wetherill *In* Lunar and Planetary Inst., Workshop on the Physics and Chemistry of Magma Oceans from 1 Bar to 4 Mbar 1992 p 74-75 (For primary document see N92-28587 19-46)
Avail: NTIS HC/MF A05

92 SOLAR PHYSICS

Includes solar activity, solar flares, solar radiation and sunspots.

For related information see *93 Space Radiation.*

N92-28520# Columbia Univ., New York, NY. Astrophysics Lab.
MATHEMATICAL MODELING OF SOLAR MAGNETO-DYNAMICS Final Report, 1 Nov. 1988 - 31 Oct. 1991
Edward A. Spiegel and Jean-Paul Zahn Jan. 1992 14 p (Grant AF-AFOSR-0012-89)
(AD-A247158; CAL-1955; AFOSR-92-0119TR) Avail: NTIS HC/MF A03

The solar cycle is a magneto-fluid-dynamical process whose intensity varies cyclically in a time of about eleven years. Its arrhythmias reveal it to be a chaotic process that has intermissions every few hundred years. Our aim in this project is to capture the

essential physical mechanisms underlying this behavior and to describe it in a mathematically simple model. We have studied the mathematical form such models may take and seen the causes of intermittency. We have isolated the probable seat of the solar cycle in the shear layer recently detected by helioseismology just below the convection zone. We call this layer the solar tachyline because of certain analogies to the oceanic thermocline. Using the methods of bifurcation theory to describe the nonlinear dynamics of this layer, we have uncovered a spatio-temporal behavior like that of the butterfly diagram characterizing the sunspot cycle. And, finally, we have uncovered in the turbulence of the tachycline, a promising mechanism for the formation of sunspots that is linked to the processes of vortex formation in geophysical fluid dynamics. GRA

N92-28869*# National Aeronautics and Space Administration. Goddard Space Flight Center, Greenbelt, MD.
FUTURE MISSION STUDIES: PRELIMINARY COMPARISONS OF SOLAR FLUX MODELS
S. Ashrafi (Computer Sciences Corp., Lanham, MD.) Dec. 1991 55 p Original contains color illustrations
(Contract NAS5-31500)
(NASA-TM-107947; Rept-544-FDD-91/004; NAS 1.15:107947; CSC/TM-91/6008) Avail: NTIS HC/MF A04; 1 functional color page

The results of comparisons of the solar flux models are presented. (The wavelength lambda = 10.7 cm radio flux is the best indicator of the strength of the ionizing radiations such as solar ultraviolet and x-ray emissions that directly affect the atmospheric density thereby changing the orbit lifetime of satellites. Thus, accurate forecasting of solar flux F sub 10.7 is crucial for orbit determination of spacecrafts.) The measured solar flux recorded by National Oceanic and Atmospheric Administration (NOAA) is compared against the forecasts made by Schatten, MSFC, and NOAA itself. The possibility of a combined linear, unbiased minimum-variance estimation that properly combines all three models into one that minimizes the variance is also discussed. All the physics inherent in each model are combined. This is considered to be the dead-end statistical approach to solar flux forecasting before any nonlinear chaotic approach. Author

N92-28870*# National Aeronautics and Space Administration. Goddard Space Flight Center, Greenbelt, MD.
NONLINEAR TECHNIQUES FOR FORECASTING SOLAR ACTIVITY DIRECTLY FROM ITS TIME SERIES
S. Ashrafi (Computer Sciences Corp., Lanham, MD.), L. Roszman (Computer Sciences Corp., Lanham, MD.), and J. Cooley 1992 18 p Presented at the Flight Mechanics/Estimation Theory Symposium, Greenbelt, MD, 5-7 May 1992
(Contract NAS5-31500)
(NASA-TM-107946; NAS 1.15:107946) Avail: NTIS HC/MF A03

Numerical techniques for constructing nonlinear predictive models to forecast solar flux directly from its time series are presented. This approach makes it possible to extract dynamical invariants of our system without reference to any underlying solar physics. We consider the dynamical evolution of solar activity in a reconstructed phase space that captures the attractor (strange), given a procedure for constructing a predictor of future solar activity, and discuss extraction of dynamical invariants such as Lyapunov exponents and attractor dimension. Author

N92-28871*# Computer Sciences Corp., Lanham, MD.
DETECTING AND DISENTANGLING NONLINEAR STRUCTURE FROM SOLAR FLUX TIME SERIES
S. Ashrafi and L. Roszman 1992 11 p
(Contract NAS5-31500)
(NASA-CR-190510; NAS 1.26:190510) Avail: NTIS HC/MF A03

Interest in solar activity has grown in the past two decades for many reasons. Most importantly for flight dynamics, solar activity changes the atmospheric density, which has important implications for spacecraft trajectory and lifetime prediction. Building upon the previously developed Rayleigh-Benard nonlinear dynamic solar model, which exhibits many dynamic behaviors observed in the Sun, this work introduces new chaotic solar forecasting techniques. Our attempt to use recently developed nonlinear chaotic techniques to model and forecast solar activity has uncovered highly entangled dynamics. Numerical techniques for decoupling additive and multiplicative white noise from deterministic dynamics and examines falloff of the power spectra at high frequencies as a possible means of distinguishing deterministic chaos from noise than spectrally white or colored are presented. The power spectral techniques presented are less cumbersome than current methods for identifying deterministic chaos, which require more computationally intensive calculations, such as those involving Lyapunov exponents and attractor dimension. Author

N92-28872*# Computer Sciences Corp., Lanham, MD.
FUTURE MISSION STUDIES: FORECASTING SOLAR FLUX DIRECTLY FROM ITS CHAOTIC TIME SERIES
S. Ashrafi Dec. 1991 43 p
(Contract NAS5-31500)
(NASA-CR-190378; Rept-554-FDD-91/113ROUDO; NAS 1.26:190378; CSC/TM-91/6167ROUDO) Avail: NTIS HC/MF A03

The mathematical structure of the programs written to construct a nonlinear predictive model to forecast solar flux directly from its time series without reference to any underlying solar physics is presented. This method and the programs are written so that one could apply the same technique to forecast other chaotic time series, such as geomagnetic data, attitude and orbit data, and even financial indexes and stock market data. Perhaps the most important application of this technique to flight dynamics is to model Goddard Trajectory Determination System (GTDS) output of residues between observed position of spacecraft and calculated position with no drag (drag flag = off). This would result in a new model of drag working directly from observed data. Author

N92-28907*# Computer Sciences Corp., Lanham, MD.
EVIDENCE OF CHAOTIC PATTERN IN SOLAR FLUX THROUGH A REPRODUCIBLE SEQUENCE OF PERIOD-DOUBLING-TYPE BIFURCATIONS
S. Ashrafi (Computer Sciences Corp., Lanham, MD.) and L. Roszman (Computer Sciences Corp., Lanham, MD.) 1991 20 p Presented at the Flight Mechanics/Estimation Theory Symposium, Greenbelt, MD, 21-23 May 1991 Sponsored by NASA. Goddard Space Flight Center
(NASA-TM-107944; NAS 1.15:107944) Avail: NTIS HC/MF A03

A preliminary study of the limits to solar flux intensity prediction, and of whether the general lack of predictability in the solar flux arises from the nonlinear chaotic nature of the Sun's physical activity is presented. Statistical analysis of a chaotic signal can extract only its most gross features, and detailed physical models fail, since even the simplest equations of motion for a nonlinear system can exhibit chaotic behavior. A recent theory by Feigenbaum suggests that nonlinear systems that can be led into chaotic behavior through a sequence of period-doubling bifurcations will exhibit a universal behavior. As the control parameter is increased, the bifurcation points occur in such a way that a proper ratio of these will approach the universal Feigenbaum number. Experimental evidence supporting the applicability of the Feigenbaum scenario to solar flux data is sparse. However, given the hypothesis that the Sun's convection zones are similar to a Rayleigh-Bernard mechanism, we can learn a great deal from the remarkable agreement observed between the prediction by theory (period doubling - a universal route to chaos) and the amplitude decrease of the signal's regular subharmonics. It is shown that period-doubling-type bifurcation is a possible route to a chaotic pattern of solar flux that is distinguishable from the logarithm of its power spectral density. This conclusion is the first positive step toward a reformulation of solar flux by a nonlinear chaotic approach. The ultimate goal of this research is to be able to predict an estimate of the upper and lower bounds for solar flux within its predictable zones. Naturally, it is an important task to identify the time horizons beyond which predictability becomes incompatible with computability. Author

93 SPACE RADIATION

Includes cosmic radiation; and inner and outer earth's radiation belts.

For biological effects of radiation see *52 Aerospace Medicine*. For theory see *73 Nuclear and High-Energy Physics*.

N92-28336# Lawrence Livermore National Lab., CA.
RESONANT COMPTON SCATTERING IN MODELS OF GAMMA RAY BURST SOURCES
P. A. Vitello Jan. 1992 7 p Presented at the Gamma Ray Burst Conference, Huntsville, AL, 17-18 Oct. 1991
(Contract W-7405-eng-48)
(DE92-010720; UCRL-JC-110087; CONF-9110310-4) Avail: NTIS HC/MF A02

We consider the spectra produced from the resonant Compton scattering of blackbody and power-law photons by a beam of relativistic electrons/positrons. The beam is assumed to be directed radially outward along the magnetic axis of a highly magnetized neutron star. We assume a dipole magnetic field geometry, and include the effects of magnetic Compton scattering energy losses on the particles in the beam during transport. A range of surface intensities for a magnetic field of 2 x 10(exp 12) Gauss are studied for a power-law electron/positron source functions of index gamma. The calculated scattered photon spectra are similar to observed gamma-ray burst spectra with a spectral index alpha which breaks from alpha approx. = 1 to alpha approx. = gamma. DOE

99 GENERAL

N92-28344*# National Aeronautics and Space Administration, Washington, DC.
NASA ENGINEERS AND THE AGE OF APOLLO
Sylvia Doughty Fries 1992 232 p
(NASA-SP-4104; NAS 1.21:4104; LC-90-39761;
ISBN-0-16-036174-5) Avail: NTIS HC/MF A11

A historical account of NASA's Apollo era engineers is presented. This book is based on interviews that were conducted with fifty-one 'typical' engineers. Author

N92-28678*# National Aeronautics and Space Administration, Washington, DC.
SPACE FLIGHT: THE FIRST 30 YEARS
Dec. 1991 39 p
(NASA-NP-150; NAS 1.83:150) Avail: NTIS HC/MF A03

A history of space flight from Project Mercury to the Space Shuttle is told from the perspective of NASA flight programs. Details are given on Mercury missions, Gemini missions, Apollo missions, Skylab missions, the Apollo-Soyuz Test Project, and the Space Shuttle missions. Author

N92-29218# Deutsche Forschungsanstalt fuer Luft- und Raumfahrt, Cologne (Germany, F.R.). Hauptabteilung Planung
[DLR RESEARCH REPORTS AND COMMUNICATIONS] Annual List, 1990 [JAHRESVERZEICHNIS 1990. DLR-FORSCHUNGSBERICHTE UND DLR-MITTEILUNGEN]
W. Wolke Jul. 1991 41 p In GERMAN
(ISSN-0939-2971; ETN-92-91391) Avail: NTIS HC/MF A03

Abstracts on the following are presented: flight mechanics, dynamics of flight systems, flight medicine, air traffic, flow mechanics, aerodynamics, propulsion, chemical propulsion, structural mechanics, aeroelasticity, materials, space simulation, high frequency, optoelectronics, physics, thermodynamics, wind tunnels, applied data technique, and data processing. ESA

N92-29219# Deutsche Forschungsanstalt fuer Luft- und Raumfahrt, Cologne (Germany, F.R.). Abt. Presse- und Oeffentlichkeitsarbeit.
[ACTIVITIES REPORT OF THE DLR] Annual Report, 1990-1991 [JAHRESBERICHT 1990/91 (DLR)]
Thomas H. Weyer Sep. 1991 97 p In GERMAN
(ISSN-0938-2194; ETN-92-91392) Avail: NTIS HC/MF A05

Subjects covered were: simulation and measuring instruments for air navigation and environment, the D2 space mission management project, satellite data for environmental research, ISIS (Intelligent Satellite Information System) for ecological mapping, robotics as a help to space navigation, and 'clean' combustion through computerized simulation of complex combustion processes. ESA

Typical Subject Index Listing

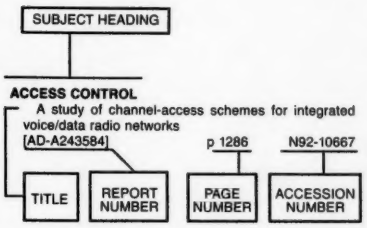

The subject heading is a key to the subject content of the document. Titles, report numbers, and accession numbers of pertinent documents are provided under each subject heading. When the title is insufficiently descriptive of the document content, a title extension has been added, separated from the title by three hyphens. The report number helps to indicate the type of document cited (e.g., NASA report, NASA translation, NASA contractor report). The accession number is the number by which the document abstracts are arranged in this journal and by which the document is sold or requested. The page number helps you locate the the citation in the abstract section. The titles, with title extensions if present, are arranged under each subject heading in ascending accession number order. The subject headings have been selected from the latest revision of the *NASA Thesaurus*.

A

A-320 AIRCRAFT
Flight simulation and digital flight controls
p 3221 N92-28526

ABILITIES
The variance of Rasch ability estimates from partially-known item parameters
[AD-A247065] p 3348 N92-28273

ABLATION
Ablation of material of solid propellant motor nozzles
[ONERA-NT-1990-13] p 3249 N92-28780

ABSORBERS (MATERIALS)
Modal element method for scattering of sound by absorbing bodies
[NASA-TM-105722] p 3353 N92-28984

ABSORPTION CROSS SECTIONS
Evidence for physics beyond the quasi-deuteron model in pion absorption
[DE92-011285] p 3354 N92-28310
Martian atmospheric chemistry during the time of low water abundance p 3376 N92-28501

ABSORPTION SPECTRA
Surface vs. atmospheric origin of 2.1-2.5 micron absorption features in the Martian spectrum
p 3373 N92-28480

ACCELERATED LIFE TESTS
Outdoor corrosion testing of aluminium-lithium alloys
[NLR-TP-90272-U] p 3260 N92-28794

ACCELERATION (PHYSICS)
KC-135 Large Motion Isolation Mount (LMIM)
p 3267 N92-28440
ACAP: Acceleration Characterization and Analysis Project p 3267 N92-28448
Early mission science support: Space Acceleration Measurement System (SAMS) p 3248 N92-28451
Empirical techniques for the study of acceleration mechanisms in the space environment
[AD-A249940] p 3248 N92-28765

ACCELERATION PROTECTION
Payload isolation and stabilization by a Suspended Experiment Mount (SEM)
[NASA-TM-107941] p 3246 N92-28369

ACCELERATION TOLERANCE
G-tolerance and spatial disorientation: Can simulation help us? p 3223 N92-28534

ACCELEROMETERS
Early mission science support: Space Acceleration Measurement System (SAMS) p 3248 N92-28451
Microgravity accelerometer characterization on Columbia STS-32 mission p 3271 N92-28452
Development of a residual acceleration data reduction and dissemination plan p 3271 N92-28453

ACCEPTABILITY
A cost-benefit analysis on the deletion of the inertial upper stage factory acceptance testing versus a decrease in mission reliability
[AD-A246620] p 3245 N92-28254
Validation of simulation systems for aircraft acceptance testing p 3222 N92-28531

ACCIDENTS
A strategy for minimizing common mode human error in executing critical functions and tasks
[DE92-011839] p 3327 N92-28775

ACCRETION DISKS
Thermal accretion disk models for active galaxies
[ETN-92-91486] p 3371 N92-29127

ACCURACY
Accuracy of shipborne kinematic GPS surveying
[AD-A245942] p 3230 N92-28317
Is choice accuracy related to information search patterns?
[IZF-1991-B-9] p 3369 N92-29162

ACETIC ACID
Conversion of acetic acid to methane by thermophiles
[DE92-010652] p 3257 N92-28942

ACHONDRITES
An ejection model for SNC meteorites: An indication for recent volcanism on Mars p 3387 N92-29038
Mid-infrared spectra of Martian komantiite
p 3390 N92-29053
Aqueous-alteration products in S-N-C meteorites and implications for volatile/regolith interactions on Mars
p 3393 N92-29071

ACID BASE EQUILIBRIUM
Electrochemical studies of Lewis acid-base systems for use in thermally regenerable fuel cells
[AD-A246457] p 3307 N92-28974
Determining the pH of Mars from the Viking labelled release reabsorption effect p 3389 N92-29049

ACID RAIN
Regional environmental impacts of methanol-fueled vehicles
[PB92-176569] p 3308 N92-29183

ACIDS
Thermodynamic and kinetic aspects of surface acidity
[DE92-011194] p 3256 N92-28893

ACOUSTIC DUCTS
Experimental validation of a line-duct acoustics model including flow
[NLR-TP-90223-U] p 3352 N92-28695

ACOUSTIC EMISSION
Magnetic remanence method and apparatus to test materials for embrittlement
[NASA-CASE-LAR-13817-4] p 3304 N92-29101
In-situ fault detection by the hybrid ray-mode method
[AD-A250213] p 3297 N92-29112
Magneto acoustic emission method for testing materials for embrittlement
[NASA-CASE-LAR-13817-2] p 3304 N92-29155

ACOUSTIC EXCITATION
Mobility power flow analysis of coupled plate structure subjected to mechanical and acoustic excitation
[NASA-CR-189635] p 3352 N92-28722

ACOUSTIC MEASUREMENT
Ultrasonic ambient noise in Australian shallow waters at frequencies up to 200 kHz
[MRL-TR-91-23] p 3351 N92-28364
Experimental validation of a line-duct acoustics model including flow
[NLR-TP-90223-U] p 3352 N92-28695

ACOUSTIC SCATTERING
Modal element method for scattering of sound by absorbing bodies
[NASA-TM-105722] p 3353 N92-28984

ACOUSTIC STREAMING
Investigation of energy exchange mechanisms between the mean and acoustic flow fields in solid rocket combustion chambers
[AD-A247402] p 3250 N92-28931

ACOUSTIC VELOCITY
Under-ice broadband transient measurements and processing
[AD-A248609] p 3351 N92-28324

ACOUSTICS
Passive acoustic range estimation of helicopters
[AD-A248033] p 3351 N92-28302
A new ocean bottom magnetometer system for continental shelf measurements
[AD-A247644] p 3321 N92-28321
Ultrasonic ambient noise in Australian shallow waters at frequencies up to 200 kHz
[MRL-TR-91-23] p 3351 N92-28364
Predicting microgravity levels for space station using VAPEPS p 3268 N92-28455
Neural network parameter estimation for the modified bistatic scattering strength model (BISSM)
[AD-A247913] p 3322 N92-28963
Modeling pulse transmission in the Monterey Bay using parabolic equation methods
[AD-A246465] p 3322 N92-28977
In-situ fault detection by the hybrid ray-mode method
[AD-A250213] p 3297 N92-29112

ACOUSTO-OPTICS
Image processing techniques for acoustic images
[AD-A247303] p 3352 N92-28559

ACRYLIC RESINS
Molecular engineering of liquid crystalline polymers by living cationic polymerization. 21: Synthesis and characterization of poly (3-((4-cyano-4'-biphenyl)oxy) propyl vinyl ether) macromonomers
[AD-A248305] p 3265 N92-29116

ACTIVATED CARBON
An investigation into techniques for the determination of moisture content on activated carbon
[AD-A245938] p 3256 N92-28882

ACTIVATION ENERGY
Dynamical solvent effects on activated electron-transfer reactions: Principles, pitfalls, and progress
[AD-A246764] p 3363 N92-28349

ACTIVE CONTROL
Microgravity vibration isolation research at the University of Virginia p 3267 N92-28446
Integrated Design Analysis and Optimisation of Aircraft Structures
[AGARD-LS-186] p 3231 N92-28469
The use and effectiveness of piloted simulation in transport aircraft research and development
p 3225 N92-28549
Structural design methodology for large space structures
[AD-A247672] p 3246 N92-28560

ACTIVE GALAXIES
Thermal accretion disk models for active galaxies
[ETN-92-91486] p 3371 N92-29127

ACTUATORS
New inertial actuator provides isolation and stabilization in microgravity conditions p 3267 N92-28443
A 6 degree-of-freedom Lorentz force vibration isolator with nonlinear controller p 3267 N92-28444
Digital control algorithms for microgravity isolation systems p 3267 N92-28445
Microgravity vibration isolation research at the University of Virginia p 3267 N92-28446
Extended H2 synthesis for microgravity vibration isolation p 3267 N92-28447
Microgravity isolation mounts based upon Piezoelectric film p 3268 N92-28454
Assessment of valve actuator motor rotor degradation by Fourier Analysis of current waveform
[DE92-013233] p 3281 N92-28814

The processing of high temperature ceramic superconducting devices, volume 2
[AD-A248159] p 3281 N92-28948
Electromechanical systems with transient high power response operating from a resonant AC link
[NASA-TM-105716] p 3238 N92-28985
ADAPTATION
New neural algorithms for self-organized learning
[AD-A249816] p 3341 N92-29198
ADAPTERS
Improvement of separations of practice bombs from a multiple bomb adapter
[NLR-TP-90307-U] p 3232 N92-28634
Modifications and results of flight tests of a practice bomb adapter
[NLR-TP-90108-U] p 3233 N92-28651
ADAPTIVE CONTROL
Reinforcement learning for the adaptive control of perception and action
[AD-A249351] p 3344 N92-28325
Adaptive and nonlinear control
[AD-A248580] p 3344 N92-28429
Ongoing Progress in Spacecraft Controls
[NASA-CP-10099] p 3247 N92-28730
Fuel optimal propulsive reboost of flexible spacecraft p 3247 N92-28734
Initial investigations of an adaptive discrete-time controller for nonlinear time-varying robotic models p 3247 N92-28736
ADAPTIVE FILTERS
Adaptive noise cancellation applied to the NUWES test ranges
[AD-A245961] p 3352 N92-28409
ADDITIVES
Effect of alumina particle additions on the aging kinetics of 2014-aluminum matrix composites
[AD-A245949] p 3252 N92-28898
Polyimide processing additives
[NASA-CASE-LAR-13669-1] p 3265 N92-29157
ADDRESSING
CESAR address generator
[FFI-91/7021] p 3334 N92-28265
ADENOSINE TRIPHOSPHATE
Conversion of acetic acid to methane by thermophiles
[DE92-010652] p 3257 N92-28942
ADHESION
Nanoscale investigation of indentation, adhesion, and fracture of diamond (111) surfaces
[AD-A250164] p 3265 N92-28916
ADHESIVE BONDING
The characterization of ceramics and ceramic/metal-joints by ultrasonic techniques
[VTT-RR-741] p 3266 N92-29194
ADSORBENTS
Substrate induced ordering of molecular adsorbates on Au(111)
[AD-A246850] p 3258 N92-29185
ADSORPTION
The impact of temperature dependent CO2 cross section measurements: A role for heterogeneous chemistry in the atmosphere of Mars? p 3372 N92-28479
The emergence of atomic-level structural information for ordered metal-solution interfaces: Some recent contributions from in-situ infrared spectroscopy and scanning tunneling microscopy
[AD-A246765] p 3364 N92-28512
Diffusion-controlled decohesion using a Cu-Sn alloy as a model system
[DE92-011645] p 3260 N92-28854
Thermodynamic and kinetic aspects of surface acidity
[DE92-011194] p 3256 N92-28893
Substrate induced ordering of molecular adsorbates on Au(111)
[AD-A246850] p 3258 N92-29185
ADVANCED VERY HIGH RESOLUTION RADIOMETER
A probabilistic neural network approach to cloud classification
[AD-A247916] p 3319 N92-28966
AEROACOUSTICS
Operational noise data for OH-58D Army helicopters
[AD-A246822] p 3351 N92-28292
The design of test-section inserts for higher speed aeroacoustic testing in the Ames 80- by 120-foot wind tunnel
[NASA-TM-103915] p 3353 N92-28909
Performance of uncoated AFRSI blankets during multiple Space Shuttle flights
[NASA-TM-103892] p 3245 N92-29104
AEROASSIST
Thermal response of rigid and flexible insulations and reflective coating in an aeroconvective heating environment
[NASA-TM-103925] p 3233 N92-28721
A generalized reusable guidance algorithm for optimal aerobraking
[NASA-TM-103590] p 3229 N92-28981
AEROBRAKING
A generalized reusable guidance algorithm for optimal aerobraking
[NASA-TM-103590] p 3229 N92-28981
AERODYNAMIC CHARACTERISTICS
NPSNET: Flight simulation dynamic modeling using quaternions
[AD-A247484] p 3333 N92-28245
Studies in general aviation aerodynamics
[NASA-CR-190431] p 3226 N92-28511
Experimental and computational ice shapes and resulting drag increase for a NACA 0012 airfoil
[NASA-TM-105743] p 3227 N92-28674
Identification of aerodynamic models for maneuvering aircraft
[NASA-CR-190444] p 3233 N92-28720
Explicit Navier-Stokes computation of turbomachinery flows
[AD-A249284] p 3286 N92-28879
AERODYNAMIC COEFFICIENTS
Experimental and computational ice shapes and resulting drag increase for a NACA 0012 airfoil
[NASA-TM-105743] p 3227 N92-28674
Calculation of support interferences on the aerodynamic coefficients for a wind tunnel calibration model
[ESA-TT-1247] p 3229 N92-29159
AERODYNAMIC CONFIGURATIONS
Constrained spanload optimization for minimum drag of multi-lifting-surface configurations
[NLR-TP-89126-U] p 3227 N92-28660
AERODYNAMIC DRAG
Experimental and computational ice shapes and resulting drag increase for a NACA 0012 airfoil
[NASA-TM-105743] p 3227 N92-28674
AERODYNAMIC LOADS
Reduction and analysis of F-111C flight data
[AD-A250341] p 3233 N92-28771
AERODYNAMIC NOISE
Boundary layer induced noise in aircraft
[ISSN-0309-7293] p 3353 N92-29201
AERODYNAMICS
Experimental aerodynamic facilities of the Aerodynamics Research and Concepts Assistance Branch
[AD-A247489] p 3240 N92-28248
Integrating aerodynamics and structures in the minimum weight design of a supersonic transport wing
[NASA-TM-107586] p 3231 N92-28435
Application of piloted simulation to high-angle-of-attack flight-dynamics research for fighter aircraft p 3225 N92-28551
Aeronautical engineering: A continuing bibliography with indexes (supplement 278)
[NASA-SP-7037(278)] p 3226 N92-28677
Aeronautical engineering: A continuing bibliography with indexes (supplement 275)
[NASA-SP-7037(275)] p 3226 N92-28679
Boundary conditions for Euler equations at internal block faces of multi-block domains using local grid refinement
[NLR-TP-90134-U] p 3284 N92-28712
Present status of computational tools for Maglev development
[DE92-013252] p 3294 N92-28815
Nonlinear normal and axial force indicial responses for a two dimensional airfoil
[AD-A247196] p 3229 N92-28888
AEROELASTICITY
Practical architecture of design optimisation software for aircraft structures taking the MBB-Lagrange code as an example p 3232 N92-28471
Structural optimization of aircraft p 3232 N92-28472
Mathematical optimization: A powerful tool for aircraft design p 3232 N92-28474
AEROMAGNETISM
Survey parameters and availability of low-level aeromagnetic data for geomagnetic field modelling p 3301 N92-28629
AERONAUTICAL ENGINEERING
Aeronautical engineering: A continuing bibliography with indexes (supplement 278)
[NASA-SP-7037(278)] p 3226 N92-28677
Aeronautical engineering: A continuing bibliography with indexes (supplement 275)
[NASA-SP-7037(275)] p 3226 N92-28679
AERONAUTICS
Aeronautical engineering: A continuing bibliography with indexes (supplement 278)
[NASA-SP-7037(278)] p 3226 N92-28677
AERONOMY
Planet-B: A Japanese Mars aeronomy observer p 3393 N92-29072
AEROSOLS
Reactions of hydrazines with chemicals found in environment
[AD-A247064] p 3308 N92-28272
An evaluation of the naval oceanic vertical aerosol model during Key90
[AD-A245943] p 3320 N92-28318
The meteoritic contribution to dust and aerosols in the atmosphere of Mars p 3383 N92-29013
The ultraviolet albedo of Mars p 3394 N92-29074
AEROSPACE ENGINEERING
The basic research simulator programme and the industrial and aerospace community: Opportunities for cooperative research
[LR-662] p 3240 N92-28579
DLR research reports and communications
[ISSN-0939-2971] p 3397 N92-29218
Activities report of the DLR
[ISSN-0938-2194] p 3397 N92-29219
AEROSPACE ENVIRONMENTS
SPEAR 2 space power data analysis
[AD-A248057] p 3250 N92-28945
AEROSPACE MEDICINE
G-tolerance and spatial disorientation: Can simulation help us? p 3223 N92-28534
Space life sciences strategic plan
[NASA-TM-107954] p 3244 N92-29100
AEROSPACE SCIENCES
Second National Space Grant Conference report, 1991
[NASA-EP-278] p 3366 N92-28864
AEROSPACE SYSTEMS
Design on an enhanced interactive satellite communications system analysis program
[AD-A245967] p 3273 N92-28410
Integrated health monitoring and controls for rocket engines
[NASA-TM-105763] p 3249 N92-28693
Scientific applications of frequency-stabilized laser technology in space
[NASA-CR-190449] p 3291 N92-28941
AEROTHERMOCHEMISTRY
Ablation of material of solid propellant motor nozzles
[ONERA-NT-1990-13] p 3249 N92-28780
AEROTHERMODYNAMICS
Steady and Transient Performance Prediction of Gas Turbine Engines
[AGARD-LS-183] p 3236 N92-28458
AGENA ROCKET VEHICLES
Development and flight history of SERT 2 spacecraft
[NASA-TM-105636] p 3250 N92-28983
AGGREGATES
Use of scrap rubber in asphalt pavement surfaces
[AD-A247419] p 3272 N92-28902
AGING (MATERIALS)
Turbine aircraft engine operational trending and JT8D static component reliability study
[DOT/FAA/CT-91/10] p 3238 N92-28686
Effect of alumina particle additions on the aging kinetics of 2014-aluminum matrix composites
[AD-A245949] p 3252 N92-28898
AGING (METALLURGY)
Phase transformations in Ti3Al based alloy
[AD-A246464] p 3261 N92-28976
AH-64 HELICOPTER
The use of a dedicated testbed to evaluate simulator training effectiveness p 3222 N92-28533
AIR DATA SYSTEMS
A simple and low cost system to measure delay times in pneumatic systems
[NLR-TP-90174-U] p 3235 N92-28644
AIR FLOW
A 2-D analysis of evaporation in laminar flow
[AD-A246467] p 3287 N92-28978
AIR LAND INTERACTIONS
Atmosphere-surface interactions and atmospheric evolution on Mars p 3383 N92-29012
AIR NAVIGATION
Loran-C performance assurance assessment program
[NASA-CR-190469] p 3230 N92-28718
DLR research reports and communications
[ISSN-0939-2971] p 3397 N92-29218
Activities report of the DLR
[ISSN-0938-2194] p 3397 N92-29219
AIR POLLUTION
Regional environmental impacts of methanol-fueled vehicles
[PB92-176569] p 3308 N92-29183
AIR PURIFICATION
Trade study of three oxygen processors for the Martian atmosphere
[AD-A246854] p 3372 N92-28393
AIR QUALITY
Identification and analysis of factors affecting the adoption of alternative transportation fuels
[PB92-164326] p 3266 N92-28914
AIR TRAFFIC
FAA aviation forecasts
[AD-A250412] p 3230 N92-29182

AIR TRAFFIC CONTROL
FAA aviation forecasts
[AD-A250412] p 3230 N92-29182
NARSIM: A real-time simulator for air traffic control research
[NLR-TP-90147-U] p 3241 N92-29204
AIR WATER INTERACTIONS
SAR-relate stress variability in the Marine Atmospheric Boundary Layer (MABL)
[AD-A247772] p 3309 N92-28567
Evaluation of a Solent sonic anemometer on RRS Charles Darwin Cruise 43
[IOS-288-1991] p 3323 N92-29213
AIRBORNE EQUIPMENT
Life cycle costs of the C-130 electrical power system upgrade
[AD-A246759] p 3221 N92-28348
Applications of ASICs to avionics
[AGARD-AG-329] p 3235 N92-28376
AIRCRAFT ACCIDENTS
Drop test: Cessna Golden Eagle 421B
[DOT/FAA/CT-TN91/32] p 3230 N92-28900
AIRCRAFT CARRIERS
Aircraft ship operations
[AGARD-AR-312] p 3231 N92-28468
AIRCRAFT COMMUNICATION
An analysis of aircrew communication patterns and content
[AD-A246618] p 3272 N92-28253
AIRCRAFT CONFIGURATIONS
Full mission simulation: A view into the future
p 3223 N92-28537
Calculation of unsteady subsonic and supersonic flow about oscillating wings and bodies by new panel methods
[NLR-TP-89119-U] p 3227 N92-28659
Modular simulation of HEI fragments and blast pressure
[AD-A248205] p 3272 N92-29191
AIRCRAFT CONTROL
Effects of cockpit lateral stick characteristics on handling qualities and pilot dynamics
[NASA-CR-4443] p 3239 N92-28584
Some longitudinal handling qualities design guidelines for active control technology transport aircraft
[NLR-TP-90129-U] p 3239 N92-28652
AIRCRAFT DESIGN
Integrating aerodynamics and structures in the minimum weight design of a supersonic transport wing
[NASA-TM-107586] p 3231 N92-28435
Practical architecture of design optimisation software for aircraft structures taking the MBB-Lagrange code as an example p 3232 N92-28471
Structural optimization of aircraft
p 3232 N92-28472
Multidisciplinary design and optimization
[AGARD-PAPER-2] p 3232 N92-28473
Mathematical optimization: A powerful tool for aircraft design p 3232 N92-28474
Use of a virtual cockpit for the development of a future transport aircraft p 3225 N92-28547
Application of piloted simulation to high-angle-of-attack flight-dynamics research for fighter aircraft
p 3225 N92-28551
Constrained spanload optimization for minimum drag of multi-lifting-surface configurations
[NLR-TP-89126-U] p 3227 N92-28660
Aeronautical engineering: A continuing bibliography with indexes (supplement 278)
[NASA-SP-7037(278)] p 3226 N92-28677
Aeronautical engineering: A continuing bibliography with indexes (supplement 275)
[NASA-SP-7037(275)] p 3226 N92-28679
Quaternion and Euler angles in kinematics
[NAL-TM-636] p 3303 N92-28836
Aerodynamic characteristics obtained from alpha sweep test of the quiet STOL experimental aircraft ASKA
[NAL-TR-1112] p 3234 N92-28901
AIRCRAFT ENGINES
Steady and Transient Performance Prediction of Gas Turbine Engines
[AGARD-LS-183] p 3236 N92-28458
Practical considerations in designing the engine cycle
p 3237 N92-28460
Steady and transient performance calculation method for prediction, analysis, and identification
p 3237 N92-28461
Inlet distortion effects in aircraft propulsion system integration p 3237 N92-28464
Engine performance and health monitoring models using steady state and transient prediction methods
p 3238 N92-28467
Turbine aircraft engine operational trending and JT8D static component reliability study
[DOT/FAA/CT-91/10] p 3238 N92-28686
AIRCRAFT INDUSTRY
Fundamentals of structural optimisation
p 3231 N92-28470
AIRCRAFT INSTRUMENTS
Microwave temperature profiler for clear air turbulence prediction
[NASA-CASE-NPO-18115-1-CU] p 3320 N92-29148
AIRCRAFT LANDING
Aircraft ship operations
[AGARD-AR-312] p 3231 N92-28468
S-76B certification for vertical take-off and landing operations from confined areas
[NLR-TP-90286-U] p 3233 N92-28714
AIRCRAFT MAINTENANCE
Application of knowledge-based systems for diagnosis of aircraft systems
[NLR-TP-90192-U] p 3230 N92-28655
Report on the workshop on Ion Implantation and Ion Beam Assisted Deposition
[AD-A250561] p 3365 N92-28923
Generation of spectra and stress histories for fatigue and damage tolerance analysis of fuselage repairs
[AD-A250390] p 3235 N92-29180
AIRCRAFT MANEUVERS
Development and evaluation of an attack and maneuvering system with combat development simulators as main development tool p 3224 N92-28541
Identification of aerodynamic models for maneuvering aircraft
[NASA-CR-190444] p 3233 N92-28720
AIRCRAFT MODELS
Integrating aerodynamics and structures in the minimum weight design of a supersonic transport wing
[NASA-TM-107586] p 3231 N92-28435
Identification of aerodynamic models for maneuvering aircraft
[NASA-CR-190444] p 3233 N92-28720
AIRCRAFT NOISE
Operational noise data for OH-58D Army helicopters
[AD-A246822] p 3351 N92-28292
Boundary layer induced noise in aircraft
[ISSN-0309-7293] p 3353 N92-29201
AIRCRAFT PARTS
A sensitivity analysis on component reliability from fatigue life computations
[AD-A247430] p 3297 N92-28425
AIRCRAFT PERFORMANCE
Effects of cockpit lateral stick characteristics on handling qualities and pilot dynamics
[NASA-CR-4443] p 3239 N92-28584
AIRCRAFT PILOTS
A study of pilot attitudes regarding the impact on mission effectiveness of using new cockpit automation technologies to replace the navigator/weapon system officer/electronic warfare officer
[AD-A246683] p 3329 N92-28286
Use of a commercially available flight simulator during aircrew performance testing
[AD-A245922] p 3240 N92-28407
Correlational analysis of survey and model-generated workload values
[AD-A247153] p 3329 N92-28518
Aircraft simulation and pilot proficiency: From surrogate flying towards effective training p 3222 N92-28532
The use of a dedicated testbed to evaluate simulator training effectiveness p 3222 N92-28533
Delays in laser glare onset differentially affect target-location performance in a visual search task
[AD-A246708] p 3327 N92-28557
Study of the loss of consciousness inflight by fighter aircraft pilots
[ONERA-RTS-11/3446-EY] p 3325 N92-28844
Neuropsychological components of object identification
[AD-A247049] p 3327 N92-28877
Methods of visual scanning with night vision goggles
[AD-A247470] p 3331 N92-28944
AIRCRAFT RELIABILITY
A sensitivity analysis on component reliability from fatigue life computations
[AD-A247430] p 3297 N92-28425
AIRCRAFT STABILITY
Aeronautical engineering: A continuing bibliography with indexes (supplement 275)
[NASA-SP-7037(275)] p 3226 N92-28679
AIRCRAFT STRUCTURES
Integrated Design Analysis and Optimisation of Aircraft Structures
[AGARD-LS-186] p 3231 N92-28469
Practical architecture of design optimisation software for aircraft structures taking the MBB-Lagrange code as an example p 3232 N92-28471
Structural optimization of aircraft
p 3232 N92-28472
Multidisciplinary design and optimization
[AGARD-PAPER-2] p 3232 N92-28473
Paint removal using cryogenic processes
[AD-A247668] p 3264 N92-28912
AIRCRAFT WAKES
Viscous effects on a vortex wake in ground effect
[NASA-CR-190400] p 3283 N92-28361
AIRFOILS
Experimental and computational ice shapes and resulting drag increase for a NACA 0012 airfoil
[NASA-TM-105743] p 3227 N92-28674
Results of a low power ice protection system test and a new method of imaging data analysis
[NASA-TM-105745] p 3227 N92-28696
Study of the leading-edge vortex dynamics in the unsteady flow over an airfoil
[AD-A247532] p 3228 N92-28865
Nonlinear normal and axial force indicial responses for a two dimensional airfoil
[AD-A247196] p 3229 N92-28888
AIRGLOW
Archival of the ECOM-721 data
[AD-A249299] p 3338 N92-28845
Atomic oxygen in the Martian thermosphere
p 3391 N92-29061
ALBEDO
Mars dust and cloud opacities and scattering properties p 3381 N92-29003
Soil texture and granulometry at the surface of Mars
p 3382 N92-29009
Mars: Wavelength-dependent dual polarization global scattering p 3384 N92-29020
Mars: Correcting surface albedo observations for effects of atmospheric dust loading p 3386 N92-29032
Simulations of the seasonal polar caps on Mars
p 3387 N92-29033
Physical properties of Deucalionis, Eos, Xanthe-type units in the central equatorial region of Mars
p 3392 N92-29063
Physical properties of Meridiani Sinus-type units in the central equatorial region of Mars p 3392 N92-29064
Physical properties of Oxia/Lunae Planum and Arabia-type units in the central equatorial region of Mars
p 3392 N92-29065
Surface photometric properties and albedo changes in the central equatorial region of Mars
p 3392 N92-29066
The ultraviolet albedo of Mars p 3394 N92-29074
ALCOHOLS
Surface crystallographic dependence of voltammetric oxidation of polyhydric alcohols and related systems at monocrystalline gold-acidic aqueous interfaces
[AD-A246763] p 3363 N92-28392
ALERTNESS
Lapses in alertness: Brain-evoked responses to task-irrelevant auditory probes
[AD-A247669] p 3328 N92-28940
ALGEBRA
A center of excellence in the mathematical sciences
[AD-A249365] p 3346 N92-28329
A discrete Fourier transform for virtual memory machines
[NASA-TM-103914] p 3349 N92-28672
Annoyance due to discrete tones in broadband background noise. Part 2: Analysis
[ISVR-TR-202-PT-2] p 3353 N92-29203
ALGORITHMS
Diagnostic reasoning within sequential circuits, volume 1
[AD-A248055] p 3278 N92-28305
The testing, analysis, and correction of the update operation of a parallel, multi-backend database supercomputer
[AD-A248320] p 3341 N92-28306
On-line point positioning with single frame camera data
[AD-A248307] p 3287 N92-28322
Multiple-valued programmable logic array minimization by simulated annealing
[AD-A248620] p 3335 N92-28353
Adaptive set-membership identification in 0(m) time for linear-in-parameters models
[AD-A249359] p 3273 N92-28358
Temporal reasoning and problem solving
[AD-A248457] p 3344 N92-28387
Studies of regional wave propagation using differential seismograms and randomized structural models
[AD-A247011] p 3309 N92-28394
Digital control algorithms for microgravity isolation systems p 3267 N92-28445
Fundamentals of structural optimisation
p 3231 N92-28470
A network flow algorithm for just-in-time project scheduling
[MEMO-COSOR-91-21] p 3336 N92-28638
Genetic algorithms in coding theory: A table for A3 (n, d)
[MEMO-COSOR-91-22] p 3336 N92-28639

Quasi-recursive dynamics equations for spacecraft-based flexible robotic manipulators
[NLR-TP-90028-U] p 3345 N92-28648
Wave drag determination in the transonic full-potential flow code MATRICS
[NLR-TP-90062-U] p 3228 N92-28709
Wavelets and numerical simulation
[ONERA-NT-1991-8] p 3347 N92-28777
Compilation and operation environment of an object based language
[ETN-92-91323] p 3338 N92-28785
A continuation method for calculating the equilibrium positions of nonlinear structures
[ONERA-RT-24/3542-RY-091-R] p 3338 N92-28790
Evaluation of drive simulator settings for DAF YA-4440
[FEL-91-B345] p 3241 N92-28828
Fast algorithms for transport models
[DE92-011432] p 3338 N92-28841
Optimization by renaming in the solution method
[ETN-92-91324] p 3338 N92-28842
Digital compression algorithms for HDTV transmission
[NASA-CR-190509] p 3275 N92-28873
Decomposition of balanced matrices. Part 7: A polynomial recognition algorithm
[AD-A247400] p 3350 N92-28930
Studies of iterated transform image compression and its application to color and DTED
[AD-A248060] p 3339 N92-28946
Diagonal forms of translation operators for helmholtz equation in three dimensions
[AD-A248422] p 3348 N92-28949
A generalized reusable guidance algorithm for optimal aerobraking
[NASA-TM-103590] p 3229 N92-28981
A rotorcraft flight database for validation of vision-based ranging algorithms
[NASA-TM-103906] p 3231 N92-29103
Mapping unstructured grid computations to massively parallel computers
[NASA-CR-190551] p 3343 N92-29109
Analysis and optimization of low-earth-orbit communication links
[DE92-013393] p 3277 N92-29131
New neural algorithms for self-organized learning
[AD-A249816] p 3341 N92-29198
Maximizing the convergence rate of the EM algorithm for the multiple broad-band signal estimation and detection
[AD-A248230] p 3341 N92-29224

ALIGNMENT
Multi-channel fiber optic rotary joint for single-mode fiber
[AD-D015273] p 3358 N92-29095

ALKALI METALS
Kinetic studies of metal combustion in propulsion
[AD-A250207] p 3256 N92-28769

ALKENES
New methodology for fluorocarbon synthesis
[AD-A247163] p 3254 N92-28261

ALKYL COMPOUNDS
New methodology for fluorocarbon synthesis
[AD-A247163] p 3254 N92-28261

ALLOCATIONS
Scheduling multiple variable-speed machines
[AD-A249362] p 3268 N92-28359

ALTERNATING CURRENT
Alternating current tokamak reactor with ohmic ignition and bootstrap current
[PPL-120] p 3361 N92-28849
Electromechanical systems with transient high power response operating from a resonant AC link
[NASA-TM-105716] p 3238 N92-28985

ALTERNATIVES
Identification and analysis of factors affecting the adoption of alternative transportation fuels
[PB92-164326] p 3266 N92-28914

ALTITUDE SICKNESS
Effects of high terrestrial altitude on military performance
[AD-A246695] p 3324 N92-28288

ALUMINIDES
Chemical vapor synthesis of niobium aluminides
[AD-A250332] p 3258 N92-29091

ALUMINUM
Weld pool flow visualization studies during gas tungsten arc welding of steel and aluminum
[AD-A249204] p 3292 N92-28293
Surface residual stress analysis of metals and alloys
[AD-A248372] p 3259 N92-28426
Underwater vapor phase burning of aluminum particles and on aluminum ignition during steam explosions
[DE92-011196] p 3257 N92-28894
Experiments in passive vibration reduction
[AD-A250397] p 3304 N92-29181

ALUMINUM ALLOYS
Surface residual stress analysis of metals and alloys
[AD-A248372] p 3259 N92-28426
The effect of intermediate heat treatments on overload induced retardation during the fatigue crack growth in an Al-alloy
[LR-651] p 3259 N92-28574
The influence of elevated temperature on the bonding quality of deformed GLARE
[LR-659] p 3252 N92-28577
The stress corrosion cracking behavior of AlLi 2090-T83 in substitute ocean water
[LR-661] p 3259 N92-28578
The compressive properties of GLARE
[LR-666] p 3252 N92-28582
Effect of cooling rate on corrosion properties of high strength aluminium alloys under atmospheric conditions
[NLR-TP-90138-U] p 3260 N92-28691
Outdoor corrosion testing of aluminium-lithium alloys
[NLR-TP-90272-U] p 3260 N92-28794
Effect of solidification technique and consolidation method on the properties of rapidly solidified Al-Fe alloys
[DLR-FB-91-24] p 3260 N92-28823
Crack resistance, fracture toughness and instability in damage tolerant Al-Li alloys
[NLR-TP-90172-U] p 3303 N92-28850
Tensile and interlaminar properties of GLARE (trade name) laminates
[AD-A250188] p 3253 N92-28921
Phase transformations in Ti3Al based alloy
[AD-A246464] p 3261 N92-28976

ALUMINUM ARSENIDES
Study of ultra short HFET devices with InP substrates
[AD-A248448] p 3279 N92-28427

ALUMINUM CARBIDES
X ray diffraction study of residual stresses in metal matrix composite-jacketed steel cylinders subjected to internal pressure
[AD-A248449] p 3251 N92-28416

ALUMINUM CHLORIDES
Electrochemical studies of Lewis acid-base systems for use in thermally regenerable fuel cells
[AD-A246457] p 3307 N92-28974

ALUMINUM GALLIUM ARSENIDES
Strained AlGaInAs semiconducting material for improved laser performance
[AD-A249379] p 3289 N92-28330
An acoustic charge transport imager for high definition television application
[AD-A250433] p 3274 N92-28773

ALUMINUM OXIDES
Microhole array electrodes based on microporous alumina membranes
[AD-A247082] p 3278 N92-28239
The effects of alumina trihydrate on the flammability characteristics of polyester, vinyl ester, and epoxy glass reinforced plastics
[AD-A247707] p 3264 N92-28563
Kinetic studies of metal combustion in propulsion
[AD-A250207] p 3256 N92-28769
Effect of alumina particle additions on the aging kinetics of 2014-aluminum matrix composites
[AD-A245949] p 3252 N92-28898
The effects of thermomechanical processing parameters on elevated-temperature behavior of a 6061 Al-Al2O3 metal matrix composite
[AD-A247889] p 3253 N92-28959
X ray photoelectron spectroscopy study on the double layer at an Al2O3-Al interface
[AD-A246454] p 3265 N92-28972
Some experiments to determine the efficiency of collection of alumina particles by electron beam button melting in a nickel-base superalloy, AP1
[NPL-DMM(A)-42] p 3261 N92-29164

ALUMINUM-LITHIUM ALLOYS
The mechanical property data base from an Air Force/industry cooperative test program on advanced aluminum alloys (IN905XL and AL905XL forgings)
[AD-A247752] p 3368 N92-28565

AMBIENT TEMPERATURE
Electrochemical studies of Lewis acid-base systems for use in thermally regenerable fuel cells
[AD-A246457] p 3307 N92-28974
Simulation of Martian surface-atmosphere interaction in a space-simulator: Technical considerations and feasibility p 3388 N92-29044

AMIDES
New methodology for fluorocarbon synthesis
[AD-A247163] p 3254 N92-28261
Substrate induced ordering of molecular adsorbates on Au(111)
[AD-A246850] p 3258 N92-29185

AMMONIA
Photochemical model for NH3 in an early Martian atmosphere p 3373 N92-28481
Was early Mars warmed by ammonia?
p 3386 N92-29030

AMMONIUM COMPOUNDS
Ion conductive polymer solid electrolytes
[DE92-010518] p 3266 N92-29195

AMORPHOUS MATERIALS
Multiphase structure of a segmented polyurethane: Effects of temperature and annealing
[AD-A247594] p 3262 N92-28250
Chain folding in EBEE semicrystalline diblock copolymers
[AD-A247595] p 3262 N92-28251
Method of intercalating large quantities of fibrous structures
[NASA-CASE-LEW-15077-1] p 3253 N92-29152

AMPLIFIERS
Multimeter-wave grid oscillators
[AD-A248430] p 3279 N92-28351

AMPLITUDES
Nonlinear sloshing and the coupled dynamics of liquid propellants and spacecraft
[AD-A250023] p 3248 N92-28967

ANAEROBES
Conversion of acetic acid to methane by thermophiles
[DE92-010652] p 3257 N92-28942

ANALOG CIRCUITS
What is an ASIC? p 3235 N92-28377

ANALOG DATA
Advanced optical fiber communication systems
[AD-A247683] p 3357 N92-28554

ANALOG TO DIGITAL CONVERTERS
Instrumentation for ultrahigh strain rate experiments
[AD-A249358] p 3298 N92-28327

ANALOGIES
Oxygen in the Martian atmosphere: Regulation of PO2 by the deposition of iron formations on Mars
p 3373 N92-28482

ANALOGS
Multiple-valued programmable logic array minimization by simulated annealing
[AD-A248620] p 3335 N92-28353

ANALYSIS (MATHEMATICS)
Analysis of constrained-layer damping of flexural and extensional waves in infinite, fluid-loaded plates
[AD-A247936] p 3304 N92-29081

ANECHOIC CHAMBERS
Microwave interactions with plasmas
[AD-A250333] p 3362 N92-29093

ANGLE OF ATTACK
Flow visualization studies of a sideslipping, canard-configured X-31A-Like fighter aircraft model
[AD-A245940] p 3228 N92-28883
Nonlinear normal and axial force indicial responses for a two dimensional airfoil
[AD-A247196] p 3229 N92-28888

ANGLES (GEOMETRY)
Feasibility study of hypersonic clinometric measurements at R3Ch
[ONERA-RSF-136/1865-AY-728-] p 3228 N92-28789

ANGULAR MOMENTUM
Angular momentum: Can be used in ballistic tracking
[AD-A247722] p 3350 N92-28400

ANIONS
Macrocyclic polycation complexes for secondary anion binding, molecular recognition, and catalysis
[AD-A246690] p 3254 N92-28287
Silicon polymers
[AD-A250201] p 3265 N92-29145

ANISOTROPIC PLATES
Programming of the complex logarithm function in the solution of the cracked anisotropic plate loaded by a point force
[LR-657] p 3299 N92-28575

ANISOTROPY
A combined experimental and analytical investigation of the theory of plasticity involving strain induced anisotropy
[AD-A248440] p 3298 N92-28352

ANNEALING
Multiphase structure of a segmented polyurethane: Effects of temperature and annealing
[AD-A247594] p 3262 N92-28250
Multiple-valued programmable logic array minimization by simulated annealing
[AD-A248620] p 3335 N92-28353

ANNUAL VARIATIONS
Ultrasonic ambient noise in Australian shallow waters at frequencies up to 200 kHz
[MRL-TR-91-23] p 3351 N92-28364
Infrared imaging of Mars for volatile distribution and seasonal variability between 2.4 and 5.1 microns
p 3379 N92-28995
Observed changes in limb clouds immediately prior to the onset of planet-encircling dust storms
p 3388 N92-29039

Is ground ice stable near the Martian equator?
p 3389 N92-29046
Short- and long-term climate changes on Mars
p 3389 N92-29051
An inventory of data collected during the NERC's North Sea Community Research Project, 1987-1992
[REPT-21-1991] p 3323 N92-29215

ANNULAR FLOW
Laser anemometer measurements and computations in an annular cascade of high turning core turbine vanes
[NASA-TP-3252] p 3229 N92-28980

ANOMALIES
Physics and technology for the investigation of properties of ultra small systems
[AD-A246772] p 3364 N92-28513
Magnetic and electromagnetic induction effects in the annual means of geomagnetic elements
p 3301 N92-28632

ANORTHOSITE
The distribution of anorthosite on the nearside of the moon p 3311 N92-28594

ANTENNA ARRAYS
Scattering and radiation analysis of three-dimensional cavity arrays via a hybrid finite element method
[NASA-CR-190408] p 3273 N92-28371
Data selection for fast projection techniques applied to adaptive nulling: A comparative study of performance
[AD-A246468] p 3276 N92-28979

ANTENNA FEEDS
Method of moments analysis of displaced-axis dual reflector antennas
[AD-A247970] p 3277 N92-29166

ANTENNA RADIATION PATTERNS
Analysis of electromagnetic propagation over variable terrain using the parabolic wave equation
[AD-A248061] p 3276 N92-28947
Method of moments analysis of displaced-axis dual reflector antennas
[AD-A247970] p 3277 N92-29166

ANTENNAS
Accuracy of shipborne kinematic GPS surveying
[AD-A245942] p 3230 N92-28317
The use of a vector network analyzer for measuring the performance of radar absorbing materials
[AD-A247194] p 3275 N92-28887
Analysis of electromagnetic propagation over variable terrain using the parabolic wave equation
[AD-A248061] p 3276 N92-28947

ANTIMISSILE DEFENSE
Optimalization of grenades with pre-formed fragments against air-targets, part 2
[PML-1990-24-PT-2] p 3349 N92-28313

ANTIRADAR COATINGS
The use of a vector network analyzer for measuring the performance of radar absorbing materials
[AD-A247194] p 3275 N92-28887

ANTISUBMARINE WARFARE
Under-ice broadband transient measurements and processing
[AD-A248609] p 3351 N92-28324

ANVILS
High temperature solder device for flat cables
[NASA-CASE-GSC-13344-1] p 3261 N92-29094

APERTURES
Scattering and radiation analysis of three-dimensional cavity arrays via a hybrid finite element method
[NASA-CR-190408] p 3273 N92-28371
Aperture coupling measurement in a test chamber for the Advanced Photon Source (APS)
[DE92-013059] p 3274 N92-28809
Water window imaging x ray microscope
[NASA-CASE-MFS-28485-1] p 3288 N92-29135

APOLLO PROJECT
NASA engineers and the age of Apollo
[NASA-SP-4104] p 3397 N92-28344

APPLICATION SPECIFIC INTEGRATED CIRCUITS
CESAR address generator
[FFI-91/7021] p 3334 N92-28265
Applications of ASICs to avionics
[AGARD-AG-329] p 3235 N92-28376
What is an ASIC? p 3235 N92-28377
The silicon compiler for designing military VLSI ASIC's
p 3235 N92-28378
A radar signal processing ASIC and a VME interface circuit p 3235 N92-28380

APPLICATIONS PROGRAMS (COMPUTERS)
An application of interactive computer graphics to the study of inferential statistics and the general linear model
[AD-A246668] p 3334 N92-28285
Computer-based assessment of schema knowledge in a flexible problem-solving environment
[AD-A246779] p 3348 N92-28516
MoCog1: A computer simulation of recognition-primed human decision making, considering emotions
[NASA-TM-107859] p 3337 N92-28758
Crystallizing FORTRAN
[AD-A250162] p 3343 N92-28915
Technological enhancements for personal computers
[AD-A247962] p 3333 N92-29083

APPROACH
Effective cueing during approach and touchdown: Comparison with flight p 3226 N92-28552

APPROACH AND LANDING TESTS (STS)
The second flight simulator test of the head-up display for NAL QSTOL experimental aircraft (ASKA)
[NAL-TM-633] p 3331 N92-28831

APPROXIMATION
Comparison of various techniques in the analysis of waveguide transitions
[AD-A247019] p 3279 N92-28367
Fourier analysis of the approximation power of principal shift-invariant spaces
[AD-A246713] p 3347 N92-28411

ARC JET ENGINES
Arcjet plume ionization effects on exposed solar array conducting surfaces
[AD-A245912] p 3307 N92-28383

ARC SPRAYING
Evaluation of plasma sprayed crucible coatings for melt processing copper-refractory metal alloys
[DE92-010871] p 3259 N92-28338

ARC WELDING
Visualization of gas tungsten arc weld pools
[AD-A245926] p 3293 N92-28384

ARCHITECTURE (COMPUTERS)
Digital hardware architecture implementation
[AD-A249194] p 3332 N92-28236
Femtosecond carrier processes in compound semiconductors and real time signal processing
[AD-A248053] p 3278 N92-28275
Numerical methods of linear and nonlinear optimization
[AD-A248579] p 3335 N92-28428
Integration of tools for the Design and Assessment of High-Performance, Highly Reliable Computing Systems (DAHPHRS), phase 1
[NASA-CR-189621] p 3336 N92-28585
SPECTOOL: A computer-aided verification tool for hardware designs, volume 1
[AD-A247492] p 3336 N92-28666
Development of a high-performance FORTRAN compiler for porting CFD codes to the Navier-Stokes computer
[AD-A250208] p 3342 N92-28770
Vector and parallel supercomputing programming
[ONERA-NT-1991-11] p 3338 N92-28779
Flexible integrated architecture for neural networks
[ETN-92-91320] p 3343 N92-28782
Fault-tolerant parallel computer systems for real-time applications
[AD-A247887] p 3343 N92-28958
VHDL and waves descriptions for a pseudo-random pattern generator
[AD-A247891] p 3349 N92-28961

ARCTIC OCEAN
Under-ice broadband transient measurements and processing
[AD-A248609] p 3351 N92-28324
Applications of passive microwave satellite data for Arctic Sea ice studies
[AD-A245966] p 3306 N92-28791

ARGON
Forsterite/melt partitioning of argon and iodine: Implications for atmosphere formation by outgassing of an early Martian magma ocean p 3313 N92-28604
Excitation of atoms and molecules in collisions with highly charged ions
[DE92-012658] p 3355 N92-28764
Computations of detonation structure: The influence of model input parameters
[AD-A248634] p 3285 N92-28803

ARGON LASERS
Delays in laser glare onset differentially affect target-location performance in a visual search task
[AD-A246708] p 3327 N92-28557
Compact, self-contained ArF lasers
[AD-A247403] p 3291 N92-28932

ARITHMETIC
Computer-based assessment of schema knowledge in a flexible problem-solving environment
[AD-A246779] p 3348 N92-28516

ARMED FORCES (UNITED STATES)
A study of pilot attitudes regarding the impact on mission effectiveness of using new cockpit automation technologies to replace the navigator/weapon system officer/electronic warfare officer
[AD-A246683] p 3329 N92-28286
Analysis of multimedia information systems for the US Coast Guard
[AD-A247890] p 3369 N92-28960

ARRAYS
Microhole array electrodes based on microporous alumina membranes
[AD-A247082] p 3278 N92-28239
Multiple-valued programmable logic array minimization by simulated annealing
[AD-A248620] p 3335 N92-28353

ARRHYTHMIA
Mathematical modeling of solar magneto-dynamics
[AD-A247158] p 3395 N92-28520

ARTIFICIAL INTELLIGENCE
Diagnostic reasoning within sequential circuits, volume 1
[AD-A248055] p 3278 N92-28305
Reinforcement learning for the adaptive control of perception and action
[AD-A249351] p 3344 N92-28325
Temporal reasoning and problem solving
[AD-A248457] p 3344 N92-28387
What is on the machine's mind? Models for reasoning with incomplete and uncertain knowledge
[NLR-TP-91099-U] p 3345 N92-28716
Learning and tuning fuzzy logic controllers through reinforcements
[NASA-TM-107875] p 3345 N92-28759
Monolithic optoelectronic implementation of neural planes
[AD-A250286] p 3345 N92-28970
Acquisition and improvement of human motor skills: Learning through observation and practice
[NASA-TM-107878] p 3329 N92-29174
Building the Scientific Modeling Assistant: An interactive environment for specialized software design
[NASA-TM-107844] p 3346 N92-29175

ARTIFICIAL SATELLITES
Space applications for contactless coilguns
[DE92-011156] p 3245 N92-29102
Analysis and optimization of low-earth-orbit communication links
[DE92-013393] p 3277 N92-29131

ASCORBIC ACID
Investigation of laser-induced retinal damage
[AD-A250173] p 3326 N92-28920

ASIA
Analysis of the effects of Eurasian crustal and upper mantle structure on regional phases using broadband seismic data
[AD-A248383] p 3309 N92-28366

ASPHALT
Use of scrap rubber in asphalt pavement surfaces
[AD-A247419] p 3272 N92-28902

ASSEMBLING
Lessons from Archimedes, a system for planning and executing mechanical assemblies
[DE92-010957] p 3335 N92-28342

ASSESSMENTS
Computer-based assessment of schema knowledge in a flexible problem-solving environment
[AD-A246779] p 3348 N92-28516

ASTRONAUTICS
Aeronautical engineering: A continuing bibliography with indexes (supplement 278)
[NASA-SP-7037(278)] p 3226 N92-28677
Aeronautical engineering: A continuing bibliography with indexes (supplement 275)
[NASA-SP-7037(275)] p 3226 N92-28679

ASTRONAUTS
Thermoregulation during spaceflight
[NASA-TM-103913] p 3325 N92-28420

ASTRONOMICAL MAPS
A Be star atlas of far UV and optical high-resolution spectra
[ESA-SP-1147] p 3371 N92-28781

ASTRONOMICAL MODELS
Thermal accretion disk models for active galaxies
[ETN-92-91486] p 3371 N92-29127

ASTRONOMY
Scientific investigations with the data base HEAO-1 scanning modulator collimator
[NASA-CR-190477] p 3370 N92-28680

ASTROPHYSICS
Secondary instability in 3D magnetic reconnection
[AD-A248630] p 3360 N92-28354
Science and application payloads in the 1990's
[NASA-TM-107937] p 3246 N92-28370
The physics of strange matter
[DE92-011734] p 3371 N92-28774

ASYMMETRY
Midlatitude weather systems on Mars: Is there a hemispheric asymmetry? p 3379 N92-28992

ATLANTIC OCEAN
CTD data from the north east Atlantic, April 1989, collected on RRS Discovery Cruise 181
[IOS-285-1991] p 3322 N92-29211

ATMOSPHERIC BOUNDARY LAYER
SAR-relate stress variability in the Marine Atmospheric Boundary Layer (MABL)
[AD-A247772] p 3309 N92-28567
A self-affine multi-fractal wave/turbulence discrimination method using data from single point fast response sensors in a nocturnal atmospheric boundary layer
[AD-A250419] p 3318 N92-28799
Influence of aerodynamic roughness length on aeolian processes: Earth, Mars, Venus p 3380 N92-28996
ATMOSPHERIC CHEMISTRY
Papers Presented to the Workshop on the Evolution of the Martian Atmosphere
[NASA-CR-190508] p 3372 N92-28478
An ion mass spectrometer for measuring isotopic adundances and loss rates of O, C and H in Mars' upper atmosphere p 3374 N92-28486
Martian atmospheric chemistry during the time of low water abundance p 3376 N92-28501
Volatile tracers of Martian atmospheric evolution: Present measurement status and requirements for future investigations p 3387 N92-29037
Regional environmental impacts of methanol-fueled vehicles
[PB92-176569] p 3308 N92-29183
ATMOSPHERIC CIRCULATION
Studies in turbulence and turbulence control
[AD-A247164] p 3282 N92-28225
High pressure experiments with a Mars general circulation model p 3374 N92-28491
Astronomical variation experiments with a Mars general circulation model p 3376 N92-28503
The thermal structure, dust loading, and meridional transport in the Martian atmosphere during late southern summer p 3377 N92-28505
A self-affine multi-fractal wave/turbulence discrimination method using data from single point fast response sensors in a nocturnal atmospheric boundary layer
[AD-A250419] p 3318 N92-28799
Simulating radar propagation through atmospheric turbulence using the Tropospheric ElectroMagnetic Parabolic Equation Routine (TEMPER)
[AD-A247408] p 3275 N92-28905
Evaluation of simple mesoscale models for use in TESS
[AD-A247914] p 3316 N92-28964
Midlatitude weather systems on Mars: Is there a hemispheric asymmetry? p 3379 N92-28992
Dust storm driven variations of the Mars thermosphere and exosphere: Coupling of atmospheric regions p 3380 N92-28997
Mars dust storm simulations: Analysis of surface stress p 3389 N92-29045
ATMOSPHERIC COMPOSITION
Papers Presented to the Workshop on the Evolution of the Martian Atmosphere
[NASA-CR-190508] p 3372 N92-28478
Surface vs. atmospheric origin of 2.1-2.5 micron absorption features in the Martian spectrum p 3373 N92-28480
Photochemical model for NH3 in an early Martian atmosphere p 3373 N92-28481
Oxygen in the Martian atmosphere: Regulation of PO2 by the deposition of iron formations on Mars p 3373 N92-28482
An ion mass spectrometer for measuring isotopic adundances and loss rates of O, C and H in Mars' upper atmosphere p 3374 N92-28486
Chemical models of volcanic outgassing on Mars p 3374 N92-28487
Time variation of the meteoritic contribution to the atmosphere of Mars p 3374 N92-28489
A reduced atmosphere for early Mars? p 3375 N92-28495
The early Martian atmosphere p 3376 N92-28502
Martian surficial carbon-constraints from isotopic measurements of shock-produced glass in EET A79001 p 3377 N92-28508
Mars atmospheric water p 3381 N92-29005
Atmosphere-surface interactions and atmospheric evolution on Mars p 3383 N92-29012
Nitrogen escape from Mars p 3383 N92-29014
Greenhouse warming by minor gases on early Mars p 3384 N92-29022
Distribution of water on Mars: Implications from SNC meteorites p 3386 N92-29027
Was early Mars warmed by ammonia? p 3386 N92-29030
Mars atmosphere evolution: Escape to space p 3387 N92-29034
Discovery concepts for Mars p 3387 N92-29035
Short- and long-term climate changes on Mars p 3389 N92-29051
Aqueous-alteration products in S-N-C meteorites and implications for volatile/regolith interactions on Mars p 3393 N92-29071
The ultraviolet albedo of Mars p 3394 N92-29074
Modeling the seasonal cycle of CO2 on Mars: A fit to the Viking lander pressure curves p 3394 N92-29076
ATMOSPHERIC DENSITY
Future mission studies: Preliminary comparisons of solar flux models
[NASA-TM-107947] p 3396 N92-28869
ATMOSPHERIC EFFECTS
Atmospheric corrections of land imagery using the extended radiosity method
[DE92-011355] p 3306 N92-28840
Influence of heat flow on early Martian climate p 3390 N92-29052
Modeling the seasonal cycle of CO2 on Mars: A fit to the Viking lander pressure curves p 3394 N92-29076
ATMOSPHERIC ENTRY
The meteoritic contribution to dust and aerosols in the atmosphere of Mars p 3383 N92-29013
ATMOSPHERIC GENERAL CIRCULATION MODELS
High pressure experiments with a Mars general circulation model p 3374 N92-28491
Astronomical variation experiments with a Mars general circulation model p 3376 N92-28503
Development of rotating shadowband spectral radiometers and GCM radiation code test data sets in support of ARM
[DE92-011438] p 3316 N92-28853
Dust storm driven variations of the Mars thermosphere and exosphere: Coupling of atmospheric regions p 3380 N92-28997
Mars dust storm simulations: Analysis of surface stress p 3389 N92-29045
Atomic oxygen in the Martian thermosphere p 3391 N92-29061
Comparison of drift potential derived from Mars GCM with rock abundance from IRTM p 3395 N92-29078
ATMOSPHERIC HEATING
Regional climatic effects of atmospheric SO2 on Mars p 3377 N92-28504
The role of SO2 on Mars and on the primordial oxygen isotope composition of water on Earth and Mars p 3377 N92-28507
Greenhouse warming by minor gases on early Mars p 3384 N92-29022
ATMOSPHERIC MODELS
An evaluation of the naval oceanic vertical aerosol model during Key90
[AD-A245943] p 3320 N92-28318
Parameterization of convective clouds, mesoscale convective systems, and convective-generated cirrus
[DE92-010951] p 3318 N92-28340
Papers Presented to the Workshop on the Evolution of the Martian Atmosphere
[NASA-CR-190508] p 3372 N92-28478
The impact of temperature dependent CO2 cross section measurements: A role for heterogeneous chemistry in the atmosphere of Mars? p 3372 N92-28479
Photochemical model for NH3 in an early Martian atmosphere p 3373 N92-28481
The production and escape of nitrogen atoms on Mars p 3374 N92-28490
A reduced atmosphere for early Mars? p 3375 N92-28495
Liquid water habitats on early Mars p 3376 N92-28500
Simulation of atmospheric frontogenesis with a semi-Lagrangian numerical model
[AD-A247151] p 3318 N92-28517
Development of an advanced representation of cumulus convection
[DE92-011031] p 3319 N92-28830
Simulating radar propagation through atmospheric turbulence using the Tropospheric ElectroMagnetic Parabolic Equation Routine (TEMPER)
[AD-A247408] p 3275 N92-28905
Wind-speed forecasting study for Westover AFB, Massachusetts
[AD-A247545] p 3319 N92-28934
Evaluation of simple mesoscale models for use in TESS
[AD-A247914] p 3316 N92-28964
Dust storm driven variations of the Mars thermosphere and exosphere: Coupling of atmospheric regions p 3380 N92-28997
Mars: Correcting surface albedo observations for effects of atmospheric dust loading p 3386 N92-29032
Simulations of the seasonal polar caps on Mars p 3387 N92-29033
Carbonate formation on Mars: History of the CO2 atmosphere from models of diffusion-limited growth in non-aqueous environments p 3391 N92-29060
Microcraters on Mars: Evidence of past climatic variations p 3394 N92-29073
The ultraviolet albedo of Mars p 3394 N92-29074
Climatic implications of the simultaneous presence of CO2 and H2O in the Martian regolith p 3395 N92-29079
ATMOSPHERIC MOISTURE
A magma ocean and the Earth's internal water budget p 3310 N92-28590
Mesoscale surface analysis of the ERICA IOP-5 cyclone
[AD-A245946] p 3319 N92-28884
VLA mapping of 1.35 cm water emission from the Mars atmospheric limb p 3381 N92-29004
Mars atmospheric water p 3381 N92-29005
ATMOSPHERIC OPTICS
Mars: Correcting surface albedo observations for effects of atmospheric dust loading p 3386 N92-29032
ATMOSPHERIC PRESSURE
High pressure experiments with a Mars general circulation model p 3374 N92-28491
Mesoscale surface analysis of the ERICA IOP-5 cyclone
[AD-A245946] p 3319 N92-28884
Ultra-high temperature stability Joule-Thomson cooler with capability to accomodate pressure variations
[NASA-CASE-NPO-18184-1-CU] p 3288 N92-29156
ATMOSPHERIC RADIATION
A new radiometer for Earth radiation budget studies
[DE92-011267] p 3306 N92-28834
ETO cloud studies for FIRE 2, part 1
[NASA-CR-190472] p 3319 N92-29087
ATMOSPHERIC SCATTERING
Atmospheric corrections of land imagery using the extended radiosity method
[DE92-011355] p 3306 N92-28840
Mars dust and cloud opacities and scattering properties p 3381 N92-29003
ATMOSPHERIC SOUNDING
ETO cloud studies for FIRE 2, part 1
[NASA-CR-190472] p 3319 N92-29087
ATMOSPHERIC STRATIFICATION
Turbulent spectra, fluxes, stability and growth of the mixed layer in the boundary layer of Mars p 3393 N92-29070
ATMOSPHERIC TEMPERATURE
Astronomical variation experiments with a Mars general circulation model p 3376 N92-28503
The thermal structure, dust loading, and meridional transport in the Martian atmosphere during late southern summer p 3377 N92-28505
Mars atmospheric water p 3381 N92-29005
Atmospheric and surface temperatures and airborne dust amounts during late southern summer from Mariner 9 IRIS data p 3390 N92-29056
Turbulent spectra, fluxes, stability and growth of the mixed layer in the boundary layer of Mars p 3393 N92-29070
ATMOSPHERIC TURBULENCE
Studies in turbulence and turbulence control
[AD-A247164] p 3282 N92-28225
Response of helicopters to gusts
[NLR-TP-90159-U] p 3239 N92-28653
Atmospheric turbulence spectra and correlation functions
[NLR-TP-89217-U] p 3316 N92-28689
Simulating radar propagation through atmospheric turbulence using the Tropospheric ElectroMagnetic Parabolic Equation Routine (TEMPER)
[AD-A247408] p 3275 N92-28905
ATMOSPHERICS
Reactions of hydrazines with chemicals found in environment
[AD-A247064] p 3308 N92-28272
Comparison of electromagnetic propagation predictions from IREPS and RPO across a coastal transition
[AD-A249331] p 3273 N92-28357
Analysis of electromagnetic propagation over variable terrain using the parabolic wave equation
[AD-A248061] p 3276 N92-28947
Microwave interactions with plasmas
[AD-A250333] p 3362 N92-29093
ATOMIC COLLISIONS
Excitation of atoms and molecules in collisions with highly charged ions
[DE92-012658] p 3355 N92-28764
ATOMIC ENERGY LEVELS
High quality Gaussian basis sets for fourth-row atoms
[NASA-TM-103918] p 3255 N92-28743
ATOMIC EXCITATIONS
Theoretical studies of the electronic and resonance structure of atomic and molecular negative ions
[AD-A247093] p 3354 N92-28259
ATOMIC STRUCTURE
Theoretical studies of the electronic and resonance structure of atomic and molecular negative ions
[AD-A247093] p 3354 N92-28259

The emergence of atomic-level structural information for ordered metal-solution interfaces: Some recent contributions from in-situ infrared spectroscopy and scanning tunneling microscopy
[AD-A246765] p 3364 N92-28512
Compositional disorder, magnetism, and their interplay in metallic alloys
[DE92-011671] p 3260 N92-28856
Electronic structure of fullerene tubules
[AD-A250166] p 3253 N92-28918
Volatile tracers of Martian atmospheric evolution: Present measurement status and requirements for future investigations p 3387 N92-29037

ATOMS
Gadolinium metastable states population distributions and atomic density under high-rate electron beam evaporation
[DE92-782008] p 3363 N92-28282

ATTENTION
Reinforcement learning for the adaptive control of perception and action
[AD-A249351] p 3344 N92-28325
Integrating the affective domain into the instructional design process
[AD-A249287] p 3327 N92-28880

ATTENUATION
Adaptive noise cancellation applied to the NUWES test ranges
[AD-A245961] p 3352 N92-28409

ATTITUDE CONTROL
Prediction of attitude stability of asymmetric dual-spin stabilized spacecraft using improved liquid slosh model
[AD-A247023] p 3246 N92-28368

ATTITUDE STABILITY
Prediction of attitude stability of asymmetric dual-spin stabilized spacecraft using improved liquid slosh model
[AD-A247023] p 3246 N92-28368

AUDIO FREQUENCIES
Examination of prosodic features in speech signal using speech fundamental frequency and loudness duration
[ETN-92-91334] p 3274 N92-28792

AUDITORY PERCEPTION
Demodulation processes in auditory perception
[AD-A250203] p 3328 N92-29146

AUDITORY STIMULI
Monaural and binaural processing of complex waveforms
[AD-A247199] p 3352 N92-28889

AUGMENTATION
Technological enhancements for personal computers
[AD-A247962] p 3333 N92-29083

AURORAS
Theoretical and experimental studies relevant to interpretation of auroral emissions
[NASA-CR-190521] p 3316 N92-28911

AUSTRALIA
Ultrasonic ambient noise in Australian shallow waters at frequencies up to 200 kHz
[MRL-TR-91-23] p 3351 N92-28364

AUTOMATIC CONTROL
Lessons from Archimedes, a system for planning and executing mechanical assemblies
[DE92-010957] p 3335 N92-28342
Software design for automated assembly of truss structures
[NASA-TP-3198] p 3344 N92-28375
Automation and remote control instrumentation development: Rocket First Motion Timing System (RFMTS)
[AD-A249970] p 3287 N92-28767
Tuning and automatic phase adjustment in external cavity diode laser beam combiners
[AD-A247421] p 3290 N92-28903
Development of an automated wire delivery system for robotic welding applications
[NASA-CR-190487] p 3295 N92-29134
Use of laser range finders and range image analysis in automated assembly tasks
[NASA-CR-186957] p 3291 N92-29139
Ultra-high temperature stability Joule-Thomson cooler with capability to accomodate pressure variations
[NASA-CASE-NPO-18184-1-CU] p 3288 N92-29156
Contribution to the design of flexible manufacturing systems: Application of the formal description technique Estelle
[LAAS-91378] p 3341 N92-29209

AUTOMATION
A probabilistic neural network approach to cloud classification
[AD-A247916] p 3319 N92-28966

AUTOMOBILE FUELS
Identification and analysis of factors affecting the adoption of alternative transportation fuels
[PB92-164326] p 3266 N92-28914
Regional environmental impacts of methanol-fueled vehicles
[PB92-176569] p 3308 N92-29183

AUTOMOBILES
Evaluation of drive simulator settings for DAF YA-4440
[FEL-91-B345] p 3241 N92-28828

AUTONOMOUS NAVIGATION
A rotorcraft flight database for validation of vision-based ranging algorithms
[NASA-TM-103906] p 3231 N92-29103

AUTONOMY
Closed-loop autonomous docking system
[NASA-CASE-MFS-28421-1] p 3248 N92-28750

AVALANCHES
Characterization of Martian near-subsurface materials by determination of cohesion and angle of internal friction p 3393 N92-29068

AVIONICS
Applications of ASICs to avionics
[AGARD-AG-329] p 3235 N92-28376
Applications of silicon hybrid multi-chip modules to avionics p 3235 N92-28379
A profile of scientist and engineer training conducted by the Naval Avionics Center
[AD-A245925] p 3326 N92-28408
A survey of high density packaging for high performance computing system
[AD-A248633] p 3332 N92-28891

AZOLES
Polyimidazoles via aromatic nucleophilic displacement
[NASA-CASE-LAR-14145-1] p 3264 N92-28751
Poly(1,3,4-oxadiazoles) via aromatic nucleophilic displacement
[NASA-CASE-LAR-14427-1] p 3250 N92-29141

B

BACKGROUND NOISE
Seafloor pressure array studies at ultra-low frequencies
[AD-A247663] p 3322 N92-28939
Annoyance due to discrete tones in broadband background noise. Part 2: Analysis
[ISVR-TR-202-PT-2] p 3353 N92-29203

BACKSCATTERING
Studies of the polarimetric dependence of enhanced backscattering from one-dimensional surfaces
[AD-A248431] p 3275 N92-28878
Neural network parameter estimation for the modified bistatic scattering strength model (BISSM)
[AD-A247913] p 3322 N92-28963

BACTERIA
Conversion of acetic acid to methane by thermophiles
[DE92-010652] p 3257 N92-28942

BAFFLES
Nonlinear sloshing and the coupled dynamics of liquid propellants and spacecraft
[AD-A250023] p 3248 N92-28967

BALL BEARINGS
Replacement bearing for Rocketdyne SSME HPOTPs using alternate self-lubricating retainer materials
[NASA-CR-184328] p 3292 N92-28362
Rolling friction robot fingers
[NASA-CASE-GSC-13261-1] p 3296 N92-29138

BANGLADESH
Multitemporal analysis of a braiding river
[NLR-TP-89235-U] p 3305 N92-28690

BARIUM OXIDES
Electrodeposition of high temperature superconductors
[AD-A250171] p 3365 N92-28919

BAROCLINIC INSTABILITY
A numerical study of time-dependent wind forcing off the west coast of Portugal, 1987-1988
[AD-A246775] p 3321 N92-28365
Midlatitude weather systems on Mars: Is there a hemispheric asymmetry? p 3379 N92-28992

BARYONS
Electroproduction of light quark baryons
[DE92-010853] p 3354 N92-28337
Inverse phase transitions: Does baryogenesis lead to dark matter?
[DE92-013022] p 3372 N92-29184

BASALT
Rates of oxidative weathering on the surface of Mars p 3380 N92-28999
Mid-infrared spectra of Martian komantiite p 3390 N92-29053

BATHING
Whole body cleaning agent containing N-acyltaurate
[NASA-CASE-MSC-21589-1] p 3332 N92-29137

BATHYMETERS
Ocean tide models for satellite geodesy and Earth rotation
[NASA-CR-190468] p 3321 N92-28867
Neural network parameter estimation for the modified bistatic scattering strength model (BISSM)
[AD-A247913] p 3322 N92-28963

BAYS (STRUCTURAL UNITS)
Payload retention device
[NASA-CASE-MSC-21906-1] p 3294 N92-28727

BEAM CURRENTS
Development of negative heavy ion sources for plasma potential measurement
[DE92-782102] p 3360 N92-28234

BEAM INTERACTIONS
Plasma beam measurements
[AD-A247892] p 3362 N92-28962

BEAMS (RADIATION)
RF impedance measurement status for the 7-GeV Advanced Photon Source (APS)
[DE92-013060] p 3274 N92-28810

BEARING (DIRECTION)
Directional wave data recorded off Flamborough Head (England)
[IOS-273-1990] p 3323 N92-29216

BEARINGS
Dynamics of a split torque helicopter transmission
[NASA-TM-105681] p 3296 N92-29136

BEDROCK
Relationships of soil, grass, and bedrock over the Kaweah serpentine melange through spectral mixture analysis of AVIRIS data
[NASA-CR-190445] p 3306 N92-28717

BEHAVIOR
Study of SCN neurochemistry using in vivo microdialysis in the conscious brain: Correlation with overt circadian rhythms
[AD-A247172] p 3325 N92-28886

BELL AIRCRAFT
An evaluation of IFR approach techniques: Generic helicopter simulation compared with actual flight p 3225 N92-28550

BEND TESTS
Tensile and interlaminar properties of GLARE (trade name) laminates
[AD-A250188] p 3253 N92-28921

BENDING FATIGUE
Fatigue strength of a glass fiber reinforced laminate structure
[VTT-RR-743] p 3251 N92-28573

BENDING VIBRATION
Exploratory flexural power flow measurements on a bar
[NLR-TP-90178-U] p 3304 N92-29176

BERYLLIUM
A Be star atlas of far UV and optical high-resolution spectra
[ESA-SP-1147] p 3371 N92-28781

BETA PARTICLES
The many aspects of neutrino physics
[DE92-011735] p 3355 N92-28858

BIAS
Magnetic and electromagnetic induction effects in the annual means of geomagnetic elements p 3301 N92-28632

BIBLIOGRAPHIES
Aeronautical engineering: A continuing bibliography with indexes (supplement 278)
[NASA-SP-7037(278)] p 3226 N92-28677
Aeronautical engineering: A continuing bibliography with indexes (supplement 275)
[NASA-SP-7037(275)] p 3226 N92-28679
Publications of the Jet Propulsion Laboratory, 1989
[NASA-CR-190457] p 3369 N92-29202

BIMETALS
Molecular recognition in the oxidation of catechols by Dicobalt-BISDIEN dioxygen complexes
[AD-A246456] p 3258 N92-28973

BINARY DATA
Binary optical filters for scale invariant pattern recognition
[NASA-TM-103902] p 3234 N92-28910

BINARY MIXTURES
Reactant conversion in homogeneous turbulence: Mathematical modeling, computational validations and practical applications p 3285 N92-28819

BINAURAL HEARING
Monaural and binaural processing of complex waveforms
[AD-A247199] p 3352 N92-28889

BINOCULAR VISION
Non-linear analysis of visual cortical neurons
[AD-A250233] p 3326 N92-29179

BIOCHEMISTRY
Study of SCN neurochemistry using in vivo microdialysis in the conscious brain: Correlation with overt circadian rhythms
[AD-A247172] p 3325 N92-28886

CTD data from the north east Atlantic, April 1989, collected on RRS Discovery Cruise 181
[IOS-285-1991] p 3322 N92-29211
BIOCONVERSION
Conversion of acetic acid to methane by thermophiles
[DE92-010652] p 3257 N92-28942
BIOLOGICAL EFFECTS
Problems in mechanistic theoretical models for cell transformation by ionizing radiation
[DE92-010265] p 3324 N92-28278
BIOLOGICAL EVOLUTION
Liquid water habitats on early Mars
p 3376 N92-28500
BIOLUMINESCENCE
Bioluminescence in the western Alboran Sea in April 1991
[AD-A250016] p 3324 N92-29089
BIOMASS
Coupling plant growth and waste recycling systems in a controlled life support system (CELSS)
[NASA-TM-107544] p 3330 N92-28670
BIOMETRICS
Technological enhancements for personal computers
[AD-A247962] p 3333 N92-29083
BIOREACTORS
Experimental measurement of the orbital paths of particles sedimenting within a rotating viscous fluid as influenced by gravity
[NASA-TP-3200] p 3331 N92-28897
Conversion of acetic acid to methane by thermophiles
[DE92-010652] p 3257 N92-28942
BIOSPHERE
Liquid water habitats on early Mars
p 3376 N92-28500
BIPOLAR TRANSISTORS
Design and realization of polysilicon emitter bipolar transistors
[LAAS-91360] p 3282 N92-29208
BIREFRINGENCE
In line optical fibre frequency shifter project
[AD-A246714] p 3357 N92-28372
BLACK HOLES (ASTRONOMY)
Quark matter and cosmology
[DE92-011736] p 3371 N92-28859
BLAST LOADS
Modular simulation of HEI fragments and blast pressure
[AD-A248205] p 3272 N92-29191
BLOCK COPOLYMERS
Chain folding in EBEE semicrystalline diblock copolymers
[AD-A247595] p 3262 N92-28251
BLOOD FLOW
Study of the loss of consciousness inflight by fighter aircraft pilots
[ONERA-RTS-11/3446-EY] p 3325 N92-28844
BLOWDOWN WIND TUNNELS
Replacement of the NAL high pressure air storage system
[NAL-TM-634] p 3241 N92-28835
BODY KINEMATICS
Linear recursive formulation of flexible multi-body space system dynamics
[NLR-TP-90284-U] p 3293 N92-28646
BODY TEMPERATURE
Modelling of heat and moisture loss through NBC ensembles
[AD-A245939] p 3329 N92-28346
Thermoregulation during spaceflight
[NASA-TM-103913] p 3325 N92-28420
BODY-WING CONFIGURATIONS
Analysis of results of an Euler-equation method applied to leading-edge vortex flow
[NLR-TP-90368-U] p 3226 N92-28657
BOILERS
Elevated temperature axial and torsional fatigue behavior of Haynes 188
[NASA-TM-105396] p 3302 N92-28701
BOMBING EQUIPMENT
Improvement of separations of practice bombs from a multiple bomb adapter
[NLR-TP-90307-U] p 3232 N92-28634
Modifications and results of flight tests of a practice bomb adapter
[NLR-TP-90108-U] p 3233 N92-28651
BOMBS (ORDNANCE)
Improvement of separations of practice bombs from a multiple bomb adapter
[NLR-TP-90307-U] p 3232 N92-28634
Modifications and results of flight tests of a practice bomb adapter
[NLR-TP-90108-U] p 3233 N92-28651
BONDING
The influence of elevated temperature on the bonding quality of deformed GLARE
[LR-659] p 3252 N92-28577
The characterization of ceramics and ceramic/metal-joints by ultrasonic techniques
[VTT-RR-741] p 3266 N92-29194
BORON
Kinetic studies of metal combustion in propulsion
[AD-A250207] p 3256 N92-28769
BORON FIBERS
Formation, structure, and properties of boron nitride fibers from polymer precursors
[AD-A247679] p 3263 N92-28553
BORON NITRIDES
Formation, structure, and properties of boron nitride fibers from polymer precursors
[AD-A247679] p 3263 N92-28553
The oxidation stability of boron nitride thin films on MgO and TiO2 substrates
[DE92-011686] p 3364 N92-28857
BOROSILICATE GLASS
Pressure transducer and system for cryogenic environments
[NASA-CASE-LAR-14579-1] p 3288 N92-29097
BOUNDARIES
Distribution of coastal morphology in the Martian northern lowlands p 3389 N92-29047
BOUNDARY CONDITIONS
A domain decomposition method for ocean/bottom interaction problems
[FFI-91/7022] p 3320 N92-28266
Development and validation of a characteristic boundary condition for a cell-centered Euler method
[NLR-TP-90144-U] p 3227 N92-28692
Boundary conditions for Euler equations at internal block faces of multi-block domains using local grid refinement
[NLR-TP-90134-U] p 3284 N92-28712
BOUNDARY ELEMENT METHOD
Hyperbolic grid generation with BEM source terms
[NLR-TP-90334-U] p 3347 N92-28635
BOUNDARY INTEGRAL METHOD
Modal analysis of plates using boundary integral equations
[NLR-TP-89211-U] p 3302 N92-28688
BOUNDARY LAYER CONTROL
Boundary layer induced noise in aircraft
[ISSN-0309-7293] p 3353 N92-29201
BOUNDARY LAYER FLOW
Air ejector experiments using the two-dimensional supersonic cascade tunnel: Zero secondary flow performance
[NAL-TM-632] p 3241 N92-28829
BOUNDARY LAYER TRANSITION
Turbulent spot generation and growth rates in a transonic boundary layer
[AD-A250221] p 3287 N92-29118
Development of instrumentation for boundary layer transition detection
[AD-A249982] p 3287 N92-29171
BOUNDARY LAYERS
Calculation of unsteady transonic flows with mild separation by viscous-inviscid interaction
[NASA-TP-3197] p 3226 N92-28477
Mesoscale surface analysis of the ERICA IOP-5 cyclone
[AD-A245946] p 3319 N92-28884
Turbulent spectra, fluxes, stability and growth of the mixed layer in the boundary layer of Mars
p 3393 N92-29070
Boundary layer induced noise in aircraft
[ISSN-0309-7293] p 3353 N92-29201
BOUNDARY LUBRICATION
Replacement bearing for Rocketdyne SSME HPOTPs using alternate self-lubricating retainer materials
[NASA-CR-184328] p 3292 N92-28362
Lubricant evaluation and performance 2
[AD-A247464] p 3262 N92-28398
BOUNDARY VALUE PROBLEMS
Calculation of chip temperatures using ELLPACK
[AD-A247156] p 3335 N92-28519
Boundary conditions for Euler equations at internal block faces of multi-block domains using local grid refinement
[NLR-TP-90134-U] p 3284 N92-28712
BOUSSINESQ APPROXIMATION
Simulation of atmospheric frontogenesis with a semi-Lagrangian numerical model
[AD-A247151] p 3318 N92-28517
BRACKETS
Removable hand hold
[NASA-CASE-LEW-15196-1] p 3295 N92-29092
BRAIN
The Coordinated Noninvasive Studies (CNS) project, phase 1
[AD-A247159] p 3324 N92-28397
Neuropsychological components of object identification
[AD-A247049] p 3327 N92-28877
Study of SCN neurochemistry using in vivo microdialysis in the conscious brain: Correlation with overt circadian rhythms
[AD-A247172] p 3325 N92-28886
BRAIN DAMAGE
Neuropsychological components of object identification
[AD-A247049] p 3327 N92-28877
BRANCHING (MATHEMATICS)
A continuation method for calculating the equilibrium positions of nonlinear structures
[ONERA-RT-24/3542-RY-091-R] p 3338 N92-28790
Bifurcations and patterns in nonlinear dissipative systems
[DE92-013502] p 3364 N92-28806
Evidence of chaotic pattern in solar flux through a reproducible sequence of period-doubling-type bifurcations
[NASA-TM-107944] p 3396 N92-28907
BREADBOARD MODELS
Telescience experiments using the Prototype Optical Diagnostic Instrument (PODI)
[NLR-TP-90199-U] p 3358 N92-28656
BRECCIA
A new angle on lunar ferroan-suite differentiation
p 3311 N92-28598
BRIGHTNESS
Surface photometric properties and albedo changes in the central equatorial region of Mars
p 3392 N92-29066
BRITTLENESS
Diffusion-controlled decohesion using a Cu-Sn alloy as a model system
[DE92-011645] p 3260 N92-28854
BROADBAND
Noise reduction in ring laser driven by a broad band pump
[DE92-622403] p 3289 N92-28228
Under-ice broadband transient measurements and processing
[AD-A248609] p 3351 N92-28324
Analysis of the effects of Eurasian crustal and upper mantle structure on regional phases using broadband seismic data
[AD-A248383] p 3309 N92-28386
Annoyance due to discrete tones in broadband background noise. Part 2: Analysis
[ISVR-TR-202-PT-2] p 3353 N92-29203
Maximizing the convergence rate of the EM algorithm for the multiple broad-band signal estimation and detection
[AD-A248230] p 3341 N92-29224
BUCKLING
Method fabricating load-bearing composites free from microbuckling deformation up to a predetermined load
[AD-D015212] p 3250 N92-28224
BUMPERS
Evaluation of Whipple bumper shields at 7 and 10 km/s
[NASA-TM-107958] p 3295 N92-28925
BUNDLES
Bundle dimensions around the internal target area
[NIKHEF-K/AMPS/91-06] p 3356 N92-28264
BURNERS
Multicomponent comparison of optical and mass spectrometric diagnostics in low-pressure flames
[AD-A250323] p 3257 N92-28954
BURNING RATE
Combustion mechanisms of solids --- solid rocket propellant
[AD-A247088] p 3254 N92-28240

C

C-130 AIRCRAFT
Life cycle costs of the C-130 electrical power system upgrade
[AD-A246759] p 3221 N92-28348
C-135 AIRCRAFT
KC-135 Large Motion Isolation Mount (LMIM)
p 3267 N92-28440
CADMIUM TELLURIDES
Thin film cadmium telluride photovoltaic cells
[DE92-001239] p 3306 N92-28277
CALCIUM OXIDES
Mg-perovskite/silicate melt partition coefficients in the CMS system at 2430 C and 226 Kbars
p 3312 N92-28601
CALCIUM SILICATES
Processing and properties of chemically derived calcium silicate cements
[AD-A249106] p 3264 N92-28570
CALDERAS
Topography of Apollinaris Patera and Ma'adim Vallis
p 3393 N92-29069

CALIBRATING
Project MAGNET high-level vector survey data reduction p 3301 N92-28628
Relationships of soil, grass, and bedrock over the Kaweah serpentine melange through spectral mixture analysis of AVIRIS data
[NASA-CR-190445] p 3306 N92-28717
Windshear radar calibration: Transmitter power and receiver gain stability
[NASA-TM-107589] p 3275 N92-28876
Wavenumber calibration tables from heterodyne frequency measurements
[NASA-CR-190422] p 3276 N92-29115
Calculation of support interferences on the aerodynamic coefficients for a wind tunnel calibration model
[ESA-TT-1247] p 3229 N92-29159
Calibration of high energy x ray detectors at the spectrum of the Crab nebula, and x ray pulsar A0535+26 examinations
[ETN-92-91484] p 3371 N92-29177
Detection of in-plane displacements of acoustic wave fields using extrinsic Fizeau fiber interferometric sensors
[NASA-CR-190493] p 3353 N92-29196

CALIFORNIA
A diagnostic study of the velocity structure of a meandering jet in the California current system using a primitive equation model
[AD-A246039] p 3320 N92-28283

CALORIMETERS
The measuring assembly for the NPL primary standard absorbed dose graphite calorimeter at therapy levels
[NPL-RSA(EXT)-23] p 3288 N92-29163

CAMERAS
On-line point positioning with single frame camera data
[AD-A248307] p 3287 N92-28322
Instrumentation for ultrahigh strain rate experiments
[AD-A249358] p 3298 N92-28327
An acoustic charge transport imager for high definition television application
[AD-A250433] p 3274 N92-28773

CAPACITANCE
Simulation in infrared imaging: Using electrical circuit principles to model heat transfer
[AD-A248290] p 3278 N92-28276

CARBON
An ion mass spectrometer for measuring isotopic adundances and loss rates of O, C and H in Mars' upper atmosphere p 3374 N92-28486
Martian surficial carbon-constraints from isotopic measurements of shock-produced glass in EET A79001 p 3377 N92-28508
The stable isotopic compositions of indigenous carbon-bearing components in EETA 79001 p 3384 N92-29021

CARBON DIOXIDE
The impact of temperature dependent CO2 cross section measurements: A role for heterogeneous chemistry in the atmosphere of Mars? p 3372 N92-28479
Surface vs. atmospheric origin of 2.1-2.5 micron absorption features in the Martian spectrum p 3373 N92-28480
Photochemical model for NH3 in an early Martian atmosphere p 3373 N92-28481
Nature and evolution of the early Martian atmosphere: Evidence from highland crater populations p 3373 N92-28485
The Mars water cycle at other epochs: History of the polar caps and layered terrain p 3375 N92-28493
A reduced atmosphere for early Mars? p 3375 N92-28495
CO2 and clathrate as past erosive agents on Mars p 3375 N92-28497
History of oxygen and carbon escape from the Martian atmosphere p 3376 N92-28498
Astronomical variation experiments with a Mars general circulation model p 3376 N92-28503
Volcanic recycling of carbonate deposits on Mars p 3377 N92-28506
Martian surficial carbon-constraints from isotopic measurements of shock-produced glass in EET A79001 p 3377 N92-28508
Spectral identification of chemisorbed CO2 and application to Mars analog materials p 3378 N92-28510
The Martian polar caps: Stability and water transport at low obliquities p 3385 N92-29023
Simulations of the seasonal polar caps on Mars p 3387 N92-29033
Recent Elysium volcanism: Effects on the Martian atmosphere p 3389 N92-29048
Influence of heat flow on early Martian climate p 3390 N92-29052
Carbonate formation on Mars: History of the CO2 atmosphere from models of diffusion-limited growth in non-aqueous environments p 3391 N92-29060
Modeling the seasonal cycle of CO2 on Mars: A fit to the Viking lander pressure curves p 3394 N92-29076
Climatic implications of the simultaneous presence of CO2 and H2O in the Martian regolith p 3395 N92-29079

CARBON DIOXIDE CONCENTRATION
Influences of CO2 sublimation/condensation processes on the long-term evolution of the Martian atmosphere p 3375 N92-28496
Martian surficial carbon-constraints from isotopic measurements of shock-produced glass in EET A79001 p 3377 N92-28508

CARBON DIOXIDE LASERS
CO2 laser frequency multiplication
[AD-A245915] p 3290 N92-28761
CO2 laser frequency multiplication
[AD-A247542] p 3291 N92-28933
Performance of the multifunctional CW CO2-laser radar at the TNO-FEL laboratory and during the BEST TWO field test
[FEL-91-A163] p 3291 N92-29160

CARBON DIOXIDE REMOVAL
Trade study of three oxygen processors for the Martian atmosphere
[AD-A246854] p 3372 N92-28393

CARBON FIBERS
Quantitative interphase study of composite materials. Interphase engineering: A scientific way of tailoring the mechanophysical properties of composite materials
[AD-A247776] p 3251 N92-28252
The application of carbon fibres in ARALL laminates
[LR-658] p 3259 N92-28576

CARBON MONOXIDE
Surface vs. atmospheric origin of 2.1-2.5 micron absorption features in the Martian spectrum p 3373 N92-28480
Excitation of atoms and molecules in collisions with highly charged ions
[DE92-012658] p 3355 N92-28764

CARBON TETRAFLUORIDE
Computations of detonation structure: The influence of model input parameters
[AD-A248634] p 3285 N92-28803

CARBON 13
Martian surficial carbon-constraints from isotopic measurements of shock-produced glass in EET A79001 p 3377 N92-28508
On the isotopic composition of magmatic carbon in SNC meteorites p 3394 N92-29077

CARBON-CARBON COMPOSITES
Ablation of material of solid propellant motor nozzles
[ONERA-NT-1990-13] p 3249 N92-28780

CARBONACEOUS CHONDRITES
High-pressure melting of carbonaceous chondrite p 3310 N92-28589

CARBONATES
Volcanic recycling of carbonate deposits on Mars p 3377 N92-28506
Spectral identification of chemisorbed CO2 and application to Mars analog materials p 3378 N92-28510
Carbonate formation on Mars: History of the CO2 atmosphere from models of diffusion-limited growth in non-aqueous environments p 3391 N92-29060

CARCINOGENS
Problems in mechanistic theoretical models for cell transformation by ionizing radiation
[DE92-010265] p 3324 N92-28278
Somatic gene mutation in the human in relation to radiation risk
[DE92-009459] p 3325 N92-28685

CARGO
Payload retention device
[NASA-CASE-MSC-21906-1] p 3294 N92-28727

CARRIER MOBILITY
Sol-gel processed multifunctional organic polymer-inorganic oxide composites for electronics and photonics
[AD-A246773] p 3263 N92-28412

CARTESIAN COORDINATES
Angular momentum: Can be used in ballistic tracking
[AD-A247722] p 3350 N92-28400

CASCADE FLOW
Explicit Navier-Stokes computation of turbomachinery flows
[AD-A249284] p 3286 N92-28879
Laser anemometer measurements and computations in an annular cascade of high turning core turbine vanes
[NASA-TP-3252] p 3229 N92-28980

CASCADE WIND TUNNELS
Air ejector experiments using the two-dimensional supersonic cascade tunnel: Zero secondary flow performance
[NAL-TM-632] p 3241 N92-28829

CASING
Diffuser casing upgrade for an advanced turbofan
[NLR-TP-90097-U] p 3238 N92-28711

CASTINGS
X ray computed tomography of full-scale castings
[AD-A247101] p 3258 N92-28241

CATALYSIS
Macrocyclic polycation complexes for secondary anion binding, molecular recognition, and catalysis
[AD-A246690] p 3254 N92-28287
Surface crystallographic dependence of voltammetric oxidation of polyhydric alcohols and related systems at monocrystalline gold-acidic aqueous interfaces
[AD-A246763] p 3363 N92-28392
Thermodynamic and kinetic aspects of surface acidity
[DE92-011194] p 3256 N92-28893

CATIONS
Macrocyclic polycation complexes for secondary anion binding, molecular recognition, and catalysis
[AD-A246690] p 3254 N92-28287
Excited negative ions and molecules and negative ion production
[AD-A247017] p 3354 N92-28414

CAVITIES
Scattering and radiation analysis of three-dimensional cavity arrays via a hybrid finite element method
[NASA-CR-190408] p 3273 N92-28371
Propellant-to-inhibitor bonding system
[AD-D015243] p 3266 N92-28739

CAVITY RESONATORS
Intense electron beam cyclotron masers with microsecond pulselengths
[AD-A247060] p 3289 N92-28271
Tunable optical sources and synthetic nonlinear media/growth and characterization of nonlinear optical materials
[AD-A249363] p 3357 N92-28328

CELLS (BIOLOGY)
Controlled method of reducing electrophoretic mobility of macromolecules, particles, or cells
[NASA-CASE-MFS-26049-2-NP] p 3255 N92-28728
Experimental measurement of the orbital paths of particles sedimenting within a rotating viscous fluid as influenced by gravity
[NASA-TP-3200] p 3331 N92-28897

CEMENTS
Processing and properties of chemically derived calcium silicate cements
[AD-A249106] p 3264 N92-28570

CENTER OF GRAVITY
Demodulation processes in auditory perception
[AD-A250203] p 3328 N92-29146

CENTRIFUGAL COMPRESSORS
Dynamic control of aerodynamic instabilities in gas turbine engines p 3238 N92-28466
Explicit Navier-Stokes computation of turbomachinery flows
[AD-A249284] p 3286 N92-28879
A 4-spot time-of-flight anemometer for small centrifugal compressor velocity measurements
[NASA-TM-105717] p 3288 N92-29105

CERAMIC FIBERS
Review and update on electrocomposites
[AD-A248050] p 3251 N92-28303
Chemical vapor deposition of yttrium borium(2) copper(3) oxygen(x) thin films for wire applications
[AD-A247013] p 3364 N92-28395

CERAMIC MATRIX COMPOSITES
Proceedings of Asilomar Conference on Polymeric Materials
[AD-A249366] p 3262 N92-28360

CERAMICS
Effect of metallic coating properties on the tribology of oil-lubricated coated-ceramics
[DE92-010904] p 3262 N92-28339
Study of high temperature failure mechanism in ceramics
[AD-A247018] p 3263 N92-28415
Mechanistic studies of superplasticity of structural ceramics
[AD-A246951] p 3263 N92-28558
Processing and properties of chemically derived calcium silicate cements
[AD-A249106] p 3264 N92-28570
EXPLOMET 90 international conference on shock-wave and high-strain-rate phenomena in materials
[AD-A248665] p 3303 N92-28892
The processing of high temperature ceramic superconducting devices, volume 2
[AD-A248159] p 3281 N92-28948
The characterization of ceramics and ceramic/metal-joints by ultrasonic techniques
[VTT-RR-741] p 3266 N92-29194

CEREBRAL CORTEX
Non-linear analysis of visual cortical neurons
[AD-A250233] p 3326 N92-29179

CERTIFICATION
Validation of simulation systems for aircraft acceptance testing p 3222 N92-28531
The use of load enhancement factors in the certification of composite aircraft structures
[NLR-TP-90068-U] p 3232 N92-28649
S-76B certification for vertical take-off and landing operations from confined areas
[NLR-TP-90286-U] p 3233 N92-28714
CESIUM 137
Operation and radiation resistance of a FOXFET biasing structure for silicon strip detectors
[DE92-011279] p 3282 N92-29197
Determination of field related transfer factors for Cs-137 and Sr-90, from the fallout of the reactor accident in Chernobyl (USSR)
[OEFZS-4581] p 3356 N92-29210
CESSNA AIRCRAFT
Drop test: Cessna Golden Eagle 421B
[DOT/FAA/CT-TN91/32] p 3230 N92-28900
CH-47 HELICOPTER
Rotorcraft In-Flight Simulation Research at NASA Ames Research Center: A Review of the 1980's and plans for the 1990's
[NASA-TM-103873] p 3234 N92-28926
CHAINS
Chain folding in EBEE semicrystalline diblock copolymers
[AD-A247595] p 3262 N92-28251
CHALLENGER (ORBITER)
Performance of uncoated AFRSI blankets during multiple Space Shuttle flights
[NASA-TM-103892] p 3245 N92-29104
CHANNEL FLOW
Chryse Planitia region, Mars: Channeling history, flood-volume estimates, and scenarios for bodies of water in the northern plains p 3390 N92-29054
CHANNELS
Martian channel networks: A revised Strahler approach for quantitative morphometry p 3380 N92-29000
Multi-channel fiber optic rotary joint for single-mode fiber
[AD-D015273] p 3358 N92-29095
CHAOS
Studies in turbulence and turbulence control
[AD-A247164] p 3282 N92-28225
Detecting and disentangling nonlinear structure from solar flux time series
[NASA-CR-190510] p 3396 N92-28871
Lagrangian turbulence: Structures and mixing in admissible model flows
[AD-A247203] p 3286 N92-28890
Evidence of chaotic pattern in solar flux through a reproducible sequence of period-doubling-type bifurcations
[NASA-TM-107944] p 3396 N92-28907
In search of a unified theory of biological organization: What does the motor system of a sea slug tell us about human motor integration?
[AD-A250223] p 3328 N92-29119
CHARACTERIZATION
The characterization of ceramics and ceramic/metal-joints by ultrasonic techniques
[VTT-RR-741] p 3266 N92-29194
CHARGE CARRIERS
Sol-gel processed multifunctional organic polymer-inorganic oxide composites for electronics and photonics
[AD-A246773] p 3263 N92-28412
CHARGE COUPLED DEVICES
Portable dynamic fundus instrument
[NASA-CASE-MSC-21675-1] p 3325 N92-28755
Split events and their influence on pn CCD energy spectra
[ETN-92-91485] p 3282 N92-29178
CHARGE TRANSFER
Secondary Li battery incorporating 12-Crown-4 ether
[NASA-CASE-NPO-17922-1-CU] p 3280 N92-28753
Molecular recognition in the oxidation of catechols by Dicobalt-BISDIEN dioxygen complexes
[AD-A246456] p 3258 N92-28973
CHARGED PARTICLES
A generalization of the K-V equilibrium for an intense, relativistic beam propagating in a solenoid
[AD-A247067] p 3350 N92-28238
Fast algorithms for transport models
[DE92-011432] p 3338 N92-28841
CHECKOUT
Comparison of three controllers applied to helicopter vibration
[NASA-TM-102192] p 3239 N92-28457
CHEMICAL ANALYSIS
The nanophase iron mineral(s) in Mars soil
p 3379 N92-28990
CHEMICAL COMPOSITION
Thermal evolution and chemical differentiation of the terrestrial magma ocean p 3310 N92-28588
High-pressure melting of carbonaceous chondrite p 3310 N92-28589
Experimental determination of the solubility of iridium in silicate melts: Preliminary results p 3310 N92-28591
Mg-perovskite/silicate melt and magnesiowuestite/silicate melt partition coefficients for KLB-1 at 250 Kbars p 3310 N92-28592
Polyimidazoles via aromatic nucleophilic displacement
[NASA-CASE-LAR-14145-1] p 3264 N92-28751
Volatile tracers of Martian atmospheric evolution: Present measurement status and requirements for future investigations p 3387 N92-29037
Poly(1,3,4-oxadiazoles) via aromatic nucleophilic displacement
[NASA-CASE-LAR-14427-1] p 3250 N92-29141
Volatile CVD precursors based on copper alkoxides and mixed group IIA-Copper alkoxides --- chemical vapor deposition
[AD-D015264] p 3261 N92-29170
CHEMICAL EVOLUTION
Workshop on the Martian Surface and Atmosphere Through Time
[NASA-CR-190418] p 3378 N92-28988
CHEMICAL FUELS
Kinetic studies of metal combustion in propulsion
[AD-A250207] p 3256 N92-28769
CHEMICAL LASERS
Relaxation dynamics of highly excited halogens in their electronic ground states
[AD-A247312] p 3254 N92-28300
CHEMICAL PROPULSION
Introduction to rocket propulsion
[AD-A250424] p 3249 N92-28800
CHEMICAL REACTIONS
Reactions of hydrazines with chemicals found in environment
[AD-A247064] p 3308 N92-28272
Polyimidazoles via aromatic nucleophilic displacement
[NASA-CASE-LAR-14145-1] p 3264 N92-28751
Reactant conversion in homogeneous turbulence: Mathematical modeling, computational validations and practical applications p 3285 N92-28819
Modeling of the reactant conversion rate in a turbulent shear flow p 3229 N92-28820
Rates of oxidative weathering on the surface of Mars p 3380 N92-28999
Chemical reaction path modeling of hydrothermal processes on Mars: Preliminary results p 3389 N92-29050
A carbonate-silicate aqueous geochemical cycle model for Mars p 3390 N92-29057
CHEMISORPTION
Spectral identification of chemisorbed CO2 and application to Mars analog materials p 3378 N92-28510
CHIPS (ELECTRONICS)
What is an ASIC? p 3235 N92-28377
Calculation of chip temperatures using ELLPACK
[AD-A247156] p 3335 N92-28519
A survey of high density packaging for high performance computing system
[AD-A248633] p 3332 N92-28891
CHROMATOGRAPHY
Humic substances in soils from Bangladesh, Namibia, and Canada
[OEFZS-4574] p 3316 N92-28740
Studies of 1,3-disilacyclobutanes as single-source CVD precursors to silicon carbide
[AD-A247111] p 3365 N92-28885
CHROMOSOMES
Primer on molecular genetics
[DE92-010680] p 3324 N92-28382
CIRCADIAN RHYTHMS
Study of SCN neurochemistry using in vivo microdialysis in the conscious brain: Correlation with overt circadian rhythms
[AD-A247172] p 3325 N92-28886
CIRCUIT DIAGRAMS
SPECTOOL: A computer-aided verification tool for hardware designs, volume 1
[AD-A247492] p 3336 N92-28666
SPECTOOL: User's manual, volume 2
[AD-A247493] p 3336 N92-28667
CIRCUITS
Simulation in infrared imaging: Using electrical circuit principles to model heat transfer
[AD-A248290] p 3278 N92-28276
Diagnostic reasoning within sequential circuits, volume 1
[AD-A248055] p 3278 N92-28305
Multimeter-wave grid oscillators
[AD-A248430] p 3279 N92-28351
Taguchi methods in electronics: A case study
[NASA-TM-103586] p 3279 N92-28456
Crosstalk correction scheme
[AD-D015251] p 3276 N92-29085
Asynchronous bidirectional network interface enabling seamless concurrent processing in a distributed heterogeneous multiprocessor system
[AD-D015274] p 3343 N92-29096
Non-linear analysis of visual cortical neurons
[AD-A250233] p 3326 N92-29179
CIRCULAR TUBES
A combined experimental and analytical investigation of the theory of plasticity involving strain induced anisotropy
[AD-A248440] p 3298 N92-28352
CIRRUS CLOUDS
Parameterization of convective clouds, mesoscale convective systems, and convective-generated cirrus
[DE92-010951] p 3318 N92-28340
ETO cloud studies for FIRE 2, part 1
[NASA-CR-190472] p 3319 N92-29087
CIVIL AVIATION
Piloted Simulation Effectiveness
[AGARD-CP-513] p 3221 N92-28522
Flight simulation and digital flight controls p 3221 N92-28526
Validation of simulation systems for aircraft acceptance testing p 3222 N92-28531
FAA aviation forecasts
[AD-A250412] p 3230 N92-29182
CLASSIFICATIONS
Magnetic repeat station data p 3301 N92-28630
Studies of iterated transform image compression and its application to color and DTED
[AD-A248060] p 3339 N92-28946
A probabilistic neural network approach to cloud classification
[AD-A247916] p 3319 N92-28966
Physical properties of Deucalionis, Eos, Xanthe-type units in the central equatorial region of Mars p 3392 N92-29063
Physical properties of Meridiani Sinus-type units in the central equatorial region of Mars p 3392 N92-29064
Physical properties of Oxia/Lunae Planum and Arabia-type units in the central equatorial region of Mars p 3392 N92-29065
Stretch and hammer neural networks for N-dimensional data generalization
[AD-A247941] p 3346 N92-29082
CLATHRATES
CO2 and clathrate as past erosive agents on Mars p 3375 N92-28497
CLAYS
The nanophase iron mineral(s) in Mars soil p 3379 N92-28990
CLEANERS
Whole body cleaning agent containing N-acyltaurate
[NASA-CASE-MSC-21589-1] p 3332 N92-29137
CLEANING
Erosion of stainless steel by ultrasonic cleaning: A preliminary study
[DE92-012566] p 3260 N92-28763
CLEAR AIR TURBULENCE
Microwave temperature profiler for clear air turbulence prediction
[NASA-CASE-NPO-18115-1-CU] p 3320 N92-29148
CLIMATE
Parameterization of convective clouds, mesoscale convective systems, and convective-generated cirrus
[DE92-010951] p 3318 N92-28340
Regional climatic effects of atmospheric SO2 on Mars p 3377 N92-28504
Workshop on the Martian Surface and Atmosphere Through Time
[NASA-CR-190418] p 3378 N92-28988
Microcraters on Mars: Evidence of past climatic variations p 3394 N92-29073
Modeling the seasonal cycle of CO2 on Mars: A fit to the Viking lander pressure curves p 3394 N92-29076
Climatic implications of the simultaneous presence of CO2 and H2O in the Martian regolith p 3395 N92-29079
Tactical line-of-sight radio propagation reliability
[AD-A245909] p 3277 N92-29165
CLIMATE CHANGE
Astronomical variation experiments with a Mars general circulation model p 3376 N92-28503
Dark material in the polar layered deposits on Mars p 3385 N92-29024
Glacial geomorphic evidence for a late climatic change on Mars p 3386 N92-29029
Discovery concepts for Mars p 3387 N92-29035
Short- and long-term climate changes on Mars p 3389 N92-29051
Microcraters on Mars: Evidence of past climatic variations p 3394 N92-29073

Climatic implications of the simultaneous presence of CO2 and H2O in the Martian regolith
p 3395 N92-29079

CLIMATOLOGY
Distribution of Martian ground-ice table: Preliminary results about climatic variations p 3373 N92-28484
A reduced atmosphere for early Mars?
p 3375 N92-28495
Regional climatic effects of atmospheric SO2 on Mars
p 3377 N92-28504
Microcraters on Mars: Evidence of past climatic variations p 3394 N92-29073
Climatic implications of the simultaneous presence of CO2 and H2O in the Martian regolith
p 3395 N92-29079

CLOSED ECOLOGICAL SYSTEMS
Coupling plant growth and waste recycling systems in a controlled life support system (CELSS)
[NASA-TM-107544] p 3330 N92-28670
Space life support engineering program
[NASA-CR-190448] p 3330 N92-28671
A study of the control problem of the shoot side environment delivery system of a closed crop growth research chamber
[NASA-CR-177597] p 3330 N92-28681

CLOSURES
Mapping closures for turbulent mixing and reaction
[AD-A247305] p 3283 N92-28274

CLOTHING
Modelling of heat and moisture loss through NBC ensembles
[AD-A245939] p 3329 N92-28346
Automated apparel specification retrieval system
[AD-A248619] p 3367 N92-28389

CLOUD PHYSICS
Multiparameter radar and aircraft based studies of the microphysical, kinematic, and electrical structure of convective clouds
[AD-A247497] p 3318 N92-28668
Development of an advanced representation of cumulus convection
[DE92-011031] p 3319 N92-28830
Mars dust and cloud opacities and scattering properties p 3381 N92-29003

CLOUDS (METEOROLOGY)
Multiparameter radar and aircraft based studies of the microphysical, kinematic, and electrical structure of convective clouds
[AD-A247497] p 3318 N92-28668
Segmentation of satellite imagery using hierarchical thresholding and neural networks
[AD-A247915] p 3319 N92-28965
A probabilistic neural network approach to cloud classification
[AD-A247916] p 3319 N92-28966

CLUTTER
An OTH radar clutter simulation
[AD-A248054] p 3272 N92-28304

COAL GASIFICATION
High temperature membranes for H2S and SO2 separations
[DE92-010451] p 3256 N92-28827

COAL UTILIZATION
High temperature membranes for H2S and SO2 separations
[DE92-010451] p 3256 N92-28827

COASTS
A diagnostic study of the velocity structure of a meandering jet in the California current system using a primitive equation model
[AD-A246039] p 3320 N92-28283
Comparison of electromagnetic propagation predictions from IREPS and RPO across a coastal transition
[AD-A249331] p 3273 N92-28357
A numerical study of time-dependent wind forcing off the west coast of Portugal, 1987-1988
[AD-A246775] p 3321 N92-28365
Evaluation of simple mesoscale models for use in TESS
[AD-A247914] p 3316 N92-28964
Distribution of coastal morphology in the Martian northern lowlands p 3389 N92-29047

COATING
Thermal response of rigid and flexible insulations and reflective coating in an aeroconvective heating environment
[NASA-TM-103925] p 3233 N92-28721

COATINGS
Chemical vapor deposition of yttrium borium(2) copper(3) oxygen(x) thin films for wire applications
[AD-A247013] p 3364 N92-28395

COBALT
Elevated temperature axial and torsional fatigue behavior of Haynes 188
[NASA-TM-105396] p 3302 N92-28701

COBALT COMPOUNDS
Method of intercalating large quantities of fibrous structures
[NASA-CASE-LEW-15077-1] p 3253 N92-29152

COCKPIT SIMULATORS
Delays in laser glare onset differentially affect target-location performance in a visual search task
[AD-A246708] p 3327 N92-28557

COCKPITS
A study of pilot attitudes regarding the impact on mission effectiveness of using new cockpit automation technologies to replace the navigator/weapon system officer/electronic warfare officer
[AD-A246683] p 3329 N92-28286
Use of a virtual cockpit for the development of a future transport aircraft p 3225 N92-28547
Effects of cockpit lateral stick characteristics on handling qualities and pilot dynamics
[NASA-CR-4443] p 3239 N92-28584
Tasking and communication flows in the F/A-18D cockpit: Issues, problems, and possible solutions
[AD-A245977] p 3234 N92-28802
Methods of visual scanning with night vision goggles
[AD-A247470] p 3331 N92-28944

CODERS
Laser optical disk position encoder with active heads
[NASA-CASE-GSC-13175-1] p 3359 N92-29133

CODING
The use of conformal subdomain basis functions in the method of moments computations for a thin wire
[AD-A245964] p 3272 N92-28347
Genetic algorithms in coding theory: A table for A3 (n, d)
[MEMO-COSOR-91-22] p 3336 N92-28639
A discrete Fourier transform for virtual memory machines
[NASA-TM-103914] p 3349 N92-28672
Neuropsychological components of object identification
[AD-A247049] p 3327 N92-28877
Laser optical disk position encoder with active heads
[NASA-CASE-GSC-13175-1] p 3359 N92-29133

COEFFICIENT OF FRICTION
Evaluation of drive simulator settings for DAF YA-4440
[FEL-91-B345] p 3241 N92-28828

COEFFICIENTS
Estimation of high temperature metal-silicate partition coefficients p 3311 N92-28599
Mg-perovskite/silicate melt partition coefficients in the CMS system at 2430 C and 226 Kbars
p 3312 N92-28601

COGNITION
Neuropsychological components of object identification
[AD-A247049] p 3327 N92-28877
Integrating the affective domain into the instructional design process
[AD-A249287] p 3327 N92-28880
Learning, teaching, and testing for complex conceptual understanding
[AD-A248728] p 3328 N92-29142

COGNITIVE PSYCHOLOGY
Studies of perceptual memory
[AD-A250200] p 3328 N92-29144
Psychophysical analyses of perceptual representations
[AD-A246945] p 3329 N92-29186

COHERENT RADIATION
Tunable optical sources and synthetic nonlinear media/growth and characterization of nonlinear optical materials
[AD-A249363] p 3357 N92-28328
Theory for the CEBAF and shipboard FELS
[AD-A245979] p 3289 N92-28662

COHESION
Characterization of Martian near-subsurface materials by determination of cohesion and angle of internal friction p 3393 N92-29068

COLLECTION
Hydrogen and carbon isotopic composition of volatiles in Nakhla: Implications for weathering on Mars
p 3394 N92-29075

COLLIMATORS
Scientific investigations with the data base HEAO-1 scanning modulator collimator
[NASA-CR-190477] p 3370 N92-28680

COLLISION AVOIDANCE
Space Station: Delays in dealing with space debris may reduce safety and increase costs
[GAO/IMTEC-92-50] p 3243 N92-28406
Use of high-fidelity simulation in the development of an F/A-18 active ground collision avoidance system
p 3222 N92-28530

COLLISIONS
Space Station: Delays in dealing with space debris may reduce safety and increase costs
[GAO/IMTEC-92-50] p 3243 N92-28406

COLOR
Studies of iterated transform image compression and its application to color and DTED
[AD-A248060] p 3339 N92-28946
Physical properties of Deucalionis, Eos, Xanthe-type units in the central equatorial region of Mars
p 3392 N92-29063
Physical properties of Meridiani Sinus-type units in the central equatorial region of Mars p 3392 N92-29064
Surface photometric properties and albedo changes in the central equatorial region of Mars
p 3392 N92-29066
Single layer multi-color luminescent display and method of making
[NASA-CASE-LAR-13616-3] p 3359 N92-29158

COLOR CODING
Studies of iterated transform image compression and its application to color and DTED
[AD-A248060] p 3339 N92-28946

COLOR PHOTOGRAPHY
Temporal variability of the surface and atmosphere of Mars: Viking Orbiter color observations
p 3388 N92-29041

COLORADO PLATEAU (US)
A seismic and integrated geophysical study of the lithosphere of the Colorado Plateau
[AD-A247091] p 3308 N92-28257

COMBAT
A study of pilot attitudes regarding the impact on mission effectiveness of using new cockpit automation technologies to replace the navigator/weapon system officer/electronic warfare officer
[AD-A246683] p 3329 N92-28286
Full mission simulation for research and development of air combat flight and attack management systems
p 3223 N92-28538
Development and evaluation of an attack and maneuvering system with combat development simulators as main development tool p 3224 N92-28541
Air combat maneuvering expert system trainer
[AD-A246459] p 3241 N92-28975

COMBINATORIAL ANALYSIS
Decomposition of balanced matrices. Part 1: Introduction
[AD-A247397] p 3349 N92-28927
Decomposition of balanced matrices. Part 2: Wheel-and-parachute-free graphs
[AD-A247398] p 3350 N92-28928
Decomposition of balanced matrices. Part 6: Even wheels
[AD-A247399] p 3350 N92-28929
Decomposition of balanced matrices. Part 7: A polynomial recognition algorithm
[AD-A247400] p 3350 N92-28930
A user's manual for MASH 1.0: A Monte Carlo adjoint shielding code system
[AD-A248204] p 3355 N92-29190

COMBUSTIBLE FLOW
Advanced diagnostics for reacting flows
[AD-A247059] p 3360 N92-28296
Kinetic studies of metal combustion in propulsion
[AD-A250207] p 3256 N92-28769

COMBUSTION
A study of the normal injection of hydrogen into a heated supersonic flow using planar laser-induced fluorescence
[DE92-010701] p 3282 N92-28268
EXPLOMET 90 international conference on shock-wave and high-strain-rate phenomena in materials
[AD-A248665] p 3303 N92-28892
Underwater vapor phase burning of aluminum particles and on aluminum ignition during steam explosions
[DE92-011196] p 3257 N92-28894
Asynchronous optical sampling for laser-based combustion diagnostics in high-pressure flames
[AD-A250206] p 3257 N92-28896

COMBUSTION CHAMBERS
An analysis of combustion studies in shock expansion tunnels and reflected shock tunnels
[NASA-TP-3224] p 3255 N92-28374
Investigation of energy exchange mechanisms between the mean and acoustic flow fields in solid rocket combustion chambers
[AD-A247402] p 3250 N92-28931

COMBUSTION CHEMISTRY
An analysis of combustion studies in shock expansion tunnels and reflected shock tunnels
[NASA-TP-3224] p 3255 N92-28374
The compositional structure and the effects of exothermicity in an unpremixed planar jet flame
p 3258 N92-28821

COMBUSTION CONTROL
Studies in turbulence and turbulence control
[AD-A247164] p 3282 N92-28225
Combustion mechanisms of solids --- solid rocket propellant
[AD-A247088] p 3254 N92-28240

COMBUSTION PHYSICS
Combustion mechanisms of solids --- solid rocket propellant
[AD-A247088] p 3254 N92-28240
An analysis of combustion studies in shock expansion tunnels and reflected shock tunnels
[NASA-TP-3224] p 3255 N92-28374
Stochastic simulation of the structure and propagation rate of turbulent premixed flames
[DE92-006682] p 3256 N92-28822
COMBUSTION PRODUCTS
Degenerate four-wave mixing using a tunable excimer laser to detect combustion gases
[DE92-005327] p 3290 N92-28852
COMBUSTION STABILITY
Investigation of energy exchange mechanisms between the mean and acoustic flow fields in solid rocket combustion chambers
[AD-A247402] p 3250 N92-28931
COMETS
How Mars lost its atmosphere p 3378 N92-28509
COMMAND AND CONTROL
Scientific applications of frequency-stabilized laser technology in space
[NASA-CR-190449] p 3291 N92-28941
COMMERCIAL AIRCRAFT
Generation of spectra and stress histories for fatigue and damage tolerance analysis of fuselage repairs
[AD-A250390] p 3235 N92-29180
FAA aviation forecasts
[AD-A250412] p 3230 N92-29182
COMMUNICATION
Information Resources Management long-range plan
[DE92-012408] p 3368 N92-28804
COMMUNICATION EQUIPMENT
Design on an enhanced interactive satellite communications system analysis program
[AD-A245967] p 3273 N92-28410
COMMUNICATION NETWORKS
Design on an enhanced interactive satellite communications system analysis program
[AD-A245967] p 3273 N92-28410
Consulting report on the NASA technology utilization network system
[NASA-CR-190367] p 3370 N92-29108
Analysis and optimization of low-earth-orbit communication links
[DE92-013393] p 3277 N92-29131
COMMUNICATION SATELLITES
Mass and power modeling of communication satellites
[NASA-CR-189186] p 3275 N92-28906
COMPARISON
Comparison of LDA and LTA applications for propeller tests in wind tunnels
[NLR-MP-88031-U] p 3226 N92-28658
COMPILERS
The silicon compiler for designing military VLSI ASIC's p 3235 N92-28378
Development of a high-performance FORTRAN compiler for porting CFD codes to the Navier-Stokes computer
[AD-A250208] p 3342 N92-28770
Compilation and operation environment of an object based language
[ETN-92-91323] p 3338 N92-28785
Crystallizing FORTRAN
[AD-A250162] p 3343 N92-28915
COMPLETENESS
Generalized quantifiers and modal logic
[ITLI-LP-91-01] p 3348 N92-29214
COMPLEX COMPOUNDS
Synthesis and study of metallonitride complexes and polymers
[AD-A248577] p 3262 N92-28323
COMPLEX SYSTEMS
Validation of knowledge based systems
[AD-A247741] p 3368 N92-28404
COMPLEX VARIABLES
Programming of the complex logarithm function in the solution of the cracked anisotropic plate loaded by a point force
[LR-657] p 3299 N92-28575
COMPONENT RELIABILITY
A sensitivity analysis on component reliability from fatigue life computations
[AD-A247430] p 3297 N92-28425
Component performance requirements p 3237 N92-28462
Turbine aircraft engine operational trending and JT8D static component reliability study
[DOT/FAA/CT-91/10] p 3238 N92-28686
COMPOSITE MATERIALS
Method fabricating load-bearing composites free from microbuckling deformation up to a predetermined load
[AD-D015212] p 3250 N92-28224
Quantitative interphase study of composite materials. Interphase engineering: A scientific way of tailoring the mechanophysical properties of composite materials
[AD-A247776] p 3251 N92-28252
Micromechanics of defects
[AD-A248432] p 3251 N92-28307
Sol-gel processed multifunctional organic polymer-inorganic oxide composites for electronics and photonics
[AD-A246773] p 3263 N92-28412
Structural optimization of aircraft p 3232 N92-28472
Mathematical optimization: A powerful tool for aircraft design p 3232 N92-28474
Simple computer programs for the design and sizing of fiber reinforced composites
[NLR-TP-91050-U] p 3252 N92-28637
The use of load enhancement factors in the certification of composite aircraft structures
[NLR-TP-90068-U] p 3232 N92-28649
National Conference on the Use of Composite Materials in Load-Bearing Marine Structures. Volume 1: Summary report
[PB92-163831] p 3252 N92-28724
National Conference on the Use of Composite Materials in Load-Bearing Marine Structures. Volume 2: Conference proceedings
[PB92-163849] p 3252 N92-28725
COMPOSITE STRUCTURES
Coupled structural/thermal/electromagnetic analysis/tailoring of graded composite structures
[NASA-CR-189153] p 3298 N92-28296
X ray diffraction study of residual stresses in metal matrix composite-jacketed steel cylinders subjected to internal pressure
[AD-A248449] p 3251 N92-28416
National Conference on the Use of Composite Materials in Load-Bearing Marine Structures. Volume 1: Summary report
[PB92-163831] p 3252 N92-28724
National Conference on the Use of Composite Materials in Load-Bearing Marine Structures. Volume 2: Conference proceedings
[PB92-163849] p 3252 N92-28725
Experimental determination of dissipated energy density as a measure of strain-induced damage in composites
[AD-A250322] p 3253 N92-28953
Development of a stratified plate model for composite panels
[AD-A248206] p 3253 N92-29192
On the use of structural dynamic experimental methods for damage inspection of a glass fibre reinforced plastic plate
[FFA-TN-1992-02] p 3253 N92-29220
COMPOSITION (PROPERTY)
The compositional structure and the effects of exothermicity in an unpremixed planar jet flame p 3258 N92-28821
The stable isotopic compositions of indigenous carbon-bearing components in EETA 79001 p 3384 N92-29021
COMPRESSIBILITY
Natural flow wing
[NASA-CASE-LAR-14281-1] p 3228 N92-28729
Turbulent spot generation and growth rates in a transonic boundary layer
[AD-A250221] p 3287 N92-29118
COMPRESSIBLE BOUNDARY LAYER
Turbulent spot generation and growth rates in a transonic boundary layer
[AD-A250221] p 3287 N92-29118
COMPRESSIBLE FLOW
Control of nonlinear distributed parameter systems with application to flow control
[AD-A250212] p 3346 N92-29149
COMPRESSION LOADS
Method fabricating load-bearing composites free from microbuckling deformation up to a predetermined load
[AD-D015212] p 3250 N92-28224
Fluids at high shock pressures and temperatures
[DE92-010709] p 3283 N92-28269
Natural flow wing
[NASA-CASE-LAR-14281-1] p 3228 N92-28729
COMPRESSIVE STRENGTH
The compressive properties of GLARE
[LR-666] p 3252 N92-28582
COMPRESSOR EFFICIENCY
Steady and transient performance calculation method for prediction, analysis, and identification p 3237 N92-28461
COMPRESSORS
Calculation of installation effects within performance computer programs p 3237 N92-28465
COMPTON EFFECT
Resonant Compton scattering in models of gamma ray burst sources
[DE92-010720] p 3397 N92-28336
COMPUTATION
A uniform approach to the semantics of concurrency
[AD-A246697] p 3334 N92-28289
A center of excellence in the mathematical sciences
[AD-A249365] p 3346 N92-28329
The use of conformal subdomain basis functions in the method of moments computations for a thin wire
[AD-A245964] p 3272 N92-28347
Constrained spanload optimization for minimum drag of multi-lifting-surface configurations
[NLR-TP-89126-U] p 3227 N92-28660
Overview of two common statistical computer packages: SAS and BMDP
[AD-A245982] p 3368 N92-28663
Center for the integration of optical computing
[AD-A250306] p 3337 N92-28719
Computations of detonation structure: The influence of model input parameters
[AD-A248634] p 3285 N92-28803
COMPUTATIONAL CHEMISTRY
High quality Gaussian basis sets for fourth-row atoms
[NASA-TM-103918] p 3255 N92-28743
COMPUTATIONAL FLUID DYNAMICS
A numerical wind tunnel study of viscous-inviscid interaction
[AD-A248429] p 3283 N92-28350
Viscous effects on a vortex wake in ground effect
[NASA-CR-190400] p 3283 N92-28361
Rocket plume flowfield characterization using laser Rayleigh scattering
[NASA-TM-105739] p 3357 N92-28475
Computation of steady and unsteady quasi-one-dimensional viscous/inviscid interacting internal flows at subsonic, transonic, and supersonic Mach numbers
[NASA-CR-189881] p 3283 N92-28555
Analysis of results of an Euler-equation method applied to leading-edge vortex flow
[NLR-TP-90368-U] p 3226 N92-28657
Calculation of unsteady subsonic and supersonic flow about oscillating wings and bodies by new panel methods
[NLR-TP-89119-U] p 3227 N92-28659
Turbulence modeling: Survey of activities in Belgium and the Netherlands, and appraisal of the status and a view on the prospects
[NLR-TP-90184-U] p 3284 N92-28694
Boundary conditions for Euler equations at internal block faces of multi-block domains using local grid refinement
[NLR-TP-90134-U] p 3284 N92-28712
Development of a high-performance FORTRAN compiler for porting CFD codes to the Navier-Stokes computer
[AD-A250208] p 3342 N92-28770
Explicit Navier-Stokes computation of turbomachinery flows
[AD-A249284] p 3286 N92-28879
Investigation of energy exchange mechanisms between the mean and acoustic flow fields in solid rocket combustion chambers
[AD-A247402] p 3250 N92-28931
Mapping unstructured grid computations to massively parallel computers
[NASA-CR-190551] p 3343 N92-29109
COMPUTATIONAL GRIDS
Wave drag determination in the transonic full-potential flow code MATRICS
[NLR-TP-90062-U] p 3228 N92-28709
Boundary conditions for Euler equations at internal block faces of multi-block domains using local grid refinement
[NLR-TP-90134-U] p 3284 N92-28712
A comparative study of the accuracy of various time domain nonorthogonal mesh methods
[DE92-007300] p 3347 N92-28824
Mapping unstructured grid computations to massively parallel computers
[NASA-CR-190551] p 3343 N92-29109
COMPUTER AIDED DESIGN
Object-oriented programming: An assessment of fundamental concepts and design considerations
[AD-A247480] p 3333 N92-28243
Applications of ASICs to avionics
[AGARD-AG-329] p 3235 N92-28376
What is an ASIC? p 3235 N92-28377
Integrated Design Analysis and Optimisation of Aircraft Structures
[AGARD-LS-186] p 3231 N92-28469
Fundamentals of structural optimisation p 3231 N92-28470
The evaluation of simulator effectiveness for the training of high speed, low level, tactical flight operations p 3223 N92-28539

Software development using a method base system
[NLR-TP-90387-U] p 3336 N92-28636
Constrained spanload optimization for minimum drag of multi-lifting-surface configurations
[NLR-TP-89126-U] p 3227 N92-28660
SPECTOOL: A computer-aided verification tool for hardware designs, volume 1
[AD-A247492] p 3336 N92-28666
SPECTOOL: User's manual, volume 2
[AD-A247493] p 3336 N92-28667
NASA Lewis steady-state heat pipe code users manual
[NASA-TM-105161] p 3249 N92-28682
Three dimensional measurements of prismatic bodies: Programming by means of a CAD system
[CRIF-MC-91] p 3337 N92-28700
Knowledge-based material selection in design
[PNR-90823] p 3337 N92-28741
Present status of computational tools for Maglev development
[DE92-013252] p 3294 N92-28815
Stretch and hammer neural networks for N-dimensional data generalization
[AD-A247941] p 3346 N92-29082

COMPUTER AIDED MANUFACTURING

Lessons from Archimedes, a system for planning and executing mechanical assemblies
[DE92-010957] p 3335 N92-28342
Automated apparel specification retrieval system
[AD-A248619] p 3367 N92-28389
Three dimensional measurements of prismatic bodies: Programming by means of a CAD system
[CRIF-MC-91] p 3337 N92-28700
Stretch and hammer neural networks for N-dimensional data generalization
[AD-A247941] p 3346 N92-29082
Contribution to the design of flexible manufacturing systems: Application of the formal description technique Estelle
[LAAS-91378] p 3341 N92-29209

COMPUTER AIDED TOMOGRAPHY

X ray computed tomography of full-scale castings
[AD-A247101] p 3258 N92-28241

COMPUTER ASSISTED INSTRUCTION

Integrating the affective domain into the instructional design process
[AD-A249287] p 3327 N92-28880
Design specifications for the Advanced Instructional Design Advisor (AIDA), volume 1
[AD-A248201] p 3340 N92-29187
Design specifications for the Advanced Instructional Design Advisor (AIDA), volume 2
[AD-A248202] p 3340 N92-29188

COMPUTER COMPONENTS

SPECTOOL: User's manual, volume 2
[AD-A247493] p 3336 N92-28667

COMPUTER GRAPHICS

HeNCE: Graphical development tools for network-based concurrent computing
[DE92-011061] p 3341 N92-28279
An application of interactive computer graphics to the study of inferential statistics and the general linear model
[AD-A246668] p 3334 N92-28285
Automated apparel specification retrieval system
[AD-A248619] p 3367 N92-28389
PC graphics generation and management tool for real-time applications
[NASA-TM-105749] p 3337 N92-28684

COMPUTER INFORMATION SECURITY

The Father Christmas worm
[NASA-TM-107938] p 3334 N92-28267

COMPUTER NETWORKS

HeNCE: Graphical development tools for network-based concurrent computing
[DE92-011061] p 3341 N92-28279
Audit trails and PC control on Novell networks
[DE92-010695] p 3335 N92-28332
Flexible integrated architecture for neural networks
[ETN-92-91320] p 3343 N92-28782
Consulting report on the NASA technology utilization network system
[NASA-CR-190387] p 3370 N92-29108
Analysis and optimization of low-earth-orbit communication links
[DE92-013393] p 3277 N92-29131

COMPUTER PROGRAM INTEGRITY

Some aerospace applications of estimation theory
[ETN-92-91281] p 3349 N92-28647

COMPUTER PROGRAMMING

SISAL: Toward resolving the parallel programming crisis
[DE92-010716] p 3342 N92-28334
An ELROS primer
[DE92-010661] p 3342 N92-28381
An experimental investigation of the effects of software size increase on software project management behavior
[AD-A248362] p 3335 N92-28385
DEPEND: A simulation-based environment for system level dependability analysis
[NASA-CR-189752] p 3297 N92-28726
SPEEDS: An approach to support programming environments using expert database systems
[AD-A247469] p 3339 N92-28943
HYPER: A domain decomposition program, version 1.0 (user's manual)
[AD-A250018] p 3340 N92-29172
Building the Scientific Modeling Assistant: An interactive environment for specialized software design
[NASA-TM-107844] p 3346 N92-29175
Development of a flight information system using the structured method
[AD-A248207] p 3236 N92-29222

COMPUTER PROGRAMS

PROPX: An x ray manipulation program
[DE92-011264] p 3334 N92-28309
On-line point positioning with single frame camera data
[AD-A248307] p 3287 N92-28322
A comparison of results from an edge-plasma model with those from a two-dimensional fluid code
[DE92-010718] p 3360 N92-28335
Selective suppression of photochemical etching: Raman spectroscopy for pre-etch process selection
[DE92-010955] p 3255 N92-28341
An experimental investigation of the effects of software size increase on software project management behavior
[AD-A248362] p 3335 N92-28385
Design on an enhanced interactive satellite communications system analysis program
[AD-A245967] p 3273 N92-28410
Calculation of installation effects within performance computer programs p 3237 N92-28465
Full mission simulation for research and development of air combat flight and attack management systems p 3223 N92-28538
Use of a virtual cockpit for the development of a future transport aircraft p 3225 N92-28547
Simple computer programs for the design and sizing of fiber reinforced composites
[NLR-TP-91050-U] p 3252 N92-28637
Calculation of unsteady subsonic and supersonic flow about oscillating wings and bodies by new panel methods
[NLR-TP-89119-U] p 3227 N92-28659
Constrained spanload optimization for minimum drag of multi-lifting-surface configurations
[NLR-TP-89126-U] p 3227 N92-28660
Overview of two common statistical computer packages: SAS and BMDP
[AD-A245982] p 3368 N92-28663
Ground Systems Development Environment (GSDE) software configuration management
[NASA-CR-190503] p 3337 N92-28710
Present status of computational tools for Maglev development
[DE92-013252] p 3294 N92-28815
Verification of satellite EGSE test-software using an application generator
[ITN-92-85131] p 3244 N92-29098
Acquisition and improvement of human motor skills: Learning through observation and practice
[NASA-TM-107878] p 3329 N92-29174
Building the Scientific Modeling Assistant: An interactive environment for specialized software design
[NASA-TM-107844] p 3346 N92-29175
A user's manual for MASH 1.0: A Monte Carlo adjoint shielding code system
[AD-A248204] p 3355 N92-29190
Development of a stratified plate model for composite panels
[AD-A248206] p 3253 N92-29192

COMPUTER STORAGE DEVICES

On-line point positioning with single frame camera data
[AD-A248307] p 3287 N92-28322
The use of conformal subdomain basis functions in the method of moments computations for a thin wire
[AD-A245964] p 3272 N92-28347
Kanerva's sparse distributed memory with multiple hamming thresholds
[NASA-CR-190552] p 3339 N92-28875
Disk memory device
[NASA-CASE-GSC-13196-1] p 3333 N92-29132

COMPUTER SYSTEMS DESIGN

DEPEND: A simulation-based environment for system level dependability analysis
[NASA-CR-189752] p 3297 N92-28726

COMPUTER SYSTEMS PERFORMANCE

Superconducting at NLR: NEC SX-2 capabilities in NLR's terminal and file-transfer network
[NLR-TP-89007-U] p 3342 N92-28706

COMPUTER SYSTEMS SIMULATION

Femtosecond carrier processes in compound semiconductors and real time signal processing
[AD-A248053] p 3278 N92-28275
An OTH radar clutter simulation
[AD-A248054] p 3272 N92-28304
The 2.0 GHz sampling rate transversal filter
[AD-A250244] p 3358 N92-28968

COMPUTER TECHNIQUES

HeNCE: Graphical development tools for network-based concurrent computing
[DE92-011061] p 3341 N92-28279
Computer assisted improvement of the estimation mean squared error with application to back propagation neural networks
[AD-A247724] p 3344 N92-28401
Fault-tolerant parallel computer systems for real-time applications
[AD-A247887] p 3343 N92-28958
Computer derivation of green's functions for structural dynamic analysis
[AD-A250249] p 3339 N92-28969
Computer recognition and analysis of photogrammetric targets
[AD-A250313] p 3339 N92-28971
Stretch and hammer neural networks for N-dimensional data generalization
[AD-A247941] p 3346 N92-29082
Development of a flight information system using the structured method
[AD-A248207] p 3236 N92-29222

COMPUTER VIRUSES

The Father Christmas worm
[NASA-TM-107938] p 3334 N92-28267

COMPUTER VISION

A theory of automated design of visual information presentations
[AD-A247425] p 3369 N92-28866
A rotorcraft flight database for validation of vision-based ranging algorithms
[NASA-TM-103906] p 3231 N92-29103
Method and apparatus for predicting the direction of movement in machine vision
[NASA-CASE-NPO-17552-1-CU] p 3331 N92-29129

COMPUTERIZED SIMULATION

A coilgun design primer
[DE92-011149] p 3244 N92-28226
Accelerator simulation using computers
[DE92-010729] p 3356 N92-28270
A diode laser pumped Nd:YAG laser
[FFI-91/7020] p 3289 N92-28315
Parameterization of convective clouds, mesoscale convective systems, and convective-generated cirrus
[DE92-010951] p 3318 N92-28340
Multiple-valued programmable logic array minimization by simulated annealing
[AD-A248620] p 3335 N92-28353
Prediction of attitude stability of asymmetric dual-spin stabilized spacecraft using improved liquid slosh model
[AD-A247023] p 3246 N92-28368
An experimental investigation of the effects of software size increase on software project management behavior
[AD-A248362] p 3335 N92-28385
Dynamic simulation of compressor and gas turbine performance p 3237 N92-28463
Aircraft ship operations
[AGARD-AR-312] p 3231 N92-28468
Simulation of atmospheric frontogenesis with a semi-Lagrangian numerical model
[AD-A247151] p 3318 N92-28517
Interest in real-time simulations for the development terrain following function of radar systems p 3222 N92-28529
Dynamics motion simulation of the Hermes robot arm subjected to constraints
[NLR-TP-90282-U] p 3293 N92-28645
Linear recursive formulation of flexible multi-body space system dynamics
[NLR-TP-90284-U] p 3293 N92-28646
S-76B certification for vertical take-off and landing operations from confined areas
[NLR-TP-90286-U] p 3233 N92-28714
DEPEND: A simulation-based environment for system level dependability analysis
[NASA-CR-189752] p 3297 N92-28726
Crew station research and development facility training for the light helicopter demonstration/validation program
[NASA-TM-103865] p 3327 N92-28744
MoCog1: A computer simulation of recognition-primed human decision making, considering emotions
[NASA-TM-107859] p 3337 N92-28758

Large Eddy Simulations (LES) and Direct Numerical Simulations (DNS) for the computational analyses of high speed reacting flows
[NASA-CR-190364] p 3285 N92-28817
Large eddy simulations and direct numerical simulations of high speed turbulent reacting flows
p 3285 N92-28818
Quaternion and Euler angles in kinematics
[NAL-TM-636] p 3303 N92-28836
Simulating radar propagation through atmospheric turbulence using the Tropospheric ElectroMagnetic Parabolic Equation Routine (TEMPER)
[AD-A247406] p 3275 N92-28905
Martian surface simulations p 3383 N92-29016
Method and apparatus for predicting the direction of movement in machine vision
[NASA-CASE-NPO-17552-1-CU] p 3331 N92-29129
Modular simulation of HEI fragments and blast pressure
[AD-A248205] p 3272 N92-29191
On some splitting schemes for wave equations
[FFI-91/7023] p 3348 N92-29193

COMPUTERS
Use of a virtual cockpit for the development of a future transport aircraft p 3225 N92-28547
A discrete Fourier transform for virtual memory machines
[NASA-TM-103914] p 3349 N92-28672
A survey of high density packaging for high performance computing system
[AD-A248633] p 3332 N92-28891
Recent advances in global optimization
[AD-A250211] p 3308 N92-29173

CONCRETES
Use of scrap rubber in asphalt pavement surfaces
[AD-A247419] p 3272 N92-28902

CONCURRENT PROCESSING
A uniform approach to the semantics of concurrency
[AD-A246697] p 3334 N92-28289
Vienna FORTRAN: A language specification, version 1.1
[NASA-CR-189629] p 3337 N92-28760
Asynchronous bidirectional network interface enabling seamless concurrent processing in a distributed heterogeneous multiprocessor system
[AD-D015274] p 3343 N92-29096

CONDENSATION
Influences of CO2 sublimation/condensation processes on the long-term evolution of the Martian atmosphere
p 3375 N92-28496

CONDUCTING POLYMERS
Ion conductive polymer solid electrolytes
[DE92-010518] p 3266 N92-29195

CONDUCTIVE HEAT TRANSFER
The nonequilibrium molecular dynamics
[DE92-011760] p 3355 N92-28860
Modeling the seasonal cycle of CO2 on Mars: A fit to the Viking lander pressure curves p 3394 N92-29076
Coupling device with improved thermal interface
[NASA-CASE-GSC-13251-1] p 3295 N92-29120

CONDUCTIVITY
Molecular dynamics calculations of optical nonlinear properties of materials
[AD-A247095] p 3354 N92-28260

CONDUCTORS
Synthesis and characterization of new low-dimensional transition metal complex conductors
[AD-A249263] p 3258 N92-28237
The effect of induced charges on low-energy particle trajectories near conducting and semiconducting plates
[NASA-TM-103589] p 3355 N92-28986

CONFERENCES
Proceedings of Asilomar Conference on Polymeric Materials
[AD-A249366] p 3262 N92-28360
International Workshop on Vibration Isolation Technology for Microgravity Science Applications
[NASA-CP-10094] p 3268 N92-28436
Types and Characteristics of Data for Geomagnetic Field Modeling
[NASA-CP-3153] p 3299 N92-28620
Turbine aircraft engine operational trending and JT8D static component reliability study
[DOT/FAA/CT-91/10] p 3238 N92-28686
Joint DOE/NSF workshop on flow of particulates and fluids
[DE92-012692] p 3285 N92-28808
EXPLOMET 90 international conference on shock-wave and high-strain-rate phenomena in materials
[AD-A248665] p 3303 N92-28892
Recent advances in global optimization
[AD-A250211] p 3308 N92-29173

CONFIGURATION MANAGEMENT
Software development using a method base system
[NLR-TP-90387-U] p 3336 N92-28636
Ground Systems Development Environment (GSDE) software configuration management
[NASA-CR-190503] p 3337 N92-28710

CONFINEMENT
Improved confinement and edge plasma fluctuations in the STOR-M tokamak
[PPL-126] p 3361 N92-28848
Simulations of solvent effects on confined electrolytes
[AD-A246851] p 3258 N92-28982

CONICAL FLOW
Natural flow wing
[NASA-CASE-LAR-14281-1] p 3228 N92-28729

CONJUGATE GRADIENT METHOD
Scattering and radiation analysis of three-dimensional cavity arrays via a hybrid finite element method
[NASA-CR-190408] p 3273 N92-28371
A look-ahead variant of the Lanczos algorithm and its application to the quasi-minimal residual method for non-Hermitian linear systems
[NASA-CR-190557] p 3340 N92-29113

CONNECTORS
Connection space reduction mechanism
[NASA-CASE-GSC-13220-1] p 3296 N92-29140

CONSOLIDATION
Effect of solidification technique and consolidation method on the properties of rapidly solidified Al-Fe alloys
[DLR-FB-91-24] p 3260 N92-28823

CONSTANTS
The evaluation of rate constants for rapid electrode reactions by using microelectrode voltammetry: Virtues of measurement at lower temperature
[AD-A246760] p 3255 N92-28391

CONSTRAINTS
Analysis of constrained-layer damping of flexural and extensional waves in infinite, fluid-loaded plates
[AD-A247936] p 3304 N92-29081

CONSTRUCTION
Software design for automated assembly of truss structures
[NASA-TP-3198] p 3344 N92-28375

CONSTRUCTION MATERIALS
Replacement of the NAL high pressure air storage system
[NAL-TM-634] p 3241 N92-28835

CONTINENTAL SHELVES
A new ocean bottom magnetometer system for continental shelf measurements
[AD-A247644] p 3321 N92-28321

CONTINUOUS WAVE LASERS
A diode laser pumped Nd:YAG laser
[FFI-91/7020] p 3289 N92-28315

CONTINUOUS WAVE RADAR
Mars: Wavelength-dependent dual polarization global scattering p 3384 N92-29020
Performance of the multifunctional CW CO2-laser radar at the TNO-FEL laboratory and during the BEST TWO field test
[FEL-91-A163] p 3291 N92-29160

CONTRACT MANAGEMENT
A review of cost performance index stability
[AD-A246821] p 3370 N92-28255

CONTRACTORS
A review of cost performance index stability
[AD-A246821] p 3370 N92-28255
Maintaining the program balance, volumes 1 and 2
[NASA-CR-190269] p 3367 N92-29111

CONTROL EQUIPMENT
A survey report for the design of biped locomotion robot: The WL-12 (Waseda Leg-12)
[DE92-782046] p 3292 N92-28233
Rotorcraft In-Flight Simulation Research at NASA Ames Research Center: A Review of the 1980's and plans for the 1990's
[NASA-TM-103873] p 3234 N92-28926
Control of nonlinear distributed parameter systems with application to flow control
[AD-A250212] p 3346 N92-29149
User friendly joystick
[NASA-CASE-GSC-13187-1] p 3281 N92-29153

CONTROL SIMULATION
Utility of ground simulation in flight control problem identification, solution development, and verification
p 3221 N92-28525
Use of high-fidelity simulation in the development of an F/A-18 active ground collision avoidance system
p 3222 N92-28530

CONTROL STICKS
User friendly joystick
[NASA-CASE-GSC-13187-1] p 3281 N92-29153

CONTROL SYSTEMS DESIGN
Digital control algorithms for microgravity isolation systems p 3267 N92-28445
Extended H2 synthesis for microgravity vibration isolation p 3267 N92-28447
Overview on basis and use of performance prediction methods p 3237 N92-28459
Anthropomorphic teleoperation: Controlling remote manipulators with the DataGlove
[NASA-TM-103588] p 3330 N92-28521
Use of a research simulator for the development of new concepts of flight control p 3224 N92-28543
A study of the control problem of the shoot side environment delivery system of a closed crop growth research chamber
[NASA-CR-177597] p 3330 N92-28681
Ongoing Progress in Spacecraft Controls
[NASA-CP-10099] p 3247 N92-28730
Sensor filter designs for large flexible spacecraft
p 3247 N92-28733
Learning and tuning fuzzy logic controllers through reinforcements
[NASA-TM-107875] p 3345 N92-28759
Electromechanical systems with transient high power response operating from a resonant AC link
[NASA-TM-105716] p 3238 N92-28985
Contribution to the design of flexible manufacturing systems: Application of the formal description technique Estelle
[LAAS-91378] p 3341 N92-29209

CONTROL THEORY
Adaptive and nonlinear control
[AD-A248580] p 3344 N92-28429
Use of high-fidelity simulation in the development of an F/A-18 active ground collision avoidance system
p 3222 N92-28530
Application of piloted simulation to high-angle-of-attack flight-dynamics research for fighter aircraft
p 3225 N92-28551
Inverse control problems: Mathematical preliminaries, system theoretical approaches, and their applications to aircraft dynamics
[LR-665] p 3345 N92-28581
Stability and optimal control theory of hereditary systems with applications from oscillating flying vehicles, mechanical systems, and robotics p 3247 N92-28732
Sensor filter designs for large flexible spacecraft
p 3247 N92-28733
Initial investigations of an adaptive discrete-time controller for nonlinear time-varying robotic models
p 3247 N92-28736
Fuzzy logic controller for manipulator systems: Preliminary results p 3247 N92-28738
Control of nonlinear distributed parameter systems with application to flow control
[AD-A250212] p 3346 N92-29149

CONTROL UNITS (COMPUTERS)
Instrumentation for ultrahigh strain rate experiments
[AD-A249358] p 3298 N92-28327

CONTROLLABILITY
The use of ground based simulation for handling qualities research: A new assessment p 3224 N92-28545
Initial validation of a R/D simulator with large amplitude motion p 3225 N92-28546
Application of piloted simulation to high-angle-of-attack flight-dynamics research for fighter aircraft
p 3225 N92-28551
Effects of cockpit lateral stick characteristics on handling qualities and pilot dynamics
[NASA-CR-4443] p 3239 N92-28584

CONTROLLERS
International Workshop on Vibration Isolation Technology for Microgravity Science Applications
[NASA-CP-10094] p 3268 N92-28436
Digital control algorithms for microgravity isolation systems p 3267 N92-28445
Extended H2 synthesis for microgravity vibration isolation p 3267 N92-28447
Taguchi methods in electronics: A case study
[NASA-TM-103586] p 3279 N92-28456
Comparison of three controllers applied to helicopter vibration
[NASA-TM-102192] p 3239 N92-28457
Initial investigations of an adaptive discrete-time controller for nonlinear time-varying robotic models
p 3247 N92-28736
Fuzzy logic controller for manipulator systems: Preliminary results p 3247 N92-28738
Closed-loop autonomous docking system
[NASA-CASE-MFS-28421-1] p 3248 N92-28750
Learning and tuning fuzzy logic controllers through reinforcements
[NASA-TM-107875] p 3345 N92-28759
Method for advanced material characterization by laser induced eddy current imaging
[NASA-CASE-GSC-13386-1] p 3298 N92-29154

CONVECTION
Parameterization of convective clouds, mesoscale convective systems, and convective-generated cirrus
[DE92-010951] p 3318 N92-28340

Mesoscale vertical structure of an explosive oceanic cyclone
[AD-A245927] p 3318 N92-28423
Numerical studies of convective transport associated with crystal growth in mirrogravity p 3267 N92-28437
Evolution of a terrestrial magma ocean: Thermodynamics, kinetics, rheology, convection, differentiation p 3314 N92-28611
The three stages of magma ocean cooling p 3315 N92-28617
Bifurcations and patterns in nonlinear dissipative systems
[DE92-013502] p 3364 N92-28806
Development of an advanced representation of cumulus convection
[DE92-011031] p 3319 N92-28830

CONVECTION CLOUDS
Parameterization of convective clouds, mesoscale convective systems, and convective-generated cirrus
[DE92-010951] p 3318 N92-28340

CONVECTIVE FLOW
Mapping closures for turbulent mixing and reaction
[AD-A247305] p 3283 N92-28274

CONVECTIVE HEAT TRANSFER
The role of hard turbulent thermal convection in the Earth's early thermal evolution p 3310 N92-28593
Mesoscale surface analysis of the ERICA IOP-5 cyclone
[AD-A245946] p 3319 N92-28884

CONVERGENCE
A look-ahead variant of the Lanczos algorithm and its application to the quasi-minimal residual method for non-Hermitian linear systems
[NASA-CR-190557] p 3340 N92-29113
Maximizing the convergence rate of the EM algorithm for the multiple broad-band signal estimation and detection
[AD-A248230] p 3341 N92-29224

COOLERS
NASA Lewis Stirling SPRE testing and analysis with reduced number of cooler tubes
[NASA-TM-105767] p 3307 N92-28837
Ultra-high temperature stability Joule-Thomson cooler with capability to accomodate pressure variations
[NASA-CASE-NPO-18184-1-CU] p 3288 N92-29156

COOLING
Modelling of heat and moisture loss through NBC ensembles
[AD-A245939] p 3329 N92-28346
Multiple-valued programmable logic array minimization by simulated annealing
[AD-A248620] p 3335 N92-28353
Calculation of chip temperatures using ELLPACK
[AD-A247156] p 3335 N92-28519
Magma ocean: Mechanisms of formation p 3312 N92-28600
Fate of a perched crystal layer in a magma ocean p 3312 N92-28602
Cooling of the magma ocean due to accretional disruption of the surface insulating layer p 3314 N92-28608
Early planetary differentiation: Geophysical consequences p 3314 N92-28609

COORDINATES
Quaternion and Euler angles in kinematics
[NAL-TM-636] p 3303 N92-28836
Coordinate systems for space and geophysical applications
[AD-A247550] p 3244 N92-28937

COPPER
Volatile CVD precursors based on copper alkoxides and mixed group IIA-Copper alkoxides --- chemical vapor deposition
[AD-D015264] p 3261 N92-29170

COPPER OXIDES
Electrodeposition of high temperature superconductors
[AD-A250171] p 3365 N92-28919
Stanford Center for research on superconductivity and superconductive electronics
[AD-A250204] p 3281 N92-29147

CORIOLIS EFFECT
Simulations of surface winds at the Viking Lander sites using a one-level model p 3380 N92-28998

CORRECTION
Injection: On-axis/off-axis
[NIKHEF-K/AMPS/91-07] p 3356 N92-28308
Crosstalk correction scheme
[AD-D015251] p 3276 N92-29085

CORRELATION
Origin of the moon and lunar core formation p 3311 N92-28596
Thermally distinct ejecta blankets from Martian craters p 3379 N92-28994

CORRELATION DETECTION
Angular momentum: Can be used in ballistic tracking
[AD-A247722] p 3350 N92-28400

CORROSION TESTS
Outdoor corrosion testing of aluminium-lithium alloys
[NLR-TP-90272-U] p 3260 N92-28794

COSMOLOGY
Quark matter and cosmology
[DE92-011736] p 3371 N92-28859

COST ANALYSIS
A cost-benefit analysis on the deletion of the inertial upper stage factory acceptance testing versus a decrease in mission reliability
[AD-A246620] p 3245 N92-28254
A review of cost performance index stability
[AD-A246621] p 3370 N92-28255
Life cycle costs of the C-130 electrical power system upgrade
[AD-A246759] p 3221 N92-28348
Trade study of three oxygen processors for the Martian atmosphere
[AD-A246854] p 3372 N92-28393

COST EFFECTIVENESS
X ray computed tomography of full-scale castings
[AD-A247101] p 3258 N92-28241
A review of cost performance index stability
[AD-A246621] p 3370 N92-28255
Life cycle costs of the C-130 electrical power system upgrade
[AD-A246759] p 3221 N92-28348

COST ESTIMATES
A review of cost performance index stability
[AD-A246621] p 3370 N92-28255
Evaluation of future space transportation systems with regard to their reliabilities and costs
[DLR-FB-91-27] p 3245 N92-28826

COSTS
Space Station: Delays in dealing with space debris may reduce safety and increase costs
[GAO/IMTEC-92-50] p 3243 N92-28406

COULOMB COLLISIONS
Simulations of solvent effects on confined electrolytes
[AD-A246851] p 3258 N92-28982

COULOMB POTENTIAL
Scattering mechanisms for semiconductor transport calculations
[AD-A249260] p 3278 N92-28295

COUPLING COEFFICIENTS
A coupled regional tide model
[AD-A247917] p 3322 N92-28913

COUPLINGS
Coupling device with improved thermal interface
[NASA-CASE-GSC-13251-1] p 3295 N92-29120
Connection space reduction mechanism
[NASA-CASE-GSC-13220-1] p 3296 N92-29140

CRAB NEBULA
Calibration of high energy x ray detectors at the spectrum of the Crab nebula, and x ray pulsar A0535+26 examinations
[ETN-92-91484] p 3371 N92-29177

CRACK PROPAGATION
Study of high temperature failure mechanism in ceramics
[AD-A247018] p 3263 N92-28415
The mechanical property data base from an Air Force/industry cooperative test program on advanced aluminum alloys (IN905XL and AL905XL forgings)
[AD-A247752] p 3368 N92-28565
The effect of intermediate heat treatments on overload induced retardation during the fatigue crack growth in an Al-alloy
[LR-651] p 3259 N92-28574
Growth of surface cracks under fatigue loading: A literature survey
[LR-664] p 3299 N92-28580
Crack resistance, fracture toughness and instability in damage tolerant Al-Li alloys
[NLR-TP-90172-U] p 3303 N92-28850
Stress analysis of plated-through-holes in rigid flex multilayer printed wiring boards
[DE92-011659] p 3303 N92-28855
Tensile and interlaminar properties of GLARE (trade name) laminates
[AD-A250188] p 3253 N92-28921
Generation of spectra and stress histories for fatigue and damage tolerance analysis of fuselage repairs
[AD-A250390] p 3235 N92-29180

CRACKING (FRACTURING)
Experimental determination of dissipated energy density as a measure of strain-induced damage in composites
[AD-A250322] p 3253 N92-28953

CRACKS
Micromechanics of defects
[AD-A248432] p 3251 N92-28307
Programming of the complex logarithm function in the solution of the cracked anisotropic plate loaded by a point force
[LR-657] p 3299 N92-28575
Pre-test analyses for pressurized thermoshock tests, vessel 1
[VTT-RR-746] p 3303 N92-28776

CRASHWORTHINESS
Drop test: Cessna Golden Eagle 421B
[DOT/FAA/CT-TN91/32] p 3230 N92-28900

CRATERING
Styles of crater gradation in Southern Ismenius Lacus, Mars: Clues from Meteor Crater, Arizona p 3384 N92-29018
Glacial and marine chronology of Mars p 3392 N92-29067

CRATERS
Nature and evolution of the early Martian atmosphere: Evidence from highland crater populations p 3373 N92-28485
Recent Elysium volcanism: Effects on the Martian atmosphere p 3389 N92-29048
Microcraters on Mars: Evidence of past climatic variations p 3394 N92-29073

CREEP PROPERTIES
Mechanisms of fracture and creep of structural alloys
[AD-A248701] p 3259 N92-28390
Regional variations in the stability and diffusion of water-ice in the Martian regolith p 3388 N92-29042

CREW PROCEDURES (INFLIGHT)
An analysis of aircrew communication patterns and content
[AD-A246618] p 3272 N92-28253
Correlational analysis of survey and model-generated workload values
[AD-A247153] p 3329 N92-28518

CRITICAL VELOCITY
Laser anemometer measurements and computations in an annular cascade of high turning core turbine vanes
[NASA-TP-3252] p 3229 N92-28980

CROP GROWTH
A study of the control problem of the shoot side environment delivery system of a closed crop growth research chamber
[NASA-CR-177597] p 3330 N92-28681

CROSS CORRELATION
Atmospheric turbulence spectra and correlation functions
[NLR-TP-89217-U] p 3316 N92-28689
Sea surface velocities from visible and infrared multispectral atmospheric mapping sensor imagery
[NASA-CR-190398] p 3305 N92-28715
Monaural and binaural processing of complex waveforms
[AD-A247199] p 3352 N92-28889

CROSSLINKING
Silicon polymers
[AD-A250201] p 3265 N92-29145

CROSSTALK
Crosstalk correction scheme
[AD-D015251] p 3276 N92-29085

CRUCIBLES
Evaluation of plasma sprayed crucible coatings for melt processing copper-refractory metal alloys
[DE92-010871] p 3259 N92-28338

CRUSTS
Discovery concepts for Mars p 3387 N92-29035

CRYOGENIC COOLING
Ultra-high temperature stability Joule-Thomson cooler with capability to accomodate pressure variations
[NASA-CASE-NPO-18184-1-CU] p 3288 N92-29156

CRYOGENIC FLUIDS
Paint removal using cryogenic processes
[AD-A247668] p 3264 N92-28912

CRYOGENIC WIND TUNNELS
Calculation of support interferences on the aerodynamic coefficients for a wind tunnel calibration model
[ESA-TT-1247] p 3229 N92-29159

CRYOGENICS
Cryogenic system operating experience review for fusion applications
[DE92-012509] p 3361 N92-28805
Pressure transducer and system for cryogenic environments
[NASA-CASE-LAR-14579-1] p 3288 N92-29097
Cryogenic shutter
[NASA-CASE-GSC-13189-2] p 3296 N92-29151

CRYOPUMPING
Cryogenic system operating experience review for fusion applications
[DE92-012509] p 3361 N92-28805

CRYOSTATS
Ultra-high temperature stability Joule-Thomson cooler with capability to accomodate pressure variations
[NASA-CASE-NPO-18184-1-CU] p 3288 N92-29156

CRYSTAL DEFECTS
Shallow states of donor impurities on periodically structured semiconductors interfaces
[DE92-622791] p 3363 N92-28312
Microgravity accelerometer characterization on Columbia STS-32 mission p 3271 N92-28452
CRYSTAL GROWTH
Numerical studies of convective transport associated with crystal growth in mirrogravity p 3267 N92-28437
The in situ observation of diamond film nucleation and growth
[AD-A248203] p 3265 N92-29189
CRYSTAL LATTICES
Energetics of nanoscale graphitic tubules
[AD-A250165] p 3252 N92-28917
CRYSTAL STRUCTURE
Shallow states of donor impurities on periodically structured semiconductors interfaces
[DE92-622791] p 3363 N92-28312
Nanoscale investigation of indentation, adhesion, and fracture of diamond (111) surfaces
[AD-A250164] p 3265 N92-28916
Energetics of nanoscale graphitic tubules
[AD-A250165] p 3252 N92-28917
CRYSTAL SURFACES
Nanoscale investigation of indentation, adhesion, and fracture of diamond (111) surfaces
[AD-A250164] p 3265 N92-28916
CRYSTALLINITY
Evidence for crystalline hematite as an accessory phase in Martian soils p 3391 N92-29059
Molecular engineering of liquid crystalline polymers by living cationic polymerization. 21: Synthesis and characterization of poly (3-((4-cyano-4'-biphenyl)oxy) propyl vinyl ether) macromonomers
[AD-A248305] p 3265 N92-29116
CRYSTALLITES
Microstructures of shocked quartz
[DE92-010710] p 3363 N92-28333
CRYSTALLIZATION
Chain folding in EBEE semicrystalline diblock copolymers
[AD-A247595] p 3262 N92-28251
Multiple-valued programmable logic array minimization by simulated annealing
[AD-A248620] p 3335 N92-28353
Phase equilibria and trace element partitioning in a magma ocean to 260 kilobars p 3311 N92-28595
Imperfect fractional crystallization of the lunar magma ocean and formation of the lunar mantle: A realistic chemical approach p 3314 N92-28610
The ferroan-anorthositic suite and the extent of primordial lunar melting p 3315 N92-28618
CRYSTALLOGRAPHY
Surface crystallographic dependence of voltammetric oxidation of polyhydric alcohols and related systems at monocrystalline gold-acidic aqueous interfaces
[AD-A246763] p 3363 N92-28392
CRYSTALS
Numerical studies of convective transport associated with crystal growth in mirrogravity p 3267 N92-28437
Fate of a perched crystal layer in a magma ocean p 3312 N92-28602
Monte Carlo optimization of depth-of-interaction resolution in PET crystals
[DE92-011147] p 3364 N92-28762
CUBIC LATTICES
Percolation conductivity of Penrose tiling by transfer-matrix Monte Carlo
[DE92-622792] p 3362 N92-28231
CUES
Initial validation of a R/D simulator with large amplitude motion p 3225 N92-28546
Effective cueing during approach and touchdown: Comparison with flight p 3226 N92-28552
CULTURE TECHNIQUES
Experimental measurement of the orbital paths of particles sedimenting within a rotating viscous fluid as influenced by gravity
[NASA-TP-3200] p 3331 N92-28897
CUMULUS CLOUDS
Development of an advanced representation of cumulus convection
[DE92-011031] p 3319 N92-28830
CURRENT DENSITY
Development of negative heavy ion sources for plasma potential measurement
[DE92-782102] p 3360 N92-28234
Arcjet plume ionization effects on exposed solar array conducting surfaces
[AD-A245912] p 3307 N92-28383
A momentum limit for electromagnetic railguns
[DE92-011380] p 3245 N92-28861
The processing of high temperature ceramic superconducting devices, volume 2
[AD-A248159] p 3281 N92-28948
CURVATURE
Curvature estimation in orientation selection
[AD-A247862] p 3328 N92-28957
CYCLES
Observed changes in limb clouds immediately prior to the onset of planet-encircling dust storms p 3388 N92-29039
A carbonate-silicate aqueous geochemical cycle model for Mars p 3390 N92-29057
Modeling the seasonal cycle of CO2 on Mars: A fit to the Viking lander pressure curves p 3394 N92-29076
CYCLIC COMPOUNDS
Macrocyclic polycation complexes for secondary anion binding, molecular recognition, and catalysis
[AD-A246690] p 3254 N92-28287
CYCLONES
Polar lows over the northeast Greenland Sea
[AD-A245360] p 3318 N92-28421
Mesoscale vertical structure of an explosive oceanic cyclone
[AD-A245927] p 3318 N92-28423
Mesoscale surface analysis of the ERICA IOP-5 cyclone
[AD-A245946] p 3319 N92-28884
CYCLOTRONS
Intense electron beam cyclotron masers with microsecond pulselengths
[AD-A247060] p 3289 N92-28271
CYLINDERS
X ray diffraction study of residual stresses in metal matrix composite-jacketed steel cylinders subjected to internal pressure
[AD-A248449] p 3251 N92-28416
CYLINDRICAL BODIES
Propellant-to-inhibitor bonding system
[AD-D015243] p 3266 N92-28739
CYTOCHROMES
Curvature estimation in orientation selection
[AD-A247862] p 3328 N92-28957

D

DAMAGE
Experimental determination of dissipated energy density as a measure of strain-induced damage in composites
[AD-A250322] p 3253 N92-28953
Performance of uncoated AFRSI blankets during multiple Space Shuttle flights
[NASA-TM-103892] p 3245 N92-29104
Generation of spectra and stress histories for fatigue and damage tolerance analysis of fuselage repairs
[AD-A250390] p 3235 N92-29180
DAMAGE ASSESSMENT
Environmental testing of the Xi Scan 1000, portable fluoroscopic and radiographic imaging system
[AD-A247167] p 3324 N92-28242
A system structure for predictive relations in penetration mechanics
[AD-A246453] p 3292 N92-28284
Study of high temperature failure mechanism in ceramics
[AD-A247018] p 3263 N92-28415
Experimental determination of dissipated energy density as a measure of strain-induced damage in composites
[AD-A250322] p 3253 N92-28953
Generation of spectra and stress histories for fatigue and damage tolerance analysis of fuselage repairs
[AD-A250390] p 3235 N92-29180
Modular simulation of HEI fragments and blast pressure
[AD-A248205] p 3272 N92-29191
On the use of structural dynamic experimental methods for damage inspection of a glass fibre reinforced plastic plate
[FFA-TN-1992-02] p 3253 N92-29220
DAMPING
Structural design methodology for large space structures
[AD-A247672] p 3246 N92-28560
Analysis of constrained-layer damping of flexural and extensional waves in infinite, fluid-loaded plates
[AD-A247936] p 3304 N92-29081
DARK MATTER
Quark matter and cosmology
[DE92-011736] p 3371 N92-28859
Inverse phase transitions: Does baryogenesis lead to dark matter?
[DE92-013022] p 3372 N92-29184
DASSAULT AIRCRAFT
The role of simulation for the study of APIS (piloting support by synthetic imagery) p 3224 N92-28544
DATA ACQUISITION
Operational noise data for OH-58D Army helicopters
[AD-A246822] p 3351 N92-28292
Project MAGNET high-level vector survey data reduction p 3301 N92-28628
Multitemporal analysis of a braiding river
[NLR-TP-89235-U] p 3305 N92-28690
An inventory of data collected during the NERC's North Sea Community Research Project, 1987-1992
[REPT-21-1991] p 3323 N92-29215
DATA BASE MANAGEMENT SYSTEMS
The instrumentation of a parallel, distributed database operation, retrieve-common, for merging two large sets of records
[AD-A247486] p 3367 N92-28246
The testing, analysis, and correction of the update operation of a parallel, multi-backend database supercomputer
[AD-A248320] p 3341 N92-28306
Audit trails and PC control on Novell networks
[DE92-010695] p 3335 N92-28332
Development of rotating shadowband spectral radiometers and GCM radiation code test data sets in support of ARM
[DE92-011438] p 3316 N92-28853
Analysis of multimedia information systems for the US Coast Guard
[AD-A247890] p 3369 N92-28960
DATA BASES
The instrumentation of a parallel, distributed database operation, retrieve-common, for merging two large sets of records
[AD-A247486] p 3367 N92-28246
The testing, analysis, and correction of the update operation of a parallel, multi-backend database supercomputer
[AD-A248320] p 3341 N92-28306
Automated apparel specification retrieval system
[AD-A248619] p 3367 N92-28389
The mechanical property data base from an Air Force/industry cooperative test program on advanced aluminum alloys (IN905XL and AL905XL forgings)
[AD-A247752] p 3368 N92-28565
Marine magnetic data holdings of World Data Center-A for Marine Geology and Geophysics p 3300 N92-28625
Scientific investigations with the data base HEAO-1 scanning modulator collimator
[NASA-CR-190477] p 3370 N92-28680
Binary optical filters for scale invariant pattern recognition
[NASA-TM-103902] p 3234 N92-28910
Calculations and databasing of molecular absorption parameters for HITRAN
[AD-A247549] p 3355 N92-28936
SPEEDS: An approach to support programming environments using expert database systems
[AD-A247469] p 3339 N92-28943
Space transportation analysis and design
[AD-A250629] p 3245 N92-28956
Analysis of multimedia information systems for the US Coast Guard
[AD-A247890] p 3369 N92-28960
Thermally distinct ejecta blankets from Martian craters p 3379 N92-28994
A rotorcraft flight database for validation of vision-based ranging algorithms
[NASA-TM-103906] p 3231 N92-29103
Consulting report on the NASA technology utilization network system
[NASA-CR-190387] p 3370 N92-29108
Development of a flight information system using the structured method
[AD-A248207] p 3236 N92-29222
DATA COMPRESSION
Transputer-based embedded system for Meteosat image data compression
[NLR-TP-90228-U] p 3305 N92-28697
Digital compression algorithms for HDTV transmission
[NASA-CR-190509] p 3275 N92-28873
DATA CORRELATION
Correlation, error-localisation, and updating of the second problem defined in GARTEUR AG11
[NLR-TP-90070-U] p 3302 N92-28650
DATA FLOW ANALYSIS
A network flow algorithm for just-in-time project scheduling
[MEMO-COSOR-91-21] p 3336 N92-28638
DATA INTEGRATION
A contribution to laser range imaging technology
[NASA-CR-190501] p 3290 N92-28707
DATA LINKS
Autonomous ocean profiler
[AD-A247657] p 3322 N92-28938
Tactical line-of-sight radio propagation reliability
[AD-A245909] p 3277 N92-29165

DATA MANAGEMENT
On-line point positioning with single frame camera data
[AD-A248307] p 3287 N92-28322
DATA PROCESSING
Digital hardware architecture implementation
[AD-A249194] p 3332 N92-28236
Measurements of declination at the Helsinki Magnetic-Meteorological Observatory 1844-1853
p 3299 N92-28622
Survey data for geomagnetic field modelling
p 3300 N92-28623
Secular variation across the oceans: A retrospective study from 35 years of shipboard total field measurements in the NE Atlantic p 3300 N92-28627
Magnetic repeat station data p 3301 N92-28630
Geomagnetic data from the US magnetic observatory network p 3301 N92-28631
Reduction and analysis of F-111C flight data
[AD-A250341] p 3233 N92-28771
Archival of the ECOM-721 data
[AD-A249299] p 3338 N92-28845
SPEEDS: An approach to support programming environments using expert database systems
[AD-A247469] p 3339 N92-28943
User's manual for the Gaussian windows program
[NASA-CR-190554] p 3340 N92-29107
CTD data from the north east Atlantic, April 1989, collected on RRS Discovery Cruise 181
[IOS-285-1991] p 3322 N92-29211
DATA PROCESSING EQUIPMENT
Digital hardware architecture implementation
[AD-A249194] p 3332 N92-28236
DATA PROCESSING TERMINALS
Upgrading the data processing section of the NAL Gust Wind Tunnel data processing system
[NAL-TM-635] p 3241 N92-28833
DATA REDUCTION
Development of a residual acceleration data reduction and dissemination plan p 3271 N92-28453
Types and Characteristics of Data for Geomagnetic Field Modeling
[NASA-CP-3153] p 3299 N92-28620
Reduction of marine magnetic data for modeling the main field of the Earth p 3300 N92-28626
Project MAGNET high-level vector survey data reduction p 3301 N92-28628
Reduction and analysis of F-111C flight data
[AD-A250341] p 3233 N92-28771
DATA SAMPLING
Microgravity accelerometer characterization on Columbia STS-32 mission p 3271 N92-28452
DATA STORAGE
Kanerva's sparse distributed memory with multiple hamming thresholds
[NASA-CR-190552] p 3339 N92-28875
Oceanographic data dictionary for netCDF files
[AD-A250017] p 3322 N92-28951
Disk memory device
[NASA-CASE-GSC-13196-1] p 3333 N92-29132
DATA STRUCTURES
HYPER: A domain decomposition program, version 1.0 (user's manual)
[AD-A250018] p 3340 N92-29172
DATA SYSTEMS
Marine magnetic data holdings of World Data Center-A for Marine Geology and Geophysics
p 3300 N92-28625
Functional requirements document for the Earth Observing System Data and Information System (EOSDIS) Scientific Computing Facilities (SCF) of the NASA/MSFC Earth Science and Applications Division, 1992
[NASA-TM-4392] p 3333 N92-28899
DATA TRANSFER (COMPUTERS)
Superconducting at NLR: NEC SX-2 capabilities in NLR's terminal and file-transfer network
[NLR-TP-89007-U] p 3342 N92-28706
DATA TRANSMISSION
Crosstalk correction scheme
[AD-D015251] p 3276 N92-29085
Verification of satellite EGSE test-software using an application generator
[ITN-92-85131] p 3244 N92-29098
Analysis and optimization of low-earth-orbit communication links
[DE92-013393] p 3277 N92-29131
DAYGLOW
An analysis of middle ultraviolet dayglow spectra
[AD-A245965] p 3309 N92-28319
Theoretical and experimental studies relevant to interpretation of auroral emissions
[NASA-CR-190521] p 3316 N92-28911
DECISION MAKING
Improved decision making through group composition
[AD-A246622] p 3366 N92-28256
A system structure for predictive relations in penetration mechanics
[AD-A246453] p 3292 N92-28284
MoCog1: A computer simulation of recognition-primed human decision making, considering emotions
[NASA-TM-107859] p 3337 N92-28758
Tasking and communication flows in the F/A-18D cockpit: Issues, problems, and possible solutions
[AD-A245977] p 3234 N92-28802
Air combat maneuvering expert system trainer
[AD-A246459] p 3241 N92-28975
Maintaining the program balance, volumes 1 and 2
[NASA-CR-190269] p 3367 N92-29111
Time pressure effects on decision making in a dynamic task environment
[IZF-1991-B-8] p 3367 N92-29161
DECISION THEORY
Time pressure effects on decision making in a dynamic task environment
[IZF-1991-B-8] p 3367 N92-29161
DECLINATION
Historical data for geomagnetic field modelling
p 3299 N92-28621
Measurements of declination at the Helsinki Magnetic-Meteorological Observatory 1844-1853
p 3299 N92-28622
DECOMPOSITION
A domain decomposition method for ocean/bottom interaction problems
[FFI-91/7022] p 3320 N92-28266
Studies of 1,3-disilacyclobutanes as single-source CVD precursors to silicon carbide
[AD-A247111] p 3365 N92-28885
DEFENSE INDUSTRY
Validation of knowledge based systems
[AD-A247741] p 3368 N92-28404
DEFENSE PROGRAM
Experimental aerodynamic facilities of the Aerodynamics Research and Concepts Assistance Branch
[AD-A247489] p 3240 N92-28248
DEFORMATION
Prediction of composite material properties using two-dimensional finite element micromechanical analysis
[AD-A250300] p 3252 N92-28702
DEGENERATION
Degenerate four-wave mixing using a tunable excimer laser to detect combustion gases
[DE92-005327] p 3290 N92-28852
DEGRADATION
Assessment of valve actuator motor rotor degradation by Fourier Analysis of current waveform
[DE92-013233] p 3281 N92-28814
DEGREES OF FREEDOM
A 6 degree-of-freedom Lorentz force vibration isolator with nonlinear controller p 3267 N92-28444
Microgravity vibration isolation research at the University of Virginia p 3267 N92-28446
Use of simulation in the USAF Test Pilot School curriculum p 3223 N92-28535
User friendly joystick
[NASA-CASE-GSC-13187-1] p 3281 N92-29153
DEICERS
Results of a low power ice protection system test and a new method of imaging data analysis
[NASA-TM-105745] p 3227 N92-28696
DEICING
Results of a low power ice protection system test and a new method of imaging data analysis
[NASA-TM-105745] p 3227 N92-28696
DELAY CIRCUITS
Delayed pulse generator
[DIGEL-1991-2] p 3278 N92-28262
Null shifting with fixed delays
[AD-A250059] p 3274 N92-28796
DELAY LINES
The 2.0 GHz sampling rate transversal filter
[AD-A250244] p 3358 N92-28968
DELTA WINGS
Analysis of results of an Euler-equation method applied to leading-edge vortex flow
[NLR-TP-90368-U] p 3226 N92-28657
Identification of aerodynamic models for maneuvering aircraft
[NASA-CR-190444] p 3233 N92-28720
Natural flow wing
[NASA-CASE-LAR-14281-1] p 3228 N92-28729
DEMAGNETIZATION
M-H characteristics and demagnetization resistance of samarium-cobalt permanent magnets to 300 C
[NASA-CR-189194] p 3280 N92-28723
DEMODULATION
Demodulation processes in auditory perception
[AD-A250203] p 3328 N92-29146
DEMOGRAPHY
Improved decision making through group composition
[AD-A246622] p 3366 N92-28256
DENSITY DISTRIBUTION
Weighted-density functional approach for the solid-liquid interfaces in electrolytes
[DE92-622662] p 3362 N92-28280
Quasi-regular impurity distribution driven by charge-density wave
[DE92-622799] p 3363 N92-28281
Gadolinium metastable states population distributions and atomic density under high-rate electron beam evaporation
[DE92-782008] p 3363 N92-28282
DEOXYRIBONUCLEIC ACID
Problems in mechanistic theoretical models for cell transformation by ionizing radiation
[DE92-010265] p 3324 N92-28278
Primer on molecular genetics
[DE92-010680] p 3324 N92-28382
DEPLETION
Martian surficial carbon-constraints from isotopic measurements of shock-produced glass in EET A79001
p 3377 N92-28508
DEPLOYMENT
Tactical line-of-sight radio propagation reliability
[AD-A245909] p 3277 N92-29165
DEPOSITION
Ionized assisted deposition of organic films for optoelectronic applications
[AD-A247744] p 3263 N92-28405
Oxygen in the Martian atmosphere: Regulation of PO2 by the deposition of iron formations on Mars
p 3373 N92-28482
A magma ocean and the Earth's internal water budget
p 3310 N92-28590
Ground deposition of liquid droplets released from a point source in the atmospheric surface layer
[ISBN-0-315-51071-4] p 3316 N92-28703
Report on the workshop on Ion Implantation and Ion Beam Assisted Deposition
[AD-A250561] p 3365 N92-28923
DEPOSITS
The distribution of anorthosite on the nearside of the moon p 3311 N92-28594
Dark material in the polar layered deposits on Mars
p 3385 N92-29024
Physical properties of Deucalionis, Eos, Xanthe-type units in the central equatorial region of Mars
p 3392 N92-29063
Physical properties of Meridiani Sinus-type units in the central equatorial region of Mars p 3392 N92-29064
Physical properties of Oxia/Lunae Planum and Arabia-type units in the central equatorial region of Mars
p 3392 N92-29065
Chemical vapor synthesis of niobium aluminides
[AD-A250332] p 3258 N92-29091
DESERTS
Tactical line-of-sight radio propagation reliability
[AD-A245909] p 3277 N92-29165
DESIGN ANALYSIS
Design on an enhanced interactive satellite communications system analysis program
[AD-A245967] p 3273 N92-28410
Taguchi methods in electronics: A case study
[NASA-TM-103586] p 3279 N92-28456
Integrated Design Analysis and Optimisation of Aircraft Structures
[AGARD-LS-186] p 3231 N92-28469
Fundamentals of structural optimisation
p 3231 N92-28470
Practical architecture of design optimisation software for aircraft structures taking the MBB-Lagrange code as an example p 3232 N92-28471
Structural optimization of aircraft
p 3232 N92-28472
Multidisciplinary design and optimization
[AGARD-PAPER-2] p 3232 N92-28473
Mathematical optimization: A powerful tool for aircraft design p 3232 N92-28474
Global minimum solution of engineering design problems
[AD-A247496] p 3337 N92-28704
Sensor filter designs for large flexible spacecraft
p 3247 N92-28733
Integrating the affective domain into the instructional design process
[AD-A249287] p 3327 N92-28880
Space transportation analysis and design
[AD-A250629] p 3245 N92-28956
Dynamics of a split torque helicopter transmission
[NASA-TM-105681] p 3296 N92-29136
Method of moments analysis of displaced-axis dual reflector antennas
[AD-A247970] p 3277 N92-29166
Design specifications for the Advanced Instructional Design Advisor (AIDA), volume 1
[AD-A248201] p 3340 N92-29187

Design specifications for the Advanced Instructional Design Advisor (AIDA), volume 2
[AD-A248202] p 3340 N92-29188
DESORPTION
Thermodynamic and kinetic aspects of surface acidity
[DE92-011194] p 3256 N92-28893
DETECTION
Reinforcement learning for the adaptive control of perception and action
[AD-A249351] p 3344 N92-28325
Lapses in alertness: Brain-evoked responses to task-irrelevant auditory probes
[AD-A247669] p 3328 N92-28940
Digital enhancement and restoration of images derived from flow visualization experiments
[AD-A250317] p 3339 N92-28952
Multicomponent comparison of optical and mass spectrometric diagnostics in low-pressure flames
[AD-A250323] p 3257 N92-28954
Development of instrumentation for boundary layer transition detection
[AD-A249982] p 3287 N92-29171
DETERIORATION
Replacement of the NAL high pressure air storage system
[NAL-TM-634] p 3241 N92-28835
DETONATION
Computations of detonation structure: The influence of model input parameters
[AD-A248634] p 3285 N92-28803
DETONATION WAVES
Computations of detonation structure: The influence of model input parameters
[AD-A248634] p 3285 N92-28803
DEUTERONS
Evidence for physics beyond the quasi-deuteron model in pion absorption
[DE92-011285] p 3354 N92-28310
DEVELOPING NATIONS
Information systems for engineering sustainable development
[DE92-011271] p 3368 N92-28838
DIAGNOSIS
Portable dynamic fundus instrument
[NASA-CASE-MSC-21675-1] p 3325 N92-28755
DIAMOND FILMS
Large-area, plasma-assisted, halogen-based diamond deposition
[AD-A247423] p 3264 N92-28904
The in situ observation of diamond film nucleation and growth
[AD-A248203] p 3265 N92-29189
DIAMONDS
Thermal wave imaging and characterization of solids
[AD-A249297] p 3297 N92-28851
Atomistic simulation of the nanoindentation of diamond and graphite surfaces
[AD-A249296] p 3355 N92-28881
Nanoscale investigation of indentation, adhesion, and fracture of diamond (111) surfaces
[AD-A250164] p 3265 N92-28916
Innovative techniques for the production of low cost 2D laser diode arrays
[AD-A248247] p 3292 N92-29226
DICARBOXYLIC ACIDS
Structural characterization of cross-linked hemoglobins developed as potential transfusion substitutes
[AD-A246777] p 3325 N92-28515
DICHLORIDES
Electrochemical studies of Lewis acid-base systems for use in thermally regenerable fuel cells
[AD-A246457] p 3307 N92-28974
DICTIONARIES
Oceanographic data dictionary for netCDF files
[AD-A250017] p 3322 N92-28951
Information technology in plain words
[AD-A250324] p 3369 N92-28955
DIELECTRIC PROPERTIES
High temperature dielectric properties of Apical, Kapton, Peek, Teflon AF, and Upilex polymers
[NASA-TM-105753] p 3280 N92-28675
DIELECTRICS
Scattering and radiation analysis of three-dimensional cavity arrays via a hybrid finite element method
[NASA-CR-190406] p 3273 N92-28371
Investigation of an equivalent circuit for the inductive strip in finline with dielectric
[AD-A247025] p 3279 N92-28373
High temperature dielectric properties of Apical, Kapton, Peek, Teflon AF, and Upilex polymers
[NASA-TM-105753] p 3280 N92-28675
DIFFERENTIAL EQUATIONS
Diagonal forms of translation operators for helmholtz equation in three dimensions
[AD-A248422] p 3348 N92-28949
DIFFRACTION PATHS
An OTH radar clutter simulation
[AD-A248054] p 3272 N92-28304
Comparison of electromagnetic propagation predictions from IREPS and RPO across a coastal transition
[AD-A249331] p 3273 N92-28357
DIFFUSERS
Diffuser casing upgrade for an advanced turbofan
[NLR-TP-90097-U] p 3238 N92-28711
DIFFUSION
Numerical studies of low temperature gallium arsenide buffer layers and their influence on device operation
[AD-A250309] p 3258 N92-29126
DIFFUSION FLAMES
The compositional structure and the effects of exothermicity in an unpremixed planar jet flame
p 3258 N92-28821
Multicomponent comparison of optical and mass spectrometric diagnostics in low-pressure flames
[AD-A250323] p 3257 N92-28954
DIFFUSIVITY
Estimation of the viscosities of silicate liquids at high pressure from measurements of oxygen diffusivity
p 3313 N92-28607
Thermal wave imaging and characterization of solids
[AD-A249297] p 3297 N92-28851
DIGITAL COMPUTERS
Digital hardware architecture implementation
[AD-A249194] p 3332 N92-28236
DIGITAL DATA
Marine magnetic data holdings of World Data Center-A for Marine Geology and Geophysics
p 3300 N92-28625
Geomagnetic data from the US magnetic observatory network p 3301 N92-28631
DIGITAL SIMULATION
Simulation of the propagation of acoustical waves through an interface separating a compressible fluid and an elastic medium
[FFI-91/7017] p 3351 N92-28314
Wavelets and numerical simulation
[ONERA-NT-1991-8] p 3347 N92-28777
Identification of weakly non-linear dynamical systems by means of random excitations
[ONERA-NT-1991-10] p 3349 N92-28778
DIGITAL SYSTEMS
CESAR address generator
[FFI-91/7021] p 3334 N92-28265
On-line point positioning with single frame camera data
[AD-A248307] p 3287 N92-28322
Digital control algorithms for microgravity isolation systems p 3267 N92-28445
Flight simulation and digital flight controls
p 3221 N92-28526
DIGITAL TELEVISION
Digital compression algorithms for HDTV transmission
[NASA-CR-190509] p 3275 N92-28873
DIISOCYANATES
Multiphase structure of a segmented polyurethane: Effects of temperature and annealing
[AD-A247594] p 3262 N92-28250
DILATOMETRY
Phase transformations in Ti3Al based alloy
[AD-A246464] p 3261 N92-28976
DIMENSIONAL MEASUREMENT
X ray computed tomography of full-scale castings
[AD-A247101] p 3258 N92-28241
DIMENSIONS
A survey of high density packaging for high performance computing system
[AD-A248633] p 3332 N92-28891
DIMETHYLHYDRAZINES
Reactions of hydrazines with chemicals found in environment
[AD-A247064] p 3308 N92-28272
DIODES
Tuning and automatic phase adjustment in external cavity diode laser beam combiners
[AD-A247421] p 3290 N92-28903
Innovative techniques for the production of low cost 2D laser diode arrays
[AD-A248247] p 3292 N92-29226
DIRECT CURRENT
The processing of high temperature ceramic superconducting devices, volume 2
[AD-A248159] p 3281 N92-28948
DIRECTION FINDING
Maximizing the convergence rate of the EM algorithm for the multiple broad-band signal estimation and detection
[AD-A248230] p 3341 N92-29224
DIRECTIONAL SOLIDIFICATION (CRYSTALS)
An examination of anticipated g-jitter on Space Station and its effects on materials processes
p 3267 N92-28438
DISCRETE FUNCTIONS
Diagonal forms of translation operators for helmholtz equation in three dimensions
[AD-A248422] p 3348 N92-28949
DISCRIMINANT ANALYSIS (STATISTICS)
Binary optical filters for scale invariant pattern recognition
[NASA-TM-103902] p 3234 N92-28910
DISILICIDES
Method of intercalating large quantities of fibrous structures
[NASA-CASE-LEW-15077-1] p 3253 N92-29152
DISK GALAXIES
Observational study and analysis of point sources found by the infrared astronomy satellite
[AD-A248416] p 3371 N92-28843
DISLOCATIONS (MATERIALS)
A combined experimental and analytical investigation of the theory of plasticity involving strain induced anisotropy
[AD-A248440] p 3298 N92-28352
DISORIENTATION
G-tolerance and spatial disorientation: Can simulation help us? p 3223 N92-28534
DISPENSERS
Modifications and results of flight tests of a practice bomb adapter
[NLR-TP-90108-U] p 3233 N92-28651
DISPERSION
Ground deposition of liquid droplets released from a point source in the atmospheric surface layer
[ISBN-0-315-51071-4] p 3316 N92-28703
DISPLACEMENT
Polyimidazoles via aromatic nucleophilic displacement
[NASA-CASE-LAR-14145-1] p 3264 N92-28751
Poly(1,3,4-oxadiazoles) via aromatic nucleophilic displacement
[NASA-CASE-LAR-14427-1] p 3250 N92-29141
Detection of in-plane displacements of acoustic wave fields using extrinsic Fizeau fiber interferometric sensors
[NASA-CR-190493] p 3353 N92-29196
DISPLAY DEVICES
Initial validation of a R/D simulator with large amplitude motion p 3225 N92-28546
Tasking and communication flows in the F/A-18D cockpit: Issues, problems, and possible solutions
[AD-A245977] p 3234 N92-28802
Single layer multi-color luminescent display and method of making
[NASA-CASE-LAR-13616-3] p 3359 N92-29158
DISSIPATION
Evaluation of a Solent sonic anemometer on RRS Charles Darwin Cruise 43
[IOS-288-1991] p 3323 N92-29213
DISSOCIATION
Excited negative ions and molecules and negative ion production
[AD-A247017] p 3354 N92-28414
History of oxygen and carbon escape from the Martian atmosphere p 3376 N92-28498
Large-area, plasma-assisted, halogen-based diamond deposition
[AD-A247423] p 3264 N92-28904
DISTANCE
The distance dependence of regional phase discriminants
[AD-A247546] p 3316 N92-28935
DISTRIBUTED PARAMETER SYSTEMS
Control of nonlinear distributed parameter systems with application to flow control
[AD-A250212] p 3346 N92-29149
DISTRIBUTED PROCESSING
The instrumentation of a parallel, distributed database operation, retrieve-common, for merging two large sets of records
[AD-A247486] p 3367 N92-28246
An ELROS primer
[DE92-010661] p 3342 N92-28381
Kanerva's sparse distributed memory with multiple hamming thresholds
[NASA-CR-190552] p 3339 N92-28875
Crystallizing FORTRAN
[AD-A250162] p 3343 N92-28915
Fault-tolerant parallel computer systems for real-time applications
[AD-A247887] p 3343 N92-28958
Asynchronous bidirectional network interface enabling seamless concurrent processing in a distributed heterogeneous multiprocessor system
[AD-D015274] p 3343 N92-29096
DISULFIDES
Orthogonal self-assembly of redox active molecules on Pt and Au: Selective reaction of disulfide with Au and isonitrile with Pt
[AD-A246698] p 3254 N92-28290

DIURNAL VARIATIONS
Simulation in infrared imaging: Using electrical circuit principles to model heat transfer
[AD-A248290] p 3278 N92-28276
Ultrasonic ambient noise in Australian shallow waters at frequencies up to 200 kHz
[MRL-TR-91-23] p 3351 N92-28364
Atomic oxygen in the Martian thermosphere
p 3391 N92-29061

DIVERTERS
A comparison of results from an edge-plasma model with those from a two-dimensional fluid code
[DE92-010718] p 3360 N92-28335
Air ejector experiments using the two-dimensional supersonic cascade tunnel: Zero secondary flow performance
[NAL-TM-632] p 3241 N92-28829

DOCUMENT STORAGE
Conversion and retrievability of hard copy and digital documents on optical disks
[AD-A247481] p 3367 N92-28244
Files improvement the NARA way
[DE92-011139] p 3368 N92-28832

DOCUMENTS
Conversion and retrievability of hard copy and digital documents on optical disks
[AD-A247481] p 3367 N92-28244
Files improvement the NARA way
[DE92-011139] p 3368 N92-28832
Publications of the Jet Propulsion Laboratory, 1989
[NASA-CR-190457] p 3369 N92-29202

DOPPLER EFFECT
Passive acoustic range estimation of helicopters
[AD-A248033] p 3351 N92-28302
Adaptive noise cancellation applied to the NUWES test ranges
[AD-A245961] p 3352 N92-28409
Analyzing noisy spectral line shapes
[DE92-011153] p 3362 N92-29086

DOPPLER RADAR
Windshear radar calibration: Transmitter power and receiver gain stability
[NASA-TM-107589] p 3275 N92-28876
Target motion detecting impulse Doppler radar system
[AD-D015263] p 3277 N92-29169

DOSAGE
Leakage current measurements in SOI devices
[AD-A247694] p 3280 N92-28561

DOSIMETERS
Somatic gene mutation in the human in relation to radiation risk
[DE92-009459] p 3325 N92-28685

DOUBLE STARS
Analysis of Mir-HEXE observations: Pulsation and energy spectra of the x ray double star SMC X-1 in 20 to 80 keV energy field
[ETN-92-91487] p 3371 N92-29128

DRAG REDUCTION
Studies in turbulence and turbulence control
[AD-A247164] p 3282 N92-28225
Constrained spanload optimization for minimum drag of multi-lifting-surface configurations
[NLR-TP-89126-U] p 3227 N92-28660

DROOPED AIRFOILS
Studies in general aviation aerodynamics
[NASA-CR-190431] p 3226 N92-28511

DROP TESTS
Drop test: Cessna Golden Eagle 421B
[DOT/FAA/CT-TN91/32] p 3230 N92-28900

DROPS (LIQUIDS)
Ground deposition of liquid droplets released from a point source in the atmospheric surface layer
[ISBN-0-315-51071-4] p 3316 N92-28703

DRUMS (CONTAINERS)
Flow rate testing of valves used with the 500 gallon collapsible drum
[AD-A250567] p 3294 N92-28924

DRY HEAT
Geothermal Progress Monitor, report No. 13
[DE92-010697] p 3307 N92-28422

DUAL SPIN SPACECRAFT
Prediction of attitude stability of asymmetric dual-spin stabilized spacecraft using improved liquid slosh model
[AD-A247023] p 3246 N92-28368

DUCT GEOMETRY
Inlet distortion effects in aircraft propulsion system integration p 3237 N92-28464

DUCTED FLOW
Experimental validation of a line-duct acoustics model including flow
[NLR-TP-90223-U] p 3352 N92-28695
Explicit Navier-Stokes computation of turbomachinery flows
[AD-A249284] p 3286 N92-28879

DUNES
Dorsa Argentea type sinuous ridges, Mars: Evidence for linear dune hypothesis p 3390 N92-29055

DUST
Using the historical record to determine dust sources
p 3376 N92-28499
The thermal structure, dust loading, and meridional transport in the Martian atmosphere during late southern summer p 3377 N92-28505
Mars dust and cloud opacities and scattering properties p 3381 N92-29003
Infrared photometric behavior and opposition effect of Mars p 3382 N92-29011
The meteoritic contribution to dust and aerosols in the atmosphere of Mars p 3383 N92-29013
Dark material in the polar layered deposits on Mars
p 3385 N92-29024
Mars: Correcting surface albedo observations for effects of atmospheric dust loading p 3386 N92-29032
Simulations of the seasonal polar caps on Mars
p 3387 N92-29033
Mars dust storm simulations: Analysis of surface stress p 3389 N92-29045
Atmospheric and surface temperatures and airborne dust amounts during late southern summer from Mariner 9 IRIS data p 3390 N92-29056
Physical properties of Oxia/Lunae Planum and Arabia-type units in the central equatorial region of Mars
p 3392 N92-29065
Surface photometric properties and albedo changes in the central equatorial region of Mars
p 3392 N92-29066

DUST STORMS
Using the historical record to determine dust sources
p 3376 N92-28499
Dust storm driven variations of the Mars thermosphere and exosphere: Coupling of atmospheric regions
p 3380 N92-28997
The composition of Martian aeolian sands: Thermal emissivity from Viking IRTM observations
p 3382 N92-29010
Nonlinear stratified flow over localized topographic obstacles on Mars p 3387 N92-29036
Observed changes in limb clouds immediately prior to the onset of planet-encircling dust storms
p 3388 N92-29039
New dust opacity maps from Viking IR thermal mapper data p 3388 N92-29040
Mars dust storm simulations: Analysis of surface stress p 3389 N92-29045

DYE LASERS
Asynchronous optical sampling for laser-based combustion diagnostics in high-pressure flames
[AD-A250206] p 3257 N92-28896

DYNAMIC CHARACTERISTICS
Inverse control problems: Mathematical preliminaries, system theoretical approaches, and their applications to aircraft dynamics
[LR-665] p 3345 N92-28581

DYNAMIC CONTROL
Dynamic control of aerodynamic instabilities in gas turbine engines p 3238 N92-28466
Inverse control problems: Mathematical preliminaries, system theoretical approaches, and their applications to aircraft dynamics
[LR-665] p 3345 N92-28581
Nonlinear sloshing and the coupled dynamics of liquid propellants and spacecraft
[AD-A250023] p 3248 N92-28967

DYNAMIC LOADS
The effect of intermediate heat treatments on overload induced retardation during the fatigue crack growth in an Al-alloy
[LR-651] p 3259 N92-28574

DYNAMIC MODELS
Optical effects on ocean mixed layer dynamics
[AD-A245941] p 3320 N92-28316
Dynamic simulation of compressor and gas turbine performance p 3237 N92-28463
Mathematical modeling of solar magneto-dynamics
[AD-A247158] p 3395 N92-28520
Dynamics motion simulation of the Hermes robot arm subjected to constraints
[NLR-TP-90282-U] p 3293 N92-28645
Linear recursive formulation of flexible multi-body space system dynamics
[NLR-TP-90284-U] p 3293 N92-28646
Quasi-recursive dynamics equations for spacecraft-based flexible robotic manipulators
[NLR-TP-90028-U] p 3345 N92-28648
Modelling and real-time simulation of the Hermes robot arm HERA
[NLR-TP-90262-U] p 3294 N92-28705
Explicit Navier-Stokes computation of turbomachinery flows
[AD-A249284] p 3286 N92-28879

DYNAMIC RESPONSE
Control and stabilization of distributed parameter systems in structural dynamics
[AD-A247097] p 3298 N92-28320
Response of helicopters to gusts
[NLR-TP-90159-U] p 3239 N92-28653
Experimental determination of dissipated energy density as a measure of strain-induced damage in composites
[AD-A250322] p 3253 N92-28953
Time pressure effects on decision making in a dynamic task environment
[IZF-1991-B-8] p 3367 N92-29161

DYNAMIC STRUCTURAL ANALYSIS
Control and stabilization of distributed parameter systems in structural dynamics
[AD-A247097] p 3298 N92-28320
Linear recursive formulation of flexible multi-body space system dynamics
[NLR-TP-90284-U] p 3293 N92-28646
Correlation, error-localisation, and updating of the second problem defined in GARTEUR AG11
[NLR-TP-90070-U] p 3302 N92-28650
Ongoing Progress in Spacecraft Controls
[NASA-CP-10099] p 3247 N92-28730
Computer derivation of green's functions for structural dynamic analysis
[AD-A250249] p 3339 N92-28969

DYNAMO THEORY
Mathematical modeling of solar magneto-dynamics
[AD-A247158] p 3395 N92-28520

E

EARTH (PLANET)
Magma ocean: Mechanisms of formation
p 3312 N92-28600
Influence of aerodynamic roughness length on aeolian processes: Earth, Mars, Venus p 3380 N92-28996

EARTH ATMOSPHERE
Remote sensing applications of the extended radiosity method
[DE92-011356] p 3306 N92-28807

EARTH CORE
Pressure regimes and core formation in the accreting earth p 3313 N92-28605
Terrestrial magma ocean and core segregation in the earth p 3313 N92-28606
Cooling of the magma ocean due to accretional disruption of the surface insulating layer
p 3314 N92-28608

EARTH CRUST
A seismic and integrated geophysical study of the lithosphere of the Colorado Plateau
[AD-A247091] p 3308 N92-28257
Analysis of the effects of Eurasian crustal and upper mantle structure on regional phases using broadband seismic data
[AD-A248383] p 3309 N92-28386
Thermal evolution and chemical differentiation of the terrestrial magma ocean p 3310 N92-28588
The three stages of magma ocean cooling
p 3315 N92-28617

EARTH MANTLE
Analysis of the effects of Eurasian crustal and upper mantle structure on regional phases using broadband seismic data
[AD-A248383] p 3309 N92-28386
Water inventories on Earth and Mars: Clues to atmosphere formation p 3373 N92-28483
A magma ocean and the Earth's internal water budget
p 3310 N92-28590
Mg-perovskite/silicate melt and magnesiowuestite/silicate melt partition coefficients for KLB-1 at 250 Kbars p 3310 N92-28592
Estimation of high temperature metal-silicate partition coefficients p 3311 N92-28599
Evidence for a high temperature differentiation in a molten earth: A preliminary appraisal
p 3312 N92-28603
Cooling of the magma ocean due to accretional disruption of the surface insulating layer
p 3314 N92-28608
On the isotopic composition of magmatic carbon in SNC meteorites p 3394 N92-29077

EARTH OBSERVATIONS (FROM SPACE)
Payload isolation and stabilization by a Suspended Experiment Mount (SEM)
[NASA-TM-107941] p 3246 N92-28369

EARTH OBSERVING SYSTEM (EOS)
Functional requirements document for the Earth Observing System Data and Information System (EOSDIS) Scientific Computing Facilities (SCF) of the NASA/MSFC Earth Science and Applications Division, 1992
[NASA-TM-4392] p 3333 N92-28899

EARTH ORBITAL ENVIRONMENTS
Cryogenic shutter
[NASA-CASE-GSC-13189-2] p 3296 N92-29151
EARTH ORBITS
Coordinate systems for space and geophysical applications
[AD-A247550] p 3244 N92-28937
Analysis and optimization of low-earth-orbit communication links
[DE92-013393] p 3277 N92-29131
EARTH PLANETARY STRUCTURE
Pressure regimes and core formation in the accreting earth p 3313 N92-28605
Terrestrial magma ocean and core segregation in the earth p 3313 N92-28606
Estimation of the viscosities of silicate liquids at high pressure from measurements of oxygen diffusivity p 3313 N92-28607
Cooling of the magma ocean due to accretional disruption of the surface insulating layer p 3314 N92-28608
Evolution of a terrestrial magma ocean: Thermodynamics, kinetics, rheology, convection, differentiation p 3314 N92-28611
Dynamics and evolution of a magma ocean p 3314 N92-28612
Evidences for the terrestrial magma ocean from high-pressure melting experiments p 3315 N92-28613
Evidence for magma oceans on asteroids, the moon, and Earth p 3315 N92-28614
EARTH RADIATION BUDGET
A new radiometer for Earth radiation budget studies
[DE92-011267] p 3306 N92-28834
EARTH ROTATION
Ocean tide models for satellite geodesy and Earth rotation
[NASA-CR-190468] p 3321 N92-28867
EARTH SCIENCES
Science and application payloads in the 1990's
[NASA-TM-107937] p 3246 N92-28370
EARTH TIDES
Ocean tide models for satellite geodesy and Earth rotation
[NASA-CR-190468] p 3321 N92-28867
EARTH-MOON SYSTEM
Origin of the moon and lunar core formation p 3311 N92-28596
Inheritance of magma ocean differentiation during lunar origin by giant impact p 3315 N92-28616
EARTHQUAKES
NORSAR basic seismological research
[AD-A248616] p 3309 N92-28569
The distance dependence of regional phase discriminants
[AD-A247546] p 3316 N92-28935
ECCENTRICITY
Laser optical disk position encoder with active heads
[NASA-CASE-GSC-13175-1] p 3359 N92-29133
ECONOMIC ANALYSIS
Information strategy plan
[AD-A247740] p 3367 N92-28403
FAA aviation forecasts
[AD-A250412] p 3230 N92-29182
ECONOMIC FACTORS
Identification and analysis of factors affecting the adoption of alternative transportation fuels
[PB92-164326] p 3266 N92-28914
EDDY CURRENTS
Method for advanced material characterization by laser induced eddy current imaging
[NASA-CASE-GSC-13386-1] p 3298 N92-29154
EDEMA
Effects of high terrestrial altitude on military performance
[AD-A246695] p 3324 N92-28288
EDUCATION
A profile of scientist and engineer training conducted by the Naval Avionics Center
[AD-A245925] p 3326 N92-28408
Second National Space Grant Conference report, 1991
[NASA-EP-278] p 3366 N92-28864
Learning, teaching, and testing for complex conceptual understanding
[AD-A248728] p 3328 N92-29142
EFFECTIVENESS
Piloted Simulation Effectiveness
[AGARD-CP-513] p 3221 N92-28522
Opportunities for flight simulation to improve operational effectiveness p 3221 N92-28523
Piloted simulation effectiveness development applications and limitations p 3221 N92-28524
Utility of ground simulation in flight control problem identification, solution development, and verification p 3221 N92-28525
Experience with piloted simulation in the development of helicopters p 3222 N92-28528
EFFECTORS
Acquisition and improvement of human motor skills: Learning through observation and practice
[NASA-TM-107878] p 3329 N92-29174
EFFECTS
Dynamical solvent effects on activated electron-transfer reactions: Principles, pitfalls, and progress
[AD-A246764] p 3363 N92-28349
EIGENVALUES
The principal part of plane vector fields with fixed Newton diagram
[DE92-622408] p 3346 N92-28311
A look-ahead variant of the Lanczos algorithm and its application to the quasi-minimal residual method for non-Hermitian linear systems
[NASA-CR-190557] p 3340 N92-29113
EJECTA
Thermally distinct ejecta blankets from Martian craters p 3379 N92-28994
Ice in the northern lowlands and southern highlands of Mars and its enrichment beneath the Elysium Lavas p 3381 N92-29001
EJECTION
An ejection model for SNC meteorites: An indication for recent volcanism on Mars p 3387 N92-29038
EJECTORS
Air ejector experiments using the two-dimensional supersonic cascade tunnel: Zero secondary flow performance
[NAL-TM-632] p 3241 N92-28829
ELASTIC BARS
Exploratory flexural power flow measurements on a bar
[NLR-TP-90178-U] p 3304 N92-29176
ELASTIC BUCKLING
The buckling behavior of a central crack in a plate under tension
[LR-667] p 3299 N92-28583
ELASTIC PLATES
The buckling behavior of a central crack in a plate under tension
[LR-667] p 3299 N92-28583
Modal analysis of plates using boundary integral equations
[NLR-TP-89211-U] p 3302 N92-28688
In-situ fault detection by the hybrid ray-mode method
[AD-A250213] p 3297 N92-29112
ELASTIC PROPERTIES
Prediction of composite material properties using two-dimensional finite element micromechanical analysis
[AD-A250300] p 3252 N92-28702
Energetics of nanoscale graphitic tubules
[AD-A250165] p 3252 N92-28917
ELASTIC WAVES
Analysis of constrained-layer damping of flexural and extensional waves in infinite, fluid-loaded plates
[AD-A247936] p 3304 N92-29081
ELASTOMERS
Multiphase structure of a segmented polyurethane: Effects of temperature and annealing
[AD-A247594] p 3262 N92-28250
Correlation between surface free energy and surface constitution
[AD-A246699] p 3262 N92-28291
Device for applying constant pressure to a surface
[NASA-CASE-GSC-13230-1] p 3294 N92-28754
ELECTRIC BATTERIES
Secondary Li battery incorporating 12-Crown-4 ether
[NASA-CASE-NPO-17922-1-CU] p 3280 N92-28753
ELECTRIC CHARGE
A generalization of the K-V equilibrium for an intense, relativistic beam propagating in a solenoid
[AD-A247067] p 3350 N92-28238
Quasi-regular impurity distribution driven by charge-density wave
[DE92-622799] p 3363 N92-28281
The effect of induced charges on low-energy particle trajectories near conducting and semiconducting plates
[NASA-TM-103589] p 3355 N92-28986
ELECTRIC CONNECTORS
A sur.ey of high density packaging for high performance computing system
[AD-A248633] p 3332 N92-28891
ELECTRIC CONTACTS
The processing of high temperature ceramic superconducting devices, volume 2
[AD-A248159] p 3281 N92-28948
ELECTRIC CURRENT
Arcjet plume ionization effects on exposed solar array conducting surfaces
[AD-A245912] p 3307 N92-28383
Assessment of valve actuator motor rotor degradation by Fourier Analysis of current waveform
[DE92-013233] p 3281 N92-28814
ELECTRIC EQUIPMENT
Life cycle costs of the C-130 electrical power system upgrade
[AD-A246759] p 3221 N92-28348
ELECTRIC GENERATORS
High power microwave generator
[AD-D015262] p 3277 N92-29199
ELECTRIC MOTOR VEHICLES
Electromechanical systems with transient high power response operating from a resonant AC link
[NASA-TM-105716] p 3238 N92-28985
ELECTRIC MOTORS
Taguchi methods in electronics: A case study
[NASA-TM-103586] p 3279 N92-28456
Assessment of valve actuator motor rotor degradation by Fourier Analysis of current waveform
[DE92-013233] p 3281 N92-28814
The processing of high temperature ceramic superconducting devices, volume 2
[AD-A248159] p 3281 N92-28948
ELECTRIC NETWORKS
Investigation of an equivalent circuit for the inductive strip in finline with dielectric
[AD-A247025] p 3279 N92-28373
ELECTRIC POTENTIAL
SPEAR 2 space power data analysis
[AD-A248057] p 3250 N92-28945
Method and apparatus for frequency spectrum analysis
[NASA-CASE-NPO-17759-1-CU] p 3276 N92-29124
ELECTRIC POWER PLANTS
Geothermal Progress Monitor, report No. 13
[DE92-010697] p 3307 N92-28422
ELECTRIC POWER SUPPLIES
Mobile electric power
[AD-A249354] p 3279 N92-28326
Limiting factors to advancing thermal battery technology for naval applications
[AD-A247773] p 3280 N92-28568
ELECTRIC PROPULSION
Development and flight history of SERT 2 spacecraft
[NASA-TM-105636] p 3250 N92-28983
ELECTRIC SWITCHES
Neutron, gamma ray, and temperature effects on the electrical characteristics of thyristors
[NASA-TM-105728] p 3279 N92-28432
ELECTRIC WELDING
High temperature solder device for flat cables
[NASA-CASE-GSC-13344-1] p 3261 N92-29094
ELECTRICAL IMPEDANCE
Aperture coupling measurement in a test chamber for the Advanced Photon Source (APS)
[DE92-013059] p 3274 N92-28809
RF impedance measurement status for the 7-GeV Advanced Photon Source (APS)
[DE92-013060] p 3274 N92-28810
ELECTRICAL MEASUREMENT
Method and apparatus for frequency spectrum analysis
[NASA-CASE-NPO-17759-1-CU] p 3276 N92-29124
ELECTRICAL PROPERTIES
Neutron, gamma ray, and temperature effects on the electrical characteristics of thyristors
[NASA-TM-105728] p 3279 N92-28432
Magnetic and electromagnetic induction effects in the annual means of geomagnetic elements p 3301 N92-28632
Simulations of solvent effects on confined electrolytes
[AD-A246851] p 3258 N92-28982
ELECTRICAL RESISTANCE
Effect of alumina particle additions on the aging kinetics of 2014-aluminum matrix composites
[AD-A245949] p 3252 N92-28898
ELECTRICAL RESISTIVITY
Percolation conductivity of Penrose tiling by transfer-matrix Monte Carlo
[DE92-622792] p 3362 N92-28231
Synthesis and characterization of new low-dimensional transition metal complex conductors
[AD-A249263] p 3258 N92-28237
Fluids at high shock pressures and temperatures
[DE92-010709] p 3283 N92-28269
ELECTRO-OPTICS
Coincident pulse techniques for hybrid electronic optical computer systems
[AD-A246774] p 3332 N92-28514
Fiber-optic interconnection networks for spacecraft
[NASA-CR-190531] p 3358 N92-28698
Monolithic optoelectronic implementation of neural planes
[AD-A250286] p 3345 N92-28970
ELECTROACOUSTIC TRANSDUCERS
In line optical fibre frequency shifter project
[AD-A246714] p 3357 N92-28372

ELECTROCHEMICAL CELLS
Trade study of three oxygen processors for the Martian atmosphere
[AD-A246854] p 3372 N92-28393
ELECTROCHEMICAL OXIDATION
Surface crystallographic dependence of voltammetric oxidation of polyhydric alcohols and related systems at monocrystalline gold-acidic aqueous interfaces
[AD-A246763] p 3363 N92-28392
ELECTROCHEMISTRY
The evaluation of rate constants for rapid electrode reactions by using microelectrode voltammetry: Virtues of measurement at lower temperature
[AD-A246760] p 3255 N92-28391
ELECTRODEPOSITION
Review and update on electrocomposites
[AD-A248050] p 3251 N92-28303
Electrodeposition of high temperature superconductors
[AD-A250171] p 3365 N92-28919
ELECTRODES
Microhole array electrodes based on microporous alumina membranes
[AD-A247082] p 3278 N92-28239
The evaluation of rate constants for rapid electrode reactions by using microelectrode voltammetry: Virtues of measurement at lower temperature
[AD-A246760] p 3255 N92-28391
The emergence of atomic-level structural information for ordered metal-solution interfaces: Some recent contributions from in-situ infrared spectroscopy and scanning tunneling microscopy
[AD-A246765] p 3364 N92-28512
High temperature solder device for flat cables
[NASA-CASE-GSC-13344-1] p 3261 N92-29094
ELECTROLUMINESCENCE
Single layer multi-color luminescent display and method of making
[NASA-CASE-LAR-13616-3] p 3359 N92-29158
ELECTROLYSIS
Water electrolysis
[NASA-CASE-MSC-21572-1-SB] p 3256 N92-28756
ELECTROLYTES
Weighted-density functional approach for the solid-liquid interfaces in electrolytes
[DE92-622662] p 3362 N92-28280
Secondary Li battery incorporating 12-Crown-4 ether
[NASA-CASE-NPO-17922-1-CU] p 3280 N92-28753
Simulations of solvent effects on confined electrolytes
[AD-A246851] p 3258 N92-28982
ELECTROLYTIC CELLS
Trade study of three oxygen processors for the Martian atmosphere
[AD-A246854] p 3372 N92-28393
Water electrolysis
[NASA-CASE-MSC-21572-1-SB] p 3256 N92-28756
ELECTROMAGNETIC ABSORPTION
The influence of the resonant electromagnetic field on the light absorption by exciton and biexciton in quantum wells
[DE92-622801] p 3366 N92-28232
Impact on the medium MTF by model estimation of beta
[AD-A247985] p 3359 N92-29167
ELECTROMAGNETIC COUPLING
Large-area, plasma-assisted, halogen-based diamond deposition
[AD-A247423] p 3264 N92-28904
ELECTROMAGNETIC FIELDS
The influence of the resonant electromagnetic field on the light absorption by exciton and biexciton in quantum wells
[DE92-622801] p 3366 N92-28232
Comparison of various techniques in the analysis of waveguide transitions
[AD-A247019] p 3279 N92-28367
Unwrapping two-dimensional phase data in contour maps
[AD-A249988] p 3338 N92-28795
Present status of computational tools for Maglev development
[DE92-013252] p 3294 N92-28815
Hydrodynamic echo in strongly inhomogeneous magnetized plasma
[DE92-621530] p 3361 N92-28816
Analysis of electromagnetic propagation over variable terrain using the parabolic wave equation
[AD-A248061] p 3276 N92-28947
ELECTROMAGNETIC INTERACTIONS
Electroproduction of light quark baryons
[DE92-010853] p 3354 N92-28337
ELECTROMAGNETIC NOISE
Fundamental noise limits in miniature acoustic and vibration sensors
[AD-A247016] p 3352 N92-28413
ELECTROMAGNETIC PROPULSION
A momentum limit for electromagnetic railguns
[DE92-011380] p 3245 N92-28861
ELECTROMAGNETIC PULSES
CO2 laser frequency multiplication
[AD-A245915] p 3290 N92-28761
Big Sky Workshop on Super-Intense Laser-Atom Physics
[AD-A248225] p 3292 N92-29223
ELECTROMAGNETIC PUMPS
Heat exchanger with oscillating flow
[NASA-CASE-LAR-14033-1] p 3284 N92-28752
ELECTROMAGNETIC RADIATION
Coupled structural/thermal/electromagnetic analysis/tailoring of graded composite structures
[NASA-CR-189153] p 3298 N92-28296
ELECTROMAGNETIC SCATTERING
Scattering and radiation analysis of three-dimensional cavity arrays via a hybrid finite element method
[NASA-CR-190408] p 3273 N92-28371
Studies of the polarimetric dependence of enhanced backscattering from one-dimensional surfaces
[AD-A248431] p 3275 N92-28878
ELECTROMAGNETIC WAVE TRANSMISSION
Comparison of electromagnetic propagation predictions from IREPS and RPO across a coastal transition
[AD-A249331] p 3273 N92-28357
Analysis of electromagnetic propagation over variable terrain using the parabolic wave equation
[AD-A248061] p 3276 N92-28947
ELECTROMAGNETISM
Present status of computational tools for Maglev development
[DE92-013252] p 3294 N92-28815
ELECTROMAGNETS
Digital control algorithms for microgravity isolation systems p 3267 N92-28445
M-H characteristics and demagnetization resistance of samarium-cobalt permanent magnets to 300 C
[NASA-CR-189194] p 3280 N92-28723
Payload retention device
[NASA-CASE-MSC-21906-1] p 3294 N92-28727
Method and apparatus for using magneto-acoustic remanence to determine embrittlement
[NASA-CASE-LAR-13817-5] p 3303 N92-28757
Magnetic remanence method and apparatus to test materials for embrittlement
[NASA-CASE-LAR-13817-4] p 3304 N92-29101
ELECTROMECHANICAL DEVICES
Electromechanical systems with transient high power response operating from a resonant AC link
[NASA-TM-105716] p 3238 N92-28985
ELECTROMECHANICS
Payload retention device
[NASA-CASE-MSC-21906-1] p 3294 N92-28727
ELECTRON ATTACHMENT
Theoretical studies of the electronic and resonance structure of atomic and molecular negative ions
[AD-A247093] p 3354 N92-28259
ELECTRON BEAMS
A generalization of the K-V equilibrium for an intense, relativistic beam propagating in a solenoid
[AD-A247067] p 3350 N92-28238
Intense electron beam cyclotron masers with microsecond pulselengths
[AD-A247060] p 3289 N92-28271
Gadolinium metastable states population distributions and atomic density under high-rate electron beam evaporation
[DE92-782008] p 3363 N92-28282
Image processing for failure analysis of integrated circuits by an electron beam
[ETN-92-91322] p 3281 N92-28784
High resolution electron beam lithography on x ray mask substrates. Effects of electron scattering and membrane heating
[ETN-92-91336] p 3272 N92-28793
Plasma beam measurements
[AD-A247892] p 3362 N92-28962
The measuring assembly for the NPL primary standard absorbed dose graphite calorimeter at therapy levels
[NPL-RSA(EXT)-23] p 3288 N92-29163
Some experiments to determine the efficiency of collection of alumina particles by electron beam button melting in a nickel-base superalloy, AP1
[NPL-DMM(A)-42] p 3261 N92-29164
ELECTRON DENSITY (CONCENTRATION)
Arcjet plume ionization effects on exposed solar array conducting surfaces
[AD-A245912] p 3307 N92-28383
Plasma beam measurements
[AD-A247892] p 3362 N92-28962
ELECTRON DENSITY PROFILES
Microwave interactions with plasmas
[AD-A250333] p 3362 N92-29093
ELECTRON MICROSCOPY
Effect of alumina particle additions on the aging kinetics of 2014-aluminum matrix composites
[AD-A245949] p 3252 N92-28898
ELECTRON ORBITALS
High quality Gaussian basis sets for fourth-row atoms
[NASA-TM-103918] p 3255 N92-28743
ELECTRON PHONON INTERACTIONS
Physics and technology for the investigation of properties of ultra small systems
[AD-A246772] p 3364 N92-28513
ELECTRON PLASMA
Plasma beam measurements
[AD-A247892] p 3362 N92-28962
ELECTRON SCATTERING
Scattering mechanisms for semiconductor transport calculations
[AD-A249260] p 3278 N92-28295
Resonant Compton scattering in models of gamma ray burst sources
[DE92-010720] p 3397 N92-28336
High resolution electron beam lithography on x ray mask substrates. Effects of electron scattering and membrane heating
[ETN-92-91336] p 3272 N92-28793
ELECTRON STATES
Relaxation dynamics of highly excited halogens in their electronic ground states
[AD-A247312] p 3254 N92-28300
Electronic structure of fullerene tubules
[AD-A250166] p 3253 N92-28918
ELECTRON TRANSFER
Dynamical solvent effects on activated electron-transfer reactions: Principles, pitfalls, and progress
[AD-A246764] p 3363 N92-28349
ELECTRON TRANSITIONS
Macrocyclic polycation complexes for secondary anion binding, molecular recognition, and catalysis
[AD-A246890] p 3254 N92-28287
ELECTRONIC EQUIPMENT
Effects of fading and data modulation on noncoherent M-sequence acquisition schemes
[AD-A247968] p 3276 N92-29084
ELECTRONIC MAIL
The Father Christmas worm
[NASA-TM-107938] p 3334 N92-28267
ELECTRONIC MODULES
Applications of silicon hybrid multi-chip modules to avionics p 3235 N92-28379
ELECTRONIC PACKAGING
Calculation of chip temperatures using ELLPACK
[AD-A247156] p 3335 N92-28519
A survey of high density packaging for high performance computing system
[AD-A248633] p 3332 N92-28891
ELECTRONICS
Sol-gel processed multifunctional organic polymer-inorganic oxide composites for electronics and photonics
[AD-A246773] p 3263 N92-28412
ELECTRONS
Scattering mechanisms for semiconductor transport calculations
[AD-A249260] p 3278 N92-28295
Numerical studies of low temperature gallium arsenide buffer layers and their influence on device operation
[AD-A250309] p 3258 N92-29126
ELECTROPHORESIS
Controlled method of reducing electrophoretic mobility of macromolecules, particles, or cells
[NASA-CASE-MFS-26049-2-NP] p 3255 N92-28728
ELECTROPHYSIOLOGY
The Coordinated Noninvasive Studies (CNS) project, phase 1
[AD-A247159] p 3324 N92-28397
ELECTROSTATIC PROBES
Empirical techniques for the study of acceleration mechanisms in the space environment
[AD-A249940] p 3248 N92-28765
ELECTROSTATICS
Simulations of solvent effects on confined electrolytes
[AD-A246851] p 3258 N92-28982
ELEMENTARY PARTICLE INTERACTIONS
Electroproduction of light quark baryons
[DE92-010853] p 3354 N92-28337
The 17 keV neutrino and neutrino tagging
[DE92-011281] p 3355 N92-28839
ELEMENTARY PARTICLES
Electroproduction of light quark baryons
[DE92-010853] p 3354 N92-28337
The physics of strange matter
[DE92-011734] p 3371 N92-28774
ELEVATION
Topography of Apollinaris Patera and Ma'adim Vallis p 3393 N92-29069

ELLIPSES
Elliptical-core two mode fiber sensors and devices incorporating photoinduced refractive index gratings
[NASA-CR-190495] p 3358 N92-28868
ELLIPSOIDS
Adaptive set-membership identification in 0(m) time for linear-in-parameters models
[AD-A249359] p 3273 N92-28358
ELLIPTIC DIFFERENTIAL EQUATIONS
A fast direct solver for a class of two-dimensional separable elliptic equations on the sphere
[NASA-TM-104567] p 3346 N92-28297
Calculation of chip temperatures using ELLPACK
[AD-A247156] p 3335 N92-28519
EMBEDDED COMPUTER SYSTEMS
Transputer-based embedded system for Meteosat image data compression
[NLR-TP-90228-U] p 3305 N92-28697
EMBEDDING
Development of an embedded Fabry Perot Fiber Optic Strain Rosette Sensor (FP-FOSRS)
[NASA-CR-190490] p 3358 N92-29088
EMBRITTLEMENT
Method and apparatus for using magneto-acoustic remanence to determine embrittlement
[NASA-CASE-LAR-13817-5] p 3303 N92-28757
Magnetic remanence method and apparatus to test materials for embrittlement
[NASA-CASE-LAR-13817-4] p 3304 N92-29101
Magneto acoustic emission method for testing materials for embrittlement
[NASA-CASE-LAR-13817-2] p 3304 N92-29155
EMISSION
Observational study and analysis of point sources found by the infrared astronomy satellite
[AD-A248416] p 3371 N92-28843
EMISSION SPECTRA
Asynchronous optical sampling for laser-based combustion diagnostics in high-pressure flames
[AD-A250206] p 3257 N92-28896
Theoretical and experimental studies relevant to interpretation of auroral emissions
[NASA-CR-190521] p 3316 N92-28911
Atmospheric and surface temperatures and airborne dust amounts during late southern summer from Mariner 9 IRIS data p 3390 N92-29056
EMISSIVITY
The composition of Martian aeolian sands: Thermal emissivity from Viking IRTM observations
p 3382 N92-29010
EMITTANCE
ETO cloud studies for FIRE 2, part 1
[NASA-CR-190472] p 3319 N92-29087
EMITTERS
Design and realization of polysilicon emitter bipolar transistors
[LAAS-91360] p 3282 N92-29208
EMOTIONS
MoCog1: A computer simulation of recognition-primed human decision making, considering emotions
[NASA-TM-107859] p 3337 N92-28758
ENCAPSULATING
Review and update on electrocomposites
[AD-A248050] p 3251 N92-28303
END EFFECTORS
Dynamics motion simulation of the Hermes robot arm subjected to constraints
[NLR-TP-90282-U] p 3293 N92-28645
Rolling friction robot fingers
[NASA-CASE-GSC-13261-1] p 3296 N92-29138
ENERGETIC PARTICLES
Empirical techniques for the study of acceleration mechanisms in the space environment
[AD-A249940] p 3248 N92-28765
ENERGY BUDGETS
A new radiometer for Earth radiation budget studies
[DE92-011267] p 3306 N92-28834
ENERGY CONVERSION EFFICIENCY
CO2 laser frequency multiplication
[AD-A245915] p 3290 N92-28761
CO2 laser frequency multiplication
[AD-A247542] p 3291 N92-28933
ENERGY DISSIPATION
Experimental determination of dissipated energy density as a measure of strain-induced damage in composites
[AD-A250322] p 3253 N92-28953
ENERGY LEVELS
Multiple-valued programmable logic array minimization by simulated annealing
[AD-A248620] p 3335 N92-28353
Analysis of Mir-HEXE observations: Pulsation and energy spectra of the x ray double star SMC X-1 in 20 to 80 keV energy field
[ETN-92-91487] p 3371 N92-29128
ENERGY METHODS
Energetics of nanoscale graphitic tubules
[AD-A250165] p 3252 N92-28917
ENERGY POLICY
Geothermal Progress Monitor, report No. 13
[DE92-010697] p 3307 N92-28422
Identification and analysis of factors affecting the adoption of alternative transportation fuels
[PB92-164326] p 3266 N92-28914
ENERGY SPECTRA
Redistribution of subsurface neutrons caused by ground ice on Mars p 3374 N92-28488
Atmospheric turbulence spectra and correlation functions
[NLR-TP-89217-U] p 3316 N92-28689
Analysis of Mir-HEXE observations: Pulsation and energy spectra of the x ray double star SMC X-1 in 20 to 80 keV energy field
[ETN-92-91487] p 3371 N92-29128
Split events and their influence on pn CCD energy spectra
[ETN-92-91485] p 3282 N92-29178
ENERGY STORAGE
Solar thermal energy receiver
[NASA-CASE-LEW-14949-1] p 3307 N92-29143
ENERGY TECHNOLOGY
Identification and analysis of factors affecting the adoption of alternative transportation fuels
[PB92-164326] p 3266 N92-28914
ENERGY TRANSFER
Secondary instability in 3D magnetic reconnection
[AD-A248630] p 3360 N92-28354
Investigation of energy exchange mechanisms between the mean and acoustic flow fields in solid rocket combustion chambers
[AD-A247402] p 3250 N92-28931
Simulation of Martian surface-atmosphere interaction in a space-simulator: Technical considerations and feasibility p 3388 N92-29044
Pulse thermal energy transport/storage system
[NASA-CASE-LEW-15235-1] p 3287 N92-29125
Solar thermal energy receiver
[NASA-CASE-LEW-14949-1] p 3307 N92-29143
ENGINE AIRFRAME INTEGRATION
The application of flight simulation models in support of rotorcraft design and development
p 3222 N92-28527
ENGINE CONTROL
Integrated health monitoring and controls for rocket engines
[NASA-TM-105763] p 3249 N92-28693
ENGINE DESIGN
Steady and Transient Performance Prediction of Gas Turbine Engines
[AGARD-LS-183] p 3236 N92-28458
Overview on basis and use of performance prediction methods p 3237 N92-28459
Practical considerations in designing the engine cycle
p 3237 N92-28460
Component performance requirements
p 3237 N92-28462
Dynamic simulation of compressor and gas turbine performance p 3237 N92-28463
ENGINE MONITORING INSTRUMENTS
An overview of in-flight plume diagnostics for rocket engines
[NASA-TM-105727] p 3248 N92-28417
Engine performance and health monitoring models using steady state and transient prediction methods
p 3238 N92-28467
ENGINE PARTS
Calculation of installation effects within performance computer programs p 3237 N92-28465
Turbine aircraft engine operational trending and JT8D static component reliability study
[DOT/FAA/CT-91/10] p 3238 N92-28686
Introduction to rocket propulsion
[AD-A250424] p 3249 N92-28800
ENGINE TESTS
An overview of in-flight plume diagnostics for rocket engines
[NASA-TM-105727] p 3248 N92-28417
Rocket plume flowfield characterization using laser Rayleigh scattering
[NASA-TM-105739] p 3357 N92-28475
ENGINEERING MANAGEMENT
NASA engineers and the age of Apollo
[NASA-SP-4104] p 3397 N92-28344
ENVIRONMENT EFFECTS
The stress corrosion cracking behavior of AlLi 2090-T83 in substitute ocean water
[LR-661] p 3259 N92-28578
Paint removal using cryogenic processes
[AD-A247668] p 3264 N92-28912
Regional environmental impacts of methanol-fueled vehicles
[PB92-176569] p 3308 N92-29183
ENVIRONMENT MODELS
The Mars water cycle at other epochs: History of the polar caps and layered terrain p 3375 N92-28493
Regional environmental impacts of methanol-fueled vehicles
[PB92-176569] p 3308 N92-29183
ENVIRONMENT PROTECTION
Identification and analysis of factors affecting the adoption of alternative transportation fuels
[PB92-164326] p 3266 N92-28914
ENVIRONMENT SIMULATORS
Simulation of Martian surface-atmosphere interaction in a space-simulator: Technical considerations and feasibility p 3388 N92-29044
ENVIRONMENTAL SURVEYS
Micro weather stations for in situ measurements in the Martian planetary boundary layer p 3382 N92-29008
Mars Environmental Survey (MESUR): Science objectives and mission description p 3385 N92-29025
ENVIRONMENTAL TESTS
Environmental testing of the Xi Scan 1000, portable fluoroscopic and radiographic imaging system
[AD-A247167] p 3324 N92-28242
Reactions of hydrazines with chemicals found in environment
[AD-A247064] p 3308 N92-28272
ENZYMES
Conversion of acetic acid to methane by thermophiles
[DE92-010652] p 3257 N92-28942
EPITAXY
Heteroepitaxy of InP on Si (001)
[ETN-92-91333] p 3364 N92-28786
Stanford Center for research on superconductivity and superconductive electronics
[AD-A250204] p 3281 N92-29147
EPOXY MATRIX COMPOSITES
Fatigue strength of a glass fiber reinforced laminate structure
[VTT-RR-743] p 3251 N92-28573
Prediction of composite material properties using two-dimensional finite element micromechanical analysis
[AD-A250300] p 3252 N92-28702
Development of an embedded Fabry Perot Fiber Optic Strain Rosette Sensor (FP-FOSRS)
[NASA-CR-190490] p 3358 N92-29088
EPOXY RESINS
The effects of alumina trihydrate on the flammability characteristics of polyester, vinyl ester, and epoxy glass reinforced plastics
[AD-A247707] p 3264 N92-28563
Propellant-to-inhibitor bonding system
[AD-D015243] p 3266 N92-28739
EQUATIONS OF STATE
Fluids at high shock pressures and temperatures
[DE92-010709] p 3283 N92-28269
EQUATORIAL REGIONS
Thermally distinct ejecta blankets from Martian craters
p 3379 N92-28994
Physical properties of Deucalionis, Eos, Xanthe-type units in the central equatorial region of Mars
p 3392 N92-29063
Physical properties of Meridiani Sinus-type units in the central equatorial region of Mars p 3392 N92-29064
Physical properties of Oxia/Lunae Planum and Arabia-type units in the central equatorial region of Mars
p 3392 N92-29065
Surface photometric properties and albedo changes in the central equatorial region of Mars
p 3392 N92-29066
EQUATORS
Is ground ice stable near the Martian equator?
p 3389 N92-29046
EQUILIBRIUM METHODS
A continuation method for calculating the equilibrium positions of nonlinear structures
[ONERA-RT-24/3542-RY-091-R] p 3338 N92-28790
EQUIVALENT CIRCUITS
Investigation of an equivalent circuit for the inductive strip in finline with dielectric
[AD-A247025] p 3279 N92-28373
EROSION
CO2 and clathrate as past erosive agents on Mars
p 3375 N92-28497
Erosion of stainless steel by ultrasonic cleaning: A preliminary study
[DE92-012566] p 3260 N92-28763
Erosional landforms on the layered terrains in Valles Marineris p 3386 N92-29031
Mars atmosphere evolution: Escape to space
p 3387 N92-29034

ERROR ANALYSIS
Correlation, error-localisation, and updating of the second problem defined in GARTEUR AG11
[NLR-TP-90070-U] p 3302 N92-28650
A strategy for minimizing common mode human error in executing critical functions and tasks
[DE92-011839] p 3327 N92-28775
ERROR CORRECTING CODES
Coding for frequency hopped spread spectrum satellite communications
[ECE-90-1] p 3274 N92-28699
ERROR SIGNALS
Adaptive set-membership identification in 0(m) time for linear-in-parameters models
[AD-A249359] p 3273 N92-28358
ERRORS
Magnetic repeat station data p 3301 N92-28630
Turbine aircraft engine operational trending and JT8D static component reliability study
[DOT/FAA/CT-91/10] p 3238 N92-28686
Initial investigations of an adaptive discrete-time controller for nonlinear time-varying robotic models p 3247 N92-28736
Lapses in alertness: Brain-evoked responses to task-irrelevant auditory probes
[AD-A247669] p 3328 N92-28940
Analysis of electromagnetic propagation over variable terrain using the parabolic wave equation
[AD-A248061] p 3276 N92-28947
ERYTHROCYTES
Structural characterization of cross-linked hemoglobins developed as potential transfusion substitutes
[AD-A246777] p 3325 N92-28515
ESTIMATES
The variance of Rasch ability estimates from partially-known item parameters
[AD-A247065] p 3348 N92-28273
Neural network parameter estimation for the modified bistatic scattering strength model (BISSM)
[AD-A247913] p 3322 N92-28963
Estimation of the point of incipient deterioration and a class of life distribution with application to cannibalization
[AD-A250216] p 3343 N92-29114
ESTIMATING
Some aerospace applications of estimation theory
[ETN-92-91281] p 3349 N92-28647
Mass and power modeling of communication satellites
[NASA-CR-189186] p 3275 N92-28906
Curvature estimation in orientation selection
[AD-A247862] p 3328 N92-28957
ETCHING
Selective suppression of photochemical etching: Raman spectroscopy for pre-etch process selection
[DE92-010955] p 3255 N92-28341
ETHERS
Secondary Li battery incorporating 12-Crown-4 ether
[NASA-CASE-NPO-17922-1-CU] p 3280 N92-28753
Molecular engineering of liquid crystalline polymers by living cationic polymerization. 21: Synthesis and characterization of poly (3-((4-cyano-4'-biphenyl)oxy) propyl vinyl ether) macromonomers
[AD-A248305] p 3265 N92-29116
ETHICS
Responsible science: Ensuring the integrity of the research process, volume 1
[ISBN-0-309-04731-5] p 3350 N92-28363
ETHYLENE
Chain folding in EBEE semicrystalline diblock copolymers
[AD-A247595] p 3262 N92-28251
EULER EQUATIONS OF MOTION
Analysis of results of an Euler-equation method applied to leading-edge vortex flow
[NLR-TP-90368-U] p 3226 N92-28657
Development and validation of a characteristic boundary condition for a cell-centered Euler method
[NLR-TP-90144-U] p 3227 N92-28692
Boundary conditions for Euler equations at internal block faces of multi-block domains using local grid refinement
[NLR-TP-90134-U] p 3284 N92-28712
EULER-LAGRANGE EQUATION
Quasi-recursive dynamics equations for spacecraft-based flexible robotic manipulators
[NLR-TP-90028-U] p 3345 N92-28648
EUROPE
Analysis of the effects of Eurasian crustal and upper mantle structure on regional phases using broadband seismic data
[AD-A248383] p 3309 N92-28386
EVALUATION
Evaluation of drive simulator settings for DAF YA-4440
[FEL-91-B345] p 3241 N92-28828
EVAPORATION
Gadolinium metastable states population distributions and atomic density under high-rate electron beam evaporation
[DE92-782008] p 3363 N92-28282
A 2-D analysis of evaporation in laminar flow
[AD-A246467] p 3287 N92-28978
Is ground ice stable near the Martian equator? p 3389 N92-29046
EVAPORATION RATE
Modelling of heat and moisture loss through NBC ensembles
[AD-A245939] p 3329 N92-28346
Is ground ice stable near the Martian equator? p 3389 N92-29046
EVAPORATORS
Pulse thermal energy transport/storage system
[NASA-CASE-LEW-15235-1] p 3287 N92-29125
EVENTS
Split events and their influence on pn CCD energy spectra
[ETN-92-91485] p 3282 N92-29178
EXCIMER LASERS
Degenerate four-wave mixing using a tunable excimer laser to detect combustion gases
[DE92-005327] p 3290 N92-28852
EXCITATION
Relaxation dynamics of highly excited halogens in their electronic ground states
[AD-A247312] p 3254 N92-28300
EXCITONS
The influence of the resonant electromagnetic field on the light absorption by exciton and biexciton in quantum wells
[DE92-622801] p 3366 N92-28232
EXHAUST SYSTEMS
Internal reversing flow in a tailpipe offtake configuration for SSTOVL aircraft
[NASA-TM-105698] p 3236 N92-28418
EXOBIOLOGY
Space life sciences strategic plan
[NASA-TM-107954] p 3244 N92-29100
EXOSPHERE
Dust storm driven variations of the Mars thermosphere and exosphere: Coupling of atmospheric regions p 3380 N92-28997
The ancient oxygen exosphere of Mars: Implications for atmosphere evolution p 3395 N92-29080
EXOTHERMIC REACTIONS
Kinetic studies of metal combustion in propulsion
[AD-A250207] p 3256 N92-28769
The compositional structure and the effects of exothermicity in an unpremixed planar jet flame p 3258 N92-28821
EXPANDABLE STRUCTURES
Flow rate testing of valves used with the 500 gallon collapsible drum
[AD-A250567] p 3294 N92-28924
EXPERIMENTATION
Evidences for the terrestrial magma ocean from high-pressure melting experiments p 3315 N92-28613
EXPERT SYSTEMS
A system structure for predictive relations in penetration mechanics
[AD-A246453] p 3292 N92-28284
Validation of knowledge based systems
[AD-A247741] p 3368 N92-28404
Application of knowledge-based systems for diagnosis of aircraft systems
[NLR-TP-90192-U] p 3230 N92-28655
PC graphics generation and management tool for real-time applications
[NASA-TM-105749] p 3337 N92-28684
Knowledge-based material selection in design
[PNR-90823] p 3337 N92-28741
Learning and tuning fuzzy logic controllers through reinforcements
[NASA-TM-107875] p 3345 N92-28759
Representation of neutron noise data using neural networks
[DE92-013232] p 3356 N92-28813
Investigations of logic of introspection and related modes of reasoning with applications
[AD-A249286] p 3345 N92-28895
SPEEDS: An approach to support programming environments using expert database systems
[AD-A247469] p 3339 N92-28943
Air combat maneuvering expert system trainer
[AD-A246459] p 3241 N92-28975
Acquisition and improvement of human motor skills: Learning through observation and practice
[NASA-TM-107878] p 3329 N92-29174
Building the Scientific Modeling Assistant: An interactive environment for specialized software design
[NASA-TM-107844] p 3346 N92-29175
EXPLOSIONS
Underwater vapor phase burning of aluminum particles and on aluminum ignition during steam explosions
[DE92-011196] p 3257 N92-28894
Modular simulation of HEI fragments and blast pressure
[AD-A248205] p 3272 N92-29191
EXPLOSIVE WELDING
EXPLOMET 90 international conference on shock-wave and high-strain-rate phenomena in materials
[AD-A248665] p 3303 N92-28892
EXPOSURE
Arcjet plume ionization effects on exposed solar array conducting surfaces
[AD-A245912] p 3307 N92-28383
The chronic effects of JP-8 jet fuel exposure on the lungs
[AD-A250308] p 3326 N92-29123
EXPULSION
How Mars lost its atmosphere p 3378 N92-28509
EXTERNAL STORES
Calculation of unsteady subsonic and supersonic flow about oscillating wings and bodies by new panel methods
[NLR-TP-89119-U] p 3227 N92-28659
Wing-extendible gliding store
[AD-D015233] p 3234 N92-28987
EXTINCTION
An evaluation of the naval oceanic vertical aerosol model during Key90
[AD-A245943] p 3320 N92-28318
How Mars lost its atmosphere p 3378 N92-28509
EXTRATERRESTRIAL LIFE
Liquid water habitats on early Mars p 3376 N92-28500
Iron Moessbauer spectroscopy: Superparamagnetism in hydrothermal vents and the search for evidence of past life on Mars p 3378 N92-28989
EXTRAVEHICULAR ACTIVITY
Removable hand hold
[NASA-CASE-LEW-15196-1] p 3295 N92-29092
EXTREME ULTRAVIOLET RADIATION
Mars atmosphere evolution: Escape to space p 3387 N92-29034
EXTREMELY HIGH FREQUENCIES
Surface vs. atmospheric origin of 2.1-2.5 micron absorption features in the Martian spectrum p 3373 N92-28480
EXTREMELY LOW RADIO FREQUENCIES
Seafloor pressure array studies at ultra-low frequencies
[AD-A247663] p 3322 N92-28939
EYE (ANATOMY)
Portable dynamic fundus instrument
[NASA-CASE-MSC-21675-1] p 3325 N92-28755
Non-linear analysis of visual cortical neurons
[AD-A250233] p 3326 N92-29179
EYE MOVEMENTS
Program Cluster: An identification of fixation cluster characteristics
[AD-A247014] p 3326 N92-28396

F

F-111 AIRCRAFT
Reduction and analysis of F-111C flight data
[AD-A250341] p 3233 N92-28771
F-16 AIRCRAFT
Improvement of separations of practice bombs from a multiple bomb adapter
[NLR-TP-90307-U] p 3232 N92-28634
Modifications and results of flight tests of a practice bomb adapter
[NLR-TP-90108-U] p 3233 N92-28651
F-18 AIRCRAFT
Use of high-fidelity simulation in the development of an F/A-18 active ground collision avoidance system p 3222 N92-28530
Identification of aerodynamic models for maneuvering aircraft
[NASA-CR-190444] p 3233 N92-28720
Tasking and communication flows in the F/A-18D cockpit: Issues, problems, and possible solutions
[AD-A245977] p 3234 N92-28802
FABRICATION
Method fabricating load-bearing composites free from microbuckling deformation up to a predetermined load
[AD-D015212] p 3250 N92-28224
FABRICS
Performance of uncoated AFRSI blankets during multiple Space Shuttle flights
[NASA-TM-103892] p 3245 N92-29104

FADING
Effects of fading and data modulation on noncoherent M-sequence acquisition schemes
[AD-A247968] p 3276 N92-29084
FAILURE
Cryogenic system operating experience review for fusion applications
[DE92-012509] p 3361 N92-28805
FAILURE ANALYSIS
Mechanisms of fracture and creep of structural alloys
[AD-A248701] p 3259 N92-28390
Study of high temperature failure mechanism in ceramics
[AD-A247018] p 3263 N92-28415
Image processing for failure analysis of integrated circuits by an electron beam
[ETN-92-91322] p 3281 N92-28784
Assessment of valve actuator motor rotor degradation by Fourier Analysis of current waveform
[DE92-013233] p 3281 N92-28814
Stress analysis of plated-through-holes in rigid flex multilayer printed wiring boards
[DE92-011659] p 3303 N92-28855
Tensile and interlaminar properties of GLARE (trade name) laminates
[AD-A250188] p 3253 N92-28921
FAILURE MODES
Study of high temperature failure mechanism in ceramics
[AD-A247018] p 3263 N92-28415
Assessment of valve actuator motor rotor degradation by Fourier Analysis of current waveform
[DE92-013233] p 3281 N92-28814
FALLOUT
Determination of field related transfer factors for Cs-137 and Sr-90, from the fallout of the reactor accident in Chernobyl (USSR)
[OEFZS-4581] p 3356 N92-29210
FAR FIELDS
Method and apparatus for phasing segmented mirror arrays
[NASA-CASE-NPO-18095-1-CU] p 3359 N92-29122
FAR ULTRAVIOLET RADIATION
The ultraviolet albedo of Mars p 3394 N92-29074
FARM CROPS
A study of the control problem of the shoot side environment delivery system of a closed crop growth research chamber
[NASA-CR-177597] p 3330 N92-28681
FAST FOURIER TRANSFORMATIONS
Diagonal forms of translation operators for helmholtz equation in three dimensions
[AD-A248422] p 3348 N92-28949
FAST NEUTRONS
Neutron, gamma ray, and temperature effects on the electrical characteristics of thyristors
[NASA-TM-105728] p 3279 N92-28432
FATIGUE (MATERIALS)
The mechanical property data base from an Air Force/industry cooperative test program on advanced aluminum alloys (IN905XL and AL905XL forgings)
[AD-A247752] p 3368 N92-28565
Fatigue strength of a glass fiber reinforced laminate structure
[VTT-RR-743] p 3251 N92-28573
Generation of spectra and stress histories for fatigue and damage tolerance analysis of fuselage repairs
[AD-A250390] p 3235 N92-29180
FATIGUE LIFE
A sensitivity analysis on component reliability from fatigue life computations
[AD-A247430] p 3297 N92-28425
Elevated temperature axial and torsional fatigue behavior of Haynes 188
[NASA-TM-105396] p 3302 N92-28701
FATIGUE TESTS
Nondestructive evaluation of damages caused by impact and fatigue loading of polymer composites
[VTT-RR-742] p 3251 N92-28572
Fatigue strength of a glass fiber reinforced laminate structure
[VTT-RR-743] p 3251 N92-28573
Growth of surface cracks under fatigue loading: A literature survey
[LR-664] p 3299 N92-28580
Spacecraft sustained load fracture control
[NLR-TP-89163-U] p 3302 N92-28643
Elevated temperature axial and torsional fatigue behavior of Haynes 188
[NASA-TM-105396] p 3302 N92-28701
FAULT TOLERANCE
Femtosecond carrier processes in compound semiconductors and real time signal processing
[AD-A248053] p 3278 N92-28275
Integration of tools for the Design and Assessment of High-Performance, Highly Reliable Computing Systems (DAHPHRS), phase 1
[NASA-CR-189621] p 3336 N92-28585
DEPEND: A simulation-based environment for system level dependability analysis
[NASA-CR-189752] p 3297 N92-28726
Payload retention device
[NASA-CASE-MSC-21906-1] p 3294 N92-28727
Fault-tolerant parallel computer systems for real-time applications
[AD-A247887] p 3343 N92-28958
FEASIBILITY ANALYSIS
Organizing plan libraries in subsumption hierarchies: Specificity based plan selection
[AD-A248711] p 3368 N92-28430
Feasibility study of hypersonic clinometric measurements at R3Ch
[ONERA-RSF-136/1865-AY-728-] p 3228 N92-28789
Evaluation of future space transportation systems with regard to their reliabilities and costs
[DLR-FB-91-27] p 3245 N92-28826
The design of test-section inserts for higher speed aeroacoustic testing in the Ames 80- by 120-foot wind tunnel
[NASA-TM-103915] p 3353 N92-28909
Compact, self-contained ArF lasers
[AD-A247403] p 3291 N92-28932
Micro weather stations for in situ measurements in the Martian planetary boundary layer p 3382 N92-29008
Mars Environmental Survey (MESUR): Science objectives and mission description p 3385 N92-29025
Technological enhancements for personal computers
[AD-A247962] p 3333 N92-29083
Feasibility of metal-oxide-semiconductor structures on Si-LPCVD thin films by low temperature (600 C) process
[LAAS-91307] p 3365 N92-29207
FEEDBACK
Nonlinear sloshing and the coupled dynamics of liquid propellants and spacecraft
[AD-A250023] p 3248 N92-28967
FEEDBACK CONTROL
Control and stabilization of distributed parameter systems in structural dynamics
[AD-A247097] p 3298 N92-28320
Adaptive and nonlinear control
[AD-A248580] p 3344 N92-28429
Digital control algorithms for microgravity isolation systems p 3267 N92-28445
Dynamic control of aerodynamic instabilities in gas turbine engines p 3238 N92-28466
Integrated health monitoring and controls for rocket engines
[NASA-TM-105763] p 3249 N92-28693
Identification of linear system models and state estimators for controls p 3247 N92-28737
Closed-loop autonomous docking system
[NASA-CASE-MFS-28421-1] p 3248 N92-28750
Heat exchanger with oscillating flow
[NASA-CASE-LAR-14033-1] p 3284 N92-28752
Superconducting bearings with levitation control configurations
[NASA-CASE-GSC-13346-1] p 3295 N92-29099
Control of nonlinear distributed parameter systems with application to flow control
[AD-A250212] p 3346 N92-29149
Ultra-high temperature stability Joule-Thomson cooler with capability to accomodate pressure variations
[NASA-CASE-NPO-18184-1-CU] p 3288 N92-29156
FEEDFORWARD CONTROL
Learning and tuning fuzzy logic controllers through reinforcements
[NASA-TM-107875] p 3345 N92-28759
FELDSPARS
The three stages of magma ocean cooling p 3315 N92-28617
FEMALES
The energetics and mechanics of load carrying
[AD-A248441] p 3332 N92-29227
FERROCENES
Orthogonal self-assembly of redox active molecules on Pt and Au: Selective reaction of disulfide with Au and isonitrile with Pt
[AD-A246698] p 3254 N92-28290
FIBER COMPOSITES
Micromechanics of defects
[AD-A248432] p 3251 N92-28307
Simple computer programs for the design and sizing of fiber reinforced composites
[NLR-TP-91050-U] p 3252 N92-28637
Prediction of composite material properties using two-dimensional finite element micromechanical analysis
[AD-A250300] p 3252 N92-28702
Tensile and interlaminar properties of GLARE (trade name) laminates
[AD-A250188] p 3253 N92-28921
Development of a stratified plate model for composite panels
[AD-A248206] p 3253 N92-29192
FIBER OPTICS
Three-axis fiber optic vector magnetometer
[AD-D015199] p 3357 N92-28223
In line optical fibre frequency shifter project
[AD-A246714] p 3357 N92-28372
Fiber-optic interconnection networks for spacecraft
[NASA-CR-190531] p 3358 N92-28698
Null shifting with fixed delays
[AD-A250059] p 3274 N92-28796
Development of an embedded Fabry Perot Fiber Optic Strain Rosette Sensor (FP-FOSRS)
[NASA-CR-190490] p 3358 N92-29088
Multi-channel fiber optic rotary joint for single-mode fiber
[AD-D015273] p 3358 N92-29095
FIBERS
Method of intercalating large quantities of fibrous structures
[NASA-CASE-LEW-15077-1] p 3253 N92-29152
FIELD EFFECT TRANSISTORS
Leakage current measurements in SOI devices
[AD-A247694] p 3280 N92-28561
Operation and radiation resistance of a FOXFET biasing structure for silicon strip detectors
[DE92-011279] p 3282 N92-29197
FIELD THEORY (PHYSICS)
Classical and quantum Liouville theory on the Riemann sphere with n greater than 3 punctures (II)
[DE92-622380] p 3366 N92-28227
The exchange algebra for Liouville theory on punctured Riemann sphere
[DE92-622409] p 3366 N92-28229
Inverse phase transitions: Does baryogenesis lead to dark matter?
[DE92-013022] p 3372 N92-29184
FIGHTER AIRCRAFT
Development and evaluation of an attack and maneuvering system with combat development simulators as main development tool p 3224 N92-28541
The role of simulation for the study of APIS (piloting support by synthetic imagery) p 3224 N92-28544
Application of piloted simulation to high-angle-of-attack flight-dynamics research for fighter aircraft p 3225 N92-28551
Flow visualization studies of a sideslipping, canard-configured X-31A-Like fighter aircraft model
[AD-A245940] p 3228 N92-28883
FILTERS
PROPX: An x ray manipulation program
[DE92-011264] p 3334 N92-28309
FILTRATION
Microhole array electrodes based on microporous alumina membranes
[AD-A247082] p 3278 N92-28239
FINES
Mars surface weathering products and spectral analogs: Palagonites and synthetic iron minerals p 3383 N92-29017
Determining the pH of Mars from the Viking labelled release reabsorption effect p 3389 N92-29049
FINITE DIFFERENCE THEORY
Calculation of chip temperatures using ELLPACK
[AD-A247156] p 3335 N92-28519
FINITE ELEMENT METHOD
Coupled structural/thermal/electromagnetic analysis/tailoring of graded composite structures
[NASA-CR-189153] p 3298 N92-28296
Modeling radiation forces acting on TOPEX/Poseidon for precision orbit determination
[NASA-TM-104564] p 3244 N92-28343
Probabilistic finite element analysis
[AD-A247721] p 3347 N92-28399
Practical architecture of design optimisation software for aircraft structures taking the MBB-Lagrange code as an example p 3232 N92-28471
The buckling behavior of a central crack in a plate under tension
[LR-667] p 3299 N92-28583
Correlation, error-localisation, and updating of the second problem defined in GARTEUR AG11
[NLR-TP-90070-U] p 3302 N92-28650
Prediction of composite material properties using two-dimensional finite element micromechanical analysis
[AD-A250300] p 3252 N92-28702
Modal element method for scattering of sound by absorbing bodies
[NASA-TM-105722] p 3353 N92-28984
FINITE VOLUME METHOD
Boundary conditions for Euler equations at internal block faces of multi-block domains using local grid refinement
[NLR-TP-90134-U] p 3284 N92-28712

FIRE CONTROL
Use of high-fidelity simulation in the development of an F/A-18 active ground collision avoidance system
p 3222 N92-28530
FIRE PREVENTION
Modular simulation of HEI fragments and blast pressure
[AD-A248205] p 3272 N92-29191
FIRING (IGNITING)
Automation and remote control instrumentation development: Rocket First Motion Timing System (RFMTS)
[AD-A249970] p 3287 N92-28767
FITTINGS
Reduction and analysis of F-111C flight data
[AD-A250341] p 3233 N92-28771
FLAME IONIZATION
Multicomponent comparison of optical and mass spectrometric diagnostics in low-pressure flames
[AD-A250323] p 3257 N92-28954
FLAME PROBES
Asynchronous optical sampling for laser-based combustion diagnostics in high-pressure flames
[AD-A250206] p 3257 N92-28896
FLAME PROPAGATION
The effects of alumina trihydrate on the flammability characteristics of polyester, vinyl ester, and epoxy glass reinforced plastics
[AD-A247707] p 3264 N92-28563
Stochastic simulation of the structure and propagation rate of turbulent premixed flames
[DE92-006682] p 3256 N92-28822
FLAME RETARDANTS
The effects of alumina trihydrate on the flammability characteristics of polyester, vinyl ester, and epoxy glass reinforced plastics
[AD-A247707] p 3264 N92-28563
FLAMES
Asynchronous optical sampling for laser-based combustion diagnostics in high-pressure flames
[AD-A250206] p 3257 N92-28896
FLAMMABILITY
The effects of alumina trihydrate on the flammability characteristics of polyester, vinyl ester, and epoxy glass reinforced plastics
[AD-A247707] p 3264 N92-28563
FLAPS (CONTROL SURFACES)
Flow gradient corrections on hot-wire measurements using an X-wire probe
[NLR-TP-90255-U] p 3228 N92-28713
FLAT SURFACES
A 2-D analysis of evaporation in laminar flow
[AD-A246467] p 3287 N92-28978
FLEXIBLE BODIES
Control and stabilization of distributed parameter systems in structural dynamics
[AD-A247097] p 3298 N92-28320
FLEXIBLE SPACECRAFT
Linear recursive formulation of flexible multi-body space system dynamics
[NLR-TP-90284-U] p 3293 N92-28646
Sensor filter designs for large flexible spacecraft
p 3247 N92-28733
Fuel optimal propulsive reboost of flexible spacecraft
p 3247 N92-28734
Fuel optimal maneuver: Experimental testbeds
p 3247 N92-28735
Identification of linear system models and state estimators for controls p 3247 N92-28737
FLIGHT CHARACTERISTICS
NPSNET: Flight simulation dynamic modeling using quaternions
[AD-A247484] p 3333 N92-28245
Flight simulation and digital flight controls
p 3221 N92-28526
Effects of cockpit lateral stick characteristics on handling qualities and pilot dynamics
[NASA-CR-4443] p 3239 N92-28584
In-flight simulation studies at the NASA Dryden Flight Research Facility
[NASA-TM-4396] p 3234 N92-29110
FLIGHT CONDITIONS
Practical considerations in designing the engine cycle
p 3237 N92-28460
Thermal response of rigid and flexible insulations and reflective coating in an aeroconvective heating environment
[NASA-TM-103925] p 3233 N92-28721
FLIGHT CONTROL
Utility of ground simulation in flight control problem identification, solution development, and verification
p 3221 N92-28525
Flight simulation and digital flight controls
p 3221 N92-28526
The application of flight simulation models in support of rotorcraft design and development
p 3222 N92-28527
Use of high-fidelity simulation in the development of an F/A-18 active ground collision avoidance system
p 3222 N92-28530
Use of simulation in the USAF Test Pilot School curriculum p 3223 N92-28535
Full mission simulation: A view into the future
p 3223 N92-28537
Development and evaluation of an attack and maneuvering system with combat development simulators as main development tool p 3224 N92-28541
Use of a research simulator for the development of new concepts of flight control p 3224 N92-28543
The role of systems simulation for the development and qualification of ATTAS p 3225 N92-28548
Effects of cockpit lateral stick characteristics on handling qualities and pilot dynamics
[NASA-CR-4443] p 3239 N92-28584
Stability and control flight testing of a half-scale Pioneer remotely piloted vehicle
[AD-A245973] p 3239 N92-28801
Rotorcraft In-Flight Simulation Research at NASA Ames Research Center: A Review of the 1980's and plans for the 1990's
[NASA-TM-103873] p 3234 N92-28926
In-flight simulation studies at the NASA Dryden Flight Research Facility
[NASA-TM-4396] p 3234 N92-29110
FLIGHT CREWS
An analysis of aircrew communication patterns and content
[AD-A246618] p 3272 N92-28253
Use of a commercially available flight simulator during aircrew performance testing
[AD-A245922] p 3240 N92-28407
G-tolerance and spatial disorientation: Can simulation help us? p 3223 N92-28534
Crew station research and development facility training for the light helicopter demonstration/validation program
[NASA-TM-103865] p 3327 N92-28744
FLIGHT OPERATIONS
Aircraft ship operations
[AGARD-AR-312] p 3231 N92-28468
The evaluation of simulator effectiveness for the training of high speed, low level, tactical flight operations
p 3223 N92-28539
FLIGHT SIMULATION
NPSNET: Flight simulation dynamic modeling using quaternions
[AD-A247484] p 3333 N92-28245
Correlational analysis of survey and model-generated workload values
[AD-A247153] p 3329 N92-28518
Piloted Simulation Effectiveness
[AGARD-CP-513] p 3221 N92-28522
Opportunities for flight simulation to improve operational effectiveness p 3221 N92-28523
Piloted simulation effectiveness development applications and limitations p 3221 N92-28524
Utility of ground simulation in flight control problem identification, solution development, and verification
p 3221 N92-28525
Flight simulation and digital flight controls
p 3221 N92-28526
The application of flight simulation models in support of rotorcraft design and development
p 3222 N92-28527
Experience with piloted simulation in the development of helicopters p 3222 N92-28528
Validation of simulation systems for aircraft acceptance testing p 3222 N92-28531
Aircraft simulation and pilot proficiency: From surrogate flying towards effective training p 3222 N92-28532
The use of a dedicated testbed to evaluate simulator training effectiveness p 3222 N92-28533
G-tolerance and spatial disorientation: Can simulation help us? p 3223 N92-28534
Use of simulation in the USAF Test Pilot School curriculum p 3223 N92-28535
AM-X flight simulator from engineering tool to training device p 3223 N92-28536
Full mission simulation for research and development of air combat flight and attack management systems
p 3223 N92-28538
The role of simulation for the study of APIS (piloting support by synthetic imagery) p 3224 N92-28544
The use of ground based simulation for handling qualities research: A new assessment p 3224 N92-28545
Initial validation of a R/D simulator with large amplitude motion p 3225 N92-28546
The use and effectiveness of piloted simulation in transport aircraft research and development
p 3225 N92-28549
Application of piloted simulation to high-angle-of-attack flight-dynamics research for fighter aircraft
p 3225 N92-28551
Effective cueing during approach and touchdown: Comparison with flight p 3226 N92-28552
Rotorcraft In-Flight Simulation Research at NASA Ames Research Center: A Review of the 1980's and plans for the 1990's
[NASA-TM-103873] p 3234 N92-28926
In-flight simulation studies at the NASA Dryden Flight Research Facility
[NASA-TM-4396] p 3234 N92-29110
FLIGHT SIMULATORS
Use of a commercially available flight simulator during aircrew performance testing
[AD-A245922] p 3240 N92-28407
Piloted Simulation Effectiveness
[AGARD-CP-513] p 3221 N92-28522
Opportunities for flight simulation to improve operational effectiveness p 3221 N92-28523
Piloted simulation effectiveness development applications and limitations p 3221 N92-28524
Utility of ground simulation in flight control problem identification, solution development, and verification
p 3221 N92-28525
Flight simulation and digital flight controls
p 3221 N92-28526
The application of flight simulation models in support of rotorcraft design and development
p 3222 N92-28527
Experience with piloted simulation in the development of helicopters p 3222 N92-28528
Use of simulation in the USAF Test Pilot School curriculum p 3223 N92-28535
AM-X flight simulator from engineering tool to training device p 3223 N92-28536
Full mission simulation: A view into the future
p 3223 N92-28537
Full mission simulation for research and development of air combat flight and attack management systems
p 3223 N92-28538
The evaluation of simulator effectiveness for the training of high speed, low level, tactical flight operations
p 3223 N92-28539
Harrier GR MK 5/7 mission simulators for the Royal Air Force p 3224 N92-28540
Development and evaluation of an attack and maneuvering system with combat development simulators as main development tool p 3224 N92-28541
Use of a research simulator for the development of new concepts of flight control p 3224 N92-28543
The use of ground based simulation for handling qualities research: A new assessment p 3224 N92-28545
Initial validation of a R/D simulator with large amplitude motion p 3225 N92-28546
The use and effectiveness of piloted simulation in transport aircraft research and development
p 3225 N92-28549
An evaluation of IFR approach techniques: Generic helicopter simulation compared with actual flight
p 3225 N92-28550
Effective cueing during approach and touchdown: Comparison with flight p 3226 N92-28552
Crew station research and development facility training for the light helicopter demonstration/validation program
[NASA-TM-103865] p 3327 N92-28744
The second flight simulator test of the head-up display for NAL QSTOL experimental aircraft (ASKA)
[NAL-TM-633] p 3331 N92-28831
Rotorcraft In-Flight Simulation Research at NASA Ames Research Center: A Review of the 1980's and plans for the 1990's
[NASA-TM-103873] p 3234 N92-28926
FLIGHT TEST INSTRUMENTS
Potential applications of laser Doppler anemometry for in-flight measurements
[NLR-TP-90163-U] p 3236 N92-28654
FLIGHT TEST VEHICLES
The role of systems simulation for the development and qualification of ATTAS p 3225 N92-28548
FLIGHT TESTS
Operational noise data for OH-58D Army helicopters
[AD-A246822] p 3351 N92-28292
Aircraft ship operations
[AGARD-AR-312] p 3231 N92-28468
Use of high-fidelity simulation in the development of an F/A-18 active ground collision avoidance system
p 3222 N92-28530
Validation of simulation systems for aircraft acceptance testing p 3222 N92-28531
Use of simulation in the USAF Test Pilot School curriculum p 3223 N92-28535
An evaluation of IFR approach techniques: Generic helicopter simulation compared with actual flight
p 3225 N92-28550

S-76B certification for vertical take-off and landing operations from confined areas
[NLR-TP-90286-U] p 3233 N92-28714
Reduction and analysis of F-111C flight data
[AD-A250341] p 3233 N92-28771
Stability and control flight testing of a half-scale Pioneer remotely piloted vehicle
[AD-A245973] p 3239 N92-28801
Aerodynamic characteristics obtained from alpha sweep test of the quiet STOL experimental aircraft ASKA
[NAL-TR-1112] p 3234 N92-28901
A rotorcraft flight database for validation of vision-based ranging algorithms
[NASA-TM-103906] p 3231 N92-29103

FLIGHT TRAINING
Piloted Simulation Effectiveness
[AGARD-CP-513] p 3221 N92-28522
Opportunities for flight simulation to improve operational effectiveness p 3221 N92-28523
Piloted simulation effectiveness development applications and limitations p 3221 N92-28524
Utility of ground simulation in flight control problem identification, solution development, and verification p 3221 N92-28525
Aircraft simulation and pilot proficiency: From surrogate flying towards effective training p 3222 N92-28532

FLIR DETECTORS
Simulation in infrared imaging: Using electrical circuit principles to model heat transfer
[AD-A248290] p 3278 N92-28276

FLOAT ZONES
An examination of anticipated g-jitter on Space Station and its effects on materials processes p 3267 N92-28438

FLOATS
The Microgravity Isolation Mount (MGIM): A Columbus facility for improving the microgravity quality of payloads p 3267 N92-28439
KC-135 Large Motion Isolation Mount (LMIM) p 3267 N92-28440

FLOODS
Chryse Planitia region, Mars: Channeling history, flood-volume estimates, and scenarios for bodies of water in the northern plains p 3390 N92-29054

FLOW CHARACTERISTICS
Polyimide processing additives
[NASA-CASE-LAR-13669-1] p 3265 N92-29157

FLOW DISTORTION
Inlet distortion effects in aircraft propulsion system integration p 3237 N92-28464

FLOW DISTRIBUTION
A diagnostic study of the velocity structure of a meandering jet in the California current system using a primitive equation model
[AD-A246039] p 3320 N92-28283
Mobile electric power
[AD-A249354] p 3279 N92-28326
Visualization of gas tungsten arc weld pools
[AD-A245926] p 3293 N92-28384
Full Navier-Stokes analysis of a two-dimensional mixer/ejector nozzle for noise suppression
[NASA-TM-105715] p 3236 N92-28419
Rocket plume flowfield characterization using laser Rayleigh scattering
[NASA-TM-105739] p 3357 N92-28475
Calculation of unsteady transonic flows with mild separation by viscous-inviscid interaction
[NASA-TP-3197] p 3226 N92-28477
Computation of steady and unsteady quasi-one-dimensional viscous/inviscid interacting internal flows at subsonic, transonic, and supersonic Mach numbers
[NASA-CR-189881] p 3283 N92-28555
Comparison of LDA and LTA applications for propeller tests in wind tunnels
[NLR-MP-88031-U] p 3226 N92-28658
Flow quality studies of the NASA Lewis Research Center 8- by 6-foot supersonic/9- by 15-foot low speed wind tunnel
[NASA-TM-105417] p 3240 N92-28673
Flow gradient corrections on hot-wire measurements using an X-wire probe
[NLR-TP-90255-U] p 3228 N92-28713
Natural flow wing
[NASA-CASE-LAR-14281-1] p 3228 N92-28729
Wall turbulence
[AD-A249973] p 3284 N92-28768
Flow visualization studies of a sideslipping, canard-configured X-31A-Like fighter aircraft model
[AD-A245940] p 3228 N92-28883
Investigation of energy exchange mechanisms between the mean and acoustic flow fields in solid rocket combustion chambers
[AD-A247402] p 3250 N92-28931

FLOW EQUATIONS
Calculation of unsteady transonic flows with mild separation by viscous-inviscid interaction
[NASA-TP-3197] p 3226 N92-28477
Explicit Navier-Stokes computation of turbomachinery flows
[AD-A249284] p 3286 N92-28879
Lagrangian turbulence: Structures and mixing in admissible model flows
[AD-A247203] p 3286 N92-28890

FLOW GEOMETRY
A combined experimental and analytical investigation of the theory of plasticity involving strain induced anisotropy
[AD-A248440] p 3298 N92-28352

FLOW MEASUREMENT
Advanced diagnostics for reacting flows
[AD-A247059] p 3360 N92-28298
Flow quality studies of the NASA Lewis Research Center 8- by 6-foot supersonic/9- by 15-foot low speed wind tunnel
[NASA-TM-105417] p 3240 N92-28673
Flow gradient corrections on hot-wire measurements using an X-wire probe
[NLR-TP-90255-U] p 3228 N92-28713
Development of instrumentation for boundary layer transition detection
[AD-A249982] p 3287 N92-29171

FLOW STABILITY
The linear and nonlinear shear instability of a fluid sheet
[AD-A247092] p 3282 N92-28258

FLOW VELOCITY
Flow gradient corrections on hot-wire measurements using an X-wire probe
[NLR-TP-90255-U] p 3228 N92-28713
Transient impeller test facility
[AD-D015249] p 3294 N92-28749
Flow rate testing of valves used with the 500 gallon collapsible drum
[AD-A250567] p 3294 N92-28924

FLOW VISUALIZATION
Weld pool flow visualization studies during gas tungsten arc welding of steel and aluminum
[AD-A249204] p 3292 N92-28293
Visualization of gas tungsten arc weld pools
[AD-A245926] p 3293 N92-28384
Flow visualization studies of a sideslipping, canard-configured X-31A-Like fighter aircraft model
[AD-A245940] p 3228 N92-28883
Digital enhancement and restoration of images derived from flow visualization experiments
[AD-A250317] p 3339 N92-28952

FLUID DYNAMICS
Nonlinear sloshing and the coupled dynamics of liquid propellants and spacecraft
[AD-A250023] p 3248 N92-28967

FLUID FLOW
Telescience experiments using the Prototype Optical Diagnostic Instrument (PODI)
[NLR-TP-90199-U] p 3358 N92-28656
Transient impeller test facility
[AD-D015249] p 3294 N92-28749
Heat exchanger with oscillating flow
[NASA-CASE-LAR-14033-1] p 3284 N92-28752
Development of a high-performance FORTRAN compiler for porting CFD codes to the Navier-Stokes computer
[AD-A250208] p 3342 N92-28770
Bifurcations and patterns in nonlinear dissipative systems
[DE92-013502] p 3364 N92-28806
Pulse thermal energy transport/storage system
[NASA-CASE-LEW-15235-1] p 3287 N92-29125

FLUID MECHANICS
Lagrangian turbulence: Structures and mixing in admissible model flows
[AD-A247203] p 3286 N92-28890

FLUID PRESSURE
Transient impeller test facility
[AD-D015249] p 3294 N92-28749

FLUIDICS
Heat exchanger with oscillating flow
[NASA-CASE-LAR-14033-1] p 3284 N92-28752
Control of nonlinear distributed parameter systems with application to flow control
[AD-A250212] p 3346 N92-29149

FLUORESCENCE
Multicomponent comparison of optical and mass spectrometric diagnostics in low-pressure flames
[AD-A250323] p 3257 N92-28954

FLUORIDES
Singlet delta oxygen pumping of iodine monofluoride in a supersonic flow
[AD-A249946] p 3284 N92-28766
Compact, self-contained ArF lasers
[AD-A247403] p 3291 N92-28932

FLUORINE ORGANIC COMPOUNDS
Ion conductive polymer solid electrolytes
[DE92-010518] p 3266 N92-29195

FLUOROCARBONS
New methodology for fluorocarbon synthesis
[AD-A247163] p 3254 N92-28261

FLUOROSCOPY
Environmental testing of the Xi Scan 1000, portable fluoroscopic and radiographic imaging system
[AD-A247167] p 3324 N92-28242

FLUTTER ANALYSIS
Coupled structural/thermal/electromagnetic analysis/tailoring of graded composite structures
[NASA-CR-189153] p 3298 N92-28296

FOLDING
Chain folding in EBEE semicrystalline diblock copolymers
[AD-A247595] p 3262 N92-28251

FORCED VIBRATION
Modal analysis of plates using boundary integral equations
[NLR-TP-89211-U] p 3302 N92-28688

FORECASTING
Future mission studies: Preliminary comparisons of solar flux models
[NASA-TM-107947] p 3396 N92-28869
Nonlinear techniques for forecasting solar activity directly from its time series
[NASA-TM-107946] p 3396 N92-28870
Detecting and disentangling nonlinear structure from solar flux time series
[NASA-CR-190510] p 3396 N92-28871
Future mission studies: Forecasting solar flux directly from its chaotic time series
[NASA-CR-190378] p 3396 N92-28872
Wind-speed forecasting study for Westover AFB, Massachusetts
[AD-A247545] p 3319 N92-28934
FAA aviation forecasts
[AD-A250412] p 3230 N92-29182

FORMALISM
Contribution to the design of flexible manufacturing systems: Application of the formal description technique Estelle
[LAAS-91378] p 3341 N92-29209
Applications and benefits of formal methods in software development
[REPT-91-33] p 3341 N92-29221

FORSTERITE
Forsterite/melt partitioning of argon and iodine: Implications for atmosphere formation by outgassing of an early Martian magma ocean p 3313 N92-28604

FORTRAN
Vienna FORTRAN: A language specification, version 1.1
[NASA-CR-189629] p 3337 N92-28760
Crystallizing FORTRAN
[AD-A250162] p 3343 N92-28915

FOUNDRIES
X ray computed tomography of full-scale castings
[AD-A247101] p 3258 N92-28241

FOUR-WAVE MIXING
Advanced optical fiber communication systems
[AD-A247683] p 3357 N92-28554
Degenerate four-wave mixing using a tunable excimer laser to detect combustion gases
[DE92-005327] p 3290 N92-28852

FOURIER ANALYSIS
Fourier analysis of the approximation power of principal shift-invariant spaces
[AD-A246713] p 3347 N92-28411
Identification of aerodynamic models for maneuvering aircraft
[NASA-CR-190444] p 3233 N92-28720
Diagonal forms of translation operators for helmholtz equation in three dimensions
[AD-A248422] p 3348 N92-28949

FOURIER SERIES
Fourier analysis of the approximation power of principal shift-invariant spaces
[AD-A246713] p 3347 N92-28411

FOURIER TRANSFORMATION
A fast direct solver for a class of two-dimensional separable elliptic equations on the sphere
[NASA-TM-104567] p 3346 N92-28297
Fourier analysis of the approximation power of principal shift-invariant spaces
[AD-A246713] p 3347 N92-28411
A discrete Fourier transform for virtual memory machines
[NASA-TM-103914] p 3349 N92-28672
Wavelets and numerical simulation
[ONERA-NT-1991-8] p 3347 N92-28777

FRACTALS
A self-affine multi-fractal wave/turbulence discrimination method using data from single point fast response sensors in a nocturnal atmospheric boundary layer
[AD-A250419] p 3318 N92-28799
Studies of iterated transform image compression and its application to color and DTED
[AD-A248060] p 3339 N92-28946
FRACTIONATION
Mars volatile evolution: Implications of the recent measurement of O-17 in water from the SNC meteorites
p 3375 N92-28492
Evidence for a high temperature differentiation in a molten earth: A preliminary appraisal
p 3312 N92-28603
FRACTOGRAPHY
Processing and properties of chemically derived calcium silicate cements
[AD-A249106] p 3264 N92-28570
FRACTURE MECHANICS
The effect of intermediate heat treatments on overload induced retardation during the fatigue crack growth in an Al-alloy
[LR-651] p 3259 N92-28574
Spacecraft sustained load fracture control
[NLR-TP-89163-U] p 3302 N92-28643
Diffusion-controlled decohesion using a Cu-Sn alloy as a model system
[DE92-011645] p 3260 N92-28854
FRACTURE STRENGTH
The mechanical property data base from an Air Force/industry cooperative test program on advanced aluminum alloys (IN905XL and AL905XL forgings)
[AD-A247752] p 3368 N92-28565
Processing and properties of chemically derived calcium silicate cements
[AD-A249106] p 3264 N92-28570
Crack resistance, fracture toughness and instability in damage tolerant Al-Li alloys
[NLR-TP-90172-U] p 3303 N92-28850
FRACTURING
Mechanisms of fracture and creep of structural alloys
[AD-A248701] p 3259 N92-28390
EXPLOMET 90 international conference on shock-wave and high-strain-rate phenomena in materials
[AD-A248665] p 3303 N92-28892
Nanoscale investigation of indentation, adhesion, and fracture of diamond (111) surfaces
[AD-A250164] p 3265 N92-28916
FRAGMENTS
Optimalization of grenades with pre-formed fragments against air-targets, part 2
[PML-1990-24-PT-2] p 3349 N92-28313
FREE CONVECTION
The role of hard turbulent thermal convection in the Earth's early thermal evolution p 3310 N92-28593
FREE ELECTRON LASERS
Theory for the CEBAF and shipboard FELS
[AD-A245979] p 3289 N92-28662
The Los Alamos POP Project: FEL oscillator experiments in the ultraviolet and beyond
[DE92-011286] p 3291 N92-29168
FREE ENERGY
Correlation between surface free energy and surface constitution
[AD-A246699] p 3262 N92-28291
FREQUENCIES
Monaural and binaural processing of complex waveforms
[AD-A247199] p 3352 N92-28889
FREQUENCY DISTRIBUTION
Method and apparatus for frequency spectrum analysis
[NASA-CASE-NPO-17759-1-CU] p 3276 N92-29124
Directional wave data recorded off Flamborough Head (England)
[IOS-273-1990] p 3323 N92-29216
FREQUENCY HOPPING
Coding for frequency hopped spread spectrum satellite communications
[ECE-90-1] p 3274 N92-28699
FREQUENCY MEASUREMENT
Wavenumber calibration tables from heterodyne frequency measurements
[NASA-CR-190422] p 3276 N92-29115
FREQUENCY RANGES
Method and apparatus for frequency spectrum analysis
[NASA-CASE-NPO-17759-1-CU] p 3276 N92-29124
FREQUENCY RESPONSE
Fundamental noise limits in miniature acoustic and vibration sensors
[AD-A247016] p 3352 N92-28413
FREQUENCY SHIFT
In line optical fibre frequency shifter project
[AD-A246714] p 3357 N92-28372
FREQUENCY STABILITY
Scientific applications of frequency-stabilized laser technology in space
[NASA-CR-190449] p 3291 N92-28941
FRICTION
Effect of metallic coating properties on the tribology of oil-lubricated coated-ceramics
[DE92-010904] p 3262 N92-28339
Rolling friction robot fingers
[NASA-CASE-GSC-13261-1] p 3296 N92-29138
FRONTAL WAVES
Moored current measurements made in the Iceland Faeroes region during July-August 1990
[IOS-286-1991] p 3323 N92-29212
FRONTS (METEOROLOGY)
Simulation of atmospheric frontogenesis with a semi-Lagrangian numerical model
[AD-A247151] p 3318 N92-28517
FUEL CELLS
Mobile electric power
[AD-A249354] p 3279 N92-28326
FUEL CONSUMPTION
Practical considerations in designing the engine cycle
p 3237 N92-28460
Fuel optimal propulsive reboost of flexible spacecraft
p 3247 N92-28734
FUEL CONTROL
Fuel optimal maneuver: Experimental testbeds
p 3247 N92-28735
FUEL INJECTION
Hydrogen no-vent fill testing in a 5 cubic foot (142 liter) tank using spray nozzle and spray bar liquid injection
[NASA-TM-105759] p 3266 N92-28433
FUEL TANKS
Flow rate testing of valves used with the 500 gallon collapsible drum
[AD-A250567] p 3294 N92-28924
FULLERENES
Energetics of nanoscale graphitic tubules
[AD-A250165] p 3252 N92-28917
Electronic structure of fullerene tubules
[AD-A250166] p 3253 N92-28918
FUNCTION SPACE
The structure of finitely generated shift-invariant spaces in L2(IR sup d)
[AD-A247314] p 3334 N92-28301
FUNCTIONAL ANALYSIS
Identification of aerodynamic models for maneuvering aircraft
[NASA-CR-190444] p 3233 N92-28720
FUNCTIONAL DESIGN SPECIFICATIONS
Some longitudinal handling qualities design guidelines for active control technology transport aircraft
[NLR-TP-90129-U] p 3239 N92-28652
Functional requirements document for the Earth Observing System Data and Information System (EOSDIS) Scientific Computing Facilities (SCF) of the NASA/MSFC Earth Science and Applications Division, 1992
[NASA-TM-4392] p 3333 N92-28899
Design specifications for the Advanced Instructional Design Advisor (AIDA), volume 1
[AD-A248201] p 3340 N92-29187
Design specifications for the Advanced Instructional Design Advisor (AIDA), volume 2
[AD-A248202] p 3340 N92-29188
Repository-based software engineering program: Concept document
[NASA-CR-190384] p 3341 N92-29200
FUNCTIONS (MATHEMATICS)
The use of conformal subdomain basis functions in the method of moments computations for a thin wire
[AD-A245964] p 3272 N92-28347
FUSELAGES
Generation of spectra and stress histories for fatigue and damage tolerance analysis of fuselage repairs
[AD-A250390] p 3235 N92-29180
FUSION REACTORS
Ignition access condition based on the generalized saddle point in a magnetic fusion reactor
[PPL-109] p 3361 N92-28665
Alternating current tokamak reactor with ohmic ignition and bootstrap current
[PPL-120] p 3361 N92-28849
FUZZY SYSTEMS
Fuzzy logic controller for manipulator systems: Preliminary results p 3247 N92-28738
Learning and tuning fuzzy logic controllers through reinforcements
[NASA-TM-107875] p 3345 N92-28759

G

GADOLINIUM
Gadolinium metastable states population distributions and atomic density under high-rate electron beam evaporation
[DE92-782008] p 3363 N92-28282
GALACTIC NUCLEI
Observational study and analysis of point sources found by the infrared astronomy satellite
[AD-A248416] p 3371 N92-28843
GALLIUM ARSENIDES
Selective suppression of photochemical etching: Raman spectroscopy for pre-etch process selection
[DE92-010955] p 3255 N92-28341
An acoustic charge transport imager for high definition television application
[AD-A250433] p 3274 N92-28773
High-performance integrated circuit evaluation system for a gallium arsenide microsupercomputer
[AD-A250385] p 3281 N92-28798
Numerical studies of low temperature gallium arsenide buffer layers and their influence on device operation
[AD-A250309] p 3258 N92-29126
GAME THEORY
An experimental investigation of the effects of software size increase on software project management behavior
[AD-A248362] p 3335 N92-28385
GAMMA RAY BURSTS
Resonant Compton scattering in models of gamma ray burst sources
[DE92-010720] p 3397 N92-28336
The physics of strange matter
[DE92-011734] p 3371 N92-28774
GAMMA RAY SPECTRA
Resonant Compton scattering in models of gamma ray burst sources
[DE92-010720] p 3397 N92-28336
GAMMA RAYS
Neutron, gamma ray, and temperature effects on the electrical characteristics of thyristors
[NASA-TM-105728] p 3279 N92-28432
Redistribution of subsurface neutrons caused by ground ice on Mars p 3374 N92-28488
GAS CHROMATOGRAPHY
Studies of 1,3-disilacyclobutanes as single-source CVD precursors to silicon carbide
[AD-A247111] p 3365 N92-28885
GAS COOLING
Ultra-high temperature stability Joule-Thomson cooler with capability to accomodate pressure variations
[NASA-CASE-NPO-18184-1-CU] p 3288 N92-29156
GAS DENSITY
Advanced diagnostics for reacting flows
[AD-A247059] p 3360 N92-28298
The effects of alumina trihydrate on the flammability characteristics of polyester, vinyl ester, and epoxy glass reinforced plastics
[AD-A247707] p 3264 N92-28563
The ancient oxygen exosphere of Mars: Implications for atmosphere evolution p 3395 N92-29080
GAS DISSOCIATION
Nitrogen escape from Mars p 3383 N92-29014
GAS GUNS
Effects of extremely high G acceleration forces on NASA's control and space exposed tomato seeds
[AD-A247488] p 3323 N92-28247
Instrumentation for ultrahigh strain rate experiments
[AD-A249358] p 3298 N92-28327
GAS INJECTION
A study of the normal injection of hydrogen into a heated supersonic flow using planar laser-induced fluorescence
[DE92-010701] p 3282 N92-28268
GAS IONIZATION
Nitrogen escape from Mars p 3383 N92-29014
GAS MIXTURES
High temperature membranes for H2S and SO2 separations
[DE92-010451] p 3256 N92-28827
GAS TRANSPORT
Influences of CO2 sublimation/condensation processes on the long-term evolution of the Martian atmosphere
p 3375 N92-28496
Simulation of Martian surface-atmosphere interaction in a space-simulator: Technical considerations and feasibility p 3388 N92-29044
GAS TUNGSTEN ARC WELDING
Weld pool flow visualization studies during gas tungsten arc welding of steel and aluminum
[AD-A249204] p 3292 N92-28293
Development of an automated wire delivery system for robotic welding applications
[NASA-CR-190487] p 3295 N92-29134

GAS TURBINE ENGINES
Lubricant evaluation and performance 2
[AD-A247464] p 3262 N92-28398
Steady and Transient Performance Prediction of Gas Turbine Engines
[AGARD-LS-183] p 3236 N92-28458
Practical considerations in designing the engine cycle p 3237 N92-28460
Steady and transient performance calculation method for prediction, analysis, and identification p 3237 N92-28461
Component performance requirements p 3237 N92-28462
Dynamic simulation of compressor and gas turbine performance p 3237 N92-28463
Calculation of installation effects within performance computer programs p 3237 N92-28465
Dynamic control of aerodynamic instabilities in gas turbine engines p 3238 N92-28466
Engine performance and health monitoring models using steady state and transient prediction methods p 3238 N92-28467
Turbine aircraft engine operational trending and JT8D static component reliability study
[DOT/FAA/CT-91/10] p 3238 N92-28686
GAS TURBINES
Overview on basis and use of performance prediction methods p 3237 N92-28459
GAS-SOLID INTERACTIONS
Carbonate formation on Mars: History of the CO2 atmosphere from models of diffusion-limited growth in non-aqueous environments p 3391 N92-29060
GEARS
Application of face-gear drives in helicopter transmissions
[NASA-TM-105655] p 3293 N92-28434
Optimum design of a gearbox for low vibration
[NASA-TM-105653] p 3293 N92-28476
Dynamics of a split torque helicopter transmission
[NASA-TM-105681] p 3296 N92-29136
GENERAL AVIATION AIRCRAFT
Studies in general aviation aerodynamics
[NASA-CR-190431] p 3226 N92-28511
FAA aviation forecasts
[AD-A250412] p 3230 N92-29182
GENES
Primer on molecular genetics
[DE92-010680] p 3324 N92-28382
Somatic gene mutation in the human in relation to radiation risk
[DE92-009459] p 3325 N92-28685
GENETIC CODE
Primer on molecular genetics
[DE92-010680] p 3324 N92-28382
GENETICS
Problems in mechanistic theoretical models for cell transformation by ionizing radiation
[DE92-010265] p 3324 N92-28278
Primer on molecular genetics
[DE92-010680] p 3324 N92-28382
Genetic algorithms in coding theory: A table for A3 (n, d)
[MEMO-COSOR-91-22] p 3336 N92-28639
Somatic gene mutation in the human in relation to radiation risk
[DE92-009459] p 3325 N92-28685
GEOCHEMISTRY
Planetary geosciences, 1989-1990
[NASA-SP-508] p 3372 N92-28345
Spectral identification of chemisorbed CO2 and application to Mars analog materials p 3378 N92-28510
Workshop on the Physics and Chemistry of Magma Oceans from 1 Bar to 4 Mbar
[NASA-CR-190419] p 3310 N92-28587
Phase equilibria and trace element partitioning in a magma ocean to 260 kilobars p 3311 N92-28595
A new angle on lunar ferroan-suite differentiation p 3311 N92-28598
Dynamics and evolution of a magma ocean p 3314 N92-28612
The ferroan-anorthositic suite and the extent of primordial lunar melting p 3315 N92-28618
A carbonate-silicate aqueous geochemical cycle model for Mars p 3390 N92-29057
Carbonate formation on Mars: History of the CO2 atmosphere from models of diffusion-limited growth in non-aqueous environments p 3391 N92-29060
Aqueous-alteration products in S-N-C meteorites and implications for volatile/regolith interactions on Mars p 3393 N92-29071
GEOCHRONOLOGY
Glacial and marine chronology of Mars p 3392 N92-29067
GEODESY
Types and Characteristics of Data for Geomagnetic Field Modeling
[NASA-CP-3153] p 3299 N92-28620
Ocean tide models for satellite geodesy and Earth rotation
[NASA-CR-190468] p 3321 N92-28867
GEODETIC SATELLITES
Modeling radiation forces acting on TOPEX/Poseidon for precision orbit determination
[NASA-TM-104564] p 3244 N92-28343
GEODETIC SURVEYS
Accuracy of shipborne kinematic GPS surveying
[AD-A245942] p 3230 N92-28317
GEODYNAMICS
Workshop on the Martian Surface and Atmosphere Through Time
[NASA-CR-190418] p 3378 N92-28988
GEOLOGICAL FAULTS
A seismic and integrated geophysical study of the lithosphere of the Colorado Plateau
[AD-A247091] p 3308 N92-28257
GEOLOGICAL SURVEYS
A seismic and integrated geophysical study of the lithosphere of the Colorado Plateau
[AD-A247091] p 3308 N92-28257
Survey parameters and availability of low-level aeromagnetic data for geomagnetic field modelling p 3301 N92-28629
Topography of Apollinaris Patera and Ma'adim Vallis p 3393 N92-29069
GEOLOGY
Planetary geosciences, 1989-1990
[NASA-SP-508] p 3372 N92-28345
GEOMAGNETISM
Types and Characteristics of Data for Geomagnetic Field Modeling
[NASA-CP-3153] p 3299 N92-28620
Historical data for geomagnetic field modelling p 3299 N92-28621
Measurements of declination at the Helsinki Magnetic-Meteorological Observatory 1844-1853 p 3299 N92-28622
Survey data for geomagnetic field modelling p 3300 N92-28623
Satellite data for geomagnetic field modeling p 3300 N92-28624
Marine magnetic data holdings of World Data Center-A for Marine Geology and Geophysics p 3300 N92-28625
Reduction of marine magnetic data for modeling the main field of the Earth p 3300 N92-28626
Secular variation across the oceans: A retrospective study from 35 years of shipboard total field measurements in the NE Atlantic p 3300 N92-28627
Project MAGNET high-level vector survey data reduction p 3301 N92-28628
Survey parameters and availability of low-level aeromagnetic data for geomagnetic field modelling p 3301 N92-28629
Magnetic repeat station data p 3301 N92-28630
Geomagnetic data from the US magnetic observatory network p 3301 N92-28631
Magnetic and electromagnetic induction effects in the annual means of geomagnetic elements p 3301 N92-28632
Future mission studies: Forecasting solar flux directly from its chaotic time series
[NASA-CR-190378] p 3396 N92-28872
Coordinate systems for space and geophysical applications
[AD-A247550] p 3244 N92-28937
GEOMETRY
A center of excellence in the mathematical sciences
[AD-A249365] p 3346 N92-28329
GEOMORPHOLOGY
Neural network parameter estimation for the modified bistatic scattering strength model (BISSM)
[AD-A247913] p 3322 N92-28963
Workshop on the Martian Surface and Atmosphere Through Time
[NASA-CR-190418] p 3378 N92-28988
Martian channel networks: A revised Strahler approach for quantitative morphometry p 3380 N92-29000
Ice in the northern lowlands and southern highlands of Mars and its enrichment beneath the Elysium Lavas p 3381 N92-29001
Soil texture and granulometry at the surface of Mars p 3382 N92-29009
Glacial geomorphic evidence for a late climatic change on Mars p 3386 N92-29029
Distribution of coastal morphology in the Martian northern lowlands p 3389 N92-29047
Chemical reaction path modeling of hydrothermal processes on Mars: Preliminary results p 3389 N92-29050
Chryse Planitia region, Mars: Channeling history, flood-volume estimates, and scenarios for bodies of water in the northern plains p 3390 N92-29054
Dorsa Argentea type sinuous ridges, Mars: Evidence for linear dune hypothesis p 3390 N92-29055
Amazonis and Utopia Planitiae: Martian Lacustrine basins p 3391 N92-29058
GEOPHYSICAL FLUIDS
Geothermal Progress Monitor, report No. 13
[DE92-010697] p 3307 N92-28422
GEOPHYSICS
A seismic and integrated geophysical study of the lithosphere of the Colorado Plateau
[AD-A247091] p 3308 N92-28257
Planetary geosciences, 1989-1990
[NASA-SP-508] p 3372 N92-28345
Pressure regimes and core formation in the accreting earth p 3313 N92-28605
Early planetary differentiation: Geophysical consequences p 3314 N92-28609
Dynamics and evolution of a magma ocean p 3314 N92-28612
Types and Characteristics of Data for Geomagnetic Field Modeling
[NASA-CP-3153] p 3299 N92-28620
Marine magnetic data holdings of World Data Center-A for Marine Geology and Geophysics p 3300 N92-28625
Reduction of marine magnetic data for modeling the main field of the Earth p 3300 N92-28626
Coordinate systems for space and geophysical applications
[AD-A247550] p 3244 N92-28937
GEOTHERMAL ENERGY CONVERSION
Geothermal Progress Monitor, report No. 13
[DE92-010697] p 3307 N92-28422
GEOTHERMAL ENERGY UTILIZATION
Geothermal Progress Monitor, report No. 13
[DE92-010697] p 3307 N92-28422
GEOTHERMAL RESOURCES
Geothermal Progress Monitor, report No. 13
[DE92-010697] p 3307 N92-28422
GERMANY
DLR research reports and communications
[ISSN-0939-2971] p 3397 N92-29218
Activities report of the DLR
[ISSN-0938-2194] p 3397 N92-29219
GERMINATION
Effects of extremely high G acceleration forces on NASA's control and space exposed tomato seeds
[AD-A247488] p 3323 N92-28247
GLACIAL DRIFT
Dorsa Argentea type sinuous ridges, Mars: Evidence for linear dune hypothesis p 3390 N92-29055
GLACIERS
Glacial geomorphic evidence for a late climatic change on Mars p 3386 N92-29029
Glacial and marine chronology of Mars p 3392 N92-29067
GLARE
Delays in laser glare onset differentially affect target-location performance in a visual search task
[AD-A246708] p 3327 N92-28557
GLASS
Mg-Si-Al oxynitride glasses
[AD-A247593] p 3261 N92-28249
Microstructures of shocked quartz
[DE92-010710] p 3363 N92-28333
Study of high temperature failure mechanism in ceramics
[AD-A247018] p 3263 N92-28415
Martian surficial carbon-constraints from isotopic measurements of shock-produced glass in EET A79001 p 3377 N92-28508
GLASS FIBER REINFORCED PLASTICS
On the use of structural dynamic experimental methods for damage inspection of a glass fibre reinforced plastic plate
[FFA-TN-1992-02] p 3253 N92-29220
GLASS FIBERS
The application of carbon fibres in ARALL laminates
[LR-658] p 3259 N92-28576
The influence of elevated temperature on the bonding quality of deformed GLARE
[LR-659] p 3252 N92-28577
GLASS TRANSITION TEMPERATURE
Multiphase structure of a segmented polyurethane: Effects of temperature and annealing
[AD-A247594] p 3262 N92-28250
GLAZES
Results of a low power ice protection system test and a new method of imaging data analysis
[NASA-TM-105745] p 3227 N92-28696
GLIDING
Wing-extendible gliding store
[AD-D015233] p 3234 N92-28987

GLOBAL POSITIONING SYSTEM
Accuracy of shipborne kinematic GPS surveying
[AD-A245942] p 3230 N92-28317
Survey parameters and availability of low-level aeromagnetic data for geomagnetic field modelling
p 3301 N92-28629
GLOVES
Anthropomorphic teleoperation: Controlling remote manipulators with the DataGlove
[NASA-TM-103588] p 3330 N92-28521
GLUONS
Electroproduction of light quark baryons
[DE92-010853] p 3354 N92-28337
GODDARD TRAJECTORY DETERMINATION SYSTEM
Future mission studies: Forecasting solar flux directly from its chaotic time series
[NASA-CR-190378] p 3396 N92-28872
GOGGLES
Methods of visual scanning with night vision goggles
[AD-A247470] p 3331 N92-28944
GOLD
Orthogonal self-assembly of redox active molecules on Pt and Au: Selective reaction of disulfide with Au and isonitrile with Pt
[AD-A246698] p 3254 N92-28290
Surface crystallographic dependence of voltammetric oxidation of polyhydric alcohols and related systems at monocrystalline gold-acidic aqueous interfaces
[AD-A246763] p 3363 N92-28392
Substrate induced ordering of molecular adsorbates on Au(111)
[AD-A246850] p 3258 N92-29185
GOLD COATINGS
Microhole array electrodes based on microporous alumina membranes
[AD-A247082] p 3278 N92-28239
GOVERNMENT/INDUSTRY RELATIONS
Maintaining the program balance, volumes 1 and 2
[NASA-CR-190269] p 3367 N92-29111
GRADIENTS
Improvement of connectionnist learning processes, working according to the gradients method
[ETN-92-91335] p 3327 N92-28787
CTD data from the north east Atlantic, April 1989, collected on RRS Discovery Cruise 181
[IOS-285-1991] p 3322 N92-29211
GRAIN BOUNDARIES
Diffusion-controlled decohesion using a Cu-Sn alloy as a model system
[DE92-011645] p 3260 N92-28854
GRAIN SIZE
Soil texture and granulometry at the surface of Mars
p 3382 N92-29009
GRANTS
Second National Space Grant Conference report, 1991
[NASA-EP-278] p 3366 N92-28864
Super auditory localization for improved human-machine interfaces
[AD-A250288] p 3331 N92-29121
GRANULAR MATERIALS
Plane wave propagation in random granular media
[AD-A247300] p 3298 N92-28424
Joint DOE/NSF workshop on flow of particulates and fluids
[DE92-012692] p 3285 N92-28808
GRAPH THEORY
Decomposition of balanced matrices. Part 2: Wheel-and-parachute-free graphs
[AD-A247398] p 3350 N92-28928
Decomposition of balanced matrices. Part 6: Even wheels
[AD-A247399] p 3350 N92-28929
Decomposition of balanced matrices. Part 7: A polynomial recognition algorithm
[AD-A247400] p 3350 N92-28930
GRAPHIC ARTS
A theory of automated design of visual information presentations
[AD-A247425] p 3369 N92-28866
Analysis of multimedia information systems for the US Coast Guard
[AD-A247890] p 3369 N92-28960
GRAPHITE
Evaluation of plasma sprayed crucible coatings for melt processing copper-refractory metal alloys
[DE92-010871] p 3259 N92-28338
Atomistic simulation of the nanoindentation of diamond and graphite surfaces
[AD-A249296] p 3355 N92-28881
Energetics of nanoscale graphitic tubules
[AD-A250165] p 3252 N92-28917
Electronic structure of fullerene tubules
[AD-A250166] p 3253 N92-28918
GRASSES
Relationships of soil, grass, and bedrock over the Kaweah serpentine melange through spectral mixture analysis of AVIRIS data
[NASA-CR-190445] p 3306 N92-28717
GRATINGS (SPECTRA)
Elliptical-core two mode fiber sensors and devices incorporating photoinduced refractive index gratings
[NASA-CR-190495] p 3358 N92-28868
GRAVITATION
Marine magnetic data holdings of World Data Center-A for Marine Geology and Geophysics
p 3300 N92-28625
GRAVITATION THEORY
Proceedings of the workshop on Quantum Gravity and Topology
[DE92-782191] p 3366 N92-28235
GRAVITATIONAL EFFECTS
New inertial actuator provides isolation and stabilization in microgravity conditions p 3267 N92-28443
Shock and vibration isolation for cyclic exercise in spacecraft p 3267 N92-28449
Microgravity accelerometer characterization on Columbia STS-32 mission p 3271 N92-28452
GRAVITY WAVES
The Navy layered ocean model users guide
[AD-A247754] p 3321 N92-28566
GREEN'S FUNCTIONS
Computer derivation of green's functions for structural dynamic analysis
[AD-A250249] p 3339 N92-28969
GREENHOUSE EFFECT
Photochemical model for NH3 in an early Martian atmosphere p 3373 N92-28481
High pressure experiments with a Mars general circulation model p 3374 N92-28491
A reduced atmosphere for early Mars?
p 3375 N92-28495
Regional climatic effects of atmospheric SO2 on Mars
p 3377 N92-28504
The role of SO2 on Mars and on the primordial oxygen isotope composition of water on Earth and Mars
p 3377 N92-28507
Spectral identification of chemisorbed CO2 and application to Mars analog materials
p 3378 N92-28510
Greenhouse warming by minor gases on early Mars
p 3384 N92-29022
Was early Mars warmed by ammonia?
p 3386 N92-29030
Influence of heat flow on early Martian climate
p 3390 N92-29052
A carbonate-silicate aqueous geochemical cycle model for Mars p 3390 N92-29057
Carbonate formation on Mars: History of the CO2 atmosphere from models of diffusion-limited growth in non-aqueous environments p 3391 N92-29060
GREENLAND
Polar lows over the northeast Greenland Sea
[AD-A245360] p 3318 N92-28421
GRENADES
Optimalization of grenades with pre-formed fragments against air-targets, part 2
[PML-1990-24-PT-2] p 3349 N92-28313
GRID GENERATION (MATHEMATICS)
Hyperbolic grid generation with BEM source terms
[NLR-TP-90334-U] p 3347 N92-28635
GROUND EFFECT (AERODYNAMICS)
Viscous effects on a vortex wake in ground effect
[NASA-CR-190400] p 3283 N92-28361
GROUND STATE
Shallow states of donor impurities on periodically structured semiconductors interfaces
[DE92-622791] p 3363 N92-28312
Singlet delta oxygen pumping of iodine monofluoride in a supersonic flow
[AD-A249946] p 3284 N92-28766
The physics of strange matter
[DE92-011734] p 3371 N92-28774
GROUND SUPPORT EQUIPMENT
Verification of satellite EGSE test-software using an application generator
[ITN-92-85131] p 3244 N92-29098
GROUND TESTS
Experimental aerodynamic facilities of the Aerodynamics Research and Concepts Assistance Branch
[AD-A247489] p 3240 N92-28248
GROUND WATER
Distribution of Martian ground-ice table: Preliminary results about climatic variations p 3373 N92-28484
The subsurface hydrologic response of Mars to the thermal evolution of its early crust p 3381 N92-29006
GROUND WIND
Simulations of surface winds at the Viking Lander sites using a one-level model p 3380 N92-28998
GROUP DYNAMICS
Tasking and communication flows in the F/A-18D cockpit: Issues, problems, and possible solutions
[AD-A245977] p 3234 N92-28802
GULF STREAM
Structure energetics and dynamics of Gulf Stream variability
[AD-A248246] p 3323 N92-29225
GUST LOADS
Response of helicopters to gusts
[NLR-TP-90159-U] p 3239 N92-28653
GUSTS
Upgrading the data processing section of the NAL Gust Wind Tunnel data processing system
[NAL-TM-635] p 3241 N92-28833

H

HABITATS
Liquid water habitats on early Mars
p 3376 N92-28500
HALIDES
Near millimeter waves and microelectronics
[AD-A250384] p 3281 N92-28797
HALOGENS
Large-area, plasma-assisted, halogen-based diamond deposition
[AD-A247423] p 3264 N92-28904
HAMSTERS
Study of SCN neurochemistry using in vivo microdialysis in the conscious brain: Correlation with overt circadian rhythms
[AD-A247172] p 3325 N92-28886
HARDENING (MATERIALS)
A combined experimental and analytical investigation of the theory of plasticity involving strain induced anisotropy
[AD-A248440] p 3298 N92-28352
HARMONIC CONTROL
Comparison of three controllers applied to helicopter vibration
[NASA-TM-102192] p 3239 N92-28457
HARMONIC GENERATIONS
CO2 laser frequency multiplication
[AD-A247542] p 3291 N92-28933
The Los Alamos POP Project: FEL oscillator experiments in the ultraviolet and beyond
[DE92-011286] p 3291 N92-29168
Big Sky Workshop on Super-Intense Laser-Atom Physics
[AD-A248225] p 3292 N92-29223
HARMONIC GENERATORS
Intense electron beam cyclotron masers with microsecond pulselengths
[AD-A247060] p 3289 N92-28271
CO2 laser frequency multiplication
[AD-A245915] p 3290 N92-28761
HARMONIC OSCILLATION
Tunable optical sources and synthetic nonlinear media/growth and characterization of nonlinear optical materials
[AD-A249363] p 3357 N92-28328
HARMONIC OSCILLATORS
CO2 laser frequency multiplication
[AD-A245915] p 3290 N92-28761
HARRIER AIRCRAFT
Harrier GR MK 5/7 mission simulators for the Royal Air Force p 3224 N92-28540
HARTREE APPROXIMATION
High quality Gaussian basis sets for fourth-row atoms
[NASA-TM-103918] p 3255 N92-28743
HAZARDS
The chronic effects of JP-8 jet fuel exposure on the lungs
[AD-A250308] p 3326 N92-29123
HEAD-UP DISPLAYS
The second flight simulator test of the head-up display for NAL QSTOL experimental aircraft (ASKA)
[NAL-TM-633] p 3331 N92-28831
HEAO 1
Scientific investigations with the data base HEAO-1 scanning modulator collimator
[NASA-CR-190477] p 3370 N92-28680
HEAT BALANCE
Modeling the seasonal cycle of CO2 on Mars: A fit to the Viking lander pressure curves p 3394 N92-29076
HEAT EXCHANGERS
Heat exchanger with oscillating flow
[NASA-CASE-LAR-14033-1] p 3284 N92-28752
Natural circulation decay heat removal from an SP-100, 550 kWe power system for a lunar outpost
[NASA-CR-190421] p 3307 N92-28863
Ultra-high temperature stability Joule-Thomson cooler with capability to accomodate pressure variations
[NASA-CASE-NPO-18184-1-CU] p 3288 N92-29156

HEAT FLUX
Heat exchanger with oscillating flow
[NASA-CASE-LAR-14033-1] p 3284 N92-28752
Mesoscale surface analysis of the ERICA IOP-5 cyclone
[AD-A245946] p 3319 N92-28884
HEAT MEASUREMENT
Multiphase structure of a segmented polyurethane: Effects of temperature and annealing
[AD-A247594] p 3262 N92-28250
Thermal analysis of selected commercial thermoplastic resins
[AD-A247711] p 3264 N92-28564
An investigation into techniques for the determination of moisture content on activated carbon
[AD-A245938] p 3256 N92-28882
Thermodynamic and kinetic aspects of surface acidity
[DE92-011194] p 3256 N92-28893
HEAT PIPES
NASA Lewis steady-state heat pipe code users manual
[NASA-TM-105161] p 3249 N92-28682
Solar thermal energy receiver
[NASA-CASE-LEW-14949-1] p 3307 N92-29143
HEAT RESISTANT ALLOYS
Mechanisms of fracture and creep of structural alloys
[AD-A248701] p 3259 N92-28390
The influence of elevated temperature on the bonding quality of deformed GLARE
[LR-659] p 3252 N92-28577
The compressive properties of GLARE
[LR-666] p 3252 N92-28582
Elevated temperature axial and torsional fatigue behavior of Haynes 188
[NASA-TM-105396] p 3302 N92-28701
Some experiments to determine the efficiency of collection of alumina particles by electron beam button melting in a nickel-base superalloy, AP1
[NPL-DMM(A)-42] p 3261 N92-29164
HEAT SINKS
Innovative techniques for the production of low cost 2D laser diode arrays
[AD-A248247] p 3292 N92-29226
HEAT SOURCES
Simulation in infrared imaging: Using electrical circuit principles to model heat transfer
[AD-A248290] p 3278 N92-28276
HEAT STORAGE
Pulse thermal energy transport/storage system
[NASA-CASE-LEW-15235-1] p 3287 N92-29125
HEAT TRANSFER
Simulation in infrared imaging: Using electrical circuit principles to model heat transfer
[AD-A248290] p 3278 N92-28276
Modelling of heat and moisture loss through NBC ensembles
[AD-A245939] p 3329 N92-28346
Practical considerations in designing the engine cycle p 3237 N92-28460
Calculation of chip temperatures using ELLPACK
[AD-A247156] p 3335 N92-28519
Heat exchanger with oscillating flow
[NASA-CASE-LAR-14033-1] p 3284 N92-28752
Natural circulation decay heat removal from an SP-100, 550 kWe power system for a lunar outpost
[NASA-CR-190421] p 3307 N92-28863
Simulations of surface winds at the Viking Lander sites using a one-level model p 3380 N92-28998
Pulse thermal energy transport/storage system
[NASA-CASE-LEW-15235-1] p 3287 N92-29125
Solar thermal energy receiver
[NASA-CASE-LEW-14949-1] p 3307 N92-29143
HEAT TRANSMISSION
Influence of heat flow on early Martian climate p 3390 N92-29052
HEAT TREATMENT
The effect of intermediate heat treatments on overload induced retardation during the fatigue crack growth in an Al-alloy
[LR-651] p 3259 N92-28574
Phase transformations in Ti3Al based alloy
[AD-A246464] p 3261 N92-28976
Feasibility of metal-oxide-semiconductor structures on Si-LPCVD thin films by low temperature (600 C) process
[LAAS-91307] p 3365 N92-29207
HEAVY IONS
Development of negative heavy ion sources for plasma potential measurement
[DE92-782102] p 3360 N92-28234
HELICOPTER DESIGN
Application of face-gear drives in helicopter transmissions
[NASA-TM-105655] p 3293 N92-28434
The application of flight simulation models in support of rotorcraft design and development p 3222 N92-28527
HELICOPTER PROPELLER DRIVE
Application of face-gear drives in helicopter transmissions
[NASA-TM-105655] p 3293 N92-28434
Dynamics of a split torque helicopter transmission
[NASA-TM-105681] p 3296 N92-29136
HELICOPTERS
An analysis of aircrew communication patterns and content
[AD-A246618] p 3272 N92-28253
Passive acoustic range estimation of helicopters
[AD-A248033] p 3351 N92-28302
A sensitivity analysis on component reliability from fatigue life computations
[AD-A247430] p 3297 N92-28425
Comparison of three controllers applied to helicopter vibration
[NASA-TM-102192] p 3239 N92-28457
Aircraft ship operations
[AGARD-AR-312] p 3231 N92-28468
Correlational analysis of survey and model-generated workload values
[AD-A247153] p 3329 N92-28518
Experience with piloted simulation in the development of helicopters p 3222 N92-28528
Full mission simulation: A view into the future p 3223 N92-28537
An evaluation of IFR approach techniques: Generic helicopter simulation compared with actual flight p 3225 N92-28550
Response of helicopters to gusts
[NLR-TP-90159-U] p 3239 N92-28653
LAH-main rotor model test at the DNW
[NLR-TP-90305-U] p 3233 N92-28687
S-76B certification for vertical take-off and landing operations from confined areas
[NLR-TP-90286-U] p 3233 N92-28714
Methods of visual scanning with night vision goggles
[AD-A247470] p 3331 N92-28944
A rotorcraft flight database for validation of vision-based ranging algorithms
[NASA-TM-103906] p 3231 N92-29103
HELIUM AFTERGLOW
Microwave interactions with plasmas
[AD-A250333] p 3362 N92-29093
HELIUM PLASMA
Microwave interactions with plasmas
[AD-A250333] p 3362 N92-29093
HELMET MOUNTED DISPLAYS
The evaluation of simulator effectiveness for the training of high speed, low level, tactical flight operations p 3223 N92-28539
HEMATITE
Oxygen in the Martian atmosphere: Regulation of PO2 by the deposition of iron formations on Mars p 3373 N92-28482
Evidence for crystalline hematite as an accessory phase in Martian soils p 3391 N92-29059
HEMOGLOBIN
Structural characterization of cross-linked hemoglobins developed as potential transfusion substitutes
[AD-A246777] p 3325 N92-28515
HERMES MANNED SPACEPLANE
Dynamics motion simulation of the Hermes robot arm subjected to constraints
[NLR-TP-90282-U] p 3293 N92-28645
Modelling and real-time simulation of the Hermes robot arm HERA
[NLR-TP-90262-U] p 3294 N92-28705
HETERODYNING
Wavenumber calibration tables from heterodyne frequency measurements
[NASA-CR-190422] p 3276 N92-29115
HETEROGENEITY
Asynchronous bidirectional network interface enabling seamless concurrent processing in a distributed heterogeneous multiprocessor system
[AD-D015274] p 3343 N92-29096
HEURISTIC METHODS
Scheduling multiple variable-speed machines
[AD-A249362] p 3268 N92-28359
Mapping unstructured grid computations to massively parallel computers
[NASA-CR-190551] p 3343 N92-29109
HIBERNATION
Limiting factors to advancing thermal battery technology for naval applications
[AD-A247773] p 3280 N92-28568
HIERARCHIES
Organizing plan libraries in subsumption hierarchies: Specificity based plan selection
[AD-A248711] p 3368 N92-28430
Segmentation of satellite imagery using hierarchical thresholding and neural networks
[AD-A247915] p 3319 N92-28965
HIGH ACCELERATION
Effects of extremely high G acceleration forces on NASA's control and space exposed tomato seeds
[AD-A247488] p 3323 N92-28247
HIGH ALTITUDE ENVIRONMENTS
Effects of high terrestrial altitude on military performance
[AD-A246695] p 3324 N92-28288
HIGH DEFINITION TELEVISION
An acoustic charge transport imager for high definition television application
[AD-A250433] p 3274 N92-28773
Digital compression algorithms for HDTV transmission
[NASA-CR-190509] p 3275 N92-28873
HIGH LEVEL LANGUAGES
A uniform approach to the semantics of concurrency
[AD-A246697] p 3334 N92-28289
Crystallizing FORTRAN
[AD-A250162] p 3343 N92-28915
HIGH POWER LASERS
Big Sky Workshop on Super-Intense Laser-Atom Physics
[AD-A248225] p 3292 N92-29223
Innovative techniques for the production of low cost 2D laser diode arrays
[AD-A248247] p 3292 N92-29226
HIGH PRESSURE
Fluids at high shock pressures and temperatures
[DE92-010709] p 3283 N92-28269
High pressure experiments with a Mars general circulation model p 3374 N92-28491
High-pressure melting of carbonaceous chondrite p 3310 N92-28589
Pressure regimes and core formation in the accreting earth p 3313 N92-28605
Terrestrial magma ocean and core segregation in the earth p 3313 N92-28606
Estimation of the viscosities of silicate liquids at high pressure from measurements of oxygen diffusivity p 3313 N92-28607
Evidences for the terrestrial magma ocean from high-pressure melting experiments p 3315 N92-28613
Asynchronous optical sampling for laser-based combustion diagnostics in high-pressure flames
[AD-A250206] p 3257 N92-28896
Paint removal using cryogenic processes
[AD-A247668] p 3264 N92-28912
HIGH RESOLUTION
A diagnostic study of the velocity structure of a meandering jet in the California current system using a primitive equation model
[AD-A246039] p 3320 N92-28283
Bioluminescence in the western Alboran Sea in April 1991
[AD-A250016] p 3324 N92-29089
Water window imaging x ray microscope
[NASA-CASE-MFS-28485-1] p 3288 N92-29135
HIGH SPEED
Evaluation of outdoor-to-indoor response to minimized sonic booms
[NASA-CR-189643] p 3352 N92-28556
HIGH STRENGTH
The effects of thermomechanical processing parameters on elevated-temperature behavior of a 6061 Al-Al2O3 metal matrix composite
[AD-A247889] p 3253 N92-28959
HIGH STRENGTH ALLOYS
Effect of cooling rate on corrosion properties of high strength aluminium alloys under atmospheric conditions
[NLR-TP-90138-U] p 3260 N92-28691
HIGH TEMPERATURE
High-temperature miniaturized turbine engine lubrication system simulator
[AD-A249259] p 3236 N92-28294
Superheat in magma oceans p 3311 N92-28597
Estimation of high temperature metal-silicate partition coefficients p 3311 N92-28599
High temperature dielectric properties of Apical, Kapton, Peek, Teflon AF, and Upilex polymers
[NASA-TM-105753] p 3280 N92-28675
M-H characteristics and demagnetization resistance of samarium-cobalt permanent magnets to 300 C
[NASA-CR-189194] p 3280 N92-28723
High temperature membranes for H2S and SO2 separations
[DE92-010451] p 3256 N92-28827
Elliptical-core two mode fiber sensors and devices incorporating photoinduced refractive index gratings
[NASA-CR-190495] p 3358 N92-28868
The processing of high temperature ceramic superconducting devices, volume 2
[AD-A248159] p 3281 N92-28948
The effects of thermomechanical processing parameters on elevated-temperature behavior of a 6061 Al-Al2O3 metal matrix composite
[AD-A247889] p 3253 N92-28959

High temperature solder device for flat cables
[NASA-CASE-GSC-13344-1] p 3261 N92-29094

HIGH TEMPERATURE FLUIDS
Lubricant evaluation and performance 2
[AD-A247464] p 3262 N92-28398

HIGH TEMPERATURE LUBRICANTS
Lubricant evaluation and performance 2
[AD-A247464] p 3262 N92-28398

HIGH TEMPERATURE PLASMAS
Advanced diagnostics for reacting flows
[AD-A247059] p 3360 N92-28298

HIGH TEMPERATURE SUPERCONDUCTORS
Chemical vapor deposition of yttrium borium(2) copper(3) oxygen(x) thin films for wire applications
[AD-A247013] p 3364 N92-28395
Magnetic hysteresis and relaxation in Ag-sheathed TlBaCaCuO (1223) and Bi(Pb)SrCaCuO (2223) superconducting tapes
[DE92-011357] p 3365 N92-28874
Electrodeposition of high temperature superconductors
[AD-A250171] p 3365 N92-28919
Superconducting bearings with levitation control configurations
[NASA-CASE-GSC-13346-1] p 3295 N92-29099

HIGH TEMPERATURE TESTS
Environmental testing of the Xi Scan 1000, portable fluoroscopic and radiographic imaging system
[AD-A247167] p 3324 N92-28242
Study of high temperature failure mechanism in ceramics
[AD-A247018] p 3263 N92-28415
The influence of elevated temperature on the bonding quality of deformed GLARE
[LR-659] p 3252 N92-28577
Pre-test analyses for pressurized thermoshock tests, vessel 1
[VTT-RR-746] p 3303 N92-28776

HIGH VOLTAGES
High voltage splitting unit for the power supplies of the vacuum pumps of AmPS
[DIGEL-1991-7] p 3278 N92-28263
Solar Array Module Plasma Interaction Experiment (SAMPIE): Technical requirements document
[NASA-TM-105660] p 3246 N92-28683
SPEAR 2 space power data analysis
[AD-A248057] p 3250 N92-28945

HIGHLANDS
Nature and evolution of the early Martian atmosphere: Evidence from highland crater populations p 3373 N92-28485

HISTORIES
NASA engineers and the age of Apollo
[NASA-SP-4104] p 3397 N92-28344
Using the historical record to determine dust sources p 3376 N92-28499
Historical data for geomagnetic field modelling p 3299 N92-28621
Space flight: The first 30 years
[NASA-NP-150] p 3397 N92-28678

HOLDERS
Removable hand hold
[NASA-CASE-LEW-15196-1] p 3295 N92-29092
Rolling friction robot fingers
[NASA-CASE-GSC-13261-1] p 3296 N92-29138

HOLOGRAPHIC INTERFEROMETRY
Instrumentation for ultrahigh strain rate experiments
[AD-A249358] p 3298 N92-28327

HOLOGRAPHY
Nondestructive evaluation of damages caused by impact and fatigue loading of polymer composites
[VTT-RR-742] p 3251 N92-28572

HOMING DEVICES
A radar signal processing ASIC and a VME interface circuit p 3235 N92-28380

HOMOGENEOUS TURBULENCE
Reactant conversion in homogeneous turbulence: Mathematical modeling, computational validations and practical applications p 3285 N92-28819

HOMOMORPHISMS
A uniform approach to the semantics of concurrency
[AD-A246697] p 3334 N92-28289

HONEYCOMB STRUCTURES
Flow quality studies of the NASA Lewis Research Center 8- by 6-foot supersonic/9- by 15-foot low speed wind tunnel
[NASA-TM-105417] p 3240 N92-28673

HORN ANTENNAS
The use of a vector network analyzer for measuring the performance of radar absorbing materials
[AD-A247194] p 3275 N92-28887

HOT-WIRE ANEMOMETERS
Flow gradient corrections on hot-wire measurements using an X-wire probe
[NLR-TP-90255-U] p 3228 N92-28713

HUBBLE SPACE TELESCOPE
Observations of Mars using Hubble Space Telescope p 3385 N92-29026

HUMAN BEHAVIOR
MoCog1: A computer simulation of recognition-primed human decision making, considering emotions
[NASA-TM-107859] p 3337 N92-28758

HUMAN CENTRIFUGES
G-tolerance and spatial disorientation: Can simulation help us? p 3223 N92-28534

HUMAN FACTORS ENGINEERING
A study of pilot attitudes regarding the impact on mission effectiveness of using new cockpit automation technologies to replace the navigator/weapon system officer/electronic warfare officer
[AD-A246683] p 3329 N92-28286
Anthropomorphic teleoperation: Controlling remote manipulators with the DataGlove
[NASA-TM-103588] p 3330 N92-28521
A strategy for minimizing common mode human error in executing critical functions and tasks
[DE92-011839] p 3327 N92-28775
A theory of automated design of visual information presentations
[AD-A247425] p 3369 N92-28866
Super auditory localization for improved human-machine interfaces
[AD-A250288] p 3331 N92-29121

HUMAN PERFORMANCE
An analysis of aircrew communication patterns and content
[AD-A246618] p 3272 N92-28253
Improved decision making through group composition
[AD-A246622] p 3366 N92-28256
Effects of high terrestrial altitude on military performance
[AD-A246695] p 3324 N92-28288
Program Cluster: An identification of fixation cluster characteristics
[AD-A247014] p 3326 N92-28396
The Coordinated Noninvasive Studies (CNS) project, phase 1
[AD-A247159] p 3324 N92-28397
Computer-based assessment of schema knowledge in a flexible problem-solving environment
[AD-A246779] p 3348 N92-28516
Correlational analysis of survey and model-generated workload values
[AD-A247153] p 3329 N92-28518
A strategy for minimizing common mode human error in executing critical functions and tasks
[DE92-011839] p 3327 N92-28775
Integrating the affective domain into the instructional design process
[AD-A249287] p 3327 N92-28880
Lapses in alertness: Brain-evoked responses to task-irrelevant auditory probes
[AD-A247669] p 3328 N92-28940
Acquisition and improvement of human motor skills: Learning through observation and practice
[NASA-TM-107878] p 3329 N92-29174
The energetics and mechanics of load carrying
[AD-A248441] p 3332 N92-29227

HUYGENS PRINCIPLE
Plane wave propagation in random granular media
[AD-A247300] p 3298 N92-28424

HYBRID CIRCUITS
A survey of high density packaging for high performance computing system
[AD-A248633] p 3332 N92-28891

HYBRID COMPUTERS
Coincident pulse techniques for hybrid electronic optical computer systems
[AD-A246774] p 3332 N92-28514

HYDRAZIDES
Poly(1,3,4-oxadiazoles) via aromatic nucleophilic displacement
[NASA-CASE-LAR-14427-1] p 3250 N92-29141

HYDRIDES
Molecular dynamics calculations of optical nonlinear properties of materials
[AD-A247095] p 3354 N92-28260
Mobile electric power
[AD-A249354] p 3279 N92-28326

HYDROCYANIC ACID
Greenhouse warming by minor gases on early Mars p 3384 N92-29022

HYDRODYNAMIC EQUATIONS
The Navy layered ocean model users guide
[AD-A247754] p 3321 N92-28566

HYDRODYNAMICS
A domain decomposition method for ocean/bottom interaction problems
[FFI-91/7022] p 3320 N92-28266
A new ocean bottom magnetometer system for continental shelf measurements
[AD-A247644] p 3321 N92-28321
How Mars lost its atmosphere p 3378 N92-28509
Hydrodynamic echo in strongly inhomogeneous magnetized plasma
[DE92-621530] p 3361 N92-28816
The nonequilibrium molecular dynamics
[DE92-011760] p 3355 N92-28860

HYDROGEN
A study of the normal injection of hydrogen into a heated supersonic flow using planar laser-induced fluorescence
[DE92-010701] p 3282 N92-28268
Hydrogen no-vent fill testing in a 5 cubic foot (142 liter) tank using spray nozzle and spray bar liquid injection
[NASA-TM-105759] p 3266 N92-28433
An ion mass spectrometer for measuring isotopic adundances and loss rates of O, C and H in Mars' upper atmosphere p 3374 N92-28486
Computations of detonation structure: The influence of model input parameters
[AD-A248634] p 3285 N92-28803

HYDROGEN EMBRITTLEMENT
Spacecraft sustained load fracture control
[NLR-TP-89163-U] p 3302 N92-28643

HYDROGEN FUELS
Mobile electric power
[AD-A249354] p 3279 N92-28326
Hydrogen no-vent fill testing in a 5 cubic foot (142 liter) tank using spray nozzle and spray bar liquid injection
[NASA-TM-105759] p 3266 N92-28433

HYDROGEN IONS
Theoretical studies of the electronic and resonance structure of atomic and molecular negative ions
[AD-A247093] p 3354 N92-28259

HYDROGEN OXYGEN ENGINES
Rocket plume flowfield characterization using laser Rayleigh scattering
[NASA-TM-105739] p 3357 N92-28475

HYDROGEN SULFIDE
High temperature membranes for H2S and SO2 separations
[DE92-010451] p 3256 N92-28827

HYDROLOGICAL CYCLE
The Mars water cycle at other epochs: History of the polar caps and layered terrain p 3375 N92-28493

HYDROLOGY
The subsurface hydrologic response of Mars to the thermal evolution of its early crust p 3381 N92-29006

HYDROLOGY MODELS
Glacial and marine chronology of Mars p 3392 N92-29067

HYDROPHONES
Under-ice broadband transient measurements and processing
[AD-A248609] p 3351 N92-28324
Seafloor pressure array studies at ultra-low frequencies
[AD-A247663] p 3322 N92-28939

HYDROPONICS
Coupling plant growth and waste recycling systems in a controlled life support system (CELSS)
[NASA-TM-107544] p 3330 N92-28670

HYDROTHERMAL SYSTEMS
Iron Moessbauer spectroscopy: Superparamagnetism in hydrothermal vents and the search for evidence of past life on Mars p 3378 N92-28989
Magmatic intrusions and hydrothermal systems on Mars p 3384 N92-29019
Chemical reaction path modeling of hydrothermal processes on Mars: Preliminary results p 3389 N92-29050

HYDROXYL RADICALS
A study of the normal injection of hydrogen into a heated supersonic flow using planar laser-induced fluorescence
[DE92-010701] p 3282 N92-28268
The impact of temperature dependent CO2 cross section measurements: A role for heterogeneous chemistry in the atmosphere of Mars? p 3372 N92-28479

HYPERBOLIC DIFFERENTIAL EQUATIONS
On some splitting schemes for wave equations
[FFI-91/7023] p 3348 N92-29193

HYPERBOLIC FUNCTIONS
Hyperbolic grid generation with BEM source terms
[NLR-TP-90334-U] p 3347 N92-28635

HYPERSONIC FLIGHT
An analysis of combustion studies in shock expansion tunnels and reflected shock tunnels
[NASA-TP-3224] p 3255 N92-28374

HYPERSONIC FLOW
Feasibility study of hypersonic clinometric measurements at R3Ch
[ONERA-RSF-136/1865-AY-728-] p 3228 N92-28789

HYPERSONIC WIND TUNNELS
Instrumentation requirements for laminar flow research in the NLR high speed wind tunnel HST
[NLR-TP-89158-U] p 3240 N92-28669
HYPERTHERMIA
Thermoregulation during spaceflight
[NASA-TM-103913] p 3325 N92-28420
HYPERVELOCITY IMPACT
Evaluation of Whipple bumper shields at 7 and 10 km/s
[NASA-TM-107958] p 3295 N92-28925
HYPOXIA
Effects of high terrestrial altitude on military performance
[AD-A246695] p 3324 N92-28288
HYSTERESIS
Magnetic hysteresis and relaxation in Ag-sheathed TlBaCaCuO (1223) and Bi(Pb)SrCaCuO (2223) superconducting tapes
[DE92-011357] p 3365 N92-28874

I

ICE
Redistribution of subsurface neutrons caused by ground ice on Mars p 3374 N92-28488
Experimental and computational ice shapes and resulting drag increase for a NACA 0012 airfoil
[NASA-TM-105743] p 3227 N92-28674
Propagation and scattering of microwaves and millimeter waves in snow based on dense random media theory
[AD-A249300] p 3274 N92-28846
Ice in the northern lowlands and southern highlands of Mars and its enrichment beneath the Elysium Lavas p 3381 N92-29001
Glacial geomorphic evidence for a late climatic change on Mars p 3386 N92-29029
Glacial and marine chronology of Mars p 3392 N92-29067
ICE FORMATION
Experimental and computational ice shapes and resulting drag increase for a NACA 0012 airfoil
[NASA-TM-105743] p 3227 N92-28674
Results of a low power ice protection system test and a new method of imaging data analysis
[NASA-TM-105745] p 3227 N92-28696
Simulations of the seasonal polar caps on Mars p 3387 N92-29033
ICE MAPPING
Distribution of Martian ground-ice table: Preliminary results about climatic variations p 3373 N92-28484
ICE PREVENTION
Results of a low power ice protection system test and a new method of imaging data analysis
[NASA-TM-105745] p 3227 N92-28696
ICEBERGS
Applications of passive microwave satellite data for Arctic Sea ice studies
[AD-A245966] p 3306 N92-28791
ICELAND
Moored current measurements made in the Iceland Faeroes region during July-August 1990
[IOS-286-1991] p 3323 N92-29212
IDENTIFYING
Reinforcement learning for the adaptive control of perception and action
[AD-A249351] p 3344 N92-28325
IGNITION
Alternating current tokamak reactor with ohmic ignition and bootstrap current
[PPL-120] p 3361 N92-28849
Underwater vapor phase burning of aluminum particles and on aluminum ignition during steam explosions
[DE92-011196] p 3257 N92-28894
IMAGE ANALYSIS
Use of laser range finders and range image analysis in automated assembly tasks
[NASA-CR-186957] p 3291 N92-29139
IMAGE CONVERTERS
Instrumentation for ultrahigh strain rate experiments
[AD-A249358] p 3298 N92-28327
IMAGE PROCESSING
Instrumentation for ultrahigh strain rate experiments
[AD-A249358] p 3298 N92-28327
A center of excellence in the mathematical sciences
[AD-A249365] p 3346 N92-28329
Image processing techniques for acoustic images
[AD-A247303] p 3352 N92-28559
Results of a low power ice protection system test and a new method of imaging data analysis
[NASA-TM-105745] p 3227 N92-28696
Transputer-based embedded system for Meteosat image data compression
[NLR-TP-90228-U] p 3305 N92-28697
A contribution to laser range imaging technology
[NASA-CR-190501] p 3290 N92-28707
Image processing for failure analysis of integrated circuits by an electron beam
[ETN-92-91322] p 3281 N92-28784
Digital compression algorithms for HDTV transmission
[NASA-CR-190509] p 3275 N92-28873
Binary optical filters for scale invariant pattern recognition
[NASA-TM-103902] p 3234 N92-28910
Studies of iterated transform image compression and its application to color and DTED
[AD-A248060] p 3339 N92-28946
Digital enhancement and restoration of images derived from flow visualization experiments
[AD-A250317] p 3339 N92-28952
Segmentation of satellite imagery using hierarchical thresholding and neural networks
[AD-A247915] p 3319 N92-28965
A probabilistic neural network approach to cloud classification
[AD-A247916] p 3319 N92-28966
Exploring compositional variations on the surface of Mars applying mixing modeling to a telescopic spectral image p 3388 N92-29043
Physical interpretation of thermal and reflected data on Martian surface units p 3391 N92-29062
Method and apparatus for predicting the direction of movement in machine vision
[NASA-CASE-NPO-17552-1-CU] p 3331 N92-29129
IMAGE RECONSTRUCTION
An acoustic charge transport imager for high definition television application
[AD-A250433] p 3274 N92-28773
IMAGE RESOLUTION
Applications of passive microwave satellite data for Arctic Sea ice studies
[AD-A245966] p 3306 N92-28791
IMAGE ROTATION
Multi-channel fiber optic rotary joint for single-mode fiber
[AD-D015273] p 3358 N92-29095
IMAGERY
The role of simulation for the study of APIS (piloting support by synthetic imagery) p 3224 N92-28544
Atmospheric corrections of land imagery using the extended radiosity method
[DE92-011355] p 3306 N92-28840
A rotorcraft flight database for validation of vision-based ranging algorithms
[NASA-TM-103906] p 3231 N92-29103
IMAGES
Thermal wave imaging and characterization of solids
[AD-A249297] p 3297 N92-28851
Studies of iterated transform image compression and its application to color and DTED
[AD-A248060] p 3339 N92-28946
Digital enhancement and restoration of images derived from flow visualization experiments
[AD-A250317] p 3339 N92-28952
IMAGING SPECTROMETERS
Remote sensing applications of the extended radiosity method
[DE92-011356] p 3306 N92-28807
Infrared photometric behavior and opposition effect of Mars p 3382 N92-29011
Exploring compositional variations on the surface of Mars applying mixing modeling to a telescopic spectral image p 3388 N92-29043
IMAGING TECHNIQUES
Environmental testing of the Xi Scan 1000, portable fluoroscopic and radiographic imaging system
[AD-A247167] p 3324 N92-28242
Quantitative interphase study of composite materials. Interphase engineering: A scientific way of tailoring the mechanophysical properties of composite materials
[AD-A247776] p 3251 N92-28252
The Coordinated Noninvasive Studies (CNS) project, phase 1
[AD-A247159] p 3324 N92-28397
Image processing techniques for acoustic images
[AD-A247303] p 3352 N92-28559
Results of a low power ice protection system test and a new method of imaging data analysis
[NASA-TM-105745] p 3227 N92-28696
A contribution to laser range imaging technology
[NASA-CR-190501] p 3290 N92-28707
Exploring compositional variations on the surface of Mars applying mixing modeling to a telescopic spectral image p 3388 N92-29043
Water window imaging x ray microscope
[NASA-CASE-MFS-28485-1] p 3288 N92-29135
Method for advanced material characterization by laser induced eddy current imaging
[NASA-CASE-GSC-13386-1] p 3298 N92-29154
IMIDES
Polyimide processing additives
[NASA-CASE-LAR-13669-1] p 3265 N92-29157
IMPACT MELTS
Superheat in magma oceans p 3311 N92-28597
Dynamics and evolution of a magma ocean p 3314 N92-28612
Evidence for magma oceans on asteroids, the moon, and Earth p 3315 N92-28614
Magma ocean formation due to giant impacts p 3315 N92-28615
Inheritance of magma ocean differentiation during lunar origin by giant impact p 3315 N92-28616
Chemical reaction path modeling of hydrothermal processes on Mars: Preliminary results p 3389 N92-29050
IMPACT TESTS
Nondestructive evaluation of damages caused by impact and fatigue loading of polymer composites
[VTT-RR-742] p 3251 N92-28572
Drop test: Cessna Golden Eagle 421B
[DOT/FAA/CT-TN91/32] p 3230 N92-28900
Evaluation of Whipple bumper shields at 7 and 10 km/s
[NASA-TM-107958] p 3295 N92-28925
IMPACTORS
Inheritance of magma ocean differentiation during lunar origin by giant impact p 3315 N92-28616
IMPEDANCE
Analysis of electromagnetic propagation over variable terrain using the parabolic wave equation
[AD-A248061] p 3276 N92-28947
IMPEDANCE MEASUREMENT
RF impedance measurement status for the 7-GeV Advanced Photon Source (APS)
[DE92-013060] p 3274 N92-28810
IMPELLERS
Transient impeller test facility
[AD-D015249] p 3294 N92-28749
IMPROVEMENT
Improvement of connectionnist learning processes, working according to the gradients method
[ETN-92-91335] p 3327 N92-28787
IMPURITIES
Quasi-regular impurity distribution driven by charge-density wave
[DE92-622799] p 3363 N92-28281
Shallow states of donor impurities on periodically structured semiconductors interfaces
[DE92-622791] p 3363 N92-28312
IN-FLIGHT MONITORING
An overview of in-flight plume diagnostics for rocket engines
[NASA-TM-105727] p 3248 N92-28417
INCENDIARY AMMUNITION
Modular simulation of HEI fragments and blast pressure
[AD-A248205] p 3272 N92-29191
INCOMPRESSIBLE FLOW
Development of instrumentation for boundary layer transition detection
[AD-A249982] p 3287 N92-29171
INDENTATION
Nanoscale investigation of indentation, adhesion, and fracture of diamond (111) surfaces
[AD-A250164] p 3265 N92-28916
INDEPENDENT VARIABLES
The variance of Rasch ability estimates from partially-known item parameters
[AD-A247065] p 3348 N92-28273
Estimation of the point of incipient deterioration and a class of life distribution with application to cannibalization
[AD-A250216] p 3343 N92-29114
INDEXES (DOCUMENTATION)
Aeronautical engineering: A continuing bibliography with indexes (supplement 278)
[NASA-SP-7037(278)] p 3226 N92-28677
Aeronautical engineering: A continuing bibliography with indexes (supplement 275)
[NASA-SP-7037(275)] p 3226 N92-28679
Publications of the Jet Propulsion Laboratory, 1989
[NASA-CR-190457] p 3369 N92-29202
INDEXES (RATIOS)
A review of cost performance index stability
[AD-A246621] p 3370 N92-28255
INDIUM ALLOYS
Strained AlGaInAs semiconducting material for improved laser performance
[AD-A249379] p 3289 N92-28330
INDIUM ARSENIDES
Study of ultra short HFET devices with InP substrates
[AD-A248448] p 3279 N92-28427
INDIUM GALLIUM ARSENIDES
Study of ultra short HFET devices with InP substrates
[AD-A248448] p 3279 N92-28427

INDIUM PHOSPHIDES
Study of ultra short HFET devices with InP substrates
[AD-A248448] p 3279 N92-28427
Heteroepitaxy of InP on Si (001)
[ETN-92-91333] p 3364 N92-28786
INDUCTION
The effect of induced charges on low-energy particle trajectories near conducting and semiconducting plates
[NASA-TM-103589] p 3355 N92-28986
INDUCTION MOTORS
Electromechanical systems with transient high power response operating from a resonant AC link
[NASA-TM-105716] p 3238 N92-28985
INELASTIC SCATTERING
The 17 keV neutrino and neutrino tagging
[DE92-011281] p 3355 N92-28839
INERTIAL COORDINATES
Angular momentum: Can be used in ballistic tracking
[AD-A247722] p 3350 N92-28400
INERTIAL UPPER STAGE
A cost-benefit analysis on the deletion of the inertial upper stage factory acceptance testing versus a decrease in mission reliability
[AD-A246620] p 3245 N92-28254
INFERENCE
Generalized quantifiers and modal logic
[ITLI-LP-91-01] p 3348 N92-29214
INFORMATION
Information Resources Management long-range plan
[DE92-012408] p 3368 N92-28804
Files improvement the NARA way
[DE92-011139] p 3368 N92-28832
A theory of automated design of visual information presentations
[AD-A247425] p 3369 N92-28866
Space transportation analysis and design
[AD-A250629] p 3245 N92-28956
INFORMATION MANAGEMENT
Automated apparel specification retrieval system
[AD-A248619] p 3367 N92-28389
Information Resources Management long-range plan
[DE92-012408] p 3368 N92-28804
Analysis of multimedia information systems for the US Coast Guard
[AD-A247890] p 3369 N92-28960
INFORMATION PROCESSING (BIOLOGY)
Studies of perceptual memory
[AD-A250200] p 3328 N92-29144
INFORMATION RETRIEVAL
Conversion and retrievability of hard copy and digital documents on optical disks
[AD-A247481] p 3367 N92-28244
The instrumentation of a parallel, distributed database operation, retrieve-common, for merging two large sets of records
[AD-A247486] p 3367 N92-28246
Files improvement the NARA way
[DE92-011139] p 3368 N92-28832
Is choice accuracy related to information search patterns?
[IZF-1991-B-9] p 3369 N92-29162
INFORMATION SYSTEMS
Information strategy plan
[AD-A247740] p 3367 N92-28403
Information Resources Management long-range plan
[DE92-012408] p 3368 N92-28804
Information systems for engineering sustainable development
[DE92-011271] p 3368 N92-28838
Functional requirements document for the Earth Observing System Data and Information System (EOSDIS) Scientific Computing Facilities (SCF) of the NASA/MSFC Earth Science and Applications Division, 1992
[NASA-TM-4392] p 3333 N92-28899
Information technology in plain words
[AD-A250324] p 3369 N92-28955
Space transportation analysis and design
[AD-A250629] p 3245 N92-28956
Analysis of multimedia information systems for the US Coast Guard
[AD-A247890] p 3369 N92-28960
Consulting report on the NASA technology utilization network system
[NASA-CR-190387] p 3370 N92-29108
INFORMATION TRANSFER
Information systems for engineering sustainable development
[DE92-011271] p 3368 N92-28838
Archival of the ECOM-721 data
[AD-A249299] p 3338 N92-28845
A theory of automated design of visual information presentations
[AD-A247425] p 3369 N92-28866
INFRARED ASTRONOMY SATELLITE
Observational study and analysis of point sources found by the infrared astronomy satellite
[AD-A248416] p 3371 N92-28843
Using Gaussian windows to explore a multivariate data set
[NASA-CR-190556] p 3339 N92-29106
INFRARED IMAGERY
Simulation in infrared imaging: Using electrical circuit principles to model heat transfer
[AD-A248290] p 3278 N92-28276
Sea surface velocities from visible and infrared multispectral atmospheric mapping sensor imagery
[NASA-CR-190398] p 3305 N92-28715
Thermally distinct ejecta blankets from Martian craters
p 3379 N92-28994
Infrared imaging of Mars for volatile distribution and seasonal variability between 2.4 and 5.1 microns
p 3379 N92-28995
INFRARED INSTRUMENTS
Physical interpretation of thermal and reflected data on Martian surface units p 3391 N92-29062
INFRARED INTERFEROMETERS
Atmospheric and surface temperatures and airborne dust amounts during late southern summer from Mariner 9 IRIS data p 3390 N92-29056
INFRARED RADIATION
Infrared photometric behavior and opposition effect of Mars p 3382 N92-29011
Physical interpretation of thermal and reflected data on Martian surface units p 3391 N92-29062
ETO cloud studies for FIRE 2, part 1
[NASA-CR-190472] p 3319 N92-29087
INFRARED SPECTRA
Spectral identification of chemisorbed CO2 and application to Mars analog materials
p 3378 N92-28510
Relationships of soil, grass, and bedrock over the Kaweah serpentine melange through spectral mixture analysis of AVIRIS data
[NASA-CR-190445] p 3306 N92-28717
Infrared imaging of Mars for volatile distribution and seasonal variability between 2.4 and 5.1 microns
p 3379 N92-28995
Mid-infrared spectra of Martian komantiite
p 3390 N92-29053
INFRARED SPECTROMETERS
Atmospheric and surface temperatures and airborne dust amounts during late southern summer from Mariner 9 IRIS data p 3390 N92-29056
INFRARED SPECTROSCOPY
The emergence of atomic-level structural information for ordered metal-solution interfaces: Some recent contributions from in-situ infrared spectroscopy and scanning tunneling microscopy
[AD-A246765] p 3364 N92-28512
Studies of 1,3-disilacyclobutanes as single-source CVD precursors to silicon carbide
[AD-A247111] p 3365 N92-28885
Infrared imaging of Mars for volatile distribution and seasonal variability between 2.4 and 5.1 microns
p 3379 N92-28995
INHIBITORS
Propellant-to-inhibitor bonding system
[AD-D015243] p 3266 N92-28739
INJECTION
Injection: On-axis/off-axis
[NIKHEF-K/AMPS/91-07] p 3356 N92-28308
INJECTION LOCKING
Phase stability of injection-locked beam of semiconductor lasers
[NASA-TT-10001] p 3290 N92-28862
INJURIES
The chronic effects of JP-8 jet fuel exposure on the lungs
[AD-A250308] p 3326 N92-29123
INLET FLOW
Inlet distortion effects in aircraft propulsion system integration p 3237 N92-28464
INLET PRESSURE
Calculation of installation effects within performance computer programs p 3237 N92-28465
INORGANIC COMPOUNDS
Sol-gel processed multifunctional organic polymer-inorganic oxide composites for electronics and photonics
[AD-A246773] p 3263 N92-28412
INSERTS
The design of test-section inserts for higher speed aeroacoustic testing in the Ames 80- by 120-foot wind tunnel
[NASA-TM-103915] p 3353 N92-28909
INSPECTION
X ray computed tomography of full-scale castings
[AD-A247101] p 3258 N92-28241
Turbine aircraft engine operational trending and JT8D static component reliability study
[DOT/FAA/CT-91/10] p 3238 N92-28686
INSTRUCTION SETS (COMPUTERS)
Compilation and operation environment of an object based language
[ETN-92-91323] p 3338 N92-28785
INSTRUMENT APPROACH
Loran-C performance assurance assessment program
[NASA-CR-190469] p 3230 N92-28718
INSULATION
High temperature dielectric properties of Apical, Kapton, Peek, Teflon AF, and Upilex polymers
[NASA-TM-105753] p 3280 N92-28675
Performance of uncoated AFRSI blankets during multiple Space Shuttle flights
[NASA-TM-103892] p 3245 N92-29104
INSULATORS
Single layer multi-color luminescent display and method of making
[NASA-CASE-LAR-13616-3] p 3359 N92-29158
INTEGRAL EQUATIONS
Modal analysis of plates using boundary integral equations
[NLR-TP-89211-U] p 3302 N92-28688
INTEGRATED CIRCUITS
Investigation of an equivalent circuit for the inductive strip in finline with dielectric
[AD-A247025] p 3279 N92-28373
Applications of silicon hybrid multi-chip modules to avionics p 3235 N92-28379
Image processing for failure analysis of integrated circuits by an electron beam
[ETN-92-91322] p 3281 N92-28784
High-performance integrated circuit evaluation system for a gallium arsenide microsupercomputer
[AD-A250385] p 3281 N92-28798
A survey of high density packaging for high performance computing system
[AD-A248633] p 3332 N92-28891
Monolithic optoelectronic implementation of neural planes
[AD-A250286] p 3345 N92-28970
INTEGRATED OPTICS
Null shifting with fixed delays
[AD-A250059] p 3274 N92-28796
INTEGRITY
Responsible science: Ensuring the integrity of the research process, volume 1
[ISBN-0-309-04731-5] p 3350 N92-28363
INTELLIGENCE
The variance of Rasch ability estimates from partially-known item parameters
[AD-A247065] p 3348 N92-28273
INTERACTIONS
Correlation between surface free energy and surface constitution
[AD-A246699] p 3262 N92-28291
INTERATOMIC FORCES
The nonequilibrium molecular dynamics
[DE92-011760] p 3355 N92-28860
INTERCALATION
Method of intercalating large quantities of fibrous structures
[NASA-CASE-LEW-15077-1] p 3253 N92-29152
INTERFACIAL ENERGY
Correlation between surface free energy and surface constitution
[AD-A246699] p 3262 N92-28291
INTERFEROMETERS
VLA mapping of 1.35 cm water emission from the Mars atmospheric limb p 3381 N92-29004
INTERFEROMETRY
Three-axis fiber optic vector magnetometer
[AD-D015199] p 3357 N92-28223
Laser optical disk position encoder with active heads
[NASA-CASE-GSC-13175-1] p 3359 N92-29133
Detection of in-plane displacements of acoustic wave fields using extrinsic Fizeau fiber interferometric sensors
[NASA-CR-190493] p 3353 N92-29196
INTERMETALLICS
Phase transformations in Ti3Al based alloy
[AD-A246464] p 3261 N92-28976
Chemical vapor synthesis of niobium aluminides
[AD-A250332] p 3258 N92-29091
INTERMITTENCY
Mathematical modeling of solar magneto-dynamics
[AD-A247158] p 3395 N92-28520
INTERNAL FRICTION
Characterization of Martian near-subsurface materials by determination of cohesion and angle of internal friction p 3393 N92-29068
INTRUSION
Magmatic intrusions and hydrothermal systems on Mars p 3384 N92-29019

INVARIANCE
Binary optical filters for scale invariant pattern recognition
[NASA-TM-103902] p 3234 N92-28910
INVENTIONS
Whole body cleaning agent containing N-acyltaurate
[NASA-CASE-MSC-21589-1] p 3332 N92-29137
INVENTORIES
An inventory of data collected during the NERC's North Sea Community Research Project, 1987-1992
[REPT-21-1991] p 3323 N92-29215
INVERSE KINEMATICS
Inverse control problems: Mathematical preliminaries, system theoretical approaches, and their applications to aircraft dynamics
[LR-665] p 3345 N92-28581
INVERSE SCATTERING
Thermal wave imaging and characterization of solids
[AD-A249297] p 3297 N92-28851
INVERTEBRATES
In search of a unified theory of biological organization: What does the motor system of a sea slug tell us about human motor integration?
[AD-A250223] p 3328 N92-29119
INVISCID FLOW
The linear and nonlinear shear instability of a fluid sheet
[AD-A247092] p 3282 N92-28258
A numerical wind tunnel study of viscous-inviscid interaction
[AD-A248429] p 3283 N92-28350
Development of an unsteady three-dimensional viscous-inviscid interaction numerical method for the calculation of airfoils vibration
[ONERA-RSF-7/3617-AY-022A] p 3229 N92-29206
IODIDES
New methodology for fluorocarbon synthesis
[AD-A247163] p 3254 N92-28261
IODINE
Relaxation dynamics of highly excited halogens in their electronic ground states
[AD-A247312] p 3254 N92-28300
IODINE COMPOUNDS
Singlet delta oxygen pumping of iodine monofluoride in a supersonic flow
[AD-A249946] p 3284 N92-28766
IODINE ISOTOPES
Forsterite/melt partitioning of argon and iodine: Implications for atmosphere formation by outgassing of an early Martian magma ocean p 3313 N92-28604
ION ATOM INTERACTIONS
Excitation of atoms and molecules in collisions with highly charged ions
[DE92-012658] p 3355 N92-28764
ION BEAMS
A generalization of the K-V equilibrium for an intense, relativistic beam propagating in a solenoid
[AD-A247067] p 3350 N92-28238
Report on the workshop on Ion Implantation and Ion Beam Assisted Deposition
[AD-A250561] p 3365 N92-28923
ION IMPLANTATION
Perspectives of ion implantation for optics
[DE92-010664] p 3357 N92-28355
Report on the workshop on Ion Implantation and Ion Beam Assisted Deposition
[AD-A250561] p 3365 N92-28923
ION PROPULSION
Development and flight history of SERT 2 spacecraft
[NASA-TM-105636] p 3250 N92-28983
ION RECOMBINATION
History of oxygen and carbon escape from the Martian atmosphere p 3376 N92-28498
ION SOURCES
Development of negative heavy ion sources for plasma potential measurement
[DE92-782102] p 3360 N92-28234
Excited negative ions and molecules and negative ion production
[AD-A247017] p 3354 N92-28414
IONIC COLLISIONS
Excitation of atoms and molecules in collisions with highly charged ions
[DE92-012658] p 3355 N92-28764
IONIC REACTIONS
Nitrogen escape from Mars p 3383 N92-29014
IONIZATION
Scattering mechanisms for semiconductor transport calculations
[AD-A249260] p 3278 N92-28295
Arcjet plume ionization effects on exposed solar array conducting surfaces
[AD-A245912] p 3307 N92-28383
Excitation of atoms and molecules in collisions with highly charged ions
[DE92-012658] p 3355 N92-28764
IONIZING RADIATION
Problems in mechanistic theoretical models for cell transformation by ionizing radiation
[DE92-010265] p 3324 N92-28278
Somatic gene mutation in the human in relation to radiation risk
[DE92-009459] p 3325 N92-28685
IONOPAUSE
The ancient oxygen exosphere of Mars: Implications for atmosphere evolution p 3395 N92-29080
IONOSPHERIC PROPAGATION
An OTH radar clutter simulation
[AD-A248054] p 3272 N92-28304
IONS
Comparison of electromagnetic propagation predictions from IREPS and RPO across a coastal transition
[AD-A249331] p 3273 N92-28357
Excitation of atoms and molecules in collisions with highly charged ions
[DE92-012658] p 3355 N92-28764
Simulations of solvent effects on confined electrolytes
[AD-A246851] p 3258 N92-28982
IRIDIUM
Experimental determination of the solubility of iridium in silicate melts: Preliminary results p 3310 N92-28591
IRON
Magma ocean: Mechanisms of formation p 3312 N92-28600
Iron Moessbauer spectroscopy: Superparamagnetism in hydrothermal vents and the search for evidence of past life on Mars p 3378 N92-28989
The nanophase iron mineral(s) in Mars soil p 3379 N92-28990
Rates of oxidative weathering on the surface of Mars p 3380 N92-28999
IRON ALLOYS
Effect of solidification technique and consolidation method on the properties of rapidly solidified Al-Fe alloys
[DLR-FB-91-24] p 3260 N92-28823
IRON COMPOUNDS
Mars: Compositional variability of ferric/ferrous minerals and polar volatiles from groundbased imaging spectroscopy p 3379 N92-28993
IRON OXIDES
Combustion mechanisms of solids --- solid rocket propellant
[AD-A247088] p 3254 N92-28240
The nanophase iron mineral(s) in Mars soil p 3379 N92-28990
Mars surface weathering products and spectral analogs: Palagonites and synthetic iron minerals p 3383 N92-29017
ISOLATION
KC-135 Large Motion Isolation Mount (LMIM) p 3267 N92-28440
New inertial actuator provides isolation and stabilization in microgravity conditions p 3267 N92-28443
Microgravity isolation mounts based upon Piezoelectric film p 3268 N92-28454
ISOTOPIC LABELING
The early Martian atmosphere p 3376 N92-28502
The stable isotopic compositions of indigenous carbon-bearing components in EETA 79001 p 3384 N92-29021
ISOTROPIC TURBULENCE
Mapping closures for turbulent mixing and reaction
[AD-A247305] p 3283 N92-28274
ISOTROPY
Prediction of composite material properties using two-dimensional finite element micromechanical analysis
[AD-A250300] p 3252 N92-28702
ITERATION
Improvement of connectionnist learning processes, working according to the gradients method
[ETN-92-91335] p 3327 N92-28787
Mapping unstructured grid computations to massively parallel computers
[NASA-CR-190551] p 3343 N92-29109
ITERATIVE SOLUTION
Fast algorithms for transport models
[DE92-011432] p 3338 N92-28841
Mapping unstructured grid computations to massively parallel computers
[NASA-CR-190551] p 3343 N92-29109

J

JAMMERS
Data selection for fast projection techniques applied to adaptive nulling: A comparative study of performance
[AD-A246468] p 3276 N92-28979
JAMMING
Design on an enhanced interactive satellite communications system analysis program
[AD-A245967] p 3273 N92-28410
Coding for frequency hopped spread spectrum satellite communications
[ECE-90-1] p 3274 N92-28699
Data selection for fast projection techniques applied to adaptive nulling: A comparative study of performance
[AD-A246468] p 3276 N92-28979
JAPAN
Planet-B: A Japanese Mars aeronomy observer p 3393 N92-29072
JET AIRCRAFT
Effective cueing during approach and touchdown: Comparison with flight p 3226 N92-28552
JET AIRCRAFT NOISE
Full Navier-Stokes analysis of a two-dimensional mixer/ejector nozzle for noise suppression
[NASA-TM-105715] p 3236 N92-28419
JET FLOW
Large Eddy Simulations (LES) and Direct Numerical Simulations (DNS) for the computational analyses of high speed reacting flows
[NASA-CR-190364] p 3285 N92-28817
The compositional structure and the effects of exothermicity in an unpremixed planar jet flame p 3258 N92-28821
JET NOZZLES
Full Navier-Stokes analysis of a two-dimensional mixer/ejector nozzle for noise suppression
[NASA-TM-105715] p 3236 N92-28419
JET PROPULSION
Publications of the Jet Propulsion Laboratory, 1989
[NASA-CR-190457] p 3369 N92-29202
JOINTS (JUNCTIONS)
The characterization of ceramics and ceramic/metal-joints by ultrasonic techniques
[VTT-RR-741] p 3266 N92-29194
JP-8 JET FUEL
The chronic effects of JP-8 jet fuel exposure on the lungs
[AD-A250308] p 3326 N92-29123

K

KALMAN FILTERS
Image processing techniques for acoustic images
[AD-A247303] p 3352 N92-28559
Identification of linear system models and state estimators for controls p 3247 N92-28737
KAONS
The 17 keV neutrino and neutrino tagging
[DE92-011281] p 3355 N92-28839
KAPTON (TRADEMARK)
High temperature dielectric properties of Apical, Kapton, Peek, Teflon AF, and Upilex polymers
[NASA-TM-105753] p 3280 N92-28675
KELVIN-HELMHOLTZ INSTABILITY
The linear and nonlinear shear instability of a fluid sheet
[AD-A247092] p 3282 N92-28258
KINEMATIC EQUATIONS
Quasi-recursive dynamics equations for spacecraft-based flexible robotic manipulators
[NLR-TP-90028-U] p 3345 N92-28648
KINEMATICS
Accuracy of shipborne kinematic GPS surveying
[AD-A245942] p 3230 N92-28317
A combined experimental and analytical investigation of the theory of plasticity involving strain induced anisotropy
[AD-A248440] p 3298 N92-28352
Quaternion and Euler angles in kinematics
[NAL-TM-636] p 3303 N92-28836
KINETIC ENERGY
A system structure for predictive relations in penetration mechanics
[AD-A246453] p 3292 N92-28284
KINETIC EQUATIONS
Numerical studies of low temperature gallium arsenide buffer layers and their influence on device operation
[AD-A250309] p 3258 N92-29126
KINETICS
Numerical studies of convective transport associated with crystal growth in mirrogravity p 3267 N92-28437
Evolution of a terrestrial magma ocean: Thermodynamics, kinetics, rheology, convection, differentiation p 3314 N92-28611
Computations of detonation structure: The influence of model input parameters
[AD-A248634] p 3285 N92-28803
Joint DOE/NSF workshop on flow of particulates and fluids
[DE92-012692] p 3285 N92-28808

Effect of alumina particle additions on the aging kinetics of 2014-aluminum matrix composites
[AD-A245949] p 3252 N92-28898

KLYSTRONS
High power microwave generator
[AD-D015262] p 3277 N92-29199

KNOWLEDGE BASES (ARTIFICIAL INTELLIGENCE)
Validation of knowledge based systems
[AD-A247741] p 3368 N92-28404
Organizing plan libraries in subsumption hierarchies: Specificity based plan selection
[AD-A248711] p 3368 N92-28430
Application of knowledge-based systems for diagnosis of aircraft systems
[NLR-TP-90192-U] p 3230 N92-28655
What is on the machine's mind? Models for reasoning with incomplete and uncertain knowledge
[NLR-TP-91099-U] p 3345 N92-28716

KNOWLEDGE REPRESENTATION
What is on the machine's mind? Models for reasoning with incomplete and uncertain knowledge
[NLR-TP-91099-U] p 3345 N92-28716
SPEEDS: An approach to support programming environments using expert database systems
[AD-A247469] p 3339 N92-28943
Air combat maneuvering expert system trainer
[AD-A246459] p 3241 N92-28975

L

LABORATORIES
Publications of the Jet Propulsion Laboratory, 1989
[NASA-CR-190457] p 3369 N92-29202

LAKES
Amazonis and Utopia Planitiae: Martian Lacustrine basins p 3391 N92-29058

LAMINAR BOUNDARY LAYER
Turbulent spot generation and growth rates in a transonic boundary layer
[AD-A250221] p 3287 N92-29118

LAMINAR FLOW
Instrumentation requirements for laminar flow research in the NLR high speed wind tunnel HST
[NLR-TP-89158-U] p 3240 N92-28669
A 2-D analysis of evaporation in laminar flow
[AD-A246467] p 3287 N92-28978

LAMINAR FLOW AIRFOILS
The windtunnel as a tool for laminar flow research
[NLR-TP-90145-U] p 3240 N92-28661
Instrumentation requirements for laminar flow research in the NLR high speed wind tunnel HST
[NLR-TP-89158-U] p 3240 N92-28669

LAMINAR HEAT TRANSFER
Development of instrumentation for boundary layer transition detection
[AD-A249982] p 3287 N92-29171

LAMINATES
Fatigue strength of a glass fiber reinforced laminate structure
[VTT-RR-743] p 3251 N92-28573
The application of carbon fibres in ARALL laminates
[LR-658] p 3259 N92-28576
The influence of elevated temperature on the bonding quality of deformed GLARE
[LR-659] p 3252 N92-28577
The compressive properties of GLARE
[LR-666] p 3252 N92-28582
Stress analysis of plated-through-holes in rigid flex multilayer printed wiring boards
[DE92-011659] p 3303 N92-28855
Tensile and interlaminar properties of GLARE (trade name) laminates
[AD-A250188] p 3253 N92-28921
In-situ fault detection by the hybrid ray-mode method
[AD-A250213] p 3297 N92-29112
Numerical studies of low temperature gallium arsenide buffer layers and their influence on device operation
[AD-A250309] p 3258 N92-29126
Development of a stratified plate model for composite panels
[AD-A248206] p 3253 N92-29192

LAND ICE
Regional variations in the stability and diffusion of water-ice in the Martian regolith p 3388 N92-29042
Is ground ice stable near the Martian equator? p 3389 N92-29046

LAND USE
Quantitative updating of land use information on 1:50,000 scale topographic maps using SPOT LANDSAT Thematic Mapper imagery
[NLR-TP-89061-U] p 3305 N92-28708

LANDFORMS
Erosional landforms on the layered terrains in Valles Marineris p 3386 N92-29031

LANDING SITES
Martian surface simulations p 3383 N92-29016

LANDSAT SATELLITES
Multitemporal analysis of a braiding river
[NLR-TP-89235-U] p 3305 N92-28690

LARGE SPACE STRUCTURES
Structural design methodology for large space structures
[AD-A247672] p 3246 N92-28560
Sensor filter designs for large flexible spacecraft p 3247 N92-28733

LASER ANEMOMETERS
Potential applications of laser Doppler anemometry for in-flight measurements
[NLR-TP-90163-U] p 3236 N92-28654
Comparison of LDA and LTA applications for propeller tests in wind tunnels
[NLR-MP-88031-U] p 3226 N92-28658
Laser anemometer measurements and computations in an annular cascade of high turning core turbine vanes
[NASA-TP-3252] p 3229 N92-28980
A 4-spot time-of-flight anemometer for small centrifugal compressor velocity measurements
[NASA-TM-105717] p 3288 N92-29105

LASER APPLICATIONS
Combustion mechanisms of solids --- solid rocket propellant
[AD-A247088] p 3254 N92-28240
Strained AlGaInAs semiconducting material for improved laser performance
[AD-A249379] p 3289 N92-28330
A contribution to laser range imaging technology
[NASA-CR-190501] p 3290 N92-28707
Asynchronous optical sampling for laser-based combustion diagnostics in high-pressure flames
[AD-A250206] p 3257 N92-28896
Scientific applications of frequency-stabilized laser technology in space
[NASA-CR-190449] p 3291 N92-28941
Use of laser range finders and range image analysis in automated assembly tasks
[NASA-CR-186957] p 3291 N92-29139

LASER BEAMS
Method for advanced material characterization by laser induced eddy current imaging
[NASA-CASE-GSC-13386-1] p 3298 N92-29154

LASER CAVITIES
Noise reduction in ring laser driven by a broad band pump
[DE92-622403] p 3289 N92-28228
Tuning and automatic phase adjustment in external cavity diode laser beam combiners
[AD-A247421] p 3290 N92-28903

LASER DAMAGE
Investigation of laser-induced retinal damage
[AD-A250173] p 3326 N92-28920

LASER DOPPLER VELOCIMETERS
Potential applications of laser Doppler anemometry for in-flight measurements
[NLR-TP-90163-U] p 3236 N92-28654
Comparison of LDA and LTA applications for propeller tests in wind tunnels
[NLR-MP-88031-U] p 3226 N92-28658
Experimental and theoretical investigations on the particle lag of particles under the influence of large velocity gradients in compressible flow
[DLR-FB-91-25] p 3286 N92-28825

LASER INDUCED FLUORESCENCE
A study of the normal injection of hydrogen into a heated supersonic flow using planar laser-induced fluorescence
[DE92-010701] p 3282 N92-28268
Advanced diagnostics for reacting flows
[AD-A247059] p 3360 N92-28298
Relaxation dynamics of highly excited halogens in their electronic ground states
[AD-A247312] p 3254 N92-28300
Multicomponent comparison of optical and mass spectrometric diagnostics in low-pressure flames
[AD-A250323] p 3257 N92-28954

LASER INTERFEROMETRY
Instrumentation for ultrahigh strain rate experiments
[AD-A249358] p 3298 N92-28327

LASER OUTPUTS
Strained AlGaInAs semiconducting material for improved laser performance
[AD-A249379] p 3289 N92-28330
CO2 laser frequency multiplication
[AD-A245915] p 3290 N92-28761
CO2 laser frequency multiplication
[AD-A247542] p 3291 N92-28933
Scientific applications of frequency-stabilized laser technology in space
[NASA-CR-190449] p 3291 N92-28941
Method for advanced material characterization by laser induced eddy current imaging
[NASA-CASE-GSC-13386-1] p 3298 N92-29154
Big Sky Workshop on Super-Intense Laser-Atom Physics
[AD-A248225] p 3292 N92-29223

LASER PLASMAS
Thin film cadmium telluride photovoltaic cells
[DE92-001239] p 3306 N92-28277
Advanced diagnostics for reacting flows
[AD-A247059] p 3360 N92-28298

LASER PUMPING
Noise reduction in ring laser driven by a broad band pump
[DE92-622403] p 3289 N92-28228
Relaxation dynamics of highly excited halogens in their electronic ground states
[AD-A247312] p 3254 N92-28300
A diode laser pumped Nd:YAG laser
[FFI-91/7020] p 3289 N92-28315
Asynchronous optical sampling for laser-based combustion diagnostics in high-pressure flames
[AD-A250206] p 3257 N92-28896

LASER RANGE FINDERS
A contribution to laser range imaging technology
[NASA-CR-190501] p 3290 N92-28707
Use of laser range finders and range image analysis in automated assembly tasks
[NASA-CR-186957] p 3291 N92-29139

LASER SPECTROSCOPY
Research studies on extreme ultraviolet and soft x ray lasers
[AD-A247309] p 3289 N92-28299

LASER TARGET INTERACTIONS
Big Sky Workshop on Super-Intense Laser-Atom Physics
[AD-A248225] p 3292 N92-29223

LASERS
Femtosecond carrier processes in compound semiconductors and real time signal processing
[AD-A248053] p 3278 N92-28275
Accuracy of shipborne kinematic GPS surveying
[AD-A245942] p 3230 N92-28317
Center for the integration of optical computing
[AD-A250306] p 3337 N92-28719
Scientific applications of frequency-stabilized laser technology in space
[NASA-CR-190449] p 3291 N92-28941
Laser optical disk position encoder with active heads
[NASA-CASE-GSC-13175-1] p 3359 N92-29133
Method for advanced material characterization by laser induced eddy current imaging
[NASA-CASE-GSC-13386-1] p 3298 N92-29154

LASING
Singlet delta oxygen pumping of iodine monofluoride in a supersonic flow
[AD-A249946] p 3284 N92-28766

LATERAL CONTROL
Initial validation of a R/D simulator with large amplitude motion p 3225 N92-28546
Effects of cockpit lateral stick characteristics on handling qualities and pilot dynamics
[NASA-CR-4443] p 3239 N92-28584

LAUNCH VEHICLES
A cost-benefit analysis on the deletion of the inertial upper stage factory acceptance testing versus a decrease in mission reliability
[AD-A246820] p 3245 N92-28254
Integrated health monitoring and controls for rocket engines
[NASA-TM-105763] p 3249 N92-28693

LAUNCHING
Rocket nozzle shield
[AD-D015248] p 3249 N92-28748
Space applications for contactless coilguns
[DE92-011156] p 3245 N92-29102

LAVA
Volcanic recycling of carbonate deposits on Mars p 3377 N92-28506
Implications of early Hesperian ages for presumed Noachian age volcanic flows on Mars p 3383 N92-29015
Recent Elysium volcanism: Effects on the Martian atmosphere p 3389 N92-29048

LAW (JURISPRUDENCE)
Identification and analysis of factors affecting the adoption of alternative transportation fuels
[PB92-164326] p 3266 N92-28914

LEADING EDGES
Study of the leading-edge vortex dynamics in the unsteady flow over an airfoil
[AD-A247532] p 3228 N92-28865

LEAKAGE
Leakage current measurements in SOI devices
[AD-A247694] p 3280 N92-28561

LEARNING
Reinforcement learning for the adaptive control of perception and action
[AD-A249351] p 3344 N92-28325

Improvement of connectionnist learning processes, working according to the gradients method
[ETN-92-91335] p 3327 N92-28787
Integrating the affective domain into the instructional design process
[AD-A249287] p 3327 N92-28880
In search of a unified theory of biological organization: What does the motor system of a sea slug tell us about human motor integration?
[AD-A250223] p 3328 N92-29119
Learning, teaching, and testing for complex conceptual understanding
[AD-A248728] p 3328 N92-29142
New neural algorithms for self-organized learning
[AD-A249816] p 3341 N92-29198

LEARNING THEORY
Computer-based assessment of schema knowledge in a flexible problem-solving environment
[AD-A246779] p 3348 N92-28516
Acquisition and improvement of human motor skills: Learning through observation and practice
[NASA-TM-107878] p 3329 N92-29174

LEAST SQUARES METHOD
Some aerospace applications of estimation theory
[ETN-92-91281] p 3349 N92-28647

LENGTH
Influence of aerodynamic roughness length on aeolian processes: Earth, Mars, Venus p 3380 N92-28996

LENSES
Portable dynamic fundus instrument
[NASA-CASE-MSC-21675-1] p 3325 N92-28755

LESIONS
Study of SCN neurochemistry using in vivo microdialysis in the conscious brain: Correlation with overt circadian rhythms
[AD-A247172] p 3325 N92-28886

LEVITATION
Present status of computational tools for Maglev development
[DE92-013252] p 3294 N92-28815
Superconducting bearings with levitation control configurations
[NASA-CASE-GSC-13346-1] p 3295 N92-29099

LIAPUNOV FUNCTIONS
The principal part of plane vector fields with fixed Newton diagram
[DE92-622408] p 3346 N92-28311

LIBRARIES
Organizing plan libraries in subsumption hierarchies: Specificity based plan selection
[AD-A248711] p 3368 N92-28430

LIE GROUPS
The exchange algebra for Liouville theory on punctured Riemann sphere
[DE92-622409] p 3366 N92-28229

LIFE (DURABILITY)
Validation of knowledge based systems
[AD-A247741] p 3368 N92-28404
Extensibility experiments with the software life-cycle support environment
[AD-A247696] p 3335 N92-28562
The use of load enhancement factors in the certification of composite aircraft structures
[NLR-TP-90068-U] p 3232 N92-28649
Ground Systems Development Environment (GSDE) software configuration management
[NASA-CR-190503] p 3337 N92-28710

LIFE CYCLE COSTS
Life cycle costs of the C-130 electrical power system upgrade
[AD-A246759] p 3221 N92-28348
Extensibility experiments with the software life-cycle support environment
[AD-A247696] p 3335 N92-28562

LIFE SCIENCES
Aeronautical engineering: A continuing bibliography with indexes (supplement 275)
[NASA-SP-7037(275)] p 3226 N92-28679
Space life sciences strategic plan
[NASA-TM-107954] p 3244 N92-29100

LIFE SUPPORT SYSTEMS
Coupling plant growth and waste recycling systems in a controlled life support system (CELSS)
[NASA-TM-107544] p 3330 N92-28670

LIFT DEVICES
Constrained spanload optimization for minimum drag of multi-lifting-surface configurations
[NLR-TP-89126-U] p 3227 N92-28660

LIFTING BODIES
In-flight simulation studies at the NASA Dryden Flight Research Facility
[NASA-TM-4396] p 3234 N92-29110

LIGANDS
Macrocyclic polycation complexes for secondary anion binding, molecular recognition, and catalysis
[AD-A246690] p 3254 N92-28287

LIGHT (VISIBLE RADIATION)
Center for the integration of optical computing
[AD-A250306] p 3337 N92-28719
A Be star atlas of far UV and optical high-resolution spectra
[ESA-SP-1147] p 3371 N92-28781

LIGHT BEAMS
Accelerator simulation using computers
[DE92-010729] p 3356 N92-28270

LIGHT GAS GUNS
A momentum limit for electromagnetic railguns
[DE92-011380] p 3245 N92-28861

LIGHT HELICOPTERS
Crew station research and development facility training for the light helicopter demonstration/validation program
[NASA-TM-103865] p 3327 N92-28744

LIGHT MODULATION
Center for the integration of optical computing
[AD-A250306] p 3337 N92-28719
Impact on the medium MTF by model estimation of beta
[AD-A247985] p 3359 N92-29167

LIGHT SCATTERING
Rocket plume flowfield characterization using laser Rayleigh scattering
[NASA-TM-105739] p 3357 N92-28475
Remote sensing applications of the extended radiosity method
[DE92-011356] p 3306 N92-28807
Impact on the medium MTF by model estimation of beta
[AD-A247985] p 3359 N92-29167

LIGHTNING
Multiparameter radar and aircraft based studies of the microphysical, kinematic, and electrical structure of convective clouds
[AD-A247497] p 3318 N92-28668

LINE OF SIGHT
Tactical line-of-sight radio propagation reliability
[AD-A245909] p 3277 N92-29165

LINE SHAPE
Analyzing noisy spectral line shapes
[DE92-011153] p 3362 N92-29086

LINE SPECTRA
VLA mapping of 1.35 cm water emission from the Mars atmospheric limb p 3381 N92-29004
Analyzing noisy spectral line shapes
[DE92-011153] p 3362 N92-29086

LINEAR ALTERNATORS
M-H characteristics and demagnetization resistance of samarium-cobalt permanent magnets to 300 C
[NASA-CR-189194] p 3280 N92-28723

LINEAR EQUATIONS
Numerical methods of linear and nonlinear optimization
[AD-A248579] p 3335 N92-28428

LINEAR PROGRAMMING
Numerical methods of linear and nonlinear optimization
[AD-A248579] p 3335 N92-28428
A network flow algorithm for just-in-time project scheduling
[MEMO-COSOR-91-21] p 3336 N92-28638
Global minimum solution of engineering design problems
[AD-A247496] p 3337 N92-28704

LINEAR SYSTEMS
Adaptive and nonlinear control
[AD-A248580] p 3344 N92-28429
Identification of linear system models and state estimators for controls p 3247 N92-28737

LINEARIZATION
Identification of weakly non-linear dynamical systems by means of random excitations
[ONERA-NT-1991-10] p 3349 N92-28778

LIOUVILLE THEOREM
Classical and quantum Liouville theory on the Riemann sphere with n greater than 3 punctures (II)
[DE92-622380] p 3366 N92-28227
The exchange algebra for Liouville theory on punctured Riemann sphere
[DE92-622409] p 3366 N92-28229

LIQUID ATOMIZATION
The linear and nonlinear shear instability of a fluid sheet
[AD-A247092] p 3282 N92-28258

LIQUID CRYSTALS
Fiber-optic interconnection networks for spacecraft
[NASA-CR-190531] p 3358 N92-28698
Bifurcations and patterns in nonlinear dissipative systems
[DE92-013502] p 3364 N92-28806
Development of instrumentation for boundary layer transition detection
[AD-A249982] p 3287 N92-29171

LIQUID INJECTION
Hydrogen no-vent fill testing in a 5 cubic foot (142 liter) tank using spray nozzle and spray bar liquid injection
[NASA-TM-105759] p 3266 N92-28433

LIQUID METALS
Underwater vapor phase burning of aluminum particles and on aluminum ignition during steam explosions
[DE92-011196] p 3257 N92-28894

LIQUID PROPELLANT ROCKET ENGINES
An overview of in-flight plume diagnostics for rocket engines
[NASA-TM-105727] p 3248 N92-28417

LIQUID SLOSHING
Prediction of attitude stability of asymmetric dual-spin stabilized spacecraft using improved liquid slosh model
[AD-A247023] p 3246 N92-28368
Nonlinear sloshing and the coupled dynamics of liquid propellants and spacecraft
[AD-A250023] p 3248 N92-28967

LIQUID SURFACES
The linear and nonlinear shear instability of a fluid sheet
[AD-A247092] p 3282 N92-28258
A 2-D analysis of evaporation in laminar flow
[AD-A246467] p 3287 N92-28978

LIQUID-SOLID INTERFACES
Weighted-density functional approach for the solid-liquid interfaces in electrolytes
[DE92-622662] p 3362 N92-28280

LIQUIDS
Fluids at high shock pressures and temperatures
[DE92-010709] p 3283 N92-28269
Estimation of the viscosities of silicate liquids at high pressure from measurements of oxygen diffusivity p 3313 N92-28607

LIQUIDUS
Phase equilibria and trace element partitioning in a magma ocean to 260 kilobars p 3311 N92-28595
A liquidus phase diagram for the groundmass of EETA 79001A (Eg), a primitive Shergottite composition p 3386 N92-29028

LITHIUM
Theoretical studies of the electronic and resonance structure of atomic and molecular negative ions
[AD-A247093] p 3354 N92-28259
Secondary Li battery incorporating 12-Crown-4 ether
[NASA-CASE-NPO-17922-1-CU] p 3280 N92-28753

LITHIUM ALLOYS
The stress corrosion cracking behavior of AlLi 2090-T83 in substitute ocean water
[LR-661] p 3259 N92-28578
Outdoor corrosion testing of aluminium-lithium alloys
[NLR-TP-90272-U] p 3260 N92-28794
Crack resistance, fracture toughness and instability in damage tolerant Al-Li alloys
[NLR-TP-90172-U] p 3303 N92-28850

LITHIUM COMPOUNDS
Ion conductive polymer solid electrolytes
[DE92-010518] p 3266 N92-29195

LITHOGRAPHY
High resolution electron beam lithography on x ray mask substrates. Effects of electron scattering and membrane heating
[ETN-92-91336] p 3272 N92-28793

LITHOLOGY
The distribution of anorthosite on the nearside of the moon p 3311 N92-28594
A new angle on lunar ferroan-suite differentiation p 3311 N92-28598

LITHOSPHERE
A seismic and integrated geophysical study of the lithosphere of the Colorado Plateau
[AD-A247091] p 3308 N92-28257

LOAD CARRYING CAPACITY
The energetics and mechanics of load carrying
[AD-A248441] p 3332 N92-29227

LOAD DISTRIBUTION (FORCES)
The energetics and mechanics of load carrying
[AD-A248441] p 3332 N92-29227

LOAD TESTS
The use of load enhancement factors in the certification of composite aircraft structures
[NLR-TP-90068-U] p 3232 N92-28649

LOADS (FORCES)
Shock and vibration isolation for cyclic exercise in spacecraft p 3267 N92-28449
Growth of surface cracks under fatigue loading: A literature survey
[LR-664] p 3299 N92-28580
Mobility power flow analysis of coupled plate structure subjected to mechanical and acoustic excitation
[NASA-CR-189635] p 3352 N92-28722
The energetics and mechanics of load carrying
[AD-A248441] p 3332 N92-29227

LOCAL AREA NETWORKS
Identification of aerodynamic models for maneuvering aircraft
[NASA-CR-190444] p 3233 N92-28720
LOCKING
Removable hand hold
[NASA-CASE-LEW-15196-1] p 3295 N92-29092
Quick application/release nut with engagement indicator
[NASA-CASE-MSC-21799-1] p 3296 N92-29150
LOCOMOTION
A survey report for the design of biped locomotion robot: The WL-12 (Waseda Leg-12)
[DE92-782046] p 3292 N92-28233
LOGARITHMS
Programming of the complex logarithm function in the solution of the cracked anisotropic plate loaded by a point force
[LR-657] p 3299 N92-28575
LOGIC
What is on the machine's mind? Models for reasoning with incomplete and uncertain knowledge
[NLR-TP-91099-U] p 3345 N92-28716
LOGIC CIRCUITS
Multiple-valued programmable logic array minimization by simulated annealing
[AD-A248620] p 3335 N92-28353
LOGIC DESIGN
Learning and tuning fuzzy logic controllers through reinforcements
[NASA-TM-107875] p 3345 N92-28759
Investigations of logic of introspection and related modes of reasoning with applications
[AD-A249286] p 3345 N92-28895
LONG DURATION EXPOSURE FACILITY
Effects of extremely high G acceleration forces on NASA's control and space exposed tomato seeds
[AD-A247488] p 3323 N92-28247
LONGITUDINAL CONTROL
Some longitudinal handling qualities design guidelines for active control technology transport aircraft
[NLR-TP-90129-U] p 3239 N92-28652
LORAN C
Survey parameters and availability of low-level aeromagnetic data for geomagnetic field modelling
p 3301 N92-28629
Loran-C performance assurance assessment program
[NASA-CR-190469] p 3230 N92-28718
LORENTZ FORCE
A 6 degree-of-freedom Lorentz force vibration isolator with nonlinear controller p 3267 N92-28444
LOSSES
Atmosphere-surface interactions and atmospheric evolution on Mars p 3383 N92-29012
Mars atmosphere evolution: Escape to space
p 3387 N92-29034
LOW ALTITUDE
Interest in real-time simulations for the development terrain following function of radar systems
p 3222 N92-28529
LOW ASPECT RATIO WINGS
Studies in general aviation aerodynamics
[NASA-CR-190431] p 3226 N92-28511
LOW COST
Innovative techniques for the production of low cost 2D laser diode arrays
[AD-A248247] p 3292 N92-29226
LOW GRAVITY MANUFACTURING
Numerical studies of convective transport associated with crystal growth in mirrogravity p 3267 N92-28437
An examination of anticipated g-jitter on Space Station and its effects on materials processes
p 3267 N92-28438
The Microgravity Isolation Mount (MGIM): A Columbus facility for improving the microgravity quality of payloads
p 3267 N92-28439
KC-135 Large Motion Isolation Mount (LMIM)
p 3267 N92-28440
Vibration isolation technology development to demonstration p 3267 N92-28442
New inertial actuator provides isolation and stabilization in microgravity conditions p 3267 N92-28443
LOW PASS FILTERS
Sensor filter designs for large flexible spacecraft
p 3247 N92-28733
LOW PRESSURE
Pressure regimes and core formation in the accreting earth p 3313 N92-28605
LOW SPEED WIND TUNNELS
Flow quality studies of the NASA Lewis Research Center 8- by 6-foot supersonic/9- by 15-foot low speed wind tunnel
[NASA-TM-105417] p 3240 N92-28673
LOW TEMPERATURE
The evaluation of rate constants for rapid electrode reactions by using microelectrode voltammetry: Virtues of measurement at lower temperature
[AD-A246760] p 3255 N92-28391
Numerical studies of low temperature gallium arsenide buffer layers and their influence on device operation
[AD-A250309] p 3258 N92-29126
LOW THRUST PROPULSION
Rocket plume flowfield characterization using laser Rayleigh scattering
[NASA-TM-105739] p 3357 N92-28475
LOW TURBULENCE
Low Reynolds number multiple-time-scale turbulence model and calculations of steady and pulsating shear layers
[NASA-CR-189176] p 3286 N92-28908
LUBRICANTS
High-temperature miniaturized turbine engine lubrication system simulator
[AD-A249259] p 3236 N92-28294
LUBRICATION
High-temperature miniaturized turbine engine lubrication system simulator
[AD-A249259] p 3236 N92-28294
Effect of metallic coating properties on the tribology of oil-lubricated coated-ceramics
[DE92-010904] p 3262 N92-28339
LUBRICATION SYSTEMS
High-temperature miniaturized turbine engine lubrication system simulator
[AD-A249259] p 3236 N92-28294
LUMINESCENCE
Short- and long-term climate changes on Mars
p 3389 N92-29051
Single layer multi-color luminescent display and method of making
[NASA-CASE-LAR-13616-3] p 3359 N92-29158
LUNAR BASED EQUIPMENT
Natural circulation decay heat removal from an SP-100, 550 kWe power system for a lunar outpost
[NASA-CR-190421] p 3307 N92-28863
LUNAR CORE
Origin of the moon and lunar core formation
p 3311 N92-28596
LUNAR CRATERS
The distribution of anorthosite on the nearside of the moon p 3311 N92-28594
A new angle on lunar ferroan-suite differentiation
p 3311 N92-28598
LUNAR CRUST
The distribution of anorthosite on the nearside of the moon p 3311 N92-28594
The ferroan-anorthositic suite and the extent of primordial lunar melting p 3315 N92-28618
LUNAR EVOLUTION
Origin of the moon and lunar core formation
p 3311 N92-28596
Evidence for magma oceans on asteroids, the moon, and Earth p 3315 N92-28614
LUNAR GEOLOGY
Imperfect fractional crystallization of the lunar magma ocean and formation of the lunar mantle: A realistic chemical approach p 3314 N92-28610
LUNAR MANTLE
Origin of the moon and lunar core formation
p 3311 N92-28596
Imperfect fractional crystallization of the lunar magma ocean and formation of the lunar mantle: A realistic chemical approach p 3314 N92-28610
LUNAR MARIA
Imperfect fractional crystallization of the lunar magma ocean and formation of the lunar mantle: A realistic chemical approach p 3314 N92-28610
LUNAR ROCKS
A new angle on lunar ferroan-suite differentiation
p 3311 N92-28598
Imperfect fractional crystallization of the lunar magma ocean and formation of the lunar mantle: A realistic chemical approach p 3314 N92-28610
LUNAR SOIL
A new angle on lunar ferroan-suite differentiation
p 3311 N92-28598
Imperfect fractional crystallization of the lunar magma ocean and formation of the lunar mantle: A realistic chemical approach p 3314 N92-28610

M

MACH NUMBER
Computation of steady and unsteady quasi-one-dimensional viscous/inviscid interacting internal flows at subsonic, transonic, and supersonic Mach numbers
[NASA-CR-189881] p 3283 N92-28555
MACH-ZEHNDER INTERFEROMETERS
Phase stability of injection-locked beam of semiconductor lasers
[NASA-TT-10001] p 3290 N92-28862
MACHINE LEARNING
Learning and tuning fuzzy logic controllers through reinforcements
[NASA-TM-107875] p 3345 N92-28759
Acquisition and improvement of human motor skills: Learning through observation and practice
[NASA-TM-107878] p 3329 N92-29174
MACHINE TOOLS
Scheduling multiple variable-speed machines
[AD-A249362] p 3268 N92-28359
Three dimensional measurements of prismatic bodies: Programming by means of a CAD system
[CRIF-MC-91] p 3337 N92-28700
MACROMOLECULES
Macrocyclic polycation complexes for secondary anion binding, molecular recognition, and catalysis
[AD-A246690] p 3254 N92-28287
MAGMA
Regional climatic effects of atmospheric SO2 on Mars
p 3377 N92-28504
Workshop on the Physics and Chemistry of Magma Oceans from 1 Bar to 4 Mbar
[NASA-CR-190419] p 3310 N92-28587
Thermal evolution and chemical differentiation of the terrestrial magma ocean p 3310 N92-28588
A magma ocean and the Earth's internal water budget
p 3310 N92-28590
Phase equilibria and trace element partitioning in a magma ocean to 260 kilobars p 3311 N92-28595
Superheat in magma oceans p 3311 N92-28597
Magma ocean: Mechanisms of formation
p 3312 N92-28600
Fate of a perched crystal layer in a magma ocean
p 3312 N92-28602
Evidence for a high temperature differentiation in a molten earth: A preliminary appraisal
p 3312 N92-28603
Forsterite/melt partitioning of argon and iodine: Implications for atmosphere formation by outgassing of an early Martian magma ocean p 3313 N92-28604
Pressure regimes and core formation in the accreting earth p 3313 N92-28605
Terrestrial magma ocean and core segregation in the earth p 3313 N92-28606
Estimation of the viscosities of silicate liquids at high pressure from measurements of oxygen diffusivity
p 3313 N92-28607
Cooling of the magma ocean due to accretional disruption of the surface insulating layer
p 3314 N92-28608
Early planetary differentiation: Geophysical consequences p 3314 N92-28609
Imperfect fractional crystallization of the lunar magma ocean and formation of the lunar mantle: A realistic chemical approach p 3314 N92-28610
Evolution of a terrestrial magma ocean: Thermodynamics, kinetics, rheology, convection, differentiation p 3314 N92-28611
Dynamics and evolution of a magma ocean
p 3314 N92-28612
Evidences for the terrestrial magma ocean from high-pressure melting experiments p 3315 N92-28613
Evidence for magma oceans on asteroids, the moon, and Earth p 3315 N92-28614
Magma ocean formation due to giant impacts
p 3315 N92-28615
Inheritance of magma ocean differentiation during lunar origin by giant impact p 3315 N92-28616
The three stages of magma ocean cooling
p 3315 N92-28617
The ferroan-anorthositic suite and the extent of primordial lunar melting p 3315 N92-28618
Magmatic intrusions and hydrothermal systems on Mars p 3384 N92-29019
MAGNESIUM OXIDES
Mg-perovskite/silicate melt partition coefficients in the CMS system at 2430 C and 226 Kbars
p 3312 N92-28601
MAGNETIC BEARINGS
Microgravity vibration isolation research at the University of Virginia p 3267 N92-28446
Superconducting bearings with levitation control configurations
[NASA-CASE-GSC-13346-1] p 3295 N92-29099
MAGNETIC CONTROL
Cryogenic shutter
[NASA-CASE-GSC-13189-2] p 3296 N92-29151
MAGNETIC DISTURBANCES
Reduction of marine magnetic data for modeling the main field of the Earth p 3300 N92-28626

MAGNETIC EFFECTS
Compositional disorder, magnetism, and their interplay in metallic alloys
[DE92-011671] p 3260 N92-28856
MAGNETIC FIELD CONFIGURATIONS
Resonant Compton scattering in models of gamma ray burst sources
[DE92-010720] p 3397 N92-28336
MAGNETIC FIELD RECONNECTION
Secondary instability in 3D magnetic reconnection
[AD-A248630] p 3360 N92-28354
MAGNETIC FIELDS
Three-axis fiber optic vector magnetometer
[AD-D015199] p 3357 N92-28223
Geomagnetic data from the US magnetic observatory network p 3301 N92-28631
Magnetic hysteresis and relaxation in Ag-sheathed TlBaCaCuO (1223) and Bi(Pb)SrCaCuO (2223) superconducting tapes
[DE92-011357] p 3365 N92-28874
Precision measurement of magnetic characteristics of an article with nullification of external magnetic fields
[NASA-CASE-NPO-18187-1-CU] p 3351 N92-29130
MAGNETIC FLUX
A momentum limit for electromagnetic railguns
[DE92-011380] p 3245 N92-28861
MAGNETIC INDUCTION
Magnetic and electromagnetic induction effects in the annual means of geomagnetic elements p 3301 N92-28632
Method and apparatus for using magneto-acoustic remanence to determine embrittlement
[NASA-CASE-LAR-13817-5] p 3303 N92-28757
Magnetic remanence method and apparatus to test materials for embrittlement
[NASA-CASE-LAR-13817-4] p 3304 N92-29101
Magneto acoustic emission method for testing materials for embrittlement
[NASA-CASE-LAR-13817-2] p 3304 N92-29155
MAGNETIC LEVITATION VEHICLES
Present status of computational tools for Maglev development
[DE92-013252] p 3294 N92-28815
MAGNETIC MATERIALS
Marine magnetic data holdings of World Data Center-A for Marine Geology and Geophysics p 3300 N92-28625
MAGNETIC MEASUREMENT
Three-axis fiber optic vector magnetometer
[AD-D015199] p 3357 N92-28223
Marine magnetic data holdings of World Data Center-A for Marine Geology and Geophysics p 3300 N92-28625
Precision measurement of magnetic characteristics of an article with nullification of external magnetic fields
[NASA-CASE-NPO-18187-1-CU] p 3351 N92-29130
MAGNETIC MOMENTS
The many aspects of neutrino physics
[DE92-011735] p 3355 N92-28858
MAGNETIC PROPERTIES
Growth and optical characterization of Zn(1-x)Mn(x)Te grown by molecular beam epitaxy
[DE92-010667] p 3363 N92-28331
Method and apparatus for using magneto-acoustic remanence to determine embrittlement
[NASA-CASE-LAR-13817-5] p 3303 N92-28757
Compositional disorder, magnetism, and their interplay in metallic alloys
[DE92-011671] p 3260 N92-28856
Precision measurement of magnetic characteristics of an article with nullification of external magnetic fields
[NASA-CASE-NPO-18187-1-CU] p 3351 N92-29130
MAGNETIC RECORDING
Disk memory device
[NASA-CASE-GSC-13196-1] p 3333 N92-29132
MAGNETIC RELAXATION
Magnetic hysteresis and relaxation in Ag-sheathed TlBaCaCuO (1223) and Bi(Pb)SrCaCuO (2223) superconducting tapes
[DE92-011357] p 3365 N92-28874
MAGNETIC STORMS
Reduction of marine magnetic data for modeling the main field of the Earth p 3300 N92-28626
MAGNETIC SURVEYS
Survey data for geomagnetic field modelling p 3300 N92-28623
Project MAGNET high-level vector survey data reduction p 3301 N92-28628
Survey parameters and availability of low-level aeromagnetic data for geomagnetic field modelling p 3301 N92-28629
MAGNETIC SUSPENSION
Vibration isolation technology development to demonstration p 3267 N92-28442
A 6 degree-of-freedom Lorentz force vibration isolator with nonlinear controller p 3267 N92-28444
MAGNETIC TAPES
Archival of the ECOM-721 data
[AD-A249299] p 3338 N92-28845
MAGNETITE
Oxygen in the Martian atmosphere: Regulation of PO2 by the deposition of iron formations on Mars p 3373 N92-28482
MAGNETOACOUSTICS
Method and apparatus for using magneto-acoustic remanence to determine embrittlement
[NASA-CASE-LAR-13817-5] p 3303 N92-28757
Magnetic remanence method and apparatus to test materials for embrittlement
[NASA-CASE-LAR-13817-4] p 3304 N92-29101
Magneto acoustic emission method for testing materials for embrittlement
[NASA-CASE-LAR-13817-2] p 3304 N92-29155
MAGNETOHYDRODYNAMIC STABILITY
Secondary instability in 3D magnetic reconnection
[AD-A248630] p 3360 N92-28354
Plasma beam measurements
[AD-A247892] p 3362 N92-28962
MAGNETOHYDRODYNAMIC TURBULENCE
Mathematical modeling of solar magneto-dynamics
[AD-A247158] p 3395 N92-28520
MAGNETOMETERS
Three-axis fiber optic vector magnetometer
[AD-D015199] p 3357 N92-28223
A new ocean bottom magnetometer system for continental shelf measurements
[AD-A247644] p 3321 N92-28321
Marine magnetic data holdings of World Data Center-A for Marine Geology and Geophysics p 3300 N92-28625
Survey parameters and availability of low-level aeromagnetic data for geomagnetic field modelling p 3301 N92-28629
MAGNETORESISTIVITY
Physics and technology for the investigation of properties of ultra small systems
[AD-A246772] p 3364 N92-28513
MAGNETOSTRICTION
Three-axis fiber optic vector magnetometer
[AD-D015199] p 3357 N92-28223
MAINTENANCE
Turbine aircraft engine operational trending and JT8D static component reliability study
[DOT/FAA/CT-91/10] p 3238 N92-28686
Diffuser casing upgrade for an advanced turbofan
[NLR-TP-90097-U] p 3238 N92-28711
A methodology for the evaluation of runway roughness for repair
[AD-A250407] p 3241 N92-28772
Design specifications for the Advanced Instructional Design Advisor (AIDA), volume 1
[AD-A248201] p 3340 N92-29187
Design specifications for the Advanced Instructional Design Advisor (AIDA), volume 2
[AD-A248202] p 3340 N92-29188
MAN MACHINE SYSTEMS
The role of simulation for the study of APIS (piloting support by synthetic imagery) p 3224 N92-28544
Super auditory localization for improved human-machine interfaces
[AD-A250288] p 3331 N92-29121
User friendly joystick
[NASA-CASE-GSC-13187-1] p 3281 N92-29153
NARSIM: A real-time simulator for air traffic control research
[NLR-TP-90147-U] p 3241 N92-29204
MAN-COMPUTER INTERFACE
Superconducting at NLR: NEC SX-2 capabilities in NLR's terminal and file-transfer network
[NLR-TP-89007-U] p 3342 N92-28706
Super auditory localization for improved human-machine interfaces
[AD-A250288] p 3331 N92-29121
HYPER: A domain decomposition program, version 1.0 (user's manual)
[AD-A250018] p 3340 N92-29172
MANAGEMENT INFORMATION SYSTEMS
Development of a flight information system using the structured method
[AD-A248207] p 3236 N92-29222
MANAGEMENT METHODS
Monitoring activities review of the Radiological Environmental Surveillance Program
[DE92-013103] p 3308 N92-28811
Consulting report on the NASA technology utilization network system
[NASA-CR-190387] p 3370 N92-29108
MANAGEMENT PLANNING
A review of cost performance index stability
[AD-A246621] p 3370 N92-28255
Ground Systems Development Environment (GSDE) software configuration management
[NASA-CR-190503] p 3337 N92-28710
Information Resources Management long-range plan
[DE92-012408] p 3368 N92-28804
Repository-based software engineering program: Concept document
[NASA-CR-190384] p 3341 N92-29200
MANAGEMENT SYSTEMS
Full mission simulation for research and development of air combat flight and attack management systems p 3223 N92-28538
MANEUVERABILITY
Study of the leading-edge vortex dynamics in the unsteady flow over an airfoil
[AD-A247532] p 3228 N92-28865
MANEUVERS
The use of ground based simulation for handling qualities research: A new assessment p 3224 N92-28545
MANGANESE COMPOUNDS
Growth and optical characterization of Zn(1-x)Mn(x)Te grown by molecular beam epitaxy
[DE92-010667] p 3363 N92-28331
MANIPULATORS
Microgravity vibration isolation research at the University of Virginia p 3267 N92-28446
Anthropomorphic teleoperation: Controlling remote manipulators with the DataGlove
[NASA-TM-103588] p 3330 N92-28521
Flow quality studies of the NASA Lewis Research Center 8- by 6-foot supersonic/9- by 15-foot low speed wind tunnel
[NASA-TM-105417] p 3240 N92-28673
MANNED MARS MISSIONS
Ongoing Progress in Spacecraft Controls
[NASA-CP-10099] p 3247 N92-28730
Review of Mars mission scenarios p 3244 N92-28731
MANNED SPACE FLIGHT
Space life support engineering program
[NASA-CR-190448] p 3330 N92-28671
MANNED SPACECRAFT
Ongoing Progress in Spacecraft Controls
[NASA-CP-10099] p 3247 N92-28730
MANNITOL
Surface crystallographic dependence of voltammetric oxidation of polyhydric alcohols and related systems at monocrystalline gold-acidic aqueous interfaces
[AD-A246763] p 3363 N92-28392
MANUAL CONTROL
User friendly joystick
[NASA-CASE-GSC-13187-1] p 3281 N92-29153
MANUFACTURING
Knowledge-based material selection in design
[PNR-90823] p 3337 N92-28741
MAPPING
Mapping closures for turbulent mixing and reaction
[AD-A247305] p 3283 N92-28274
Quantitative updating of land use information on 1:50,000 scale topographic maps using SPOT LANDSAT Thematic Mapper imagery
[NLR-TP-89061-U] p 3305 N92-28708
Sea surface velocities from visible and infrared multispectral atmospheric mapping sensor imagery
[NASA-CR-190398] p 3305 N92-28715
Use of laser range finders and range image analysis in automated assembly tasks
[NASA-CR-186957] p 3291 N92-29139
MARINE METEOROLOGY
An evaluation of the naval oceanic vertical aerosol model during Key90
[AD-A245943] p 3320 N92-28318
MARINE TECHNOLOGY
National Conference on the Use of Composite Materials in Load-Bearing Marine Structures. Volume 1: Summary report
[PB92-163831] p 3252 N92-28724
National Conference on the Use of Composite Materials in Load-Bearing Marine Structures. Volume 2: Conference proceedings
[PB92-163849] p 3252 N92-28725
MARINER 9 SPACE PROBE
Atomic oxygen in the Martian thermosphere p 3391 N92-29061
MARS (PLANET)
Water inventories on Earth and Mars: Clues to atmosphere formation p 3373 N92-28483
Regional climatic effects of atmospheric SO2 on Mars p 3377 N92-28504
The thermal structure, dust loading, and meridional transport in the Martian atmosphere during late southern summer p 3377 N92-28505
Volcanic recycling of carbonate deposits on Mars p 3377 N92-28506

The role of SO2 on Mars and on the primordial oxygen isotope composition of water on Earth and Mars
p 3377 N92-28507
Martian surficial carbon-constraints from isotopic measurements of shock-produced glass in EET A79001
p 3377 N92-28508
How Mars lost its atmosphere p 3378 N92-28509
Forsterite/melt partitioning of argon and iodine: Implications for atmosphere formation by outgassing of an early Martian magma ocean p 3313 N92-28604
Early planetary differentiation: Geophysical consequences p 3314 N92-28609
Workshop on the Martian Surface and Atmosphere Through Time
[NASA-CR-190418] p 3378 N92-28988
Influence of aerodynamic roughness length on aeolian processes: Earth, Mars, Venus p 3380 N92-28996
MARSNET surface and atmosphere investigations
p 3381 N92-29002
The subsurface hydrologic response of Mars to the thermal evolution of its early crust p 3381 N92-29006
Micro weather stations for in situ measurements in the Martian planetary boundary layer p 3382 N92-29008
Observations of Mars using Hubble Space Telescope
p 3385 N92-29026
Glacial geomorphic evidence for a late climatic change on Mars p 3386 N92-29029
Observed changes in limb clouds immediately prior to the onset of planet-encircling dust storms
p 3388 N92-29039
Mid-infrared spectra of Martian komantiite
p 3390 N92-29053
A carbonate-silicate aqueous geochemical cycle model for Mars p 3390 N92-29057
Amazonis and Utopia Planitiae: Martian Lacustrine basins p 3391 N92-29058
Carbonate formation on Mars: History of the CO2 atmosphere from models of diffusion-limited growth in non-aqueous environments p 3391 N92-29060
Atomic oxygen in the Martian thermosphere
p 3391 N92-29061
Physical interpretation of thermal and reflected data on Martian surface units p 3391 N92-29062
Physical properties of Deucalionis, Eos, Xanthe-type units in the central equatorial region of Mars
p 3392 N92-29063
Physical properties of Meridiani Sinus-type units in the central equatorial region of Mars p 3392 N92-29064
Physical properties of Oxia/Lunae Planum and Arabia-type units in the central equatorial region of Mars
p 3392 N92-29065
Glacial and marine chronology of Mars
p 3392 N92-29067
Characterization of Martian near-subsurface materials by determination of cohesion and angle of internal friction p 3393 N92-29068
Topography of Apollinaris Patera and Ma'adim Vallis
p 3393 N92-29069
Turbulent spectra, fluxes, stability and growth of the mixed layer in the boundary layer of Mars
p 3393 N92-29070
Aqueous-alteration products in S-N-C meteorites and implications for volatile/regolith interactions on Mars
p 3393 N92-29071
Planet-B: A Japanese Mars aeronomy observer
p 3393 N92-29072
Microcraters on Mars: Evidence of past climatic variations p 3394 N92-29073
Hydrogen and carbon isotopic composition of volatiles in Nakhla: Implications for weathering on Mars
p 3394 N92-29075
Modeling the seasonal cycle of CO2 on Mars: A fit to the Viking lander pressure curves p 3394 N92-29076
On the isotopic composition of magmatic carbon in SNC meteorites p 3394 N92-29077
Climatic implications of the simultaneous presence of CO2 and H2O in the Martian regolith
p 3395 N92-29079
The ancient oxygen exosphere of Mars: Implications for atmosphere evolution p 3395 N92-29080

MARS ATMOSPHERE

Trade study of three oxygen processors for the Martian atmosphere
[AD-A246854] p 3372 N92-28393
Papers Presented to the Workshop on the Evolution of the Martian Atmosphere
[NASA-CR-190508] p 3372 N92-28478
The impact of temperature dependent CO2 cross section measurements: A role for heterogeneous chemistry in the atmosphere of Mars? p 3372 N92-28479
Surface vs. atmospheric origin of 2.1-2.5 micron absorption features in the Martian spectrum
p 3373 N92-28480
Photochemical model for NH3 in an early Martian atmosphere p 3373 N92-28481
Oxygen in the Martian atmosphere: Regulation of PO2 by the deposition of iron formations on Mars
p 3373 N92-28482
Nature and evolution of the early Martian atmosphere: Evidence from highland crater populations
p 3373 N92-28485
An ion mass spectrometer for measuring isotopic adundances and loss rates of O, C and H in Mars' upper atmosphere p 3374 N92-28486
Chemical models of volcanic outgassing on Mars
p 3374 N92-28487
Time variation of the meteoritic contribution to the atmosphere of Mars p 3374 N92-28489
The production and escape of nitrogen atoms on Mars
p 3374 N92-28490
High pressure experiments with a Mars general circulation model p 3374 N92-28491
Mars volatile evolution: Implications of the recent measurement of O-17 in water from the SNC meteorites
p 3375 N92-28492
The Mars water cycle at other epochs: History of the polar caps and layered terrain p 3375 N92-28493
Mars global reference atmosphere model (Mars-GRAM) p 3375 N92-28494
A reduced atmosphere for early Mars?
p 3375 N92-28495
Influences of CO2 sublimation/condensation processes on the long-term evolution of the Martian atmosphere
p 3375 N92-28496
CO2 and clathrate as past erosive agents on Mars
p 3375 N92-28497
History of oxygen and carbon escape from the Martian atmosphere p 3376 N92-28498
Using the historical record to determine dust sources
p 3376 N92-28499
Martian atmospheric chemistry during the time of low water abundance p 3376 N92-28501
The early Martian atmosphere p 3376 N92-28502
Astronomical variation experiments with a Mars general circulation model p 3376 N92-28503
Regional climatic effects of atmospheric SO2 on Mars
p 3377 N92-28504
The thermal structure, dust loading, and meridional transport in the Martian atmosphere during late southern summer p 3377 N92-28505
Volcanic recycling of carbonate deposits on Mars
p 3377 N92-28506
The role of SO2 on Mars and on the primordial oxygen isotope composition of water on Earth and Mars
p 3377 N92-28507
Martian surficial carbon-constraints from isotopic measurements of shock-produced glass in EET A79001
p 3377 N92-28508
How Mars lost its atmosphere p 3378 N92-28509
Spectral identification of chemisorbed CO2 and application to Mars analog materials
p 3378 N92-28510
Forsterite/melt partitioning of argon and iodine: Implications for atmosphere formation by outgassing of an early Martian magma ocean p 3313 N92-28604
Workshop on the Martian Surface and Atmosphere Through Time
[NASA-CR-190418] p 3378 N92-28988
Midlatitude weather systems on Mars: Is there a hemispheric asymmetry? p 3379 N92-28992
Dust storm driven variations of the Mars thermosphere and exosphere: Coupling of atmospheric regions
p 3380 N92-28997
MARSNET surface and atmosphere investigations
p 3381 N92-29002
VLA mapping of 1.35 cm water emission from the Mars atmospheric limb p 3381 N92-29004
Mars atmospheric water p 3381 N92-29005
Analysis of Martian atmospheric and surface optical properties between 4.4 and 5.1 microns
p 3382 N92-29007
Atmosphere-surface interactions and atmospheric evolution on Mars p 3383 N92-29012
The meteoritic contribution to dust and aerosols in the atmosphere of Mars p 3383 N92-29013
Nitrogen escape from Mars p 3383 N92-29014
Greenhouse warming by minor gases on early Mars
p 3384 N92-29022
The Martian polar caps: Stability and water transport at low obliquities p 3385 N92-29023
Mars Environmental Survey (MESUR): Science objectives and mission description p 3385 N92-29025
Observations of Mars using Hubble Space Telescope
p 3385 N92-29026
Distribution of water on Mars: Implications from SNC meteorites p 3386 N92-29027
Was early Mars warmed by ammonia?
p 3386 N92-29030
Mars: Correcting surface albedo observations for effects of atmospheric dust loading p 3386 N92-29032
Mars atmosphere evolution: Escape to space
p 3387 N92-29034
Discovery concepts for Mars p 3387 N92-29035
Volatile tracers of Martian atmospheric evolution: Present measurement status and requirements for future investigations p 3387 N92-29037
New dust opacity maps from Viking IR thermal mapper data p 3388 N92-29040
Temporal variability of the surface and atmosphere of Mars: Viking Orbiter color observations
p 3388 N92-29041
Mars dust storm simulations: Analysis of surface stress p 3389 N92-29045
Recent Elysium volcanism: Effects on the Martian atmosphere p 3389 N92-29048
Influence of heat flow on early Martian climate
p 3390 N92-29052
Atmospheric and surface temperatures and airborne dust amounts during late southern summer from Mariner 9 IRIS data p 3390 N92-29056
Carbonate formation on Mars: History of the CO2 atmosphere from models of diffusion-limited growth in non-aqueous environments p 3391 N92-29060
Atomic oxygen in the Martian thermosphere
p 3391 N92-29061
Turbulent spectra, fluxes, stability and growth of the mixed layer in the boundary layer of Mars
p 3393 N92-29070
Aqueous-alteration products in S-N-C meteorites and implications for volatile/regolith interactions on Mars
p 3393 N92-29071
Planet-B: A Japanese Mars aeronomy observer
p 3393 N92-29072
Microcraters on Mars: Evidence of past climatic variations p 3394 N92-29073
The ultraviolet albedo of Mars p 3394 N92-29074
Hydrogen and carbon isotopic composition of volatiles in Nakhla: Implications for weathering on Mars
p 3394 N92-29075
Modeling the seasonal cycle of CO2 on Mars: A fit to the Viking lander pressure curves p 3394 N92-29076
Climatic implications of the simultaneous presence of CO2 and H2O in the Martian regolith
p 3395 N92-29079
The ancient oxygen exosphere of Mars: Implications for atmosphere evolution p 3395 N92-29080

MARS CRATERS

Martian impact crater degradation studies: Implications for localized obliteration episodes p 3379 N92-28991
Thermally distinct ejecta blankets from Martian craters
p 3379 N92-28994
Ice in the northern lowlands and southern highlands of Mars and its enrichment beneath the Elysium Lavas
p 3381 N92-29001
The composition of Martian aeolian sands: Thermal emissivity from Viking IRTM observations
p 3382 N92-29010
Styles of crater gradation in Southern Ismenius Lacus, Mars: Clues from Meteor Crater, Arizona
p 3384 N92-29018

MARS ENVIRONMENT

The Mars water cycle at other epochs: History of the polar caps and layered terrain p 3375 N92-28493
Regional climatic effects of atmospheric SO2 on Mars
p 3377 N92-28504
Spectral identification of chemisorbed CO2 and application to Mars analog materials
p 3378 N92-28510
Micro weather stations for in situ measurements in the Martian planetary boundary layer p 3382 N92-29008
Infrared photometric behavior and opposition effect of Mars p 3382 N92-29011
Dark material in the polar layered deposits on Mars
p 3385 N92-29024
Mars Environmental Survey (MESUR): Science objectives and mission description p 3385 N92-29025
Nonlinear stratified flow over localized topographic obstacles on Mars p 3387 N92-29036
Mars dust storm simulations: Analysis of surface stress p 3389 N92-29045
Short- and long-term climate changes on Mars
p 3389 N92-29051
Influence of heat flow on early Martian climate
p 3390 N92-29052
Microcraters on Mars: Evidence of past climatic variations p 3394 N92-29073

MARS LANDING

MARSNET surface and atmosphere investigations
p 3381 N92-29002
Martian surface simulations p 3383 N92-29016
Mars Environmental Survey (MESUR): Science objectives and mission description p 3385 N92-29025

MARS PHOTOGRAPHS

Distribution of coastal morphology in the Martian northern lowlands p 3389 N92-29047

Surface photometric properties and albedo changes in the central equatorial region of Mars
p 3392 N92-29066

MARS PROBES
Mars Environmental Survey (MESUR): Science objectives and mission description p 3385 N92-29025
Planet-B; A Japanese Mars aeronomy observer
p 3393 N92-29072

MARS SURFACE
Water inventories on Earth and Mars: Clues to atmosphere formation p 3373 N92-28483
Distribution of Martian ground-ice table: Preliminary results about climatic variations p 3373 N92-28484
Chemical models of volcanic outgassing on Mars
p 3374 N92-28487
Redistribution of subsurface neutrons caused by ground ice on Mars p 3374 N92-28488
The Mars water cycle at other epochs: History of the polar caps and layered terrain p 3375 N92-28493
Influences of CO2 sublimation/condensation processes on the long-term evolution of the Martian atmosphere
p 3375 N92-28496
CO2 and clathrate as past erosive agents on Mars
p 3375 N92-28497
Using the historical record to determine dust sources
p 3376 N92-28499
Liquid water habitats on early Mars
p 3376 N92-28500
Regional climatic effects of atmospheric SO2 on Mars
p 3377 N92-28504
Volcanic recycling of carbonate deposits on Mars
p 3377 N92-28506
The role of SO2 on Mars and on the primordial oxygen isotope composition of water on Earth and Mars
p 3377 N92-28507
Spectral identification of chemisorbed CO2 and application to Mars analog materials
p 3378 N92-28510
Workshop on the Martian Surface and Atmosphere Through Time
[NASA-CR-190418] p 3378 N92-28988
Iron Moessbauer spectroscopy: Superparamagnetism in hydrothermal vents and the search for evidence of past life on Mars p 3378 N92-28989
The nanophase iron mineral(s) in Mars soil
p 3379 N92-28990
Martian impact crater degradation studies: Implications for localized obliteration episodes p 3379 N92-28991
Mars: Compositional variability of ferric/ferrous minerals and polar volatiles from groundbased imaging spectroscopy p 3379 N92-28993
Thermally distinct ejecta blankets from Martian craters
p 3379 N92-28994
Infrared imaging of Mars for volatile distribution and seasonal variability between 2.4 and 5.1 microns
p 3379 N92-28995
Simulations of surface winds at the Viking Lander sites using a one-level model p 3380 N92-28998
Rates of oxidative weathering on the surface of Mars
p 3380 N92-28999
Martian channel networks: A revised Strahler approach for quantitative morphometry p 3380 N92-29000
Ice in the northern lowlands and southern highlands of Mars and its enrichment beneath the Elysium Lavas
p 3381 N92-29001
MARSNET surface and atmosphere investigations
p 3381 N92-29002
Mars dust and cloud opacities and scattering properties p 3381 N92-29003
Mars atmospheric water p 3381 N92-29005
The subsurface hydrologic response of Mars to the thermal evolution of its early crust p 3381 N92-29006
Analysis of Martian atmospheric and surface optical properties between 4.4 and 5.1 microns
p 3382 N92-29007
Soil texture and granulometry at the surface of Mars
p 3382 N92-29009
The composition of Martian aeolian sands: Thermal emissivity from Viking IRTM observations
p 3382 N92-29010
Implications of early Hesperian ages for presumed Noachian age volcanic flows on Mars
p 3383 N92-29015
Martian surface simulations p 3383 N92-29016
Mars surface weathering products and spectral analogs: Palagonites and synthetic iron minerals
p 3383 N92-29017
Styles of crater gradation in Southern Ismenius Lacus, Mars: Clues from Meteor Crater, Arizona
p 3384 N92-29018
Magmatic intrusions and hydrothermal systems on Mars p 3384 N92-29019
Mars: Wavelength-dependent dual polarization global scattering p 3384 N92-29020
The stable isotopic compositions of indigenous carbon-bearing components in EETA 79001
p 3384 N92-29021
The Martian polar caps: Stability and water transport at low obliquities p 3385 N92-29023
Dark material in the polar layered deposits on Mars
p 3385 N92-29024
Mars Environmental Survey (MESUR): Science objectives and mission description p 3385 N92-29025
Distribution of water on Mars: Implications from SNC meteorites p 3386 N92-29027
Glacial geomorphic evidence for a late climatic change on Mars p 3386 N92-29029
Was early Mars warmed by ammonia?
p 3386 N92-29030
Erosional landforms on the layered terrains in Valles Marineris p 3386 N92-29031
Mars: Correcting surface albedo observations for effects of atmospheric dust loading p 3386 N92-29032
Simulations of the seasonal polar caps on Mars
p 3387 N92-29033
Nonlinear stratified flow over localized topographic obstacles on Mars p 3387 N92-29036
An ejection model for SNC meteorites: An indication for recent volcanism on Mars p 3387 N92-29038
New dust opacity maps from Viking IR thermal mapper data p 3388 N92-29040
Temporal variability of the surface and atmosphere of Mars: Viking Orbiter color observations
p 3388 N92-29041
Regional variations in the stability and diffusion of water-ice in the Martian regolith p 3388 N92-29042
Exploring compositional variations on the surface of Mars applying mixing modeling to a telescopic spectral image p 3388 N92-29043
Simulation of Martian surface-atmosphere interaction in a space-simulator: Technical considerations and feasibility p 3388 N92-29044
Mars dust storm simulations: Analysis of surface stress p 3389 N92-29045
Is ground ice stable near the Martian equator?
p 3389 N92-29046
Distribution of coastal morphology in the Martian northern lowlands p 3389 N92-29047
Recent Elysium volcanism: Effects on the Martian atmosphere p 3389 N92-29048
Chemical reaction path modeling of hydrothermal processes on Mars: Preliminary results
p 3389 N92-29050
Chryse Planitia region, Mars: Channeling history, flood-volume estimates, and scenarios for bodies of water in the northern plains p 3390 N92-29054
Amazonis and Utopia Planitiae: Martian Lacustrine basins p 3391 N92-29058
Evidence for crystalline hematite as an accessory phase in Martian soils p 3391 N92-29059
Carbonate formation on Mars: History of the CO2 atmosphere from models of diffusion-limited growth in non-aqueous environments p 3391 N92-29060
Atomic oxygen in the Martian thermosphere
p 3391 N92-29061
Physical interpretation of thermal and reflected data on Martian surface units p 3391 N92-29062
Physical properties of Deucalionis, Eos, Xanthe-type units in the central equatorial region of Mars
p 3392 N92-29063
Physical properties of Meridiani Sinus-type units in the central equatorial region of Mars p 3392 N92-29064
Physical properties of Oxia/Lunae Planum and Arabia-type units in the central equatorial region of Mars
p 3392 N92-29065
Surface photometric properties and albedo changes in the central equatorial region of Mars
p 3392 N92-29066
Glacial and marine chronology of Mars
p 3392 N92-29067
Characterization of Martian near-subsurface materials by determination of cohesion and angle of internal friction p 3393 N92-29068
Topography of Apollinaris Patera and Ma'adim Vallis
p 3393 N92-29069
Aqueous-alteration products in S-N-C meteorites and implications for volatile/regolith interactions on Mars
p 3393 N92-29071
Microcraters on Mars: Evidence of past climatic variations p 3394 N92-29073
Modeling the seasonal cycle of CO2 on Mars: A fit to the Viking lander pressure curves p 3394 N92-29076
On the isotopic composition of magmatic carbon in SNC meteorites p 3394 N92-29077
Climatic implications of the simultaneous presence of CO2 and H2O in the Martian regolith
p 3395 N92-29079

MARS VOLCANOES
Chemical models of volcanic outgassing on Mars
p 3374 N92-28487
Implications of early Hesperian ages for presumed Noachian age volcanic flows on Mars
p 3383 N92-29015
Magmatic intrusions and hydrothermal systems on Mars p 3384 N92-29019
An ejection model for SNC meteorites: An indication for recent volcanism on Mars p 3387 N92-29038
Topography of Apollinaris Patera and Ma'adim Vallis
p 3393 N92-29069

MASERS
Intense electron beam cyclotron masers with microsecond pulselengths
[AD-A247060] p 3289 N92-28271

MASKS
Thermal analysis of selected commercial thermoplastic resins
[AD-A247711] p 3264 N92-28564

MASS
Mass and power modeling of communication satellites
[NASA-CR-189186] p 3275 N92-28906

MASS SPECTROMETERS
Ionized assisted deposition of organic films for optoelectronic applications
[AD-A247744] p 3263 N92-28405
An ion mass spectrometer for measuring isotopic adundances and loss rates of O, C and H in Mars' upper atmosphere p 3374 N92-28486

MASS SPECTROSCOPY
Studies of 1,3-disilacyclobutanes as single-source CVD precursors to silicon carbide
[AD-A247111] p 3365 N92-28885
Multicomponent comparison of optical and mass spectrometric diagnostics in low-pressure flames
[AD-A250323] p 3257 N92-28954

MASS TRANSFER
The thermal structure, dust loading, and meridional transport in the Martian atmosphere during late southern summer p 3377 N92-28505

MASSACHUSETTS
Wind-speed forecasting study for Westover AFB, Massachusetts
[AD-A247545] p 3319 N92-28934

MASSIVELY PARALLEL PROCESSORS
Mapping unstructured grid computations to massively parallel computers
[NASA-CR-190551] p 3343 N92-29109

MATERIALS TESTS
Use of scrap rubber in asphalt pavement surfaces
[AD-A247419] p 3272 N92-28902
Magneto acoustic emission method for testing materials for embrittlement
[NASA-CASE-LAR-13817-2] p 3304 N92-29155

MATHEMATICAL LOGIC
Generalized quantifiers and modal logic
[ITLI-LP-91-01] p 3348 N92-29214

MATHEMATICAL MODELS
A coilgun design primer
[DE92-011149] p 3244 N92-28226
The linear and nonlinear shear instability of a fluid sheet
[AD-A247092] p 3282 N92-28258
A diagnostic study of the velocity structure of a meandering jet in the California current system using a primitive equation model
[AD-A246039] p 3320 N92-28283
A system structure for predictive relations in penetration mechanics
[AD-A246453] p 3292 N92-28284
An application of interactive computer graphics to the study of inferential statistics and the general linear model
[AD-A246668] p 3334 N92-28285
Evidence for physics beyond the quasi-deuteron model in pion absorption
[DE92-011285] p 3354 N92-28310
Simulation of the propagation of acoustical waves through an interface separating a compressible fluid and an elastic medium
[FFI-91/7017] p 3351 N92-28314
A center of excellence in the mathematical sciences
[AD-A249365] p 3346 N92-28329
A comparison of results from an edge-plasma model with those from a two-dimensional fluid code
[DE92-010718] p 3360 N92-28335
Resonant Compton scattering in models of gamma ray burst sources
[DE92-010720] p 3397 N92-28336
Modeling radiation forces acting on TOPEX/Poseidon for precision orbit determination
[NASA-TM-104564] p 3244 N92-28343
Prediction of attitude stability of asymmetric dual-spin stabilized spacecraft using improved liquid slosh model
[AD-A247023] p 3246 N92-28368
Calculation of unsteady transonic flows with mild separation by viscous-inviscid interaction
[NASA-TP-3197] p 3226 N92-28477

Mars global reference atmosphere model (Mars-GRAM) p 3375 N92-28494
Calculation of chip temperatures using ELLPACK
[AD-A247156] p 3335 N92-28519
Mathematical modeling of solar magneto-dynamics
[AD-A247158] p 3395 N92-28520
Inverse control problems: Mathematical preliminaries, system theoretical approaches, and their applications to aircraft dynamics
[LR-665] p 3345 N92-28581
Origin of the moon and lunar core formation p 3311 N92-28596
Magma ocean formation due to giant impacts p 3315 N92-28615
Experimental validation of a line-duct acoustics model including flow
[NLR-TP-90223-U] p 3352 N92-28695
Stability and optimal control theory of hereditary systems with applications from oscillating flying vehicles, mechanical systems, and robotics p 3247 N92-28732
Sensor filter designs for large flexible spacecraft p 3247 N92-28733
Fuel optimal maneuver: Experimental testbeds p 3247 N92-28735
Models for recall and recognition
[IZF-1991-B-4] p 3342 N92-28746
MoCog1: A computer simulation of recognition-primed human decision making, considering emotions
[NASA-TM-107859] p 3337 N92-28758
Joint DOE/NSF workshop on flow of particulates and fluids
[DE92-012692] p 3285 N92-28808
Representation of neutron noise data using neural networks
[DE92-013232] p 3356 N92-28813
Reactant conversion in homogeneous turbulence: Mathematical modeling, computational validations and practical applications p 3285 N92-28819
Mass and power modeling of communication satellites
[NASA-CR-189186] p 3275 N92-28906
A coupled regional tide model
[AD-A247917] p 3322 N92-28913
Calculations and databasing of molecular absorption parameters for HITRAN
[AD-A247549] p 3355 N92-28936
Simulations of surface winds at the Viking Lander sites using a one-level model p 3380 N92-28998
Magmatic intrusions and hydrothermal systems on Mars p 3384 N92-29019
Analysis of constrained-layer damping of flexural and extensional waves in infinite, fluid-loaded plates
[AD-A247936] p 3304 N92-29081
Demodulation processes in auditory perception
[AD-A250203] p 3328 N92-29146
Calculation of support interferences on the aerodynamic coefficients for a wind tunnel calibration model
[ESA-TT-1247] p 3229 N92-29159
Impact on the medium MTF by model estimation of beta
[AD-A247985] p 3359 N92-29167
Building the Scientific Modeling Assistant: An interactive environment for specialized software design
[NASA-TM-107844] p 3346 N92-29175
Development of a stratified plate model for composite panels
[AD-A248206] p 3253 N92-29192
Boundary layer induced noise in aircraft
[ISSN-0309-7293] p 3353 N92-29201

MATHEMATICAL PROGRAMMING
Mathematical optimization: A powerful tool for aircraft design p 3232 N92-28474
Programming of the complex logarithm function in the solution of the cracked anisotropic plate loaded by a point force
[LR-657] p 3299 N92-28575
Genetic algorithms in coding theory: A table for A3 (n, d)
[MEMO-COSOR-91-22] p 3336 N92-28639
Optimization by renaming in the solution method
[ETN-92-91324] p 3338 N92-28842

MATRICES (CIRCUITS)
Crosstalk correction scheme
[AD-D015251] p 3276 N92-29085

MATRICES (MATHEMATICS)
Percolation conductivity of Penrose tiling by transfer-matrix Monte Carlo
[DE92-622792] p 3362 N92-28231
Decomposition of balanced matrices. Part 1: Introduction
[AD-A247397] p 3349 N92-28927
Decomposition of balanced matrices. Part 2: Wheel-and-parachute-free graphs
[AD-A247398] p 3350 N92-28928
Decomposition of balanced matrices. Part 6: Even wheels
[AD-A247399] p 3350 N92-28929
Decomposition of balanced matrices. Part 7: A polynomial recognition algorithm
[AD-A247400] p 3350 N92-28930
Mapping unstructured grid computations to massively parallel computers
[NASA-CR-190551] p 3343 N92-29109
A look-ahead variant of the Lanczos algorithm and its application to the quasi-minimal residual method for non-Hermitian linear systems
[NASA-CR-190557] p 3340 N92-29113

MATRIX MATERIALS
Method fabricating load-bearing composites free from microbuckling deformation up to a predetermined load
[AD-D015212] p 3250 N92-28224
Development of a stratified plate model for composite panels
[AD-A248206] p 3253 N92-29192

MATTER (PHYSICS)
The physics of strange matter
[DE92-011734] p 3371 N92-28774

MAXIMUM LIKELIHOOD ESTIMATES
Some aerospace applications of estimation theory
[ETN-92-91281] p 3349 N92-28647

MAXWELL EQUATION
Hyper-Raman scattering and 3-photon resonant ionization: Competitive effects
[DE92-622671] p 3366 N92-28230
A comparative study of the accuracy of various time domain nonorthogonal mesh methods
[DE92-007300] p 3347 N92-28824

MEAN SQUARE VALUES
Computer assisted improvement of the estimation mean squared error with application to back propagation neural networks
[AD-A247724] p 3344 N92-28401
Some aerospace applications of estimation theory
[ETN-92-91281] p 3349 N92-28647

MEASURE AND INTEGRATION
A comparative study of the accuracy of various time domain nonorthogonal mesh methods
[DE92-007300] p 3347 N92-28824

MEASURING INSTRUMENTS
A simple and low cost system to measure delay times in pneumatic systems
[NLR-TP-90174-U] p 3235 N92-28644
Space life support engineering program
[NASA-CR-190448] p 3330 N92-28671
Flow quality studies of the NASA Lewis Research Center 8- by 6-foot supersonic/9- by 15-foot low speed wind tunnel
[NASA-TM-105417] p 3240 N92-28673
Seafloor pressure array studies at ultra-low frequencies
[AD-A247663] p 3322 N92-28939

MECHANICAL DEVICES
Payload retention device
[NASA-CASE-MSC-21906-1] p 3294 N92-28727
Device for applying constant pressure to a surface
[NASA-CASE-GSC-13230-1] p 3294 N92-28754

MECHANICAL ENGINEERING
The 1991 research program (of the Faculty of Mechanical Engineering)
[ETN-92-91353] p 3296 N92-29217

MECHANICAL PROPERTIES
Mechanistic studies of superplasticity of structural ceramics
[AD-A246951] p 3263 N92-28558
The mechanical property data base from an Air Force/industry cooperative test program on advanced aluminum alloys (IN905XL and AL905XL forgings)
[AD-A247752] p 3368 N92-28565
The application of carbon fibres in ARALL laminates
[LR-658] p 3259 N92-28576
Effect of solidification technique and consolidation method on the properties of rapidly solidified Al-Fe alloys
[DLR-FB-91-24] p 3260 N92-28823
Crack resistance, fracture toughness and instability in damage tolerant Al-Li alloys
[NLR-TP-90172-U] p 3303 N92-28850
The effects of thermomechanical processing parameters on elevated-temperature behavior of a 6061 Al-Al2O3 metal matrix composite
[AD-A247889] p 3253 N92-28959
Development of a stratified plate model for composite panels
[AD-A248206] p 3253 N92-29192

MECHANICAL SHOCK
Effects of extremely high G acceleration forces on NASA's control and space exposed tomato seeds
[AD-A247488] p 3323 N92-28247

MEDIA
Analysis of multimedia information systems for the US Coast Guard
[AD-A247890] p 3369 N92-28960

MEDITERRANEAN SEA
Bioluminescence in the western Alboran Sea in April 1991
[AD-A250016] p 3324 N92-29089

MELANIN
Investigation of laser-induced retinal damage
[AD-A250173] p 3326 N92-28920

MELTING
Thermal evolution and chemical differentiation of the terrestrial magma ocean p 3310 N92-28588
High-pressure melting of carbonaceous chondrite p 3310 N92-28589
Pressure regimes and core formation in the accreting earth p 3313 N92-28605
Terrestrial magma ocean and core segregation in the earth p 3313 N92-28606
Evidences for the terrestrial magma ocean from high-pressure melting experiments p 3315 N92-28613
The ferroan-anorthositic suite and the extent of primordial lunar melting p 3315 N92-28618

MELTS (CRYSTAL GROWTH)
Workshop on the Physics and Chemistry of Magma Oceans from 1 Bar to 4 Mbar
[NASA-CR-190419] p 3310 N92-28587
Experimental determination of the solubility of iridium in silicate melts: Preliminary results p 3310 N92-28591
Mg-perovskite/silicate melt and magnesiowuestite/silicate melt partition coefficients for KLB-1 at 250 Kbars p 3310 N92-28592
Mg-perovskite/silicate melt partition coefficients in the CMS system at 2430 C and 226 Kbars p 3312 N92-28601

MEMBRANE STRUCTURES
Mobile electric power
[AD-A249354] p 3279 N92-28326

MEMBRANES
Microhole array electrodes based on microporous alumina membranes
[AD-A247082] p 3278 N92-28239
High temperature membranes for H2S and SO2 separations
[DE92-010451] p 3256 N92-28827

MEMORY
Models for recall and recognition
[IZF-1991-B-4] p 3342 N92-28746
Studies of perceptual memory
[AD-A250200] p 3328 N92-29144

MEMORY (COMPUTERS)
Vienna FORTRAN: A language specification, version 1.1
[NASA-CR-189629] p 3337 N92-28760
Kanerva's sparse distributed memory with multiple hamming thresholds
[NASA-CR-190552] p 3339 N92-28875
Crystallizing FORTRAN
[AD-A250162] p 3343 N92-28915

MENTAL PERFORMANCE
Effects of high terrestrial altitude on military performance
[AD-A246695] p 3324 N92-28288
Investigations of logic of introspection and related modes of reasoning with applications
[AD-A249286] p 3345 N92-28895

MESOMETEOROLOGY
Evaluation of simple mesoscale models for use in TESS
[AD-A247914] p 3316 N92-28964

MESOSCALE PHENOMENA
Parameterization of convective clouds, mesoscale convective systems, and convective-generated cirrus
[DE92-010951] p 3318 N92-28340
A numerical study of time-dependent wind forcing off the west coast of Portugal, 1987-1988
[AD-A246775] p 3321 N92-28365
Mesoscale vertical structure of an explosive oceanic cyclone
[AD-A245927] p 3318 N92-28423
Simulation of atmospheric frontogenesis with a semi-Lagrangian numerical model
[AD-A247151] p 3318 N92-28517
Mesoscale surface analysis of the ERICA IOP-5 cyclone
[AD-A245946] p 3319 N92-28884
Evaluation of simple mesoscale models for use in TESS
[AD-A247914] p 3316 N92-28964

METABOLISM
Conversion of acetic acid to methane by thermophiles
[DE92-010652] p 3257 N92-28942
The energetics and mechanics of load carrying
[AD-A248441] p 3332 N92-29227

METAL COATINGS
Effect of metallic coating properties on the tribology of oil-lubricated coated-ceramics
[DE92-010904] p 3262 N92-28339

METAL FILMS
Method of intercalating large quantities of fibrous structures
[NASA-CASE-LEW-15077-1] p 3253 N92-29152
METAL FOILS
Chemical vapor synthesis of niobium aluminides
[AD-A250332] p 3258 N92-29091
METAL FUELS
Kinetic studies of metal combustion in propulsion
[AD-A250207] p 3256 N92-28769
METAL IONS
Formation, structure, and properties of boron nitride fibers from polymer precursors
[AD-A247679] p 3263 N92-28553
METAL MATRIX COMPOSITES
Review and update on electrocomposites
[AD-A248050] p 3251 N92-28303
X ray diffraction study of residual stresses in metal matrix composite-jacketed steel cylinders subjected to internal pressure
[AD-A248449] p 3251 N92-28416
Effect of alumina particle additions on the aging kinetics of 2014-aluminum matrix composites
[AD-A245949] p 3252 N92-28898
The effects of thermomechanical processing parameters on elevated-temperature behavior of a 6061 Al-Al2O3 metal matrix composite
[AD-A247889] p 3253 N92-28959
Oxidation resistant coating for titanium alloys and titanium alloy matrix composites
[NASA-CASE-LEW-15155-1] p 3265 N92-29090
Chemical vapor synthesis of niobium aluminides
[AD-A250332] p 3258 N92-29091
METAL OXIDE SEMICONDUCTORS
Leakage current measurements in SOI devices
[AD-A247694] p 3280 N92-28561
Feasibility of metal-oxide-semiconductor structures on Si-LPCVD thin films by low temperature (600 C) process
[LAAS-91307] p 3365 N92-29207
METAL OXIDES
Volatile CVD precursors based on copper alkoxides and mixed group IIA-Copper alkoxides --- chemical vapor deposition
[AD-D015264] p 3261 N92-29170
METAL PARTICLES
Underwater vapor phase burning of aluminum particles and on aluminum ignition during steam explosions
[DE92-011196] p 3257 N92-28894
METAL PLATES
Weld pool flow visualization studies during gas tungsten arc welding of steel and aluminum
[AD-A249204] p 3292 N92-28293
Surface residual stress analysis of metals and alloys
[AD-A248372] p 3259 N92-28426
METAL STRIPS
High temperature solder device for flat cables
[NASA-CASE-GSC-13344-1] p 3261 N92-29094
METAL SURFACES
The emergence of atomic-level structural information for ordered metal-solution interfaces: Some recent contributions from in-situ infrared spectroscopy and scanning tunneling microscopy
[AD-A246765] p 3364 N92-28512
X ray photoelectron spectroscopy study on the double layer at an Al2O3-Al interface
[AD-A246454] p 3265 N92-28972
METAL WORKING
EXPLOMET 90 international conference on shock-wave and high-strain-rate phenomena in materials
[AD-A248665] p 3303 N92-28892
METAL-WATER REACTIONS
Underwater vapor phase burning of aluminum particles and on aluminum ignition during steam explosions
[DE92-011196] p 3257 N92-28894
METALORGANIC CHEMICAL VAPOR DEPOSITION
Volatile CVD precursors based on copper alkoxides and mixed group IIA-Copper alkoxides --- chemical vapor deposition
[AD-D015264] p 3261 N92-29170
METALS
Synthesis and study of metallonitride complexes and polymers
[AD-A248577] p 3262 N92-28323
Surface residual stress analysis of metals and alloys
[AD-A248372] p 3259 N92-28426
Estimation of high temperature metal-silicate partition coefficients p 3311 N92-28599
The characterization of ceramics and ceramic/metal-joints by ultrasonic techniques
[VTT-RR-741] p 3266 N92-29194
METASTABLE STATE
Theoretical studies of the electronic and resonance structure of atomic and molecular negative ions
[AD-A247093] p 3354 N92-28259
Gadolinium metastable states population distributions and atomic density under high-rate electron beam evaporation
[DE92-782008] p 3363 N92-28282
Excited negative ions and molecules and negative ion production
[AD-A247017] p 3354 N92-28414
METATHESIS
Silicon polymers
[AD-A250201] p 3265 N92-29145
METEORITE COLLISIONS
Time variation of the meteoritic contribution to the atmosphere of Mars p 3374 N92-28489
Magma ocean formation due to giant impacts p 3315 N92-28615
METEORITE CRATERS
Giant and large impacts in the context of planetary formation theory p 3315 N92-28619
Styles of crater gradation in Southern Ismenius Lacus, Mars: Clues from Meteor Crater, Arizona p 3384 N92-29018
Chemical reaction path modeling of hydrothermal processes on Mars: Preliminary results p 3389 N92-29050
METEORITES
A new angle on lunar ferroan-suite differentiation p 3311 N92-28598
The meteoritic contribution to dust and aerosols in the atmosphere of Mars p 3383 N92-29013
Distribution of water on Mars: Implications from SNC meteorites p 3386 N92-29027
An ejection model for SNC meteorites: An indication for recent volcanism on Mars p 3387 N92-29038
Microcraters on Mars: Evidence of past climatic variations p 3394 N92-29073
Hydrogen and carbon isotopic composition of volatiles in Nakhla: Implications for weathering on Mars p 3394 N92-29075
On the isotopic composition of magmatic carbon in SNC meteorites p 3394 N92-29077
METEORITIC COMPOSITION
Time variation of the meteoritic contribution to the atmosphere of Mars p 3374 N92-28489
Mars volatile evolution: Implications of the recent measurement of O-17 in water from the SNC meteorites p 3375 N92-28492
The stable isotopic compositions of indigenous carbon-bearing components in EETA 79001 p 3384 N92-29021
A liquidus phase diagram for the groundmass of EETA 79001A (Eg), a primitive Shergottite composition p 3386 N92-29028
Mid-infrared spectra of Martian komantiite p 3390 N92-29053
Aqueous-alteration products in S-N-C meteorites and implications for volatile/regolith interactions on Mars p 3393 N92-29071
METEORITIC DAMAGE
Origin of the moon and lunar core formation p 3311 N92-28596
Superheat in magma oceans p 3311 N92-28597
Styles of crater gradation in Southern Ismenius Lacus, Mars: Clues from Meteor Crater, Arizona p 3384 N92-29018
METEOROLOGICAL CHARTS
Polar lows over the northeast Greenland Sea
[AD-A245360] p 3318 N92-28421
METEOROLOGICAL PARAMETERS
MARSNET surface and atmosphere investigations p 3381 N92-29002
METEOROLOGICAL RADAR
Windshear radar calibration: Transmitter power and receiver gain stability
[NASA-TM-107589] p 3275 N92-28876
METEOROLOGICAL SATELLITES
EUMETSAT: The European Organization for Meteorological Satellites
[ETN-92-91069] p 3318 N92-28745
METEOROLOGY
Regional climatic effects of atmospheric SO2 on Mars p 3377 N92-28504
Simulation of atmospheric frontogenesis with a semi-Lagrangian numerical model
[AD-A247151] p 3318 N92-28517
EUMETSAT: The European Organization for Meteorological Satellites
[ETN-92-91069] p 3318 N92-28745
Midlatitude weather systems on Mars: Is there a hemispheric asymmetry? p 3379 N92-28992
Micro weather stations for in situ measurements in the Martian planetary boundary layer p 3382 N92-29008
Observations of Mars using Hubble Space Telescope p 3385 N92-29026
Planet-B: A Japanese Mars aeronomy observer p 3393 N92-29072
METEOSAT SATELLITE
Transputer-based embedded system for Meteosat image data compression
[NLR-TP-90228-U] p 3305 N92-28697
EUMETSAT: The European Organization for Meteorological Satellites
[ETN-92-91069] p 3318 N92-28745
METHOD OF MOMENTS
The use of conformal subdomain basis functions in the method of moments computations for a thin wire
[AD-A245964] p 3272 N92-28347
Method of moments analysis of displaced-axis dual reflector antennas
[AD-A247970] p 3277 N92-29166
METHYL ALCOHOL
Regional environmental impacts of methanol-fueled vehicles
[PB92-176569] p 3308 N92-29183
METHYL COMPOUNDS
Near millimeter waves and microelectronics
[AD-A250384] p 3281 N92-28797
Substrate induced ordering of molecular adsorbates on Au(111)
[AD-A246850] p 3258 N92-29185
METHYL POLYSILOXANES
Correlation between surface free energy and surface constitution
[AD-A246699] p 3262 N92-28291
MICROCOMPUTERS
High-performance integrated circuit evaluation system for a gallium arsenide microsupercomputer
[AD-A250385] p 3281 N92-28798
Technological enhancements for personal computers
[AD-A247962] p 3333 N92-29083
MICROCRACKS
Study of high temperature failure mechanism in ceramics
[AD-A247018] p 3263 N92-28415
MICROELECTRONICS
Near millimeter waves and microelectronics
[AD-A250384] p 3281 N92-28797
Monolithic optoelectronic implementation of neural planes
[AD-A250286] p 3345 N92-28970
MICROGRAVITY APPLICATIONS
Space Station Freedom microgravity environment requirements and assessment methods p 3268 N92-28450
MICROHARDNESS
Mg-Si-Al oxynitride glasses
[AD-A247593] p 3261 N92-28249
MICROMECHANICS
Micromechanics of defects
[AD-A248432] p 3251 N92-28307
Prediction of composite material properties using two-dimensional finite element micromechanical analysis
[AD-A250300] p 3252 N92-28702
MICROMETEOROIDS
The meteoritic contribution to dust and aerosols in the atmosphere of Mars p 3383 N92-29013
MICROPOROSITY
Microhole array electrodes based on microporous alumina membranes
[AD-A247082] p 3278 N92-28239
MICROSCOPES
Woelter x ray microscope characterization measurements on Nova
[DE92-013207] p 3288 N92-28812
Water window imaging x ray microscope
[NASA-CASE-MFS-28485-1] p 3288 N92-29135
MICROSCOPY
Woelter x ray microscope characterization measurements on Nova
[DE92-013207] p 3288 N92-28812
MICROSTRIP DEVICES
Operation and radiation resistance of a FOXFET biasing structure for silicon strip detectors
[DE92-011279] p 3282 N92-29197
MICROSTRUCTURE
Chain folding in EBEE semicrystalline diblock copolymers
[AD-A247595] p 3262 N92-28251
Microstructures of shocked quartz
[DE92-010710] p 3363 N92-28333
Plane wave propagation in random granular media
[AD-A247300] p 3298 N92-28424
Mechanistic studies of superplasticity of structural ceramics
[AD-A246951] p 3263 N92-28558
Phase transformations in Ti3Al based alloy
[AD-A246464] p 3261 N92-28976
The characterization of ceramics and ceramic/metal-joints by ultrasonic techniques
[VTT-RR-741] p 3266 N92-29194

MICROWAVE ATTENUATION
Microwave interactions with plasmas
[AD-A250333] p 3362 N92-29093
MICROWAVE EQUIPMENT
High power microwave generator
[AD-D015262] p 3277 N92-29199
MICROWAVE PLASMA PROBES
Microwave interactions with plasmas
[AD-A250333] p 3362 N92-29093
MICROWAVE RADIOMETERS
Microwave temperature profiler for clear air turbulence prediction
[NASA-CASE-NPO-18115-1-CU] p 3320 N92-29148
MICROWAVE SCATTERING
Comparison of various techniques in the analysis of waveguide transitions
[AD-A247019] p 3279 N92-28367
Propagation and scattering of microwaves and millimeter waves in snow based on dense random media theory
[AD-A249300] p 3274 N92-28846
MICROWAVE TRANSMISSION
Comparison of various techniques in the analysis of waveguide transitions
[AD-A247019] p 3279 N92-28367
Propagation and scattering of microwaves and millimeter waves in snow based on dense random media theory
[AD-A249300] p 3274 N92-28846
MICROWAVES
Intense electron beam cyclotron masers with microsecond pulselengths
[AD-A247060] p 3289 N92-28271
Applications of passive microwave satellite data for Arctic Sea ice studies
[AD-A245966] p 3306 N92-28791
Microwave derived rainrates in typhoons and their use in the diagnosis and prediction of typhoon intensity
[AD-A250556] p 3319 N92-28922
Analysis of electromagnetic propagation over variable terrain using the parabolic wave equation
[AD-A248061] p 3276 N92-28947
MIE SCATTERING
Analysis of Martian atmospheric and surface optical properties between 4.4 and 5.1 microns
p 3382 N92-29007
MILITARY HELICOPTERS
Report on the workshop on Ion Implantation and Ion Beam Assisted Deposition
[AD-A250561] p 3365 N92-28923
MILITARY OPERATIONS
Information strategy plan
[AD-A247740] p 3367 N92-28403
Opportunities for flight simulation to improve operational effectiveness p 3221 N92-28523
Methods of visual scanning with night vision goggles
[AD-A247470] p 3331 N92-28944
MILITARY TECHNOLOGY
Limiting factors to advancing thermal battery technology for naval applications
[AD-A247773] p 3280 N92-28568
MILITARY VEHICLES
A user's manual for MASH 1.0: A Monte Carlo adjoint shielding code system
[AD-A248204] p 3355 N92-29190
MILLIMETER WAVES
Multimeter-wave grid oscillators
[AD-A248430] p 3279 N92-28351
Scattering measurements and predictions for a Delta stage 2 rocket nozzle
[AD-A246776] p 3248 N92-28366
Monolithic mm-wave phase shifter using optically activated superconducting switches
[NASA-CASE-LEW-14878-1] p 3358 N92-28571
Near millimeter waves and microelectronics
[AD-A250384] p 3281 N92-28797
Propagation and scattering of microwaves and millimeter waves in snow based on dense random media theory
[AD-A249300] p 3274 N92-28846
MINERAL DEPOSITS
The composition of Martian aeolian sands: Thermal emissivity from Viking IRTM observations
p 3382 N92-29010
MINERALOGY
A new angle on lunar ferroan-suite differentiation
p 3311 N92-28598
Mars: Compositional variability of ferric/ferrous minerals and polar volatiles from groundbased imaging spectroscopy p 3379 N92-28993
A carbonate-silicate aqueous geochemical cycle model for Mars p 3390 N92-29057
MINERALS
A new angle on lunar ferroan-suite differentiation
p 3311 N92-28598
Coupling plant growth and waste recycling systems in a controlled life support system (CELSS)
[NASA-TM-107544] p 3330 N92-28670
The nanophase iron mineral(s) in Mars soil
p 3379 N92-28990
Mars: Compositional variability of ferric/ferrous minerals and polar volatiles from groundbased imaging spectroscopy p 3379 N92-28993
Rates of oxidative weathering on the surface of Mars
p 3380 N92-28999
Mars surface weathering products and spectral analogs: Palagonites and synthetic iron minerals
p 3383 N92-29017
Aqueous-alteration products in S-N-C meteorites and implications for volatile/regolith interactions on Mars
p 3393 N92-29071
MINIATURIZATION
High-temperature miniaturized turbine engine lubrication system simulator
[AD-A249259] p 3236 N92-28294
Fundamental noise limits in miniature acoustic and vibration sensors
[AD-A247016] p 3352 N92-28413
MINIMUM DRAG
Constrained spanload optimization for minimum drag of multi-lifting-surface configurations
[NLR-TP-89126-U] p 3227 N92-28660
MIR SPACE STATION
Analysis of Mir-HEXE observations: Pulsation and energy spectra of the x ray double star SMC X-1 in 20 to 80 keV energy field
[ETN-92-91487] p 3371 N92-29128
MIRRORS
Method and apparatus for phasing segmented mirror arrays
[NASA-CASE-NPO-18095-1-CU] p 3359 N92-29122
Water window imaging x ray microscope
[NASA-CASE-MFS-28485-1] p 3288 N92-29135
Method for advanced material characterization by laser induced eddy current imaging
[NASA-CASE-GSC-13386-1] p 3298 N92-29154
MISSILES
Rocket nozzle shield
[AD-D015248] p 3249 N92-28748
MISSION PLANNING
Information strategy plan
[AD-A247740] p 3367 N92-28403
Review of Mars mission scenarios
p 3244 N92-28731
Martian surface simulations p 3383 N92-29016
MISSISSIPPI DELTA (LA)
Sea surface velocities from visible and infrared multispectral atmospheric mapping sensor imagery
[NASA-CR-190398] p 3305 N92-28715
MIXING
Lagrangian turbulence: Structures and mixing in admissible model flows
[AD-A247203] p 3286 N92-28890
MIXING LENGTH FLOW THEORY
Turbulence modeling: Survey of activities in Belgium and the Netherlands, and appraisal of the status and a view on the prospects
[NLR-TP-90184-U] p 3284 N92-28694
MOBILITY
Controlled method of reducing electrophoretic mobility of macromolecules, particles, or cells
[NASA-CASE-MFS-26049-2-NP] p 3255 N92-28728
MODAL RESPONSE
Optimum design of a gearbox for low vibration
[NASA-TM-105653] p 3293 N92-28476
Modal analysis of plates using boundary integral equations
[NLR-TP-89211-U] p 3302 N92-28688
MODFETS
Study of ultra short HFET devices with InP substrates
[AD-A248448] p 3279 N92-28427
MODULATION
Scientific investigations with the data base HEAO-1 scanning modulator collimator
[NASA-CR-190477] p 3370 N92-28680
MODULATION TRANSFER FUNCTION
Impact on the medium MTF by model estimation of beta
[AD-A247985] p 3359 N92-29167
MODULATORS
Scientific investigations with the data base HEAO-1 scanning modulator collimator
[NASA-CR-190477] p 3370 N92-28680
Non-mechanical optical path switching and its application to dual beam spectroscopy including gas filter correlation radiometry
[NASA-CASE-LAR-14588-1-CU] p 3359 N92-29117
Method for advanced material characterization by laser induced eddy current imaging
[NASA-CASE-GSC-13386-1] p 3298 N92-29154
MODULUS OF ELASTICITY
Mg-Si-Al oxynitride glasses
[AD-A247593] p 3261 N92-28249
The compressive properties of GLARE
[LR-666] p 3252 N92-28582
MOISTURE CONTENT
Water inventories on Earth and Mars: Clues to atmosphere formation p 3373 N92-28483
Redistribution of subsurface neutrons caused by ground ice on Mars p 3374 N92-28488
A magma ocean and the Earth's internal water budget
p 3310 N92-28590
An investigation into techniques for the determination of moisture content on activated carbon
[AD-A245938] p 3256 N92-28882
Ice in the northern lowlands and southern highlands of Mars and its enrichment beneath the Elysium Lavas
p 3381 N92-29001
MOLECULAR ABSORPTION
Calculations and databasing of molecular absorption parameters for HITRAN
[AD-A247549] p 3355 N92-28936
MOLECULAR BEAM EPITAXY
Growth and optical characterization of Zn(1-x)Mn(x)Te grown by molecular beam epitaxy
[DE92-010667] p 3363 N92-28331
Study of ultra short HFET devices with InP substrates
[AD-A248448] p 3279 N92-28427
Center for the integration of optical computing
[AD-A250306] p 3337 N92-28719
Innovative techniques for the production of low cost 2D laser diode arrays
[AD-A248247] p 3292 N92-29226
MOLECULAR BEAMS
Multicomponent comparison of optical and mass spectrometric diagnostics in low-pressure flames
[AD-A250323] p 3257 N92-28954
MOLECULAR COLLISIONS
Excitation of atoms and molecules in collisions with highly charged ions
[DE92-012658] p 3355 N92-28764
The nonequilibrium molecular dynamics
[DE92-011760] p 3355 N92-28860
MOLECULAR DIFFUSION
Mapping closures for turbulent mixing and reaction
[AD-A247305] p 3283 N92-28274
MOLECULAR EXCITATION
Dynamical solvent effects on activated electron-transfer reactions: Principles, pitfalls, and progress
[AD-A246764] p 3363 N92-28349
Excited negative ions and molecules and negative ion production
[AD-A247017] p 3354 N92-28414
Excitation of atoms and molecules in collisions with highly charged ions
[DE92-012658] p 3355 N92-28764
MOLECULAR FLOW
Mapping closures for turbulent mixing and reaction
[AD-A247305] p 3283 N92-28274
Stochastic simulation of the structure and propagation rate of turbulent premixed flames
[DE92-006682] p 3256 N92-28822
MOLECULAR GASES
Molecular recognition in the oxidation of catechols by Dicobalt-BISDIEN dioxygen complexes
[AD-A246456] p 3258 N92-28973
Volatile tracers of Martian atmospheric evolution: Present measurement status and requirements for future investigations p 3387 N92-29037
MOLECULAR INTERACTIONS
Nanoscale investigation of indentation, adhesion, and fracture of diamond (111) surfaces
[AD-A250164] p 3265 N92-28916
MOLECULAR IONS
Theoretical studies of the electronic and resonance structure of atomic and molecular negative ions
[AD-A247093] p 3354 N92-28259
MOLECULAR SPECTROSCOPY
Calculations and databasing of molecular absorption parameters for HITRAN
[AD-A247549] p 3355 N92-28936
MOLECULAR WEIGHT
Polyimidazoles via aromatic nucleophilic displacement
[NASA-CASE-LAR-14145-1] p 3264 N92-28751
MOLECULES
Molecular dynamics calculations of optical nonlinear properties of materials
[AD-A247095] p 3354 N92-28260
Orthogonal self-assembly of redox active molecules on Pt and Au: Selective reaction of disulfide with Au and isonitrile with Pt
[AD-A246698] p 3254 N92-28290
Controlled method of reducing electrophoretic mobility of macromolecules, particles, or cells
[NASA-CASE-MFS-26049-2-NP] p 3255 N92-28728
MOLTEN SALT ELECTROLYTES
Limiting factors to advancing thermal battery technology for naval applications
[AD-A247773] p 3280 N92-28568

MOLTEN SALTS
Electrochemical studies of Lewis acid-base systems for use in thermally regenerable fuel cells
[AD-A246457] p 3307 N92-28974
MOMENTUM
A momentum limit for electromagnetic railguns
[DE92-011380] p 3245 N92-28861
MONITORS
Microgravity accelerometer characterization on Columbia STS-32 mission p 3271 N92-28452
Integrated health monitoring and controls for rocket engines
[NASA-TM-105763] p 3249 N92-28693
MONKEYS
Non-linear analysis of visual cortical neurons
[AD-A250233] p 3326 N92-29179
MONTE CARLO METHOD
Percolation conductivity of Penrose tiling by transfer-matrix Monte Carlo
[DE92-622792] p 3362 N92-28231
Scattering mechanisms for semiconductor transport calculations
[AD-A249260] p 3278 N92-28295
Selective suppression of photochemical etching: Raman spectroscopy for pre-etch process selection
[DE92-010955] p 3255 N92-28341
Monte Carlo optimization of depth-of-interaction resolution in PET crystals
[DE92-011147] p 3364 N92-28762
Simulations of solvent effects on confined electrolytes
[AD-A246851] p 3258 N92-28982
Analyzing noisy spectral line shapes
[DE92-011153] p 3362 N92-29086
A user's manual for MASH 1.0: A Monte Carlo adjoint shielding code system
[AD-A248204] p 3355 N92-29190
MONTEREY BAY (CA)
Modeling pulse transmission in the Monterey Bay using parabolic equation methods
[AD-A246465] p 3322 N92-28977
MOON
Origin of the moon and lunar core formation
p 3311 N92-28596
Early planetary differentiation: Geophysical consequences p 3314 N92-28609
MORPHOLOGY
Studies of 1,3-disilacyclobutanes as single-source CVD precursors to silicon carbide
[AD-A247111] p 3365 N92-28885
Styles of crater gradation in Southern Ismenius Lacus, Mars: Clues from Meteor Crater, Arizona
p 3384 N92-29018
Erosional landforms on the layered terrains in Valles Marineris p 3386 N92-29031
Regional variations in the stability and diffusion of water-ice in the Martian regolith p 3388 N92-29042
Amazonis and Utopia Planitiae: Martian Lacustrine basins p 3391 N92-29058
MOSAICS
Temporal variability of the surface and atmosphere of Mars: Viking Orbiter color observations
p 3388 N92-29041
Surface photometric properties and albedo changes in the central equatorial region of Mars
p 3392 N92-29066
MOSSBAUER EFFECT
Iron Moessbauer spectroscopy: Superparamagnetism in hydrothermal vents and the search for evidence of past life on Mars p 3378 N92-28989
MOTION SIMULATION
The basic research simulator programme and the industrial and aerospace community: Opportunities for cooperative research
[LR-662] p 3240 N92-28579
Dynamics motion simulation of the Hermes robot arm subjected to constraints
[NLR-TP-90282-U] p 3293 N92-28645
Curvature estimation in orientation selection
[AD-A247862] p 3328 N92-28957
Nonlinear sloshing and the coupled dynamics of liquid propellants and spacecraft
[AD-A250023] p 3248 N92-28967
MOTIVATION
Integrating the affective domain into the instructional design process
[AD-A249287] p 3327 N92-28880
MOUNTING
Removable hand hold
[NASA-CASE-LEW-15196-1] p 3295 N92-29092
MOVING TARGET INDICATORS
Target motion detecting impulse Doppler radar system
[AD-D015263] p 3277 N92-29169
MRCA AIRCRAFT
The evaluation of simulator effectiveness for the training of high speed, low level, tactical flight operations
p 3223 N92-28539
MULTICHANNEL COMMUNICATION
Crosstalk correction scheme
[AD-D015251] p 3276 N92-29085
MULTIPATH TRANSMISSION
Fade durations in satellite-path mobile radio propagation
[NASA-CR-190484] p 3273 N92-28586
MULTIPHASE FLOW
Joint DOE/NSF workshop on flow of particulates and fluids
[DE92-012692] p 3285 N92-28808
MULTIPLEXING
Elliptical-core two mode fiber sensors and devices incorporating photoinduced refractive index gratings
[NASA-CR-190495] p 3358 N92-28868
MULTIPROCESSING (COMPUTERS)
HeNCE: Graphical development tools for network-based concurrent computing
[DE92-011061] p 3341 N92-28279
SISAL: Toward resolving the parallel programming crisis
[DE92-010716] p 3342 N92-28334
Coincident pulse techniques for hybrid electronic optical computer systems
[AD-A246774] p 3332 N92-28514
Vienna FORTRAN: A language specification, version 1.1
[NASA-CR-189629] p 3337 N92-28760
Functional requirements document for the Earth Observing System Data and Information System (EOSDIS) Scientific Computing Facilities (SCF) of the NASA/MSFC Earth Science and Applications Division, 1992
[NASA-TM-4392] p 3333 N92-28899
Asynchronous bidirectional network interface enabling seamless concurrent processing in a distributed heterogeneous multiprocessor system
[AD-D015274] p 3343 N92-29096
MULTIPROGRAMMING
Analysing multiprogramming queues by generating functions
[MEMO-COSOR-91-25] p 3342 N92-28642
MULTISPECTRAL BAND SCANNERS
Sea surface velocities from visible and infrared multispectral atmospheric mapping sensor imagery
[NASA-CR-190398] p 3305 N92-28715
MULTISTATIC RADAR
Neural network parameter estimation for the modified bistatic scattering strength model (BISSM)
[AD-A247913] p 3322 N92-28963
MULTIVARIATE STATISTICAL ANALYSIS
Full mission simulation: A view into the future
p 3223 N92-28537
Using Gaussian windows to explore a multivariate data set
[NASA-CR-190556] p 3339 N92-29106
User's manual for the Gaussian windows program
[NASA-CR-190554] p 3340 N92-29107
MUONS
The 17 keV neutrino and neutrino tagging
[DE92-011281] p 3355 N92-28839
MUTATIONS
Problems in mechanistic theoretical models for cell transformation by ionizing radiation
[DE92-010265] p 3324 N92-28278
Primer on molecular genetics
[DE92-010680] p 3324 N92-28382
Somatic gene mutation in the human in relation to radiation risk
[DE92-009459] p 3325 N92-28685

N

NAKHLITES
Mid-infrared spectra of Martian komantiite
p 3390 N92-29053
Aqueous-alteration products in S-N-C meteorites and implications for volatile/regolith interactions on Mars
p 3393 N92-29071
NASA PROGRAMS
Space flight: The first 30 years
[NASA-NP-150] p 3397 N92-28678
Second National Space Grant Conference report, 1991
[NASA-EP-278] p 3366 N92-28864
Space life sciences strategic plan
[NASA-TM-107954] p 3244 N92-29100
Consulting report on the NASA technology utilization network system
[NASA-CR-190387] p 3370 N92-29108
Maintaining the program balance, volumes 1 and 2
[NASA-CR-190269] p 3367 N92-29111
NASA SPACE PROGRAMS
Ongoing Progress in Spacecraft Controls
[NASA-CP-10099] p 3247 N92-28730
Review of Mars mission scenarios
p 3244 N92-28731
NAVIER-STOKES EQUATION
Viscous effects on a vortex wake in ground effect
[NASA-CR-190400] p 3283 N92-28361
Full Navier-Stokes analysis of a two-dimensional mixer/ejector nozzle for noise suppression
[NASA-TM-105715] p 3236 N92-28419
Computation of steady and unsteady quasi-one-dimensional viscous/inviscid interacting internal flows at subsonic, transonic, and supersonic Mach numbers
[NASA-CR-189881] p 3283 N92-28555
Development of a high-performance FORTRAN compiler for porting CFD codes to the Navier-Stokes computer
[AD-A250208] p 3342 N92-28770
Explicit Navier-Stokes computation of turbomachinery flows
[AD-A249284] p 3286 N92-28879
NAVIGATION AIDS
Loran-C performance assurance assessment program
[NASA-CR-190469] p 3230 N92-28718
NAVY
Information strategy plan
[AD-A247740] p 3367 N92-28403
The Navy layered ocean model users guide
[AD-A247754] p 3321 N92-28566
Limiting factors to advancing thermal battery technology for naval applications
[AD-A247773] p 3280 N92-28568
NEGATIVE IONS
Development of negative heavy ion sources for plasma potential measurement
[DE92-782102] p 3360 N92-28234
Theoretical studies of the electronic and resonance structure of atomic and molecular negative ions
[AD-A247093] p 3354 N92-28259
Excited negative ions and molecules and negative ion production
[AD-A247017] p 3354 N92-28414
NETWORK ANALYSIS
The Father Christmas worm
[NASA-TM-107938] p 3334 N92-28267
Investigation of an equivalent circuit for the inductive strip in finline with dielectric
[AD-A247025] p 3279 N92-28373
NETWORKS
Coincident pulse techniques for hybrid electronic optical computer systems
[AD-A246774] p 3332 N92-28514
NEURAL NETS
Computer assisted improvement of the estimation mean squared error with application to back propagation neural networks
[AD-A247724] p 3344 N92-28401
Center for the integration of optical computing
[AD-A250306] p 3337 N92-28719
Flexible integrated architecture for neural networks
[ETN-92-91320] p 3343 N92-28782
Improvement of connectionnist learning processes, working according to the gradients method
[ETN-92-91335] p 3327 N92-28787
Representation of neutron noise data using neural networks
[DE92-013232] p 3356 N92-28813
Neural network parameter estimation for the modified bistatic scattering strength model (BISSM)
[AD-A247913] p 3322 N92-28963
Segmentation of satellite imagery using hierarchical thresholding and neural networks
[AD-A247915] p 3319 N92-28965
A probabilistic neural network approach to cloud classification
[AD-A247916] p 3319 N92-28966
Monolithic optoelectronic implementation of neural planes
[AD-A250286] p 3345 N92-28970
Stretch and hammer neural networks for N-dimensional data generalization
[AD-A247941] p 3346 N92-29082
Estimation of the point of incipient deterioration and a class of life distribution with application to cannibalization
[AD-A250216] p 3343 N92-29114
Method and apparatus for predicting the direction of movement in machine vision
[NASA-CASE-NPO-17552-1-CU] p 3331 N92-29129
New neural algorithms for self-organized learning
[AD-A249816] p 3341 N92-29198
NEUROLOGY
Study of SCN neurochemistry using in vivo microdialysis in the conscious brain: Correlation with overt circadian rhythms
[AD-A247172] p 3325 N92-28886

NEURONS
In search of a unified theory of biological organization: What does the motor system of a sea slug tell us about human motor integration?
[AD-A250223] p 3328 N92-29119
Non-linear analysis of visual cortical neurons
[AD-A250233] p 3326 N92-29179
NEUROPHYSIOLOGY
The Coordinated Noninvasive Studies (CNS) project, phase 1
[AD-A247159] p 3324 N92-28397
Neuropsychological components of object identification
[AD-A247049] p 3327 N92-28877
NEUROTRANSMITTERS
In search of a unified theory of biological organization: What does the motor system of a sea slug tell us about human motor integration?
[AD-A250223] p 3328 N92-29119
NEUTRAL SHEETS
Secondary instability in 3D magnetic reconnection
[AD-A248630] p 3360 N92-28354
NEUTRINOS
The 17 keV neutrino and neutrino tagging
[DE92-011281] p 3355 N92-28839
The many aspects of neutrino physics
[DE92-011735] p 3355 N92-28858
Quark matter and cosmology
[DE92-011736] p 3371 N92-28859
NEUTRON SPECTRA
Redistribution of subsurface neutrons caused by ground ice on Mars p 3374 N92-28488
NEUTRON STARS
Resonant Compton scattering in models of gamma ray burst sources
[DE92-010720] p 3397 N92-28336
NEUTRONS
Redistribution of subsurface neutrons caused by ground ice on Mars p 3374 N92-28488
Compositional disorder, magnetism, and their interplay in metallic alloys
[DE92-011671] p 3260 N92-28856
NEW MEXICO
A seismic and integrated geophysical study of the lithosphere of the Colorado Plateau
[AD-A247091] p 3308 N92-28257
NEWTON METHODS
The principal part of plane vector fields with fixed Newton diagram
[DE92-622408] p 3346 N92-28311
NEWTONIAN FLUIDS
The role of hard turbulent thermal convection in the Earth's early thermal evolution p 3310 N92-28593
NICKEL ALLOYS
Some experiments to determine the efficiency of collection of alumina particles by electron beam button melting in a nickel-base superalloy, AP1
[NPL-DMM(A)-42] p 3261 N92-29164
NIGHT VISION
Methods of visual scanning with night vision goggles
[AD-A247470] p 3331 N92-28944
NIOBIUM
Chemical vapor synthesis of niobium aluminides
[AD-A250332] p 3258 N92-29091
NITINOL ALLOYS
Coupling device with improved thermal interface
[NASA-CASE-GSC-13251-1] p 3295 N92-29120
NITROGEN
Nitrogen escape from Mars p 3383 N92-29014
NITROGEN ATOMS
Synthesis and study of metallonitride complexes and polymers
[AD-A248577] p 3262 N92-28323
The production and escape of nitrogen atoms on Mars p 3374 N92-28490
NITROGEN ISOTOPES
The production and escape of nitrogen atoms on Mars p 3374 N92-28490
NITROGEN OXIDES
Greenhouse warming by minor gases on early Mars p 3384 N92-29022
NITROGEN POLYMERS
Synthesis and study of metallonitride complexes and polymers
[AD-A248577] p 3262 N92-28323
NITROGEN 15
Nitrogen escape from Mars p 3383 N92-29014
NITROGENATION
Poly(1,3,4-oxadiazoles) via aromatic nucleophilic displacement
[NASA-CASE-LAR-14427-1] p 3250 N92-29141
NOAA SATELLITES
ETO cloud studies for FIRE 2, part 1
[NASA-CR-190472] p 3319 N92-29087
NOISE GENERATORS
Boundary layer induced noise in aircraft
[ISSN-0309-7293] p 3353 N92-29201
NOISE INTENSITY
Operational noise data for OH-58D Army helicopters
[AD-A246822] p 3351 N92-28292
Fundamental noise limits in miniature acoustic and vibration sensors
[AD-A247016] p 3352 N92-28413
Annoyance due to discrete tones in broadband background noise. Part 2: Analysis
[ISVR-TR-202-PT-2] p 3353 N92-29203
NOISE MEASUREMENT
Operational noise data for OH-58D Army helicopters
[AD-A246822] p 3351 N92-28292
NOISE PROPAGATION
Under-ice broadband transient measurements and processing
[AD-A248609] p 3351 N92-28324
Adaptive noise cancellation applied to the NUWES test ranges
[AD-A245961] p 3352 N92-28409
NOISE REDUCTION
Noise reduction in ring laser driven by a broad band pump
[DE92-622403] p 3289 N92-28228
Full Navier-Stokes analysis of a two-dimensional mixer/ejector nozzle for noise suppression
[NASA-TM-105715] p 3236 N92-28419
NOISE SPECTRA
Operational noise data for OH-58D Army helicopters
[AD-A246822] p 3351 N92-28292
Demodulation processes in auditory perception
[AD-A250203] p 3328 N92-29146
NONCONSERVATIVE FORCES
Modeling radiation forces acting on TOPEX/Poseidon for precision orbit determination
[NASA-TM-104564] p 3244 N92-28343
NONDESTRUCTIVE TESTS
X ray computed tomography of full-scale castings
[AD-A247101] p 3258 N92-28241
Nondestructive evaluation of damages caused by impact and fatigue loading of polymer composites
[VTT-RR-742] p 3251 N92-28572
Diffuser casing upgrade for an advanced turbofan
[NLR-TP-90097-U] p 3238 N92-28711
Magnetic remanence method and apparatus to test materials for embrittlement
[NASA-CASE-LAR-13817-4] p 3304 N92-29101
Method for advanced material characterization by laser induced eddy current imaging
[NASA-CASE-GSC-13386-1] p 3298 N92-29154
Magneto acoustic emission method for testing materials for embrittlement
[NASA-CASE-LAR-13817-2] p 3304 N92-29155
The characterization of ceramics and ceramic/metal-joints by ultrasonic techniques
[VTT-RR-741] p 3266 N92-29194
NONLINEAR FEEDBACK
Adaptive and nonlinear control
[AD-A248580] p 3344 N92-28429
Control of nonlinear distributed parameter systems with application to flow control
[AD-A250212] p 3346 N92-29149
NONLINEAR OPTICS
Research studies on extreme ultraviolet and soft x ray lasers
[AD-A247309] p 3289 N92-28299
Tunable optical sources and synthetic nonlinear media/growth and characterization of nonlinear optical materials
[AD-A249363] p 3357 N92-28328
NONLINEAR PROGRAMMING
Numerical methods of linear and nonlinear optimization
[AD-A248579] p 3335 N92-28428
Global minimum solution of engineering design problems
[AD-A247496] p 3337 N92-28704
NONLINEAR SYSTEMS
Noise reduction in ring laser driven by a broad band pump
[DE92-622403] p 3289 N92-28228
Identification of weakly non-linear dynamical systems by means of random excitations
[ONERA-NT-1991-10] p 3349 N92-28778
A continuation method for calculating the equilibrium positions of nonlinear structures
[ONERA-RT-24/3542-RY-091-R] p 3338 N92-28790
Future mission studies: Forecasting solar flux directly from its chaotic time series
[NASA-CR-190378] p 3396 N92-28872
Evidence of chaotic pattern in solar flux through a reproducible sequence of period-doubling-type bifurcations
[NASA-TM-107944] p 3396 N92-28907
Control of nonlinear distributed parameter systems with application to flow control
[AD-A250212] p 3346 N92-29149
Optical switching devices
[AD-D015261] p 3360 N92-29205
NONLINEARITY
Molecular dynamics calculations of optical nonlinear properties of materials
[AD-A247095] p 3354 N92-28260
Computer assisted improvement of the estimation mean squared error with application to back propagation neural networks
[AD-A247724] p 3344 N92-28401
Adaptive and nonlinear control
[AD-A248580] p 3344 N92-28429
Initial investigations of an adaptive discrete-time controller for nonlinear time-varying robotic models p 3247 N92-28736
Nonlinear techniques for forecasting solar activity directly from its time series
[NASA-TM-107946] p 3396 N92-28870
Detecting and disentangling nonlinear structure from solar flux time series
[NASA-CR-190510] p 3396 N92-28871
Nonlinear normal and axial force indicial responses for a two dimensional airfoil
[AD-A247196] p 3229 N92-28888
Nonlinear sloshing and the coupled dynamics of liquid propellants and spacecraft
[AD-A250023] p 3248 N92-28967
Nonlinear stratified flow over localized topographic obstacles on Mars p 3387 N92-29036
NONPARAMETRIC STATISTICS
Estimation of the point of incipient deterioration and a class of life distribution with application to cannibalization
[AD-A250216] p 3343 N92-29114
NORMAL DENSITY FUNCTIONS
High quality Gaussian basis sets for fourth-row atoms
[NASA-TM-103918] p 3255 N92-28743
NORTH SEA
An inventory of data collected during the NERC's North Sea Community Research Project, 1987-1992
[REPT-21-1991] p 3323 N92-29215
Directional wave data recorded off Flamborough Head (England)
[IOS-273-1990] p 3323 N92-29216
NORTHERN HEMISPHERE
Midlatitude weather systems on Mars: Is there a hemispheric asymmetry? p 3379 N92-28992
NOZZLE FLOW
Rocket nozzle shield
[AD-D015248] p 3249 N92-28748
Flow rate testing of valves used with the 500 gallon collapsible drum
[AD-A250567] p 3294 N92-28924
NUCLEAR EXPLOSIONS
Studies of regional wave propagation using differential seismograms and randomized structural models
[AD-A247011] p 3309 N92-28394
NORSAR basic seismological research
[AD-A248616] p 3309 N92-28569
NUCLEAR FUSION
Cryogenic system operating experience review for fusion applications
[DE92-012509] p 3361 N92-28805
NUCLEAR MAGNETIC RESONANCE
Quantitative interphase study of composite materials. Interphase engineering: A scientific way of tailoring the mechanophysical properties of composite materials
[AD-A247776] p 3251 N92-28252
NUCLEAR PHYSICS
Evidence for physics beyond the quasi-deuteron model in pion absorption
[DE92-011285] p 3354 N92-28310
NUCLEAR POWER PLANTS
Representation of neutron noise data using neural networks
[DE92-013232] p 3356 N92-28813
NUCLEAR POWER REACTORS
Natural circulation decay heat removal from an SP-100, 550 kWe power system for a lunar outpost
[NASA-CR-190421] p 3307 N92-28863
NUCLEAR REACTIONS
Evidence for physics beyond the quasi-deuteron model in pion absorption
[DE92-011285] p 3354 N92-28310
NUCLEAR REACTORS
A strategy for minimizing common mode human error in executing critical functions and tasks
[DE92-011839] p 3327 N92-28775
Pre-test analyses for pressurized thermoshock tests, vessel 1
[VTT-RR-746] p 3303 N92-28776

NUCLEATION
The in situ observation of diamond film nucleation and growth
[AD-A248203] p 3265 N92-29189
NULL ZONES
Null shifting with fixed delays
[AD-A250059] p 3274 N92-28796
Data selection for fast projection techniques applied to adaptive nulling: A comparative study of performance
[AD-A246468] p 3276 N92-28979
NUMERICAL ANALYSIS
Mapping closures for turbulent mixing and reaction
[AD-A247305] p 3283 N92-28274
Computation of steady and unsteady quasi-one-dimensional viscous/inviscid interacting internal flows at subsonic, transonic, and supersonic Mach numbers
[NASA-CR-189881] p 3283 N92-28555
A comparative study of the accuracy of various time domain nonorthogonal mesh methods
[DE92-007300] p 3347 N92-28824
Diagonal forms of translation operators for helmholtz equation in three dimensions
[AD-A248422] p 3348 N92-28949
NUMERICAL CONTROL
Audit trails and PC control on Novell networks
[DE92-010695] p 3335 N92-28332
NUMERICAL FLOW VISUALIZATION
Construction of a numerical optimization method for the definition of hypersupported profiles
[ONERA-RSF-43/1736-AY-146A] p 3284 N92-28788
Development of an unsteady three-dimensional viscous-inviscid interaction numerical method for the calculation of airfoils vibration
[ONERA-RSF-7/3617-AY-022A] p 3229 N92-29206
NUMERICAL INTEGRATION
On some splitting schemes for wave equations
[FFI-91/7023] p 3348 N92-29193
NUMERICAL WEATHER FORECASTING
Simulation of atmospheric frontogenesis with a semi-Lagrangian numerical model
[AD-A247151] p 3318 N92-28517
NUTS (FASTENERS)
Quick application/release nut with engagement indicator
[NASA-CASE-MSC-21799-1] p 3296 N92-29150

O

OBJECT PROGRAMS
Object-oriented programming: An assessment of fundamental concepts and design considerations
[AD-A247480] p 3333 N92-28243
OBJECT-ORIENTED PROGRAMMING
Object-oriented programming: An assessment of fundamental concepts and design considerations
[AD-A247480] p 3333 N92-28243
OBLIQUENESS
The Martian polar caps: Stability and water transport at low obliquities p 3385 N92-29023
OBSERVATION
The in situ observation of diamond film nucleation and growth
[AD-A248203] p 3265 N92-29189
OBSERVATORIES
Measurements of declination at the Helsinki Magnetic-Meteorological Observatory 1844-1853
p 3299 N92-28622
Magnetic repeat station data p 3301 N92-28630
Geomagnetic data from the US magnetic observatory network p 3301 N92-28631
Magnetic and electromagnetic induction effects in the annual means of geomagnetic elements
p 3301 N92-28632
Independent constituents in observatory time series in characterizing the secular variation
p 3302 N92-28633
OCEAN BOTTOM
A new ocean bottom magnetometer system for continental shelf measurements
[AD-A247644] p 3321 N92-28321
Test of the new ONR ocean bottom seismographs on the Juan de Fuca Ridge
[AD-A247733] p 3321 N92-28402
The Navy layered ocean model users guide
[AD-A247754] p 3321 N92-28566
Pressure regimes and core formation in the accreting earth p 3313 N92-28605
Marine magnetic data holdings of World Data Center-A for Marine Geology and Geophysics
p 3300 N92-28625
Reduction of marine magnetic data for modeling the main field of the Earth p 3300 N92-28626
Seafloor pressure array studies at ultra-low frequencies
[AD-A247663] p 3322 N92-28939
OCEAN CURRENTS
A diagnostic study of the velocity structure of a meandering jet in the California current system using a primitive equation model
[AD-A246039] p 3320 N92-28283
The Navy layered ocean model users guide
[AD-A247754] p 3321 N92-28566
Applications of passive microwave satellite data for Arctic Sea ice studies
[AD-A245966] p 3306 N92-28791
Structure energetics and dynamics of Gulf Stream variability
[AD-A248246] p 3323 N92-29225
OCEAN DATA ACQUISITIONS SYSTEMS
EUMETSAT: The European Organization for Meteorological Satellites
[ETN-92-91069] p 3318 N92-28745
Autonomous ocean profiler
[AD-A247657] p 3322 N92-28938
CTD data from the north east Atlantic, April 1989, collected on RRS Discovery Cruise 181
[IOS-285-1991] p 3322 N92-29211
Moored current measurements made in the Iceland Faeroes region during July-August 1990
[IOS-286-1991] p 3323 N92-29212
Evaluation of a Solent sonic anemometer on RRS Charles Darwin Cruise 43
[IOS-288-1991] p 3323 N92-29213
Directional wave data recorded off Flamborough Head (England)
[IOS-273-1990] p 3323 N92-29216
OCEAN DYNAMICS
Optical effects on ocean mixed layer dynamics
[AD-A245941] p 3320 N92-28316
TOPEX/POSEIDON science investigations plan
[NASA-CR-190456] p 3305 N92-28950
Structure energetics and dynamics of Gulf Stream variability
[AD-A248246] p 3323 N92-29225
OCEAN MODELS
A numerical study of time-dependent wind forcing off the west coast of Portugal, 1987-1988
[AD-A246775] p 3321 N92-28365
The Navy layered ocean model users guide
[AD-A247754] p 3321 N92-28566
Ocean tide models for satellite geodesy and Earth rotation
[NASA-CR-190468] p 3321 N92-28867
A coupled regional tide model
[AD-A247917] p 3322 N92-28913
OCEAN SURFACE
SAR-relate stress variability in the Marine Atmospheric Boundary Layer (MABL)
[AD-A247772] p 3309 N92-28567
Sea surface velocities from visible and infrared multispectral atmospheric mapping sensor imagery
[NASA-CR-190398] p 3305 N92-28715
OCEAN TEMPERATURE
Autonomous ocean profiler
[AD-A247657] p 3322 N92-28938
OCEANOGRAPHIC PARAMETERS
Autonomous ocean profiler
[AD-A247657] p 3322 N92-28938
Oceanographic data dictionary for netCDF files
[AD-A250017] p 3322 N92-28951
Neural network parameter estimation for the modified bistatic scattering strength model (BISSM)
[AD-A247913] p 3322 N92-28963
Bioluminescence in the western Alboran Sea in April 1991
[AD-A250016] p 3324 N92-29089
OCEANOGRAPHY
Optical effects on ocean mixed layer dynamics
[AD-A245941] p 3320 N92-28316
Autonomous ocean profiler
[AD-A247657] p 3322 N92-28938
TOPEX/POSEIDON science investigations plan
[NASA-CR-190456] p 3305 N92-28950
CTD data from the north east Atlantic, April 1989, collected on RRS Discovery Cruise 181
[IOS-285-1991] p 3322 N92-29211
Evaluation of a Solent sonic anemometer on RRS Charles Darwin Cruise 43
[IOS-288-1991] p 3323 N92-29213
Structure energetics and dynamics of Gulf Stream variability
[AD-A248246] p 3323 N92-29225
OCEANS
A new ocean bottom magnetometer system for continental shelf measurements
[AD-A247644] p 3321 N92-28321
Ultrasonic ambient noise in Australian shallow waters at frequencies up to 200 kHz
[MRL-TR-91-23] p 3351 N92-28364
Mesoscale vertical structure of an explosive oceanic cyclone
[AD-A245927] p 3318 N92-28423
Terrestrial magma ocean and core segregation in the earth p 3313 N92-28606
Estimation of the viscosities of silicate liquids at high pressure from measurements of oxygen diffusivity
p 3313 N92-28607
Cooling of the magma ocean due to accretional disruption of the surface insulating layer
p 3314 N92-28608
Early planetary differentiation: Geophysical consequences p 3314 N92-28609
Imperfect fractional crystallization of the lunar magma ocean and formation of the lunar mantle: A realistic chemical approach p 3314 N92-28610
Evolution of a terrestrial magma ocean: Thermodynamics, kinetics, rheology, convection, differentiation p 3314 N92-28611
Dynamics and evolution of a magma ocean
p 3314 N92-28612
Evidences for the terrestrial magma ocean from high-pressure melting experiments p 3315 N92-28613
Evidence for magma oceans on asteroids, the moon, and Earth p 3315 N92-28614
Magma ocean formation due to giant impacts
p 3315 N92-28615
Inheritance of magma ocean differentiation during lunar origin by giant impact p 3315 N92-28616
The three stages of magma ocean cooling
p 3315 N92-28617
The ferroan-anorthositic suite and the extent of primordial lunar melting p 3315 N92-28618
Secular variation across the oceans: A retrospective study from 35 years of shipboard total field measurements in the NE Atlantic p 3300 N92-28627
Bioluminescence in the western Alboran Sea in April 1991
[AD-A250016] p 3324 N92-29089
OH-58 HELICOPTER
Operational noise data for OH-58D Army helicopters
[AD-A246822] p 3351 N92-28292
OILS
Effect of metallic coating properties on the tribology of oil-lubricated coated-ceramics
[DE92-010904] p 3262 N92-28339
OLIVINE
Fate of a perched crystal layer in a magma ocean
p 3312 N92-28602
ON-LINE SYSTEMS
On-line point positioning with single frame camera data
[AD-A248307] p 3287 N92-28322
ONBOARD DATA PROCESSING
Future benefits and applications of intelligent on-board processing to VSAT services
[NASA-CR-189185] p 3273 N92-28431
ONBOARD EQUIPMENT
Potential applications of laser Doppler anemometry for in-flight measurements
[NLR-TP-90163-U] p 3236 N92-28654
Loran-C performance assurance assessment program
[NASA-CR-190469] p 3230 N92-28718
OPACITY
Mars dust and cloud opacities and scattering properties p 3381 N92-29003
Greenhouse warming by minor gases on early Mars
p 3384 N92-29022
OPERATING TEMPERATURE
Calculation of installation effects within performance computer programs p 3237 N92-28465
OPERATIONS RESEARCH
Recent advances in global optimization
[AD-A250211] p 3308 N92-29173
OPTICAL ACTIVITY
Monolithic mm-wave phase shifter using optically activated superconducting switches
[NASA-CASE-LEW-14878-1] p 3358 N92-28571
OPTICAL COMMUNICATION
Advanced optical fiber communication systems
[AD-A247683] p 3357 N92-28554
Fiber-optic interconnection networks for spacecraft
[NASA-CR-190531] p 3358 N92-28698
The 2.0 GHz sampling rate transversal filter
[AD-A250244] p 3358 N92-28968
OPTICAL COMPUTERS
Coincident pulse techniques for hybrid electronic optical computer systems
[AD-A246774] p 3332 N92-28514
Center for the integration of optical computing
[AD-A250306] p 3337 N92-28719

OPTICAL COUPLING
In line optical fibre frequency shifter project
[AD-A246714] p 3357 N92-28372
OPTICAL DATA PROCESSING
Coincident pulse techniques for hybrid electronic optical computer systems
[AD-A246774] p 3332 N92-28514
Center for the integration of optical computing
[AD-A250306] p 3337 N92-28719
Null shifting with fixed delays
[AD-A250059] p 3274 N92-28796
OPTICAL DISKS
Conversion and retrievability of hard copy and digital documents on optical disks
[AD-A247481] p 3367 N92-28244
Laser optical disk position encoder with active heads
[NASA-CASE-GSC-13175-1] p 3359 N92-29133
OPTICAL EQUIPMENT
Monolithic optoelectronic implementation of neural planes
[AD-A250286] p 3345 N92-28970
OPTICAL FIBERS
Three-axis fiber optic vector magnetometer
[AD-D015199] p 3357 N92-28223
In line optical fibre frequency shifter project
[AD-A246714] p 3357 N92-28372
Advanced optical fiber communication systems
[AD-A247683] p 3357 N92-28554
Elliptical-core two mode fiber sensors and devices incorporating photoinduced refractive index gratings
[NASA-CR-190495] p 3358 N92-28868
Detection of in-plane displacements of acoustic wave fields using extrinsic Fizeau fiber interferometric sensors
[NASA-CR-190493] p 3353 N92-29196
OPTICAL FILTERS
Null shifting with fixed delays
[AD-A250059] p 3274 N92-28796
Binary optical filters for scale invariant pattern recognition
[NASA-TM-103902] p 3234 N92-28910
OPTICAL HETERODYNING
Performance of the multifunctional CW CO2-laser radar at the TNO-FEL laboratory and during the BEST TWO field test
[FEL-91-A163] p 3291 N92-29160
OPTICAL MATERIALS
Optical switching devices
[AD-D015261] p 3360 N92-29205
OPTICAL MEASURING INSTRUMENTS
Perspectives of ion implantation for optics
[DE92-010664] p 3357 N92-28355
OPTICAL MEMORY (DATA STORAGE)
Disk memory device
[NASA-CASE-GSC-13196-1] p 3333 N92-29132
OPTICAL PATHS
Multi-channel fiber optic rotary joint for single-mode fiber
[AD-D015273] p 3358 N92-29095
Non-mechanical optical path switching and its application to dual beam spectroscopy including gas filter correlation radiometry
[NASA-CASE-LAR-14588-1-CU] p 3359 N92-29117
OPTICAL PROPERTIES
Molecular dynamics calculations of optical nonlinear properties of materials
[AD-A247095] p 3354 N92-28260
Tunable optical sources and synthetic nonlinear media/growth and characterization of nonlinear optical materials
[AD-A249363] p 3357 N92-28328
Perspectives of ion implantation for optics
[DE92-010664] p 3357 N92-28355
Theory for the CEBAF and shipboard FELS
[AD-A245979] p 3289 N92-28662
CO2 laser frequency multiplication
[AD-A247542] p 3291 N92-28933
Analysis of Martian atmospheric and surface optical properties between 4.4 and 5.1 microns
p 3382 N92-29007
Bioluminescence in the western Alboran Sea in April 1991
[AD-A250016] p 3324 N92-29089
OPTICAL PUMPING
Singlet delta oxygen pumping of iodine monofluoride in a supersonic flow
[AD-A249946] p 3284 N92-28766
OPTICAL RADAR
An evaluation of the naval oceanic vertical aerosol model during Key90
[AD-A245943] p 3320 N92-28318
ETO cloud studies for FIRE 2, part 1
[NASA-CR-190472] p 3319 N92-29087
Use of laser range finders and range image analysis in automated assembly tasks
[NASA-CR-186957] p 3291 N92-29139
Performance of the multifunctional CW CO2-laser radar at the TNO-FEL laboratory and during the BEST TWO field test
[FEL-91-A163] p 3291 N92-29160
OPTICAL SWITCHING
Non-mechanical optical path switching and its application to dual beam spectroscopy including gas filter correlation radiometry
[NASA-CASE-LAR-14588-1-CU] p 3359 N92-29117
Optical switching devices
[AD-D015261] p 3360 N92-29205
OPTICAL THICKNESS
Mars dust and cloud opacities and scattering properties p 3381 N92-29003
Atmospheric and surface temperatures and airborne dust amounts during late southern summer from Mariner 9 IRIS data p 3390 N92-29056
Comparison of drift potential derived from Mars GCM with rock abundance from IRTM p 3395 N92-29078
OPTIMAL CONTROL
Stability and optimal control theory of hereditary systems with applications from oscillating flying vehicles, mechanical systems, and robotics p 3247 N92-28732
Fuel optimal propulsive reboost of flexible spacecraft p 3247 N92-28734
Fuel optimal maneuver: Experimental testbeds p 3247 N92-28735
A generalized reusable guidance algorithm for optimal aerobraking
[NASA-TM-103590] p 3229 N92-28981
OPTIMIZATION
Optimalization of grenades with pre-formed fragments against air-targets, part 2
[PML-1990-24-PT-2] p 3349 N92-28313
Adaptive set-membership identification in 0(m) time for linear-in-parameters models
[AD-A249359] p 3273 N92-28358
Scheduling multiple variable-speed machines
[AD-A249362] p 3268 N92-28359
Numerical methods of linear and nonlinear optimization
[AD-A248579] p 3335 N92-28426
Taguchi methods in electronics: A case study
[NASA-TM-103586] p 3279 N92-28456
Integrated Design Analysis and Optimisation of Aircraft Structures
[AGARD-LS-186] p 3231 N92-28469
Fundamentals of structural optimisation p 3231 N92-28470
Practical architecture of design optimisation software for aircraft structures taking the MBB-Lagrange code as an example p 3232 N92-28471
Structural optimization of aircraft p 3232 N92-28472
Multidisciplinary design and optimization
[AGARD-PAPER-2] p 3232 N92-28473
Mathematical optimization: A powerful tool for aircraft design p 3232 N92-28474
Optimum design of a gearbox for low vibration
[NASA-TM-105653] p 3293 N92-28476
Constrained spanload optimization for minimum drag of multi-lifting-surface configurations
[NLR-TP-89126-U] p 3227 N92-28660
Global minimum solution of engineering design problems
[AD-A247496] p 3337 N92-28704
Fuel optimal propulsive reboost of flexible spacecraft p 3247 N92-28734
Monte Carlo optimization of depth-of-interaction resolution in PET crystals
[DE92-011147] p 3364 N92-28762
Construction of a numerical optimization method for the definition of hypersupported profiles
[ONERA-RSF-43/1736-AY-146A] p 3284 N92-28788
Optimization by renaming in the solution method
[ETN-92-91324] p 3338 N92-28842
Decomposition of balanced matrices. Part 1: Introduction
[AD-A247397] p 3349 N92-28927
Decomposition of balanced matrices. Part 6: Even wheels
[AD-A247399] p 3350 N92-28929
Estimation of the point of incipient deterioration and a class of life distribution with application to cannibalization
[AD-A250216] p 3343 N92-29114
Recent advances in global optimization
[AD-A250211] p 3308 N92-29173
ORBIT CALCULATION
Modeling radiation forces acting on TOPEX/Poseidon for precision orbit determination
[NASA-TM-104564] p 3244 N92-28343
Future mission studies: Preliminary comparisons of solar flux models
[NASA-TM-107947] p 3396 N92-28869
ORBIT TRANSFER VEHICLES
Thermal response of rigid and flexible insulations and reflective coating in an aeroconvective heating environment
[NASA-TM-103925] p 3233 N92-28721
ORBITAL ASSEMBLY
Software design for automated assembly of truss structures
[NASA-TP-3198] p 3344 N92-28375
Quick application/release nut with engagement indicator
[NASA-CASE-MSC-21799-1] p 3296 N92-29150
ORDER-DISORDER TRANSFORMATIONS
Compositional disorder, magnetism, and their interplay in metallic alloys
[DE92-011671] p 3260 N92-28856
ORGANIC COMPOUNDS
Sol-gel processed multifunctional organic polymer-inorganic oxide composites for electronics and photonics
[AD-A246773] p 3263 N92-28412
Ion conductive polymer solid electrolytes
[DE92-010518] p 3266 N92-29195
ORGANIC MATERIALS
Ionized assisted deposition of organic films for optoelectronic applications
[AD-A247744] p 3263 N92-28405
ORGANOMETALLIC COMPOUNDS
New methodology for fluorocarbon synthesis
[AD-A247163] p 3254 N92-28261
Volatile CVD precursors based on copper alkoxides and mixed group IIA-Copper alkoxides --- chemical vapor deposition
[AD-D015264] p 3261 N92-29170
ORTHOGONALITY
The structure of finitely generated shift-invariant spaces in L2(IR sup d)
[AD-A247314] p 3334 N92-28301
OSCILLATING FLOW
Heat exchanger with oscillating flow
[NASA-CASE-LAR-14033-1] p 3284 N92-28752
Wall turbulence
[AD-A249973] p 3284 N92-28768
OSCILLATIONS
Microgravity accelerometer characterization on Columbia STS-32 mission p 3271 N92-28452
Independent constituents in observatory time series in characterizing the secular variation p 3302 N92-28633
The many aspects of neutrino physics
[DE92-011735] p 3355 N92-28858
OSCILLATORS
Multimeter-wave grid oscillators
[AD-A248430] p 3279 N92-28351
The Los Alamos POP Project: FEL oscillator experiments in the ultraviolet and beyond
[DE92-011286] p 3291 N92-29168
OUTGASSING
Chemical models of volcanic outgassing on Mars p 3374 N92-28487
Forsterite/melt partitioning of argon and iodine: Implications for atmosphere formation by outgassing of an early Martian magma ocean p 3313 N92-28604
Atmosphere-surface interactions and atmospheric evolution on Mars p 3383 N92-29012
Was early Mars warmed by ammonia? p 3386 N92-29030
OVER-THE-HORIZON RADAR
An OTH radar clutter simulation
[AD-A248054] p 3272 N92-28304
OVERPRESSURE
Rocket nozzle shield
[AD-D015248] p 3249 N92-28748
OXIDASE
Curvature estimation in orientation selection
[AD-A247862] p 3328 N92-28957
OXIDATION
Macrocyclic polycation complexes for secondary anion binding, molecular recognition, and catalysis
[AD-A246690] p 3254 N92-28287
Mechanisms of fracture and creep of structural alloys
[AD-A248701] p 3259 N92-28390
Oxygen in the Martian atmosphere: Regulation of PO2 by the deposition of iron formations on Mars p 3373 N92-28482
High-pressure melting of carbonaceous chondrite p 3310 N92-28589
Kinetic studies of metal combustion in propulsion
[AD-A250207] p 3256 N92-28769
Investigation of laser-induced retinal damage
[AD-A250173] p 3326 N92-28920
Molecular recognition in the oxidation of catechols by Dicobalt-BISDIEN dioxygen complexes
[AD-A246456] p 3258 N92-28973
Rates of oxidative weathering on the surface of Mars p 3380 N92-28999

Oxidation resistant coating for titanium alloys and titanium alloy matrix composites
[NASA-CASE-LEW-15155-1] p 3265 N92-29090

OXIDATION RESISTANCE
The oxidation stability of boron nitride thin films on MgO and TiO2 substrates
[DE92-011686] p 3364 N92-28857
Oxidation resistant coating for titanium alloys and titanium alloy matrix composites
[NASA-CASE-LEW-15155-1] p 3265 N92-29090

OXIDATION-REDUCTION REACTIONS
Macrocyclic polycation complexes for secondary anion binding, molecular recognition, and catalysis
[AD-A246690] p 3254 N92-28287
Orthogonal self-assembly of redox active molecules on Pt and Au: Selective reaction of disulfide with Au and isonitrile with Pt
[AD-A246698] p 3254 N92-28290
The evaluation of rate constants for rapid electrode reactions by using microelectrode voltammetry: Virtues of measurement at lower temperature
[AD-A246760] p 3255 N92-28391
Estimation of high temperature metal-silicate partition coefficients p 3311 N92-28599
Conversion of acetic acid to methane by thermophiles
[DE92-010652] p 3257 N92-28942
Molecular recognition in the oxidation of catechols by Dicobalt-BISDIEN dioxygen complexes
[AD-A246456] p 3258 N92-28973
Determining the pH of Mars from the Viking labelled release reabsorption effect p 3389 N92-29049

OXIDE FILMS
Feasibility of metal-oxide-semiconductor structures on Si-LPCVD thin films by low temperature (600 C) process
[LAAS-91307] p 3365 N92-29207

OXIDES
Sol-gel processed multifunctional organic polymer-inorganic oxide composites for electronics and photonics
[AD-A246773] p 3263 N92-28412

OXYGEN
Oxygen in the Martian atmosphere: Regulation of PO2 by the deposition of iron formations on Mars p 3373 N92-28482
An ion mass spectrometer for measuring isotopic adundances and loss rates of O, C and H in Mars' upper atmosphere p 3374 N92-28486
Estimation of the viscosities of silicate liquids at high pressure from measurements of oxygen diffusivity p 3313 N92-28607
Singlet delta oxygen pumping of iodine monofluoride in a supersonic flow
[AD-A249946] p 3284 N92-28766
Computations of detonation structure: The influence of model input parameters
[AD-A248634] p 3285 N92-28803
The ancient oxygen exosphere of Mars: Implications for atmosphere evolution p 3395 N92-29080

OXYGEN ATOMS
History of oxygen and carbon escape from the Martian atmosphere p 3376 N92-28498
Atomic oxygen in the Martian thermosphere p 3391 N92-29061

OXYGEN PRODUCTION
Trade study of three oxygen processors for the Martian atmosphere
[AD-A246854] p 3372 N92-28393
Compact, self-contained ArF lasers
[AD-A247403] p 3291 N92-28932

OXYGEN RECOMBINATION
The impact of temperature dependent CO2 cross section measurements: A role for heterogeneous chemistry in the atmosphere of Mars? p 3372 N92-28479

OXYGEN SPECTRA
An analysis of middle ultraviolet dayglow spectra
[AD-A245965] p 3309 N92-28319

OXYGEN 17
Mars volatile evolution: Implications of the recent measurement of O-17 in water from the SNC meteorites p 3375 N92-28492

OXYHEMOGLOBIN
Structural characterization of cross-linked hemoglobins developed as potential transfusion substitutes
[AD-A246777] p 3325 N92-28515

OXYNITRIDES
Mg-Si-Al oxynitride glasses
[AD-A247593] p 3261 N92-28249

OZONE
Reactions of hydrazines with chemicals found in environment
[AD-A247064] p 3308 N92-28272
Simulations of the seasonal polar caps on Mars p 3387 N92-29033

P

P-N JUNCTIONS
Split events and their influence on pn CCD energy spectra
[ETN-92-91485] p 3282 N92-29178

PAINTS
Paint removal using cryogenic processes
[AD-A247668] p 3264 N92-28912

PANEL METHOD (FLUID DYNAMICS)
Calculation of unsteady subsonic and supersonic flow about oscillating wings and bodies by new panel methods
[NLR-TP-89119-U] p 3227 N92-28659

PARABOLIC DIFFERENTIAL EQUATIONS
Simulating radar propagation through atmospheric turbulence using the Tropospheric ElectroMagnetic Parabolic Equation Routine (TEMPER)
[AD-A247408] p 3275 N92-28905

PARABOLIC REFLECTORS
Method of moments analysis of displaced-axis dual reflector antennas
[AD-A247970] p 3277 N92-29166

PARALLEL COMPUTERS
Digital hardware architecture implementation
[AD-A249194] p 3332 N92-28236
Fault-tolerant parallel computer systems for real-time applications
[AD-A247887] p 3343 N92-28958

PARALLEL PROCESSING (COMPUTERS)
Digital hardware architecture implementation
[AD-A249194] p 3332 N92-28236
The instrumentation of a parallel, distributed database operation, retrieve-common, for merging two large sets of records
[AD-A247486] p 3367 N92-28246
HeNCE: Graphical development tools for network-based concurrent computing
[DE92-011061] p 3341 N92-28279
The testing, analysis, and correction of the update operation of a parallel, multi-backend database supercomputer
[AD-A248320] p 3341 N92-28306
SISAL: Toward resolving the parallel programming crisis
[DE92-010716] p 3342 N92-28334
Adaptive set-membership identification in 0(m) time for linear-in-parameters models
[AD-A249359] p 3273 N92-28358
Integration of tools for the Design and Assessment of High-Performance, Highly Reliable Computing Systems (DAHPHRS), phase 1
[NASA-CR-189621] p 3336 N92-28585
Mentat/A: Medium grain parallel processing
[NASA-CR-190486] p 3342 N92-28676
Development of a high-performance FORTRAN compiler for porting CFD codes to the Navier-Stokes computer
[AD-A250208] p 3342 N92-28770
Vector and parallel supercomputing programming
[ONERA-NT-1991-11] p 3338 N92-28779
Kanerva's sparse distributed memory with multiple hamming thresholds
[NASA-CR-190552] p 3339 N92-28875
Crystallizing FORTRAN
[AD-A250162] p 3343 N92-28915
Fault-tolerant parallel computer systems for real-time applications
[AD-A247887] p 3343 N92-28958
Mapping unstructured grid computations to massively parallel computers
[NASA-CR-190551] p 3343 N92-29109

PARALLEL PROGRAMMING
HeNCE: Graphical development tools for network-based concurrent computing
[DE92-011061] p 3341 N92-28279
Vector and parallel supercomputing programming
[ONERA-NT-1991-11] p 3338 N92-28779

PARAMAGNETISM
Iron Moessbauer spectroscopy: Superparamagnetism in hydrothermal vents and the search for evidence of past life on Mars p 3378 N92-28989

PARAMETER IDENTIFICATION
Adaptive set-membership identification in 0(m) time for linear-in-parameters models
[AD-A249359] p 3273 N92-28358

PARAMETERIZATION
Parameterization of convective clouds, mesoscale convective systems, and convective-generated cirrus
[DE92-010951] p 3318 N92-28340
Fundamentals of structural optimisation p 3231 N92-28470
A 2-D analysis of evaporation in laminar flow
[AD-A246467] p 3287 N92-28978
Estimation of the point of incipient deterioration and a class of life distribution with application to cannibalization
[AD-A250216] p 3343 N92-29114

PARTIAL DIFFERENTIAL EQUATIONS
A domain decomposition method for ocean/bottom interaction problems
[FFI-91/7022] p 3320 N92-28266
Simulation of the propagation of acoustical waves through an interface separating a compressible fluid and an elastic medium
[FFI-91/7017] p 3351 N92-28314
Wavelets and numerical simulation
[ONERA-NT-1991-8] p 3347 N92-28777
On some splitting schemes for wave equations
[FFI-91/7023] p 3348 N92-29193

PARTICLE ACCELERATOR TARGETS
Bundle dimensions around the internal target area
[NIKHEF-K/AMPS/91-06] p 3356 N92-28264
Woelter x ray microscope characterization measurements on Nova
[DE92-013207] p 3288 N92-28812

PARTICLE ACCELERATORS
High voltage splitting unit for the power supplies of the vacuum pumps of AmPS
[DIGEL-1991-7] p 3278 N92-28263
Bundle dimensions around the internal target area
[NIKHEF-K/AMPS/91-06] p 3356 N92-28264
Accelerator simulation using computers
[DE92-010729] p 3356 N92-28270
Injection: On-axis/off-axis
[NIKHEF-K/AMPS/91-07] p 3356 N92-28308
Cryogenic system operating experience review for fusion applications
[DE92-012509] p 3361 N92-28805
Analyzing noisy spectral line shapes
[DE92-011153] p 3362 N92-29086

PARTICLE BEAMS
Analyzing noisy spectral line shapes
[DE92-011153] p 3362 N92-29086

PARTICLE INTERACTIONS
Scattering mechanisms for semiconductor transport calculations
[AD-A249260] p 3278 N92-28295

PARTICLE LADEN JETS
Experimental and theoretical investigations on the particle lag of particles under the influence of large velocity gradients in compressible flow
[DLR-FB-91-25] p 3286 N92-28825

PARTICLE PRODUCTION
The production and escape of nitrogen atoms on Mars p 3374 N92-28490
Some experiments to determine the efficiency of collection of alumina particles by electron beam button melting in a nickel-base superalloy, AP1
[NPL-DMM(A)-42] p 3261 N92-29164

PARTICLE THEORY
Proceedings of the workshop on Quantum Gravity and Topology
[DE92-782191] p 3366 N92-28235
Electroproduction of light quark baryons
[DE92-010853] p 3354 N92-28337

PARTICLE TRACKS
The solenoidal detector collaboration silicon detector system
[DE92-011237] p 3356 N92-28356

PARTICLE TRAJECTORIES
Experimental and theoretical investigations on the particle lag of particles under the influence of large velocity gradients in compressible flow
[DLR-FB-91-25] p 3286 N92-28825
The effect of induced charges on low-energy particle trajectories near conducting and semiconducting plates
[NASA-TM-103589] p 3355 N92-28966

PARTICLES
Controlled method of reducing electrophoretic mobility of macromolecules, particles, or cells
[NASA-CASE-MFS-26049-2-NP] p 3255 N92-28728

PARTICULATES
Joint DOE/NSF workshop on flow of particulates and fluids
[DE92-012692] p 3285 N92-28808

PARTITIONS
Estimation of high temperature metal-silicate partition coefficients p 3311 N92-28599
Mg-perovskite/silicate melt partition coefficients in the CMS system at 2430 C and 226 Kbars p 3312 N92-28601

PARTITIONS (MATHEMATICS)
Origin of the moon and lunar core formation p 3311 N92-28596

PASSIVE SATELLITES
Applications of passive microwave satellite data for Arctic Sea ice studies
[AD-A245966] p 3306 N92-28791

PASTES
Whole body cleaning agent containing N-acyltaurate
[NASA-CASE-MSC-21589-1] p 3332 N92-29137
PATHOGENESIS
Problems in mechanistic theoretical models for cell transformation by ionizing radiation
[DE92-010265] p 3324 N92-28278
Somatic gene mutation in the human in relation to radiation risk
[DE92-009459] p 3325 N92-28685
PATTERN RECOGNITION
NORSAR basic seismological research
[AD-A248616] p 3309 N92-28569
Binary optical filters for scale invariant pattern recognition
[NASA-TM-103902] p 3234 N92-28910
Stretch and hammer neural networks for N-dimensional data generalization
[AD-A247941] p 3346 N92-29082
Method and apparatus for predicting the direction of movement in machine vision
[NASA-CASE-NPO-17552-1-CU] p 3331 N92-29129
Use of laser range finders and range image analysis in automated assembly tasks
[NASA-CR-186957] p 3291 N92-29139
Psychophysical analyses of perceptual representations
[AD-A246945] p 3329 N92-29186
PATTERN REGISTRATION
Neuropsychological components of object identification
[AD-A247049] p 3327 N92-28877
PATTERNS
Evidence of chaotic pattern in solar flux through a reproducible sequence of period-doubling-type bifurcations
[NASA-TM-107944] p 3396 N92-28907
VHDL and waves descriptions for a pseudo-random pattern generator
[AD-A247891] p 3349 N92-28961
PAVEMENTS
A methodology for the evaluation of runway roughness for repair
[AD-A250407] p 3241 N92-28772
Use of scrap rubber in asphalt pavement surfaces
[AD-A247419] p 3272 N92-28902
PAYLOAD STATIONS
SPEAR 2 space power data analysis
[AD-A248057] p 3250 N92-28945
PAYLOADS
Science and application payloads in the 1990's
[NASA-TM-107937] p 3246 N92-28370
The Microgravity Isolation Mount (MGIM): A Columbus facility for improving the microgravity quality of payloads p 3267 N92-28439
Vibration isolation technology development to demonstration p 3267 N92-28442
ACAP: Acceleration Characterization and Analysis Project p 3267 N92-28448
Predicting microgravity levels for space station using VAPEPS p 3268 N92-28455
Payload retention device
[NASA-CASE-MSC-21906-1] p 3294 N92-28727
PEEK
High temperature dielectric properties of Apical, Kapton, Peek, Teflon AF, and Upilex polymers
[NASA-TM-105753] p 3280 N92-28675
PENETRATION
Optical effects on ocean mixed layer dynamics
[AD-A245941] p 3320 N92-28316
PERCEPTION
Reinforcement learning for the adaptive control of perception and action
[AD-A249351] p 3344 N92-28325
Studies of perceptual memory
[AD-A250200] p 3328 N92-29144
PERFORMANCE
The design of test-section inserts for higher speed aeroacoustic testing in the Ames 80- by 120-foot wind tunnel
[NASA-TM-103915] p 3353 N92-28909
PERFORMANCE PREDICTION
Prediction of attitude stability of asymmetric dual-spin stabilized spacecraft using improved liquid slosh model
[AD-A247023] p 3246 N92-28368
Steady and Transient Performance Prediction of Gas Turbine Engines
[AGARD-LS-183] p 3236 N92-28458
Overview on basis and use of performance prediction methods p 3237 N92-28459
Steady and transient performance calculation method for prediction, analysis, and identification p 3237 N92-28461
Component performance requirements p 3237 N92-28462
Dynamic simulation of compressor and gas turbine performance p 3237 N92-28463
Calculation of installation effects within performance computer programs p 3237 N92-28465
NASA Lewis steady-state heat pipe code users manual
[NASA-TM-105161] p 3249 N92-28682
Introduction to rocket propulsion
[AD-A250424] p 3249 N92-28800
PERFORMANCE TESTS
A cost-benefit analysis on the deletion of the inertial upper stage factory acceptance testing versus a decrease in mission reliability
[AD-A246620] p 3245 N92-28254
Improved decision making through group composition
[AD-A246622] p 3366 N92-28256
An application of interactive computer graphics to the study of inferential statistics and the general linear model
[AD-A246668] p 3334 N92-28285
In line optical fibre frequency shifter project
[AD-A246714] p 3357 N92-28372
The Coordinated Noninvasive Studies (CNS) project, phase 1
[AD-A247159] p 3324 N92-28397
Internal reversing flow in a tailpipe offtake configuration for SSTOVL aircraft
[NASA-TM-105698] p 3236 N92-28418
Delays in laser glare onset differentially affect target-location performance in a visual search task
[AD-A246708] p 3327 N92-28557
LAH-main rotor model test at the DNW
[NLR-TP-90305-U] p 3233 N92-28687
Tasking and communication flows in the F/A-18D cockpit: Issues, problems, and possible solutions
[AD-A245977] p 3234 N92-28802
A coupled regional tide model
[AD-A247917] p 3322 N92-28913
Flow rate testing of valves used with the 500 gallon collapsible drum
[AD-A250567] p 3294 N92-28924
Lapses in alertness: Brain-evoked responses to task-irrelevant auditory probes
[AD-A247669] p 3328 N92-28940
The effects of thermomechanical processing parameters on elevated-temperature behavior of a 6061 Al-Al2O3 metal matrix composite
[AD-A247889] p 3253 N92-28959
VHDL and waves descriptions for a pseudo-random pattern generator
[AD-A247891] p 3349 N92-28961
Performance of the multifunctional CW CO2-laser radar at the TNO-FEL laboratory and during the BEST TWO field test
[FEL-91-A163] p 3291 N92-29160
PERIOD DOUBLING
Evidence of chaotic pattern in solar flux through a reproducible sequence of period-doubling-type bifurcations
[NASA-TM-107944] p 3396 N92-28907
PERIODIC VARIATIONS
Astronomical variation experiments with a Mars general circulation model p 3376 N92-28503
Observations of Mars using Hubble Space Telescope p 3385 N92-29026
PERIODICALS
Super auditory localization for improved human-machine interfaces
[AD-A250288] p 3331 N92-29121
PERIPHERAL EQUIPMENT (COMPUTERS)
Upgrading the data processing section of the NAL Gust Wind Tunnel data processing system
[NAL-TM-635] p 3241 N92-28833
Technological enhancements for personal computers
[AD-A247962] p 3333 N92-29083
PERMAFROST
Distribution of Martian ground-ice table: Preliminary results about climatic variations p 3373 N92-28484
PERMANENT MAGNETS
M-H characteristics and demagnetization resistance of samarium-cobalt permanent magnets to 300 C
[NASA-CR-189194] p 3280 N92-28723
PEROVSKITES
Mg-perovskite/silicate melt partition coefficients in the CMS system at 2430 C and 226 Kbars p 3312 N92-28601
PERSONAL COMPUTERS
Audit trails and PC control on Novell networks
[DE92-010695] p 3335 N92-28332
PC graphics generation and management tool for real-time applications
[NASA-TM-105749] p 3337 N92-28684
Technological enhancements for personal computers
[AD-A247962] p 3333 N92-29083
PERSONNEL
NASA engineers and the age of Apollo
[NASA-SP-4104] p 3397 N92-28344
PERTURBATION THEORY
Probabilistic finite element analysis
[AD-A247721] p 3347 N92-28399
PETROLOGY
A liquidus phase diagram for the groundmass of EETA 79001A (Eg), a primitive Shergottite composition p 3386 N92-29028
PH
Determining the pH of Mars from the Viking labelled release reabsorption effect p 3389 N92-29049
PHASE DEVIATION
The distance dependence of regional phase discriminants
[AD-A247546] p 3316 N92-28935
PHASE DIAGRAMS
A liquidus phase diagram for the groundmass of EETA 79001A (Eg), a primitive Shergottite composition p 3386 N92-29028
PHASE MATCHING
CO2 laser frequency multiplication
[AD-A247542] p 3291 N92-28933
Effects of fading and data modulation on noncoherent M-sequence acquisition schemes
[AD-A247968] p 3276 N92-29084
PHASE MODULATION
Effects of fading and data modulation on noncoherent M-sequence acquisition schemes
[AD-A247968] p 3276 N92-29084
PHASE SHIFT
Monolithic mm-wave phase shifter using optically activated superconducting switches
[NASA-CASE-LEW-14878-1] p 3358 N92-28571
Tuning and automatic phase adjustment in external cavity diode laser beam combiners
[AD-A247421] p 3290 N92-28903
PHASE SHIFT KEYING
Coding for frequency hopped spread spectrum satellite communications
[ECE-90-1] p 3274 N92-28699
PHASE TRANSFORMATIONS
The nonequilibrium molecular dynamics
[DE92-011760] p 3355 N92-28860
Phase transformations in Ti3Al based alloy
[AD-A246464] p 3261 N92-28976
Inverse phase transitions: Does baryogenesis lead to dark matter?
[DE92-013022] p 3372 N92-29184
PHENYLS
Poly(1,3,4-oxadiazoles) via aromatic nucleophilic displacement
[NASA-CASE-LAR-14427-1] p 3250 N92-29141
PHOSPHORS
Single layer multi-color luminescent display and method of making
[NASA-CASE-LAR-13616-3] p 3359 N92-29158
PHOTOCATHODES
PROPX: An x ray manipulation program
[DE92-011264] p 3334 N92-28309
PHOTOCHEMICAL REACTIONS
Selective suppression of photochemical etching: Raman spectroscopy for pre-etch process selection
[DE92-010955] p 3255 N92-28341
Photochemical model for NH3 in an early Martian atmosphere p 3373 N92-28481
Martian atmospheric chemistry during the time of low water abundance p 3376 N92-28501
Elliptical-core two mode fiber sensors and devices incorporating photoinduced refractive index gratings
[NASA-CR-190495] p 3358 N92-28868
Investigation of laser-induced retinal damage
[AD-A250173] p 3326 N92-28920
PHOTODIODES
Monte Carlo optimization of depth-of-interaction resolution in PET crystals
[DE92-011147] p 3364 N92-28762
PHOTODISSOCIATION
Nitrogen escape from Mars p 3383 N92-29014
PHOTOELECTRON SPECTROSCOPY
X ray photoelectron spectroscopy study on the double layer at an Al2O3-Al interface
[AD-A246454] p 3265 N92-28972
PHOTOGRAMMETRY
Computer recognition and analysis of photogrammetric targets
[AD-A250313] p 3339 N92-28971
Martian impact crater degradation studies: Implications for localized obliteration episodes p 3379 N92-28991
PHOTOGRAPHS
Instrumentation for ultrahigh strain rate experiments
[AD-A249358] p 3298 N92-28327
PHOTOIONIZATION
Hyper-Raman scattering and 3-photon resonant ionization: Competitive effects
[DE92-622671] p 3366 N92-28230
Nitrogen escape from Mars p 3383 N92-29014

Microwave interactions with plasmas
[AD-A250333] p 3362 N92-29093
Big Sky Workshop on Super-Intense Laser-Atom Physics
[AD-A248225] p 3292 N92-29223
PHOTOLUMINESCENCE
Growth and optical characterization of Zn(1-x)Mn(x)Te grown by molecular beam epitaxy
[DE92-010667] p 3363 N92-28331
PHOTOLYSIS
The impact of temperature dependent CO2 cross section measurements: A role for heterogeneous chemistry in the atmosphere of Mars? p 3372 N92-28479
Photochemical model for NH3 in an early Martian atmosphere p 3373 N92-28481
Martian atmospheric chemistry during the time of low water abundance p 3376 N92-28501
PHOTOMASKS
High resolution electron beam lithography on x ray mask substrates. Effects of electron scattering and membrane heating
[ETN-92-91336] p 3272 N92-28793
PHOTOMETRY
Infrared photometric behavior and opposition effect of Mars p 3382 N92-29011
Temporal variability of the surface and atmosphere of Mars: Viking Orbiter color observations p 3388 N92-29041
Surface photometric properties and albedo changes in the central equatorial region of Mars p 3392 N92-29066
PHOTON BEAMS
The measuring assembly for the NPL primary standard absorbed dose graphite calorimeter at therapy levels
[NPL-RSA(EXT)-23] p 3288 N92-29163
PHOTONICS
Sol-gel processed multifunctional organic polymer-inorganic oxide composites for electronics and photonics
[AD-A246773] p 3263 N92-28412
Fiber-optic interconnection networks for spacecraft
[NASA-CR-190531] p 3358 N92-28698
PHOTONS
Resonant Compton scattering in models of gamma ray burst sources
[DE92-010720] p 3397 N92-28336
Aperture coupling measurement in a test chamber for the Advanced Photon Source (APS)
[DE92-013059] p 3274 N92-28809
RF impedance measurement status for the 7-GeV Advanced Photon Source (APS)
[DE92-013060] p 3274 N92-28810
Split events and their influence on pn CCD energy spectra
[ETN-92-91485] p 3282 N92-29178
Operation and radiation resistance of a FOXFET biasing structure for silicon strip detectors
[DE92-011279] p 3282 N92-29197
PHTHALOCYANIN
Optical switching devices
[AD-D015261] p 3360 N92-29205
PHYSICAL EXERCISE
Thermoregulation during spaceflight
[NASA-TM-103913] p 3325 N92-28420
Shock and vibration isolation for cyclic exercise in spacecraft p 3267 N92-28449
PHYSICAL OPTICS
Accelerator simulation using computers
[DE92-010729] p 3356 N92-28270
PHYSICAL PROPERTIES
Structure energetics and dynamics of Gulf Stream variability
[AD-A248246] p 3323 N92-29225
PHYSICS
Aeronautical engineering: A continuing bibliography with indexes (supplement 275)
[NASA-SP-7037(275)] p 3226 N92-28679
PHYSIOLOGICAL EFFECTS
Effects of high terrestrial altitude on military performance
[AD-A246695] p 3324 N92-28288
Study of the loss of consciousness inflight by fighter aircraft pilots
[ONERA-RTS-11/3446-EY] p 3325 N92-28844
PHYSIOLOGY
Modelling of heat and moisture loss through NBC ensembles
[AD-A245939] p 3329 N92-28346
PHYTOTRONS
A study of the control problem of the shoot side environment delivery system of a closed crop growth research chamber
[NASA-CR-177597] p 3330 N92-28681
PIEZOELECTRICITY
Microgravity isolation mounts based upon Piezoelectric film p 3268 N92-28454
PILOT PERFORMANCE
A study of pilot attitudes regarding the impact on mission effectiveness of using new cockpit automation technologies to replace the navigator/weapon system officer/electronic warfare officer
[AD-A246883] p 3329 N92-28286
Use of a commercially available flight simulator during aircrew performance testing
[AD-A245922] p 3240 N92-28407
Study of the loss of consciousness inflight by fighter aircraft pilots
[ONERA-RTS-11/3446-EY] p 3325 N92-28844
Neuropsychological components of object identification
[AD-A247049] p 3327 N92-28877
PILOT TRAINING
Use of a commercially available flight simulator during aircrew performance testing
[AD-A245922] p 3240 N92-28407
Piloted Simulation Effectiveness
[AGARD-CP-513] p 3221 N92-28522
Opportunities for flight simulation to improve operational effectiveness p 3221 N92-28523
Utility of ground simulation in flight control problem identification, solution development, and verification p 3221 N92-28525
Experience with piloted simulation in the development of helicopters p 3222 N92-28528
Harrier GR MK 5/7 mission simulators for the Royal Air Force p 3224 N92-28540
Shipboard mission training effectiveness of the Naval Air Test Center's V-22 government test pilot trainer p 3224 N92-28542
Methods of visual scanning with night vision goggles
[AD-A247470] p 3331 N92-28944
PINS
Coupling device with improved thermal interface
[NASA-CASE-GSC-13251-1] p 3295 N92-29120
PIONS
Evidence for physics beyond the quasi-deuteron model in pion absorption
[DE92-011285] p 3354 N92-28310
PIPELINING (COMPUTERS)
CESAR address generator
[FFI-91/7021] p 3334 N92-28265
Mentat/A: Medium grain parallel processing
[NASA-CR-190486] p 3342 N92-28676
PIPES (TUBES)
NASA Lewis Stirling SPRE testing and analysis with reduced number of cooler tubes
[NASA-TM-105767] p 3307 N92-28837
PISTON ENGINES
NASA Lewis Stirling SPRE testing and analysis with reduced number of cooler tubes
[NASA-TM-105767] p 3307 N92-28837
PITCH
Annoyance due to discrete tones in broadband background noise. Part 2: Analysis
[ISVR-TR-202-PT-2] p 3353 N92-29203
PITCH (INCLINATION)
Stability and control flight testing of a half-scale Pioneer remotely piloted vehicle
[AD-A245973] p 3239 N92-28801
Nonlinear normal and axial force indicial responses for a two dimensional airfoil
[AD-A247196] p 3229 N92-28888
PIVOTS
Reduction and analysis of F-111C flight data
[AD-A250341] p 3233 N92-28771
PLAINS
Distribution of coastal morphology in the Martian northern lowlands p 3389 N92-29047
Chryse Planitia region, Mars: Channeling history, flood-volume estimates, and scenarios for bodies of water in the northern plains p 3390 N92-29054
PLANE WAVES
The use of conformal subdomain basis functions in the method of moments computations for a thin wire
[AD-A245964] p 3272 N92-28347
Plane wave propagation in random granular media
[AD-A247300] p 3298 N92-28424
PLANETARY ATMOSPHERES
Water inventories on Earth and Mars: Clues to atmosphere formation p 3373 N92-28483
PLANETARY BOUNDARY LAYER
Micro weather stations for in situ measurements in the Martian planetary boundary layer p 3382 N92-29008
PLANETARY COMPOSITION
Time variation of the meteoritic contribution to the atmosphere of Mars p 3374 N92-28489
Mars: Compositional variability of ferric/ferrous minerals and polar volatiles from groundbased imaging spectroscopy p 3379 N92-28993
Infrared imaging of Mars for volatile distribution and seasonal variability between 2.4 and 5.1 microns p 3379 N92-28995
Mars surface weathering products and spectral analogs: Palagonites and synthetic iron minerals p 3383 N92-29017
PLANETARY CRATERS
Superheat in magma oceans p 3311 N92-28597
PLANETARY CRUSTS
Fate of a perched crystal layer in a magma ocean p 3312 N92-28602
The subsurface hydrologic response of Mars to the thermal evolution of its early crust p 3381 N92-29006
PLANETARY EVOLUTION
Papers Presented to the Workshop on the Evolution of the Martian Atmosphere
[NASA-CR-190508] p 3372 N92-28478
Water inventories on Earth and Mars: Clues to atmosphere formation p 3373 N92-28483
Distribution of Martian ground-ice table: Preliminary results about climatic variations p 3373 N92-28484
Nature and evolution of the early Martian atmosphere: Evidence from highland crater populations p 3373 N92-28485
Time variation of the meteoritic contribution to the atmosphere of Mars p 3374 N92-28489
Mars volatile evolution: Implications of the recent measurement of O-17 in water from the SNC meteorites p 3375 N92-28492
CO2 and clathrate as past erosive agents on Mars p 3375 N92-28497
History of oxygen and carbon escape from the Martian atmosphere p 3376 N92-28498
The early Martian atmosphere p 3376 N92-28502
Workshop on the Physics and Chemistry of Magma Oceans from 1 Bar to 4 Mbar
[NASA-CR-190419] p 3310 N92-28587
Thermal evolution and chemical differentiation of the terrestrial magma ocean p 3310 N92-28588
A magma ocean and the Earth's internal water budget p 3310 N92-28590
The role of hard turbulent thermal convection in the Earth's early thermal evolution p 3310 N92-28593
Magma ocean: Mechanisms of formation p 3312 N92-28600
Evolution of a terrestrial magma ocean: Thermodynamics, kinetics, rheology, convection, differentiation p 3314 N92-28611
Dynamics and evolution of a magma ocean p 3314 N92-28612
Evidences for the terrestrial magma ocean from high-pressure melting experiments p 3315 N92-28613
Evidence for magma oceans on asteroids, the moon, and Earth p 3315 N92-28614
Magma ocean formation due to giant impacts p 3315 N92-28615
Inheritance of magma ocean differentiation during lunar origin by giant impact p 3315 N92-28616
The ferroan-anorthositic suite and the extent of primordial lunar melting p 3315 N92-28618
Giant and large impacts in the context of planetary formation theory p 3315 N92-28619
Workshop on the Martian Surface and Atmosphere Through Time
[NASA-CR-190418] p 3378 N92-28988
The subsurface hydrologic response of Mars to the thermal evolution of its early crust p 3381 N92-29006
Atmosphere-surface interactions and atmospheric evolution on Mars p 3383 N92-29012
Implications of early Hesperian ages for presumed Noachian age volcanic flows on Mars p 3383 N92-29015
Styles of crater gradation in Southern Ismenius Lacus, Mars: Clues from Meteor Crater, Arizona p 3384 N92-29018
Magmatic intrusions and hydrothermal systems on Mars p 3384 N92-29019
Dark material in the polar layered deposits on Mars p 3385 N92-29024
Distribution of water on Mars: Implications from SNC meteorites p 3386 N92-29027
A liquidus phase diagram for the groundmass of EETA 79001A (Eg), a primitive Shergottite composition p 3386 N92-29028
Glacial geomorphic evidence for a late climatic change on Mars p 3386 N92-29029
Was early Mars warmed by ammonia? p 3386 N92-29030
Erosional landforms on the layered terrains in Valles Marineris p 3386 N92-29031
Mars atmosphere evolution: Escape to space p 3387 N92-29034
Dorsa Argentea type sinuous ridges, Mars: Evidence for linear dune hypothesis p 3390 N92-29055
PLANETARY GEOLOGY
Planetary geosciences, 1989-1990
[NASA-SP-508] p 3372 N92-28345
Chemical models of volcanic outgassing on Mars p 3374 N92-28487

Volcanic recycling of carbonate deposits on Mars
p 3377 N92-28506
Workshop on the Martian Surface and Atmosphere Through Time
[NASA-CR-190418] p 3378 N92-28988
Mars: Compositional variability of ferric/ferrous minerals and polar volatiles from groundbased imaging spectroscopy p 3379 N92-28993
Rates of oxidative weathering on the surface of Mars
p 3380 N92-28999
Ice in the northern lowlands and southern highlands of Mars and its enrichment beneath the Elysium Lavas
p 3381 N92-29001
The subsurface hydrologic response of Mars to the thermal evolution of its early crust p 3381 N92-29006
Implications of early Hesperian ages for presumed Noachian age volcanic flows on Mars
p 3383 N92-29015
Mars surface weathering products and spectral analogs: Palagonites and synthetic iron minerals
p 3383 N92-29017
Dark material in the polar layered deposits on Mars
p 3385 N92-29024
An ejection model for SNC meteorites: An indication for recent volcanism on Mars p 3387 N92-29038
Regional variations in the stability and diffusion of water-ice in the Martian regolith p 3388 N92-29042
Chryse Planitia region, Mars: Channeling history, flood-volume estimates, and scenarios for bodies of water in the northern plains p 3390 N92-29054
Physical properties of Deucalionis, Eos, Xanthe-type units in the central equatorial region of Mars
p 3392 N92-29063
Physical properties of Meridiani Sinus-type units in the central equatorial region of Mars p 3392 N92-29064
Physical properties of Oxia/Lunae Planum and Arabia-type units in the central equatorial region of Mars
p 3392 N92-29065
Surface photometric properties and albedo changes in the central equatorial region of Mars
p 3392 N92-29066
Characterization of Martian near-subsurface materials by determination of cohesion and angle of internal friction p 3393 N92-29068
Topography of Apollinaris Patera and Ma'adim Vallis
p 3393 N92-29069
Aqueous-alteration products in S-N-C meteorites and implications for volatile/regolith interactions on Mars
p 3393 N92-29071
Microcraters on Mars: Evidence of past climatic variations p 3394 N92-29073
Hydrogen and carbon isotopic composition of volatiles in Nakhla: Implications for weathering on Mars
p 3394 N92-29075
Climatic implications of the simultaneous presence of CO2 and H2O in the Martian regolith
p 3395 N92-29079

PLANETARY IONOSPHERES
The production and escape of nitrogen atoms on Mars
p 3374 N92-28490
Discovery concepts for Mars p 3387 N92-29035

PLANETARY MANTLES
Forsterite/melt partitioning of argon and iodine: Implications for atmosphere formation by outgassing of an early Martian magma ocean p 3313 N92-28604
A liquidus phase diagram for the groundmass of EETA 79001A (Eg), a primitive Shergottite composition
p 3386 N92-29028

PLANETARY MAPPING
Physical properties of Deucalionis, Eos, Xanthe-type units in the central equatorial region of Mars
p 3392 N92-29063
Physical properties of Meridiani Sinus-type units in the central equatorial region of Mars p 3392 N92-29064
Physical properties of Oxia/Lunae Planum and Arabia-type units in the central equatorial region of Mars
p 3392 N92-29065
Surface photometric properties and albedo changes in the central equatorial region of Mars
p 3392 N92-29066

PLANETARY METEOROLOGY
Papers Presented to the Workshop on the Evolution of the Martian Atmosphere
[NASA-CR-190508] p 3372 N92-28478
Observed changes in limb clouds immediately prior to the onset of planet-encircling dust storms
p 3388 N92-29039

PLANETARY STRUCTURE
Forsterite/melt partitioning of argon and iodine: Implications for atmosphere formation by outgassing of an early Martian magma ocean p 3313 N92-28604

PLANETARY TEMPERATURE
Influences of CO2 sublimation/condensation processes on the long-term evolution of the Martian atmosphere
p 3375 N92-28496
Superheat in magma oceans p 3311 N92-28597

PLANNING
Lessons from Archimedes, a system for planning and executing mechanical assemblies
[DE92-010957] p 3335 N92-28342
Organizing plan libraries in subsumption hierarchies: Specificity based plan selection
[AD-A248711] p 3368 N92-28430
Information Resources Management long-range plan
[DE92-012408] p 3368 N92-28804

PLASMA ARC WELDING
Development of an automated wire delivery system for robotic welding applications
[NASA-CR-190487] p 3295 N92-29134

PLASMA CONTROL
Ohmic ignition in a tokamak reactor with the confinement degradation effect due to alpha heating
[PPL-124] p 3360 N92-28664

PLASMA CURRENTS
Development of negative heavy ion sources for plasma potential measurement
[DE92-782102] p 3360 N92-28234
Solar Array Module Plasma Interaction Experiment (SAMPIE): Technical requirements document
[NASA-TM-105660] p 3246 N92-28683
Plasma density scaling at the current reversal in the STOR-1M tokamak with AC operation
[PPL-127] p 3361 N92-28847
Alternating current tokamak reactor with ohmic ignition and bootstrap current
[PPL-120] p 3361 N92-28849
Plasma beam measurements
[AD-A247892] p 3362 N92-28962

PLASMA DENSITY
Plasma density scaling at the current reversal in the STOR-1M tokamak with AC operation
[PPL-127] p 3361 N92-28847
Improved confinement and edge plasma fluctuations in the STOR-M tokamak
[PPL-126] p 3361 N92-28848
Microwave interactions with plasmas
[AD-A250333] p 3362 N92-29093

PLASMA DIAGNOSTICS
Woelter x ray microscope characterization measurements on Nova
[DE92-013207] p 3288 N92-28812
Analyzing noisy spectral line shapes
[DE92-011153] p 3362 N92-29086

PLASMA DIODES
Advanced diagnostics for reacting flows
[AD-A247059] p 3360 N92-28298

PLASMA DYNAMICS
A comparison of results from an edge-plasma model with those from a two-dimensional fluid code
[DE92-010718] p 3360 N92-28335

PLASMA GUNS
Plasma beam measurements
[AD-A247892] p 3362 N92-28962

PLASMA HEATING
Ohmic ignition in a tokamak reactor with the confinement degradation effect due to alpha heating
[PPL-124] p 3360 N92-28664
Ignition access condition based on the generalized saddle point in a magnetic fusion reactor
[PPL-109] p 3361 N92-28665

PLASMA INTERACTION EXPERIMENT
Solar Array Module Plasma Interaction Experiment (SAMPIE): Technical requirements document
[NASA-TM-105660] p 3246 N92-28683

PLASMA INTERACTIONS
Solar Array Module Plasma Interaction Experiment (SAMPIE): Technical requirements document
[NASA-TM-105660] p 3246 N92-28683
The theory of the long waveguide structures radiating the LH waves into a plasma
[IPPCZ-314] p 3361 N92-28742
Microwave interactions with plasmas
[AD-A250333] p 3362 N92-29093

PLASMA JETS
Thermal response of rigid and flexible insulations and reflective coating in an aeroconvective heating environment
[NASA-TM-103925] p 3233 N92-28721

PLASMA LAYERS
Orthogonal self-assembly of redox active molecules on Pt and Au: Selective reaction of disulfide with Au and isonitrile with Pt
[AD-A246698] p 3254 N92-28290
Secondary instability in 3D magnetic reconnection
[AD-A248630] p 3360 N92-28354

PLASMA PHYSICS
A comparison of results from an edge-plasma model with those from a two-dimensional fluid code
[DE92-010718] p 3360 N92-28335

PLASMA POTENTIALS
Development of negative heavy ion sources for plasma potential measurement
[DE92-782102] p 3360 N92-28234

PLASMA PROPULSION
Development and flight history of SERT 2 spacecraft
[NASA-TM-105636] p 3250 N92-28983

PLASMA SPRAYING
Large-area, plasma-assisted, halogen-based diamond deposition
[AD-A247423] p 3264 N92-28904

PLASMA WAVES
The theory of the long waveguide structures radiating the LH waves into a plasma
[IPPCZ-314] p 3361 N92-28742

PLASMAS (PHYSICS)
Hydrodynamic echo in strongly inhomogeneous magnetized plasma
[DE92-621530] p 3361 N92-28816
Plasma beam measurements
[AD-A247892] p 3362 N92-28962

PLASTIC AIRCRAFT STRUCTURES
The use of load enhancement factors in the certification of composite aircraft structures
[NLR-TP-90068-U] p 3232 N92-28649

PLASTIC DEFORMATION
The nonequilibrium molecular dynamics
[DE92-011760] p 3355 N92-28860

PLASTIC FLOW
A combined experimental and analytical investigation of the theory of plasticity involving strain induced anisotropy
[AD-A248440] p 3298 N92-28352
Polyimide processing additives
[NASA-CASE-LAR-13669-1] p 3265 N92-29157

PLASTIC PROPERTIES
A combined experimental and analytical investigation of the theory of plasticity involving strain induced anisotropy
[AD-A248440] p 3298 N92-28352
Nanoscale investigation of indentation, adhesion, and fracture of diamond (111) surfaces
[AD-A250164] p 3265 N92-28916

PLASTICS
Polyimide processing additives
[NASA-CASE-LAR-13669-1] p 3265 N92-29157

PLATE THEORY
Analysis of constrained-layer damping of flexural and extensional waves in infinite, fluid-loaded plates
[AD-A247936] p 3304 N92-29081

PLATES
The effect of induced charges on low-energy particle trajectories near conducting and semiconducting plates
[NASA-TM-103589] p 3355 N92-28986

PLATES (STRUCTURAL MEMBERS)
Mobility power flow analysis of coupled plate structure subjected to mechanical and acoustic excitation
[NASA-CR-189635] p 3352 N92-28722

PLATINUM
Orthogonal self-assembly of redox active molecules on Pt and Au: Selective reaction of disulfide with Au and isonitrile with Pt
[AD-A246698] p 3254 N92-28290

PLAYBACKS
Disk memory device
[NASA-CASE-GSC-13196-1] p 3333 N92-29132

PLUMES
Arcjet plume ionization effects on exposed solar array conducting surfaces
[AD-A245912] p 3307 N92-28383
An overview of in-flight plume diagnostics for rocket engines
[NASA-TM-105727] p 3248 N92-28417

PNEUMATIC CIRCUITS
A simple and low cost system to measure delay times in pneumatic systems
[NLR-TP-90174-U] p 3235 N92-28644

POINT SPREAD FUNCTIONS
Atmospheric corrections of land imagery using the extended radiosity method
[DE92-011355] p 3306 N92-28840

POISSON DENSITY FUNCTIONS
Matrix-geometric analysis of the shortest queue problem with threshold jockeying
[MEMO-COSOR-91-24] p 3347 N92-28641

POLAR CAPS
High pressure experiments with a Mars general circulation model p 3374 N92-28491
The Mars water cycle at other epochs: History of the polar caps and layered terrain p 3375 N92-28493
Midlatitude weather systems on Mars: Is there a hemispheric asymmetry? p 3379 N92-28992
Mars: Compositional variability of ferric/ferrous minerals and polar volatiles from groundbased imaging spectroscopy p 3379 N92-28993

Infrared imaging of Mars for volatile distribution and seasonal variability between 2.4 and 5.1 microns p 3379 N92-28995
The Martian polar caps: Stability and water transport at low obliquities p 3385 N92-29023
Simulations of the seasonal polar caps on Mars p 3387 N92-29033

POLAR REGIONS
Polar lows over the northeast Greenland Sea [AD-A245360] p 3318 N92-28421
Distribution of Martian ground-ice table: Preliminary results about climatic variations p 3373 N92-28484
Applications of passive microwave satellite data for Arctic Sea ice studies [AD-A245966] p 3306 N92-28791
Dark material in the polar layered deposits on Mars p 3385 N92-29024

POLAR SUBSTORMS
Polar lows over the northeast Greenland Sea [AD-A245360] p 3318 N92-28421

POLARIMETRY
Studies of the polarimetric dependence of enhanced backscattering from one-dimensional surfaces [AD-A248431] p 3275 N92-28878
Soil texture and granulometry at the surface of Mars p 3382 N92-29009

POLARIZED ELECTROMAGNETIC RADIATION
Studies of the polarimetric dependence of enhanced backscattering from one-dimensional surfaces [AD-A248431] p 3275 N92-28878

POLARIZED RADIATION
Analysis of electromagnetic propagation over variable terrain using the parabolic wave equation [AD-A248061] p 3276 N92-28947

POLARIZERS
Non-mechanical optical path switching and its application to dual beam spectroscopy including gas filter correlation radiometry [NASA-CASE-LAR-14588-1-CU] p 3359 N92-29117

POLICIES
Space life sciences strategic plan [NASA-TM-107954] p 3244 N92-29100
Maintaining the program balance, volumes 1 and 2 [NASA-CR-190269] p 3367 N92-29111

POLLUTION TRANSPORT
Regional environmental impacts of methanol-fueled vehicles [PB92-176569] p 3308 N92-29183

POLYCRYSTALS
Design and realization of polysilicon emitter bipolar transistors [LAAS-91360] p 3282 N92-29208

POLYESTER RESINS
Proceedings of Asilomar Conference on Polymeric Materials [AD-A249366] p 3262 N92-28360

POLYESTERS
The effects of alumina trihydrate on the flammability characteristics of polyester, vinyl ester, and epoxy glass reinforced plastics [AD-A247707] p 3264 N92-28563

POLYETHYLENES
Proceedings of Asilomar Conference on Polymeric Materials [AD-A249366] p 3262 N92-28360

POLYIMIDES
Polyimidazoles via aromatic nucleophilic displacement [NASA-CASE-LAR-14145-1] p 3264 N92-28751
Polyimide processing additives [NASA-CASE-LAR-13669-1] p 3265 N92-29157

POLYMER CHEMISTRY
Synthesis and study of metallonitride complexes and polymers [AD-A248577] p 3262 N92-28323
Formation, structure, and properties of boron nitride fibers from polymer precursors [AD-A247679] p 3263 N92-28553
Controlled method of reducing electrophoretic mobility of macromolecules, particles, or cells [NASA-CASE-MFS-26049-2-NP] p 3255 N92-28728

POLYMERIC FILMS
Microgravity isolation mounts based upon Piezoelectric film p 3268 N92-28454

POLYMERIZATION
Molecular engineering of liquid crystalline polymers by living cationic polymerization. 21: Synthesis and characterization of poly (3-((4-cyano-4'-biphenyl)oxy) propyl vinyl ether) macromonomers [AD-A248305] p 3265 N92-29116
Poly(1,3,4-oxadiazoles) via aromatic nucleophilic displacement [NASA-CASE-LAR-14427-1] p 3250 N92-29141
Silicon polymers [AD-A250201] p 3265 N92-29145

POLYMERS
Molecular dynamics calculations of optical nonlinear properties of materials [AD-A247095] p 3354 N92-28260
Sol-gel processed multifunctional organic polymer-inorganic oxide composites for electronics and photonics [AD-A246773] p 3263 N92-28412
Formation, structure, and properties of boron nitride fibers from polymer precursors [AD-A247679] p 3263 N92-28553

POLYNOMIALS
Fourier analysis of the approximation power of principal shift-invariant spaces [AD-A246713] p 3347 N92-28411
Optimization by renaming in the solution method [ETN-92-91324] p 3338 N92-28842

POPULATION THEORY
Distribution theory for selection from logistic populations [MEMO-COSOR-91-23] p 3348 N92-28640

POPULATIONS
Gadolinium metastable states population distributions and atomic density under high-rate electron beam evaporation [DE92-782008] p 3363 N92-28282
Distribution theory for selection from logistic populations [MEMO-COSOR-91-23] p 3348 N92-28640

PORTABLE EQUIPMENT
Mobile electric power [AD-A249354] p 3279 N92-28326

PORTUGAL
A numerical study of time-dependent wind forcing off the west coast of Portugal, 1987-1988 [AD-A246775] p 3321 N92-28365

POSEIDON SATELLITE
Modeling radiation forces acting on TOPEX/Poseidon for precision orbit determination [NASA-TM-104564] p 3244 N92-28343
TOPEX/POSEIDON science investigations plan [NASA-CR-190456] p 3305 N92-28950

POSITION (LOCATION)
On-line point positioning with single frame camera data [AD-A248307] p 3287 N92-28322
Scattering measurements and predictions for a Delta stage 2 rocket nozzle [AD-A246776] p 3248 N92-28366

POSITION SENSING
Laser optical disk position encoder with active heads [NASA-CASE-GSC-13175-1] p 3359 N92-29133

POSITIONING
On-line point positioning with single frame camera data [AD-A248307] p 3287 N92-28322

POTENTIAL FLOW
Viscous effects on a vortex wake in ground effect [NASA-CR-190400] p 3283 N92-28361
Wave drag determination in the transonic full-potential flow code MATRICS [NLR-TP-90062-U] p 3228 N92-28709

POWDER (PARTICLES)
Magnetic hysteresis and relaxation in Ag-sheathed TlBaCaCuO (1223) and Bi(Pb)SrCaCuO (2223) superconducting tapes [DE92-011357] p 3365 N92-28874

POWER CONDITIONING
Intense electron beam cyclotron masers with microsecond pulselengths [AD-A247060] p 3289 N92-28271

POWER CONVERTERS
M-H characteristics and demagnetization resistance of samarium-cobalt permanent magnets to 300 C [NASA-CR-189194] p 3280 N92-28723
NASA Lewis Stirling SPRE testing and analysis with reduced number of cooler tubes [NASA-TM-105767] p 3307 N92-28837

POWER GAIN
Windshear radar calibration: Transmitter power and receiver gain stability [NASA-TM-107589] p 3275 N92-28876

POWER SUPPLIES
Mass and power modeling of communication satellites [NASA-CR-189186] p 3275 N92-28906

POWER SUPPLY CIRCUITS
High voltage splitting unit for the power supplies of the vacuum pumps of AmPS [DIGEL-1991-7] p 3278 N92-28263

POWER TRANSMISSION
Mobility power flow analysis of coupled plate structure subjected to mechanical and acoustic excitation [NASA-CR-189635] p 3352 N92-28722

POWERED LIFT AIRCRAFT
Internal reversing flow in a tailpipe offtake configuration for SSTOVL aircraft [NASA-TM-105698] p 3236 N92-28418
Aerodynamic characteristics obtained from alpha sweep test of the quiet STOL experimental aircraft ASKA [NAL-TR-1112] p 3234 N92-28901

PRANDTL NUMBER
The role of hard turbulent thermal convection in the Earth's early thermal evolution p 3310 N92-28593

PRECIPITATES
Mg-Si-Al oxynitride glasses [AD-A247593] p 3261 N92-28249

PRECIPITATION HARDENING
Mechanisms of fracture and creep of structural alloys [AD-A248701] p 3259 N92-28390

PRECISION
Modeling radiation forces acting on TOPEX/Poseidon for precision orbit determination [NASA-TM-104564] p 3244 N92-28343

PREDICTION ANALYSIS TECHNIQUES
A coilgun design primer [DE92-011149] p 3244 N92-28226
A comparison of results from an edge-plasma model with those from a two-dimensional fluid code [DE92-010718] p 3360 N92-28335
Selective suppression of photochemical etching: Raman spectroscopy for pre-etch process selection [DE92-010955] p 3255 N92-28341
Polar lows over the northeast Greenland Sea [AD-A245360] p 3318 N92-28421
Predicting microgravity levels for space station using VAPEPS p 3268 N92-28455
Steady and Transient Performance Prediction of Gas Turbine Engines [AGARD-LS-183] p 3236 N92-28458
Overview on basis and use of performance prediction methods p 3237 N92-28459
Engine performance and health monitoring models using steady state and transient prediction methods p 3238 N92-28467
Experimental and computational ice shapes and resulting drag increase for a NACA 0012 airfoil [NASA-TM-105743] p 3227 N92-28674
The theory of the long waveguide structures radiating the LH waves into a plasma [IPPCZ-314] p 3361 N92-28742
Nonlinear techniques for forecasting solar activity directly from its time series [NASA-TM-107946] p 3396 N92-28870
Detecting and disentangling nonlinear structure from solar flux time series [NASA-CR-190510] p 3396 N92-28871
Future mission studies: Forecasting solar flux directly from its chaotic time series [NASA-CR-190378] p 3396 N92-28872
Evidence of chaotic pattern in solar flux through a reproducible sequence of period-doubling-type bifurcations [NASA-TM-107944] p 3396 N92-28907
Microwave derived rainrates in typhoons and their use in the diagnosis and prediction of typhoon intensity [AD-A250556] p 3319 N92-28922

PREDICTIONS
A system structure for predictive relations in penetration mechanics [AD-A246453] p 3292 N92-28284
Prediction of composite material properties using two-dimensional finite element micromechanical analysis [AD-A250300] p 3252 N92-28702
Models for recall and recognition [IZF-1991-B-4] p 3342 N92-28746
Pre-test analyses for pressurized thermoshock tests, vessel 1 [VTT-RR-746] p 3303 N92-28776
Method and apparatus for predicting the direction of movement in machine vision [NASA-CASE-NPO-17552-1-CU] p 3331 N92-29129
Microwave temperature profiler for clear air turbulence prediction [NASA-CASE-NPO-18115-1-CU] p 3320 N92-29148

PREDICTOR-CORRECTOR METHODS
A continuation method for calculating the equilibrium positions of nonlinear structures [ONERA-RT-24/3542-RY-091-R] p 3338 N92-28790

PREMIXED FLAMES
Stochastic simulation of the structure and propagation rate of turbulent premixed flames [DE92-006682] p 3256 N92-28822

PREMIXING
Stochastic simulation of the structure and propagation rate of turbulent premixed flames [DE92-006682] p 3256 N92-28822

PRESSURE BROADENING
VLA mapping of 1.35 cm water emission from the Mars atmospheric limb p 3381 N92-29004

PRESSURE DISTRIBUTION
Calculation of installation effects within performance computer programs p 3237 N92-28465
Seafloor pressure array studies at ultra-low frequencies
[AD-A247663] p 3322 N92-28939
PRESSURE EFFECTS
High pressure experiments with a Mars general circulation model p 3374 N92-28491
Device for applying constant pressure to a surface
[NASA-CASE-GSC-13230-1] p 3294 N92-28754
PRESSURE GRADIENTS
Fate of a perched crystal layer in a magma ocean p 3312 N92-28602
PRESSURE MEASUREMENT
Estimation of the viscosities of silicate liquids at high pressure from measurements of oxygen diffusivity p 3313 N92-28607
Study of the leading-edge vortex dynamics in the unsteady flow over an airfoil
[AD-A247532] p 3228 N92-28865
Pressure transducer and system for cryogenic environments
[NASA-CASE-LAR-14579-1] p 3288 N92-29097
PRESSURE SENSORS
Asynchronous optical sampling for laser-based combustion diagnostics in high-pressure flames
[AD-A250206] p 3257 N92-28896
Seafloor pressure array studies at ultra-low frequencies
[AD-A247663] p 3322 N92-28939
Pressure transducer and system for cryogenic environments
[NASA-CASE-LAR-14579-1] p 3288 N92-29097
PRESSURE VESSELS
Hydrogen no-vent fill testing in a 5 cubic foot (142 liter) tank using spray nozzle and spray bar liquid injection
[NASA-TM-105759] p 3266 N92-28433
Elevated temperature axial and torsional fatigue behavior of Haynes 188
[NASA-TM-105396] p 3302 N92-28701
Pre-test analyses for pressurized thermoshock tests, vessel 1
[VTT-RR-746] p 3303 N92-28776
Replacement of the NAL high pressure air storage system
[NAL-TM-634] p 3241 N92-28835
PRIMARY BATTERIES
Ion conductive polymer solid electrolytes
[DE92-010518] p 3266 N92-29195
PRIMITIVE EQUATIONS
A numerical study of time-dependent wind forcing off the west coast of Portugal, 1987-1988
[AD-A246775] p 3321 N92-28365
The Navy layered ocean model users guide
[AD-A247754] p 3321 N92-28566
PRINTED CIRCUITS
Stress analysis of plated-through-holes in rigid flex multilayer printed wiring boards
[DE92-011659] p 3303 N92-28855
PROBABILITY DENSITY FUNCTIONS
Mapping closures for turbulent mixing and reaction
[AD-A247305] p 3283 N92-28274
Modeling of the reactant conversion rate in a turbulent shear flow p 3229 N92-28820
PROBABILITY THEORY
Hyper-Raman scattering and 3-photon resonant ionization: Competitive effects
[DE92-622671] p 3366 N92-28230
The influence of the resonant electromagnetic field on the light absorption by exciton and biexciton in quantum wells
[DE92-622801] p 3366 N92-28232
Quasi-regular impurity distribution driven by charge-density wave
[DE92-622799] p 3363 N92-28281
Distribution theory for selection from logistic populations
[MEMO-COSOR-91-23] p 3348 N92-28640
Matrix-geometric analysis of the shortest queue problem with threshold jockeying
[MEMO-COSOR-91-24] p 3347 N92-28641
Reactant conversion in homogeneous turbulence: Mathematical modeling, computational validations and practical applications p 3285 N92-28819
PROBLEM SOLVING
Improved decision making through group composition
[AD-A246622] p 3366 N92-28256
Temporal reasoning and problem solving
[AD-A248457] p 3344 N92-28387
Computer-based assessment of schema knowledge in a flexible problem-solving environment
[AD-A246779] p 3348 N92-28516
A network flow algorithm for just-in-time project scheduling
[MEMO-COSOR-91-21] p 3336 N92-28638
PROCEDURES
Files improvement the NARA way
[DE92-011139] p 3368 N92-28832
PROCESS CONTROL (INDUSTRY)
Scheduling multiple variable-speed machines
[AD-A249362] p 3268 N92-28359
PROCESSES
Chemical vapor deposition of yttrium borium(2) copper(3) oxygen(x) thin films for wire applications
[AD-A247013] p 3364 N92-28395
Polyimide processing additives
[NASA-CASE-LAR-13669-1] p 3265 N92-29157
PROCUREMENT
Archival of the ECOM-721 data
[AD-A249299] p 3338 N92-28845
PRODUCT DEVELOPMENT
X ray computed tomography of full-scale castings
[AD-A247101] p 3258 N92-28241
Delayed pulse generator
[DIGEL-1991-2] p 3278 N92-28262
Piloted Simulation Effectiveness
[AGARD-CP-513] p 3221 N92-28522
Flight simulation and digital flight controls p 3221 N92-28526
The application of flight simulation models in support of rotorcraft design and development p 3222 N92-28527
Experience with piloted simulation in the development of helicopters p 3222 N92-28528
Information systems for engineering sustainable development
[DE92-011271] p 3368 N92-28838
Applications and benefits of formal methods in software development
[REPT-91-33] p 3341 N92-29221
PRODUCTION ENGINEERING
A cost-benefit analysis on the deletion of the inertial upper stage factory acceptance testing versus a decrease in mission reliability
[AD-A246620] p 3245 N92-28254
PRODUCTION MANAGEMENT
Scheduling multiple variable-speed machines
[AD-A249362] p 3268 N92-28359
Automated apparel specification retrieval system
[AD-A248619] p 3367 N92-28389
PRODUCTIVITY
Taguchi methods in electronics: A case study
[NASA-TM-103586] p 3279 N92-28456
PROGRAM VERIFICATION (COMPUTERS)
Extensibility experiments with the software life-cycle support environment
[AD-A247696] p 3335 N92-28562
Verification of satellite EGSE test-software using an application generator
[ITN-92-65131] p 3244 N92-29098
PROGRAMMING LANGUAGES
Object-oriented programming: An assessment of fundamental concepts and design considerations
[AD-A247480] p 3333 N92-28243
A uniform approach to the semantics of concurrency
[AD-A246697] p 3334 N92-28289
SISAL: Toward resolving the parallel programming crisis
[DE92-010716] p 3342 N92-28334
An ELROS primer
[DE92-010661] p 3342 N92-28381
Mentat/A: Medium grain parallel processing
[NASA-CR-190486] p 3342 N92-28676
Development of a flight information system using the structured method
[AD-A248207] p 3236 N92-29222
PROJECT MANAGEMENT
An experimental investigation of the effects of software size increase on software project management behavior
[AD-A248362] p 3335 N92-28385
Monitoring activities review of the Radiological Environmental Surveillance Program
[DE92-013103] p 3308 N92-28811
Maintaining the program balance, volumes 1 and 2
[NASA-CR-190269] p 3367 N92-29111
Repository-based software engineering program: Concept document
[NASA-CR-190384] p 3341 N92-29200
PROJECTILES
A system structure for predictive relations in penetration mechanics
[AD-A246453] p 3292 N92-28284
PROPAGATION MODES
Experimental validation of a line-duct acoustics model including flow
[NLR-TP-90223-U] p 3352 N92-28695
PROPELLANT CHEMISTRY
Multicomponent comparison of optical and mass spectrometric diagnostics in low-pressure flames
[AD-A250323] p 3257 N92-28954
PROPELLANT DECOMPOSITION
Combustion mechanisms of solids --- solid rocket propellant
[AD-A247088] p 3254 N92-28240
PROPELLANT STORAGE
Nonlinear sloshing and the coupled dynamics of liquid propellants and spacecraft
[AD-A250023] p 3248 N92-28967
PROPELLANT TANKS
Hydrogen no-vent fill testing in a 5 cubic foot (142 liter) tank using spray nozzle and spray bar liquid injection
[NASA-TM-105759] p 3266 N92-28433
PROPELLANT TRANSFER
Hydrogen no-vent fill testing in a 5 cubic foot (142 liter) tank using spray nozzle and spray bar liquid injection
[NASA-TM-105759] p 3266 N92-28433
PROPELLERS
Comparison of LDA and LTA applications for propeller tests in wind tunnels
[NLR-MP-88031-U] p 3226 N92-28658
PROPORTIONAL COUNTERS
Scientific investigations with the data base HEAO-1 scanning modulator collimator
[NASA-CR-190477] p 3370 N92-28680
PROPULSION
Kinetic studies of metal combustion in propulsion
[AD-A250207] p 3256 N92-28769
Introduction to rocket propulsion
[AD-A250424] p 3249 N92-28800
PROPULSION SYSTEM CONFIGURATIONS
Integrated health monitoring and controls for rocket engines
[NASA-TM-105763] p 3249 N92-28693
Solid-propellant-powered maneuvering system for spacecraft
[AD-D015245] p 3249 N92-28747
PROPULSION SYSTEM PERFORMANCE
Component performance requirements p 3237 N92-28462
Inlet distortion effects in aircraft propulsion system integration p 3237 N92-28464
Engine performance and health monitoring models using steady state and transient prediction methods p 3238 N92-28467
Integrated health monitoring and controls for rocket engines
[NASA-TM-105763] p 3249 N92-28693
PROTECTION
Space Station: Delays in dealing with space debris may reduce safety and increase costs
[GAO/IMTEC-92-50] p 3243 N92-28406
PROTECTIVE CLOTHING
Modelling of heat and moisture loss through NBC ensembles
[AD-A245939] p 3329 N92-28346
PROTECTIVE COATINGS
Oxidation resistant coating for titanium alloys and titanium alloy matrix composites
[NASA-CASE-LEW-15155-1] p 3265 N92-29090
PROTEIN CRYSTAL GROWTH
An examination of anticipated g-jitter on Space Station and its effects on materials processes p 3267 N92-28438
PROTEINS
Numerical studies of convective transport associated with crystal growth in microgravity p 3267 N92-28437
PROTOCOL (COMPUTERS)
Contribution to the design of flexible manufacturing systems: Application of the formal description technique Estelle
[LAAS-91378] p 3341 N92-29209
PROTOPLANETS
A magma ocean and the Earth's internal water budget p 3310 N92-28590
PROTOTYPES
Extensibility experiments with the software life-cycle support environment
[AD-A247696] p 3335 N92-28562
A knowledge based approach for testing VLSI circuits: Application to the validation of prototypes for a non-contact test
[ETN-92-91321] p 3280 N92-28783
PROVING
SPECTOOL: A computer-aided verification tool for hardware designs, volume 1
[AD-A247492] p 3336 N92-28666
SPECTOOL: User's manual, volume 2
[AD-A247493] p 3336 N92-28667
Experimental validation of a line-duct acoustics model including flow
[NLR-TP-90223-U] p 3352 N92-28695
A knowledge based approach for testing VLSI circuits: Application to the validation of prototypes for a non-contact test
[ETN-92-91321] p 3280 N92-28783

PROXIMITY EFFECT (ELECTRICITY)
Physics and technology for the investigation of properties of ultra small systems
[AD-A246772] p 3364 N92-28513
PSEUDORANDOM SEQUENCES
VHDL and waves descriptions for a pseudo-random pattern generator
[AD-A247891] p 3349 N92-28961
PSYCHOLOGICAL TESTS
Improved decision making through group composition
[AD-A246622] p 3366 N92-28256
The variance of Rasch ability estimates from partially-known item parameters
[AD-A247065] p 3348 N92-28273
PSYCHOMETRICS
The variance of Rasch ability estimates from partially-known item parameters
[AD-A247065] p 3348 N92-28273
PSYCHOMOTOR PERFORMANCE
Effects of high terrestrial altitude on military performance
[AD-A246695] p 3324 N92-28288
PSYCHOPHYSIOLOGY
Psychophysical analyses of perceptual representations
[AD-A246945] p 3329 N92-29186
PULMONARY FUNCTIONS
The chronic effects of JP-8 jet fuel exposure on the lungs
[AD-A250308] p 3326 N92-29123
PULSARS
Calibration of high energy x ray detectors at the spectrum of the Crab nebula, and x ray pulsar A0535+26 examinations
[ETN-92-91484] p 3371 N92-29177
PULSE GENERATORS
Delayed pulse generator
[DIGEL-1991-2] p 3278 N92-28262
PULSED LASERS
Advanced diagnostics for reacting flows
[AD-A247059] p 3360 N92-28298
Visualization of gas tungsten arc weld pools
[AD-A245926] p 3293 N92-28384
Compact, self-contained ArF lasers
[AD-A247403] p 3291 N92-28932
Big Sky Workshop on Super-Intense Laser-Atom Physics
[AD-A248225] p 3292 N92-29223
PULSES
Coincident pulse techniques for hybrid electronic optical computer systems
[AD-A246774] p 3332 N92-28514
CO2 laser frequency multiplication
[AD-A245915] p 3290 N92-28761
Automation and remote control instrumentation development: Rocket First Motion Timing System (RFMTS)
[AD-A249970] p 3287 N92-28767
SPEAR 2 space power data analysis
[AD-A248057] p 3250 N92-28945
Analysis of Mir-HEXE observations: Pulsation and energy spectra of the x ray double star SMC X-1 in 20 to 80 keV energy field
[ETN-92-91487] p 3371 N92-29128
PYROCERAM (TRADEMARK)
Study of high temperature failure mechanism in ceramics
[AD-A247018] p 3263 N92-28415
PYROLYSIS
Combustion mechanisms of solids --- solid rocket propellant
[AD-A247088] p 3254 N92-28240
Studies of 1,3-disilacyclobutanes as single-source CVD precursors to silicon carbide
[AD-A247111] p 3365 N92-28885
PYROMETALLURGY
Effect of solidification technique and consolidation method on the properties of rapidly solidified Al-Fe alloys
[DLR-FB-91-24] p 3260 N92-28823
PYRRHOTITE
Rates of oxidative weathering on the surface of Mars
p 3380 N92-28999

Q

QUADRATIC PROGRAMMING
Numerical methods of linear and nonlinear optimization
[AD-A248579] p 3335 N92-28428
QUALIFICATIONS
Diffuser casing upgrade for an advanced turbofan
[NLR-TP-90097-U] p 3238 N92-28711
QUALITY CONTROL
Three dimensional measurements of prismatic bodies: Programming by means of a CAD system
[CRIF-MC-91] p 3337 N92-28700
QUANTITATIVE ANALYSIS
Humic substances in soils from Bangladesh, Namibia, and Canada
[OEFZS-4574] p 3316 N92-28740
QUANTUM CHEMISTRY
High quality Gaussian basis sets for fourth-row atoms
[NASA-TM-103918] p 3255 N92-28743
QUANTUM CHROMODYNAMICS
The principal part of plane vector fields with fixed Newton diagram
[DE92-622408] p 3346 N92-28311
QUANTUM MECHANICS
Classical and quantum Liouville theory on the Riemann sphere with n greater than 3 punctures (II)
[DE92-622380] p 3366 N92-28227
Hyper-Raman scattering and 3-photon resonant ionization: Competitive effects
[DE92-622671] p 3366 N92-28230
QUANTUM NUMBERS
Inverse phase transitions: Does baryogenesis lead to dark matter?
[DE92-013022] p 3372 N92-29184
QUANTUM THEORY
Classical and quantum Liouville theory on the Riemann sphere with n greater than 3 punctures (II)
[DE92-622380] p 3366 N92-28227
Proceedings of the workshop on Quantum Gravity and Topology
[DE92-782191] p 3366 N92-28235
Research studies on extreme ultraviolet and soft x ray lasers
[AD-A247309] p 3289 N92-28299
Hydrodynamic echo in strongly inhomogeneous magnetized plasma
[DE92-621530] p 3361 N92-28816
QUANTUM WELLS
The influence of the resonant electromagnetic field on the light absorption by exciton and biexciton in quantum wells
[DE92-622801] p 3366 N92-28232
Center for the integration of optical computing
[AD-A250306] p 3337 N92-28719
QUARK MODELS
Electroproduction of light quark baryons
[DE92-010853] p 3354 N92-28337
QUARKS
Electroproduction of light quark baryons
[DE92-010853] p 3354 N92-28337
The physics of strange matter
[DE92-011734] p 3371 N92-28774
Quark matter and cosmology
[DE92-011736] p 3371 N92-28859
QUARTZ
Microstructures of shocked quartz
[DE92-010710] p 3363 N92-28333
QUATERNIONS
NPSNET: Flight simulation dynamic modeling using quaternions
[AD-A247484] p 3333 N92-28245
Quaternion and Euler angles in kinematics
[NAL-TM-636] p 3303 N92-28836
QUENCHING (COOLING)
Effect of cooling rate on corrosion properties of high strength aluminium alloys under atmospheric conditions
[NLR-TP-90138-U] p 3260 N92-28691
QUEUEING THEORY
Matrix-geometric analysis of the shortest queue problem with threshold jockeying
[MEMO-COSOR-91-24] p 3347 N92-28641
Analysing multiprogramming queues by generating functions
[MEMO-COSOR-91-25] p 3342 N92-28642

R

RADAR ABSORBERS
The use of a vector network analyzer for measuring the performance of radar absorbing materials
[AD-A247194] p 3275 N92-28887
RADAR CROSS SECTIONS
The use of a vector network analyzer for measuring the performance of radar absorbing materials
[AD-A247194] p 3275 N92-28887
RADAR DATA
Scattering measurements and predictions for a Delta stage 2 rocket nozzle
[AD-A246776] p 3248 N92-28366
Multiparameter radar and aircraft based studies of the microphysical, kinematic, and electrical structure of convective clouds
[AD-A247497] p 3318 N92-28668
RADAR DETECTION
Target motion detecting impulse Doppler radar system
[AD-D015263] p 3277 N92-29169
RADAR IMAGERY
Scattering measurements and predictions for a Delta stage 2 rocket nozzle
[AD-A246776] p 3248 N92-28366
Interest in real-time simulations for the development terrain following function of radar systems
p 3222 N92-28529
SAR-relate stress variability in the Marine Atmospheric Boundary Layer (MABL)
[AD-A247772] p 3309 N92-28567
RADAR MEASUREMENT
Scattering measurements and predictions for a Delta stage 2 rocket nozzle
[AD-A246776] p 3248 N92-28366
TOPEX/POSEIDON science investigations plan
[NASA-CR-190456] p 3305 N92-28950
Mars: Wavelength-dependent dual polarization global scattering p 3384 N92-29020
Target motion detecting impulse Doppler radar system
[AD-D015263] p 3277 N92-29169
RADAR NAVIGATION
Interest in real-time simulations for the development terrain following function of radar systems
p 3222 N92-28529
RADAR NETWORKS
The use of a vector network analyzer for measuring the performance of radar absorbing materials
[AD-A247194] p 3275 N92-28887
RADAR SCATTERING
Scattering measurements and predictions for a Delta stage 2 rocket nozzle
[AD-A246776] p 3248 N92-28366
Simulating radar propagation through atmospheric turbulence using the Tropospheric ElectroMagnetic Parabolic Equation Routine (TEMPER)
[AD-A247408] p 3275 N92-28905
Mars: Wavelength-dependent dual polarization global scattering p 3384 N92-29020
RADAR TRACKING
Mars: Wavelength-dependent dual polarization global scattering p 3384 N92-29020
Target motion detecting impulse Doppler radar system
[AD-D015263] p 3277 N92-29169
RADIANCE
Simulation in infrared imaging: Using electrical circuit principles to model heat transfer
[AD-A248290] p 3278 N92-28276
Microwave derived rainrates in typhoons and their use in the diagnosis and prediction of typhoon intensity
[AD-A250556] p 3319 N92-28922
RADIANT COOLING
The three stages of magma ocean cooling
p 3315 N92-28617
RADIANT FLUX DENSITY
Target motion detecting impulse Doppler radar system
[AD-D015263] p 3277 N92-29169
RADIATION ABSORPTION
PROPX: An x ray manipulation program
[DE92-011264] p 3334 N92-28309
Evidence for physics beyond the quasi-deuteron model in pion absorption
[DE92-011285] p 3354 N92-28310
Calculations and databasing of molecular absorption parameters for HITRAN
[AD-A247549] p 3355 N92-28936
Microwave interactions with plasmas
[AD-A250333] p 3362 N92-29093
RADIATION BELTS
Coordinate systems for space and geophysical applications
[AD-A247550] p 3244 N92-28937
RADIATION COUNTERS
Empirical techniques for the study of acceleration mechanisms in the space environment
[AD-A249940] p 3248 N92-28765
RADIATION DAMAGE
Neutron, gamma ray, and temperature effects on the electrical characteristics of thyristors
[NASA-TM-105728] p 3279 N92-28432
RADIATION DETECTORS
PROPX: An x ray manipulation program
[DE92-011264] p 3334 N92-28309
The solenoidal detector collaboration silicon detector system
[DE92-011237] p 3356 N92-28356
RADIATION DISTRIBUTION
Analysis of electromagnetic propagation over variable terrain using the parabolic wave equation
[AD-A248061] p 3276 N92-28947
RADIATION DOSAGE
Review of Mars mission scenarios
p 3244 N92-28731

The measuring assembly for the NPL primary standard absorbed dose graphite calorimeter at therapy levels
[NPL-RSA(EXT)-23] p 3288 N92-29163

RADIATION EFFECTS
Problems in mechanistic theoretical models for cell transformation by ionizing radiation
[DE92-010265] p 3324 N92-28278
PROPX: An x ray manipulation program
[DE92-011264] p 3334 N92-28309
Perspectives of ion implantation for optics
[DE92-010664] p 3357 N92-28355
Neutron, gamma ray, and temperature effects on the electrical characteristics of thyristors
[NASA-TM-105728] p 3279 N92-28432
Somatic gene mutation in the human in relation to radiation risk
[DE92-009459] p 3325 N92-28685

RADIATION MEASUREMENT
Monitoring activities review of the Radiological Environmental Surveillance Program
[DE92-013103] p 3308 N92-28811
Development of rotating shadowband spectral radiometers and GCM radiation code test data sets in support of ARM
[DE92-011438] p 3316 N92-28853
Theoretical and experimental studies relevant to interpretation of auroral emissions
[NASA-CR-190521] p 3316 N92-28911

RADIATION MEASURING INSTRUMENTS
Calibration of high energy x ray detectors at the spectrum of the Crab nebula, and x ray pulsar A0535+26 examinations
[ETN-92-91484] p 3371 N92-29177

RADIATION PROTECTION
A user's manual for MASH 1.0: A Monte Carlo adjoint shielding code system
[AD-A248204] p 3355 N92-29190

RADIATION SHIELDING
Cryogenic shutter
[NASA-CASE-GSC-13189-2] p 3296 N92-29151
A user's manual for MASH 1.0: A Monte Carlo adjoint shielding code system
[AD-A248204] p 3355 N92-29190

RADIATION SOURCES
Theory for the CEBAF and shipboard FELS
[AD-A245979] p 3289 N92-28662
Aperture coupling measurement in a test chamber for the Advanced Photon Source (APS)
[DE92-013059] p 3274 N92-28809
RF impedance measurement status for the 7-GeV Advanced Photon Source (APS)
[DE92-013060] p 3274 N92-28810

RADIATION SPECTRA
PROPX: An x ray manipulation program
[DE92-011264] p 3334 N92-28309

RADIATION TOLERANCE
Operation and radiation resistance of a FOXFET biasing structure for silicon strip detectors
[DE92-011279] p 3282 N92-29197

RADIATIVE HEAT TRANSFER
The three stages of magma ocean cooling
p 3315 N92-28617
Remote sensing applications of the extended radiosity method
[DE92-011356] p 3306 N92-28807
Atmospheric corrections of land imagery using the extended radiosity method
[DE92-011355] p 3306 N92-28840

RADIATIVE TRANSFER
Development of an advanced representation of cumulus convection
[DE92-011031] p 3319 N92-28830
Mars dust and cloud opacities and scattering properties p 3381 N92-29003
Mars: Correcting surface albedo observations for effects of atmospheric dust loading p 3386 N92-29032

RADIO ALTIMETERS
TOPEX/POSEIDON science investigations plan
[NASA-CR-190456] p 3305 N92-28950

RADIO DIRECTION FINDERS
Maximizing the convergence rate of the EM algorithm for the multiple broad-band signal estimation and detection
[AD-A248230] p 3341 N92-29224

RADIO FREQUENCY DISCHARGE
Large-area, plasma-assisted, halogen-based diamond deposition
[AD-A247423] p 3264 N92-28904

RADIO TELEMETRY
Verification of satellite EGSE test-software using an application generator
[ITN-92-85131] p 3244 N92-29098

RADIO TRANSMISSION
Comparison of electromagnetic propagation predictions from IREPS and RPO across a coastal transition
[AD-A249331] p 3273 N92-28357
Fade durations in satellite-path mobile radio propagation
[NASA-CR-190484] p 3273 N92-28586
Tactical line-of-sight radio propagation reliability
[AD-A245909] p 3277 N92-29165

RADIOACTIVE DECAY
The many aspects of neutrino physics
[DE92-011735] p 3355 N92-28858

RADIOACTIVE WASTES
Monitoring activities review of the Radiological Environmental Surveillance Program
[DE92-013103] p 3308 N92-28811

RADIOGENIC MATERIALS
Forsterite/melt partitioning of argon and iodine: Implications for atmosphere formation by outgassing of an early Martian magma ocean p 3313 N92-28604

RADIOGRAPHY
Environmental testing of the Xi Scan 1000, portable fluoroscopic and radiographic imaging system
[AD-A247167] p 3324 N92-28242

RADIOLOGY
Monitoring activities review of the Radiological Environmental Surveillance Program
[DE92-013103] p 3308 N92-28811

RADIOMETERS
A new radiometer for Earth radiation budget studies
[DE92-011267] p 3306 N92-28834
Development of rotating shadowband spectral radiometers and GCM radiation code test data sets in support of ARM
[DE92-011438] p 3316 N92-28853
ETO cloud studies for FIRE 2, part 1
[NASA-CR-190472] p 3319 N92-29087
Non-mechanical optical path switching and its application to dual beam spectroscopy including gas filter correlation radiometry
[NASA-CASE-LAR-14588-1-CU] p 3359 N92-29117

RAIL TRANSPORTATION
Present status of computational tools for Maglev development
[DE92-013252] p 3294 N92-28815

RAILGUN ACCELERATORS
A coilgun design primer
[DE92-011149] p 3244 N92-28226
A momentum limit for electromagnetic railguns
[DE92-011380] p 3245 N92-28861
Space applications for contactless coilguns
[DE92-011156] p 3245 N92-29102

RAIN
Microwave derived rainrates in typhoons and their use in the diagnosis and prediction of typhoon intensity
[AD-A250556] p 3319 N92-28922

RAMAN LASERS
Noise reduction in ring laser driven by a broad band pump
[DE92-622403] p 3289 N92-28228

RAMAN SPECTRA
Hyper-Raman scattering and 3-photon resonant ionization: Competitive effects
[DE92-622671] p 3366 N92-28230

RAMAN SPECTROSCOPY
Selective suppression of photochemical etching: Raman spectroscopy for pre-etch process selection
[DE92-010955] p 3255 N92-28341

RANDOM LOADS
Probabilistic finite element analysis
[AD-A247721] p 3347 N92-28399
Identification of weakly non-linear dynamical systems by means of random excitations
[ONERA-NT-1991-10] p 3349 N92-28778

RANDOM NOISE
Comparison of three controllers applied to helicopter vibration
[NASA-TM-102192] p 3239 N92-28457

RANDOM PROCESSES
Probabilistic finite element analysis
[AD-A247721] p 3347 N92-28399

RANGE (EXTREMES)
Passive acoustic range estimation of helicopters
[AD-A248033] p 3351 N92-28302

RANGEFINDING
Passive acoustic range estimation of helicopters
[AD-A248033] p 3351 N92-28302
A rotorcraft flight database for validation of vision-based ranging algorithms
[NASA-TM-103906] p 3231 N92-29103

RARE GASES
The early Martian atmosphere p 3376 N92-28502
Volatile tracers of Martian atmospheric evolution: Present measurement status and requirements for future investigations p 3387 N92-29037

RASTER SCANNING
Method for advanced material characterization by laser induced eddy current imaging
[NASA-CASE-GSC-13386-1] p 3298 N92-29154

RATES (PER TIME)
Microwave derived rainrates in typhoons and their use in the diagnosis and prediction of typhoon intensity
[AD-A250556] p 3319 N92-28922
Disk memory device
[NASA-CASE-GSC-13196-1] p 3333 N92-29132

RAY TRACING
An OTH radar clutter simulation
[AD-A248054] p 3272 N92-28304
NORSAR basic seismological research
[AD-A248616] p 3309 N92-28569

RAYLEIGH SCATTERING
Rocket plume flowfield characterization using laser Rayleigh scattering
[NASA-TM-105739] p 3357 N92-28475
Photochemical model for NH3 in an early Martian atmosphere p 3373 N92-28481

REACTING FLOW
Large Eddy Simulations (LES) and Direct Numerical Simulations (DNS) for the computational analyses of high speed reacting flows
[NASA-CR-190364] p 3285 N92-28817
Large eddy simulations and direct numerical simulations of high speed turbulent reacting flows
p 3285 N92-28818
Modeling of the reactant conversion rate in a turbulent shear flow p 3229 N92-28820
The compositional structure and the effects of exothermicity in an unpremixed planar jet flame
p 3258 N92-28821

REACTION KINETICS
Mapping closures for turbulent mixing and reaction
[AD-A247305] p 3283 N92-28274
An analysis of combustion studies in shock expansion tunnels and reflected shock tunnels
[NASA-TP-3224] p 3255 N92-28374
The evaluation of rate constants for rapid electrode reactions by using microelectrode voltammetry: Virtues of measurement at lower temperature
[AD-A246760] p 3255 N92-28391
Surface crystallographic dependence of voltammetric oxidation of polyhydric alcohols and related systems at monocrystalline gold-acidic aqueous interfaces
[AD-A246763] p 3363 N92-28392
Martian atmospheric chemistry during the time of low water abundance p 3376 N92-28501
Estimation of high temperature metal-silicate partition coefficients p 3311 N92-28599
Kinetic studies of metal combustion in propulsion
[AD-A250207] p 3256 N92-28769
Thermodynamic and kinetic aspects of surface acidity
[DE92-011194] p 3256 N92-28893
Rates of oxidative weathering on the surface of Mars
p 3380 N92-28999

REACTION TIME
Time pressure effects on decision making in a dynamic task environment
[IZF-1991-B-8] p 3367 N92-29161

REACTOR CORES
Natural circulation decay heat removal from an SP-100, 550 kWe power system for a lunar outpost
[NASA-CR-190421] p 3307 N92-28863

REACTOR DESIGN
Cryogenic system operating experience review for fusion applications
[DE92-012509] p 3361 N92-28805
Natural circulation decay heat removal from an SP-100, 550 kWe power system for a lunar outpost
[NASA-CR-190421] p 3307 N92-28863

REACTOR SAFETY
A strategy for minimizing common mode human error in executing critical functions and tasks
[DE92-011839] p 3327 N92-28775
Cryogenic system operating experience review for fusion applications
[DE92-012509] p 3361 N92-28805
Underwater vapor phase burning of aluminum particles and on aluminum ignition during steam explosions
[DE92-011196] p 3257 N92-28894
Determination of field related transfer factors for Cs-137 and Sr-90, from the fallout of the reactor accident in Chernobyl (USSR)
[OEFZS-4581] p 3356 N92-29210

REAL TIME OPERATION
NPSNET: Flight simulation dynamic modeling using quaternions
[AD-A247484] p 3333 N92-28245
A radar signal processing ASIC and a VME interface circuit p 3235 N92-28380
Anthropomorphic teleoperation: Controlling remote manipulators with the DataGlove
[NASA-TM-103588] p 3330 N92-28521
Interest in real-time simulations for the development terrain following function of radar systems
p 3222 N92-28529

The role of simulation for the study of APIS (piloting support by synthetic imagery) p 3224 N92-28544
PC graphics generation and management tool for real-time applications
[NASA-TM-105749] p 3337 N92-28684
Modelling and real-time simulation of the Hermes robot arm HERA
[NLR-TP-90262-U] p 3294 N92-28705
Fault-tolerant parallel computer systems for real-time applications
[AD-A247887] p 3343 N92-28958
A generalized reusable guidance algorithm for optimal aerobraking
[NASA-TM-103590] p 3229 N92-28981
Analysis and optimization of low-earth-orbit communication links
[DE92-013393] p 3277 N92-29131
NARSIM: A real-time simulator for air traffic control research
[NLR-TP-90147-U] p 3241 N92-29204

RECEIVERS
Data selection for fast projection techniques applied to adaptive nulling: A comparative study of performance
[AD-A246468] p 3276 N92-28979
Effects of fading and data modulation on noncoherent M-sequence acquisition schemes
[AD-A247968] p 3276 N92-29084
Crosstalk correction scheme
[AD-D015251] p 3276 N92-29085
Solar thermal energy receiver
[NASA-CASE-LEW-14949-1] p 3307 N92-29143

RECOGNITION
Models for recall and recognition
[IZF-1991-B-4] p 3342 N92-28746

RECOMMENDATIONS
Responsible science: Ensuring the integrity of the research process, volume 1
[ISBN-0-309-04731-5] p 3350 N92-28363
Monitoring activities review of the Radiological Environmental Surveillance Program
[DE92-013103] p 3308 N92-28811

RECONNAISSANCE AIRCRAFT
Reduction and analysis of F-111C flight data
[AD-A250341] p 3233 N92-28771

RECORDS MANAGEMENT
Files improvement the NARA way
[DE92-011139] p 3368 N92-28832

RECTANGULAR WAVEGUIDES
Comparison of various techniques in the analysis of waveguide transitions
[AD-A247019] p 3279 N92-28367

RECURSIVE FUNCTIONS
Linear recursive formulation of flexible multi-body space system dynamics
[NLR-TP-90284-U] p 3293 N92-28646

RECYCLING
Coupling plant growth and waste recycling systems in a controlled life support system (CELSS)
[NASA-TM-107544] p 3330 N92-28670

REDUCED GRAVITY
Thermoregulation during spaceflight
[NASA-TM-103913] p 3325 N92-28420
Hydrogen no-vent fill testing in a 5 cubic foot (142 liter) tank using spray nozzle and spray bar liquid injection
[NASA-TM-105759] p 3266 N92-28433
International Workshop on Vibration Isolation Technology for Microgravity Science Applications
[NASA-CP-10094] p 3268 N92-28436
Numerical studies of convective transport associated with crystal growth in mirrogravity p 3267 N92-28437
The Microgravity Isolation Mount (MGIM): A Columbus facility for improving the microgravity quality of payloads p 3267 N92-28439
Vibration isolation technology development to demonstration p 3267 N92-28442
New inertial actuator provides isolation and stabilization in microgravity conditions p 3267 N92-28443
A 6 degree-of-freedom Lorentz force vibration isolator with nonlinear controller p 3267 N92-28444
Digital control algorithms for microgravity isolation systems p 3267 N92-28445
Microgravity vibration isolation research at the University of Virginia p 3267 N92-28446
Extended H2 synthesis for microgravity vibration isolation p 3267 N92-28447
ACAP: Acceleration Characterization and Analysis Project p 3267 N92-28448
Space Station Freedom microgravity environment requirements and assessment methods p 3268 N92-28450
Early mission science support: Space Acceleration Measurement System (SAMS) p 3248 N92-28451
Microgravity accelerometer characterization on Columbia STS-32 mission p 3271 N92-28452
Development of a residual acceleration data reduction and dissemination plan p 3271 N92-28453
Microgravity isolation mounts based upon Piezoelectric film p 3268 N92-28454
Predicting microgravity levels for space station using VAPEPS p 3268 N92-28455
Review of Mars mission scenarios p 3244 N92-28731
Experimental measurement of the orbital paths of particles sedimenting within a rotating viscous fluid as influenced by gravity
[NASA-TP-3200] p 3331 N92-28897

REDUCTION (CHEMISTRY)
Thermodynamic and kinetic aspects of surface acidity
[DE92-011194] p 3256 N92-28893

REDUNDANCY ENCODING
DEPEND: A simulation-based environment for system level dependability analysis
[NASA-CR-189752] p 3297 N92-28726

REDUNDANT COMPONENTS
Validation of knowledge based systems
[AD-A247741] p 3368 N92-28404

REFERENCE ATMOSPHERES
Mars global reference atmosphere model (Mars-GRAM) p 3375 N92-28494

REFLECTANCE
The use of a vector network analyzer for measuring the performance of radar absorbing materials
[AD-A247194] p 3275 N92-28887
Theoretical and experimental studies relevant to interpretation of auroral emissions
[NASA-CR-190521] p 3316 N92-28911
Infrared photometric behavior and opposition effect of Mars p 3382 N92-29011
Water window imaging x ray microscope
[NASA-CASE-MFS-28485-1] p 3288 N92-29135

REFLECTION
Thermal response of rigid and flexible insulations and reflective coating in an aeroconvective heating environment
[NASA-TM-103925] p 3233 N92-28721
Modal element method for scattering of sound by absorbing bodies
[NASA-TM-105722] p 3353 N92-28984
Physical interpretation of thermal and reflected data on Martian surface units p 3391 N92-29062
In-situ fault detection by the hybrid ray-mode method
[AD-A250213] p 3297 N92-29112

REFLECTOR ANTENNAS
Method of moments analysis of displaced-axis dual reflector antennas
[AD-A247970] p 3277 N92-29166

REFLECTORS
Accuracy of shipborne kinematic GPS surveying
[AD-A245942] p 3230 N92-28317
Method and apparatus for phasing segmented mirror arrays
[NASA-CASE-NPO-18095-1-CU] p 3359 N92-29122

REFRACTION
Optical effects on ocean mixed layer dynamics
[AD-A245941] p 3320 N92-28316
The distance dependence of regional phase discriminants
[AD-A247546] p 3316 N92-28935

REFRACTIVITY
Perspectives of ion implantation for optics
[DE92-010664] p 3357 N92-28355
Elliptical-core two mode fiber sensors and devices incorporating photoinduced refractive index gratings
[NASA-CR-190495] p 3358 N92-28868

REFRACTORY MATERIALS
Evaluation of plasma sprayed crucible coatings for melt processing copper-refractory metal alloys
[DE92-010871] p 3259 N92-28338
High temperature dielectric properties of Apical, Kapton, Peek, Teflon AF, and Upilex polymers
[NASA-TM-105753] p 3280 N92-28675

REFRIGERATING
Ultra-high temperature stability Joule-Thomson cooler with capability to accomodate pressure variations
[NASA-CASE-NPO-18184-1-CU] p 3288 N92-29156

REFUELING
Flow rate testing of valves used with the 500 gallon collapsible drum
[AD-A250567] p 3294 N92-28924

REGENERATIVE FUEL CELLS
Electrochemical studies of Lewis acid-base systems for use in thermally regenerable fuel cells
[AD-A246457] p 3307 N92-28974

REGOLITH
How Mars lost its atmosphere p 3378 N92-28509
Regional variations in the stability and diffusion of water-ice in the Martian regolith p 3388 N92-29042
Determining the pH of Mars from the Viking labelled release reabsorption effect p 3389 N92-29049
Climatic implications of the simultaneous presence of CO2 and H2O in the Martian regolith p 3395 N92-29079

REGRESSION ANALYSIS
An application of interactive computer graphics to the study of inferential statistics and the general linear model
[AD-A246668] p 3334 N92-28285
A study of pilot attitudes regarding the impact on mission effectiveness of using new cockpit automation technologies to replace the navigator/weapon system officer/electronic warfare officer
[AD-A246683] p 3329 N92-28286
Overview of two common statistical computer packages: SAS and BMDP
[AD-A245982] p 3368 N92-28663
Microwave derived rainrates in typhoons and their use in the diagnosis and prediction of typhoon intensity
[AD-A250556] p 3319 N92-28922

REGULATORS
Adaptive and nonlinear control
[AD-A248580] p 3344 N92-28429

REINFORCING FIBERS
Method fabricating load-bearing composites free from microbuckling deformation up to a predetermined load
[AD-D015212] p 3250 N92-28224
The application of carbon fibres in ARALL laminates
[LR-658] p 3259 N92-28576

RELATIVISTIC PARTICLES
A generalization of the K-V equilibrium for an intense, relativistic beam propagating in a solenoid
[AD-A247067] p 3350 N92-28238

RELAXATION TIME
Dynamical solvent effects on activated electron-transfer reactions: Principles, pitfalls, and progress
[AD-A246764] p 3363 N92-28349

RELIABILITY
A cost-benefit analysis on the deletion of the inertial upper stage factory acceptance testing versus a decrease in mission reliability
[AD-A246620] p 3245 N92-28254
Turbine aircraft engine operational trending and JT8D static component reliability study
[DOT/FAA/CT-91/10] p 3238 N92-28686
Fiber-optic interconnection networks for spacecraft
[NASA-CR-190531] p 3358 N92-28698
Tactical line-of-sight radio propagation reliability
[AD-A245909] p 3277 N92-29165

RELIABILITY ANALYSIS
A sensitivity analysis on component reliability from fatigue life computations
[AD-A247430] p 3297 N92-28425
Integration of tools for the Design and Assessment of High-Performance, Highly Reliable Computing Systems (DAHPHRS), phase 1
[NASA-CR-189621] p 3336 N92-28585
DEPEND: A simulation-based environment for system level dependability analysis
[NASA-CR-189752] p 3297 N92-28726

RELIABILITY ENGINEERING
Integration of tools for the Design and Assessment of High-Performance, Highly Reliable Computing Systems (DAHPHRS), phase 1
[NASA-CR-189621] p 3336 N92-28585
Evaluation of future space transportation systems with regard to their reliabilities and costs
[DLR-FB-91-27] p 3245 N92-28826

RELIEF MAPS
Survey parameters and availability of low-level aeromagnetic data for geomagnetic field modelling p 3301 N92-28629
Unwrapping two-dimensional phase data in contour maps
[AD-A249988] p 3338 N92-28795

RELIEF VALVES
Ultra-high temperature stability Joule-Thomson cooler with capability to accomodate pressure variations
[NASA-CASE-NPO-18184-1-CU] p 3288 N92-29156

REMANENCE
Method and apparatus for using magneto-acoustic remanence to determine embrittlement
[NASA-CASE-LAR-13817-5] p 3303 N92-28757
Discovery concepts for Mars p 3387 N92-29035
Magnetic remanence method and apparatus to test materials for embrittlement
[NASA-CASE-LAR-13817-4] p 3304 N92-29101

REMOTE CONTROL
Anthropomorphic teleoperation: Controlling remote manipulators with the DataGlove
[NASA-TM-103588] p 3330 N92-28521
Automation and remote control instrumentation development: Rocket First Motion Timing System (RFMTS)
[AD-A249970] p 3287 N92-28767

REMOTE SENSING
The distribution of anorthosite on the nearside of the moon p 3311 N92-28594

Remote sensing applications of the extended radiosity method
[DE92-011356] p 3306 N92-28807
VLA mapping of 1.35 cm water emission from the Mars atmospheric limb p 3381 N92-29004
Micro weather stations for in situ measurements in the Martian planetary boundary layer p 3382 N92-29008
Physical properties of Oxia/Lunae Planum and Arabia-type units in the central equatorial region of Mars p 3392 N92-29065
ETO cloud studies for FIRE 2, part 1
[NASA-CR-190472] p 3319 N92-29087

REMOTE SENSORS
ETO cloud studies for FIRE 2, part 1
[NASA-CR-190472] p 3319 N92-29087

REMOTELY PILOTED VEHICLES
Stability and control flight testing of a half-scale Pioneer remotely piloted vehicle
[AD-A245973] p 3239 N92-28801

REMOVAL
Paint removal using cryogenic processes
[AD-A247668] p 3264 N92-28912

RENAL FUNCTION
The chronic effects of JP-8 jet fuel exposure on the lungs
[AD-A250308] p 3326 N92-29123

REPLACING
Replacement bearing for Rocketdyne SSME HPOTPs using alternate self-lubricating retainer materials
[NASA-CR-184328] p 3292 N92-28362

REPORTS
The 1991 research program (of the Faculty of Mechanical Engineering)
[ETN-92-91353] p 3296 N92-29217
DLR research reports and communications
[ISSN-0939-2971] p 3397 N92-29218

REQUIREMENTS
Mass and power modeling of communication satellites
[NASA-CR-189186] p 3275 N92-28906
Nonlinear sloshing and the coupled dynamics of liquid propellants and spacecraft
[AD-A250023] p 3248 N92-28967

RESEARCH
Responsible science: Ensuring the integrity of the research process, volume 1
[ISBN-0-309-04731-5] p 3350 N92-28363

RESEARCH AIRCRAFT
The second flight simulator test of the head-up display for NAL QSTOL experimental aircraft (ASKA)
[NAL-TM-633] p 3331 N92-28831
Aerodynamic characteristics obtained from alpha sweep test of the quiet STOL experimental aircraft ASKA
[NAL-TR-1112] p 3234 N92-28901

RESEARCH AND DEVELOPMENT
Maintaining the program balance, volumes 1 and 2
[NASA-CR-190269] p 3367 N92-29111

RESEARCH FACILITIES
Experimental aerodynamic facilities of the Aerodynamics Research and Concepts Assistance Branch
[AD-A247489] p 3240 N92-28248
Expand turbulence laboratory facilities to meet new DOD research interest
[AD-A248581] p 3240 N92-28388
Use of a research simulator for the development of new concepts of flight control p 3224 N92-28543
The basic research simulator programme and the industrial and aerospace community: Opportunities for cooperative research
[LR-662] p 3240 N92-28579

RESEARCH MANAGEMENT
Information Resources Management long-range plan
[DE92-012408] p 3368 N92-28804

RESEARCH PROJECTS
Responsible science: Ensuring the integrity of the research process, volume 1
[ISBN-0-309-04731-5] p 3350 N92-28363
The 1991 research program (of the Faculty of Mechanical Engineering)
[ETN-92-91353] p 3296 N92-29217
DLR research reports and communications
[ISSN-0939-2971] p 3397 N92-29218
Activities report of the DLR
[ISSN-0938-2194] p 3397 N92-29219

RESEARCH VEHICLES
Rotorcraft In-Flight Simulation Research at NASA Ames Research Center: A Review of the 1980's and plans for the 1990's
[NASA-TM-103873] p 3234 N92-28926

RESIDUAL STRESS
X ray diffraction study of residual stresses in metal matrix composite-jacketed steel cylinders subjected to internal pressure
[AD-A248449] p 3251 N92-28416
Surface residual stress analysis of metals and alloys
[AD-A248372] p 3259 N92-28426

RESIN BONDING
Propellant-to-inhibitor bonding system
[AD-D015243] p 3266 N92-28739

RESISTORS
Percolation conductivity of Penrose tiling by transfer-matrix Monte Carlo
[DE92-622792] p 3362 N92-28231

RESOLUTION
High resolution electron beam lithography on x ray mask substrates. Effects of electron scattering and membrane heating
[ETN-92-91336] p 3272 N92-28793

RESONANCE
Theoretical studies of the electronic and resonance structure of atomic and molecular negative ions
[AD-A247093] p 3354 N92-28259

RESONANT FREQUENCIES
Experiments in passive vibration reduction
[AD-A250397] p 3304 N92-29181

RESONANT VIBRATION
Fundamental noise limits in miniature acoustic and vibration sensors
[AD-A247016] p 3352 N92-28413

RESOURCES MANAGEMENT
Information Resources Management long-range plan
[DE92-012408] p 3368 N92-28804

RESPONSES
The variance of Rasch ability estimates from partially-known item parameters
[AD-A247065] p 3348 N92-28273

RESTORATION
Digital enhancement and restoration of images derived from flow visualization experiments
[AD-A250317] p 3339 N92-28952

RETAINING
Payload retention device
[NASA-CASE-MSC-21906-1] p 3294 N92-28727

RETINA
Portable dynamic fundus instrument
[NASA-CASE-MSC-21675-1] p 3325 N92-28755
Investigation of laser-induced retinal damage
[AD-A250173] p 3326 N92-28920

REVERSED FLOW
Internal reversing flow in a tailpipe offtake configuration for SSTOVL aircraft
[NASA-TM-105698] p 3236 N92-28418

RHEOLOGY
Evolution of a terrestrial magma ocean: Thermodynamics, kinetics, rheology, convection, differentiation p 3314 N92-28611

RIDGES
Test of the new ONR ocean bottom seismographs on the Juan de Fuca Ridge
[AD-A247733] p 3321 N92-28402
Dorsa Argentea type sinuous ridges, Mars: Evidence for linear dune hypothesis p 3390 N92-29055

RIEMANN MANIFOLD
Classical and quantum Liouville theory on the Riemann sphere with n greater than 3 punctures (II)
[DE92-622380] p 3366 N92-28227
The exchange algebra for Liouville theory on punctured Riemann sphere
[DE92-622409] p 3366 N92-28229

RIGID STRUCTURES
Quaternion and Euler angles in kinematics
[NAL-TM-636] p 3303 N92-28836

RING LASERS
Noise reduction in ring laser driven by a broad band pump
[DE92-622403] p 3289 N92-28228

RIO GRANDE (NORTH AMERICA)
A seismic and integrated geophysical study of the lithosphere of the Colorado Plateau
[AD-A247091] p 3308 N92-28257

RISK
Cryogenic system operating experience review for fusion applications
[DE92-012509] p 3361 N92-28805

RIVERS
Multitemporal analysis of a braiding river
[NLR-TP-89235-U] p 3305 N92-28690

ROBOT ARMS
Dynamics motion simulation of the Hermes robot arm subjected to constraints
[NLR-TP-90282-U] p 3293 N92-28645
Modelling and real-time simulation of the Hermes robot arm HERA
[NLR-TP-90262-U] p 3294 N92-28705
Rolling friction robot fingers
[NASA-CASE-GSC-13261-1] p 3296 N92-29138

ROBOT CONTROL
A survey report for the design of biped locomotion robot: The WL-12 (Waseda Leg-12)
[DE92-782046] p 3292 N92-28233
Lessons from Archimedes, a system for planning and executing mechanical assemblies
[DE92-010957] p 3335 N92-28342
Anthropomorphic teleoperation: Controlling remote manipulators with the DataGlove
[NASA-TM-103588] p 3330 N92-28521
Acquisition and improvement of human motor skills: Learning through observation and practice
[NASA-TM-107878] p 3329 N92-29174

ROBOT DYNAMICS
A survey report for the design of biped locomotion robot: The WL-12 (Waseda Leg-12)
[DE92-782046] p 3292 N92-28233

ROBOTICS
Quasi-recursive dynamics equations for spacecraft-based flexible robotic manipulators
[NLR-TP-90028-U] p 3345 N92-28648
Ongoing Progress in Spacecraft Controls
[NASA-CP-10099] p 3247 N92-28730
Fuzzy logic controller for manipulator systems: Preliminary results p 3247 N92-28738
Method and apparatus for predicting the direction of movement in machine vision
[NASA-CASE-NPO-17552-1-CU] p 3331 N92-29129
Development of an automated wire delivery system for robotic welding applications
[NASA-CR-190487] p 3295 N92-29134

ROBOTS
A survey report for the design of biped locomotion robot: The WL-12 (Waseda Leg-12)
[DE92-782046] p 3292 N92-28233
Lessons from Archimedes, a system for planning and executing mechanical assemblies
[DE92-010957] p 3335 N92-28342
Mars Environmental Survey (MESUR): Science objectives and mission description p 3385 N92-29025

ROCKET ENGINE DESIGN
Introduction to rocket propulsion
[AD-A250424] p 3249 N92-28800

ROCKET ENGINES
An overview of in-flight plume diagnostics for rocket engines
[NASA-TM-105727] p 3248 N92-28417
Integrated health monitoring and controls for rocket engines
[NASA-TM-105763] p 3249 N92-28893
Kinetic studies of metal combustion in propulsion
[AD-A250207] p 3256 N92-28769

ROCKET EXHAUST
Rocket plume flowfield characterization using laser Rayleigh scattering
[NASA-TM-105739] p 3357 N92-28475

ROCKET LAUNCHERS
Automation and remote control instrumentation development: Rocket First Motion Timing System (RFMTS)
[AD-A249970] p 3287 N92-28767

ROCKET NOZZLES
Scattering measurements and predictions for a Delta stage 2 rocket nozzle
[AD-A246776] p 3248 N92-28366
Rocket nozzle shield
[AD-D015248] p 3249 N92-28748
Ablation of material of solid propellant motor nozzles
[ONERA-NT-1990-13] p 3249 N92-28780

ROCKET OXIDIZERS
Kinetic studies of metal combustion in propulsion
[AD-A250207] p 3256 N92-28769

ROCKS
Comparison of drift potential derived from Mars GCM with rock abundance from IRTM p 3395 N92-29078

ROLLER BEARINGS
Rolling friction robot fingers
[NASA-CASE-GSC-13261-1] p 3296 N92-29138

ROLLING
Device for applying constant pressure to a surface
[NASA-CASE-GSC-13230-1] p 3294 N92-28754

ROTARY STABILITY
Explicit Navier-Stokes computation of turbomachinery flows
[AD-A249284] p 3286 N92-28879

ROTARY WING AIRCRAFT
The application of flight simulation models in support of rotorcraft design and development p 3222 N92-28527
Rotorcraft In-Flight Simulation Research at NASA Ames Research Center: A Review of the 1980's and plans for the 1990's
[NASA-TM-103873] p 3234 N92-28926

ROTATING FLUIDS
Experimental measurement of the orbital paths of particles sedimenting within a rotating viscous fluid as influenced by gravity
[NASA-TP-3200] p 3331 N92-28897

ROTATING STALLS
Dynamic control of aerodynamic instabilities in gas turbine engines p 3238 N92-28466
ROTOR AERODYNAMICS
LAH-main rotor model test at the DNW
[NLR-TP-90305-U] p 3233 N92-28687
ROTOR BLADES
LAH-main rotor model test at the DNW
[NLR-TP-90305-U] p 3233 N92-28687
ROTOR SPEED
Explicit Navier-Stokes computation of turbomachinery flows
[AD-A249284] p 3286 N92-28879
ROTORS
Assessment of valve actuator motor rotor degradation by Fourier Analysis of current waveform
[DE92-013233] p 3281 N92-28814
Multi-channel fiber optic rotary joint for single-mode fiber
[AD-D015273] p 3358 N92-29095
Superconducting bearings with levitation control configurations
[NASA-CASE-GSC-13346-1] p 3295 N92-29099
RUBBER
Use of scrap rubber in asphalt pavement surfaces
[AD-A247419] p 3272 N92-28902
RUNGE-KUTTA METHOD
Comparison of various techniques in the analysis of waveguide transitions
[AD-A247019] p 3279 N92-28367
On some splitting schemes for wave equations
[FFI-91/7023] p 3348 N92-29193
RUNWAYS
A methodology for the evaluation of runway roughness for repair
[AD-A250407] p 3241 N92-28772
RYDBERG SERIES
Excited negative ions and molecules and negative ion production
[AD-A247017] p 3354 N92-28414

S

S MATRIX THEORY
Comparison of various techniques in the analysis of waveguide transitions
[AD-A247019] p 3279 N92-28367
S WAVES
The distance dependence of regional phase discriminants
[AD-A247546] p 3316 N92-28935
SADDLE POINTS
Using Gaussian windows to explore a multivariate data set
[NASA-CR-190556] p 3339 N92-29106
SAFETY
Space Station: Delays in dealing with space debris may reduce safety and increase costs
[GAO/IMTEC-92-50] p 3243 N92-28406
SAFETY FACTORS
Probabilistic finite element analysis
[AD-A247721] p 3347 N92-28399
SAMPLED DATA SYSTEMS
Unwrapping two-dimensional phase data in contour maps
[AD-A249988] p 3338 N92-28795
SAMPLING
The variance of Rasch ability estimates from partially-known item parameters
[AD-A247065] p 3348 N92-28273
Reduction of marine magnetic data for modeling the main field of the Earth p 3300 N92-28626
An investigation into techniques for the determination of moisture content on activated carbon
[AD-A245938] p 3256 N92-28882
The 2.0 GHz sampling rate transversal filter
[AD-A250244] p 3358 N92-28968
SANDS
The composition of Martian aeolian sands: Thermal emissivity from Viking IRTM observations p 3382 N92-29010
Surface photometric properties and albedo changes in the central equatorial region of Mars p 3392 N92-29066
SATELLITE ALTIMETRY
TOPEX/POSEIDON science investigations plan
[NASA-CR-190456] p 3305 N92-28950
SATELLITE COMMUNICATION
Design on an enhanced interactive satellite communications system analysis program
[AD-A245967] p 3273 N92-28410
Fade durations in satellite-path mobile radio propagation
[NASA-CR-190484] p 3273 N92-28586
Coding for frequency hopped spread spectrum satellite communications
[ECE-90-1] p 3274 N92-28699
SATELLITE DESIGN
Quaternion and Euler angles in kinematics
[NAL-TM-636] p 3303 N92-28836
SATELLITE GROUND SUPPORT
Verification of satellite EGSE test-software using an application generator
[ITN-92-85131] p 3244 N92-29098
SATELLITE IMAGERY
Quantitative updating of land use information on 1:50,000 scale topographic maps using SPOT LANDSAT Thematic Mapper imagery
[NLR-TP-89061-U] p 3305 N92-28708
Sea surface velocities from visible and infrared multispectral atmospheric mapping sensor imagery
[NASA-CR-190398] p 3305 N92-28715
Theoretical and experimental studies relevant to interpretation of auroral emissions
[NASA-CR-190521] p 3316 N92-28911
Segmentation of satellite imagery using hierarchical thresholding and neural networks
[AD-A247915] p 3319 N92-28965
A probabilistic neural network approach to cloud classification
[AD-A247916] p 3319 N92-28966
SATELLITE INSTRUMENTS
Atmospheric corrections of land imagery using the extended radiosity method
[DE92-011355] p 3306 N92-28840
SATELLITE NETWORKS
EUMETSAT: The European Organization for Meteorological Satellites
[ETN-92-91069] p 3318 N92-28745
SATELLITE OBSERVATION
Satellite data for geomagnetic field modeling p 3300 N92-28624
Ocean tide models for satellite geodesy and Earth rotation
[NASA-CR-190468] p 3321 N92-28867
Microwave derived rainrates in typhoons and their use in the diagnosis and prediction of typhoon intensity
[AD-A250556] p 3319 N92-28922
Observations of Mars using Hubble Space Telescope p 3385 N92-29026
SATELLITE ORBITS
Future mission studies: Preliminary comparisons of solar flux models
[NASA-TM-107947] p 3396 N92-28869
SCALARS
Mapping closures for turbulent mixing and reaction
[AD-A247305] p 3283 N92-28274
Modeling of the reactant conversion rate in a turbulent shear flow p 3229 N92-28820
SCALE MODELS
Low Reynolds number multiple-time-scale turbulence model and calculations of steady and pulsating shear layers
[NASA-CR-189176] p 3286 N92-28908
SCANNERS
Scientific investigations with the data base HEAO-1 scanning modulator collimator
[NASA-CR-190477] p 3370 N92-28680
SCANNING
Methods of visual scanning with night vision goggles
[AD-A247470] p 3331 N92-28944
SCANNING TUNNELING MICROSCOPY
The emergence of atomic-level structural information for ordered metal-solution interfaces: Some recent contributions from in-situ infrared spectroscopy and scanning tunneling microscopy
[AD-A246765] p 3364 N92-28512
SCATTER PROPAGATION
Propagation and scattering of microwaves and millimeter waves in snow based on dense random media theory
[AD-A249300] p 3274 N92-28846
In-situ fault detection by the hybrid ray-mode method
[AD-A250213] p 3297 N92-29112
SCATTERING
The use of conformal subdomain basis functions in the method of moments computations for a thin wire
[AD-A245964] p 3272 N92-28347
Thermal wave imaging and characterization of solids
[AD-A249297] p 3297 N92-28851
SCATTERING FUNCTIONS
Propagation and scattering of microwaves and millimeter waves in snow based on dense random media theory
[AD-A249300] p 3274 N92-28846
SCHEDULING
Scheduling multiple variable-speed machines
[AD-A249362] p 3268 N92-28359
A network flow algorithm for just-in-time project scheduling
[MEMO-COSOR-91-21] p 3336 N92-28638
SCHLIEREN PHOTOGRAPHY
Telescience experiments using the Prototype Optical Diagnostic Instrument (PODI)
[NLR-TP-90199-U] p 3358 N92-28656
SCHUMANN-RUNGE BANDS
Degenerate four-wave mixing using a tunable excimer laser to detect combustion gases
[DE92-005327] p 3290 N92-28852
SCIENTISTS
NASA engineers and the age of Apollo
[NASA-SP-4104] p 3397 N92-28344
A profile of scientist and engineer training conducted by the Naval Avionics Center
[AD-A245925] p 3326 N92-28408
SEA ICE
Under-ice broadband transient measurements and processing
[AD-A248609] p 3351 N92-28324
SEA LEVEL
TOPEX/POSEIDON science investigations plan
[NASA-CR-190456] p 3305 N92-28950
SEAS
Test of the new ONR ocean bottom seismographs on the Juan de Fuca Ridge
[AD-A247733] p 3321 N92-28402
SEASONS
Modeling the seasonal cycle of CO2 on Mars: A fit to the Viking lander pressure curves p 3394 N92-29076
SECONDARY FLOW
Heat exchanger with oscillating flow
[NASA-CASE-LAR-14033-1] p 3284 N92-28752
SECULAR VARIATIONS
Secular variation across the oceans: A retrospective study from 35 years of shipboard total field measurements in the NE Atlantic p 3300 N92-28627
Magnetic repeat station data p 3301 N92-28630
Magnetic and electromagnetic induction effects in the annual means of geomagnetic elements p 3301 N92-28632
Independent constituents in observatory time series in characterizing the secular variation p 3302 N92-28633
SEDIMENTS
Experimental measurement of the orbital paths of particles sedimenting within a rotating viscous fluid as influenced by gravity
[NASA-TP-3200] p 3331 N92-28897
SEEDS
Effects of extremely high G acceleration forces on NASA's control and space exposed tomato seeds
[AD-A247488] p 3323 N92-28247
SEGMENTS
Segmentation of satellite imagery using hierarchical thresholding and neural networks
[AD-A247915] p 3319 N92-28965
Method and apparatus for phasing segmented mirror arrays
[NASA-CASE-NPO-18095-1-CU] p 3359 N92-29122
SEISMIC WAVES
Analysis of the effects of Eurasian crustal and upper mantle structure on regional phases using broadband seismic data
[AD-A248383] p 3309 N92-28386
Studies of regional wave propagation using differential seismograms and randomized structural models
[AD-A247011] p 3309 N92-28394
NORSAR basic seismological research
[AD-A248616] p 3309 N92-28569
The distance dependence of regional phase discriminants
[AD-A247546] p 3316 N92-28935
SEISMOGRAMS
Studies of regional wave propagation using differential seismograms and randomized structural models
[AD-A247011] p 3309 N92-28394
The distance dependence of regional phase discriminants
[AD-A247546] p 3316 N92-28935
SEISMOGRAPHS
Test of the new ONR ocean bottom seismographs on the Juan de Fuca Ridge
[AD-A247733] p 3321 N92-28402
SEISMOLOGY
Analysis of the effects of Eurasian crustal and upper mantle structure on regional phases using broadband seismic data
[AD-A248383] p 3309 N92-28386
NORSAR basic seismological research
[AD-A248616] p 3309 N92-28569
The distance dependence of regional phase discriminants
[AD-A247546] p 3316 N92-28935
MARSNET surface and atmosphere investigations p 3381 N92-29002

SELECTION
Is choice accuracy related to information search patterns?
[IZF-1991-B-9] p 3369 N92-29162
SELF LUBRICATING MATERIALS
Replacement bearing for Rocketdyne SSME HPOTPs using alternate self-lubricating retainer materials
[NASA-CR-184328] p 3292 N92-28362
SELF ORGANIZING SYSTEMS
New neural algorithms for self-organized learning
[AD-A249816] p 3341 N92-29198
SEMANTICS
A uniform approach to the semantics of concurrency
[AD-A246697] p 3334 N92-28289
What is on the machine's mind? Models for reasoning with incomplete and uncertain knowledge
[NLR-TP-91099-U] p 3345 N92-28716
Generalized quantifiers and modal logic
[ITLI-LP-91-01] p 3348 N92-29214
SEMICONDUCTOR DEVICES
Neutron, gamma ray, and temperature effects on the electrical characteristics of thyristors
[NASA-TM-105728] p 3279 N92-28432
The effect of induced charges on low-energy particle trajectories near conducting and semiconducting plates
[NASA-TM-103589] p 3355 N92-28986
Operation and radiation resistance of a FOXFET biasing structure for silicon strip detectors
[DE92-011279] p 3282 N92-29197
SEMICONDUCTOR DIODES
Advanced diagnostics for reacting flows
[AD-A247059] p 3360 N92-28298
SEMICONDUCTOR LASERS
A diode laser pumped Nd:YAG laser
[FFI-91/7020] p 3289 N92-28315
Strained AlGaInAs semiconducting material for improved laser performance
[AD-A249379] p 3289 N92-28330
Phase stability of injection-locked beam of semiconductor lasers
[NASA-TT-10001] p 3290 N92-28862
Tuning and automatic phase adjustment in external cavity diode laser beam combiners
[AD-A247421] p 3290 N92-28903
Innovative techniques for the production of low cost 2D laser diode arrays
[AD-A248247] p 3292 N92-29226
SEMICONDUCTOR PLASMAS
Advanced diagnostics for reacting flows
[AD-A247059] p 3360 N92-28298
SEMICONDUCTORS (MATERIALS)
The influence of the resonant electromagnetic field on the light absorption by exciton and biexciton in quantum wells
[DE92-622801] p 3366 N92-28232
Femtosecond carrier processes in compound semiconductors and real time signal processing
[AD-A248053] p 3278 N92-28275
Scattering mechanisms for semiconductor transport calculations
[AD-A249260] p 3278 N92-28295
Shallow states of donor impurities on periodically structured semiconductors interfaces
[DE92-622791] p 3363 N92-28312
Strained AlGaInAs semiconducting material for improved laser performance
[AD-A249379] p 3289 N92-28330
Growth and optical characterization of Zn(1-x)Mn(x)Te grown by molecular beam epitaxy
[DE92-010667] p 3363 N92-28331
Center for the integration of optical computing
[AD-A250306] p 3337 N92-28719
Studies of 1,3-disilacyclobutanes as single-source CVD precursors to silicon carbide
[AD-A247111] p 3365 N92-28885
A survey of high density packaging for high performance computing system
[AD-A248633] p 3332 N92-28891
Monolithic optoelectronic implementation of neural planes
[AD-A250286] p 3345 N92-28970
SENSITIVITY
A sensitivity analysis on component reliability from fatigue life computations
[AD-A247430] p 3297 N92-28425
SENSORIMOTOR PERFORMANCE
Acquisition and improvement of human motor skills: Learning through observation and practice
[NASA-TM-107878] p 3329 N92-29174
SENSORS
Fundamental noise limits in miniature acoustic and vibration sensors
[AD-A247016] p 3352 N92-28413
A contribution to laser range imaging technology
[NASA-CR-190501] p 3290 N92-28707
Elliptical-core two mode fiber sensors and devices incorporating photoinduced refractive index gratings
[NASA-CR-190495] p 3358 N92-28868
Detection of in-plane displacements of acoustic wave fields using extrinsic Fizeau fiber interferometric sensors
[NASA-CR-190493] p 3353 N92-29196
SENSORY PERCEPTION
Psychophysical analyses of perceptual representations
[AD-A246945] p 3329 N92-29186
SEPARATED FLOW
A numerical wind tunnel study of viscous-inviscid interaction
[AD-A248429] p 3283 N92-28350
Inlet distortion effects in aircraft propulsion system integration p 3237 N92-28464
SEROTONIN
Study of SCN neurochemistry using in vivo microdialysis in the conscious brain: Correlation with overt circadian rhythms
[AD-A247172] p 3325 N92-28886
SERT 2 SPACECRAFT
Development and flight history of SERT 2 spacecraft
[NASA-TM-105636] p 3250 N92-28983
SET THEORY
The structure of finitely generated shift-invariant spaces in L2(IR sup d)
[AD-A247314] p 3334 N92-28301
Adaptive set-membership identification in 0(m) time for linear-in-parameters models
[AD-A249359] p 3273 N92-28058
SHADOWS
Fade durations in satellite-path mobile radio propagation
[NASA-CR-190484] p 3273 N92-28586
SHAFTS (MACHINE ELEMENTS)
Application of face-gear drives in helicopter transmissions
[NASA-TM-105655] p 3293 N92-28434
SHALLOW WATER
A new ocean bottom magnetometer system for continental shelf measurements
[AD-A247644] p 3321 N92-28321
Ultrasonic ambient noise in Australian shallow waters at frequencies up to 200 kHz
[MRL-TR-91-23] p 3351 N92-28364
Sea surface velocities from visible and infrared multispectral atmospheric mapping sensor imagery
[NASA-CR-190398] p 3305 N92-28715
SHAPED CHARGES
EXPLOMET 90 international conference on shock-wave and high-strain-rate phenomena in materials
[AD-A248665] p 3303 N92-28892
SHAPES
Experimental and computational ice shapes and resulting drag increase for a NACA 0012 airfoil
[NASA-TM-105743] p 3227 N92-28674
Neuropsychological components of object identification
[AD-A247049] p 3327 N92-28877
Curvature estimation in orientation selection
[AD-A247862] p 3328 N92-28957
X ray photoelectron spectroscopy study on the double layer at an Al2O3-Al interface
[AD-A246454] p 3265 N92-28972
SHARP LEADING EDGES
Analysis of results of an Euler-equation method applied to leading-edge vortex flow
[NLR-TP-90368-U] p 3226 N92-28657
SHEAR FLOW
The linear and nonlinear shear instability of a fluid sheet
[AD-A247092] p 3282 N92-28258
Large eddy simulations and direct numerical simulations of high speed turbulent reacting flows
p 3285 N92-28818
Modeling of the reactant conversion rate in a turbulent shear flow p 3229 N92-28820
SHEAR LAYERS
Low Reynolds number multiple-time-scale turbulence model and calculations of steady and pulsating shear layers
[NASA-CR-189176] p 3286 N92-28908
SHEAR STRENGTH
Tensile and interlaminar properties of GLARE (trade name) laminates
[AD-A250188] p 3253 N92-28921
SHEAR STRESS
Comparison of drift potential derived from Mars GCM with rock abundance from IRTM p 3395 N92-29078
SHELLFISH
Ultrasonic ambient noise in Australian shallow waters at frequencies up to 200 kHz
[MRL-TR-91-23] p 3351 N92-28364
SHELLS (STRUCTURAL FORMS)
Optimum design of a gearbox for low vibration
[NASA-TM-105653] p 3293 N92-28476
SHERGOTTITES
The stable isotopic compositions of indigenous carbon-bearing components in EETA 79001
p 3384 N92-29021
A liquidus phase diagram for the groundmass of EETA 79001A (Eg), a primitive Shergottite composition
p 3386 N92-29028
SHIELDING
Space Station: Delays in dealing with space debris may reduce safety and increase costs
[GAO/IMTEC-92-50] p 3243 N92-28406
SHIFT REGISTERS
VHDL and waves descriptions for a pseudo-random pattern generator
[AD-A247891] p 3349 N92-28961
SHIP HULLS
A numerical wind tunnel study of viscous-inviscid interaction
[AD-A248429] p 3283 N92-28350
SHIPS
Accuracy of shipborne kinematic GPS surveying
[AD-A245942] p 3230 N92-28317
SHOCK TUNNELS
An analysis of combustion studies in shock expansion tunnels and reflected shock tunnels
[NASA-TP-3224] p 3255 N92-28374
SHOCK WAVE PROFILES
Evaluation of outdoor-to-indoor response to minimized sonic booms
[NASA-CR-189643] p 3352 N92-28556
SHOCK WAVES
Fluids at high shock pressures and temperatures
[DE92-010709] p 3283 N92-28269
Microstructures of shocked quartz
[DE92-010710] p 3363 N92-28333
EXPLOMET 90 international conference on shock-wave and high-strain-rate phenomena in materials
[AD-A248665] p 3303 N92-28892
SHORELINES
Distribution of coastal morphology in the Martian northern lowlands p 3389 N92-29047
SHORT TAKEOFF AIRCRAFT
Internal reversing flow in a tailpipe offtake configuration for SSTOVL aircraft
[NASA-TM-105698] p 3236 N92-28418
The second flight simulator test of the head-up display for NAL QSTOL experimental aircraft (ASKA)
[NAL-TM-633] p 3331 N92-28831
Aerodynamic characteristics obtained from alpha sweep test of the quiet STOL experimental aircraft ASKA
[NAL-TR-1112] p 3234 N92-28901
SHUTTERS
Cryogenic shutter
[NASA-CASE-GSC-13189-2] p 3296 N92-29151
SIDESLIP
Flow visualization studies of a sideslipping, canard-configured X-31A-Like fighter aircraft model
[AD-A245940] p 3228 N92-28883
SIERRA NEVADA MOUNTAINS (CA)
Relationships of soil, grass, and bedrock over the Kaweah serpentine melange through spectral mixture analysis of AVIRIS data
[NASA-CR-190445] p 3306 N92-28717
SIGNAL ANALYZERS
The use of a vector network analyzer for measuring the performance of radar absorbing materials
[AD-A247194] p 3275 N92-28887
The 2.0 GHz sampling rate transversal filter
[AD-A250244] p 3358 N92-28968
SIGNAL DETECTION
Under-ice broadband transient measurements and processing
[AD-A248609] p 3351 N92-28324
Studies of regional wave propagation using differential seismograms and randomized structural models
[AD-A247011] p 3309 N92-28394
Effects of fading and data modulation on noncoherent M-sequence acquisition schemes
[AD-A247968] p 3276 N92-29084
Maximizing the convergence rate of the EM algorithm for the multiple broad-band signal estimation and detection
[AD-A248230] p 3341 N92-29224
SIGNAL DETECTORS
Passive acoustic range estimation of helicopters
[AD-A248033] p 3351 N92-28302
Neural network parameter estimation for the modified bistatic scattering strength model (BISSM)
[AD-A247913] p 3322 N92-28963
SIGNAL ENCODING
Examination of prosodic features in speech signal using speech fundamental frequency and loudness duration
[ETN-92-91334] p 3274 N92-28792

SIGNAL FADING
Fade durations in satellite-path mobile radio propagation
[NASA-CR-190484] p 3273 N92-28586
SIGNAL PROCESSING
Digital hardware architecture implementation
[AD-A249194] p 3332 N92-28236
CESAR address generator
[FFI-91/7021] p 3334 N92-28265
Femtosecond carrier processes in compound semiconductors and real time signal processing
[AD-A248053] p 3278 N92-28275
Adaptive set-membership identification in 0(m) time for linear-in-parameters models
[AD-A249359] p 3273 N92-28358
A radar signal processing ASIC and a VME interface circuit p 3235 N92-28380
Development of a residual acceleration data reduction and dissemination plan p 3271 N92-28453
Closed-loop autonomous docking system
[NASA-CASE-MFS-28421-1] p 3248 N92-28750
Null shifting with fixed delays
[AD-A250059] p 3274 N92-28796
Monaural and binaural processing of complex waveforms
[AD-A247199] p 3352 N92-28889
Diagonal forms of translation operators for helmholtz equation in three dimensions
[AD-A248422] p 3348 N92-28949
The 2.0 GHz sampling rate transversal filter
[AD-A250244] p 3358 N92-28968
SIGNAL REFLECTION
The use of a vector network analyzer for measuring the performance of radar absorbing materials
[AD-A247194] p 3275 N92-28887
SIGNAL TO NOISE RATIOS
Fundamental noise limits in miniature acoustic and vibration sensors
[AD-A247016] p 3352 N92-28413
Mars: Wavelength-dependent dual polarization global scattering p 3384 N92-29020
SIGNAL TRANSMISSION
Modeling pulse transmission in the Monterey Bay using parabolic equation methods
[AD-A246465] p 3322 N92-28977
SIGNATURE ANALYSIS
Evaluation of outdoor-to-indoor response to minimized sonic booms
[NASA-CR-189643] p 3352 N92-28556
SIGNATURES
Evaluation of outdoor-to-indoor response to minimized sonic booms
[NASA-CR-189643] p 3352 N92-28556
SILANES
Silicon polymers
[AD-A250201] p 3265 N92-29145
SILICATES
Experimental determination of the solubility of iridium in silicate melts: Preliminary results p 3310 N92-28591
Mg-perovskite/silicate melt and magnesiowuestite/silicate melt partition coefficients for KLB-1 at 250 Kbars p 3310 N92-28592
Estimation of high temperature metal-silicate partition coefficients p 3311 N92-28599
Magma ocean: Mechanisms of formation p 3312 N92-28600
Mg-perovskite/silicate melt partition coefficients in the CMS system at 2430 C and 226 Kbars p 3312 N92-28601
Evidence for a high temperature differentiation in a molten earth: A preliminary appraisal p 3312 N92-28603
Pressure regimes and core formation in the accreting earth p 3313 N92-28605
Terrestrial magma ocean and core segregation in the earth p 3313 N92-28606
Estimation of the viscosities of silicate liquids at high pressure from measurements of oxygen diffusivity p 3313 N92-28607
Inheritance of magma ocean differentiation during lunar origin by giant impact p 3315 N92-28616
SILICON
The solenoidal detector collaboration silicon detector system
[DE92-011237] p 3356 N92-28356
The silicon compiler for designing military VLSI ASIC's p 3235 N92-28378
Applications of silicon hybrid multi-chip modules to avionics p 3235 N92-28379
Heteroepitaxy of InP on Si (001)
[ETN-92-91333] p 3364 N92-28786
Pressure transducer and system for cryogenic environments
[NASA-CASE-LAR-14579-1] p 3288 N92-29097
Operation and radiation resistance of a FOXFET biasing structure for silicon strip detectors
[DE92-011279] p 3282 N92-29197
Design and realization of polysilicon emitter bipolar transistors
[LAAS-91360] p 3282 N92-29208
SILICON CARBIDES
X ray diffraction study of residual stresses in metal matrix composite-jacketed steel cylinders subjected to internal pressure
[AD-A248449] p 3251 N92-28416
Studies of 1,3-disilacyclobutanes as single-source CVD precursors to silicon carbide
[AD-A247111] p 3365 N92-28885
SILICON CONTROLLED RECTIFIERS
Neutron, gamma ray, and temperature effects on the electrical characteristics of thyristors
[NASA-TM-105728] p 3279 N92-28432
SILICON DIOXIDE
Mg-perovskite/silicate melt partition coefficients in the CMS system at 2430 C and 226 Kbars p 3312 N92-28601
SILICON NITRIDES
Mechanistic studies of superplasticity of structural ceramics
[AD-A246951] p 3263 N92-28558
SILICON POLYMERS
Silicon polymers
[AD-A250201] p 3265 N92-29145
SIMD (COMPUTERS)
Vienna FORTRAN: A language specification, version 1.1
[NASA-CR-189629] p 3337 N92-28760
SIMULATION
Accelerator simulation using computers
[DE92-010729] p 3356 N92-28270
Simulation in infrared imaging: Using electrical circuit principles to model heat transfer
[AD-A248290] p 3278 N92-28276
Coupled structural/thermal/electromagnetic analysis/tailoring of graded composite structures
[NASA-CR-189153] p 3298 N92-28296
An OTH radar clutter simulation
[AD-A248054] p 3272 N92-28304
Taguchi methods in electronics: A case study
[NASA-TM-103586] p 3279 N92-28456
Full mission simulation: A view into the future p 3223 N92-28537
Computations of detonation structure: The influence of model input parameters
[AD-A248634] p 3285 N92-28803
Joint DOE/NSF workshop on flow of particulates and fluids
[DE92-012692] p 3285 N92-28808
The second flight simulator test of the head-up display for NAL QSTOL experimental aircraft (ASKA)
[NAL-TM-633] p 3331 N92-28831
Atomistic simulation of the nanoindentation of diamond and graphite surfaces
[AD-A249296] p 3355 N92-28881
Simulations of surface winds at the Viking Lander sites using a one-level model p 3380 N92-28998
SIMULATORS
High-temperature miniaturized turbine engine lubrication system simulator
[AD-A249259] p 3236 N92-28294
Full mission simulation: A view into the future p 3223 N92-28537
Use of a virtual cockpit for the development of a future transport aircraft p 3225 N92-28547
The role of systems simulation for the development and qualification of ATTAS p 3225 N92-28548
The basic research simulator programme and the industrial and aerospace community: Opportunities for cooperative research
[LR-662] p 3240 N92-28579
NARSIM: A real-time simulator for air traffic control research
[NLR-TP-90147-U] p 3241 N92-29204
SINGLE CRYSTALS
Microstructures of shocked quartz
[DE92-010710] p 3363 N92-28333
Thermal wave imaging and characterization of solids
[AD-A249297] p 3297 N92-28851
Method of intercalating large quantities of fibrous structures
[NASA-CASE-LEW-15077-1] p 3253 N92-29152
SITE SELECTION
Martian surface simulations p 3383 N92-29016
SIZE DISTRIBUTION
The meteoritic contribution to dust and aerosols in the atmosphere of Mars p 3383 N92-29013
SKIN (STRUCTURAL MEMBER)
Generation of spectra and stress histories for fatigue and damage tolerance analysis of fuselage repairs
[AD-A250390] p 3235 N92-29180
SKIN TEMPERATURE (BIOLOGY)
Thermoregulation during spaceflight
[NASA-TM-103913] p 3325 N92-28420
SLABS
Fast algorithms for transport models
[DE92-011432] p 3338 N92-28841
SLEEP
Lapses in alertness: Brain-evoked responses to task-irrelevant auditory probes
[AD-A247669] p 3328 N92-28940
SLOPES
Characterization of Martian near-subsurface materials by determination of cohesion and angle of internal friction p 3393 N92-29068
SNOW
Propagation and scattering of microwaves and millimeter waves in snow based on dense random media theory
[AD-A249300] p 3274 N92-28846
SODIUM COMPOUNDS
Ion conductive polymer solid electrolytes
[DE92-010518] p 3266 N92-29195
SOFTWARE ENGINEERING
Software design for automated assembly of truss structures
[NASA-TP-3198] p 3344 N92-28375
Program Cluster: An identification of fixation cluster characteristics
[AD-A247014] p 3326 N92-28396
Extensibility experiments with the software life-cycle support environment
[AD-A247696] p 3335 N92-28562
Software development using a method base system
[NLR-TP-90387-U] p 3336 N92-28636
Ground Systems Development Environment (GSDE) software configuration management
[NASA-CR-190503] p 3337 N92-28710
Knowledge-based material selection in design
[PNR-90823] p 3337 N92-28741
Development of a high-performance FORTRAN compiler for porting CFD codes to the Navier-Stokes computer
[AD-A250208] p 3342 N92-28770
Compilation and operation environment of an object based language
[ETN-92-91323] p 3338 N92-28785
Repository-based software engineering program: Concept document
[NASA-CR-190384] p 3341 N92-29200
Applications and benefits of formal methods in software development
[REPT-91-33] p 3341 N92-29221
SOFTWARE REUSE
Software development using a method base system
[NLR-TP-90387-U] p 3336 N92-28636
SOFTWARE TOOLS
Object-oriented programming: An assessment of fundamental concepts and design considerations
[AD-A247480] p 3333 N92-28243
HeNCE: Graphical development tools for network-based concurrent computing
[DE92-011061] p 3341 N92-28279
A system structure for predictive relations in penetration mechanics
[AD-A246453] p 3292 N92-28284
An application of interactive computer graphics to the study of inferential statistics and the general linear model
[AD-A246668] p 3334 N92-28285
Extensibility experiments with the software life-cycle support environment
[AD-A247696] p 3335 N92-28562
Software development using a method base system
[NLR-TP-90387-U] p 3336 N92-28636
SPECTOOL: A computer-aided verification tool for hardware designs, volume 1
[AD-A247492] p 3336 N92-28666
Present status of computational tools for Maglev development
[DE92-013252] p 3294 N92-28815
Building the Scientific Modeling Assistant: An interactive environment for specialized software design
[NASA-TM-107844] p 3346 N92-29175
SOIL MOISTURE
Humic substances in soils from Bangladesh, Namibia, and Canada
[OEFZS-4574] p 3316 N92-28740
SOIL SCIENCE
Humic substances in soils from Bangladesh, Namibia, and Canada
[OEFZS-4574] p 3316 N92-28740
SOILS
Relationships of soil, grass, and bedrock over the Kaweah serpentine melange through spectral mixture analysis of AVIRIS data
[NASA-CR-190445] p 3306 N92-28717

The nanophase iron mineral(s) in Mars soil
p 3379 N92-28990
Soil texture and granulometry at the surface of Mars
p 3382 N92-29009
Evidence for crystalline hematite as an accessory phase in Martian soils
p 3391 N92-29059
Surface photometric properties and albedo changes in the central equatorial region of Mars
p 3392 N92-29066

SOL-GEL PROCESSES
Sol-gel processed multifunctional organic polymer-inorganic oxide composites for electronics and photonics
[AD-A246773] p 3263 N92-28412
Formation, structure, and properties of boron nitride fibers from polymer precursors
[AD-A247679] p 3263 N92-28553

SOLAR ACTIVITY
Nonlinear techniques for forecasting solar activity directly from its time series
[NASA-TM-107946] p 3396 N92-28870
Detecting and disentangling nonlinear structure from solar flux time series
[NASA-CR-190510] p 3396 N92-28871

SOLAR ARRAYS
Arcjet plume ionization effects on exposed solar array conducting surfaces
[AD-A245912] p 3307 N92-28383
Solar Array Module Plasma Interaction Experiment (SAMPIE): Technical requirements document
[NASA-TM-105660] p 3246 N92-28683

SOLAR CELLS
Thin film cadmium telluride photovoltaic cells
[DE92-001239] p 3306 N92-28277
Solar Array Module Plasma Interaction Experiment (SAMPIE): Technical requirements document
[NASA-TM-105660] p 3246 N92-28683

SOLAR CYCLES
Mathematical modeling of solar magneto-dynamics
[AD-A247158] p 3395 N92-28520

SOLAR ENERGY
Solar thermal energy receiver
[NASA-CASE-LEW-14949-1] p 3307 N92-29143

SOLAR FLUX
Future mission studies: Preliminary comparisons of solar flux models
[NASA-TM-107947] p 3396 N92-28869
Nonlinear techniques for forecasting solar activity directly from its time series
[NASA-TM-107946] p 3396 N92-28870
Detecting and disentangling nonlinear structure from solar flux time series
[NASA-CR-190510] p 3396 N92-28871
Future mission studies: Forecasting solar flux directly from its chaotic time series
[NASA-CR-190378] p 3396 N92-28872
Evidence of chaotic pattern in solar flux through a reproducible sequence of period-doubling-type bifurcations
[NASA-TM-107944] p 3396 N92-28907

SOLAR NEUTRINOS
The many aspects of neutrino physics
[DE92-011735] p 3355 N92-28858

SOLAR OBSERVATORIES
Science and application payloads in the 1990's
[NASA-TM-107937] p 3246 N92-28370

SOLAR RADIATION
Optical effects on ocean mixed layer dynamics
[AD-A245941] p 3320 N92-28316
Short- and long-term climate changes on Mars
p 3389 N92-29051

SOLAR SYSTEM
Planetary geosciences, 1989-1990
[NASA-SP-508] p 3372 N92-28345

SOLAR WIND
Mars atmosphere evolution: Escape to space
p 3387 N92-29034

SOLAR X-RAYS
Future mission studies: Preliminary comparisons of solar flux models
[NASA-TM-107947] p 3396 N92-28869

SOLDERING
High temperature solder device for flat cables
[NASA-CASE-GSC-13344-1] p 3261 N92-29094

SOLENOIDS
A generalization of the K-V equilibrium for an intense, relativistic beam propagating in a solenoid
[AD-A247067] p 3350 N92-28238

SOLID CRYOGENS
Relaxation dynamics of highly excited halogens in their electronic ground states
[AD-A247312] p 3254 N92-28300

SOLID ELECTROLYTES
Secondary Li battery incorporating 12-Crown-4 ether
[NASA-CASE-NPO-17922-1-CU] p 3280 N92-28753
Ion conductive polymer solid electrolytes
[DE92-010518] p 3266 N92-29195

SOLID LUBRICANTS
Effect of metallic coating properties on the tribology of oil-lubricated coated-ceramics
[DE92-010904] p 3262 N92-28339

SOLID PROPELLANT COMBUSTION
Combustion mechanisms of solids --- solid rocket propellant
[AD-A247088] p 3254 N92-28240

SOLID PROPELLANT ROCKET ENGINES
Solid-propellant-powered maneuvering system for spacecraft
[AD-D015245] p 3249 N92-28747
Ablation of material of solid propellant motor nozzles
[ONERA-NT-1990-13] p 3249 N92-28780
Introduction to rocket propulsion
[AD-A250424] p 3249 N92-28800
Investigation of energy exchange mechanisms between the mean and acoustic flow fields in solid rocket combustion chambers
[AD-A247402] p 3250 N92-28931

SOLID PROPELLANTS
Propellant-to-inhibitor bonding system
[AD-D015243] p 3266 N92-28739
Investigation of energy exchange mechanisms between the mean and acoustic flow fields in solid rocket combustion chambers
[AD-A247402] p 3250 N92-28931

SOLID ROCKET PROPELLANTS
Kinetic studies of metal combustion in propulsion
[AD-A250207] p 3256 N92-28769
Introduction to rocket propulsion
[AD-A250424] p 3249 N92-28800

SOLID-SOLID INTERFACES
Shallow states of donor impurities on periodically structured semiconductors interfaces
[DE92-622791] p 3363 N92-28312

SOLIDIFICATION
Workshop on the Physics and Chemistry of Magma Oceans from 1 Bar to 4 Mbar
[NASA-CR-190419] p 3310 N92-28587
Thermal evolution and chemical differentiation of the terrestrial magma ocean
p 3310 N92-28588
Fate of a perched crystal layer in a magma ocean
p 3312 N92-28602
Effect of solidification technique and consolidation method on the properties of rapidly solidified Al-Fe alloys
[DLR-FB-91-24] p 3260 N92-28823

SOLIDS
Multiple-valued programmable logic array minimization by simulated annealing
[AD-A248620] p 3335 N92-28353
Thermal wave imaging and characterization of solids
[AD-A249297] p 3297 N92-28851

SOLIDS FLOW
Joint DOE/NSF workshop on flow of particulates and fluids
[DE92-012692] p 3285 N92-28808

SOLUBILITY
Experimental determination of the solubility of iridium in silicate melts: Preliminary results
p 3310 N92-28591

SOLVATION
Dynamical solvent effects on activated electron-transfer reactions: Principles, pitfalls, and progress
[AD-A246764] p 3363 N92-28349

SOLVENTS
Dynamical solvent effects on activated electron-transfer reactions: Principles, pitfalls, and progress
[AD-A246764] p 3363 N92-28349
Erosion of stainless steel by ultrasonic cleaning: A preliminary study
[DE92-012566] p 3260 N92-28763
An investigation into techniques for the determination of moisture content on activated carbon
[AD-A245938] p 3256 N92-28882
Simulations of solvent effects on confined electrolytes
[AD-A246851] p 3258 N92-28982

SONAR
Image processing techniques for acoustic images
[AD-A247303] p 3352 N92-28559
Lapses in alertness: Brain-evoked responses to task-irrelevant auditory probes
[AD-A247669] p 3328 N92-28940

SONIC ANEMOMETERS
Evaluation of a Solent sonic anemometer on RRS Charles Darwin Cruise 43
[IOS-288-1991] p 3323 N92-29213

SONIC BOOMS
Evaluation of outdoor-to-indoor response to minimized sonic booms
[NASA-CR-189643] p 3352 N92-28556

SOUND FIELDS
Detection of in-plane displacements of acoustic wave fields using extrinsic Fizeau fiber interferometric sensors
[NASA-CR-190493] p 3353 N92-29196

SOUND PRESSURE
Fundamental noise limits in miniature acoustic and vibration sensors
[AD-A247016] p 3352 N92-28413
Modal element method for scattering of sound by absorbing bodies
[NASA-TM-105722] p 3353 N92-28984
Annoyance due to discrete tones in broadband background noise. Part 2: Analysis
[ISVR-TR-202-PT-2] p 3353 N92-29203

SOUND TRANSMISSION
Modeling pulse transmission in the Monterey Bay using parabolic equation methods
[AD-A246465] p 3322 N92-28977

SOUND WAVES
A new ocean bottom magnetometer system for continental shelf measurements
[AD-A247644] p 3321 N92-28321
In line optical fibre frequency shifter project
[AD-A246714] p 3357 N92-28372
Mobility power flow analysis of coupled plate structure subjected to mechanical and acoustic excitation
[NASA-CR-189635] p 3352 N92-28722
Investigation of energy exchange mechanisms between the mean and acoustic flow fields in solid rocket combustion chambers
[AD-A247402] p 3250 N92-28931
Modeling pulse transmission in the Monterey Bay using parabolic equation methods
[AD-A246465] p 3322 N92-28977
Detection of in-plane displacements of acoustic wave fields using extrinsic Fizeau fiber interferometric sensors
[NASA-CR-190493] p 3353 N92-29196

SOUNDING
Mesoscale vertical structure of an explosive oceanic cyclone
[AD-A245927] p 3318 N92-28423

SPACE DEBRIS
Space Station: Delays in dealing with space debris may reduce safety and increase costs
[GAO/IMTEC-92-50] p 3243 N92-28406

SPACE ELECTRIC ROCKET TESTS
Development and flight history of SERT 2 spacecraft
[NASA-TM-105636] p 3250 N92-28983

SPACE ERECTABLE STRUCTURES
Software design for automated assembly of truss structures
[NASA-TP-3198] p 3344 N92-28375

SPACE EXPLORATION
Ongoing Progress in Spacecraft Controls
[NASA-CP-10099] p 3247 N92-28730
Review of Mars mission scenarios
p 3244 N92-28731
MARSNET surface and atmosphere investigations
p 3381 N92-29002

SPACE FLIGHT
Thermoregulation during spaceflight
[NASA-TM-103913] p 3325 N92-28420
Space flight: The first 30 years
[NASA-NP-150] p 3397 N92-28678
Whole body cleaning agent containing N-acyltaurate
[NASA-CASE-MSC-21589-1] p 3332 N92-29137

SPACE LABORATORIES
Development of a residual acceleration data reduction and dissemination plan
p 3271 N92-28453

SPACE LAW
Space life sciences strategic plan
[NASA-TM-107954] p 3244 N92-29100

SPACE MANUFACTURING
International Workshop on Vibration Isolation Technology for Microgravity Science Applications
[NASA-CP-10094] p 3268 N92-28436

SPACE MISSIONS
Space life support engineering program
[NASA-CR-190448] p 3330 N92-28671

SPACE NAVIGATION
Some aerospace applications of estimation theory
[ETN-92-91281] p 3349 N92-28647
DLR research reports and communications
[ISSN-0939-2971] p 3397 N92-29218
Activities report of the DLR
[ISSN-0938-2194] p 3397 N92-29219

SPACE PERCEPTION
Neuropsychological components of object identification
[AD-A247049] p 3327 N92-28877

SPACE PLASMAS
SPEAR 2 space power data analysis
[AD-A248057] p 3250 N92-28945
The effect of induced charges on low-energy particle trajectories near conducting and semiconducting plates
[NASA-TM-103589] p 3355 N92-28986

SPACE PLATFORMS
Science and application payloads in the 1990's
[NASA-TM-107937] p 3246 N92-28370
Vibration isolation technology development to demonstration p 3267 N92-28442
New inertial actuator provides isolation and stabilization in microgravity conditions p 3267 N92-28443
Theoretical and experimental studies relevant to interpretation of auroral emissions
[NASA-CR-190521] p 3316 N92-28911
SPACE POWER REACTORS
Natural circulation decay heat removal from an SP-100, 550 kWe power system for a lunar outpost
[NASA-CR-190421] p 3307 N92-28863
SPACE PROCESSING
Numerical studies of convective transport associated with crystal growth in mirrogravity p 3267 N92-28437
An examination of anticipated g-jitter on Space Station and its effects on materials processes
p 3267 N92-28438
The Microgravity Isolation Mount (MGIM): A Columbus facility for improving the microgravity quality of payloads
p 3267 N92-28439
SPACE SHUTTLE MAIN ENGINE
Replacement bearing for Rocketdyne SSME HPOTPs using alternate self-lubricating retainer materials
[NASA-CR-184328] p 3292 N92-28362
Integrated health monitoring and controls for rocket engines
[NASA-TM-105763] p 3249 N92-28693
SPACE SHUTTLE MISSIONS
Empirical techniques for the study of acceleration mechanisms in the space environment
[AD-A249940] p 3248 N92-28765
SPACE SHUTTLE ORBITERS
Extended H2 synthesis for microgravity vibration isolation p 3267 N92-28447
ACAP: Acceleration Characterization and Analysis Project p 3267 N92-28448
SPACE SHUTTLE PAYLOADS
Payload isolation and stabilization by a Suspended Experiment Mount (SEM)
[NASA-TM-107941] p 3246 N92-28369
SPACE SHUTTLES
International Workshop on Vibration Isolation Technology for Microgravity Science Applications
[NASA-CP-10094] p 3268 N92-28436
Microgravity accelerometer characterization on Columbia STS-32 mission p 3271 N92-28452
In-flight simulation studies at the NASA Dryden Flight Research Facility
[NASA-TM-4396] p 3234 N92-29110
SPACE SIMULATORS
Simulation of Martian surface-atmosphere interaction in a space-simulator: Technical considerations and feasibility p 3388 N92-29044
SPACE STATION FREEDOM
International Workshop on Vibration Isolation Technology for Microgravity Science Applications
[NASA-CP-10094] p 3268 N92-28436
An examination of anticipated g-jitter on Space Station and its effects on materials processes
p 3267 N92-28438
Space Station Freedom microgravity environment requirements and assessment methods
p 3268 N92-28450
Predicting microgravity levels for space station using VAPEPS p 3268 N92-28455
SPACE STATION PAYLOADS
Payload isolation and stabilization by a Suspended Experiment Mount (SEM)
[NASA-TM-107941] p 3246 N92-28369
SPACE STATIONS
Space Station: Delays in dealing with space debris may reduce safety and increase costs
[GAO/IMTEC-92-50] p 3243 N92-28406
NASDA's activities on vibration isolation technology
p 3267 N92-28441
A 6 degree-of-freedom Lorentz force vibration isolator with nonlinear controller p 3267 N92-28444
SPACE TOOLS
Quick application/release nut with engagement indicator
[NASA-CASE-MSC-21799-1] p 3296 N92-29150
SPACE TRANSPORTATION
Evaluation of future space transportation systems with regard to their reliabilities and costs
[DLR-FB-91-27] p 3245 N92-28826
SPACE TRANSPORTATION SYSTEM
Space transportation analysis and design
[AD-A250629] p 3245 N92-28956
SPACE TRANSPORTATION SYSTEM FLIGHTS
Microgravity accelerometer characterization on Columbia STS-32 mission p 3271 N92-28452
Performance of uncoated AFRSI blankets during multiple Space Shuttle flights
[NASA-TM-103892] p 3245 N92-29104
SPACEBORNE ASTRONOMY
Analysis of Mir-HEXE observations: Pulsation and energy spectra of the x ray double star SMC X-1 in 20 to 80 keV energy field
[ETN-92-91487] p 3371 N92-29128
Calibration of high energy x ray detectors at the spectrum of the Crab nebula, and x ray pulsar A0535+26 examinations
[ETN-92-91484] p 3371 N92-29177
SPACEBORNE EXPERIMENTS
Science and application payloads in the 1990's
[NASA-TM-107937] p 3246 N92-28370
NASDA's activities on vibration isolation technology
p 3267 N92-28441
Extended H2 synthesis for microgravity vibration isolation p 3267 N92-28447
Telescience experiments using the Prototype Optical Diagnostic Instrument (PODI)
[NLR-TP-90199-U] p 3358 N92-28656
Solar Array Module Plasma Interaction Experiment (SAMPIE): Technical requirements document
[NASA-TM-105660] p 3246 N92-28683
SPACECRAFT COMMUNICATION
Scientific applications of frequency-stabilized laser technology in space
[NASA-CR-190449] p 3291 N92-28941
SPACECRAFT CONTROL
Ongoing Progress in Spacecraft Controls
[NASA-CP-10099] p 3247 N92-28730
Fuel optimal propulsive reboost of flexible spacecraft
p 3247 N92-28734
Fuel optimal maneuver: Experimental testbeds
p 3247 N92-28735
Identification of linear system models and state estimators for controls p 3247 N92-28737
Scientific applications of frequency-stabilized laser technology in space
[NASA-CR-190449] p 3291 N92-28941
A generalized reusable guidance algorithm for optimal aerobraking
[NASA-TM-103590] p 3229 N92-28981
SPACECRAFT DOCKING
Closed-loop autonomous docking system
[NASA-CASE-MFS-28421-1] p 3248 N92-28750
SPACECRAFT ENVIRONMENTS
Shock and vibration isolation for cyclic exercise in spacecraft p 3267 N92-28449
Spacecraft sustained load fracture control
[NLR-TP-89163-U] p 3302 N92-28643
SPACECRAFT GUIDANCE
A generalized reusable guidance algorithm for optimal aerobraking
[NASA-TM-103590] p 3229 N92-28981
SPACECRAFT MANEUVERS
Fuel optimal maneuver: Experimental testbeds
p 3247 N92-28735
SPACECRAFT MODELS
Predicting microgravity levels for space station using VAPEPS p 3268 N92-28455
SPACECRAFT ORBITS
Coordinate systems for space and geophysical applications
[AD-A247550] p 3244 N92-28937
SPACECRAFT POWER SUPPLIES
High temperature dielectric properties of Apical, Kapton, Peek, Teflon AF, and Upilex polymers
[NASA-TM-105753] p 3280 N92-28675
Solar Array Module Plasma Interaction Experiment (SAMPIE): Technical requirements document
[NASA-TM-105660] p 3246 N92-28683
NASA Lewis Stirling SPRE testing and analysis with reduced number of cooler tubes
[NASA-TM-105767] p 3307 N92-28837
SPEAR 2 space power data analysis
[AD-A248057] p 3250 N92-28945
SPACECRAFT PROPULSION
Solid-propellant-powered maneuvering system for spacecraft
[AD-D015245] p 3249 N92-28747
Development and flight history of SERT 2 spacecraft
[NASA-TM-105636] p 3250 N92-28983
SPACECRAFT SHIELDING
Evaluation of Whipple bumper shields at 7 and 10 km/s
[NASA-TM-107958] p 3295 N92-28925
SPACECRAFT STABILITY
Prediction of attitude stability of asymmetric dual-spin stabilized spacecraft using improved liquid slosh model
[AD-A247023] p 3246 N92-28368
SPACECRAFT TRACKING
Scientific applications of frequency-stabilized laser technology in space
[NASA-CR-190449] p 3291 N92-28941
SPACECRAFT TRAJECTORIES
A generalized reusable guidance algorithm for optimal aerobraking
[NASA-TM-103590] p 3229 N92-28981
SPALLATION
Quark matter and cosmology
[DE92-011736] p 3371 N92-28859
SPATIAL DISTRIBUTION
Curvature estimation in orientation selection
[AD-A247862] p 3328 N92-28957
Substrate induced ordering of molecular adsorbates on Au(111)
[AD-A246850] p 3258 N92-29185
SPATIAL RESOLUTION
Thermally distinct ejecta blankets from Martian craters
p 3379 N92-28994
SPECIFICATIONS
Automated apparel specification retrieval system
[AD-A248619] p 3367 N92-28389
SPECTRA
Development of rotating shadowband spectral radiometers and GCM radiation code test data sets in support of ARM
[DE92-011438] p 3316 N92-28853
Analyzing noisy spectral line shapes
[DE92-011153] p 3362 N92-29086
Calibration of high energy x ray detectors at the spectrum of the Crab nebula, and x ray pulsar A0535+26 examinations
[ETN-92-91484] p 3371 N92-29177
SPECTRAL BANDS
Spectral identification of chemisorbed CO2 and application to Mars analog materials
p 3378 N92-28510
SPECTRAL EMISSION
A Be star atlas of far UV and optical high-resolution spectra
[ESA-SP-1147] p 3371 N92-28781
SPECTRAL ENERGY DISTRIBUTION
Relaxation dynamics of highly excited halogens in their electronic ground states
[AD-A247312] p 3254 N92-28300
SPECTRAL METHODS
On some splitting schemes for wave equations
[FFI-91/7023] p 3348 N92-29193
SPECTRAL REFLECTANCE
Relationships of soil, grass, and bedrock over the Kaweah serpentine melange through spectral mixture analysis of AVIRIS data
[NASA-CR-190445] p 3306 N92-28717
Remote sensing applications of the extended radiosity method
[DE92-011356] p 3306 N92-28807
The nanophase iron mineral(s) in Mars soil
p 3379 N92-28990
Mars surface weathering products and spectral analogs: Palagonites and synthetic iron minerals
p 3383 N92-29017
Exploring compositional variations on the surface of Mars applying mixing modeling to a telescopic spectral image p 3388 N92-29043
SPECTRAL RESOLUTION
Surface vs. atmospheric origin of 2.1-2.5 micron absorption features in the Martian spectrum
p 3373 N92-28480
SPECTRAL SIGNATURES
Spectral identification of chemisorbed CO2 and application to Mars analog materials
p 3378 N92-28510
SPECTROMETERS
The solenoidal detector collaboration silicon detector system
[DE92-011237] p 3356 N92-28356
The 17 keV neutrino and neutrino tagging
[DE92-011281] p 3355 N92-28839
Multicomponent comparison of optical and mass spectrometric diagnostics in low-pressure flames
[AD-A250323] p 3257 N92-28954
SPECTROSCOPIC ANALYSIS
An overview of in-flight plume diagnostics for rocket engines
[NASA-TM-105727] p 3248 N92-28417
Mars: Compositional variability of ferric/ferrous minerals and polar volatiles from groundbased imaging spectroscopy p 3379 N92-28993
SPECTROSCOPY
An overview of in-flight plume diagnostics for rocket engines
[NASA-TM-105727] p 3248 N92-28417
Asynchronous optical sampling for laser-based combustion diagnostics in high-pressure flames
[AD-A250206] p 3257 N92-28896
Iron Moessbauer spectroscopy: Superparamagnetism in hydrothermal vents and the search for evidence of past life on Mars p 3378 N92-28989

Mars: Compositional variability of ferric/ferrous minerals and polar volatiles from groundbased imaging spectroscopy p 3379 N92-28993
Non-mechanical optical path switching and its application to dual beam spectroscopy including gas filter correlation radiometry
[NASA-CASE-LAR-14588-1-CU] p 3359 N92-29117

SPECTRUM ANALYSIS
An analysis of middle ultraviolet dayglow spectra
[AD-A245965] p 3309 N92-28319
Surface vs. atmospheric origin of 2.1-2.5 micron absorption features in the Martian spectrum p 3373 N92-28480
Relationships of soil, grass, and bedrock over the Kaweah serpentine melange through spectral mixture analysis of AVIRIS data
[NASA-CR-190445] p 3306 N92-28717
Diagonal forms of translation operators for helmholtz equation in three dimensions
[AD-A248422] p 3348 N92-28949
The 2.0 GHz sampling rate transversal filter
[AD-A250244] p 3358 N92-28968
Exploring compositional variations on the surface of Mars applying mixing modeling to a telescopic spectral image p 3388 N92-29043
Method and apparatus for frequency spectrum analysis
[NASA-CASE-NPO-17759-1-CU] p 3276 N92-29124
Demodulation processes in auditory perception
[AD-A250203] p 3328 N92-29146
Generation of spectra and stress histories for fatigue and damage tolerance analysis of fuselage repairs
[AD-A250390] p 3235 N92-29180
Directional wave data recorded off Flamborough Head (England)
[IOS-273-1990] p 3323 N92-29216

SPEECH
Examination of prosodic features in speech signal using speech fundamental frequency and loudness duration
[ETN-92-91334] p 3274 N92-28792

SPHERES
A fast direct solver for a class of two-dimensional separable elliptic equations on the sphere
[NASA-TM-104567] p 3346 N92-28297

SPHERICAL COORDINATES
A comparative study of the accuracy of various time domain nonorthogonal mesh methods
[DE92-007300] p 3347 N92-28824

SPIRAL ANTENNAS
The use of conformal subdomain basis functions in the method of moments computations for a thin wire
[AD-A245964] p 3272 N92-28347

SPLINE FUNCTIONS
Fourier analysis of the approximation power of principal shift-invariant spaces
[AD-A246713] p 3347 N92-28411

SPLIT FLAPS
Construction of a numerical optimization method for the definition of hypersupported profiles
[ONERA-RSF-43/1736-AY-146A] p 3284 N92-28788

SPLITTING
Split events and their influence on pn CCD energy spectra
[ETN-92-91485] p 3282 N92-29178
On some splitting schemes for wave equations
[FFI-91/7023] p 3348 N92-29193

SPRAY CHARACTERISTICS
Ground deposition of liquid droplets released from a point source in the atmospheric surface layer
[ISBN-0-315-51071-4] p 3316 N92-28703

SPRAY NOZZLES
Hydrogen no-vent fill testing in a 5 cubic foot (142 liter) tank using spray nozzle and spray bar liquid injection
[NASA-TM-105759] p 3266 N92-28433

SPRAYED COATINGS
Evaluation of plasma sprayed crucible coatings for melt processing copper-refractory metal alloys
[DE92-010871] p 3259 N92-28338

SPRAYERS
Ground deposition of liquid droplets released from a point source in the atmospheric surface layer
[ISBN-0-315-51071-4] p 3316 N92-28703

SPREAD SPECTRUM TRANSMISSION
Effects of fading and data modulation on noncoherent M-sequence acquisition schemes
[AD-A247968] p 3276 N92-29084

SPUTTERING
Thin film cadmium telluride photovoltaic cells
[DE92-001239] p 3306 N92-28277
History of oxygen and carbon escape from the Martian atmosphere p 3376 N92-28498

STABILITY
Stability and optimal control theory of hereditary systems with applications from oscillating flying vehicles, mechanical systems, and robotics p 3247 N92-28732
Phase stability of injection-locked beam of semiconductor lasers
[NASA-TT-10001] p 3290 N92-28862
Windshear radar calibration: Transmitter power and receiver gain stability
[NASA-TM-107589] p 3275 N92-28876
Tuning and automatic phase adjustment in external cavity diode laser beam combiners
[AD-A247421] p 3290 N92-28903
The Martian polar caps: Stability and water transport at low obliquities p 3385 N92-29023
Turbulent spectra, fluxes, stability and growth of the mixed layer in the boundary layer of Mars p 3393 N92-29070

STABILITY TESTS
Digital control algorithms for microgravity isolation systems p 3267 N92-28445
Stability and control flight testing of a half-scale Pioneer remotely piloted vehicle
[AD-A245973] p 3239 N92-28801

STABILIZATION
Control and stabilization of distributed parameter systems in structural dynamics
[AD-A247097] p 3298 N92-28320
New inertial actuator provides isolation and stabilization in microgravity conditions p 3267 N92-28443

STABILIZED PLATFORMS
Payload isolation and stabilization by a Suspended Experiment Mount (SEM)
[NASA-TM-107941] p 3246 N92-28369

STAINLESS STEELS
Erosion of stainless steel by ultrasonic cleaning: A preliminary study
[DE92-012566] p 3260 N92-28763

STANDARDS
Responsible science: Ensuring the integrity of the research process, volume 1
[ISBN-0-309-04731-5] p 3350 N92-28363
Applications and benefits of formal methods in software development
[REPT-91-33] p 3341 N92-29221

STAR DISTRIBUTION
Observational study and analysis of point sources found by the infrared astronomy satellite
[AD-A248416] p 3371 N92-28843

STARS
The physics of strange matter
[DE92-011734] p 3371 N92-28774
A Be star atlas of far UV and optical high-resolution spectra
[ESA-SP-1147] p 3371 N92-28781

STATE ESTIMATION
Identification of linear system models and state estimators for controls p 3247 N92-28737

STATIC STABILITY
Stability and control flight testing of a half-scale Pioneer remotely piloted vehicle
[AD-A245973] p 3239 N92-28801
Calculation of support interferences on the aerodynamic coefficients for a wind tunnel calibration model
[ESA-TT-1247] p 3229 N92-29159

STATISTICAL ANALYSIS
Computer assisted improvement of the estimation mean squared error with application to back propagation neural networks
[AD-A247724] p 3344 N92-28401
Predicting microgravity levels for space station using VAPEPS p 3268 N92-28455
Atmospheric turbulence spectra and correlation functions
[NLR-TP-89217-U] p 3316 N92-28689
Future mission studies: Preliminary comparisons of solar flux models
[NASA-TM-107947] p 3396 N92-28869
Evidence of chaotic pattern in solar flux through a reproducible sequence of period-doubling-type bifurcations
[NASA-TM-107944] p 3396 N92-28907
Computer recognition and analysis of photogrammetric targets
[AD-A250313] p 3339 N92-28971
Martian channel networks: A revised Strahler approach for quantitative morphometry p 3380 N92-29000

STATISTICAL DISTRIBUTIONS
Distribution theory for selection from logistic populations
[MEMO-COSOR-91-23] p 3348 N92-28640
Estimation of the point of incipient deterioration and a class of life distribution with application to cannibalization
[AD-A250216] p 3343 N92-29114
Substrate induced ordering of molecular adsorbates on Au(111)
[AD-A246850] p 3258 N92-29185

STATISTICAL MECHANICS
Multiple-valued programmable logic array minimization by simulated annealing
[AD-A248620] p 3335 N92-28353
The nonequilibrium molecular dynamics
[DE92-011760] p 3355 N92-28860

STEADY FLOW
Low Reynolds number multiple-time-scale turbulence model and calculations of steady and pulsating shear layers
[NASA-CR-189176] p 3286 N92-28908

STEADY STATE
Engine performance and health monitoring models using steady state and transient prediction methods p 3238 N92-28467
NASA Lewis steady-state heat pipe code users manual
[NASA-TM-105161] p 3249 N92-28682

STEAM
Underwater vapor phase burning of aluminum particles and on aluminum ignition during steam explosions
[DE92-011196] p 3257 N92-28894

STEEL STRUCTURES
X ray diffraction study of residual stresses in metal matrix composite-jacketed steel cylinders subjected to internal pressure
[AD-A248449] p 3251 N92-28416

STEELS
Weld pool flow visualization studies during gas tungsten arc welding of steel and aluminum
[AD-A249204] p 3292 N92-28293
Surface residual stress analysis of metals and alloys
[AD-A248372] p 3259 N92-28426
Method and apparatus for using magneto-acoustic remanence to determine embrittlement
[NASA-CASE-LAR-13817-5] p 3303 N92-28757
Magnetic remanence method and apparatus to test materials for embrittlement
[NASA-CASE-LAR-13817-4] p 3304 N92-29101
Magneto acoustic emission method for testing materials for embrittlement
[NASA-CASE-LAR-13817-2] p 3304 N92-29155

STEERING
Closed-loop autonomous docking system
[NASA-CASE-MFS-28421-1] p 3248 N92-28750

STELLAR LUMINOSITY
Observational study and analysis of point sources found by the infrared astronomy satellite
[AD-A248416] p 3371 N92-28843

STELLAR MODELS
Observational study and analysis of point sources found by the infrared astronomy satellite
[AD-A248416] p 3371 N92-28843
Future mission studies: Preliminary comparisons of solar flux models
[NASA-TM-107947] p 3396 N92-28869
Nonlinear techniques for forecasting solar activity directly from its time series
[NASA-TM-107946] p 3396 N92-28870
Detecting and disentangling nonlinear structure from solar flux time series
[NASA-CR-190510] p 3396 N92-28871

STELLAR STRUCTURE
Observational study and analysis of point sources found by the infrared astronomy satellite
[AD-A248416] p 3371 N92-28843

STELLARATORS
Ignition access condition based on the generalized saddle point in a magnetic fusion reactor
[PPL-109] p 3361 N92-28665

STIRLING CYCLE
NASA Lewis Stirling SPRE testing and analysis with reduced number of cooler tubes
[NASA-TM-105767] p 3307 N92-28837

STIRLING ENGINES
M-H characteristics and demagnetization resistance of samarium-cobalt permanent magnets to 300 C
[NASA-CR-189194] p 3280 N92-28723
NASA Lewis Stirling SPRE testing and analysis with reduced number of cooler tubes
[NASA-TM-105767] p 3307 N92-28837
Solar thermal energy receiver
[NASA-CASE-LEW-14949-1] p 3307 N92-29143

STOCHASTIC PROCESSES
Plane wave propagation in random granular media
[AD-A247300] p 3298 N92-28424
Matrix-geometric analysis of the shortest queue problem with threshold jockeying
[MEMO-COSOR-91-24] p 3347 N92-28641
Global minimum solution of engineering design problems
[AD-A247496] p 3337 N92-28704
Stochastic simulation of the structure and propagation rate of turbulent premixed flames
[DE92-006682] p 3256 N92-28822

STOICHIOMETRY
Reactant conversion in homogeneous turbulence: Mathematical modeling, computational validations and practical applications p 3285 N92-28819
STORAGE BATTERIES
Secondary Li battery incorporating 12-Crown-4 ether [NASA-CASE-NPO-17922-1-CU] p 3280 N92-28753
STORAGE RINGS (PARTICLE ACCELERATORS)
Aperture coupling measurement in a test chamber for the Advanced Photon Source (APS) [DE92-013059] p 3274 N92-28809
RF impedance measurement status for the 7-GeV Advanced Photon Source (APS) [DE92-013060] p 3274 N92-28810
STORAGE TANKS
Replacement of the NAL high pressure air storage system [NAL-TM-634] p 3241 N92-28835
STRAIN GAGE BALANCES
Studies in general aviation aerodynamics [NASA-CR-190431] p 3226 N92-28511
STRAIN GAGES
Development of an embedded Fabry Perot Fiber Optic Strain Rosette Sensor (FP-FOSRS) [NASA-CR-190490] p 3358 N92-29088
STRAIN MEASUREMENT
Development of an embedded Fabry Perot Fiber Optic Strain Rosette Sensor (FP-FOSRS) [NASA-CR-190490] p 3358 N92-29088
STRAIN RATE
Instrumentation for ultrahigh strain rate experiments [AD-A249358] p 3298 N92-28327
The stress corrosion cracking behavior of AlLi 2090-T83 in substitute ocean water [LR-661] p 3259 N92-28578
EXPLOMET 90 international conference on shock-wave and high-strain-rate phenomena in materials [AD-A248665] p 3303 N92-28892
STRATA
Development of a stratified plate model for composite panels [AD-A248206] p 3253 N92-29192
STRATIGRAPHY
The distribution of anorthosite on the nearside of the moon p 3311 N92-28594
Amazonis and Utopia Planitiae: Martian Lacustrine basins p 3391 N92-29056
STRESS ANALYSIS
A combined experimental and analytical investigation of the theory of plasticity involving strain induced anisotropy [AD-A248440] p 3298 N92-28352
Replacement bearing for Rocketdyne SSME HPOTPs using alternate self-lubricating retainer materials [NASA-CR-184328] p 3292 N92-28362
X ray diffraction study of residual stresses in metal matrix composite-jacketed steel cylinders subjected to internal pressure [AD-A248449] p 3251 N92-28416
Surface residual stress analysis of metals and alloys [AD-A248372] p 3259 N92-28426
Stress analysis of plated-through-holes in rigid flex multilayer printed wiring boards [DE92-011659] p 3303 N92-28855
Generation of spectra and stress histories for fatigue and damage tolerance analysis of fuselage repairs [AD-A250390] p 3235 N92-29180
STRESS CORROSION CRACKING
The stress corrosion cracking behavior of AlLi 2090-T83 in substitute ocean water [LR-661] p 3259 N92-28578
Spacecraft sustained load fracture control [NLR-TP-89163-U] p 3302 N92-28643
Effect of cooling rate on corrosion properties of high strength aluminium alloys under atmospheric conditions [NLR-TP-90138-U] p 3260 N92-28691
STRESS INTENSITY FACTORS
The buckling behavior of a central crack in a plate under tension [LR-667] p 3299 N92-28583
Pre-test analyses for pressurized thermoshock tests, vessel 1 [VTT-RR-746] p 3303 N92-28776
STRESS WAVES
Method for advanced material characterization by laser induced eddy current imaging [NASA-CASE-GSC-13386-1] p 3298 N92-29154
STRESS-STRAIN RELATIONSHIPS
Multiphase structure of a segmented polyurethane: Effects of temperature and annealing [AD-A247594] p 3262 N92-28250
Elevated temperature axial and torsional fatigue behavior of Haynes 188 [NASA-TM-105396] p 3302 N92-28701
STRING THEORY
Proceedings of the workshop on Quantum Gravity and Topology [DE92-782191] p 3366 N92-28235
STRIP TRANSMISSION LINES
Investigation of an equivalent circuit for the inductive strip in finline with dielectric [AD-A247025] p 3279 N92-28373
STRONTIUM 90
Determination of field related transfer factors for Cs-137 and Sr-90, from the fallout of the reactor accident in Chernobyl (USSR) [OEFZS-4581] p 3356 N92-29210
STRUCTURAL ANALYSIS
Coupled structural/thermal/electromagnetic analysis/tailoring of graded composite structures [NASA-CR-189153] p 3298 N92-28296
Control and stabilization of distributed parameter systems in structural dynamics [AD-A247097] p 3298 N92-28320
Probabilistic finite element analysis [AD-A247721] p 3347 N92-28399
Integrated Design Analysis and Optimisation of Aircraft Structures [AGARD-LS-186] p 3231 N92-28469
Fundamentals of structural optimisation p 3231 N92-28470
Structural optimization of aircraft p 3232 N92-28472
Multidisciplinary design and optimization [AGARD-PAPER-2] p 3232 N92-28473
Structural characterization of cross-linked hemoglobins developed as potential transfusion substitutes [AD-A246777] p 3325 N92-28515
Structural design methodology for large space structures [AD-A247672] p 3246 N92-28560
Experimental determination of dissipated energy density as a measure of strain-induced damage in composites [AD-A250322] p 3253 N92-28953
Computer recognition and analysis of photogrammetric targets [AD-A250313] p 3339 N92-28971
Mapping unstructured grid computations to massively parallel computers [NASA-CR-190551] p 3343 N92-29109
STRUCTURAL BASINS
Dorsa Argentea type sinuous ridges, Mars: Evidence for linear dune hypothesis p 3390 N92-29055
STRUCTURAL DESIGN
A survey report for the design of biped locomotion robot: The WL-12 (Waseda Leg-12) [DE92-782046] p 3292 N92-28233
Multidisciplinary design and optimization [AGARD-PAPER-2] p 3232 N92-28473
Mathematical optimization: A powerful tool for aircraft design p 3232 N92-28474
Optimum design of a gearbox for low vibration [NASA-TM-105653] p 3293 N92-28476
Structural design methodology for large space structures [AD-A247672] p 3246 N92-28560
Simple computer programs for the design and sizing of fiber reinforced composites [NLR-TP-91050-U] p 3252 N92-28637
STRUCTURAL DESIGN CRITERIA
National Conference on the Use of Composite Materials in Load-Bearing Marine Structures. Volume 1: Summary report [PB92-163831] p 3252 N92-28724
National Conference on the Use of Composite Materials in Load-Bearing Marine Structures. Volume 2: Conference proceedings [PB92-163849] p 3252 N92-28725
STRUCTURAL ENGINEERING
Structural design methodology for large space structures [AD-A247672] p 3246 N92-28560
National Conference on the Use of Composite Materials in Load-Bearing Marine Structures. Volume 1: Summary report [PB92-163831] p 3252 N92-28724
National Conference on the Use of Composite Materials in Load-Bearing Marine Structures. Volume 2: Conference proceedings [PB92-163849] p 3252 N92-28725
A methodology for the evaluation of runway roughness for repair [AD-A250407] p 3241 N92-28772
STRUCTURAL FAILURE
Turbine aircraft engine operational trending and JT8D static component reliability study [DOT/FAA/CT-91/10] p 3238 N92-28686
A methodology for the evaluation of runway roughness for repair [AD-A250407] p 3241 N92-28772
STRUCTURAL MEMBERS
Experimental determination of dissipated energy density as a measure of strain-induced damage in composites [AD-A250322] p 3253 N92-28953
STRUCTURAL PROPERTIES (GEOLOGY)
Soil texture and granulometry at the surface of Mars p 3382 N92-29009
STRUCTURAL STABILITY
Method fabricating load-bearing composites free from microbuckling deformation up to a predetermined load [AD-D015212] p 3250 N92-28224
STRUCTURAL STRAIN
Experimental determination of dissipated energy density as a measure of strain-induced damage in composites [AD-A250322] p 3253 N92-28953
STRUCTURAL VIBRATION
An examination of anticipated g-jitter on Space Station and its effects on materials processes p 3267 N92-28438
Mobility power flow analysis of coupled plate structure subjected to mechanical and acoustic excitation [NASA-CR-189635] p 3352 N92-28722
Computer derivation of green's functions for structural dynamic analysis [AD-A250249] p 3339 N92-28969
Computer recognition and analysis of photogrammetric targets [AD-A250313] p 3339 N92-28971
STUDENTS
Design on an enhanced interactive satellite communications system analysis program [AD-A245967] p 3273 N92-28410
Computer-based assessment of schema knowledge in a flexible problem-solving environment [AD-A246779] p 3348 N92-28516
SUBLIMATION
The Mars water cycle at other epochs: History of the polar caps and layered terrain p 3375 N92-28493
Influences of CO2 sublimation/condensation processes on the long-term evolution of the Martian atmosphere p 3375 N92-28496
The Martian polar caps: Stability and water transport at low obliquities p 3385 N92-29023
Simulations of the seasonal polar caps on Mars p 3387 N92-29033
SUBSONIC FLOW
Computation of steady and unsteady quasi-one-dimensional viscous/inviscid interacting internal flows at subsonic, transonic, and supersonic Mach numbers [NASA-CR-189881] p 3283 N92-28555
SUBSONIC WIND TUNNELS
Calculation of support interferences on the aerodynamic coefficients for a wind tunnel calibration model [ESA-TT-1247] p 3229 N92-29159
SUBSTITUTES
Structural characterization of cross-linked hemoglobins developed as potential transfusion substitutes [AD-A246777] p 3325 N92-28515
SUBSTRATES
High resolution electron beam lithography on x ray mask substrates. Effects of electron scattering and membrane heating [ETN-92-91336] p 3272 N92-28793
The oxidation stability of boron nitride thin films on MgO and TiO2 substrates [DE92-011686] p 3364 N92-28857
Molecular recognition in the oxidation of catechols by Dicobalt-BISDIEN dioxygen complexes [AD-A246456] p 3258 N92-28973
Pressure transducer and system for cryogenic environments [NASA-CASE-LAR-14579-1] p 3288 N92-29097
Substrate induced ordering of molecular adsorbates on Au(111) [AD-A246850] p 3258 N92-29185
SUBSTRUCTURES
Mobility power flow analysis of coupled plate structure subjected to mechanical and acoustic excitation [NASA-CR-189635] p 3352 N92-28722
SULFUR DIOXIDES
Regional climatic effects of atmospheric SO2 on Mars p 3377 N92-28504
The role of SO2 on Mars and on the primordial oxygen isotope composition of water on Earth and Mars p 3377 N92-28507
High temperature membranes for H2S and SO2 separations [DE92-010451] p 3256 N92-28827
SULFUR OXIDES
High temperature membranes for H2S and SO2 separations [DE92-010451] p 3256 N92-28827
SUNSPOT CYCLE
Mathematical modeling of solar magneto-dynamics [AD-A247158] p 3395 N92-28520

SUPERCOMPUTERS
The instrumentation of a parallel, distributed database operation, retrieve-common, for merging two large sets of records
[AD-A247486] p 3367 N92-28246
The testing, analysis, and correction of the update operation of a parallel, multi-backend database supercomputer
[AD-A248320] p 3341 N92-28306
Superconducting at NLR: NEC SX-2 capabilities in NLR's terminal and file-transfer network
[NLR-TP-89007-U] p 3342 N92-28706
Development of a high-performance FORTRAN compiler for porting CFD codes to the Navier-Stokes computer
[AD-A250208] p 3342 N92-28770
Vector and parallel supercomputing programming
[ONERA-NT-1991-11] p 3338 N92-28779
High-performance integrated circuit evaluation system for a gallium arsenide microsupercomputer
[AD-A250385] p 3281 N92-28798
Functional requirements document for the Earth Observing System Data and Information System (EOSDIS) Scientific Computing Facilities (SCF) of the NASA/MSFC Earth Science and Applications Division, 1992
[NASA-TM-4392] p 3333 N92-28899
SUPERCONDUCTING FILMS
Stanford Center for research on superconductivity and superconductive electronics
[AD-A250204] p 3281 N92-29147
SUPERCONDUCTING MAGNETS
Superconducting bearings with levitation control configurations
[NASA-CASE-GSC-13346-1] p 3295 N92-29099
SUPERCONDUCTING SUPER COLLIDER
The solenoidal detector collaboration silicon detector system
[DE92-011237] p 3356 N92-28356
SUPERCONDUCTIVITY
Synthesis and characterization of new low-dimensional transition metal complex conductors
[AD-A249263] p 3258 N92-28237
Physics and technology for the investigation of properties of ultra small systems
[AD-A246772] p 3364 N92-28513
Monolithic mm-wave phase shifter using optically activated superconducting switches
[NASA-CASE-LEW-14878-1] p 3358 N92-28571
EXPLOMET 90 international conference on shock-wave and high-strain-rate phenomena in materials
[AD-A248665] p 3303 N92-28892
The processing of high temperature ceramic superconducting devices, volume 2
[AD-A248159] p 3281 N92-28948
Superconducting bearings with levitation control configurations
[NASA-CASE-GSC-13346-1] p 3295 N92-29099
Stanford Center for research on superconductivity and superconductive electronics
[AD-A250204] p 3281 N92-29147
SUPERCONDUCTORS
Stanford Center for research on superconductivity and superconductive electronics
[AD-A250204] p 3281 N92-29147
SUPERCRITICAL AIRFOILS
Development and validation of a characteristic boundary condition for a cell-centered Euler method
[NLR-TP-90144-U] p 3227 N92-28692
SUPERGRAVITY
Proceedings of the workshop on Quantum Gravity and Topology
[DE92-782191] p 3366 N92-28235
SUPERLATTICES
Shallow states of donor impurities on periodically structured semiconductors interfaces
[DE92-622791] p 3363 N92-28312
SUPERPLASTICITY
Mechanistic studies of superplasticity of structural ceramics
[AD-A246951] p 3263 N92-28558
SUPERSONIC FLOW
A study of the normal injection of hydrogen into a heated supersonic flow using planar laser-induced fluorescence
[DE92-010701] p 3282 N92-28268
Computation of steady and unsteady quasi-one-dimensional viscous/inviscid interacting internal flows at subsonic, transonic, and supersonic Mach numbers
[NASA-CR-189881] p 3283 N92-28555
Singlet delta oxygen pumping of iodine monofluoride in a supersonic flow
[AD-A249946] p 3284 N92-28766
SUPERSONIC TRANSPORTS
Full Navier-Stokes analysis of a two-dimensional mixer/ejector nozzle for noise suppression
[NASA-TM-105715] p 3236 N92-28419
Integrating aerodynamics and structures in the minimum weight design of a supersonic transport wing
[NASA-TM-107586] p 3231 N92-28435
Evaluation of outdoor-to-indoor response to minimized sonic booms
[NASA-CR-189643] p 3352 N92-28556
SUPERSONIC WIND TUNNELS
Air ejector experiments using the two-dimensional supersonic cascade tunnel: Zero secondary flow performance
[NAL-TM-632] p 3241 N92-28829
SUPPORT INTERFERENCE
Calculation of support interferences on the aerodynamic coefficients for a wind tunnel calibration model
[ESA-TT-1247] p 3229 N92-29159
SUPPORT SYSTEMS
The role of simulation for the study of APIS (piloting support by synthetic imagery) p 3224 N92-28544
Tasking and communication flows in the F/A-18D cockpit: Issues, problems, and possible solutions
[AD-A245977] p 3234 N92-28802
SPEEDS: An approach to support programming environments using expert database systems
[AD-A247469] p 3339 N92-28943
SUPPORTS
The Microgravity Isolation Mount (MGIM): A Columbus facility for improving the microgravity quality of payloads p 3267 N92-28439
KC-135 Large Motion Isolation Mount (LMIM) p 3267 N92-28440
Microgravity isolation mounts based upon Piezoelectric film p 3268 N92-28454
SURFACE CRACKS
Growth of surface cracks under fatigue loading: A literature survey
[LR-664] p 3299 N92-28580
SURFACE DIFFUSION
Simulations of surface winds at the Viking Lander sites using a one-level model p 3380 N92-28998
SURFACE ENERGY
Correlation between surface free energy and surface constitution
[AD-A246699] p 3262 N92-28291
Simulation of Martian surface-atmosphere interaction in a space-simulator: Technical considerations and feasibility p 3388 N92-29044
SURFACE LAYERS
The emergence of atomic-level structural information for ordered metal-solution interfaces: Some recent contributions from in-situ infrared spectroscopy and scanning tunneling microscopy
[AD-A246765] p 3364 N92-28512
X ray photoelectron spectroscopy study on the double layer at an Al2O3-Al interface
[AD-A246454] p 3265 N92-28972
Turbulent spectra, fluxes, stability and growth of the mixed layer in the boundary layer of Mars p 3393 N92-29070
The in situ observation of diamond film nucleation and growth
[AD-A248203] p 3265 N92-29189
SURFACE PROPERTIES
Orthogonal self-assembly of redox active molecules on Pt and Au: Selective reaction of disulfide with Au and isonitrile with Pt
[AD-A246698] p 3254 N92-28290
Atomistic simulation of the nanoindentation of diamond and graphite surfaces
[AD-A249296] p 3355 N92-28881
Martian impact crater degradation studies: Implications for localized obliteration episodes p 3379 N92-28991
Analysis of Martian atmospheric and surface optical properties between 4.4 and 5.1 microns p 3382 N92-29007
Use of laser range finders and range image analysis in automated assembly tasks
[NASA-CR-186957] p 3291 N92-29139
SURFACE REACTIONS
Correlation between surface free energy and surface constitution
[AD-A246699] p 3262 N92-28291
Surface crystallographic dependence of voltammetric oxidation of polyhydric alcohols and related systems at monocrystalline gold-acidic aqueous interfaces
[AD-A246763] p 3363 N92-28392
Thermodynamic and kinetic aspects of surface acidity
[DE92-011194] p 3256 N92-28893
SURFACE ROUGHNESS
A methodology for the evaluation of runway roughness for repair
[AD-A250407] p 3241 N92-28772
Studies of the polarimetric dependence of enhanced backscattering from one-dimensional surfaces
[AD-A248431] p 3275 N92-28878
Influence of aerodynamic roughness length on aeolian processes: Earth, Mars, Venus p 3380 N92-28996
SURFACE STABILITY
The linear and nonlinear shear instability of a fluid sheet
[AD-A247092] p 3282 N92-28258
SURFACE TEMPERATURE
Simulations of surface winds at the Viking Lander sites using a one-level model p 3380 N92-28998
Was early Mars warmed by ammonia? p 3386 N92-29030
Atmospheric and surface temperatures and airborne dust amounts during late southern summer from Mariner 9 IRIS data p 3390 N92-29056
Turbulent spectra, fluxes, stability and growth of the mixed layer in the boundary layer of Mars p 3393 N92-29070
SURFACE TREATMENT
Quantitative interphase study of composite materials. Interphase engineering: A scientific way of tailoring the mechanophysical properties of composite materials
[AD-A247776] p 3251 N92-28252
Orthogonal self-assembly of redox active molecules on Pt and Au: Selective reaction of disulfide with Au and isonitrile with Pt
[AD-A246698] p 3254 N92-28290
SURFACE WATER
Nature and evolution of the early Martian atmosphere: Evidence from highland crater populations p 3373 N92-28485
SURFACE WAVES
SAR-relate stress variability in the Marine Atmospheric Boundary Layer (MABL)
[AD-A247772] p 3309 N92-28567
SURGES
Dynamic control of aerodynamic instabilities in gas turbine engines p 3238 N92-28466
SURVEILLANCE
Monitoring activities review of the Radiological Environmental Surveillance Program
[DE92-013103] p 3308 N92-28811
SURVEYS
A study of pilot attitudes regarding the impact on mission effectiveness of using new cockpit automation technologies to replace the navigator/weapon system officer/electronic warfare officer
[AD-A246683] p 3329 N92-28286
Accuracy of shipborne kinematic GPS surveying
[AD-A245942] p 3230 N92-28317
A profile of scientist and engineer training conducted by the Naval Avionics Center
[AD-A245925] p 3326 N92-28408
Correlational analysis of survey and model-generated workload values
[AD-A247153] p 3329 N92-28518
Historical data for geomagnetic field modelling p 3299 N92-28621
Survey data for geomagnetic field modelling p 3300 N92-28623
Satellite data for geomagnetic field modeling p 3300 N92-28624
Reduction of marine magnetic data for modeling the main field of the Earth p 3300 N92-28626
An inventory of data collected during the NERC's North Sea Community Research Project, 1987-1992
[REPT-21-1991] p 3323 N92-29215
SWEEP FREQUENCY
Method and apparatus for frequency spectrum analysis
[NASA-CASE-NPO-17759-1-CU] p 3276 N92-29124
SWEPT WINGS
Natural flow wing
[NASA-CASE-LAR-14281-1] p 3228 N92-28729
SWITCHES
Monolithic mm-wave phase shifter using optically activated superconducting switches
[NASA-CASE-LEW-14878-1] p 3358 N92-28571
Optical switching devices
[AD-D015261] p 3360 N92-29205
SWITCHING CIRCUITS
Fiber-optic interconnection networks for spacecraft
[NASA-CR-190531] p 3358 N92-28698
Design and realization of polysilicon emitter bipolar transistors
[LAAS-91360] p 3282 N92-29208
SYMBOLS
Investigations of logic of introspection and related modes of reasoning with applications
[AD-A249286] p 3345 N92-28895
SYNCHRONISM
Asynchronous bidirectional network interface enabling seamless concurrent processing in a distributed heterogeneous multiprocessor system
[AD-D015274] p 3343 N92-29096
SYNCHRONOUS PLATFORMS
Science and application payloads in the 1990's
[NASA-TM-107937] p 3246 N92-28370

SYNCHROTRON RADIATION
Aperture coupling measurement in a test chamber for the Advanced Photon Source (APS)
[DE92-013059] p 3274 N92-28809
RF impedance measurement status for the 7-GeV Advanced Photon Source (APS)
[DE92-013060] p 3274 N92-28810
SYNTHESIS (CHEMISTRY)
New methodology for fluorocarbon synthesis
[AD-A247163] p 3254 N92-28261
Synthesis and study of metallonitride complexes and polymers
[AD-A248577] p 3262 N92-28323
Polyimidazoles via aromatic nucleophilic displacement
[NASA-CASE-LAR-14145-1] p 3264 N92-28751
Thermodynamic and kinetic aspects of surface acidity
[DE92-011194] p 3256 N92-28893
Molecular engineering of liquid crystalline polymers by living cationic polymerization. 21: Synthesis and characterization of poly (3-((4-cyano-4'-biphenyl)oxy) propyl vinyl ether) macromonomers
[AD-A248305] p 3265 N92-29116
Poly(1,3,4-oxadiazoles) via aromatic nucleophilic displacement
[NASA-CASE-LAR-14427-1] p 3250 N92-29141
SYNTHETIC FIBERS
Proceedings of Asilomar Conference on Polymeric Materials
[AD-A249366] p 3262 N92-28360
SYSTEM IDENTIFICATION
The role of systems simulation for the development and qualification of ATTAS p 3225 N92-28548
Identification of linear system models and state estimators for controls p 3247 N92-28737
Fuzzy logic controller for manipulator systems: Preliminary results p 3247 N92-28738
Identification of weakly non-linear dynamical systems by means of random excitations
[ONERA-NT-1991-10] p 3349 N92-28778
SYSTEMS ANALYSIS
Information strategy plan
[AD-A247740] p 3367 N92-28403
Design on an enhanced interactive satellite communications system analysis program
[AD-A245967] p 3273 N92-28410
Software development using a method base system
[NLR-TP-90387-U] p 3336 N92-28636
Analysing multiprogramming queues by generating functions
[MEMO-COSOR-91-25] p 3342 N92-28642
A survey of high density packaging for high performance computing system
[AD-A248633] p 3332 N92-28891
Mass and power modeling of communication satellites
[NASA-CR-189186] p 3275 N92-28906
Space transportation analysis and design
[AD-A250629] p 3245 N92-28956
SYSTEMS ENGINEERING
Integrated Design Analysis and Optimisation of Aircraft Structures
[AGARD-LS-186] p 3231 N92-28469
Multidisciplinary design and optimization
[AGARD-PAPER-2] p 3232 N92-28473
Design specifications for the Advanced Instructional Design Advisor (AIDA), volume 1
[AD-A248201] p 3340 N92-29187
Design specifications for the Advanced Instructional Design Advisor (AIDA), volume 2
[AD-A248202] p 3340 N92-29188
Development of a flight information system using the structured method
[AD-A248207] p 3236 N92-29222
SYSTEMS INTEGRATION
Inlet distortion effects in aircraft propulsion system integration p 3237 N92-28464
Ground Systems Development Environment (GSDE) software configuration management
[NASA-CR-190503] p 3337 N92-28710
Verification of satellite EGSE test-software using an application generator
[ITN-92-85131] p 3244 N92-29098
SYSTEMS SIMULATION
Harrier GR MK 5/7 mission simulators for the Royal Air Force p 3224 N92-28540
The role of systems simulation for the development and qualification of ATTAS p 3225 N92-28548
A study of the control problem of the shoot side environment delivery system of a closed crop growth research chamber
[NASA-CR-177597] p 3330 N92-28681
Crew station research and development facility training for the light helicopter demonstration/validation program
[NASA-TM-103865] p 3327 N92-28744
SYSTEMS STABILITY
Windshear radar calibration: Transmitter power and receiver gain stability
[NASA-TM-107589] p 3275 N92-28876

T

TABLES (DATA)
Wavenumber calibration tables from heterodyne frequency measurements
[NASA-CR-190422] p 3276 N92-29115
TARGET ACQUISITION
Delays in laser glare onset differentially affect target-location performance in a visual search task
[AD-A246708] p 3327 N92-28557
Performance of the multifunctional CW CO2-laser radar at the TNO-FEL laboratory and during the BEST TWO field test
[FEL-91-A163] p 3291 N92-29160
TARGET MASKING
Delays in laser glare onset differentially affect target-location performance in a visual search task
[AD-A246708] p 3327 N92-28557
Monaural and binaural processing of complex waveforms
[AD-A247199] p 3352 N92-28889
TARGET RECOGNITION
Program Cluster: An identification of fixation cluster characteristics
[AD-A247014] p 3326 N92-28396
Delays in laser glare onset differentially affect target-location performance in a visual search task
[AD-A246708] p 3327 N92-28557
TARGETS
Target motion detecting impulse Doppler radar system
[AD-D015263] p 3277 N92-29169
TASK COMPLEXITY
Is choice accuracy related to information search patterns?
[IZF-1991-B-9] p 3369 N92-29162
TAYLOR SERIES
The variance of Rasch ability estimates from partially-known item parameters
[AD-A247065] p 3348 N92-28273
TEAMS
Improved decision making through group composition
[AD-A246622] p 3366 N92-28256
TECHNOLOGICAL FORECASTING
Evaluation of future space transportation systems with regard to their reliabilities and costs
[DLR-FB-91-27] p 3245 N92-28826
TECHNOLOGY ASSESSMENT
Piloted simulation effectiveness development applications and limitations p 3221 N92-28524
TECHNOLOGY TRANSFER
National Conference on the Use of Composite Materials in Load-Bearing Marine Structures. Volume 1: Summary report
[PB92-163831] p 3252 N92-28724
National Conference on the Use of Composite Materials in Load-Bearing Marine Structures. Volume 2: Conference proceedings
[PB92-163849] p 3252 N92-28725
TECHNOLOGY UTILIZATION
Consulting report on the NASA technology utilization network system
[NASA-CR-190387] p 3370 N92-29108
TECTONICS
CO2 and clathrate as past erosive agents on Mars p 3375 N92-28497
TEFLON (TRADEMARK)
High temperature dielectric properties of Apical, Kapton, Peek, Teflon AF, and Upilex polymers
[NASA-TM-105753] p 3280 N92-28675
TELECOMMUNICATION
Advanced optical fiber communication systems
[AD-A247683] p 3357 N92-28554
Fade durations in satellite-path mobile radio propagation
[NASA-CR-190484] p 3273 N92-28586
Tasking and communication flows in the F/A-18D cockpit: Issues, problems, and possible solutions
[AD-A245977] p 3234 N92-28802
TELEMETRY
Applications of passive microwave satellite data for Arctic Sea ice studies
[AD-A245966] p 3306 N92-28791
Stability and control flight testing of a half-scale Pioneer remotely piloted vehicle
[AD-A245973] p 3239 N92-28801
TELEOPERATORS
Anthropomorphic teleoperation: Controlling remote manipulators with the DataGlove
[NASA-TM-103588] p 3330 N92-28521
Telescience experiments using the Prototype Optical Diagnostic Instrument (PODI)
[NLR-TP-90199-U] p 3358 N92-28656
Modelling and real-time simulation of the Hermes robot arm HERA
[NLR-TP-90262-U] p 3294 N92-28705
Super auditory localization for improved human-machine interfaces
[AD-A250288] p 3331 N92-29121
TELEROBOTICS
Anthropomorphic teleoperation: Controlling remote manipulators with the DataGlove
[NASA-TM-103588] p 3330 N92-28521
TELESCOPES
Method and apparatus for phasing segmented mirror arrays
[NASA-CASE-NPO-18095-1-CU] p 3359 N92-29122
TELEVISION EQUIPMENT
An acoustic charge transport imager for high definition television application
[AD-A250433] p 3274 N92-28773
TELEVISION TRANSMISSION
Digital compression algorithms for HDTV transmission
[NASA-CR-190509] p 3275 N92-28873
TELLURIDES
Growth and optical characterization of Zn(1-x)Mn(x)Te grown by molecular beam epitaxy
[DE92-010667] p 3363 N92-28331
TEMPERATURE DEPENDENCE
The impact of temperature dependent CO2 cross section measurements: A role for heterogeneous chemistry in the atmosphere of Mars? p 3372 N92-28479
Martian atmospheric chemistry during the time of low water abundance p 3376 N92-28501
Magnetic hysteresis and relaxation in Ag-sheathed TlBaCaCuO (1223) and Bi(Pb)SrCaCuO (2223) superconducting tapes
[DE92-011357] p 3365 N92-28874
Calculations and databasing of molecular absorption parameters for HITRAN
[AD-A247549] p 3355 N92-28936
TEMPERATURE DISTRIBUTION
The thermal structure, dust loading, and meridional transport in the Martian atmosphere during late southern summer p 3377 N92-28505
Wall turbulence
[AD-A249973] p 3284 N92-28768
TEMPERATURE EFFECTS
Neutron, gamma ray, and temperature effects on the electrical characteristics of thyristors
[NASA-TM-105728] p 3279 N92-28432
Experimental and computational ice shapes and resulting drag increase for a NACA 0012 airfoil
[NASA-TM-105743] p 3227 N92-28674
Thermal response of rigid and flexible insulations and reflective coating in an aeroconvective heating environment
[NASA-TM-103925] p 3233 N92-28721
M-H characteristics and demagnetization resistance of samarium-cobalt permanent magnets to 300 C
[NASA-CR-189194] p 3280 N92-28723
Influence of heat flow on early Martian climate p 3390 N92-29052
TEMPERATURE GRADIENTS
Optical effects on ocean mixed layer dynamics
[AD-A245941] p 3320 N92-28316
The thermal structure, dust loading, and meridional transport in the Martian atmosphere during late southern summer p 3377 N92-28505
TEMPERATURE MEASUREMENT
The evaluation of rate constants for rapid electrode reactions by using microelectrode voltammetry: Virtues of measurement at lower temperature
[AD-A246760] p 3255 N92-28391
Lubricant evaluation and performance 2
[AD-A247464] p 3262 N92-28398
Autonomous ocean profiler
[AD-A247657] p 3322 N92-28938
Turbulent spectra, fluxes, stability and growth of the mixed layer in the boundary layer of Mars p 3393 N92-29070
The measuring assembly for the NPL primary standard absorbed dose graphite calorimeter at therapy levels
[NPL-RSA(EXT)-23] p 3288 N92-29163
TEMPERATURE MEASURING INSTRUMENTS
The measuring assembly for the NPL primary standard absorbed dose graphite calorimeter at therapy levels
[NPL-RSA(EXT)-23] p 3288 N92-29163
TEMPERATURE PROBES
Thermal wave imaging and characterization of solids
[AD-A249297] p 3297 N92-28851
TEMPERATURE PROFILES
Multicomponent comparison of optical and mass spectrometric diagnostics in low-pressure flames
[AD-A250323] p 3257 N92-28954

Microwave temperature profiler for clear air turbulence prediction
[NASA-CASE-NPO-18115-1-CU] p 3320 N92-29148
TEMPERATURE SENSORS
Ultra-high temperature stability Joule-Thomson cooler with capability to accomodate pressure variations
[NASA-CASE-NPO-18184-1-CU] p 3288 N92-29156
TEMPORAL RESOLUTION
Multitemporal analysis of a braiding river
[NLR-TP-89235-U] p 3305 N92-28690
TENSILE PROPERTIES
Tensile and interlaminar properties of GLARE (trade name) laminates
[AD-A250188] p 3253 N92-28921
TENSILE STRESS
Diffusion-controlled decohesion using a Cu-Sn alloy as a model system
[DE92-011645] p 3260 N92-28854
TENSILE TESTS
Study of high temperature failure mechanism in ceramics
[AD-A247018] p 3263 N92-28415
The buckling behavior of a central crack in a plate under tension
[LR-667] p 3299 N92-28583
TERMINAL BALLISTICS
A system structure for predictive relations in penetration mechanics
[AD-A246453] p 3292 N92-28284
Evaluation of Whipple bumper shields at 7 and 10 km/s
[NASA-TM-107958] p 3295 N92-28925
TERMINAL FACILITIES
FAA aviation forecasts
[AD-A250412] p 3230 N92-29182
TERMINOLOGY
Information systems for engineering sustainable development
[DE92-011271] p 3368 N92-28838
Information technology in plain words
[AD-A250324] p 3369 N92-28955
TERMS
Information technology in plain words
[AD-A250324] p 3369 N92-28955
TERRACES (LANDFORMS)
Erosional landforms on the layered terrains in Valles Marineris p 3386 N92-29031
TERRAIN
Propagation and scattering of microwaves and millimeter waves in snow based on dense random media theory
[AD-A249300] p 3274 N92-28846
Studies of iterated transform image compression and its application to color and DTED
[AD-A248060] p 3339 N92-28946
Analysis of electromagnetic propagation over variable terrain using the parabolic wave equation
[AD-A248061] p 3276 N92-28947
Influence of aerodynamic roughness length on aeolian processes: Earth, Mars, Venus p 3380 N92-28996
Simulations of surface winds at the Viking Lander sites using a one-level model p 3380 N92-28998
Mars: Wavelength-dependent dual polarization global scattering p 3384 N92-29020
Erosional landforms on the layered terrains in Valles Marineris p 3386 N92-29031
TERRAIN ANALYSIS
Interest in real-time simulations for the development terrain following function of radar systems
p 3222 N92-28529
Implications of early Hesperian ages for presumed Noachian age volcanic flows on Mars
p 3383 N92-29015
TERRAIN FOLLOWING AIRCRAFT
Interest in real-time simulations for the development terrain following function of radar systems
p 3222 N92-28529
TERRESTRIAL PLANETS
Evidence for magma oceans on asteroids, the moon, and Earth p 3315 N92-28614
Magma ocean formation due to giant impacts
p 3315 N92-28615
Giant and large impacts in the context of planetary formation theory p 3315 N92-28619
TEST CHAMBERS
The design of test-section inserts for higher speed aeroacoustic testing in the Ames 80- by 120-foot wind tunnel
[NASA-TM-103915] p 3353 N92-28909
TEST EQUIPMENT
Method and apparatus for using magneto-acoustic remanence to determine embrittlement
[NASA-CASE-LAR-13817-5] p 3303 N92-28757
High-performance integrated circuit evaluation system for a gallium arsenide microsupercomputer
[AD-A250385] p 3281 N92-28798
Magneto acoustic emission method for testing materials for embrittlement
[NASA-CASE-LAR-13817-2] p 3304 N92-29155
TEST FACILITIES
Transient impeller test facility
[AD-D015249] p 3294 N92-28749
TEST PILOTS
Use of simulation in the USAF Test Pilot School curriculum p 3223 N92-28535
TEST RANGES
Adaptive noise cancellation applied to the NUWES test ranges
[AD-A245961] p 3352 N92-28409
TESTS
Fuel optimal maneuver: Experimental testbeds
p 3247 N92-28735
TETHERED SATELLITES
Empirical techniques for the study of acceleration mechanisms in the space environment
[AD-A249940] p 3248 N92-28765
TEXTS
Conversion and retrievability of hard copy and digital documents on optical disks
[AD-A247481] p 3367 N92-28244
Introduction to rocket propulsion
[AD-A250424] p 3249 N92-28800
TEXTURES
Soil texture and granulometry at the surface of Mars
p 3382 N92-29009
THEMATIC MAPPERS (LANDSAT)
Quantitative updating of land use information on 1:50,000 scale topographic maps using SPOT LANDSAT Thematic Mapper imagery
[NLR-TP-89061-U] p 3305 N92-28708
THEMATIC MAPPING
Comparison of drift potential derived from Mars GCM with rock abundance from IRTM p 3395 N92-29078
THEOREM PROVING
Fourier analysis of the approximation power of principal shift-invariant spaces
[AD-A246713] p 3347 N92-28411
Decomposition of balanced matrices. Part 1: Introduction
[AD-A247397] p 3349 N92-28927
Decomposition of balanced matrices. Part 2: Wheel-and-parachute-free graphs
[AD-A247398] p 3350 N92-28928
Decomposition of balanced matrices. Part 6: Even wheels
[AD-A247399] p 3350 N92-28929
Decomposition of balanced matrices. Part 7: A polynomial recognition algorithm
[AD-A247400] p 3350 N92-28930
THEOREMS
Stability and optimal control theory of hereditary systems with applications from oscillating flying vehicles, mechanical systems, and robotics p 3247 N92-28732
THEORETICAL PHYSICS
The physics of strange matter
[DE92-011734] p 3371 N92-28774
THERMAL ANALYSIS
Coupled structural/thermal/electromagnetic analysis/tailoring of graded composite structures
[NASA-CR-189153] p 3298 N92-28296
Lubricant evaluation and performance 2
[AD-A247464] p 3262 N92-28398
Thermal analysis of selected commercial thermoplastic resins
[AD-A247711] p 3264 N92-28564
Thermal response of rigid and flexible insulations and reflective coating in an aeroconvective heating environment
[NASA-TM-103925] p 3233 N92-28721
THERMAL BATTERIES
Limiting factors to advancing thermal battery technology for naval applications
[AD-A247773] p 3280 N92-28568
THERMAL CONDUCTIVITY
Simulation in infrared imaging: Using electrical circuit principles to model heat transfer
[AD-A248290] p 3278 N92-28276
Coupling device with improved thermal interface
[NASA-CASE-GSC-13251-1] p 3295 N92-29120
THERMAL DECOMPOSITION
Mg-Si-Al oxynitride glasses
[AD-A247593] p 3261 N92-28249
Volcanic recycling of carbonate deposits on Mars
p 3377 N92-28506
THERMAL DIFFUSION
The subsurface hydrologic response of Mars to the thermal evolution of its early crust p 3381 N92-29006
THERMAL EMISSION
The thermal structure, dust loading, and meridional transport in the Martian atmosphere during late southern summer p 3377 N92-28505
Mid-infrared spectra of Martian komantiite
p 3390 N92-29053
Physical properties of Oxia/Lunae Planum and Arabia-type units in the central equatorial region of Mars
p 3392 N92-29065
THERMAL ENERGY
Pulse thermal energy transport/storage system
[NASA-CASE-LEW-15235-1] p 3287 N92-29125
Thermal accretion disk models for active galaxies
[ETN-92-91486] p 3371 N92-29127
Solar thermal energy receiver
[NASA-CASE-LEW-14949-1] p 3307 N92-29143
THERMAL ENVIRONMENTS
Performance of uncoated AFRSI blankets during multiple Space Shuttle flights
[NASA-TM-103892] p 3245 N92-29104
THERMAL FATIGUE
Elevated temperature axial and torsional fatigue behavior of Haynes 188
[NASA-TM-105396] p 3302 N92-28701
THERMAL INSULATION
Thermal response of rigid and flexible insulations and reflective coating in an aeroconvective heating environment
[NASA-TM-103925] p 3233 N92-28721
THERMAL MAPPING
The thermal structure, dust loading, and meridional transport in the Martian atmosphere during late southern summer p 3377 N92-28505
Thermal wave imaging and characterization of solids
[AD-A249297] p 3297 N92-28851
Thermally distinct ejecta blankets from Martian craters
p 3379 N92-28994
Mars dust and cloud opacities and scattering properties p 3381 N92-29003
Soil texture and granulometry at the surface of Mars
p 3382 N92-29009
The composition of Martian aeolian sands: Thermal emissivity from Viking IRTM observations
p 3382 N92-29010
Mars: Correcting surface albedo observations for effects of atmospheric dust loading p 3386 N92-29032
New dust opacity maps from Viking IR thermal mapper data p 3388 N92-29040
Physical interpretation of thermal and reflected data on Martian surface units p 3391 N92-29062
Comparison of drift potential derived from Mars GCM with rock abundance from IRTM p 3395 N92-29078
THERMAL NOISE
Fundamental noise limits in miniature acoustic and vibration sensors
[AD-A247016] p 3352 N92-28413
THERMAL PROTECTION
Thermal response of rigid and flexible insulations and reflective coating in an aeroconvective heating environment
[NASA-TM-103925] p 3233 N92-28721
THERMAL RADIATION
Physics and technology for the investigation of properties of ultra small systems
[AD-A246772] p 3364 N92-28513
THERMAL RESISTANCE
Elliptical-core two mode fiber sensors and devices incorporating photoinduced refractive index gratings
[NASA-CR-190495] p 3358 N92-28868
THERMAL SHOCK
Pre-test analyses for pressurized thermoshock tests, vessel 1
[VTT-RR-746] p 3303 N92-28776
Paint removal using cryogenic processes
[AD-A247668] p 3264 N92-28912
THERMAL STABILITY
New methodology for fluorocarbon synthesis
[AD-A247163] p 3254 N92-28261
Ultra-high temperature stability Joule-Thomson cooler with capability to accomodate pressure variations
[NASA-CASE-NPO-18184-1-CU] p 3288 N92-29156
THERMAL STRESSES
Method for advanced material characterization by laser induced eddy current imaging
[NASA-CASE-GSC-13386-1] p 3298 N92-29154
THERMISTORS
The measuring assembly for the NPL primary standard absorbed dose graphite calorimeter at therapy levels
[NPL-RSA(EXT)-23] p 3288 N92-29163
THERMODYNAMIC CYCLES
Practical considerations in designing the engine cycle
p 3237 N92-28460
THERMODYNAMIC PROPERTIES
An investigation into techniques for the determination of moisture content on activated carbon
[AD-A245938] p 3256 N92-28882
Energetics of nanoscale graphitic tubules
[AD-A250165] p 3252 N92-28917

THERMODYNAMICS
Steady and transient performance calculation method for prediction, analysis, and identification
p 3237 N92-28461
Evolution of a terrestrial magma ocean: Thermodynamics, kinetics, rheology, convection, differentiation p 3314 N92-28611
Thermodynamic and kinetic aspects of surface acidity
[DE92-011194] p 3256 N92-28893
THERMOGRAPHY
Nondestructive evaluation of damages caused by impact and fatigue loading of polymer composites
[VTT-RR-742] p 3251 N92-28572
THERMOGRAVIMETRY
Thermal analysis of selected commercial thermoplastic resins
[AD-A247711] p 3264 N92-28564
THERMOMECHANICAL TREATMENT
The effects of thermomechanical processing parameters on elevated-temperature behavior of a 6061 Al-Al2O3 metal matrix composite
[AD-A247889] p 3253 N92-28959
THERMOPHILES
Conversion of acetic acid to methane by thermophiles
[DE92-010652] p 3257 N92-28942
THERMOPLASTIC RESINS
Proceedings of Asilomar Conference on Polymeric Materials
[AD-A249366] p 3262 N92-28360
Thermal analysis of selected commercial thermoplastic resins
[AD-A247711] p 3264 N92-28564
THERMOPLASTICITY
Thermal analysis of selected commercial thermoplastic resins
[AD-A247711] p 3264 N92-28564
THERMOREGULATION
Thermoregulation during spaceflight
[NASA-TM-103913] p 3325 N92-28420
THERMOSPHERE
Dust storm driven variations of the Mars thermosphere and exosphere: Coupling of atmospheric regions
p 3380 N92-28997
Atomic oxygen in the Martian thermosphere
p 3391 N92-29061
THESAURI
Information technology in plain words
[AD-A250324] p 3369 N92-28955
THICK FILMS
The processing of high temperature ceramic superconducting devices, volume 2
[AD-A248159] p 3281 N92-28948
THICK PLATES
Weld pool flow visualization studies during gas tungsten arc welding of steel and aluminum
[AD-A249204] p 3292 N92-28293
THIN FILMS
Thin film cadmium telluride photovoltaic cells
[DE92-001239] p 3306 N92-28277
Perspectives of ion implantation for optics
[DE92-010664] p 3357 N92-28355
Chemical vapor deposition of yttrium borium(2) copper(3) oxygen(x) thin films for wire applications
[AD-A247013] p 3364 N92-28395
Ionized assisted deposition of organic films for optoelectronic applications
[AD-A247744] p 3263 N92-28405
Physics and technology for the investigation of properties of ultra small systems
[AD-A246772] p 3364 N92-28513
The oxidation stability of boron nitride thin films on MgO and TiO2 substrates
[DE92-011686] p 3364 N92-28857
The processing of high temperature ceramic superconducting devices, volume 2
[AD-A248159] p 3281 N92-28948
Stanford Center for research on superconductivity and superconductive electronics
[AD-A250204] p 3281 N92-29147
Volatile CVD precursors based on copper alkoxides and mixed group IIA-Copper alkoxides --- chemical vapor deposition
[AD-D015264] p 3261 N92-29170
Feasibility of metal-oxide-semiconductor structures on Si-LPCVD thin films by low temperature (600 C) process
[LAAS-91307] p 3365 N92-29207
THREADS
Quick application/release nut with engagement indicator
[NASA-CASE-MSC-21799-1] p 3296 N92-29150
THREE DIMENSIONAL BODIES
Three dimensional measurements of prismatic bodies: Programming by means of a CAD system
[CRIF-MC-91] p 3337 N92-28700
THREE DIMENSIONAL BOUNDARY LAYER
SAR-relate stress variability in the Marine Atmospheric Boundary Layer (MABL)
[AD-A247772] p 3309 N92-28567
THREE DIMENSIONAL FLOW
A diagnostic study of the velocity structure of a meandering jet in the California current system using a primitive equation model
[AD-A246039] p 3320 N92-28283
Calculation of unsteady transonic flows with mild separation by viscous-inviscid interaction
[NASA-TP-3197] p 3226 N92-28477
Development and validation of a characteristic boundary condition for a cell-centered Euler method
[NLR-TP-90144-U] p 3227 N92-28692
Development of an unsteady three-dimensional viscous-inviscid interaction numerical method for the calculation of airfoils vibration
[ONERA-RSF-7/3617-AY-022A] p 3229 N92-29206
THREE DIMENSIONAL MODELS
NPSNET: Flight simulation dynamic modeling using quaternions
[AD-A247484] p 3333 N92-28245
Plane wave propagation in random granular media
[AD-A247300] p 3298 N92-28424
Stretch and hammer neural networks for N-dimensional data generalization
[AD-A247941] p 3346 N92-29082
THUNDERSTORMS
An evaluation of the naval oceanic vertical aerosol model during Key90
[AD-A245943] p 3320 N92-28318
Multiparameter radar and aircraft based studies of the microphysical, kinematic, and electrical structure of convective clouds
[AD-A247497] p 3318 N92-28668
THYRISTORS
Neutron, gamma ray, and temperature effects on the electrical characteristics of thyristors
[NASA-TM-105728] p 3279 N92-28432
TIDES
A coupled regional tide model
[AD-A247917] p 3322 N92-28913
TIME
Temporal reasoning and problem solving
[AD-A248457] p 3344 N92-28387
TIME DEPENDENCE
A numerical study of time-dependent wind forcing off the west coast of Portugal, 1987-1988
[AD-A246775] p 3321 N92-28365
Initial investigations of an adaptive discrete-time controller for nonlinear time-varying robotic models
p 3247 N92-28736
Time pressure effects on decision making in a dynamic task environment
[IZF-1991-B-8] p 3367 N92-29161
TIME LAG
Ionized assisted deposition of organic films for optoelectronic applications
[AD-A247744] p 3263 N92-28405
A simple and low cost system to measure delay times in pneumatic systems
[NLR-TP-90174-U] p 3235 N92-28644
The 2.0 GHz sampling rate transversal filter
[AD-A250244] p 3358 N92-28968
TIME OF FLIGHT SPECTROMETERS
Ionized assisted deposition of organic films for optoelectronic applications
[AD-A247744] p 3263 N92-28405
TIME SERIES ANALYSIS
Development of a residual acceleration data reduction and dissemination plan p 3271 N92-28453
Independent constituents in observatory time series in characterizing the secular variation
p 3302 N92-28633
Multiparameter radar and aircraft based studies of the microphysical, kinematic, and electrical structure of convective clouds
[AD-A247497] p 3318 N92-28668
A self-affine multi-fractal wave/turbulence discrimination method using data from single point fast response sensors in a nocturnal atmospheric boundary layer
[AD-A250419] p 3318 N92-28799
Nonlinear techniques for forecasting solar activity directly from its time series
[NASA-TM-107946] p 3396 N92-28870
Detecting and disentangling nonlinear structure from solar flux time series
[NASA-CR-190510] p 3396 N92-28871
Future mission studies: Forecasting solar flux directly from its chaotic time series
[NASA-CR-190378] p 3396 N92-28872
TIME SHARING
Crystallizing FORTRAN
[AD-A250162] p 3343 N92-28915
TIME TEMPERATURE PARAMETER
Lubricant evaluation and performance 2
[AD-A247464] p 3262 N92-28398
TIMING DEVICES
Automation and remote control instrumentation development: Rocket First Motion Timing System (RFMTS)
[AD-A249970] p 3287 N92-28767
TISSUES (BIOLOGY)
Experimental measurement of the orbital paths of particles sedimenting within a rotating viscous fluid as influenced by gravity
[NASA-TP-3200] p 3331 N92-28897
TITANIUM ALLOYS
Mechanisms of fracture and creep of structural alloys
[AD-A248701] p 3259 N92-28390
Surface residual stress analysis of metals and alloys
[AD-A248372] p 3259 N92-28426
Phase transformations in Ti3Al based alloy
[AD-A246464] p 3261 N92-28976
Oxidation resistant coating for titanium alloys and titanium alloy matrix composites
[NASA-CASE-LEW-15155-1] p 3265 N92-29090
TOKAMAK DEVICES
A comparison of results from an edge-plasma model with those from a two-dimensional fluid code
[DE92-010718] p 3360 N92-28335
Ohmic ignition in a tokamak reactor with the confinement degradation effect due to alpha heating
[PPL-124] p 3360 N92-28664
Ignition access condition based on the generalized saddle point in a magnetic fusion reactor
[PPL-109] p 3361 N92-28665
Plasma density scaling at the current reversal in the STOR-1M tokamak with AC operation
[PPL-127] p 3361 N92-28847
Improved confinement and edge plasma fluctuations in the STOR-M tokamak
[PPL-126] p 3361 N92-28848
Alternating current tokamak reactor with ohmic ignition and bootstrap current
[PPL-120] p 3361 N92-28849
TOLERANCES (MECHANICS)
Generation of spectra and stress histories for fatigue and damage tolerance analysis of fuselage repairs
[AD-A250390] p 3235 N92-29180
TOLUENE
An investigation into techniques for the determination of moisture content on activated carbon
[AD-A245938] p 3256 N92-28882
TOMATOES
Effects of extremely high G acceleration forces on NASA's control and space exposed tomato seeds
[AD-A247488] p 3323 N92-28247
TOMOGRAPHY
NORSAR basic seismological research
[AD-A248616] p 3309 N92-28569
Pressure regimes and core formation in the accreting earth p 3313 N92-28605
Thermal wave imaging and characterization of solids
[AD-A249297] p 3297 N92-28851
Modeling pulse transmission in the Monterey Bay using parabolic equation methods
[AD-A246465] p 3322 N92-28977
TOPEX
Modeling radiation forces acting on TOPEX/Poseidon for precision orbit determination
[NASA-TM-104564] p 3244 N92-28343
TOPEX/POSEIDON science investigations plan
[NASA-CR-190456] p 3305 N92-28950
TOPOGRAPHY
The Navy layered ocean model users guide
[AD-A247754] p 3321 N92-28566
Survey parameters and availability of low-level aeromagnetic data for geomagnetic field modelling
p 3301 N92-28629
Quantitative updating of land use information on 1:50,000 scale topographic maps using SPOT LANDSAT Thematic Mapper imagery
[NLR-TP-89061-U] p 3305 N92-28708
Implications of early Hesperian ages for presumed Noachian age volcanic flows on Mars
p 3383 N92-29015
Characterization of Martian near-subsurface materials by determination of cohesion and angle of internal friction p 3393 N92-29068
Topography of Apollinaris Patera and Ma'adim Vallis
p 3393 N92-29069
TOPOLOGY
Proceedings of the workshop on Quantum Gravity and Topology
[DE92-782191] p 3366 N92-28235
A center of excellence in the mathematical sciences
[AD-A249365] p 3346 N92-28329

TORQUE
Dynamics of a split torque helicopter transmission
[NASA-TM-105681] p 3296 N92-29136
TORSION
Elevated temperature axial and torsional fatigue behavior of Haynes 188
[NASA-TM-105396] p 3302 N92-28701
TOTAL QUALITY MANAGEMENT
Taguchi methods in electronics: A case study
[NASA-TM-103586] p 3279 N92-28456
TOUCHDOWN
Effective cueing during approach and touchdown: Comparison with flight p 3226 N92-28552
TOUGHNESS
Processing and properties of chemically derived calcium silicate cements
[AD-A249106] p 3264 N92-28570
TRACE ELEMENTS
Mg-perovskite/silicate melt and magnesiowuestite/silicate melt partition coefficients for KLB-1 at 250 Kbars p 3310 N92-28592
Phase equilibria and trace element partitioning in a magma ocean to 260 kilobars p 3311 N92-28595
Evidence for a high temperature differentiation in a molten earth: A preliminary appraisal p 3312 N92-28603
Greenhouse warming by minor gases on early Mars p 3384 N92-29022
TRACKING (POSITION)
Passive acoustic range estimation of helicopters
[AD-A248033] p 3351 N92-28302
Angular momentum: Can be used in ballistic tracking
[AD-A247722] p 3350 N92-28400
Applications of passive microwave satellite data for Arctic Sea ice studies
[AD-A245966] p 3306 N92-28791
TRACKING PROBLEM
Angular momentum: Can be used in ballistic tracking
[AD-A247722] p 3350 N92-28400
TRADEOFFS
Integration of tools for the Design and Assessment of High-Performance, Highly Reliable Computing Systems (DAHPHRS), phase 1
[NASA-CR-189621] p 3336 N92-28585
Time pressure effects on decision making in a dynamic task environment
[IZF-1991-B-8] p 3367 N92-29161
TRAINING ANALYSIS
Learning, teaching, and testing for complex conceptual understanding
[AD-A248728] p 3328 N92-29142
TRAINING DEVICES
Piloted Simulation Effectiveness
[AGARD-CP-513] p 3221 N92-28522
AM-X flight simulator from engineering tool to training device p 3223 N92-28536
Shipboard mission training effectiveness of the Naval Air Test Center's V-22 government test pilot trainer p 3224 N92-28542
Air combat maneuvering expert system trainer
[AD-A246459] p 3241 N92-28975
TRAINING SIMULATORS
Piloted simulation effectiveness development applications and limitations p 3221 N92-28524
Experience with piloted simulation in the development of helicopters p 3222 N92-28528
Validation of simulation systems for aircraft acceptance testing p 3222 N92-28531
Aircraft simulation and pilot proficiency: From surrogate flying towards effective training p 3222 N92-28532
The use of a dedicated testbed to evaluate simulator training effectiveness p 3222 N92-28533
AM-X flight simulator from engineerng tool to training device p 3223 N92-28536
The evaluation of simulator effectiveness for the training of high speed, low level, tactical flight operations p 3223 N92-28539
Harrier GR MK 5/7 mission simulators for the Royal Air Force p 3224 N92-28540
Crew station research and development facility training for the light helicopter demonstration/validation program
[NASA-TM-103865] p 3327 N92-28744
TRAJECTORIES
Accelerator simulation using computers
[DE92-010729] p 3356 N92-28270
TRAJECTORY CONTROL
Initial investigations of an adaptive discrete-time controller for nonlinear time-varying robotic models p 3247 N92-28736
A generalized reusable guidance algorithm for optimal aerobraking
[NASA-TM-103590] p 3229 N92-28981
TRANSDUCERS
Pressure transducer and system for cryogenic environments
[NASA-CASE-LAR-14579-1] p 3288 N92-29097
TRANSFER OF TRAINING
The use of a dedicated testbed to evaluate simulator training effectiveness p 3222 N92-28533
G-tolerance and spatial disorientation: Can simulation help us? p 3223 N92-28534
AM-X flight simulator from engineering tool to training device p 3223 N92-28536
TRANSFERRING
Secondary instability in 3D magnetic reconnection
[AD-A248630] p 3360 N92-28354
TRANSFORMATIONS (MATHEMATICS)
Studies of iterated transform image compression and its application to color and DTED
[AD-A248060] p 3339 N92-28946
TRANSFORMERS
SPEAR 2 space power data analysis
[AD-A248057] p 3250 N92-28945
TRANSFUSION
Structural characterization of cross-linked hemoglobins developed as potential transfusion substitutes
[AD-A246777] p 3325 N92-28515
TRANSIENT RESPONSE
Electromechanical systems with transient high power response operating from a resonant AC link
[NASA-TM-105716] p 3238 N92-28985
TRANSISTORS
Study of ultra short HFET devices with InP substrates
[AD-A248448] p 3279 N92-28427
TRANSITION METALS
Synthesis and characterization of new low-dimensional transition metal complex conductors
[AD-A249263] p 3258 N92-28237
Synthesis and study of metallonitride complexes and polymers
[AD-A248577] p 3262 N92-28323
Molecular recognition in the oxidation of catechols by Dicobalt-BISDIEN dioxygen complexes
[AD-A246456] p 3258 N92-28973
TRANSITION TEMPERATURE
Physics and technology for the investigation of properties of ultra small systems
[AD-A246772] p 3364 N92-28513
TRANSLATIONAL MOTION
Connection space reduction mechanism
[NASA-CASE-GSC-13220-1] p 3296 N92-29140
TRANSMISSIONS (MACHINE ELEMENTS)
Application of face-gear drives in helicopter transmissions
[NASA-TM-105655] p 3293 N92-28434
Dynamics of a split torque helicopter transmission
[NASA-TM-105681] p 3296 N92-29136
TRANSMITTANCE
Theoretical and experimental studies relevant to interpretation of auroral emissions
[NASA-CR-190521] p 3316 N92-28911
TRANSMITTER RECEIVERS
Windshear radar calibration: Transmitter power and receiver gain stability
[NASA-TM-107589] p 3275 N92-28876
TRANSONIC FLOW
Calculation of unsteady transonic flows with mild separation by viscous-inviscid interaction
[NASA-TP-3197] p 3226 N92-28477
Computation of steady and unsteady quasi-one-dimensional viscous/inviscid interacting internal flows at subsonic, transonic, and supersonic Mach numbers
[NASA-CR-189881] p 3283 N92-28555
Analysis of results of an Euler-equation method applied to leading-edge vortex flow
[NLR-TP-90368-U] p 3226 N92-28657
Wave drag determination in the transonic full-potential flow code MATRICS
[NLR-TP-90062-U] p 3228 N92-28709
Explicit Navier-Stokes computation of turbomachinery flows
[AD-A249284] p 3286 N92-28879
Turbulent spot generation and growth rates in a transonic boundary layer
[AD-A250221] p 3287 N92-29118
TRANSONIC WIND TUNNELS
The windtunnel as a tool for laminar flow research
[NLR-TP-90145-U] p 3240 N92-28661
Replacement of the NAL high pressure air storage system
[NAL-TM-634] p 3241 N92-28835
TRANSPORT AIRCRAFT
Use of a virtual cockpit for the development of a future transport aircraft p 3225 N92-28547
The use and effectiveness of piloted simulation in transport aircraft research and development p 3225 N92-28549
Hyperbolic grid generation with BEM source terms
[NLR-TP-90334-U] p 3347 N92-28635
Some longitudinal handling qualities design guidelines for active control technology transport aircraft
[NLR-TP-90129-U] p 3239 N92-28652
TRANSPORT PROPERTIES
A generalization of the K-V equilibrium for an intense, relativistic beam propagating in a solenoid
[AD-A247067] p 3350 N92-28238
Scattering mechanisms for semiconductor transport calculations
[AD-A249260] p 3278 N92-28295
Numerical studies of convective transport associated with crystal growth in mirrogravity p 3267 N92-28437
TRANSPORT THEORY
Fast algorithms for transport models
[DE92-011432] p 3338 N92-28841
TRANSPORT VEHICLES
A user's manual for MASH 1.0: A Monte Carlo adjoint shielding code system
[AD-A248204] p 3355 N92-29190
TRANSPUTERS
Transputer-based embedded system for Meteosat image data compression
[NLR-TP-90228-U] p 3305 N92-28697
TRIANGULATION
On-line point positioning with single frame camera data
[AD-A248307] p 3287 N92-28322
TRIBOLOGY
High-temperature miniaturized turbine engine lubrication system simulator
[AD-A249259] p 3236 N92-28294
Effect of metallic coating properties on the tribology of oil-lubricated coated-ceramics
[DE92-010904] p 3262 N92-28339
TRIBUTARIES
Martian channel networks: A revised Strahler approach for quantitative morphometry p 3380 N92-29000
TRUSSES
Control and stabilization of distributed parameter systems in structural dynamics
[AD-A247097] p 3298 N92-28320
Software design for automated assembly of truss structures
[NASA-TP-3198] p 3344 N92-28375
Structural design methodology for large space structures
[AD-A247672] p 3246 N92-28560
Correlation, error-localisation, and updating of the second problem defined in GARTEUR AG11
[NLR-TP-90070-U] p 3302 N92-28650
TUNABLE LASERS
Tunable optical sources and synthetic nonlinear media/growth and characterization of nonlinear optical materials
[AD-A249363] p 3357 N92-28328
Degenerate four-wave mixing using a tunable excimer laser to detect combustion gases
[DE92-005327] p 3290 N92-28852
Tuning and automatic phase adjustment in external cavity diode laser beam combiners
[AD-A247421] p 3290 N92-28903
TUNGSTEN
Visualization of gas tungsten arc weld pools
[AD-A245926] p 3293 N92-28384
TUNING
Learning and tuning fuzzy logic controllers through reinforcements
[NASA-TM-107875] p 3345 N92-28759
TURBINE BLADES
Laser anemometer measurements and computations in an annular cascade of high turning core turbine vanes
[NASA-TP-3252] p 3229 N92-28980
TURBINE ENGINES
High-temperature miniaturized turbine engine lubrication system simulator
[AD-A249259] p 3236 N92-28294
TURBINE PUMPS
Replacement bearing for Rocketdyne SSME HPOTPs using alternate self-lubricating retainer materials
[NASA-CR-184328] p 3292 N92-28362
Transient impeller test facility
[AD-D015249] p 3294 N92-28749
TURBOCOMPRESSORS
Dynamic simulation of compressor and gas turbine performance p 3237 N92-28463
TURBOFAN ENGINES
Diffuser casing upgrade for an advanced turbofan
[NLR-TP-90097-U] p 3238 N92-28711
TURBOFANS
Steady and transient performance calculation method for prediction, analysis, and identification p 3237 N92-28461
Component performance requirements p 3237 N92-28462

TURBOMACHINERY
Laser anemometer measurements and computations in an annular cascade of high turning core turbine vanes
[NASA-TP-3252] p 3229 N92-28980
TURBULENCE
Secondary instability in 3D magnetic reconnection
[AD-A248630] p 3360 N92-28354
Expand turbulence laboratory facilities to meet new DOD research interest
[AD-A248581] p 3240 N92-28388
The role of hard turbulent thermal convection in the Earth's early thermal evolution p 3310 N92-28593
Wall turbulence
[AD-A249973] p 3284 N92-28768
Wavelets and numerical simulation
[ONERA-NT-1991-8] p 3347 N92-28777
A self-affine multi-fractal wave/turbulence discrimination method using data from single point fast response sensors in a nocturnal atmospheric boundary layer
[AD-A250419] p 3318 N92-28799
Lagrangian turbulence: Structures and mixing in admissible model flows
[AD-A247203] p 3286 N92-28890
Laser anemometer measurements and computations in an annular cascade of high turning core turbine vanes
[NASA-TP-3252] p 3229 N92-28980
Turbulent spectra, fluxes, stability and growth of the mixed layer in the boundary layer of Mars
p 3393 N92-29070
TURBULENCE EFFECTS
Viscous effects on a vortex wake in ground effect
[NASA-CR-190400] p 3283 N92-28361
TURBULENCE MODELS
Turbulence modeling: Survey of activities in Belgium and the Netherlands, and appraisal of the status and a view on the prospects
[NLR-TP-90184-U] p 3284 N92-28694
Lagrangian turbulence: Structures and mixing in admissible model flows
[AD-A247203] p 3286 N92-28890
Low Reynolds number multiple-time-scale turbulence model and calculations of steady and pulsating shear layers
[NASA-CR-189176] p 3286 N92-28908
TURBULENT BOUNDARY LAYER
A numerical wind tunnel study of viscous-inviscid interaction
[AD-A248429] p 3283 N92-28350
Turbulence modeling: Survey of activities in Belgium and the Netherlands, and appraisal of the status and a view on the prospects
[NLR-TP-90184-U] p 3284 N92-28694
A self-affine multi-fractal wave/turbulence discrimination method using data from single point fast response sensors in a nocturnal atmospheric boundary layer
[AD-A250419] p 3318 N92-28799
Turbulent spot generation and growth rates in a transonic boundary layer
[AD-A250221] p 3287 N92-29118
TURBULENT FLOW
Studies in turbulence and turbulence control
[AD-A247164] p 3282 N92-28225
Flow gradient corrections on hot-wire measurements using an X-wire probe
[NLR-TP-90255-U] p 3228 N92-28713
Wall turbulence
[AD-A249973] p 3284 N92-28768
Large Eddy Simulations (LES) and Direct Numerical Simulations (DNS) for the computational analyses of high speed reacting flows
[NASA-CR-190364] p 3285 N92-28817
Large eddy simulations and direct numerical simulations of high speed turbulent reacting flows
p 3285 N92-28818
Modeling of the reactant conversion rate in a turbulent shear flow p 3229 N92-28820
Low Reynolds number multiple-time-scale turbulence model and calculations of steady and pulsating shear layers
[NASA-CR-189176] p 3286 N92-28908
Laser anemometer measurements and computations in an annular cascade of high turning core turbine vanes
[NASA-TP-3252] p 3229 N92-28980
TURBULENT HEAT TRANSFER
Turbulent spot generation and growth rates in a transonic boundary layer
[AD-A250221] p 3287 N92-29118
TURBULENT MIXING
Mapping closures for turbulent mixing and reaction
[AD-A247305] p 3283 N92-28274
Stochastic simulation of the structure and propagation rate of turbulent premixed flames
[DE92-006682] p 3256 N92-28822
TWO DIMENSIONAL BODIES
Construction of a numerical optimization method for the definition of hypersupported profiles
[ONERA-RSF-43/1736-AY-146A] p 3284 N92-28788
TWO DIMENSIONAL FLOW
The linear and nonlinear shear instability of a fluid sheet
[AD-A247092] p 3282 N92-28258
Explicit Navier-Stokes computation of turbomachinery flows
[AD-A249284] p 3286 N92-28879
TWO DIMENSIONAL MODELS
Plane wave propagation in random granular media
[AD-A247300] p 3298 N92-28424
A comparative study of the accuracy of various time domain nonorthogonal mesh methods
[DE92-007300] p 3347 N92-28824
Air ejector experiments using the two-dimensional supersonic cascade tunnel: Zero secondary flow performance
[NAL-TM-632] p 3241 N92-28829
A coupled regional tide model
[AD-A247917] p 3322 N92-28913
TYPHOONS
Microwave derived rainrates in typhoons and their use in the diagnosis and prediction of typhoon intensity
[AD-A250556] p 3319 N92-28922

U

U.S.S.R.
Determination of field related transfer factors for Cs-137 and Sr-90, from the fallout of the reactor accident in Chernobyl (USSR)
[OEFZS-4581] p 3356 N92-29210
UH-60A HELICOPTER
Rotorcraft In-Flight Simulation Research at NASA Ames Research Center: A Review of the 1980's and plans for the 1990's
[NASA-TM-103873] p 3234 N92-28926
ULTRASONIC CLEANING
Erosion of stainless steel by ultrasonic cleaning: A preliminary study
[DE92-012566] p 3260 N92-28763
ULTRASONIC FLAW DETECTION
In-situ fault detection by the hybrid ray-mode method
[AD-A250213] p 3297 N92-29112
ULTRASONIC RADIATION
Detection of in-plane displacements of acoustic wave fields using extrinsic Fizeau fiber interferometric sensors
[NASA-CR-190493] p 3353 N92-29196
ULTRASONIC TESTS
Nondestructive evaluation of damages caused by impact and fatigue loading of polymer composites
[VTT-RR-742] p 3251 N92-28572
In-situ fault detection by the hybrid ray-mode method
[AD-A250213] p 3297 N92-29112
The characterization of ceramics and ceramic/metal-joints by ultrasonic techniques
[VTT-RR-741] p 3266 N92-29194
ULTRASONICS
Instrumentation for ultrahigh strain rate experiments
[AD-A249358] p 3298 N92-28327
Ultrasonic ambient noise in Australian shallow waters at frequencies up to 200 kHz
[MRL-TR-91-23] p 3351 N92-28364
ULTRAVIOLET EMISSION
Future mission studies: Preliminary comparisons of solar flux models
[NASA-TM-107947] p 3396 N92-28869
ULTRAVIOLET LASERS
Research studies on extreme ultraviolet and soft x ray lasers
[AD-A247309] p 3289 N92-28299
Compact, self-contained ArF lasers
[AD-A247403] p 3291 N92-28932
ULTRAVIOLET RADIATION
Research studies on extreme ultraviolet and soft x ray lasers
[AD-A247309] p 3289 N92-28299
The impact of temperature dependent CO2 cross section measurements: A role for heterogeneous chemistry in the atmosphere of Mars? p 3372 N92-28479
Theoretical and experimental studies relevant to interpretation of auroral emissions
[NASA-CR-190521] p 3316 N92-28911
ULTRAVIOLET SPECTRA
An analysis of middle ultraviolet dayglow spectra
[AD-A245965] p 3309 N92-28319
A Be star atlas of far UV and optical high-resolution spectra
[ESA-SP-1147] p 3371 N92-28781
ULTRAVIOLET SPECTROMETERS
Atomic oxygen in the Martian thermosphere
p 3391 N92-29061
UNCONSCIOUSNESS
Study of the loss of consciousness inflight by fighter aircraft pilots
[ONERA-RTS-11/3446-EY] p 3325 N92-28844
UNDERGROUND EXPLOSIONS
Studies of regional wave propagation using differential seismograms and randomized structural models
[AD-A247011] p 3309 N92-28394
UNDERWATER ACOUSTICS
A domain decomposition method for ocean/bottom interaction problems
[FFI-91/7022] p 3320 N92-28266
Simulation of the propagation of acoustical waves through an interface separating a compressible fluid and an elastic medium
[FFI-91/7017] p 3351 N92-28314
Under-ice broadband transient measurements and processing
[AD-A248609] p 3351 N92-28324
UNDERWATER ENGINEERING
Rocket nozzle shield
[AD-D015248] p 3249 N92-28748
UNDERWATER EXPLOSIONS
Under-ice broadband transient measurements and processing
[AD-A248609] p 3351 N92-28324
UNDERWATER OPTICS
Impact on the medium MTF by model estimation of beta
[AD-A247985] p 3359 N92-29167
UNITED NATIONS
Information systems for engineering sustainable development
[DE92-011271] p 3368 N92-28838
UNIX (OPERATING SYSTEM)
DEPEND: A simulation-based environment for system level dependability analysis
[NASA-CR-189752] p 3297 N92-28726
UNSTEADY AERODYNAMICS
Studies in turbulence and turbulence control
[AD-A247164] p 3282 N92-28225
Study of the leading-edge vortex dynamics in the unsteady flow over an airfoil
[AD-A247532] p 3228 N92-28865
UNSTEADY FLOW
Calculation of unsteady transonic flows with mild separation by viscous-inviscid interaction
[NASA-TP-3197] p 3226 N92-28477
Computation of steady and unsteady quasi-one-dimensional viscous/inviscid interacting internal flows at subsonic, transonic, and supersonic Mach numbers
[NASA-CR-189881] p 3283 N92-28555
Study of the leading-edge vortex dynamics in the unsteady flow over an airfoil
[AD-A247532] p 3228 N92-28865
Low Reynolds number multiple-time-scale turbulence model and calculations of steady and pulsating shear layers
[NASA-CR-189176] p 3286 N92-28908
Development of an unsteady three-dimensional viscous-inviscid interaction numerical method for the calculation of airfoils vibration
[ONERA-RSF-7/3617-AY-022A] p 3229 N92-29206
UPGRADING
Life cycle costs of the C-130 electrical power system upgrade
[AD-A246759] p 3221 N92-28348
UPPER ATMOSPHERE
An ion mass spectrometer for measuring isotopic adundances and loss rates of O, C and H in Mars' upper atmosphere p 3374 N92-28486
Dust storm driven variations of the Mars thermosphere and exosphere: Coupling of atmospheric regions
p 3380 N92-28997
The ultraviolet albedo of Mars p 3394 N92-29074
UPPER SURFACE BLOWING
Aerodynamic characteristics obtained from alpha sweep test of the quiet STOL experimental aircraft ASKA
[NAL-TR-1112] p 3234 N92-28901
UPWELLING WATER
A numerical study of time-dependent wind forcing off the west coast of Portugal, 1987-1988
[AD-A246775] p 3321 N92-28365
USER MANUALS (COMPUTER PROGRAMS)
The Navy layered ocean model users guide
[AD-A247754] p 3321 N92-28566
SPECTOOL: User's manual, volume 2
[AD-A247493] p 3336 N92-28667
NASA Lewis steady-state heat pipe code users manual
[NASA-TM-105161] p 3249 N92-28682
User's manual for the Gaussian windows program
[NASA-CR-190554] p 3340 N92-29107

HYPER: A domain decomposition program, version 1.0 (user's manual)
[AD-A250018] p 3340 N92-29172
A user's manual for MASH 1.0: A Monte Carlo adjoint shielding code system
[AD-A248204] p 3355 N92-29190

USER REQUIREMENTS
Instrumentation requirements for laminar flow research in the NLR high speed wind tunnel HST
[NLR-TP-89158-U] p 3240 N92-28669
Superconducting at NLR: NEC SX-2 capabilities in NLR's terminal and file-transfer network
[NLR-TP-89007-U] p 3342 N92-28706
Development of a flight information system using the structured method
[AD-A248207] p 3236 N92-29222

V

V-22 AIRCRAFT
Shipboard mission training effectiveness of the Naval Air Test Center's V-22 government test pilot trainer p 3224 N92-28542

VACUUM
Non-mechanical optical path switching and its application to dual beam spectroscopy including gas filter correlation radiometry
[NASA-CASE-LAR-14588-1-CU] p 3359 N92-29117

VACUUM CHAMBERS
Water window imaging x ray microscope
[NASA-CASE-MFS-28485-1] p 3288 N92-29135

VACUUM MELTING
Some experiments to determine the efficiency of collection of alumina particles by electron beam button melting in a nickel-base superalloy, AP1
[NPL-DMM(A)-42] p 3261 N92-29164

VACUUM PUMPS
High voltage splitting unit for the power supplies of the vacuum pumps of AmPS
[DIGEL-1991-7] p 3278 N92-28263

VALENCE
High quality Gaussian basis sets for fourth-row atoms
[NASA-TM-103918] p 3255 N92-28743

VALVES
Solid-propellant-powered maneuvering system for spacecraft
[AD-D015245] p 3249 N92-28747
Assessment of valve actuator motor rotor degradation by Fourier Analysis of current waveform
[DE92-013233] p 3281 N92-28814
Flow rate testing of valves used with the 500 gallon collapsible drum
[AD-A250567] p 3294 N92-28924

VANADIUM ALLOYS
Surface residual stress analysis of metals and alloys
[AD-A248372] p 3259 N92-28426

VANES
Laser anemometer measurements and computations in an annular cascade of high turning core turbine vanes
[NASA-TP-3252] p 3229 N92-28980

VAPOR DEPOSITION
Thin film cadmium telluride photovoltaic cells
[DE92-001239] p 3306 N92-28277
Chemical vapor deposition of yttrium borium(2) copper(3) oxygen(x) thin films for wire applications
[AD-A247013] p 3364 N92-28395
Heteroepitaxy of InP on Si (001)
[ETN-92-91333] p 3364 N92-28786
Studies of 1,3-disilacyclobutanes as single-source CVD precursors to silicon carbide
[AD-A247111] p 3365 N92-28885
Large-area, plasma-assisted, halogen-based diamond deposition
[AD-A247423] p 3264 N92-28904
Chemical vapor synthesis of niobium aluminides
[AD-A250332] p 3258 N92-29091
The in situ observation of diamond film nucleation and growth
[AD-A248203] p 3265 N92-29189
Feasibility of metal-oxide-semiconductor structures on Si-LPCVD thin films by low temperature (600 C) process
[LAAS-91307] p 3365 N92-29207

VAPOR PHASE EPITAXY
The in situ observation of diamond film nucleation and growth
[AD-A248203] p 3265 N92-29189

VAPOR PHASES
Near millimeter waves and microelectronics
[AD-A250384] p 3281 N92-28797
Volatile CVD precursors based on copper alkoxides and mixed group IIA-Copper alkoxides — chemical vapor deposition
[AD-D015264] p 3261 N92-29170

VAPORS
The subsurface hydrologic response of Mars to the thermal evolution of its early crust p 3381 N92-29006

VARIABILITY
Structure energetics and dynamics of Gulf Stream variability
[AD-A248246] p 3323 N92-29225

VASODILATION
Thermoregulation during spaceflight
[NASA-TM-103913] p 3325 N92-28420

VECTOR PROCESSING (COMPUTERS)
CESAR address generator
[FFI-91/7021] p 3334 N92-28265
Vector and parallel supercomputing programming
[ONERA-NT-1991-11] p 3338 N92-28779
Functional requirements document for the Earth Observing System Data and Information System (EOSDIS) Scientific Computing Facilities (SCF) of the NASA/MSFC Earth Science and Applications Division, 1992
[NASA-TM-4392] p 3333 N92-28899

VECTOR SPACES
An application of interactive computer graphics to the study of inferential statistics and the general linear model
[AD-A246668] p 3334 N92-28285

VECTORS (MATHEMATICS)
An application of interactive computer graphics to the study of inferential statistics and the general linear model
[AD-A246668] p 3334 N92-28285
The principal part of plane vector fields with fixed Newton diagram
[DE92-622408] p 3346 N92-28311
A look-ahead variant of the Lanczos algorithm and its application to the quasi-minimal residual method for non-Hermitian linear systems
[NASA-CR-190557] p 3340 N92-29113

VEGETATION GROWTH
Coupling plant growth and waste recycling systems in a controlled life support system (CELSS)
[NASA-TM-107544] p 3330 N92-28670

VELOCITY DISTRIBUTION
Giant and large impacts in the context of planetary formation theory p 3315 N92-28619
Wall turbulence
[AD-A249973] p 3284 N92-28768
Experimental and theoretical investigations on the particle lag of particles under the influence of large velocity gradients in compressible flow
[DLR-FB-91-25] p 3286 N92-28825

VELOCITY MEASUREMENT
Wall turbulence
[AD-A249973] p 3284 N92-28768
Experimental and theoretical investigations on the particle lag of particles under the influence of large velocity gradients in compressible flow
[DLR-FB-91-25] p 3286 N92-28825
Study of the leading-edge vortex dynamics in the unsteady flow over an airfoil
[AD-A247532] p 3228 N92-28865
A 4-spot time-of-flight anemometer for small centrifugal compressor velocity measurements
[NASA-TM-105717] p 3288 N92-29105

VENTS
Iron Moessbauer spectroscopy: Superparamagnetism in hydrothermal vents and the search for evidence of past life on Mars p 3378 N92-28989

VENUS (PLANET)
Influence of aerodynamic roughness length on aeolian processes: Earth, Mars, Venus p 3380 N92-28996

VERBAL COMMUNICATION
An analysis of aircrew communication patterns and content
[AD-A246618] p 3272 N92-28253

VERTICAL DISTRIBUTION
Mesoscale vertical structure of an explosive oceanic cyclone
[AD-A245927] p 3318 N92-28423
Feasibility study of hypersonic clinometric measurements at R3Ch
[ONERA-RSF-136/1865-AY-728-] p 3228 N92-28789
Mars atmospheric water p 3381 N92-29005

VERTICAL LANDING
Internal reversing flow in a tailpipe offtake configuration for SSTOVL aircraft
[NASA-TM-105698] p 3236 N92-28418

VERTICAL MOTION SIMULATORS
The use of ground based simulation for handling qualities research: A new assessment p 3224 N92-28545

VERTICAL TAKEOFF
S-76B certification for vertical take-off and landing operations from confined areas
[NLR-TP-90286-U] p 3233 N92-28714

VERTICAL TAKEOFF AIRCRAFT
Aircraft ship operations
[AGARD-AR-312] p 3231 N92-28468

VERY LARGE ARRAY (VLA)
VLA mapping of 1.35 cm water emission from the Mars atmospheric limb p 3381 N92-29004

VERY LARGE SCALE INTEGRATION
Femtosecond carrier processes in compound semiconductors and real time signal processing
[AD-A248053] p 3278 N92-28275
Multiple-valued programmable logic array minimization by simulated annealing
[AD-A248620] p 3335 N92-28353
The silicon compiler for designing military VLSI ASIC's p 3235 N92-28378
Applications of silicon hybrid multi-chip modules to avionics p 3235 N92-28379
A knowledge based approach for testing VLSI circuits: Application to the validation of prototypes for a non-contact test
[ETN-92-91321] p 3280 N92-28783
VHDL and waves descriptions for a pseudo-random pattern generator
[AD-A247891] p 3349 N92-28961

VIBRATION
Comparison of three controllers applied to helicopter vibration
[NASA-TM-102192] p 3239 N92-28457
Optimum design of a gearbox for low vibration
[NASA-TM-105653] p 3293 N92-28476

VIBRATION DAMPING
Payload isolation and stabilization by a Suspended Experiment Mount (SEM)
[NASA-TM-107941] p 3246 N92-28369
NASDA's activities on vibration isolation technology p 3267 N92-28441
Shock and vibration isolation for cyclic exercise in spacecraft p 3267 N92-28449
Comparison of three controllers applied to helicopter vibration
[NASA-TM-102192] p 3239 N92-28457
Optimum design of a gearbox for low vibration
[NASA-TM-105653] p 3293 N92-28476
Experiments in passive vibration reduction
[AD-A250397] p 3304 N92-29181

VIBRATION ISOLATORS
Payload isolation and stabilization by a Suspended Experiment Mount (SEM)
[NASA-TM-107941] p 3246 N92-28369
International Workshop on Vibration Isolation Technology for Microgravity Science Applications
[NASA-CP-10094] p 3268 N92-28436
The Microgravity Isolation Mount (MGIM): A Columbus facility for improving the microgravity quality of payloads p 3267 N92-28439
NASDA's activities on vibration isolation technology p 3267 N92-28441
Vibration isolation technology development to demonstration p 3267 N92-28442
New inertial actuator provides isolation and stabilization in microgravity conditions p 3267 N92-28443
A 6 degree-of-freedom Lorentz force vibration isolator with nonlinear controller p 3267 N92-28444
Digital control algorithms for microgravity isolation systems p 3267 N92-28445
Microgravity vibration isolation research at the University of Virginia p 3267 N92-28446
Extended H2 synthesis for microgravity vibration isolation p 3267 N92-28447
Shock and vibration isolation for cyclic exercise in spacecraft p 3267 N92-28449
Early mission science support: Space Acceleration Measurement System (SAMS) p 3248 N92-28451

VIBRATION MEASUREMENT
Computer recognition and analysis of photogrammetric targets
[AD-A250313] p 3339 N92-28971

VIBRATION TESTS
Environmental testing of the Xi Scan 1000, portable fluoroscopic and radiographic imaging system
[AD-A247167] p 3324 N92-28242
Exploratory flexural power flow measurements on a bar
[NLR-TP-90178-U] p 3304 N92-29176
On the use of structural dynamic experimental methods for damage inspection of a glass fibre reinforced plastic plate
[FFA-TN-1992-02] p 3253 N92-29220

VIBRATIONAL STRESS
Predicting microgravity levels for space station using VAPEPS p 3268 N92-28455
Exploratory flexural power flow measurements on a bar
[NLR-TP-90178-U] p 3304 N92-29176

VIKING LANDER SPACECRAFT
Micro weather stations for in situ measurements in the Martian planetary boundary layer p 3382 N92-29008

Surface photometric properties and albedo changes in the central equatorial region of Mars
p 3392 N92-29066
Modeling the seasonal cycle of CO2 on Mars: A fit to the Viking lander pressure curves p 3394 N92-29076

VIKING MARS PROGRAM
Determining the pH of Mars from the Viking labelled release reabsorption effect p 3389 N92-29049
Physical properties of Deucalionis, Eos, Xanthe-type units in the central equatorial region of Mars
p 3392 N92-29063
The ultraviolet albedo of Mars p 3394 N92-29074

VIKING ORBITER SPACECRAFT
Temporal variability of the surface and atmosphere of Mars: Viking Orbiter color observations
p 3388 N92-29041
Physical interpretation of thermal and reflected data on Martian surface units p 3391 N92-29062
Physical properties of Meridiani Sinus-type units in the central equatorial region of Mars p 3392 N92-29064

VIKING ORBITER 2
Surface photometric properties and albedo changes in the central equatorial region of Mars
p 3392 N92-29066

VIRTUAL MEMORY SYSTEMS
A discrete Fourier transform for virtual memory machines
[NASA-TM-103914] p 3349 N92-28672

VISCOMETRY
Estimation of the viscosities of silicate liquids at high pressure from measurements of oxygen diffusivity
p 3313 N92-28607

VISCOSITY
Estimation of the viscosities of silicate liquids at high pressure from measurements of oxygen diffusivity
p 3313 N92-28607

VISCOUS FLOW
A numerical wind tunnel study of viscous-inviscid interaction
[AD-A248429] p 3283 N92-28350
Viscous effects on a vortex wake in ground effect
[NASA-CR-190400] p 3283 N92-28361
Calculation of unsteady transonic flows with mild separation by viscous-inviscid interaction
[NASA-TP-3197] p 3226 N92-28477
Computation of steady and unsteady quasi-one-dimensional viscous/inviscid interacting internal flows at subsonic, transonic, and supersonic Mach numbers
[NASA-CR-189881] p 3283 N92-28555
Control of nonlinear distributed parameter systems with application to flow control
[AD-A250212] p 3346 N92-29149
Development of an unsteady three-dimensional viscous-inviscid interaction numerical method for the calculation of airfoils vibration
[ONERA-RSF-7/3617-AY-022A] p 3229 N92-29206

VISCOUS FLUIDS
Experimental measurement of the orbital paths of particles sedimenting within a rotating viscous fluid as influenced by gravity
[NASA-TP-3200] p 3331 N92-28897

VISIBLE SPECTRUM
Relationships of soil, grass, and bedrock over the Kaweah serpentine melange through spectral mixture analysis of AVIRIS data
[NASA-CR-190445] p 3306 N92-28717

VISUAL FIELDS
Program Cluster: An identification of fixation cluster characteristics
[AD-A247014] p 3326 N92-28396

VISUAL PERCEPTION
Program Cluster: An identification of fixation cluster characteristics
[AD-A247014] p 3326 N92-28396
Delays in laser glare onset differentially affect target-location performance in a visual search task
[AD-A246708] p 3327 N92-28557
A theory of automated design of visual information presentations
[AD-A247425] p 3369 N92-28866
Neuropsychological components of object identification
[AD-A247049] p 3327 N92-28877

VISUAL TASKS
Program Cluster: An identification of fixation cluster characteristics
[AD-A247014] p 3326 N92-28396

VLASOV EQUATIONS
A generalization of the K-V equilibrium for an intense, relativistic beam propagating in a solenoid
[AD-A247067] p 3350 N92-28238

VOICE DATA PROCESSING
Examination of prosodic features in speech signal using speech fundamental frequency and loudness duration
[ETN-92-91334] p 3274 N92-28792

VOLATILITY
Atmosphere-surface interactions and atmospheric evolution on Mars p 3383 N92-29012

VOLCANOES
Volcanic recycling of carbonate deposits on Mars
p 3377 N92-28506
The role of SO2 on Mars and on the primordial oxygen isotope composition of water on Earth and Mars
p 3377 N92-28507
Was early Mars warmed by ammonia?
p 3386 N92-29030

VOLCANOLOGY
Volcanic recycling of carbonate deposits on Mars
p 3377 N92-28506
Recent Elysium volcanism: Effects on the Martian atmosphere p 3389 N92-29048

VOLT-AMPERE CHARACTERISTICS
Leakage current measurements in SOI devices
[AD-A247694] p 3280 N92-28561

VORTEX ALLEVIATION
Flow visualization studies of a sideslipping, canard-configured X-31A-Like fighter aircraft model
[AD-A245940] p 3228 N92-28883

VORTEX GENERATORS
Aerodynamic characteristics obtained from alpha sweep test of the quiet STOL experimental aircraft ASKA
[NAL-TR-1112] p 3234 N92-28901

VORTICES
Viscous effects on a vortex wake in ground effect
[NASA-CR-190400] p 3283 N92-28361
Wall turbulence
[AD-A249973] p 3284 N92-28768
Large Eddy Simulations (LES) and Direct Numerical Simulations (DNS) for the computational analyses of high speed reacting flows
[NASA-CR-190364] p 3285 N92-28817
Large eddy simulations and direct numerical simulations of high speed turbulent reacting flows
p 3285 N92-28818
Study of the leading-edge vortex dynamics in the unsteady flow over an airfoil
[AD-A247532] p 3228 N92-28865

VORTICITY
Studies in turbulence and turbulence control
[AD-A247164] p 3282 N92-28225

VSAT (NETWORK)
Future benefits and applications of intelligent on-board processing to VSAT services
[NASA-CR-189185] p 3273 N92-28431

W

WAFERS
Strained AlGaInAs semiconducting material for improved laser performance
[AD-A249379] p 3289 N92-28330
A survey of high density packaging for high performance computing system
[AD-A248633] p 3332 N92-28891

WALL FLOW
A numerical wind tunnel study of viscous-inviscid interaction
[AD-A248429] p 3283 N92-28350
Wall turbulence
[AD-A249973] p 3284 N92-28768
Lagrangian turbulence: Structures and mixing in admissible model flows
[AD-A247203] p 3286 N92-28890

WASTE TREATMENT
Monitoring activities review of the Radiological Environmental Surveillance Program
[DE92-013103] p 3308 N92-28811

WATER
Papers Presented to the Workshop on the Evolution of the Martian Atmosphere
[NASA-CR-190508] p 3372 N92-28478
Redistribution of subsurface neutrons caused by ground ice on Mars p 3374 N92-28488
Mars volatile evolution: Implications of the recent measurement of O-17 in water from the SNC meteorites
p 3375 N92-28492
The Mars water cycle at other epochs: History of the polar caps and layered terrain p 3375 N92-28493
Liquid water habitats on early Mars
p 3376 N92-28500
Martian atmospheric chemistry during the time of low water abundance p 3376 N92-28501
Astronomical variation experiments with a Mars general circulation model p 3376 N92-28503
The role of SO2 on Mars and on the primordial oxygen isotope composition of water on Earth and Mars
p 3377 N92-28507
Space life support engineering program
[NASA-CR-190448] p 3330 N92-28671
Magmatic intrusions and hydrothermal systems on Mars p 3384 N92-29019
Distribution of water on Mars: Implications from SNC meteorites p 3386 N92-29027
A carbonate-silicate aqueous geochemical cycle model for Mars p 3390 N92-29057
Amazonis and Utopia Planitiae: Martian Lacustrine basins p 3391 N92-29058
Water window imaging x ray microscope
[NASA-CASE-MFS-28485-1] p 3288 N92-29135
Impact on the medium MTF by model estimation of beta
[AD-A247985] p 3359 N92-29167

WATER CURRENTS
Moored current measurements made in the Iceland Faeroes region during July-August 1990
[IOS-286-1991] p 3323 N92-29212

WATER FLOW
Chryse Planitia region, Mars: Channeling history, flood-volume estimates, and scenarios for bodies of water in the northern plains p 3390 N92-29054

WATER MANAGEMENT
An inventory of data collected during the NERC's North Sea Community Research Project, 1987-1992
[REPT-21-1991] p 3323 N92-29215

WATER MASERS
Intense electron beam cyclotron masers with microsecond pulselengths
[AD-A247060] p 3289 N92-28271

WATER RECLAMATION
Space life support engineering program
[NASA-CR-190448] p 3330 N92-28671
Whole body cleaning agent containing N-acyltaurate
[NASA-CASE-MSC-21589-1] p 3332 N92-29137

WATER RESOURCES
Water inventories on Earth and Mars: Clues to atmosphere formation p 3373 N92-28483
The Martian polar caps: Stability and water transport at low obliquities p 3385 N92-29023

WATER SPLITTING
Water electrolysis
[NASA-CASE-MSC-21572-1-SB] p 3256 N92-28756

WATER TEMPERATURE
Moored current measurements made in the Iceland Faeroes region during July-August 1990
[IOS-286-1991] p 3323 N92-29212

WATER VAPOR
VLA mapping of 1.35 cm water emission from the Mars atmospheric limb p 3381 N92-29004
Mars atmospheric water p 3381 N92-29005
Recent Elysium volcanism: Effects on the Martian atmosphere p 3389 N92-29048
Carbonate formation on Mars: History of the CO2 atmosphere from models of diffusion-limited growth in non-aqueous environments p 3391 N92-29060

WATER WAVES
Directional wave data recorded off Flamborough Head (England)
[IOS-273-1990] p 3323 N92-29216

WAVE DRAG
Wave drag determination in the transonic full-potential flow code MATRICS
[NLR-TP-90062-U] p 3228 N92-28709

WAVE EQUATIONS
Analysis of electromagnetic propagation over variable terrain using the parabolic wave equation
[AD-A248061] p 3276 N92-28947
On some splitting schemes for wave equations
[FFI-91/7023] p 3348 N92-29193

WAVE FRONTS
Plane wave propagation in random granular media
[AD-A247300] p 3298 N92-28424

WAVE INTERACTION
The theory of the long waveguide structures radiating the LH waves into a plasma
[IPPCZ-314] p 3361 N92-28742

WAVE PROPAGATION
A domain decomposition method for ocean/bottom interaction problems
[FFI-91/7022] p 3320 N92-28266
Simulation of the propagation of acoustical waves through an interface separating a compressible fluid and an elastic medium
[FFI-91/7017] p 3351 N92-28314
Analysis of the effects of Eurasian crustal and upper mantle structure on regional phases using broadband seismic data
[AD-A248383] p 3309 N92-28386
Studies of regional wave propagation using differential seismograms and randomized structural models
[AD-A247011] p 3309 N92-28394
Plane wave propagation in random granular media
[AD-A247300] p 3298 N92-28424
NORSAR basic seismological research
[AD-A248616] p 3309 N92-28569

Aperture coupling measurement in a test chamber for the Advanced Photon Source (APS)
[DE92-013059] p 3274 N92-28809
Hydrodynamic echo in strongly inhomogeneous magnetized plasma
[DE92-621530] p 3361 N92-28816
Simulating radar propagation through atmospheric turbulence using the Tropospheric ElectroMagnetic Parabolic Equation Routine (TEMPER)
[AD-A247408] p 3275 N92-28905
The distance dependence of regional phase discriminants
[AD-A247546] p 3316 N92-28935
Analysis of constrained-layer damping of flexural and extensional waves in infinite, fluid-loaded plates
[AD-A247936] p 3304 N92-29081
Detection of in-plane displacements of acoustic wave fields using extrinsic Fizeau fiber interferometric sensors
[NASA-CR-190493] p 3353 N92-29196

WAVE SCATTERING
Studies of regional wave propagation using differential seismograms and randomized structural models
[AD-A247011] p 3309 N92-28394

WAVEFORMS
Assessment of valve actuator motor rotor degradation by Fourier Analysis of current waveform
[DE92-013233] p 3281 N92-28814
Monaural and binaural processing of complex waveforms
[AD-A247199] p 3352 N92-28889

WAVEGUIDE LASERS
Perspectives of ion implantation for optics
[DE92-010664] p 3357 N92-28355
Compact, self-contained ArF lasers
[AD-A247403] p 3291 N92-28932

WAVEGUIDES
Perspectives of ion implantation for optics
[DE92-010664] p 3357 N92-28355
Investigation of an equivalent circuit for the inductive strip in finline with dielectric
[AD-A247025] p 3279 N92-28373
The theory of the long waveguide structures radiating the LH waves into a plasma
[IPPCZ-314] p 3361 N92-28742

WAVELENGTH DIVISION MULTIPLEXING
Advanced optical fiber communication systems
[AD-A247683] p 3357 N92-28554

WEAPON SYSTEMS
Development and evaluation of an attack and maneuvering system with combat development simulators as main development tool p 3224 N92-28541

WEAPONS
A survey of high density packaging for high performance computing system
[AD-A248633] p 3332 N92-28891
Wing-extendible gliding store
[AD-D015233] p 3234 N92-28987

WEAPONS INDUSTRY
A survey of high density packaging for high performance computing system
[AD-A248633] p 3332 N92-28891

WEAR
Effect of metallic coating properties on the tribology of oil-lubricated coated-ceramics
[DE92-010904] p 3262 N92-28339
Turbine aircraft engine operational trending and JT8D static component reliability study
[DOT/FAA/CT-91/10] p 3238 N92-28686

WEATHER
Midlatitude weather systems on Mars: Is there a hemispheric asymmetry? p 3379 N92-28992

WEATHER FORECASTING
Polar lows over the northeast Greenland Sea
[AD-A245360] p 3318 N92-28421
Microwave derived rainrates in typhoons and their use in the diagnosis and prediction of typhoon intensity
[AD-A250556] p 3319 N92-28922
Evaluation of simple mesoscale models for use in TESS
[AD-A247914] p 3316 N92-28964

WEATHER STATIONS
Micro weather stations for in situ measurements in the Martian planetary boundary layer p 3382 N92-29008

WEATHERING
Rates of oxidative weathering on the surface of Mars p 3380 N92-28999
Mars surface weathering products and spectral analogs: Palagonites and synthetic iron minerals p 3383 N92-29017
Characterization of Martian near-subsurface materials by determination of cohesion and angle of internal friction p 3393 N92-29068
Aqueous-alteration products in S-N-C meteorites and implications for volatile/regolith interactions on Mars p 3393 N92-29071
Hydrogen and carbon isotopic composition of volatiles in Nakhla: Implications for weathering on Mars p 3394 N92-29075

WEIGHTING FUNCTIONS
Weighted-density functional approach for the solid-liquid interfaces in electrolytes
[DE92-622662] p 3362 N92-28280

WEIGHTLESSNESS
Shock and vibration isolation for cyclic exercise in spacecraft p 3267 N92-28449
Whole body cleaning agent containing N-acyltaurate
[NASA-CASE-MSC-21589-1] p 3332 N92-29137
Cryogenic shutter
[NASA-CASE-GSC-13189-2] p 3296 N92-29151

WELDED JOINTS
Weld pool flow visualization studies during gas tungsten arc welding of steel and aluminum
[AD-A249204] p 3292 N92-28293
Development of an automated wire delivery system for robotic welding applications
[NASA-CR-190487] p 3295 N92-29134

WELDING MACHINES
High temperature solder device for flat cables
[NASA-CASE-GSC-13344-1] p 3261 N92-29094

WETTING
Whole body cleaning agent containing N-acyltaurate
[NASA-CASE-MSC-21589-1] p 3332 N92-29137

WHEATSTONE BRIDGES
Pressure transducer and system for cryogenic environments
[NASA-CASE-LAR-14579-1] p 3288 N92-29097

WHEELS
Device for applying constant pressure to a surface
[NASA-CASE-GSC-13230-1] p 3294 N92-28754

WHITE NOISE
Non-linear analysis of visual cortical neurons
[AD-A250233] p 3326 N92-29179

WIND (METEOROLOGY)
Wind-speed forecasting study for Westover AFB, Massachusetts
[AD-A247545] p 3319 N92-28934
Evaluation of simple mesoscale models for use in TESS
[AD-A247914] p 3316 N92-28964
The composition of Martian aeolian sands: Thermal emissivity from Viking IRTM observations p 3382 N92-29010
Observed changes in limb clouds immediately prior to the onset of planet-encircling dust storms p 3388 N92-29039
Turbulent spectra, fluxes, stability and growth of the mixed layer in the boundary layer of Mars p 3393 N92-29070

WIND EFFECTS
Influence of aerodynamic roughness length on aeolian processes: Earth, Mars, Venus p 3380 N92-28996
The composition of Martian aeolian sands: Thermal emissivity from Viking IRTM observations p 3382 N92-29010
Infrared photometric behavior and opposition effect of Mars p 3382 N92-29011
Nonlinear stratified flow over localized topographic obstacles on Mars p 3387 N92-29036
Aqueous-alteration products in S-N-C meteorites and implications for volatile/regolith interactions on Mars p 3393 N92-29071

WIND EROSION
Nonlinear stratified flow over localized topographic obstacles on Mars p 3387 N92-29036

WIND MEASUREMENT
Expand turbulence laboratory facilities to meet new DOD research interest
[AD-A248581] p 3240 N92-28388
Evaluation of a Solent sonic anemometer on RRS Charles Darwin Cruise 43
[IOS-288-1991] p 3323 N92-29213

WIND PROFILES
Influence of aerodynamic roughness length on aeolian processes: Earth, Mars, Venus p 3380 N92-28996

WIND SHEAR
A numerical study of time-dependent wind forcing off the west coast of Portugal, 1987-1988
[AD-A248775] p 3321 N92-28365
Windshear radar calibration: Transmitter power and receiver gain stability
[NASA-TM-107589] p 3275 N92-28876
Comparison of drift potential derived from Mars GCM with rock abundance from IRTM p 3395 N92-29078

WIND TUNNEL APPARATUS
Studies in general aviation aerodynamics
[NASA-CR-190431] p 3226 N92-28511
Instrumentation requirements for laminar flow research in the NLR high speed wind tunnel HST
[NLR-TP-89158-U] p 3240 N92-28669
Flow quality studies of the NASA Lewis Research Center 8- by 6-foot supersonic/9- by 15-foot low speed wind tunnel
[NASA-TM-105417] p 3240 N92-28673
Upgrading the data processing section of the NAL Gust Wind Tunnel data processing system
[NAL-TM-635] p 3241 N92-28833
The design of test-section inserts for higher speed aeroacoustic testing in the Ames 80- by 120-foot wind tunnel
[NASA-TM-103915] p 3353 N92-28909

WIND TUNNEL MODELS
Instrumentation requirements for laminar flow research in the NLR high speed wind tunnel HST
[NLR-TP-89158-U] p 3240 N92-28669
LAH-main rotor model test at the DNW
[NLR-TP-90305-U] p 3233 N92-28687

WIND TUNNEL TESTS
A numerical wind tunnel study of viscous-inviscid interaction
[AD-A248429] p 3283 N92-28350
Studies in general aviation aerodynamics
[NASA-CR-190431] p 3226 N92-28511
Comparison of LDA and LTA applications for propeller tests in wind tunnels
[NLR-MP-88031-U] p 3226 N92-28658
The windtunnel as a tool for laminar flow research
[NLR-TP-90145-U] p 3240 N92-28661
LAH-main rotor model test at the DNW
[NLR-TP-90305-U] p 3233 N92-28687
Feasibility study of hypersonic clinometric measurements at R3Ch
[ONERA-RSF-136/1865-AY-728-] p 3228 N92-28789
Aerodynamic characteristics obtained from alpha sweep test of the quiet STOL experimental aircraft ASKA
[NAL-TR-1112] p 3234 N92-28901
Calculation of support interferences on the aerodynamic coefficients for a wind tunnel calibration model
[ESA-TT-1247] p 3229 N92-29159

WIND TUNNELS
Experimental aerodynamic facilities of the Aerodynamics Research and Concepts Assistance Branch
[AD-A247489] p 3240 N92-28248
Expand turbulence laboratory facilities to meet new DOD research interest
[AD-A248581] p 3240 N92-28388
The design of test-section inserts for higher speed aeroacoustic testing in the Ames 80- by 120-foot wind tunnel
[NASA-TM-103915] p 3353 N92-28909
Turbulent spot generation and growth rates in a transonic boundary layer
[AD-A250221] p 3287 N92-29118

WIND VELOCITY
SAR-relate stress variability in the Marine Atmospheric Boundary Layer (MABL)
[AD-A247772] p 3309 N92-28567
Wind-speed forecasting study for Westover AFB, Massachusetts
[AD-A247545] p 3319 N92-28934
Turbulent spectra, fluxes, stability and growth of the mixed layer in the boundary layer of Mars p 3393 N92-29070

WIND VELOCITY MEASUREMENT
Potential applications of laser Doppler anemometry for in-flight measurements
[NLR-TP-90163-U] p 3236 N92-28654

WING PLANFORMS
Studies in general aviation aerodynamics
[NASA-CR-190431] p 3226 N92-28511

WING TIP VORTICES
Analysis of results of an Euler-equation method applied to leading-edge vortex flow
[NLR-TP-90368-U] p 3226 N92-28657

WINGS
Integrating aerodynamics and structures in the minimum weight design of a supersonic transport wing
[NASA-TM-107586] p 3231 N92-28435
Turbulence modeling: Survey of activities in Belgium and the Netherlands, and appraisal of the status and a view on the prospects
[NLR-TP-90184-U] p 3284 N92-28694
Reduction and analysis of F-111C flight data
[AD-A250341] p 3233 N92-28771

WIRE
The use of conformal subdomain basis functions in the method of moments computations for a thin wire
[AD-A245964] p 3272 N92-28347
Chemical vapor deposition of yttrium borium(2) copper(3) oxygen(x) thin films for wire applications
[AD-A247013] p 3364 N92-28395
Coupling device with improved thermal interface
[NASA-CASE-GSC-13251-1] p 3295 N92-29120
Development of an automated wire delivery system for robotic welding applications
[NASA-CR-190487] p 3295 N92-29134

WIRING
Stress analysis of plated-through-holes in rigid flex multilayer printed wiring boards
[DE92-011659] p 3303 N92-28855
WORDS (LANGUAGE)
Information technology in plain words
[AD-A250324] p 3369 N92-28955
WORK FUNCTIONS
X ray photoelectron spectroscopy study on the double layer at an Al2O3-Al interface
[AD-A246454] p 3265 N92-28972
WORKLOADS (PSYCHOPHYSIOLOGY)
Correlational analysis of survey and model-generated workload values
[AD-A247153] p 3329 N92-28518
Shipboard mission training effectiveness of the Naval Air Test Center's V-22 government test pilot trainer
p 3224 N92-28542
WORKSTATIONS
Functional requirements document for the Earth Observing System Data and Information System (EOSDIS) Scientific Computing Facilities (SCF) of the NASA/MSFC Earth Science and Applications Division, 1992
[NASA-TM-4392] p 3333 N92-28899

X

X RAY ANALYSIS
Woelter x ray microscope characterization measurements on Nova
[DE92-013207] p 3288 N92-28812
Water window imaging x ray microscope
[NASA-CASE-MFS-28485-1] p 3288 N92-29135
X RAY APPARATUS
Environmental testing of the Xi Scan 1000, portable fluoroscopic and radiographic imaging system
[AD-A247167] p 3324 N92-28242
Woelter x ray microscope characterization measurements on Nova
[DE92-013207] p 3288 N92-28812
X RAY ASTRONOMY
Analysis of Mir-HEXE observations: Pulsation and energy spectra of the x ray double star SMC X-1 in 20 to 80 keV energy field
[ETN-92-91487] p 3371 N92-29128
Calibration of high energy x ray detectors at the spectrum of the Crab nebula, and x ray pulsar A0535+26 examinations
[ETN-92-91484] p 3371 N92-29177
X RAY DIFFRACTION
Growth and optical characterization of Zn(1-x)Mn(x)Te grown by molecular beam epitaxy
[DE92-010667] p 3363 N92-28331
X ray diffraction study of residual stresses in metal matrix composite-jacketed steel cylinders subjected to internal pressure
[AD-A248449] p 3251 N92-28416
X RAY INSPECTION
X ray computed tomography of full-scale castings
[AD-A247101] p 3258 N92-28241
X RAY LASERS
Research studies on extreme ultraviolet and soft x ray lasers
[AD-A247309] p 3289 N92-28299
Instrumentation for ultrahigh strain rate experiments
[AD-A249358] p 3298 N92-28327
X RAY SOURCES
Scientific investigations with the data base HEAO-1 scanning modulator collimator
[NASA-CR-190477] p 3370 N92-28680
X RAY SPECTROSCOPY
X ray photoelectron spectroscopy study on the double layer at an Al2O3-Al interface
[AD-A246454] p 3265 N92-28972
X RAYS
PROPX: An x ray manipulation program
[DE92-011264] p 3334 N92-28309
High resolution electron beam lithography on x ray mask substrates. Effects of electron scattering and membrane heating
[ETN-92-91336] p 3272 N92-28793
Water window imaging x ray microscope
[NASA-CASE-MFS-28485-1] p 3288 N92-29135

Y

YAG LASERS
A diode laser pumped Nd:YAG laser
[FFI-91/7020] p 3289 N92-28315
YIELD STRENGTH
The compressive properties of GLARE
[LR-666] p 3252 N92-28582
YTTRIUM
Chemical vapor deposition of yttrium borium(2) copper(3) oxygen(x) thin films for wire applications
[AD-A247013] p 3364 N92-28395
YTTRIUM OXIDES
Chemical vapor deposition of yttrium borium(2) copper(3) oxygen(x) thin films for wire applications
[AD-A247013] p 3364 N92-28395
Electrodeposition of high temperature superconductors
[AD-A250171] p 3365 N92-28919

Z

ZINC TELLURIDES
Growth and optical characterization of Zn(1-x)Mn(x)Te grown by molecular beam epitaxy
[DE92-010667] p 3363 N92-28331
ZIRCONIUM OXIDES
Effect of metallic coating properties on the tribology of oil-lubricated coated-ceramics
[DE92-010904] p 3262 N92-28339
Mechanistic studies of superplasticity of structural ceramics
[AD-A246951] p 3263 N92-28558
ZONE MELTING
Microgravity accelerometer characterization on Columbia STS-32 mission p 3271 N92-28452

Typical Personal Author Index Listing

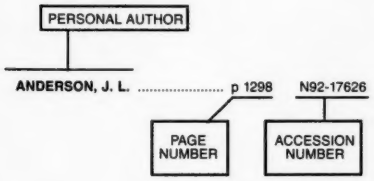

Listings in this index are arranged alphabetically by personal author. The page number helps you locate the citation in the abstract section. The accession number denotes the number by which the citation is identified.

A

AARTS, E. H. L. ..... p 3336 N92-28639
ABE, Y. ..... p 3310 N92-28588
ABHIRAMAN, A. S. ..... p 3263 N92-28553
ABRAMS, EVE M. ..... p 3294 N92-28754
ABRUNA, HECTOR D. ..... p 3258 N92-29185
ACORD, J. M. ..... p 3386 N92-29030
ADAIR, J. H. ..... p 3264 N92-28570
ADAN, I. J. B. F. ..... p 3347 N92-28641
p 3342 N92-28642
ADKINS, KENNETH C. ..... p 3275 N92-28873
ADVANI, S. ..... p 3225 N92-28550
ADVANI, S. K. ..... p 3240 N92-28579
AGEE, CARL B. ..... p 3310 N92-28587
p 3310 N92-28589
AGRESTI, DAVID G. ..... p 3378 N92-28989
AHLERS, GUENTER ..... p 3364 N92-28806
AHRENS, THOMAS J. ..... p 3310 N92-28590
AIKEN, EDWIN W. ..... p 3234 N92-28926
AITCHESON, KENT ROBERT ..... p 3239 N92-28801
AJAYI, O. O. ..... p 3262 N92-28339
ALAPHILIPPE, M. ..... p 3228 N92-28789
ALEXANDER, M. J. ..... p 3391 N92-29061
ALLAIRE, PAUL E. ..... p 3267 N92-28446
ALLAN, A. PETER ..... p 3267 N92-28446
ALLARD, L. F. ..... p 3364 N92-28857
ALLEN, CHERYL L. ..... p 3344 N92-28375
ALLEN, M. ..... p 3372 N92-28479
ALLEN, MARK ..... p 3376 N92-28501
ALLISON, SIDNEY G. ..... p 3303 N92-28757
p 3304 N92-29101
p 3304 N92-29155
ALVELID, MAGNUS ..... p 3253 N92-29220
ALVERTOS, NICOLAS ..... p 3291 N92-29139
AMES, GREGORY H. ..... p 3358 N92-29095
ANBAR, A. D. ..... p 3372 N92-28479
ANDERSEN, KEVIN ROBERT ..... p 3273 N92-28410
ANDERSON, THOMAS W. ..... p 3249 N92-28748
ANDREASSEN, OEYVIND ..... p 3351 N92-28314
ANDREESCU, MARIA ..... p 3301 N92-28632
ANG, J. A. ..... p 3295 N92-28925
ANGUS, J. E. ..... p 3344 N92-28401
ANTIOCHOS, S. K. ..... p 3360 N92-28354
ANTREASIAN, P. G. ..... p 3244 N92-28343
APONSO, BIMAL L. ..... p 3239 N92-28584
ARANA, CLAUDIA R. ..... p 3258 N92-29185
ARISAWA, TAKASHI ..... p 3363 N92-28282
ARMANDO, A. ..... p 3223 N92-28536
ARNOLD, G. W. ..... p 3357 N92-28355
ARNONE, R. ..... p 3359 N92-29167
ARRINGTON, E. ALLEN ..... p 3240 N92-28673
ARTNER, CHRISTOPH ..... p 3356 N92-29210
ASAY, A. A. ..... p 3221 N92-28525
ASH, ROBERT L. ..... p 3283 N92-28361
ASHBY, C. I. H. ..... p 3255 N92-28341
ASHRAFI, S. ..... p 3396 N92-28869
p 3396 N92-28870
p 3396 N92-28871
p 3396 N92-28872
p 3396 N92-28907
ATENCIO, ADOLPH, JR. ..... p 3224 N92-28545
AUERBACH, DAVID I. ..... p 3254 N92-28290
AUERKARI, PERTTI ..... p 3251 N92-28573
AVERA, WILL ..... p 3321 N92-28321

B

BABA, SHIGEO ..... p 3241 N92-28835
BABALIEVSKI, F. V. ..... p 3362 N92-28231
BABER, BURL B. ..... p 3236 N92-28294
BADALIANCE, ROBERT ..... p 3253 N92-28953
BADESCU, M. ..... p 3363 N92-28281
BADILLA, G. ..... p 3268 N92-28455
BAER, ERIC ..... p 3262 N92-28360
BAILEY, J. E. ..... p 3362 N92-29086
BAILEY, WAYNE L. ..... p 3246 N92-28369
BAKER, DAVID D., JR. ..... p 3324 N92-28242
BAKER, DIANA L. ..... p 3335 N92-28385
BAKER, KARL W. ..... p 3249 N92-28682
p 3307 N92-29143
BAKER, MARK R. ..... p 3308 N92-28257
BAKER, R. ..... p 3336 N92-28585
BALDEA, I. ..... p 3363 N92-28281
BALDWIN, R. T. ..... p 3299 N92-28620
p 3300 N92-28624
p 3300 N92-28626
BAMKIN, R. J. ..... p 3337 N92-28741
BANACH, ANTONI S. ..... p 3346 N92-29149
BANDERET, LOUIS E. ..... p 3324 N92-28288
BANDOU, TOSHIO ..... p 3234 N92-28901
BANE, JOHN M. ..... p 3323 N92-29225
BANERJEE, BIBHUTI B. ..... p 3267 N92-28446
BANIN, A. ..... p 3379 N92-28990
BANKERT, R. L. ..... p 3319 N92-28966
BARD, STEVEN ..... p 3288 N92-29156
BAREFIELD, E. K. ..... p 3364 N92-28395
BARLOW, N. G. ..... p 3379 N92-28991
BARNES, J. R. ..... p 3379 N92-28992
BARNETT, WILLIAM T. ..... p 3277 N92-29165
BARNETTE, B. D. ..... p 3326 N92-28396
BARNEY, RICHARD D. ..... p 3296 N92-29151
BARR, W. L. ..... p 3360 N92-28335
BARRACLOUGH, B. L. ..... p 3374 N92-28486
BARRACLOUGH, D. R. ..... p 3300 N92-28623
BARTH, C. A. ..... p 3387 N92-29035
BARTHELEMY, JEAN-FRANCOIS M. ..... p 3231 N92-28435
BARTON, C. E. ..... p 3301 N92-28630
BARTOSH, BRADY J. ..... p 3240 N92-28407
BARYLAK, M. ..... p 3371 N92-28781
BATTRICK, BRUCE ..... p 3371 N92-28781
BAUER, STEVEN X. S. ..... p 3228 N92-28729
BAUGHER, CHARLES R. ..... p 3267 N92-28448
BAUM, JOSEPH D. ..... p 3250 N92-28931
BAUMANN, E. D. ..... p 3280 N92-28675
BAUMANN, WILLIAM T. ..... p 3346 N92-29149
BAUMEISTER, KENNETH J. ..... p 3353 N92-28984
BAYLESS, JOHN R. ..... p 3250 N92-28945
BEARD, S. ..... p 3245 N92-29102
BEASLEY, M. R. ..... p 3281 N92-29147
BECHTEL, ROBERT J. ..... p 3241 N92-28975
BECKETT, PETER ..... p 3226 N92-28552
BEGUELIN, A. ..... p 3341 N92-28279
BELIAN, T. ..... p 3308 N92-29183
BELL, JAMES F., III ..... p 3373 N92-28480
p 3379 N92-28993
BELL, MICHAEL J. ..... p 3351 N92-28364
BELTRACCHI, L. ..... p 3327 N92-28775
BEN-SHLOMO, T. ..... p 3379 N92-28990
BENDER, S. C. ..... p 3291 N92-29168
BENNEMA, P. ..... p 3362 N92-28280
BENSON, L. J. ..... p 3351 N92-28292
BERENJI, HAMID R. ..... p 3345 N92-28759
BEREZOVSKAYA, F. ..... p 3346 N92-28311
BERGEN, T. ..... p 3268 N92-28455
BERNSTEIN, LESLIE R. ..... p 3352 N92-28869
BERNSTEIN, R. H. ..... p 3355 N92-28839
BERRY, M. H. ..... p 3274 N92-28796
p 3358 N92-28968
BERWICK, M. ..... p 3357 N92-28372
BETTS, B. H. ..... p 3379 N92-28994
BHARGAVA, VIJAY K. ..... p 3274 N92-28699
BHASIN, KUL B. ..... p 3358 N92-28571
BHAVNANI, K. H. ..... p 3244 N92-28937
BIBRING, J-P. ..... p 3382 N92-29011
BIBYK, STEVEN B. ..... p 3275 N92-28873
BICE, CARL A. ..... p 3289 N92-28682
BICKFORD, MARK ..... p 3336 N92-28666
p 3336 N92-28667
BICKFORD, R. L. ..... p 3248 N92-28417
BIEDERMAN, IRVING ..... p 3329 N92-29186
BIKA, D. ..... p 3260 N92-28854
BIRCH, K. G. ..... p 3323 N92-29213
BIRKMIRE, DEBORAH P. ..... p 3326 N92-28396
BITTNER, LAWRENCE P. ..... p 3367 N92-28244
BLACKBURN, JOHN ..... p 3267 N92-28443
BLACKBURN, ROBERT R. ..... p 3272 N92-28902
BLACKLEY, M. W. L. ..... p 3323 N92-29215
BLACKWELL, A. L. ..... p 3330 N92-28681
BLACKWELL, C. C. ..... p 3330 N92-28681
BLAKE, D. F. ..... p 3379 N92-28990
BLAKE, IAN F. ..... p 3274 N92-28699
BLANAS, PANAGIOTIS ..... p 3252 N92-28702
BLANEY, DIANA L. ..... p 3379 N92-28995
p 3382 N92-29007
BLOM, HARALD ..... p 3334 N92-28265
BLOOMFIELD, DAVID P. ..... p 3279 N92-28326
BLOOMFIELD, VALERIE J. ..... p 3279 N92-28326
BLOOR, J. E. ..... p 3354 N92-28260
BLOSSER, MAX L. ..... p 3284 N92-28752
BLUMBERG, DAN G. ..... p 3380 N92-28996
BOBRYSHEVA, A. I. ..... p 3366 N92-28232
BOERSTOEL, J. W. ..... p 3227 N92-28692
BOGERT, PHILIP ..... p 3268 N92-28450
BOHN, R. ..... p 3306 N92-28277
BONACUSE, PETER J. ..... p 3302 N92-28701
BOND, THOMAS H. ..... p 3227 N92-28674
p 3227 N92-28696
BOOGERS, J. A. M. ..... p 3260 N92-28794
BOREL, C. C. ..... p 3306 N92-28807
p 3306 N92-28840
BORIE, V. ..... p 3249 N92-28780
BORISOV, ALEXANDER ..... p 3310 N92-28591
BOROWSKI, RICHARD A. ..... p 3221 N92-28524
BOSS, R. D. ..... p 3339 N92-28946
BOSSI, RICHARD H. ..... p 3258 N92-28241
BOSSLER, R. B., JR. ..... p 3293 N92-28434
BOSTIAN, CHARLES W. ..... p 3273 N92-28586
BOTTS, MICHAEL E. ..... p 3333 N92-28899
BOUGHER, S. W. ..... p 3376 N92-28498
p 3380 N92-28997
p 3391 N92-29061
p 3395 N92-29080
BOURGEOIS, B. S. ..... p 3322 N92-28963
BOXALL, RONALD A. ..... p 3339 N92-28943
BOYDELATOUR, THIERRY ..... p 3338 N92-28842
BOYES, J. ..... p 3245 N92-29102
BOYLE, MICHAEL E. ..... p 3360 N92-29205
BOYNTON, W. V. ..... p 3374 N92-28488
BRACE, L. H. ..... p 3387 N92-29035
BRANSTETTER, M. L. ..... p 3342 N92-28381
BRENNAN, K. F. ..... p 3274 N92-28773
BRENNER, D. W. ..... p 3355 N92-28881
p 3265 N92-28916
p 3252 N92-28917
p 3253 N92-28918
BREZANY, PETER ..... p 3337 N92-28760
BRICE, J. M. ..... p 3235 N92-28377
p 3235 N92-28378
BRIDGER, ALISON F. C. ..... p 3380 N92-28998
BRINDLEY, WILLIAM J. ..... p 3265 N92-29090
BRINGI, V. N. ..... p 3318 N92-28668
BROCKEL, KENNETH H. ..... p 3277 N92-29165
BROEK, DAVID ..... p 3235 N92-29180
BROGAN, F. A. ..... p 3299 N92-28583
BROOKS, N. KENT ..... p 3230 N92-28718
BROWN, DAVID ..... p 3352 N92-28556
BROWN, L. L. ..... p 3373 N92-28481
p 3386 N92-29030
BROWN, RICHARD B. ..... p 3281 N92-28796
BROWN, WAYNE M. ..... p 3249 N92-28748
BRUMLIK, CHARLES J. ..... p 3278 N92-28239
BRUNNER, MICHAEL T. ..... p 3222 N92-28530

BUCHOLTZ, FRANK p 3357 N92-28223
BUDE, JEFF p 3278 N92-28295
BUI, BANG DOAN p 3289 N92-28228
BUIS, A. p 3259 N92-28578
BULMER, R. H. p 3360 N92-28335
BURCHETT, S. N. p 3303 N92-28855
BURGETT, RICHARD p 3321 N92-28321
BURKERT, V. D. p 3354 N92-28337
BURKS, HAROLD D. p 3265 N92-29157
BURNS, ROGER G. p 3373 N92-28482
p 3380 N92-28999
BURRELL, W. R. p 3367 N92-28403
BURROWS, LINDA M. p 3238 N92-28985
BURSE, RICHARD L. p 3324 N92-28288
BURSTEIN, N. M. p 3281 N92-28814
BURTON, DONALD J. p 3254 N92-28261
BURZYNSKI, RYSZARD p 3263 N92-28412
BUSBY, JUDY A. p 3283 N92-28555
BUSS, STEPHEN L. p 3321 N92-28365
BUTLER, JON T. p 3335 N92-28353
BUZZO, BRUCE p 3287 N92-28767
BYER, ROBERT L. p 3357 N92-28328
BYMAN, DAVID p 3321 N92-28321
BYRNES, CHRISTOPHER I. p 3344 N92-28429

C

CABOT, A. p 3335 N92-28332
CABROL, N. A. p 3380 N92-29000
CADWALLADER, L. C. p 3361 N92-28805
CAIN, BRAD p 3329 N92-28346
p 3287 N92-28978
CAIRELLI, JAMES E. p 3307 N92-28837
CAMARDA, CHARLES J. p 3284 N92-28752
CAMERON, L. E. p 3256 N92-28882
CAMPBELL, BRYCE p 3273 N92-28357
CANN, D. p 3342 N92-28334
CANNELL, DAVID S. p 3364 N92-28806
CANTRELL, JOHN H. p 3303 N92-28757
p 3304 N92-29101
p 3304 N92-29155
CAO, LONG VAN p 3289 N92-28228
CAPOBIANCO, CHRISTOPHER J. p 3311 N92-28599
CAPSIMALIS, G. p 3251 N92-28416
CAPUTO, MICHAEL P. p 3325 N92-28755
CARLSTEN, B. E. p 3291 N92-29168
CARMAN, GREGORY P. p 3358 N92-29088
CARR, M. H. p 3373 N92-28483
p 3381 N92-29006
CARRILLO, RENE p 3237 N92-28461
CARROLL, BILL D. p 3343 N92-28958
CARROLL, M. R. p 3313 N92-28607
CARTER, W. B. p 3364 N92-28395
CARTER, WILLIAM H. p 3338 N92-28795
CARVALHODEALMEIDA, RICARDO p 3318 N92-28517
CASE, SCOTT W. p 3358 N92-29088
CASSTEVENS, MARTIN K. p 3263 N92-28412
CASTOLDI, P. p 3223 N92-28536
CATO, DOUGLAS H. p 3351 N92-28364
CAVE, JULIE A. p 3381 N92-29001
CECERE, THOMAS H. p 3320 N92-28318
CEZAR, F. S. p 3258 N92-28973
CHAKRABARTI, SUPRIYA p 3338 N92-28845
CHAKRAVORTY, S. p 3261 N92-29164
CHAMBERLAIN, V. E. p 3375 N92-28497
CHAMPAGNE, FRANK H. p 3240 N92-28388
CHAN, KWAI S. p 3263 N92-28415
CHANDLER, D. W. p 3290 N92-28852
CHANEY, KENNETH D. p 3277 N92-29165
CHANG, SI-CHUNG p 3363 N92-28392
p 3364 N92-28512
CHAPMAN, BARBARA p 3337 N92-28760
CHAPMAN, JOHN J. p 3288 N92-29097
CHAPMAN, MARY G. p 3391 N92-29058
CHATRENET, D. p 3221 N92-28526
CHATTERJEE, A. p 3324 N92-28278
CHAUDHURY, MANOJ K. p 3262 N92-28291
CHEN, CHUNG-WEN p 3247 N92-28737
CHEN, DONG-YUAN p 3343 N92-28915
CHEN, I.-WEI p 3263 N92-28558
CHEN, MARINA C. p 3343 N92-28915
CHEN, S. S. p 3294 N92-28815
CHEN, Y.-J. D. p 3293 N92-28434
CHEREPANOVA, T. A. p 3362 N92-28280
CHERN, ENGMIN J. p 3298 N92-29154
CHERNOFF, H. p 3266 N92-28914
CHESSER, B. LAWRENCE p 3283 N92-28555
CHHABILDAS, L. C. p 3295 N92-28925
CHIARULLI, D. M. p 3332 N92-28514
CHICARRO, A. F. p 3381 N92-29002
CHILDS, R. L. p 3355 N92-29190
CHIN, J. p 3258 N92-29091
CHIU, S. A. p 3233 N92-28721
CHOCHOD, A. p 3235 N92-28380
CHRISTENSEN, C. P. p 3291 N92-28932
CHRISTENSEN, PHILIP R. p 3382 N92-29010
CHRISTIANSEN, E. L. p 3295 N92-28925
CHU, BENJAMIN p 3262 N92-28250
CHU, NHI-ANH p 3332 N92-28891
CHUKWU, ETHELBERT NWAKUCHE p 3247 N92-28732
CHURCH, VICTOR E. p 3337 N92-28710
CLANCY, R. T. p 3381 N92-29003
p 3381 N92-29004
p 3381 N92-29005
p 3386 N92-29032
CLANCY, R. TODD p 3376 N92-28501
p 3385 N92-29026
CLARK, J. P. p 3287 N92-29118
CLAUS, R. O. p 3353 N92-29196
CLAUS, RICHARD O. p 3358 N92-28868
p 3358 N92-29088
CLAYSON, C. H. p 3323 N92-29216
CLIFFORD, B. R. p 3224 N92-28540
CLIFFORD, S. M. p 3381 N92-29006
CNARE, E. C. p 3245 N92-29102
COEN, PETER G. p 3231 N92-28435
COFFEY, VICTORIA N. p 3355 N92-28986
COHEN, R. E. p 3262 N92-28251
COHEN, S. A. p 3360 N92-28335
COLE, STEVEN W. p 3276 N92-29124
COLEMAN, RACHEL J. p 3301 N92-28628
COLLYER, J. C. p 3264 N92-28564
COLLYER, P. D. p 3327 N92-28557
COLTON, R. J. p 3355 N92-28881
p 3265 N92-28916
COMPAAN, A. p 3306 N92-28277
CONARD, DIDIER p 3281 N92-28784
CONFORTI, MICHELE p 3349 N92-28927
p 3350 N92-28928
p 3350 N92-28929
p 3350 N92-28930
CONNELL, JOHN W. p 3264 N92-28751
p 3250 N92-29141
CONWAY, G. D. p 3361 N92-28848
COOK, A. p 3393 N92-29069
COOK, JEFFREY p 3253 N92-28921
COOKE, JOSEPH M. p 3333 N92-28245
COOLEY, J. p 3396 N92-28870
COOPER, LANCE p 3332 N92-28236
CORBETT, W. p 3356 N92-28270
CORNUAULT, C. p 3232 N92-28472
CORNUEJOLS, GERARD p 3349 N92-28927
p 3350 N92-28928
p 3350 N92-28929
p 3350 N92-28930
CORRIGAN, ROBERT D. p 3295 N92-29092
CORYNEN, G. C. p 3277 N92-29131
COSTARD, F. M. p 3373 N92-28484
COTTON, W. R. p 3318 N92-28340
COULSON, RICHARD L. p 3328 N92-29142
COULTER, J. Y. p 3365 N92-28874
COUR-PALAIS, B. G. p 3295 N92-28925
COUWENBERG, M. J. H. p 3293 N92-28645
p 3294 N92-28705
COWAN, M. p 3245 N92-28861
p 3245 N92-29102
COY, JOHN J. p 3293 N92-28476
CRADDOCK, ROBERT A. p 3373 N92-28485
CRESS, DANIEL H. p 3351 N92-28302
CREWS, J. L. p 3295 N92-28925
CRISCOE, J. C. p 3281 N92-28814
CRISP, D. p 3377 N92-28505
p 3382 N92-29008
p 3390 N92-29056
CRISP, DAVE p 3382 N92-29007
CRISP, DAVID p 3373 N92-28480
CRISP, J. p 3389 N92-29048
CRISP, N. A. p 3323 N92-29212
CROISETIERE, P. p 3224 N92-28542
CUELLAR, JOHN P. p 3236 N92-28294
CUSCHIERI, J. M. p 3352 N92-28722
CYNADER, MAX S. p 3328 N92-28957

D

DABNEY, RICHARD W. p 3248 N92-28750
DAHLBURG, R. B. p 3360 N92-28354
DAMIANO, B. p 3356 N92-28813
DAMSCHEN, DONALD E. p 3308 N92-28272
DANDREA, J. A. p 3327 N92-28557
DANLEY, DAVID L. p 3324 N92-28242
DARDY, HENRY p 3332 N92-28891
DASCH, E. JULIUS p 3366 N92-28864
DATYE, A. K. p 3364 N92-28857
DAVIDSON, THOMAS F. p 3266 N92-28739
DAVIS, H. T. p 3258 N92-28982
DAVIS, PATRICK B. p 3280 N92-28568
DAVIS, W. M. p 3300 N92-28626
DAVIS, WANDA L. p 3376 N92-28500
DAY, T. p 3393 N92-29069
DAYTON, DAVID C. p 3257 N92-28954
DCUNHA, IVAN p 3291 N92-29139
DEARNALEY, G. p 3365 N92-28923
DEBOER, A. p 3302 N92-28650
DEBOER, W. P. p 3222 N92-28532
p 3239 N92-28652
DEBONIS, JAMES R. p 3236 N92-28419
DEBOOR, CARL p 3334 N92-28301
p 3347 N92-28411
DEFIGUEIREDO, RUI J. P. p 3290 N92-28707
DEFRANCO, CARL p 3323 N92-28247
DEGNAN, J. H. p 3362 N92-28962
DEJONG, S. p 3336 N92-28636
DELEEUW, J. H. p 3225 N92-28550
DELLER, J. R., JR. p 3273 N92-28358
DELOMBARD, RICHARD p 3248 N92-28451
DELUCIA, FRANK C. p 3281 N92-28797
DEMETRESCU, CRISAN p 3301 N92-28632
DENBRAVEN, W. p 3241 N92-29204
DENERY, DALLAS G. p 3234 N92-28926
DENNEY, BRADLEY S. p 3290 N92-28707
DERENZO, S. E. p 3364 N92-28762
DERIJKE, MAARTEN p 3348 N92-29214
DERUIZ, KAYE A. p 3368 N92-28663
DESAI, PRASHANT p 3263 N92-28553
DESANCTIS, CARMINE E. p 3246 N92-28369
p 3246 N92-28370
DESCHAMPS, M. p 3382 N92-29009
DESPER, C. R. p 3262 N92-28250
DEVOL, T. A. p 3364 N92-28762
DEVON, RICHARD F. p 3366 N92-28864
DEVORE, RONALD A. p 3334 N92-28301
DHAWAN, R. p 3353 N92-29196
DICKMAN, STEVEN R. p 3321 N92-28867
DIELEMAN, P. p 3294 N92-28705
DIETZ, D. p 3362 N92-28962
DINGWELL, DONALD B. p 3310 N92-28591
DISTEFANO, SALVADOR p 3280 N92-28753
DOAZAN, V. p 3371 N92-28781
DODELSON, S. p 3372 N92-29184
DOEBERLING, THOMAS J. p 3307 N92-28837
DOEHNEL, W. p 3222 N92-28528
DOERRER, THOMAS p 3371 N92-29127
DOGGETT, WILLIAM R. p 3344 N92-28375
DOHERTY, NANCY M. p 3262 N92-28323
DOHM, JAMES M. p 3391 N92-29058
DOKOUPIL, T. M. p 3241 N92-28828
DOLLFUS, A. p 3382 N92-29009
DONGARRA, J. p 3341 N92-28279
DONKER, J. C. p 3230 N92-28655
DONNELLAN, MARY E. p 3253 N92-28921
DORMAN, LEROY M. p 3321 N92-28402
DORNSIFE, RALPH J. p 3246 N92-28560
DOSER, DIANE I. p 3308 N92-28257
DOUZINAS, K. C. p 3262 N92-28251
DOVI, AUGUSTINE R. p 3231 N92-28435
DOWNIE, JOHN D. p 3234 N92-28910
DOXBECK, M. p 3251 N92-28416
DRAKE, MICHAEL J. p 3310 N92-28592
p 3311 N92-28599
p 3312 N92-28601
p 3313 N92-28604
DRAVNIEKS, OLAF p 3274 N92-28699
DREIBUS, G. p 3377 N92-28507
DROSSART, P. p 3382 N92-29011
DUBBELDAY, PIETER S. p 3304 N92-29081
DUBOIS, NEIL J. p 3250 N92-28224
DUECK, GERHARD W. p 3335 N92-28353
DUFRANE, K. p 3292 N92-28362
DUGGIN, B. W. p 3245 N92-29102
DUKEMAN, G. A. p 3229 N92-28981
DUKES, MICHAEL A. p 3349 N92-28961
DUMESIC, J. A. p 3256 N92-28893
DUNBAR, BONNIE p 3271 N92-28452
DUNCAN, D. B. p 3248 N92-28417
DUNLAP, B. I. p 3253 N92-28918
DUPONCHEL, JEAN PIERRE p 3237 N92-28461
DURLACH, NATHANIEL p 3331 N92-29121
DUSAUTOY, A. R. p 3288 N92-29163
DUSTIN, MILES O. p 3307 N92-29143

E

EARLE, ROBERT C. p 3335 N92-28353
EASTMAN, LESTER F. p 3279 N92-28427
EATON, ROBERT A. p 3272 N92-28902
EBERLY, J. H. p 3292 N92-29223
ECCLES, E. S. p 3235 N92-28379
ECKSTROM, D. J. p 3362 N92-29093
EDGETT, KENNETH S. p 3382 N92-29010
EDWARD, RON p 3273 N92-28431
EIBL, HERBERT p 3224 N92-28541
EKLUND, WAYNE D. p 3281 N92-29153

EL-GENK, MOHAMED S. ..... p 3307 N92-28863
ELKINS, T. J. ..... p 3272 N92-28304
ELLENBROEK, M. H. W. ..... p 3302 N92-28650
ELLIOTT, C. M. ..... p 3258 N92-29185
ELLIOTT, F. S. ..... p 3328 N92-28940
ELLIS, T. W. ..... p 3259 N92-28338
ELPHIC, R. C. ..... p 3374 N92-28486
ELPHICK, S. C. ..... p 3313 N92-28607
ELSENAAR, A. ..... p 3240 N92-28661
p 3240 N92-28669
EMANUEL, K. A. ..... p 3319 N92-28830
EMERY, W. J. ..... p 3305 N92-28715
EMMETT, M. B. ..... p 3355 N92-29190
ENGELS, E., JR. ..... p 3282 N92-29197
EPSTEIN, A. H. ..... p 3238 N92-28466
EPSTEIN, M. ..... p 3257 N92-28894
EPSTEIN, S. ..... p 3394 N92-29075
ERARD, S. ..... p 3382 N92-29011
ERCK, R. A. ..... p 3262 N92-28339
ERDEMIR, A. ..... p 3262 N92-28339
ESHOW, MICHELLE M. ..... p 3234 N92-28926
ESKER, BARBARA S. ..... p 3236 N92-28418
ESPINOSA, DANIEL C. ..... p 3293 N92-28384
ESTEP, LEE ..... p 3359 N92-29167
EVANS, RONALD J. ..... p 3278 N92-28276
EVERT, RICHARD W. ..... p 3307 N92-28383
EWING, J. A. ..... p 3323 N92-29216

F

FABUNMI, JAMES A. ..... p 3339 N92-28969
FAEGRI, KNUT, JR. ..... p 3255 N92-28743
FANALE, F. P. ..... p 3377 N92-28504
FANALE, FRASER P. ..... p 3390 N92-29052
FANG, K. C. ..... p 3229 N92-28888
FARIS, F. ..... p 3273 N92-28431
FARNHAM, JAMES M. ..... p 3328 N92-29144
FASSI, F. ..... p 3223 N92-28536
FAULKNER, A. ..... p 3222 N92-28528
FAVRO, L. D. ..... p 3297 N92-28851
FEDUTENKO, E. A. ..... p 3361 N92-28816
FEGLEY, BRUCE, JR. ..... p 3374 N92-28487
p 3383 N92-29012
FEIGELSON, ROBERT S. ..... p 3357 N92-28328
FELDMAN, D. W. ..... p 3291 N92-29168
FELDMAN, W. C. ..... p 3374 N92-28488
FELSEN, LEOPOLD B. ..... p 3297 N92-29112
FELTOVICH, PAUL J. ..... p 3328 N92-29142
FENN, RALPH ..... p 3267 N92-28444
FENSKE, G. R. ..... p 3262 N92-28339
FEO, J. ..... p 3342 N92-28334
FERGUSON, DALE C. ..... p 3246 N92-28683
FERRANTI, MICHAEL J. ..... p 3223 N92-28537
FESEN, C. G. ..... p 3380 N92-28997
p 3391 N92-29061
FETH, LAWRENCE L. ..... p 3328 N92-29146
FIELDS, B. ..... p 3371 N92-28859
FILLATRE, OLLIVIER ..... p 3349 N92-28778
FILUK, A. B. ..... p 3362 N92-29086
FINGER, HAROLD ..... p 3367 N92-29111
FINK, ALAN L. ..... p 3333 N92-28243
FITZGERALD, TIMOTHY R. ..... p 3222 N92-28530
FLETCHER, JAMES C. ..... p 3265 N92-29157
FLOM, YURY ..... p 3295 N92-29099
FLOUDAS, C. A. ..... p 3308 N92-29173
FLYNN, G. J. ..... p 3374 N92-28489
p 3383 N92-29013
FOGG, BRIAN ..... p 3358 N92-29088
FOGG, BRIAN R. ..... p 3358 N92-28868
FONTIJN, ARTHUR ..... p 3256 N92-28769
FORREST, L. ..... p 3245 N92-28956
FORTNEY, SUZANNE M. ..... p 3325 N92-28420
FOSTER, JOHN V. ..... p 3225 N92-28551
FOX, J. L. ..... p 3374 N92-28490
p 3383 N92-29014
FRALEY, DAN ..... p 3321 N92-28321
FRANK, G. ..... p 3336 N92-28585
FRANKEL, S. H. ..... p 3285 N92-28817
p 3285 N92-28818
p 3285 N92-28819
p 3229 N92-28820
FRASCA, A. J. ..... p 3279 N92-28432
FREY, H. V. ..... p 3383 N92-29015
FRIEDMAN, D. ..... p 3266 N92-28914
FRIEMAN, J. A. ..... p 3355 N92-28858
FRIES, SYLVIA DOUGHTY ..... p 3397 N92-28344
FROST, MICHAEL ..... p 3289 N92-28330
FUJIEDA, HIROTOSHI ..... p 3241 N92-28833
FUJISAWA, A. ..... p 3360 N92-28234
FUJITA, J. ..... p 3360 N92-28234
FUJITA, TOSHIMI ..... p 3241 N92-28833
FULLER, MARVIN G. ..... p 3333 N92-29083

G

GABRIELSON, THOMAS B. ..... p 3352 N92-28413
GAFFIE, DANIEL ..... p 3325 N92-28844
GAIER, JAMES R. ..... p 3253 N92-29152
GAINER, CHARLES ..... p 3222 N92-28533
GALANT, DAVID C. ..... p 3349 N92-28672
GALLOWAY, GORDON L. ..... p 3272 N92-29191
GALVAN, PAUL A. ..... p 3249 N92-28747
GALVIN, JAMES J., JR. ..... p 3329 N92-28518
GAMACHE, ROBERT R. ..... p 3355 N92-28936
GAMBLE, M. T. ..... p 3356 N92-28356
GAO, TONG ..... p 3262 N92-28250
GAO, XIAOPING ..... p 3363 N92-28392
p 3364 N92-28512
GARDNER, ELIZABETH B. ..... p 3318 N92-28423
GARDNER, TIMOTHY J. ..... p 3254 N92-28290
GARLAND, JAY L. ..... p 3330 N92-28670
GARY, BRUCE L. ..... p 3320 N92-29148
GASKA, JAMES P. ..... p 3326 N92-29179
GASKELL, R. W. ..... p 3383 N92-29016
GASPARIK, TIBOR ..... p 3312 N92-28601
GEHRING, A. U. ..... p 3379 N92-28990
GEIST, A. ..... p 3341 N92-28279
GEORGESON, GARY E. ..... p 3258 N92-28241
GERBER, D. ..... p 3247 N92-28738
GERSTL, S. A. W. ..... p 3306 N92-28807
p 3306 N92-28840
GERZABEK, MARTIN H. ..... p 3316 N92-28740
p 3356 N92-29210
GEVARTER, WILLIAM B. ..... p 3337 N92-28758
GHOSH, DAVE ..... p 3247 N92-28730
GIANG, S. S. ..... p 3247 N92-28736
GIBSON, C. ROBERT ..... p 3325 N92-28755
GILGENBACH, RONALD M. ..... p 3289 N92-28271
GIRARD, R. ..... p 3338 N92-28790
GIRODROUX-LAVIGNE, P. ..... p 3229 N92-29206
GIVI, P. ..... p 3285 N92-28818
p 3285 N92-28819
p 3229 N92-28820
GIVI, PEYMAN ..... p 3258 N92-28821
GLASER, R. E. ..... p 3285 N92-28817
GLASS, DAVID J. ..... p 3277 N92-29131
GLEASON, DANIEL ..... p 3325 N92-28886
GLEESON, J. ..... p 3223 N92-28535
GLEISNER, ROBERT P. ..... p 3292 N92-28362
GLENDINNING, S. G. ..... p 3261 N92-28249
GLICKMAN, RANDOLPH D. ..... p 3288 N92-28812
GODDARD, CHARLES W. ..... p 3326 N92-28920
GODDARD, DANIEL G. ..... p 3249 N92-28747
GODWIN, R. B. ..... p 3223 N92-28538
GOLDEN, D. C. ..... p 3272 N92-28304
GOLDMAN, A. ..... p 3383 N92-29017
GOLDMAN, LOUIS J. ..... p 3304 N92-29181
GOLDSTEIN, HOWARD E. ..... p 3229 N92-28980
GOLDSTEIN, J. C. ..... p 3245 N92-29104
GOODEN, J. H. M. ..... p 3291 N92-29168
p 3226 N92-28658
p 3228 N92-28713
GOODING, J. L. ..... p 3393 N92-29071
GOOKIN, D. M. ..... p 3274 N92-28796
p 3358 N92-28968
GORSLINE, D. S. ..... p 3389 N92-29047
GOSWAMI, KUMAR ..... p 3297 N92-28726
GRADY, M. M. ..... p 3394 N92-29077
GRAHAM, G. M. ..... p 3229 N92-28888
GRAHAM, W. R. ..... p 3353 N92-29201
GRANT, J. A. ..... p 3384 N92-29018
GRANTHAM, CAROLYN ..... p 3344 N92-28375
GRATZ, A. J. ..... p 3363 N92-28333
GRAY, G. ..... p 3336 N92-28585
GRECO, V. P. ..... p 3251 N92-28303
GREELEY, RONALD ..... p 3380 N92-28996
p 3395 N92-29078
GREEN, CORDELL ..... p 3369 N92-28866
GREEN, JAMES L. ..... p 3334 N92-28267
GREENE, B. R. ..... p 3372 N92-29184
GREENE, JONATHAN A. ..... p 3358 N92-28868
GREENHALGCH, SAMUEL ..... p 3234 N92-28987
GREENLEAF, JOHN E. ..... p 3325 N92-28420
GREER, SUSAN N. ..... p 3319 N92-28884
GREGORY, MICHAEL L. ..... p 3326 N92-28408
GREITZER, E. M. ..... p 3237 N92-28464
p 3238 N92-28466
GRIFFITHS, G. ..... p 3323 N92-29212
GRIGGER, DAVID J. ..... p 3256 N92-28756
GRIMSHAW, ANDREW S. ..... p 3342 N92-28676
GRIN, E. A. ..... p 3380 N92-29000
GRINKER, BARRY ..... p 3230 N92-28317
GRODSINSKY, CARLOS ..... p 3267 N92-28442
GROSSMAN, A. W. ..... p 3381 N92-29004
p 3381 N92-29005
GROT, ANNETTE ..... p 3345 N92-28970
GRUBIN, H. L. ..... p 3258 N92-29126
GRUEN, A. ..... p 3287 N92-28322
GRUNDMANN, MARIUS ..... p 3364 N92-28786
GU, SHIWEI ..... p 3363 N92-28312
GUDIVADA, V. N. ..... p 3344 N92-28387
GUENETTE, G. R. ..... p 3238 N92-28466
GUICHETEAU, PH. ..... p 3224 N92-28543
GULICK, V. C. ..... p 3384 N92-29019
p 3386 N92-29031
GULLIVER, T. AARON ..... p 3274 N92-28699
GUNTHER, M. F. ..... p 3353 N92-29196
GUO, T. H. ..... p 3249 N92-28693
GUSE, J. A. ..... p 3342 N92-28381
GUSTAFSON, STEVEN C. ..... p 3346 N92-29082
GUSTAVSSON, LARS ..... p 3253 N92-29220
GUTIERREZ, PIERRE J. ..... p 3236 N92-28294
GUTMANOVITZ, AVI ..... p 3244 N92-29098
GUZMAN, A. M. ..... p 3366 N92-28230
GYORFFY, B. L. ..... p 3260 N92-28856
GYSLING, D. L. ..... p 3238 N92-28466

H

HABERLE, R. M. ..... p 3374 N92-28491
p 3376 N92-28503
HABERLE, ROBERT M. ..... p 3378 N92-28988
p 3380 N92-28998
HADFIELD, P. ..... p 3267 N92-28439
HAEHNER, CARL L. ..... p 3261 N92-29094
HAGER, G. ..... p 3284 N92-28766
HALE, J. P., II ..... p 3330 N92-28521
HALL, J. R. ..... p 3225 N92-28546
HALL, LAURA E. ..... p 3231 N92-28435
HAMEETMAN, G. J. ..... p 3342 N92-28706
HAMELIN, ANTOINETTE ..... p 3363 N92-28392
p 3364 N92-28512
HAMMOND, GREGORY A. ..... p 3367 N92-28246
HAMMOND, STEVEN WARREN .. p 3343 N92-29109
HAMMOUD, A. N. ..... p 3280 N92-28675
HAMPTON, R. DAVID ..... p 3267 N92-28446
p 3267 N92-28447
HANEL, ROBERT P. ..... p 3385 N92-29025
HANIGOFSKY, J. A. ..... p 3364 N92-28395
HANKE, D. ..... p 3225 N92-28548
HANKO, L. ..... p 3284 N92-28766
HANSEN, IRVING G. ..... p 3238 N92-28985
HANSEN, ULLI ..... p 3310 N92-28593
HANSON, R. K. ..... p 3360 N92-28298
HARDING, W. B. ..... p 3260 N92-28763
HARMON, J. K. ..... p 3384 N92-29020
HARPER, CHRISTOPHER P. ..... p 3252 N92-28898
HARRIS, S. E. ..... p 3289 N92-28299
HARRISON, J. A. ..... p 3355 N92-28881
p 3265 N92-28916
HARRISON, L. ..... p 3316 N92-28853
HARRISON, STEVEN B. ..... p 3267 N92-29171
HARTENSTEIN, RAY ..... p 3337 N92-28710
HARTLE, M. S. ..... p 3298 N92-28296
HARTMETZ, C. P. ..... p 3377 N92-28508
p 3384 N92-29021
HARTUNIAN, R. ..... p 3245 N92-28956
HARVEY, DANNY J. ..... p 3309 N92-28394
HARVEY, MICHELS H. ..... p 3354 N92-28259
HATFIELD, WILLIAM E. ..... p 3258 N92-28237
HAUER, ROBERT L. ..... p 3295 N92-29092
HAWKE, B. R. ..... p 3311 N92-28594
HAWLEY, KEVIN J. ..... p 3328 N92-29144
HAYDL, W. ..... p 3279 N92-28427
HAYNES, J. ..... p 3238 N92-28466
HEATH, G. ..... p 3293 N92-28434
HEAVEN, MICHAEL ..... p 3254 N92-28300
HEBERS, H. ..... p 3291 N92-29160
HEGLUND, NORMAN C. ..... p 3332 N92-29227
HEIMSOTH, JEFFREY T. ..... p 3366 N92-28864
HEINRICH, M. N. ..... p 3384 N92-29022
HEISE, SCOTT R. ..... p 3370 N92-28255
HELMS, C. A. ..... p 3284 N92-28766
HENDERSON, B. G. ..... p 3385 N92-29023
HENDERSON, BRADLEY G. ..... p 3375 N92-28493
HENDRICKS, G. J. ..... p 3238 N92-28466
HERDEGEN, DALE W. ..... p 3352 N92-28409
HERGENROTHER, PAUL M. ..... p 3264 N92-28751
p 3250 N92-29141
HERKENHOFF, KEN ..... p 3385 N92-29024
HERMANS, C. ..... p 3233 N92-28687
HERSTROM, CATHERINE L. ..... p 3344 N92-28375
HERZBERG, CLAUDE ..... p 3311 N92-28595
HERZOG, DONALD C. ..... p 3301 N92-28631
HESS, KARL ..... p 3278 N92-28295
HEYDEN, J. ..... p 3221 N92-28523
HICKEY, ALBERT E. ..... p 3340 N92-29187
p 3340 N92-29188
HICKMAN, JAMES J. ..... p 3254 N92-28290
HIGGINS, R. WAYNE ..... p 3346 N92-28297
HILDEBRAND, JOHN A. ..... p 3321 N92-28402
HILL, D. N. ..... p 3364 N92-28395
HILLARD, G. BARRY ..... p 3246 N92-28683

HILLGREN, VALERIE J. p 3311 N92-28596
HINDSON, WILLIAM S. p 3234 N92-28926
HINE, BUTLER P. p 3234 N92-28910
HINOJOSA, JUAN H. p 3308 N92-28257
HIROSE, AKIRA p 3360 N92-28664
p 3361 N92-28665
p 3361 N92-28847
p 3361 N92-28848
p 3361 N92-28849
HIRST, C. p 3322 N92-29211
HLAVA, MARJORIE M. K. p 3370 N92-29108
HO, YEUNGHAW p 3363 N92-28392
HODGKINSON, J. p 3225 N92-28549
HODIAMONT, SUSANNA p 3260 N92-28823
HOEG, J. G. p 3231 N92-28468
HOEIJMAKERS, H. W. M. p 3226 N92-28657
HOFFLER, KEITH D. p 3225 N92-28551
HOGENDOORN, R. A. p 3305 N92-28697
HOH, ROGER H. p 3224 N92-28545
HOLLEY, W. R. p 3324 N92-28278
HOLMES, J. L. p 3362 N92-28962
HOLT, R. p 3298 N92-28296
HOLTZBLATT, LESTER J. p 3278 N92-28305
HONESS, SHAWN B. p 3351 N92-29130
HONG, SUN p 3363 N92-28312
HOOD, PETER p 3301 N92-28629
HOOVER, RICHARD B. p 3288 N92-29135
HOOVER, W. G. p 3355 N92-28860
HORAK, OTHMAR p 3356 N92-29210
HORN, MICHAEL H. p 3245 N92-28254
HOUNJET, M. H. L. p 3347 N92-28635
p 3227 N92-28659
HOWARD, RICHARD T. p 3248 N92-28750
HOWARD, STEPHEN L. p 3257 N92-28954
HOWLETT, JAMES T. p 3226 N92-28477
HSIEH, J. H. p 3262 N92-28339
HSU, Y. L. p 3322 N92-28913
HU, C. C. p 3233 N92-28720
HUANG, H. p 3298 N92-28296
HUBBARD, G. SCOTT p 3385 N92-29025
HUBER, ALAN C. p 3248 N92-28765
HUDDLESTON, DAVID H. p 3283 N92-28555
HUDSON, DAVID F. p 3277 N92-29169
HUDSON, R. S. p 3384 N92-29020
HULBERT, M. S. p 3324 N92-29089
HUMPHRIS, ROBERT R. p 3267 N92-28446
HUNT, W. D. p 3274 N92-28773
HUNTER, NORWOOD R. p 3325 N92-28755
HURTAK, O. p 3361 N92-28742
HUTING, WILLIAM A. p 3279 N92-28367
HUYNH, H. T. p 3239 N92-28652

I

IBA, WAYNE p 3329 N92-29174
IBANNAIN, MOHAMED p 3282 N92-29208
IGNACZAK, LOUIS R. p 3250 N92-28983
IGUCHI, H. p 3360 N92-28234
ILIFFE, J. C. p 3393 N92-29069
INLOW, MARK p 3328 N92-28940
INOUE, KATSUMI p 3293 N92-28476
INSERRA, JOSEPH R. p 3277 N92-29165
INTERRANTE, LEONARD V. p 3365 N92-28885
INUKAI, TOM p 3273 N92-28431
ISHIDA, HATSUO p 3251 N92-28252
ISLAM, M. p 3229 N92-28888
IVERSON, D. J. p 3233 N92-28721
IWASAKI, AKIHITO p 3241 N92-28833
IYER, RAVISHANKAR K. p 3297 N92-28726
IZUCHI, HIDEKAZU p 3266 N92-29195

J

JACHIMOWSKI, CASIMIR J. p 3255 N92-28374
JACKSON, ANDREW p 3299 N92-28621
JACKSON, D. A. p 3357 N92-28372
JACKSON, P. p 3224 N92-28540
JACOBS, E. W. p 3339 N92-28946
JACOBS, J. M. J. W. p 3226 N92-28657
JACOBSEN, LOWELL D. p 3326 N92-29179
JAECKEL, LOUIS A. p 3339 N92-29106
p 3340 N92-29107
JAGOUTZ, E. p 3377 N92-28507
JAKES, PETR p 3311 N92-28597
JAKOSKY, B. M. p 3374 N92-28488
p 3385 N92-29023
p 3387 N92-29035
JAKOSKY, BRUCE M. p 3375 N92-28492
p 3375 N92-28493
p 3378 N92-28988
p 3388 N92-29042
JAMES, BONNIE F. p 3375 N92-28494
JAMES, ODETTE B. p 3372 N92-28345
JAMES, P. B. p 3388 N92-29039
JAMES, PHILIP B. p 3385 N92-29026
JANSWEIJER, P. P. M. p 3278 N92-28262
JANZEN, D. B. p 3221 N92-28525
JEHLE, ROBERT E. p 3277 N92-29169
JENTINK, H. W. p 3236 N92-28654
JESKANEN, HARRI p 3251 N92-28572
p 3266 N92-29194
JIANG, XUDONG p 3364 N92-28512
JIN, JIAN-MING p 3273 N92-28371
JOHNSON, BRADLEY Q. p 3279 N92-28326
JOHNSON, BRUCE p 3267 N92-28444
JOHNSON, D. D. p 3260 N92-28856
JOHNSON, J. O. p 3355 N92-29190
JOHNSON, NATASHA p 3392 N92-29067
JOHNSON, R. E. p 3376 N92-28498
JOHNSTON, WILLIAM A. p 3328 N92-29144
JOLLIFF, B. L. p 3311 N92-28598
JONES, D. I. p 3267 N92-28439
JONES, E. D. p 3363 N92-28331
JONES, J. H. p 3386 N92-29027
p 3386 N92-29028
JONES, JOHN H. p 3311 N92-28599
JONES, RICHARD T. p 3325 N92-28515
JONES, T. V. p 3287 N92-29118
JORNA, P. G. A. M. p 3222 N92-28532
JOYCE, G. p 3350 N92-28238
JUDEIKIS, HENRY S. p 3308 N92-28272
JUREWICZ, A. J. G. p 3386 N92-29028
JUSTUS, C. G. p 3375 N92-28494

K

KAHN, RALPH p 3385 N92-29026
KAILASANATH, K. p 3285 N92-28803
KAISER, W. J. p 3382 N92-29008
KALLEMEYN, GREGORY W. p 3315 N92-28618
KALLURI, SREERAMESH p 3302 N92-28701
KAMADA, R. F. p 3318 N92-28799
KAMPA, K. p 3222 N92-28528
KANGAS, TUULIKKI p 3299 N92-28622
KANNEL, J. p 3292 N92-28362
KARGEL, J. S. p 3386 N92-29029
KARGEL, JEFFREY S. p 3392 N92-29067
KARSH, ROBERT p 3326 N92-28396
KASKI, KIMMO p 3339 N92-28875
KASSIES, A. p 3284 N92-28712
KASTING, J. F. p 3373 N92-28481
p 3375 N92-28495
p 3386 N92-29030
KATO, ICHIRO p 3292 N92-28233
KAUFFMAN, R. E. p 3262 N92-28398
KAULA, W. M. p 3312 N92-28600
KAUPPINEN, PENTTI p 3251 N92-28572
p 3251 N92-28573
p 3266 N92-29194
KAYE, R. J. p 3245 N92-29102
KAZOVSKY, LEONID p 3357 N92-28554
KEFFER, CHARLES E. p 3316 N92-28911
KEFFER, LYNNE p 3366 N92-28864
KEINANEN, HEIKKI p 3251 N92-28573
p 3303 N92-28776
KELLER, G. RANDY p 3308 N92-28257
KELLER, K. L. p 3221 N92-28525
KELLER, M. A. p 3262 N92-28398
KELLER, RICHARD M. p 3346 N92-29175
KELLEY, M. C. p 3272 N92-28304
KENDALL, E. R. p 3225 N92-28549
KENNETT, BRIAN L. p 3316 N92-28935
KENNY, T. W. p 3382 N92-29008
KERLEY, JAMES J. p 3281 N92-29153
KERN, D. p 3268 N92-28455
KERSLAKE, WILLIAM R. p 3250 N92-28983
KERSTEIN, A. R. p 3256 N92-28822
KERSTHOLT, J. H. p 3367 N92-29161
p 3369 N92-29162
KETOLA, ANNELI p 3299 N92-28622
KEY, DAVID L. p 3224 N92-28545
KHACHEN, W. p 3280 N92-28675
KHEDKAR, PRATAP p 3345 N92-28759
KIDA, TAKASHI p 3303 N92-28836
KIM, CHANG H. p 3228 N92-28883
KIM, DO HOON p 3290 N92-28862
KIM, SANG-WOOK p 3286 N92-28908
KING, G. B. p 3257 N92-28896
KIRTS, RICHARD E. p 3264 N92-28912
KISSEL, R. p 3279 N92-28456
KIUTTU, G. F. p 3362 N92-28962
KLEINMANN, S. G. p 3371 N92-28843
KLYDE, DAVID H. p 3239 N92-28584
KNIGHT, CHRISTINE p 3392 N92-29067
KNOSPE, CARL R. p 3267 N92-28446
p 3267 N92-28447
KOBUS, DAVID p 3328 N92-28940
KOCHAN, H. p 3388 N92-29044
KOENIG, JACK L. p 3251 N92-28252
KOLBE, R. L. p 3350 N92-28400
KOMATSU, G. p 3386 N92-29031
KOO, K. P. p 3357 N92-28223
KOOI, J. W. p 3226 N92-28658
KOOL, G. A. p 3238 N92-28711
KORDESCH, MARTIN E. p 3265 N92-29189
KORJACK, THOMAS A. p 3292 N92-28284
KORSAH, K. p 3356 N92-28813
KOSS, D. A. p 3259 N92-28390
KOSSACKI, K. p 3375 N92-28496
KOSSLYN, STEPHEN M. p 3327 N92-28877
KOTULAK, JOHN C. p 3331 N92-28944
KOURTIDES, D. A. p 3233 N92-28721
KRALL, J. p 3350 N92-28238
KRAMMER, J. p 3232 N92-28471
KRANTZ, TIMOTHY p 3296 N92-29136
KREIDER, KEVIN L. p 3353 N92-28984
KREMPL, E. p 3298 N92-28352
KRESKOVSKY, J. P. p 3258 N92-29126
KRETSCHMAR, PETER p 3371 N92-29177
KRICKE, DIETER p 3225 N92-28547
KRUSIUS, J. P. p 3278 N92-28275
KUECK, J. D. p 3281 N92-28814
KUIJPERS, E. A. p 3358 N92-28656
KUME, ETSUO p 3292 N92-28233
KUNG, P. J. p 3365 N92-28874
KUNZ, MATHIAS p 3371 N92-29128
KUNZ, ROBERT p 3286 N92-28879
KUO, P. K. p 3297 N92-28851
KURTS, DAVID p 3222 N92-28533
KURZKE, J. p 3237 N92-28465
KUSTOM, R. L. p 3274 N92-28809
p 3274 N92-28810
KWAK, YEONG-LAE p 3236 N92-29222
KWAN, ROBERT K. p 3273 N92-28431
KWON, JIN HYUK p 3290 N92-28862
KYRALA, G. A. p 3334 N92-28309

L

LAABS, F. C. p 3259 N92-28338
LAAKSO, M. p 3282 N92-29197
LACKEY, W. J. p 3364 N92-28395
LAGHARI, J. R. p 3280 N92-28675
LAGNESE, JOHN E. p 3298 N92-28320
LAIBINIS, PAUL E. p 3254 N92-28290
LAKATOS, THOMAS F. p 3307 N92-28837
LAKSHMINARAYANA, B. p 3286 N92-28879
LAM, KWOK-WAI p 3326 N92-28920
LAMBERT, D. p 3249 N92-28780
LAMBERT, R. ST.J. p 3375 N92-28497
LAMERIS, J. p 3232 N92-28649
LAMPE, M. p 3350 N92-28238
LAN, C. EDWARD p 3233 N92-28720
LANDBERG, LARS p 3393 N92-29070
LANGE, H.-H. p 3225 N92-28548
LANGEL, R. A. p 3299 N92-28620
p 3300 N92-28624
LANGER, H.-J. p 3233 N92-28687
LANKFORD, JAMES p 3263 N92-28415
LAPSHIN, V. I. p 3361 N92-28816
LARKIN, DAVID J. p 3365 N92-28885
LARROQUE, PIERRE p 3224 N92-28544
LARSEN, SOREN E. p 3393 N92-29070
LAUER, H. V., JR. p 3383 N92-29017
LAURENDEAU, N. M. p 3257 N92-28896
LAUTER, JUDITH L. p 3324 N92-28397
LAVOIE, D. M. p 3324 N92-29089
LAWTON, TERI B. p 3331 N92-29129
LAY, THORNE p 3309 N92-28386
LE, L. p 3386 N92-29028
LEBACQZ, J. VICTOR p 3234 N92-28926
LEBALLEUR, J. C. p 3229 N92-29206
LEE, E. H. p 3298 N92-28352
LEE, GORDON K. F. p 3247 N92-28736
LEE, H. p 3374 N92-28491
p 3376 N92-28503
LEE, JA H. p 3290 N92-28862
LEE, M. p 3356 N92-28270
LEE, M. F. p 3339 N92-28952
LEE, MYONGSOO p 3265 N92-29116
LEE, S. L. p 3251 N92-28416
LEE, S. W. p 3381 N92-29003
p 3386 N92-29032
LEE, STEVEN W. p 3385 N92-29026
LEFEBVRE, MICHEL H. p 3285 N92-28803
LEFEBVRE, PAUL J. p 3294 N92-28749
LEGRAFF, J. E. p 3287 N92-29118
LEIDECKER, H. p 3390 N92-29057
LELIWA-KOPYSTYNSKI, J. p 3375 N92-28496
LENGELLE, G. p 3249 N92-28780
LENTSCH, STEVEN E. p 3332 N92-29137
LEON-SALAMANCA, TEODORO p 3259 N92-28426
LEONARD, R. S. p 3368 N92-28838
LEOVY, C. B. p 3389 N92-29045

LESKO, JOHN J. p 3358 N92-29088
LESMERISES, ALAN L. p 3253 N92-29192
LEU, M-T. p 3372 N92-28479
LEVITAN, S. P. p 3332 N92-28514
LEVNER, E. V. p 3336 N92-28638
LEWICKI, D. G. p 3293 N92-28434
LEWIS, DAVID W. p 3267 N92-28446
LEWIS, J. K. p 3322 N92-28913
LEYLAND, JANE A. p 3239 N92-28457
LI, GANG p 3274 N92-28699
LI, YINGJIE p 3262 N92-28250
LIANG, S. H. p 3256 N92-28882
LIE, IVAR p 3320 N92-28266
p 3351 N92-28314
p 3348 N92-29193
LIGOCKI, M. P. p 3308 N92-29183
LILLEY, ROBERT W. p 3230 N92-28718
LIN, STEVEN p 3345 N92-28970
LINDNER, BERNHARD LEE p 3387 N92-29033
LINDSAY, R. W. p 3327 N92-28775
LING, M. R. p 3259 N92-28574
LINLIU, KUNG p 3262 N92-28250
LINZEY, MICHAEL R. p 3279 N92-28373
LIPINSKI, R. J. p 3245 N92-29102
LITTLE, GORDON R. p 3346 N92-29082
LITVIN, F. L. p 3293 N92-28434
LIU, JIAN p 3262 N92-28250
LO, JAMES T. p 3341 N92-29224
LOCHER, ROBERT J. p 3277 N92-29165
LOCKE, RANDY J. p 3257 N92-28954
LOGANANTHARAJ, R. p 3344 N92-28387
LOISY, JEAN p 3237 N92-28461
LONG, D. p 3337 N92-28710
LONG, JAMES H., JR. p 3281 N92-28948
LONGHI, JOHN p 3310 N92-28587
LONGLEY, J. P. p 3237 N92-28464
LOOIJE, C. E. W. p 3238 N92-28711
LOUIS, D. p 3338 N92-28790
LOUTON, STEVEN E. p 3223 N92-28535
LOWE, CALVIN W. p 3263 N92-28405
LOWE, D. M. p 3233 N92-28721
LOWEN, S. V. p 3264 N92-28564
LOWRY, R. K. p 3323 N92-29215
LUBOMSKI, JOSEPH F. p 3268 N92-28436
LUCAS, JOHN T. p 3249 N92-28747
LUCEY, P. G. p 3311 N92-28594
LUHMANN, J. G. p 3376 N92-28498
p 3387 N92-29034
p 3387 N92-29035
p 3395 N92-29080
LUNINE, JONATHAN I. p 3372 N92-28345
LUTHCKE, S. B. p 3244 N92-28343
LYON, J. M. p 3249 N92-28800
LYTLE, F. E. p 3257 N92-28896

M

MAADS, R. p 3356 N92-28264
MAAS, R. p 3356 N92-28308
MACARTHUR, PAUL D. p 3319 N92-28922
MACISAAC, B. D. p 3238 N92-28467
MACKENZIE, ANNE I. p 3275 N92-28876
MACMILLAN, S. p 3300 N92-28623
MACNAB, R. p 3300 N92-28627
MACPHERSON, GLENN J. p 3372 N92-28345
MADI, FRANK J. p 3307 N92-28837
MADNIA, C. K. p 3285 N92-28818
p 3285 N92-28819
p 3229 N92-28820
MADNIA, CYRUS K. p 3285 N92-28817
MADZSAR, G. C. p 3248 N92-28417
MAGALHAES, J. A. p 3387 N92-29036
MAGNER, THOMAS J. p 3296 N92-29151
MAHAFFY, PAUL p 3387 N92-29037
MAIN, ROBERT G. p 3327 N92-28880
MAISONNEUVE, Y. p 3249 N92-28780
MAKEIG, SCOTT p 3328 N92-28940
MAKI, A. G. p 3276 N92-29115
MALEVSKY, ANDREI V. p 3310 N92-28593
MALEY, M. P. p 3365 N92-28874
MALLETTE, JAMES R., JR. p 3320 N92-28283
MANCHEK, R. p 3341 N92-28279
MANHART, PAUL K. p 3359 N92-29122
MANKER, J. P. p 3387 N92-29038
MANTEUFFEL, T. p 3338 N92-28841
MARCOTTE, RICHARD A. p 3278 N92-28305
MARDER, B. p 3244 N92-28226
MAREK, VICTOR W. p 3345 N92-28895
MARGULIES, L. p 3379 N92-28990
MARKOU, C. P. p 3254 N92-28240
MARKS, TIMOTHY S. p 3249 N92-28682
MARSHALL, J. A. p 3244 N92-28343
MARSHALL, SANDRA P. p 3348 N92-28516
MARTELL, ARTHUR E. p 3254 N92-28287
p 3258 N92-28973
MARTIN, CHARLES R. p 3278 N92-28239
MARTIN, L. J. p 3376 N92-28499
p 3388 N92-29039
MARTIN, LEONARD p 3385 N92-29026
MARTIN, T. Z. p 3388 N92-29040
MARTINET, T. p 3222 N92-28529
MARZOUKI, MERYEM p 3280 N92-28783
MAST, PHILLIP W. p 3253 N92-28953
MASUI, KAZUYA p 3331 N92-28831
MATSUMOTO, JOY HAMERMAN p 3327 N92-28744
MATTHEWS, WILLIAM T. p 3297 N92-28425
MAUERSBERGER, KONRAD p 3387 N92-29037
MAXWELL, TED A. p 3373 N92-28485
MAZZOLA, VITORIO BRUNO p 3341 N92-29209
MCARDLE, JACK G. p 3236 N92-28418
MCAULEY, JAMES M. p 3351 N92-29130
MCCAULEY, MICHAEL p 3327 N92-28744
MCCOMAS, D. J. p 3374 N92-28486
MCCUTCHEON, K. M. p 3264 N92-28564
MCEWEN, A. S. p 3388 N92-29041
MCFARLANE, ELISABETH A. p 3310 N92-28592
p 3312 N92-28601
MCGARITY, JOHN O. p 3248 N92-28765
MCGUIRE, ROBERT p 3230 N92-28900
MCHENRY, M. E. p 3365 N92-28874
MCKAY, CHRISTOPHER P. p 3376 N92-28500
MCKEON, MARK F. p 3234 N92-28802
MCKNIGHT, R. L. p 3298 N92-28296
MCMAHON, C. J., JR. p 3260 N92-28854
MECHOLSKY, J. J. p 3264 N92-28570
MEEHAN, RICHARD T. p 3325 N92-28755
MEHROTRA, PIYUSH p 3337 N92-28760
MEIER, R. R. p 3391 N92-29061
MEIJER, G. p 3290 N92-28852
MEIJER, P. G. p 3305 N92-28708
MELHEM, R. G. p 3332 N92-28514
MELLON, M. T. p 3374 N92-28488
MELLON, MICHAEL T. p 3375 N92-28493
p 3388 N92-29042
MELOSH, H. J. p 3315 N92-28615
MENDELSOHN, M. L. p 3325 N92-28685
MENON, S. p 3256 N92-28822
MEREDITH, ROGER W. p 3351 N92-28324
MERENYI, E. p 3388 N92-29043
MERIENNE, M. C. p 3228 N92-28789
MERRILL, W. C. p 3249 N92-28603
MESANDER, GEERT A. p 3227 N92-28696
MESSIER, DONALD R. p 3261 N92-28249
METCALF, ANDREW C. p 3369 N92-28960
METZGER, DAN p 3300 N92-28625
MEYER, JOHN L. p 3247 N92-28735
MEYERS, MARC A. p 3303 N92-28892
MICHALSKY, J. p 3316 N92-28853
MICHEL, THIERRY R. p 3275 N92-28878
MICHOPOULOS, JOHN p 3253 N92-28953
MIGINIAC, ROLAND p 3224 N92-28544
MILAM, MALCOLM BRUCE p 3295 N92-29120
p 3296 N92-29140
MILAVEC, T. J. p 3394 N92-29073
MILLER, C. p 3224 N92-28542
MILLER, J. S. p 3388 N92-29043
p 3391 N92-29059
MILLER, MARK S. p 3358 N92-28868
MILLER, MILES C. p 3240 N92-28248
MILLER, R. J. p 3316 N92-28964
MILLER, W. O. p 3356 N92-28356
MING, D. W. p 3383 N92-29017
MINTMIRE, J. W. p 3252 N92-28917
p 3253 N92-28918
MISLEVY, ROBERT J. p 3348 N92-28273
MISLOVE, MICHAEL W. p 3334 N92-28289
MITARAI, OSAMU p 3360 N92-28664
p 3361 N92-28665
p 3361 N92-28847
p 3361 N92-28848
p 3361 N92-28849
MITCHELL, A. C. p 3283 N92-28269
MITCHELL, DAVID G. p 3224 N92-28545
p 3239 N92-28584
MITTAL, VIBHU p 3368 N92-28430
MIZIOLEK, ANDRZEJ W. p 3257 N92-28954
MOEHLMANN, D. p 3388 N92-29044
MOEK, GEERT p 3349 N92-28647
MOENS, F. p 3284 N92-28788
MOISE, M. p 3363 N92-28281
MONFORD, LEO G., JR. p 3294 N92-28727
MONKEL, A. p 3305 N92-28697
MOODY, JOHN E. p 3341 N92-29198
MOORE, C. FRED p 3354 N92-28310
MOORE, K. p 3341 N92-28279
MOORE, THOMAS E. p 3355 N92-28986
MOORE, THOMAS G. p 3248 N92-28366
MOORTHI, SHRINIVAS p 3346 N92-28297
MORALES, R. p 3288 N92-28812
MORAN, MATTHEW E. p 3266 N92-28433
MORCHAT, RICHARD M. p 3264 N92-28563
MORGAN, BEN B., JR. p 3272 N92-28253
MORGAN, R. M. p 3245 N92-29102
MORRIS, A. J. p 3231 N92-28470
MORRIS, ANDREW p 3223 N92-28539
MORRIS, C. L. p 3354 N92-28310
MORRIS, R. E. p 3308 N92-29183
MORRIS, R. V. p 3383 N92-29017
MORRIS, TIMOTHY B. p 3295 N92-29134
MORSE, S. A. p 3312 N92-28602
MOSES, CLIFFORD A. p 3236 N92-28294
MOSES, W. W. p 3364 N92-28762
MOSS, B. p 3245 N92-28956
MOWREY, R. C. p 3253 N92-28918
MPITSOS, GEORGE J. p 3328 N92-29119
MUECK, KONRAD p 3356 N92-29210
MUHLEMAN, D. O. p 3381 N92-29004
p 3381 N92-29005
MUKHIN, L. M. p 3377 N92-28507
MULLER, J.-P. p 3393 N92-29069
MULLER, RONALD M. p 3333 N92-29132
MUMM, R. H. p 3335 N92-28562
MURA, T. p 3251 N92-28307
MURAIDA, DANIEL J. p 3340 N92-29187
p 3340 N92-29188
MURPHY, BRIAN P. p 3352 N92-28559
MURPHY, J. R. p 3374 N92-28491
p 3376 N92-28503
p 3389 N92-29045
MURPHY, KENT A. p 3358 N92-28868
MURPHY, KEVIN J. p 3351 N92-28292
MURR, LAWRENCE E. p 3303 N92-28892
MURRAY, B. C. p 3379 N92-28994
MURRAY, J. B. p 3393 N92-29069
MURTHY, V. RAMA p 3312 N92-28603
MUSGRAVE, J. L. p 3249 N92-28693
MUSSELWHITE, DONALD S. p 3313 N92-28604
MUSTARD, JOHN F. p 3306 N92-28717
MYERS, D. R. p 3255 N92-28341
MYERS, I. T. p 3280 N92-28675
MYKKELTVEIT, SVEIN p 3309 N92-28569

N

NACHTIGAL, NOEL M. p 3340 N92-29113
NAGASUBRAMANIAN, GANESAN p 3280 N92-28753
NAGY, A. F. p 3376 N92-28498
p 3387 N92-29035
p 3395 N92-29080
NAIR, H. p 3372 N92-28479
NAIR, HARI p 3376 N92-28501
NAMKUNG, MIN p 3303 N92-28757
p 3304 N92-29101
p 3304 N92-29155
NARVAEZ, PABLO p 3351 N92-29130
NASH, GERALD E. p 3253 N92-28953
NEAL, DONALD M. p 3297 N92-28425
NEIBERG, MAURINE J. p 3278 N92-28305
NELLIS, W. J. p 3283 N92-28269
p 3363 N92-28333
NELSON, EMILY p 3267 N92-28438
NELSON, JAMES H. p 3324 N92-28242
NEMAT-NASSER, S. p 3298 N92-28327
NEMIROVSKY, A. S. p 3336 N92-28638
NERODE, ANIL p 3346 N92-28329
NESSETT, D. M. p 3342 N92-28381
NEVANLINNA, HEIKKI p 3299 N92-28622
NEWNAM, B. E. p 3291 N92-29168
NEWSOM, H. E. p 3313 N92-28605
NGUYEN, HONG QUANG p 3366 N92-28232
NGUYENVAN, HIEP p 3338 N92-28785
NICAISE, PLACIDE D. p 3246 N92-28369
NICHOLAS, O. P. p 3239 N92-28652
NICHOLS, F. A. p 3262 N92-28339
NICOGOSSIAN, ARNAULD E. p 3244 N92-29100
NIEDRA, JANIS M. p 3280 N92-28723
NIEDZWECKI, JOHN M. p 3347 N92-28399
NIMMO, NANCY A. p 3247 N92-28733
NISHIMURA, AKIHIKO p 3363 N92-28282
NISSLEY, WILLIAM p 3230 N92-28900
NOBACK, R. p 3239 N92-28653
p 3316 N92-28689
NODA, TOMOHIKO p 3266 N92-29195
NOORBERGEN, H. H. S. p 3305 N92-28690
NORDHOLT, J. E. p 3374 N92-28486
NORMAN, J. H. p 3258 N92-29091
NORMAN, MARC D. p 3315 N92-28614
NOSENCHUCK, DANIEL M. p 3342 N92-28770
NYLAND, TED W. p 3266 N92-28433

O

OBERMAYER, M. p 3222 N92-28528
OBRIEN, WALTER F. p 3237 N92-28463

ODA, ICHIRO p 3366 N92-28235
ODEHL, S. F. p 3273 N92-28356
ODONNELL, KEVIN A. p 3275 N92-28678
OFFENBECK, HANS-GUENTER p 3224 N92-28541
OGBURN, MARILYN E. p 3225 N92-28551
OHBA, HIRONORI p 3363 N92-28282
OHTANI, EIJI p 3313 N92-28606
OKABE, Y. p 3360 N92-28234
OKAMOTO, OSAMU p 3303 N92-28836
OLINTO, A. V. p 3371 N92-28774
OLSON, LARRY E. p 3353 N92-28909
OLSON, REO p 3351 N92-28302
OLTHOFF, J. p 3252 N92-28637
ONEILL, HUGH ST.C. p 3310 N92-28591
OOKAMI, YOSHIAKI p 3303 N92-28836
ORAN, ELAINE S. p 3285 N92-28803
ORCUTT, JOHN A. p 3322 N92-28939
OSBORNE, ERIC P. p 3359 N92-29133
OSCZEVSKI, RANDALL p 3329 N92-28346
OSER, RANDALL L. p 3272 N92-28253
OSHEA, P. G. p 3291 N92-29168
OSTERYOUNG, ROBERT A. p 3307 N92-28974
OSTOJA-STARZEWSKI, MARTIN p 3298 N92-28424
OTTINO, JULIO M. p 3286 N92-28890
OUALI, JAMEL EDDINE p 3343 N92-28782
OUTKA, D. p 3245 N92-29102
OVERTON, E. p 3280 N92-28675
OWEN, R. G. p 3267 N92-28439
OWENS, A. R. p 3267 N92-28439

P

PADUANO, J. p 3238 N92-28466
PAGE, RICHARD A. p 3263 N92-28415
PAGE, WILLIAM E., III p 3366 N92-28256
PAGNIEZ, PIERRE p 3224 N92-28544
PAIGE, D. A. p 3389 N92-29046
p 3394 N92-29073
p 3394 N92-29076
PAINE, R. T. p 3364 N92-28857
PALME, HERBERT p 3310 N92-28591
PALOUNEK, A. P. T. p 3356 N92-28356
PANKAKOSKI, PEKKA H. p 3251 N92-28573
PANNETON, BERNARD p 3316 N92-28703
PANTAZIS, JOHN A. p 3248 N92-28765
PARAMITHAS, GEORGE p 3332 N92-28236
PARDALOS, P. M. p 3308 N92-29173
PARIS, CECIL p 3368 N92-28430
PARK, H. p 3279 N92-28427
PARKER, JOHN V. p 3333 N92-28899
PARKER, S. A. p 3335 N92-28562
PARKER, T. J. p 3386 N92-29031
p 3389 N92-29047
PARPIA, J. M. p 3364 N92-28513
PARTRIDGE, HARRY p 3255 N92-28743
PASCAL, R. W. p 3323 N92-29213
PASTERCZYK, C. p 3368 N92-28832
PATIL, RAMESH p 3368 N92-28430
PATIN, MAX p 3332 N92-28236
PAXTON, L. J. p 3391 N92-29061
PEAK, JAMES E. p 3319 N92-28965
PEARCE, STEPHEN D. p 3334 N92-28285
PEDERSEN, TORBEN S. p 3318 N92-28421
PEPIN, ROBERT O. p 3376 N92-28502
PERCE, VIRGIL p 3265 N92-29116
PERDUE, WILLIAM D. p 3294 N92-28924
PEREZ-DAVILA, ALFREDO p 3337 N92-28710
PERKINS, A. L. p 3322 N92-28951
p 3340 N92-29172
PERKINS, L. J. p 3360 N92-28335
PERRAM, G. P. p 3284 N92-28766
PERRIER, VALERIE p 3347 N92-28777
PETACH, HELEN H. p 3258 N92-29185
PETERS, W. C. p 3285 N92-28808
PETERSON, D. E. p 3365 N92-28874
PETERSON, JAMES R. p 3354 N92-28414
PETIAU, C. p 3232 N92-28472
PHILLIPS, MARY A. p 3368 N92-28565
PHILLIPS, ROGER J. p 3372 N92-28345
PHILLIPS, RON J. p 3333 N92-28899
PHILPOT, M. G. p 3237 N92-28460
PIAZZA, RICHARD L. p 3278 N92-28305
PICKETT, MARK T. p 3240 N92-28673
PIDGEON, DAVID p 3275 N92-28906
PIERCEY, B. J. p 3337 N92-28741
PIERS, M. A. p 3230 N92-28655
PILLALAMARRI, RAMAKRISHNA S. p 3326 N92-28396
PILLINGER, C. T. p 3377 N92-28508
p 3384 N92-29021
p 3394 N92-29077
PINSKI, F. J. p 3260 N92-28856
PINTER, RON Y. p 3343 N92-28915
PINTER, SHLOMIT S. p 3343 N92-28915
PIPERIAS, P. p 3233 N92-28771
p 3304 N92-29181
PLASYNSKI, S. I. p 3285 N92-28808
PLAT, NICO p 3341 N92-29221
PLESCIA, J. B. p 3389 N92-29048
PLUMB, ROBERT C. p 3389 N92-29049
PLUMLEE, GEOFFREY S. p 3389 N92-29050
PLYSTAK, STEVEN R. p 3372 N92-28393
POESTKOKE, R. p 3240 N92-28669
POHJA, SEPPO p 3339 N92-28875
POLLACK, J. B. p 3374 N92-28491
p 3376 N92-28503
p 3386 N92-29030
POLLACK, JAMES B. p 3389 N92-29051
POLLARD, R. T. p 3322 N92-29211
POLLEN, DANIEL A. p 3326 N92-29179
PONGRATZ, HANS W. p 3224 N92-28541
POPE, P. A. p 3305 N92-28715
POPE, S. B. p 3283 N92-28274
POSTAWKO, S. E. p 3377 N92-28504
POSTAWKO, SUSAN p 3390 N92-29052
POTTER, D. p 3245 N92-29102
POVEY, L. A. p 3323 N92-29212
POWERS, ROBERT S. p 3358 N92-28698
PRATT, J. RICHARD p 3265 N92-29157
PRATT, LOZELLE L p 3249 N92-28748
PREINHAELTER, J. p 3361 N92-28742
PRICE, D. W. p 3362 N92-28962
PRICE, E. W. p 3254 N92-28240
PRICE, KENT M. p 3273 N92-28431
p 3275 N92-28906
PRINCE, CAROLYN p 3272 N92-28253
PROVIDAKES, J. p 3272 N92-28304
PSALTIS, DEMETRI p 3345 N92-28970
PURDY, ANDREW p 3261 N92-29170
PURTELL, L. P. p 3284 N92-28768
PUTERBAUGH, TODD S. p 3346 N92-29082
PUTNAM, ROGER S. p 3290 N92-28903
PUTRA, ICHSAN S. p 3299 N92-28580

Q

QIU, XIAOMEI p 3364 N92-28857
QUANDIEU, P. p 3325 N92-28844
QUELLMANN, WILFRIED p 3225 N92-28547
QUESTED, P. N. p 3261 N92-29164

R

RAAIJMAKERS, J. G. W. p 3342 N92-28746
RABINDRA, P. p 3319 N92-28966
RADEBAUGH, M. p 3305 N92-28715
RADEMAKER, E. R. p 3352 N92-28695
RAETH, PETER G. p 3346 N92-29082
RAIDT, URBAN p 3282 N92-29178
RAMACHANDRAN, N. p 3267 N92-28437
RAMAKER, DAVID E. p 3265 N92-28972
RAMAPRAIN, B. R. p 3228 N92-28865
RAMBO, P. W. p 3347 N92-28824
RAMIREZ, C. p 3366 N92-28230
RAMOS, RUBEN p 3385 N92-29025
RANGEL, R. H. p 3282 N92-28258
RANKIN, C. C. p 3299 N92-28583
RANSOME, R. D. p 3354 N92-28310
RAO, M. R. p 3349 N92-28927
p 3350 N92-28928
p 3350 N92-28929
p 3350 N92-28930
RASHIDI, MAJID p 3296 N92-29136
RASMUSSEN, ERIK A. p 3318 N92-28421
RATTRAY, A. p 3369 N92-28955
RAY, S. L. p 3347 N92-28824
READ, J. F. p 3322 N92-29211
REDDIX, M. D. p 3327 N92-28557
REDMOND, JIM p 3247 N92-28734
REDOLFI, J. p 3235 N92-28377
REID, L. D. p 3225 N92-28550
REID, MAX B. p 3234 N92-28910
REIMER, KLAUS p 3272 N92-28793
REINHART, EUGENE R. p 3259 N92-28426
REMINGTON, B. A. p 3288 N92-28812
RENO, J. L. p 3363 N92-28331
REYES, DAVID P. p 3390 N92-29053
REYNAUD, JUAN p 3321 N92-28321
REYNOLDS, G. H. p 3258 N92-29091
RHOADES, W. A. p 3355 N92-29190
RHODES, JAMES A. p 3236 N92-28418
RICE, JAMES W., JR. p 3391 N92-29058
RICE, RICHARD C. p 3235 N92-29180
RICHARDSON, M. I. p 3388 N92-29040
RICHARDSON, R. C. p 3364 N92-28513
RICHTER, A. BRUCE p 3238 N92-28686
RICKARDS, L. J. p 3323 N92-29215
RIDENOUR-BENDER, MARGARET p 3238 N92-28686
RIDER, C. D. p 3304 N92-29181
RIDGWAY, J. R. p 3300 N92-28626
RIDLEY, W. IAN p 3389 N92-29050
RIECHERS, JOHN T. p 3241 N92-28772
RIJZEBOL, K. R. p 3232 N92-28634
p 3233 N92-28651
RIKS, E. p 3299 N92-28583
RINGENBACH, DANIEL P. p 3223 N92-28535
RITCHIE, B. G. p 3354 N92-28310
RITTER, P. D. p 3308 N92-28811
ROBERTS, G. p 3267 N92-28439
ROBERTS, H. p 3247 N92-28738
ROBERTS, RICHARD J. p 3272 N92-28902
ROBERTSON, D. H. p 3252 N92-28917
p 3253 N92-28918
ROBERTSON, JAMES B. p 3359 N92-29158
ROBINSON, D. W. p 3353 N92-29203
ROCO, MIKE C. p 3285 N92-28808
ROGERS, MELISSA J. B. p 3271 N92-28453
ROGERS, STEVEN p 3327 N92-28744
ROHNE, P. B. p 3240 N92-28669
ROJO, JAVIER p 3343 N92-29114
ROKHLIN, V. p 3348 N92-28949
ROMANOFSKY, ROBERT R. p 3358 N92-28571
RON, AMOS p 3334 N92-28301
p 3347 N92-28411
ROOS, N. p 3345 N92-28716
ROSBOROUGH, G. W. p 3244 N92-28343
ROSEN, J. B. p 3337 N92-28704
ROSS, C. R., II p 3313 N92-28607
ROSSITTO, K. F. p 3225 N92-28549
ROSZMAN, L. p 3396 N92-28870
p 3396 N92-28871
p 3396 N92-28907
ROTE, D. M. p 3294 N92-28815
ROTHERY, D. A. p 3393 N92-29089
ROTHMAN, S. p 3288 N92-28812
ROTHSTEIN, A. D. p 3282 N92-28268
ROTTO, SUSAN L. p 3390 N92-29054
ROUGE, CARL J. p 3265 N92-29090
ROUSEFF, DANIEL p 3275 N92-28905
ROUSH, T. L. p 3378 N92-28510
ROUX, FRANCOIS-XAVIER p 3338 N92-28779
ROYSTON, JAMES D. p 3295 N92-29099
ROZENDAL, D. p 3240 N92-28669
RUBIE, D. C. p 3313 N92-28607
RUBIE, DAVID C. p 3310 N92-28592
RUDALEVIGE, TREVOR p 3297 N92-28425
RUDDER, R. A. p 3264 N92-28904
RUFF, STEVEN W. p 3390 N92-29055
RUSCH, MARTIN p 3274 N92-28792
RUSCONI, L. p 3371 N92-28781
RUSSELL, C. T. p 3387 N92-29035
RUTLEDGE, DAVID p 3279 N92-28351
RYALL, T. G. p 3339 N92-28971
RYAN, FRANK J. p 3276 N92-28947

S

SAAGER, P. p 3225 N92-28548
SABA, COSTANDY S. p 3262 N92-28398
SACHSE, GLEN W. p 3359 N92-29117
SAFFORD, LANCE K. p 3255 N92-28391
SAGAN, C. p 3384 N92-29022
SAKAGUCHI, HAJIME p 3241 N92-28829
SALINAS, AL p 3327 N92-28744
SALOMON, RALF p 3327 N92-28787
SAMBE, HIDEO p 3265 N92-28972
SAMPSON, C. R. p 3316 N92-28964
SANTAOJA, KARI p 3251 N92-28573
SANTEE, M. p 3377 N92-28505
p 3390 N92-29056
SARAVANAMUTTOO, H. I. H. p 3237 N92-28459
p 3237 N92-28462
SARKISSAN, A. p 3361 N92-28848
SARVER, GEORGE L. p 3385 N92-29025
SASAKI, SHO p 3314 N92-28608
SASAO, M. p 3360 N92-28234
SASSEN, KENNETH p 3319 N92-29087
SAUSA, ROSARIO C. p 3257 N92-28954
SAWCHUK, A. A. p 3337 N92-28719
SAWKO, PAUL M. p 3245 N92-29104
SCHAEFER, M. W. p 3377 N92-28506
p 3390 N92-29057
SCHAEFFER, J. p 3374 N92-28491
p 3376 N92-28503
SCHAFRANEK, D. p 3239 N92-28652
SCHARTON, T. p 3268 N92-28455
SCHAUB, WILLIAM R., JR. p 3319 N92-28934
SCHAUDER, THOMAS J. p 3253 N92-28959
SCHEETZ, B. E. p 3264 N92-28570
SCHEPER, C. p 3336 N92-28585
SCHIJVE, J. p 3259 N92-28574
p 3259 N92-28578
SCHIPPERS, H. p 3302 N92-28688
SCHMIER, ROBERT G. p 3273 N92-28586

SCHMITT, M. J. p 3291 N92-29168
SCHOESS, JEFF p 3271 N92-28452
SCHRA, L. p 3260 N92-28691
p 3260 N92-28794
p 3303 N92-28850
SCHRAMM, D. N. p 3371 N92-28859
SCHUBERT, FRANZ H. p 3256 N92-28756
SCHUBERT, G. p 3314 N92-28609
SCHULTZ, DAVID N. p 3246 N92-28369
SCHULTZ, P. H. p 3384 N92-29018
SCHUMAKER, BONNY L. p 3291 N92-28941
SCHUPP, PETER E. p 3292 N92-28293
SCHUSTER, GREGORY p 3290 N92-28862
SCHWALD, ANDREAS p 3337 N92-28760
SCHWARTZ, DANIEL A. p 3370 N92-28680
SCHWARTZ, SUSAN p 3309 N92-28386
SCHWARZ, RAY P. p 3331 N92-28897
SCHWARZE, G. E. p 3279 N92-28432
SCOTT, DAVID H. p 3391 N92-29058
SCOTT, JOACHIM H. p 3258 N92-29185
SCOTT, W. H., JR. p 3355 N92-29190
SCOTTI, STEPHEN J. p 3284 N92-28752
SEAGRAVE, RICHARD C. p 3330 N92-28671
SEASHOLTZ, RICHARD G. p 3229 N92-28980
SEDMAK, G. p 3371 N92-28781
SENGUPTA, S. K. p 3319 N92-28966
SENSBURG, OTTO p 3232 N92-28474
SERAFINO, KAREN M. p 3349 N92-28961
SEYMOUR, THEODORE D. p 3221 N92-28348
SHAFER, MARY F. p 3234 N92-29110
SHAFF, WILLIAM p 3289 N92-28330
SHALKHAUSER, MARY JO p 3275 N92-28873
SHAM, T. L. p 3298 N92-28352
SHANNO, DAVID F. p 3335 N92-28428
SHANTHAKUMARAN, P. p 3222 N92-28527
SHAPPELL, SCOTT A. p 3240 N92-28407
SHARMAN, GEORGE F. p 3300 N92-28625
SHEN, JIANMIN p 3366 N92-28227
p 3366 N92-28229
SHENG, ZHENGMAO p 3366 N92-28229
SHEPARD, P. p 3282 N92-29197
SHIBATA, TAKEMASA p 3363 N92-28282
SHIFFRIN, R. M. p 3342 N92-28746
SHIN, JAIWON p 3227 N92-28674
p 3227 N92-28696
SHIRER, HAMPTON N. p 3309 N92-28567
SHIRK, JAMES S. p 3360 N92-29205
SIGEL, G. H. p 3357 N92-28223
SIGMAN, R. K. p 3254 N92-28240
SILDER, STEPHEN H., JR. p 3223 N92-28537
SILETZKY, STEPHAN p 3273 N92-28357
SIMON, J. S. p 3238 N92-28466
SIMPSON, STEVEN S. p 3272 N92-28253
SINGER, R. B. p 3388 N92-29043
p 3391 N92-29059
SINGER, ROBERT p 3385 N92-29026
SINGH, P. p 3282 N92-29197
SINHA, ALOK p 3267 N92-28445
SIRIGNANO, W. A. p 3282 N92-28258
SISSON, PATRICIA L. p 3334 N92-28267
SKARSGARD, HARVEY M. p 3360 N92-28664
p 3361 N92-28665
p 3361 N92-28847
p 3361 N92-28848
p 3361 N92-28849
SKOCH, GARY J. p 3288 N92-29105
SKOGSTROEM, ROAR p 3334 N92-28265
SLADE, M. A. p 3384 N92-29020
SLINKER, S. p 3350 N92-28238
SMIALEK, JAMES L. p 3265 N92-29090
SMIT, J. p 3223 N92-28534
SMITH, H. A. p 3262 N92-28398
SMITH, PHILLIP N. p 3231 N92-29103
SMITH, SAMUEL H. p 3235 N92-29180
SNYDER, GREGORY A. p 3314 N92-28610
SOBIESZCZANSKI-SOBIESKI, JAROSLAW p 3232 N92-28473
SODERMAN, PAUL T. p 3353 N92-28909
SOINILA, SEPPO p 3328 N92-29119
SOLOMATOV, V. S. p 3314 N92-28611
SONG, J. J. p 3274 N92-28809
p 3274 N92-28810
SORDELET, D. J. p 3259 N92-28338
SPECTOR, J. M. p 3340 N92-29187
SPECTOR, J. MICHAEL p 3340 N92-29188
SPIEGEL, EDWARD A. p 3395 N92-28520
SPIRO, RAND J. p 3328 N92-29142
SPUDIS, P. D. p 3311 N92-28594
SREENIVASAN, K. R. p 3282 N92-28225
SRIVAS, MANDAYAM p 3336 N92-28666
p 3336 N92-28667
ST.CLAIR, TERRY L. p 3265 N92-29157
STALDER, K. R. p 3362 N92-29093
STANIER, JEFFREY p 3275 N92-28887
STANLEY, R. J., II p 3247 N92-28738
STARR, SUZANNE E. p 3358 N92-28868
STARR, WILLIAM K. p 3329 N92-28286
STATSINGER, J. p 3245 N92-28956
STAUDHAMMER, KARL P. p 3303 N92-28892
STAUNTON, J. B. p 3260 N92-28856
STEIER, W. H. p 3337 N92-28719
STEINBACH, DIETER p 3229 N92-29159
STEINBERGER, C. J. p 3285 N92-28817
p 3285 N92-28818
p 3258 N92-28821
STEKOLNIKOV, A. V. p 3362 N92-28280
STEPHENS, STUART K. p 3391 N92-29060
STEVENS, BRUCE W. p 3343 N92-29096
STEVENS, J. M. G. F. p 3233 N92-28714
STEVENSON, D. J. p 3314 N92-28611
p 3314 N92-28612
STEVENSON, DAVID J. p 3391 N92-29060
STEWART, A. I. F. p 3391 N92-29061
STOAKLEY, DIANE M. p 3265 N92-29157
STODDARD, J. A. p 3355 N92-29190
STOKER, I. p 3288 N92-29163
STOLPER, E. M. p 3394 N92-29075
STOLTE, J. p 3278 N92-28262
STONE, PHILIP L. p 3264 N92-28912
STORMVANLEEUWEN, S. p 3235 N92-28644
STREIT, ROY L. p 3276 N92-29085
STRICKLAND, EDWIN L., III p 3391 N92-29062
p 3392 N92-29063
p 3392 N92-29064
p 3392 N92-29065
p 3392 N92-29066
STRIFFLER, FOSTER L. p 3276 N92-29085
STRIP, D. p 3335 N92-28342
STROM, R. G. p 3386 N92-29029
p 3386 N92-29031
STROM, ROBERT G. p 3392 N92-29067
SU, TSUNG-CHOW p 3248 N92-28967
SUENAGA, HISASHI p 3241 N92-28835
SULLIVAN, EVESTER p 3266 N92-28739
SULLIVAN, R. J. p 3393 N92-29068
SUMMERS, C. J. p 3274 N92-28773
SURYA, CHARLES p 3280 N92-28561
SUTHAR, J. L. p 3280 N92-28675
SUTHERLAND, LOUIS C. p 3352 N92-28556
SUZUKI, MASAMITU p 3241 N92-28835
SWAFFORD, TIMOTHY W. p 3283 N92-28555
SWARTOUT, WILLIAM p 3368 N92-28430
SWEC, DIANE M. p 3307 N92-28837
SWINDLE, TIMOTHY D. p 3313 N92-28604
SZOSTAK, MICHAEL J. p 3246 N92-28368
SZPOGANICZ, BRUNO p 3258 N92-28973

T

TAGLIARINI, GENE A. p 3367 N92-28389
TAKAHASHI, EIICHI p 3315 N92-28613
TAKAMORI, SUSUMU p 3241 N92-28829
TAKANISHI, ATSUO p 3292 N92-28233
TALJA, HELI p 3303 N92-28776
TANAKA, KEIJI p 3331 N92-28831
TANAKA, KENNETH L. p 3390 N92-29054
TARVAINEN, REINO p 3251 N92-28572
TAURINES, PHILIPPE p 3365 N92-29207
TAYLOR, G. J. p 3311 N92-28594
TAYLOR, G. JEFFREY p 3315 N92-28614
TAYLOR, GERALD R. p 3325 N92-28755
TAYLOR, LAWRENCE A. p 3314 N92-28610
TAYLOR, P. K. p 3323 N92-29213
TENCH, D. M. p 3365 N92-28919
TENDAM, A. A. p 3293 N92-28645
TENHAVE, J. M. p 3241 N92-29204
THART, W. G. J. p 3260 N92-28691
p 3260 N92-28794
p 3303 N92-28850
THOMAS, D. p 3371 N92-28859
THOMAS, DON p 3271 N92-28452
THOMAS, PETER p 3286 N92-28825
THOMAS, R. L. p 3297 N92-28851
THOMAS, RAY W. p 3253 N92-28953
THOMPSON, STEVEN R. p 3368 N92-28565
THOMPSON, T. C. p 3356 N92-28356
THOMPSON, W. R. p 3384 N92-29022
THORNHILL, G. D. p 3393 N92-29069
THORNTON, W. p 3267 N92-28449
TILLMAN, J. E. p 3382 N92-29008
TILLMAN, JAMES E. p 3393 N92-29070
TIRUMALAI, PARTHASARATHY p 3335 N92-28353
TODA, NOBUHIRO p 3241 N92-28835
TOETENEL, HANS p 3341 N92-29221
TOGNACCINI, R. p 3284 N92-28712
TOKUDA, KOICHI p 3278 N92-28239
TOMAZOS, DIMITRIS p 3265 N92-29116
TOMLINSON, B. N. p 3225 N92-28546
TONKS, W. B. p 3315 N92-28615
TORABI, A. p 3274 N92-28773
TOTH, D. K. p 3262 N92-28398
TOULGOAT, MYLENE p 3276 N92-28979
TOWER, LEONARD K. p 3249 N92-28682
TOWNSEND, DENNIS P. p 3293 N92-28476
TRAHIOTIS, CONSTANTINE p 3352 N92-28889
TREIMAN, A. H. p 3393 N92-29071
TRICK, MICHAEL A. p 3268 N92-28359
TRIMBLE, CURTIS A. p 3288 N92-29156
TRUONG, LONG V. p 3337 N92-28684
TRUSZCZYNSKI, MIROSLAW p 3345 N92-28895
TRYGGVASON, BJARNI V. p 3267 N92-28440
TSANG, LEUNG p 3274 N92-28846
TSAO, ALEX p 3275 N92-28906
TSAO, MIKE p 3238 N92-28686
TSOURDALAKIS, EMMANUEL p 3261 N92-28976
TSURUDA, K. p 3393 N92-29072
TURNER, ROSS M. p 3276 N92-28979

U

UHM, HAN S. p 3277 N92-29199
ULLAH, SHAH M. p 3316 N92-28740
UUTTU, TERO p 3251 N92-28573

V

VAESSENS, R. J. M. p 3336 N92-28639
VALAVANI, L. p 3238 N92-28466
VANALSTINE, JAMES M. p 3255 N92-28728
VANCOUR, R. P. p 3244 N92-28937
VANDENBERG, J. I. p 3226 N92-28657
p 3227 N92-28692
VANDENDAM, R. F. p 3227 N92-28660
VANDENHOUDT, GEERT p 3337 N92-28700
VANDERBERG, B. p 3284 N92-28694
VANDERHOEK, WIEBE p 3348 N92-29214
VANDERLAAN, F. p 3294 N92-28705
VANDERLAAN, F. B. p 3305 N92-28708
VANDERLAAN, PAUL p 3348 N92-28640
VANDERVLIET, G. p 3224 N92-28542
VANDERVOOREN, J. p 3228 N92-28709
VANDERWAL, H. M. M. p 3304 N92-29176
VANDERWEES, A. J. p 3228 N92-28709
VANENGELEN, J. A. J. p 3239 N92-28652
VANES, J. T. p 3278 N92-28263
VANGEL, MARK G. p 3297 N92-28425
VANHEMEL, PAUL E. p 3223 N92-28539
VANJOOLEN, VINCENT J. p 3335 N92-28519
VANKATWIJK, JAN p 3341 N92-29221
VANKLEEF, E. R. A. p 3222 N92-28532
VANLENT, M. p 3228 N92-28713
VANLINT, J. H. p 3336 N92-28639
VANNUNEN, J. W. G. p 3233 N92-28687
VANPATTEN, ROBERT E. p 3223 N92-28534
VANPRAAG, R. p 3252 N92-28577
VANTRIGT, J. H. p 3278 N92-28263
VANWOERKOM, P. T. L. M. p 3293 N92-28646
p 3345 N92-28648
VANZANDT, T. R. p 3382 N92-29008
VASAVADA, A. R. p 3394 N92-29073
VAYDA, G. A. p 3322 N92-28913
VENGSARKAR, ASHISH M. p 3358 N92-28868
VENKATASUBRAMANIAN, N. p 3263 N92-28553
VENTERS, STUART p 3332 N92-28236
VERED, NISSAN p 3277 N92-29166
VERHOEF, J. p 3300 N92-28627
VERMEEREN, C. A. J. R. p 3259 N92-28576
VEROLME, J. L. p 3252 N92-28582
VERSLUIS, M. p 3290 N92-28852
VERSTEEG, M. H. J. B. p 3305 N92-28697
VIDMAR, R. J. p 3362 N92-29093
VIDONI, T. J. p 3258 N92-28821
VINCENT, PATRICK J. p 3276 N92-29084
VITELLO, P. A. p 3397 N92-28336
VODEGEL, H. J. G. C. p 3233 N92-28714
VOLAKIS, JOHN L. p 3273 N92-28371
VOLLERSEN, CARL A. p 3249 N92-28748
VONENTRESS-FUERSTENECK, LUTZ p 3245 N92-28826
VONFLOTOW, ANDREAS p 3268 N92-28454
VRANISH, JOHN M. p 3296 N92-29138

W

WADA, M. p 3360 N92-28234
WADE, BRUCE p 3263 N92-28553
WADE, R. p 3341 N92-28279
WAENKE, H. p 3377 N92-28507
WAGENER, R. p 3394 N92-29074
WAITE, J. H. p 3387 N92-29035
WALBERG, GERALD p 3244 N92-28731
WALDEN, BILLIE S. p 3309 N92-28319
WALLACE, R. J. p 3288 N92-28812
WALLCRAFT, ALAN J. p 3321 N92-28566
WALTER, BRUCE A. p 3272 N92-28347

WANG, J.-C. p 3293 N92-28434
WANG, LIANG-GUO p 3359 N92-29117
WANG, QIANG p 3274 N92-28699
WANG, YUNG-PENG p 3287 N92-28445
WANG, Z. p 3294 N92-28815
WANG, ZHONGHUA p 3366 N92-28227
WANHILL, R. J. H. p 3302 N92-28643
p 3238 N92-28711
p 3303 N92-28850
WARREN, PAUL H. p 3315 N92-28616
p 3315 N92-28617
p 3315 N92-28618
WARREN, R. W. p 3291 N92-29168
WATSON, D. L. p 3354 N92-28310
WATSON, L. L. p 3394 N92-29075
WATSON, R. L. p 3355 N92-28764
WDOWIAK, THOMAS J. p 3378 N92-28989
WEAVER, MICHAEL J. p 3363 N92-28349
p 3255 N92-28391
p 3363 N92-28392
p 3364 N92-28512
WEBER, P. G. p 3306 N92-28834
WEBER, WILLIAM P. p 3265 N92-29145
WEBERS, W. p 3302 N92-28633
WEDBERG, TOROLF C. p 3289 N92-28315
WEISLOGEL, MARK W. p 3287 N92-29125
WEISS, JONATHAN M. p 3357 N92-28475
WELCH, DONALD A. p 3329 N92-28286
WELLS, J. S. p 3276 N92-29115
WENDLAND, W. L. p 3302 N92-28688
WENTLING, ROGER p 3323 N92-28247
WERCINSKI, PAUL F. p 3385 N92-29025
WERLEY, K. A. p 3360 N92-28335
WERNET, MARK P. p 3288 N92-29105
WESSELS, J. p 3347 N92-28641
p 3342 N92-28642
WESTFOLD, STEPHEN p 3369 N92-28866
WESTREICH, ERIC L. p 3322 N92-28977
WETHERILL, G. W. p 3315 N92-28619
WEYER, THOMAS H. p 3397 N92-29219
WHITE, A. D. p 3225 N92-28546
WHITE, C. T. p 3355 N92-28881
p 3265 N92-28916
WHITE, HENRY S. p 3258 N92-28982
WHITE, JONATHAN W. p 3320 N92-28316
WHITE, MICHEAL J. p 3351 N92-28292
WHITEHEAD, STEVEN D. p 3344 N92-28325
WHITESIDES, GEORGE M. p 3262 N92-28291
WHITTEN, G. Z. p 3308 N92-29183
WIDROW, L. M. p 3372 N92-29184
WILCOX, DAVID C. p 3283 N92-28350
WILDENBERG, A. P. p 3349 N92-28313
WILL, RALPH W. p 3344 N92-28375
WILLIAMS, A. L. p 3323 N92-29213
WILLIAMS, C. A. p 3300 N92-28627
WILLIAMS, MICHAEL A. p 3341 N92-28306
WILLIS, J. O. p 3365 N92-28874
WILSON, ANTHONY p 3230 N92-28900
WILSON, C. B. p 3367 N92-28403
WINCHESTER, CLINTON S. p 3280 N92-28568
WINDSOR, J. C. p 3247 N92-28738
WINKELMANN, ALLEN E. p 3226 N92-28511
WINNICK, J. p 3256 N92-28827
WIRYOHADIATMOJO, E. S. L. H. p 3345 N92-28581
WITTEN, MARK L. p 3326 N92-29123
WOLF, DAVID A. p 3331 N92-28897
WOLF, PETER p 3250 N92-29141
WOLFE, M. p 3245 N92-28956
WOLKE, W. p 3397 N92-29218
WOLSKI, R. p 3342 N92-28334
WONG, WAYNE A. p 3307 N92-28837
WOOD, R. T. p 3356 N92-28813
WOOD, RICHARD M. p 3228 N92-28729
WOOD, S. E. p 3394 N92-29076
WOODFIELD, A. A. p 3222 N92-28531
WOODYATT, B. A. p 3339 N92-28971
WRENN, GREGORY A. p 3231 N92-28435
WRIGHT, I. P. p 3377 N92-28508
p 3384 N92-29021
p 3394 N92-29077
WRIGHT, JAY M. p 3296 N92-29150
WRIGHT, PATRICK D. p 3333 N92-28899
WRIGHT, WILLIAM A. p 3306 N92-28791
WU, JIUNN-JENG p 3288 N92-29156

X

XIAO, C. p 3361 N92-28848
XU, PENGYANG p 3395 N92-29078
XUE, HUIMIN p 3307 N92-28863

Y

YALAMANCHILI, S. p 3336 N92-28585
YAMAGUCHI, ISAO p 3303 N92-28836
YAMAOKA, H. p 3360 N92-28234
YANG, S. M. p 3343 N92-28958
YARCHI, ZOHAR p 3244 N92-29098
YAZAWA, KENJI p 3331 N92-28831
YELLAND, M. J. p 3323 N92-29213
YOST, WILLIAM T. p 3303 N92-28757
p 3304 N92-29101
p 3304 N92-29155
YOUNG, D. K. p 3324 N92-29089
YOUNG, GEORGE S. p 3309 N92-28567
YOUNG, R. E. p 3387 N92-29036
YUEN, DAVID A. p 3310 N92-28593
YUNG, Y. L. p 3372 N92-28479
YUNG, YUK L. p 3376 N92-28501
YURIMOTO, NAOYOSHI p 3313 N92-28606

Z

ZAAL, K. J. J. M. p 3299 N92-28575
ZAHN, JEAN-PAUL p 3395 N92-28520
ZAHNLE, KEVIN p 3378 N92-28509
ZAMBRE, Y. p 3356 N92-28270
ZANG, T. A. p 3360 N92-28354
ZEH, JAMES M. p 3223 N92-28538
ZENT, A. P. p 3378 N92-28510
p 3395 N92-29079
ZHANG, L. p 3361 N92-28848
ZHANG, LIANRUI p 3258 N92-28982
ZHANG, M. H. G. p 3376 N92-28498
p 3395 N92-29080
ZHANG, W. p 3361 N92-28848
ZHAO, WULING p 3310 N92-28593
ZHENG, Z. p 3283 N92-28361
ZHOU, J. H. p 3274 N92-28809
ZIJM, W. H. M. p 3347 N92-28641
p 3342 N92-28642
ZIMA, HANS p 3337 N92-28760
ZIMBELMAN, J. p 3382 N92-29009
ZINDER, S. p 3257 N92-28942
ZIOCK, H. J. p 3356 N92-28356
ZOU, CHAOFENG p 3254 N92-28290
ZUBER, MARIA T. p 3372 N92-28345
ZUCKER, STEVEN W. p 3328 N92-28957
ZUMBRO, J. D. p 3354 N92-28310
ZUPANC, FRANK J. p 3357 N92-28475
ZUREK, R. W. p 3380 N92-28997
p 3388 N92-29039
ZUREK, RICHARD p 3385 N92-29026

Typical Corporate Source Index Listing

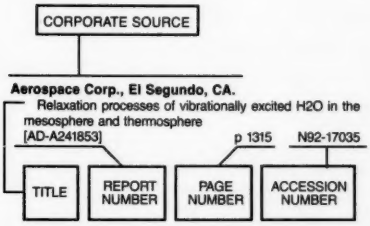

Listings in this index are arranged alphabetically by corporate source. The title of the document provides the user with a brief description of the subject matter. The report number helps to indicate the type of document cited (e.g., NASA report, translation, NASA contractor report). The accession number denotes the number by which the citation is identified. The page number helps you locate the citation in the abstract section. The titles are arranged under each corporate source in ascending accession number order.

A

ACADEMY OF SCIENCES, POTSDAM (GERMAN D.R.).
Independent constituents in observatory time series in characterizing the secular variation
p 3302 N92-28633

ACADEMY OF SCIENCES OF THE UKRAINIAN SSR, KIEV.
Hydrodynamic echo in strongly inhomogeneous magnetized plasma
[DE92-621530] p 3361 N92-28816

ACADEMY OF SCIENCES (USSR), MOSCOW.
Experimental determination of the solubility of iridium in silicate melts: Preliminary results
p 3310 N92-28591

ADVISORY GROUP FOR AEROSPACE RESEARCH AND DEVELOPMENT, NEUILLY-SUR-SEINE (FRANCE).
Applications of ASICs to avionics
[AGARD-AG-329] p 3235 N92-28376
Steady and Transient Performance Prediction of Gas Turbine Engines
[AGARD-LS-183] p 3236 N92-28458
Aircraft ship operations
[AGARD-AR-312] p 3231 N92-28468
Integrated Design Analysis and Optimisation of Aircraft Structures
[AGARD-LS-186] p 3231 N92-28469
Piloted Simulation Effectiveness
[AGARD-CP-513] p 3221 N92-28522

AEDAR CORP., LANDOVER, MD.
Computer derivation of green's functions for structural dynamic analysis
[AD-A250249] p 3339 N92-28969

AERITALIA S.P.A., NAPLES (ITALY).
Boundary conditions for Euler equations at internal block faces of multi-block domains using local grid refinement
[NLR-TP-90134-U] p 3284 N92-28712

AERODYNE RESEARCH, INC., BILLERICA, MA.
Tuning and automatic phase adjustment in external cavity diode laser beam combiners
[AD-A247421] p 3290 N92-28903

AERONAUTICAL RESEARCH INST. OF SWEDEN, STOCKHOLM.
On the use of structural dynamic experimental methods for damage inspection of a glass fibre reinforced plastic plate
[FFA-TN-1992-02] p 3253 N92-29220

AERONAUTICAL RESEARCH LABS., MELBOURNE (AUSTRALIA).
Reduction and analysis of F-111C flight data
[AD-A250341] p 3233 N92-28771
Digital enhancement and restoration of images derived from flow visualization experiments
[AD-A250317] p 3339 N92-28952
Computer recognition and analysis of photogrammetric targets
[AD-A250313] p 3339 N92-28971
Experiments in passive vibration reduction
[AD-A250397] p 3304 N92-29181

AEROSPACE CORP., EL SEGUNDO, CA.
Reactions of hydrazines with chemicals found in environment
[AD-A247064] p 3308 N92-28272
Space transportation analysis and design
[AD-A250629] p 3245 N92-28956

AEROSPATIALE, TOULOUSE (FRANCE).
Flight simulation and digital flight controls
p 3221 N92-28526

AIR FORCE ACADEMY, CO.
Overview of two common statistical computer packages: SAS and BMDP
[AD-A245982] p 3368 N92-28663

AIR FORCE ENVIRONMENTAL TECHNICAL APPLICATIONS CENTER, SCOTT AFB, IL.
Wind-speed forecasting study for Westover AFB, Massachusetts
[AD-A247545] p 3319 N92-28934

AIR FORCE FLIGHT TEST CENTER, EDWARDS AFB, CA.
Utility of ground simulation in flight control problem identification, solution development, and verification
p 3221 N92-28525
Use of simulation in the USAF Test Pilot School curriculum p 3223 N92-28535

AIR FORCE INST. OF TECH., WRIGHT-PATTERSON AFB, OH.
A cost-benefit analysis on the deletion of the inertial upper stage factory acceptance testing versus a decrease in mission reliability
[AD-A246620] p 3245 N92-28254
A review of cost performance index stability
[AD-A246621] p 3370 N92-28255
Improved decision making through group composition
[AD-A246622] p 3366 N92-28256
An application of interactive computer graphics to the study of inferential statistics and the general linear model
[AD-A246668] p 3334 N92-28285
A study of pilot attitudes regarding the impact on mission effectiveness of using new cockpit automation technologies to replace the navigator/weapon system officer/electronic warfare officer
[AD-A246683] p 3329 N92-28286
Life cycle costs of the C-130 electrical power system upgrade
[AD-A246759] p 3221 N92-28348
Microwave derived rainrates in typhoons and their use in the diagnosis and prediction of typhoon intensity
[AD-A250556] p 3319 N92-28922
Development of instrumentation for boundary layer transition detection
[AD-A249982] p 3287 N92-29171
Modular simulation of HEI fragments and blast pressure
[AD-A248205] p 3272 N92-29191
Development of a stratified plate model for composite panels
[AD-A248206] p 3253 N92-29192
Development of a flight information system using the structured method
[AD-A248207] p 3236 N92-29222

AIR FORCE SYSTEMS COMMAND, KIRTLAND AFB, NM.
Plasma beam measurements
[AD-A247892] p 3362 N92-28962

ALABAMA UNIV., BIRMINGHAM.
Iron Moessbauer spectroscopy: Superparamagnetism in hydrothermal vents and the search for evidence of past life on Mars p 3378 N92-28989

ALABAMA UNIV., HUNTSVILLE.
Development of a residual acceleration data reduction and dissemination plan p 3271 N92-28453
Theoretical and experimental studies relevant to interpretation of auroral emissions
[NASA-CR-190521] p 3316 N92-28911

ALBERTA UNIV., EDMONTON.
CO2 and clathrate as past erosive agents on Mars
p 3375 N92-28497

ALENIA, TORINO (ITALY).
AM-X flight simulator from engineering tool to training device p 3223 N92-28536

ALLIED-SIGNAL AEROSPACE CO., KANSAS CITY, MO.
Erosion of stainless steel by ultrasonic cleaning: A preliminary study
[DE92-012566] p 3260 N92-28763

AMERICAN MAGNETICS, INC., OAK RIDGE, TN.
Chemical vapor deposition of yttrium borium(2) copper(3) oxygen(x) thin films for wire applications
[AD-A247013] p 3364 N92-28395

AMES LAB., IA.
Evaluation of plasma sprayed crucible coatings for melt processing copper-refractory metal alloys
[DE92-010871] p 3259 N92-28338

AMPTEK, INC., BEDFORD, MA.
Empirical techniques for the study of acceleration mechanisms in the space environment
[AD-A249940] p 3248 N92-28765

AMSTERDAM UNIV. (NETHERLANDS).
Generalized quantifiers and modal logic
[ITLI-LP-91-01] p 3348 N92-29214

ANALYTIC POWER CORP., BOSTON, MA.
Mobile electric power
[AD-A249354] p 3279 N92-28326

APPLIED EXPERTISE, INC., ARLINGTON, VA.
Consulting report on the NASA technology utilization network system
[NASA-CR-190387] p 3370 N92-29108
Repository-based software engineering program: Concept document
[NASA-CR-190384] p 3341 N92-29200

APPLIED TECHNOLOGY ASSOCIATES, INC., ALBUQUERQUE, NM.
New inertial actuator provides isolation and stabilization in microgravity conditions p 3267 N92-28443

ARGONNE NATIONAL LAB., IL.
Effect of metallic coating properties on the tribology of oil-lubricated coated-ceramics
[DE92-010904] p 3262 N92-28339
A strategy for minimizing common mode human error in executing critical functions and tasks
[DE92-011839] p 3327 N92-28775
Aperture coupling measurement in a test chamber for the Advanced Photon Source (APS)
[DE92-013059] p 3274 N92-28809
RF impedance measurement status for the 7-GeV Advanced Photon Source (APS)
[DE92-013060] p 3274 N92-28810
Present status of computational tools for Maglev development
[DE92-013252] p 3294 N92-28815

ARIZONA STATE UNIV., TEMPE.
Influence of aerodynamic roughness length on aeolian processes: Earth, Mars, Venus p 3380 N92-28996
The composition of Martian aeolian sands: Thermal emissivity from Viking IRTM observations
p 3382 N92-29010
Mid-infrared spectra of Martian komantiite
p 3390 N92-29053
Dorsa Argentea type sinuous ridges, Mars: Evidence for linear dune hypothesis p 3390 N92-29055

Characterization of Martian near-subsurface materials by determination of cohesion and angle of internal friction p 3393 N92-29068
Comparison of drift potential derived from Mars GCM with rock abundance from IRTM p 3395 N92-29078

ARIZONA UNIV., TUCSON.
Expand turbulence laboratory facilities to meet new DOD research interest
[AD-A248581] p 3240 N92-28388
The Coordinated Noninvasive Studies (CNS) project, phase 1
[AD-A247159] p 3324 N92-28397
Mg-perovskite/silicate melt and magnesiowuestite/silicate melt partition coefficients for KLB-1 at 250 Kbars p 3310 N92-28592
Origin of the moon and lunar core formation p 3311 N92-28596
Mg-perovskite/silicate melt partition coefficients in the CMS system at 2430 C and 226 Kbars p 3312 N92-28601
Forsterite/melt partitioning of argon and iodine: Implications for atmosphere formation by outgassing of an early Martian magma ocean p 3313 N92-28604
Magma ocean formation due to giant impacts p 3315 N92-28615
Dust storm driven variations of the Mars thermosphere and exosphere: Coupling of atmospheric regions p 3380 N92-28997
Magmatic intrusions and hydrothermal systems on Mars p 3384 N92-29019
Glacial geomorphic evidence for a late climatic change on Mars p 3386 N92-29029
Erosional landforms on the layered terrains in Valles Marineris p 3386 N92-29031
Exploring compositional variations on the surface of Mars applying mixing modeling to a telescopic spectral image p 3388 N92-29043
Evidence for crystalline hematite as an accessory phase in Martian soils p 3391 N92-29059
Glacial and marine chronology of Mars p 3392 N92-29067
The chronic effects of JP-8 jet fuel exposure on the lungs
[AD-A250308] p 3326 N92-29123

ARMY AEROMEDICAL RESEARCH LAB., FORT RUCKER, AL.
Methods of visual scanning with night vision goggles
[AD-A247470] p 3331 N92-28944

ARMY ARMAMENT RESEARCH, DEVELOPMENT AND ENGINEERING CENTER, PICATINNY ARSENAL, NJ.
Effects of extremely high G acceleration forces on NASA's control and space exposed tomato seeds
[AD-A247488] p 3323 N92-28247

ARMY ARMAMENT RESEARCH, DEVELOPMENT AND ENGINEERING CENTER, WATERVLIET, NY.
Review and update on electrocomposites
[AD-A248050] p 3251 N92-28303
X ray diffraction study of residual stresses in metal matrix composite-jacketed steel cylinders subjected to internal pressure
[AD-A248449] p 3251 N92-28416

ARMY BELVOIR RESEARCH AND DEVELOPMENT CENTER, FORT BELVOIR, VA.
Flow rate testing of valves used with the 500 gallon collapsible drum
[AD-A250567] p 3294 N92-28924

ARMY BIOMEDICAL RESEARCH AND DEVELOPMENT LAB., FORT DETRICK, MD.
Environmental testing of the Xi Scan 1000, portable fluoroscopic and radiographic imaging system
[AD-A247167] p 3324 N92-28242

ARMY CHEMICAL RESEARCH AND DEVELOPMENT CENTER, ABERDEEN PROVING GROUND, MD.
Multicomponent comparison of optical and mass spectrometric diagnostics in low-pressure flames
[AD-A250323] p 3257 N92-28954

ARMY COLD REGIONS RESEARCH AND ENGINEERING LAB., HANOVER, NH.
Use of scrap rubber in asphalt pavement surfaces
[AD-A247419] p 3272 N92-28902

ARMY COMMUNICATIONS-ELECTRONICS COMMAND, FORT MONMOUTH, NJ.
Tactical line-of-sight radio propagation reliability
[AD-A245909] p 3277 N92-29165

ARMY CONSTRUCTION ENGINEERING RESEARCH LAB., CHAMPAIGN, IL.
Operational noise data for OH-58D Army helicopters
[AD-A246822] p 3351 N92-28292
Structural design methodology for large space structures
[AD-A247672] p 3246 N92-28560

ARMY ENGINEER WATERWAYS EXPERIMENT STATION, VICKSBURG, MS.
Passive acoustic range estimation of helicopters
[AD-A248033] p 3351 N92-28302

ARMY LAB. COMMAND, WATERTOWN, MA.
A sensitivity analysis on component reliability from fatigue life computations
[AD-A247430] p 3297 N92-28425
Prediction of composite material properties using two-dimensional finite element micromechanical analysis
[AD-A250300] p 3252 N92-28702

ARMY MATERIALS TECHNOLOGY LAB., WATERTOWN, MA.
Mg-Si-Al oxynitride glasses
[AD-A247593] p 3261 N92-28249
Multiphase structure of a segmented polyurethane: Effects of temperature and annealing
[AD-A247594] p 3262 N92-28250

ARMY MISSILE COMMAND, REDSTONE ARSENAL, AL.
Introduction to rocket propulsion
[AD-A250424] p 3249 N92-28800

ARMY RESEARCH INST. FOR THE BEHAVIORAL AND SOCIAL SCIENCES, ALEXANDRIA, VA.
Effects of high terrestrial altitude on military performance
[AD-A246695] p 3324 N92-28288

ATMOSPHERIC AND ENVIRONMENTAL RESEARCH, INC., CAMBRIDGE, MA.
Simulations of the seasonal polar caps on Mars p 3387 N92-29033

AUSTRALIAN NATIONAL UNIV., CANBERRA.
The distance dependence of regional phase discriminants
[AD-A247546] p 3316 N92-28935

B

BALLISTIC RESEARCH LABS., ABERDEEN PROVING GROUND, MD.
A system structure for predictive relations in penetration mechanics
[AD-A246453] p 3292 N92-28284

BATTELLE COLUMBUS LABS., OH.
Replacement bearing for Rocketdyne SSME HPOTPs using alternate self-lubricating retainer materials
[NASA-CR-184328] p 3292 N92-28362

BATTELLE MEMORIAL INST., COLUMBUS, OH.
Generation of spectra and stress histories for fatigue and damage tolerance analysis of fuselage repairs
[AD-A250390] p 3235 N92-29180

BAYREUTH UNIV. (GERMANY, F.R.).
Estimation of the viscosities of silicate liquids at high pressure from measurements of oxygen diffusivity p 3313 N92-28607

BIDSTON OBSERVATORY, MERSEYSIDE (ENGLAND).
An inventory of data collected during the NERC's North Sea Community Research Project, 1987-1992
[REPT-21-1991] p 3323 N92-29215

BIONETICS CORP., COCOA BEACH, FL.
Coupling plant growth and waste recycling systems in a controlled life support system (CELSS)
[NASA-TM-107544] p 3330 N92-28670

BOEING CO., SEATTLE, WA.
X ray computed tomography of full-scale castings
[AD-A247101] p 3258 N92-28241

BRITISH AEROSPACE PUBLIC LTD. CO., LANCASHIRE (ENGLAND).
Effective cueing during approach and touchdown: Comparison with flight p 3226 N92-28552

BROOKHAVEN NATIONAL LAB., UPTON, NY.
The ultraviolet albedo of Mars p 3394 N92-29074

BROWN UNIV., PROVIDENCE, RI.
Relationships of soil, grass, and bedrock over the Kaweah serpentine melange through spectral mixture analysis of AVIRIS data
[NASA-CR-190445] p 3306 N92-28717
Styles of crater gradation in Southern Ismenius Lacus, Mars: Clues from Meteor Crater, Arizona p 3384 N92-29018

BROWN UNIV., WORCESTER, MA.
Determining the pH of Mars from the Viking labelled release reabsorption effect p 3389 N92-29049

BUREAU OF MINERAL RESOURCES, GEOLOGY AND GEOPHYSICS, CANBERRA (AUSTRALIA).
Magnetic repeat station data p 3301 N92-28630

C

CAE ELECTRONICS LTD., MONTREAL (QUEBEC).
The use of a dedicated testbed to evaluate simulator training effectiveness p 3222 N92-28533

CAE ELECTRONICS LTD., SAINT LAURENT (QUEBEC).
The evaluation of simulator effectiveness for the training of high speed, low level, tactical flight operations p 3223 N92-28539

CALIFORNIA INST. OF TECH., PASADENA.
Multimeter-wave grid oscillators
[AD-A248430] p 3279 N92-28351
The impact of temperature dependent CO2 cross section measurements: A role for heterogeneous chemistry in the atmosphere of Mars? p 3372 N92-28479
Martian atmospheric chemistry during the time of low water abundance p 3376 N92-28501
A magma ocean and the Earth's internal water budget p 3310 N92-28590
Evolution of a terrestrial magma ocean: Thermodynamics, kinetics, rheology, convection, differentiation p 3314 N92-28611
Dynamics and evolution of a magma ocean p 3314 N92-28612
Monolithic optoelectronic implementation of neural planes
[AD-A250286] p 3345 N92-28970
Thermally distinct ejecta blankets from Martian craters p 3379 N92-28994
Carbonate formation on Mars: History of the CO2 atmosphere from models of diffusion-limited growth in non-aqueous environments p 3391 N92-29060
Hydrogen and carbon isotopic composition of volatiles in Nakhla: Implications for weathering on Mars p 3394 N92-29075

CALIFORNIA STATE UNIV., CHICO.
Integrating the affective domain into the instructional design process
[AD-A249287] p 3327 N92-28880

CALIFORNIA UNIV., BERKELEY.
Archival of the ECOM-721 data
[AD-A249299] p 3338 N92-28845

CALIFORNIA UNIV., BERKELEY. LAWRENCE BERKELEY LAB.
Problems in mechanistic theoretical models for cell transformation by ionizing radiation
[DE92-010265] p 3324 N92-28278
Monte Carlo optimization of depth-of-interaction resolution in PET crystals
[DE92-011147] p 3364 N92-28762

CALIFORNIA UNIV., IRVINE.
The linear and nonlinear shear instability of a fluid sheet
[AD-A247092] p 3282 N92-28258
Synthesis and study of metallonitride complexes and polymers
[AD-A248577] p 3262 N92-28323

CALIFORNIA UNIV., LOS ANGELES.
History of oxygen and carbon escape from the Martian atmosphere p 3376 N92-28498
Magma ocean: Mechanisms of formation p 3312 N92-28600
Early planetary differentiation: Geophysical consequences p 3314 N92-28609
Inheritance of magma ocean differentiation during lunar origin by giant impact p 3315 N92-28616
The three stages of magma ocean cooling p 3315 N92-28617
The ferroan-anorthositic suite and the extent of primordial lunar melting p 3315 N92-28618
Mars atmosphere evolution: Escape to space p 3387 N92-29034
Discovery concepts for Mars p 3387 N92-29035
Is ground ice stable near the Martian equator? p 3389 N92-29046
Microcraters on Mars: Evidence of past climatic variations p 3394 N92-29073
Modeling the seasonal cycle of CO2 on Mars: A fit to the Viking lander pressure curves p 3394 N92-29076
The ancient oxygen exosphere of Mars: Implications for atmosphere evolution p 3395 N92-29080

CALIFORNIA UNIV., SAN DIEGO.
EXPLOMET 90 international conference on shock-wave and high-strain-rate phenomena in materials
[AD-A248665] p 3303 N92-28892

CALIFORNIA UNIV., SAN DIEGO, LA JOLLA.
Instrumentation for ultrahigh strain rate experiments
[AD-A249358] p 3298 N92-28327
Seafloor pressure array studies at ultra-low frequencies
[AD-A247663] p 3322 N92-28939

CALIFORNIA UNIV., SANTA BARBARA.
Bifurcations and patterns in nonlinear dissipative systems
[DE92-013502] p 3364 N92-28806

CALIFORNIA UNIV., SANTA CRUZ.
Analysis of the effects of Eurasian crustal and upper mantle structure on regional phases using broadband seismic data
[AD-A248383] p 3309 N92-28386

CAMBRIDGE UNIV. (ENGLAND).
Inlet distortion effects in aircraft propulsion system integration p 3237 N92-28464
Secular variation across the oceans: A retrospective study from 35 years of shipboard total field measurements in the NE Atlantic p 3300 N92-28627
Boundary layer induced noise in aircraft
[ISSN-0309-7293] p 3353 N92-29201

CANADIAN SPACE AGENCY, OTTAWA (ONTARIO).
KC-135 Large Motion Isolation Mount (LMIM)
p 3267 N92-28440
CARLETON UNIV., OTTAWA (ONTARIO).
Overview on basis and use of performance prediction methods p 3237 N92-28459
Component performance requirements
p 3237 N92-28462
CARNEGIE INSTITUTION OF WASHINGTON, DC.
Giant and large impacts in the context of planetary formation theory p 3315 N92-28619
CARNEGIE-MELLON UNIV., PITTSBURGH, PA.
Scheduling multiple variable-speed machines
[AD-A249362] p 3268 N92-28359
Decomposition of balanced matrices. Part 1: Introduction
[AD-A247397] p 3349 N92-28927
Decomposition of balanced matrices. Part 2: Wheel-and-parachute-free graphs
[AD-A247398] p 3350 N92-28928
Decomposition of balanced matrices. Part 6: Even wheels
[AD-A247399] p 3350 N92-28929
Decomposition of balanced matrices. Part 7: A polynomial recognition algorithm
[AD-A247400] p 3350 N92-28930
CASE WESTERN RESERVE UNIV., CLEVELAND, OH.
Quantitative interphase study of composite materials. Interphase engineering: A scientific way of tailoring the mechanophysical properties of composite materials
[AD-A247776] p 3251 N92-28252
Proceedings of Asilomar Conference on Polymeric Materials
[AD-A249366] p 3262 N92-28360
Molecular engineering of liquid crystalline polymers by living cationic polymerization. 21: Synthesis and characterization of poly (3-((4-cyano-4'-biphenyl)oxy) propyl vinyl ether) macromonomers
[AD-A248305] p 3265 N92-29116
CENTRE DE RECHERCHES SCIENTIFIQUES ET TECHNIQUES DE L'INDUSTRIE DES FABRICATIONS METALLIQUES, BRUSSELS (BELGIUM).
Three dimensional measurements of prismatic bodies: Programming by means of a CAD system
[CRIF-MC-91] p 3337 N92-28700
CENTRE NATIONAL DE LA RECHERCHE SCIENTIFIQUE, MEUDON-BELLEVUE (FRANCE).
Distribution of Martian ground-ice table: Preliminary results about climatic variations p 3373 N92-28484
CENTRE NATIONAL DE LA RECHERCHE SCIENTIFIQUE, ORSAY (FRANCE).
Infrared photometric behavior and opposition effect of Mars p 3382 N92-29011
CHEMICAL RESEARCH AND DEVELOPMENT CENTER, ABERDEEN PROVING GROUND, MD.
Experimental aerodynamic facilities of the Aerodynamics Research and Concepts Assistance Branch
[AD-A247489] p 3240 N92-28248
CLEMSON UNIV., SC.
Automated apparel specification retrieval system
[AD-A248619] p 3367 N92-28389
COLOGNE UNIV. (GERMANY, F.R.).
The role of hard turbulent thermal convection in the Earth's early thermal evolution p 3310 N92-28593
COLORADO STATE UNIV., FORT COLLINS.
Microhole array electrodes based on microporous alumina membranes
[AD-A247082] p 3278 N92-28239
Parameterization of convective clouds, mesoscale convective systems, and convective-generated cirrus
[DE92-010951] p 3318 N92-28340
Multiparameter radar and aircraft based studies of the microphysical, kinematic, and electrical structure of convective clouds
[AD-A247497] p 3318 N92-28668
COLORADO UNIV., BOULDER.
Studies of regional wave propagation using differential seismograms and randomized structural models
[AD-A247011] p 3309 N92-28394
Mars volatile evolution: Implications of the recent measurement of O-17 in water from the SNC meteorites
p 3375 N92-28492
The Mars water cycle at other epochs: History of the polar caps and layered terrain p 3375 N92-28493
Sea surface velocities from visible and infrared multispectral atmospheric mapping sensor imagery
[NASA-CR-190398] p 3305 N92-28715
Mars dust and cloud opacities and scattering properties p 3381 N92-29003
VLA mapping of 1.35 cm water emission from the Mars atmospheric limb p 3381 N92-29004
The Martian polar caps: Stability and water transport at low obliquities p 3385 N92-29023
Mars: Correcting surface albedo observations for effects of atmospheric dust loading p 3386 N92-29032
Regional variations in the stability and diffusion of water-ice in the Martian regolith p 3388 N92-29042
Atomic oxygen in the Martian thermosphere
p 3391 N92-29061
COLORADO UNIV., DENVER.
Fast algorithms for transport models
[DE92-011432] p 3338 N92-28841
COLSA, INC., HUNTSVILLE, AL.
Digital hardware architecture implementation
[AD-A249194] p 3332 N92-28236
COLUMBIA UNIV., NEW YORK, NY.
Mathematical modeling of solar magneto-dynamics
[AD-A247158] p 3395 N92-28520
COMPUTER SCIENCES CORP., LANHAM, MD.
Detecting and disentangling nonlinear structure from solar flux time series
[NASA-CR-190510] p 3396 N92-28871
Future mission studies: Forecasting solar flux directly from its chaotic time series
[NASA-CR-190378] p 3396 N92-28872
Evidence of chaotic pattern in solar flux through a reproducible sequence of period-doubling-type bifurcations
[NASA-TM-107944] p 3396 N92-28907
CONNECTICUT UNIV., FARMINGTON.
Monaural and binaural processing of complex waveforms
[AD-A247199] p 3352 N92-28889
CONTINUOUS ELECTRON BEAM ACCELERATOR FACILITY, NEWPORT NEW, VA.
Electroproduction of light quark baryons
[DE92-010853] p 3354 N92-28337
COPENHAGEN UNIV. (DENMARK).
Polar lows over the northeast Greenland Sea
[AD-A245360] p 3318 N92-28421
CORNELL UNIV., ITHACA, NY.
Mapping closures for turbulent mixing and reaction
[AD-A247305] p 3283 N92-28274
Femtosecond carrier processes in compound semiconductors and real time signal processing
[AD-A248053] p 3278 N92-28275
A center of excellence in the mathematical sciences
[AD-A249365] p 3346 N92-28329
Study of ultra short HFET devices with InP substrates
[AD-A248448] p 3279 N92-28427
Physics and technology for the investigation of properties of ultra small systems
[AD-A246772] p 3364 N92-28513
Conversion of acetic acid to methane by thermophiles
[DE92-010652] p 3257 N92-28942
Greenhouse warming by minor gases on early Mars
p 3384 N92-29022
CRANFIELD INST. OF TECH., BEDFORD (ENGLAND).
Fundamentals of structural optimisation
p 3231 N92-28470

D

DASSAULT (E. M.) CO., SAINT CLOUD (FRANCE).
Structural optimization of aircraft
p 3232 N92-28472
DASSAULT-BREGUET AVIATION, SAINT CLOUD (FRANCE).
The role of simulation for the study of APIS (piloting support by synthetic imagery) p 3224 N92-28544
DAYTON UNIV., OH.
Lubricant evaluation and performance 2
[AD-A247464] p 3262 N92-28398
Stretch and hammer neural networks for N-dimensional data generalization
[AD-A247941] p 3346 N92-29082
DAYTON UNIV. RESEARCH INST., OH.
Simulation in infrared imaging: Using electrical circuit principles to model heat transfer
[AD-A248290] p 3278 N92-28276
DCW INDUSTRIES, LA CANADA, CA.
A numerical wind tunnel study of viscous-inviscid interaction
[AD-A248429] p 3283 N92-28350
DEFENCE RESEARCH AGENCY, BEDFORD (ENGLAND).
Initial validation of a R/D simulator with large amplitude motion p 3225 N92-28546
DEFENCE RESEARCH ESTABLISHMENT ATLANTIC, DARTMOUTH (NOVA SCOTIA).
The effects of alumina trihydrate on the flammability characteristics of polyester, vinyl ester, and epoxy glass reinforced plastics
[AD-A247707] p 3264 N92-28563
DEFENCE RESEARCH ESTABLISHMENT, OTTAWA (ONTARIO).
Modelling of heat and moisture loss through NBC ensembles
[AD-A245939] p 3329 N92-28346
Thermal analysis of selected commercial thermoplastic resins
[AD-A247711] p 3264 N92-28564
An investigation into techniques for the determination of moisture content on activated carbon
[AD-A245938] p 3256 N92-28882
The use of a vector network analyzer for measuring the performance of radar absorbing materials
[AD-A247194] p 3275 N92-28887
A 2-D analysis of evaporation in laminar flow
[AD-A246467] p 3287 N92-28978
Data selection for fast projection techniques applied to adaptive nulling: A comparative study of performance
[AD-A246468] p 3276 N92-28979
DEPARTMENT OF ENERGY, WASHINGTON, DC.
Primer on molecular genetics
[DE92-010680] p 3324 N92-28382
Geothermal Progress Monitor, report No. 13
[DE92-010697] p 3307 N92-28422
Information Resources Management long-range plan
[DE92-012408] p 3368 N92-28804
DEPARTMENT OF THE NAVY, WASHINGTON, DC.
Three-axis fiber optic vector magnetometer
[AD-D015199] p 3357 N92-28223
Method fabricating load-bearing composites free from microbuckling deformation up to a predetermined load
[AD-D015212] p 3250 N92-28224
Propellant-to-inhibitor bonding system
[AD-D015243] p 3266 N92-28739
Solid-propellant-powered maneuvering system for spacecraft
[AD-D015245] p 3249 N92-28747
Rocket nozzle shield
[AD-D015248] p 3249 N92-28748
Transient impeller test facility
[AD-D015249] p 3294 N92-28749
Wing-extendible gliding store
[AD-D015233] p 3234 N92-28987
Crosstalk correction scheme
[AD-D015251] p 3276 N92-29085
Multi-channel fiber optic rotary joint for single-mode fiber
[AD-D015273] p 3358 N92-29095
Asynchronous bidirectional network interface enabling seamless concurrent processing in a distributed heterogeneous multiprocessor system
[AD-D015274] p 3343 N92-29096
Target motion detecting impulse Doppler radar system
[AD-D015263] p 3277 N92-29169
Volatile CVD precursors based on copper alkoxides and mixed group IIA-Copper alkoxides
[AD-D015264] p 3261 N92-29170
High power microwave generator
[AD-D015262] p 3277 N92-29199
Optical switching devices
[AD-D015261] p 3360 N92-29205
DEUTSCHE AIRBUS G.M.B.H., HAMBURG (GERMANY, F.R.).
Use of a virtual cockpit for the development of a future transport aircraft p 3225 N92-28547
DEUTSCHE FORSCHUNGSANSTALT FUER LUFT- UND RAUMFAHRT, BRUNSWICK (GERMANY, F.R.).
The role of systems simulation for the development and qualification of ATTAS p 3225 N92-28548
DEUTSCHE FORSCHUNGSANSTALT FUER LUFT- UND RAUMFAHRT, COLOGNE (GERMANY, F.R.).
Effect of solidification technique and consolidation method on the properties of rapidly solidified Al-Fe alloys
[DLR-FB-91-24] p 3260 N92-28823
Simulation of Martian surface-atmosphere interaction in a space-simulator: Technical considerations and feasibility p 3388 N92-29044
DLR research reports and communications
[ISSN-0939-2971] p 3397 N92-29218
Activities report of the DLR
[ISSN-0938-2194] p 3397 N92-29219
DEUTSCHE FORSCHUNGSANSTALT FUER LUFT- UND RAUMFAHRT, GOETTINGEN (GERMANY, F.R.).
Experimental and theoretical investigations on the particle lag of particles under the influence of large velocity gradients in compressible flow
[DLR-FB-91-25] p 3286 N92-28825
DEUTSCHE FORSCHUNGSANSTALT FUER LUFT- UND RAUMFAHRT, LAMPOLDSHAUSEN (GERMANY, F.R.).
Evaluation of future space transportation systems with regard to their reliabilities and costs
[DLR-FB-91-27] p 3245 N92-28826
DOUGLAS AIRCRAFT CO., INC., LONG BEACH, CA.
The use and effectiveness of piloted simulation in transport aircraft research and development
p 3225 N92-28549
DUKE UNIV., DURHAM, NC.
Near millimeter waves and microelectronics
[AD-A250384] p 3281 N92-28797

E

EDGERTON, GERMESHAUSEN AND GRIER, INC., IDAHO FALLS, ID.
Cryogenic system operating experience review for fusion applications
[DE92-012509] p 3361 N92-28805
Monitoring activities review of the Radiological Environmental Surveillance Program
[DE92-013103] p 3308 N92-28811
EDUCATIONAL TESTING SERVICE, PRINCETON, NJ.
The variance of Rasch ability estimates from partially-known item parameters
[AD-A247065] p 3348 N92-28273
EIDGENOESSISCHE TECHNISCHE HOCHSCHULE, ZURICH (SWITZERLAND).
On-line point positioning with single frame camera data
[AD-A248307] p 3287 N92-28322
ELECTRONICS RESEARCH LAB., ADELAIDE (AUSTRALIA).
Information technology in plain words
[AD-A250324] p 3369 N92-28955
EMORY UNIV., ATLANTA, GA.
Relaxation dynamics of highly excited halogens in their electronic ground states
[AD-A247312] p 3254 N92-28300
EUROPEAN ORGANIZATION FOR THE EXPLOITATION OF METEOROLOGICAL SATELLITES, DARMSTADT (GERMANY, F.R.).
EUMETSAT: The European Organization for Meteorological Satellites
[ETN-92-91069] p 3318 N92-28745
EUROPEAN SPACE AGENCY, PARIS (FRANCE).
A Be star atlas of far UV and optical high-resolution spectra
[ESA-SP-1147] p 3371 N92-28781
Calculation of support interferences on the aerodynamic coefficients for a wind tunnel calibration model
[ESA-TT-1247] p 3229 N92-29159
EUROPEAN SPACE AGENCY. EUROPEAN SPACE RESEARCH AND TECHNOLOGY CENTER, ESTEC, NOORDWIJK (NETHERLANDS).
MARSNET surface and atmosphere investigations
p 3381 N92-29002

F

FEDERAL AVIATION ADMINISTRATION, ATLANTIC CITY, NJ.
Drop test: Cessna Golden Eagle 421B
[DOT/FAA/CT-TN91/32] p 3230 N92-28900
FEDERAL AVIATION ADMINISTRATION, WASHINGTON, DC.
FAA aviation forecasts
[AD-A250412] p 3230 N92-29182
FEDERAL MINISTRY FOR DEFENCE, BONN (GERMANY, F.R.).
Opportunities for flight simulation to improve operational effectiveness p 3221 N92-28523
FERMI NATIONAL ACCELERATOR LAB., BATAVIA, IL.
The physics of strange matter
[DE92-011734] p 3371 N92-28774
The 17 keV neutrino and neutrino tagging
[DE92-011281] p 3355 N92-28839
The many aspects of neutrino physics
[DE92-011735] p 3355 N92-28858
Quark matter and cosmology
[DE92-011736] p 3371 N92-28859
Inverse phase transitions: Does baryogenesis lead to dark matter?
[DE92-013022] p 3372 N92-29184
Operation and radiation resistance of a FOXFET biasing structure for silicon strip detectors
[DE92-011279] p 3282 N92-29197
FINNISH METEOROLOGICAL INST., HELSINKI.
Measurements of declination at the Helsinki Magnetic-Meteorological Observatory 1844-1853
p 3299 N92-28622
FLORIDA ATLANTIC UNIV., BOCA RATON.
Mobility power flow analysis of coupled plate structure subjected to mechanical and acoustic excitation
[NASA-CR-189635] p 3352 N92-28722
Nonlinear sloshing and the coupled dynamics of liquid propellants and spacecraft
[AD-A250023] p 3248 N92-28967

G

GASTOPS LTD., GLOUCESTER (ONTARIO).
Engine performance and health monitoring models using steady state and transient prediction methods
p 3238 N92-28467
GENERAL ACCOUNTING OFFICE, WASHINGTON, DC.
Space Station: Delays in dealing with space debris may reduce safety and increase costs
[GAO/IMTEC-92-50] p 3243 N92-28406
GENERAL ELECTRIC CO., CINCINNATI, OH.
Coupled structural/thermal/electromagnetic analysis/tailoring of graded composite structures
[NASA-CR-189153] p 3298 N92-28296
GEOLOGICAL SURVEY, DENVER, CO.
Geomagnetic data from the US magnetic observatory network p 3301 N92-28631
Chemical reaction path modeling of hydrothermal processes on Mars: Preliminary results
p 3389 N92-29050
GEOLOGICAL SURVEY, FLAGSTAFF, AZ.
Temporal variability of the surface and atmosphere of Mars: Viking Orbiter color observations
p 3388 N92-29041
Chryse Planitia region, Mars: Channeling history, flood-volume estimates, and scenarios for bodies of water in the northern plains p 3390 N92-29054
Amazonis and Utopia Planitiae: Martian Lacustrine basins p 3391 N92-29058
GEOLOGICAL SURVEY, MENLO PARK, CA.
Water inventories on Earth and Mars: Clues to atmosphere formation p 3373 N92-28483
GEOLOGICAL SURVEY OF CANADA, OTTAWA (ONTARIO).
Survey parameters and availability of low-level aeromagnetic data for geomagnetic field modelling
p 3301 N92-28629
GEORGE WASHINGTON UNIV., WASHINGTON, DC.
X ray photoelectron spectroscopy study on the double layer at an Al2O3-Al interface
[AD-A246454] p 3265 N92-28972
GEORGETOWN UNIV., WASHINGTON, DC.
Control and stabilization of distributed parameter systems in structural dynamics
[AD-A247097] p 3298 N92-28320
GEORGIA INST. OF TECH., ATLANTA.
Combustion mechanisms of solids
[AD-A247088] p 3254 N92-28240
Chemical vapor deposition of yttrium borium(2) copper(3) oxygen(x) thin films for wire applications
[AD-A247013] p 3364 N92-28395
Formation, structure, and properties of boron nitride fibers from polymer precursors
[AD-A247679] p 3263 N92-28553
An acoustic charge transport imager for high definition television application
[AD-A250433] p 3274 N92-28773
High temperature membranes for H2S and SO2 separations
[DE92-010451] p 3256 N92-28827
Studies of the polarimetric dependence of enhanced backscattering from one-dimensional surfaces
[AD-A248431] p 3275 N92-28878
GEORGIA SOUTHWESTERN COLL., AMERICUS.
An ejection model for SNC meteorites: An indication for recent volcanism on Mars p 3387 N92-29038

H

HAMPTON UNIV., VA.
Ionized assisted deposition of organic films for optoelectronic applications
[AD-A247744] p 3263 N92-28405
HARRIS CORP., MELBOURNE, FL.
SPECTOOL: A computer-aided verification tool for hardware designs, volume 1
[AD-A247492] p 3336 N92-28666
SPECTOOL: User's manual, volume 2
[AD-A247493] p 3336 N92-28667
HARVARD COLL. OBSERVATORY, CAMBRIDGE, MA.
The energetics and mechanics of load carrying
[AD-A248441] p 3332 N92-29227
HARVARD UNIV., CAMBRIDGE, MA.
Orthogonal self-assembly of redox active molecules on Pt and Au: Selective reaction of disulfide with Au and isonitrile with Pt
[AD-A246698] p 3254 N92-28290
Correlation between surface free energy and surface constitution
[AD-A246699] p 3262 N92-28291
High-pressure melting of carbonaceous chondrite
p 3310 N92-28589
HAWAII UNIV., HONOLULU.
Evidence for magma oceans on asteroids, the moon, and Earth p 3315 N92-28614
Mars: Compositional variability of ferric/ferrous minerals and polar volatiles from groundbased imaging spectroscopy p 3379 N92-28993
Influence of heat flow on early Martian climate
p 3390 N92-29052
HELSINKI UNIV. (FINLAND).
Operation and radiation resistance of a FOXFET biasing structure for silicon strip detectors
[DE92-011279] p 3282 N92-29197
HIROSHIMA UNIV. (JAPAN).
Cooling of the magma ocean due to accretional disruption of the surface insulating layer
p 3314 N92-28608
HOUSTON UNIV., TX.
Superheat in magma oceans p 3311 N92-28597
HOWARD UNIV., WASHINGTON, DC.
Neuropsychological components of object identification
[AD-A247049] p 3327 N92-28877
HUGHES STX, INC., LANHAM, MD.
Reduction of marine magnetic data for modeling the main field of the Earth p 3300 N92-28626
HUMAN ENGINEERING LABS., ABERDEEN PROVING GROUND, MD.
Program Cluster: An identification of fixation cluster characteristics
[AD-A247014] p 3326 N92-28396

I

ILLINOIS UNIV., URBANA.
Scattering mechanisms for semiconductor transport calculations
[AD-A249260] p 3278 N92-28295
Wall turbulence
[AD-A249973] p 3284 N92-28768
ILLINOIS UNIV., URBANA-CHAMPAIGN.
DEPEND: A simulation-based environment for system level dependability analysis
[NASA-CR-189752] p 3297 N92-28726
INDIANA UNIV., BLOOMINGTON.
Models for recall and recognition
[IZF-1991-B-4] p 3342 N92-28746
INSTITUT NATIONAL POLYTECHNIQUE, GRENOBLE (FRANCE).
Flexible integrated architecture for neural networks
[ETN-92-91320] p 3343 N92-28782
A knowledge based approach for testing VLSI circuits: Application to the validation of prototypes for a non-contact test
[ETN-92-91321] p 3280 N92-28783
Image processing for failure analysis of integrated circuits by an electron beam
[ETN-92-91322] p 3281 N92-28784
Compilation and operation environment of an object based language
[ETN-92-91323] p 3338 N92-28785
Optimization by renaming in the solution method
[ETN-92-91324] p 3338 N92-28842
INSTITUTE FOR COMPUTER APPLICATIONS IN SCIENCE AND ENGINEERING, HAMPTON, VA.
Vienna FORTRAN: A language specification, version 1.1
[NASA-CR-189629] p 3337 N92-28760
INSTITUTE FOR NAVAL OCEANOGRAPHY, BAY SAINT LOUIS, MS.
Oceanographic data dictionary for netCDF files
[AD-A250017] p 3322 N92-28951
HYPER: A domain decomposition program, version 1.0 (user's manual)
[AD-A250018] p 3340 N92-29172
INSTITUTE FOR PERCEPTION RVO-TNO, SOESTERBERG (NETHERLANDS).
Models for recall and recognition
[IZF-1991-B-4] p 3342 N92-28746
Time pressure effects on decision making in a dynamic task environment
[IZF-1991-B-8] p 3367 N92-29161
Is choice accuracy related to information search patterns?
[IZF-1991-B-9] p 3369 N92-29162
INSTITUTE OF GEODYNAMICS, BUCHAREST (ROMANIA).
Magnetic and electromagnetic induction effects in the annual means of geomagnetic elements
p 3301 N92-28632
INSTITUTE OF OCEANOGRAPHIC SCIENCES, WORMLEY (ENGLAND).
CTD data from the north east Atlantic, April 1989, collected on RRS Discovery Cruise 181
[IOS-285-1991] p 3322 N92-29211
Moored current measurements made in the Iceland Faeroes region during July-August 1990
[IOS-286-1991] p 3323 N92-29212
Evaluation of a Solent sonic anemometer on RRS Charles Darwin Cruise 43
[IOS-288-1991] p 3323 N92-29213
Directional wave data recorded off Flamborough Head (England)
[IOS-273-1990] p 3323 N92-29216

INSTITUTE OF PLASMA PHYSICS, PRAGUE (CZECHOSLOVAKIA).
The theory of the long waveguide structures radiating the LH waves into a plasma
[IPPCZ-314] p 3361 N92-28742
INTERNATIONAL CENTRE FOR THEORETICAL PHYSICS, TRIESTE (ITALY).
Classical and quantum Liouville theory on the Riemann sphere with n greater than 3 punctures (II)
[DE92-622380] p 3366 N92-28227
Noise reduction in ring laser driven by a broad band pump
[DE92-622403] p 3289 N92-28228
The exchange algebra for Liouville theory on punctured Riemann sphere
[DE92-622409] p 3366 N92-28229
Hyper-Raman scattering and 3-photon resonant ionization: Competitive effects
[DE92-622671] p 3366 N92-28230
Percolation conductivity of Penrose tiling by transfer-matrix Monte Carlo
[DE92-622792] p 3362 N92-28231
The influence of the resonant electromagnetic field on the light absorption by exciton and biexciton in quantum wells
[DE92-622801] p 3366 N92-28232
Weighted-density functional approach for the solid-liquid interfaces in electrolytes
[DE92-622662] p 3362 N92-28280
Quasi-regular impurity distribution driven by charge-density wave
[DE92-622799] p 3363 N92-28281
The principal part of plane vector fields with fixed Newton diagram
[DE92-622408] p 3346 N92-28311
Shallow states of donor impurities on periodically structured semiconductors interfaces
[DE92-622791] p 3363 N92-28312
IOWA STATE UNIV. OF SCIENCE AND TECHNOLOGY, AMES.
Space life support engineering program
[NASA-CR-190448] p 3330 N92-28671
IOWA UNIV., IOWA CITY.
New methodology for fluorocarbon synthesis
[AD-A247163] p 3254 N92-28261
ISHIKAWAJIMA-HARIMA HEAVY INDUSTRIES CO. LTD., TOKYO (JAPAN).
NASDA's activities on vibration isolation technology p 3267 N92-28441
ISRAEL AIRCRAFT INDUSTRIES LTD., LOD.
Verification of satellite EGSE test-software using an application generator
[ITN-92-85131] p 3244 N92-29098

J

JACKSON STATE UNIV., MS.
Temporal reasoning and problem solving
[AD-A248457] p 3344 N92-28387
JAPAN ATOMIC ENERGY RESEARCH INST., TOKYO.
A survey report for the design of biped locomotion robot: The WL-12 (Waseda Leg-12)
[DE92-782046] p 3292 N92-28233
Gadolinium metastable states population distributions and atomic density under high-rate electron beam evaporation
[DE92-782008] p 3363 N92-28282
JAPAN SPACE UTILIZATION PROMOTION CENTER, TOKYO.
NASDA's activities on vibration isolation technology p 3267 N92-28441
JET PROPULSION LAB., CALIFORNIA INST. OF TECH., PASADENA.
Predicting microgravity levels for space station using VAPEPS p 3268 N92-28455
Surface vs. atmospheric origin of 2.1-2.5 micron absorption features in the Martian spectrum p 3373 N92-28480
The thermal structure, dust loading, and meridional transport in the Martian atmosphere during late southern summer p 3377 N92-28505
Secondary Li battery incorporating 12-Crown-4 ether
[NASA-CASE-NPO-17922-1-CU] p 3280 N92-28753
Scientific applications of frequency-stabilized laser technology in space
[NASA-CR-190449] p 3291 N92-28941
TOPEX/POSEIDON science investigations plan
[NASA-CR-190456] p 3305 N92-28950
Infrared imaging of Mars for volatile distribution and seasonal variability between 2.4 and 5.1 microns p 3379 N92-28995
Analysis of Martian atmospheric and surface optical properties between 4.4 and 5.1 microns p 3382 N92-29007
Micro weather stations for in situ measurements in the Martian planetary boundary layer p 3382 N92-29008
Martian surface simulations p 3383 N92-29016
Dark material in the polar layered deposits on Mars p 3385 N92-29024
Observations of Mars using Hubble Space Telescope p 3385 N92-29026
New dust opacity maps from Viking IR thermal mapper data p 3388 N92-29040
Recent Elysium volcanism: Effects on the Martian atmosphere p 3389 N92-29048
Atmospheric and surface temperatures and airborne dust amounts during late southern summer from Mariner 9 IRIS data p 3390 N92-29056
Method and apparatus for phasing segmented mirror arrays
[NASA-CASE-NPO-18095-1-CU] p 3359 N92-29122
Method and apparatus for frequency spectrum analysis
[NASA-CASE-NPO-17759-1-CU] p 3276 N92-29124
Method and apparatus for predicting the direction of movement in machine vision
[NASA-CASE-NPO-17552-1-CU] p 3331 N92-29129
Precision measurement of magnetic characteristics of an article with nullification of external magnetic fields
[NASA-CASE-NPO-18187-1-CU] p 3351 N92-29130
Microwave temperature profiler for clear air turbulence prediction
[NASA-CASE-NPO-18115-1-CU] p 3320 N92-29148
Ultra-high temperature stability Joule-Thomson cooler with capability to accomodate pressure variations
[NASA-CASE-NPO-18184-1-CU] p 3288 N92-29156
Publications of the Jet Propulsion Laboratory, 1989
[NASA-CR-190457] p 3369 N92-29202
JEWISH HOSPITAL OF BROOKLYN, NY.
Study of SCN neurochemistry using in vivo microdialysis in the conscious brain: Correlation with overt circadian rhythms
[AD-A247172] p 3325 N92-28886
JOHNS HOPKINS UNIV., LAUREL, MD.
Comparison of various techniques in the analysis of waveguide transitions
[AD-A247019] p 3279 N92-28367
Unwrapping two-dimensional phase data in contour maps
[AD-A249988] p 3338 N92-28795
Simulating radar propagation through atmospheric turbulence using the Tropospheric ElectroMagnetic Parabolic Equation Routine (TEMPER)
[AD-A247408] p 3275 N92-28905

K

KANSAS UNIV. CENTER FOR RESEARCH, INC., LAWRENCE.
Identification of aerodynamic models for maneuvering aircraft
[NASA-CR-190444] p 3233 N92-28720
KENT UNIV., CANTERBURY (ENGLAND).
In line optical fibre frequency shifter project
[AD-A246714] p 3357 N92-28372
KENTUCKY UNIV., LEXINGTON.
Investigations of logic of introspection and related modes of reasoning with applications
[AD-A249286] p 3345 N92-28895

L

LABORATOIRE D'AUTOMATIQUE ET D'ANALYSE DES SYSTEMES, TOULOUSE (FRANCE).
Feasibility of metal-oxide-semiconductor structures on Si-LPCVD thin films by low temperature (600 C) process
[LAAS-91307] p 3365 N92-29207
Design and realization of polysilicon emitter bipolar transistors
[LAAS-91360] p 3282 N92-29208
Contribution to the design of flexible manufacturing systems: Application of the formal description technique Estelle
[LAAS-91378] p 3341 N92-29209
LASER PHOTONICS TECHNOLOGY, INC., AMHERST, NY.
Sol-gel processed multifunctional organic polymer-inorganic oxide composites for electronics and photonics
[AD-A246773] p 3263 N92-28412
LAWRENCE LIVERMORE NATIONAL LAB., CA.
Fluids at high shock pressures and temperatures
[DE92-010709] p 3283 N92-28269
Microstructures of shocked quartz
[DE92-010710] p 3363 N92-28333
SISAL: Toward resolving the parallel programming crisis
[DE92-010716] p 3342 N92-28334
A comparison of results from an edge-plasma model with those from a two-dimensional fluid code
[DE92-010718] p 3360 N92-28335
Resonant Compton scattering in models of gamma ray burst sources
[DE92-010720] p 3397 N92-28336
An ELROS primer
[DE92-010661] p 3342 N92-28381
Somatic gene mutation in the human in relation to radiation risk
[DE92-009459] p 3325 N92-28685
Woelter x ray microscope characterization measurements on Novs
[DE92-013207] p 3288 N92-28812
A comparative study of the accuracy of various time domain nonorthogonal mesh methods
[DE92-007300] p 3347 N92-28824
The nonequilibrium molecular dynamics
[DE92-011760] p 3355 N92-28860
Analysis and optimization of low-earth-orbit communication links
[DE92-013393] p 3277 N92-29131
LOCKHEED MISSILES AND SPACE CO., AUSTIN, TX.
Validation of knowledge based systems
[AD-A247741] p 3368 N92-28404
LOS ALAMOS NATIONAL LAB., NM.
A study of the normal injection of hydrogen into a heated supersonic flow using planar laser-induced fluorescence
[DE92-010701] p 3282 N92-28268
PROPX: An x ray manipulation program
[DE92-011264] p 3334 N92-28309
Evidence for physics beyond the quasi-deuteron model in pion absorption
[DE92-011285] p 3354 N92-28310
The solenoidal detector collaboration silicon detector system
[DE92-011237] p 3356 N92-28356
An ion mass spectrometer for measuring isotopic adundances and loss rates of O, C and H in Mars' upper atmosphere p 3374 N92-28486
Redistribution of subsurface neutrons caused by ground ice on Mars p 3374 N92-28488
Remote sensing applications of the extended radiosity method
[DE92-011356] p 3306 N92-28807
A new radiometer for Earth radiation budget studies
[DE92-011267] p 3306 N92-28834
Information systems for engineering sustainable development
[DE92-011271] p 3368 N92-28838
Atmospheric corrections of land imagery using the extended radiosity method
[DE92-011355] p 3306 N92-28840
Magnetic hysteresis and relaxation in Ag-sheathed TlBaCaCuO (1223) and Bi(Pb)SrCaCuO (2223) superconducting tapes
[DE92-011357] p 3365 N92-28874
The Los Alamos POP Project: FEL oscillator experiments in the ultraviolet and beyond
[DE92-011286] p 3291 N92-29168
LOWELL OBSERVATORY, FLAGSTAFF, AZ.
Using the historical record to determine dust sources p 3376 N92-28499
Observed changes in limb clouds immediately prior to the onset of planet-encircling dust storms p 3388 N92-29039
LOWELL UNIV., MA.
Calculations and databasing of molecular absorption parameters for HITRAN
[AD-A247549] p 3355 N92-28936
LUNAR AND PLANETARY INST., HOUSTON, TX.
Papers Presented to the Workshop on the Evolution of the Martian Atmosphere
[NASA-CR-190508] p 3372 N92-28478
Workshop on the Physics and Chemistry of Magma Oceans from 1 Bar to 4 Mbar
[NASA-CR-190419] p 3310 N92-28587
The distribution of anorthosite on the nearside of the moon p 3311 N92-28594
Superheat in magma oceans p 3311 N92-28597
Workshop on the Martian Surface and Atmosphere Through Time
[NASA-CR-190418] p 3378 N92-28988
Mars atmospheric water p 3381 N92-29005
The subsurface hydrologic response of Mars to the thermal evolution of its early crust p 3381 N92-29006

M

MARYLAND UNIV., COLLEGE PARK.
Volcanic recycling of carbonate deposits on Mars p 3377 N92-28506
Studies in general aviation aerodynamics
[NASA-CR-190431] p 3226 N92-28511

MARYLAND UNIV. BALTIMORE COUNTY, CATONSVILLE.
Maximizing the convergence rate of the EM algorithm for the multiple broad-band signal estimation and detection
[AD-A248230] p 3341 N92-29224
MASSACHUSETTS INST. OF TECH., CAMBRIDGE.
Chain folding in EBEE semicrystalline diblock copolymers
[AD-A247595] p 3262 N92-28251
Microgravity isolation mounts based upon Piezoelectric film p 3268 N92-28454
Dynamic control of aerodynamic instabilities in gas turbine engines p 3238 N92-28466
Oxygen in the Martian atmosphere: Regulation of PO2 by the deposition of iron formations on Mars p 3373 N92-28482
Development of an advanced representation of cumulus convection
[DE92-011031] p 3319 N92-28830
Rates of oxidative weathering on the surface of Mars p 3380 N92-28999
Super auditory localization for improved human-machine interfaces
[AD-A250288] p 3331 N92-29121
MASSACHUSETTS INST. OF TECH., LEXINGTON.
Scattering measurements and predictions for a Delta stage 2 rocket nozzle
[AD-A246776] p 3248 N92-28366
MASSACHUSETTS UNIV., AMHERST.
Fate of a perched crystal layer in a magma ocean p 3312 N92-28602
Observational study and analysis of point sources found by the infrared astronomy satellite
[AD-A248416] p 3371 N92-28843
Lagrangian turbulence: Structures and mixing in admissible model flows
[AD-A247203] p 3286 N92-28890
MASSACHUSETTS UNIV., WORCESTER.
Non-linear analysis of visual cortical neurons
[AD-A250233] p 3326 N92-29179
MATERIALS RESEARCH LABS., ASCOT VALE (AUSTRALIA).
Ultrasonic ambient noise in Australian shallow waters at frequencies up to 200 kHz
[MRL-TR-91-23] p 3351 N92-28364
MAX-PLANCK-INST. FUER CHEMIE, MAINZ (GERMANY, F.R.).
The role of SO2 on Mars and on the primordial oxygen isotope composition of water on Earth and Mars p 3377 N92-28507
MCDONNELL-DOUGLAS CORP., LONG BEACH, CA.
Evaluation of outdoor-to-indoor response to minimized sonic booms
[NASA-CR-189643] p 3352 N92-28556
MCDONNELL-DOUGLAS HELICOPTER CO., MESA, AZ.
The application of flight simulation models in support of rotorcraft design and development p 3222 N92-28527
MCGILL UNIV., MONTREAL (QUEBEC).
Curvature estimation in orientation selection
[AD-A247862] p 3328 N92-28957
MEI ASSOCIATES, INC., LEXINGTON, MA.
Design specifications for the Advanced Instructional Design Advisor (AIDA), volume 1
[AD-A248201] p 3340 N92-29187
Design specifications for the Advanced Instructional Design Advisor (AIDA), volume 2
[AD-A248202] p 3340 N92-29188
MERIT TECHNOLOGY, INC., PLANO, TX.
Air combat maneuvering expert system trainer
[AD-A246459] p 3241 N92-28975
MESSERSCHMITT-BOELKOW-BLOHM G.M.B.H., MUNICH (GERMANY, F.R.).
Practical architecture of design optimisation software for aircraft structures taking the MBB-Lagrange code as an example p 3232 N92-28471
Mathematical optimization: A powerful tool for aircraft design p 3232 N92-28474
Experience with piloted simulation in the development of helicopters p 3222 N92-28526
MESSERSCHMITT-BOELKOW-BLOHM G.M.B.H., OTTOBRUNN (GERMANY, F.R.).
Development and evaluation of an attack and maneuvering system with combat development simulators as main development tool p 3224 N92-28541
MICHIGAN STATE UNIV., EAST LANSING.
Adaptive set-membership identification in 0(m) time for linear-in-parameters models
[AD-A249359] p 3273 N92-28358
MICHIGAN UNIV., ANN ARBOR.
Intense electron beam cyclotron masers with microsecond pulselengths
[AD-A247060] p 3289 N92-28271
Scattering and radiation analysis of three-dimensional cavity arrays via a hybrid finite element method
[NASA-CR-190408] p 3273 N92-28371
Mechanistic studies of superplasticity of structural ceramics
[AD-A246951] p 3263 N92-28558
High-performance integrated circuit evaluation system for a gallium arsenide microsupercomputer
[AD-A250385] p 3281 N92-28798
MICRO CIRCUIT ENGINEERING LTD., TEWKESBURY (ENGLAND).
Applications of silicon hybrid multi-chip modules to avionics p 3235 N92-28379
MIDWEST RESEARCH INST., GOLDEN, CO.
Thin film cadmium telluride photovoltaic cells
[DE92-001239] p 3306 N92-28277
MIDWEST RESEARCH INST., KANSAS CITY, MO.
Use of scrap rubber in asphalt pavement surfaces
[AD-A247419] p 3272 N92-28902
MINISTRY OF DEFENCE, LONDON (ENGLAND).
Harrier GR MK 5/7 mission simulators for the Royal Air Force p 3224 N92-28540
MINNESOTA UNIV., MINNEAPOLIS.
The early Martian atmosphere p 3376 N92-28502
Evidence for a high temperature differentiation in a molten earth: A preliminary appraisal p 3312 N92-28603
Global minimum solution of engineering design problems
[AD-A247496] p 3337 N92-28704
Simulations of solvent effects on confined electrolytes
[AD-A246851] p 3258 N92-28982
Substrate induced ordering of molecular adsorbates on Au(111)
[AD-A246850] p 3258 N92-29185
Psychophysical analyses of perceptual representations
[AD-A246945] p 3329 N92-29186
MISSISSIPPI STATE UNIV., MISSISSIPPI STATE.
Computation of steady and unsteady quasi-one-dimensional viscous/inviscid interacting internal flows at subsonic, transonic, and supersonic Mach numbers
[NASA-CR-189881] p 3283 N92-28555
MITRE CORP., BEDFORD, MA.
An OTH radar clutter simulation
[AD-A248054] p 3272 N92-28304
Diagnostic reasoning within sequential circuits, volume 1
[AD-A248055] p 3278 N92-28305
MSNW, INC., SAN MARCOS, CA.
Chemical vapor synthesis of niobium aluminides
[AD-A250332] p 3258 N92-29091

N

NAGOYA UNIV. (JAPAN).
Thermal evolution and chemical differentiation of the terrestrial magma ocean p 3310 N92-28588
NATIONAAL INST. VOOR KERNFYSICA EN HOGE ENERGIEFYSICA, AMSTERDAM (NETHERLANDS).
Delayed pulse generator
[DIGEL-1991-2] p 3278 N92-28262
High voltage splitting unit for the power supplies of the vacuum pumps of AmPS
[DIGEL-1991-7] p 3278 N92-28263
Bundle dimensions around the internal target area
[NIKHEF-K/AMPS/91-06] p 3356 N92-28264
Injection: On-axis/off-axis
[NIKHEF-K/AMPS/91-07] p 3356 N92-28308
NATIONAL ACADEMY OF PUBLIC ADMINISTRATION, WASHINGTON, DC.
Maintaining the program balance, volumes 1 and 2
[NASA-CR-190269] p 3367 N92-29111
NATIONAL ACADEMY OF SCIENCES - NATIONAL RESEARCH COUNCIL, WASHINGTON, DC.
Responsible science: Ensuring the integrity of the research process, volume 1
[ISBN-0-309-04731-5] p 3350 N92-28363
National Conference on the Use of Composite Materials in Load-Bearing Marine Structures. Volume 1: Summary report
[PB92-163831] p 3252 N92-28724
National Conference on the Use of Composite Materials in Load-Bearing Marine Structures. Volume 2: Conference proceedings
[PB92-163849] p 3252 N92-28725
NATIONAL AERONAUTICS AND SPACE ADMINISTRATION, WASHINGTON, DC.
NASA engineers and the age of Apollo
[NASA-SP-4104] p 3397 N92-28344
Planetary geosciences, 1989-1990
[NASA-SP-508] p 3372 N92-28345
Space Station Freedom microgravity environment requirements and assessment methods p 3268 N92-28450
Aeronautical engineering: A continuing bibliography with indexes (supplement 278)
[NASA-SP-7037(278)] p 3226 N92-28677
Space flight: The first 30 years
[NASA-NP-150] p 3397 N92-28678
Aeronautical engineering: A continuing bibliography with indexes (supplement 275)
[NASA-SP-7037(275)] p 3226 N92-28679
NATIONAL AERONAUTICS AND SPACE ADMINISTRATION. AMES RESEARCH CENTER, MOFFETT FIELD, CA.
Thermoregulation during spaceflight
[NASA-TM-103913] p 3325 N92-28420
Comparison of three controllers applied to helicopter vibration
[NASA-TM-102192] p 3239 N92-28457
High pressure experiments with a Mars general circulation model p 3374 N92-28491
Liquid water habitats on early Mars p 3376 N92-28500
Astronomical variation experiments with a Mars general circulation model p 3376 N92-28503
How Mars lost its atmosphere p 3378 N92-28509
Spectral identification of chemisorbed CO2 and application to Mars analog materials p 3378 N92-28510
A discrete Fourier transform for virtual memory machines
[NASA-TM-103914] p 3349 N92-28672
Thermal response of rigid and flexible insulations and reflective coating in an aeroconvective heating environment
[NASA-TM-103925] p 3233 N92-28721
High quality Gaussian basis sets for fourth-row atoms
[NASA-TM-103918] p 3255 N92-28743
Crew station research and development facility training for the light helicopter demonstration/validation program
[NASA-TM-103865] p 3327 N92-28744
MoCog1: A computer simulation of recognition-primed human decision making, considering emotions
[NASA-TM-107859] p 3337 N92-28758
Learning and tuning fuzzy logic controllers through reinforcements
[NASA-TM-107875] p 3345 N92-28759
The design of test-section inserts for higher speed aeroacoustic testing in the Ames 80- by 120-foot wind tunnel
[NASA-TM-103915] p 3353 N92-28909
Binary optical filters for scale invariant pattern recognition
[NASA-TM-103902] p 3234 N92-28910
Rotorcraft In-Flight Simulation Research at NASA Ames Research Center: A Review of the 1980's and plans for the 1990's
[NASA-TM-103873] p 3224 N92-28926
The nanophase iron mineral(s) in Mars soil p 3379 N92-28990
Simulations of surface winds at the Viking Lander sites using a one-level model p 3380 N92-28998
Mars Environmental Survey (MESUR): Science objectives and mission description p 3385 N92-29025
Was early Mars warmed by ammonia? p 3386 N92-29030
Nonlinear stratified flow over localized topographic obstacles on Mars p 3387 N92-29036
Mars dust storm simulations: Analysis of surface stress p 3389 N92-29045
Short- and long-term climate changes on Mars p 3389 N92-29051
Climatic implications of the simultaneous presence of CO2 and H2O in the Martian regolith p 3395 N92-29079
A rotorcraft flight database for validation of vision-based ranging algorithms
[NASA-TM-103906] p 3231 N92-29103
Performance of uncoated AFRSI blankets during multiple Space Shuttle flights
[NASA-TM-103892] p 3245 N92-29104
Acquisition and improvement of human motor skills: Learning through observation and practice
[NASA-TM-107878] p 3329 N92-29174
Building the Scientific Modeling Assistant: An interactive environment for specialized software design
[NASA-TM-107844] p 3346 N92-29175
NATIONAL AERONAUTICS AND SPACE ADMINISTRATION. GODDARD SPACE FLIGHT CENTER, GREENBELT, MD.
The Father Christmas worm
[NASA-TM-107938] p 3334 N92-28267
A fast direct solver for a class of two-dimensional separable elliptic equations on the sphere
[NASA-TM-104567] p 3346 N92-28297
Modeling radiation forces acting on TOPEX/Poseidon for precision orbit determination
[NASA-TM-104564] p 3244 N92-28343

Volcanic recycling of carbonate deposits on Mars
p 3377 N92-28506
Types and Characteristics of Data for Geomagnetic Field Modeling
[NASA-CP-3153] p 3299 N92-28620
Satellite data for geomagnetic field modeling
p 3300 N92-28624
Device for applying constant pressure to a surface
[NASA-CASE-GSC-13230-1] p 3294 N92-28754
Future mission studies: Preliminary comparisons of solar flux models
[NASA-TM-107947] p 3396 N92-28869
Nonlinear techniques for forecasting solar activity directly from its time series
[NASA-TM-107946] p 3396 N92-28870
Implications of early Hesperian ages for presumed Noachian age volcanic flows on Mars
p 3383 N92-29015
Volatile tracers of Martian atmospheric evolution: Present measurement status and requirements for future investigations p 3387 N92-29037
A carbonate-silicate aqueous geochemical cycle model for Mars p 3390 N92-29057
High temperature solder device for flat cables
[NASA-CASE-GSC-13344-1] p 3261 N92-29094
Superconducting bearings with levitation control configurations
[NASA-CASE-GSC-13346-1] p 3295 N92-29099
Coupling device with improved thermal interface
[NASA-CASE-GSC-13251-1] p 3295 N92-29120
Disk memory device
[NASA-CASE-GSC-13196-1] p 3333 N92-29132
Laser optical disk position encoder with active heads
[NASA-CASE-GSC-13175-1] p 3359 N92-29133
Rolling friction robot fingers
[NASA-CASE-GSC-13261-1] p 3296 N92-29138
Connection space reduction mechanism
[NASA-CASE-GSC-13220-1] p 3296 N92-29140
Cryogenic shutter
[NASA-CASE-GSC-13189-2] p 3296 N92-29151
User friendly joystick
[NASA-CASE-GSC-13187-1] p 3281 N92-29153
Method for advanced material characterization by laser induced eddy current imaging
[NASA-CASE-GSC-13386-1] p 3298 N92-29154

NATIONAL AERONAUTICS AND SPACE ADMINISTRATION. HUGH L. DRYDEN FLIGHT RESEARCH CENTER, EDWARDS, CA.

In-flight simulation studies at the NASA Dryden Flight Research Facility
[NASA-TM-4396] p 3234 N92-29110

NATIONAL AERONAUTICS AND SPACE ADMINISTRATION. LYNDON B. JOHNSON SPACE CENTER, HOUSTON, TX.

Shock and vibration isolation for cyclic exercise in spacecraft p 3267 N92-28449
Microgravity accelerometer characterization on Columbia STS-32 mission p 3271 N92-28452
Estimation of high temperature metal-silicate partition coefficients p 3311 N92-28599
Payload retention device
[NASA-CASE-MSC-21906-1] p 3294 N92-28727
Portable dynamic fundus instrument
[NASA-CASE-MSC-21675-1] p 3325 N92-28755
Water electrolysis
[NASA-CASE-MSC-21572-1-SB] p 3256 N92-28756
Experimental measurement of the orbital paths of particles sedimenting within a rotating viscous fluid as influenced by gravity
[NASA-TP-3200] p 3331 N92-28897
Evaluation of Whipple bumper shields at 7 and 10 km/s
[NASA-TM-107958] p 3295 N92-28925
Martian impact crater degradation studies: Implications for localized obliteration episodes p 3379 N92-28991
Mars surface weathering products and spectral analogs: Palagonites and synthetic iron minerals
p 3383 N92-29017
Distribution of water on Mars: Implications from SNC meteorites p 3386 N92-29027
A liquidus phase diagram for the groundmass of EETA 79001A (Eg), a primitive Shergottite composition
p 3386 N92-29028
Aqueous-alteration products in S-N-C meteorites and implications for volatile/regolith interactions on Mars
p 3393 N92-29071
Whole body cleaning agent containing N-acyltaurate
[NASA-CASE-MSC-21589-1] p 3332 N92-29137
Quick application/release nut with engagement indicator
[NASA-CASE-MSC-21799-1] p 3296 N92-29150

NATIONAL AERONAUTICS AND SPACE ADMINISTRATION. LANGLEY RESEARCH CENTER, HAMPTON, VA.

An analysis of combustion studies in shock expansion tunnels and reflected shock tunnels
[NASA-TP-3224] p 3255 N92-28374
Software design for automated assembly of truss structures
[NASA-TP-3198] p 3344 N92-28375
Integrating aerodynamics and structures in the minimum weight design of a supersonic transport wing
[NASA-TM-107586] p 3231 N92-28435
Multidisciplinary design and optimization
[AGARD-PAPER-2] p 3232 N92-28473
Calculation of unsteady transonic flows with mild separation by viscous-inviscid interaction
[NASA-TP-3197] p 3226 N92-28477
Application of piloted simulation to high-angle-of-attack flight-dynamics research for fighter aircraft
p 3225 N92-28551
Natural flow wing
[NASA-CASE-LAR-14281-1] p 3228 N92-28729
Ongoing Progress in Spacecraft Controls
[NASA-CP-10099] p 3247 N92-28730
Sensor filter designs for large flexible spacecraft
p 3247 N92-28733
Fuel optimal propulsive reboost of flexible spacecraft
p 3247 N92-28734
Fuel optimal maneuver: Experimental testbeds
p 3247 N92-28735
Polyimidazoles via aromatic nucleophilic displacement
[NASA-CASE-LAR-14145-1] p 3264 N92-28751
Heat exchanger with oscillating flow
[NASA-CASE-LAR-14033-1] p 3284 N92-28752
Method and apparatus for using magneto-acoustic remanence to determine embrittlement
[NASA-CASE-LAR-13817-5] p 3303 N92-28757
Phase stability of injection-locked beam of semiconductor lasers
[NASA-TT-10001] p 3290 N92-28862
Windshear radar calibration: Transmitter power and receiver gain stability
[NASA-TM-107589] p 3275 N92-28876
Pressure transducer and system for cryogenic environments
[NASA-CASE-LAR-14579-1] p 3288 N92-29097
Magnetic remanence method and apparatus to test materials for embrittlement
[NASA-CASE-LAR-13817-4] p 3304 N92-29101
Non-mechanical optical path switching and its application to dual beam spectroscopy including gas filter correlation radiometry
[NASA-CASE-LAR-14588-1-CU] p 3359 N92-29117
Poly(1,3,4-oxadiazoles) via aromatic nucleophilic displacement
[NASA-CASE-LAR-14427-1] p 3250 N92-29141
Magneto acoustic emission method for testing materials for embrittlement
[NASA-CASE-LAR-13817-2] p 3304 N92-29155
Polyimide processing additives
[NASA-CASE-LAR-13669-1] p 3265 N92-29157
Single layer multi-color luminescent display and method of making
[NASA-CASE-LAR-13616-3] p 3359 N92-29158

NATIONAL AERONAUTICS AND SPACE ADMINISTRATION. LEWIS RESEARCH CENTER, CLEVELAND, OH.

An overview of in-flight plume diagnostics for rocket engines
[NASA-TM-105727] p 3248 N92-28417
Internal reversing flow in a tailpipe offtake configuration for SSTOVL aircraft
[NASA-TM-105698] p 3236 N92-28418
Full Navier-Stokes analysis of a two-dimensional mixer/ejector nozzle for noise suppression
[NASA-TM-105715] p 3236 N92-28419
Neutron, gamma ray, and temperature effects on the electrical characteristics of thyristors
[NASA-TM-105728] p 3279 N92-28432
Hydrogen no-vent fill testing in a 5 cubic foot (142 liter) tank using spray nozzle and spray bar liquid injection
[NASA-TM-105759] p 3266 N92-28433
Application of face-gear drives in helicopter transmissions
[NASA-TM-105655] p 3293 N92-28434
International Workshop on Vibration Isolation Technology for Microgravity Science Applications
[NASA-CP-10094] p 3268 N92-28436
An examination of anticipated g-jitter on Space Station and its effects on materials processes
p 3267 N92-28438
Vibration isolation technology development to demonstration p 3267 N92-28442
Early mission science support: Space Acceleration Measurement System (SAMS) p 3248 N92-28451
Rocket plume flowfield characterization using laser Rayleigh scattering
[NASA-TM-105739] p 3357 N92-28475
Optimum design of a gearbox for low vibration
[NASA-TM-105653] p 3293 N92-28476
Monolithic mm-wave phase shifter using optically activated superconducting switches
[NASA-CASE-LEW-14878-1] p 3358 N92-28571
Flow quality studies of the NASA Lewis Research Center 8- by 6-foot supersonic/9- by 15-foot low speed wind tunnel
[NASA-TM-105417] p 3240 N92-28673
Experimental and computational ice shapes and resulting drag increase for a NACA 0012 airfoil
[NASA-TM-105743] p 3227 N92-28674
High temperature dielectric properties of Apical, Kapton, Peek, Teflon AF, and Upilex polymers
[NASA-TM-105753] p 3280 N92-28675
NASA Lewis steady-state heat pipe code users manual
[NASA-TM-105161] p 3249 N92-28682
Solar Array Module Plasma Interaction Experiment (SAMPIE): Technical requirements document
[NASA-TM-105660] p 3246 N92-28683
PC graphics generation and management tool for real-time applications
[NASA-TM-105749] p 3337 N92-28684
Integrated health monitoring and controls for rocket engines
[NASA-TM-105763] p 3249 N92-28693
Results of a low power ice protection system test and a new method of imaging data analysis
[NASA-TM-105745] p 3227 N92-28696
Elevated temperature axial and torsional fatigue behavior of Haynes 188
[NASA-TM-105396] p 3302 N92-28701
NASA Lewis Stirling SPRE testing and analysis with reduced number of cooler tubes
[NASA-TM-105787] p 3307 N92-28837
Laser anemometer measurements and computations in an annular cascade of high turning core turbine vanes
[NASA-TP-3252] p 3229 N92-28980
Development and flight history of SERT 2 spacecraft
[NASA-TM-105636] p 3250 N92-28983
Modal element method for scattering of sound by absorbing bodies
[NASA-TM-105722] p 3353 N92-28984
Electromechanical systems with transient high power response operating from a resonant AC link
[NASA-TM-105716] p 3238 N92-28985
Oxidation resistant coating for titanium alloys and titanium alloy matrix composites
[NASA-CASE-LEW-15155-1] p 3265 N92-29090
Removable hand hold
[NASA-CASE-LEW-15196-1] p 3295 N92-29092
A 4-spot time-of-flight anemometer for small centrifugal compressor velocity measurements
[NASA-TM-105717] p 3288 N92-29105
Pulse thermal energy transport/storage system
[NASA-CASE-LEW-15235-1] p 3287 N92-29125
Dynamics of a split torque helicopter transmission
[NASA-TM-105681] p 3296 N92-29136
Solar thermal energy receiver
[NASA-CASE-LEW-14949-1] p 3307 N92-29143
Method of intercalating large quantities of fibrous structures
[NASA-CASE-LEW-15077-1] p 3253 N92-29152

NATIONAL AERONAUTICS AND SPACE ADMINISTRATION. MARSHALL SPACE FLIGHT CENTER, HUNTSVILLE, AL.

Payload isolation and stabilization by a Suspended Experiment Mount (SEM)
[NASA-TM-107941] p 3246 N92-28369
Science and application payloads in the 1990's
[NASA-TM-107937] p 3246 N92-28370
ACAP: Acceleration Characterization and Analysis Project p 3267 N92-28448
Taguchi methods in electronics: A case study
[NASA-TM-103586] p 3279 N92-28456
Mars global reference atmosphere model (Mars-GRAM) p 3375 N92-28494
Anthropomorphic teleoperation: Controlling remote manipulators with the DataGlove
[NASA-TM-103588] p 3330 N92-28521
Controlled method of reducing electrophoretic mobility of macromolecules, particles, or cells
[NASA-CASE-MFS-26049-2-NP] p 3255 N92-28728
Closed-loop autonomous docking system
[NASA-CASE-MFS-28421-1] p 3248 N92-28750
Second National Space Grant Conference report, 1991
[NASA-EP-278] p 3366 N92-28864

Functional requirements document for the Earth Observing System Data and Information System (EOSDIS) Scientific Computing Facilities (SCF) of the NASA/MSFC Earth Science and Applications Division, 1992
[NASA-TM-4392] p 3333 N92-28899
A generalized reusable guidance algorithm for optimal aerobraking
[NASA-TM-103590] p 3229 N92-28981
The effect of induced charges on low-energy particle trajectories near conducting and semiconducting plates
[NASA-TM-103589] p 3355 N92-28986
Water window imaging x ray microscope
[NASA-CASE-MFS-28485-1] p 3288 N92-29135

NATIONAL AERONAUTICS AND SPACE ADMINISTRATION. PASADENA OFFICE, CA.
Secondary Li battery incorporating 12-Crown-4 ether
[NASA-CASE-NPO-17922-1-CU] p 3280 N92-28753
Method and apparatus for phasing segmented mirror arrays
[NASA-CASE-NPO-18095-1-CU] p 3359 N92-29122
Method and apparatus for frequency spectrum analysis
[NASA-CASE-NPO-17759-1-CU] p 3276 N92-29124
Method and apparatus for predicting the direction of movement in machine vision
[NASA-CASE-NPO-17552-1-CU] p 3331 N92-29129
Precision measurement of magnetic characteristics of an article with nullification of external magnetic fields
[NASA-CASE-NPO-18187-1-CU] p 3351 N92-29130
Microwave temperature profiler for clear air turbulence prediction
[NASA-CASE-NPO-18115-1-CU] p 3320 N92-29148
Ultra-high temperature stability Joule-Thomson cooler with capability to accomodate pressure variations
[NASA-CASE-NPO-18184-1-CU] p 3288 N92-29156

NATIONAL AEROSPACE LAB., AMSTERDAM (NETHERLANDS).
Aircraft simulation and pilot proficiency: From surrogate flying towards effective training p 3222 N92-28532
Improvement of separations of practice bombs from a multiple bomb adapter
[NLR-TP-90307-U] p 3232 N92-28634
Hyperbolic grid generation with BEM source terms
[NLR-TP-90334-U] p 3347 N92-28635
Software development using a method base system
[NLR-TP-90387-U] p 3336 N92-28636
Simple computer programs for the design and sizing of fiber reinforced composites
[NLR-TP-91050-U] p 3252 N92-28637
Spacecraft sustained load fracture control
[NLR-TP-89163-U] p 3302 N92-28643
A simple and low cost system to measure delay times in pneumatic systems
[NLR-TP-90174-U] p 3235 N92-28644
Dynamics motion simulation of the Hermes robot arm subjected to constraints
[NLR-TP-90282-U] p 3293 N92-28645
Linear recursive formulation of flexible multi-body space system dynamics
[NLR-TP-90284-U] p 3293 N92-28646
Quasi-recursive dynamics equations for spacecraft-based flexible robotic manipulators
[NLR-TP-90028-U] p 3345 N92-28648
The use of load enhancement factors in the certification of composite aircraft structures
[NLR-TP-90068-U] p 3232 N92-28649
Correlation, error-localisation, and updating of the second problem defined in GARTEUR AG11
[NLR-TP-90070-U] p 3302 N92-28650
Modifications and results of flight tests of a practice bomb adapter
[NLR-TP-90108-U] p 3233 N92-28651
Some longitudinal handling qualities design guidelines for active control technology transport aircraft
[NLR-TP-90129-U] p 3239 N92-28652
Response of helicopters to gusts
[NLR-TP-90159-U] p 3239 N92-28653
Potential applications of laser Doppler anemometry for in-flight measurements
[NLR-TP-90163-U] p 3236 N92-28654
Application of knowledge-based systems for diagnosis of aircraft systems
[NLR-TP-90192-U] p 3230 N92-28655
Telescience experiments using the Prototype Optical Diagnostic Instrument (PODI)
[NLR-TP-90199-U] p 3358 N92-28656
Analysis of results of an Euler-equation method applied to leading-edge vortex flow
[NLR-TP-90368-U] p 3226 N92-28657
Comparison of LDA and LTA applications for propeller tests in wind tunnels
[NLR-MP-88031-U] p 3226 N92-28658
Calculation of unsteady subsonic and supersonic flow about oscillating wings and bodies by new panel methods
[NLR-TP-89119-U] p 3227 N92-28659
Constrained spanload optimization for minimum drag of multi-lifting-surface configurations
[NLR-TP-89126-U] p 3227 N92-28660
The windtunnel as a tool for laminar flow research
[NLR-TP-90145-U] p 3240 N92-28661
Instrumentation requirements for laminar flow research in the NLR high speed wind tunnel HST
[NLR-TP-89158-U] p 3240 N92-28669
LAH-main rotor model test at the DNW
[NLR-TP-90305-U] p 3233 N92-28687
Modal analysis of plates using boundary integral equations
[NLR-TP-89211-U] p 3302 N92-28688
Atmospheric turbulence spectra and correlation functions
[NLR-TP-89217-U] p 3316 N92-28689
Multitemporal analysis of a braiding river
[NLR-TP-89235-U] p 3305 N92-28690
Effect of cooling rate on corrosion properties of high strength aluminium alloys under atmospheric conditions
[NLR-TP-90138-U] p 3260 N92-28691
Development and validation of a characteristic boundary condition for a cell-centered Euler method
[NLR-TP-90144-U] p 3227 N92-28692
Turbulence modeling: Survey of activities in Belgium and the Netherlands, and appraisal of the status and a view on the prospects
[NLR-TP-90184-U] p 3264 N92-28694
Experimental validation of a line-duct acoustics model including flow
[NLR-TP-90223-U] p 3352 N92-28695
Transputer-based embedded system for Meteosat image data compression
[NLR-TP-90228-U] p 3305 N92-28697
Modelling and real-time simulation of the Hermes robot arm HERA
[NLR-TP-90262-U] p 3294 N92-28705
Superconducting at NLR: NEC SX-2 capabilities in NLR's terminal and file-transfer network
[NLR-TP-89007-U] p 3342 N92-28706
Quantitative updating of land use information on 1:50,000 scale topographic maps using SPOT LANDSAT Thematic Mapper imagery
[NLR-TP-89061-U] p 3305 N92-28708
Wave drag determination in the transonic full-potential flow code MATRICS
[NLR-TP-90062-U] p 3228 N92-28709
Diffuser casing upgrade for an advanced turbofan
[NLR-TP-90097-U] p 3238 N92-28711
Boundary conditions for Euler equations at internal block faces of multi-block domains using local grid refinement
[NLR-TP-90134-U] p 3264 N92-28712
Flow gradient corrections on hot-wire measurements using an X-wire probe
[NLR-TP-90255-U] p 3228 N92-28713
S-76B certification for vertical take-off and landing operations from confined areas
[NLR-TP-90286-U] p 3233 N92-28714
What is on the machine's mind? Models for reasoning with incomplete and uncertain knowledge
[NLR-TP-91099-U] p 3345 N92-28716
Outdoor corrosion testing of aluminium-lithium alloys
[NLR-TP-90272-U] p 3260 N92-28794
Crack resistance, fracture toughness and instability in damage tolerant Al-Li alloys
[NLR-TP-90172-U] p 3303 N92-28850
NARSIM: A real-time simulator for air traffic control research
[NLR-TP-90147-U] p 3241 N92-29204

NATIONAL AEROSPACE LAB., EMMELOORD (NETHERLANDS).
Exploratory flexural power flow measurements on a bar
[NLR-TP-90178-U] p 3304 N92-29176

NATIONAL AEROSPACE LAB., TOKYO (JAPAN).
Air ejector experiments using the two-dimensional supersonic cascade tunnel: Zero secondary flow performance
[NAL-TM-632] p 3241 N92-28829
The second flight simulator test of the head-up display for NAL QSTOL experimental aircraft (ASKA)
[NAL-TM-633] p 3331 N92-28831
Upgrading the data processing section of the NAL Gust Wind Tunnel data processing system
[NAL-TM-635] p 3241 N92-28833
Replacement of the NAL high pressure air storage system
[NAL-TM-634] p 3241 N92-28835
Quaternion and Euler angles in kinematics
[NAL-TM-636] p 3303 N92-28836
Aerodynamic characteristics obtained from alpha sweep test of the quiet STOL experimental aircraft ASKA
[NAL-TR-1112] p 3234 N92-28901

NATIONAL AIR AND SPACE MUSEUM, WASHINGTON, DC.
Nature and evolution of the early Martian atmosphere: Evidence from highland crater populations p 3373 N92-28485

NATIONAL ENVIRONMENTAL RESEARCH COUNCIL, EDINBURGH (SCOTLAND).
Survey data for geomagnetic field modelling p 3300 N92-28623

NATIONAL GEOPHYSICAL DATA CENTER, BOULDER, CO.
Marine magnetic data holdings of World Data Center-A for Marine Geology and Geophysics p 3300 N92-28625

NATIONAL INST. FOR FUSION SCIENCE, NAGOYA (JAPAN).
Development of negative heavy ion sources for plasma potential measurement
[DE92-782102] p 3360 N92-28234

NATIONAL INST. OF STANDARDS AND TECHNOLOGY, GAITHERSBURG, MD.
Wavenumber calibration tables from heterodyne frequency measurements
[NASA-CR-190422] p 3276 N92-29115

NATIONAL PHYSICAL LAB., TEDDINGTON (ENGLAND).
The measuring assembly for the NPL primary standard absorbed dose graphite calorimeter at therapy levels
[NPL-RSA(EXT)-23] p 3288 N92-29163
Some experiments to determine the efficiency of collection of alumina particles by electron beam button melting in a nickel-base superalloy, AP1
[NPL-DMM(A)-42] p 3261 N92-29164

NATIONAL SCIENCE FOUNDATION, WASHINGTON, DC.
Joint DOE/NSF workshop on flow of particulates and fluids
[DE92-012692] p 3285 N92-28808

NATIONAL SPACE DEVELOPMENT AGENCY, TOKYO (JAPAN).
NASDA's activities on vibration isolation technology p 3267 N92-28441

NAVAL AEROSPACE MEDICAL RESEARCH LAB., PENSACOLA, FL.
Use of a commercially available flight simulator during aircrew performance testing
[AD-A245922] p 3240 N92-28407
Delays in laser glare onset differentially affect target-location performance in a visual search task
[AD-A246706] p 3327 N92-28557

NAVAL AIR DEVELOPMENT CENTER, WARMINSTER, PA.
Fundamental noise limits in miniature acoustic and vibration sensors
[AD-A247016] p 3352 N92-28413
Tensile and interlaminar properties of GLARE (trade name) laminates
[AD-A250188] p 3253 N92-28921

NAVAL AIR TEST CENTER, PATUXENT RIVER, MD.
Use of high-fidelity simulation in the development of an F/A-18 active ground collision avoidance system p 3222 N92-28530
Shipboard mission training effectiveness of the Naval Air Test Center's V-22 government test pilot trainer p 3224 N92-28542

NAVAL CIVIL ENGINEERING LAB., PORT HUENEME, CA.
Paint removal using cryogenic processes
[AD-A247668] p 3264 N92-28912

NAVAL HEALTH RESEARCH CENTER, SAN DIEGO, CA.
Computer assisted improvement of the estimation mean squared error with application to back propagation neural networks
[AD-A247724] p 3344 N92-28401
Lapses in alertness: Brain-evoked responses to task-irrelevant auditory probes
[AD-A247669] p 3328 N92-28940

NAVAL OCEAN SYSTEMS CENTER, SAN DIEGO, CA.
Extensibility experiments with the software life-cycle support environment
[AD-A247696] p 3335 N92-28562
Null shifting with fixed delays
[AD-A250059] p 3274 N92-28796
Studies of iterated transform image compression and its application to color and DTED
[AD-A248060] p 3339 N92-28946
Analysis of electromagnetic propagation over variable terrain using the parabolic wave equation
[AD-A248061] p 3276 N92-28947
The 2.0 GHz sampling rate transversal filter
[AD-A250244] p 3358 N92-28968

NAVAL OCEANOGRAPHIC AND ATMOSPHERIC RESEARCH LAB., BAY SAINT LOUIS, MS.
A new ocean bottom magnetometer system for continental shelf measurements
[AD-A247644] p 3321 N92-28321

Under-ice broadband transient measurements and processing
[AD-A248609] p 3351 N92-28324
A coupled regional tide model
[AD-A247917] p 3322 N92-28913
Neural network parameter estimation for the modified bistatic scattering strength model (BISSM)
[AD-A247913] p 3322 N92-28963
Bioluminescence in the western Alboran Sea in April 1991
[AD-A250016] p 3324 N92-29089
Impact on the medium MTF by model estimation of beta
[AD-A247985] p 3359 N92-29167

NAVAL OCEANOGRAPHIC AND ATMOSPHERIC RESEARCH LAB., MONTEREY, CA.
Evaluation of simple mesoscale models for use in TESS
[AD-A247914] p 3316 N92-28964
Segmentation of satellite imagery using hierarchical thresholding and neural networks
[AD-A247915] p 3319 N92-28965
A probabilistic neural network approach to cloud classification
[AD-A247916] p 3319 N92-28966

NAVAL OCEANOGRAPHIC OFFICE, BAY SAINT LOUIS, MS.
Project MAGNET high-level vector survey data reduction p 3301 N92-28628

NAVAL POSTGRADUATE SCHOOL, MONTEREY, CA.
Object-oriented programming: An assessment of fundamental concepts and design considerations
[AD-A247480] p 3333 N92-28243
Conversion and retrievability of hard copy and digital documents on optical disks
[AD-A247481] p 3367 N92-28244
NPSNET: Flight simulation dynamic modeling using quaternions
[AD-A247484] p 3333 N92-28245
The instrumentation of a parallel, distributed database operation, retrieve-common, for merging two large sets of records
[AD-A247486] p 3367 N92-28246
A diagnostic study of the velocity structure of a meandering jet in the California current system using a primitive equation model
[AD-A246039] p 3320 N92-28283
Weld pool flow visualization studies during gas tungsten arc welding of steel and aluminum
[AD-A249204] p 3292 N92-28293
The testing, analysis, and correction of the update operation of a parallel, multi-backend database supercomputer
[AD-A248320] p 3341 N92-28306
Optical effects on ocean mixed layer dynamics
[AD-A245941] p 3320 N92-28316
Accuracy of shipborne kinematic GPS surveying
[AD-A245942] p 3230 N92-28317
An evaluation of the naval oceanic vertical aerosol model during Key90
[AD-A245943] p 3320 N92-28318
An analysis of middle ultraviolet dayglow spectra
[AD-A245965] p 3309 N92-28319
The use of conformal subdomain basis functions in the method of moments computations for a thin wire
[AD-A245964] p 3272 N92-28347
Multiple-valued programmable logic array minimization by simulated annealing
[AD-A248620] p 3335 N92-28353
Comparison of electromagnetic propagation predictions from IREPS and RPO across a coastal transition
[AD-A249331] p 3273 N92-28357
A numerical study of time-dependent wind forcing off the west coast of Portugal, 1987-1988
[AD-A246775] p 3321 N92-28365
Prediction of attitude stability of asymmetric dual-spin stabilized spacecraft using improved liquid slosh model
[AD-A247023] p 3246 N92-28368
Investigation of an equivalent circuit for the inductive strip in finline with dielectric
[AD-A247025] p 3279 N92-28373
Arcjet plume ionization effects on exposed solar array conducting surfaces
[AD-A245912] p 3307 N92-28383
Visualization of gas tungsten arc weld pools
[AD-A245926] p 3293 N92-28384
An experimental investigation of the effects of software size increase on software project management behavior
[AD-A248362] p 3335 N92-28385
Trade study of three oxygen processors for the Martian atmosphere
[AD-A246854] p 3372 N92-28393
A profile of scientist and engineer training conducted by the Naval Avionics Center
[AD-A245925] p 3326 N92-28408
Adaptive noise cancellation applied to the NUWES test ranges
[AD-A245961] p 3352 N92-28409
Design on an enhanced interactive satellite communications system analysis program
[AD-A245967] p 3273 N92-28410
Mesoscale vertical structure of an explosive oceanic cyclone
[AD-A245927] p 3318 N92-28423
Simulation of atmospheric frontogenesis with a semi-Lagrangian numerical model
[AD-A247151] p 3318 N92-28517
Correlational analysis of survey and model-generated workload values
[AD-A247153] p 3329 N92-28518
Calculation of chip temperatures using ELLPACK
[AD-A247156] p 3335 N92-28519
Image processing techniques for acoustic images
[AD-A247303] p 3352 N92-28559
Theory for the CEBAF and shipboard FELS
[AD-A245979] p 3289 N92-28662
Applications of passive microwave satellite data for Arctic Sea ice studies
[AD-A245966] p 3306 N92-28791
A self-affine multi-fractal wave/turbulence discrimination method using data from single point fast response sensors in a nocturnal atmospheric boundary layer
[AD-A250419] p 3318 N92-28799
Stability and control flight testing of a half-scale Pioneer remotely piloted vehicle
[AD-A245973] p 3239 N92-28801
Tasking and communication flows in the F/A-18D cockpit: Issues, problems, and possible solutions
[AD-A245977] p 3234 N92-28802
Flow visualization studies of a sideslipping, canard-configured X-31A-Like fighter aircraft model
[AD-A245940] p 3228 N92-28883
Mesoscale surface analysis of the ERICA IOP-5 cyclone
[AD-A245946] p 3319 N92-28884
Effect of alumina particle additions on the aging kinetics of 2014-aluminum matrix composites
[AD-A245949] p 3252 N92-28898
SPEEDS: An approach to support programming environments using expert database systems
[AD-A247469] p 3339 N92-28943
The effects of thermomechanical processing parameters on elevated-temperature behavior of a 6061 Al-Al2O3 metal matrix composite
[AD-A247889] p 3253 N92-28959
Analysis of multimedia information systems for the US Coast Guard
[AD-A247890] p 3369 N92-28960
Phase transformations in Ti3Al based alloy
[AD-A246464] p 3261 N92-28976
Modeling pulse transmission in the Monterey Bay using parabolic equation methods
[AD-A246465] p 3322 N92-28977
Technological enhancements for personal computers
[AD-A247962] p 3333 N92-29083
Effects of fading and data modulation on noncoherent M-sequence acquisition schemes
[AD-A247968] p 3276 N92-29084
Method of moments analysis of displaced-axis dual reflector antennas
[AD-A247970] p 3277 N92-29166

NAVAL RESEARCH LAB., ORLANDO, FL.
Analysis of constrained-layer damping of flexural and extensional waves in infinite, fluid-loaded plates
[AD-A247936] p 3304 N92-29081

NAVAL RESEARCH LAB., WASHINGTON, DC.
A generalization of the K-V equilibrium for an intense, relativistic beam propagating in a solenoid
[AD-A247067] p 3350 N92-28238
Secondary instability in 3D magnetic reconnection
[AD-A248630] p 3360 N92-28354
Angular momentum: Can be used in ballistic tracking
[AD-A247722] p 3350 N92-28400
Computations of detonation structure: The influence of model input parameters
[AD-A248634] p 3285 N92-28803
Atomistic simulation of the nanoindentation of diamond and graphite surfaces
[AD-A249296] p 3355 N92-28881
A survey of high density packaging for high performance computing system
[AD-A248633] p 3332 N92-28891
Nanoscale investigation of indentation, adhesion, and fracture of diamond (111) surfaces
[AD-A250164] p 3265 N92-28916
Energetics of nanoscale graphitic tubules
[AD-A250165] p 3252 N92-28917
Electronic structure of fullerene tubules
[AD-A250166] p 3253 N92-28918
Experimental determination of dissipated energy density as a measure of strain-induced damage in composites
[AD-A250322] p 3253 N92-28953

NAVAL SURFACE WARFARE CENTER, DAHLGREN, VA.
Information strategy plan
[AD-A247740] p 3367 N92-28403

NAVAL SURFACE WARFARE CENTER, SILVER SPRING, MD.
Limiting factors to advancing thermal battery technology for naval applications
[AD-A247773] p 3280 N92-28568

NAVAL TRAINING SYSTEMS CENTER, ORLANDO, FL.
An analysis of aircrew communication patterns and content
[AD-A246618] p 3272 N92-28253

NETHERLANDS AEROSPACE MEDICAL CENTRE, SOESTERBERG.
G-tolerance and spatial disorientation: Can simulation help us? p 3223 N92-28534

NEW MEXICO UNIV., ALBUQUERQUE.
Pressure regimes and core formation in the accreting earth p 3313 N92-28605
Natural circulation decay heat removal from an SP-100, 550 kWe power system for a lunar outpost
[NASA-CR-190421] p 3307 N92-28863

NICHOLS RESEARCH CORP., HUNTSVILLE, AL.
Development of an automated wire delivery system for robotic welding applications
[NASA-CR-190487] p 3295 N92-29134

NIPPON ELECTRIC CO. LTD., TOKYO (JAPAN).
NASDA's activities on vibration isolation technology p 3267 N92-28441

NORTH CAROLINA STATE UNIV., RALEIGH.
Review of Mars mission scenarios p 3244 N92-28731
Stability and optimal control theory of hereditary systems with applications from oscillating flying vehicles, mechanical systems, and robotics p 3247 N92-28732
Initial investigations of an adaptive discrete-time controller for nonlinear time-varying robotic models p 3247 N92-28736
Identification of linear system models and state estimators for controls p 3247 N92-28737
Fuzzy logic controller for manipulator systems: Preliminary results p 3247 N92-28738

NORTH CAROLINA UNIV., CHAPEL HILL.
Synthesis and characterization of new low-dimensional transition metal complex conductors
[AD-A249263] p 3258 N92-28237
Structure energetics and dynamics of Gulf Stream variability
[AD-A248246] p 3323 N92-29225

NORTHEAST ARTIFICIAL INTELLIGENCE CONSORTIUM, ARECIBO (PUERTO RICO).
Mars: Wavelength-dependent dual polarization global scattering p 3384 N92-29020

NORTHEAST SEMICONDUCTOR, INC., ITHACA, NY.
Strained AlGaInAs semiconducting material for improved laser performance
[AD-A249379] p 3289 N92-28330
Innovative techniques for the production of low cost 2D laser diode arrays
[AD-A248247] p 3292 N92-29226

NORTHWESTERN UNIV., EVANSTON, IL.
Micromechanics of defects
[AD-A248432] p 3251 N92-28307

NORWEGIAN DEFENCE RESEARCH ESTABLISHMENT, KJELLER.
CESAR address generator
[FFI-91/7021] p 3334 N92-28265
A domain decomposition method for ocean/bottom interaction problems
[FFI-91/7022] p 3320 N92-28266
Simulation of the propagation of acoustical waves through an interface separating a compressible fluid and an elastic medium
[FFI-91/7017] p 3351 N92-28314
A diode laser pumped Nd:YAG laser
[FFI-91/7020] p 3289 N92-28315
On some splitting schemes for wave equations
[FFI-91/7023] p 3348 N92-29193

O

OAK RIDGE NATIONAL LAB., TN.
HeNCE: Graphical development tools for network-based concurrent computing
[DE92-011061] p 3341 N92-29279
Primer on molecular genetics
[DE92-010680] p 3324 N92-28382
Representation of neutron noise data using neural networks
[DE92-013232] p 3356 N92-28813

Assessment of valve actuator motor rotor degradation by Fourier Analysis of current waveform
[DE92-013233] p 3281 N92-28814
Compositional disorder, magnetism, and their interplay in metallic alloys
[DE92-011671] p 3260 N92-28856
The oxidation stability of boron nitride thin films on MgO and TiO2 substrates
[DE92-011686] p 3364 N92-28857
A user's manual for MASH 1.0: A Monte Carlo adjoint shielding code system
[AD-A248204] p 3355 N92-29190

OBSERVATOIRE DE PARIS-MEUDON (FRANCE).
Martian channel networks: A revised Strahler approach for quantitative morphometry p 3380 N92-29000
Soil texture and granulometry at the surface of Mars p 3382 N92-29009

OESTERREICHISCHES FORSCHUNGSZENTRUM SEIBERSDORF G.M.B.H., VIENNA.
Humic substances in soils from Bangladesh, Namibia, and Canada
[OEFZS-4574] p 3316 N92-28740
Determination of field related transfer factors for Cs-137 and Sr-90, from the fallout of the reactor accident in Chernobyl (USSR)
[OEFZS-4581] p 3356 N92-29210

OFFICE NATIONAL D'ETUDES ET DE RECHERCHES AEROSPATIALES, PARIS (FRANCE).
Use of a research simulator for the development of new concepts of flight control p 3224 N92-28543
Wavelets and numerical simulation
[ONERA-NT-1991-8] p 3347 N92-28777
Identification of weakly non-linear dynamical systems by means of random excitations
[ONERA-NT-1991-10] p 3349 N92-28778
Vector and parallel supercomputing programming
[ONERA-NT-1991-11] p 3338 N92-28779
Ablation of material of solid propellant motor nozzles
[ONERA-NT-1990-13] p 3249 N92-28780
Construction of a numerical optimization method for the definition of hypersupported profiles
[ONERA-RSF-43/1736-AY-146A] p 3284 N92-28788
Feasibility study of hypersonic clinometric measurements at R3Ch
[ONERA-RSF-136/1865-AY-728-] p 3228 N92-28789
A continuation method for calculating the equilibrium positions of nonlinear structures
[ONERA-RT-24/3542-RY-091-R] p 3338 N92-28790
Study of the loss of consciousness inflight by fighter aircraft pilots
[ONERA-RTS-11/3446-EY] p 3325 N92-28844
Development of an unsteady three-dimensional viscous-inviscid interaction numerical method for the calculation of airfoils vibration
[ONERA-RSF-7/3617-AY-022A] p 3229 N92-29206

OFFICE OF SPACE SCIENCE AND APPLICATIONS, WASHINGTON, DC.
Space life sciences strategic plan
[NASA-TM-107954] p 3244 N92-29100

OHIO STATE UNIV., COLUMBUS.
Digital compression algorithms for HDTV transmission
[NASA-CR-190509] p 3275 N92-28873
Demodulation processes in auditory perception
[AD-A250203] p 3328 N92-29146

OHIO UNIV., ATHENS.
Loran-C performance assurance assessment program
[NASA-CR-190469] p 3230 N92-28718
Nonlinear normal and axial force indicial responses for a two dimensional airfoil
[AD-A247196] p 3229 N92-28888
The in situ observation of diamond film nucleation and growth
[AD-A248203] p 3265 N92-29189

OKLAHOMA UNIV., NORMAN.
Regional climatic effects of atmospheric SO2 on Mars p 3377 N92-28504

OLD DOMINION UNIV., NORFOLK, VA.
Viscous effects on a vortex wake in ground effect
[NASA-CR-190400] p 3283 N92-28361
Use of laser range finders and range image analysis in automated assembly tasks
[NASA-CR-186957] p 3291 N92-29139

OPEN UNIV., MILTON (ENGLAND).
Martian surficial carbon-constraints from isotopic measurements of shock-produced glass in EET A79001 p 3377 N92-28508
The stable isotopic compositions of indigenous carbon-bearing components in EETA 79001 p 3384 N92-29021
Topography of Apollinaris Patera and Ma'adim Vallis p 3393 N92-29069
On the isotopic composition of magmatic carbon in SNC meteorites p 3394 N92-29077

OPTIVISION, INC., PALO ALTO, CA.
Fiber-optic interconnection networks for spacecraft
[NASA-CR-190531] p 3358 N92-28698

ORA CORP., ITHACA, NY.
SPECTOOL: A computer-aided verification tool for hardware designs, volume 1
[AD-A247492] p 3336 N92-28666
SPECTOOL: User's manual, volume 2
[AD-A247493] p 3336 N92-28667

OREGON HEALTH SCIENCES UNIV., PORTLAND.
Structural characterization of cross-linked hemoglobins developed as potential transfusion substitutes
[AD-A246777] p 3325 N92-28515

OREGON STATE UNIV., CORVALLIS.
Midlatitude weather systems on Mars: Is there a hemispheric asymmetry? p 3379 N92-28992

OREGON STATE UNIV., NEWPORT.
In search of a unified theory of biological organization: What does the motor system of a sea slug tell us about human motor integration?
[AD-A250223] p 3328 N92-29119

OXFORD UNIV. (ENGLAND).
Historical data for geomagnetic field modelling p 3299 N92-28621
Turbulent spot generation and growth rates in a transonic boundary layer
[AD-A250221] p 3287 N92-29118

P

PENNSYLVANIA STATE UNIV., UNIVERSITY PARK.
Mechanisms of fracture and creep of structural alloys
[AD-A248701] p 3259 N92-28390
Digital control algorithms for microgravity isolation systems p 3267 N92-28445
Photochemical model for NH3 in an early Martian atmosphere p 3373 N92-28481
A reduced atmosphere for early Mars? p 3375 N92-28495
SAR-relate stress variability in the Marine Atmospheric Boundary Layer (MABL)
[AD-A247772] p 3309 N92-28567
Processing and properties of chemically derived calcium silicate cements
[AD-A249106] p 3264 N92-28570
Explicit Navier-Stokes computation of turbomachinery flows
[AD-A249284] p 3286 N92-28879

PENNSYLVANIA UNIV., PHILADELPHIA.
Diffusion-controlled decohesion using a Cu-Sn alloy as a model system
[DE92-011645] p 3260 N92-28854

PHILLIPS LAB., KIRKLAND AFB, NM.
Singlet delta oxygen pumping of iodine monofluoride in a supersonic flow
[AD-A249946] p 3284 N92-28766

PHYSICS AND ELECTRONICS LAB. TNO, THE HAGUE (NETHERLANDS).
Evaluation of drive simulator settings for DAF YA-4440
[FEL-91-B345] p 3241 N92-28828
Performance of the multifunctional CW CO2-laser radar at the TNO-FEL laboratory and during the BEST TWO field test
[FEL-91-A163] p 3291 N92-29160

PITTSBURGH ENERGY TECHNOLOGY CENTER, PA.
Joint DOE/NSF workshop on flow of particulates and fluids
[DE92-012692] p 3285 N92-28808

PITTSBURGH UNIV., PA.
Coincident pulse techniques for hybrid electronic optical computer systems
[AD-A246774] p 3332 N92-28514

PLANNING SYSTEMS, INC., SLIDELL, LA.
The Navy layered ocean model users guide
[AD-A247754] p 3321 N92-28566

POLYTECHNIC UNIV., FARMINGDALE, NY.
In-situ fault detection by the hybrid ray-mode method
[AD-A250213] p 3297 N92-29112

POTOMAC PHOTONICS, INC., LANHAM, MD.
Compact, self-contained ArF lasers
[AD-A247403] p 3291 N92-28932

PRINCETON UNIV., NJ.
Development of a high-performance FORTRAN compiler for porting CFD codes to the Navier-Stokes computer
[AD-A250208] p 3342 N92-28770
Recent advances in global optimization
[AD-A250211] p 3308 N92-29173

PRINS MAURITS LAB. TNO, RIJSWIJK (NETHERLANDS).
Optimalization of grenades with pre-formed fragments against air-targets, part 2
[PML-1990-24-PT-2] p 3349 N92-28313

PULSE SCIENCES, INC., AGOURA HILLS, CA.
SPEAR 2 space power data analysis
[AD-A248057] p 3250 N92-28945

PURDUE UNIV., WEST LAFAYETTE, IN.
Dynamical solvent effects on activated electron-transfer reactions: Principles, pitfalls, and progress
[AD-A246764] p 3363 N92-28349
The evaluation of rate constants for rapid electrode reactions by using microelectrode voltammetry: Virtues of measurement at lower temperature
[AD-A246760] p 3255 N92-28391
Surface crystallographic dependence of voltammetric oxidation of polyhydric alcohols and related systems at monocrystalline gold-acidic aqueous interfaces
[AD-A246763] p 3363 N92-28392
Plane wave propagation in random granular media
[AD-A247300] p 3298 N92-28424
The emergence of atomic-level structural information for ordered metal-solution interfaces: Some recent contributions from in-situ infrared spectroscopy and scanning tunneling microscopy
[AD-A246765] p 3364 N92-28512
Asynchronous optical sampling for laser-based combustion diagnostics in high-pressure flames
[AD-A250206] p 3257 N92-28896

R

RADEX, INC., BEDFORD, MA.
Coordinate systems for space and geophysical applications
[AD-A247550] p 3244 N92-28937

REINHART AND ASSOCIATES, INC., AUSTIN, TX.
Surface residual stress analysis of metals and alloys
[AD-A248372] p 3259 N92-28426

RENSSELAER POLYTECHNIC INST., TROY, NY.
A combined experimental and analytical investigation of the theory of plasticity involving strain induced anisotropy
[AD-A248440] p 3298 N92-28352
Kinetic studies of metal combustion in propulsion
[AD-A250207] p 3256 N92-28769
Studies of 1,3-disilacyclobutanes as single-source CVD precursors to silicon carbide
[AD-A247111] p 3365 N92-28885

RESEARCH INST. FOR ADVANCED COMPUTER SCIENCE, MOFFETT FIELD, CA.
Kanerva's sparse distributed memory with multiple hamming thresholds
[NASA-CR-190552] p 3339 N92-28875
Using Gaussian windows to explore a multivariate data set
[NASA-CR-190556] p 3339 N92-29106
User's manual for the Gaussian windows program
[NASA-CR-190554] p 3340 N92-29107
Mapping unstructured grid computations to massively parallel computers
[NASA-CR-190551] p 3343 N92-29109
A look-ahead variant of the Lanczos algorithm and its application to the quasi-minimal residual method for non-Hermitian linear systems
[NASA-CR-190557] p 3340 N92-29113

RESEARCH INST. FOR COMPUTING AND INFORMATION SYSTEMS, HOUSTON, TX.
A contribution to laser range imaging technology
[NASA-CR-190501] p 3290 N92-28707
Ground Systems Development Environment (GSDE) software configuration management
[NASA-CR-190503] p 3337 N92-28710
Consulting report on the NASA technology utilization network system
[NASA-CR-190387] p 3370 N92-29108
Repository-based software engineering program: Concept document
[NASA-CR-190384] p 3341 N92-29200

RESEARCH TRIANGLE INST., RESEARCH TRIANGLE PARK, NC.
Integration of tools for the Design and Assessment of High-Performance, Highly Reliable Computing Systems (DAHPHRS), phase 1
[NASA-CR-189621] p 3336 N92-28585
Large-area, plasma-assisted, halogen-based diamond deposition
[AD-A247423] p 3264 N92-28904

ROCHESTER UNIV., NY.
Reinforcement learning for the adaptive control of perception and action
[AD-A249351] p 3344 N92-28325
Big Sky Workshop on Super-Intense Laser-Atom Physics
[AD-A248225] p 3292 N92-29223

ROCKWELL INTERNATIONAL SCIENCE CENTER, THOUSAND OAKS, CA.
Electrodeposition of high temperature superconductors
[AD-A250171] p 3365 N92-28919

ROLLS-ROYCE LTD., DERBY (ENGLAND).
Knowledge-based material selection in design
[PNR-90823] p 3337 N92-28741
ROYAL AEROSPACE ESTABLISHMENT, BEDFORD (ENGLAND).
Validation of simulation systems for aircraft acceptance testing p 3222 N92-28531
ROYAL AEROSPACE ESTABLISHMENT, FARNBOROUGH (ENGLAND).
Practical considerations in designing the engine cycle p 3237 N92-28460
ROYAL NETHERLANDS AIR FORCE, THE HAGUE.
Diffuser casing upgrade for an advanced turbofan
[NLR-TP-90097-U] p 3238 N92-28711
ROYAL NORWEGIAN COUNCIL FOR SCIENTIFIC AND INDUSTRIAL RESEARCH, KJELLER.
NORSAR basic seismological research
[AD-A248616] p 3309 N92-28569
RUTGERS - THE STATE UNIV., NEW BRUNSWICK, NJ.
Numerical methods of linear and nonlinear optimization
[AD-A248579] p 3335 N92-28428
Phase equilibria and trace element partitioning in a magma ocean to 260 kilobars p 3311 N92-28595

S

SAN DIEGO STATE UNIV., CA.
Computer-based assessment of schema knowledge in a flexible problem-solving environment
[AD-A246779] p 3348 N92-28516
SANDIA NATIONAL LABS., ALBUQUERQUE, NM.
A coilgun design primer
[DE92-011149] p 3244 N92-28226
Growth and optical characterization of Zn(1-x)Mn(x)Te grown by molecular beam epitaxy
[DE92-010667] p 3363 N92-28331
Selective suppression of photochemical etching: Raman spectroscopy for pre-etch process selection
[DE92-010955] p 3255 N92-28341
Lessons from Archimedes, a system for planning and executing mechanical assemblies
[DE92-010957] p 3335 N92-28342
Perspectives of ion implantation for optics
[DE92-010664] p 3357 N92-28355
Files improvement the NARA way
[DE92-011139] p 3368 N92-28832
Stress analysis of plated-through-holes in rigid flex multilayer printed wiring boards
[DE92-011659] p 3303 N92-28855
A momentum limit for electromagnetic railguns
[DE92-011380] p 3245 N92-28861
Analyzing noisy spectral line shapes
[DE92-011153] p 3362 N92-29086
Space applications for contactless coilguns
[DE92-011156] p 3245 N92-29102
Ion conductive polymer solid electrolytes
[DE92-010518] p 3266 N92-29195
SANDIA NATIONAL LABS., LIVERMORE, CA.
Stochastic simulation of the structure and propagation rate of turbulent premixed flames
[DE92-006682] p 3256 N92-28822
Degenerate four-wave mixing using a tunable excimer laser to detect combustion gases
[DE92-005327] p 3290 N92-28852
SASKATCHEWAN UNIV., SASKATOON.
Ohmic ignition in a tokamak reactor with the confinement degradation effect due to alpha heating
[PPL-124] p 3360 N92-28664
Ignition access condition based on the generalized saddle point in a magnetic fusion reactor
[PPL-109] p 3361 N92-28665
Plasma density scaling at the current reversal in the STOR-1M tokamak with AC operation
[PPL-127] p 3361 N92-28847
Improved confinement and edge plasma fluctuations in the STOR-M tokamak
[PPL-126] p 3361 N92-28848
Alternating current tokamak reactor with ohmic ignition and bootstrap current
[PPL-120] p 3361 N92-28849
SATCON TECHNOLOGY CORP., CAMBRIDGE, MA.
A 6 degree-of-freedom Lorentz force vibration isolator with nonlinear controller p 3267 N92-28444
SCIENCE APPLICATIONS, INC., MCLEAN, VA.
Identification and analysis of factors affecting the adoption of alternative transportation fuels
[PB92-164326] p 3266 N92-28914
SCIENCE APPLICATIONS INTERNATIONAL CORP., MCLEAN, VA.
Investigation of energy exchange mechanisms between the mean and acoustic flow fields in solid rocket combustion chambers
[AD-A247402] p 3250 N92-28931
SCIENCE APPLICATIONS INTERNATIONAL CORP., SAN ANTONIO, TX.
Turbine aircraft engine operational trending and JT8D static component reliability study
[DOT/FAA/CT-91/10] p 3238 N92-28686
SCIENTIFIC MEASUREMENT SYSTEMS, INC., AUSTIN, TX.
Physical interpretation of thermal and reflected data on Martian surface units p 3391 N92-29062
Physical properties of Deucalionis, Eos, Xanthe-type units in the central equatorial region of Mars p 3392 N92-29063
Physical properties of Meridiani Sinus-type units in the central equatorial region of Mars p 3392 N92-29064
Physical properties of Oxia/Lunae Planum and Arabia-type units in the central equatorial region of Mars p 3392 N92-29065
Surface photometric properties and albedo changes in the central equatorial region of Mars p 3392 N92-29066
SCIENTIFIC RESEARCH ASSOCIATES, INC., GLASTONBURY, CT.
Numerical studies of low temperature gallium arsenide buffer layers and their influence on device operation
[AD-A250309] p 3258 N92-29126
SCRIPPS INSTITUTION OF OCEANOGRAPHY, LA JOLLA, CA.
Test of the new ONR ocean bottom seismographs on the Juan de Fuca Ridge
[AD-A247733] p 3321 N92-28402
Autonomous ocean profiler
[AD-A247657] p 3322 N92-28938
SIKORSKY AIRCRAFT, STRATFORD, CT.
Full mission simulation: A view into the future p 3223 N92-28537
SMITHSONIAN ASTROPHYSICAL OBSERVATORY, CAMBRIDGE, MA.
Scientific investigations with the data base HEAO-1 scanning modulator collimator
[NASA-CR-190477] p 3370 N92-28680
SOCIETE NATIONALE D'ETUDE ET DE CONSTRUCTION DE MOTEURS D'AVIATION, MOISSY-CRAMAYEL (FRANCE).
Steady and transient performance calculation method for prediction, analysis, and identification p 3237 N92-28461
SOUTHAMPTON UNIV. (ENGLAND).
Annoyance due to discrete tones in broadband background noise. Part 2: Analysis
[ISVR-TR-202-PT-2] p 3353 N92-29203
SOUTHWEST RESEARCH INST., SAN ANTONIO, TX.
High-temperature miniaturized turbine engine lubrication system simulator
[AD-A249259] p 3236 N92-28294
Study of high temperature failure mechanism in ceramics
[AD-A247018] p 3263 N92-28415
SPACE SYSTEMS/LORAL, PALO ALTO, CA.
Future benefits and applications of intelligent on-board processing to VSAT services
[NASA-CR-189185] p 3273 N92-28431
Mass and power modeling of communication satellites
[NASA-CR-189186] p 3275 N92-28906
SRI INTERNATIONAL CORP., MENLO PARK, CA.
Excited negative ions and molecules and negative ion production
[AD-A247017] p 3354 N92-28414
Microwave interactions with plasmas
[AD-A250333] p 3362 N92-29093
STANFORD LINEAR ACCELERATOR CENTER, CA.
Accelerator simulation using computers
[DE92-010729] p 3356 N92-28270
STANFORD UNIV., CA.
Advanced diagnostics for reacting flows
[AD-A247059] p 3360 N92-28298
Research studies on extreme ultraviolet and soft x ray lasers
[AD-A247309] p 3289 N92-28299
Tunable optical sources and synthetic nonlinear media/growth and characterization of nonlinear optical materials
[AD-A249363] p 3357 N92-28328
Advanced optical fiber communication systems
[AD-A247683] p 3357 N92-28554
Stanford Center for research on superconductivity and superconductive electronics
[AD-A250204] p 3281 N92-29147
STATE UNIV. OF NEW YORK, ALBANY.
Development of rotating shadowband spectral radiometers and GCM radiation code test data sets in support of ARM
[DE92-011438] p 3316 N92-28853
STATE UNIV. OF NEW YORK, BINGHAMTON.
Ocean tide models for satellite geodesy and Earth rotation
[NASA-CR-190468] p 3321 N92-28867
STATE UNIV. OF NEW YORK, BUFFALO.
Large Eddy Simulations (LES) and Direct Numerical Simulations (DNS) for the computational analyses of high speed reacting flows
[NASA-CR-190364] p 3285 N92-28817
Large eddy simulations and direct numerical simulations of high speed turbulent reacting flows p 3285 N92-28818
Reactant conversion in homogeneous turbulence: Mathematical modeling, computational validations and practical applications p 3285 N92-28819
Modeling of the reactant conversion rate in a turbulent shear flow p 3229 N92-28820
The compositional structure and the effects of exothermicity in an unpremixed planar jet flame p 3258 N92-28821
Electrochemical studies of Lewis acid-base systems for use in thermally regenerable fuel cells
[AD-A246457] p 3307 N92-28974
STATE UNIV. OF NEW YORK, PLATTSBURGH.
Time variation of the meteoritic contribution to the atmosphere of Mars p 3374 N92-28489
The meteoritic contribution to dust and aerosols in the atmosphere of Mars p 3383 N92-29013
STATE UNIV. OF NEW YORK, STONY BROOK.
The production and escape of nitrogen atoms on Mars p 3374 N92-28490
Nitrogen escape from Mars p 3383 N92-29014
SUPERCONDUCTOR TECHNOLOGIES, INC., SANTA BARBARA, CA.
The processing of high temperature ceramic superconducting devices, volume 2
[AD-A248159] p 3281 N92-28948
SVERDRUP TECHNOLOGY, INC., BROOK PARK, OH.
M-H characteristics and demagnetization resistance of samarium-cobalt permanent magnets to 300 C
[NASA-CR-189194] p 3280 N92-28723
SYRACUSE UNIV., NY.
Leakage current measurements in SOI devices
[AD-A247694] p 3280 N92-28561
SYSTEMS APPLICATIONS INTERNATIONAL, SAN RAFAEL, CA.
Regional environmental impacts of methanol-fueled vehicles
[PB92-176569] p 3308 N92-29183
SYSTEMS EXPLORATION, INC., DAYTON, OH.
A theory of automated design of visual information presentations
[AD-A247425] p 3369 N92-28866
SYSTEMS TECHNOLOGY, INC., HAWTHORNE, CA.
The use of ground based simulation for handling qualities research: A new assessment p 3224 N92-28545
Effects of cockpit lateral stick characteristics on handling qualities and pilot dynamics
[NASA-CR-4443] p 3239 N92-28584

T

TECHNICAL RESEARCH CENTRE OF FINLAND, ESPOO.
Nondestructive evaluation of damages caused by impact and fatigue loading of polymer composites
[VTT-RR-742] p 3251 N92-28572
Fatigue strength of a glass fiber reinforced laminate structure
[VTT-RR-743] p 3251 N92-28573
Pre-test analyses for pressurized thermoshock tests, vessel 1
[VTT-RR-746] p 3303 N92-28776
The characterization of ceramics and ceramic/metal-joints by ultrasonic techniques
[VTT-RR-741] p 3266 N92-29194
TECHNISCHE UNIV., BERLIN (GERMANY, F.R.).
Heteroepitaxy of InP on Si (001)
[ETN-92-91333] p 3364 N92-28786
Improvement of connectionnist learning processes, working according to the gradients method
[ETN-92-91335] p 3327 N92-28787
Examination of prosodic features in speech signal using speech fundamental frequency and loudness duration
[ETN-92-91334] p 3274 N92-28792
High resolution electron beam lithography on x ray mask substrates. Effects of electron scattering and membrane heating
[ETN-92-91336] p 3272 N92-28793
TECHNISCHE UNIV., DELFT (NETHERLANDS).
The effect of intermediate heat treatments on overload induced retardation during the fatigue crack growth in an Al-alloy
[LR-651] p 3259 N92-28574
Programming of the complex logarithm function in the solution of the cracked anisotropic plate loaded by a point force
[LR-657] p 3299 N92-28575

The application of carbon fibres in ARALL laminates
[LR-658] p 3259 N92-28576
The influence of elevated temperature on the bonding quality of deformed GLARE
[LR-659] p 3252 N92-28577
The stress corrosion cracking behavior of AlLi 2090-T83 in substitute ocean water
[LR-661] p 3259 N92-28578
The basic research simulator programme and the industrial and aerospace community: Opportunities for cooperative research
[LR-662] p 3240 N92-28579
Growth of surface cracks under fatigue loading: A literature survey
[LR-664] p 3299 N92-28580
Inverse control problems: Mathematical preliminaries, system theoretical approaches, and their applications to aircraft dynamics
[LR-665] p 3345 N92-28581
The compressive properties of GLARE
[LR-666] p 3252 N92-28582
The buckling behavior of a central crack in a plate under tension
[LR-667] p 3299 N92-28583
Some aerospace applications of estimation theory
[ETN-92-91281] p 3349 N92-28647
Applications and benefits of formal methods in software development
[REPT-91-33] p 3341 N92-29221

TECHNISCHE UNIV., EINDHOVEN (NETHERLANDS).
A network flow algorithm for just-in-time project scheduling
[MEMO-COSOR-91-21] p 3336 N92-28638
Genetic algorithms in coding theory: A table for A3 (n, d)
[MEMO-COSOR-91-22] p 3336 N92-28639
Distribution theory for selection from logistic populations
[MEMO-COSOR-91-23] p 3348 N92-28640
Matrix-geometric analysis of the shortest queue problem with threshold jockeying
[MEMO-COSOR-91-24] p 3347 N92-28641
Analysing multiprogramming queues by generating functions
[MEMO-COSOR-91-25] p 3342 N92-28642

TECHNISCHE UNIV., MUNICH (GERMANY, F.R.).
Calculation of installation effects within performance computer programs p 3237 N92-28465

TENNESSEE UNIV., KNOXVILLE.
Molecular dynamics calculations of optical nonlinear properties of materials
[AD-A247095] p 3354 N92-28260
Imperfect fractional crystallization of the lunar magma ocean and formation of the lunar mantle: A realistic chemical approach p 3314 N92-28610

TEXAS A&M UNIV., COLLEGE STATION.
Macrocyclic polycation complexes for secondary anion binding, molecular recognition, and catalysis
[AD-A246690] p 3254 N92-28287
Probabilistic finite element analysis
[AD-A247721] p 3347 N92-28399
Excitation of atoms and molecules in collisions with highly charged ions
[DE92-012658] p 3355 N92-28764
Molecular recognition in the oxidation of catechols by Dicobalt-BISDIEN dioxygen complexes
[AD-A246456] p 3258 N92-28973

TEXAS UNIV., ARLINGTON.
A study of the control problem of the shoot side environment delivery system of a closed crop growth research chamber
[NASA-CR-177597] p 3330 N92-28681
Fault-tolerant parallel computer systems for real-time applications
[AD-A247887] p 3343 N92-28958

TEXAS UNIV., EL PASO.
A seismic and integrated geophysical study of the lithosphere of the Colorado Plateau
[AD-A247091] p 3308 N92-28257
Estimation of the point of incipient deterioration and a class of life distribution with application to cannibalization
[AD-A250216] p 3343 N92-29114

TEXAS UNIV. HEALTH SCIENCE CENTER, SAN ANTONIO.
Investigation of laser-induced retinal damage
[AD-A250173] p 3326 N92-28920

TEXTRON DEFENSE SYSTEMS, EVERETT, MA.
CO2 laser frequency multiplication
[AD-A245915] p 3290 N92-28761
CO2 laser frequency multiplication
[AD-A247542] p 3291 N92-28933

THOMSON COMPOSANTS, SAINT EGREVE (FRANCE).
What is an ASIC? p 3235 N92-28377
The silicon compiler for designing military VLSI ASIC's p 3235 N92-28378

THOMSON-CSF, MALAKOFF (FRANCE).
Interest in real-time simulations for the development terrain following function of radar systems p 3222 N92-28529

THOMSON-CSF, MONTROUGE (FRANCE).
A radar signal processing ASIC and a VME interface circuit p 3235 N92-28380

TOHOKU UNIV., SENDAI (JAPAN).
Terrestrial magma ocean and core segregation in the earth p 3313 N92-28606

TOKYO INST. OF TECH. (JAPAN).
Evidences for the terrestrial magma ocean from high-pressure melting experiments p 3315 N92-28613

TOKYO UNIV., SAGAMIHARA (JAPAN).
Planet-B: A Japanese Mars aeronomy observer p 3393 N92-29072

TOKYO UNIV., TANASHI (JAPAN).
Proceedings of the workshop on Quantum Gravity and Topology
[DE92-782191] p 3366 N92-28235

TOLEDO UNIV., OH.
Low Reynolds number multiple-time-scale turbulence model and calculations of steady and pulsating shear layers
[NASA-CR-189176] p 3286 N92-28908

TORONTO UNIV., DOWNSVIEW (ONTARIO).
An evaluation of IFR approach techniques: Generic helicopter simulation compared with actual flight p 3225 N92-28550

TORONTO UNIV. (ONTARIO).
Ground deposition of liquid droplets released from a point source in the atmospheric surface layer
[ISBN-0-315-51071-4] p 3316 N92-28703

TUEBINGEN UNIV. (GERMANY, F.R.).
Thermal accretion disk models for active galaxies
[ETN-92-91486] p 3371 N92-29127
Analysis of Mir-HEXE observations: Pulsation and energy spectra of the x ray double star SMC X-1 in 20 to 80 keV energy field
[ETN-92-91487] p 3371 N92-29128
Calibration of high energy x ray detectors at the spectrum of the Crab nebula, and x ray pulsar A0535+26 examinations
[ETN-92-91484] p 3371 N92-29177
Split events and their influence on pn CCD energy spectra
[ETN-92-91485] p 3282 N92-29178

TULANE UNIV., NEW ORLEANS, LA.
A uniform approach to the semantics of concurrency
[AD-A246697] p 3334 N92-28289

TURBINE SUPPORT EUROPA, TILBURG (NETHERLANDS).
Diffuser casing upgrade for an advanced turbofan
[NLR-TP-90097-U] p 3238 N92-28711

U

UNITED KINGDOM ATOMIC ENERGY AUTHORITY, HARWELL (ENGLAND).
Report on the workshop on Ion Implantation and Ion Beam Assisted Deposition
[AD-A250561] p 3365 N92-28923

UNITED TECHNOLOGIES RESEARCH CENTER, EAST HARTFORD, CT.
Theoretical studies of the electronic and resonance structure of atomic and molecular negative ions
[AD-A247093] p 3354 N92-28259

UNIVERSITEIT TWENTE, ENSCHEDE (NETHERLANDS).
The 1991 research program (of the Faculty of Mechanical Engineering)
[ETN-92-91353] p 3296 N92-29217

UNIVERSITIES SPACE RESEARCH ASSOCIATION, HUNTSVILLE, AL.
Numerical studies of convective transport associated with crystal growth in microgravity p 3267 N92-28437

UNIVERSITY COLL., LONDON (ENGLAND).
Ice in the northern lowlands and southern highlands of Mars and its enrichment beneath the Elysium Lavas p 3381 N92-29001

UNIVERSITY COLL. OF NORTH WALES, BANGOR.
The Microgravity Isolation Mount (MGIM): A Columbus facility for improving the microgravity quality of payloads p 3267 N92-28439

UNIVERSITY OF SOUTHERN CALIFORNIA, LOS ANGELES.
Center for the integration of optical computing
[AD-A250306] p 3337 N92-28719
Distribution of coastal morphology in the Martian northern lowlands p 3389 N92-29047
Silicon polymers
[AD-A250201] p 3265 N92-29145

UNIVERSITY OF SOUTHERN CALIFORNIA, MARINA DEL REY.
Organizing plan libraries in subsumption hierarchies: Specificity based plan selection
[AD-A248711] p 3368 N92-28430

UNIVERSITY OF SOUTHERN ILLINOIS, SPRINGFIELD.
Learning, teaching, and testing for complex conceptual understanding
[AD-A248728] p 3328 N92-29142

UTAH UNIV., SALT LAKE CITY.
ETO cloud studies for FIRE 2, part 1
[NASA-CR-190472] p 3319 N92-29087
Studies of perceptual memory
[AD-A250200] p 3328 N92-29144

V

VICTORIA UNIV. (BRITISH COLUMBIA).
Coding for frequency hopped spread spectrum satellite communications
[ECE-90-1] p 3274 N92-28699

VIRGINIA POLYTECHNIC INST. AND STATE UNIV., BLACKSBURG.
Dynamic simulation of compressor and gas turbine performance p 3237 N92-28463
Fade durations in satellite-path mobile radio propagation
[NASA-CR-190484] p 3273 N92-28586
Elliptical-core two mode fiber sensors and devices incorporating photoinduced refractive index gratings
[NASA-CR-190495] p 3358 N92-28868
Development of an embedded Fabry Perot Fiber Optic Strain Rosette Sensor (FP-FOSRS)
[NASA-CR-190490] p 3358 N92-29088
Control of nonlinear distributed parameter systems with application to flow control
[AD-A250212] p 3346 N92-29149
Detection of in-plane displacements of acoustic wave fields using extrinsic Fizeau fiber interferometric sensors
[NASA-CR-190493] p 3353 N92-29196

VIRGINIA UNIV., CHARLOTTESVILLE.
Microgravity vibration isolation research at the University of Virginia p 3267 N92-28446
Extended H2 synthesis for microgravity vibration isolation p 3267 N92-28447
Mentat/A: Medium grain parallel processing
[NASA-CR-190486] p 3342 N92-28676

W

WARSAW UNIV. (POLAND).
Influences of CO2 sublimation/condensation processes on the long-term evolution of the Martian atmosphere p 3375 N92-28496

WASHINGTON STATE UNIV., PULLMAN.
Study of the leading-edge vortex dynamics in the unsteady flow over an airfoil
[AD-A247532] p 3228 N92-28865

WASHINGTON UNIV., SAINT LOUIS, MO.
Adaptive and nonlinear control
[AD-A248580] p 3344 N92-28429
Chemical models of volcanic outgassing on Mars p 3374 N92-28487
A new angle on lunar ferroan-suite differentiation p 3311 N92-28598
Atmosphere-surface interactions and atmospheric evolution on Mars p 3383 N92-29012

WASHINGTON UNIV., SEATTLE.
Propagation and scattering of microwaves and millimeter waves in snow based on dense random media theory
[AD-A249300] p 3274 N92-28846
Mars: Compositional variability of ferric/ferrous minerals and polar volatiles from groundbased imaging spectroscopy p 3379 N92-28993
Turbulent spectra, fluxes, stability and growth of the mixed layer in the boundary layer of Mars p 3393 N92-29070

WAYNE STATE UNIV., DETROIT, MI.
Thermal wave imaging and characterization of solids
[AD-A249297] p 3297 N92-28851

WESTINGHOUSE SAVANNAH RIVER CO., AIKEN, SC.
Audit trails and PC control on Novell networks
[DE92-010695] p 3335 N92-28332
Underwater vapor phase burning of aluminum particles and on aluminum ignition during steam explosions
[DE92-011196] p 3257 N92-28894

WISCONSIN UNIV., MADISON.
The structure of finitely generated shift-invariant spaces in L2(IR sup d)
[AD-A247314] p 3334 N92-28301
Fourier analysis of the approximation power of principal shift-invariant spaces
[AD-A246713] p 3347 N92-28411

Thermodynamic and kinetic aspects of surface acidity
[DE92-011194] p 3256 N92-28893
WORCESTER POLYTECHNIC INST., MA.
Determining the pH of Mars from the Viking labelled release reabsorption effect p 3389 N92-29049
WRIGHT LAB., WRIGHT-PATTERSON AFB, OH.
Piloted simulation effectiveness development applications and limitations p 3221 N92-28524
Full mission simulation for research and development of air combat flight and attack management systems p 3223 N92-28538
The mechanical property data base from an Air Force/industry cooperative test program on advanced aluminum alloys (IN905XL and AL905XL forgings)
[AD-A247752] p 3368 N92-28565
A methodology for the evaluation of runway roughness for repair
[AD-A250407] p 3241 N92-28772
VHDL and waves descriptions for a pseudo-random pattern generator
[AD-A247891] p 3349 N92-28961
Stretch and hammer neural networks for N-dimensional data generalization
[AD-A247941] p 3346 N92-29082
WYLE LABS., INC., EL SEGUNDO, CA.
Evaluation of outdoor-to-indoor response to minimized sonic booms
[NASA-CR-189643] p 3352 N92-28556

Y

YALE UNIV., NEW HAVEN, CT.
Studies in turbulence and turbulence control
[AD-A247164] p 3282 N92-28225
Crystallizing FORTRAN
[AD-A250162] p 3343 N92-28915
Diagonal forms of translation operators for helmholtz equation in three dimensions
[AD-A248422] p 3348 N92-28949
New neural algorithms for self-organized learning
[AD-A249816] p 3341 N92-29198
YUMA PROVING GROUND, AZ.
Automation and remote control instrumentation development: Rocket First Motion Timing System (RFMTS)
[AD-A249970] p 3287 N92-28767

Typical Contract Number Index Listing

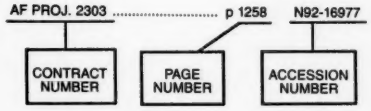

Listings in this index are arranged alphanumerically by contract number. Under each contract number the accession numbers denoting documents that have been produced as a result of research done under that contract are arranged in ascending order. The page number helps to locate the citation in the abstract section. The accession number denotes the number by which the citation is identified.

AF PROJ. 2418 ..... p 3368 N92-28565
AF PROJ. 3151 ..... p 3284 N92-28766
AF PROJ. 5797 ..... p 3362 N92-28962
AF PROJ. 6096 ..... p 3349 N92-28961
AF-AFOSR-0003-91 ..... p 3342 N92-28770
AF-AFOSR-0004-87 ..... p 3240 N92-28388
AF-AFOSR-0007-89 ..... p 3265 N92-29145
AF-AFOSR-0012-89 ..... p 3395 N92-28520
AF-AFOSR-0016-86 ..... p 3282 N92-28258
AF-AFOSR-0030-89 ..... p 3352 N92-28889
AF-AFOSR-0047-90 ..... p 3325 N92-28886
AF-AFOSR-0051-89 ..... p 3257 N92-28896
AF-AFOSR-0052-88 ..... p 3283 N92-28274
AF-AFOSR-0067-89 ..... p 3360 N92-28298
AF-AFOSR-0070-88 ..... p 3371 N92-28843
AF-AFOSR-0086-89 ..... p 3256 N92-28769
AF-AFOSR-0088-90 ..... p 3297 N92-29112
AF-AFOSR-0089-87 ..... p 3342 N92-28746
AF-AFOSR-0100-91 ..... p 3327 N92-28877
AF-AFOSR-0105-92 ..... p 3329 N92-29186
AF-AFOSR-0111-90 ..... p 3364 N92-28513
AF-AFOSR-0114-91 ..... p 3357 N92-28372
AF-AFOSR-0116-87 ..... p 3282 N92-28225
AF-AFOSR-0116-91 ..... p 3308 N92-29173
AF-AFOSR-0127-87 ..... p 3337 N92-28704
AF-AFOSR-0131-90 ..... p 3228 N92-28865
AF-AFOSR-0133-90 ..... p 3337 N92-28719
AF-AFOSR-0134-89 ..... p 3254 N92-28261
AF-AFOSR-0141-91 ..... p 3318 N92-28668
AF-AFOSR-0179-91 ..... p 3262 N92-28323
AF-AFOSR-0184-88 ..... p 3264 N92-28570
AF-AFOSR-0208-91 ..... p 3326 N92-28920
AF-AFOSR-0215-87 ..... p 3335 N92-28428
AF-AFOSR-0227-89 ..... p 3328 N92-29146
AF-AFOSR-0247-89 ..... p 3326 N92-29179
AF-AFOSR-0249-88 ..... p 3254 N92-28300
AF-AFOSR-0251-89 ..... p 3286 N92-28890
AF-AFOSR-0260-89 ..... p 3328 N92-28957
AF-AFOSR-0262-89 ..... p 3328 N92-29119
AF-AFOSR-0275-89 ..... p 3328 N92-29144
AF-AFOSR-0276-88 ..... p 3289 N92-28271
AF-AFOSR-0289-87 ..... p 3263 N92-28558
AF-AFOSR-0309-88 ..... p 3344 N92-28429
AF-AFOSR-0312-90 ..... p 3331 N92-29121
AF-AFOSR-0337-88 ..... p 3298 N92-28320
AF-AFOSR-0352-88 ..... p 3324 N92-28397
AF-AFOSR-0352-90 ..... p 3316 N92-28935
AF-AFOSR-0427-89 ..... p 3287 N92-29118
AF-AFOSR-0444-89 ..... p 3248 N92-28967
AF-AFOSR-0469-89 ..... p 3332 N92-28514
AF-AFOSR-0495-89 ..... p 3346 N92-29149
AF-AFOSR-0502-89 ..... p 3229 N92-28888
ARPA ORDER 06266 ..... p 3281 N92-28948
ATD-90-STI-6401 ..... p 3239 N92-28584
A81KL131 ..... p 3241 N92-28828
A85/KM/118 ..... p 3349 N92-28313
A90KL621 ..... p 3291 N92-29160
DA PROJ. RS3-4-S-91 ..... p 3253 N92-28953
DA PROJ. RV3-6-I-21 ..... p 3339 N92-28946
DA PROJ. 1L1-61102-AH-42 ..... p 3261 N92-28249
p 3262 N92-28250
DA PROJ. 1L1-61102-AH-43 ..... p 3257 N92-28954
DA PROJ. 1L1-61102-BH-57 ..... p 3287 N92-28322
p 3275 N92-28878
DA PROJ. 1L1-62211-A-47-A ..... p 3293 N92-28434
p 3293 N92-28476
p 3288 N92-29105
p 3296 N92-29136
DA PROJ. 3M1-62787-A-874 ..... p 3324 N92-28242
p 3325 N92-28515
DA PROJ. 3M1-62787-A-879 ..... p 3331 N92-28944
DAAG29-85-C-0018 ..... p 3346 N92-28329
DAAL03-G-90-0090 ..... p 3334 N92-28301
DAAL03-86-G-0019 ..... p 3281 N92-28797
DAAL03-86-G-0044 ..... p 3286 N92-28879
DAAL03-88-G-0007 ..... p 3298 N92-28327
DAAL03-88-K-0032 ..... p 3332 N92-29227
DAAL03-88-K-0041 ..... p 3298 N92-28352
DAAL03-88-K-0089 ..... p 3297 N92-28851
DAAL03-88-K-0113 ..... p 3357 N92-28328
DAAL03-89-K-0003 ..... p 3279 N92-28351
DAAL03-89-K-0006 ..... p 3279 N92-28427
DAAL03-89-K-0019 ..... p 3251 N92-28307
DAAL03-89-K-0037 ..... p 3278 N92-28295
DAAL03-89-K-0055 ..... p 3274 N92-28846
DAAL03-89-K-0124 ..... p 3345 N92-28895
DAAL03-90-G-0068 ..... p 3303 N92-28892
DAAL03-90-G-0090 ..... p 3347 N92-28411
DAAL03-90-G-0217 ..... p 3344 N92-28387
DAAL03-90-G-0233 ..... p 3338 N92-28845
DAAL03-91-C-0031 ..... p 3289 N92-28330
DAAL03-91-C-0036 ..... p 3279 N92-28326
DAAL03-91-G-0220 ..... p 3275 N92-28878
DAAL03-91-G-0223 ..... p 3281 N92-28798
DAAL03-92-C-0028 ..... p 3262 N92-28360
DABT63-91-C-0025 ..... p 3368 N92-28430
DACA39-89-M-1309 ..... p 3298 N92-28424
DAJA45-89-C-0004 ..... p 3287 N92-28322
DAMD17-89-C-9002 ..... p 3325 N92-28515
DASG60-91-C-0006 ..... p 3332 N92-28236
DE-AC01-87EI-19800 ..... p 3266 N92-28914
DE-AC02-76CH-03000 ..... p 3371 N92-28774
p 3355 N92-28839
p 3355 N92-28858
p 3371 N92-28859
p 3372 N92-29184
p 3282 N92-29197
DE-AC02-83CH-10093 ..... p 3306 N92-28277
DE-AC02-83ER-40105 ..... p 3354 N92-28337
DE-AC03-76SF-00098 ..... p 3356 N92-28270
p 3324 N92-28278
p 3364 N92-28762
DE-AC03-76SF-00515 ..... p 3356 N92-28270
DE-AC04-76DP-00613 ..... p 3260 N92-28763
DE-AC04-76DP-00789 ..... p 3244 N92-28226
p 3363 N92-28331
p 3255 N92-28341
p 3335 N92-28342
p 3357 N92-28355
p 3368 N92-28832
p 3303 N92-28855
p 3245 N92-28861
p 3295 N92-28925
p 3362 N92-29086
p 3245 N92-29102
p 3266 N92-29195
DE-AC04-76DR-00789 ..... p 3256 N92-28822
p 3290 N92-28852
DE-AC05-84OR-21400 ..... p 3341 N92-28279
p 3324 N92-28382
p 3356 N92-28813
p 3281 N92-28814
p 3260 N92-28856
p 3364 N92-28857
p 3355 N92-29190
DE-AC07-76ID-01570 ..... p 3361 N92-28805
p 3308 N92-28811
DE-AC09-89SR-18035 ..... p 3335 N92-28332
p 3257 N92-28894
DE-AM03-76SF-00010 ..... p 3356 N92-28270
DE-FG02-84ER-13183 ..... p 3256 N92-28893
DE-FG02-85ER-13370 ..... p 3257 N92-28942
DE-FG02-87ER-45290 ..... p 3260 N92-28854
DE-FG02-90ER-25086 ..... p 3338 N92-28841
DE-FG02-90ER-61066 ..... p 3318 N92-28340
DE-FG02-90ER-61072 ..... p 3316 N92-28853
DE-FG02-91ER-40606 ..... p 3371 N92-28774
p 3371 N92-28859
DE-FG02-91ER-61220 ..... p 3319 N92-28830
DE-FG03-87ER-13738 ..... p 3364 N92-28806
DE-FG05-84ER-13262 ..... p 3355 N92-28764
DE-FG05-91ER-25105 ..... p 3341 N92-28279
DE-FG22-90PC-90293 ..... p 3256 N92-28827
DLA900-87-D-0017 ..... p 3367 N92-28389
DNA001-90-C-0084 ..... p 3250 N92-28945
DRET-89-1208 ..... p 3325 N92-28844
DRET-89-34-001 ..... p 3284 N92-28788
p 3228 N92-28789
p 3338 N92-28790
DSS-36001-8-359/01-SS ..... p 3274 N92-28699
DTCG-23-88-C-20025 ..... p 3252 N92-28725
DTCG-23-88-C-20055 ..... p 3252 N92-28724
DTRS-57-89-C-00006 ..... p 3235 N92-29180
EAS-7222/87/NL ..... p 3294 N92-28705
ESA-A0/2-1162-NL/PH ..... p 3302 N92-28643
F04606-89-D-0036 ..... p 3238 N92-28686
F04701-88-C-0089 ..... p 3308 N92-28272
p 3245 N92-28956
F19628-86-C-0029 ..... p 3248 N92-28765
F19628-88-K-0030 ..... p 3355 N92-28936
F19628-89-C-0001 ..... p 3272 N92-28304
p 3278 N92-28305
F19628-89-C-0068 ..... p 3244 N92-28937
F19628-90-C-0002 ..... p 3248 N92-28366
F19628-90-K-0023 ..... p 3309 N92-28394
F19628-90-K-0041 ..... p 3309 N92-28386
F30602-88-C-0130 ..... p 3368 N92-28404
F30602-88-D-0027 ..... p 3280 N92-28561
F30602-89-D-0096 ..... p 3336 N92-28666
p 3336 N92-28667
F33615-88-C-0003 ..... p 3340 N92-29187
p 3340 N92-29188
F33615-88-C-0004 ..... p 3369 N92-28866
F33615-88-C-0011 ..... p 3241 N92-28975
F33615-88-C-2816 ..... p 3236 N92-28294
F33615-88-C-2817 ..... p 3262 N92-28398
F33615-88-C-5404 ..... p 3258 N92-28241
F33615-89-C-5607 ..... p 3258 N92-29091
F33615-90-C-0005 ..... p 3278 N92-28276
F49620-88-C-0081 ..... p 3263 N92-28415
F49620-88-C-0120 ..... p 3289 N92-28299
F49620-89-C-0001 ..... p 3281 N92-29147
F49620-89-C-0019 ..... p 3354 N92-28259
F49620-89-C-0038 ..... p 3309 N92-28569
F49620-89-C-0076 ..... p 3308 N92-28257
F49620-89-C-0085 ..... p 3343 N92-29114
F49620-89-C-0112 ..... p 3339 N92-28969
F49620-89-C-0124 ..... p 3250 N92-28931
F49620-89-K-0002 ..... p 3354 N92-28414
F49620-90-C-0039 ..... p 3278 N92-28275
F49620-90-C-0041 ..... p 3362 N92-29093
F49620-90-C-0076 ..... p 3327 N92-28880
F49620-91-C-0023 ..... p 3258 N92-29126
F49620-91-C-0035 ..... p 3263 N92-28412
F49620-91-0040 ..... p 3291 N92-28932
GRI-5090-810-2037 ..... p 3266 N92-28914
JPL-956512 ..... p 3273 N92-28586
MIPR-FY76169100412 ..... p 3318 N92-28799
NAGW-1118 ..... p 3306 N92-28717
NAGW-2257 ..... p 3388 N92-29039
NAG1-1077 ..... p 3352 N92-28722
NAG1-1087 ..... p 3233 N92-28720
NAG1-1122 ..... p 3285 N92-28817
p 3285 N92-28818
NAG1-1181 ..... p 3342 N92-28676
NAG1-1348 ..... p 3358 N92-28868
p 3358 N92-29088
p 3353 N92-29196
NAG1-613 ..... p 3297 N92-28726
NAG1-681 ..... p 3226 N92-28511
NAG1-685 ..... p 3352 N92-28722
NAG1-816 ..... p 3230 N92-28718
NAG1-868 ..... p 3319 N92-29087
NAG1-987 ..... p 3283 N92-28361
NAG2-722 ..... p 3330 N92-28671
NAG3-1082 ..... p 3275 N92-28873
NAG3-1170 ..... p 3283 N92-28555

NAG3-992 p 3307 N92-28863
NAG5-145 p 3321 N92-28867
NAG8-496 p 3370 N92-28680
NAG8-806 p 3305 N92-28715
NAG8-834 p 3316 N92-28911
NAG9-39 p 3313 N92-28604
NAG9-56 p 3311 N92-28598
NASW-4254 p 3367 N92-29111
NASW-4574 p 3372 N92-28478
p 3310 N92-28587
p 3378 N92-28988
NAS1-17964 p 3336 N92-28585
NAS1-18584 p 3291 N92-29139
NAS1-18605 p 3337 N92-28760
NAS1-19060 p 3352 N92-28556
NAS10-11624 p 3330 N92-28670
NAS2-12722 p 3239 N92-28584
NAS2-12849 p 3327 N92-28744
NAS2-13127 p 3224 N92-28545
NAS2-13210 p 3346 N92-29175
NAS3-24538 p 3298 N92-28296
NAS3-25092 p 3273 N92-28431
p 3275 N92-28906
NAS3-25266 p 3240 N92-28673
p 3280 N92-28723
NAS5-30896 p 3358 N92-28698
NAS5-31500 p 3396 N92-28869
p 3396 N92-28870
p 3396 N92-28871
p 3396 N92-28872
NAS7-918 p 3291 N92-28941
p 3305 N92-28950
p 3369 N92-29202
NAS8-36996 p 3292 N92-28362
NAS8-38477 p 3295 N92-29134
NCA2-484 p 3330 N92-28681
NCA2-543 p 3273 N92-28371
NCC2-387 p 3339 N92-29106
p 3340 N92-29107
p 3343 N92-29109
p 3340 N92-29113
NCC2-408 p 3339 N92-29106
p 3340 N92-29107
NCC3-229 p 3286 N92-28908
NCC9-16 p 3290 N92-28707
p 3337 N92-28710
p 3370 N92-29108
p 3341 N92-29200
NERC-GR3/7704 p 3300 N92-28627
NIMH-12717 p 3342 N92-28746
NIVR-RB-311.1-01501-N p 3228 N92-28709
NIVR-01101-N p 3227 N92-28660
NIVR-01404-N p 3260 N92-28794
NIVR-01502-N p 3228 N92-28713
NIVR-01604-N p 3284 N92-28712
NIVR-01708-N p 3230 N92-28655
NIVR-01803-N p 3352 N92-28695
NIVR-01808-N p 3304 N92-29176
NIVR-01904-N p 3347 N92-28635
NIVR-02506-N p 3293 N92-28645
p 3293 N92-28646
p 3345 N92-28648
NIVR-02904-N p 3302 N92-28650
NIVR-03601-N p 3226 N92-28658
NIVR-1869 p 3260 N92-28691
NR PROJ. RM3-3-T-21 p 3272 N92-28253
NR PROJ. RR0-1301 p 3265 N92-28916
p 3252 N92-28917
NR PROJ. RR0-2203 p 3253 N92-28918
NSF CCR-89-08285 p 3343 N92-28915
NSF DDM-88-00281 p 3349 N92-28927
p 3350 N92-28928
p 3350 N92-28929
p 3350 N92-28930
NSF DDM-89-01495 p 3349 N92-28927
p 3350 N92-28928
p 3350 N92-28929
p 3350 N92-28930
NSF DDM-90-01705 p 3349 N92-28927
p 3350 N92-28928
p 3350 N92-28929
p 3350 N92-28930
NSF DMS-90-00053 p 3334 N92-28301
NSF IRI-89-03582 p 3344 N92-28325
NSF MIP-90-16734 p 3273 N92-28358
N00014-80-C-0190 p 3344 N92-28325
N00014-82-K-0324 p 3284 N92-28768
N00014-82-K-0812 p 3278 N92-28239
N00014-85-K-0198 p 3268 N92-28359
N00014-85-K-0803 p 3254 N92-28240
N00014-86-K-0756 p 3254 N92-28290
p 3262 N92-28291
N00014-87-G-0232 p 3318 N92-28421
N00014-88-C-0615 p 3364 N92-28395
N00014-88-C-0713 p 3281 N92-28948
N00014-88-K-0077 p 3328 N92-29142
N00014-88-K-0304 p 3348 N92-28273
N00014-88-K-0451 p 3254 N92-28287
p 3258 N92-28973
N00014-88-K-0490 p 3341 N92-29224
N00014-88-K-0495 p 3263 N92-28553
N00014-88-K-0499 p 3334 N92-28289
N00014-88-K-0622 p 3343 N92-28958
N00014-88-K-2023 p 3345 N92-28970
N00014-88-R-0330 p 3251 N92-28252
N00014-89-C-6002 p 3321 N92-28566
N00014-89-C-6014 p 3322 N92-28938
N00014-89-J-1586 p 3347 N92-28399
N00014-89-J-1734 p 3258 N92-28237
N00014-90-C-0225 p 3365 N92-28919
N00014-90-J-1143 p 3348 N92-28516
N00014-90-J-1228 p 3322 N92-28939
N00014-90-J-1596 p 3323 N92-29225
N00014-90-J-1828 p 3265 N92-29116
N00014-90-J-1881 p 3321 N92-28402
N00014-91-C-0025 p 3290 N92-28903
N00014-91-C-0177 p 3264 N92-28904
N00014-91-C-0222 p 3292 N92-29226
N00014-91-C-2279 p 3290 N92-28761
p 3291 N92-28933
N00014-91-J-1045 p 3262 N92-28251
N00014-91-J-1329 p 3273 N92-28358
N00014-91-J-1409 p 3363 N92-28349
p 3255 N92-28391
p 3363 N92-28392
p 3364 N92-28512
N00014-91-J-1414 p 3259 N92-28390
N00014-91-J-1483 p 3263 N92-28405
N00014-91-J-1559 p 3343 N92-28915
N00014-91-J-1596 p 3265 N92-29189
N00014-91-J-1668 p 3292 N92-29223
N00014-91-J-1857 p 3357 N92-28554
N00014-91-J-1896 p 3265 N92-28972
N00014-91-J-1917 p 3365 N92-28885
N00014-91-J-1927 p 3258 N92-28982
p 3258 N92-29185
N00015-89-K-0056 p 3307 N92-28974
N00019-88-C-0174 p 3354 N92-28260
N00019-91-C-0062 p 3259 N92-28426
N00039-89-C-5301 p 3279 N92-28367
p 3275 N92-28905
N00039-91-C-0001 p 3338 N92-28795
OV/RLD-937/1 p 3316 N92-28689
OV/RLD-987 p 3232 N92-28649
PROJ. 89-06 p 3330 N92-28521
RICIS PROJ. AI-11 p 3290 N92-28707
RICIS PROJ. RB-04 p 3370 N92-29108
p 3341 N92-29200
RICIS PROJ. SE-34 p 3337 N92-28710
RNLAF-RB-KLU-1990/A.5 p 3239 N92-28653
RTOP 144-50-50 p 3273 N92-28431
p 3275 N92-28906
RTOP 199-18-12-07 p 3325 N92-28420
RTOP 505-59-36 p 3234 N92-28926
RTOP 505-59-52 p 3353 N92-28909
RTOP 505-61-51 p 3239 N92-28457
p 3327 N92-28744
RTOP 505-62-40-04 p 3255 N92-28374
RTOP 505-62-50 p 3288 N92-29105
RTOP 505-62-52 p 3229 N92-28980
p 3353 N92-28984
RTOP 505-62-84 p 3240 N92-28673
RTOP 505-62-91 p 3298 N92-28296
RTOP 505-63-36-05 p 3352 N92-28722
RTOP 505-63-36 p 3293 N92-28434
p 3293 N92-28476
p 3296 N92-29136
RTOP 505-63-50-06 p 3231 N92-28435
RTOP 505-64-12-02 p 3275 N92-28876
RTOP 505-64-30 p 3239 N92-28584
p 3234 N92-29110
RTOP 505-64-36 p 3231 N92-29103
RTOP 505-64-54-01 p 3336 N92-28585
RTOP 505-68-10 p 3227 N92-28674
p 3227 N92-28696
RTOP 505-68-32 p 3236 N92-28418
RTOP 505-90-52-01 p 3337 N92-28760
RTOP 506-41-41-01 p 3290 N92-28862
RTOP 506-41-41 p 3280 N92-28675
p 3337 N92-28684
RTOP 506-42-31 p 3357 N92-28475
p 3250 N92-28983
RTOP 506-42-72 p 3249 N92-28693
RTOP 506-42-73 p 3266 N92-28433
RTOP 506-43-11 p 3255 N92-28743
RTOP 506-43-31 p 3233 N92-28721
p 3245 N92-29104
RTOP 506-43-41-02 p 3344 N92-28375
RTOP 506-51-31 p 3234 N92-28910
RTOP 506-59-31 p 3349 N92-28672
RTOP 506-59-61-01 p 3247 N92-28730
RTOP 509-10-02-03 p 3226 N92-28477
RTOP 537-02-23 p 3236 N92-28419
RTOP 537-03-21-03 p 3352 N92-28556
RTOP 553-13-00 p 3302 N92-28701
RTOP 578-41-16-20 p 3346 N92-28297
RTOP 579-31-02 p 3300 N92-28624
RTOP 589-01-1B p 3246 N92-28683
RTOP 590-11-21-02 p 3291 N92-29139
RTOP 590-13-11 p 3280 N92-28723
p 3307 N92-28837
RTOP 590-13-21 p 3249 N92-28682
RTOP 590-13-31 p 3279 N92-28432
RTOP 590-21-41 p 3248 N92-28417
RTOP 650-60-21 p 3275 N92-28873
RTOP 694-01-23-05 p 3331 N92-28897
RTOP 694-03-0C p 3268 N92-28436
RTOP 906-11-03 p 3238 N92-28985
STPA-85-95-009 p 3229 N92-29206
W-31-109-ENG-38 p 3262 N92-28339
p 3327 N92-28775
p 3274 N92-28809
p 3274 N92-28810
p 3294 N92-28815
W-7405-ENG-36 p 3282 N92-28268
p 3334 N92-28309
p 3354 N92-28310
p 3356 N92-28356
p 3306 N92-28807
p 3306 N92-28834
p 3368 N92-28838
p 3306 N92-28840
p 3365 N92-28874
p 3291 N92-29168
W-7405-ENG-48 p 3283 N92-28269
p 3363 N92-28333
p 3342 N92-28334
p 3360 N92-28335
p 3397 N92-28336
p 3342 N92-28381
p 3325 N92-28685
p 3288 N92-28812
p 3347 N92-28824
p 3355 N92-28860
p 3277 N92-29131
W-7405-ENG-82 p 3259 N92-28338
W2207-7-AF69/01-SS p 3225 N92-28550

REPORT NUMBER INDEX

Typical Report Number Index Listing

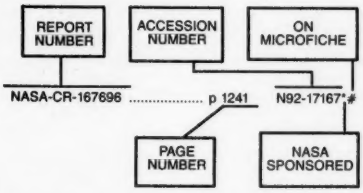

Listings in this index are arranged alphanumerically by report number. The accession number denotes the number by which the citation is identified. The page number helps to locate the citation in the abstract section. An asterisk (*) indicates that the item is a NASA report. A pound sign (#) indicates that the item is available on microfiche.

A-89130 ..... p 3239 N92-28457 * #
A-91153 ..... p 3327 N92-28744 * #
A-91178 ..... p 3234 N92-28926 * #
A-91237 ..... p 3245 N92-29104 * #
A-92014 ..... p 3234 N92-28910 * #
A-92021 ..... p 3231 N92-29103 * #
A-92043 ..... p 3325 N92-28420 * #
A-92048 ..... p 3349 N92-28672 * #
A-92052 ..... p 3353 N92-28909 * #
A-92056 ..... p 3255 N92-28743 * #
A-92064 ..... p 3233 N92-28721 * #
A-92138 ..... p 3330 N92-28681 * #

AD-A245360 ..... p 3318 N92-28421 #
AD-A245909 ..... p 3277 N92-29165 #
AD-A245912 ..... p 3307 N92-28383 #
AD-A245915 ..... p 3290 N92-28761 #
AD-A245922 ..... p 3240 N92-28407 #
AD-A245925 ..... p 3326 N92-28408 #
AD-A245926 ..... p 3293 N92-28384 #
AD-A245927 ..... p 3318 N92-28423 #
AD-A245938 ..... p 3256 N92-28882 #
AD-A245939 ..... p 3329 N92-28346 #
AD-A245940 ..... p 3228 N92-28883 #
AD-A245941 ..... p 3320 N92-28316 #
AD-A245942 ..... p 3230 N92-28317 #
AD-A245943 ..... p 3320 N92-28318 #
AD-A245946 ..... p 3319 N92-28884 #
AD-A245949 ..... p 3252 N92-28898 #
AD-A245961 ..... p 3352 N92-28409 #
AD-A245964 ..... p 3272 N92-28347 #
AD-A245965 ..... p 3309 N92-28319 #
AD-A245966 ..... p 3306 N92-28791 #
AD-A245967 ..... p 3273 N92-28410 #
AD-A245973 ..... p 3239 N92-28801 #
AD-A245977 ..... p 3234 N92-28802 #
AD-A245979 ..... p 3289 N92-28662 #
AD-A245982 ..... p 3368 N92-28663 #
AD-A246039 ..... p 3320 N92-28283 #
AD-A246453 ..... p 3292 N92-28284 #
AD-A246454 ..... p 3265 N92-28972 #
AD-A246456 ..... p 3258 N92-28973 #
AD-A246457 ..... p 3307 N92-28974 #
AD-A246459 ..... p 3241 N92-28975 #
AD-A246464 ..... p 3261 N92-28976 #
AD-A246465 ..... p 3322 N92-28977 #
AD-A246467 ..... p 3287 N92-28978 #
AD-A246468 ..... p 3276 N92-28979 #
AD-A246618 ..... p 3272 N92-28253 #
AD-A246620 ..... p 3245 N92-28254 #
AD-A246621 ..... p 3370 N92-28255 #
AD-A246622 ..... p 3366 N92-28256 #
AD-A246668 ..... p 3334 N92-28285 #
AD-A246683 ..... p 3329 N92-28286 #
AD-A246690 ..... p 3254 N92-28287 #
AD-A246695 ..... p 3324 N92-28288 #
AD-A246697 ..... p 3334 N92-28289 #
AD-A246698 ..... p 3254 N92-28290 #
AD-A246699 ..... p 3262 N92-28291 #
AD-A246708 ..... p 3327 N92-28557 #
AD-A246713 ..... p 3347 N92-28411 #
AD-A246714 ..... p 3357 N92-28372 #
AD-A246759 ..... p 3221 N92-28348 #
AD-A246760 ..... p 3255 N92-28391 #
AD-A246763 ..... p 3363 N92-28392 #
AD-A246764 ..... p 3363 N92-28349 #
AD-A246765 ..... p 3364 N92-28512 #
AD-A246772 ..... p 3364 N92-28513 #
AD-A246773 ..... p 3263 N92-28412 #
AD-A246774 ..... p 3332 N92-28514 #
AD-A246775 ..... p 3321 N92-28365 #
AD-A246776 ..... p 3248 N92-28366 #
AD-A246777 ..... p 3325 N92-28515 #
AD-A246779 ..... p 3348 N92-28516 #
AD-A246822 ..... p 3351 N92-28292 #
AD-A246850 ..... p 3258 N92-29185 #
AD-A246851 ..... p 3258 N92-28982 #
AD-A246854 ..... p 3372 N92-28393 #
AD-A246945 ..... p 3329 N92-29186 #
AD-A246951 ..... p 3263 N92-28558 #
AD-A247011 ..... p 3309 N92-28394 #
AD-A247013 ..... p 3364 N92-28395 #
AD-A247014 ..... p 3326 N92-28396 #
AD-A247016 ..... p 3352 N92-28413 #
AD-A247017 ..... p 3354 N92-28414 #
AD-A247018 ..... p 3263 N92-28415 #
AD-A247019 ..... p 3279 N92-28367 #
AD-A247023 ..... p 3246 N92-28368 #
AD-A247025 ..... p 3279 N92-28373 #
AD-A247049 ..... p 3327 N92-28877 #
AD-A247059 ..... p 3360 N92-28298 #
AD-A247060 ..... p 3289 N92-28271 #
AD-A247064 ..... p 3308 N92-28272 #
AD-A247065 ..... p 3348 N92-28273 #
AD-A247067 ..... p 3350 N92-28238 #
AD-A247082 ..... p 3278 N92-28239 #
AD-A247088 ..... p 3254 N92-28240 #
AD-A247091 ..... p 3308 N92-28257 #
AD-A247092 ..... p 3282 N92-28258 #
AD-A247093 ..... p 3354 N92-28259 #
AD-A247095 ..... p 3354 N92-28260 #
AD-A247097 ..... p 3298 N92-28320 #
AD-A247101 ..... p 3258 N92-28241 #
AD-A247111 ..... p 3365 N92-28885 #
AD-A247151 ..... p 3318 N92-28517 #
AD-A247153 ..... p 3329 N92-28518 #
AD-A247156 ..... p 3335 N92-28519 #
AD-A247158 ..... p 3395 N92-28520 #
AD-A247159 ..... p 3324 N92-28397 #
AD-A247163 ..... p 3254 N92-28261 #
AD-A247164 ..... p 3282 N92-28225 #
AD-A247167 ..... p 3324 N92-28242 #
AD-A247172 ..... p 3325 N92-28886 #
AD-A247194 ..... p 3275 N92-28887 #
AD-A247196 ..... p 3229 N92-28888 #
AD-A247199 ..... p 3352 N92-28889 #
AD-A247203 ..... p 3286 N92-28890 #
AD-A247300 ..... p 3298 N92-28424 #
AD-A247303 ..... p 3352 N92-28559 #
AD-A247305 ..... p 3283 N92-28274 #
AD-A247309 ..... p 3289 N92-28299 #
AD-A247312 ..... p 3254 N92-28300 #
AD-A247314 ..... p 3334 N92-28301 #
AD-A247397 ..... p 3349 N92-28927 #
AD-A247398 ..... p 3350 N92-28928 #
AD-A247399 ..... p 3350 N92-28929 #
AD-A247400 ..... p 3350 N92-28930 #
AD-A247402 ..... p 3250 N92-28931 #
AD-A247403 ..... p 3291 N92-28932 #
AD-A247408 ..... p 3275 N92-28905 #
AD-A247419 ..... p 3272 N92-28902 #
AD-A247421 ..... p 3290 N92-28903 #
AD-A247423 ..... p 3264 N92-28904 #
AD-A247425 ..... p 3369 N92-28866 #
AD-A247430 ..... p 3297 N92-28425 #
AD-A247464 ..... p 3262 N92-28398 #
AD-A247469 ..... p 3339 N92-28943 #
AD-A247470 ..... p 3331 N92-28944 #
AD-A247480 ..... p 3333 N92-28243 #
AD-A247481 ..... p 3367 N92-28244 #
AD-A247484 ..... p 3333 N92-28245 #
AD-A247486 ..... p 3367 N92-28246 #
AD-A247488 ..... p 3323 N92-28247 #
AD-A247489 ..... p 3240 N92-28248 #
AD-A247492 ..... p 3336 N92-28666 #
AD-A247493 ..... p 3336 N92-28667 #
AD-A247496 ..... p 3337 N92-28704 #
AD-A247497 ..... p 3318 N92-28668 #
AD-A247532 ..... p 3228 N92-28865 #
AD-A247542 ..... p 3291 N92-28933 #
AD-A247545 ..... p 3319 N92-28934 #
AD-A247546 ..... p 3316 N92-28935 #
AD-A247549 ..... p 3355 N92-28936 #
AD-A247550 ..... p 3244 N92-28937 #
AD-A247593 ..... p 3261 N92-28249 #
AD-A247594 ..... p 3262 N92-28250 #
AD-A247595 ..... p 3262 N92-28251 #
AD-A247644 ..... p 3321 N92-28321 #
AD-A247657 ..... p 3322 N92-28938 #
AD-A247663 ..... p 3322 N92-28939 #
AD-A247668 ..... p 3264 N92-28912 #
AD-A247669 ..... p 3328 N92-28940 #
AD-A247672 ..... p 3246 N92-28560 #
AD-A247679 ..... p 3263 N92-28553 #
AD-A247683 ..... p 3357 N92-28554 #
AD-A247694 ..... p 3280 N92-28561 #
AD-A247696 ..... p 3335 N92-28562 #
AD-A247707 ..... p 3264 N92-28563 #
AD-A247711 ..... p 3264 N92-28564 #
AD-A247721 ..... p 3347 N92-28399 #
AD-A247722 ..... p 3350 N92-28400 #
AD-A247724 ..... p 3344 N92-28401 #
AD-A247733 ..... p 3321 N92-28402 #
AD-A247740 ..... p 3367 N92-28403 #
AD-A247741 ..... p 3368 N92-28404 #
AD-A247744 ..... p 3263 N92-28405 #
AD-A247752 ..... p 3368 N92-28565 #
AD-A247754 ..... p 3321 N92-28566 #
AD-A247772 ..... p 3309 N92-28567 #
AD-A247773 ..... p 3280 N92-28568 #
AD-A247776 ..... p 3251 N92-28252 #
AD-A247862 ..... p 3328 N92-28957 #
AD-A247887 ..... p 3343 N92-28958 #
AD-A247889 ..... p 3253 N92-28959 #
AD-A247890 ..... p 3369 N92-28960 #
AD-A247891 ..... p 3349 N92-28961 #
AD-A247892 ..... p 3362 N92-28962 #
AD-A247913 ..... p 3322 N92-28963 #
AD-A247914 ..... p 3316 N92-28964 #
AD-A247915 ..... p 3319 N92-28965 #
AD-A247916 ..... p 3319 N92-28966 #
AD-A247917 ..... p 3322 N92-28913 #
AD-A247936 ..... p 3304 N92-29081 #
AD-A247941 ..... p 3346 N92-29082 #
AD-A247962 ..... p 3333 N92-29083 #
AD-A247968 ..... p 3276 N92-29084 #
AD-A247970 ..... p 3277 N92-29166 #
AD-A247985 ..... p 3359 N92-29167 #
AD-A248033 ..... p 3351 N92-28302 #
AD-A248050 ..... p 3251 N92-28303 #
AD-A248053 ..... p 3278 N92-28275 #
AD-A248054 ..... p 3272 N92-28304 #
AD-A248055 ..... p 3278 N92-28305 #
AD-A248057 ..... p 3250 N92-28945 #
AD-A248060 ..... p 3339 N92-28946 #
AD-A248061 ..... p 3276 N92-28947 #
AD-A248159 ..... p 3281 N92-28948 #
AD-A248201 ..... p 3340 N92-29187 #
AD-A248202 ..... p 3340 N92-29188 #
AD-A248203 ..... p 3265 N92-29189 #
AD-A248204 ..... p 3355 N92-29190 #
AD-A248205 ..... p 3272 N92-29191 #
AD-A248206 ..... p 3253 N92-29192 #
AD-A248207 ..... p 3236 N92-29222 #
AD-A248225 ..... p 3292 N92-29223 #
AD-A248230 ..... p 3341 N92-29224 #
AD-A248246 ..... p 3323 N92-29225 #
AD-A248247 ..... p 3292 N92-29226 #
AD-A248290 ..... p 3278 N92-28276 #
AD-A248305 ..... p 3265 N92-29116 #
AD-A248307 ..... p 3287 N92-28322 #

AD-A248320 ..... p 3341 N92-28306 #
AD-A248362 ..... p 3335 N92-28385 #
AD-A248372 ..... p 3259 N92-28426 #
AD-A248383 ..... p 3309 N92-28386 #
AD-A248416 ..... p 3371 N92-28843 #
AD-A248422 ..... p 3348 N92-28949 #
AD-A248429 ..... p 3283 N92-28350 #
AD-A248430 ..... p 3279 N92-28351 #
AD-A248431 ..... p 3275 N92-28878 #
AD-A248432 ..... p 3251 N92-28307 #
AD-A248440 ..... p 3298 N92-28352 #
AD-A248441 ..... p 3332 N92-29227 #
AD-A248448 ..... p 3279 N92-28427 #
AD-A248449 ..... p 3251 N92-28416 #
AD-A248457 ..... p 3344 N92-28387 #
AD-A248577 ..... p 3262 N92-28323 #
AD-A248579 ..... p 3335 N92-28428 #
AD-A248580 ..... p 3344 N92-28429 #
AD-A248581 ..... p 3240 N92-28388 #
AD-A248609 ..... p 3351 N92-28324 #
AD-A248616 ..... p 3309 N92-28569 #
AD-A248619 ..... p 3367 N92-28389 #
AD-A248620 ..... p 3335 N92-28353 #
AD-A248630 ..... p 3360 N92-28354 #
AD-A248633 ..... p 3332 N92-28891 #
AD-A248634 ..... p 3285 N92-28803 #
AD-A248665 ..... p 3303 N92-28892 #
AD-A248701 ..... p 3259 N92-28390 #
AD-A248711 ..... p 3368 N92-28430 #
AD-A248728 ..... p 3328 N92-29142 #
AD-A249106 ..... p 3264 N92-28570 #
AD-A249194 ..... p 3332 N92-28236 #
AD-A249204 ..... p 3292 N92-28293 #
AD-A249259 ..... p 3236 N92-28294 #
AD-A249260 ..... p 3278 N92-28295 #
AD-A249263 ..... p 3258 N92-28237 #
AD-A249284 ..... p 3286 N92-28879 #
AD-A249286 ..... p 3345 N92-28895 #
AD-A249287 ..... p 3327 N92-28880 #
AD-A249296 ..... p 3355 N92-28881 #
AD-A249297 ..... p 3297 N92-28851 #
AD-A249299 ..... p 3338 N92-28845 #
AD-A249300 ..... p 3274 N92-28846 #
AD-A249331 ..... p 3273 N92-28357 #
AD-A249351 ..... p 3344 N92-28325 #
AD-A249354 ..... p 3279 N92-28326 #
AD-A249358 ..... p 3298 N92-28327 #
AD-A249359 ..... p 3273 N92-28358 #
AD-A249362 ..... p 3268 N92-28359 #
AD-A249363 ..... p 3357 N92-28328 #
AD-A249365 ..... p 3346 N92-28329 #
AD-A249366 ..... p 3262 N92-28360 #
AD-A249379 ..... p 3289 N92-28330 #
AD-A249816 ..... p 3341 N92-29198 #
AD-A249940 ..... p 3248 N92-28765 #
AD-A249946 ..... p 3284 N92-28766 #
AD-A249970 ..... p 3287 N92-28767 #
AD-A249973 ..... p 3284 N92-28768 #
AD-A249982 ..... p 3287 N92-29171 #
AD-A249988 ..... p 3338 N92-28795 #
AD-A250016 ..... p 3324 N92-29089 #
AD-A250017 ..... p 3322 N92-28951 #
AD-A250018 ..... p 3340 N92-29172 #
AD-A250023 ..... p 3248 N92-28967 #
AD-A250059 ..... p 3274 N92-28796 #
AD-A250162 ..... p 3343 N92-28915 #
AD-A250164 ..... p 3265 N92-28916 #
AD-A250165 ..... p 3252 N92-28917 #
AD-A250166 ..... p 3253 N92-28918 #
AD-A250171 ..... p 3365 N92-28919 #
AD-A250173 ..... p 3326 N92-28920 #
AD-A250188 ..... p 3253 N92-28921 #
AD-A250200 ..... p 3328 N92-29144 #
AD-A250201 ..... p 3265 N92-29145 #
AD-A250203 ..... p 3328 N92-29146 #
AD-A250204 ..... p 3281 N92-29147 #
AD-A250206 ..... p 3257 N92-28896 #
AD-A250207 ..... p 3256 N92-28769 #
AD-A250208 ..... p 3342 N92-28770 #
AD-A250211 ..... p 3308 N92-29173 #
AD-A250212 ..... p 3346 N92-29149 #
AD-A250213 ..... p 3297 N92-29112 #
AD-A250216 ..... p 3343 N92-29114 #
AD-A250221 ..... p 3287 N92-29118 #
AD-A250223 ..... p 3328 N92-29119 #
AD-A250233 ..... p 3326 N92-29179 #
AD-A250244 ..... p 3358 N92-28968 #
AD-A250249 ..... p 3339 N92-28969 #
AD-A250286 ..... p 3345 N92-28970 #
AD-A250288 ..... p 3331 N92-29121 #
AD-A250300 ..... p 3252 N92-28702 #
AD-A250306 ..... p 3337 N92-28719 #
AD-A250308 ..... p 3326 N92-29123 #
AD-A250309 ..... p 3258 N92-29126 #
AD-A250313 ..... p 3339 N92-26971 #
AD-A250317 ..... p 3339 N92-28952 #
AD-A250322 ..... p 3253 N92-28953 #
AD-A250323 ..... p 3257 N92-28954 #
AD-A250324 ..... p 3369 N92-28955 #
AD-A250332 ..... p 3258 N92-29091 #
AD-A250333 ..... p 3362 N92-29093 #
AD-A250341 ..... p 3233 N92-28771 #
AD-A250384 ..... p 3281 N92-28797 #
AD-A250385 ..... p 3281 N92-28798 #
AD-A250390 ..... p 3235 N92-29180 #
AD-A250397 ..... p 3304 N92-29181 #
AD-A250407 ..... p 3241 N92-28772 #
AD-A250412 ..... p 3230 N92-29182 #
AD-A250419 ..... p 3318 N92-28799 #
AD-A250424 ..... p 3249 N92-28800 #
AD-A250433 ..... p 3274 N92-28773 #
AD-A250556 ..... p 3319 N92-28922 #
AD-A250561 ..... p 3365 N92-28923 #
AD-A250567 ..... p 3294 N92-28924 #
AD-A250629 ..... p 3245 N92-28956 #

AD-D015199 ..... p 3357 N92-28223 #
AD-D015212 ..... p 3250 N92-28224 #
AD-D015233 ..... p 3234 N92-28987
AD-D015243 ..... p 3266 N92-28739
AD-D015245 ..... p 3249 N92-28747
AD-D015248 ..... p 3249 N92-28748
AD-D015249 ..... p 3294 N92-28749
AD-D015251 ..... p 3276 N92-29085
AD-D015261 ..... p 3360 N92-29205 #
AD-D015262 ..... p 3277 N92-29199 #
AD-D015263 ..... p 3277 N92-29169 #
AD-D015264 ..... p 3261 N92-29170 #
AD-D015273 ..... p 3358 N92-29095 #
AD-D015274 ..... p 3343 N92-29096 #

AD-E200862 ..... p 3355 N92-28936 #
AD-E200869 ..... p 3309 N92-28394 #
AD-E200896 ..... p 3244 N92-28937 #
AD-E200901 ..... p 3316 N92-28935 #
AD-E200947 ..... p 3309 N92-28386 #
AD-E200950 ..... p 3309 N92-28569 #
AD-E200955 ..... p 3264 N92-28766 #
AD-E200993 ..... p 3248 N92-28765 #
AD-E951808 ..... p 3249 N92-28800 #

AEDAR-FTR-91-02 ..... p 3339 N92-28969 #

AFIT/CI/CIA-91-100 ..... p 3287 N92-29171 #
AFIT/CI/CIA-91-118 ..... p 3319 N92-28922 #

AFIT/GA/ENY/92M-02 ..... p 3253 N92-29192 #

AFIT/GCS/ENG/92M-03 ..... p 3236 N92-29222 #

AFIT/GLM/LSQ/91S-57 ..... p 3221 N92-28348 #

AFIT/GLM/LSR/91S-62 ..... p 3329 N92-28286 #

AFIT/GOR/ENS/92M-11 ..... p 3272 N92-29191 #

AFIT/GSM/ENC/91S-22 ..... p 3334 N92-28285 #

AFIT/GSM/LSM/91S-21 ..... p 3366 N92-28256 #

AFIT/GSM/LSY/91S-12 ..... p 3370 N92-28255 #

AFOSR-92-0007TR ..... p 3263 N92-28412 #
AFOSR-92-0009TR ..... p 3308 N92-28257 #
AFOSR-92-0011TR ..... p 3354 N92-28414 #
AFOSR-92-0012TR ..... p 3263 N92-28415 #
AFOSR-92-0014TR ..... p 3289 N92-28299 #
AFOSR-92-0016TR ..... p 3354 N92-28259 #
AFOSR-92-0017TR ..... p 3291 N92-28932 #
AFOSR-92-0032TR ..... p 3283 N92-28274 #
AFOSR-92-0041TR ..... p 3282 N92-28258 #
AFOSR-92-0077TR ..... p 3229 N92-28888 #
AFOSR-92-0079TR ..... p 3298 N92-28320 #
AFOSR-92-0080TR ..... p 3286 N92-28890 #
AFOSR-92-0084TR ..... p 3289 N92-28271 #
AFOSR-92-0087TR ..... p 3263 N92-28558 #
AFOSR-92-0104TR ..... p 3325 N92-28886 #
AFOSR-92-0105TR ..... p 3329 N92-29186 #
AFOSR-92-0116TR ..... p 3352 N92-28889 #
AFOSR-92-0119TR ..... p 3395 N92-28520 #
AFOSR-92-0123TR ..... p 3360 N92-28298 #
AFOSR-92-0136TR ..... p 3327 N92-28877 #
AFOSR-92-0137TR ..... p 3332 N92-28514 #
AFOSR-92-0145TR ..... p 3282 N92-28225 #
AFOSR-92-0146TR-PHASE-1 ..... p 3324 N92-28397 #
AFOSR-92-0161TR ..... p 3254 N92-28300 #
AFOSR-92-0162TR ..... p 3254 N92-28261 #
AFOSR-92-0165TR ..... p 3364 N92-28513 #
AFOSR-92-0194TR ..... p 3371 N92-28843 #
AFOSR-92-0211TR ..... p 3328 N92-28957 #
AFOSR-92-0216TR ..... p 3337 N92-28704 #
AFOSR-92-0220TR ..... p 3318 N92-28668 #
AFOSR-92-0222TR ..... p 3228 N92-28865 #
AFOSR-92-0223TR ..... p 3264 N92-28570 #
AFOSR-92-0224TR ..... p 3262 N92-28323 #
AFOSR-92-0229TR ..... p 3248 N92-28967 #
AFOSR-92-0259TR ..... p 3240 N92-28388 #
AFOSR-92-0262TR ..... p 3344 N92-28429 #
AFOSR-92-0263TR ..... p 3335 N92-28428 #
AFOSR-92-0279TR ..... p 3337 N92-28719 #
AFOSR-92-0289TR ..... p 3265 N92-29145 #
AFOSR-92-0291TR ..... p 3343 N92-29114 #
AFOSR-92-0293TR ..... p 3281 N92-29147 #
AFOSR-92-0299TR ..... p 3328 N92-29119 #
AFOSR-92-0300TR ..... p 3328 N92-29146 #
AFOSR-92-0307TR ..... p 3326 N92-29179 #
AFOSR-92-0308TR ..... p 3328 N92-29144 #
AFOSR-92-0311TR ..... p 3258 N92-29126 #
AFOSR-92-0314TR ..... p 3326 N92-29123 #
AFOSR-92-0316TR ..... p 3326 N92-28920 #
AFOSR-92-0342TR ..... p 3339 N92-28969 #
AFOSR-92-0343TR ..... p 3362 N92-29093 #
AFOSR-92-0349TR ..... p 3297 N92-29112 #
AFOSR-92-0354TR ..... p 3308 N92-29173 #
AFOSR-92-0365TR ..... p 3287 N92-29118 #
AFOSR-92-0371TR ..... p 3346 N92-29149 #
AFOSR-92-0389TR ..... p 3342 N92-28770 #
AFOSR-92-0390TR ..... p 3256 N92-28769 #
AFOSR-92-0391TR ..... p 3257 N92-28896 #
AFOSR-92-0392TR ..... p 3331 N92-29121 #

AF030-FR-LPT(1/92) ..... p 3263 N92-28412 #

AGARD-AG-329 ..... p 3235 N92-28376 #

AGARD-AR-312 ..... p 3231 N92-28468 #

AGARD-CP-513 ..... p 3221 N92-28522 #

AGARD-LS-183 ..... p 3236 N92-28458 #
AGARD-LS-186 ..... p 3231 N92-28469 #

AGARD-PAPER-2 ..... p 3232 N92-28473 * #

AIAA PAPER 92-3063 ..... p 3266 N92-28433 * #
AIAA PAPER 92-3351 ..... p 3357 N92-28475 * #
AIAA PAPER 92-3516 ..... p 3250 N92-28983 * #
AIAA PAPER 92-3570 ..... p 3236 N92-28419 * #
AIAA PAPER 92-3785 ..... p 3248 N92-28417 * #
AIAA PAPER 92-3790 ..... p 3236 N92-28418 * #
AIAA PAPER 92-3916 ..... p 3240 N92-28673 * #

AL-TP-1991-0050 ..... p 3369 N92-28866 #
AL-TP-1991-0058 ..... p 3241 N92-28975 #
AL-TP-1992-0004 ..... p 3327 N92-28880 #

AL-TR-1991-0085-VOL-1 ..... p 3340 N92-29187 #
AL-TR-1991-0085-VOL-2 ..... p 3340 N92-29188 #
AL-TR-1991-0103 ..... p 3278 N92-28276 #

ALS/TR-92-009 ..... p 3266 N92-29195 #

AMSMI-TR-RD-PR-91-17 ..... p 3249 N92-28800 #

ANL/CP-75335 ..... p 3327 N92-28775 #
ANL/CP-75375 ..... p 3262 N92-28339 #
ANL/CP-75861 ..... p 3274 N92-28810 #
ANL/CP-75862 ..... p 3274 N92-28809 #

ANL/ESD/TM-24 ..... p 3294 N92-28815 #

AR-006-376 ..... p 3351 N92-28364 #

ARAED-SP-91002 ..... p 3323 N92-28247 #

ARCCB-TR-92005 ..... p 3251 N92-28303 #
ARCCB-TR-92007 ..... p 3251 N92-28416 #

ARL-FLIGHT-MECH-TM-452 ..... p 3339 N92-28952 #

ARL-STRUC-TM-531 ..... p 3304 N92-29181 #
ARL-STRUC-TM-544 ..... p 3233 N92-28771 #
ARL-STRUC-TM-549 ..... p 3339 N92-28971 #

ARO-23306.531-MA ..... p 3346 N92-28329 #
ARO-23756.3-PH-F ..... p 3281 N92-28797 #
ARO-24981.33-MS ..... p 3297 N92-28851 #
ARO-25408.17-PH ..... p 3357 N92-28328 #
ARO-25786.1-MS-A ..... p 3298 N92-28327 #
ARO-26057.16-EG ..... p 3251 N92-28307 #
ARO-26384.11-GS ..... p 3274 N92-28846 #
ARO-26438.16-EL ..... p 3345 N92-28895 #
ARO-26711.17-EL ..... p 3278 N92-28295 #
ARO-28197.9-MA-SAH ..... p 3344 N92-28387 #
ARO-28637.1-GS-EQ ..... p 3338 N92-28845 #
ARO-28866.1-CH-SBI ..... p 3279 N92-28326 #
ARO-29004.1-EL-SBI ..... p 3289 N92-28330 #
ARO-29305.1-EL ..... p 3281 N92-28798 #

ARO-29648.1-MS-CF ..... p 3262 N92-28360 #

AVSCOM-TR-91-C-027 ..... p 3293 N92-28478 * #
AVSCOM-TR-91-C-036 ..... p 3293 N92-28434 * #
AVSCOM-TR-91-C-043 ..... p 3296 N92-29136 * #
AVSCOM-TR-91-C-045 ..... p 3302 N92-28701 * #
AVSCOM-TR-92-C-026 ..... p 3288 N92-29105 * #

B-237832 ..... p 3243 N92-28406 #

BRDEC-2525 ..... p 3294 N92-28924 #

BRL-TR-3317 ..... p 3292 N92-28284 #
BRL-TR-3328 ..... p 3257 N92-28954 #

CAL-1955 ..... p 3395 N92-28520 #

CEBAF-PR-92-001 ..... p 3354 N92-28337 #

CECOM-TR-91-3 ..... p 3277 N92-29165 #

CERL-M-92/12 ..... p 3246 N92-28560 #

CERL-N-92/07 ..... p 3351 N92-28292 #

CI-2071-92-0012 ..... p 3332 N92-28236 #

CLNS-92-1133 ..... p 3372 N92-29184 #

CMS-TSR-92-01 ..... p 3347 N92-28411 #
CMS-TSR-92-08 ..... p 3334 N92-28301 #

CONF-9102158 ..... p 3366 N92-28235 #
CONF-9104298-2 ..... p 3325 N92-28685 #
CONF-9105126-6 ..... p 3335 N92-28332 #
CONF-9106194-8 ..... p 3354 N92-28310 #
CONF-9107105-59 ..... p 3363 N92-28333 #
CONF-9108118-48 ..... p 3291 N92-29168 #
CONF-9108175-3 ..... p 3372 N92-29184 #
CONF-9108186-3 ..... p 3371 N92-28774 #
CONF-9109107-5 ..... p 3324 N92-28278 #
CONF-9109127-1 ..... p 3354 N92-28337 #
CONF-9110228-8 ..... p 3283 N92-28269 #
CONF-9110310-4 ..... p 3397 N92-28336 #
CONF-9110369 ..... p 3285 N92-28808 #
CONF-9111106-92 ..... p 3364 N92-28762 #
CONF-9111141-SUMM ..... p 3355 N92-28858 #
CONF-9111141-6 ..... p 3355 N92-28839 #
CONF-9111165-12 ..... p 3371 N92-28859 #
CONF-9111203-1 ..... p 3356 N92-28270 #
CONF-9111204-1 ..... p 3257 N92-28894 #
CONF-9111210-SUMM ..... p 3355 N92-28858 #
CONF-911202-71 ..... p 3260 N92-28854 #
CONF-911202-72 ..... p 3364 N92-28857 #
CONF-911202-74 ..... p 3260 N92-28856 #
CONF-920240-4 ..... p 3365 N92-28874 #
CONF-920299-1 ..... p 3282 N92-29197 #
CONF-9203113-1 ..... p 3368 N92-28832 #
CONF-9203126-1 ..... p 3368 N92-28838 #
CONF-920315-31 ..... p 3274 N92-28810 #
CONF-920315-32 ..... p 3274 N92-28809 #
CONF-920318-1 ..... p 3355 N92-28860 #
CONF-920331-3 ..... p 3356 N92-28356 #
CONF-920362-10 ..... p 3362 N92-29086 #
CONF-920362-15 ..... p 3334 N92-28309 #
CONF-920362-28 ..... p 3288 N92-28812 #
CONF-920373-3 ..... p 3295 N92-28925 * #
CONF-920390-2 ..... p 3342 N92-28334 #
CONF-9204102-3 ..... p 3244 N92-28226 #
CONF-9204102-4 ..... p 3245 N92-29102 #
CONF-9204102-6 ..... p 3245 N92-28861 #
CONF-9204106-3 ..... p 3341 N92-28279 #
CONF-9204115-1 ..... p 3303 N92-28855 #
CONF-920432-11 ..... p 3281 N92-28814 #
CONF-9205132-1 ..... p 3262 N92-28339 #
CONF-9205136-1 ..... p 3306 N92-28834 #
CONF-9205136-2 ..... p 3306 N92-28807 #
CONF-9205136-3 ..... p 3306 N92-28840 #
CONF-920538-18 ..... p 3327 N92-28775 #
CONF-920538-24 ..... p 3356 N92-28813 #
CONF-920540-16 ..... p 3335 N92-28342 #
CONF-920607-6 ..... p 3360 N92-28335 #
CONF-9206135-2 ..... p 3259 N92-28338 #
CONF-9206141-1 ..... p 3357 N92-28355 #
CONF-920657-2 ..... p 3255 N92-28341 #
CONF-920676-1 ..... p 3363 N92-28331 #
CONF-920707-14 ..... p 3256 N92-28822 #
CONF-920707-4 ..... p 3290 N92-28852 #
CONF-920750-1 ..... p 3347 N92-28824 #

CRDEC-TR-309 ..... p 3240 N92-28248 #

CRHC-92-11 ..... p 3297 N92-28726 * #

CRIF-MC-91 ..... p 3337 N92-28700 #

CRMSE-91-01 ..... p 3348 N92-28516 #

CRREL-SR-91-27 ..... p 3272 N92-28902 #

CSC/TM-91/6008 ..... p 3396 N92-28869 * #
CSC/TM-91/6167ROUDO ..... p 3396 N92-28872 * #

CSC/TR-92/6054 ..... p 3337 N92-28710 * #

CTN-91-60077 ..... p 3274 N92-28699 #
CTN-92-60460 ..... p 3316 N92-28703 #
CTN-92-60497 ..... p 3361 N92-28847 #
CTN-92-60498 ..... p 3361 N92-28848 #
CTN-92-60500 ..... p 3360 N92-28664 #
CTN-92-60504 ..... p 3361 N92-28849 #
CTN-92-60513 ..... p 3361 N92-28665 #

CUED/A-AERO/TR-18 ..... p 3353 N92-29201 #

DCW-R-33-01 ..... p 3283 N92-28350 #

DE92-001239 ..... p 3306 N92-28277 #
DE92-005327 ..... p 3290 N92-28852 #
DE92-006682 ..... p 3256 N92-28822 #
DE92-007300 ..... p 3347 N92-28824 #
DE92-009459 ..... p 3325 N92-28685 #
DE92-010265 ..... p 3324 N92-28278 #
DE92-010451 ..... p 3256 N92-28827 #
DE92-010518 ..... p 3266 N92-29195 #
DE92-010652 ..... p 3257 N92-28942 #
DE92-010661 ..... p 3342 N92-28381 #
DE92-010663 ..... p 3295 N92-28925 * #
DE92-010684 ..... p 3357 N92-28355 #
DE92-010667 ..... p 3363 N92-28331 #
DE92-010680 ..... p 3324 N92-28382 #
DE92-010695 ..... p 3335 N92-28332 #
DE92-010697 ..... p 3307 N92-28422 #
DE92-010701 ..... p 3282 N92-28268 #
DE92-010709 ..... p 3283 N92-28269 #
DE92-010710 ..... p 3363 N92-28333 #
DE92-010716 ..... p 3342 N92-28334 #
DE92-010718 ..... p 3360 N92-28335 #
DE92-010720 ..... p 3397 N92-28336 #
DE92-010729 ..... p 3356 N92-28270 #
DE92-010853 ..... p 3354 N92-28337 #
DE92-010871 ..... p 3259 N92-28338 #
DE92-010904 ..... p 3262 N92-28339 #
DE92-010951 ..... p 3318 N92-28340 #
DE92-010955 ..... p 3255 N92-28341 #
DE92-010957 ..... p 3335 N92-28342 #
DE92-011031 ..... p 3319 N92-28830 #
DE92-011061 ..... p 3341 N92-28279 #
DE92-011139 ..... p 3368 N92-28832 #
DE92-011147 ..... p 3364 N92-28762 #
DE92-011149 ..... p 3244 N92-28226 #
DE92-011153 ..... p 3362 N92-29086 #
DE92-011156 ..... p 3245 N92-29102 #
DE92-011194 ..... p 3256 N92-28893 #
DE92-011196 ..... p 3257 N92-28894 #
DE92-011237 ..... p 3356 N92-28356 #
DE92-011264 ..... p 3334 N92-28309 #
DE92-011267 ..... p 3306 N92-28834 #
DE92-011271 ..... p 3368 N92-28838 #
DE92-011279 ..... p 3282 N92-29197 #
DE92-011281 ..... p 3355 N92-28839 #
DE92-011285 ..... p 3354 N92-28310 #
DE92-011286 ..... p 3291 N92-29168 #
DE92-011355 ..... p 3306 N92-28840 #
DE92-011356 ..... p 3306 N92-28807 #
DE92-011357 ..... p 3365 N92-28874 #
DE92-011380 ..... p 3245 N92-28861 #
DE92-011432 ..... p 3338 N92-28841 #
DE92-011438 ..... p 3316 N92-28853 #
DE92-011645 ..... p 3260 N92-28854 #
DE92-011659 ..... p 3303 N92-28855 #
DE92-011671 ..... p 3260 N92-28856 #
DE92-011686 ..... p 3364 N92-28857 #
DE92-011734 ..... p 3371 N92-28774 #
DE92-011735 ..... p 3355 N92-28858 #
DE92-011736 ..... p 3371 N92-28859 #
DE92-011760 ..... p 3355 N92-28860 #
DE92-011839 ..... p 3327 N92-28775 #
DE92-012408 ..... p 3368 N92-28804 #
DE92-012509 ..... p 3361 N92-28805 #
DE92-012566 ..... p 3260 N92-28763 #
DE92-012658 ..... p 3355 N92-28764 #
DE92-012692 ..... p 3285 N92-28808 #
DE92-013022 ..... p 3372 N92-29184 #
DE92-013059 ..... p 3274 N92-28809 #
DE92-013060 ..... p 3274 N92-28810 #
DE92-013103 ..... p 3308 N92-28811 #
DE92-013207 ..... p 3288 N92-28812 #
DE92-013232 ..... p 3356 N92-28813 #
DE92-013233 ..... p 3281 N92-28814 #
DE92-013252 ..... p 3294 N92-28815 #
DE92-013393 ..... p 3277 N92-29131 #

DE92-013502 ..... p 3364 N92-28806 #
DE92-621530 ..... p 3361 N92-28816 #
DE92-622380 ..... p 3366 N92-28227 #
DE92-622403 ..... p 3289 N92-28228 #
DE92-622408 ..... p 3346 N92-28311 #
DE92-622409 ..... p 3366 N92-28229 #
DE92-622662 ..... p 3362 N92-28280 #
DE92-622671 ..... p 3366 N92-28230 #
DE92-622791 ..... p 3363 N92-28312 #
DE92-622792 ..... p 3362 N92-28231 #
DE92-622799 ..... p 3363 N92-28281 #
DE92-622801 ..... p 3366 N92-28232 #
DE92-782008 ..... p 3363 N92-28282 #
DE92-782046 ..... p 3292 N92-28233 #
DE92-782102 ..... p 3360 N92-28234 #
DE92-782191 ..... p 3366 N92-28235 #

DIGEL-1991-2 ..... p 3278 N92-28262 #
DIGEL-1991-7 ..... p 3278 N92-28263 #

DLR-FB-90-26 ..... p 3229 N92-29159 #
DLR-FB-91-24 ..... p 3260 N92-28823 #
DLR-FB-91-25 ..... p 3286 N92-28825 #
DLR-FB-91-27 ..... p 3245 N92-28826 #

DNA-TR-91-71 ..... p 3250 N92-28945 #

DODA-AR-006-150 ..... p 3304 N92-29181 #
DODA-AR-006-633 ..... p 3233 N92-28771 #
DODA-AR-006-656 ..... p 3339 N92-28952 #
DODA-AR-006-659 ..... p 3339 N92-28971 #
DODA-AR-006-927 ..... p 3369 N92-28955 #

DOE/AD-0019 ..... p 3368 N92-28804 #

DOE/CE-0532 ..... p 3307 N92-28422 #

DOE/ER-13183/T1 ..... p 3256 N92-28893 #
DOE/ER-13262/8 ..... p 3355 N92-28764 #
DOE/ER-13370/T1 ..... p 3257 N92-28942 #
DOE/ER-13738/T2 ..... p 3364 N92-28806 #
DOE/ER-25086/2 ..... p 3338 N92-28841 #
DOE/ER-40105/181 ..... p 3354 N92-28337 #
DOE/ER-61066/T1 ..... p 3318 N92-28340 #
DOE/ER-61072/2 ..... p 3316 N92-28853 #
DOE/ER-61220/1 ..... p 3319 N92-28830 #

DOE/PC-90293/T3 ..... p 3256 N92-28827 #

DOT/FAA/CT-TN91/32 ..... p 3230 N92-28900 #

DOT/FAA/CT-91/10 ..... p 3238 N92-28686 #

DOT/VNTSC-FAA-91-16 ..... p 3235 N92-29180 #

DREA-TM-91/214 ..... p 3264 N92-28563 #

DREO-TN-91-25 ..... p 3256 N92-28882 #
DREO-TN-91-32 ..... p 3275 N92-28687 #
DREO-TN-91-9 ..... p 3264 N92-28564 #

DREO-1093 ..... p 3287 N92-28978 #
DREO-1100 ..... p 3276 N92-28979 #

E-6354 ..... p 3229 N92-28980 * #
E-6450 ..... p 3249 N92-28682 * #
E-6622 ..... p 3293 N92-28476 * #
E-6788 ..... p 3302 N92-28701 * #
E-6827 ..... p 3240 N92-28673 * #
E-6839 ..... p 3250 N92-28983 * #
E-6930 ..... p 3227 N92-28696 * #
E-7019 ..... p 3293 N92-28434 * #
E-7033 ..... p 3246 N92-28683 * #
E-7035 ..... p 3268 N92-28436 * #
E-7038 ..... p 3286 N92-28908 * #
E-7053 ..... p 3337 N92-28684 * #
E-7060 ..... p 3296 N92-29136 * #
E-7086 ..... p 3236 N92-28418 * #
E-7109 ..... p 3236 N92-28419 * #
E-7112 ..... p 3288 N92-29105 * #
E-7113 ..... p 3238 N92-28985 * #
E-7126 ..... p 3353 N92-28984 * #
E-7130 ..... p 3248 N92-28417 * #
E-7131 ..... p 3279 N92-28432 * #
E-7144 ..... p 3280 N92-28723 * #
E-7145 ..... p 3357 N92-28475 * #
E-7148 ..... p 3227 N92-28674 * #
E-7161 ..... p 3280 N92-28675 * #
E-7173 ..... p 3266 N92-28433 * #
E-7180 ..... p 3249 N92-28693 * #
E-7184 ..... p 3307 N92-28837 * #

ECE-90-1 ..... p 3274 N92-28699 #

EE-SATCOM-86-5 ..... p 3273 N92-28586 * #

EGG-ESQ-10167 ..... p 3308 N92-28811 #

EGG-FSP-10048 ..... p 3361 N92-28805 #

EOARD-TR-92-04 ..... p 3357 N92-28372 #

ERL-0594-GD ..... p 3369 N92-28955 #

ESA-SP-1147 ..... p 3371 N92-28781 #

ESA-TT-1247 ..... p 3229 N92-29159 #

ESD-TR-91-161 ..... p 3248 N92-28366 #

ETN-92-90643 ..... p 3316 N92-28740 #
ETN-92-90846 ..... p 3337 N92-28741 #
ETN-92-91022 ..... p 3337 N92-28700 #
ETN-92-91065 ..... p 3260 N92-28823 #
ETN-92-91066 ..... p 3286 N92-28825 #
ETN-92-91067 ..... p 3245 N92-28826 #
ETN-92-91069 ..... p 3318 N92-28745
ETN-92-91207 ..... p 3229 N92-29159 #
ETN-92-91215 ..... p 3291 N92-29160
ETN-92-91228 ..... p 3241 N92-28828
ETN-92-91229 ..... p 3278 N92-28262 #
ETN-92-91230 ..... p 3342 N92-28746
ETN-92-91231 ..... p 3367 N92-29161
ETN-92-91232 ..... p 3369 N92-29162
ETN-92-91235 ..... p 3278 N92-28263 #
ETN-92-91237 ..... p 3356 N92-28264 #
ETN-92-91238 ..... p 3356 N92-28308 #
ETN-92-91241 ..... p 3351 N92-28314 #
ETN-92-91242 ..... p 3289 N92-28315 #
ETN-92-91243 ..... p 3334 N92-28265 #
ETN-92-91244 ..... p 3320 N92-28266 #
ETN-92-91245 ..... p 3348 N92-29193 #
ETN-92-91265 ..... p 3266 N92-29194 #
ETN-92-91266 ..... p 3251 N92-28572 #
ETN-92-91267 ..... p 3251 N92-28573 #
ETN-92-91268 ..... p 3303 N92-28776 #
ETN-92-91269 ..... p 3347 N92-28777 #
ETN-92-91270 ..... p 3349 N92-28778 #
ETN-92-91271 ..... p 3338 N92-28779 #
ETN-92-91272 ..... p 3249 N92-28780 #
ETN-92-91276 ..... p 3371 N92-28781 #
ETN-92-91281 ..... p 3349 N92-28647 #
ETN-92-91320 ..... p 3343 N92-28782 #
ETN-92-91321 ..... p 3280 N92-28783 #
ETN-92-91322 ..... p 3281 N92-28784 #
ETN-92-91323 ..... p 3338 N92-28785 #
ETN-92-91324 ..... p 3338 N92-28842 #
ETN-92-91325 ..... p 3229 N92-29206 #
ETN-92-91326 ..... p 3284 N92-28788 #
ETN-92-91327 ..... p 3228 N92-28789 #
ETN-92-91328 ..... p 3325 N92-28844 #
ETN-92-91329 ..... p 3338 N92-28790 #
ETN-92-91330 ..... p 3365 N92-29207 #
ETN-92-91331 ..... p 3282 N92-29208 #
ETN-92-91332 ..... p 3341 N92-29209 #
ETN-92-91333 ..... p 3364 N92-28786 #
ETN-92-91334 ..... p 3274 N92-28792 #
ETN-92-91335 ..... p 3327 N92-28787 #
ETN-92-91336 ..... p 3272 N92-28793 #
ETN-92-91340 ..... p 3356 N92-29210 #
ETN-92-91344 ..... p 3323 N92-29215 #
ETN-92-91345 ..... p 3323 N92-29216 #
ETN-92-91346 ..... p 3322 N92-29211 #
ETN-92-91347 ..... p 3323 N92-29212 #
ETN-92-91348 ..... p 3323 N92-29213 #
ETN-92-91349 ..... p 3348 N92-29214 #
ETN-92-91353 ..... p 3296 N92-29217 #
ETN-92-91373 ..... p 3288 N92-29163
ETN-92-91376 ..... p 3261 N92-29164
ETN-92-91391 ..... p 3397 N92-29218 #
ETN-92-91392 ..... p 3397 N92-29219 #
ETN-92-91394 ..... p 3253 N92-29220 #
ETN-92-91395 ..... p 3260 N92-28794 #
ETN-92-91396 ..... p 3259 N92-28574 #
ETN-92-91397 ..... p 3299 N92-28575 #
ETN-92-91398 ..... p 3259 N92-28576 #
ETN-92-91399 ..... p 3252 N92-28577 #
ETN-92-91400 ..... p 3259 N92-28578 #
ETN-92-91401 ..... p 3240 N92-28579 #
ETN-92-91402 ..... p 3299 N92-28580 #
ETN-92-91403 ..... p 3345 N92-28581 #
ETN-92-91404 ..... p 3252 N92-28582 #
ETN-92-91405 ..... p 3299 N92-28583 #
ETN-92-91406 ..... p 3341 N92-29221 #
ETN-92-91431 ..... p 3345 N92-28648 #
ETN-92-91432 ..... p 3232 N92-28649 #
ETN-92-91433 ..... p 3302 N92-28650 #
ETN-92-91434 ..... p 3233 N92-28651 #
ETN-92-91435 ..... p 3239 N92-28652 #
ETN-92-91436 ..... p 3239 N92-28653 #
ETN-92-91437 ..... p 3236 N92-28654 #
ETN-92-91438 ..... p 3235 N92-28644 #

ETN-92-91439 ..... p 3230 N92-28655 #
ETN-92-91441 ..... p 3358 N92-28656 #
ETN-92-91442 ..... p 3294 N92-28705 #
ETN-92-91444 ..... p 3293 N92-28645 #
ETN-92-91445 ..... p 3293 N92-28646 #
ETN-92-91446 ..... p 3233 N92-28687 #
ETN-92-91447 ..... p 3232 N92-28634 #
ETN-92-91448 ..... p 3347 N92-28635 #
ETN-92-91450 ..... p 3226 N92-28657 #
ETN-92-91451 ..... p 3336 N92-28636 #
ETN-92-91452 ..... p 3252 N92-28637 #
ETN-92-91455 ..... p 3336 N92-28638 #
ETN-92-91456 ..... p 3336 N92-28639 #
ETN-92-91457 ..... p 3348 N92-28640 #
ETN-92-91458 ..... p 3347 N92-28641 #
ETN-92-91459 ..... p 3342 N92-28642 #
ETN-92-91484 ..... p 3371 N92-29177 #
ETN-92-91485 ..... p 3282 N92-29178 #
ETN-92-91486 ..... p 3371 N92-29127 #
ETN-92-91487 ..... p 3371 N92-29128 #
ETN-92-91512 ..... p 3226 N92-28658 #
ETN-92-91515 ..... p 3342 N92-28706 #
ETN-92-91516 ..... p 3305 N92-28708 #
ETN-92-91518 ..... p 3227 N92-28659 #
ETN-92-91519 ..... p 3227 N92-28660 #
ETN-92-91520 ..... p 3240 N92-28669 #
ETN-92-91521 ..... p 3302 N92-28643 #
ETN-92-91522 ..... p 3302 N92-28688 #
ETN-92-91523 ..... p 3316 N92-28689 #
ETN-92-91524 ..... p 3305 N92-28690 #
ETN-92-91530 ..... p 3228 N92-28709 #
ETN-92-91531 ..... p 3238 N92-28711 #
ETN-92-91533 ..... p 3284 N92-28712 #
ETN-92-91534 ..... p 3260 N92-28691 #
ETN-92-91535 ..... p 3227 N92-28692 #
ETN-92-91536 ..... p 3240 N92-28661 #
ETN-92-91537 ..... p 3241 N92-29204 #
ETN-92-91538 ..... p 3303 N92-28850 #
ETN-92-91539 ..... p 3304 N92-29176 #
ETN-92-91540 ..... p 3284 N92-28694 #
ETN-92-91541 ..... p 3352 N92-28695 #
ETN-92-91542 ..... p 3305 N92-28697 #
ETN-92-91543 ..... p 3228 N92-28713 #
ETN-92-91544 ..... p 3233 N92-28714 #
ETN-92-91545 ..... p 3345 N92-28716 #
ETN-92-98303 ..... p 3349 N92-28313 #

ETS-RR-92-9-ONR ..... p 3348 N92-28273 #

FAA-APO-92-1 ..... p 3230 N92-29182 #

FEL-91-A163 ..... p 3291 N92-29160
FEL-91-B345 ..... p 3241 N92-28828

FFA-TN-1992-02 ..... p 3253 N92-29220 #

FFI-91/7017 ..... p 3351 N92-28314 #
FFI-91/7020 ..... p 3289 N92-28315 #
FFI-91/7021 ..... p 3334 N92-28265 #
FFI-91/7022 ..... p 3320 N92-28266 #
FFI-91/7023 ..... p 3348 N92-29193 #

FFP-2-91 ..... p 3361 N92-28849 #
FFP-4-91 ..... p 3360 N92-28664 #

FIA-91-13 ..... p 3346 N92-29175 * #
FIA-92-02 ..... p 3345 N92-28759 * #
FIA-92-13 ..... p 3337 N92-28758 * #

FNAL/C-91/349-A ..... p 3371 N92-28774 #
FNAL/C-92/20-A ..... p 3371 N92-28859 #
FNAL/C-92/26A ..... p 3355 N92-28858 #
FNAL/C-92/62 ..... p 3355 N92-28839 #
FNAL/C-92/66 ..... p 3262 N92-29197 #
FNAL/C-92/72-A ..... p 3372 N92-29184 #

GAO/IMTEC-92-50 ..... p 3243 N92-28406 #

GARTEUR/TP-056 ..... p 3239 N92-28652 #

GRI-92/0064 ..... p 3266 N92-28914 #

H-1769 ..... p 3239 N92-28584 * #
H-1833 ..... p 3234 N92-29110 * #

HEL-TN-1-92 ..... p 3326 N92-28396 #

IC-91/234 ..... p 3289 N92-28228 #
IC-91/282 ..... p 3363 N92-28281 #
IC-91/287 ..... p 3363 N92-28312 #
IC-91/292 ..... p 3362 N92-28231 #
IC-91/304 ..... p 3346 N92-28311 #
IC-91/308 ..... p 3362 N92-28280 #
IC-91/376 ..... p 3366 N92-28229 #
IC-91/389 ..... p 3366 N92-28232 #
IC-91/396 ..... p 3366 N92-28227 #

ICASE-IR-21 ..... p 3337 N92-28760 * #

INO-SP-4 ..... p 3340 N92-29172 #

INO-TM-7 ..... p 3322 N92-28951 #

INS-T-506 ..... p 3366 N92-28235 #

INT-PATENT-CLASS-A47H-1/144 p 3295 N92-29092 *
INT-PATENT-CLASS-A61B-3/14 . p 3325 N92-28755 *

INT-PATENT-CLASS-B05C-17/02 p 3294 N92-28754 *
INT-PATENT-CLASS-B23K-1/00 . p 3261 N92-29094 *
INT-PATENT-CLASS-B25G-3/00 . p 3296 N92-29140 *
INT-PATENT-CLASS-B32B-15/01 p 3265 N92-29090 *
INT-PATENT-CLASS-B32B-15/20 p 3265 N92-29090 *
INT-PATENT-CLASS-B32B-5/02 . p 3265 N92-29090 *
INT-PATENT-CLASS-B64C-3/14 . p 3228 N92-28729 *
INT-PATENT-CLASS-B64G-1/62 . p 3294 N92-28727 *
INT-PATENT-CLASS-B64G-1/64 . p 3248 N92-28750 *
INT-PATENT-CLASS-B66C-1/62 . p 3296 N92-29138 *

INT-PATENT-CLASS-C07D-271/10 p 3250 N92-29141 *
INT-PATENT-CLASS-C08F-283/04 p 3265 N92-29157 *
INT-PATENT-CLASS-C08G-73/08 p 3250 N92-29141 *
INT-PATENT-CLASS-C25B-1/04 . p 3256 N92-28756 *
INT-PATENT-CLASS-C25B-1/12 . p 3256 N92-28756 *

INT-PATENT-CLASS-F03G-6/00 . p 3307 N92-29143 *
INT-PATENT-CLASS-F16B-37/08 p 3296 N92-29150 *
INT-PATENT-CLASS-F16C-32/04 p 3295 N92-29099 *
INT-PATENT-CLASS-F16C-9/00 . p 3295 N92-29120 *
INT-PATENT-CLASS-F25B-19/02 p 3288 N92-29156 *
INT-PATENT-CLASS-F28D-15/02 p 3287 N92-29125 *
INT-PATENT-CLASS-F28D-17/00 p 3284 N92-28752 *

INT-PATENT-CLASS-G01C-21/00 p 3320 N92-29148 *
INT-PATENT-CLASS-G01D-5/34 . p 3359 N92-29133 *
INT-PATENT-CLASS-G01J-1/20 . p 3359 N92-29122 *
INT-PATENT-CLASS-G01L-7/08 . p 3288 N92-29097 *
INT-PATENT-CLASS-G01L-9/06 . p 3288 N92-29097 *
INT-PATENT-CLASS-G01N-27/26 p 3255 N92-28728 *
INT-PATENT-CLASS-G01N-27/72 p 3351 N92-29130 *
INT-PATENT-CLASS-G01N-27/80 p 3303 N92-28757 *
INT-PATENT-CLASS-G01R-23/16 p 3276 N92-29124 *
INT-PATENT-CLASS-G01R-27/72 p 3304 N92-29101 *
INT-PATENT-CLASS-G01R-33/12 p 3303 N92-28757 *
INT-PATENT-CLASS-G01R-33/12 p 3304 N92-29101 *
INT-PATENT-CLASS-G01R-35/00 p 3298 N92-29154 *
INT-PATENT-CLASS-G02B-26/02 p 3296 N92-29151 *
INT-PATENT-CLASS-G02F-1/01 . p 3359 N92-29117 *
INT-PATENT-CLASS-G05G-9/00 p 3281 N92-29153 *
INT-PATENT-CLASS-G06K-9/00 . p 3331 N92-29129 *
INT-PATENT-CLASS-G11B-17/22 p 3333 N92-29132 *
INT-PATENT-CLASS-G11B-3/74 . p 3333 N92-29132 *
INT-PATENT-CLASS-G11B-5/09 . p 3333 N92-29132 *
INT-PATENT-CLASS-G21K-7/00 . p 3288 N92-29135 *

INT-PATENT-CLASS-H01M-10/40 p 3280 N92-28753 *
INT-PATENT-CLASS-H01P-1/18 . p 3358 N92-28571 *
INT-PATENT-CLASS-H02K-1/14 . p 3295 N92-29099 *

IOS-273-1990 ..... p 3323 N92-29216 #
IOS-285-1991 ..... p 3322 N92-29211 #
IOS-286-1991 ..... p 3323 N92-29212 #
IOS-288-1991 ..... p 3323 N92-29213 #

IPPCZ-314 ..... p 3361 N92-28742 #

IS-M-700 ..... p 3259 N92-28338 #

ISBN-0-16-036173-7 ..... p 3372 N92-28345 * #
ISBN-0-16-036174-5 ..... p 3397 N92-28344 * #
ISBN-0-309-04731-5 ..... p 3350 N92-28363 #
ISBN-0-315-51071-4 ..... p 3316 N92-28703 #
ISBN-92-835-0656-1 ..... p 3221 N92-28522 #
ISBN-92-835-0657-X ..... p 3235 N92-28376 #
ISBN-92-835-0668-5 ..... p 3231 N92-28468 #
ISBN-92-835-0674-X ..... p 3236 N92-28458 #
ISBN-92-835-0675-8 ..... p 3231 N92-28469 #
ISBN-92-9092-025-4 ..... p 3371 N92-28781 #
ISBN-951-38-3989-3 ..... p 3266 N92-29194 #
ISBN-951-38-3990-7 ..... p 3251 N92-28572 #
ISBN-951-38-3991-5 ..... p 3251 N92-28573 #
ISBN-951-38-3994-X ..... p 3303 N92-28776 #

ISSN-0078-3781 ..... p 3347 N92-28777 #
ISSN-0078-3781 ..... p 3349 N92-28778 #
ISSN-0078-3781 ..... p 3338 N92-28779 #
ISSN-0078-3781 ..... p 3249 N92-28780 #
ISSN-0171-1342 ..... p 3229 N92-29159 #
ISSN-0309-7293 ..... p 3353 N92-29201 #
ISSN-0358-5077 ..... p 3251 N92-28572 #
ISSN-0358-5077 ..... p 3251 N92-28573 #
ISSN-0358-5077 ..... p 3303 N92-28776 #
ISSN-0358-5077 ..... p 3266 N92-29194 #

ISSN-0389-4010 ..... p 3234 N92-28901 #
ISSN-0452-2982 ..... p 3241 N92-28829 #
ISSN-0452-2982 ..... p 3331 N92-28831 #
ISSN-0452-2982 ..... p 3241 N92-28833 #
ISSN-0452-2982 ..... p 3241 N92-28835 #
ISSN-0452-2982 ..... p 3303 N92-28836 #
ISSN-0602-2437 ..... p 3334 N92-28265 #
ISSN-0802-2437 ..... p 3320 N92-28266 #
ISSN-0802-2437 ..... p 3351 N92-28314 #
ISSN-0802-2437 ..... p 3289 N92-28315 #
ISSN-0802-2437 ..... p 3348 N92-29193 #
ISSN-0922-5641 ..... p 3341 N92-29221 #
ISSN-0924-2082 ..... p 3348 N92-29214 #
ISSN-0926-4493 ..... p 3336 N92-28638 #
ISSN-0926-4493 ..... p 3336 N92-28639 #
ISSN-0926-4493 ..... p 3348 N92-28640 #
ISSN-0938-2194 ..... p 3397 N92-29219 #
ISSN-0939-2963 ..... p 3260 N92-28823 #
ISSN-0939-2963 ..... p 3286 N92-28825 #
ISSN-0939-2963 ..... p 3245 N92-28826 #
ISSN-0939-2971 ..... p 3397 N92-29218 #
ISSN-0955-9655 ..... p 3288 N92-29163
ISSN-0959-2423 ..... p 3261 N92-29164

ISVR-TR-202-PT-2 ..... p 3353 N92-29203 #

ITF-91-28 ..... p 3361 N92-28816 #

ITLI-LP-91-01 ..... p 3348 N92-29214 #

ITN-92-85131 ..... p 3244 N92-29098 #

IZF-1991-B-4 ..... p 3342 N92-28746
IZF-1991-B-8 ..... p 3367 N92-29161
IZF-1991-B-9 ..... p 3369 N92-29162

JAERI-M-91-178 ..... p 3363 N92-28282 #
JAERI-M-91-197 ..... p 3292 N92-28233 #

JHU/APL-TG-1379 ..... p 3279 N92-28367 #
JHU/APL-TG-1380 ..... p 3338 N92-28795 #
JHU/APL-TG-1381 ..... p 3275 N92-28905 #

JPL-BIBL-39-31 ..... p 3369 N92-29202 * #

JPL-PUBL-90-50 ..... p 3291 N92-28941 * #
JPL-PUBL-91-27 ..... p 3305 N92-28950 * #

JPL-9950-1382 ..... p 3273 N92-28586 * #

JTN-92-80350 ..... p 3241 N92-28829 #
JTN-92-80351 ..... p 3331 N92-28831 #
JTN-92-80352 ..... p 3241 N92-28833 #
JTN-92-80362 ..... p 3241 N92-28835 #
JTN-92-80363 ..... p 3303 N92-28836 #
JTN-92-80381 ..... p 3234 N92-28901 #

KCP-613-4547 ..... p 3260 N92-28763 #

KU-FRL-872-5 ..... p 3233 N92-28720 * #

L-16967 ..... p 3290 N92-28862 * #
L-16983 ..... p 3344 N92-28375 * #
L-16996 ..... p 3226 N92-28477 * #
L-17025 ..... p 3255 N92-28374 * #

LA-UR-92-653 ..... p 3368 N92-28838 #
LA-UR-92-706 ..... p 3365 N92-28874 #
LA-UR-92-708 ..... p 3306 N92-28807 #
LA-UR-92-709 ..... p 3306 N92-28840 #
LA-UR-92-751 ..... p 3354 N92-28310 #
LA-UR-92-754 ..... p 3291 N92-29168 #
LA-UR-92-764 ..... p 3306 N92-28834 #
LA-UR-92-837 ..... p 3334 N92-28309 #
LA-UR-92-936 ..... p 3356 N92-28356 #

LA-12287-T ..... p 3282 N92-28268 #

LAAS-91307 ..... p 3365 N92-29207 #
LAAS-91360 ..... p 3282 N92-29208 #
LAAS-91378 ..... p 3341 N92-29209 #

LAMP-91/9 ..... p 3366 N92-28230 #

LBL-31398 ..... p 3324 N92-28278 #
LBL-31457 ..... p 3364 N92-28762 #

LC-90-39761 ..... p 3397 N92-28344 * #
LC-91-33408 ..... p 3372 N92-28345 * #
LC-92-10780 ..... p 3350 N92-28363 #

LPI-CONTRIB-787 ..... p 3372 N92-28478 * #

LPI-TR-92-02 ..... p 3378 N92-28988 * #
LPI-TR-92-03 ..... p 3310 N92-28587 * #

LR-651 ..... p 3259 N92-28574 #
LR-657 ..... p 3299 N92-28575 #
LR-658 ..... p 3259 N92-28576 #
LR-659 ..... p 3252 N92-28577 #
LR-661 ..... p 3259 N92-28578 #
LR-662 ..... p 3240 N92-28579 #
LR-664 ..... p 3299 N92-28580 #
LR-665 ..... p 3345 N92-28581 #
LR-666 ..... p 3252 N92-28582 #
LR-667 ..... p 3299 N92-28583 #

M-692 ..... p 3333 N92-28899 * #

MEMO-COSOR-91-21 ..... p 3336 N92-28638 #
MEMO-COSOR-91-22 ..... p 3336 N92-28639 #
MEMO-COSOR-91-23 ..... p 3348 N92-28640 #
MEMO-COSOR-91-24 ..... p 3347 N92-28641 #
MEMO-COSOR-91-25 ..... p 3342 N92-28642 #

MPL-U-10/92 ..... p 3321 N92-28402 #

MRL-TR-91-23 ..... p 3351 N92-28364 #

MSRR-569 ..... p 3349 N92-28927 #
MSRR-570 ..... p 3350 N92-28928 #
MSRR-574 ..... p 3350 N92-28929 #
MSRR-575 ..... p 3350 N92-28930 #
MSRR-578 ..... p 3268 N92-28359 #

MSSU-EIRS-ERC-91-1 ..... p 3283 N92-28555 * #

MTL-TR-92-18 ..... p 3252 N92-28702 #
MTL-TR-92-4 ..... p 3262 N92-28250 #
MTL-TR-92-5 ..... p 3297 N92-28425 #
MTL-TR-92-6 ..... p 3261 N92-28249 #

MTR-11227-VOL-1 ..... p 3278 N92-28305 #

M91-114 ..... p 3272 N92-28304 #

NADC-91087-60 ..... p 3253 N92-28921 #
NADC-91113-50 ..... p 3352 N92-28413 #

NAL-TM-632 ..... p 3241 N92-28829 #
NAL-TM-633 ..... p 3331 N92-28831 #
NAL-TM-634 ..... p 3241 N92-28835 #
NAL-TM-635 ..... p 3241 N92-28833 #
NAL-TM-636 ..... p 3303 N92-28836 #

NAL-TR-1112 ..... p 3234 N92-28901 #

NAMRL-TM-91-2 ..... p 3240 N92-28407 #

NAMRL-1367 ..... p 3327 N92-28557 #

NAS 1.15:102192 ..... p 3239 N92-28457 * #
NAS 1.15:103586 ..... p 3279 N92-28456 * #
NAS 1.15:103588 ..... p 3330 N92-28521 * #
NAS 1.15:103589 ..... p 3355 N92-28986 * #
NAS 1.15:103590 ..... p 3229 N92-28981 * #
NAS 1.15:103865 ..... p 3327 N92-28744 * #
NAS 1.15:103873 ..... p 3234 N92-28926 * #
NAS 1.15:103892 ..... p 3245 N92-29104 * #
NAS 1.15:103902 ..... p 3234 N92-28910 * #
NAS 1.15:103906 ..... p 3231 N92-29103 * #
NAS 1.15:103913 ..... p 3325 N92-28420 * #
NAS 1.15:103914 ..... p 3349 N92-28672 * #
NAS 1.15:103915 ..... p 3353 N92-28909 * #
NAS 1.15:103918 ..... p 3255 N92-28743 * #
NAS 1.15:103925 ..... p 3233 N92-28721 * #
NAS 1.15:104564 ..... p 3244 N92-28343 * #
NAS 1.15:104567 ..... p 3346 N92-28297 * #
NAS 1.15:105161 ..... p 3249 N92-28682 * #
NAS 1.15:105396 ..... p 3302 N92-28701 * #
NAS 1.15:105417 ..... p 3240 N92-28673 * #
NAS 1.15:105636 ..... p 3250 N92-28983 * #
NAS 1.15:105653 ..... p 3293 N92-28476 * #
NAS 1.15:105655 ..... p 3293 N92-28434 * #
NAS 1.15:105660 ..... p 3246 N92-28683 * #
NAS 1.15:105681 ..... p 3296 N92-29136 * #
NAS 1.15:105698 ..... p 3236 N92-28418 * #
NAS 1.15:105715 ..... p 3236 N92-28419 * #
NAS 1.15:105716 ..... p 3238 N92-28985 * #
NAS 1.15:105717 ..... p 3288 N92-29105 * #
NAS 1.15:105722 ..... p 3353 N92-28984 * #
NAS 1.15:105727 ..... p 3248 N92-28417 * #
NAS 1.15:105728 ..... p 3279 N92-28432 * #
NAS 1.15:105739 ..... p 3357 N92-28475 * #
NAS 1.15:105743 ..... p 3227 N92-28674 * #
NAS 1.15:105745 ..... p 3227 N92-28696 * #
NAS 1.15:105749 ..... p 3337 N92-28684 * #
NAS 1.15:105753 ..... p 3280 N92-28675 * #
NAS 1.15:105759 ..... p 3266 N92-28433 * #
NAS 1.15:105763 ..... p 3249 N92-28693 * #
NAS 1.15:105767 ..... p 3307 N92-28837 * #
NAS 1.15:107544 ..... p 3330 N92-28670 * #

NAS 1.15:107586 ..... p 3231 N92-28435 * #
NAS 1.15:107589 ..... p 3275 N92-28876 * #
NAS 1.15:107844 ..... p 3346 N92-29175 * #
NAS 1.15:107859 ..... p 3337 N92-28758 * #
NAS 1.15:107875 ..... p 3345 N92-28759 * #
NAS 1.15:107878 ..... p 3329 N92-29174 * #
NAS 1.15:107937 ..... p 3246 N92-28370 * #
NAS 1.15:107938 ..... p 3334 N92-28267 * #
NAS 1.15:107941 ..... p 3246 N92-28369 * #
NAS 1.15:107944 ..... p 3396 N92-28907 * #
NAS 1.15:107946 ..... p 3396 N92-28870 * #
NAS 1.15:107947 ..... p 3396 N92-28869 * #
NAS 1.15:107954 ..... p 3244 N92-29100 * #
NAS 1.15:107958 ..... p 3295 N92-28925 * #
NAS 1.15:4392 ..... p 3333 N92-28899 * #
NAS 1.15:4396 ..... p 3234 N92-29110 * #
NAS 1.19:278 ..... p 3366 N92-28864 * #
NAS 1.21:4104 ..... p 3397 N92-28344 * #
NAS 1.21:508 ..... p 3372 N92-28345 * #
NAS 1.21:7037(275) ..... p 3226 N92-28679 *
NAS 1.21:7037(278) ..... p 3226 N92-28677 *
NAS 1.26:177597 ..... p 3330 N92-28681 * #
NAS 1.26:184328 ..... p 3292 N92-28362 * #
NAS 1.26:186957 ..... p 3291 N92-29139 * #
NAS 1.26:189153 ..... p 3298 N92-28296 * #
NAS 1.26:189176 ..... p 3286 N92-28908 * #
NAS 1.26:189185 ..... p 3273 N92-28431 * #
NAS 1.26:189186 ..... p 3275 N92-28906 * #
NAS 1.26:189194 ..... p 3280 N92-28723 * #
NAS 1.26:189621 ..... p 3336 N92-28585 * #
NAS 1.26:189629 ..... p 3337 N92-28760 * #
NAS 1.26:189635 ..... p 3352 N92-28722 * #
NAS 1.26:189643 ..... p 3352 N92-28556 * #
NAS 1.26:189752 ..... p 3297 N92-28726 * #
NAS 1.26:189881 ..... p 3283 N92-28555 * #
NAS 1.26:190269 ..... p 3367 N92-29111 * #
NAS 1.26:190364 ..... p 3285 N92-28817 * #
NAS 1.26:190378 ..... p 3396 N92-28872 * #
NAS 1.26:190384 ..... p 3341 N92-29200 * #
NAS 1.26:190387 ..... p 3370 N92-29108 * #
NAS 1.26:190398 ..... p 3305 N92-28715 * #
NAS 1.26:190400 ..... p 3283 N92-28361 * #
NAS 1.26:190408 ..... p 3273 N92-28371 * #
NAS 1.26:190418 ..... p 3378 N92-28988 * #
NAS 1.26:190419 ..... p 3310 N92-28587 * #
NAS 1.26:190421 ..... p 3307 N92-28863 * #
NAS 1.26:190422 ..... p 3276 N92-29115 * #
NAS 1.26:190431 ..... p 3226 N92-28511 * #
NAS 1.26:190444 ..... p 3233 N92-28720 * #
NAS 1.26:190445 ..... p 3306 N92-28717 * #
NAS 1.26:190448 ..... p 3330 N92-28671 * #
NAS 1.26:190449 ..... p 3291 N92-28941 * #
NAS 1.26:190456 ..... p 3305 N92-28950 * #
NAS 1.26:190457 ..... p 3369 N92-29202 * #
NAS 1.26:190468 ..... p 3321 N92-28867 * #
NAS 1.26:190469 ..... p 3230 N92-28718 * #
NAS 1.26:190472 ..... p 3319 N92-29087 * #
NAS 1.26:190477 ..... p 3370 N92-28680 * #
NAS 1.26:190484 ..... p 3273 N92-28586 * #
NAS 1.26:190486 ..... p 3342 N92-28676 * #
NAS 1.26:190487 ..... p 3295 N92-29134 * #
NAS 1.26:190490 ..... p 3358 N92-29088 * #
NAS 1.26:190493 ..... p 3353 N92-29196 * #
NAS 1.26:190495 ..... p 3358 N92-28868 * #
NAS 1.26:190501 ..... p 3290 N92-28707 * #
NAS 1.26:190503 ..... p 3337 N92-28710 * #
NAS 1.26:190508 ..... p 3372 N92-28478 * #
NAS 1.26:190509 ..... p 3275 N92-28873 * #
NAS 1.26:190510 ..... p 3396 N92-28871 * #
NAS 1.26:190521 ..... p 3316 N92-28911 * #
NAS 1.26:190531 ..... p 3358 N92-28698 * #
NAS 1.26:190551 ..... p 3343 N92-29109 * #
NAS 1.26:190552 ..... p 3339 N92-28875 * #
NAS 1.26:190554 ..... p 3340 N92-29107 * #
NAS 1.26:190556 ..... p 3339 N92-29106 * #
NAS 1.26:190557 ..... p 3340 N92-29113 * #
NAS 1.26:4443 ..... p 3239 N92-28584 * #
NAS 1.55:10094 ..... p 3268 N92-28436 * #
NAS 1.55:10099 ..... p 3247 N92-28730 * #
NAS 1.55:3153 ..... p 3299 N92-28620 * #
NAS 1.60:3197 ..... p 3226 N92-28477 * #
NAS 1.60:3198 ..... p 3344 N92-28375 * #
NAS 1.60:3200 ..... p 3331 N92-28897 * #
NAS 1.60:3224 ..... p 3255 N92-28374 * #
NAS 1.60:3252 ..... p 3229 N92-28980 * #
NAS 1.77:10001 ..... p 3290 N92-28862 * #
NAS 1.83:150 ..... p 3397 N92-28678 * #

NASA-CASE-GSC-13175-1 ..... p 3359 N92-29133 *
NASA-CASE-GSC-13187-1 ..... p 3281 N92-29153 *
NASA-CASE-GSC-13189-2 ..... p 3296 N92-29151 *
NASA-CASE-GSC-13196-1 ..... p 3333 N92-29132 *
NASA-CASE-GSC-13220-1 ..... p 3296 N92-29140 *
NASA-CASE-GSC-13230-1 ..... p 3294 N92-28754 *
NASA-CASE-GSC-13251-1 ..... p 3295 N92-29120 *
NASA-CASE-GSC-13261-1 ..... p 3296 N92-29138 *

NASA-CASE-GSC-13344-1 ..... p 3261 N92-29094 *
NASA-CASE-GSC-13346-1 ..... p 3295 N92-29099 *
NASA-CASE-GSC-13366-1 ..... p 3298 N92-29154 *

NASA-CASE-LAR-13616-3 ..... p 3359 N92-29158 *
NASA-CASE-LAR-13669-1 ..... p 3265 N92-29157 *
NASA-CASE-LAR-13817-2 ..... p 3304 N92-29155 *
NASA-CASE-LAR-13817-4 ..... p 3304 N92-29101 *
NASA-CASE-LAR-13817-5 ..... p 3303 N92-28757 *
NASA-CASE-LAR-14033-1 ..... p 3284 N92-28752 *
NASA-CASE-LAR-14145-1 ..... p 3264 N92-28751 *
NASA-CASE-LAR-14281-1 ..... p 3228 N92-28729 *
NASA-CASE-LAR-14427-1 ..... p 3250 N92-29141 *
NASA-CASE-LAR-14579-1 ..... p 3288 N92-29097 *
NASA-CASE-LAR-14588-1-CU ..... p 3359 N92-29117 *

NASA-CASE-LEW-14878-1 ..... p 3358 N92-28571 *
NASA-CASE-LEW-14949-1 ..... p 3307 N92-29143 *
NASA-CASE-LEW-15077-1 ..... p 3253 N92-29152 *
NASA-CASE-LEW-15155-1 ..... p 3265 N92-29090 *
NASA-CASE-LEW-15196-1 ..... p 3295 N92-29092 *
NASA-CASE-LEW-15235-1 ..... p 3287 N92-29125 *

NASA-CASE-MFS-26049-2-NP .... p 3255 N92-28728 *
NASA-CASE-MFS-28421-1 ..... p 3248 N92-28750 *
NASA-CASE-MFS-28485-1 ..... p 3288 N92-29135 *

NASA-CASE-MSC-21572-1-SB .... p 3256 N92-28756 *
NASA-CASE-MSC-21589-1 ..... p 3332 N92-29137 *
NASA-CASE-MSC-21675-1 ..... p 3325 N92-28755 *
NASA-CASE-MSC-21799-1 ..... p 3296 N92-29150 *
NASA-CASE-MSC-21906-1 ..... p 3294 N92-28727 *

NASA-CASE-NPO-17552-1-CU .... p 3331 N92-29129 *
NASA-CASE-NPO-17759-1-CU .... p 3276 N92-29124 *
NASA-CASE-NPO-17922-1-CU .... p 3280 N92-28753 *
NASA-CASE-NPO-18095-1-CU .... p 3359 N92-29122 *
NASA-CASE-NPO-18115-1-CU .... p 3320 N92-29148 *
NASA-CASE-NPO-18184-1-CU .... p 3288 N92-29156 *
NASA-CASE-NPO-18187-1-CU .... p 3351 N92-29130 *

NASA-CP-10094 ..... p 3268 N92-28436 * #
NASA-CP-10099 ..... p 3247 N92-28730 * #
NASA-CP-3153 ..... p 3299 N92-28620 * #

NASA-CR-177597 ..... p 3330 N92-28681 * #
NASA-CR-184328 ..... p 3292 N92-28362 * #
NASA-CR-186957 ..... p 3291 N92-29139 * #
NASA-CR-189153 ..... p 3298 N92-28296 * #
NASA-CR-189176 ..... p 3286 N92-28908 * #
NASA-CR-189185 ..... p 3273 N92-28431 * #
NASA-CR-189186 ..... p 3275 N92-28906 * #
NASA-CR-189194 ..... p 3280 N92-28723 * #
NASA-CR-189621 ..... p 3336 N92-28585 * #
NASA-CR-189629 ..... p 3337 N92-28760 * #
NASA-CR-189635 ..... p 3352 N92-28722 * #
NASA-CR-189643 ..... p 3352 N92-28556 * #
NASA-CR-189752 ..... p 3297 N92-28726 * #
NASA-CR-189861 ..... p 3283 N92-28555 * #
NASA-CR-190269 ..... p 3367 N92-29111 * #
NASA-CR-190364 ..... p 3285 N92-28817 * #
NASA-CR-190378 ..... p 3396 N92-28872 * #
NASA-CR-190384 ..... p 3341 N92-29200 * #
NASA-CR-190387 ..... p 3370 N92-29108 * #
NASA-CR-190398 ..... p 3305 N92-28715 * #
NASA-CR-190400 ..... p 3283 N92-28361 * #
NASA-CR-190408 ..... p 3273 N92-28371 * #
NASA-CR-190418 ..... p 3378 N92-28988 * #
NASA-CR-190419 ..... p 3310 N92-28587 * #
NASA-CR-190421 ..... p 3307 N92-28863 * #
NASA-CR-190422 ..... p 3276 N92-29115 * #
NASA-CR-190431 ..... p 3226 N92-28511 * #
NASA-CR-190444 ..... p 3233 N92-28720 * #
NASA-CR-190445 ..... p 3306 N92-28717 * #
NASA-CR-190448 ..... p 3330 N92-28671 * #
NASA-CR-190449 ..... p 3291 N92-28941 * #
NASA-CR-190456 ..... p 3305 N92-28950 * #
NASA-CR-190457 ..... p 3369 N92-29202 * #
NASA-CR-190468 ..... p 3321 N92-28867 * #
NASA-CR-190469 ..... p 3230 N92-28718 * #
NASA-CR-190472 ..... p 3319 N92-29087 * #
NASA-CR-190477 ..... p 3370 N92-28680 * #
NASA-CR-190484 ..... p 3273 N92-28586 * #
NASA-CR-190486 ..... p 3342 N92-28676 * #
NASA-CR-190487 ..... p 3295 N92-29134 * #
NASA-CR-190490 ..... p 3358 N92-29088 * #
NASA-CR-190493 ..... p 3353 N92-29196 * #
NASA-CR-190495 ..... p 3358 N92-28868 * #
NASA-CR-190501 ..... p 3290 N92-28707 * #
NASA-CR-190503 ..... p 3337 N92-28710 * #
NASA-CR-190508 ..... p 3372 N92-28478 * #
NASA-CR-190509 ..... p 3275 N92-28873 * #
NASA-CR-190510 ..... p 3396 N92-28871 * #
NASA-CR-190521 ..... p 3316 N92-28911 * #
NASA-CR-190531 ..... p 3358 N92-28698 * #
NASA-CR-190551 ..... p 3343 N92-29109 * #
NASA-CR-190552 ..... p 3339 N92-28875 * #
NASA-CR-190554 ..... p 3340 N92-29107 * #
NASA-CR-190556 ..... p 3339 N92-29106 * #
NASA-CR-190557 ..... p 3340 N92-29113 * #
NASA-CR-4443 ..... p 3239 N92-28584 * #

NASA-EP-278 ..... p 3366 N92-28864 * #

NASA-NP-150 ..... p 3397 N92-28678 * #

NASA-SP-4104 ..... p 3397 N92-28344 * #
NASA-SP-508 ..... p 3372 N92-28345 * #
NASA-SP-7037(275) ..... p 3226 N92-28679 *
NASA-SP-7037(278) ..... p 3226 N92-28677 *

NASA-TM-102192 ..... p 3239 N92-28457 * #
NASA-TM-103586 ..... p 3279 N92-28456 * #
NASA-TM-103588 ..... p 3330 N92-28521 * #
NASA-TM-103589 ..... p 3355 N92-28986 * #
NASA-TM-103590 ..... p 3229 N92-28981 * #
NASA-TM-103865 ..... p 3327 N92-28744 * #
NASA-TM-103873 ..... p 3234 N92-28926 * #
NASA-TM-103892 ..... p 3245 N92-29104 * #
NASA-TM-103902 ..... p 3234 N92-28910 * #
NASA-TM-103906 ..... p 3231 N92-29103 * #
NASA-TM-103913 ..... p 3325 N92-28420 * #
NASA-TM-103914 ..... p 3349 N92-28672 * #
NASA-TM-103915 ..... p 3353 N92-28909 * #
NASA-TM-103918 ..... p 3255 N92-28743 * #
NASA-TM-103925 ..... p 3233 N92-28721 * #
NASA-TM-104564 ..... p 3244 N92-28343 * #
NASA-TM-104567 ..... p 3346 N92-28297 * #
NASA-TM-105161 ..... p 3249 N92-28682 * #
NASA-TM-105396 ..... p 3302 N92-28701 * #
NASA-TM-105417 ..... p 3240 N92-28673 * #
NASA-TM-105636 ..... p 3250 N92-28983 * #
NASA-TM-105653 ..... p 3293 N92-28476 * #
NASA-TM-105655 ..... p 3293 N92-28434 * #
NASA-TM-105660 ..... p 3246 N92-28683 * #
NASA-TM-105681 ..... p 3296 N92-29136 * #
NASA-TM-105698 ..... p 3236 N92-28418 * #
NASA-TM-105715 ..... p 3236 N92-28419 * #
NASA-TM-105716 ..... p 3238 N92-28985 * #
NASA-TM-105717 ..... p 3288 N92-29105 * #
NASA-TM-105722 ..... p 3353 N92-28984 * #
NASA-TM-105727 ..... p 3248 N92-28417 * #
NASA-TM-105728 ..... p 3279 N92-28432 * #
NASA-TM-105739 ..... p 3357 N92-28475 * #
NASA-TM-105743 ..... p 3227 N92-28674 * #
NASA-TM-105745 ..... p 3227 N92-28696 * #
NASA-TM-105749 ..... p 3337 N92-28684 * #
NASA-TM-105753 ..... p 3280 N92-28675 * #
NASA-TM-105759 ..... p 3266 N92-28433 * #
NASA-TM-105763 ..... p 3249 N92-28693 * #
NASA-TM-105767 ..... p 3307 N92-28837 * #
NASA-TM-107544 ..... p 3330 N92-28670 * #
NASA-TM-107586 ..... p 3231 N92-28435 * #
NASA-TM-107589 ..... p 3275 N92-28876 * #
NASA-TM-107844 ..... p 3346 N92-29175 * #
NASA-TM-107859 ..... p 3337 N92-28758 * #
NASA-TM-107875 ..... p 3345 N92-28759 * #
NASA-TM-107878 ..... p 3329 N92-29174 * #
NASA-TM-107937 ..... p 3246 N92-28370 * #
NASA-TM-107938 ..... p 3334 N92-28267 * #
NASA-TM-107941 ..... p 3246 N92-28369 * #
NASA-TM-107944 ..... p 3396 N92-28907 * #
NASA-TM-107946 ..... p 3396 N92-28870 * #
NASA-TM-107947 ..... p 3396 N92-28869 * #
NASA-TM-107954 ..... p 3244 N92-29100 * #
NASA-TM-107958 ..... p 3295 N92-28925 * #
NASA-TM-4392 ..... p 3333 N92-28899 * #
NASA-TM-4396 ..... p 3234 N92-29110 * #

NASA-TP-3197 ..... p 3226 N92-28477 * #
NASA-TP-3198 ..... p 3344 N92-28375 * #
NASA-TP-3200 ..... p 3331 N92-28897 * #
NASA-TP-3224 ..... p 3255 N92-28374 * #
NASA-TP-3252 ..... p 3229 N92-28980 * #

NASA-TT-10001 ..... p 3290 N92-28862 * #

NAVSWC-TR-91-614 ..... p 3280 N92-28568 #

NAVY-CASE-68711 ..... p 3357 N92-28223 #
NAVY-CASE-72815 ..... p 3250 N92-28224 #

NCEL-TN-1839 ..... p 3264 N92-28912 #

NHRC-90-39 ..... p 3328 N92-28940 #
NHRC-91-17 ..... p 3344 N92-28401 #

NIFS-112 ..... p 3360 N92-28234 #

NIKHEF-K/AMPS/91-06 ..... p 3356 N92-28264 #
NIKHEF-K/AMPS/91-07 ..... p 3356 N92-28308 #

NIST/SP-821 ..... p 3276 N92-29115 * #

NLR-MP-88031-U ..... p 3226 N92-28658 #

NLR-TP-89007-U ..... p 3342 N92-28706 #
NLR-TP-89061-U ..... p 3305 N92-28708 #
NLR-TP-89119-U ..... p 3227 N92-28659 #
NLR-TP-89126-U ..... p 3227 N92-28660 #
NLR-TP-89158-U ..... p 3240 N92-28669 #
NLR-TP-89163-U ..... p 3302 N92-28643 #
NLR-TP-89211-U ..... p 3302 N92-28688 #
NLR-TP-89217-U ..... p 3316 N92-28689 #
NLR-TP-89235-U ..... p 3305 N92-28690 #
NLR-TP-90028-U ..... p 3345 N92-28648 #
NLR-TP-90062-U ..... p 3228 N92-28709 #
NLR-TP-90068-U ..... p 3232 N92-28649 #
NLR-TP-90070-U ..... p 3302 N92-28650 #
NLR-TP-90097-U ..... p 3238 N92-28711 #
NLR-TP-90108-U ..... p 3233 N92-28651 #
NLR-TP-90129-U ..... p 3239 N92-28652 #
NLR-TP-90134-U ..... p 3284 N92-28712 #
NLR-TP-90138-U ..... p 3260 N92-28691 #
NLR-TP-90144-U ..... p 3227 N92-28692 #
NLR-TP-90145-U ..... p 3240 N92-28661 #
NLR-TP-90147-U ..... p 3241 N92-29204 #
NLR-TP-90159-U ..... p 3239 N92-28653 #
NLR-TP-90163-U ..... p 3236 N92-28654 #
NLR-TP-90172-U ..... p 3303 N92-28650 #
NLR-TP-90174-U ..... p 3235 N92-28644 #
NLR-TP-90178-U ..... p 3304 N92-29176 #
NLR-TP-90184-U ..... p 3284 N92-28694 #
NLR-TP-90192-U ..... p 3230 N92-28655 #
NLR-TP-90199-U ..... p 3358 N92-28656 #
NLR-TP-90223-U ..... p 3352 N92-28695 #
NLR-TP-90228-U ..... p 3305 N92-28697 #
NLR-TP-90255-U ..... p 3228 N92-28713 #
NLR-TP-90262-U ..... p 3294 N92-28705 #
NLR-TP-90272-U ..... p 3260 N92-28794 #
NLR-TP-90282-U ..... p 3293 N92-28645 #
NLR-TP-90284-U ..... p 3293 N92-28646 #
NLR-TP-90286-U ..... p 3233 N92-28714 #
NLR-TP-90305-U ..... p 3233 N92-28687 #
NLR-TP-90307-U ..... p 3232 N92-28634 #
NLR-TP-90334-U ..... p 3347 N92-28635 #
NLR-TP-90368-U ..... p 3226 N92-28657 #
NLR-TP-90387-U ..... p 3336 N92-28636 #
NLR-TP-91050-U ..... p 3252 N92-28637 #
NLR-TP-91099-U ..... p 3345 N92-28716 #

NOARL-CR-011-92 ..... p 3322 N92-28938 #

NOARL-PR-91-024-352 ..... p 3359 N92-29167 #
NOARL-PR-91-054-352 ..... p 3321 N92-28321 #

NOARL-TN-173 ..... p 3319 N92-28966 #
NOARL-TN-185 ..... p 3319 N92-28965 #
NOARL-TN-195 ..... p 3316 N92-28964 #
NOARL-TN-212 ..... p 3324 N92-29089 #
NOARL-TN-214 ..... p 3322 N92-28963 #
NOARL-TN-221 ..... p 3322 N92-28913 #

NOARL-15 ..... p 3351 N92-28324 #
NOARL-35 ..... p 3321 N92-28566 #

NOSC-TR-1463 ..... p 3335 N92-28562 #

NOSC/TR-1453 ..... p 3276 N92-28947 #
NOSC/TR-1468 ..... p 3339 N92-28946 #

NPL-DMM(A)-42 ..... p 3261 N92-29164

NPL-RSA(EXT)-23 ..... p 3288 N92-29163

NPS-EC-92-004 ..... p 3335 N92-28353 #

NPS-OC-91-002 ..... p 3321 N92-28365 #

NPS-PH-92-008 ..... p 3318 N92-28799 #

NRC-TR-92-143 ..... p 3295 N92-29134 * #

NREL/TP-451-4797 ..... p 3306 N92-28277 #

NRL-MR-6922 ..... p 3350 N92-28238 #

NRL-TR-3 ..... p 3355 N92-28881 #

NRL/FR/5560-92-9329 ..... p 3332 N92-28891 #
NRL/FR/6383-92-9369 ..... p 3253 N92-28953 #

NRL/MR/4404-92-6961 ..... p 3285 N92-28803 #
NRL/MR/4440-92-6952 ..... p 3350 N92-28400 #
NRL/MR/4440-92-6966 ..... p 3360 N92-28354 #

NSWCDD/TR-92/47 ..... p 3367 N92-28403 #

NTSC-TR-90-09 ..... p 3272 N92-28253 #

OEFZS-4574 ..... p 3316 N92-28740 #
OEFZS-4581 ..... p 3356 N92-29210 #

ONERA-NT-1990-13 ..... p 3249 N92-28780 #
ONERA-NT-1991-10 ..... p 3349 N92-28778 #
ONERA-NT-1991-11 ..... p 3338 N92-28779 #
ONERA-NT-1991-8 ..... p 3347 N92-28777 #

ONERA-RSF-136/1865-AY-728-A p 3228 N92-28789 #
ONERA-RSF-43/1736-AY-146A .. p 3284 N92-28788 #
ONERA-RSF-7/3617-AY-022A .... p 3229 N92-29206 #

ONERA-RT-24/3542-RY-091-R ... p 3338 N92-28790 #

ONERA-RTS-11/3446-EY ..... p 3325 N92-28844 #

ORNL/M-2026 ..... p 3324 N92-28382 #

ORNL/TM-11778 ..... p 3355 N92-29190 #

OU/AEC-EER-92-2 ..... p 3230 N92-28718 * #

PB92-163831 ..... p 3252 N92-28724 #
PB92-163849 ..... p 3252 N92-28725 #
PB92-164326 ..... p 3266 N92-28914 #
PB92-176569 ..... p 3308 N92-29183 #

PL-TR-91-1044 ..... p 3284 N92-28766 #
PL-TR-91-2126 ..... p 3309 N92-28394 #
PL-TR-91-2216 ..... p 3355 N92-28936 #
PL-TR-91-2250 ..... p 3316 N92-28935 #
PL-TR-91-2273 ..... p 3248 N92-28765 #
PL-TR-91-2281 ..... p 3309 N92-28386 #
PL-TR-91-2296 ..... p 3244 N92-28937 #
PL-TR-92-2005 ..... p 3309 N92-28569 #

PML-1990-24-PT-2 ..... p 3349 N92-28313 #

PNR-90823 ..... p 3337 N92-28741 #

POLY-WRI-1589-92 ..... p 3297 N92-29112 #

PPL-109 ..... p 3361 N92-28665 #
PPL-120 ..... p 3361 N92-28849 #
PPL-124 ..... p 3360 N92-28664 #
PPL-126 ..... p 3361 N92-28848 #
PPL-127 ..... p 3361 N92-28847 #

PSI-FR-2567-1 ..... p 3250 N92-28945 #

PSU-TURBO-R-9201 ..... p 3286 N92-28879 #

R/D-6907-EE-06 ..... p 3365 N92-28923 #

REPT-21-1991 ..... p 3323 N92-29215 #
REPT-26151-EL ..... p 3279 N92-28427 #
REPT-2 ..... p 3365 N92-28885 #
REPT-544-FDD-91/004 ..... p 3396 N92-28869 * #
REPT-554-FDD-91/113ROUDO ... p 3396 N92-28872 * #
REPT-91-33 ..... p 3341 N92-29221 #
REPT-92B00061 ..... p 3299 N92-28620 * #
REPT-92B00089 ..... p 3244 N92-28343 * #
REPT-92B00092 ..... p 3346 N92-28297 * #

RIA-91-29 ..... p 3329 N92-29174 * #

RIACS-TR-91.19 ..... p 3340 N92-29113 * #
RIACS-TR-91.22 ..... p 3339 N92-29106 * #
RIACS-TR-92.05 ..... p 3340 N92-29107 * #
RIACS-TR-92.14 ..... p 3343 N92-29109 * #
RIACS-TR-92-06 ..... p 3339 N92-28875 * #

RL-TR-91-339-VOL-1 ..... p 3336 N92-28666 #
RL-TR-91-339-VOL-2 ..... p 3336 N92-28667 #
RL-TR-91-340 ..... p 3280 N92-28561 #
RL-TR-91-361 ..... p 3368 N92-28404 #

RTI-83U-5123 ..... p 3264 N92-28904 #

RTI/5123/91-29 ..... p 3264 N92-28904 #

RXR-91121 ..... p 3244 N92-28937 #

R92-928101 ..... p 3354 N92-28259 #

S-668 ..... p 3331 N92-28897 * #

SAIC-91/1286 ..... p 3250 N92-28931 #

SAND-91-1717C ..... p 3295 N92-28925 * #
SAND-91-2155C ..... p 3244 N92-28226 #
SAND-91-2285C ..... p 3245 N92-28861 #
SAND-91-8712 ..... p 3290 N92-28852 #
SAND-91-8742 ..... p 3256 N92-28822 #

SAND-92-0066C ..... p 3362 N92-29086 #
SAND-92-0271C ..... p 3303 N92-28855 #
SAND-92-0384C ..... p 3363 N92-28331 #
SAND-92-0393C ..... p 3357 N92-28355 #
SAND-92-0447C ..... p 3255 N92-28341 #
SAND-92-0460C ..... p 3245 N92-29102 #
SAND-92-0477C ..... p 3368 N92-28832 #
SAND-92-0520C ..... p 3335 N92-28342 #

SR-11 ..... p 3309 N92-28569 #
SR-1 ..... p 3309 N92-28386 #

SRA-R92-910034-1 ..... p 3258 N92-29126 #

SS/L-TR00820 ..... p 3273 N92-28431 * #
SS/L-TR00821 ..... p 3275 N92-28906 * #

SSD-TR-92-03 ..... p 3308 N92-28272 #

SU-SLAC-PUB-5701 ..... p 3356 N92-28270 #

SWRI-2253/3 ..... p 3263 N92-28415 #

SYSAPP-91/151 ..... p 3308 N92-29183 #

TD-90-1700-PT-2 ..... p 3349 N92-28313 #

TD91-2156 ..... p 3342 N92-28746
TD91-2168 ..... p 3367 N92-29161
TD91-2169 ..... p 3369 N92-29162
TD91-2230 ..... p 3291 N92-29160
TD91-3887 ..... p 3241 N92-28828

TOR-92(2464)-1 ..... p 3245 N92-28956 #

TR-0091(6448)-1 ..... p 3308 N92-28272 #
TR-114 ..... p 3363 N92-28392 #
TR-115 ..... p 3363 N92-28349 #
TR-118 ..... p 3364 N92-28512 #
TR-120 ..... p 3255 N92-28391 #
TR-14 ..... p 3258 N92-28973 #
TR-406 ..... p 3344 N92-28325 #
TR-46 ..... p 3254 N92-28290 #
TR-47 ..... p 3262 N92-28291 #
TR-4 ..... p 3253 N92-28916 #
TR-56 ..... p 3265 N92-28972 #
TR-59 ..... p 3265 N92-29116 #
TR-5 ..... p 3252 N92-28917 #
TR-65 ..... p 3278 N92-28239 #
TR-6 ..... p 3328 N92-29142 #
TR-7 ..... p 3262 N92-28251 #
TR-84 ..... p 3287 N92-28322 #
TR-934 ..... p 3248 N92-28366 #

UCRL-JC-109095 ..... p 3288 N92-28812 #
UCRL-JC-109289 ..... p 3363 N92-28333 #
UCRL-JC-109291 ..... p 3283 N92-28269 #
UCRL-JC-109505 ..... p 3347 N92-28824 #
UCRL-JC-109513 ..... p 3325 N92-28685 #
UCRL-JC-109774 ..... p 3342 N92-28334 #
UCRL-JC-109808 ..... p 3360 N92-28335 #
UCRL-JC-110087 ..... p 3397 N92-28336 #
UCRL-JC-110189 ..... p 3355 N92-28860 #

UCRL-LR-109784 ..... p 3277 N92-29131 #

UCRL-MA-108543 ..... p 3342 N92-28381 #

UDR-TR-91-53 ..... p 3262 N92-28398 #

UILU-ENG-92-2217 ..... p 3297 N92-28726 * #

UMICH-027723-5-T ..... p 3273 N92-28371 * #

UNM-ISNPS-4-92 ..... p 3307 N92-28863 * #

US-PATENT-APPL-SN-084064 ..... p 3265 N92-29157 *
US-PATENT-APPL-SN-140185 ..... p 3359 N92-29158 *
US-PATENT-APPL-SN-210486 ..... p 3303 N92-28757 *
US-PATENT-APPL-SN-210486 ..... p 3304 N92-29101 *
US-PATENT-APPL-SN-210486 ..... p 3304 N92-29155 *
US-PATENT-APPL-SN-251500 ..... p 3331 N92-29129 *
US-PATENT-APPL-SN-331119 ..... p 3296 N92-29151 *
US-PATENT-APPL-SN-337768 ..... p 3359 N92-29158 *
US-PATENT-APPL-SN-357928 ..... p 3333 N92-29132 *
US-PATENT-APPL-SN-376270 ..... p 3276 N92-29085
US-PATENT-APPL-SN-376487 ..... p 3255 N92-28728 *
US-PATENT-APPL-SN-449209 ..... p 3304 N92-29155 *
US-PATENT-APPL-SN-449211 ..... p 3303 N92-28757 *
US-PATENT-APPL-SN-449211 ..... p 3304 N92-29101 *
US-PATENT-APPL-SN-481537 ..... p 3248 N92-28750 *
US-PATENT-APPL-SN-501909 ..... p 3284 N92-28752 *
US-PATENT-APPL-SN-506636 ..... p 3359 N92-29133 *
US-PATENT-APPL-SN-508316 ..... p 3264 N92-28751 *
US-PATENT-APPL-SN-529427 ..... p 3332 N92-29137 *
US-PATENT-APPL-SN-531374 ..... p 3294 N92-28754 *

US-PATENT-APPL-SN-560923 ..... p 3228 N92-28729 *
US-PATENT-APPL-SN-562095 ..... p 3325 N92-28755 *
US-PATENT-APPL-SN-587921 ..... p 3358 N92-28571 *
US-PATENT-APPL-SN-596139 ..... p 3280 N92-28753 *
US-PATENT-APPL-SN-599601 ..... p 3255 N92-28728 *
US-PATENT-APPL-SN-606988 ..... p 3288 N92-29135 *
US-PATENT-APPL-SN-608493 ..... p 3253 N92-29152 *
US-PATENT-APPL-SN-608504 ..... p 3304 N92-29101 *
US-PATENT-APPL-SN-613188 ..... p 3296 N92-29151 *
US-PATENT-APPL-SN-618789 ..... p 3351 N92-29130 *
US-PATENT-APPL-SN-618790 ..... p 3320 N92-29148 *
US-PATENT-APPL-SN-621256 ..... p 3266 N92-28739
US-PATENT-APPL-SN-628529 ..... p 3296 N92-29138 *
US-PATENT-APPL-SN-632442 ..... p 3234 N92-28987
US-PATENT-APPL-SN-632709 ..... p 3294 N92-28749
US-PATENT-APPL-SN-636076 ..... p 3288 N92-29156 *
US-PATENT-APPL-SN-636532 ..... p 3296 N92-29140 *
US-PATENT-APPL-SN-645089 ..... p 3250 N92-29141 *
US-PATENT-APPL-SN-648933 ..... p 3256 N92-28756 *
US-PATENT-APPL-SN-653605 ..... p 3359 N92-29117 *
US-PATENT-APPL-SN-657790 ..... p 3281 N92-29153 *
US-PATENT-APPL-SN-660361 ..... p 3249 N92-28747
US-PATENT-APPL-SN-660371 ..... p 3276 N92-29124 *
US-PATENT-APPL-SN-665509 ..... p 3359 N92-29122 *
US-PATENT-APPL-SN-674271 ..... p 3249 N92-28748
US-PATENT-APPL-SN-676910 ..... p 3307 N92-29143 *
US-PATENT-APPL-SN-682160 ..... p 3265 N92-29090 *
US-PATENT-APPL-SN-686263 ..... p 3303 N92-28757 *
US-PATENT-APPL-SN-687606 ..... p 3295 N92-29092 *
US-PATENT-APPL-SN-690198 ..... p 3288 N92-29097 *
US-PATENT-APPL-SN-691609 ..... p 3295 N92-29099 *
US-PATENT-APPL-SN-693049 ..... p 3359 N92-29158 *
US-PATENT-APPL-SN-714814 ..... p 3295 N92-29120 *
US-PATENT-APPL-SN-718046 ..... p 3261 N92-29094 *
US-PATENT-APPL-SN-725717 ..... p 3250 N92-28224 #
US-PATENT-APPL-SN-732884 ..... p 3264 N92-28751 *
US-PATENT-APPL-SN-736145 ..... p 3287 N92-29125 *
US-PATENT-APPL-SN-758143 ..... p 3360 N92-29205 #
US-PATENT-APPL-SN-758977 ..... p 3298 N92-29154 *
US-PATENT-APPL-SN-759367 ..... p 3296 N92-29150 *
US-PATENT-APPL-SN-760635 ..... p 3358 N92-29095 #
US-PATENT-APPL-SN-767955 ..... p 3357 N92-28223 #
US-PATENT-APPL-SN-783661 ..... p 3343 N92-29096 #
US-PATENT-APPL-SN-813558 ..... p 3294 N92-28727 *
US-PATENT-APPL-SN-819699 ..... p 3277 N92-29199 #
US-PATENT-APPL-SN-828634 ..... p 3261 N92-29170 #
US-PATENT-APPL-SN-857536 ..... p 3277 N92-29169 #

US-PATENT-CLASS-118-416 ..... p 3253 N92-29152 *
US-PATENT-CLASS-126-433 ..... p 3307 N92-29143 *
US-PATENT-CLASS-126-436 ..... p 3307 N92-29143 *
US-PATENT-CLASS-15-230.11 ..... p 3294 N92-28754 *
US-PATENT-CLASS-16-111R ..... p 3295 N92-29092 *
US-PATENT-CLASS-16-114R ..... p 3295 N92-29092 *
US-PATENT-CLASS-165-104.14 .. p 3287 N92-29125 *
US-PATENT-CLASS-165-104.22 .. p 3287 N92-29125 *
US-PATENT-CLASS-165-104.31 .. p 3284 N92-28752 *
US-PATENT-CLASS-165-104.34 .. p 3284 N92-28752 *
US-PATENT-CLASS-165-109.1 .... p 3284 N92-28752 *
US-PATENT-CLASS-165-110 ..... p 3284 N92-28752 *
US-PATENT-CLASS-165-41 ..... p 3284 N92-28752 *
US-PATENT-CLASS-165-41 ..... p 3287 N92-29125 *
US-PATENT-CLASS-165-4 ..... p 3284 N92-28752 *
US-PATENT-CLASS-204-129 ..... p 3256 N92-28756 *
US-PATENT-CLASS-204-180.1 .... p 3255 N92-28728 *
US-PATENT-CLASS-204-183.3 .... p 3255 N92-28728 *
US-PATENT-CLASS-204-299R .... p 3255 N92-28728 *
US-PATENT-CLASS-219-85.15 .... p 3261 N92-29094 *
US-PATENT-CLASS-219-85.19 .... p 3261 N92-29094 *
US-PATENT-CLASS-244-161 ..... p 3294 N92-28727 *
US-PATENT-CLASS-244-161 ..... p 3248 N92-28750 *
US-PATENT-CLASS-244-169 ..... p 3249 N92-28747
US-PATENT-CLASS-244-3.27 ..... p 3234 N92-28987
US-PATENT-CLASS-244-35R ..... p 3228 N92-28729 *
US-PATENT-CLASS-244-36 ..... p 3228 N92-28729 *
US-PATENT-CLASS-248-222.1 .... p 3295 N92-29092 *
US-PATENT-CLASS-248-251 ..... p 3295 N92-29092 *
US-PATENT-CLASS-248-65 ..... p 3281 N92-29153 *
US-PATENT-CLASS-248-68.1 ..... p 3281 N92-29153 *
US-PATENT-CLASS-250-201.9 .... p 3359 N92-29122 *
US-PATENT-CLASS-250-231.14 .. p 3359 N92-29133 *
US-PATENT-CLASS-252-DIG.13 . p 3332 N92-29137 *
US-PATENT-CLASS-252-DIG.14 . p 3332 N92-29137 *
US-PATENT-CLASS-252-DIG.5 .... p 3332 N92-29137 *
US-PATENT-CLASS-252-502 ..... p 3253 N92-29152 *
US-PATENT-CLASS-252-545 ..... p 3332 N92-29137 *
US-PATENT-CLASS-252-547 ..... p 3332 N92-29137 *
US-PATENT-CLASS-252-62.2 ..... p 3280 N92-28753 *
US-PATENT-CLASS-256-59 ..... p 3295 N92-29092 *
US-PATENT-CLASS-273-148B .... p 3281 N92-29153 *
US-PATENT-CLASS-285-381 ..... p 3295 N92-29120 *
US-PATENT-CLASS-29-110.5 ..... p 3294 N92-28754 *
US-PATENT-CLASS-29-123 ..... p 3294 N92-28754 *
US-PATENT-CLASS-29-132 ..... p 3294 N92-28754 *
US-PATENT-CLASS-292-DIG.66 . p 3295 N92-29120 *
US-PATENT-CLASS-294-119.1 .... p 3296 N92-29138 *

US-PATENT-CLASS-294-65.5 ..... p 3294 N92-28727 *
US-PATENT-CLASS-294-86.4 ..... p 3294 N92-28727 *
US-PATENT-CLASS-294-902 ..... p 3296 N92-29138 *
US-PATENT-CLASS-310-90.5 ..... p 3295 N92-29099 *
US-PATENT-CLASS-324-205 ..... p 3351 N92-29130 *
US-PATENT-CLASS-324-209 ..... p 3304 N92-29155 *
US-PATENT-CLASS-324-224 ..... p 3298 N92-29154 *
US-PATENT-CLASS-324-226 ..... p 3303 N92-28757 *
US-PATENT-CLASS-324-226 ..... p 3298 N92-29154 *
US-PATENT-CLASS-324-226 ..... p 3304 N92-29155 *
US-PATENT-CLASS-324-227 ..... p 3304 N92-29155 *
US-PATENT-CLASS-324-235 ..... p 3303 N92-28757 *
US-PATENT-CLASS-324-235 ..... p 3304 N92-29155 *
US-PATENT-CLASS-324-239 ..... p 3304 N92-29101 *
US-PATENT-CLASS-324-239 ..... p 3304 N92-29155 *
US-PATENT-CLASS-324-244 ..... p 3351 N92-29130 *
US-PATENT-CLASS-324-261 ..... p 3351 N92-29130 *
US-PATENT-CLASS-324-262 ..... p 3298 N92-29154 *
US-PATENT-CLASS-324-77CS .... p 3276 N92-29124 *
US-PATENT-CLASS-324-77C ..... p 3276 N92-29124 *
US-PATENT-CLASS-324-78D ..... p 3276 N92-29124 *
US-PATENT-CLASS-324-78F ..... p 3276 N92-29124 *
US-PATENT-CLASS-333-161 ..... p 3358 N92-28571 *
US-PATENT-CLASS-333-995 ..... p 3358 N92-28571 *
US-PATENT-CLASS-338-128 ..... p 3281 N92-29153 *
US-PATENT-CLASS-338-4 ..... p 3288 N92-29097 *
US-PATENT-CLASS-351-206 ..... p 3325 N92-28755 *
US-PATENT-CLASS-351-221 ..... p 3325 N92-28755 *
US-PATENT-CLASS-356-370 ..... p 3359 N92-29117 *
US-PATENT-CLASS-356-414 ..... p 3359 N92-29117 *
US-PATENT-CLASS-356-432 ..... p 3298 N92-29154 *
US-PATENT-CLASS-358-103 ..... p 3248 N92-28750 *
US-PATENT-CLASS-358-105 ..... p 3331 N92-29129 *
US-PATENT-CLASS-359.849 ..... p 3359 N92-29122 *
US-PATENT-CLASS-359-230 ..... p 3296 N92-29151 *
US-PATENT-CLASS-359-236 ..... p 3296 N92-29151 *
US-PATENT-CLASS-359-246 ..... p 3359 N92-29117 *
US-PATENT-CLASS-359-247 ..... p 3359 N92-29117 *
US-PATENT-CLASS-359-261 ..... p 3359 N92-29117 *
US-PATENT-CLASS-360-48 ..... p 3333 N92-29132 *
US-PATENT-CLASS-360-98.01 .... p 3333 N92-29132 *
US-PATENT-CLASS-361-148 ..... p 3351 N92-29130 *
US-PATENT-CLASS-361-149 ..... p 3351 N92-29130 *
US-PATENT-CLASS-361-267 ..... p 3351 N92-29130 *
US-PATENT-CLASS-364-424.01 .. p 3331 N92-29129 *
US-PATENT-CLASS-364-443 ..... p 3320 N92-29148 *
US-PATENT-CLASS-364-459 ..... p 3248 N92-28750 *
US-PATENT-CLASS-369-32 ..... p 3333 N92-29132 *
US-PATENT-CLASS-369-44.26 .... p 3359 N92-29133 *
US-PATENT-CLASS-369-95 ..... p 3333 N92-29132 *
US-PATENT-CLASS-370-6 ..... p 3276 N92-29085
US-PATENT-CLASS-374-112 ..... p 3320 N92-29148 *
US-PATENT-CLASS-374-45 ..... p 3298 N92-29154 *
US-PATENT-CLASS-374-4 ..... p 3298 N92-29154 *
US-PATENT-CLASS-378-210 ..... p 3288 N92-29135 *
US-PATENT-CLASS-378-43 ..... p 3288 N92-29135 *
US-PATENT-CLASS-382-1 ..... p 3331 N92-29129 *
US-PATENT-CLASS-382-22 ..... p 3331 N92-29129 *
US-PATENT-CLASS-4-661 ..... p 3332 N92-29137 *
US-PATENT-CLASS-403-13 ..... p 3296 N92-29140 *
US-PATENT-CLASS-403-24 ..... p 3296 N92-29140 *
US-PATENT-CLASS-403-28 ..... p 3295 N92-29120 *
US-PATENT-CLASS-403-404 ..... p 3295 N92-29120 *
US-PATENT-CLASS-411-14 ..... p 3296 N92-29150 *
US-PATENT-CLASS-411-267 ..... p 3296 N92-29150 *
US-PATENT-CLASS-411-433 ..... p 3296 N92-29150 *
US-PATENT-CLASS-411-909 ..... p 3295 N92-29120 *
US-PATENT-CLASS-417-209 ..... p 3287 N92-29125 *
US-PATENT-CLASS-423-447.2 .... p 3253 N92-29152 *
US-PATENT-CLASS-423-448 ..... p 3253 N92-29152 *
US-PATENT-CLASS-423-460 ..... p 3253 N92-29152 *
US-PATENT-CLASS-424-70 ..... p 3332 N92-29137 *
US-PATENT-CLASS-427-108 ..... p 3359 N92-29158 *
US-PATENT-CLASS-427-109 ..... p 3359 N92-29158 *
US-PATENT-CLASS-427-294 ..... p 3253 N92-29152 *
US-PATENT-CLASS-427-38 ..... p 3359 N92-29158 *
US-PATENT-CLASS-427-443.2 .... p 3253 N92-29152 *
US-PATENT-CLASS-427-66 ..... p 3359 N92-29158 *
US-PATENT-CLASS-427-68 ..... p 3359 N92-29158 *
US-PATENT-CLASS-428-614 ..... p 3265 N92-29090 *
US-PATENT-CLASS-428-660 ..... p 3265 N92-29090 *
US-PATENT-CLASS-428-661 ..... p 3265 N92-29090 *
US-PATENT-CLASS-429-192 ..... p 3280 N92-28753 *
US-PATENT-CLASS-505-1 ..... p 3358 N92-28571 *
US-PATENT-CLASS-505-703 ..... p 3358 N92-28571 *
US-PATENT-CLASS-505-848 ..... p 3358 N92-28571 *
US-PATENT-CLASS-505-866 ..... p 3358 N92-28571 *
US-PATENT-CLASS-505-876 ..... p 3295 N92-29099 *
US-PATENT-CLASS-525-420 ..... p 3265 N92-29157 *
US-PATENT-CLASS-525-432 ..... p 3265 N92-29157 *
US-PATENT-CLASS-528-125 ..... p 3264 N92-28751 *
US-PATENT-CLASS-528-126 ..... p 3264 N92-28751 *
US-PATENT-CLASS-528-127 ..... p 3264 N92-28751 *
US-PATENT-CLASS-528-128 ..... p 3264 N92-28751 *
US-PATENT-CLASS-528-179 ..... p 3265 N92-29157 *
US-PATENT-CLASS-528-185 ..... p 3250 N92-29141 *
US-PATENT-CLASS-528-185 ..... p 3265 N92-29157 *
US-PATENT-CLASS-528-220 ..... p 3264 N92-28751 *
US-PATENT-CLASS-528-224 ..... p 3264 N92-28751 *
US-PATENT-CLASS-528-352 ..... p 3265 N92-29157 *
US-PATENT-CLASS-528-353 ..... p 3265 N92-29157 *
US-PATENT-CLASS-548-143 ..... p 3250 N92-29141 *
US-PATENT-CLASS-60-641.8 ..... p 3307 N92-29143 *
US-PATENT-CLASS-60-659 ..... p 3307 N92-29143 *
US-PATENT-CLASS-62.224 ..... p 3288 N92-29156 *
US-PATENT-CLASS-62-51.2 ..... p 3288 N92-29156 *
US-PATENT-CLASS-73-168 ..... p 3294 N92-28749
US-PATENT-CLASS-73-178R ..... p 3320 N92-29148 *
US-PATENT-CLASS-73-601 ..... p 3303 N92-28757 *
US-PATENT-CLASS-73-708 ..... p 3288 N92-29097 *
US-PATENT-CLASS-73-721 ..... p 3288 N92-29097 *
US-PATENT-CLASS-73-727 ..... p 3288 N92-29097 *
US-PATENT-CLASS-73-756 ..... p 3288 N92-29097 *
US-PATENT-CLASS-73-801 ..... p 3304 N92-29155 *
US-PATENT-CLASS-74-471XY .... p 3281 N92-29153 *
US-PATENT-CLASS-82-20-14 ..... p 3266 N92-28739
US-PATENT-CLASS-89-1.809 ..... p 3249 N92-28748
US-PATENT-CLASS-901-1 ..... p 3331 N92-29129 *
US-PATENT-CLASS-901-30 ..... p 3294 N92-28727 *
US-PATENT-CLASS-901-39 ..... p 3296 N92-29138 *
US-PATENT-CLASS-901-46 ..... p 3294 N92-28727 *

US-PATENT-5,056,405 ..... p 3266 N92-28739
US-PATENT-5,062,593 ..... p 3249 N92-28747
US-PATENT-5,068,951 ..... p 3294 N92-28754 *
US-PATENT-5,073,412 ..... p 3253 N92-29152 *
US-PATENT-5,074,187 ..... p 3249 N92-28748
US-PATENT-5,074,493 ..... p 3234 N92-28987
US-PATENT-5,078,009 ..... p 3294 N92-28749
US-PATENT-5,086,423 ..... p 3276 N92-29085
US-PATENT-5,104,683 ..... p 3359 N92-29158 *
US-PATENT-5,107,107 ..... p 3359 N92-29133 *
US-PATENT-5,107,526 ..... p 3288 N92-29135 *
US-PATENT-5,107,920 ..... p 3284 N92-28752 *
US-PATENT-5,108,214 ..... p 3295 N92-29120 *
US-PATENT-5,108,568 ..... p 3255 N92-28728 *
US-PATENT-5,109,195 ..... p 3304 N92-29155 *
US-PATENT-5,109,345 ..... p 3248 N92-28750 *
US-PATENT-5,109,425 ..... p 3331 N92-29129 *
US-PATENT-5,110,436 ..... p 3256 N92-28756 *
US-PATENT-5,110,694 ..... p 3280 N92-28753 *
US-PATENT-5,111,345 ..... p 3333 N92-29132 *
US-PATENT-5,112,120 ..... p 3228 N92-28729 *
US-PATENT-5,112,154 ..... p 3296 N92-29140 *
US-PATENT-5,113,064 ..... p 3359 N92-29122 *
US-PATENT-5,113,659 ..... p 3307 N92-29143 *
US-PATENT-5,113,714 ..... p 3281 N92-29153 *
US-PATENT-5,116,331 ..... p 3288 N92-29097 *
US-PATENT-5,116,543 ..... p 3332 N92-29137 *
US-PATENT-5,116,690 ..... p 3265 N92-29090 *
US-PATENT-5,116,807 ..... p 3358 N92-28571 *
US-PATENT-5,116,934 ..... p 3264 N92-28751 *
US-PATENT-5,116,939 ..... p 3265 N92-29157 *
US-PATENT-5,117,139 ..... p 3295 N92-29099 *
US-PATENT-5,117,184 ..... p 3304 N92-29101 *
US-PATENT-5,117,689 ..... p 3320 N92-29148 *
US-PATENT-5,118,237 ..... p 3296 N92-29150 *
US-PATENT-5,118,781 ..... p 3250 N92-29141 *
US-PATENT-5,119,637 ..... p 3288 N92-29156 *
US-PATENT-5,120,101 ..... p 3296 N92-29138 *
US-PATENT-5,121,058 ..... p 3303 N92-28757 *
US-PATENT-5,122,731 ..... p 3276 N92-29124 *
US-PATENT-5,124,640 ..... p 3298 N92-29154 *
US-PATENT-5,125,601 ..... p 3294 N92-28727 *
US-PATENT-5,125,730 ..... p 3325 N92-28755 *
US-PATENT-5,126,131 ..... p 3295 N92-29092 *
US-PATENT-5,126,527 ..... p 3261 N92-29094 *
US-PATENT-5,126,669 ..... p 3351 N92-29130 *
US-PATENT-5,127,471 ..... p 3287 N92-29125 *
US-PATENT-5,128,796 ..... p 3296 N92-29151 *
US-PATENT-5,128,797 ..... p 3359 N92-29117 *

USAARL-92-10 ..... p 3331 N92-28944 #

USAAVSCOM-TR-92-A-003 ..... p 3327 N92-28744 * #

USABRDL-9201 ..... p 3324 N92-28242 #

USAFA-TR-91-19 ..... p 3368 N92-28663 #

USAFETAC/PR-91/023 ..... p 3319 N92-28934 #

USARIEM-T2-92 ..... p 3324 N92-28288 #

VTT-RR-741 ..... p 3266 N92-29194 #
VTT-RR-742 ..... p 3251 N92-28572 #
VTT-RR-743 ..... p 3251 N92-28573 #
VTT-RR-746 ..... p 3303 N92-28776 #

WES/CR/SL-92-2 ..... p 3298 N92-28424 #

WES/TR/EL-92-13 ..... p 3351 N92-28302 #

WL-TM-02-307-FIBE ..... p 3241 N92-28772 #

WL-TR-90-83 ..... p 3362 N92-28962 #
WL-TR-91-1146 ..... p 3346 N92-29082 #
WL-TR-91-2103 ..... p 3236 N92-28294 #
WL-TR-91-2111 ..... p 3262 N92-28398 #
WL-TR-91-4049 ..... p 3258 N92-28241 #
WL-TR-91-4103 ..... p 3258 N92-29091 #
WL-TR-91-4132 ..... p 3368 N92-28565 #
WL-TR-91-5037 ..... p 3349 N92-28961 #

WSRC-MS-91-086 ..... p 3335 N92-28332 #

WSRC-RP-91-1001 ..... p 3257 N92-28894 #

WYLE-TN-91-8 ..... p 3352 N92-28556 * #

YALEU/DCS/RR-894 ..... p 3348 N92-28949 #

Typical Accession Number Index Listing

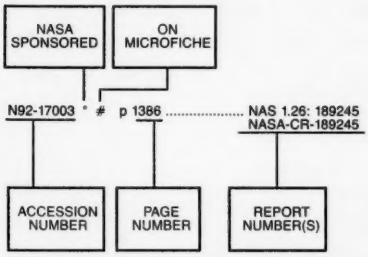

Listings in this index are arranged alphanumerically by accession number. The page number helps to locate the citation in the abstract section. An asterisk (*) indicates that the item is a NASA report. A pound sign (#) indicates that the item is available on microfiche.

N92-28223 # p 3357 AD-D015199
N92-28223 # p 3357 NAVY-CASE-68711
US-PATENT-APPL-SN-767955
N92-28224 # p 3250 AD-D015212
NAVY-CASE-72815
US-PATENT-APPL-SN-725717
N92-28225 # p 3282 AD-A247164
AFOSR-92-0145TR
N92-28226 # p 3244 CONF-9204102-3
DE92-011149
SAND-91-2155C
N92-28227 # p 3366 DE92-622380
IC-91/396
N92-28228 # p 3289 DE92-622403
IC-91/234
N92-28229 # p 3366 DE92-622409
IC-91/376
N92-28230 # p 3366 DE92-622671
LAMP-91/9
N92-28231 # p 3362 DE92-622792
IC-91/292
N92-28232 # p 3366 DE92-622801
IC-91/389
N92-28233 # p 3292 DE92-782046
JAERI-M-91-197
N92-28234 # p 3360 DE92-782102
NIFS-112
N92-28235 # p 3366 CONF-9102158
DE92-782191
INS-T-506
N92-28236 # p 3332 AD-A249194
CI-2071-92-0012
N92-28237 # p 3258 AD-A249263
N92-28238 # p 3350 AD-A247067
NRL-MR-6922
N92-28239 # p 3278 AD-A247082
TR-65
N92-28240 # p 3254 AD-A247088
N92-28241 # p 3258 AD-A247101
WL-TR-91-4049
N92-28242 # p 3324 AD-A247167
USABRDL-9201
N92-28243 # p 3333 AD-A247480
N92-28244 # p 3367 AD-A247481
N92-28245 # p 3333 AD-A247484
N92-28246 # p 3367 AD-A247486
N92-28247 # p 3323 AD-A247488
ARAED-SP-91002
N92-28248 # p 3240 AD-A247489
CRDEC-TR-309
N92-28249 # p 3261 AD-A247593
MTL-TR-92-6
N92-28250 # p 3262 AD-A247594
MTL-TR-92-4
N92-28251 # p 3262 AD-A247595
TR-7
N92-28252 # p 3251 AD-A247776
N92-28253 # p 3272 AD-A246618
NTSC-TR-90-09
N92-28254 # p 3245 AD-A246620
N92-28255 # p 3370 AD-A246621
AFIT/GSM/LSY/91S-12
N92-28256 # p 3366 AD-A246622
AFIT/GSM/LSM/91S-21
N92-28257 # p 3308 AD-A247091
AFOSR-92-0009TR
N92-28258 # p 3282 AD-A247092
AFOSR-92-0041TR
N92-28259 # p 3354 AD-A247093
AFOSR-92-0016TR
R92-928101
N92-28260 # p 3354 AD-A247095
N92-28261 # p 3254 AD-A247163
AFOSR-92-0162TR
N92-28262 # p 3278 DIGEL-1991-2
ETN-92-91229
N92-28263 # p 3278 DIGEL-1991-7
ETN-92-91235
N92-28264 # p 3356 ETN-92-91237
NIKHEF-K/AMPS/91-06
N92-28265 # p 3334 ETN-92-91243
FFI-91/7021
ISSN-0802-2437
N92-28266 # p 3320 ETN-92-91244
FFI-91/7022
ISSN-0802-2437
N92-28267* # p 3334 NAS 1.15:107938
NASA-TM-107938
N92-28268 # p 3282 DE92-010701
LA-12287-T
N92-28269 # p 3283 CONF-9110228-8
DE92-010709
UCRL-JC-109291
N92-28270 # p 3356 CONF-9111203-1
DE92-010729
SU-SLAC-PUB-5701
N92-28271 # p 3289 AD-A247060
AFOSR-92-0084TR
N92-28272 # p 3308 AD-A247064
SSD-TR-92-03
TR-0091(6448)-1
N92-28273 # p 3348 AD-A247065
ETS-RR-92-9-ONR
N92-28274 # p 3283 AD-A247305
AFOSR-92-0032TR
N92-28275 # p 3278 AD-A248053
N92-28276 # p 3278 AD-A248290
AL-TR-1991-0103
N92-28277 # p 3306 DE92-001239
NREL/TP-451-4797
N92-28278 # p 3324 CONF-9109107-5
DE92-010265
LBL-31398
N92-28279 # p 3341 CONF-9204106-3
DE92-011061
N92-28280 # p 3362 DE92-622662
IC-91/308
N92-28281 # p 3363 DE92-622799
IC-91/282
N92-28282 # p 3363 DE92-782008
JAERI-M-91-178
N92-28283 # p 3320 AD-A246039
N92-28284 # p 3292 AD-A246453
BRL-TR-3317
N92-28285 # p 3334 AD-A246668
AFIT/GSM/ENC/91S-22
N92-28286 # p 3329 AD-A246683
AFIT/GLM/LSR/91S-62
N92-28287 # p 3254 AD-A246690
N92-28288 # p 3324 AD-A246695
USARIEM-T2-92
N92-28289 # p 3334 AD-A246697
N92-28290 # p 3254 AD-A246698
TR-46
N92-28291 # p 3262 AD-A246699
TR-47
N92-28292 # p 3351 AD-A246822
CERL-N-92/07
N92-28293 # p 3292 AD-A249204
N92-28294 # p 3236 AD-A249259
WL-TR-91-2103
N92-28295 # p 3278 AD-A249260
ARO-26711.17-EL
N92-28296* # p 3298 NAS 1.26:189153
NASA-CR-189153
N92-28297* # p 3346 NAS 1.15:104567
NASA-TM-104567
REPT-92B00092
N92-28298 # p 3360 AD-A247059
AFOSR-92-0123TR
N92-28299 # p 3289 AD-A247309
AFOSR-92-0014TR
N92-28300 # p 3254 AD-A247312
AFOSR-92-0161TR
N92-28301 # p 3334 AD-A247314
CMS-TSR-92-08
N92-28302 # p 3351 AD-A248033
WES/TR/EL-92-13
N92-28303 # p 3251 AD-A248050
ARCCB-TR-92005
N92-28304 # p 3272 AD-A248054
M91-114
N92-28305 # p 3278 AD-A248055
MTR-11227-VOL-1
N92-28306 # p 3341 AD-A248320
N92-28307 # p 3251 AD-A248432
ARO-26057.16-EG
N92-28308 # p 3356 ETN-92-91238
NIKHEF-K/AMPS/91-07
N92-28309 # p 3334 CONF-920362-15
DE92-011264
LA-UR-92-837
N92-28310 # p 3354 CONF-9106194-8
DE92-011285
LA-UR-92-751
N92-28311 # p 3346 DE92-622408
IC-91/304
N92-28312 # p 3363 DE92-622791
IC-91/287
N92-28313 # p 3349 ETN-92-98303
PML-1990-24-PT-2
TD-90-1700-PT-2
N92-28314 # p 3351 ETN-92-91241
FFI-91/7017
ISSN-0802-2437
N92-28315 # p 3289 ETN-92-91242
FFI-91/7020
ISSN-0802-2437
N92-28316 # p 3320 AD-A245941
N92-28317 # p 3230 AD-A245942
N92-28318 # p 3320 AD-A245943
N92-28319 # p 3309 AD-A245965
N92-28320 # p 3298 AD-A247097
AFOSR-92-0079TR
N92-28321 # p 3321 AD-A247644
NOARL-PR-91-054-352
N92-28322 # p 3287 AD-A248307
TR-84
N92-28323 # p 3262 AD-A248577
AFOSR-92-0224TR
N92-28324 # p 3351 AD-A248609
NOARL-15
N92-28325 # p 3344 AD-A249351
TR-406
N92-28326 # p 3279 AD-A249354
ARO-28866.1-CH-SBI
N92-28327 # p 3298 AD-A249358
ARO-25786.1-MS-A
N92-28328 # p 3357 AD-A249363
ARO-25408.17-PH
N92-28329 # p 3346 AD-A249365
ARO-23306.531-MA
N92-28330 # p 3289 AD-A249379
ARO-29004.1-EL-SBI
N92-28331 # p 3363 CONF-920676-1
DE92-010667
SAND-92-0384C
N92-28332 # p 3335 CONF-9105126-6
DE92-010695
WSRC-MS-91-086
N92-28333 # p 3363 CONF-9107105-59

DE92-010710
UCRL-JC-109289
N92-28334 # p 3342 ..... CONF-920390-2
DE92-010716
UCRL-JC-109774
N92-28335 # p 3360 ..... CONF-920607-6
DE92-010718
UCRL-JC-109808
N92-28336 # p 3397 ..... CONF-9110310-4
DE92-010720
UCRL-JC-110087
N92-28337 # p 3354 ..... CEBAF-PR-92-001
CONF-9109127-1
DE92-010853
DOE/ER-40105/181
N92-28338 # p 3259 ..... CONF-9206135-2
DE92-010871
IS-M-700
N92-28339 # p 3262 ..... ANL/CP-75375
CONF-9205132-1
DE92-010904
N92-28340 # p 3318 ..... DE92-010951
DOE/ER-61066/T1
N92-28341 # p 3255 ..... CONF-920657-2
DE92-010955
SAND-92-0447C
N92-28342 # p 3335 ..... CONF-920540-16
DE92-010957
SAND-92-0520C
N92-28343* # p 3244 ..... NAS 1.15:104564
NASA-TM-104564
REPT-92B00089
N92-28344* # p 3397 ..... ISBN-0-16-036174-5
LC-90-39761
NAS 1.21:4104
NASA-SP-4104
N92-28345* # p 3372 ..... ISBN-0-16-036173-7
LC-91-33408
NAS 1.21:508
NASA-SP-508
N92-28346 # p 3329 ..... AD-A245939
N92-28347 # p 3272 ..... AD-A245964
N92-28348 # p 3221 ..... AD-A246759
AFIT/GLM/LSQ/91S-57
N92-28349 # p 3363 ..... AD-A246764
TR-115
N92-28350 # p 3283 ..... AD-A248429
DCW-R-33-01
N92-28351 # p 3279 ..... AD-A248430
N92-28352 # p 3298 ..... AD-A248440
N92-28353 # p 3335 ..... AD-A248620
NPS-EC-92-004
N92-28354 # p 3360 ..... AD-A248630
NRL/MR/4440-92-6966
N92-28355 # p 3357 ..... CONF-9206141-1
DE92-010664
SAND-92-0393C
N92-28356 # p 3356 ..... CONF-920331-3
DE92-011237
LA-UR-92-936
N92-28357 # p 3273 ..... AD-A249331
N92-28358 # p 3273 ..... AD-A249359
N92-28359 # p 3268 ..... AD-A249362
MSRR-578
N92-28360 # p 3262 ..... AD-A249366
ARO-29648.1-MS-CF
N92-28361* # p 3283 ..... NAS 1.26:190400
NASA-CR-190400
N92-28362* # p 3292 ..... NAS 1.26:184328
NASA-CR-184328
N92-28363 # p 3350 ..... ISBN-0-309-04731-5
LC-92-10780
N92-28364 # p 3351 ..... AR-006-376
MRL-TR-91-23
N92-28365 # p 3321 ..... AD-A246775
NPS-OC-91-002
N92-28366 # p 3248 ..... AD-A246776
ESD-TR-91-161
TR-934
N92-28367 # p 3279 ..... AD-A247019
JHU/APL-TG-1379
N92-28368 # p 3246 ..... AD-A247023
N92-28369* # p 3246 ..... NAS 1.15:107941
NASA-TM-107941
N92-28370* # p 3246 ..... NAS 1.15:107937
NASA-TM-107937
N92-28371* # p 3273 ..... NAS 1.26:190408
NASA-CR-190408
UMICH-027723-5-T
N92-28372 # p 3357 ..... AD-A246714
EOARD-TR-92-04
N92-28373 # p 3279 ..... AD-A247025
N92-28374* # p 3255 ..... L-17025
NAS 1.60:3224
NASA-TP-3224
N92-28375* # p 3344 ..... L-16983
NAS 1.60:3198
NASA-TP-3198
N92-28376 # p 3235 ..... AGARD-AG-329
ISBN-92-835-0657-X
N92-28377 # p 3235 ..... NO REPORT NUMBER
N92-28378 # p 3235 ..... NO REPORT NUMBER
N92-28379 # p 3235 ..... NO REPORT NUMBER
N92-28380 # p 3235 ..... NO REPORT NUMBER
N92-28381 # p 3342 ..... DE92-010661
UCRL-MA-108543
N92-28382 # p 3324 ..... DE92-010680
ORNL/M-2026
N92-28383 # p 3307 ..... AD-A245912
N92-28384 # p 3293 ..... AD-A245926
N92-28385 # p 3335 ..... AD-A248362
N92-28386 # p 3309 ..... AD-A248383
AD-E200947
PL-TR-91-2281
SR-1
N92-28387 # p 3344 ..... AD-A248457
ARO-28197.9-MA-SAH
N92-28388 # p 3240 ..... AD-A248581
AFOSR-92-0259TR
N92-28389 # p 3367 ..... AD-A248619
N92-28390 # p 3259 ..... AD-A248701
N92-28391 # p 3255 ..... AD-A246760
TR-120
N92-28392 # p 3363 ..... AD-A246763
TR-114
N92-28393 # p 3372 ..... AD-A246854
N92-28394 # p 3309 ..... AD-A247011
AD-E200869
PL-TR-91-2126
N92-28395 # p 3364 ..... AD-A247013
N92-28396 # p 3326 ..... AD-A247014
HEL-TN-1-92
N92-28397 # p 3324 ..... AD-A247159
AFOSR-92-0146TR-PHASE-1
N92-28398 # p 3262 ..... AD-A247464
UDR-TR-91-53
WL-TR-91-2111
N92-28399 # p 3347 ..... AD-A247721
N92-28400 # p 3350 ..... AD-A247722
NRL/MR/4440-92-6952
N92-28401 # p 3344 ..... AD-A247724
NHRC-91-17
N92-28402 # p 3321 ..... AD-A247733
MPL-U-10/92
N92-28403 # p 3367 ..... AD-A247740
NSWCDD/TR-92/47
N92-28404 # p 3368 ..... AD-A247741
RL-TR-91-361
N92-28405 # p 3263 ..... AD-A247744
N92-28406 # p 3243 ..... B-237832
GAO/IMTEC-92-50
N92-28407 # p 3240 ..... AD-A245922
NAMRL-TM-91-2
N92-28408 # p 3326 ..... AD-A245925
N92-28409 # p 3352 ..... AD-A245961
N92-28410 # p 3273 ..... AD-A245967
N92-28411 # p 3347 ..... AD-A246713
CMS-TSR-92-01
N92-28412 # p 3263 ..... AD-A246773
AFOSR-92-0007TR
AF030-FR-LPT(1/92)
N92-28413 # p 3352 ..... AD-A247016
NADC-91113-50
N92-28414 # p 3354 ..... AD-A247017
AFOSR-92-0011TR
N92-28415 # p 3263 ..... AD-A247018
AFOSR-92-0012TR
SWRI-2253/3
N92-28416 # p 3251 ..... AD-A248449
ARCCB-TR-92007
N92-28417* # p 3248 ..... AIAA PAPER 92-3785
E-7130
NAS 1.15:105727
NASA-TM-105727
N92-28418* # p 3236 ..... AIAA PAPER 92-3790
E-7086
NAS 1.15:105698
NASA-TM-105698
N92-28419* # p 3236 ..... AIAA PAPER 92-3570
E-7109
NAS 1.15:105715
NASA-TM-105715
N92-28420* # p 3325 ..... A-92043
NAS 1.15:103913
NASA-TM-103913
N92-28421 # p 3318 ..... AD-A245360
N92-28422 # p 3307 ..... DE92-010697
DOE/CE-0532
N92-28423 # p 3318 ..... AD-A245927
N92-28424 # p 3298 ..... AD-A247300
WES/CR/SL-92-2
N92-28425 # p 3297 ..... AD-A247430
MTL-TR-92-5
N92-28426 # p 3259 ..... AD-A248372
N92-28427 # p 3279 ..... AD-A248448
REPT-26151-EL
N92-28428 # p 3335 ..... AD-A248579
AFOSR-92-0263TR
N92-28429 # p 3344 ..... AD-A248580
AFOSR-92-0262TR
N92-28430 # p 3368 ..... AD-A248711
N92-28431* # p 3273 ..... NAS 1.26:189185
NASA-CR-189185
SS/L-TR00820
N92-28432* # p 3279 ..... E-7131
NAS 1.15:105728
NASA-TM-105728
N92-28433* # p 3266 ..... AIAA PAPER 92-3063
E-7173
NAS 1.15:105759
NASA-TM-105759
N92-28434* # p 3293 ..... AVSCOM-TR-91-C-036
E-7019
NAS 1.15:105655
NASA-TM-105655
N92-28435* # p 3231 ..... NAS 1.15:107586
NASA-TM-107586
N92-28436* # p 3268 ..... E-7035
NAS 1.55:10094
NASA-CP-10094
N92-28437* # p 3267 ..... NO REPORT NUMBER
N92-28438* # p 3267 ..... NO REPORT NUMBER
N92-28439* # p 3267 ..... NO REPORT NUMBER
N92-28440* # p 3267 ..... NO REPORT NUMBER
N92-28441* # p 3267 ..... NO REPORT NUMBER
N92-28442* # p 3267 ..... NO REPORT NUMBER
N92-28443* # p 3267 ..... NO REPORT NUMBER
N92-28444* # p 3267 ..... NO REPORT NUMBER
N92-28445* # p 3267 ..... NO REPORT NUMBER
N92-28446* # p 3267 ..... NO REPORT NUMBER
N92-28447* # p 3267 ..... NO REPORT NUMBER
N92-28448* # p 3267 ..... NO REPORT NUMBER
N92-28449* # p 3267 ..... NO REPORT NUMBER
N92-28450* # p 3268 ..... NO REPORT NUMBER
N92-28451* # p 3248 ..... NO REPORT NUMBER
N92-28452* # p 3271 ..... NO REPORT NUMBER
N92-28453* # p 3271 ..... NO REPORT NUMBER
N92-28454* # p 3268 ..... NO REPORT NUMBER
N92-28455* # p 3268 ..... NO REPORT NUMBER
N92-28456* # p 3279 ..... NAS 1.15:103586
NASA-TM-103586
N92-28457* # p 3239 ..... A-89130
NAS 1.15:102192
NASA-TM-102192
N92-28458 # p 3236 ..... AGARD-LS-183
ISBN-92-835-0674-X
N92-28459 # p 3237 ..... NO REPORT NUMBER
N92-28460 # p 3237 ..... NO REPORT NUMBER
N92-28461 # p 3237 ..... NO REPORT NUMBER
N92-28462 # p 3237 ..... NO REPORT NUMBER
N92-28463 # p 3237 ..... NO REPORT NUMBER
N92-28464* # p 3237 ..... NO REPORT NUMBER
N92-28465 # p 3237 ..... NO REPORT NUMBER
N92-28466* # p 3238 ..... NO REPORT NUMBER
N92-28467 # p 3238 ..... NO REPORT NUMBER
N92-28468 # p 3231 ..... AGARD-AR-312
ISBN-92-835-0668-5
N92-28469 # p 3231 ..... AGARD-LS-186
ISBN-92-835-0675-8
N92-28470 # p 3231 ..... NO REPORT NUMBER
N92-28471 # p 3232 ..... NO REPORT NUMBER
N92-28472 # p 3232 ..... NO REPORT NUMBER
N92-28473* # p 3232 ..... AGARD-PAPER-2
N92-28474 # p 3232 ..... NO REPORT NUMBER
N92-28475* # p 3357 ..... AIAA PAPER 92-3351
E-7145
NAS 1.15:105739
NASA-TM-105739
N92-28476* # p 3293 ..... AVSCOM-TR-91-C-027
E-6622
NAS 1.15:105653
NASA-TM-105653
N92-28477* # p 3226 ..... L-16996
NAS 1.60:3197
NASA-TP-3197
N92-28478* # p 3372 ..... LPI-CONTRIB-787
NAS 1.26:190508
NASA-CR-190508
N92-28479* # p 3372 ..... NO REPORT NUMBER
N92-28480* # p 3373 ..... NO REPORT NUMBER
N92-28481* # p 3373 ..... NO REPORT NUMBER
N92-28482* # p 3373 ..... NO REPORT NUMBER
N92-28483* # p 3373 ..... NO REPORT NUMBER
N92-28484* # p 3373 ..... NO REPORT NUMBER
N92-28485* # p 3373 ..... NO REPORT NUMBER
N92-28486* # p 3374 ..... NO REPORT NUMBER
N92-28487* # p 3374 ..... NO REPORT NUMBER
N92-28488* # p 3374 ..... NO REPORT NUMBER

N92-28489* # p 3374 ..... NO REPORT NUMBER
N92-28490* # p 3374 ..... NO REPORT NUMBER
N92-28491* # p 3374 ..... NO REPORT NUMBER
N92-28492* # p 3375 ..... NO REPORT NUMBER
N92-28493* # p 3375 ..... NO REPORT NUMBER
N92-28494* # p 3375 ..... NO REPORT NUMBER
N92-28495* # p 3375 ..... NO REPORT NUMBER
N92-28496* # p 3375 ..... NO REPORT NUMBER
N92-28497* # p 3375 ..... NO REPORT NUMBER
N92-28498* # p 3376 ..... NO REPORT NUMBER
N92-28499* # p 3376 ..... NO REPORT NUMBER
N92-28500* # p 3376 ..... NO REPORT NUMBER
N92-28501* # p 3376 ..... NO REPORT NUMBER
N92-28502* # p 3376 ..... NO REPORT NUMBER
N92-28503* # p 3376 ..... NO REPORT NUMBER
N92-28504* # p 3377 ..... NO REPORT NUMBER
N92-28505* # p 3377 ..... NO REPORT NUMBER
N92-28506* # p 3377 ..... NO REPORT NUMBER
N92-28507* # p 3377 ..... NO REPORT NUMBER
N92-28508* # p 3377 ..... NO REPORT NUMBER
N92-28509* # p 3378 ..... NO REPORT NUMBER
N92-28510* # p 3378 ..... NO REPORT NUMBER
N92-28511* # p 3226 ..... NAS 1.26:190431
NASA-CR-190431
N92-28512 # p 3364 ..... AD-A246765
TR-118
N92-28513 # p 3364 ..... AD-A246772
AFOSR-92-0165TR
N92-28514 # p 3332 ..... AD-A246774
AFOSR-92-0137TR
N92-28515 # p 3325 ..... AD-A246777
N92-28516 # p 3348 ..... AD-A246779
CRMSE-91-01
N92-28517 # p 3318 ..... AD-A247151
N92-28518 # p 3329 ..... AD-A247153
N92-28519 # p 3335 ..... AD-A247156
N92-28520 # p 3395 ..... AD-A247158
AFOSR-92-0119TR
CAL-1955
N92-28521* # p 3330 ..... NAS 1.15:103588
NASA-TM-103588
N92-28522 # p 3221 ..... AGARD-CP-513
ISBN-92-835-0656-1
N92-28523 # p 3221 ..... NO REPORT NUMBER
N92-28524 # p 3221 ..... NO REPORT NUMBER
N92-28525 # p 3221 ..... NO REPORT NUMBER
N92-28526 # p 3221 ..... NO REPORT NUMBER
N92-28527 # p 3222 ..... NO REPORT NUMBER
N92-28528 # p 3222 ..... NO REPORT NUMBER
N92-28529 # p 3222 ..... NO REPORT NUMBER
N92-28530 # p 3222 ..... NO REPORT NUMBER
N92-28531 # p 3222 ..... NO REPORT NUMBER
N92-28532 # p 3222 ..... NO REPORT NUMBER
N92-28533 # p 3222 ..... NO REPORT NUMBER
N92-28534 # p 3223 ..... NO REPORT NUMBER
N92-28535 # p 3223 ..... NO REPORT NUMBER
N92-28536 # p 3223 ..... NO REPORT NUMBER
N92-28537 # p 3223 ..... NO REPORT NUMBER
N92-28538 # p 3223 ..... NO REPORT NUMBER
N92-28539 # p 3223 ..... NO REPORT NUMBER
N92-28540 # p 3224 ..... NO REPORT NUMBER
N92-28541 # p 3224 ..... NO REPORT NUMBER
N92-28542 # p 3224 ..... NO REPORT NUMBER
N92-28543 # p 3224 ..... NO REPORT NUMBER
N92-28544 # p 3224 ..... NO REPORT NUMBER
N92-28545* # p 3224 ..... NO REPORT NUMBER
N92-28546 # p 3225 ..... NO REPORT NUMBER
N92-28547 # p 3225 ..... NO REPORT NUMBER
N92-28548 # p 3225 ..... NO REPORT NUMBER
N92-28549 # p 3225 ..... NO REPORT NUMBER
N92-28550 # p 3225 ..... NO REPORT NUMBER
N92-28551* # p 3225 ..... NO REPORT NUMBER
N92-28552 # p 3226 ..... NO REPORT NUMBER
N92-28553 # p 3263 ..... AD-A247679
N92-28554 # p 3357 ..... AD-A247683
N92-28555* # p 3283 ..... MSSU-EIRS-ERC-91-1
NAS 1.26:189881
NASA-CR-189881
N92-28556* # p 3352 ..... NAS 1.26:189643
NASA-CR-189643
WYLE-TN-91-8
N92-28557 # p 3327 ..... AD-A246708
NAMRL-1367
N92-28558 # p 3263 ..... AD-A246951
AFOSR-92-0087TR
N92-28559 # p 3352 ..... AD-A247303
N92-28560 # p 3246 ..... AD-A247672
CERL-M-92/12
N92-28561 # p 3280 ..... AD-A247694
RL-TR-91-340
N92-28562 # p 3335 ..... AD-A247696
NOSC-TR-1463
N92-28563 # p 3264 ..... AD-A247707
DREA-TM-91/214
N92-28564 # p 3264 ..... AD-A247711
DREO-TN-91-9
N92-28565 # p 3368 ..... AD-A247752
WL-TR-91-4132
N92-28566 # p 3321 ..... AD-A247754
NOARL-35
N92-28567 # p 3309 ..... AD-A247772
N92-28568 # p 3280 ..... AD-A247773
NAVSWC-TR-91-614
N92-28569 # p 3309 ..... AD-A248616
AD-E200950
PL-TR-92-2005
SR-11
N92-28570 # p 3264 ..... AD-A249106
AFOSR-92-0223TR
N92-28571* p 3358 INT-PATENT-CLASS-H01P-1/18
NASA-CASE-LEW-14878-1
US-PATENT-APPL-SN-587921
US-PATENT-CLASS-333-161
US-PATENT-CLASS-333-995
US-PATENT-CLASS-505-1
US-PATENT-CLASS-505-703
US-PATENT-CLASS-505-848
US-PATENT-CLASS-505-866
US-PATENT-5,116,807
N92-28572 # p 3251 ..... ETN-92-91266
ISBN-951-38-3990-7
ISSN-0358-5077
VTT-RR-742
N92-28573 # p 3251 ..... ETN-92-91267
ISBN-951-38-3991-5
ISSN-0358-5077
VTT-RR-743
N92-28574 # p 3259 ..... ETN-92-91396
LR-651
N92-28575 # p 3299 ..... ETN-92-91397
LR-657
N92-28576 # p 3259 ..... ETN-92-91398
LR-658
N92-28577 # p 3252 ..... ETN-92-91399
LR-659
N92-28578 # p 3259 ..... ETN-92-91400
LR-661
N92-28579 # p 3240 ..... ETN-92-91401
LR-662
N92-28580 # p 3299 ..... ETN-92-91402
LR-664
N92-28581 # p 3345 ..... ETN-92-91403
LR-665
N92-28582 # p 3252 ..... ETN-92-91404
LR-666
N92-28583 # p 3299 ..... ETN-92-91405
LR-667
N92-28584* # p 3239 ..... H-1769
NAS 1.26:4443
NASA-CR-4443
N92-28585* # p 3336 ..... NAS 1.26:189621
NASA-CR-189621
N92-28586* # p 3273 ..... EE-SATCOM-86-5
JPL-9950-1382
NAS 1.26:190484
NASA-CR-190484
N92-28587* # p 3310 ..... LPI-TR-92-03
NAS 1.26:190419
NASA-CR-190419
N92-28588* # p 3310 ..... NO REPORT NUMBER
N92-28589* # p 3310 ..... NO REPORT NUMBER
N92-28590* # p 3310 ..... NO REPORT NUMBER
N92-28591* # p 3310 ..... NO REPORT NUMBER
N92-28592* # p 3310 ..... NO REPORT NUMBER
N92-28593* # p 3310 ..... NO REPORT NUMBER
N92-28594* # p 3311 ..... NO REPORT NUMBER
N92-28595* # p 3311 ..... NO REPORT NUMBER
N92-28596* # p 3311 ..... NO REPORT NUMBER
N92-28597* # p 3311 ..... NO REPORT NUMBER
N92-28598* # p 3311 ..... NO REPORT NUMBER
N92-28599* # p 3311 ..... NO REPORT NUMBER
N92-28600* # p 3312 ..... NO REPORT NUMBER
N92-28601* # p 3312 ..... NO REPORT NUMBER
N92-28602* # p 3312 ..... NO REPORT NUMBER
N92-28603* # p 3312 ..... NO REPORT NUMBER
N92-28604* # p 3313 ..... NO REPORT NUMBER
N92-28605* # p 3313 ..... NO REPORT NUMBER
N92-28606* # p 3313 ..... NO REPORT NUMBER
N92-28607* # p 3313 ..... NO REPORT NUMBER
N92-28608* # p 3314 ..... NO REPORT NUMBER
N92-28609* # p 3314 ..... NO REPORT NUMBER
N92-28610* # p 3314 ..... NO REPORT NUMBER
N92-28611* # p 3314 ..... NO REPORT NUMBER
N92-28612* # p 3314 ..... NO REPORT NUMBER
N92-28613* # p 3315 ..... NO REPORT NUMBER
N92-28614* # p 3315 ..... NO REPORT NUMBER
N92-28615* # p 3315 ..... NO REPORT NUMBER
N92-28616* # p 3315 ..... NO REPORT NUMBER
N92-28617* # p 3315 ..... NO REPORT NUMBER
N92-28618* # p 3315 ..... NO REPORT NUMBER
N92-28619* # p 3315 ..... NO REPORT NUMBER
N92-28620* # p 3299 ..... NAS 1.55:3153
NASA-CP-3153
REPT-92B00061
N92-28621* # p 3299 ..... NO REPORT NUMBER
N92-28622* # p 3299 ..... NO REPORT NUMBER
N92-28623* # p 3300 ..... NO REPORT NUMBER
N92-28624* # p 3300 ..... NO REPORT NUMBER
N92-28625* # p 3300 ..... NO REPORT NUMBER
N92-28626* # p 3300 ..... NO REPORT NUMBER
N92-28627* # p 3300 ..... NO REPORT NUMBER
N92-28628* # p 3301 ..... NO REPORT NUMBER
N92-28629* # p 3301 ..... NO REPORT NUMBER
N92-28630* # p 3301 ..... NO REPORT NUMBER
N92-28631* # p 3301 ..... NO REPORT NUMBER
N92-28632* # p 3301 ..... NO REPORT NUMBER
N92-28633* # p 3302 ..... NO REPORT NUMBER
N92-28634 # p 3232 ..... ETN-92-91447
NLR-TP-90307-U
N92-28635 # p 3347 ..... ETN-92-91448
NLR-TP-90334-U
N92-28636 # p 3336 ..... ETN-92-91451
NLR-TP-90387-U
N92-28637 # p 3252 ..... ETN-92-91452
NLR-TP-91050-U
N92-28638 # p 3336 ..... ETN-92-91455
ISSN-0926-4493
MEMO-COSOR-91-21
N92-28639 # p 3336 ..... ETN-92-91456
ISSN-0926-4493
MEMO-COSOR-91-22
N92-28640 # p 3348 ..... ETN-92-91457
ISSN-0926-4493
MEMO-COSOR-91-23
N92-28641 # p 3347 ..... ETN-92-91458
MEMO-COSOR-91-24
N92-28642 # p 3342 ..... ETN-92-91459
MEMO-COSOR-91-25
N92-28643 # p 3302 ..... ETN-92-91521
NLR-TP-89163-U
N92-28644 # p 3235 ..... ETN-92-91438
NLR-TP-90174-U
N92-28645 # p 3293 ..... ETN-92-91444
NLR-TP-90282-U
N92-28646 # p 3293 ..... ETN-92-91445
NLR-TP-90284-U
N92-28647 # p 3349 ..... ETN-92-91281
N92-28648 # p 3345 ..... ETN-92-91431
NLR-TP-90028-U
N92-28649 # p 3232 ..... ETN-92-91432
NLR-TP-90068-U
N92-28650 # p 3302 ..... ETN-92-91433
NLR-TP-90070-U
N92-28651 # p 3233 ..... ETN-92-91434
NLR-TP-90108-U
N92-28652 # p 3239 ..... ETN-92-91435
GARTEUR/TP-056
NLR-TP-90129-U
N92-28653 # p 3239 ..... ETN-92-91436
NLR-TP-90159-U
N92-28654 # p 3236 ..... ETN-92-91437
NLR-TP-90163-U
N92-28655 # p 3230 ..... ETN-92-91439
NLR-TP-90192-U
N92-28656 # p 3358 ..... ETN-92-91441
NLR-TP-90199-U
N92-28657 # p 3226 ..... ETN-92-91450
NLR-TP-90368-U
N92-28658 # p 3226 ..... ETN-92-91512
NLR-MP-88031-U
N92-28659 # p 3227 ..... ETN-92-91518
NLR-TP-89119-U
N92-28660 # p 3227 ..... ETN-92-91519
NLR-TP-89126-U
N92-28661 # p 3240 ..... ETN-92-91536
NLR-TP-90145-U
N92-28662 # p 3289 ..... AD-A245979
N92-28663 # p 3368 ..... AD-A245982
USAFA-TR-91-19
N92-28664 # p 3360 ..... CTN-92-60500
FFP-4-91
PPL-124
N92-28665 # p 3361 ..... CTN-92-60513
PPL-109
N92-28666 # p 3336 ..... AD-A247492
RL-TR-91-339-VOL-1
N92-28667 # p 3336 ..... AD-A247493
RL-TR-91-339-VOL-2
N92-28668 # p 3318 ..... AD-A247497
AFOSR-92-0220TR
N92-28669 # p 3240 ..... ETN-92-91520
NLR-TP-89158-U
N92-28670* # p 3330 ..... NAS 1.15:107544
NASA-TM-107544
N92-28671* # p 3330 ..... NAS 1.26:190448
NASA-CR-190448
N92-28672* # p 3349 ..... A-92048
NAS 1.15:103914

NASA-TM-103914
N92-28673* # p 3240 ..... AIAA PAPER 92-3916
E-6827
NAS 1.15:105417
NASA-TM-105417
N92-28674* # p 3227 ..... E-7148
NAS 1.15:105743
NASA-TM-105743
N92-28675* # p 3280 ..... E-7161
NAS 1.15:105753
NASA-TM-105753
N92-28676* # p 3342 ..... NAS 1.26:190486
NASA-CR-190486
N92-28677* p 3226 ..... NAS 1.21:7037(278)
NASA-SP-7037(278)
N92-28678* # p 3397 ..... NAS 1.83:150
NASA-NP-150
N92-28679* p 3226 ..... NAS 1.21:7037(275)
NASA-SP-7037(275)
N92-28680* # p 3370 ..... NAS 1.26:190477
NASA-CR-190477
N92-28681* # p 3330 ..... A-92138
NAS 1.26:177597
NASA-CR-177597
N92-28682* # p 3249 ..... E-6450
NAS 1.15:105161
NASA-TM-105161
N92-28683* # p 3246 ..... E-7033
NAS 1.15:105660
NASA-TM-105660
N92-28684* # p 3337 ..... E-7053
NAS 1.15:105749
NASA-TM-105749
N92-28685 # p 3325 ..... CONF-9104298-2
DE92-009459
UCRL-JC-109513
N92-28686 # p 3238 ..... DOT/FAA/CT-91/10
N92-28687 # p 3233 ..... ETN-92-91446
NLR-TP-90305-U
N92-28688 # p 3302 ..... ETN-92-91522
NLR-TP-89211-U
N92-28689 # p 3316 ..... ETN-92-91523
NLR-TP-89217-U
N92-28690 # p 3305 ..... ETN-92-91524
NLR-TP-89235-U
N92-28691 # p 3260 ..... ETN-92-91534
NLR-TP-90138-U
N92-28692 # p 3227 ..... ETN-92-91535
NLR-TP-90144-U
N92-28693* # p 3249 ..... E-7180
NAS 1.15:105763
NASA-TM-105763
N92-28694 # p 3284 ..... ETN-92-91540
NLR-TP-90184-U
N92-28695 # p 3352 ..... ETN-92-91541
NLR-TP-90223-U
N92-28696* # p 3227 ..... E-6930
NAS 1.15:105745
NASA-TM-105745
N92-28697 # p 3305 ..... ETN-92-91542
NLR-TP-90228-U
N92-28698* # p 3358 ..... NAS 1.26:190531
NASA-CR-190531
N92-28699 # p 3274 ..... CTN-91-60077
ECE-90-1
N92-28700 # p 3337 ..... CRIF-MC-91
ETN-92-91022
N92-28701* # p 3302 ..... AVSCOM-TR-91-C-045
E-6788
NAS 1.15:105396
NASA-TM-105396
N92-28702 # p 3252 ..... AD-A250300
MTL-TR-92-18
N92-28703 # p 3316 ..... CTN-92-60460
ISBN-0-315-51071-4
N92-28704 # p 3337 ..... AD-A247496
AFOSR-92-0216TR
N92-28705 # p 3294 ..... ETN-92-91442
NLR-TP-90262-U
N92-28706 # p 3342 ..... ETN-92-91515
NLR-TP-89007-U
N92-28707* # p 3290 ..... NAS 1.26:190501
NASA-CR-190501
N92-28708 # p 3305 ..... ETN-92-91516
NLR-TP-89061-U
N92-28709 # p 3228 ..... ETN-92-91530
NLR-TP-90062-U
N92-28710* # p 3337 ..... CSC/TR-92/6054
NAS 1.26:190503
NASA-CR-190503
N92-28711 # p 3236 ..... ETN-92-91531
NLR-TP-90097-U
N92-28712 # p 3284 ..... ETN-92-91533
NLR-TP-90134-U
N92-28713 # p 3228 ..... ETN-92-91543
NLR-TP-90255-U
N92-28714 # p 3233 ..... ETN-92-91544
NLR-TP-90286-U
N92-28715* # p 3305 ..... NAS 1.26:190398
NASA-CR-190398
N92-28716 # p 3345 ..... ETN-92-91545
NLR-TP-91099-U
N92-28717* # p 3306 ..... NAS 1.26:190445
NASA-CR-190445
N92-28718* # p 3230 ..... NAS 1.26:190469
NASA-CR-190469
OU/AEC-EER-92-2
N92-28719 # p 3337 ..... AD-A250306
AFOSR-92-0279TR
N92-28720* # p 3233 ..... KU-FRL-872-5
NAS 1.26:190444
NASA-CR-190444
N92-28721* # p 3233 ..... A-92064
NAS 1.15:103925
NASA-TM-103925
N92-28722* # p 3352 ..... NAS 1.26:189635
NASA-CR-189635
N92-28723* # p 3280 ..... E-7144
NAS 1.26:189194
NASA-CR-189194
N92-28724 # p 3252 ..... PB92-163831
N92-28725 # p 3252 ..... PB92-163849
N92-28726* # p 3297 ..... CRHC-92-11
NAS 1.26:189752
NASA-CR-189752
UILU-ENG-92-2217
N92-28727* p 3294 INT-PATENT-CLASS-B64G-1/62
NASA-CASE-MSC-21906-1
US-PATENT-APPL-SN-813558
US-PATENT-CLASS-244-161
US-PATENT-CLASS-294-65.5
US-PATENT-CLASS-294-86.4
US-PATENT-CLASS-901-30
US-PATENT-CLASS-901-46
US-PATENT-5,125,601
N92-28728* p 3255 ..... INT-PATENT-CLASS-G01N-27/26
NASA-CASE-MFS-26049-2-NP
US-PATENT-APPL-SN-376487
US-PATENT-APPL-SN-599601
US-PATENT-CLASS-204-180.1
US-PATENT-CLASS-204-183.3
US-PATENT-CLASS-204-299R
US-PATENT-5,108,568
N92-28729* p 3228 INT-PATENT-CLASS-B64C-3/14
NASA-CASE-LAR-14281-1
US-PATENT-APPL-SN-560923
US-PATENT-CLASS-244-35R
US-PATENT-CLASS-244-36
US-PATENT-5,112,120
N92-28730* # p 3247 ..... NAS 1.55:10099
NASA-CP-10099
N92-28731* # p 3244 ..... NO REPORT NUMBER
N92-28732* # p 3247 ..... NO REPORT NUMBER
N92-28733* # p 3247 ..... NO REPORT NUMBER
N92-28734* # p 3247 ..... NO REPORT NUMBER
N92-28735* # p 3247 ..... NO REPORT NUMBER
N92-28736* # p 3247 ..... NO REPORT NUMBER
N92-28737* # p 3247 ..... NO REPORT NUMBER
N92-28738* # p 3247 ..... NO REPORT NUMBER
N92-28739 p 3266 ..... AD-D015243
US-PATENT-APPL-SN-621256
US-PATENT-CLASS-82-20-14
US-PATENT-5,056,405
N92-28740 # p 3316 ..... ETN-92-90643
OEFZS-4574
N92-28741 # p 3337 ..... ETN-92-90846
PNR-90823
N92-28742 # p 3361 ..... IPPCZ-314
N92-28743* # p 3255 ..... A-92056
NAS 1.15:103918
NASA-TM-103918
N92-28744* # p 3327 ..... A-91153
NAS 1.15:103865
NASA-TM-103865
USAAVSCOM-TR-92-A-003
N92-28745 p 3318 ..... ETN-92-91069
N92-28746 p 3342 ..... ETN-92-91230
IZF-1991-B-4
TD91-2156
N92-28747 p 3249 ..... AD-D015245
US-PATENT-APPL-SN-660361
US-PATENT-CLASS-244-169
US-PATENT-5,062,593
N92-28748 p 3249 ..... AD-D015248
US-PATENT-APPL-SN-674271
US-PATENT-CLASS-89-1.809
US-PATENT-5,074,187
N92-28749 p 3294 ..... AD-D015249
US-PATENT-APPL-SN-632709
US-PATENT-CLASS-73-168
US-PATENT-5,078,009
N92-28750* p 3248 INT-PATENT-CLASS-B64G-1/64
NASA-CASE-MFS-28421-1
US-PATENT-APPL-SN-481537
US-PATENT-CLASS-244-161
US-PATENT-CLASS-358-103
US-PATENT-CLASS-364-459
US-PATENT-5,109,345
N92-28751* p 3264 ..... NASA-CASE-LAR-14145-1
US-PATENT-APPL-SN-508316
US-PATENT-APPL-SN-732884
US-PATENT-CLASS-528-125
US-PATENT-CLASS-528-126
US-PATENT-CLASS-528-127
US-PATENT-CLASS-528-128
US-PATENT-CLASS-528-220
US-PATENT-CLASS-528-224
US-PATENT-5,116,934
N92-28752* p 3284 INT-PATENT-CLASS-F28D-17/00
NASA-CASE-LAR-14033-1
US-PATENT-APPL-SN-501909
US-PATENT-CLASS-165-104.31
US-PATENT-CLASS-165-104.34
US-PATENT-CLASS-165-109.1
US-PATENT-CLASS-165-110
US-PATENT-CLASS-165-4
US-PATENT-CLASS-165-41
US-PATENT-5,107,920
N92-28753* p 3280 ..... INT-PATENT-CLASS-H01M-10/40
NASA-CASE-NPO-17922-1-CU
US-PATENT-APPL-SN-596139
US-PATENT-CLASS-252-62.2
US-PATENT-CLASS-429-192
US-PATENT-5,110,694
N92-28754* p 3294 ..... INT-PATENT-CLASS-B05C-17/02
NASA-CASE-GSC-13230-1
US-PATENT-APPL-SN-531374
US-PATENT-CLASS-15-230.11
US-PATENT-CLASS-29-110.5
US-PATENT-CLASS-29-123
US-PATENT-CLASS-29-132
US-PATENT-5,068,951
N92-28755* p 3325 INT-PATENT-CLASS-A61B-3/14
NASA-CASE-MSC-21675-1
US-PATENT-APPL-SN-562095
US-PATENT-CLASS-351-206
US-PATENT-CLASS-351-221
US-PATENT-5,125,730
N92-28756* p 3256 INT-PATENT-CLASS-C25B-1/04
INT-PATENT-CLASS-C25B-1/12
NASA-CASE-MSC-21572-1-SB
US-PATENT-APPL-SN-648933
US-PATENT-CLASS-204-129
US-PATENT-5,110,436
N92-28757* p 3303 ..... INT-PATENT-CLASS-G01N-27/80
INT-PATENT-CLASS-G01R-33/12
NASA-CASE-LAR-13617-5
US-PATENT-APPL-SN-210486
US-PATENT-APPL-SN-449211
US-PATENT-APPL-SN-686263
US-PATENT-CLASS-324-226
US-PATENT-CLASS-324-235
US-PATENT-CLASS-73-601
US-PATENT-5,121,058
N92-28758* # p 3337 ..... FIA-92-13
NAS 1.15:107859
NASA-TM-107859
N92-28759* # p 3345 ..... FIA-92-02
NAS 1.15:107875
NASA-TM-107875
N92-28760* # p 3337 ..... ICASE-IR-21
NAS 1.26:189629
NASA-CR-189629
N92-28761 # p 3290 ..... AD-A245915
N92-28762 # p 3364 ..... CONF-911106-92
DE92-011147
LBL-31457
N92-28763 # p 3260 ..... DE92-012566
KCP-613-4547
N92-28764 # p 3355 ..... DE92-012658
DOE/ER-13262/8
N92-28765 # p 3248 ..... AD-A249940
AD-E200993
PL-TR-91-2273
N92-28766 # p 3284 ..... AD-A249946
AD-E200955
PL-TR-91-1044
N92-28767 # p 3287 ..... AD-A249970
N92-28768 # p 3284 ..... AD-A249973
N92-28769 # p 3256 ..... AD-A250207
AFOSR-92-0390TR
N92-28770 # p 3342 ..... AD-A250208
AFOSR-92-0389TR
N92-28771 # p 3233 ..... AD-A250341

ARL-STRUC-TM-544
DODA-AR-006-633
N92-28772 # p 3241 ..... AD-A250407
WL-TM-02-307-FIBE
N92-28773 # p 3274 ..... AD-A250433
N92-28774 # p 3371 ..... CONF-9108186-3
DE92-011734
FNAL/C-91/349-A
N92-28775 # p 3327 ..... ANL/CP-75335
CONF-920538-18
DE92-011839
N92-28776 # p 3303 ..... ETN-92-91268
ISBN-951-38-3994-X
ISSN-0358-5077
VTT-RR-746
N92-28777 # p 3347 ..... ETN-92-91269
ISSN-0078-3781
ONERA-NT-1991-8
N92-28778 # p 3349 ..... ETN-92-91270
ISSN-0078-3781
ONERA-NT-1991-10
N92-28779 # p 3338 ..... ETN-92-91271
ISSN-0078-3781
ONERA-NT-1991-11
N92-28780 # p 3249 ..... ETN-92-91272
ISSN-0078-3781
ONERA-NT-1990-13
N92-28781 # p 3371 ..... ESA-SP-1147
ETN-92-91276
ISBN-92-9092-025-4
N92-28782 # p 3343 ..... ETN-92-91320
N92-28783 # p 3260 ..... ETN-92-91321
N92-28784 # p 3281 ..... ETN-92-91322
N92-28785 # p 3338 ..... ETN-92-91323
N92-28786 # p 3364 ..... ETN-92-91333
N92-28787 # p 3327 ..... ETN-92-91335
N92-28788 # p 3284 ..... ETN-92-91326
ONERA-RSF-43/1736-AY-146A
N92-28789 # p 3228 ..... ETN-92-91327
ONERA-RSF-136/1865-AY-728-A
N92-28790 # p 3338 ..... ETN-92-91329
ONERA-RT-24/3542-RY-091-R
N92-28791 # p 3306 ..... AD-A245966
N92-28792 # p 3274 ..... ETN-92-91334
N92-28793 # p 3272 ..... ETN-92-91336
N92-28794 # p 3260 ..... ETN-92-91395
NLR-TP-90272-U
N92-28795 # p 3338 ..... AD-A249988
JHU/APL-TG-1380
N92-28796 # p 3274 ..... AD-A250059
N92-28797 # p 3281 ..... AD-A250384
ARO-23756.3-PH-F
N92-28798 # p 3281 ..... AD-A250385
ARO-29305.1-EL
N92-28799 # p 3318 ..... AD-A250419
NPS-PH-92-008
N92-28800 # p 3249 ..... AD-A250424
AD-E951808
AMSMI-TR-RD-PR-91-17
N92-28801 # p 3239 ..... AD-A245973
N92-28802 # p 3234 ..... AD-A245977
N92-28803 # p 3285 ..... AD-A248634
NRL/MR/4404-92-6961
N92-28804 # p 3368 ..... DE92-012408
DOE/AD-0019
N92-28805 # p 3361 ..... DE92-012509
EGG-FSP-10048
N92-28806 # p 3364 ..... DE92-013502
DOE/ER-13738/T2
N92-28807 # p 3306 ..... CONF-9205136-2
DE92-011356
LA-UR-92-708
N92-28808 # p 3285 ..... CONF-9110369
DE92-012692
N92-28809 # p 3274 ..... ANL/CP-75862
CONF-920315-32
DE92-013059
N92-28810 # p 3274 ..... ANL/CP-75861
CONF-920315-31
DE92-013060
N92-28811 # p 3308 ..... DE92-013103
EGG-ESQ-10167
N92-28812 # p 3288 ..... CONF-920362-28
DE92-013207
UCRL-JC-109095
N92-28813 # p 3356 ..... CONF-920538-24
DE92-013232
N92-28814 # p 3281 ..... CONF-920432-11
DE92-013233
N92-28815 # p 3294 ..... ANL/ESD/TM-24
DE92-013252
N92-28816 # p 3361 ..... DE92-621530
ITF-91-28
N92-28817*# p 3285 ..... NAS 1.26:190364
NASA-CR-190364
N92-28818*# p 3285 ..... NO REPORT NUMBER
N92-28819*# p 3285 ..... NO REPORT NUMBER
N92-28820*# p 3229 ..... NO REPORT NUMBER
N92-28821*# p 3258 ..... NO REPORT NUMBER
N92-28822 # p 3256 ..... CONF-920707-14
DE92-006682
SAND-91-8742
N92-28823 # p 3260 ..... DLR-FB-91-24
ETN-92-91065
ISSN-0939-2963
N92-28824 # p 3347 ..... CONF-920750-1
DE92-007300
UCRL-JC-109505
N92-28825 # p 3286 ..... DLR-FB-91-25
ETN-92-91066
ISSN-0939-2963
N92-28826 # p 3245 ..... DLR-FB-91-27
ETN-92-91067
ISSN-0939-2963
N92-28827 # p 3256 ..... DE92-010451
DOE/PC-90293/T3
N92-28828 p 3241 ..... ETN-92-91228
FEL-91-B345
TD91-3887
N92-28829 # p 3241 ..... ISSN-0452-2982
JTN-92-80350
NAL-TM-632
N92-28830 # p 3319 ..... DE92-011031
DOE/ER-61220/1
N92-28831 # p 3331 ..... ISSN-0452-2982
JTN-92-80351
NAL-TM-633
N92-28832 # p 3368 ..... CONF-9203113-1
DE92-011139
SAND-92-0477C
N92-28833 # p 3241 ..... ISSN-0452-2982
JTN-92-80352
NAL-TM-635
N92-28834 # p 3306 ..... CONF-9205136-1
DE92-011267
LA-UR-92-764
N92-28835 # p 3241 ..... ISSN-0452-2982
JTN-92-80362
NAL-TM-634
N92-28836 # p 3303 ..... ISSN-0452-2982
JTN-92-80363
NAL-TM-636
N92-28837*# p 3307 ..... E-7184
NAS 1.15:105767
NASA-TM-105767
N92-28838 # p 3368 ..... CONF-9203126-1
DE92-011271
LA-UR-92-653
N92-28839 # p 3355 ..... CONF-9111141-6
DE92-011281
FNAL/C-92/62
N92-28840 # p 3306 ..... CONF-9205136-3
DE92-011355
LA-UR-92-709
N92-28841 # p 3338 ..... DE92-011432
DOE/ER-25086/2
N92-28842 # p 3338 ..... ETN-92-91324
N92-28843 # p 3371 ..... AD-A248416
AFOSR-92-0194TR
N92-28844 # p 3325 ..... ETN-92-91328
ONERA-RTS-11/3446-EY
N92-28845 # p 3336 ..... AD-A249299
ARO-28637.1-GS-EQ
N92-28846 # p 3274 ..... AD-A249300
ARO-26384.11-GS
N92-28847 # p 3361 ..... CTN-92-60497
PPL-127
N92-28848 # p 3361 ..... CTN-92-60498
PPL-126
N92-28849 # p 3361 ..... CTN-92-60504
FFP-2-91
PPL-120
N92-28850 # p 3303 ..... ETN-92-91538
NLR-TP-90172-U
N92-28851 # p 3297 ..... AD-A249297
ARO-24981.33-MS
N92-28852 # p 3290 ..... CONF-920707-4
DE92-005327
SAND-91-8712
N92-28853 # p 3316 ..... DE92-011438
DOE/ER-61072/2
N92-28854 # p 3260 ..... CONF-911202-71
DE92-011645
N92-28855 # p 3303 ..... CONF-9204115-1
DE92-011659
SAND-92-0271C
N92-28856 # p 3260 ..... CONF-911202-74
DE92-011671
N92-28857 # p 3364 ..... CONF-911202-72
DE92-011686
N92-28858 # p 3355 ..... CONF-9111141-SUMM
CONF-9111210-SUMM
DE92-011735
FNAL/C-92/26A
N92-28859 # p 3371 ..... CONF-9111165-12
DE92-011736
FNAL/C-92/20-A
N92-28860 # p 3355 ..... CONF-920318-1
DE92-011760
UCRL-JC-110189
N92-28861 # p 3245 ..... CONF-9204102-6
DE92-011380
SAND-91-2285C
N92-28862*# p 3290 ..... L-16967
NAS 1.77:10001
NASA-TT-10001
N92-28863*# p 3307 ..... NAS 1.26:190421
NASA-CR-190421
UNM-ISNPS-4-92
N92-28864*# p 3366 ..... NAS 1.19:278
NASA-EP-278
N92-28865 # p 3228 ..... AD-A247532
AFOSR-92-0222TR
N92-28866 # p 3369 ..... AD-A247425
AL-TP-1991-0050
N92-28867*# p 3321 ..... NAS 1.26:190488
NASA-CR-190488
N92-28868*# p 3358 ..... NAS 1.26:190495
NASA-CR-190495
N92-28869*# p 3396 ..... CSC/TM-91/6008
NAS 1.15:107947
NASA-TM-107947
REPT-544-FDD-91/004
N92-28870*# p 3396 ..... NAS 1.15:107946
NASA-TM-107946
N92-28871*# p 3396 ..... NAS 1.26:190510
NASA-CR-190510
N92-28872*# p 3396 ..... CSC/TM-91/6167ROUDO
NAS 1.26:190378
NASA-CR-190378
REPT-554-FDD-91/113ROUDO
N92-28873*# p 3275 ..... NAS 1.26:190509
NASA-CR-190509
N92-28874 # p 3365 ..... CONF-920240-4
DE92-011357
LA-UR-92-706
N92-28875*# p 3339 ..... NAS 1.26:190552
NASA-CR-190552
RIACS-TR-92-06
N92-28876*# p 3275 ..... NAS 1.15:107589
NASA-TM-107589
N92-28877 # p 3327 ..... AD-A247049
AFOSR-92-0136TR
N92-28878 # p 3275 ..... AD-A248431
N92-28879 # p 3286 ..... AD-A249284
PSU-TURBO-R-9201
N92-28880 # p 3327 ..... AD-A249287
AL-TP-1992-0004
N92-28881 # p 3355 ..... AD-A249296
NRL-TR-3
N92-28882 # p 3256 ..... AD-A245938
DREO-TN-91-25
N92-28883 # p 3228 ..... AD-A245940
N92-28884 # p 3319 ..... AD-A245946
N92-28885 # p 3365 ..... AD-A247111
REPT-2
N92-28886 # p 3325 ..... AD-A247172
AFOSR-92-0104TR
N92-28887 # p 3275 ..... AD-A247194
DREO-TN-91-32
N92-28888 # p 3229 ..... AD-A247196
AFOSR-92-0077TR
N92-28889 # p 3352 ..... AD-A247199
AFOSR-92-0116TR
N92-28890 # p 3286 ..... AD-A247203
AFOSR-92-0080TR
N92-28891 # p 3332 ..... AD-A248633
NRL/FR/5560-92-9329
N92-28892 # p 3303 ..... AD-A248665
N92-28893 # p 3256 ..... DE92-011194
DOE/ER-13183/T1
N92-28894 # p 3257 ..... CONF-9111204-1
DE92-011196
WSRC-RP-91-1001
N92-28895 # p 3345 ..... AD-A249286
ARO-26436.16-EL
N92-28896 # p 3257 ..... AD-A250206
AFOSR-92-0391TR
N92-28897*# p 3331 ..... NAS 1.60:3200
NASA-TP-3200
S-668
N92-28898 # p 3252 ..... AD-A245949
N92-28899*# p 3333 ..... M-692
NAS 1.15:4392
NASA-TM-4392
N92-28900 # p 3230 ..... DOT/FAA/CT-TN91/32
N92-28901 # p 3234 ..... ISSN-0389-4010
JTN-92-80381

NAL-TR-1112
N92-28902 # p 3272 ..... AD-A247419
CRREL-SR-91-27
N92-28903 # p 3290 ..... AD-A247421
N92-28904 # p 3264 ..... AD-A247423
RTI-83U-5123
RTI/5123/91-29
N92-28905 # p 3275 ..... AD-A247408
JHU/APL-TG-1381
N92-28906* # p 3275 ..... NAS 1.26:189186
NASA-CR-189186
SS/L-TR00821
N92-28907* # p 3396 ..... NAS 1.15:107944
NASA-TM-107944
N92-28908* # p 3286 ..... E-7038
NAS 1.26:189176
NASA-CR-189176
N92-28909* # p 3353 ..... A-92052
NAS 1.15:103915
NASA-TM-103915
N92-28910* # p 3234 ..... A-92014
NAS 1.15:103902
NASA-TM-103902
N92-28911* # p 3316 ..... NAS 1.26:190521
NASA-CR-190521
N92-28912 # p 3264 ..... AD-A247668
NCEL-TN-1839
N92-28913 # p 3322 ..... AD-A247917
NOARL-TN-221
N92-28914 # p 3266 ..... GRI-92/0064
PB92-164326
N92-28915 # p 3343 ..... AD-A250162
N92-28916 # p 3265 ..... AD-A250164
N92-28917 # p 3252 ..... AD-A250165
TR-5
N92-28918 # p 3253 ..... AD-A250166
TR-4
N92-28919 # p 3365 ..... AD-A250171
N92-28920 # p 3326 ..... AD-A250173
AFOSR-92-0316TR
N92-28921 # p 3253 ..... AD-A250188
NADC-91087-60
N92-28922 # p 3319 ..... AD-A250556
AFIT/CI/CIA-91-118
N92-28923 # p 3365 ..... AD-A250561
R/D-6907-EE-06
N92-28924 # p 3294 ..... AD-A250567
BRDEC-2525
N92-28925* # p 3295 ..... CONF-920373-3
DE92-010663
NAS 1.15:107958
NASA-TM-107958
SAND-91-1717C
N92-28926* # p 3234 ..... A-91178
NAS 1.15:103873
NASA-TM-103873
N92-28927 # p 3349 ..... AD-A247397
MSRR-569
N92-28928 # p 3350 ..... AD-A247398
MSRR-570
N92-28929 # p 3350 ..... AD-A247399
MSRR-574
N92-28930 # p 3350 ..... AD-A247400
MSRR-575
N92-28931 # p 3250 ..... AD-A247402
SAIC-91/1286
N92-28932 # p 3291 ..... AD-A247403
AFOSR-92-0017TR
N92-28933 # p 3291 ..... AD-A247542
N92-28934 # p 3319 ..... AD-A247545
USAFETAC/PR-91/023
N92-28935 # p 3316 ..... AD-A247546
AD-E200901
PL-TR-91-2250
N92-28936 # p 3355 ..... AD-A247549
AD-E200862
PL-TR-91-2216
N92-28937 # p 3244 ..... AD-A247550
AD-E200896
PL-TR-91-2296
RXR-91121
N92-28938 # p 3322 ..... AD-A247657
NOARL-CR-011-92
N92-28939 # p 3322 ..... AD-A247663
N92-28940 # p 3328 ..... AD-A247669
NHRC-90-39
N92-28941* # p 3291 ..... JPL-PUBL-90-50
NAS 1.26:190449
NASA-CR-190449
N92-28942 # p 3257 ..... DE92-010652
DOE/ER-13370/T1
N92-28943 # p 3339 ..... AD-A247469
N92-28944 # p 3331 ..... AD-A247470
USAARL-92-10
N92-28945 # p 3250 ..... AD-A248057
DNA-TR-91-71
PSI-FR-2567-1
N92-28946 # p 3339 ..... AD-A248060
NOSC/TR-1468
N92-28947 # p 3276 ..... AD-A248061
NOSC/TR-1453
N92-28948 # p 3281 ..... AD-A248159
N92-28949 # p 3348 ..... AD-A248422
YALEU/DCS/RR-894
N92-28950* # p 3305 ..... JPL-PUBL-91-27
NAS 1.26:190456
NASA-CR-190456
N92-28951 # p 3322 ..... AD-A250017
INO-TM-7
N92-28952 # p 3339 ..... AD-A250317
ARL-FLIGHT-MECH-TM-452
DODA-AR-006-656
N92-28953 # p 3253 ..... AD-A250322
NRL/FR/6383-92-9369
N92-28954 # p 3257 ..... AD-A250323
BRL-TR-3328
N92-28955 # p 3369 ..... AD-A250324
DODA-AR-006-927
ERL-0594-GD
N92-28956 # p 3245 ..... AD-A250629
TOR-92(2464)-1
N92-28957 # p 3328 ..... AD-A247862
AFOSR-92-0211TR
N92-28958 # p 3343 ..... AD-A247887
N92-28959 # p 3253 ..... AD-A247889
N92-28960 # p 3369 ..... AD-A247890
N92-28961 # p 3349 ..... AD-A247891
WL-TR-91-5037
N92-28962 # p 3362 ..... AD-A247892
WL-TR-90-83
N92-28963 # p 3322 ..... AD-A247913
NOARL-TN-214
N92-28964 # p 3316 ..... AD-A247914
NOARL-TN-195
N92-28965 # p 3319 ..... AD-A247915
NOARL-TN-185
N92-28966 # p 3319 ..... AD-A247916
NOARL-TN-173
N92-28967 # p 3248 ..... AD-A250023
AFOSR-92-0229TR
N92-28968 # p 3358 ..... AD-A250244
N92-28969 # p 3339 ..... AD-A250249
AEDAR-FTR-91-02
AFOSR-92-0342TR
N92-28970 # p 3345 ..... AD-A250286
N92-28971 # p 3339 ..... AD-A250313
ARL-STRUC-TM-549
DODA-AR-006-659
N92-28972 # p 3265 ..... AD-A246454
TR-56
N92-28973 # p 3258 ..... AD-A246456
TR-14
N92-28974 # p 3307 ..... AD-A246457
N92-28975 # p 3241 ..... AD-A246459
AL-TP-1991-0058
N92-28976 # p 3261 ..... AD-A246464
N92-28977 # p 3322 ..... AD-A246465
N92-28978 # p 3287 ..... AD-A246467
DREO-1093
N92-28979 # p 3276 ..... AD-A246468
DREO-1100
N92-28980* # p 3229 ..... E-6354
NAS 1.60:3252
NASA-TP-3252
N92-28981* # p 3229 ..... NAS 1.15:103590
NASA-TM-103590
N92-28982 # p 3258 ..... AD-A246851
N92-28983* # p 3250 ..... AIAA PAPER 92-3516
E-6839
NAS 1.15:105636
NASA-TM-105636
N92-28984* # p 3353 ..... E-7126
NAS 1.15:105722
NASA-TM-105722
N92-28985* # p 3238 ..... E-7113
NAS 1.15:105716
NASA-TM-105716
N92-28986* # p 3355 ..... NAS 1.15:103589
NASA-TM-103589
N92-28987 p 3234 ..... AD-D015233
US-PATENT-APPL-SN-632442
US-PATENT-CLASS-244-3.27
US-PATENT-5,074,493
N92-28988* # p 3378 ..... LPI-TR-92-02
NAS 1.26:190418
NASA-CR-190418
N92-28989* # p 3378 ..... NO REPORT NUMBER
N92-28990* # p 3379 ..... NO REPORT NUMBER
N92-28991* # p 3379 ..... NO REPORT NUMBER
N92-28992* # p 3379 ..... NO REPORT NUMBER
N92-28993* # p 3379 ..... NO REPORT NUMBER
N92-28994* # p 3379 ..... NO REPORT NUMBER
N92-28995* # p 3379 ..... NO REPORT NUMBER
N92-28996* # p 3380 ..... NO REPORT NUMBER
N92-28997* # p 3380 ..... NO REPORT NUMBER
N92-28998* # p 3380 ..... NO REPORT NUMBER
N92-28999* # p 3380 ..... NO REPORT NUMBER
N92-29000* # p 3380 ..... NO REPORT NUMBER
N92-29001* # p 3381 ..... NO REPORT NUMBER
N92-29002* # p 3381 ..... NO REPORT NUMBER
N92-29003* # p 3381 ..... NO REPORT NUMBER
N92-29004* # p 3381 ..... NO REPORT NUMBER
N92-29005* # p 3381 ..... NO REPORT NUMBER
N92-29006* # p 3381 ..... NO REPORT NUMBER
N92-29007* # p 3382 ..... NO REPORT NUMBER
N92-29008* # p 3382 ..... NO REPORT NUMBER
N92-29009* # p 3382 ..... NO REPORT NUMBER
N92-29010* # p 3382 ..... NO REPORT NUMBER
N92-29011* # p 3382 ..... NO REPORT NUMBER
N92-29012* # p 3383 ..... NO REPORT NUMBER
N92-29013* # p 3383 ..... NO REPORT NUMBER
N92-29014* # p 3383 ..... NO REPORT NUMBER
N92-29015* # p 3383 ..... NO REPORT NUMBER
N92-29016* # p 3383 ..... NO REPORT NUMBER
N92-29017* # p 3383 ..... NO REPORT NUMBER
N92-29018* # p 3384 ..... NO REPORT NUMBER
N92-29019* # p 3384 ..... NO REPORT NUMBER
N92-29020* # p 3384 ..... NO REPORT NUMBER
N92-29021* # p 3384 ..... NO REPORT NUMBER
N92-29022* # p 3384 ..... NO REPORT NUMBER
N92-29023* # p 3385 ..... NO REPORT NUMBER
N92-29024* # p 3385 ..... NO REPORT NUMBER
N92-29025* # p 3385 ..... NO REPORT NUMBER
N92-29026* # p 3385 ..... NO REPORT NUMBER
N92-29027* # p 3386 ..... NO REPORT NUMBER
N92-29028* # p 3386 ..... NO REPORT NUMBER
N92-29029* # p 3386 ..... NO REPORT NUMBER
N92-29030* # p 3386 ..... NO REPORT NUMBER
N92-29031* # p 3386 ..... NO REPORT NUMBER
N92-29032* # p 3386 ..... NO REPORT NUMBER
N92-29033* # p 3387 ..... NO REPORT NUMBER
N92-29034* # p 3387 ..... NO REPORT NUMBER
N92-29035* # p 3387 ..... NO REPORT NUMBER
N92-29036* # p 3387 ..... NO REPORT NUMBER
N92-29037* # p 3387 ..... NO REPORT NUMBER
N92-29038* # p 3387 ..... NO REPORT NUMBER
N92-29039* # p 3388 ..... NO REPORT NUMBER
N92-29040* # p 3388 ..... NO REPORT NUMBER
N92-29041* # p 3388 ..... NO REPORT NUMBER
N92-29042* # p 3388 ..... NO REPORT NUMBER
N92-29043* # p 3388 ..... NO REPORT NUMBER
N92-29044* # p 3388 ..... NO REPORT NUMBER
N92-29045* # p 3389 ..... NO REPORT NUMBER
N92-29046* # p 3389 ..... NO REPORT NUMBER
N92-29047* # p 3389 ..... NO REPORT NUMBER
N92-29048* # p 3389 ..... NO REPORT NUMBER
N92-29049* # p 3389 ..... NO REPORT NUMBER
N92-29050* # p 3389 ..... NO REPORT NUMBER
N92-29051* # p 3389 ..... NO REPORT NUMBER
N92-29052* # p 3390 ..... NO REPORT NUMBER
N92-29053* # p 3390 ..... NO REPORT NUMBER
N92-29054* # p 3390 ..... NO REPORT NUMBER
N92-29055* # p 3390 ..... NO REPORT NUMBER
N92-29056* # p 3390 ..... NO REPORT NUMBER
N92-29057* # p 3390 ..... NO REPORT NUMBER
N92-29058* # p 3391 ..... NO REPORT NUMBER
N92-29059* # p 3391 ..... NO REPORT NUMBER
N92-29060* # p 3391 ..... NO REPORT NUMBER
N92-29061* # p 3391 ..... NO REPORT NUMBER
N92-29062* # p 3391 ..... NO REPORT NUMBER
N92-29063* # p 3392 ..... NO REPORT NUMBER
N92-29064* # p 3392 ..... NO REPORT NUMBER
N92-29065* # p 3392 ..... NO REPORT NUMBER
N92-29066* # p 3392 ..... NO REPORT NUMBER
N92-29067* # p 3392 ..... NO REPORT NUMBER
N92-29068* # p 3393 ..... NO REPORT NUMBER
N92-29069* # p 3393 ..... NO REPORT NUMBER
N92-29070* # p 3393 ..... NO REPORT NUMBER
N92-29071* # p 3393 ..... NO REPORT NUMBER
N92-29072* # p 3393 ..... NO REPORT NUMBER
N92-29073* # p 3394 ..... NO REPORT NUMBER
N92-29074* # p 3394 ..... NO REPORT NUMBER
N92-29075* # p 3394 ..... NO REPORT NUMBER
N92-29076* # p 3394 ..... NO REPORT NUMBER
N92-29077* # p 3394 ..... NO REPORT NUMBER
N92-29078* # p 3395 ..... NO REPORT NUMBER
N92-29079* # p 3395 ..... NO REPORT NUMBER
N92-29080* # p 3395 ..... NO REPORT NUMBER
N92-29081 # p 3304 ..... AD-A247936
N92-29082 # p 3346 ..... AD-A247941
WL-TR-91-1146
N92-29083 # p 3333 ..... AD-A247962
N92-29084 # p 3276 ..... AD-A247968
N92-29085 p 3276 ..... AD-D015251
US-PATENT-APPL-SN-376270
US-PATENT-CLASS-370-6
US-PATENT-5,086,423
N92-29086 # p 3362 ..... CONF-920362-10

DE92-011153
SAND-92-0066C
N92-29087* # p 3319 NAS 1.26:190472
NASA-CR-190472
N92-29088* # p 3358 NAS 1.26:190490
NASA-CR-190490
N92-29089 # p 3324 AD-A250016
NOARL-TN-212
N92-29090* p 3265 INT-PATENT-CLASS-B32B-15/01
INT-PATENT-CLASS-B32B-15/20
INT-PATENT-CLASS-B32B-5/02
NASA-CASE-LEW-15155-1
US-PATENT-APPL-SN-682160
US-PATENT-CLASS-428-614
US-PATENT-CLASS-428-680
US-PATENT-CLASS-428-661
US-PATENT-5,116,690
N92-29091 # p 3258 AD-A250332
WL-TR-91-4103
N92-29092* p 3295 INT-PATENT-CLASS-A47H-1/144
NASA-CASE-LEW-15196-1
US-PATENT-APPL-SN-687606
US-PATENT-CLASS-16-111R
US-PATENT-CLASS-16-114R
US-PATENT-CLASS-248-222.1
US-PATENT-CLASS-248-251
US-PATENT-CLASS-256-59
US-PATENT-5,126,131
N92-29093 # p 3362 AD-A250333
AFOSR-92-0343TR
N92-29094* p 3261 INT-PATENT-CLASS-B23K-1/00
NASA-CASE-GSC-13344-1
US-PATENT-APPL-SN-718046
US-PATENT-CLASS-219-85.15
US-PATENT-CLASS-219-85.19
US-PATENT-5,126,527
N92-29095 # p 3358 AD-D015273
US-PATENT-APPL-SN-760635
N92-29096 # p 3343 AD-D015274
US-PATENT-APPL-SN-783661
N92-29097* p 3288 INT-PATENT-CLASS-G01L-7/08
INT-PATENT-CLASS-G01L-9/06
NASA-CASE-LAR-14579-1
US-PATENT-APPL-SN-690198
US-PATENT-CLASS-338-4
US-PATENT-CLASS-73-708
US-PATENT-CLASS-73-721
US-PATENT-CLASS-73-727
US-PATENT-CLASS-73-756
US-PATENT-5,116,331
N92-29098 # p 3244 ITN-92-85131
N92-29099* p 3295 INT-PATENT-CLASS-F16C-32/04
INT-PATENT-CLASS-H02K-1/14
NASA-CASE-GSC-13346-1
US-PATENT-APPL-SN-691609
US-PATENT-CLASS-310-90.5
US-PATENT-CLASS-505-876
US-PATENT-5,117,139
N92-29100* # p 3244 NAS 1.15:107954
NASA-TM-107954
N92-29101* p 3304 INT-PATENT-CLASS-G01R-27/72
INT-PATENT-CLASS-G01R-33/12
NASA-CASE-LAR-13817-4
US-PATENT-APPL-SN-210486
US-PATENT-APPL-SN-449211
US-PATENT-APPL-SN-608504
US-PATENT-CLASS-324-239
US-PATENT-5,117,184
N92-29102 # p 3245 CONF-9204102-4
DE92-011156
SAND-92-0460C
N92-29103* # p 3231 A-92021
NAS 1.15:103906
NASA-TM-103906
N92-29104* # p 3245 A-91237
NAS 1.15:103892
NASA-TM-103892
N92-29105* # p 3288 AVSCOM-TR-92-C-026
E-7112
NAS 1.15:105717
NASA-TM-105717
N92-29106* # p 3339 NAS 1.26:190556
NASA-CR-190556
RIACS-TR-91.22
N92-29107* # p 3340 NAS 1.26:190554
NASA-CR-190554
RIACS-TR-92.05
N92-29108* # p 3370 NAS 1.26:190387
NASA-CR-190387
N92-29109* # p 3343 NAS 1.26:190551
NASA-CR-190551
RIACS-TR-92.14
N92-29110* # p 3234 H-1833
NAS 1.15:4396
NASA-TM-4396
N92-29111* # p 3367 NAS 1.26:190269
NASA-CR-190269
N92-29112 # p 3297 AD-A250213
AFOSR-92-0349TR
POLY-WRI-1589-92
N92-29113* # p 3340 NAS 1.26:190557
NASA-CR-190557
RIACS-TR-91.19
N92-29114 # p 3343 AD-A250216
AFOSR-92-0291TR
N92-29115* # p 3276 NAS 1.26:190422
NASA-CR-190422
NIST/SP-821
N92-29116 # p 3265 AD-A248305
TR-59
N92-29117* p 3359 INT-PATENT-CLASS-G02F-1/01
NASA-CASE-LAR-14588-1-CU
US-PATENT-APPL-SN-653605
US-PATENT-CLASS-356-370
US-PATENT-CLASS-356-414
US-PATENT-CLASS-359-246
US-PATENT-CLASS-359-247
US-PATENT-CLASS-359-281
US-PATENT-5,126,797
N92-29118 # p 3267 AD-A250221
AFOSR-92-0365TR
N92-29119 # p 3328 AD-A250223
AFOSR-92-0299TR
N92-29120* p 3295 INT-PATENT-CLASS-F16C-9/00
NASA-CASE-GSC-13251-1
US-PATENT-APPL-SN-714814
US-PATENT-CLASS-285-381
US-PATENT-CLASS-292-DIG.66
US-PATENT-CLASS-403-28
US-PATENT-CLASS-403-404
US-PATENT-CLASS-411-909
US-PATENT-5,108,214
N92-29121 # p 3331 AD-A250288
AFOSR-92-0392TR
N92-29122* p 3359 INT-PATENT-CLASS-G01J-1/20
NASA-CASE-NPO-18095-1-CU
US-PATENT-APPL-SN-665509
US-PATENT-CLASS-250-201.9
US-PATENT-CLASS-359.849
US-PATENT-5,113,064
N92-29123 # p 3326 AD-A250308
AFOSR-92-0314TR
N92-29124* p 3276 INT-PATENT-CLASS-G01R-23/16
NASA-CASE-NPO-17759-1-CU
US-PATENT-APPL-SN-660371
US-PATENT-CLASS-324-77C
US-PATENT-CLASS-324-77CS
US-PATENT-CLASS-324-78D
US-PATENT-CLASS-324-78F
US-PATENT-5,122,731
N92-29125* p 3287 INT-PATENT-CLASS-F28D-15/02
NASA-CASE-LEW-15235-1
US-PATENT-APPL-SN-736145
US-PATENT-CLASS-165-104.14
US-PATENT-CLASS-165-104.22
US-PATENT-CLASS-165-41
US-PATENT-CLASS-417-209
US-PATENT-5,127,471
N92-29126 # p 3258 AD-A250309
AFOSR-92-0311TR
SRA-R92-910034-1
N92-29127 # p 3371 ETN-92-91486
N92-29128 # p 3371 ETN-92-91487
N92-29129* p 3331 INT-PATENT-CLASS-G06K-9/00
NASA-CASE-NPO-17552-1-CU
US-PATENT-APPL-SN-251500
US-PATENT-CLASS-358-105
US-PATENT-CLASS-364-424.01
US-PATENT-CLASS-382-1
US-PATENT-CLASS-382-22
US-PATENT-CLASS-901-1
US-PATENT-5,109,425
N92-29130* p 3351 INT-PATENT-CLASS-G01N-27/72
NASA-CASE-NPO-18187-1-CU
US-PATENT-APPL-SN-618789
US-PATENT-CLASS-324-205
US-PATENT-CLASS-324-244
US-PATENT-CLASS-324-261
US-PATENT-CLASS-361-148
US-PATENT-CLASS-361-149
US-PATENT-CLASS-361-267
US-PATENT-5,126,669
N92-29131 # p 3277 DE92-013393
UCRL-LR-109784
N92-29132* p 3333 INT-PATENT-CLASS-G11B-17/22
INT-PATENT-CLASS-G11B-3/74
INT-PATENT-CLASS-G11B-5/09
NASA-CASE-GSC-13196-1
US-PATENT-APPL-SN-357928
US-PATENT-CLASS-360-48
US-PATENT-CLASS-360-98.01
US-PATENT-CLASS-369-32
US-PATENT-CLASS-369-95
US-PATENT-5,111,345
N92-29133* p 3359 INT-PATENT-CLASS-G01D-5/34
NASA-CASE-GSC-13175-1
US-PATENT-APPL-SN-506636
US-PATENT-CLASS-250-231.14
US-PATENT-CLASS-369-44.26
US-PATENT-5,107,107
N92-29134* # p 3295 NAS 1.26:190487
NASA-CR-190487
NRC-TR-92-143
N92-29135* p 3288 INT-PATENT-CLASS-G21K-7/00
NASA-CASE-MFS-26485-1
US-PATENT-APPL-SN-606988
US-PATENT-CLASS-378-210
US-PATENT-CLASS-378-43
US-PATENT-5,107,526
N92-29136* # p 3296 AVSCOM-TR-91-C-043
E-7060
NAS 1.15:105681
NASA-TM-105681
N92-29137* p 3332 NASA-CASE-MSC-21589-1
US-PATENT-APPL-SN-529427
US-PATENT-CLASS-252-DIG.13
US-PATENT-CLASS-252-DIG.14
US-PATENT-CLASS-252-DIG.5
US-PATENT-CLASS-252-545
US-PATENT-CLASS-252-547
US-PATENT-CLASS-4-661
US-PATENT-CLASS-424-70
US-PATENT-5,116,543
N92-29138* p 3296 INT-PATENT-CLASS-B66C-1/62
NASA-CASE-GSC-13251-1
US-PATENT-APPL-SN-628529
US-PATENT-CLASS-294-119.1
US-PATENT-CLASS-294-902
US-PATENT-CLASS-901-39
US-PATENT-5,120,101
N92-29139* # p 3291 NAS 1.26:186957
NASA-CR-186957
N92-29140* p 3296 INT-PATENT-CLASS-B25G-3/00
NASA-CASE-GSC-13220-1
US-PATENT-APPL-SN-636532
US-PATENT-CLASS-403-13
US-PATENT-CLASS-403-24
US-PATENT-5,112,154
N92-29141* p 3250 INT-PATENT-CLASS-C07D-271/10
INT-PATENT-CLASS-C08G-73/06
NASA-CASE-LAR-14427-1
US-PATENT-APPL-SN-645089
US-PATENT-CLASS-528-185
US-PATENT-CLASS-548-143
US-PATENT-5,118,781
N92-29142 # p 3328 AD-A248726
TR-6
N92-29143* p 3307 INT-PATENT-CLASS-F03G-6/00
NASA-CASE-LEW-14949-1
US-PATENT-APPL-SN-676910
US-PATENT-CLASS-126-433
US-PATENT-CLASS-126-436
US-PATENT-CLASS-60-641.8
US-PATENT-CLASS-60-659
US-PATENT-5,113,659
N92-29144 # p 3328 AD-A250200
AFOSR-92-0308TR
N92-29145 # p 3265 AD-A250201
AFOSR-92-0289TR
N92-29146 # p 3328 AD-A250203
AFOSR-92-0300TR
N92-29147 # p 3281 AD-A250204
AFOSR-92-0293TR
N92-29148* p 3320 INT-PATENT-CLASS-G01C-21/00
NASA-CASE-NPO-18115-1-CU
US-PATENT-APPL-SN-618790
US-PATENT-CLASS-364-443
US-PATENT-CLASS-374-112
US-PATENT-CLASS-73-178R
US-PATENT-5,117,889
N92-29149 # p 3346 AD-A250212
AFOSR-92-0371TR
N92-29150* p 3296 INT-PATENT-CLASS-F16B-37/08
NASA-CASE-MSC-21799-1
US-PATENT-APPL-SN-759367
US-PATENT-CLASS-411-14
US-PATENT-CLASS-411-267
US-PATENT-CLASS-411-433
US-PATENT-5,118,237
N92-29151* p 3296 INT-PATENT-CLASS-G02B-26/02

NASA-CASE-GSC-13189-2
US-PATENT-APPL-SN-331119
US-PATENT-APPL-SN-613188
US-PATENT-CLASS-359-230
US-PATENT-CLASS-359-236
US-PATENT-5,128,796
N92-29152* p 3253 ..... NASA-CASE-LEW-15077-1
US-PATENT-APPL-SN-608493
US-PATENT-CLASS-118-416
US-PATENT-CLASS-252-502
US-PATENT-CLASS-423-447.2
US-PATENT-CLASS-423-448
US-PATENT-CLASS-423-460
US-PATENT-CLASS-427-294
US-PATENT-CLASS-427-443.2
US-PATENT-5,073,412
N92-29153* p 3281 INT-PATENT-CLASS-G05G-9/00
NASA-CASE-GSC-13187-1
US-PATENT-APPL-SN-657790
US-PATENT-CLASS-248-65
US-PATENT-CLASS-248-68.1
US-PATENT-CLASS-273-148B
US-PATENT-CLASS-338-128
US-PATENT-CLASS-74-471XY
US-PATENT-5,113,714
N92-29154* p 3298
..... INT-PATENT-CLASS-G01R-35/00
NASA-CASE-GSC-13386-1
US-PATENT-APPL-SN-758977
US-PATENT-CLASS-324-224
US-PATENT-CLASS-324-226
US-PATENT-CLASS-324-262
US-PATENT-CLASS-356-432
US-PATENT-CLASS-374-4
US-PATENT-CLASS-374-45
US-PATENT-5,124,640
N92-29155* p 3304 ..... NASA-CASE-LAR-13817-2
US-PATENT-APPL-SN-210486
US-PATENT-APPL-SN-449209
US-PATENT-CLASS-324-209
US-PATENT-CLASS-324-226
US-PATENT-CLASS-324-227
US-PATENT-CLASS-324-235
US-PATENT-CLASS-324-239
US-PATENT-CLASS-73-801
US-PATENT-5,109,195
N92-29156* p 3288 INT-PATENT-CLASS-F25B-19/02
NASA-CASE-NPO-18184-1-CU
US-PATENT-APPL-SN-636076
US-PATENT-CLASS-62.224
US-PATENT-CLASS-62-51.2
US-PATENT-5,119,637
N92-29157* p 3265
..... INT-PATENT-CLASS-C08F-283/04
NASA-CASE-LAR-13669-1
US-PATENT-APPL-SN-084064
US-PATENT-CLASS-525-420
US-PATENT-CLASS-525-432
US-PATENT-CLASS-528-179
US-PATENT-CLASS-528-185
US-PATENT-CLASS-528-352
US-PATENT-CLASS-528-353
US-PATENT-5,116,939
N92-29158* p 3359 ..... NASA-CASE-LAR-13616-3
US-PATENT-APPL-SN-140185
US-PATENT-APPL-SN-337768
US-PATENT-APPL-SN-693049
US-PATENT-CLASS-427-108
US-PATENT-CLASS-427-109
US-PATENT-CLASS-427-38
US-PATENT-CLASS-427-66
US-PATENT-CLASS-427-68
US-PATENT-5,104,683
N92-29159 # p 3229 ..... DLR-FB-90-26
ESA-TT-1247
ETN-92-91207
ISSN-0171-1342
N92-29160 p 3291 ..... ETN-92-91215
FEL-91-A163
TD91-2230
N92-29161 p 3367 ..... ETN-92-91231
IZF-1991-B-8
TD91-2168
N92-29162 p 3369 ..... ETN-92-91232
IZF-1991-B-9
TD91-2169
N92-29163 p 3288 ..... ETN-92-91373
ISSN-0955-9655
NPL-RSA(EXT)-23
N92-29164 p 3261 ..... ETN-92-91378
ISSN-0959-2423
NPL-DMM(A)-42
N92-29165 # p 3277 ..... AD-A245909
CECOM-TR-91-3
N92-29166 # p 3277 ..... AD-A247970
N92-29167 # p 3359 ..... AD-A247985
NOARL-PR-91-024-352
N92-29168 # p 3291 ..... CONF-9108118-48
DE92-011286
LA-UR-92-754
N92-29169 # p 3277 ..... AD-D015263
US-PATENT-APPL-SN-857536
N92-29170 # p 3261 ..... AD-D015264
US-PATENT-APPL-SN-828634
N92-29171 # p 3287 ..... AD-A249982
AFIT/CI/CIA-91-100
N92-29172 # p 3340 ..... AD-A250018
INO-SP-4
N92-29173 # p 3308 ..... AD-A250211
AFOSR-92-0354TR
N92-29174* # p 3329 ..... NAS 1.15:107878
NASA-TM-107878
RIA-91-29
N92-29175* # p 3346 ..... FIA-91-13
NAS 1.15:107844
NASA-TM-107844
N92-29176 # p 3304 ..... ETN-92-91539
NLR-TP-90178-U
N92-29177 # p 3371 ..... ETN-92-91484
N92-29178 # p 3282 ..... ETN-92-91485
N92-29179 # p 3326 ..... AD-A250233
AFOSR-92-0307TR
N92-29180 # p 3235 ..... AD-A250390
DOT/VNTSC-FAA-91-16
N92-29181 # p 3304 ..... AD-A250397
ARL-STRUC-TM-531
DODA-AR-006-150
N92-29182 # p 3230 ..... AD-A250412
FAA-APO-92-1
N92-29183 # p 3308 ..... PB92-176569
SYSAPP-91/151
N92-29184 # p 3372 ..... CLNS-92-1133
CONF-9108175-3
DE92-013022
FNAL/C-92/72-A
N92-29185 # p 3258 ..... AD-A246850
N92-29186 # p 3329 ..... AD-A246945
AFOSR-92-0105TR
N92-29187 # p 3340 ..... AD-A248201
AL-TR-1991-0085-VOL-1
N92-29188 # p 3340 ..... AD-A248202
AL-TR-1991-0085-VOL-2
N92-29189 # p 3265 ..... AD-A248203
N92-29190 # p 3355 ..... AD-A248204
ORNL/TM-11778
N92-29191 # p 3272 ..... AD-A248205
AFIT/GOR/ENS/92M-11
N92-29192 # p 3253 ..... AD-A248206
AFIT/GA/ENY/92M-02
N92-29193 # p 3348 ..... ETN-92-91245
FFI-91/7023
ISSN-0802-2437
N92-29194 # p 3266 ..... ETN-92-91265
ISBN-951-38-3989-3
ISSN-0358-5077
VTT-RR-741
N92-29195 # p 3266 ..... ALS/TR-92-009
DE92-010518
N92-29196* # p 3353 ..... NAS 1.26:190493
NASA-CR-190493
N92-29197 # p 3282 ..... CONF-920299-1
DE92-011279
FNAL/C-92/66
N92-29198 # p 3341 ..... AD-A249816
N92-29199 # p 3277 ..... AD-D015262
US-PATENT-APPL-SN-819699
N92-29200* # p 3341 ..... NAS 1.26:190384
NASA-CR-190384
N92-29201 # p 3353 ..... CUED/A-AERO/TR-18
ISSN-0309-7293
N92-29202* # p 3369 ..... JPL-BIBL-39-31
NAS 1.26:190457
NASA-CR-190457
N92-29203 # p 3353 ..... ISVR-TR-202-PT-2
N92-29204 # p 3241 ..... ETN-92-91537
NLR-TP-90147-U
N92-29205 # p 3360 ..... AD-D015261
US-PATENT-APPL-SN-758143
N92-29206 # p 3229 ..... ETN-92-91325
ONERA-RSF-7/3617-AY-022A
N92-29207 # p 3365 ..... ETN-92-91330
LAAS-91307
N92-29208 # p 3282 ..... ETN-92-91331
LAAS-91360
N92-29209 # p 3341 ..... ETN-92-91332
LAAS-91378
N92-29210 # p 3356 ..... ETN-92-91340
OEFZS-4581
N92-29211 # p 3322 ..... ETN-92-91346
IOS-285-1991
N92-29212 # p 3323 ..... ETN-92-91347
IOS-286-1991
N92-29213 # p 3323 ..... ETN-92-91348
IOS-288-1991
N92-29214 # p 3348 ..... ETN-92-91349
ISSN-0924-2082
ITLI-LP-91-01
N92-29215 # p 3323 ..... ETN-92-91344
REPT-21-1991
N92-29216 # p 3323 ..... ETN-92-91345
IOS-273-1990
N92-29217 # p 3296 ..... ETN-92-91353
N92-29218 # p 3397 ..... ETN-92-91391
ISSN-0939-2971
N92-29219 # p 3397 ..... ETN-92-91392
ISSN-0938-2194
N92-29220 # p 3253 ..... ETN-92-91394
FFA-TN-1992-02
N92-29221 # p 3341 ..... ETN-92-91408
ISSN-0922-5641
REPT-91-33
N92-29222 # p 3236 ..... AD-A248207
AFIT/GCS/ENG/92M-03
N92-29223 # p 3292 ..... AD-A248225
N92-29224 # p 3341 ..... AD-A248230
N92-29225 # p 3323 ..... AD-A248246
N92-29226 # p 3292 ..... AD-A248247
N92-29227 # p 3332 ..... AD-A248441

Appendix

NASA SCIENTIFIC AND TECHNICAL INFORMATION PROGRAM PRODUCTS AND SERVICES

The NASA Scientific and Technical Information (STI) Program provides for the collection and announcement of aerospace-related reports and literature obtained worldwide through agreements and exchanges. The result of the collection is the comprehensive NASA STI Database that covers aeronautics, space, and supporting disciplines.

The STI Database, documents generated or obtained by NASA, and products and services derived from or supporting the database are made available to the NASA research community and to the public. Descriptions and sources of these items are presented in the following pages.

Scientific and Technical Aerospace Reports (*STAR*) is an abstract journal, listing citations with abstracts for aerospace-related reports obtained from worldwide sources. *STAR* is issued on the 8th and 23rd of each month and announces current documents that have been entered into the NASA STI Database during the previous two weeks. The reports are of the following types:

- NASA, NASA contractor, and NASA grantee reports;
- Reports issued by other U.S. Government agencies, domestic and foreign institutions, universities, and private firms;
- Translations in report form;
- NASA-owned patents and patent applications;
- Other U.S. Government agency and foreign patents and patent applications;
- Domestic and foreign dissertations and theses.

Journal, book, and conference literature, journal translations, and certain foreign dissertations having the same subject scope as *STAR* are announced in a companion journal, *International Aerospace Abstracts* (*IAA*). *IAA* is issued on the 1st and 15th of each month and is available from the American Institute of Aeronautics and Astronautics, Technical Information Service, 555 West 57th Street, 12th Floor, New York, NY 10019.

ELIGIBILITY AND REGISTRATION FOR NASA STI PRODUCTS AND SERVICES

Organizations of the type listed below that have registered with NASA can receive products and services.

- NASA offices and installations, contractors, subcontractors, grantees, and consultants;
- Other U.S. Government agencies and their contractors;
- Libraries in the United States that have arrangements with NASA to maintain collections of NASA documents for public reference;
- Other organizations in the United States having a need for NASA documents in work related to aeronautics and space research;
- Organizations abroad that have established reciprocal documents exchange arrangements with NASA.

Only the central service points or central points of document acquisition and control within qualified organizations are eligible to register for NASA STI products and services. Domestic organizations that may be eligible to receive various classes of NASA publications and services should address their requests for registration or further information to:

NASA Center for AeroSpace Information
ATTN: Registration Services
P.O. Box 8757
Baltimore, MD 21240-0757
301-621-0153

Organizations abroad should direct requests to:

National Aeronautics and Space Administration
Director, Scientific and Technical Information Program
Code JTT
Washington, DC 20546
USA
703-271-5640

SUBJECT SCOPE

The subject scope of *STAR* and *IAA* includes all aspects of aeronautics and space research and development, supporting basic and applied research, and applications. Aerospace aspects of Earth resources, energy development, conservation, oceanography, environmental protection, urban transportation, and other topics of high national priority are also covered.

HOW TO USE *STAR* SUBJECT CATEGORIES

Abstracts in *STAR* are categorized by 10 major subject divisions that are divided further into 76 specific subject categories. The subject divisions and categories are listed in the Table of Contents together with a note for each that defines its scope and provides any cross-references. For example:

16 SPACE TRANSPORTATION
Includes passenger and cargo space transportation, e.g., shuttle operations; and space rescue techniques. For related information see also *03 Air Transportation and Safety* and *18 Spacecraft Design, Testing and Performance.* For space suits see *54 Man/System Technology and Life Support.*

CROSS-REFERENCES

Individual *STAR* abstracts are not ordinarily cross-referenced, except for certain conference reports or book translations that have had separate abstracts written for their component papers or chapters. Citations and abstracts of the components follow immediately after those of the parent document. When the subject content of a component differs sufficiently from the general content of the parent, a cross-reference citation also is printed at the end of the category to which it normally would have been assigned if it were independent.

DOCUMENTS ON MICROFICHE

Documents available on microfiche are designated by a pound sign (#) following the accession number.

LIMITED REPRODUCIBILITY

A note of limited reproducibility appears in the citation, if there are factors affecting the reproducibility of more than 20% of the document. These factors include faint or broken type, color photographs, black and white photographs, foldouts, dot matrix print, or some other factor that limits the reproducibility of the document. This notation also appears on the microfiche header with the specific factor checked off on a list visible in the second frame.

COLOR COPIES

An increasing number of NASA scientific and technical reports are being produced with color graphs, charts, illustrations, and photographs. An indication that a document has color pages follows the source and pricing (SAP) information in the *STAR* citation.

Registered users of the NASA Scientific and Technical Information Program will receive ordered documents with color at no additional cost, as long as stock copies of the document are available. Otherwise, an additional fee of $2.00 per color page will be charged. The NASA Center for AeroSpace Information staff will contact registered users to determine individual user's needs.

NASA PATENTS AND PATENT APPLICATIONS

Patents and patent applications owned by NASA are announced in *STAR* under appropriate subject categories and are referenced in the *STAR* indexes. In the Report/Accession Number Index, patents are indexed by the NASA Case Number, and the U.S. Patent Class. Patent applications are indexed by the NASA Case Number and the U.S. Patent Application Serial Number.

Printed copies of patents (which are not microfiched) are available for purchase from the U.S. Patent and Trademark Office.

NASA patent application specifications are sold in both paper copy and microfiche by the National Technical Information Service (NTIS). The US-Patent-Appl-SN-number should be used in ordering either paper copy or microfiche from NTIS.

When ordering patents, the U.S. Patent Number should be used, and payment must be remitted in advance, by money order or check payable to the Commissioner of Patents and Trademarks. Prepaid purchase coupons for ordering are also available from the U.S. Patent and Trademark Office.

The patents and patent applications announced in *STAR* are owned by NASA and are available for royalty-free licensing. Requests for licensing terms and further information should be addressed to:

National Aeronautics and Space Administration
Associate General Counsel for Intellectual Property
Code GP
Washington, DC 20546

SOURCES FOR DOCUMENTS

One or more sources from which a document announced in *STAR* is available to the public is given in each citation. The most commonly indicated sources and their acronyms or abbreviations are listed on page A-6. If the publication is available from a source other than those listed, the publisher and address will be displayed on the availability line or in combination with the corporate source line.

Avail: NTIS. Sold by the National Technical Information Service. Prices for hard copy (HC) and microfiche (MF) are indicated by a price code following the letters HC or MF in the *STAR* citation. Current values for the price codes are given in the tables on page A-7.

Initially distributed microfiche under the NTIS SRIM (Selected Research in Microfiche) is available at greatly reduced unit prices. For this service and for information concerning subscription to NASA printed reports, consult the NTIS Subscription Section, Springfield, VA 22161.

NOTE ON ORDERING DOCUMENTS: When ordering NASA publications (those followed by the * symbol), use the N accession number. NASA patent applications (only the specifications are offered) should be ordered by the US-Patent-Appl-SN number. Non-NASA publications (no asterisk) should be ordered by the AD, PB, or other *report number* shown on the last line of the citation, not by the N accession number. It is also advisable to cite the title and other bibliographic identification.

Avail: SOD (or GPO). Sold by the Superintendent of Documents, U.S. Government Printing Office, in hard copy. The current price and order number are given following the availability line. (NTIS will fill microfiche requests, as indicated above, for those documents identified by a # symbol.)

Avail: BLL (formerly NLL): British Library Lending Division, Boston Spa, Wetherby, Yorkshire, England. Photocopies available from this organization at the price shown. (If none is given, address inquiry to the BLL.)

Avail: DOE Depository Libraries. Organizations in U.S. cities and abroad that maintain collections of Department of Energy reports, usually in microfiche form, are listed in *Energy Research Abstracts.* Services available from the DOE and its depositories are described in a booklet, *DOE Technical Information Center - Its Functions and Services* (TID-4660), which may be obtained without charge from the DOE Technical Information Center.

Avail: ESDU. Pricing information on specific data, computer programs, and details on Engineering Sciences Data Unit (ESDU) topic categories can be obtained from ESDU International Ltd. Requesters in North America should use the Virginia address while all other requesters should use the London address, both of which are on page A-6.

Avail: Fachinformationszentrum, Karlsruhe. Sold by the Fachinformationszentrum Energie, Physik, Mathematik GMBH, Eggenstein Leopoldshafen, Federal Republic of Germany, at the price shown in deutschmarks (DM).

Avail: HMSO. Publications of Her Majesty's Stationery Office are sold in the U.S. by Pendragon House, Inc. (PHI), Redwood City, CA. The U.S. price (including a service and mailing charge) is given, or a conversion table may be obtained from PHI.

Avail: NASA Public Document Rooms. Documents so indicated may be examined at or purchased from the National Aeronautics and Space Administration, Public Documents Room (Room 126), 600 Independence Ave., S.W., Washington, DC 20546, or public document rooms located at NASA installations, and the NASA Pasadena Office at the Jet Propulsion Laboratory.

Avail: Univ. Microfilms. Documents so indicated are dissertations selected from *Dissertation Abstracts* and are sold by University Microfilms as xerographic copy (HC) and microfilm. All requests should cite the author and the Order Number as they appear in the citation.

Avail: US Patent and Trademark Office. Sold by Commissioner of Patents and Trademarks, U.S. Patent and Trademark Office, at the standard price of $1.50 each, postage free. (See discussion of NASA patents and patent applications below.)

Avail: (US Sales Only). These foreign documents are available to users within the United States from the National Technical Information Service (NTIS). They are available to users outside the United States through the International Nuclear Information Service (INIS) representative in their country, or by applying directly to the issuing organization.

Avail: USGS. Originals of many reports from the U.S. Geological Survey, which may contain color illustrations, or otherwise may not have the quality of illustrations preserved in the microfiche or facsimile reproduction, may be examined by the public at the libraries of the USGS field offices whose addresses are listed on page A-6. The libraries may be queried concerning the availability of specific documents and the possible utilization of local copying services, such as color reproduction.

Avail: Issuing Activity, or Corporate Author, or no indication of availability. Inquiries as to the availability of these documents should be addressed to the organization shown in the citation as the corporate author of the document.

FEDERAL DEPOSITORY LIBRARIES: To provide the general public with greater access to U.S. Government publications, Congress established the Federal Depository Library Program under the Government Printing Office (GPO), with 53 regional depositories responsible for permanent retention of material, inter-library loan, and reference services. (These libraries are not sales outlets.) At least one copy of nearly every NASA and NASA-sponsored publication, either in printed or microfiche format, is received and retained by the 53 regional depositories. A list of the regional GPO libraries, appears on page A-8. A local library can contact a regional depository library to help locate specific reports, or direct contact may be made by an individual.

PUBLIC COLLECTION OF NASA DOCUMENTS

An extensive collection of NASA and NASA-sponsored publications is maintianed by the British Library Lending Divison, Boston Spa, Wetherby, Yorkshire, England, for public access. The British Library Lending Division also has available many of the non-NASA publications cited in *STAR*.

European requesters may purchase facsimile copy or microfiche of NASA and NASA-sponsored documents, those identified by both the symbols # and * from ESA—Information Retrieval Service, European Space Agency, 8-10 rue Mario-Nikis, 75738 Paris CEDEX 15, France.

SUBMITTING DOCUMENTS

All users of this abstract service are urged to forward reports to be considered for announcement in *STAR*. This will aid NASA in its efforts to provide the fullest possible coverage of all scientific and technical publications that might support aeronautics and space research and development. If you have prepared relevant reports (other than those you will transmit to NASA, DOD, or DOE through the usual contract- or grant-reporting channels), please send them for consideration to the NASA Center for AeroSpace Information, P.O. Box 8757, Baltimore, MD 21240-0757.

Reprints of journal articles, book chapters, and conference papers are also welcome. These will be considered for announcement in *STAR*'s companion journal, *IAA*.

You may specify a particular source to be included in a report announcement if you wish; otherwise the report will be placed on a public sale at the National Technical Information Service. Copyrighted publications will be announced but not distributed or sold.

PURCHASE OF *STAR*

STAR is publicly available on annual subscription from the Superintendent of Documents, U.S. Government Printing Office, Washington, DC 20402.

STAR is available to registered users on annual subscription from the NASA Center for AeroSpace Information, ATTN: Registration Services, P.O. Box 8757, Baltimore, MD 21240-0757.

Microfiche of the abstract sections of *STAR* are available, on annual subscription only, from NTIS as PB92-911300, Attn: Subscriptions, 5285 Port Royal Road, Springfield, VA 22161. Annual subscription rates are $100.00 North America; $200.00 foreign. Abstract sections for previous years retroactive to 1964 are available at the current rates.

ADDRESSES OF ORGANIZATIONS

American Institute of Aeronautics and Astronautics
Technical Information Service
555 West 57th Street, 12th Floor
New York, New York 10019

British Library Lending Division,
Boston Spa, Wetherby, Yorkshire,
England

Commissioner of Patents and Trademarks
U.S. Patent and Trademark Office
Washington, DC 20231

Department of Energy
Technical Information Center
P.O. Box 62
Oak Ridge, Tennessee 37830

European Space Agency-Information Retrieval Service
ESRIN
Via Galileo Galilei
00044 Frascati (Rome) Italy

Engineering Sciences Data Unit International
P.O. Box 1633
Manassas, Virginia 22110

Engineering Sciences Data Unit International, Ltd.
251-259 Regent Street
London, W1R 7AD, England

Fachinformationszentrum Energie, Physik, Mathematik
GMBH
7514 Eggenstein Leopoldshafen
Federal Republic of Germany

Her Majesty's Stationery Office
P.O. Box 569, S.E. 1
London, England

NASA Center for AeroSpace Information
P.O. Box 8757
Baltimore, Maryland 21240-0757

National Aeronautics and Space Administration
Scientific and Technical Information Program (JTT)
Washington, DC 20546-0001

National Technical Information Service
5285 Port Royal Road
Springfield, Virginia 22161

Pendragon House, Inc.
899 Broadway Avenue
Redwood City, California 94063

Superintendent of Documents
U.S. Government Printing Office
Washington, DC 20402

University Microfilms
A Xerox Company
300 North Zeeb Road
Ann Arbor, Michigan 48106

University Microfilms, Ltd.
Tylers Green
London, England

U.S. Geological Survey Library National Center
MS 950
12201 Sunrise Valley Drive
Reston, Virginia 22092

U.S. Geological Survey Library
2255 North Gemini Drive
Flagstaff, Arizona 86001

U.S. Geological Survey
345 Middlefield Road
Menlo Park, California 94025

U.S. Geological Survey Library
Box 25046
Denver Federal Center, MS914
Denver, Colorado 80225

NTIS PRICE SCHEDULES

(Effective October 1, 1991)

Schedule A
STANDARD PRICE DOCUMENTS AND MICROFICHE**

PRICE CODE	NORTH AMERICAN PRICE	FOREIGN PRICE
A01	$ 9.00	$ 18.00
A02	12.50	25.00
A03	17.00	34.00
A04-A05	19.00	38.00
A06-A09	26.00	52.00
A10-A13	35.00	70.00
A14-A17	43.00	86.00
A18-A21	50.00	100.00
A22-A25	59.00	118.00
A99	*	*
N01	60.00	120.00
N02	59.00	118.00
N03	20.00	40.00

Schedule E
EXCEPTION PRICE DOCUMENTS AND MICROFICHE**

PRICE CODE	NORTH AMERICAN PRICE	FOREIGN PRICE
E01	$11.00	$ 22.00
E02	14.00	28.00
E03	16.00	32.00
E04	19.00	38.00
E05	21.00	42.00
E06	24.00	48.00
E07	27.00	54.00
E08	30.00	60.00
E09	33.00	66.00
E10	36.00	72.00
E11	39.00	78.00
E12	43.00	86.00
E13	46.00	92.00
E14	50.00	100.00
E15	54.00	108.00
E16	59.00	118.00
E17	64.00	128.00
E18	69.00	138.00
E19	76.00	152.00
E20	88.00	176.00
E99	*	*

* Contact NTIS for price quote.

** Effective January 1, 1991, the microfiche copy of any new document entering the NTIS collection will be priced the same as the paper copy of the document.

IMPORTANT NOTICE

NTIS Shipping and Handling Charges

U.S., Canada, Mexico — ADD $3.00 per TOTAL ORDER

All Other Countries — ADD $4.00 per TOTAL ORDER

Exceptions — Does NOT apply to:

ORDERS REQUESTING NTIS RUSH HANDLING

ORDERS FOR SUBSCRIPTION OR STANDING ORDER PRODUCTS *ONLY*

NOTE: Each additional delivery address on an order requires a separate shipping and handling charge.

FEDERAL REGIONAL DEPOSITORY LIBRARIES

ALABAMA

AUBURN UNIV. AT MONTGOMERY LIBRARY
Documents Dept.
7300 University Drive
Montgomery, AL 36117-3596
(205) 244-3650 FAX: (205) 244-0678

UNIV. OF ALABAMA
Amelia Gayle Gorgas Library
Govt. Documents
Box 870266
Tuscaloosa, AL 35487-0266
(205) 348-6046 FAX: (205) 348-8833

ARIZONA

DEPT. OF LIBRARY, ARCHIVES, AND PUBLIC RECORDS
Federal Documents
Third Floor State Capitol
1700 West Washington
Phoenix, AZ 85007
(602) 542-4121 FAX: (602) 542-4400; 542-4500

ARKANSAS

ARKANSAS STATE LIBRARY
State Library Services
One Capitol Mall
Little Rock, AR 72201
(501) 682-2869

CALIFORNIA

CALIFORNIA STATE LIBRARY
Govt. Publications Section
914 Capitol Mall - P.O. Box 942837
Sacramento, CA 94237-0001
(916) 322-4572 FAX: (916) 324-8120

COLORADO

UNIV. OF COLORADO - BOULDER
Norlin Library
Govt. Publications
Campus Box 184
Boulder, CO 80309-0184
(303) 492-8834 FAX: (303) 492-2185

DENVER PUBLIC LIBRARY
Govt. Publications Dept. BS/GPD
1357 Broadway
Denver, CO 80203
(303) 571-2135

CONNECTICUT

CONNECTICUT STATE LIBRARY
231 Capitol Avenue
Hartford, CT 06106
(203) 566-4971 FAX: (203) 566-3322

FLORIDA

UNIV. OF FLORIDA LIBRARIES
Documents Dept.
Library West
Gainesville, FL 32611-2048
(904) 392-0366 FAX: (904) 392-7251

GEORGIA

UNIV. OF GEORGIA LIBRARIES
Govt. Documents Dept.
Jackson Street
Athens, GA 30602
(404) 542-8949 FAX: (404) 542-6522

HAWAII

UNIV. OF HAWAII
Hamilton Library
Govt. Documents Collection
2550 The Mall
Honolulu, HI 96822
(808) 948-8230 FAX: (808) 956-5968

IDAHO

UNIV. OF IDAHO LIBRARY
Documents Section
Moscow, ID 83843
(208) 885-6344 FAX: (208) 885-6817

ILLINOIS

ILLINOIS STATE LIBRARY
Reference Dept.
300 South Second
Springfield, IL 62701-1796
(217) 782-7596 FAX: (217) 524-0041

INDIANA

INDIANA STATE LIBRARY
Serials/Documents Section
140 North Senate Avenue
Indianapolis, IN 46204
(317) 232-3678 FAX: (317) 232-3728

IOWA

UNIV. OF IOWA LIBRARIES
Govt. Publications Dept.
Washington & Madison Streets
Iowa City, IA 52242
(319) 335-5926 FAX: (319) 335-5830

KANSAS

UNIV. OF KANSAS
Govt. Documents & Map Library
6001 Malatt Hall
Lawrence, KS 66045-2800
(913) 864-4660 FAX: (913) 864-5380

KENTUCKY

UNIV. OF KENTUCKY LIBRARIES
Govt. Publications/Maps Dept.
Lexington, KY 40506-0039
(606) 257-3139 FAX: (606) 257-1563; 257-8379

LOUISIANA

LOUISIANA STATE UNIV.
Middleton Library
Govt. Documents Dept.
Baton Rouge, LA 70803
(504) 388-2570 FAX: (504) 388-6992

LOUISIANA TECHNICAL UNIV.
Prescott Memorial Library
Govt. Documents Dept.
305 Wisteria Street
Ruston, LA 71270-9985
(318) 257-4962 FAX: (318) 257-2447

MAINE

TRI-STATE DOCUMENTS DEPOSITORY
Raymond H. Fogler Library
Govt. Documents & Microforms Dept.
Univ. of Maine
Orono, ME 04469
(207) 581-1680

MARYLAND

UNIV. OF MARYLAND
Hornbake Library
Govt. Documents/Maps Unit
College Park, MD 20742
(301) 454-3034 FAX: (301) 454-4985

MASSACHUSETTS

BOSTON PUBLIC LIBRARY
Govt. Documents Dept.
666 Boylston Street
Boston, MA 02117
(617) 536-5400 ext. 226
FAX: (617) 267-8273; 267-8248

MICHIGAN

DETROIT PUBLIC LIBRARY
5201 Woodward Avenue
Detroit, MI 48202-4093
(313) 833-1440; 833-1409
FAX: (313) 833-5039

LIBRARY OF MICHIGAN
Govt. Documents Unit
P.O. Box 30007
Lansing, MI 48909
(517) 373-0640 FAX: (517) 373-3381

MINNESOTA

UNIV. OF MINNESOTA
Wilson Library
Govt. Publications Library
309 19th Avenue South
Minneapolis, MN 55455
(612) 624-5073 FAX: (612) 626-9353

MISSISSIPPI

UNIV. OF MISSISSIPPI
J.D. Williams Library
Federal Documents Dept.
106 Old Gym Bldg.
University, MS 38677
(601) 232-5857 FAX: (601) 232-5453

MISSOURI

UNIV. OF MISSOURI - COLUMBIA
Ellis Library
Govt. Documents
Columbia, MO 65201
(314) 882-6733 FAX: (314) 882-8044

MONTANA

UNIV. OF MONTANA
Maureen & Mike Mansfield Library
Documents Div.
Missoula, MT 59812-1195
(406) 243-6700 FAX: (406) 243-2060

NEBRASKA

UNIV. OF NEBRASKA - LINCOLN
D.L. Love Memorial Library
Documents Dept.
Lincoln, NE 68588
(402) 472-2562

NEVADA

UNIV. OF NEVADA
Reno Library
Govt. Publications Dept.
Reno, NV 89557
(702) 784-6579 FAX: (702) 784-1751

NEW JERSEY

NEWARK PUBLIC LIBRARY
U.S. Documents Div.
5 Washington Street -
P.O. Box 630
Newark, NJ 07101-0630
(201) 733-7812 FAX: (201) 733-5648

NEW MEXICO

UNIV. OF NEW MEXICO
General Library
Govt. Publications Dept.
Albuquerque, NM 87131-1466
(505) 277-5441 FAX: (505) 277-6019

NEW MEXICO STATE LIBRARY
325 Don Gaspar Avenue
Santa Fe, NM 87503
(505) 827-3826 FAX: (505) 827-3820

NEW YORK

NEW YORK STATE LIBRARY
Documents/Gift & Exchange Section
Federal Depository Program
Cultural Education Center
Albany, NY 12230
(518) 474-5563 FAX: (518) 474-5786

NORTH CAROLINA

UNIV. OF NORTH CAROLINA - CHAPEL HILL
CB#3912, Davis Library
BA/SS Dept.—Documents
Chapel Hill, NC 27599
(919) 962-1151 FAX: (919) 962-0484

NORTH DAKOTA

NORTH DAKOTA STATE UNIV. LIBRARY
Documents Office
Fargo, ND 58105
(701) 237-8886 FAX: (701) 237-7138
In cooperation with Univ. of North Dakota, Chester Fritz Library
Grand Forks

OHIO

STATE LIBRARY OF OHIO
Documents Dept.
65 South Front Street
Columbus, OH 43266
(614) 644-7051 FAX: (614) 752-9178

OKLAHOMA

OKLAHOMA DEPT. OF LIBRARIES
U.S. Govt. Information Div.
200 NE 18th Street
Oklahoma City, OK 73105-3298
(405) 521-2502, ext. 252, 253
FAX: (405) 525-7804

OKLAHOMA STATE UNIV.
Edmon Low Library
Documents Dept.
Stillwater, OK 74078
(405) 744-6546 FAX: (405) 744-5183

OREGON

PORTLAND STATE UNIV.
Millar Library
934 SW Harrison - P.O. Box 1151
Portland, OR 97207
(503) 725-3673 FAX: (503) 725-4527

PENNSYLVANIA

STATE LIBRARY OF PENN.
Govt. Publications Section
Walnut St. & Commonwealth Ave. - P.O. Box 1601
Harrisburg, PA 17105
(717) 787-3752

SOUTH CAROLINA

CLEMSON UNIV.
Cooper Library
Public Documents Unit
Clemson, SC 29634-3001
(803) 656-5174 FAX: (803) 656-3025
In cooperation with Univ. of South Carolina, Thomas Cooper Library, Columbia

TENNESSEE

MEMPHIS STATE UNIV. LIBRARIES
Govt. Documents
Memphis, TN 38152
(901) 678-2586 FAX: (901) 678-2511

TEXAS

TEXAS STATE LIBRARY
United States Documents
P.O. Box 12927 - 1201 Brazos
Austin, TX 78711
(512) 463-5455 FAX: (512) 463-5436

TEXAS TECH. UNIV. LIBRARY
Documents Dept.
Lubbock, TX 79409
(806) 742-2268 FAX: (806) 742-1920

UTAH

UTAH STATE UNIV.
Merrill Library & Learning Resources Center, UMC-3000
Documents Dept.
Logan, UT 84322-3000
(801) 750-2684 FAX: (801) 750-2677

VIRGINIA

UNIV. OF VIRGINIA
Alderman Library
Govt. Documents
Charlottesville, VA 22903-2498
(804) 924-3133 FAX: (804) 924-4337

WASHINGTON

WASHINGTON STATE LIBRARY
Document Section
MS AJ-11
Olympia, WA 98504-0111
(206) 753-4027 FAX: (206) 753-3546

WEST VIRGINIA

WEST VIRGINIA UNIV. LIBRARY
Govt. Documents Section
P.O. Box 6069
Morgantown, WV 26506
(304) 293-3640

WISCONSIN

ST. HIST. SOC. OF WISCONSIN LIBRARY
Govt. Publications Section
816 State Street
Madison, WI 53706
(608) 262-2781 FAX: (608) 262-4711
In cooperation with Univ. of Wisconsin-Madison, Memorial Library

MILWAUKEE PUBLIC LIBRARY
Documents Div.
814 West Wisconsin Avenue
Milwaukee, WI 53233
(414) 278-2167 FAX: (414) 278-2137

* U.S. G.P.O.:1992-313-125:60019

National Aeronautics and
Space Administration
Code JTT
Washington, D.C.
20546-0001

Official Business
Penalty for Private Use, $300

SPECIAL FOURTH-CLASS RATE
POSTAGE & FEES PAID
NASA
PERMIT No. G27

POSTMASTER: If Undeliverable (Section 158
Postal Manual) Do Not Return